

## INTERNATIONAL TMF-WORKSHOP

# 3<sup>RD</sup> WORKSHOP ON THERMO-MECHANICAL FATIGUE

## DATE

27.04.2016 - 29.04.2016

## VENUE

Bundesanstalt für Materialforschung und -prüfung  
Unter den Eichen 87  
12205 Berlin

## JOINT ORGANIZERS

High Temperature Mechanical Testing Committee (HTMTC)  
Bundesanstalt für Materialforschung und -prüfung (BAM), Department Materials Engineering

## SCOPE

Components in the Aerospace, Power and Automotive engineering sectors are frequently subjected to cyclic stresses induced by thermal fluctuations and mechanical loads. For the design of such components, reliable material property data are required which need to be acquired using well accepted and reproducible test procedures for thermo-mechanical fatigue (TMF) loading. Available materials TMF property data are limited so that there is a need for further TMF data generated by TMF testing. The TMF behaviour of materials is often desired to be simulated in models which describe the cyclic stress-strain behaviour, the fatigue life and the cyclic crack growth behaviour. There is a continuous need for the development and amendment of such models. Models can be validated by using materials in industrial applications which are subjected to TMF loading.

## TOPICS

- TMF of steels, cast irons, aluminium-, titanium-, nickel base and other alloys
- Cyclic stress strain behaviour at TMF
- TMF life
- TMF crack growth
- Comparison of TMF and LCF life
- TMF and superimposed HCF

- TMF and creep interactions
- TMF and environmental interactions
- Multiaxial TMF
- TMF of coated materials
- TMF and thermal fatigue of components
- TMF damage mechanisms
- Interpretation of TMF data
- TMF life and crack growth models
- TMF crack growth measurement
- Stress or strain controlled TMF testing
- Service-cycle TMF testing
- TMF testing procedures and standardisation
- Applications

## TARGET GROUP

The TMF-Workshops address engineers, scientists and technical staff of research institutes and industry who have an interest in the numerous aspects of thermo-mechanical fatigue.

## PARTNERS

ESIS European Structural Integrity Society

DVM German Association for Materials Research and Testing

## SPONSORS

INSTRON

MTS

## HISTORY

International Workshops on Thermo-Mechanical Fatigue were successfully held at BAM in 2016, 2011 and 2005.

The first TMF-Workshop was held on the occasion of the development of a European Code of Practice for strain-controlled TMF testing. It brought together approx. 70 European and international experts.

The 2<sup>nd</sup> TMF-Workshop was successful as well with approx. 100 international participants.

From 2012 to 2015, a Code of Practice for Force Controlled TMF testing was developed by a European group of experts. The paper was presented and discussed on the 3<sup>rd</sup> International Workshop on Thermo-Mechanical Fatigue in 2016.

## CONTACT

Bundesanstalt für Materialforschung und -prüfung (BAM)  
Department Materials Engineering  
Dr.-Ing. Hellmuth Klingelhöffer  
Email: [hellmuth.klingelhoeffler@bam.de](mailto:hellmuth.klingelhoeffler@bam.de)



# TMF-Workshop 2016, BAM, Berlin

## Programme

Chairman: Dr.-Ing. Hellmuth Klingelhöffer  
Phone: + 49 30 8104 1501

co-organized by



co-sponsored by



### Wednesday April 27, 2016:

Time Start	Time End	Author(s)/Speaker	Affiliation(s)	Title
09:00	09:10	Klingelhöffer	BAM, chairman	Welcome and Opening
09:10	09:20	Portella	BAM, head of department 5 - Materials Engineering	Welcome to BAM
09:20	09:30	Olbricht	BAM, Berlin, Germany	Development of TMF testing - a little look back
<b>Session 1</b>		<b>Chairman: M. Bache</b>		<b>Thermal Barrier Coatings / Thermal Gradient Mechanical Fatigue</b>
09:35	10:00	Okazaki et al.	Nagaoka Tech. University/... (JP)	Effect of ceramic top coat on thermo-mechanical fatigue failure of TBCed superalloy specimen
10:00	10:25	Mauget et al.	CNRS - ENSMA, Univ. Poitiers (F)	Damage mechanisms in an EB-PVD thermal barrier coating system during TMF and TGMF testing conditions under hot gas flow
10:25	10:50	Bartsch et al.	DLR, Köln /... (D)	In situ-strain measurement in a coated superalloy by synchrotron x-ray diffraction during thermal mechanical cycling with superposed thermal gradient (TGMF)
10:50	11:20	Coffee break and poster session		The poster authors and titles can be found on the last page of the program
<b>Session 2</b>		<b>Chairman: T. Beck</b>		<b>TMF properties I: steels, Al- and Mg-alloys</b>
11:20	11:45	Moverare et al.	Linköping Univ. / Sandvik (S)	Thermo-mechanical fatigue behaviour of an advanced heat resistant austenitic stainless steel
11:45	12:10	Azadi et al.	Semnan Univ., Semnan (Iran)	Study of thermo-mechanical fatigue behaviors in light alloys with and without heat treatment
12:10	12:35	Nagesha et al.	Indira Gandhi Centre for Atomic Research, Kalpakkam (India)	Thermomechanical fatigue studies on Indian RAFM steel including dwell effects
12:35	13:00	Hübsch et al.	Fraunhofer IWM, VDM Metals (D)	Impact of phasing, creep effects and microstructural evolution on the thermomechanical fatigue behaviour of alloy 800H
13:00	14:00	Lunch break		

<b>Session 3</b>		<b>Chairman: E. Affeldt</b>		<b>Industrial applications</b>
14:00	14:25	Remy et al.	Mines ParisTech et al	Thermal Mechanical Fatigue of welded ferritic stainless steel structures
14:25	14:50	Rudolph et al.	AREVA, Erlangen (D)	TMF/SHM for thermal power plants
14:50	15:15	Vacchieri, Holdsworth, Poggio, Villari	Ansaldo Sviluppo Energia (I), EMPA, Dübendorf (CH)	Service-like TMF tests for the validation and assessment of a creep-fatigue life procedure developed for GT blades and vanes
15:15	15:45	Coffee break and poster session		The poster authors and titles can be found on the last page of the program
<b>Session 4</b>		<b>Chairman: K.-H. Lang</b>		<b>TMF + HCF</b>
15:45	16:10	Fedelich, Kühn et al.	BAM, Berlin (D)	Experimental and analytical investigation of the TMF-HCF lifetime behavior of two cast iron alloys
16:10	16:35	Hosseini, Holdsworth	Inspire Centre for Mech. Integrity, EMPA, Dübendorf (CH)	Cracking due to combined HCF and TMF loading in cast iron
16:35	17:00	Norman, Skoglund, Leidermark, Moverare	Linköping Univ.; Scania, Södertälje (S)	Combined thermo-mechanical and high-cycle fatigue of high-Silicon-Molybdenum spheroidal graphite irons

<b>Thursday, April 28, 2016:</b>				
<b>Time</b>		<b>Author(s)/Speaker</b>	<b>Affiliation(s)</b>	<b>Title</b>
<b>Start</b>	<b>End</b>			
<b>Session 5</b>		<b>Chairman M. McGaw</b>		<b>Advanced TMF testing techniques / TMF properties Ni-alloys</b>
09:00	09:25	Jones, Whittaker, Brookes, Lancaster et al	Swansea University (UK), Rolls-Royce MTOC (D)	Infrared thermography for cyclic high-temperature measurement and control
09:25	09:50	Brookes et al.	Rolls Royce MTOC (D) et al.	A new code of practice for force controlled thermo-mechanical fatigue testing
09:50	10:15	Hormozi, Biglari, Nikbin	Imperial College London (UK), Amirkabir Univ. of Technology Tehran (Iran)	Experimental procedures of conducting strain-controlled thermo mechanical fatigue & low cycle fatigue tests on type 316 stainless steel
10:15	10:40	Jones, Whittaker, Lancaster, Williams	Swansea University (UK), Rolls-Royce, Derby (UK)	The influence of phase angle, strain range and peak cycle temperature on the TMF crack initiation behaviour and damage mechanisms of the Nickel-based superalloy RR1000
10:40	11:10	Coffee break and poster session		The poster authors and titles can be found on the last page of the program

Session 6		Chairman P.D.Portella		TMF crack growth	
11:10	11:35	Whittaker, Pretty, Williams	Swansea University, Rolls-Royce (UK)	Thermo-mechanical fatigue crack growth of RR1000	
11:35	12:00	Schlesinger, Seifert, Preußner	Fraunhofer IWM, Offenburg University (D)	Experimental investigation of the time and temperature dependent growth of small fatigue cracks in Inconel 718 and mechanism based lifetime prediction	
12:00	12:25	Eckmann, Schweizer	Fraunhofer IWM, Freiburg (D)	Characterisation of damage mechanisms of Nickel-base alloy MAR-M247 CC (HIP) under thermomechanical creep-fatigue loading using digital image processing	
12:25	12:50	Hyde, Buss	Nottingham Univ. (UK)	Thermo-mechanical fatigue crack growth testing of high temperature materials	
13:00	14:00	Lunch break			
14:00	14:25	Fischer, Kuhn, Mutschler, Rieck et al	FZ Jülich, Univ. Rostock, TÜV NORD GROUP (D)	Thermo-mechanical fatigue crack growth of power plant steels	
14:25	14:50	Kraemer, Mueller et al.	IWK Darmstadt (D), Ansaldo Sviluppo Energia (I)	Estimation of thermo-mechanical fatigue crack growth using an accumulative approach based on isothermal test data	
14:50	15:15	Stekovic, Whittaker, Hyde, Messe, Pattison	Linköping Univ. (S), Swansea Univ., Nottingham Univ. Cambridge Univ., Rolls Royce (UK)	Towards the elaboration of the European Code of Practice for thermo-mechanical fatigue crack growth	
15:15	15:30	Coffee break and poster session		The poster authors and titles can be found on the last page of the program	
<b>Round table discussion</b>					
15:30	17:00	discussion chairmen: M. McGaw, E.Affeldt, T.Beck, H.Klingelhöffer		Discussion of potential amendments of TMF testing standards ISO 12111 and ASTM E 2368	
17:00	18:00				Discussion of potential needs for future research and development in the regime of Thermo-Mechanical Fatigue
<b>Buffet dinner</b>					
18:00	Get together reception in the BAM conference center				
21:00					

Friday, April 29, 2016:

Time Start	Time End	Author(s)/Speaker	Affiliation(s)	Title
<b>Session 7</b>		<b>Chairman L. Remy</b>		<b>TMF Modelling and Lifetime Prediction I</b>
09:00	09:25	Christ et al.	Univ. Siegen (D)	Assessing the thermomechanical fatigue life of TiAl-based alloy TNB-V2
09:25	09:50	Faivre, Santacreu et al.	Aperam Isbergues, ArcelorMittal (F)	TMF life prediction model of a Nickel-Chromium alloy
09:50	10:15	Barrett, O'Hara, Li, O'Donoghue, Leen	NUI Gaway (Ireland), Shenzhen Graduate School (China)	A physically based model for microstructural degradation and life prediction in 9-12Cr steels und thermo-mechanical fatigue
10:15	10:40	Grützner, Fedelich, Rehmer	BAM, Berlin (D)	Constitutive modelling and lifetime prediction for a conventionally cast Ni-base superalloy under TMF loading
10:40	11:10	Coffee break and poster session		The poster authors and titles can be found on the last page of the program
<b>Session 8</b>		<b>Chairman H.-J. Christ</b>		<b>TMF Modelling and Lifetime Prediction II / TMF properties</b>
11:10	11:35	Fischer, Schweizer, Seifert	Fraunhofer IWM, Freiburg; Offenburg University (D)	A crack opening stress equation for in-phase and out-of-phase thermomechanical fatigue loading
11:35	12:00	Okrajni et al.	Silesian Univ. of Technology, Katowice (PL)	Local stress-strain behaviour of power plant components
12:00	12:25	Lang, Guth	Karlsruhe Institute Techn. (D)	An approach to lifetime prediction for a wrought Ni-base alloy under thermo-mechanical fatigue with various phase angles between temperature and mechanical strain
12:25	12:50	Kühn, Rehmer, Skrotzki	BAM, Berlin (D)	Thermo-mechanical fatigue of heat resistant austenitic cast iron EN-GJSA-NiSiCr35-5-2 (Ni-Resist D-5S)
12:50	13:00	Closing remarks		
13:00	14:00	Lunch break		
14:00	15:00	Visit of BAM laboratories	Visit options: five parallel visits (please register for one tour at the registration desk; for each visit only a limited number of persons can be accepted)	<a href="#">1. Visit of BAM division 5.2: High temperature mechanical testing incl. TMF testing</a> <a href="#">2. Visit of BAM division 5.1: High temperature corrosion</a> <a href="#">3. Visit of BAM division 2.3: Pyrotechnics for vehicles</a> <a href="#">4. Visit of BAM division 4.1: Biological damage of materials</a> <a href="#">5. Visit of BAM division 8.5: Micro non-destructive testing</a>
15:00	End of event			

<b>Session P</b>	<b>Author(s)/Speaker</b>	<b>Affiliation(s)</b>	<b>Poster Session at coffee breaks Title</b>
P1	von Hartrott, Vorndran, Tandler	Fraunhofer IWM, Freiburg (D)	Investigation on the thermocyclic plasticity of metallic materials for cryogenic hydrogen pressure tanks
P2	Smith, Lancaster, Jones, Mason-Flucke, Bagnall, Jones	Swansea University, Rolls-Royce (UK)	Lifting the thermo-mechanical fatigue behaviour of single crystal superalloys
P3	Prashanth CS, Ragupathy Kannusamy et al.	Honeywell Turbo Technologies, Honeywell Technology Solutions Lab, Bangalore, India	Sensitivity study on effect of cooling and heating rates to control thermal gradient for generation of material data under TMF loading conditions
P4	E.Lopez, S.Ghodrat, L.Kestens, Y.Wu, H.Pirgazi	Ghent University, Ghent, Belgium; Delft University, Delft, The Netherlands	3D EBSD of thermo-mechanical fatigue cracks in compacted graphite iron
P5	Jim Banks, Matt Brooks, Tony Fry, Dave Gorman, John Nunn	National Physical Laboratory, Teddington, UK	Influence of Aluminide coatings on the TMF performance of T91 Steel



In The Name of God



Article Title:

# **Study of Thermo-Mechanical Fatigue Behaviors in Light Alloys with and without Heat Treatments**

**Mohammad Azadi**

*Faculty of Mechanical Engineering, Semnan University, Semnan, Iran*

*Fatigue and Wear in Materials Workgroup, Irankhodro Powertrain Company, Tehran, Iran*

*Research Visitor at Chair of Mechanical Engineering, University of Leoben (Montan-Universitaet), Leoben, Austria*

**Mahboobeh Azadi**

*Faculty of Materials and Metallurgical Engineering, Semnan University, Semnan, Iran*

## Contents

- ❑ Introduction
- ❑ Materials
- ❑ TMF Testing
- ❑ Results and Discussions
- ❑ Conclusions

## Contents

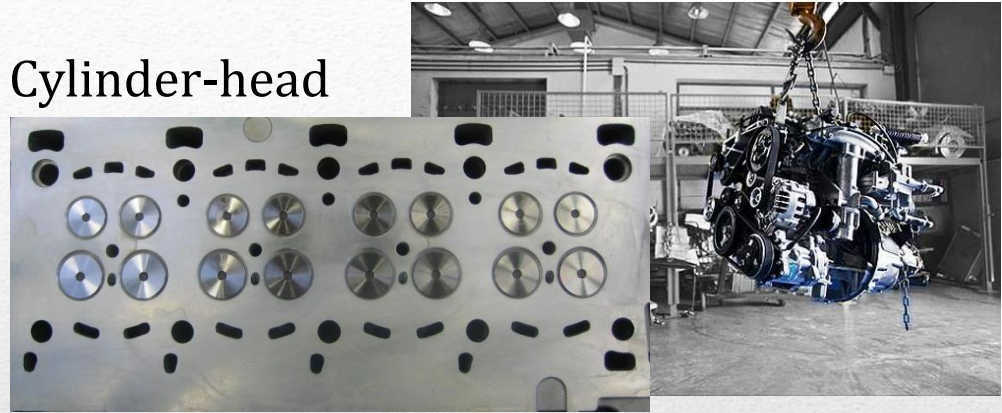
- ❑ **Introduction**
- ❑ Materials
- ❑ TMF Testing
- ❑ Results and Discussions
- ❑ Conclusions

## Introduction

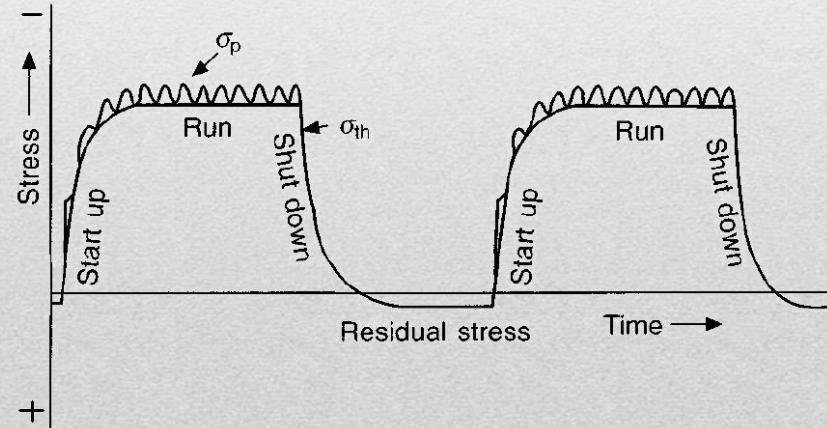
- ❑ Nowadays, light alloys have been utilized in powertrain industries due to their low strength to weight ratio.
- ❑ As such these materials,
  - ❖ aluminum alloys have extensively applied and
  - ❖ magnesium alloys have been considered as a target to use in near futures.
- ❑ Engine components, especially cylinder heads and blocks made of such light alloys, are usually imposed by low-cycle unisothermal fatigue loadings.
- ❑ Therefore, the study of fatigue behaviors in such parts has a high importance in their design and manufacturing processes.

## Introduction

### ❑ Case Study: Diesel Engine Cylinder-head



### ❑ Loadings in Cylinder-head



## Contents

- ❑ Introduction
- ❑ **Materials**
- ❑ TMF Testing
- ❑ Results and Discussions
- ❑ Conclusions

## Materials

Two types of materials:

### ☐ *Material 1: Aluminum alloy*

- ❖ a cast aluminum–silicon–magnesium alloy
- ❖ A356.0 (Al–Si7–Mg0.3)
- ❖ Chemical composition:
  - 7.06% Si, 0.37% Mg, 0.15% Fe, 0.01% Cu, 0.02% Mn, 0.13% Ti and Al is the remainder.
- ❖ Production method:
  - a gravity casting process in permanent molds
- ❖ Heat treatment:
  - 8 h solution at 535 C, water quench and 3 h ageing at 180 C (entitled T6)

## Materials

Two types of materials:

### ❑ **Material 1: Aluminum alloy**

- ❖ a cast aluminum–silicon–magnesium alloy
- ❖ A356.0 (Al–Si7–Mg0.3)

### **What is the problem?**

**In the mass production, suppliers request to eliminate the heat treatment process for the cylinder head to reduce the production time and costs!**

- ❖ Production method:
  - a gravity casting process in permanent molds
- ❖ Heat treatment:
  - 8 h solution at 535 C, water quench and 3 h ageing at 180 C (entitled T6)



## Materials

Two types of materials:

### □ *Material 2: Magnesium alloy*

- ❖ A gravity die cast magnesium alloy
- ❖ AZ91C alloy with RE elements, entitled AZE911
- ❖ Chemical composition:
  - 9.00% Al, 1.05% Zn, 0.06% Mn, 0.04% Si, 1.00% Ca, 0.68% RE and Mg is the remainder.
- ❖ Production method:
  - a gravity manner in permanent molds
- ❖ Heat treatment:
  - 5 h solution at 415 C, quenching in the compressed air (entitled T4) and 5 h ageing at 215 C (entitled T6)

## Materials

Two types of materials:

### ❑ *Material 2: Magnesium alloy*

- ❖ A gravity die cast magnesium alloy
- ❖ AZ91C alloy with RE elements, entitled AZE911

### What is the problem?

**For the mass production of the cylinder head by magnesium alloys, tensile and fatigue properties should be the same as aluminum alloys...**

- ❖ Production method:
  - a gravity manner in permanent molds
- ❖ Heat treatment:
  - 5 h solution at 415 C, quenching in the compressed air (entitled T4) and 5 h ageing at 215 C (entitled T6)

## Contents

- ❑ Introduction
- ❑ Materials
- ❑ **TMF Testing**
- ❑ Results and Discussions
- ❑ Conclusions

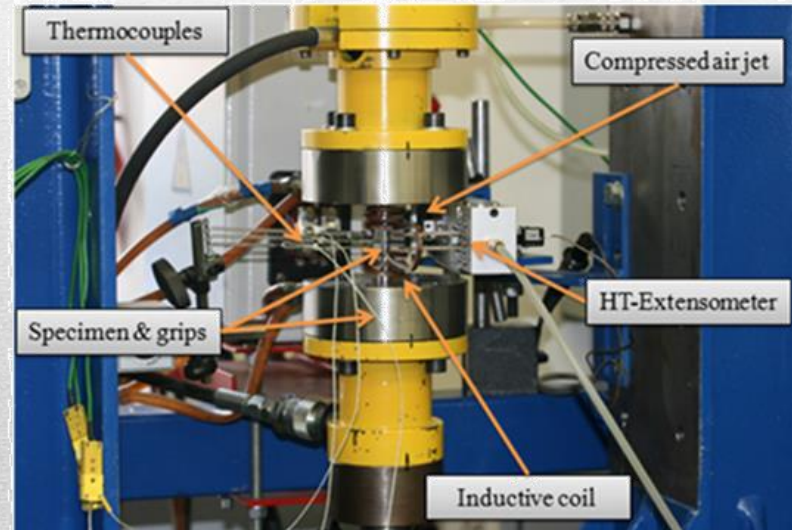
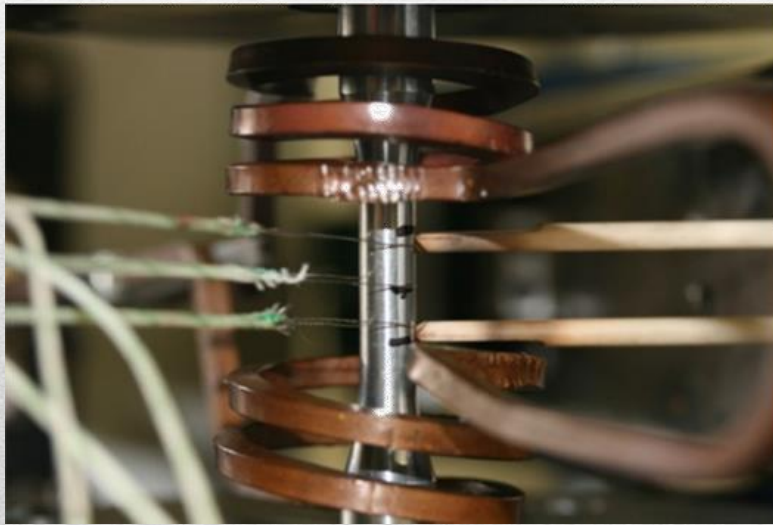
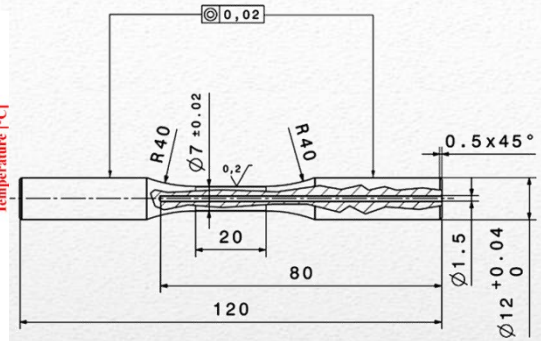
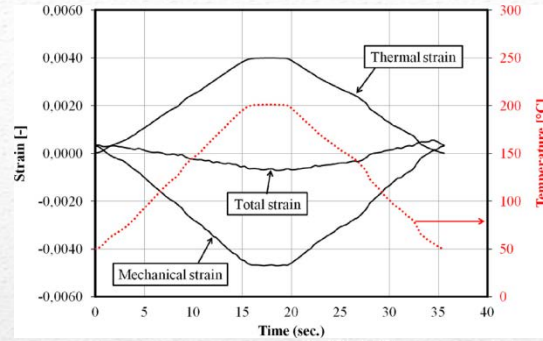
## TMF Testing

- ❑ OP-TMF tests standard: COP-EUR22281-EN procedure
- ❑ Heating/cooling rate: 10 C/s
- ❑ Initial mechanical strain: 0.03%
- ❑ Minimum temperature: 50 C
- ❑ Maximum temperature:
  - Aluminum alloys: 200, 225 and 250 C
  - Magnesium alloys: 200 C
- ❑ Thermo-mechanical loading factor ( $K_{TM}$ ):
  - Aluminum alloys: 125 and 150 %
  - Magnesium alloys: 125 %
- ❑ Holding time (dwell time) at maximum temperatures
  - Aluminum alloys: 5 and 60 s
  - Magnesium alloys: 5 s

$$K_{TM} = \frac{\varepsilon_{a,mech}}{\varepsilon_{a,th}} = \frac{\varepsilon_{mech}(T = T_{max}) - \varepsilon_{mech}(T = T_{min})}{\alpha_{th}(T_{max} - T_{min})}$$

## TMF Testing

- ❑ Specimen
- ❑ Equipment
- ❑ Loadings

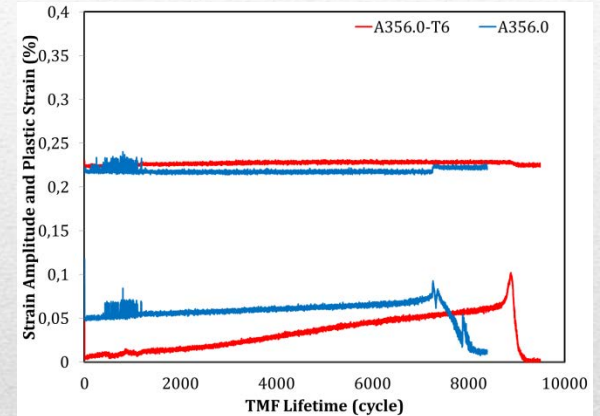
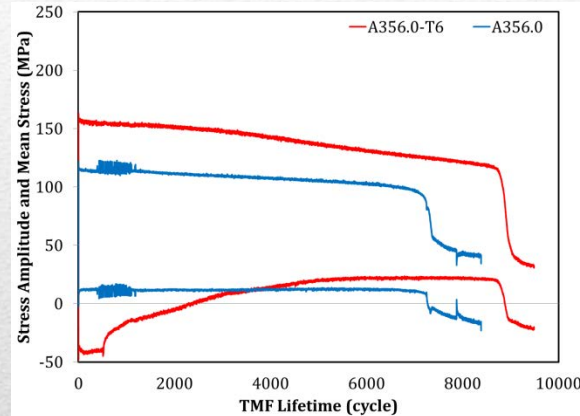
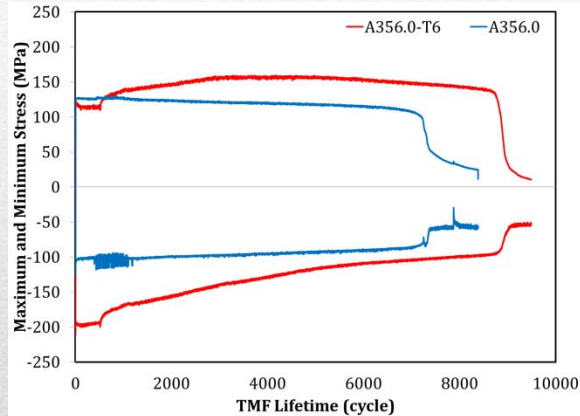


## Contents

- ❑ Introduction
- ❑ Materials
- ❑ TMF Testing
- ❑ **Results and Discussions**
- ❑ Conclusions

## Results and Discussions

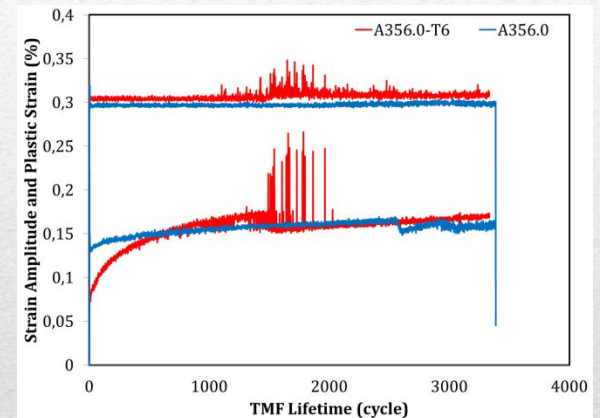
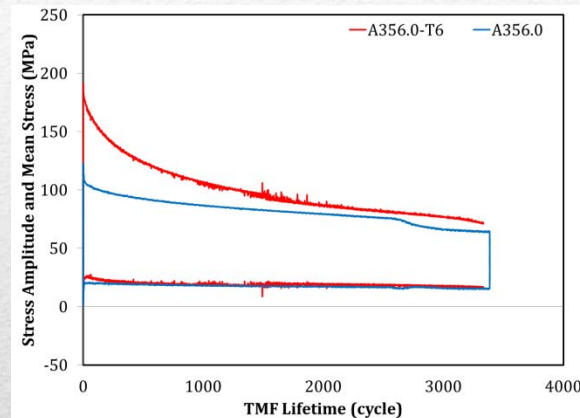
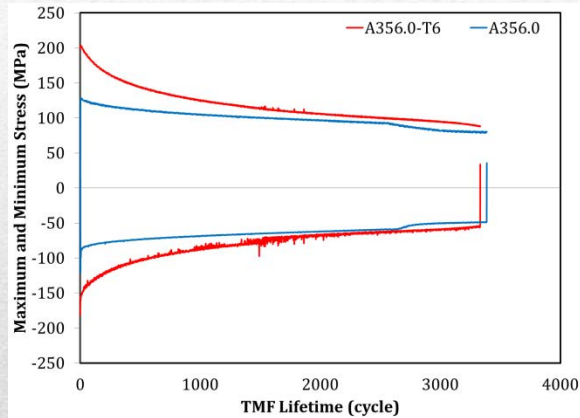
### □ Results for Aluminum alloy



- ❖ Maximum temperature: 200 C
- ❖ Thermo-mechanical loading factor ( $K_{TM}$ ): 125 %
- ❖ Holding time (dwell time) at maximum temperatures: 5 s

## Results and Discussions

### □ Results for Aluminum alloy

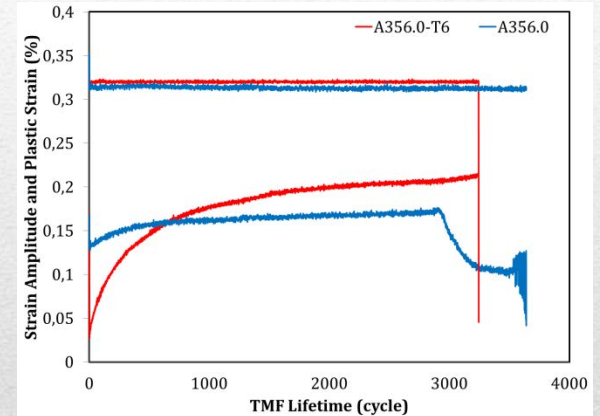
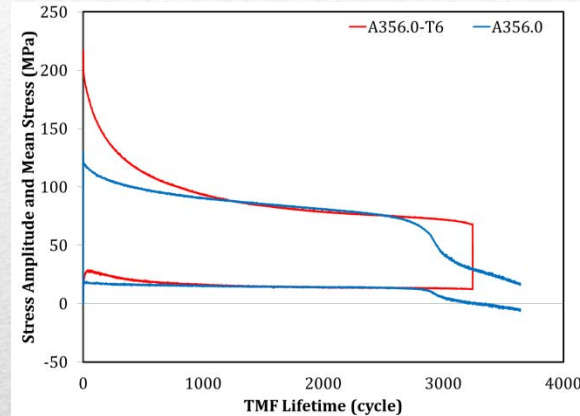
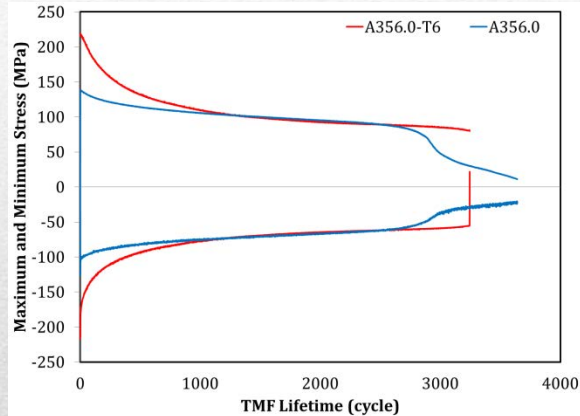


- ❖ Maximum temperature: 250 C
- ❖ Thermo-mechanical loading factor ( $K_{TM}$ ): 125 %
- ❖ Holding time (dwell time) at maximum temperatures: 5 s



## Results and Discussions

### □ Results for Aluminum alloy

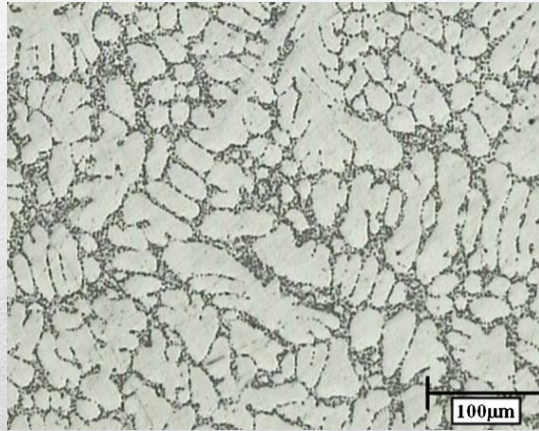


- ❖ Maximum temperature: 225 C
- ❖ Thermo-mechanical loading factor ( $K_{TM}$ ): 150 %
- ❖ Holding time (dwell time) at maximum temperatures: 60 s

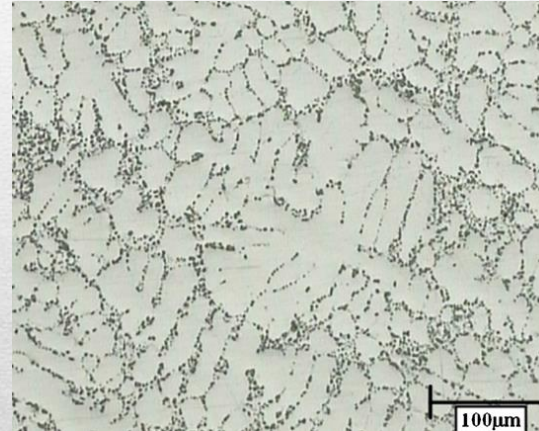
## Results and Discussions

### □ Results for Aluminum alloy

**A356.0 (as-cast)**



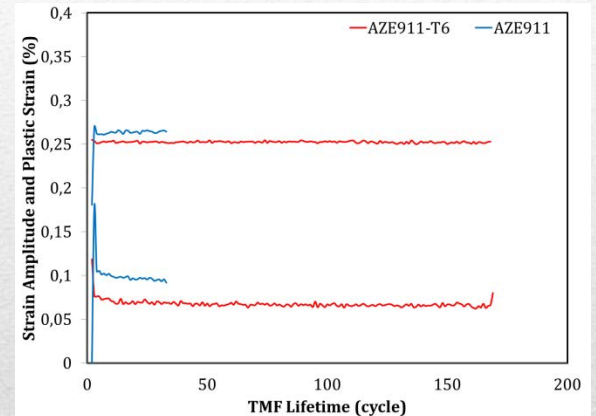
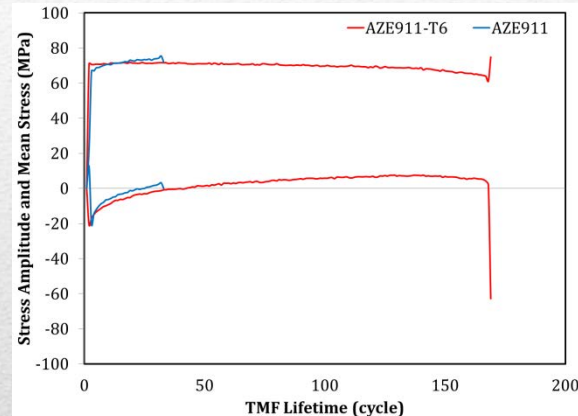
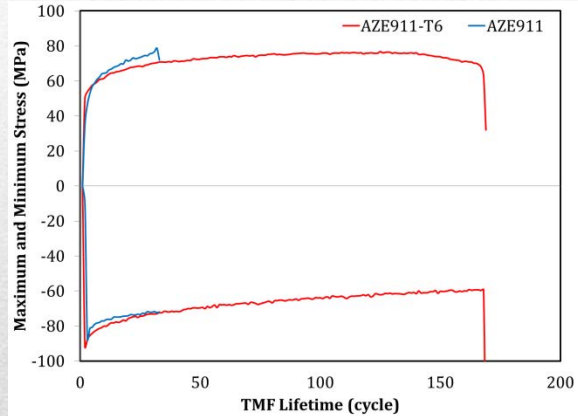
**A356.0-T6**



Irregular eutectic silicon phase → Fine spherodized silicon particles  
Over-ageing in A356.0-T6 → A significant reduction in the strength

## Results and Discussions

### □ Results for Magnesium alloy

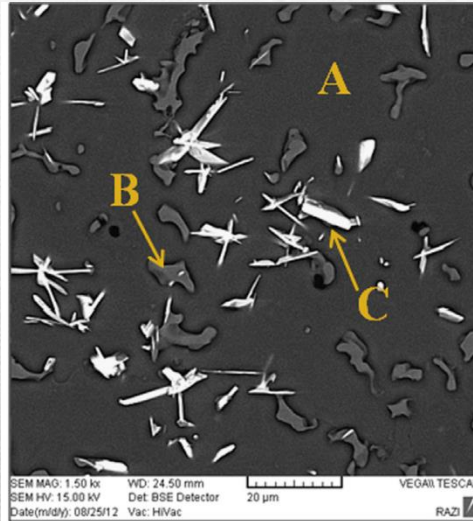


- ❖ Maximum temperature: 200 C
- ❖ Thermo-mechanical loading factor ( $K_{TM}$ ): 125 %
- ❖ Holding time (dwell time) at maximum temperatures: 5 s

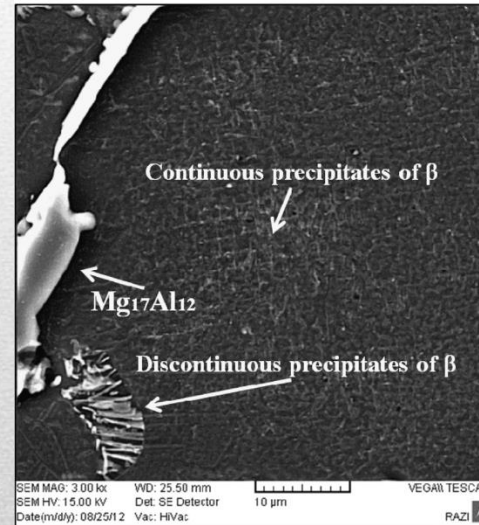
## Results and Discussions

### □ Results for Magnesium alloy

#### AZE911 (as-cast)



#### AZE911-T6

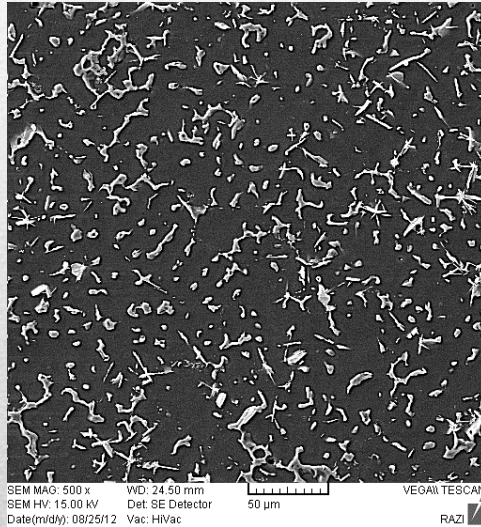


A:  $\alpha$ -Mg matrix , B:  $\beta$ - $Mg_{17}Al_{12}$  phase, C:  $Al_{11}RE_3$  intermetallic

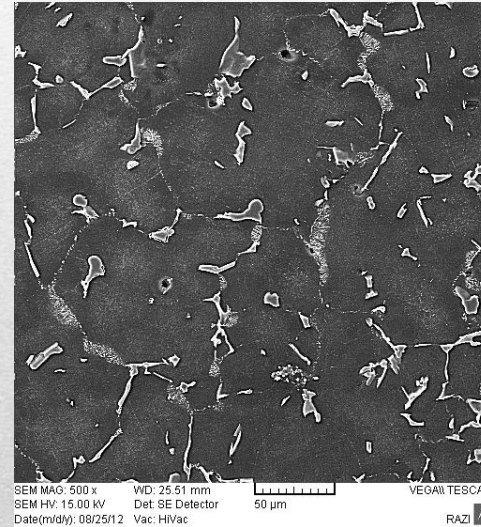
## Results and Discussions

### □ Results for Magnesium alloy

#### AZE911 (as-cast)



#### AZE911-T6

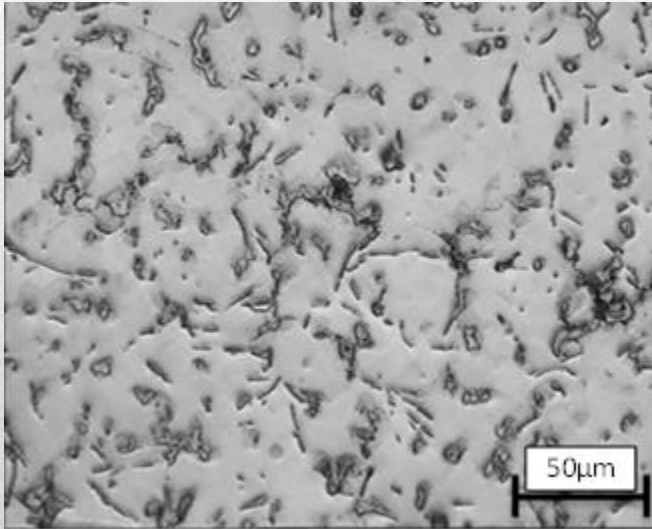


Al<sub>11</sub>-RE<sub>3</sub> intermetallic brittle phase was dissolved in the matrix!

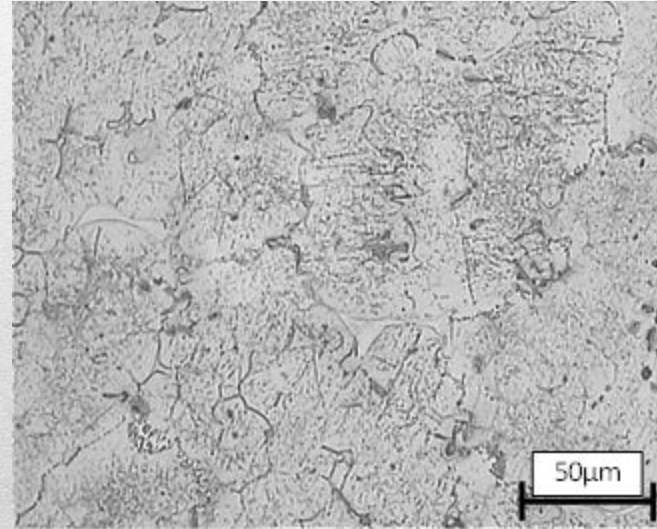
## Results and Discussions

### □ Results for Magnesium alloy

**AZE911 (as-cast)**



**AZE911-T6**



Al<sub>11</sub>-RE<sub>3</sub> intermetallic brittle phase was dissolved in the matrix!

## Contents

- ❑ Introduction
- ❑ Materials
- ❑ TMF Testing
- ❑ Results and Discussions
- ❑ **Conclusions**

## Conclusions

- ❑ For aluminum alloys, the heat treatment can be eliminated, if the design target is the TMF lifetime of the cylinder head.
- ❑ Magnesium alloys, with rare earth elements and a special heat treatment can be used for cylinder heads instead of aluminum alloys, if the combustion temperature is not too high.



**Thank You for Your Attentions**  
**Any Question?**

# A Physically-Based Model for Microstructural Degradation in 9-12Cr Steels Under TMF

R.A. Barrett<sup>1,2</sup>, D.-F. Li<sup>3</sup>, N.P. O'Dowd<sup>4</sup>, P.E. O'Donoghue<sup>2,5</sup>, S.B. Leen<sup>1,2</sup>

<sup>1</sup>Mechanical Engineering, National University of Ireland, Galway, Ireland

<sup>2</sup>Ryan Institute for Environmental, Marine and Energy Research, National University of Ireland, Galway, Ireland

<sup>3</sup>Shenzhen Graduate School, Harbin Institute of Technology, Shenzhen 518055, China

<sup>4</sup>Dept. Of Mechanical, Aeronautical and Biomedical Engineering, MSSI, University of Limerick, Ireland

<sup>5</sup>Civil Engineering, National University of Ireland, Galway, Ireland



OÉ Gaillimh  
NUI Galway



Ryan  
Institute



UNIVERSITY of LIMERICK  
OLLSCOIL LUIMNIGH



# Next Generation Power Plants

**Fossil fuel power generation is in transition to:**

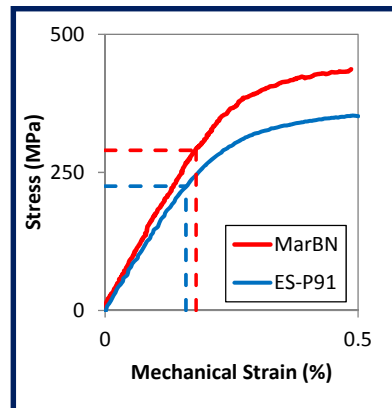
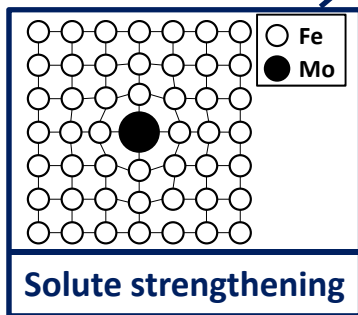
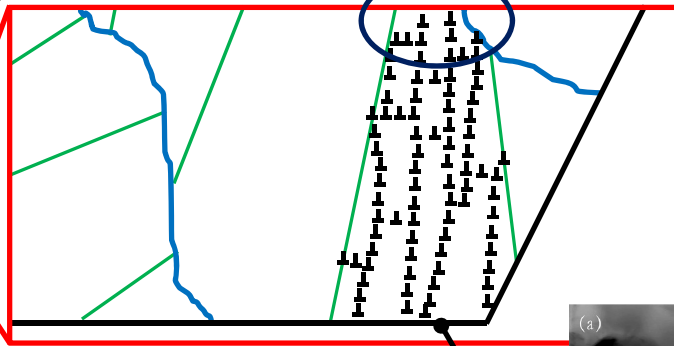
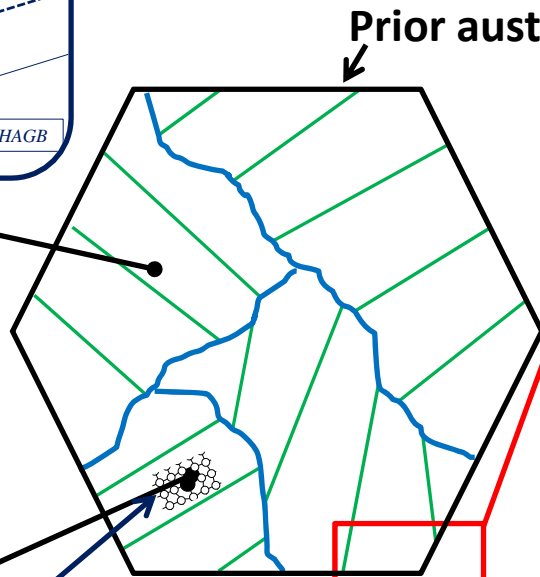
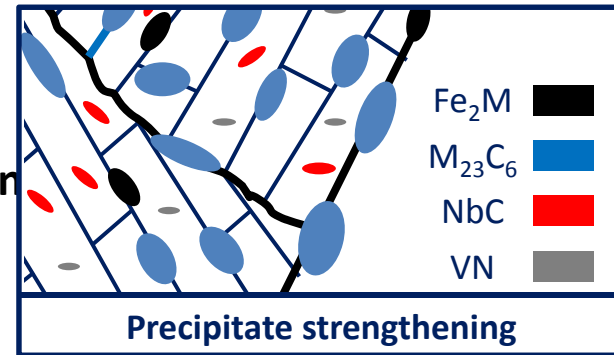
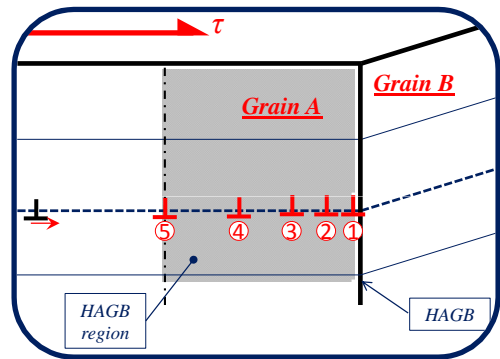
- 1. Higher temperatures and pressures to increase plant efficiencies:**  
→ *Creep, creep-corrosion.*
- 2. Increased flexible operation to accommodate renewable energy sources:**  
→ *Thermal transients, TMF-creep-oxidation deformation.*

**This transition to flexible operation at higher temperatures leads to:**

- 1. More complex mechanisms of deformation.*
- 2. Evolution of the microstructure & microstructural degradation.*
- 3. Ultimately premature failure of components.*

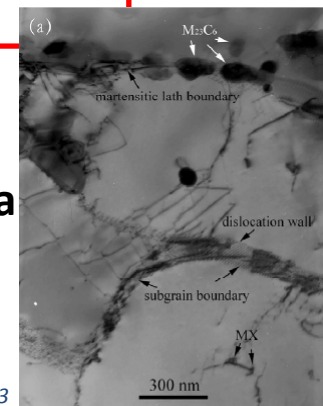
**Requirement for advanced materials with increased  
resistance to microstructural degradation**

# Microstructure of 9Cr Steels



LAB strengthening:  $M_a$

$$\tau_w = \alpha_1 \mu b \sqrt{\rho_w} = \frac{\alpha_2 \mu b}{w}$$

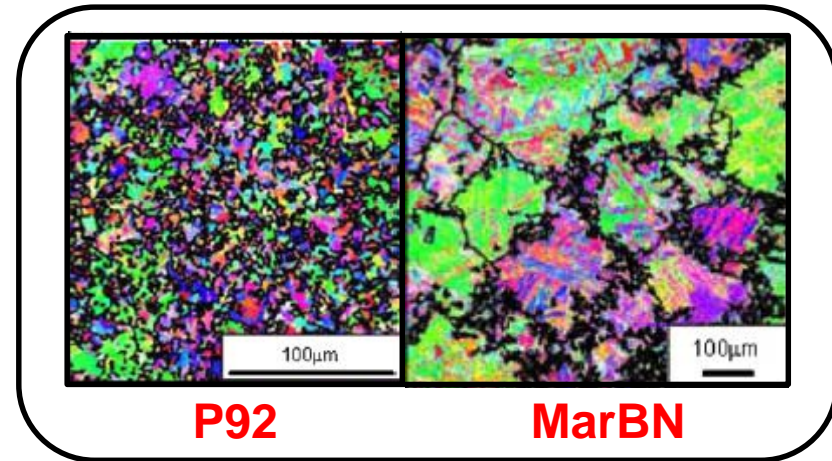
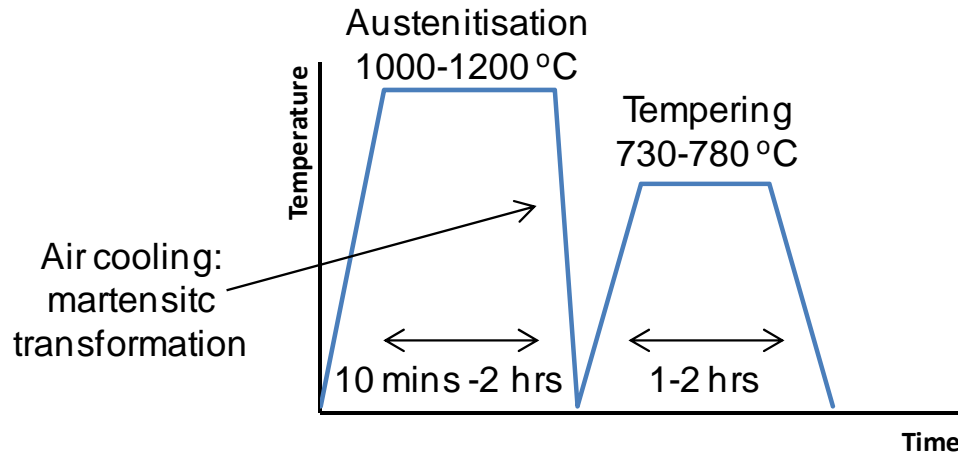


Hu et al., 2013

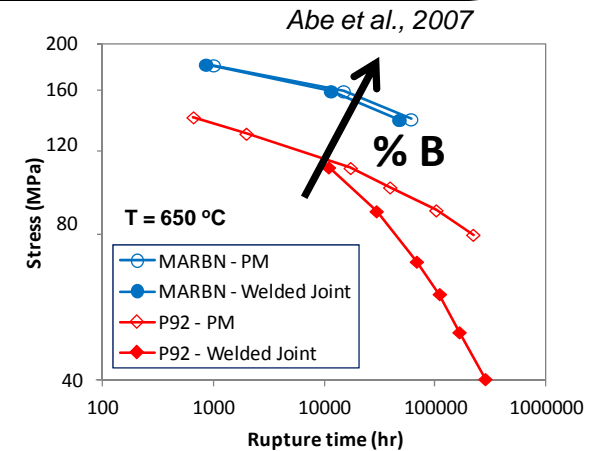
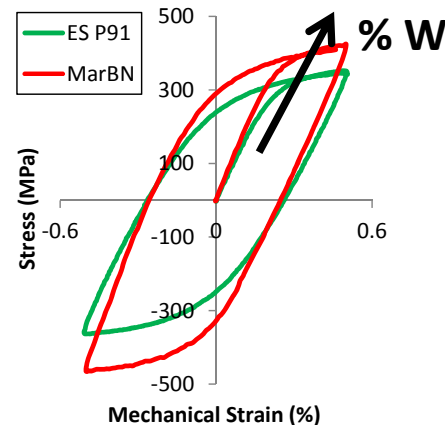
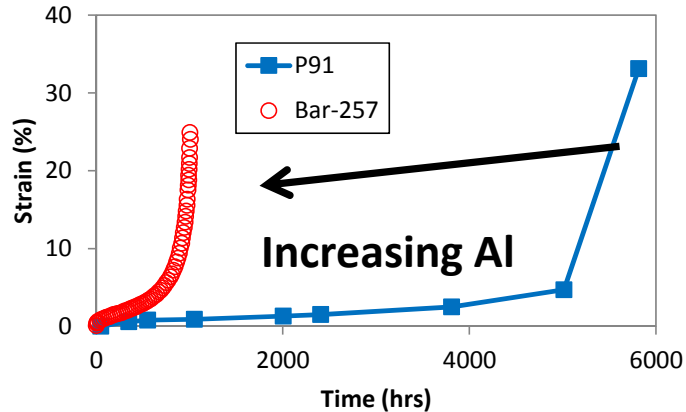
# 9Cr Steels: Composition & HT

	Al	B	C	Co	Cr	Mn	Mo	N	Nb	P	Si	V	W
<b>ES-P91</b>	0.007	-	0.10	-	8.48	0.42	0.94	0.058	0.07	0.013	0.26	0.204	-
<b>MarBN</b>	-	0.018	0.081	3.10	9.08	0.51	-	0.065	0.055	-	0.31	0.2	3.13

MarBN composition: Abe et al., 2008

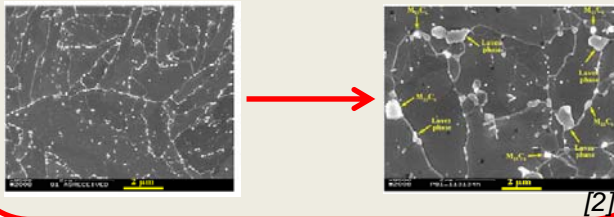


- Hyde et al., 2006.
- Abd El-Azim et al., 2013.



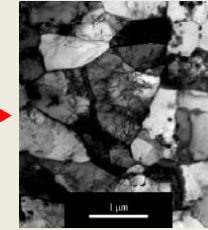
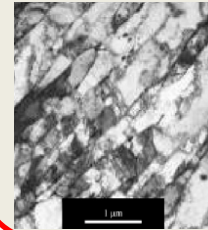
# Evolution of Microstructure

## Precipitate coarsening & Laves phase formation

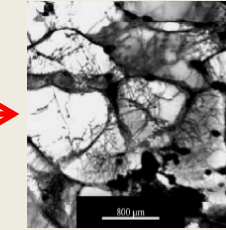


[2]

## Subgrain formation

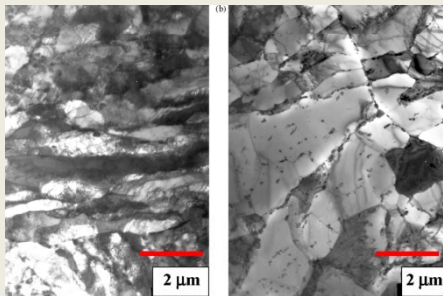


## Subgrain growth

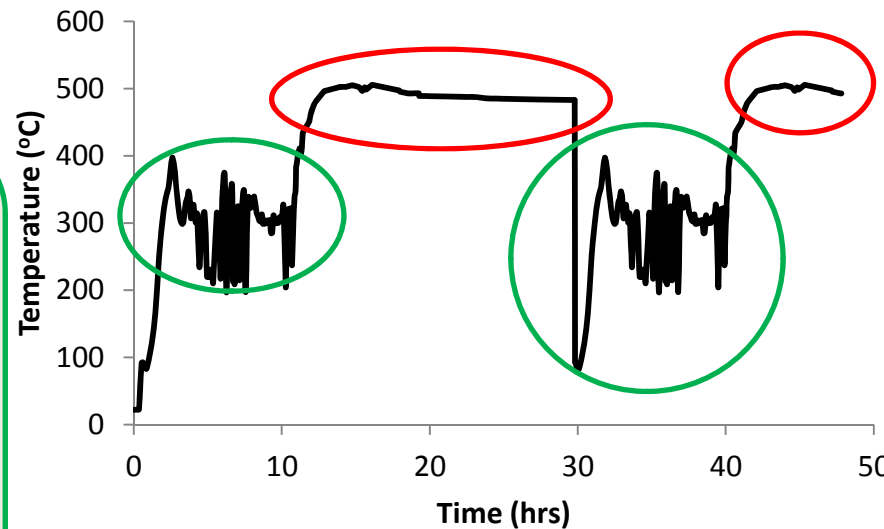


[3]

## Martensitic lath widening

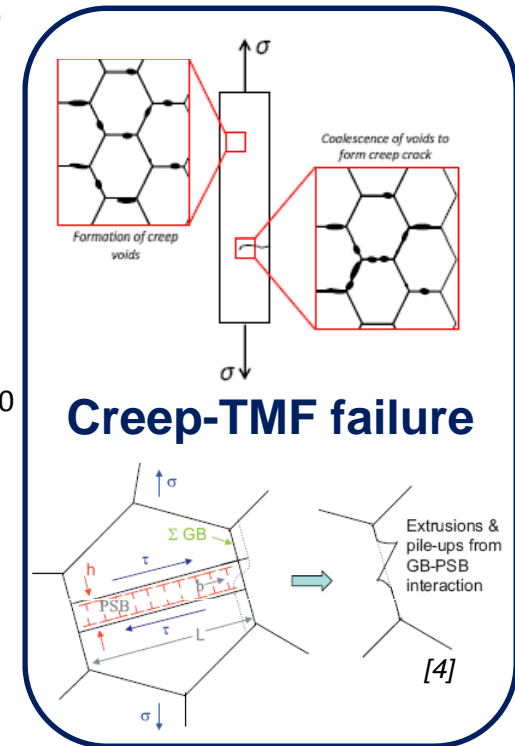


[1]



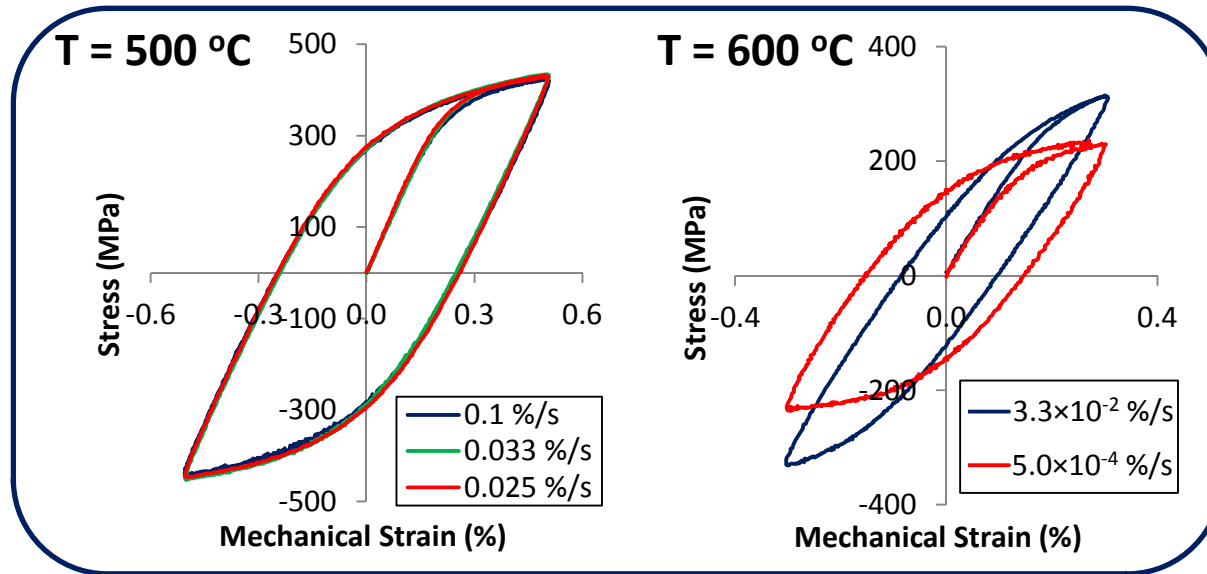
## Creep-TMF deformation & microstructural degradation

1. Sauzay et al., 2008.
2. Panait et al., 2010.
3. Yan et al., 2013.
4. Sangid et al., 2011.



[4]

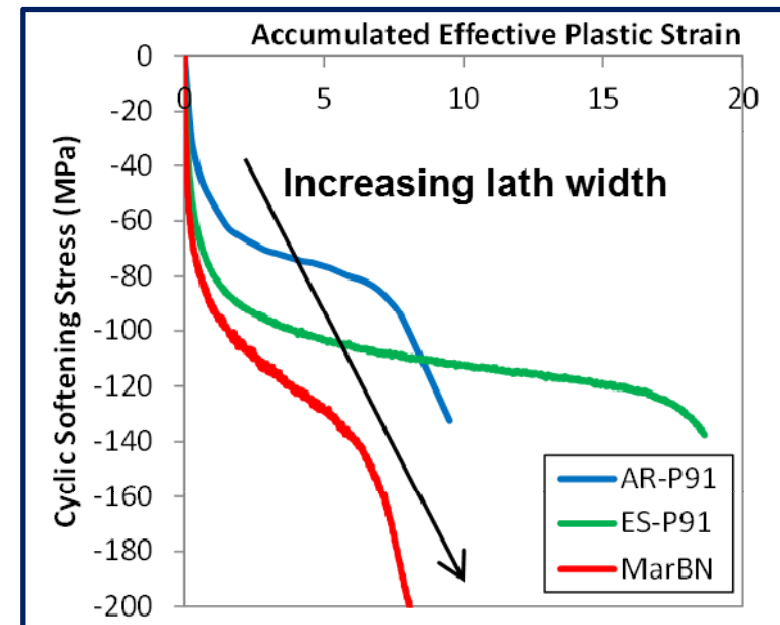
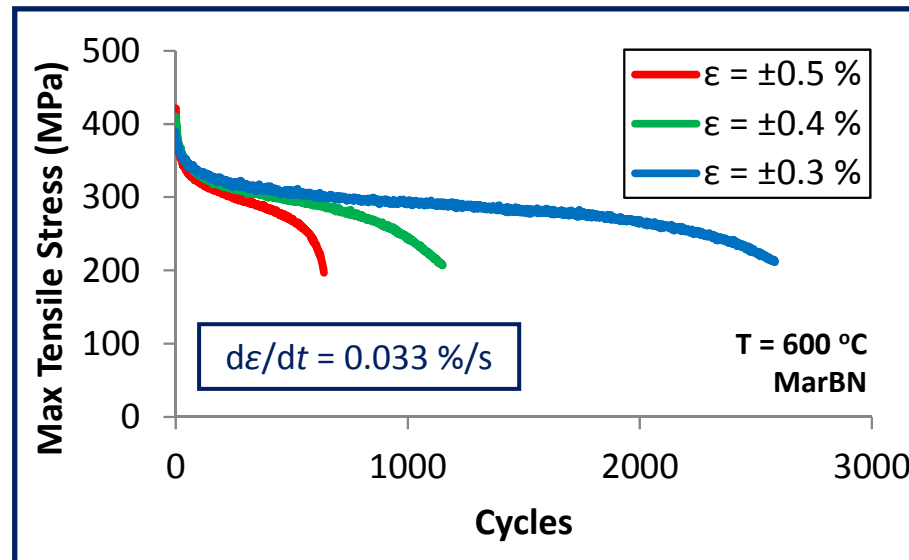
# Experimental Testing – 9Cr Steels



ES-P91 Testing carried out by Dr. C.J. Hyde, University of Nottingham.

**Strain-rate effect**

**Cyclic softening**

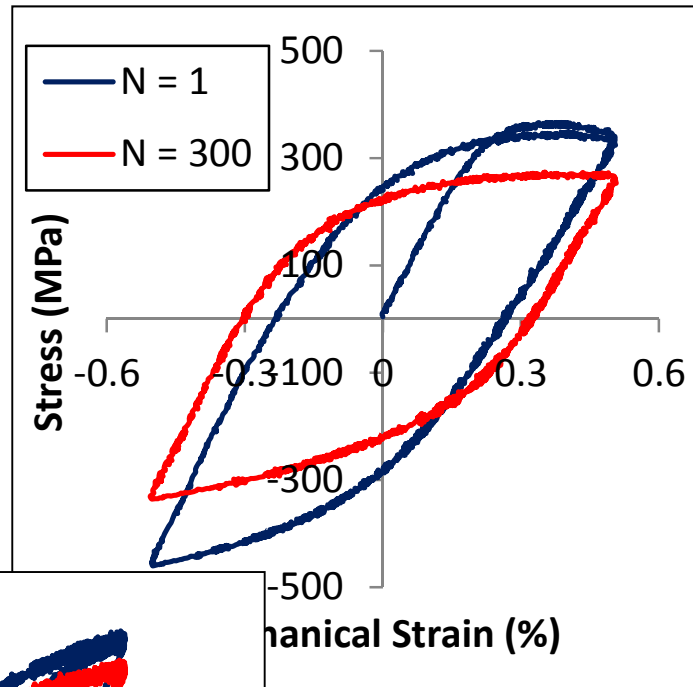


AR-P91 Data: Saad, PhD thesis, University of Nottingham (2012).

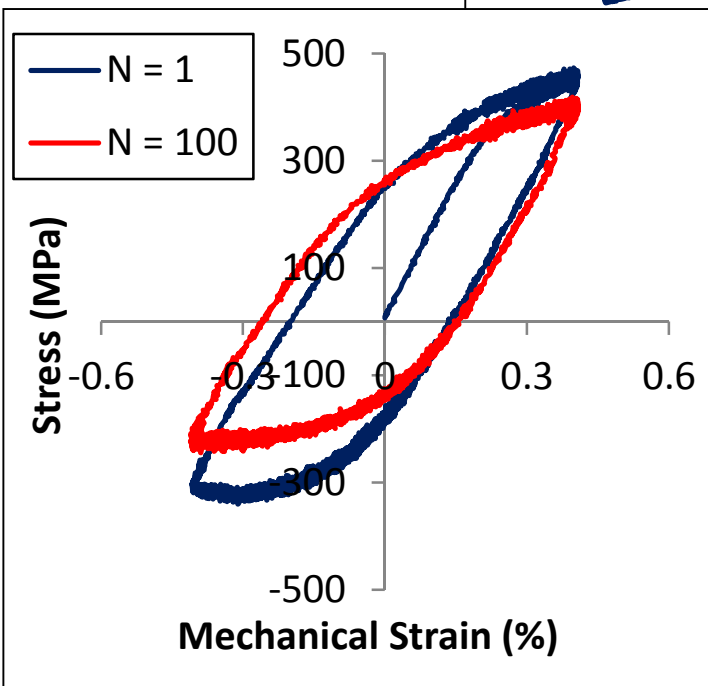
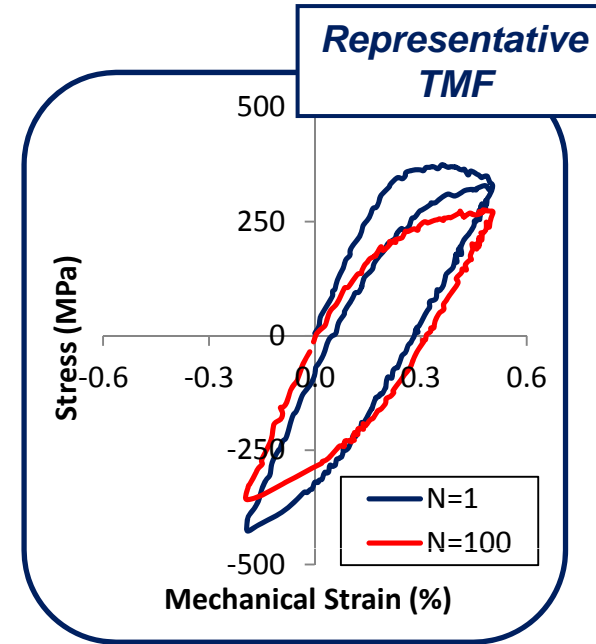
# Experimental Testing - TMF

## TMF-IP

$\epsilon = \pm 0.5\%$   
 $d\epsilon/dt = 0.025\%/s$

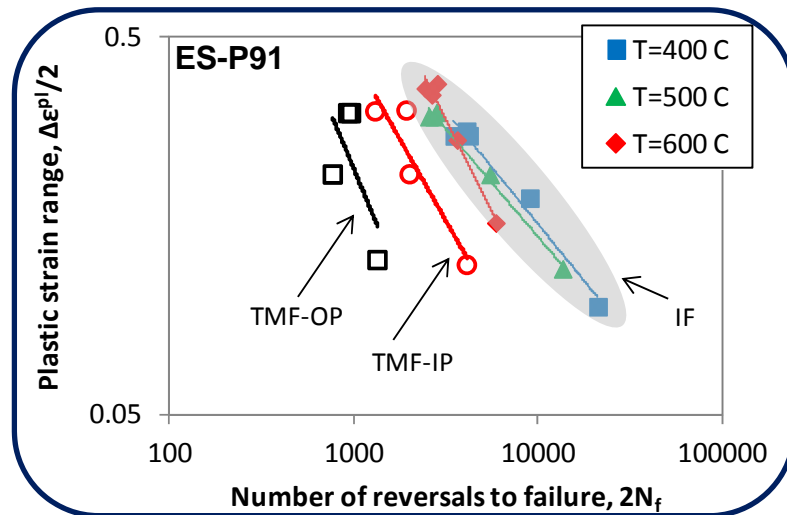


## Representative TMF



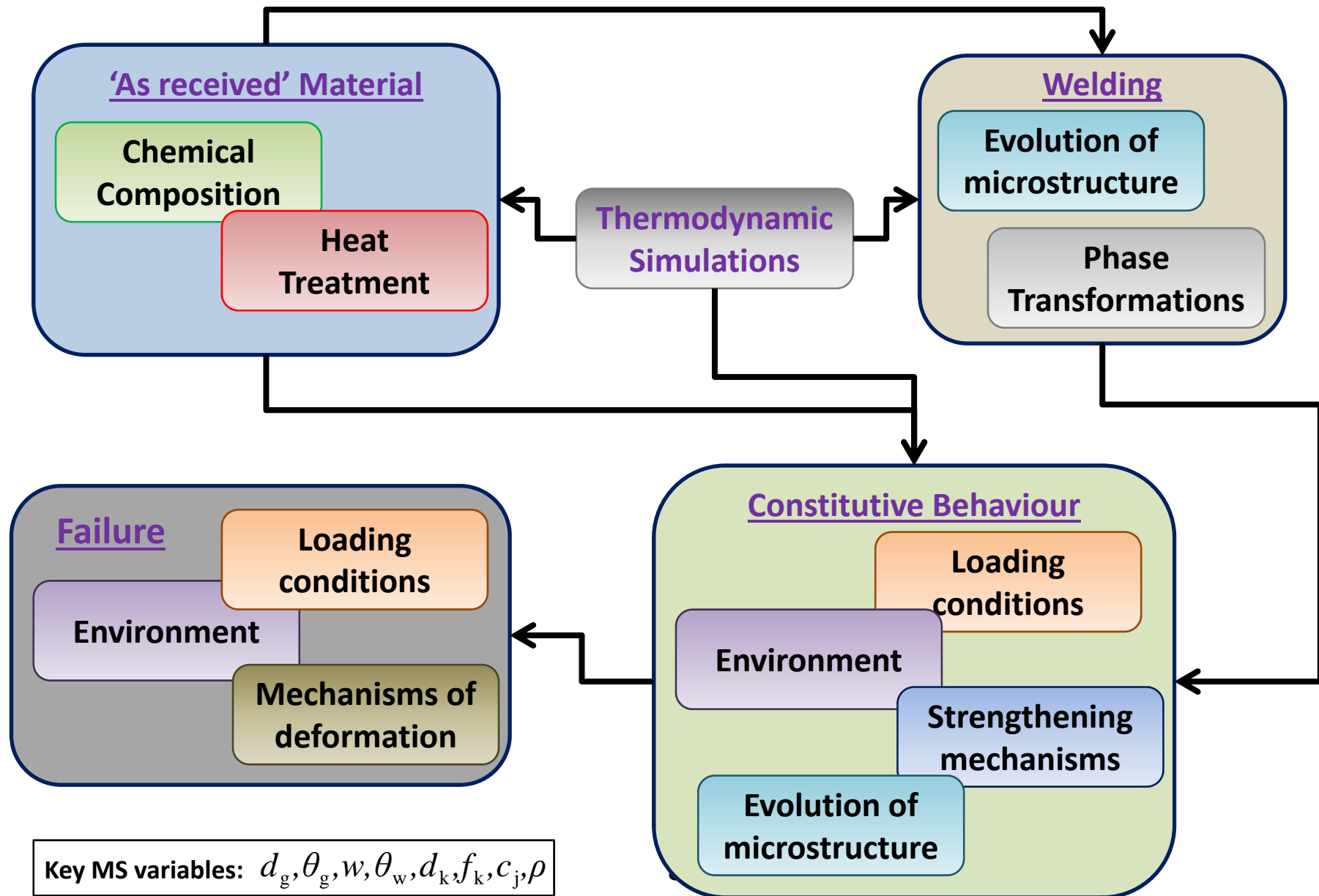
## TMF-OP

$\epsilon = \pm 0.4\%$   
 $d\epsilon/dt = 0.033\%/s$





# MECHANNICS Modelling Framework



# CP Modelling of 9Cr Steels

## □ Kinematics of single crystal (block)

$$\mathbf{F} = \mathbf{F}^p \mathbf{F}^e$$

Plastic flow

$$\mathbf{L}^p = \dot{\mathbf{F}}^p \mathbf{F}^{p-1} = \sum_{\alpha} \dot{\gamma}^{\alpha} \mathbf{m}^{\alpha} \otimes \mathbf{n}^{\alpha}$$

$$\dot{\gamma}^{\alpha} = \dot{\gamma}_0 \exp \left[ -\frac{F}{kT} \left\langle 1 - \left\langle \frac{|\tau^{\alpha} - B^{\alpha}| - S^{\alpha}}{\hat{\tau}_0 + C_{\tau} \sqrt{\sum_{\beta} \rho_S^{\beta} + \rho_G^{\beta}}} \right\rangle \right\rangle \right] \text{sgn}(\tau^{\alpha} - B^{\alpha})$$

$$S^{\alpha} = \mu b \sqrt{\sum_{\beta} h^{\alpha\beta} (\rho_S^{\alpha} + \rho_G^{\alpha})}$$

Elastic deformation

$$\boldsymbol{\sigma} = \mathbf{C} \mathbf{E}^e$$

$$\mathbf{E}^e = \frac{1}{2} (\mathbf{F}^{eT} \mathbf{F}^e - \mathbf{I})$$

Temperature-dependent parameters:  $\mathbf{C}$  and  $h_b$

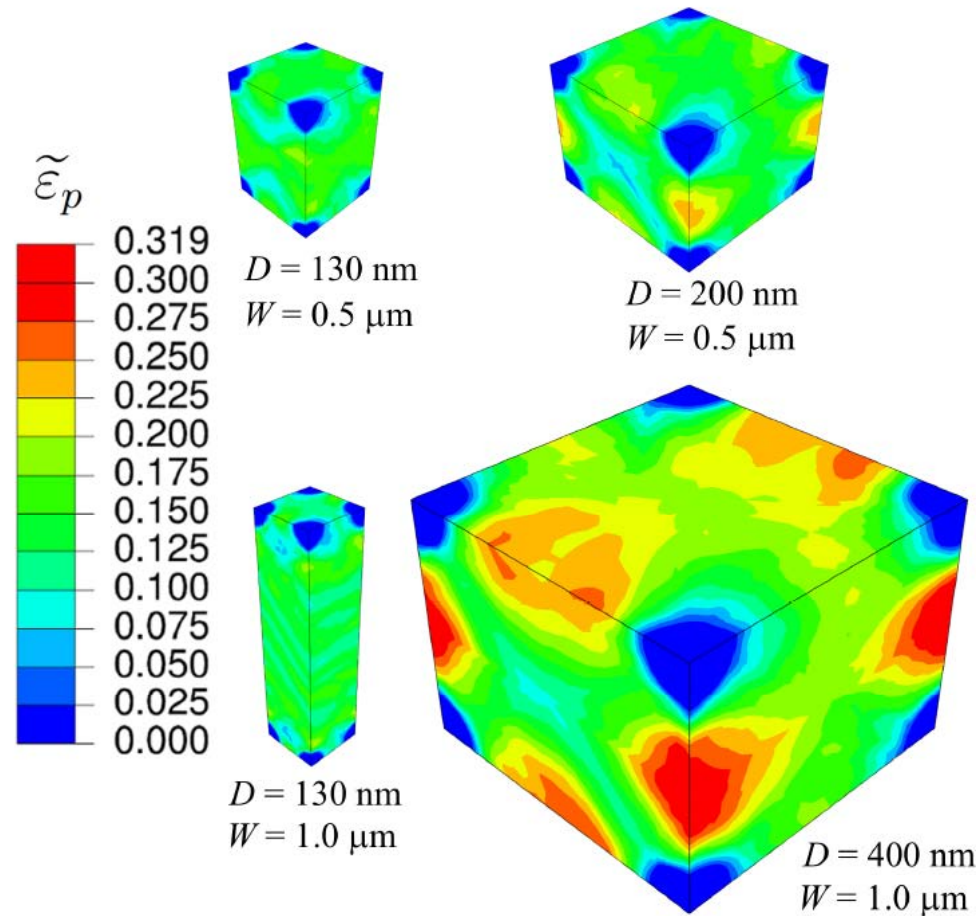
Back stress evolution:

$$\dot{B}^{\alpha} = h_b \dot{\gamma}^{\alpha} - r_D B^{\alpha} / S^{\alpha} |\dot{\gamma}^{\alpha}| \quad \longrightarrow \quad \text{(not necessary at the microscale)}$$

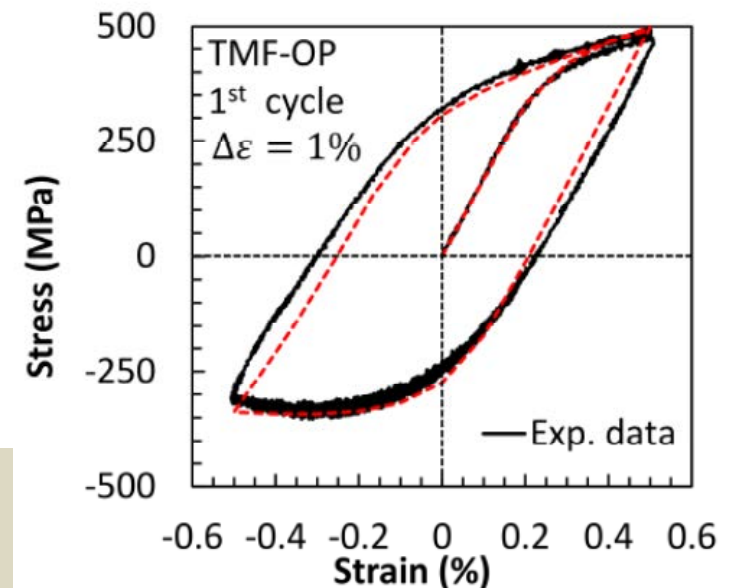
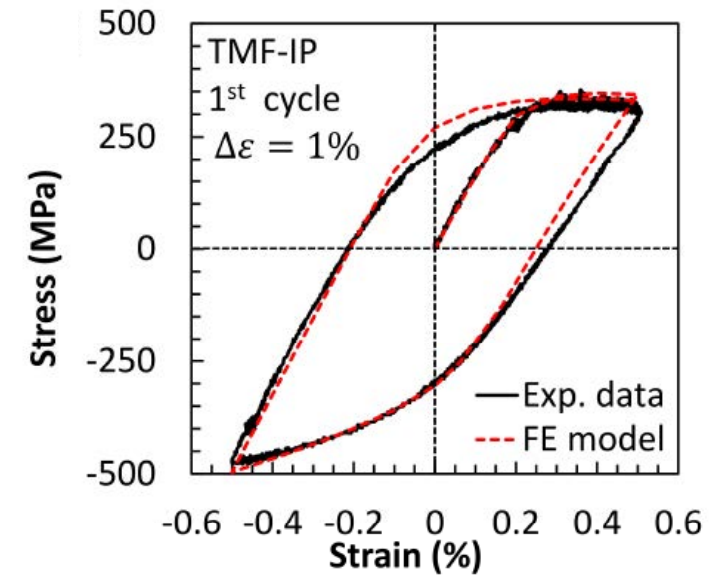
$$\dot{\rho}_S^{\alpha} = \frac{1}{b} \left[ K \sqrt{\sum_{\beta} (\rho_S^{\beta} + \rho_G^{\beta})} - l \rho_S^{\alpha} \right] |\dot{\gamma}^{\alpha}|;$$

$$\dot{\rho}_G^{\alpha} = \frac{1}{b} \nabla \times (\dot{\gamma}^{\alpha} \mathbf{n}^{\alpha} \mathbf{F}^p)$$

# A CP Model for TMF of P91 Steel

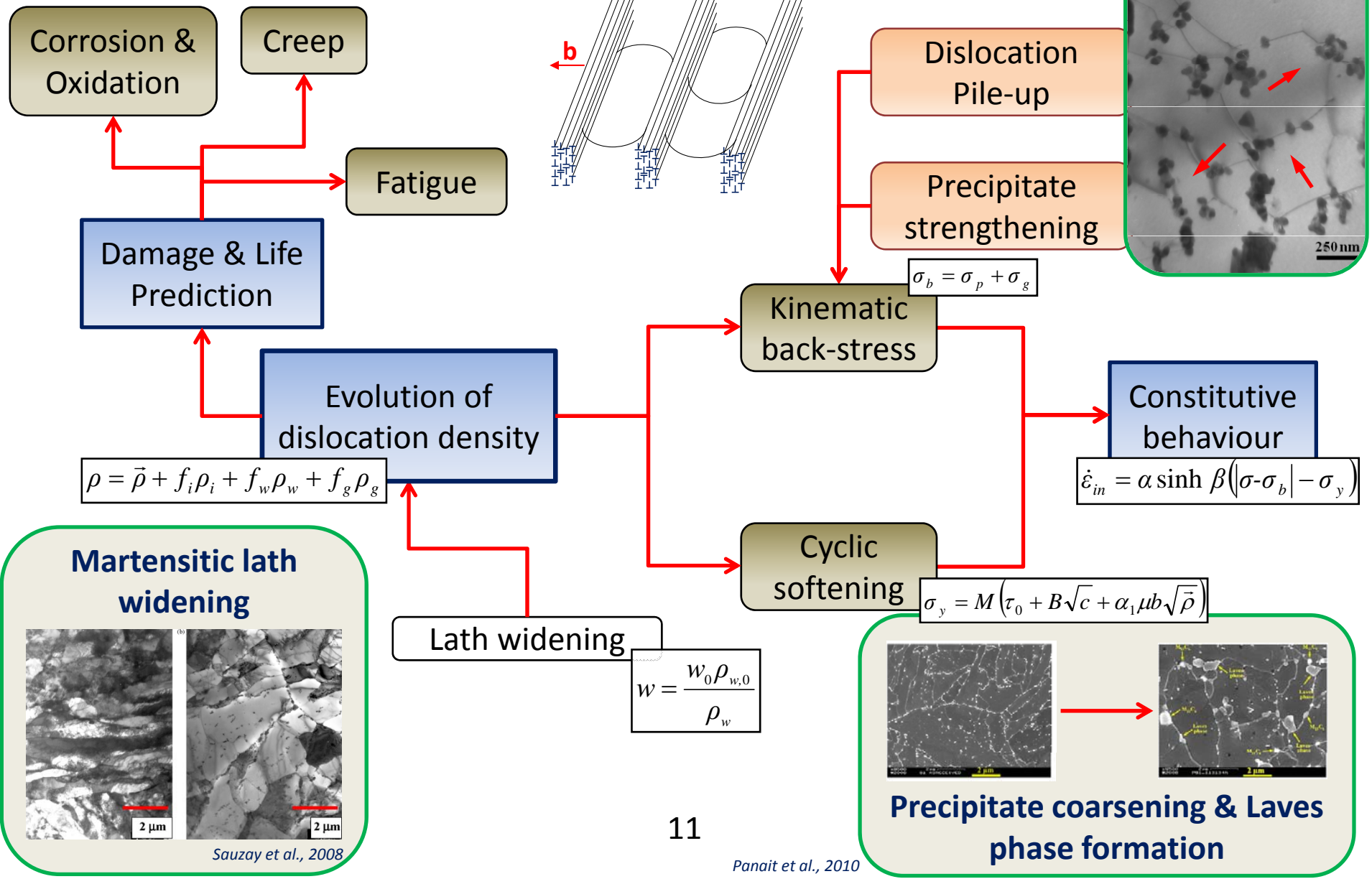


Simulating size effects in 9-12Cr steels



# Dislocation-Mechanics Model

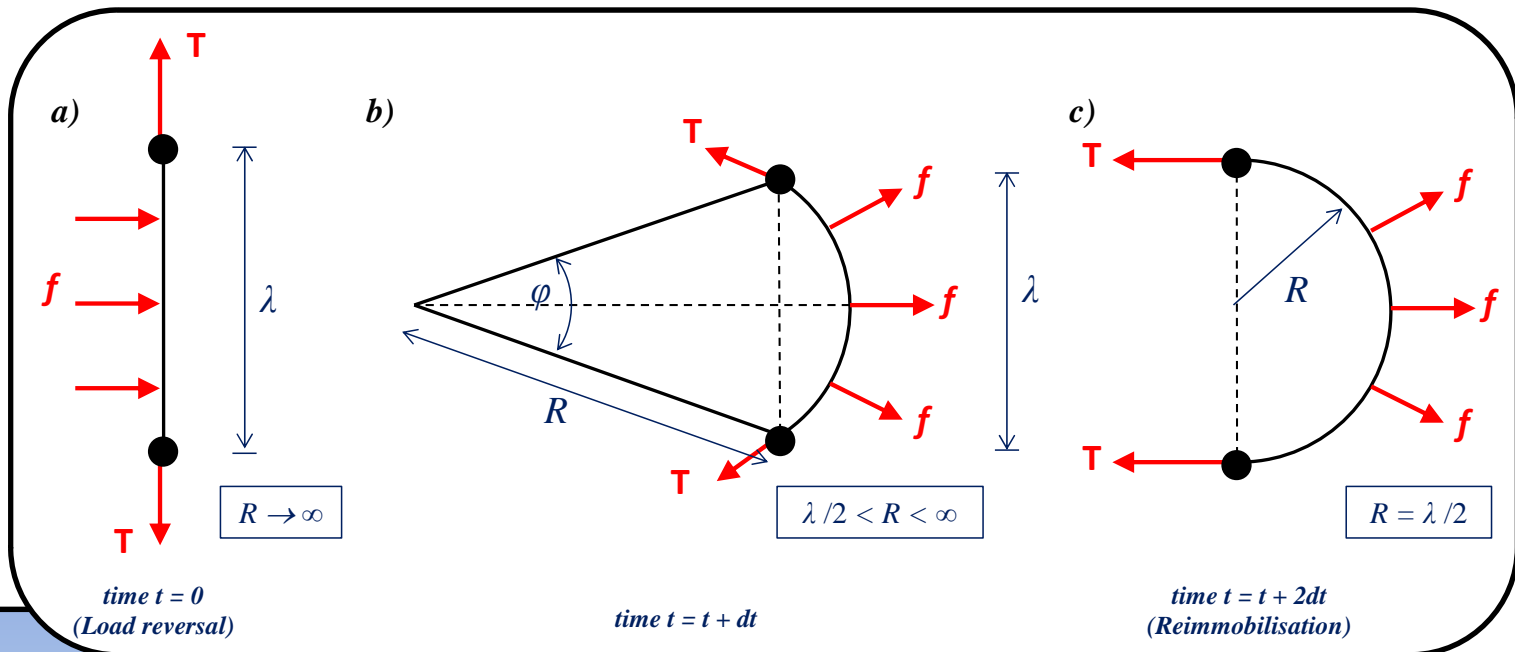
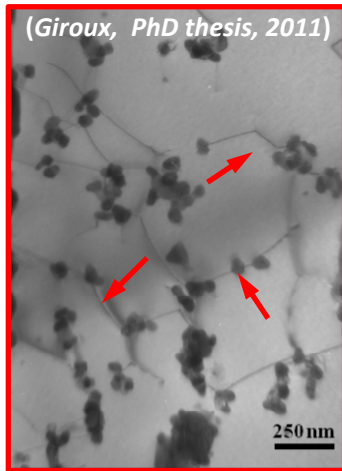
(Giroux, PhD thesis, 2011)



Sauzay et al., 2008

Panait et al., 2010

# Back-Stress: Precipitates



## Orowan stress & precipitate back-stress:

$$\sigma_{\max} = \frac{Mb\mu}{\lambda} \quad \text{and} \quad \sigma_p = (f_g + f_w)\sigma_{p,bd} + f_i\sigma_{p,i}$$

## Kinematic back-stress due to precipitate strengthening:

$$\dot{\sigma}_{p,k} = \frac{2}{\bar{\rho}b\lambda_k} \frac{|\sigma_{p,k}^3|}{\sigma_{\max,k}^2} \frac{\dot{p}M}{n} \left[ \left( \frac{\sigma_{\max,k}^2}{\sigma_{p,k}^2} - 1 \right) - \tan^{-1} \left( \frac{\sigma_{\max,k}^2}{\sigma_{p,k}^2} - 1 \right) \right]^{-1}$$

## Spacing of precipitates:

$$\lambda_k = \frac{0.5d_k}{\sqrt{f_k}}$$

	Diameter	Volume Fraction
$M_{23}C_6$	70 nm	0.019
$MX$	20 nm	0.005

# Back-Stress: Dislocation Pile-Ups

Number of dislocations in a pile-up:

$$n_g = M \frac{\alpha_g d_g}{b\mu} \sigma_g$$

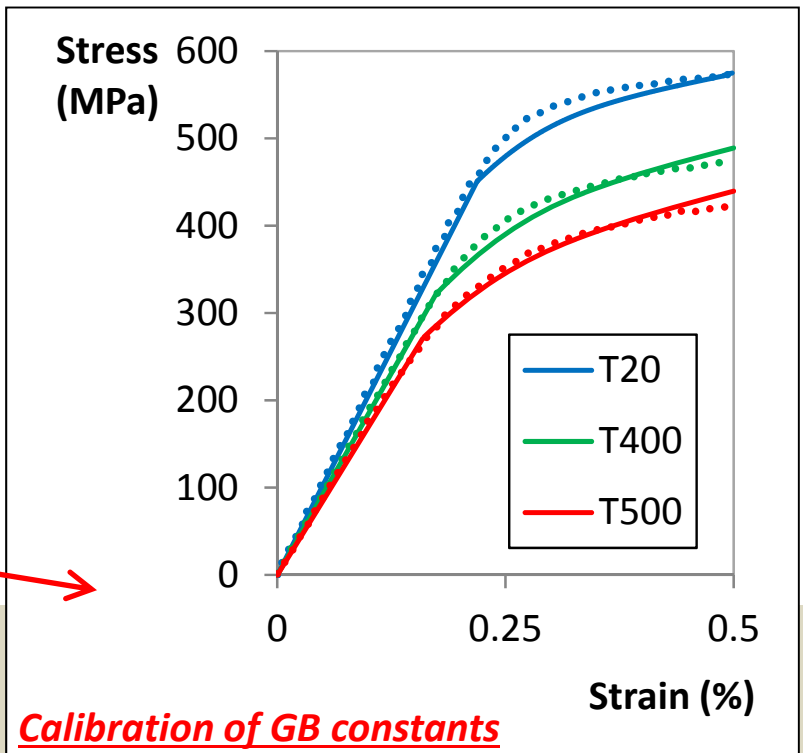
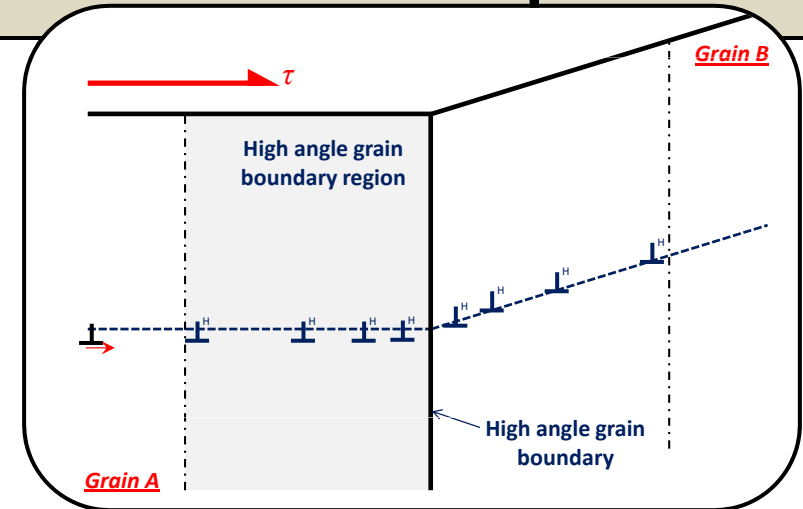
Time rate change of dislocation pile-up formation (*Bardel, 2015*):

$$\dot{n}_g = \frac{M\lambda_g}{b} \left( \text{sgn}(\sigma - \sigma_b) - \frac{n_g}{n_g^*} \right) \dot{p}$$

Kinematic back-stress due to dislocation pile-up:

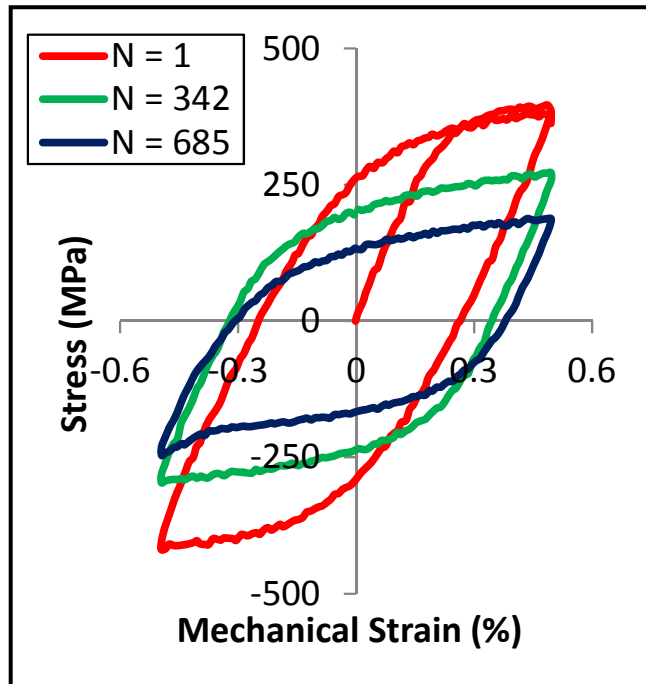
$$\dot{\sigma}_g = \frac{2M^2\alpha_g\lambda_g\mu}{d_g} \left( \text{sgn}(\sigma - \sigma_b) - \frac{n_g}{n_g^*} \right) \dot{p}$$

where  $\lambda_g$  and  $n_g^*$  are material constants.



*Calibration of GB constants*

# Evolution of Dislocation Density



## Cyclic softening in 9Cr steels:

1. Decrease in dislocation density.
2. LAB dislocation annihilation.
3. Widening of martensitic lath structure.

Evolution of martensitic lath width due to LAB dislocation annihilation<sup>[1]</sup>:

$$w = \frac{w_0 \rho_{w,0}}{\rho_w}$$

Taylor hardening model used to define the cyclic yield stress:

$$\dot{\sigma}_y = M \frac{\alpha_1 \mu b}{2\sqrt{\bar{\rho}}} \dot{\bar{\rho}}$$

Overall dislocation density:

$$\rho = \bar{\rho} + f_i \rho_i + f_w \rho_w + f_g \rho_g$$

# Results: Constitutive Behaviour

## Step 1: Elastic parameters

$$E, \nu, \sigma_{y,0}$$

## Step 2: Fundamental constants

$$n, M, b, \alpha_1$$

## Step 3: Precipitate strengthening

$$d_{M_{23}C_6}, f_{M_{23}C_6}, d_{MX}, f_{MX}$$

## Step 4: Dislocation pile-up constants

$$\lambda_g, n_g^*, d_g$$

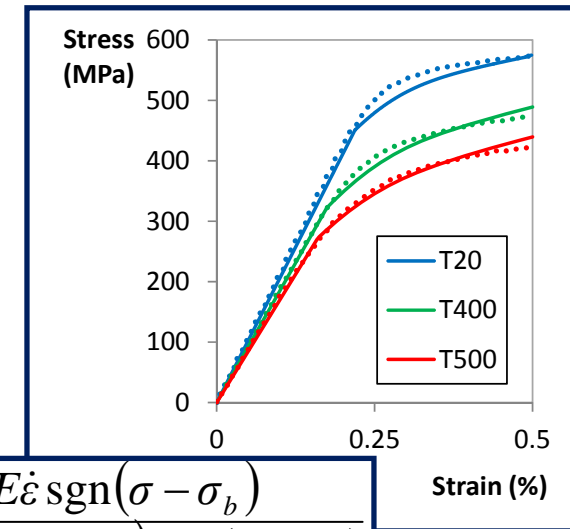
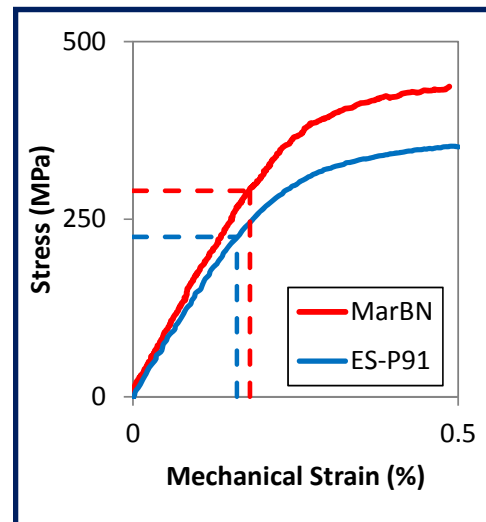
## Step 5: Dislocation density evolution

$$w_0, \vec{\rho}_0, \rho_{g,0}, \rho_{i,0}, d_l, \theta_0$$

## Step 6: Cyclic viscoplastic

$$\alpha, \beta$$

22 fitted parameters

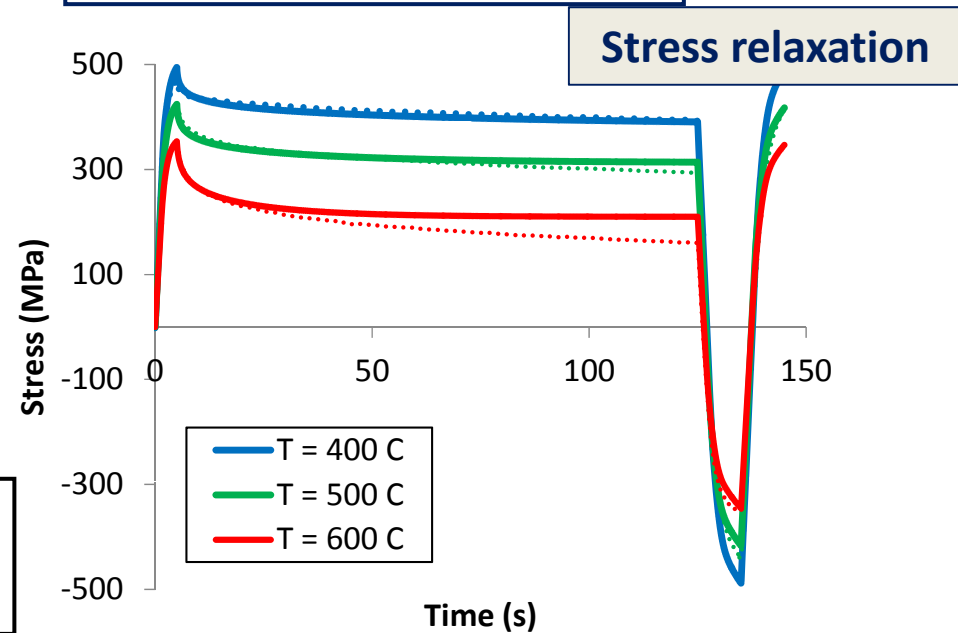
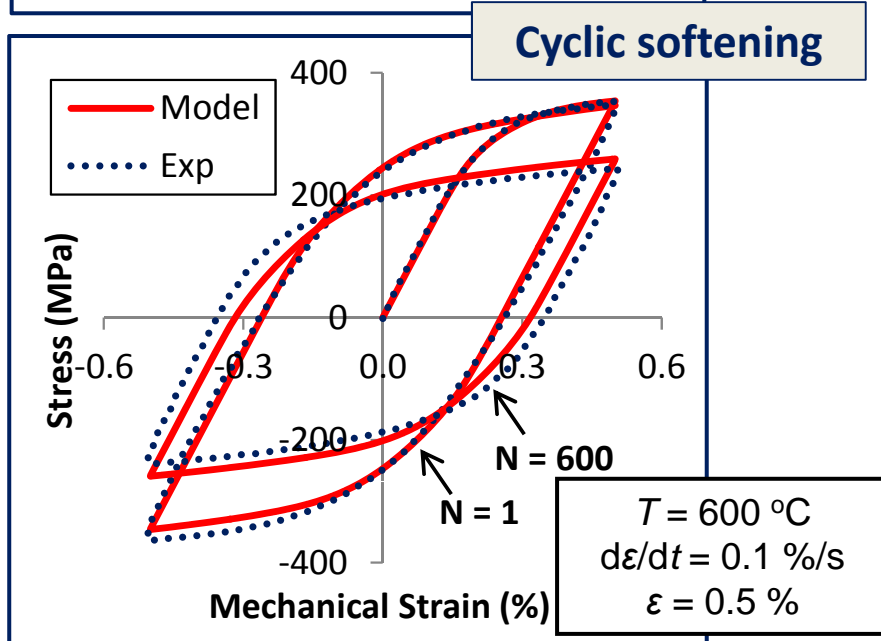
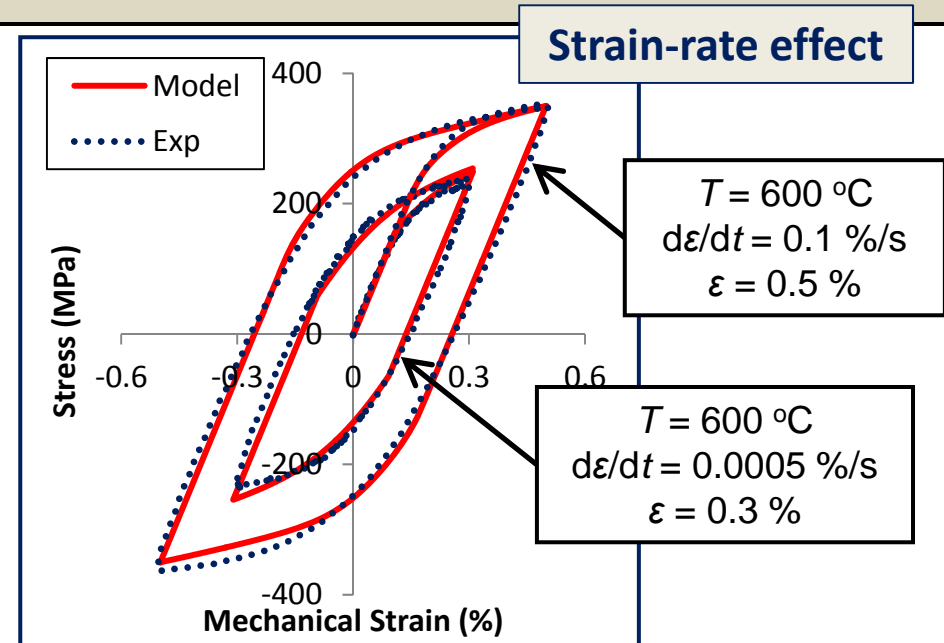
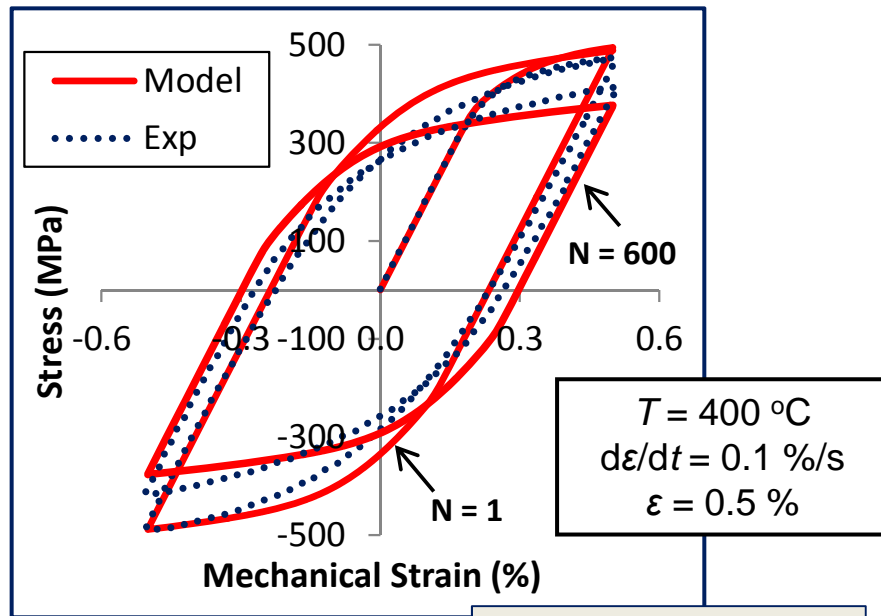


$$\dot{p} = \frac{E\dot{\epsilon} \operatorname{sgn}(\sigma - \sigma_b)}{E + (\Omega_g + \Omega_p) \operatorname{sgn}(\sigma - \sigma_b)}$$

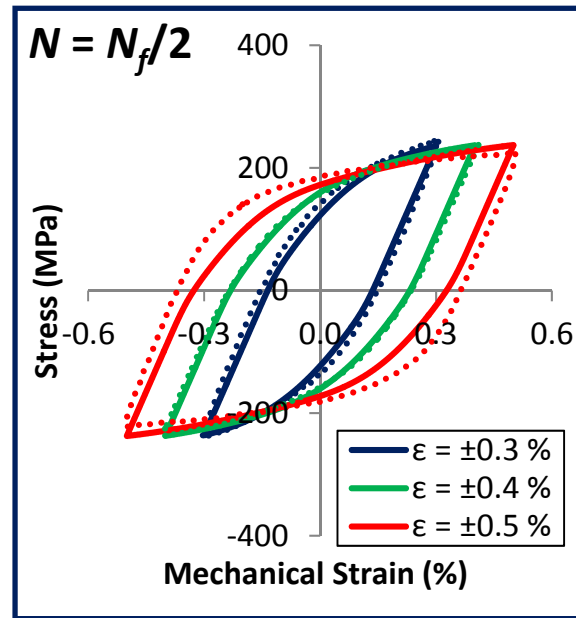
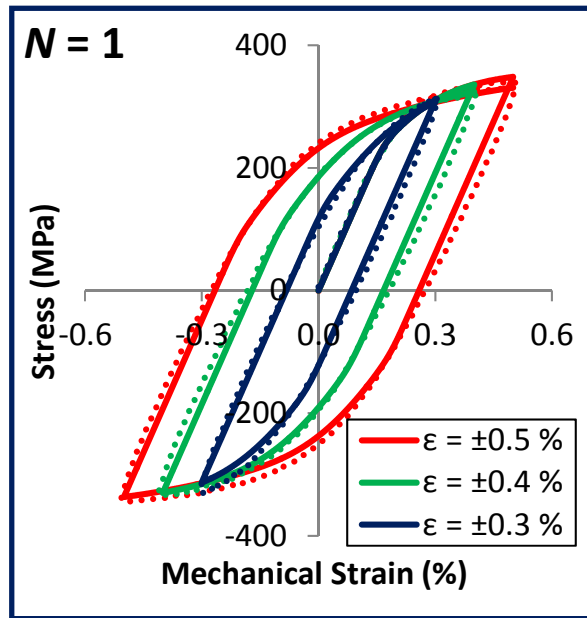
- 22 parameters.
- 8 parameters identified from EBSD/SEM/TEM.
- ONLY 7 fitted parameters.
- ONLY 4 temperature-dependent parameters.



# Results: Constitutive Behaviour

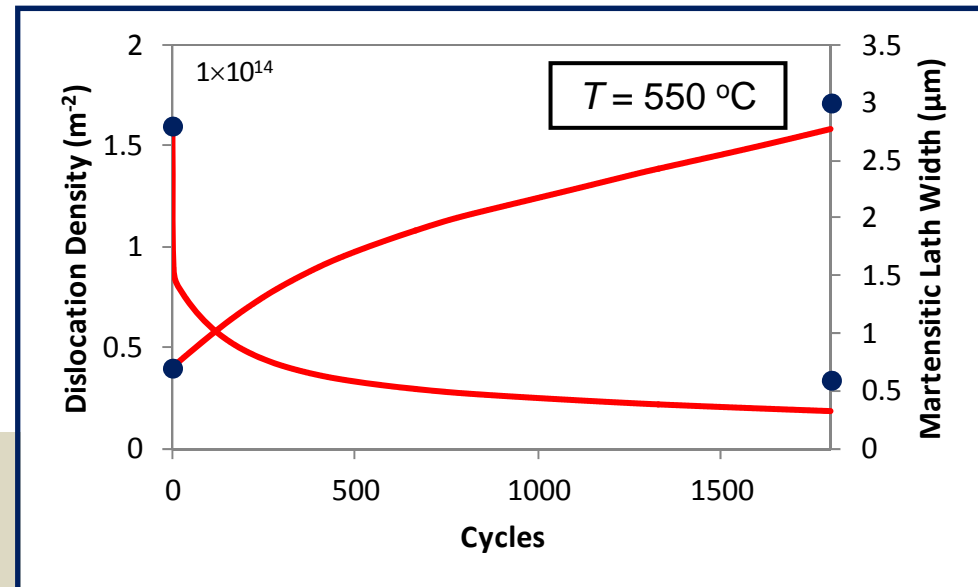


# Results: Microstructure Evolution

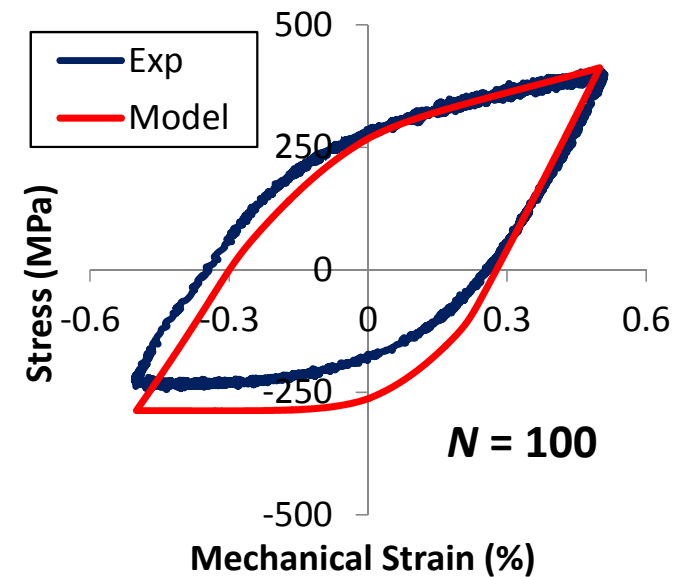
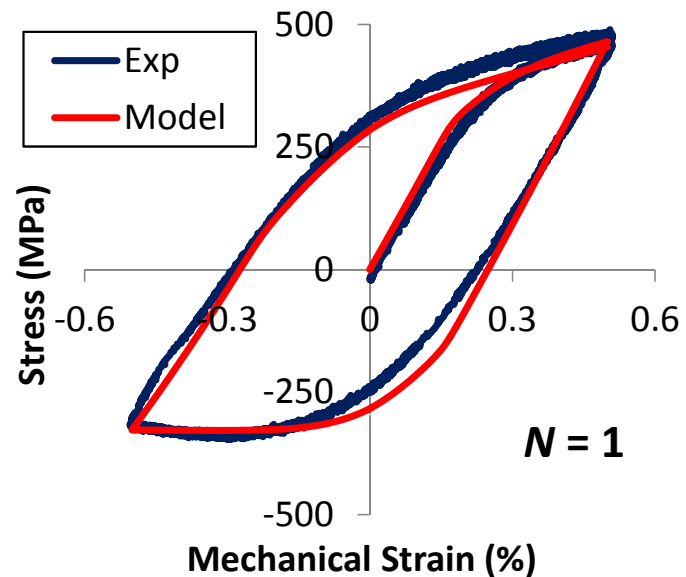
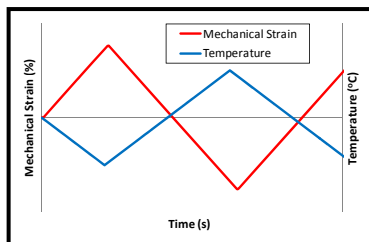
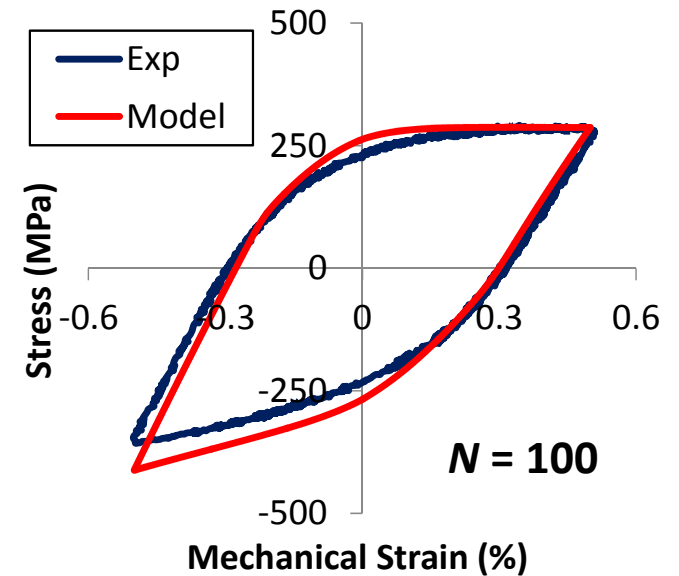
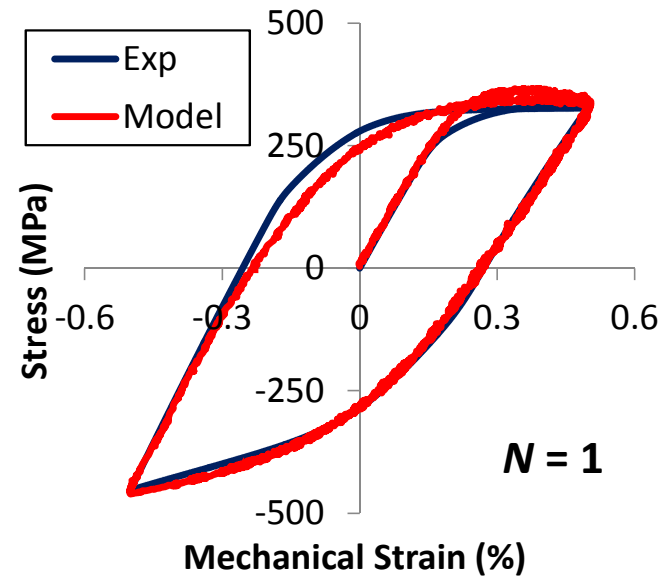
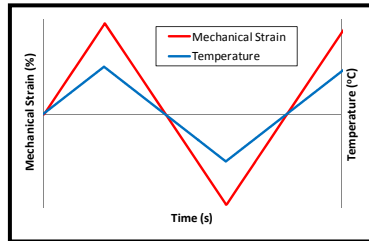


$T = 600 \text{ }^\circ\text{C}$   
 $d\varepsilon/dt = 0.1 \text{ } \%/s$   
 $\varepsilon = 0.5 \%$

**Cyclic softening controlled by martensitic lath width**



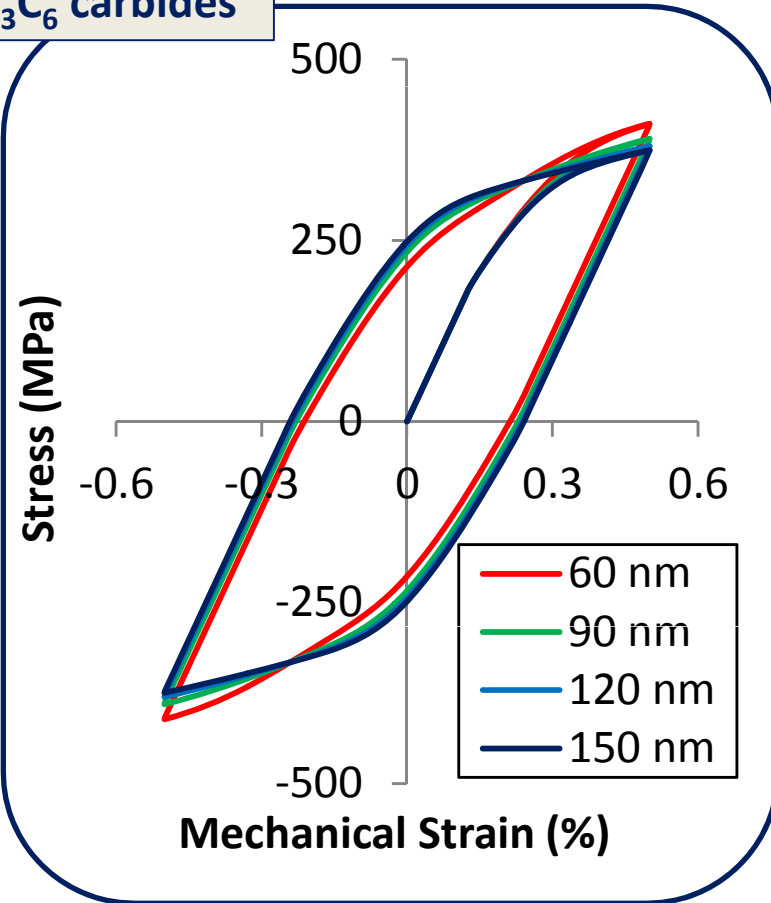
# Results: Modelling TMF



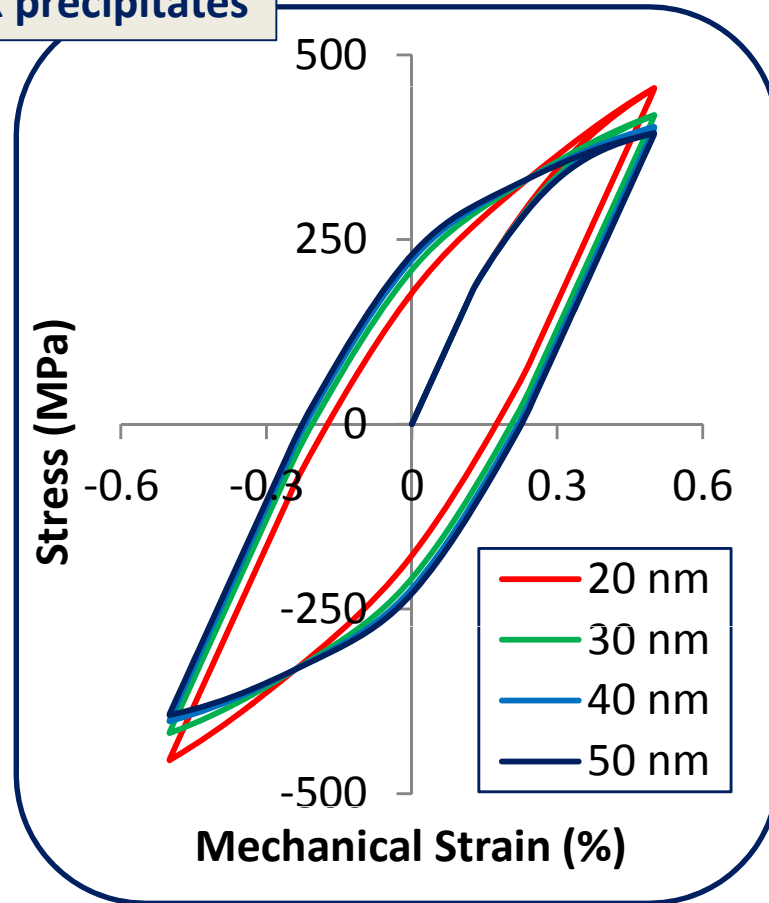
$T = 400\text{ }^{\circ}\text{C} - 600\text{ }^{\circ}\text{C}$   
 $d\varepsilon/dt = 0.025\text{ } \%/s$

# Results: Effect of Microstructure

$M_{23}C_6$  carbides



MX precipitates



# Summary & Conclusions

- **Development of a multi-scale modelling framework for microstructural degradation of 9-12Cr steels**
  - *Physically-based yield stress.*
  - *Cyclic softening via dislocation density evolution & LAB widening.*
  - *NLKH via physical mechanisms of (i) dislocation pile-ups & (ii) pinning of dislocations at precipitates.*
- **Model predicts evolution of key microstructural variables under TMF.**
- **Methodology is applicable to creep-TMF 9-12Cr steels.**

# Acknowledgements

This publication has emanated from research conducted with the financial support of Science Foundation Ireland under Grant Numbers SFI/10/IN.1/I3015 and SFI/IA/2604.



The Open University



# In situ-strain measurement in a coated superalloy by synchrotron X-ray diffraction during thermal mechanical cycling with superposed thermal gradient (TGMF)



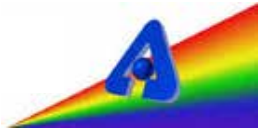
M. Bartsch, J. Wischek, C. Meid  
German Aerospace Center, Cologne



A. Manero, S. Sofronsky, K. Knipe, S. Raghavan  
Mechanical and Aerospace Engineering, University of Central Florida,  
Orlando, Florida



A. M. Karlsson  
Fenn College of Engineering, Cleveland State University, Ohio



J. Okasinski, J. Almer  
Advanced Photon Source  
Argonne National Laboratory  
Argonne, Illinois



Knowledge for Tomorrow

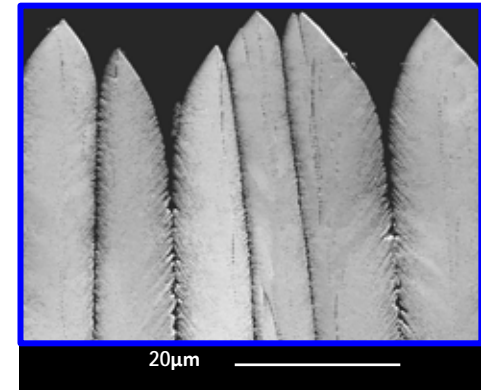
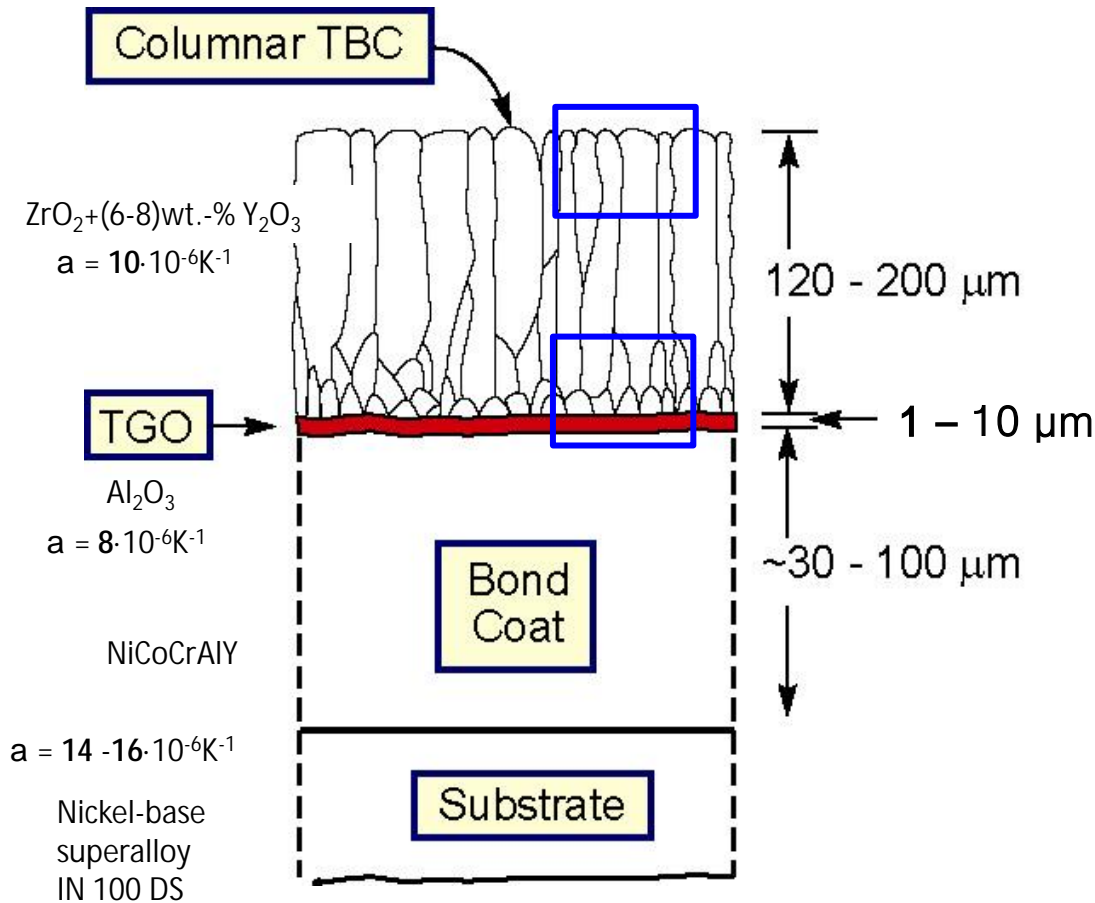
# Outline

- Ø Experimental findings in a TBC-system after thermomechanical testing with thermal gradients (TGMF)
  
- Ø Numerical Modeling of TGMF-tests
  - Open questions due to missing data on material properties
  
- Ø In situ measuring of local strain during TGMF cycles via synchrotron X-ray diffraction

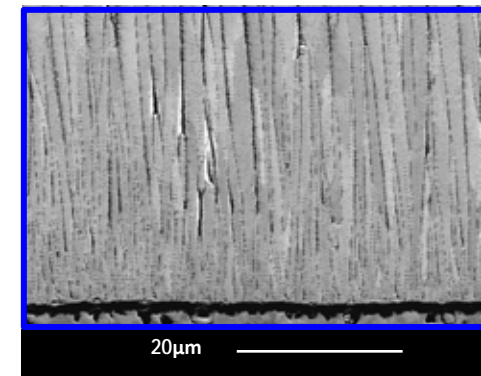




# Investigated coating system



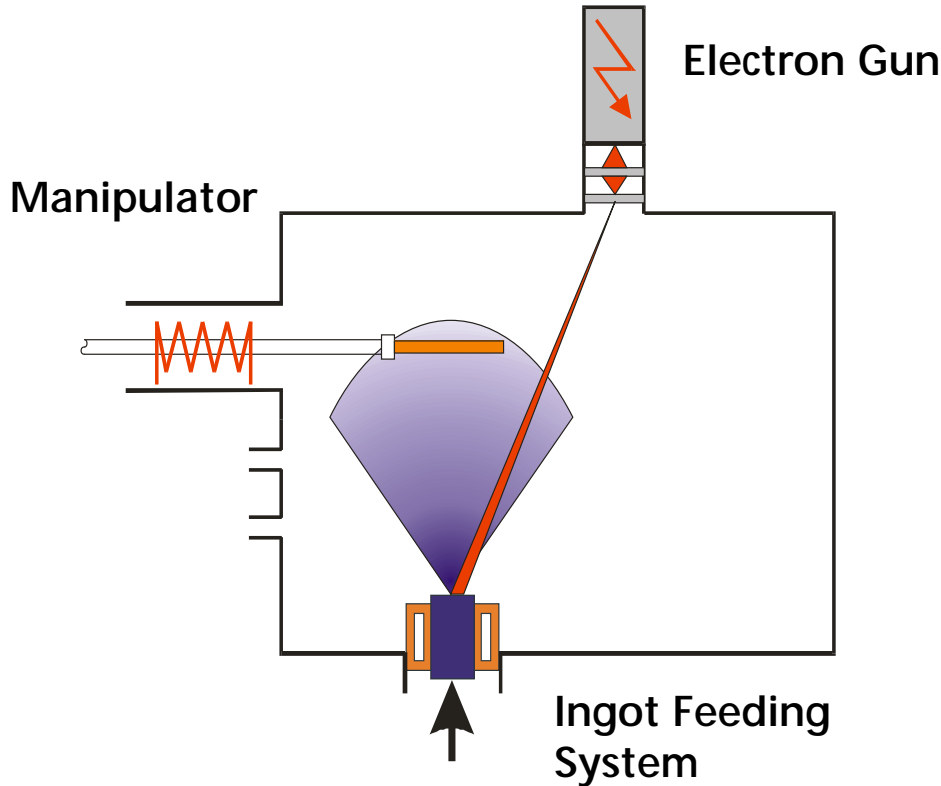
near surface



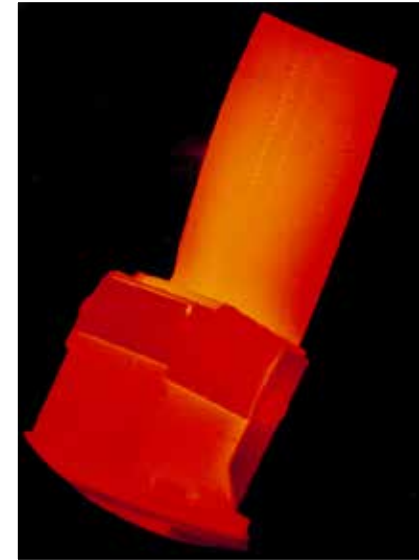
near TGO



# Stress free at homogenous temperature of 1000°C



Electron Beam - Physical Vapor Deposition (EB-PVD)



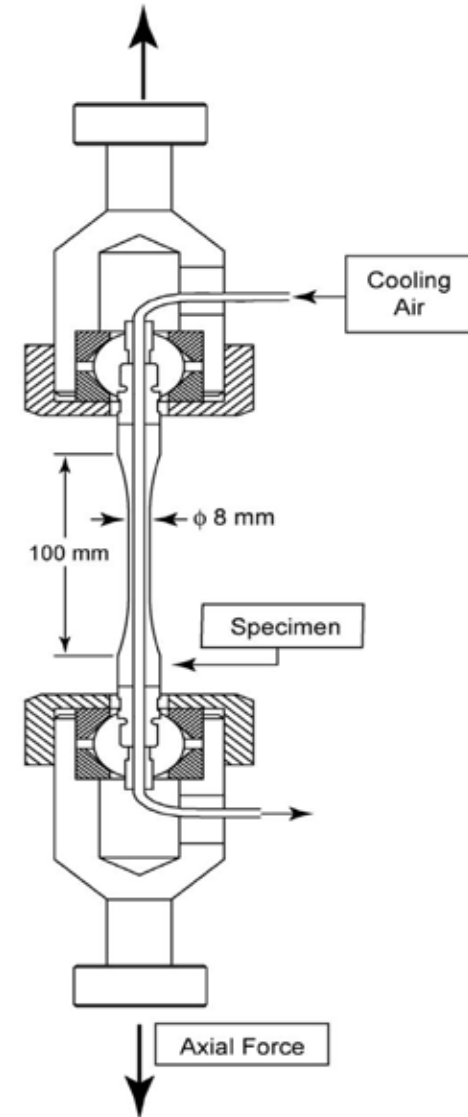
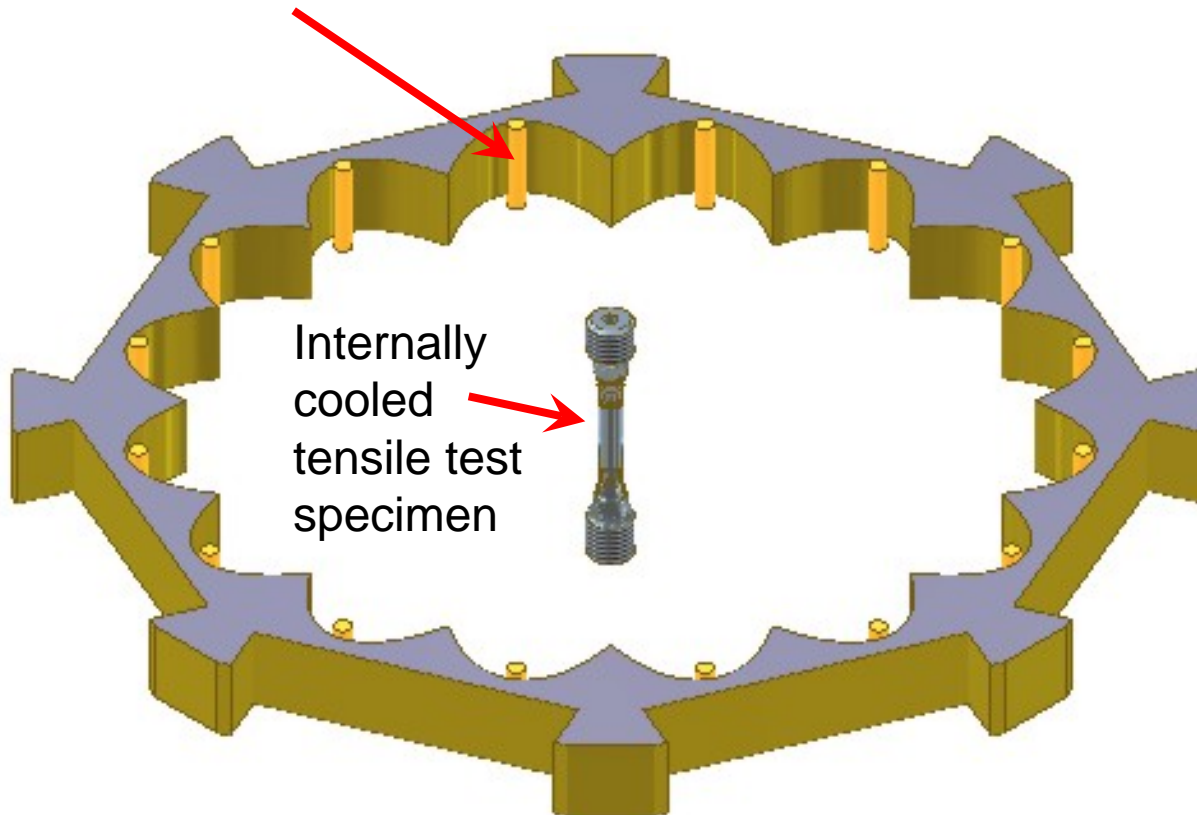
Deposition temperature: ca. 1000°C

↳ compressive residual in plane stresses in ceramic top coat at ambient temperature



# Test facility for thermal gradient mechanical fatigue

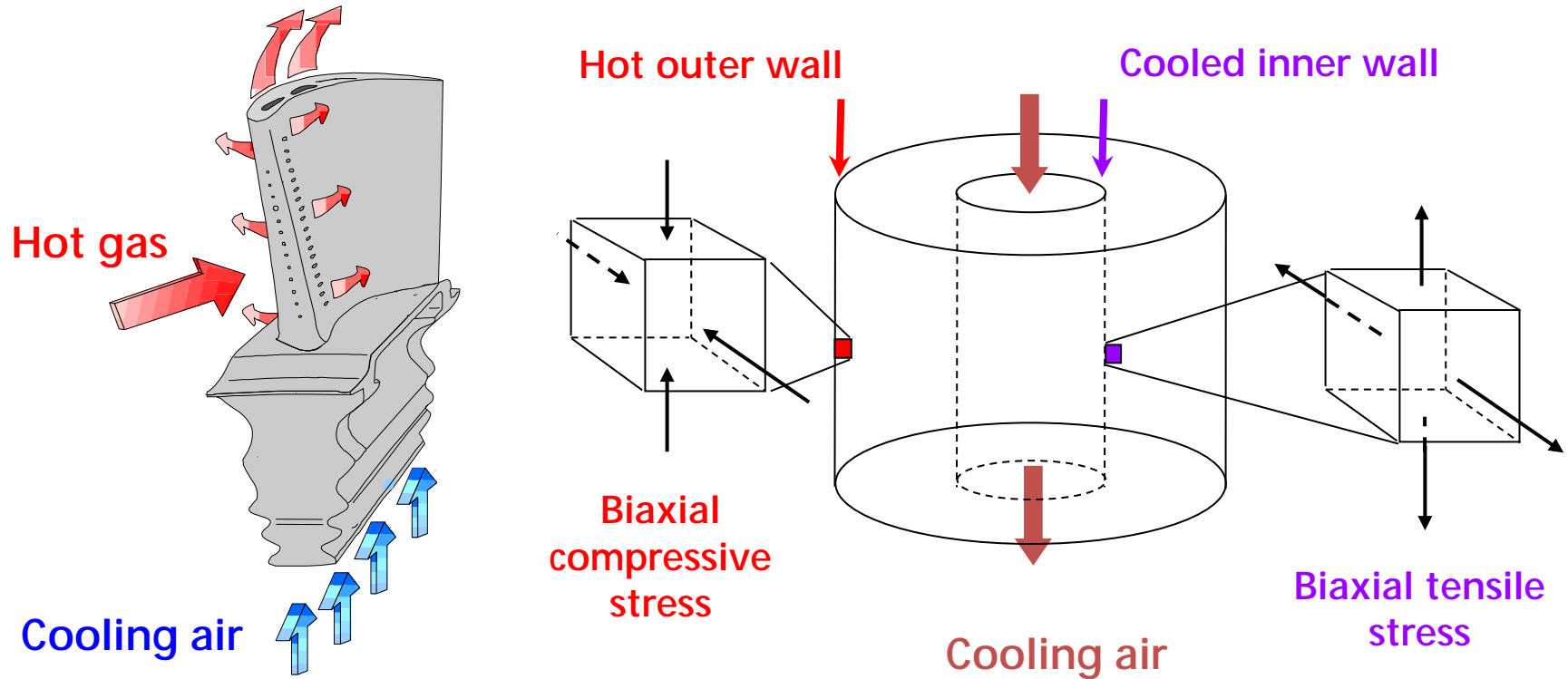
16 Quartz lamps, 1 kW each



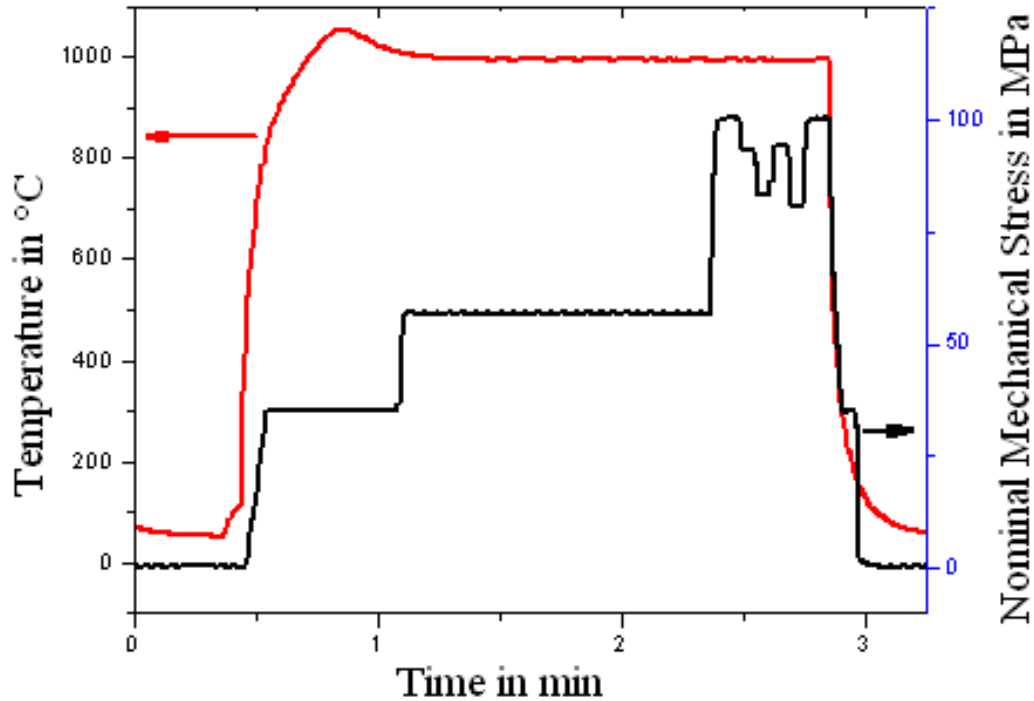
Thermal Gradient Mechanical Fatigue = TGMF



# Stress distribution due to thermal gradient



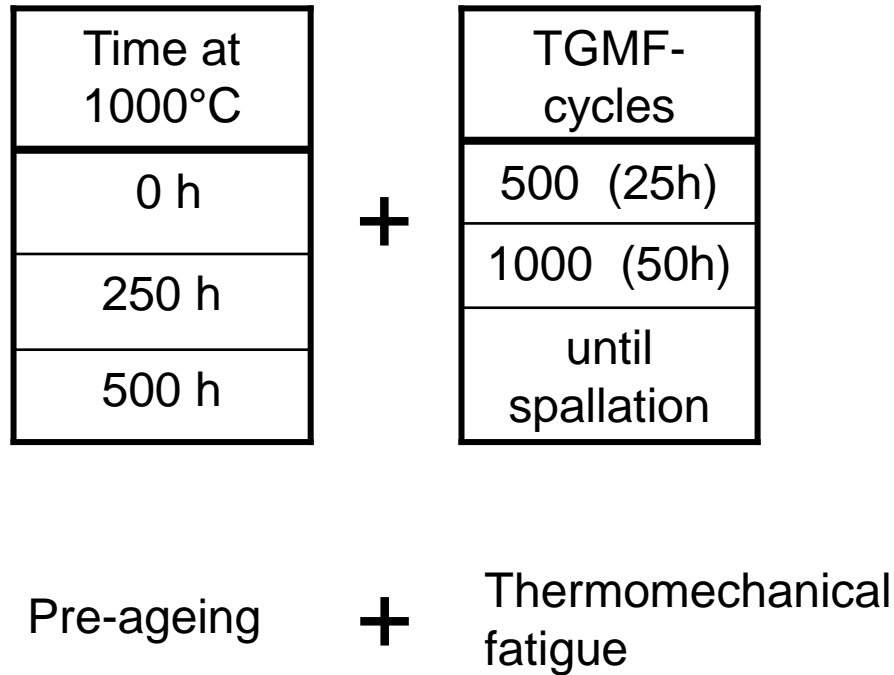
# Thermal mechanical load cycle



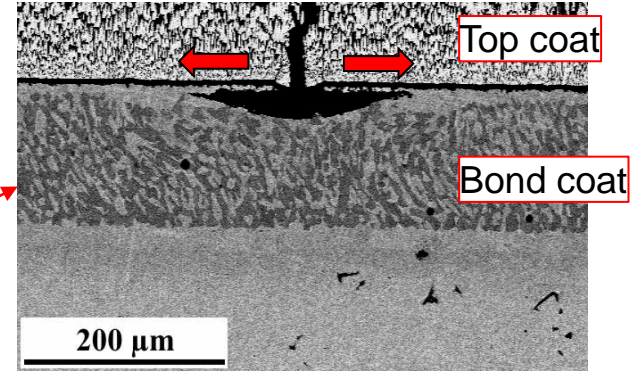
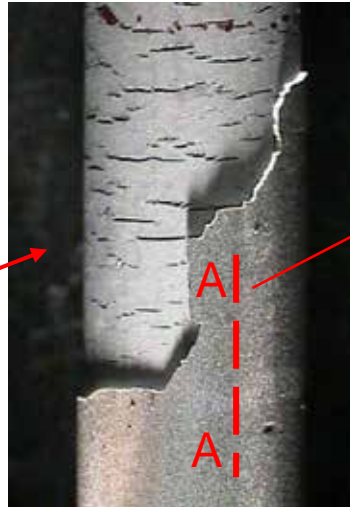
- Representing a flight cycle with reduced dwell times (3 min instead of It 2 - 10 hours)
- time at high temperature imposed by systematic pre-ageing



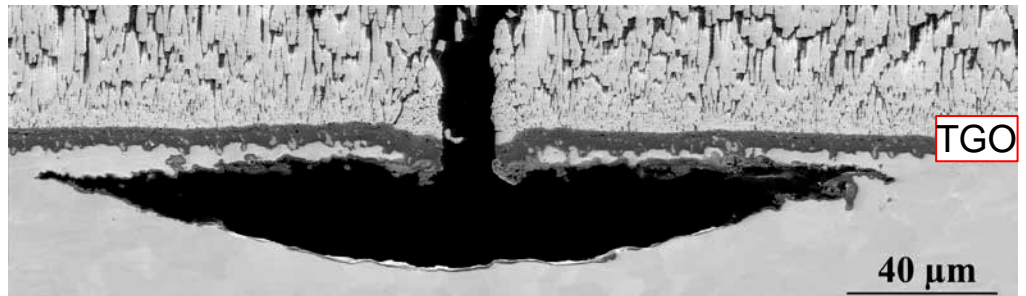
# Considering time dependent effects by pre-ageing



# Experimental findings



Length sections with adhering top coat



After 933 TGMF-cycles +  
500h pre-ageing at 1000°C



# Experimental findings

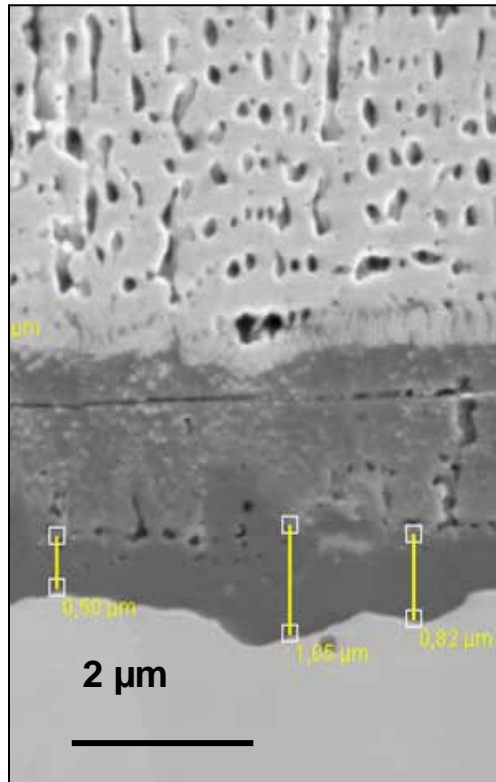
- Evolution of the ‚smiley‘ cracks is linked to cracks in the TGO, perpendicular to the applied mechanical load
- Initial TGO cracks are generated due to axial tensile stresses
- 250h (500h) pre-ageing + 1000 cycles
  - top coat spallation
  - crack pattern perpendicular to mechanical load
  - accumulated time at high temperature: 300h (550h)
- No pre-ageing + 7000 cycles
  - no spontaneous spallation
  - forced spallation during sample cutting revealed traces of similar crack pattern
  - accumulated time at HT: ca. 350h

**How can axial tensile stresses evolve in the TGO during TGMF?  
Why do cracks evolve faster in pre-aged specimens?**

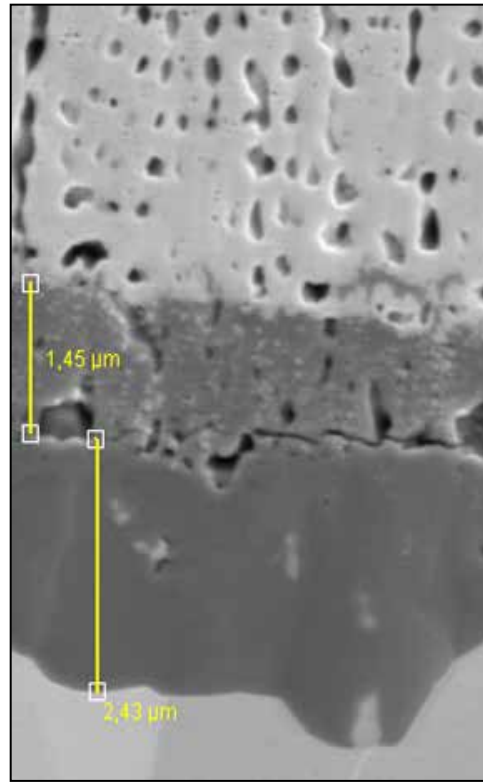




# After pre-oxidation: bi-layer of thermally grown oxide



50h/1000°C



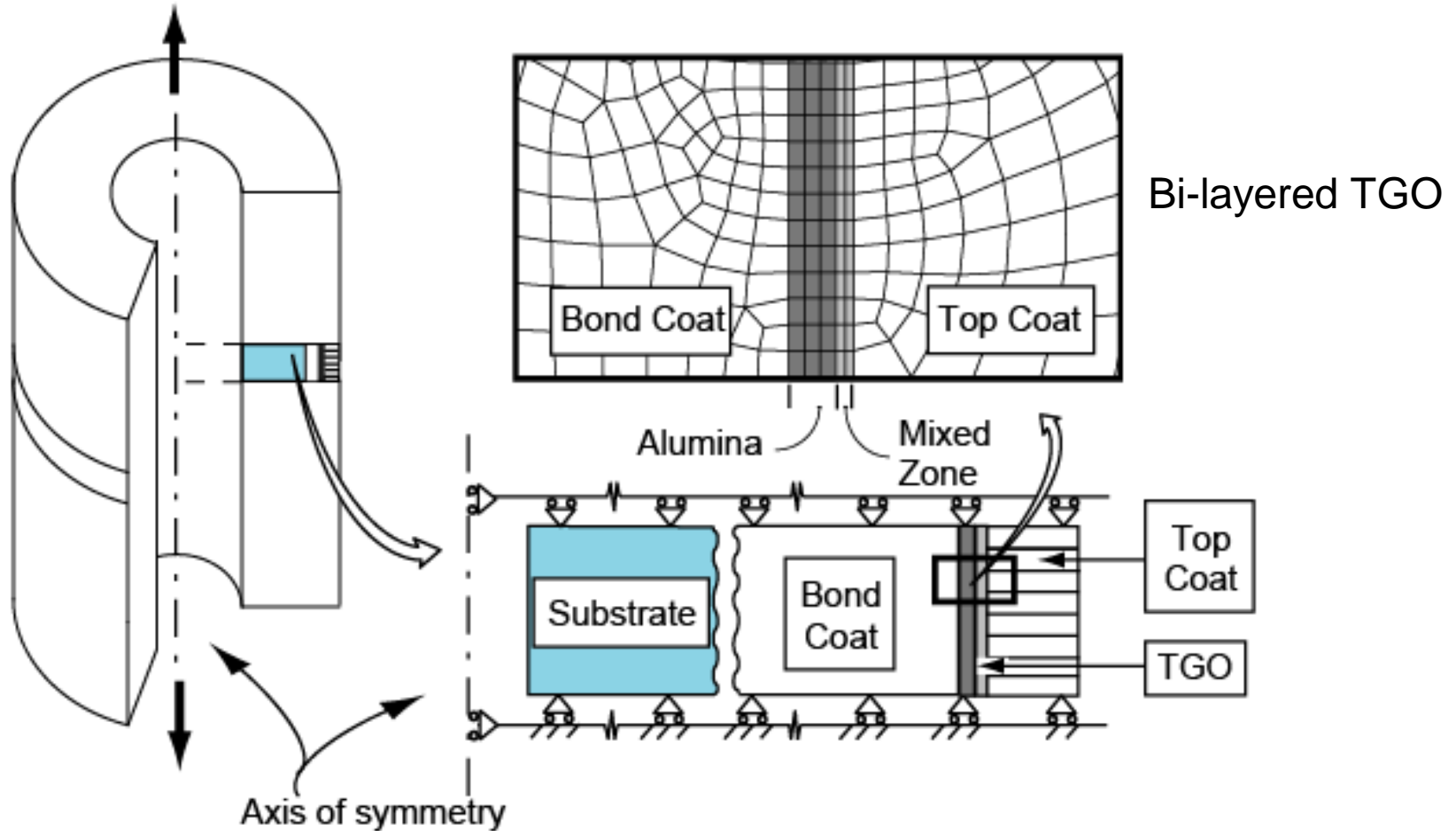
200h/1000°C

Fine grained  
intermixed zone  
 $\text{Al}_2\text{O}_3 + \text{ZrO}_2$

Coarse grained  
 $\text{Al}_2\text{O}_3$



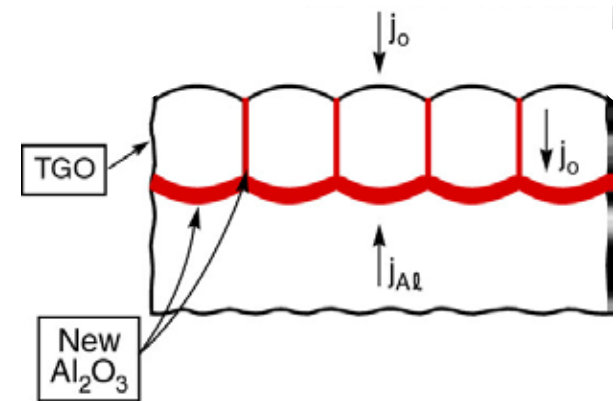
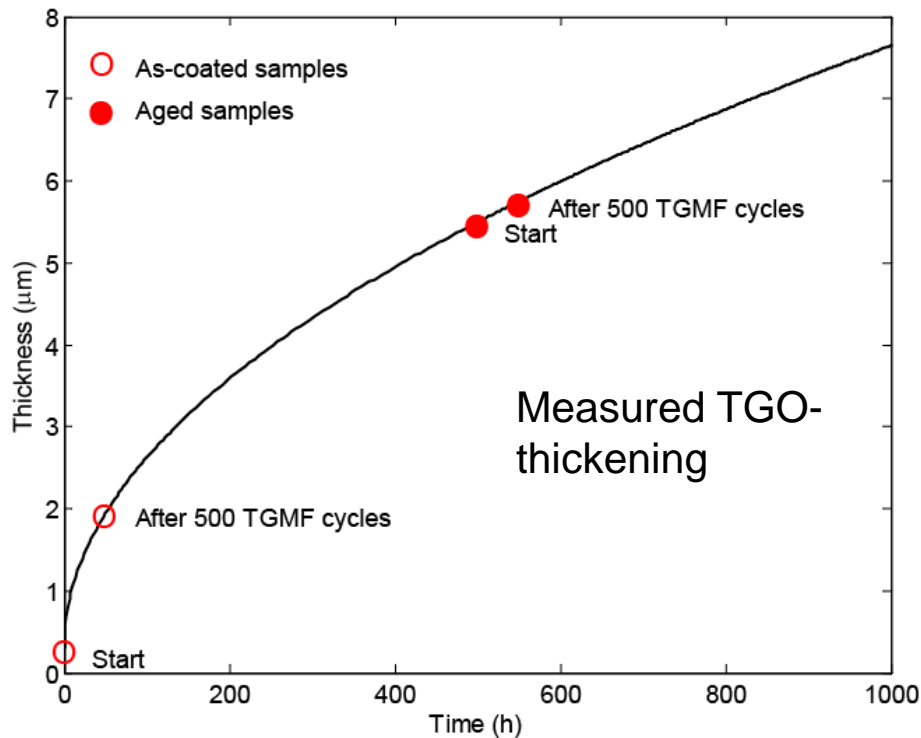
# Numerical model: Geometry and boundary conditions



[M. Hernandez, A.M. Karlsson, M. Bartsch: *Surface Coatings & Technology* 203, 3549-58, 2009]



# Time dependent TGO properties: (1) growth strain



Thickening  $\epsilon_t$  and lengthening  $\epsilon_l$  growth strain

$$\epsilon_l = 0.1 \cdot \epsilon_t$$

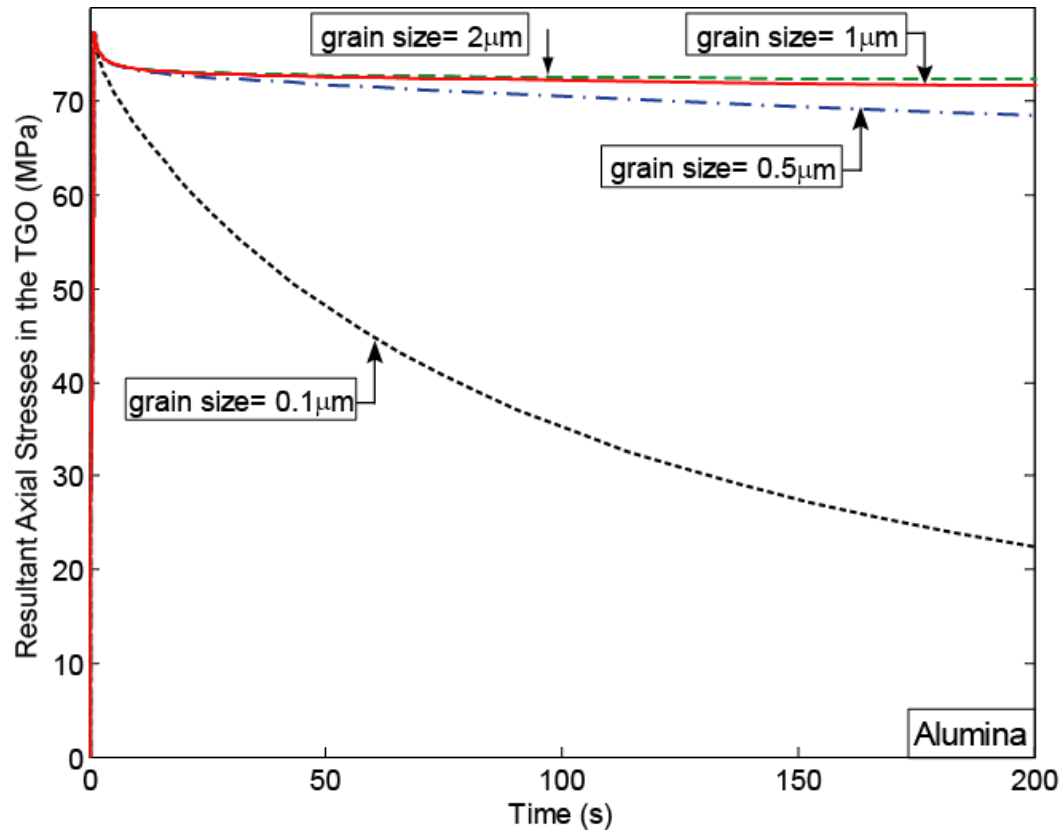
M. Hernandez, A.M. Karlsson, M. Bartsch: *Surface Coatings & Technology* 203, 2009, 3549-58

A.M. Karlsson and A.G. Evans, *Acta Materialia*, 2001 49(10) 1793-1804

**Growth strain increases the compressive stress in TGO with time!**



# Time dependent TGO properties: (2) relaxation/creep



Relaxation behavior depends on

- Grain size of TGO
  - as-coated:  $< 0.1 \mu\text{m}$
  - aged:  $0.1 - 2 \mu\text{m}$
- Chemical composition

Relaxation decreases the compressive stress in TGO with time!

Data from: J.D. French, J.H. Zhao, M.P. Harmer, H.M Chan, G.A. Miller. *J. American Ceramic Society* 77 (1994)



# Material properties used in FEM-Calculation

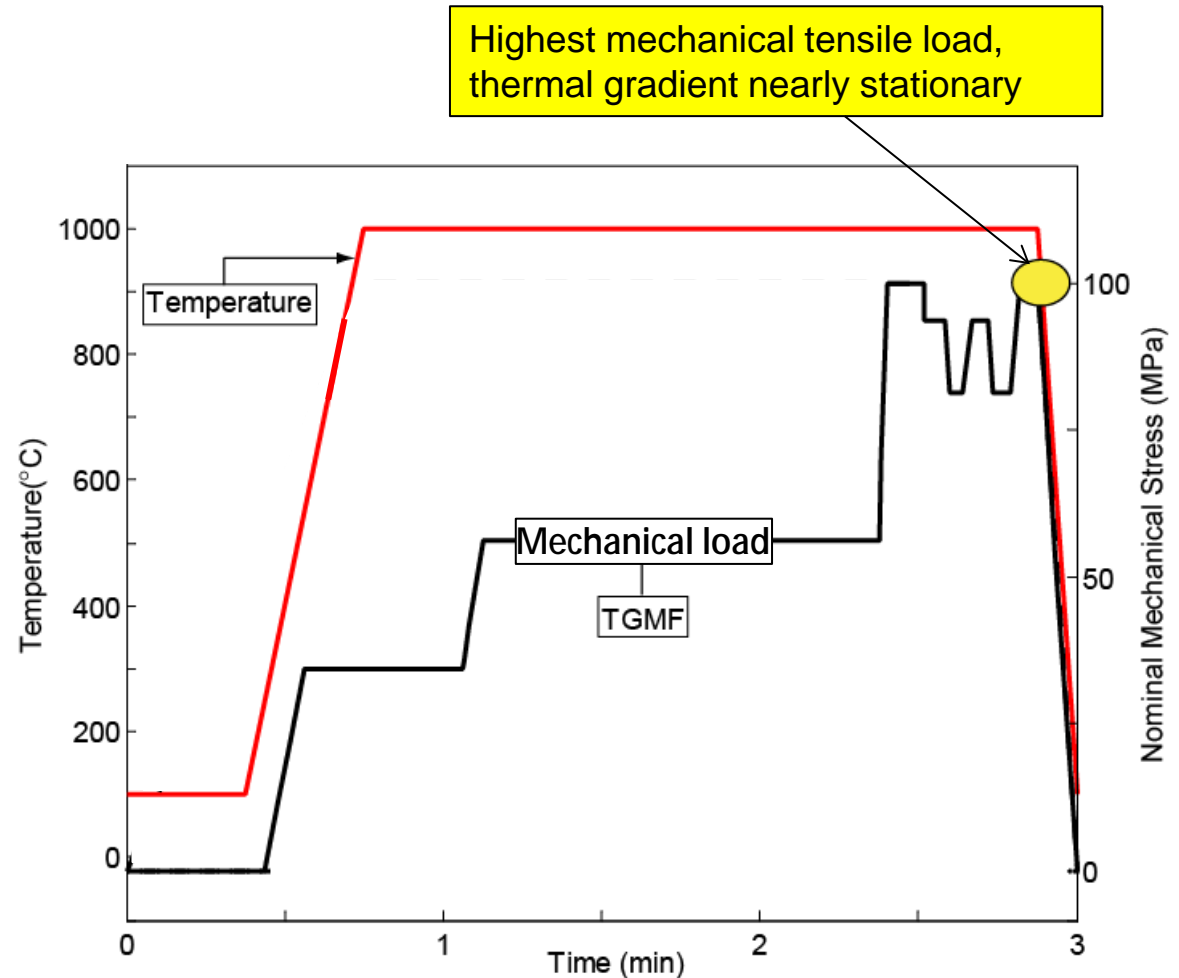
	Substrate		Bond coat		TGO		Top coat	
	RT	HT	RT	HT	RT	HT	RT	HT
Elastic modulus, $E$ , radial or isotropic [GPa]	215	148	140	70	360	340	13	16
Elastic modulus, $E$ , axial [GPa]	120	80	–	–	–	–	–	–
Poisson ratio, $\nu$	0.3	0.3	0.322	0.351	0.24	0.24	0.22	0.28
Coefficient of thermal expansion, $\alpha$ [ $10^{-6}$ 1/K]	11.5	18.8	8.6	16.6	6.0	8.7	9.0	11.5
Thermal conductivity, $\lambda$ [W/mK]	15	30	8.7	27.5	23	5	1.88	1.60
Density, $\rho$ [g/cm <sup>3</sup> ]	7.75	7.29	7.80	7.43	4.00	4.00	5.00	4.84
Heat capacity, $C_p$ [J/kgK]	400	580	390	700	769	1261	500	630
Creep law	Bond coat at high temperature						$n$	$B$
$\dot{\epsilon} = B\theta^n$							3	5.31E-9
Creep law	Material		$P$	$n$	$\Delta H_c$ [kJ/mol]			
$\dot{\epsilon} = Ad^{-p}\theta^n e^{\left(\frac{-Q}{RT}\right)}$	Mixed zone		2.2	1.8	633			
	Alumina		2.2	1.7	453			

[M. Hernandez, A.M. Karlsson, M. Bartsch: *Surface Coatings & Technology* 203, 3549-58, 2009]

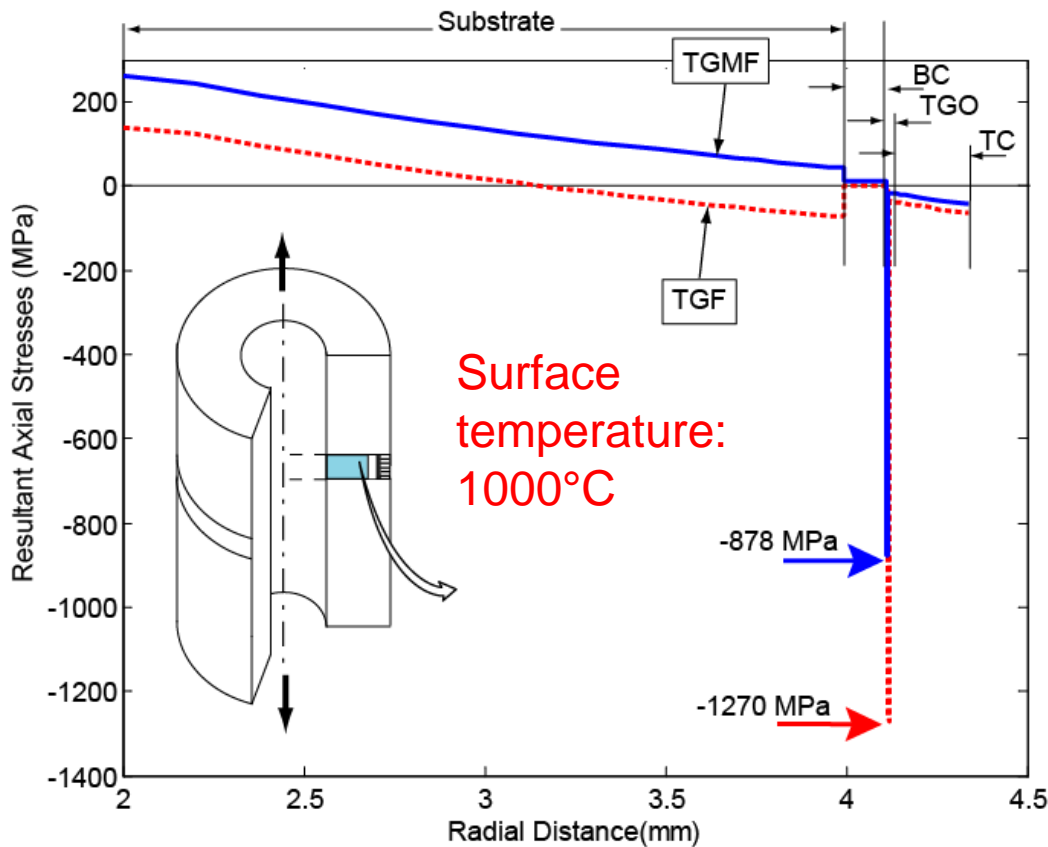


# Numerical model: load cycle

- Cyclic thermal load (temperature at the outer surface is shown)
- Thermal gradient: time dependent temperature difference between outer and inner wall (not shown)
- Cyclic mechanical load



# Axial stresses in first cycle



Axial stresses across the specimen wall due to

- thermal gradient (TGF)
- mechanical load (TGMF)
- property mismatch

**→** TGO always under compression

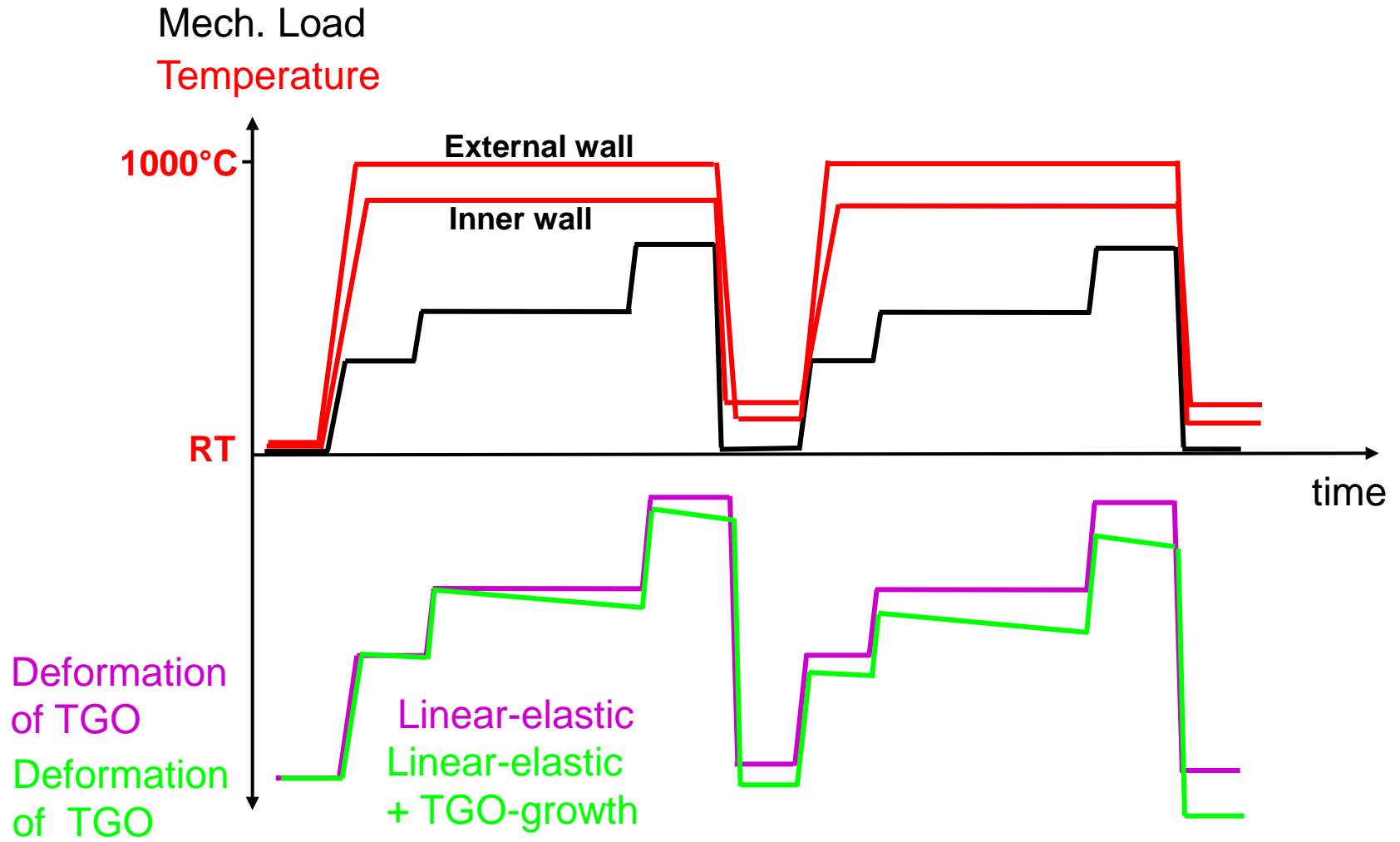
Stress free conditions:

- no mechanical load
- 1000°C, homogenous

[M. Hernandez, A.M. Karlsson, M. Bartsch: *Surface Coatings & Technology* 203, 3549-58, 2009]

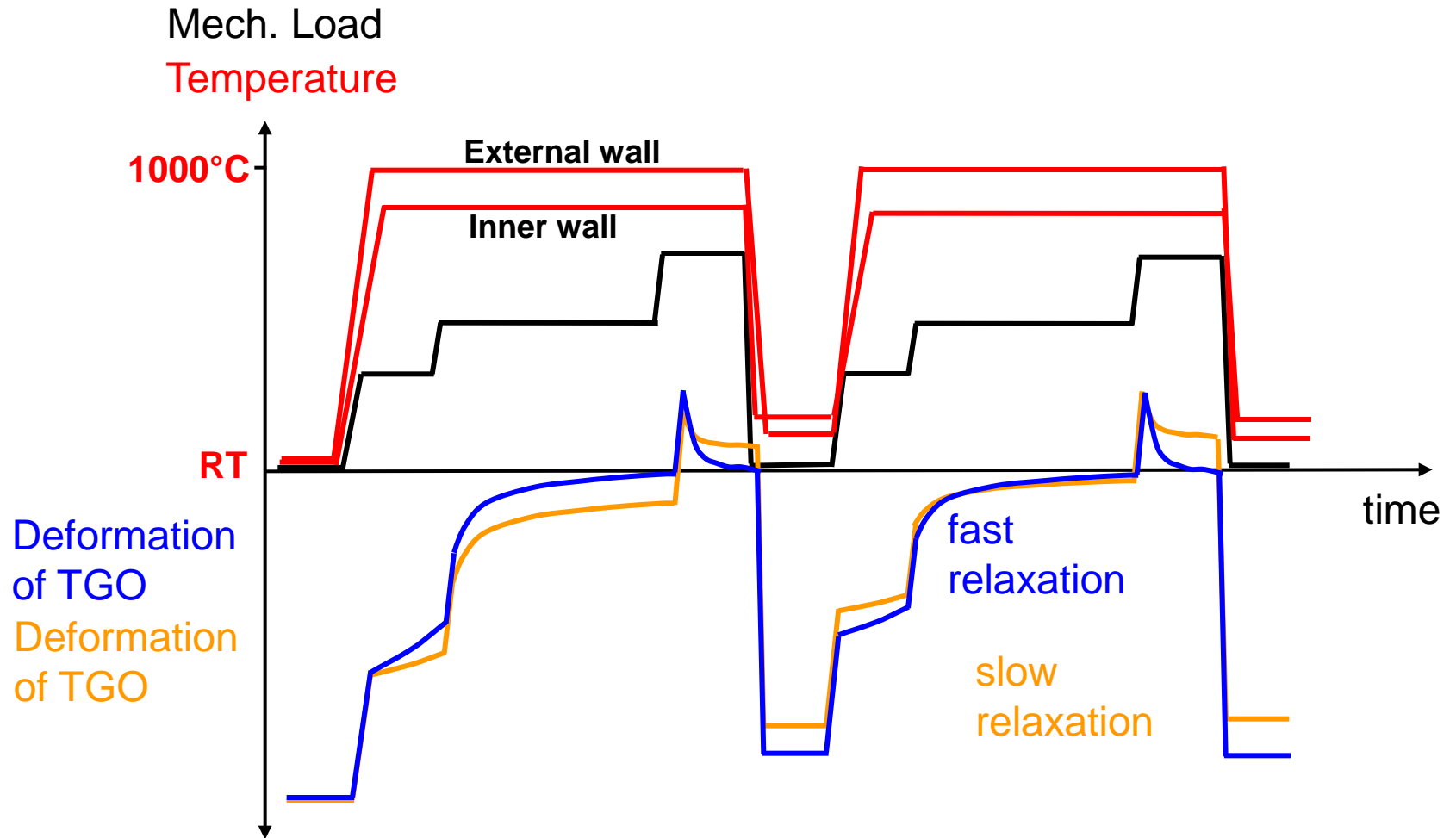


# Effect of TGO properties on cyclic stress accumulation

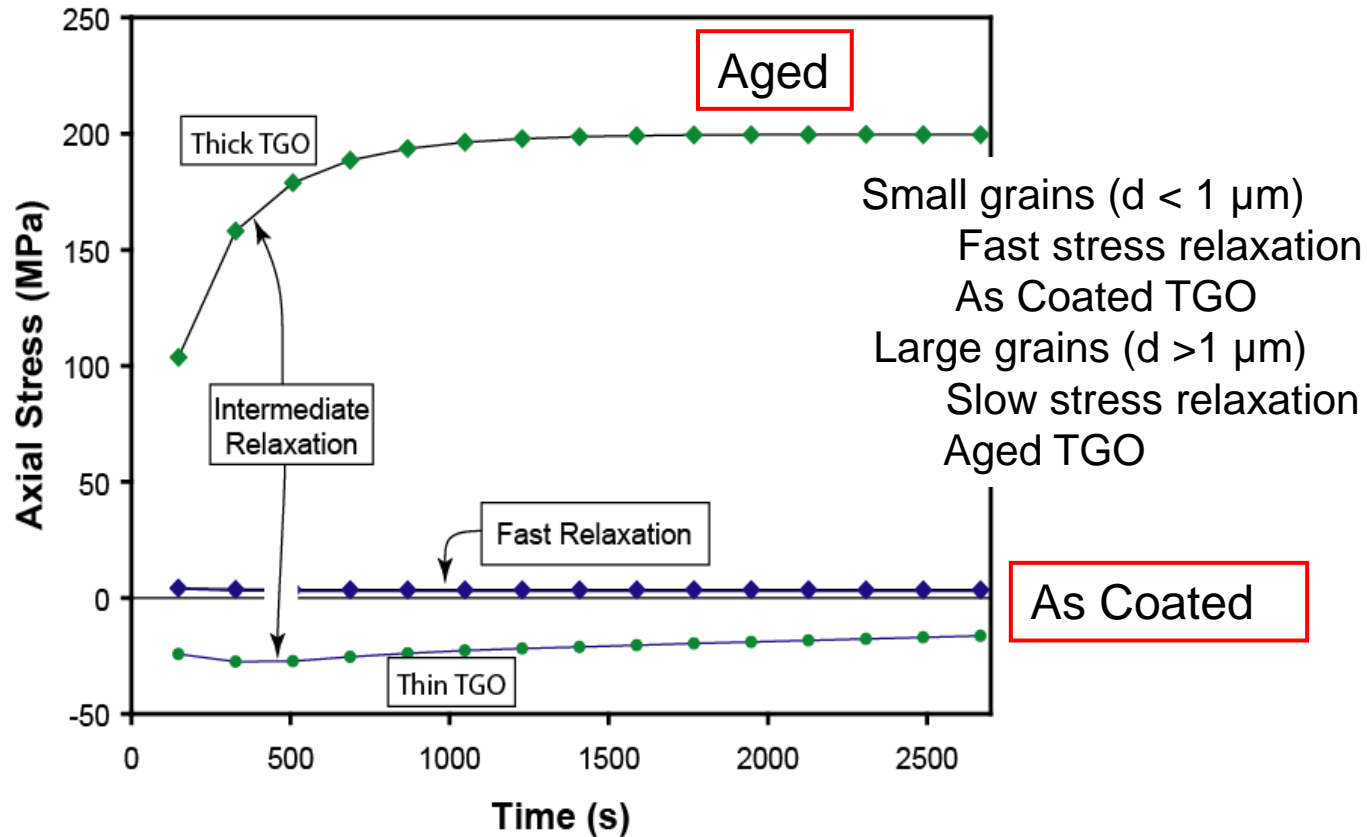




# Effect of TGO properties on cyclic stress accumulation



# Evolution of axial TGO-stresses



Hypothesis: Initiation of fatigue crack in TGO due to accumulation of tensile stress during subsequent TGMF-cycles → Material data missing



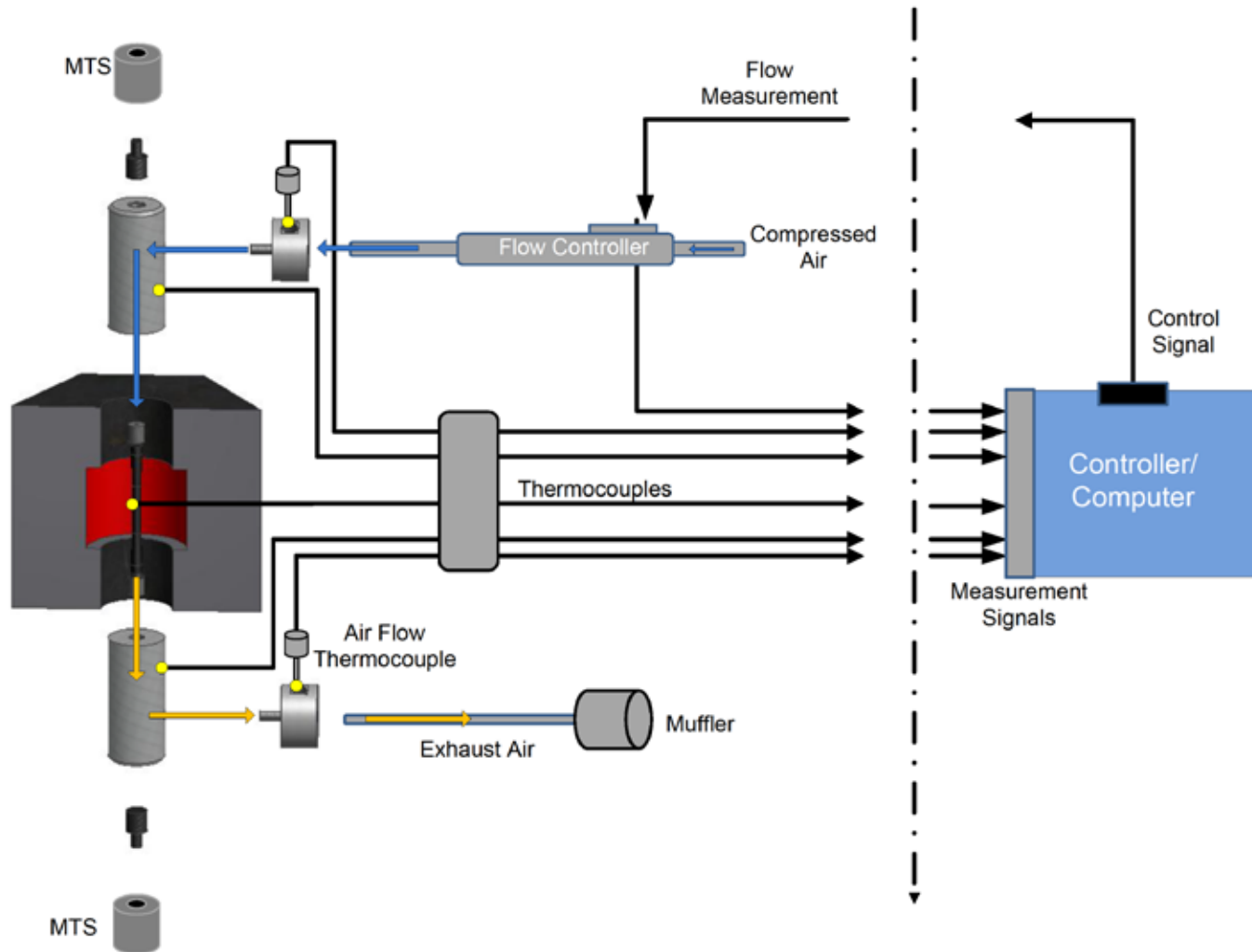
# In situ strain measurement : combining TGMF test setup with synchrotron X-ray diffractometry



- Argonne National Laboratory, Argonne, Illinois
- Synchrotron high energy monochromatic X-Ray beam-line; 65 keV beam energy

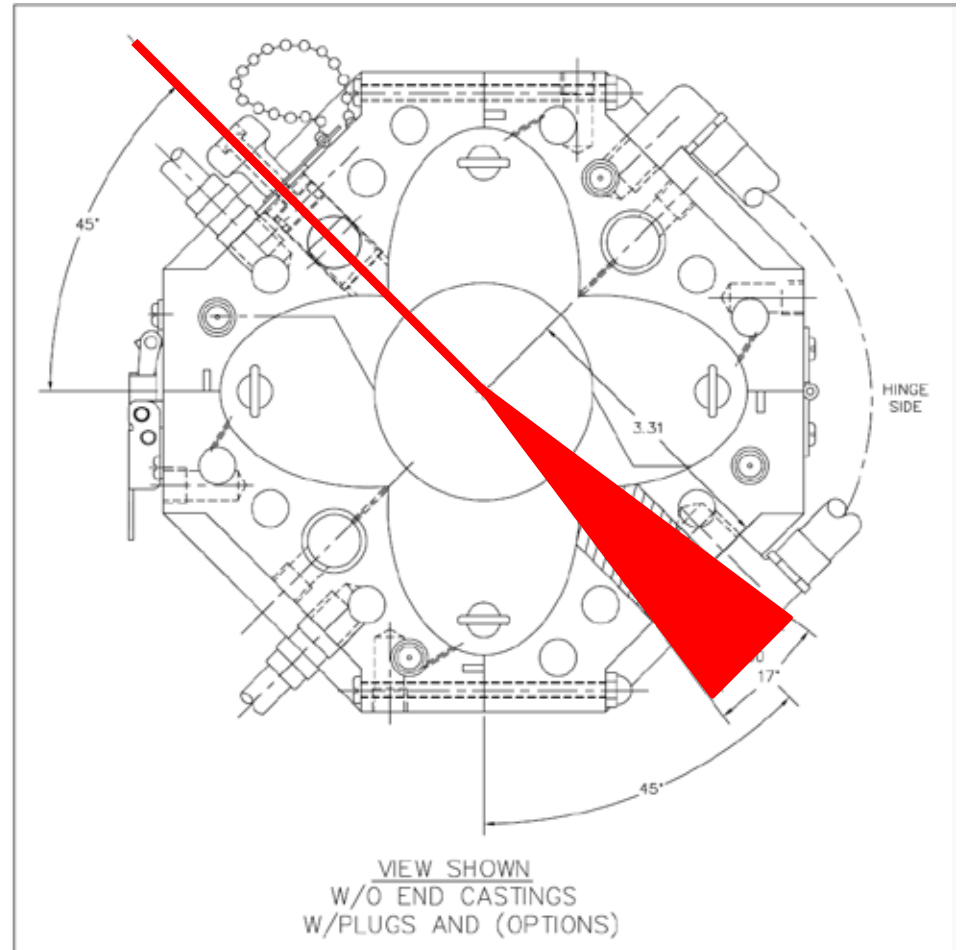
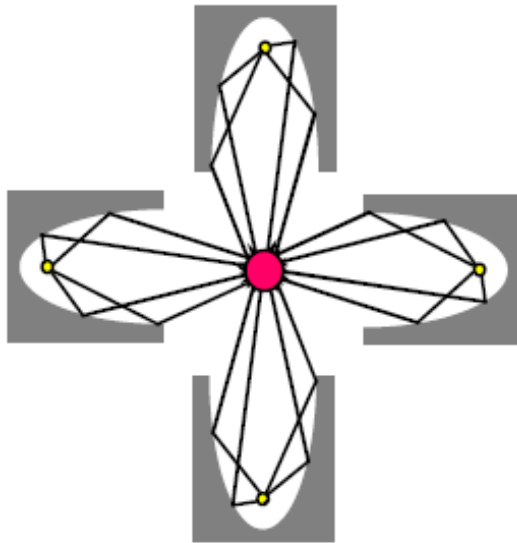


# Schematic of test facility configuration



# Top view of heater and beam

- 4 focused infrared lamps
  - 8 kW total
- Beam exit window
  - $17^{\circ} 40'$



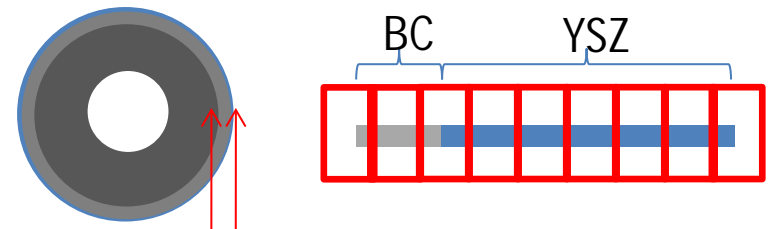
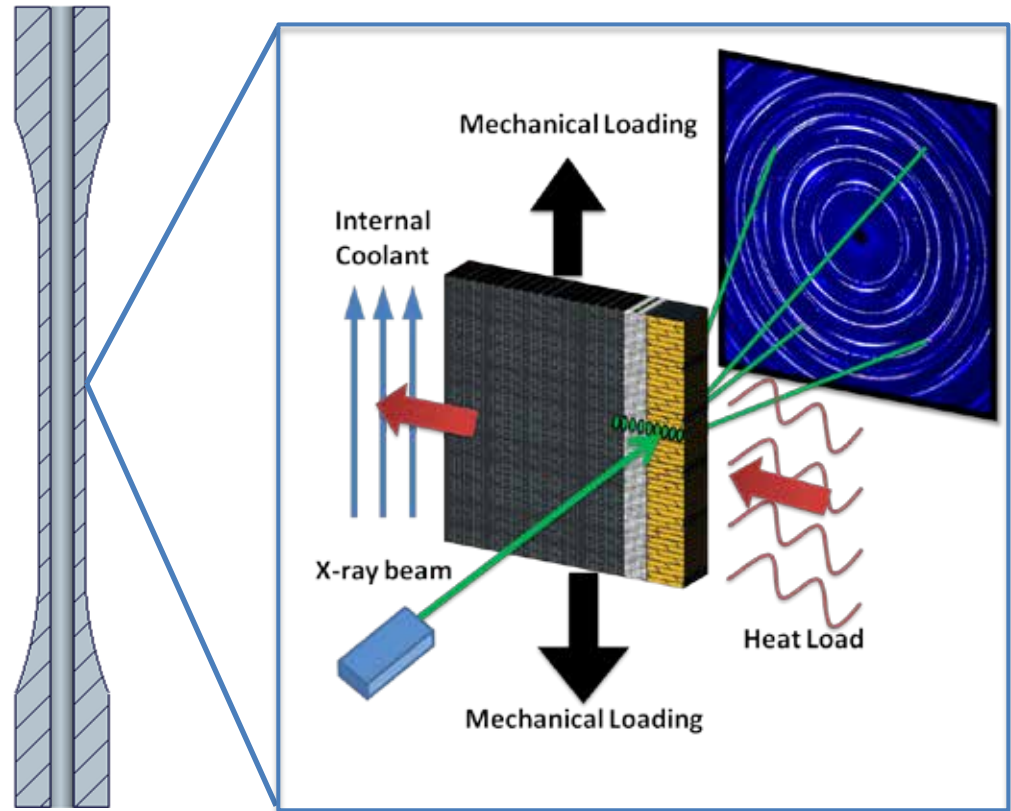
# Measurement method

## Loading parameter:

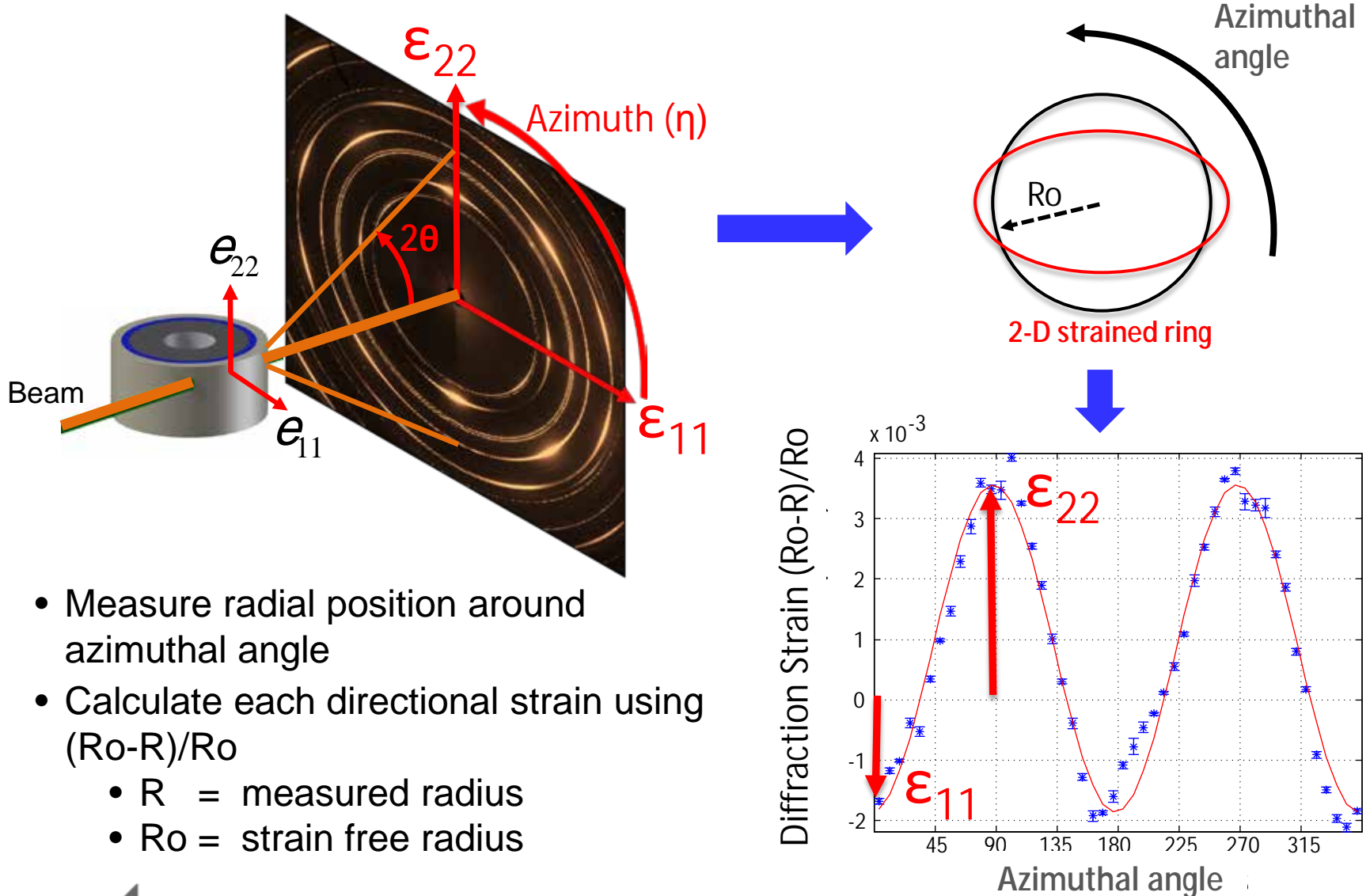
- thermal cycle (80 min)
- outer surface temperature max. 1000°C,  $\Delta T$  between outer and inner surface ca. 150°C
- variation of thermal gradient by cooling flow rate
- superposing mechanical load

## Beam parameter:

- 65 keV beam energy
- X-Ray scan through coating thickness every 3.5 minutes
- 10 windows a (30 x 300)  $\mu\text{m}^2$



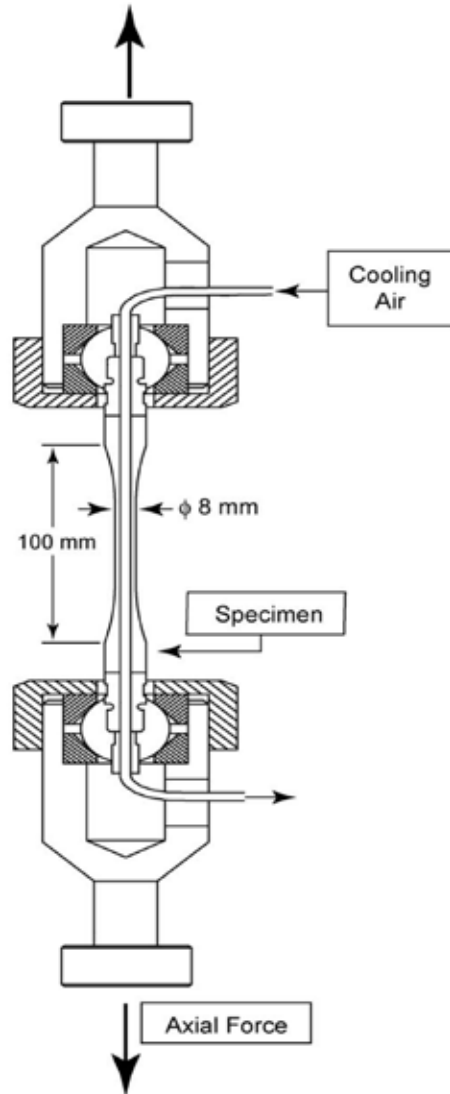
# X-Ray diffraction 2-D strain measurements



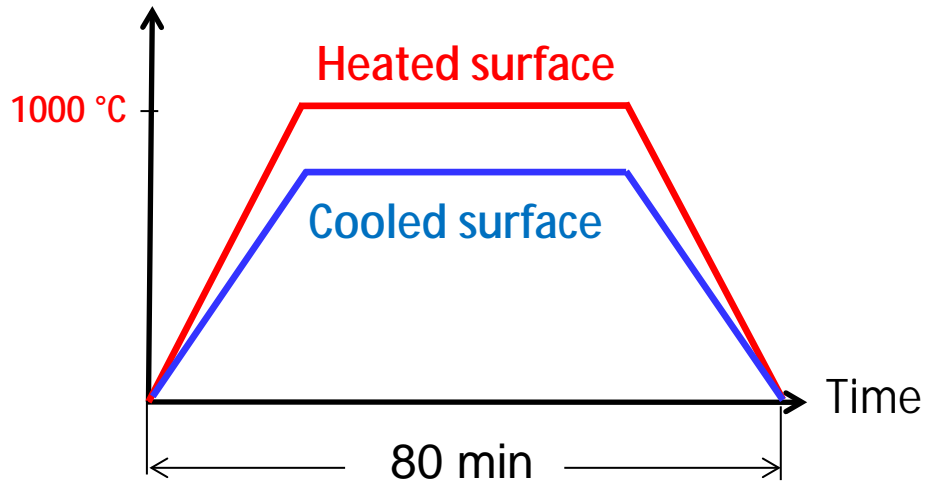
- Measure radial position around azimuthal angle
- Calculate each directional strain using  $(R_o-R)/R_o$ 
  - $R$  = measured radius
  - $R_o$  = strain free radius



# Strain measurement during cyclic loading



Temperature

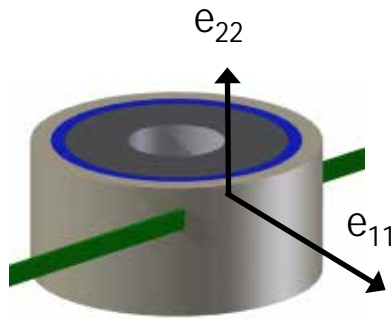


- Outer surface ramped up to  $1000\text{ }^{\circ}\text{C}$
- Constant coolant flow rate  
(30, 50, and 75 % max. flow, 100 SLPM max)
- Constant nominal mechanical stress  
(32, 64 and 128 MPa applied)





# Strain in YSZ during thermal cycle



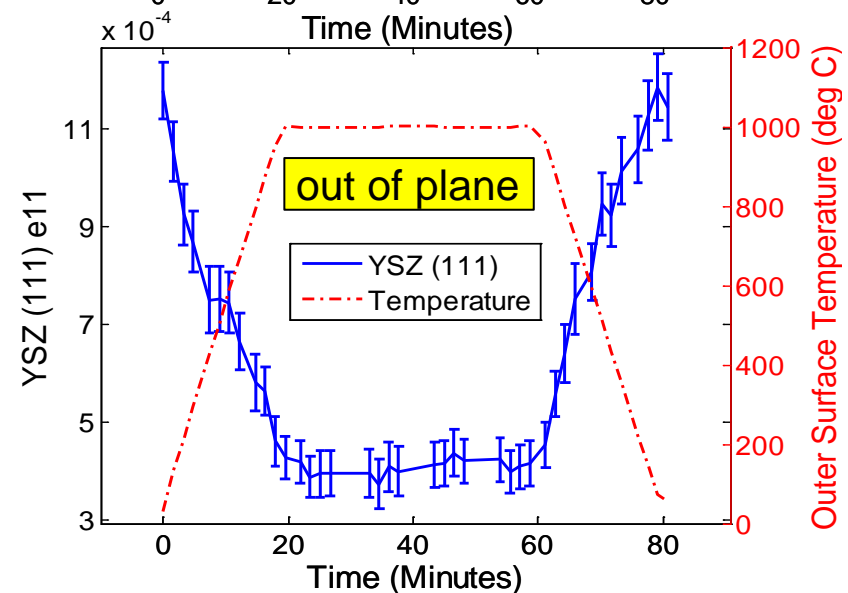
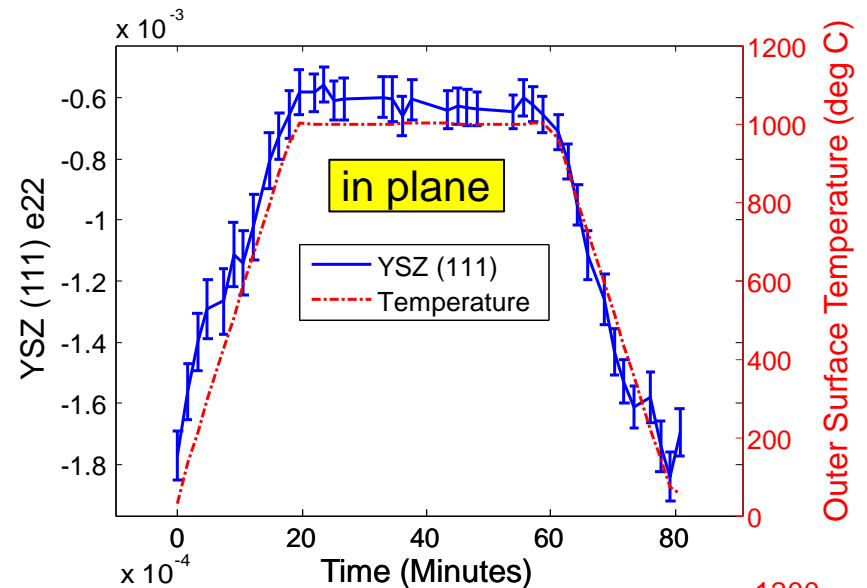
- 64 MPa
- 75% cooling air flow rate

at room temperature:

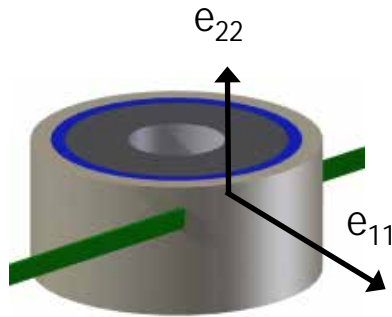
- compressive in plane strain  $e_{22}$
- tensile out of plane strain  $e_{11}$

at high temperature:

- strain reduces (closer to stress free condition at manufacturing temperature)



# Strain in bond coat $\beta$ -NiAl during thermal cycle



- 64 MPa
- 75% cooling air flow rate

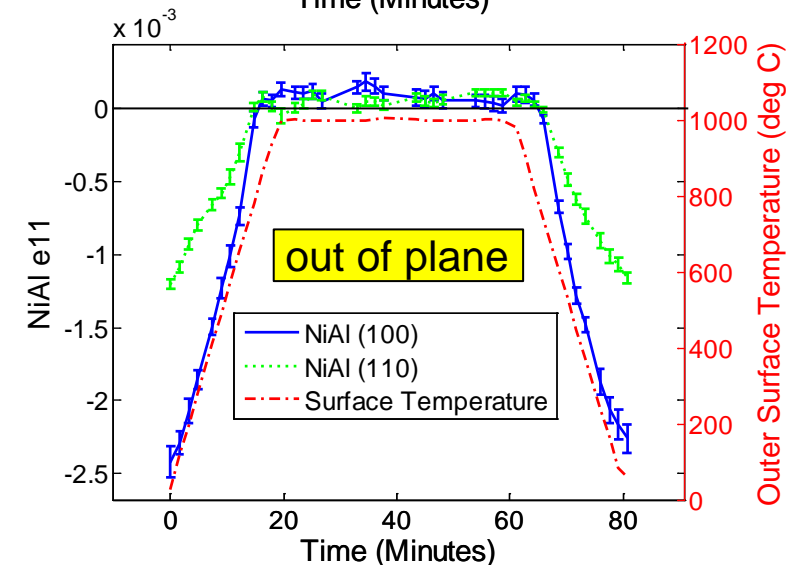
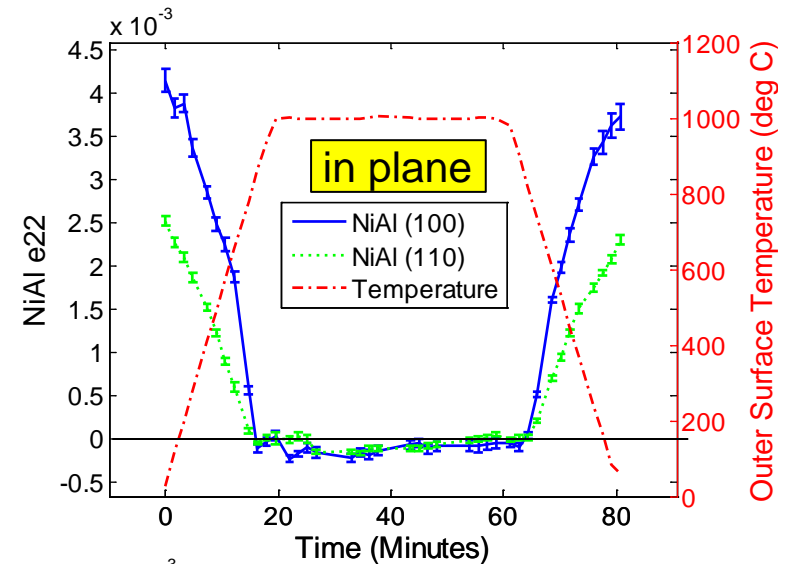
at room temperature:

- tensile in plane strain  $e_{22}$
- compressive out of plane strain  $e_{11}$

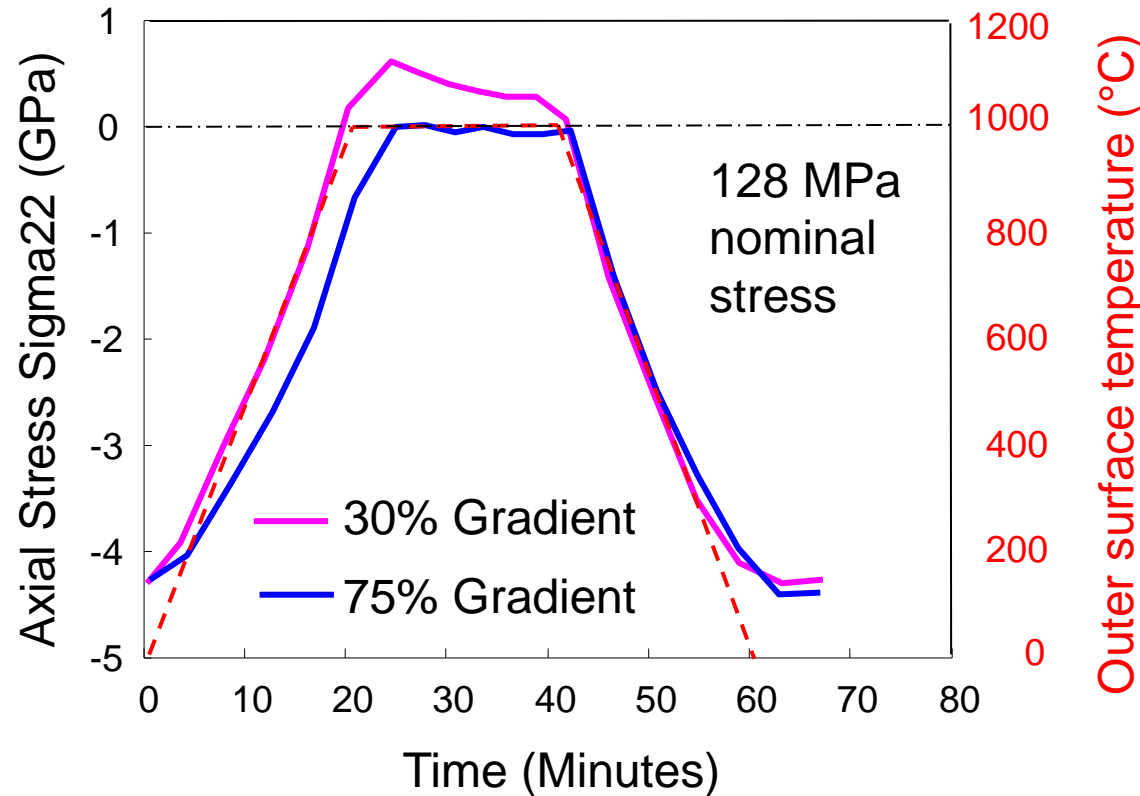
at high temperature:

- strain reduces (closer to stress free temperature, relaxation)

Thermal expansion in Bond coat higher than in substrate



# TGO stress in pre-aged specimen during thermal cycle



Pre-aged specimen:  
304h at 1000 $^{\circ}\text{C}$

- the TGO experience tensile stresses under TGMF loading depending on applied mechanical tensile load and thermal gradient.
- Relaxation occurs during dwell time at high temperature, which is a condition for accumulating tensile stress during cycling.



# Conclusions

- Local mechanical behavior of the coating materials has been captured at RT and high temperature, based on in-situ X-ray diffraction data
  - TGO relaxation has been observed
- In situ strain measurement provide evidence for supposed damage mechanisms - support hypotheses based on FEM calculations
- Further evaluation of data and improvement of methods  $\Rightarrow$  ongoing



# Thank you for your attention!

## Questions?

### Acknowledgements:

- This material is based upon work supported by the National Science Foundation Grants OISE 1157619 and CMMI 1125696
- German Science Foundation (DFG) grant SFB-TRR103, project A3
- Use of the Advanced Photon Source, an Office of Science User Facility operated for the U.S. Department of Energy (DOE) Office of Science by Argonne National Laboratory, was supported by the U.S. DOE under Contract No. DE-AC02-06CH11357.



# Publications

- M.Bartsch, B. Baufeld, M. Heinzelmann, A. M. Karlsson, S. Dalkilic, L. Chernova: Multiaxial thermo-mechanical fatigue on material systems for gas turbines, *Materialwiss. & Werkstofftechnik* 38, (2007) 712-719
- M. Bartsch, B. Baufeld, S. Dalkilic, L. Chernova, M. Heinzelmann: Fatigue cracks in a thermal barrier coating system on a super alloy in multiaxial thermomechanical testing, *Int. J. fatigue* 30 (2008) 211-218
- M. Hernandez, A. Karlsson, M. Bartsch: On TGO creep and the initiation of a class of fatigue cracks in thermal barrier coatings, *Surf. Coat. Techn.* 203 (2009) 3549-3558
- M. T. Hernandez, D. Cojocar, A. M. Karlsson, M. Bartsch: On the crack opening of a characteristic crack due to thermo-mechanical fatigue testing of thermal barrier coatings, *Comp. Mat. Sci.* (50) (2011) 2561-2572
- S. F. Siddiqui, K. Knipe, A. Manero, C. Meid, J. Schneider, J. Okasinski, J. Almer, A.M. Karlsson, M. Bartsch, S. Raghavan: Synchrotron X-Ray Measurement Techniques for Thermal Barrier Coated Cylindrical Samples under Thermal Gradients, *Review of Scientific Instruments*, (2013) 84, 083904
- K. Knipe, A. Manero, S. F. Siddiqui, C. Meid, J. Wischek, J. Okasinski, J. Almer, A. M. Karlsson, M. Bartsch & S. Raghavan: Strain response of Thermal Barrier Coatings captured under extreme engine environments through Synchrotron X-ray Diffraction, *Nature Communications* 5 (2014), article number 4559
- A. Manero, S. Sofronsky, K. Knipe, C. Meid, J. Wischek, J. Okasinski, J. Almer, A. M. Karlsson, S. Raghavan & M. Bartsch: Monitoring Local Strain in a Thermal Barrier Coating System Under Thermal Mechanical Gas Turbine Operating Conditions, *Journal of Materials* 67, Issue 7 (2015) 1528-39

**Contact:** Prof. Dr.-Ing. Marion Bartsch  
German Aerospace Center (DLR)  
Institute of Materials Research  
Linder Höhe  
D-51147 Köln  
Phone: +49-(0)2203-601-2436  
e-mail: [marion.bartsch@dlr.de](mailto:marion.bartsch@dlr.de)



# A new code of Practice for Force Controlled Thermo-mechanical Fatigue Testing

## **AUTHORS:**

**S. Brookes, A. Scholz, H. Klingelhöffer, R. Lohr,  
M. Whittaker, M. Loveday, A. Wisby, N. Ryder,  
S. Stekovic, J. Moverare, S. Holdsworth, D. Dudzinski.**

**CoP Co-Ordinator:  
Dr Stephen Brookes**



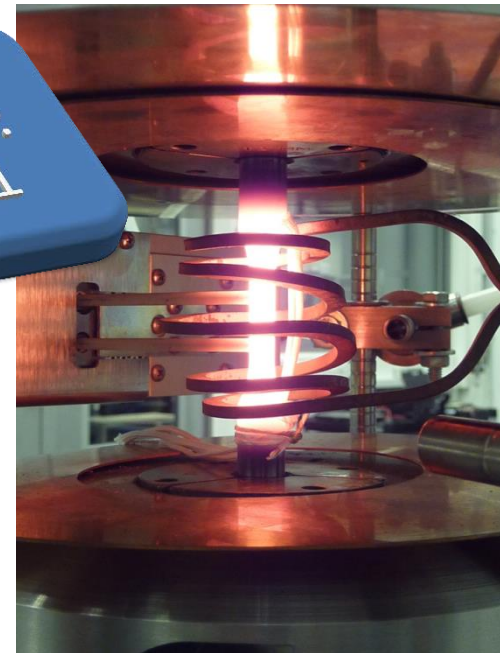
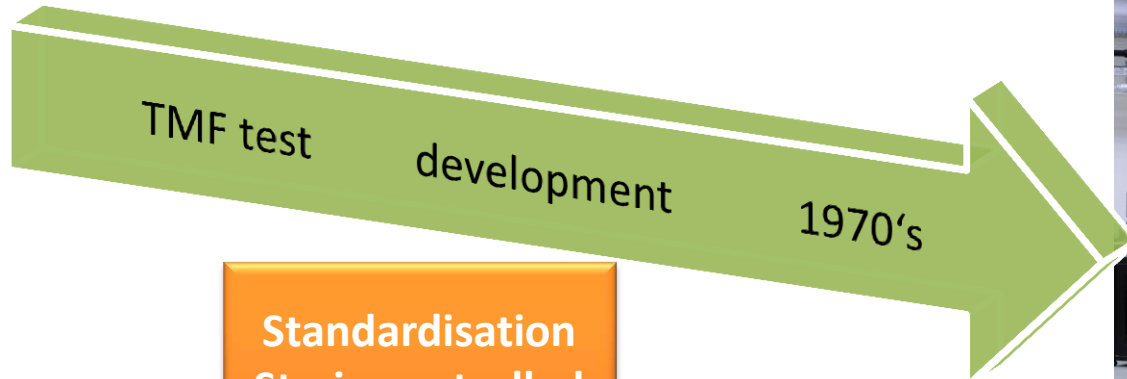
**Rolls-Royce**

**Mechanical Test Operations Centre**

<b>PARTNERS</b>	
<b>Rolls-Royce Mechanical Test Operations Centre, Dahlewitz</b>	<b>Germany</b>
<b>Technical University of Darmstadt, Darmstadt</b>	<b>Germany</b>
<b>Federal Institute for Materials Research and Testing (BAM), Berlin</b>	<b>Germany</b>
<b>University of Swansea, Swansea</b>	<b>United Kingdom</b>
<b>National Physical Laboratory (NPL), Teddington</b>	<b>United Kingdom</b>
<b>High Temperature Mechanical Testing Committee</b>	<b>United Kingdom</b>
<b>AMEC, Warrington</b>	<b>United Kingdom</b>
<b>Severn Thermal Solutions, Bristol</b>	<b>United Kingdom</b>
<b>Raymond Lohr Consulting Engineer</b>	<b>United Kingdom</b>
<b>Linköping University, Linköping</b>	<b>Sweden</b>
<b>Siemens Industrial Turbomachinery AB, Finspong</b>	<b>Sweden</b>
<b>EMPA, Swiss Federal Laboratories for Materials Science and Technology, Dübendorf</b>	<b>Switzerland</b>
<b>Derivation Research Laboratory, Ottawa</b>	<b>Canada</b>



# Background



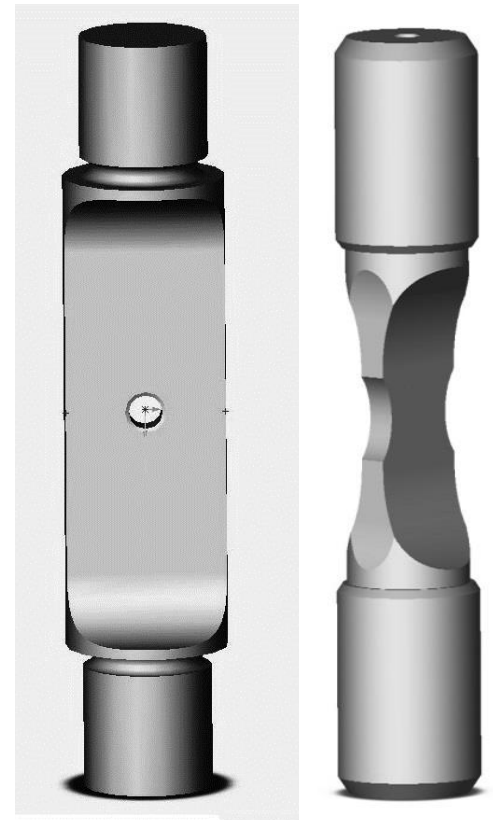
# Why the need for a new Code of Practice for Force controlled TMF?

- **Accommodate Feature Based (Specimen) Fatigue Testing where extensometers are difficult to apply**

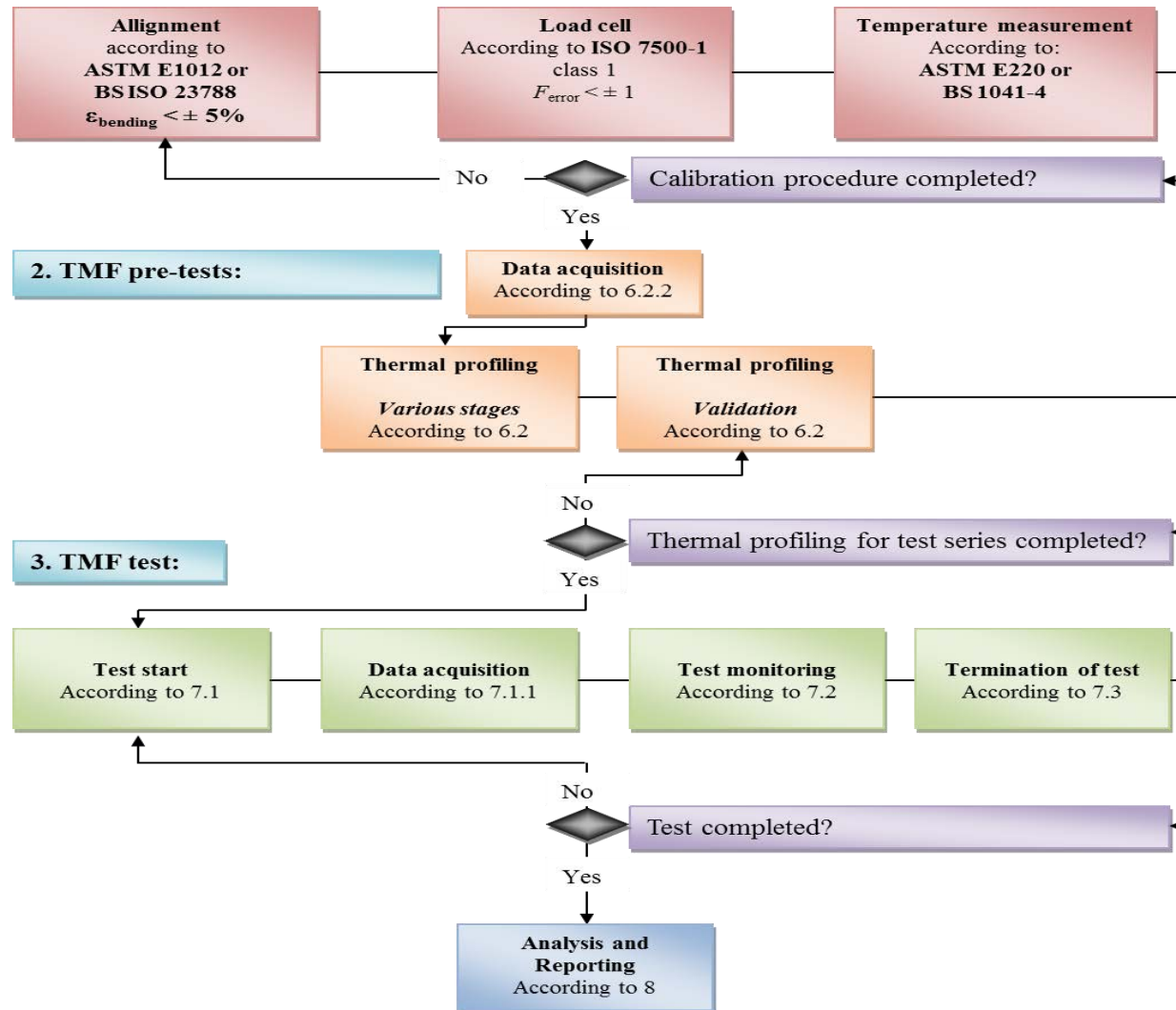
Specimens are carefully made to be as representative of the real production components:

- Surface finish
- Manufacturing technique
- Volume of material tested
- Part or full feature (hole)

- **Ensures a standardised approach.**
- **Amendments to strain TMF standards would require greater revision when changes are incorporated to either types.**
- **Strain and force controlled tests are historically separate standards.**

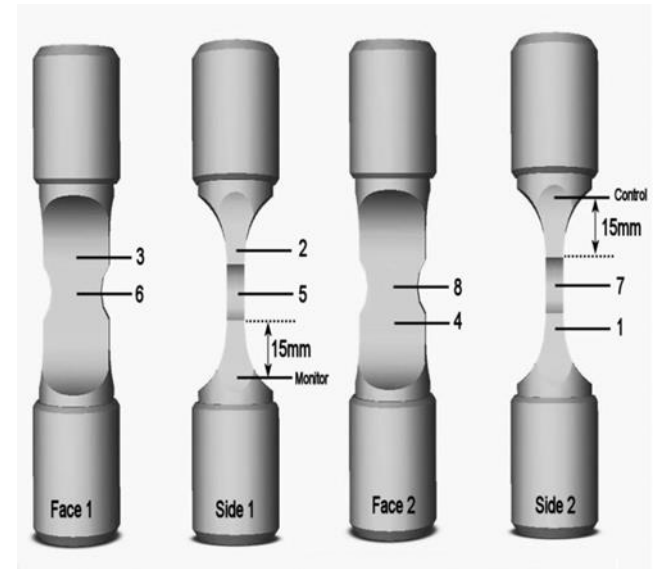


# The various steps in undertaking a force-controlled TMF test according to this new code of practice



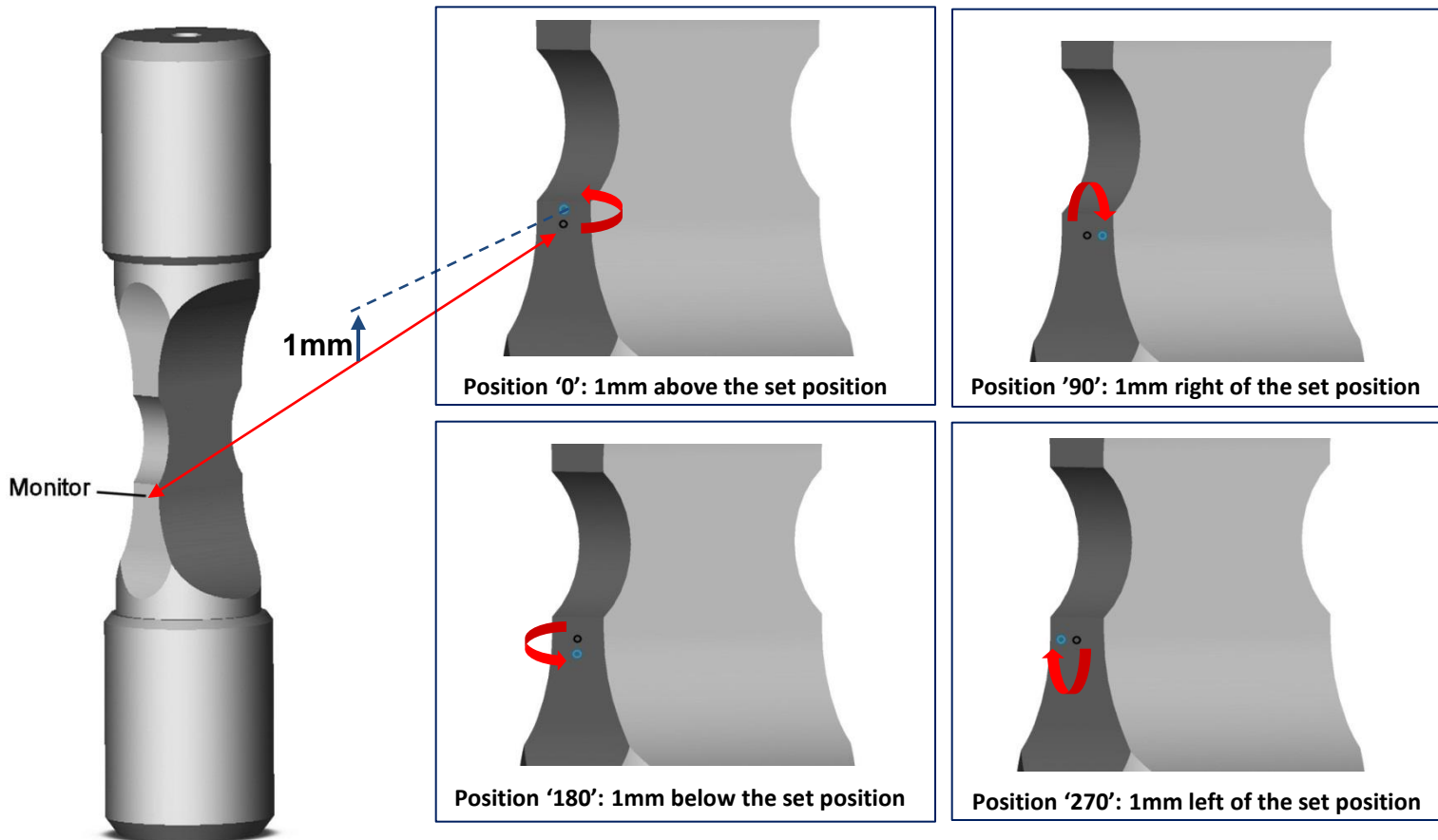
## An important inclusion in the new Code of Practice: TMF Pre-tests Section 6.2 - Verification of temperature uniformity - Thermal profiling

- **TMF test specimens containing a feature such as a notch naturally cause an uneven temperature distribution across the specimen surface.**
- **A dummy specimen with numerous thermocouples is exposed to the desired thermal cycle.**
- **Adjustments can be made to the furnace position, cooling air flow, heating ramps and specimen orientation to gain the best profile.**
- **Further profiles are performed with a reduced number of thermocouples and only adjusting the heating ramps.**
- **The final profile will only have 2 thermocouples. This will be identical to the final setup on the test specimen.**

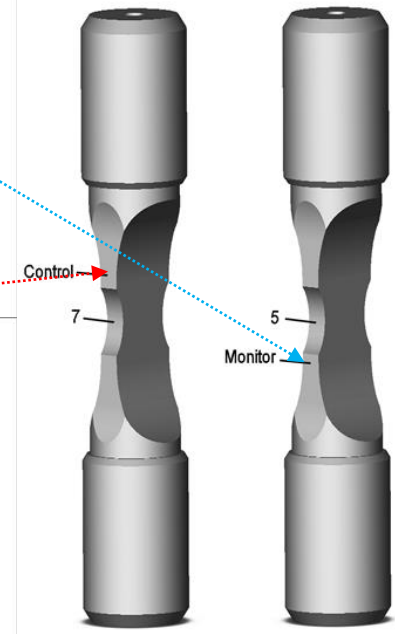
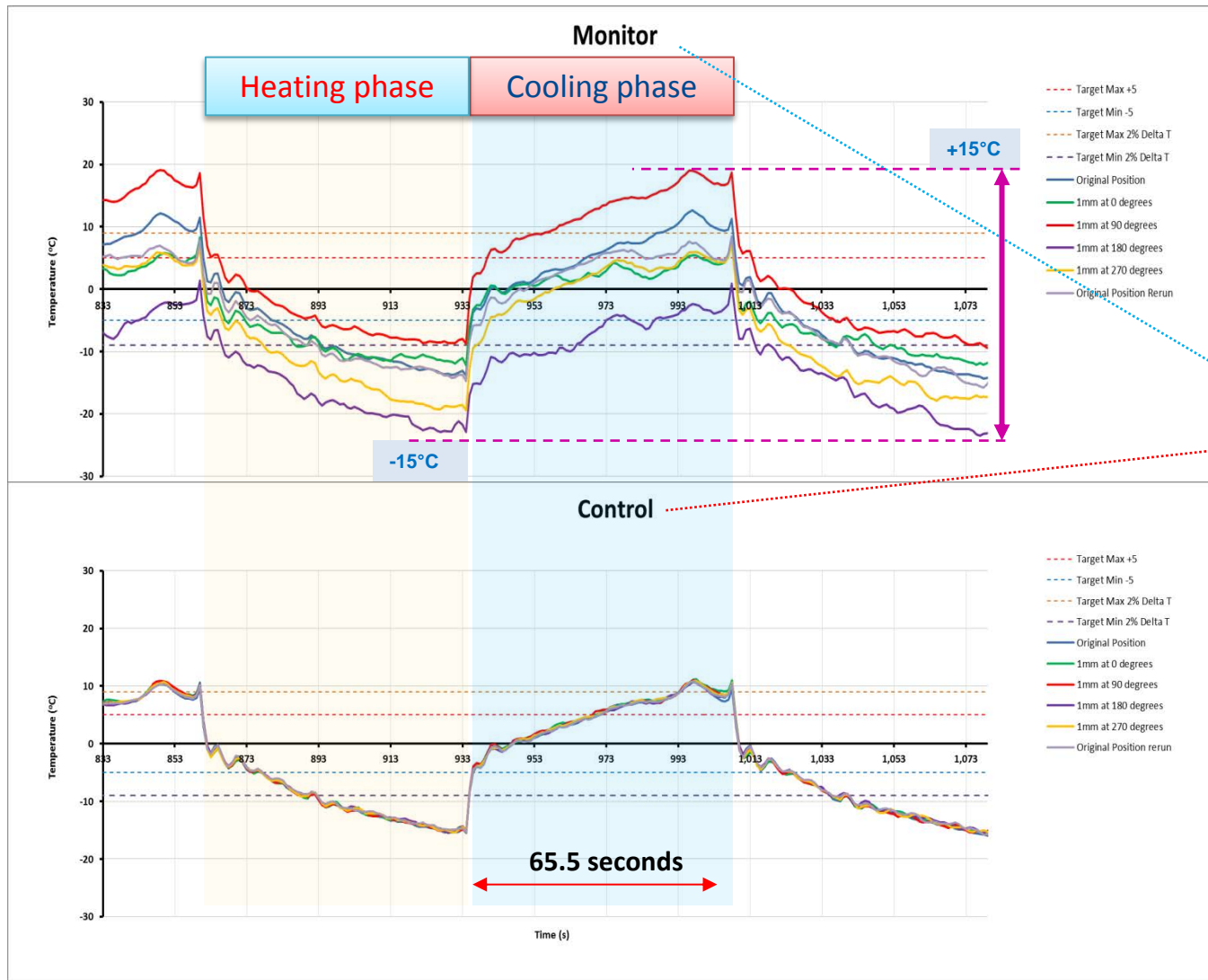


# An Example: The position of monitor thermocouples and their effects on the temperature measurement

A set of experimental trials were conducted at Rolls-Royce to highlight the effect of the monitor TC position and the subsequent effects on the temperature measurement.



# The effects on the Monitor thermocouple position on temperature measurement



At the monitor TC the most effect on temperature is seen when this TC is situated at 90° and 1 mm below the correct position.

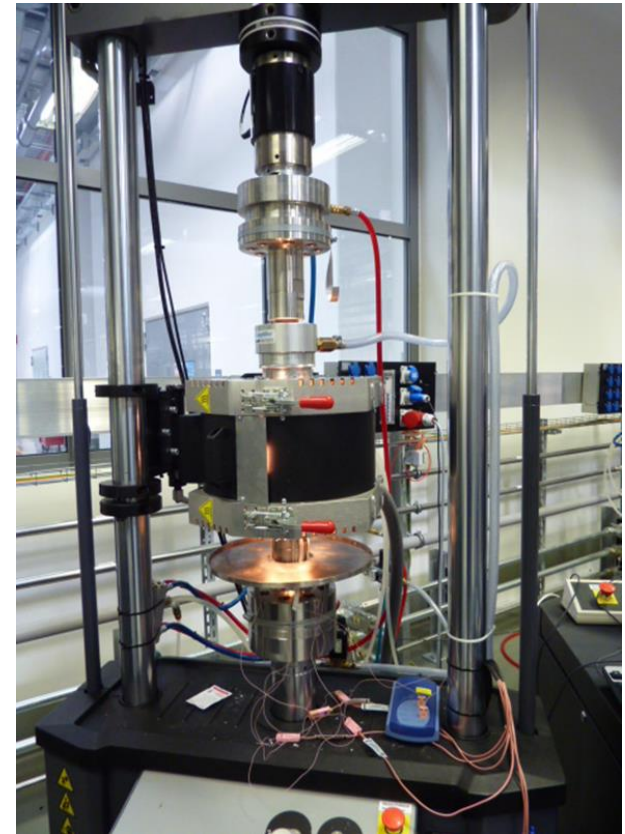
# The effects of the monitor thermocouple position on the centre notch temperature measurement



At the notch the most effect on temperature is seen when the TC's are 1mm above and below the correct position.

# The new Code of Practice – The justification

- A vital new test method for materials testing.
- It meets the growing demand of industry for more complex testing methods.
- Major contribution by the international testing community which clearly indicates the requirements for such a new test method.





# The new Code of Practice – – The next steps

- **This CoP is open to discussion during this TMF workshop.**
- **This CoP is to be brought to the attention of the international standards organisation committee ISO TC 164 SC5, in October 2016, which is responsible for developing fatigue standards. With the aim to initiate a new ISO standard for Force Controlled Thermo-Mechanical Fatigue Testing.**



# Thank you for your attention And A big thank you to the partners for their contributions



SIEMENS



Where to find the new TMF Code of Practice

[http://www.tmf-workshop.bam.de/en/tmf media/code of practice for force controlled thermo-mechanical fatigue \(2\).pdf](http://www.tmf-workshop.bam.de/en/tmf_media/code_of_practice_for_force_controlled_thermo-mechanical_fatigue_(2).pdf)



# Assessing the thermomechanical fatigue life of TiAl-based alloy TNB-V2



**TMF-Workshop 2016**  
BAM, Berlin, April 27-29

Ali El Chaikh<sup>a</sup>, Björn Wollny<sup>a</sup>, Fritz Appel<sup>b</sup>, Hans-Jürgen Christ<sup>a</sup>

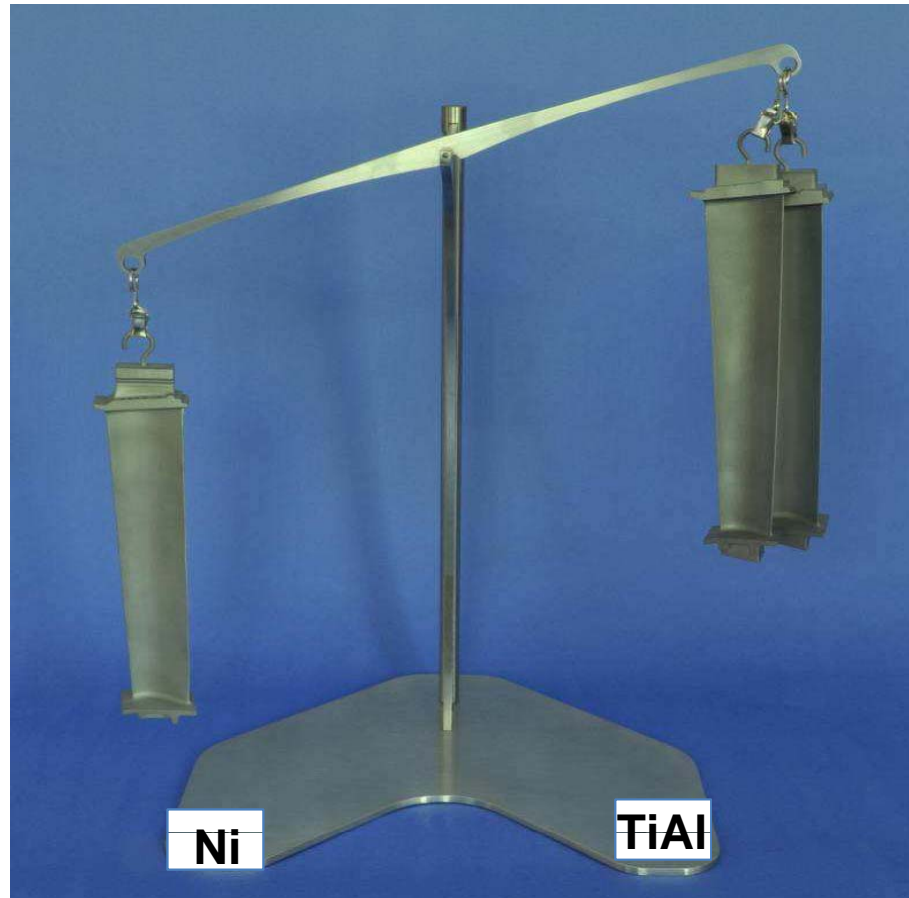
<sup>a</sup>Institut für Werkstofftechnik, Universität Siegen

<sup>b</sup>Institut für Werkstoffforschung, Helmholtz-Zentrum Geesthacht

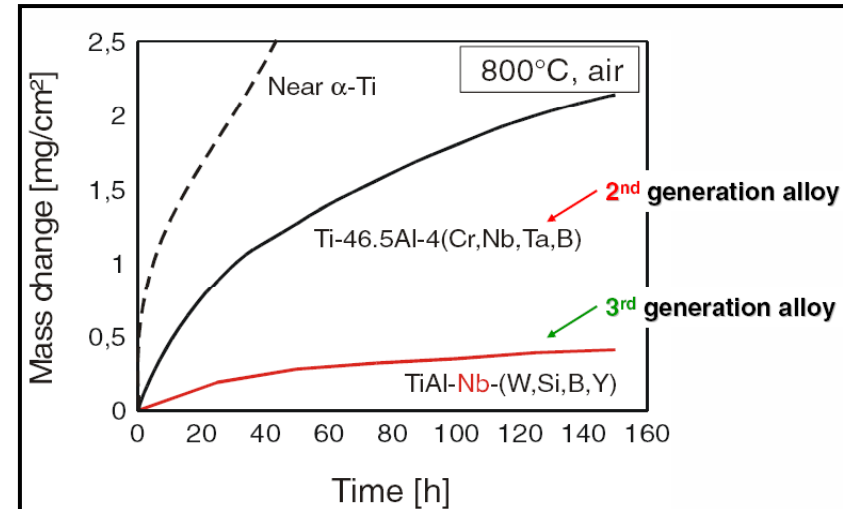


## Content:

- **Introduction**
  - Background
- **Experimental**
  - Material (TNB-V2), testing system
- **Cyclic Stress-Strain Behaviour / Fatigue Life**
  - LCF and TMF results (at different  $\Delta\varepsilon/2$ , air and vacuum)
  - Microstructural changes
- **Modelling of CSS Behaviour**
- **Fatigue Life Assessment**
- **Conclusions**

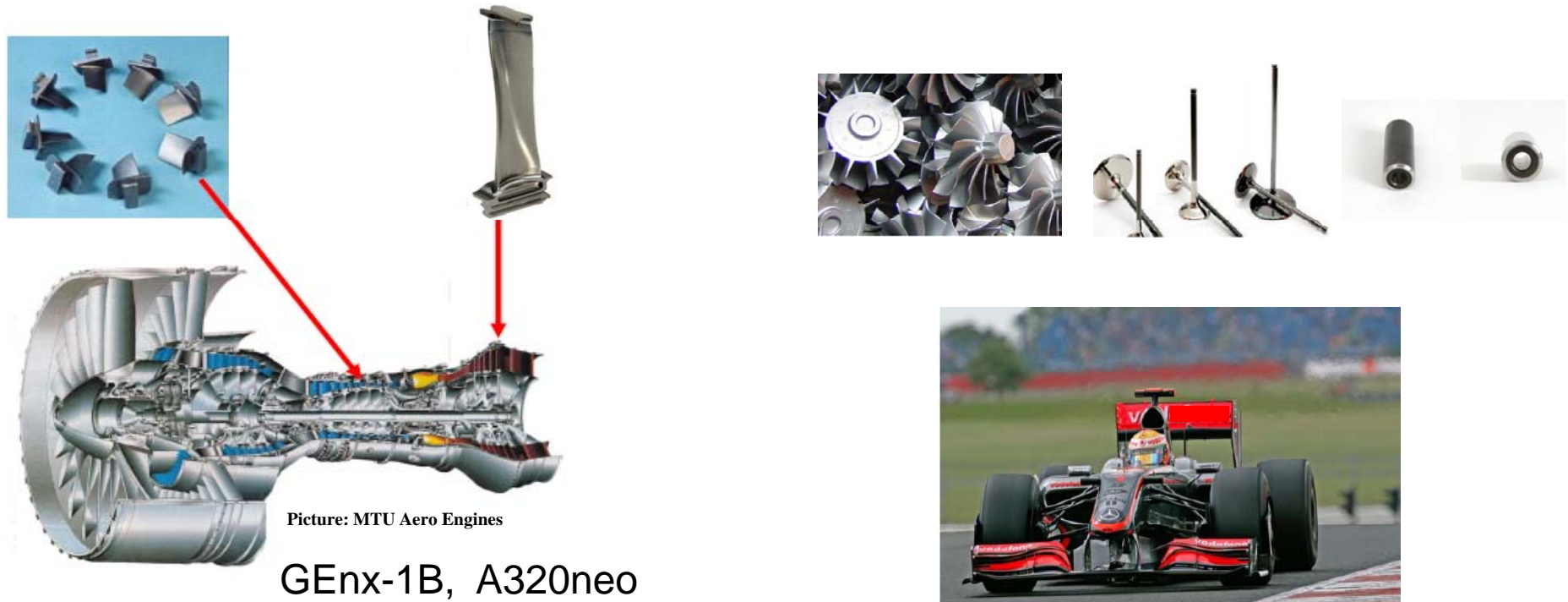


Picture: courtesy of Tital, Bestwig



## Drawbacks:

- Pronounced BDTT
- Below BDTT very brittle
- Low damage tolerance
- Microstructure depends very sensitively on heat treatment
- Variation in mechanical behaviour



Picture: MTU Aero Engines  
**GEnx-1B, A320neo**

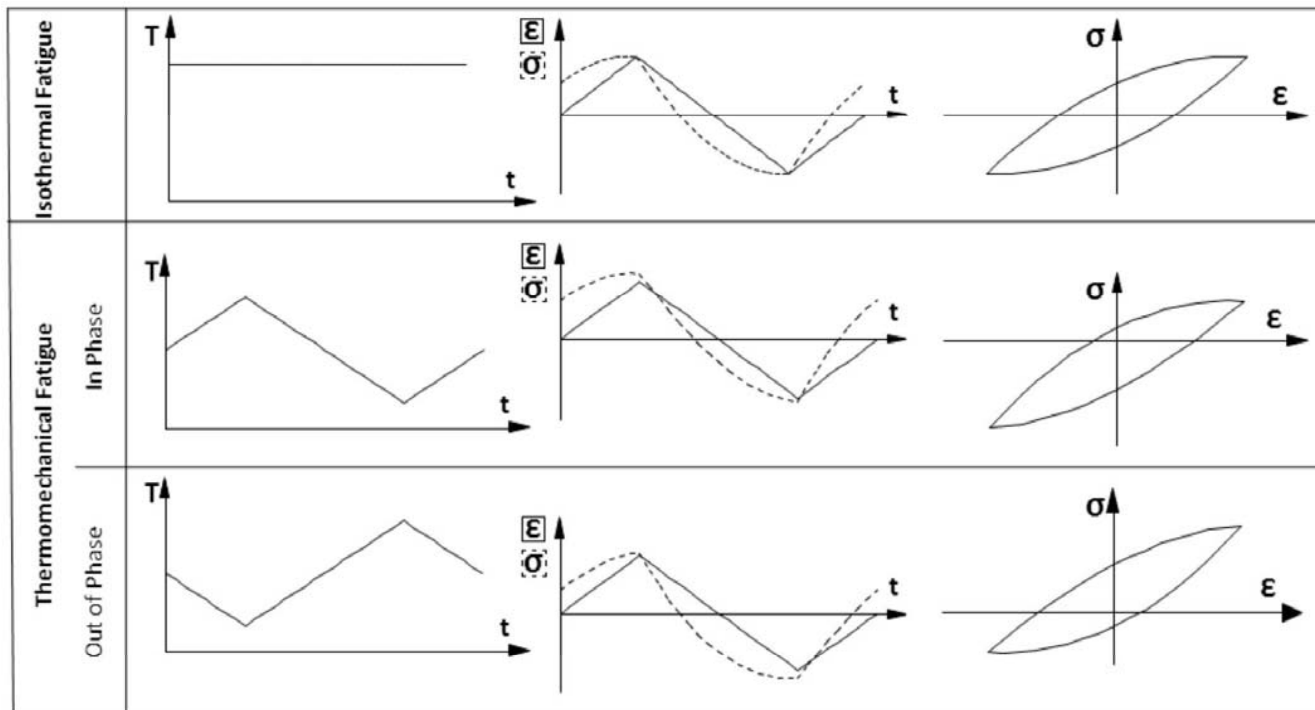
- Reduction in CO<sub>2</sub> emissions (-15 to -20%)
- Reduction in NO<sub>x</sub> emissions (-80%)
- noise reduction (-20 to -25%)
- Significant maintenance cost reduction (-30%)

- Higher efficiency

## Content:

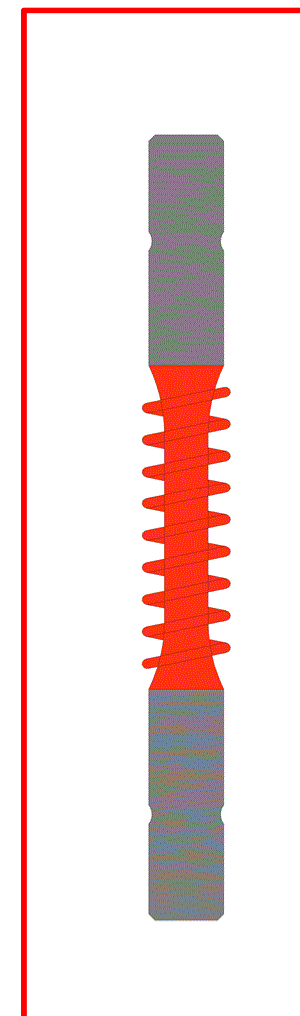
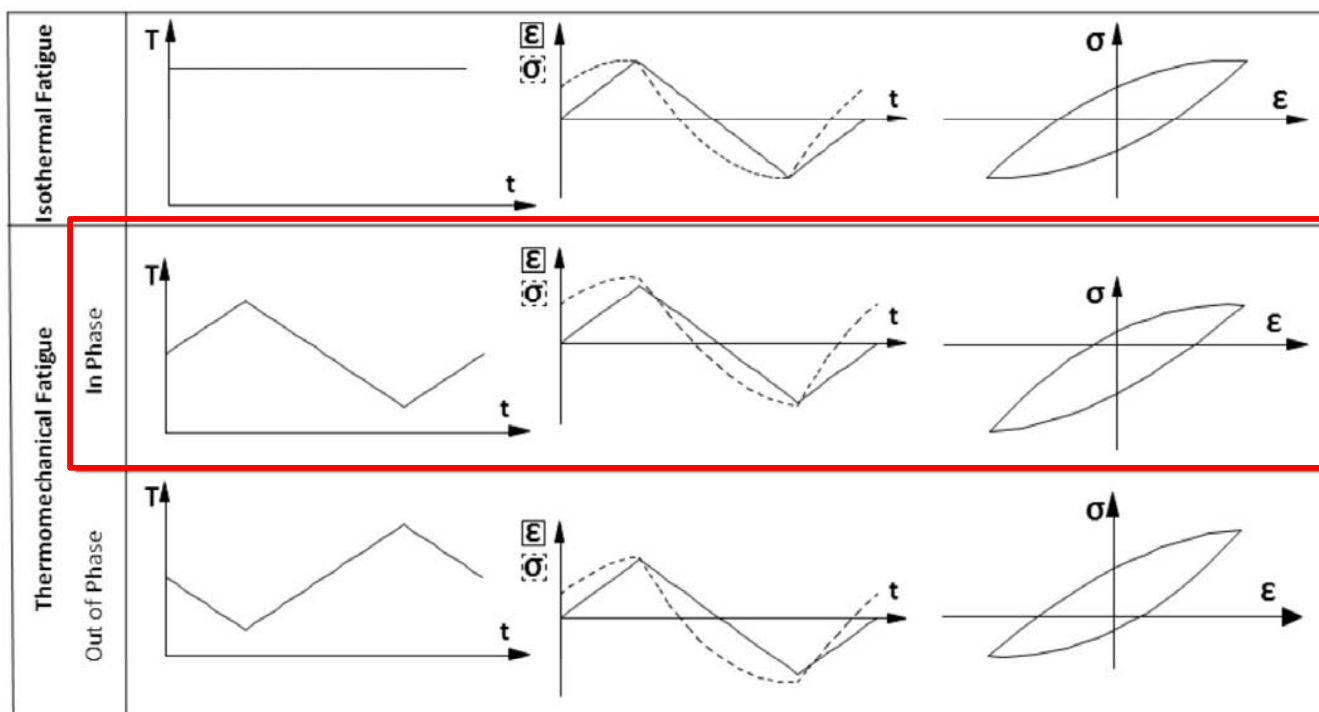
- **Introduction**
  - Background
- **Experimental**
  - **Material (TNB-V2), testing system**
- **Cyclic Stress-Strain Behaviour / Fatigue Life**
  - LCF and TMF results (at different  $\Delta\epsilon/2$ , air and vacuum)
  - Microstructural changes
- **Modelling of CSS Behaviour**
- **Fatigue Life Assessment**
- **Conclusions**

## High temperature fatigue

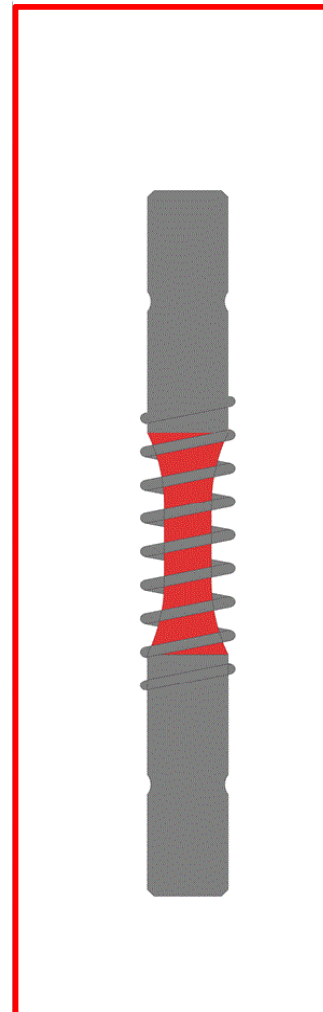
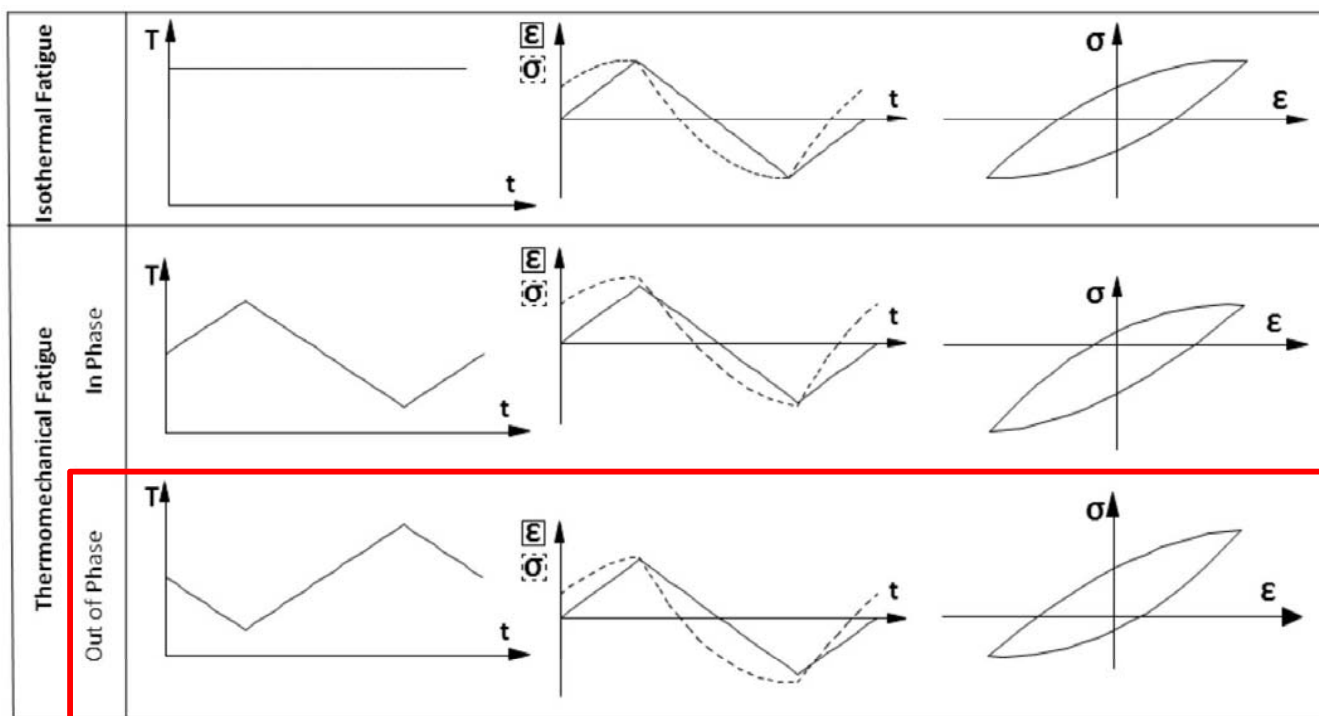




# High temperature fatigue

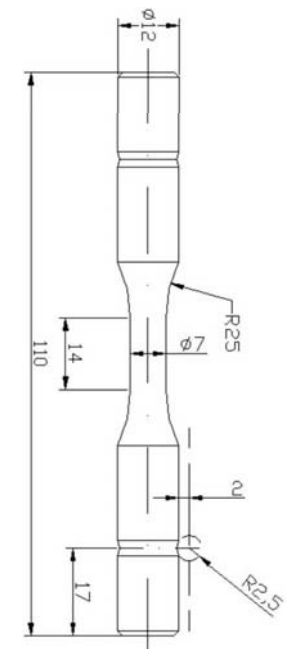
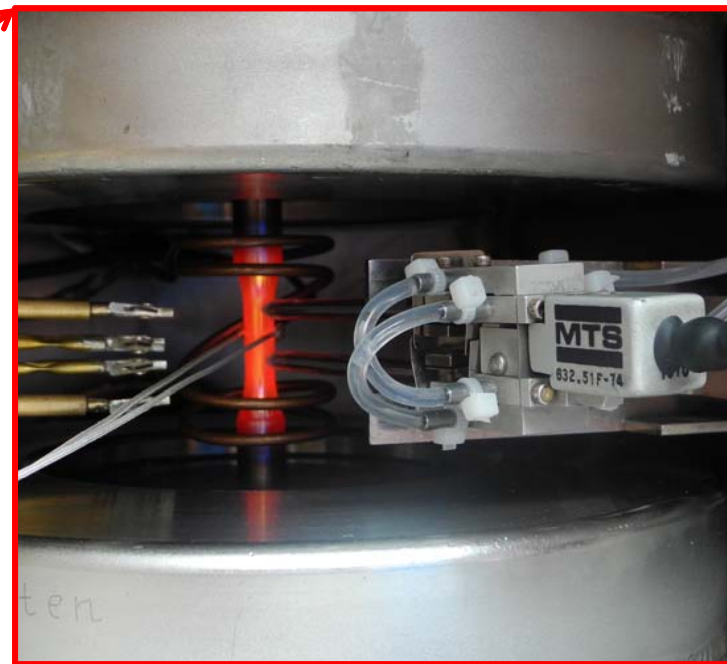
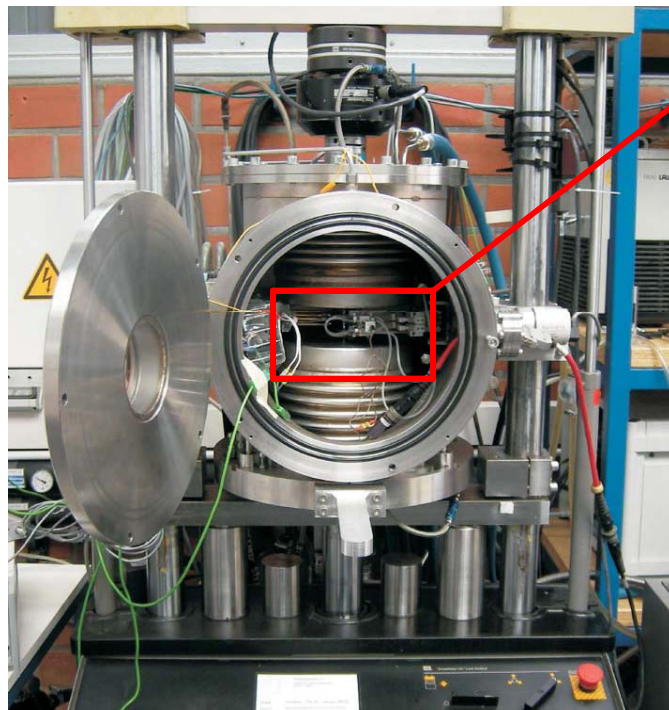


## High temperature fatigue



➤ Experimental

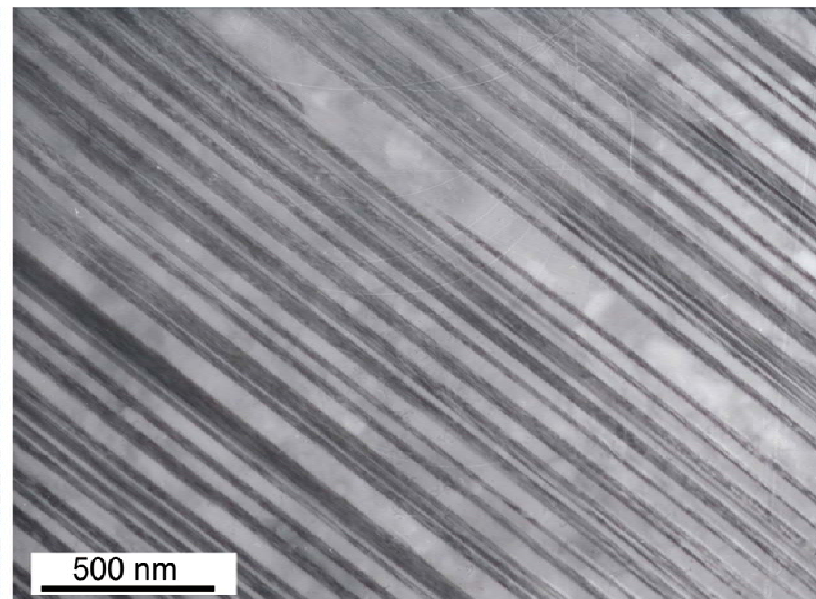
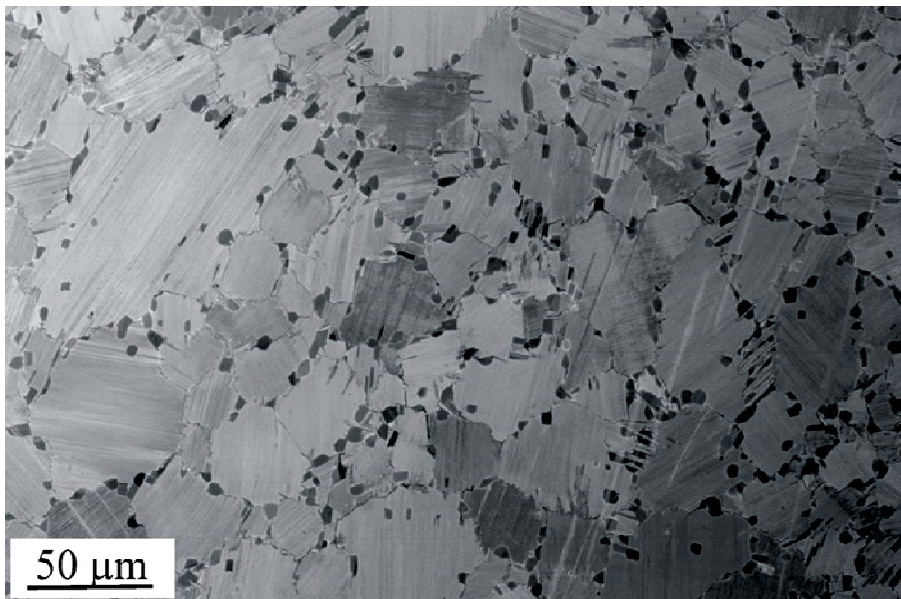
- 16 isothermal LCF and 16 thermomechanical experiments:  
 mostly  $R = -1$ ,  $\Delta\epsilon/2 = 0.4 \dots 0.7\%$ ,  $T_{\min} = 350^\circ\text{C}$  and  $T_{\max} = 650, 750$  and  $850^\circ\text{C}$   
 strain controlled, in air and in high vacuum ( $10^{-5}$  mbar)



## ➤ Experimental

### - Material

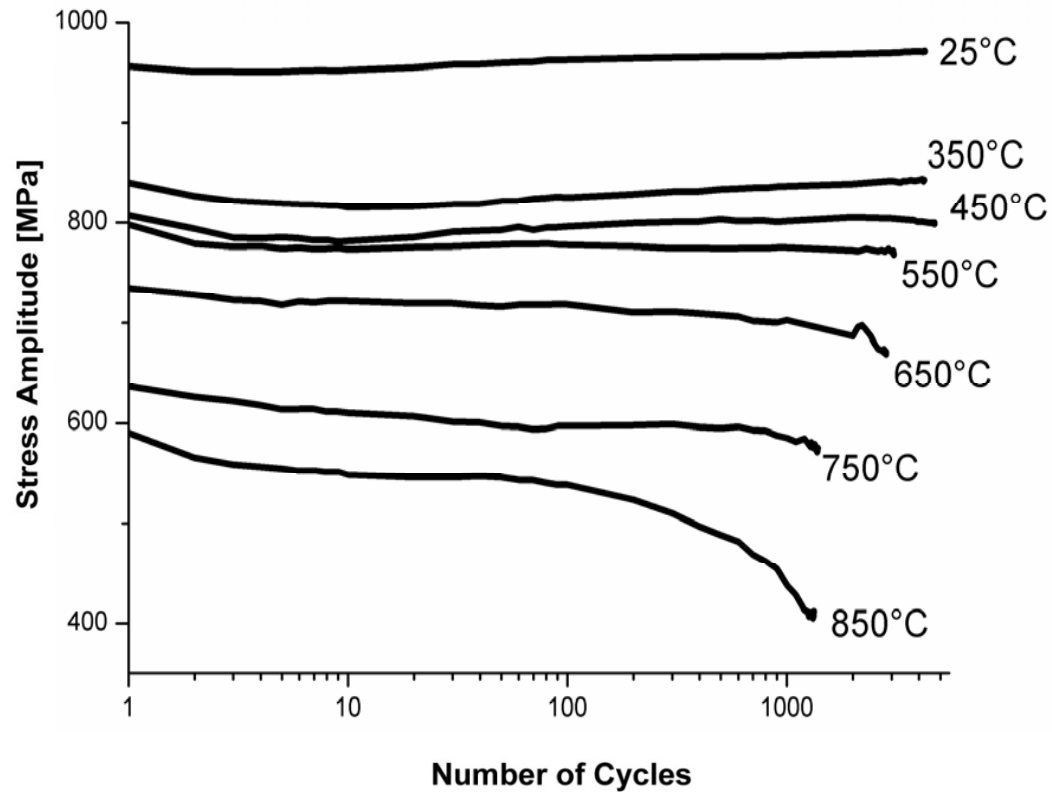
- 3rd Generation of TiAl: TNB-V2:Ti-45Al-8Nb-0,2C (at%), GfE, HZ Geesthacht
- Nearly lamellar microstructure ~ 66 vol.% lamellar colonies,  $\varnothing$  6  $\mu\text{m}$



## Content:

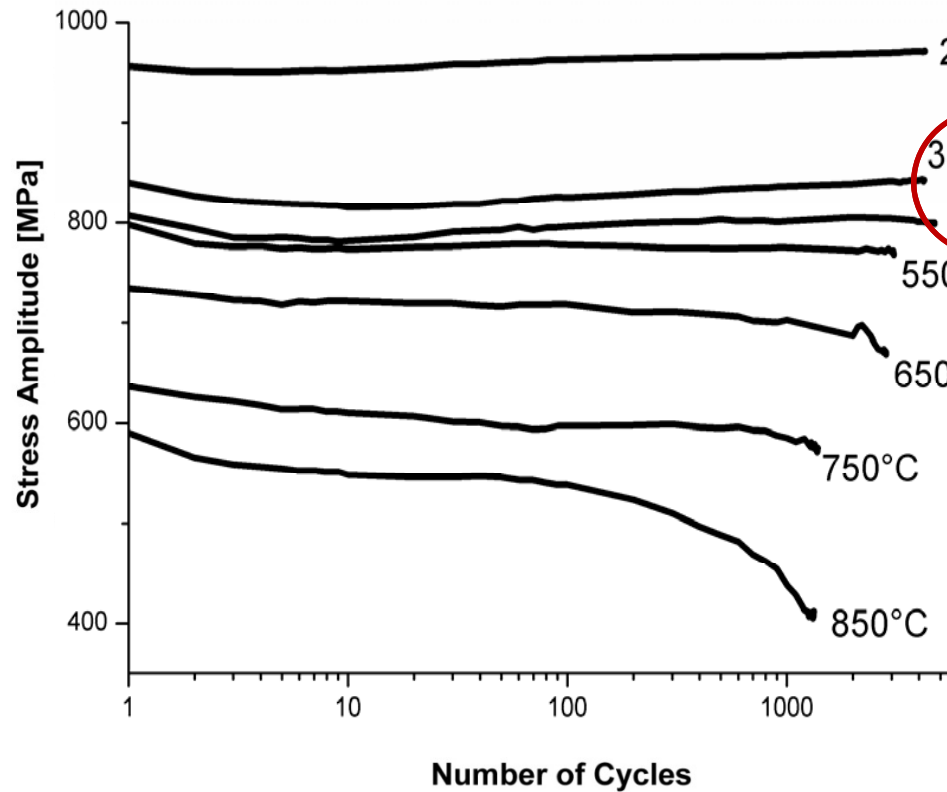
- **Introduction**
  - Background
- **Experimental**
  - Material (TNB-V2), testing system
- **Cyclic Stress-Strain Behaviour / Fatigue Life**
  - LCF and TMF results (at different  $\Delta\varepsilon/2$ , air and vacuum)
  - Microstructural changes
- **Modelling of CSS Behaviour**
- **Fatigue Life Assessment**
- **Conclusions**

Isothermal LCF at  $\Delta\epsilon/2 = 0.6\%$

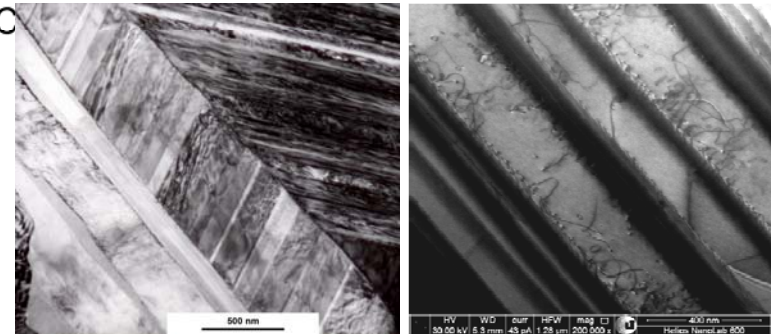


At room temperature:  
 Slight cyclic hardening  
 1. Dislocations lock each other through intersecting → additional glide obstacles  
 2. High lattice friction

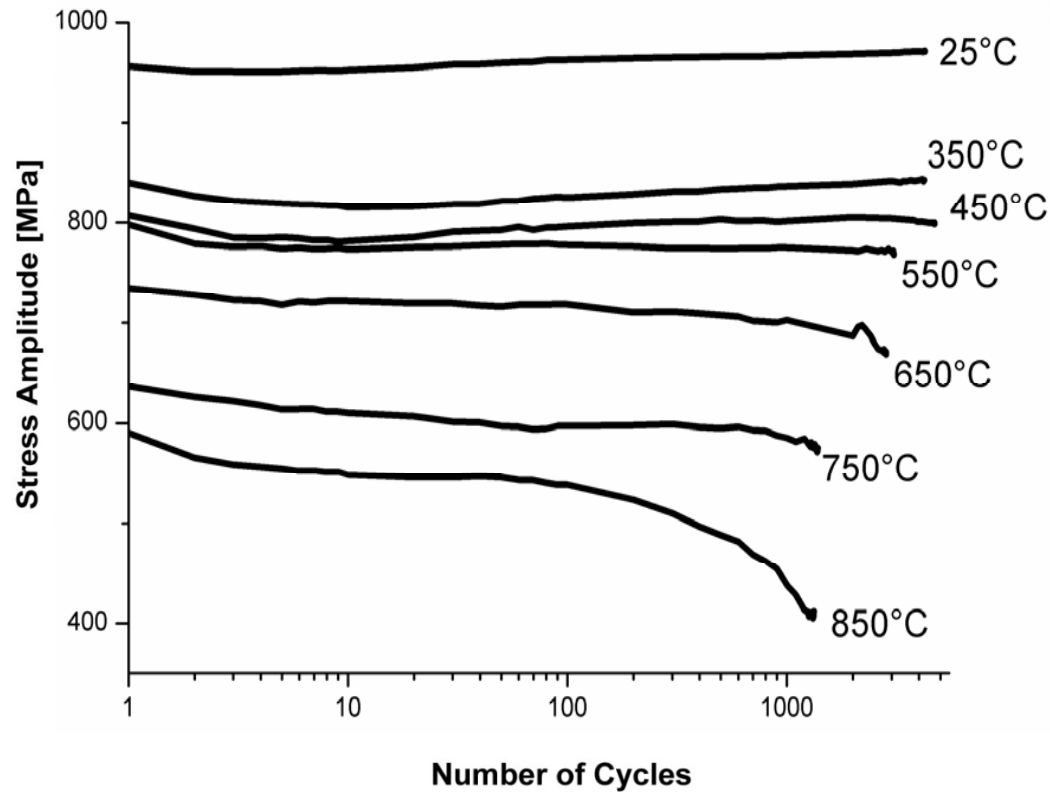
Isothermal LCF at  $\Delta\epsilon/2 = 0.6\%$



At 350 and 450°C  
 Dynamic strain ageing results in hardening, pinning of dislocations by interaction between vacancies and  $Ti_{Al}$  antisite atoms



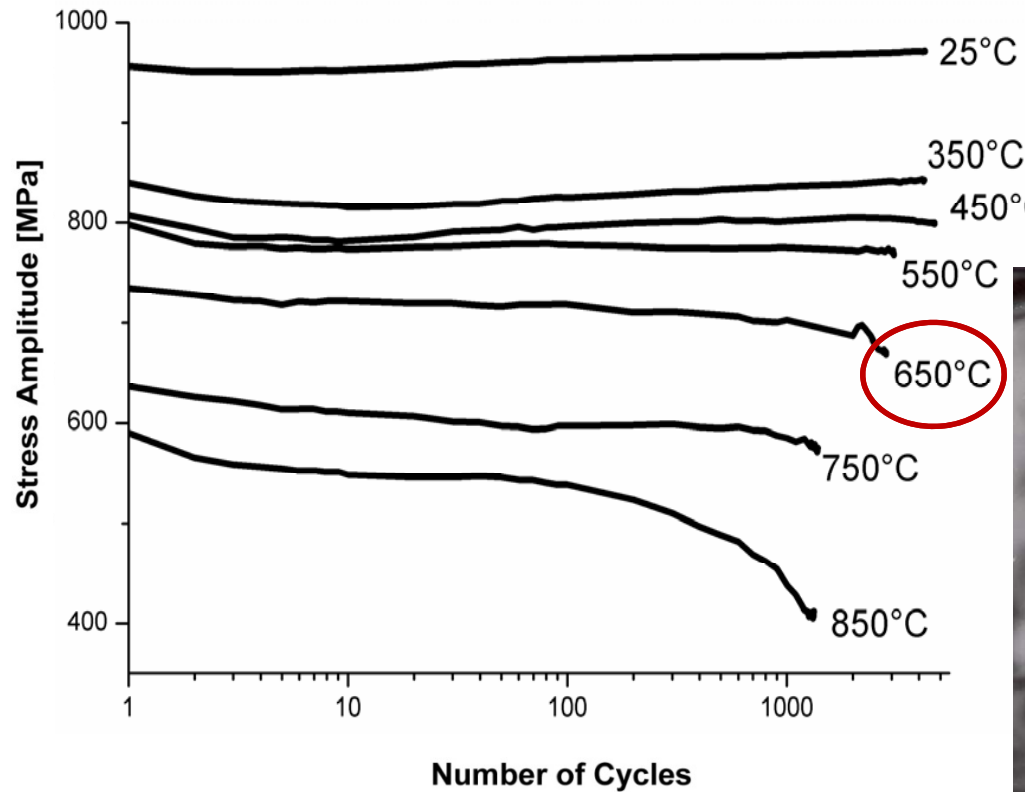
Isothermal LCF at  $\Delta\epsilon/2 = 0.6\%$



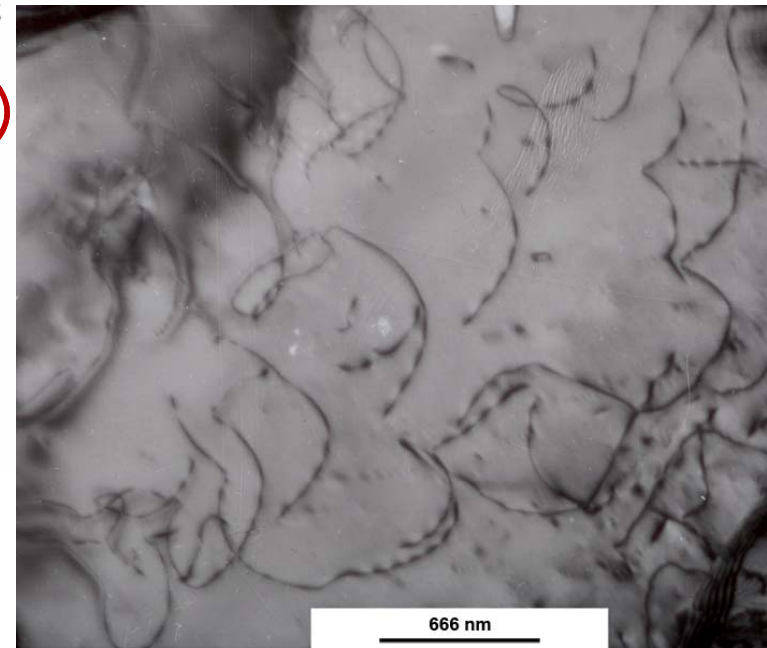
At 550°C:  
 Saturated stress response until failure



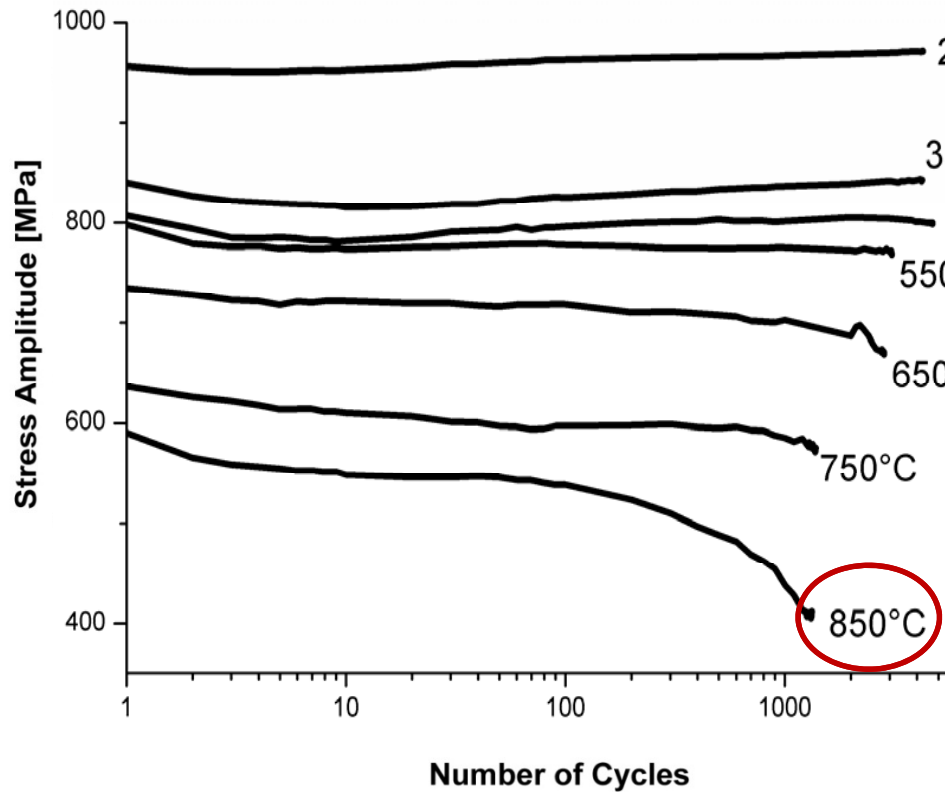
Isothermal LCF at  $\Delta\epsilon/2 = 0.6\%$



At high temperatures 650-850°C  
 Cyclic softening  
 Most evident above DBTT



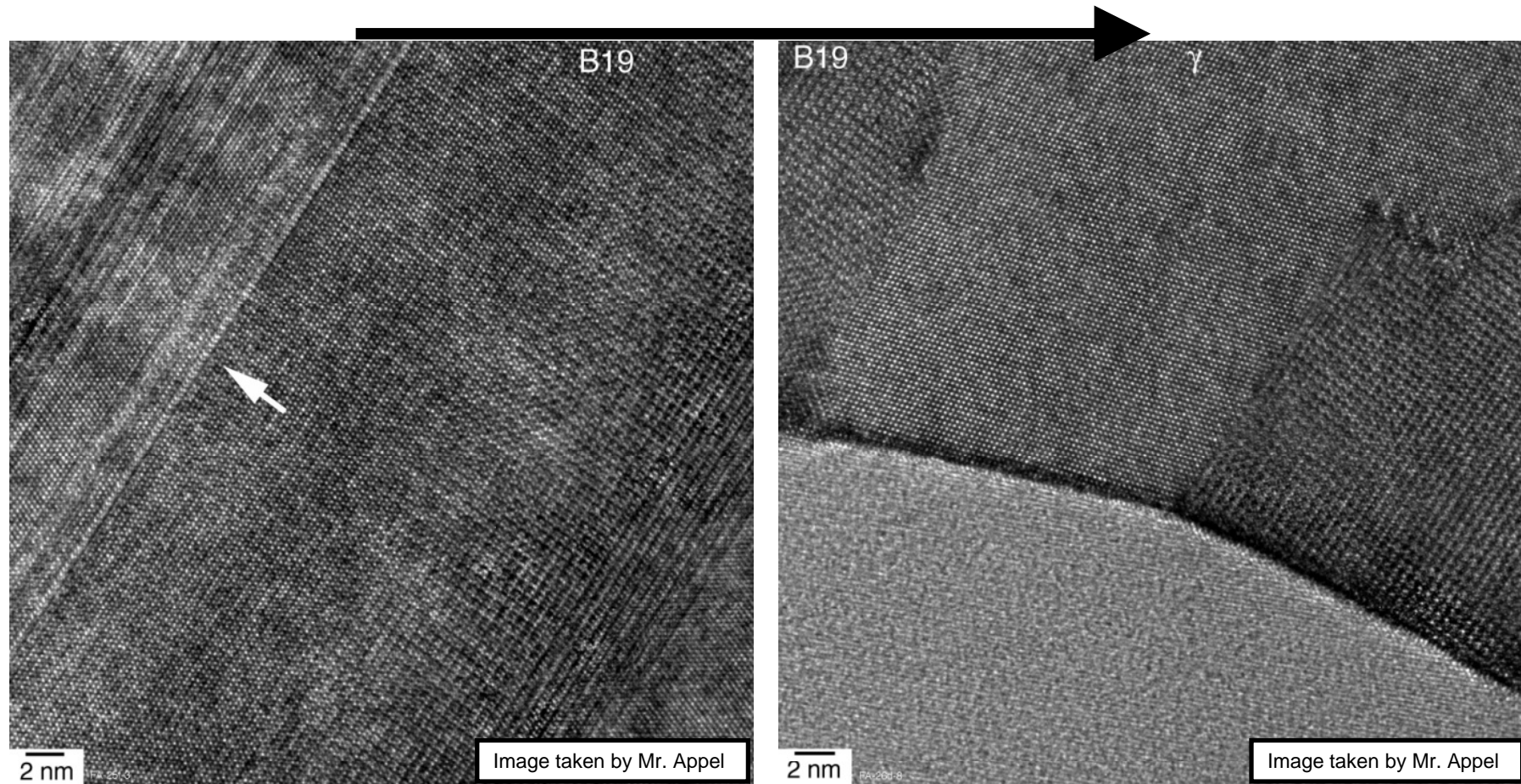
Isothermal LCF at  $\Delta\epsilon/2 = 0.6\%$



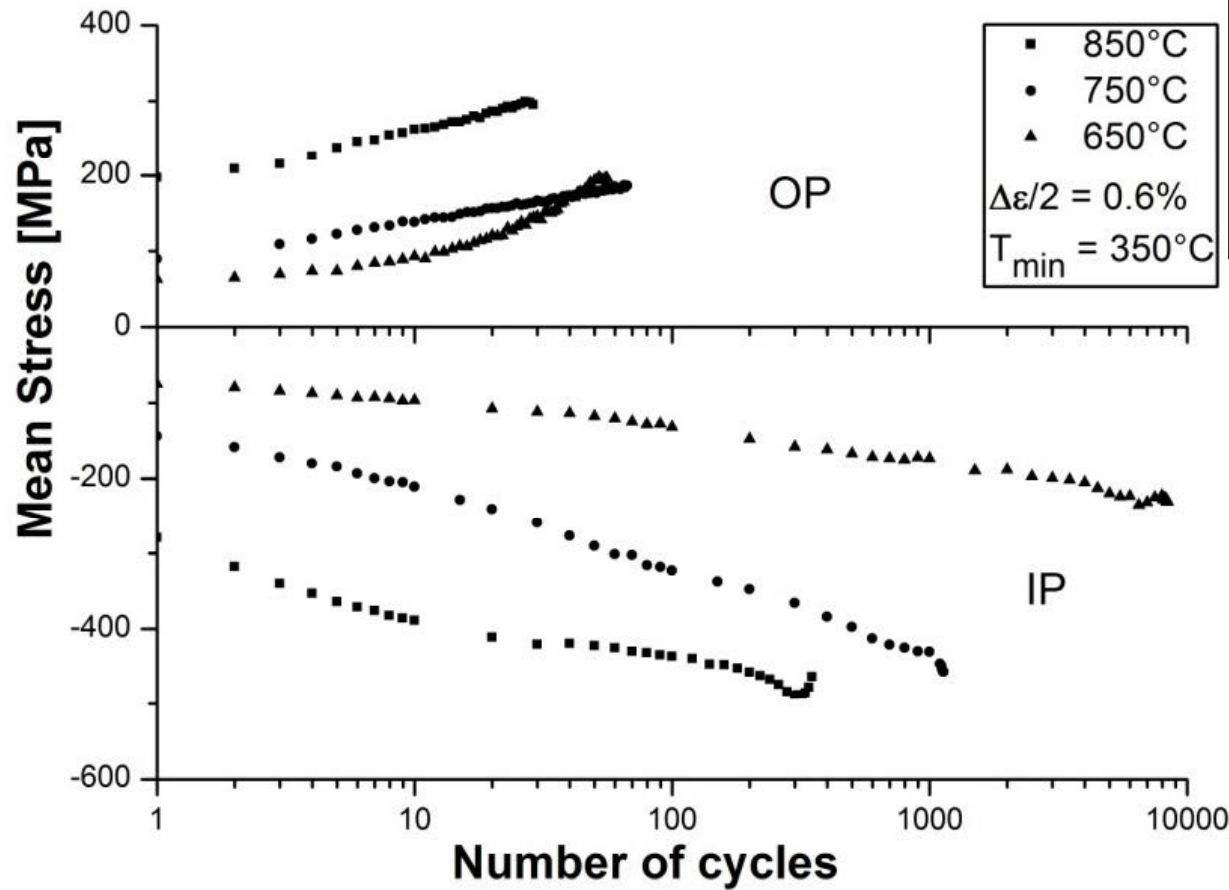
At high temperatures 650-850°C  
 Cyclic softening  
 Most evident above DBTT



Transformation of B19 phase into  $\gamma$  phase during fatigue

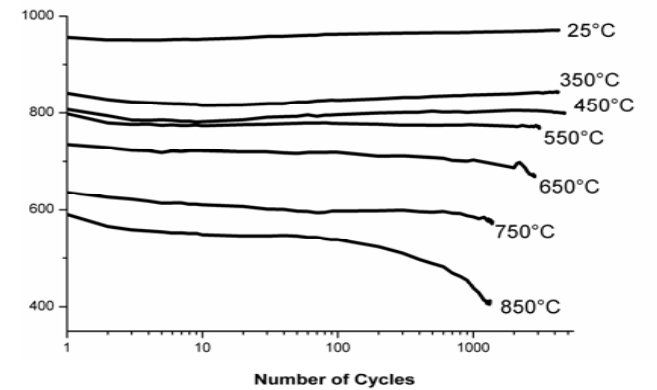


TMF-Results

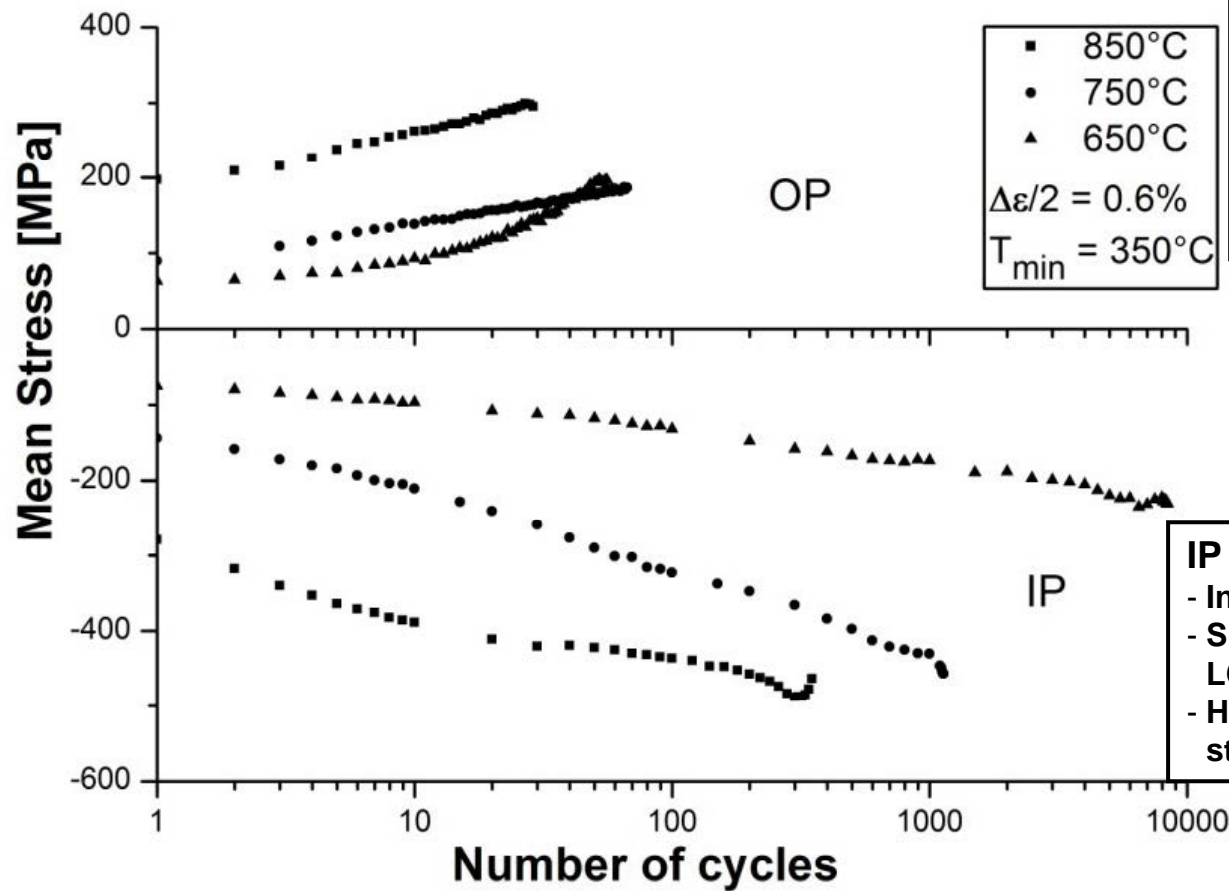


**OP**

- Increasing tensile mean stress
- Low fatigue lives under OP loading
- Formation of oxide scale in the compression part leads to early crack initiation in tension (low temperature).



TMF-Results



**OP**

- Increasing tensile mean stress
- Low fatigue lives under OP loading
- Formation of oxide scale in the compression part leads to early crack initiation in tension (low temperature).

**IP**

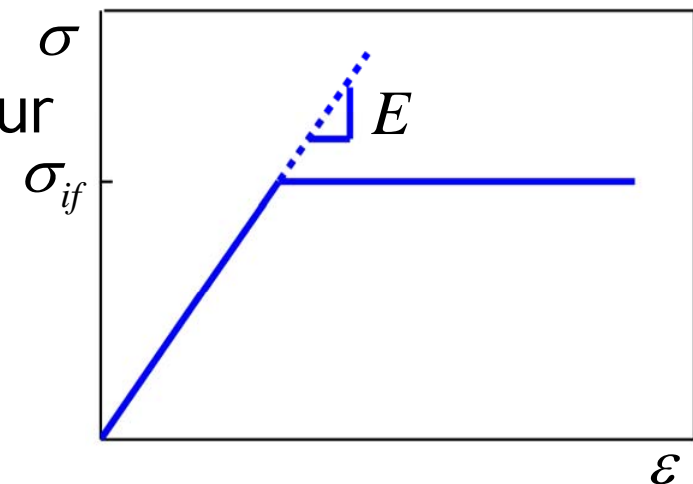
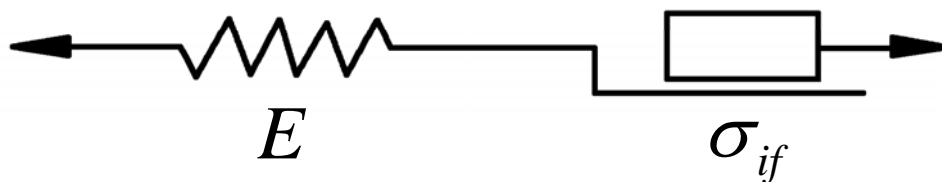
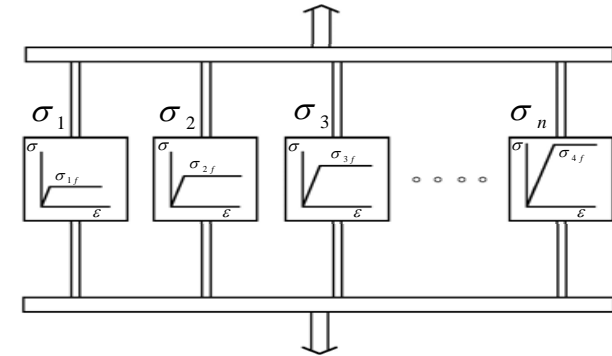
- Increasing compressive mean stress
- Similar fatigue life as under isothermal LCF-loading
- High  $\Delta T$  leads to high compressive mean stresses, but reduces the fatigue life.

## Content:

- **Introduction**
  - Background
- **Experimental**
  - Material (TNB-V2), testing system
- **Cyclic Stress-Strain Behaviour / Fatigue Life**
  - LCF and TMF results (at different  $\Delta\varepsilon/2$ , air and vacuum)
  - Microstructural changes
- **Modelling of CSS Behaviour**
- **Fatigue Life Assessment**
- **Conclusions**

## The Masing Model Assumptions

- Materials consists of elementary volumes in parallel arrangement.
- Each element has an element-specific strength (microscopic flow stress).
- Identical Young's Modulus for all elements
- Isotropic material
- Linear elastic ideal-plastic behaviour of each element



## Simplified Statistical Theory

Probability density function of elementary flow stresses:  $f_p(\sigma_{if})$

$f_p(\sigma_{if}) d\sigma_{if}$  is the area fraction of elements of yield stress between  $\sigma_{if}^*$  and  $\sigma_{if}^* + d\sigma_{if}$

Using the second integral functions

$$G_p(x) = \int_0^x \int_0^x f_p(x') dx'$$

$$\sigma_r = E \varepsilon_r - 2G_p \left( \frac{E \varepsilon_r}{2} \right)$$

with relative stress/strain coordinates (related to the last load reversal).

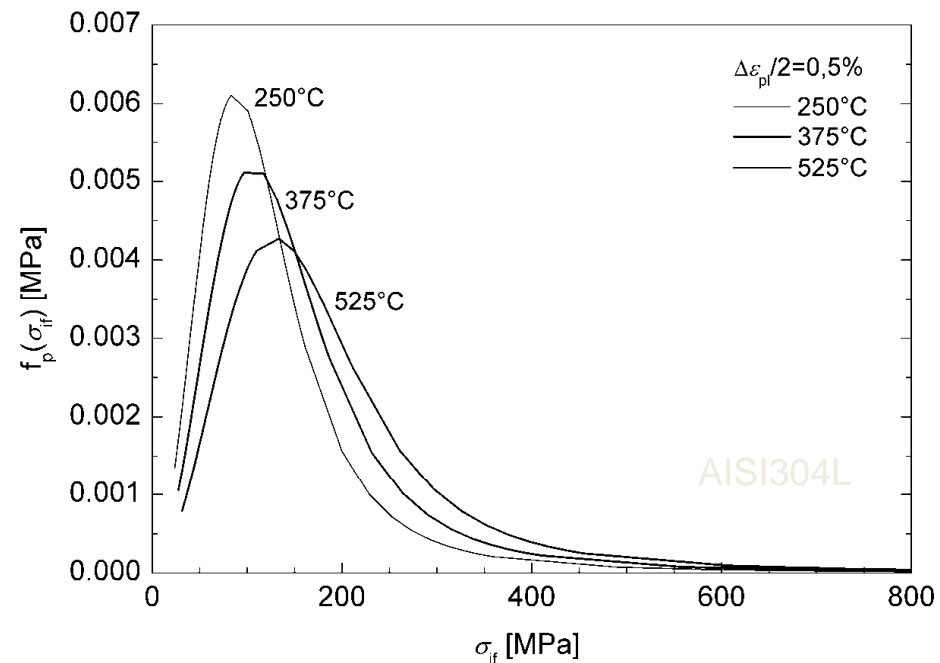
Conversely, the distribution density function of the microscopic yield stresses can directly be obtained from a double differentiation of a single branch of a hysteresis loop:

$$f_p \left( \frac{E \varepsilon_r}{2} \right) = - \frac{2}{E^2} \frac{d^2 \sigma_r}{d\varepsilon_r^2}$$



## Procedure for Pseudoisothermal TMF calculation

- ◆ The yield stress distribution function is determined from isothermal fatigue tests (at various temperatures).



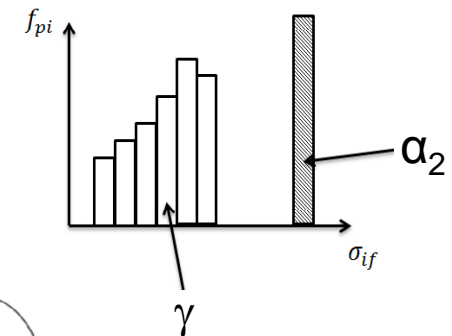
## Procedure for Pseudoisothermal TMF calculation

- ◆ The yield stress distribution function is determined from isothermal fatigue tests (at various temperatures).
- ◆ The distribution function is interpolated regarding the temperature.
- ◆ The distribution function is transformed into a discrete distribution (e.g. 30 elements).
- ◆  $T(t)$  and  $\varepsilon(t)$  is defined.
- ◆ The stress-strain relationship is stepwise calculated by
  - changing strain and temperature in each element
  - calculating the total stress from the stresses acting in each element

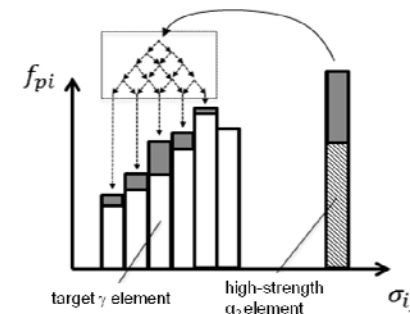
## Expansion of the CSS model with respect to TNB-V2

- Nonlinearity of elastic deformation  $\sigma = E_o \varepsilon_{el} + k_{el} \varepsilon_{el}^2$
- Creep/Stress Relaxation  $\dot{\varepsilon}_{creep}(\sigma, T) = C \cdot \sigma^n \cdot e^{-\frac{Q_{eff}}{RT}}$

- Extrapolation of yield stress distribution function  $f_p(\sigma_{if})$

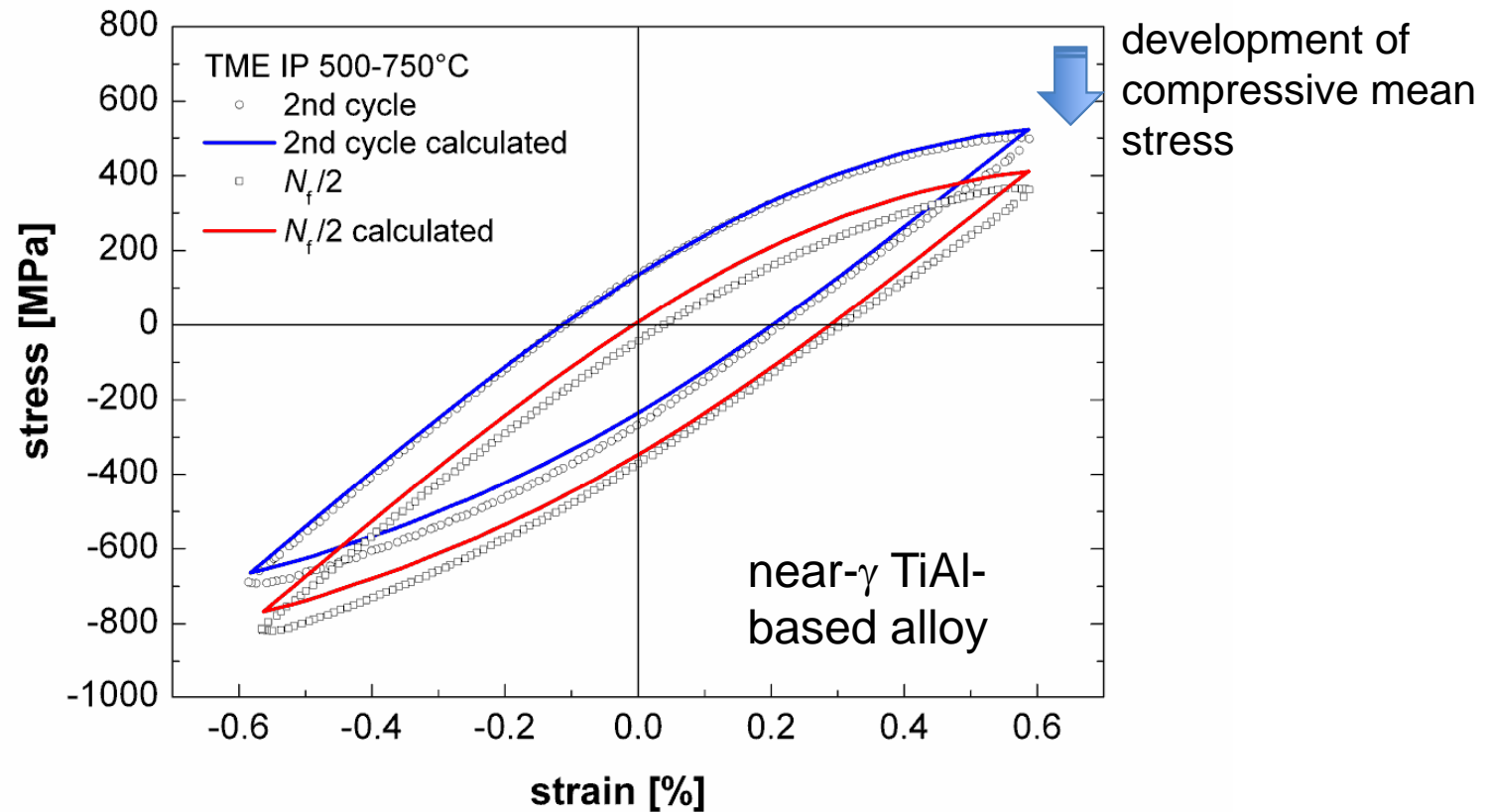


- Incorporation of strengthening and hardening effects



- Microstructural instability at  $T > 800^\circ\text{C}$   
 (dissolution of lamellar microstructure)

## Modelling of the TMF hysteresis loop



## Content:

- **Introduction**
  - Background
- **Experimental**
  - Material (TNB-V2), testing system
- **Cyclic Stress-Strain Behaviour / Fatigue Life**
  - LCF and TMF results (at different  $\Delta\varepsilon/2$ , air and vacuum)
  - Microstructural changes
- **Modelling of CSS Behaviour**
- **Fatigue Life Assessment**
- **Conclusions**

## Idea for a life prediction model

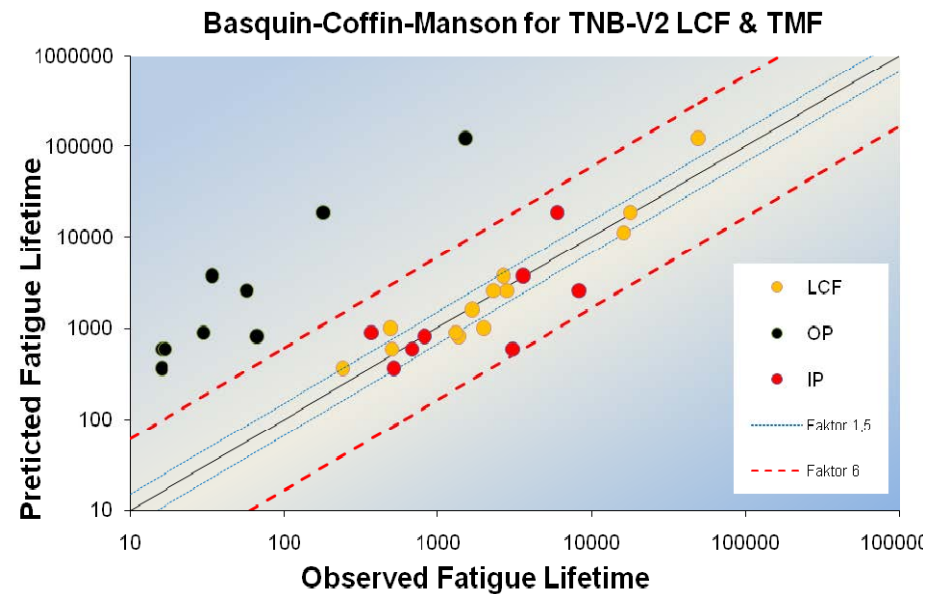
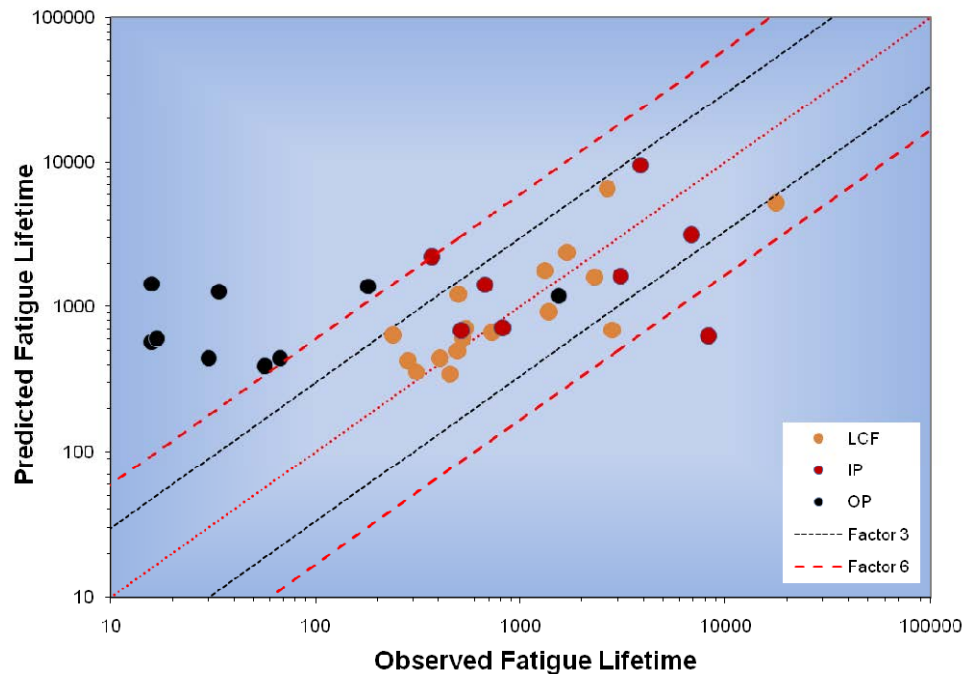
### Max. stress as a damage parameter

$$P_{SWT} = \sqrt{\sigma_{\max} \cdot \frac{\Delta \varepsilon_{\text{mech}}}{2} \cdot E}$$

PSWT for TNB-V2 LCF & TMF

### Strain as a damage parameter

$$\frac{\Delta \varepsilon}{2} = \frac{\Delta \varepsilon_{el}}{2} + \frac{\Delta \varepsilon_{pl}}{2} = \frac{\sigma_f'}{E} (2N_f)^{-b} + \varepsilon_f' (2N_f)^{-c}$$



Idea for a life prediction model

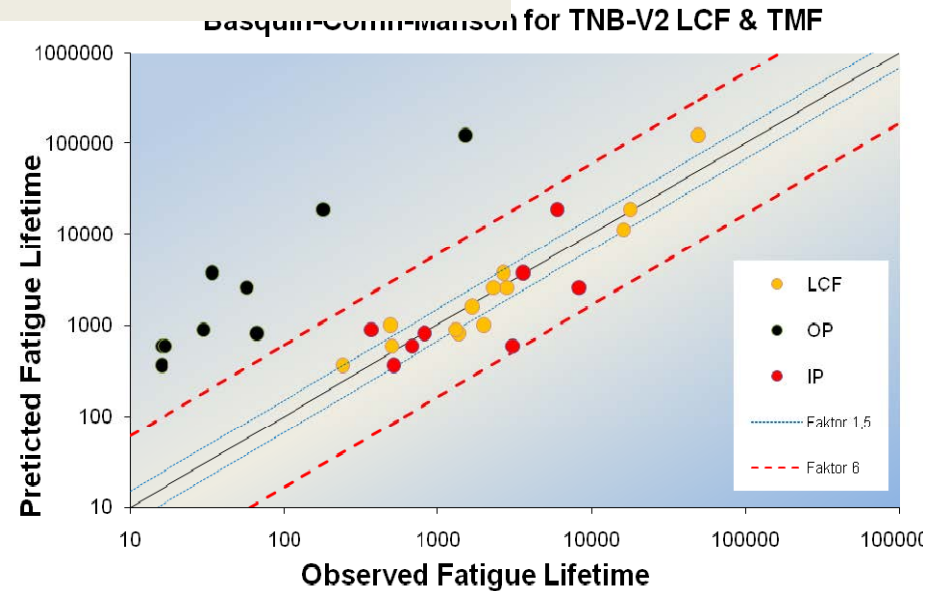
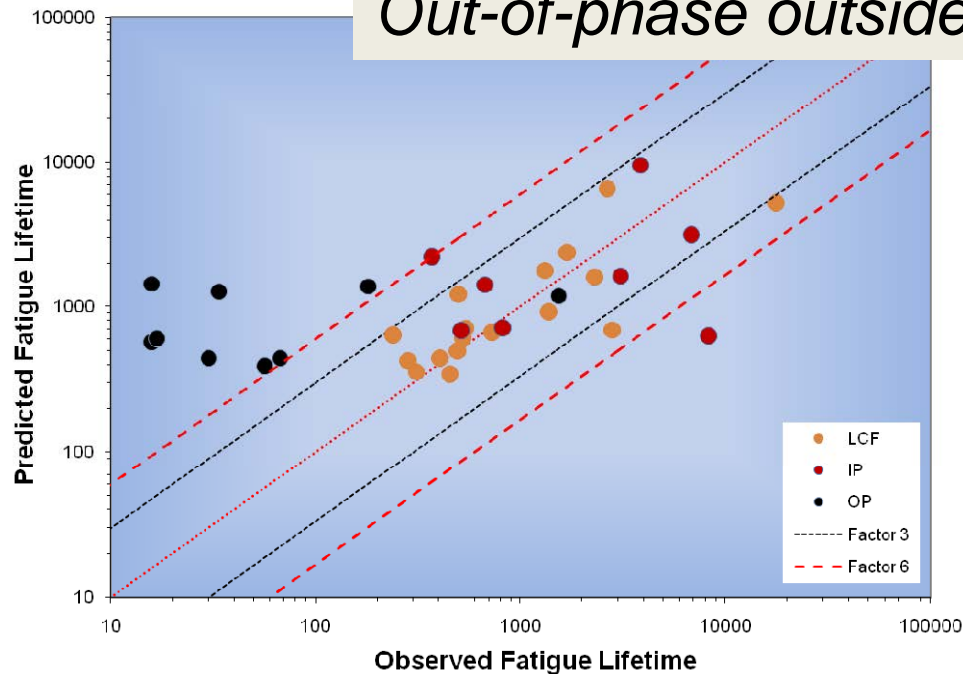
Max. stress as a damage parameter

$$P_{SWT} = \sqrt{\sigma_{\max} \cdot \frac{\Delta \varepsilon_{mech} \cdot E}{2}}$$

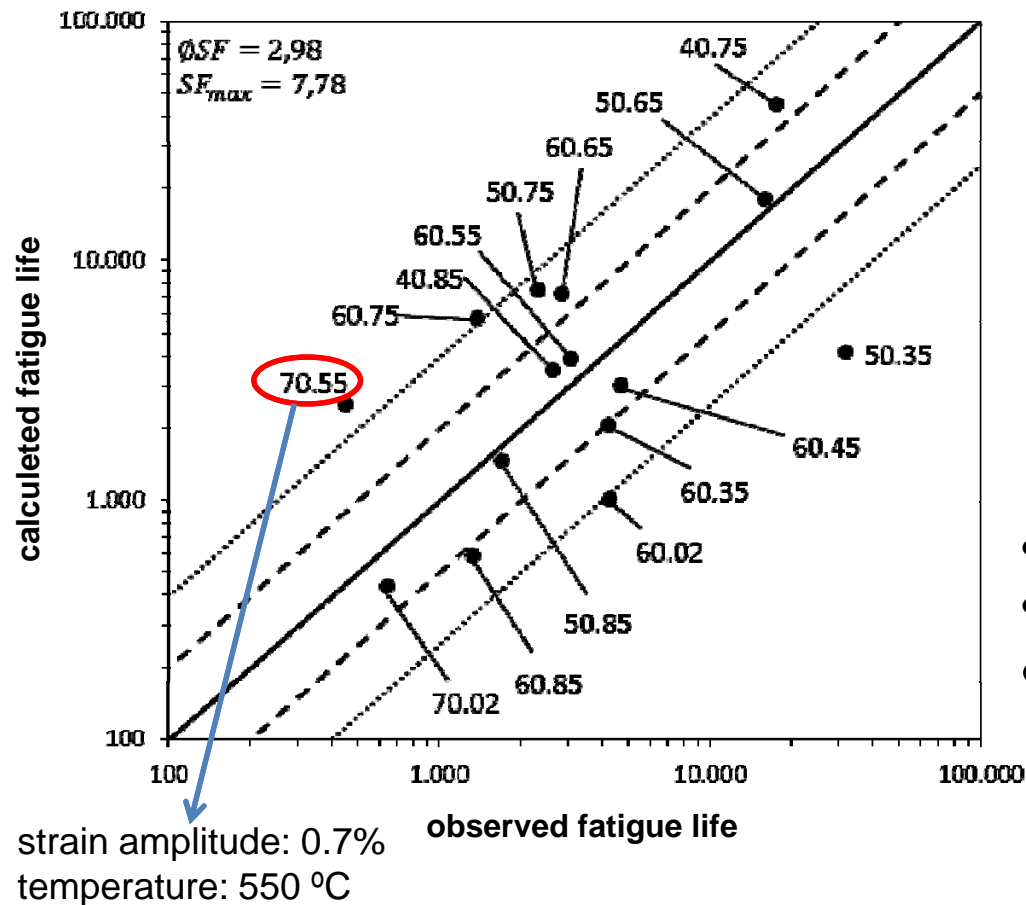
Strain as a damage parameter

$$\frac{\Delta \varepsilon}{2} = \frac{\Delta \varepsilon_{el}}{2} + \frac{\Delta \varepsilon_{pl}}{2} = \frac{\sigma_f'}{E} (2N_f)^{-b} + \varepsilon_f' (2N_f)^{-c}$$

PSWT for TNB-V2 LCF & TMF  
*Out-of-phase outside the scatter band*



## Model of Buchholz (Diss. Dresden, 2012) developed for a Ni-base alloy



$$P = w \left( \frac{\sigma_{tlrp}}{R_m(T_{tlrp})} \right)^x + y \left( \frac{\sigma_{clrp}}{R_m(T_{clrp})} \right)^z$$

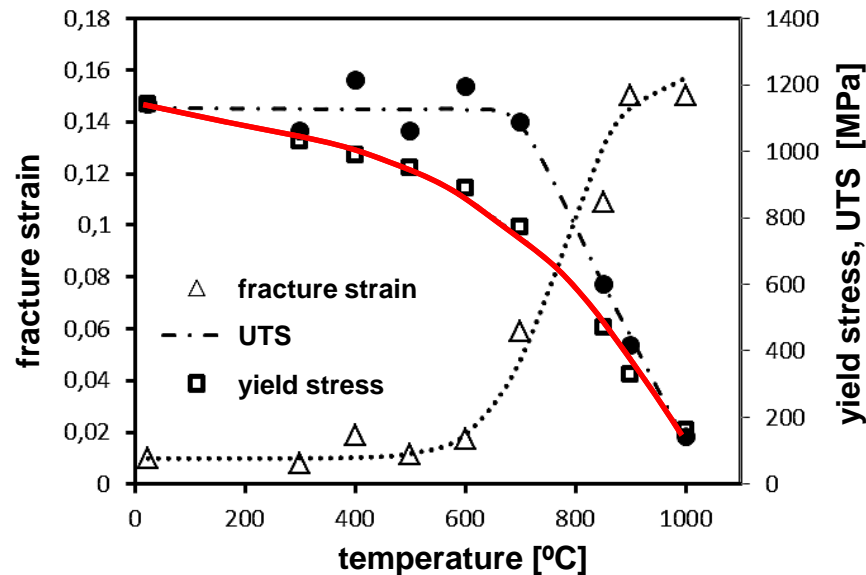
tlrp: tensile load reversal point  
 clrp: compression load reversal point

$$P = \frac{C}{1 + \left( \frac{N_f}{D} \right)^E} + F$$

- 8 fitting parameters (w,x,y,z,C,D,E,F)
- suitable for isothermal life data
- **non suitable for TMF life**



## Modified Buchholz Model



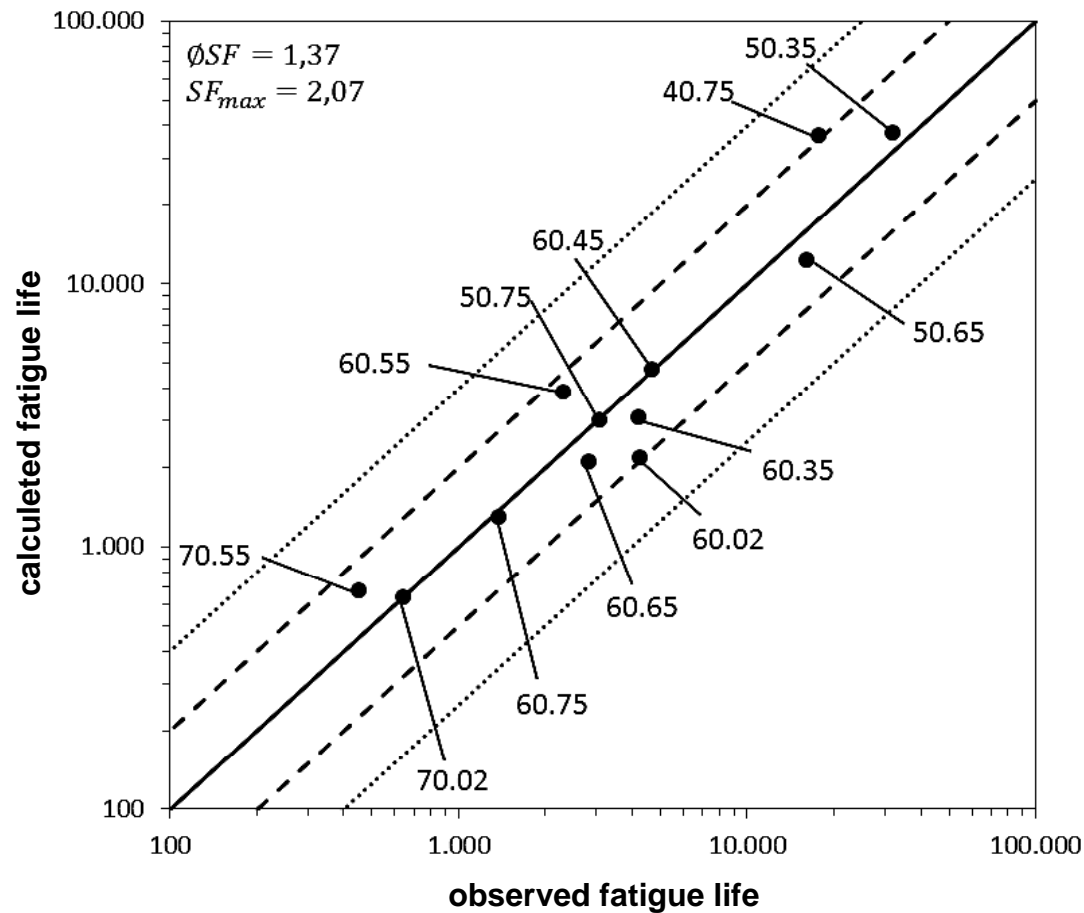
TNB-V2: Yield stress represents the effect of temperature better than UTS!

$$P = \frac{1}{2} \left( \frac{\sigma_{tlrp}}{R_{p0.2}(T_{tlrp})} + \frac{\sigma_{clrp}}{R_{p0.2}(T_{clrp})} \right) + \left( \frac{\sigma_m}{R_{p0.2}(T_m)} \right)^\alpha$$

$$P = A \cdot N_f^b$$

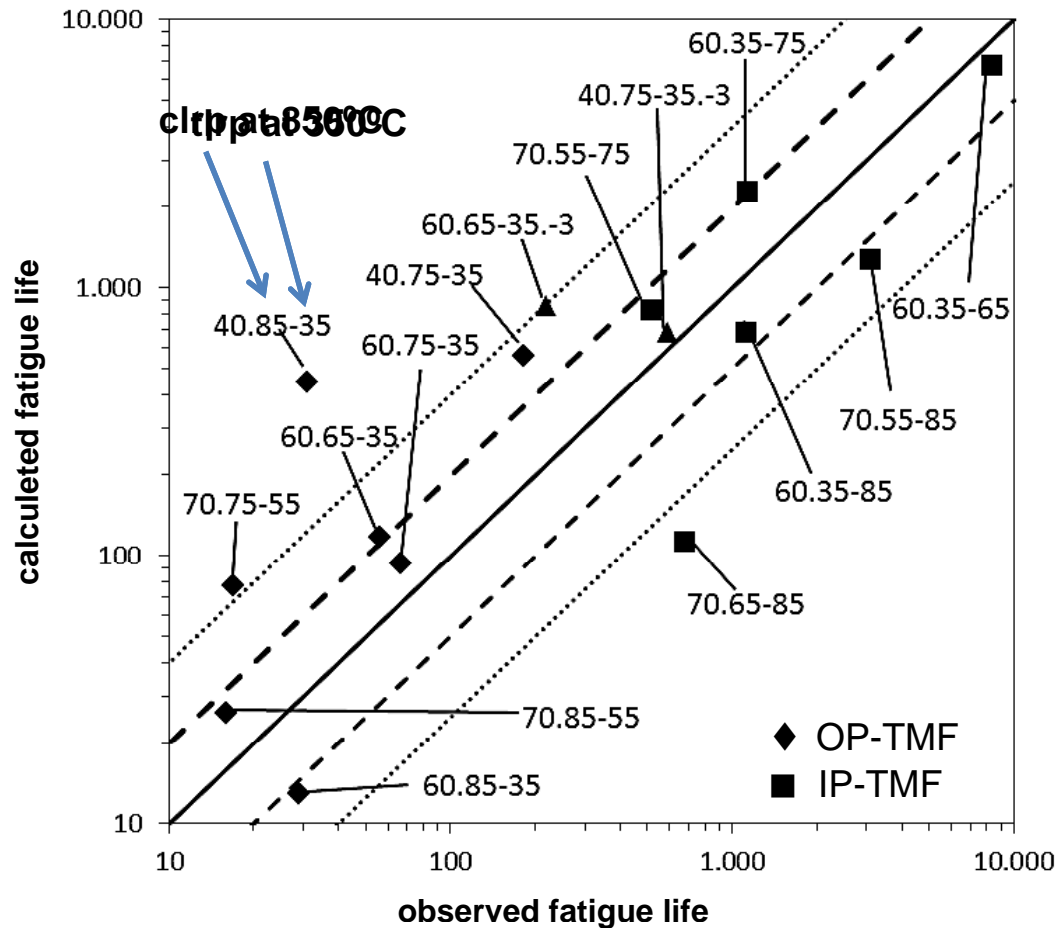
tlrp: tensile load reversal point  
 clrp: compression load reversal point

## Modified Buchholz Model: Isothermal Data



Excellent predictive capability!

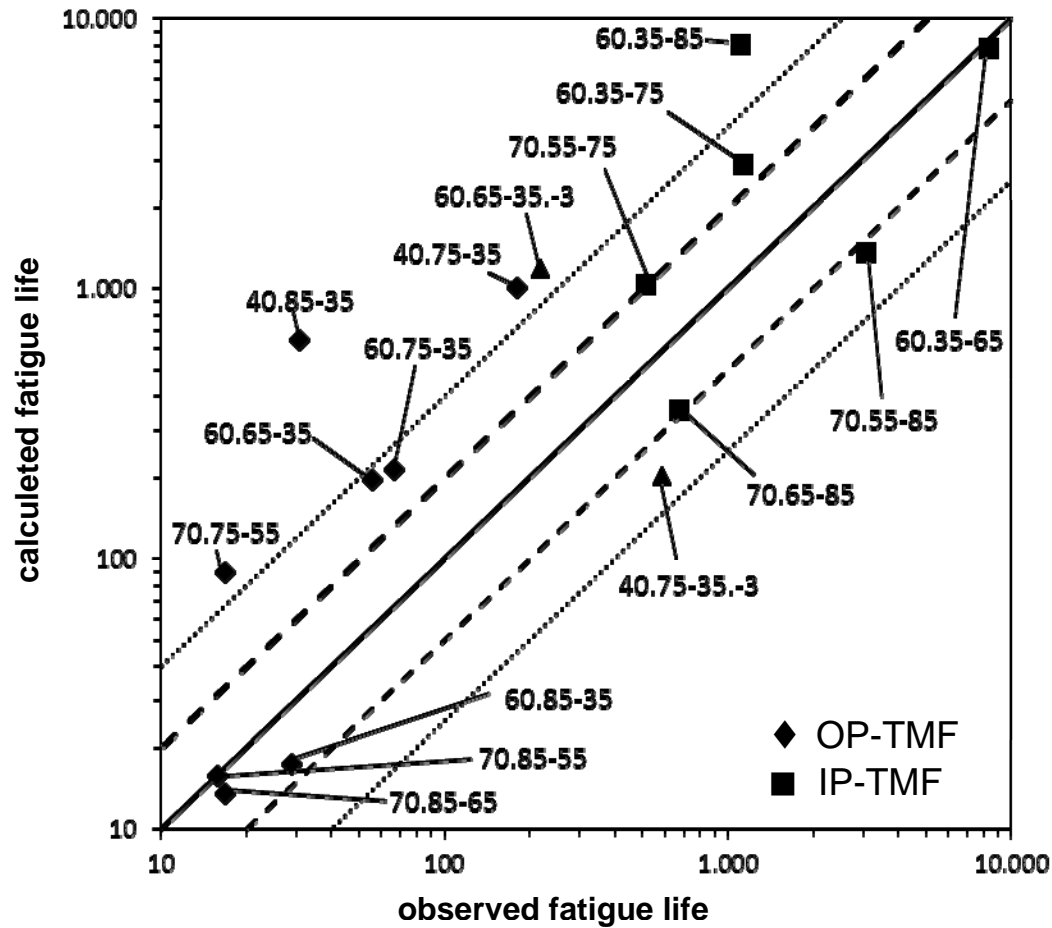
## Modified Buchholz Model: TMF Data



- Mean stress exponent  $\alpha$  was determined by TMF test at  $R_\varepsilon = -3$ .
- Linear damage accumulation was applied.
- Reversal points were taken from the test data.

Reasonable predictive capability!

## Modified Buchholz Model: Calculated TMF CSS



Cyclic stress-strain behaviour was calculated on the basis of the advanced multicomposite model.

Predictive capability is still o.k.!

## Content:

- **Introduction**
  - Background
- **Experimental**
  - Material (TNB-V2), testing system
- **Cyclic Stress-Strain Behaviour / Fatigue Life**
  - LCF and TMF results (at different  $\Delta\varepsilon/2$ , air and vacuum)
  - Microstructural changes
- **Modelling of CSS Behaviour**
- **Fatigue Life Assessment**
- **Conclusions**

- Isothermal fatigue of TiAl-based alloy TNB-V2:
  - Slight cyclic hardening at low temperatures
  - Cyclic softening at high temperature
  - Microstructural instability above 800°C
- TMF behaviour:
  - IP: development of negative mean stress
  - OP: development of positiv mean stress
  - Tremendously low TMF life under OP conditions
- Modelling:
  - CSS behaviour can be reproduced by means of a composite model (based on the statistical theory of the model of Masing)
  - A new model was developed which allows for the prediction of TMF lives (IP **and** OP) from isothermal data.



---

# Thank you for your attention!

Financial support by  
Deutsche Forschungsgemeinschaft  
is gratefully acknowledged.

---

# CHARACTERIZATION OF DAMAGE MECHANISMS OF NICKEL-BASE ALLOY MAR-M247 CC (HIP) UNDER THERMOMECHANICAL CREEP-FATIGUE LOADING USING DIGITAL IMAGE PROCESSING

---

Stefan Eckmann, Christoph Schweizer

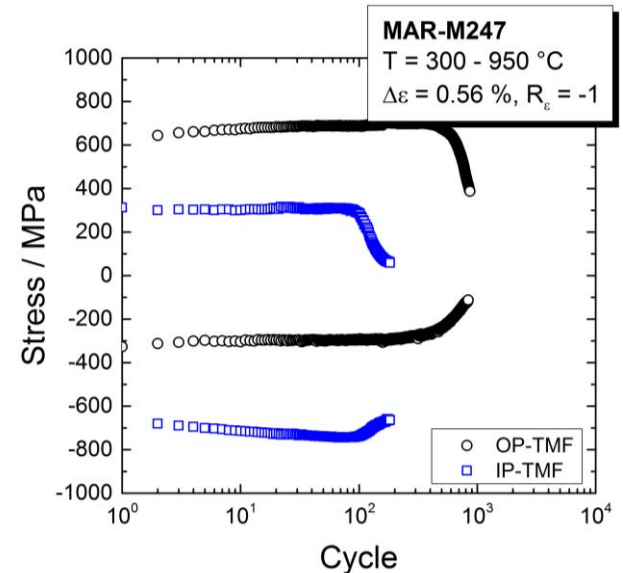
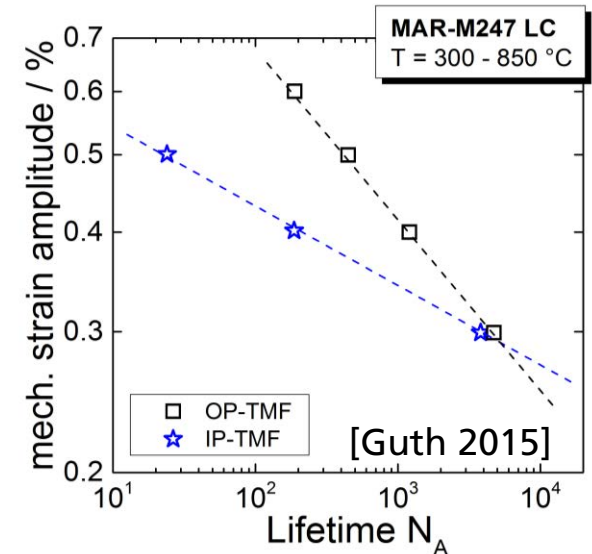
Fraunhofer Institute of Mechanics of Materials IWM, Freiburg, Germany

3<sup>rd</sup> TMF-Workshop, Berlin, 27<sup>th</sup> - 29<sup>th</sup> April 2016



# Motivation

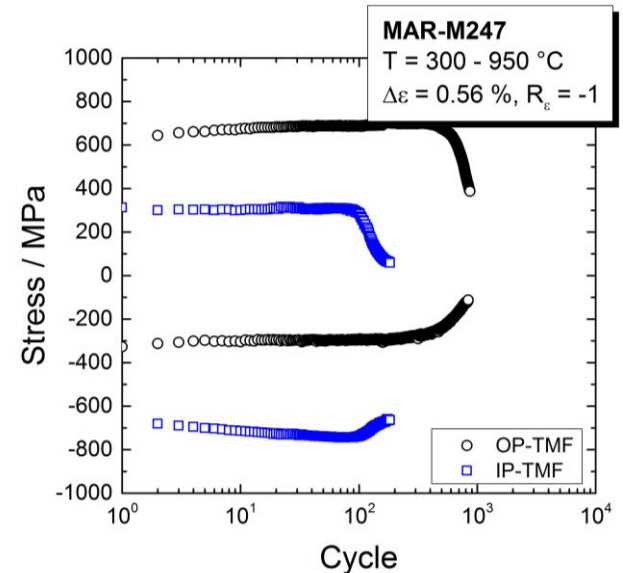
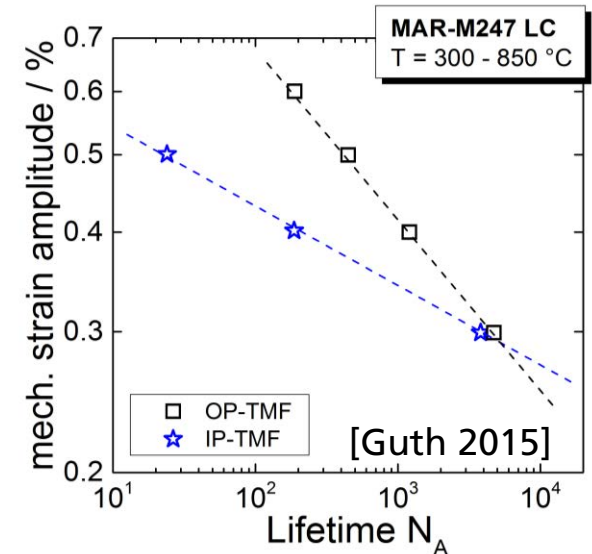
- Comprehensive database for thermo-mechanical fatigue (TMF) for nickel-base alloys available
- TMF lifetime is strongly influenced by phase angle (IP, OP) and time dependent effects



# Motivation

- Comprehensive database for thermo-mechanical fatigue (TMF) for nickel-base alloys available
- TMF lifetime is strongly influenced by phase angle (IP, OP) and time dependent effects

→ Investigation of influences of phase angle and time dependent effects on damage mechanisms and fatigue crack growth rate



---

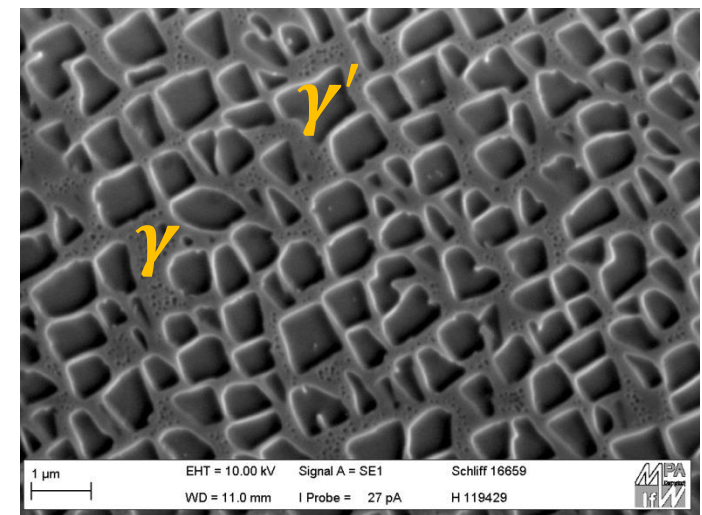
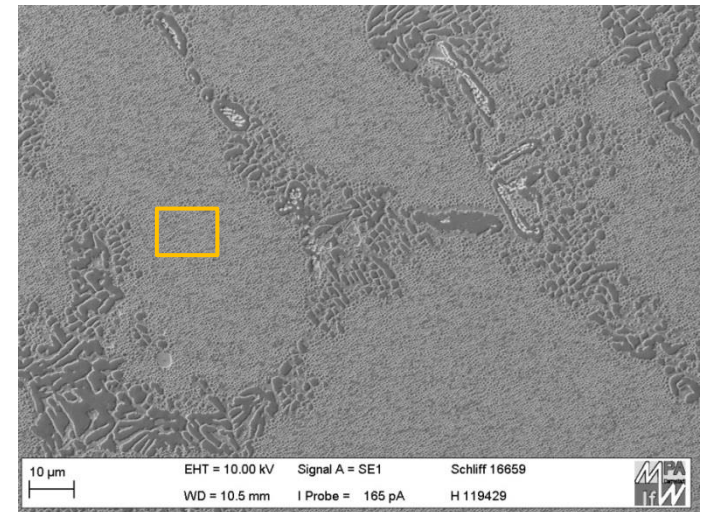
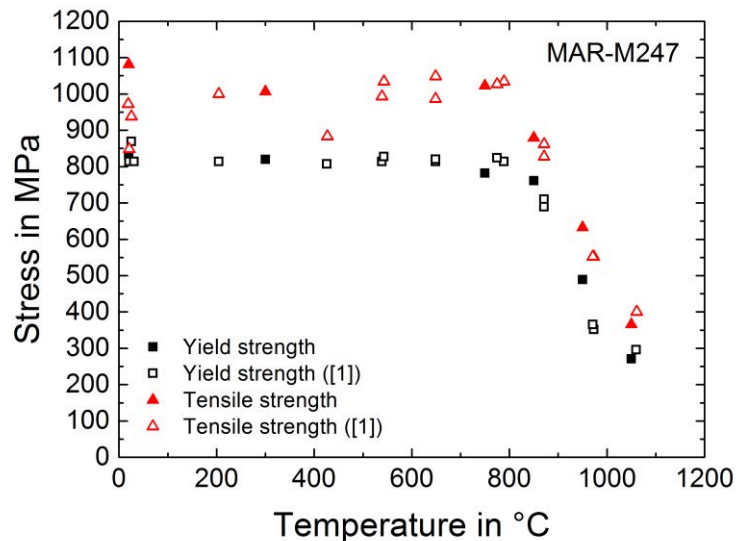
# OUTLINE

---

- Investigated material
- Nonisothermal crack growth measurements
  - Influence of phase angle and load ratio
  - Influence of time dependent effects
- Outlook – Digital image processing

# Investigated material

- Nickel-base superalloy MAR-M247 CC (HIP)
- Elements: 60-70% Ni, Cr, Co, Al, Ti
- High strength at wide temperature range (> 1000 °C) due to  $\gamma'$ -precipitates within  $\gamma$ -Matrix)

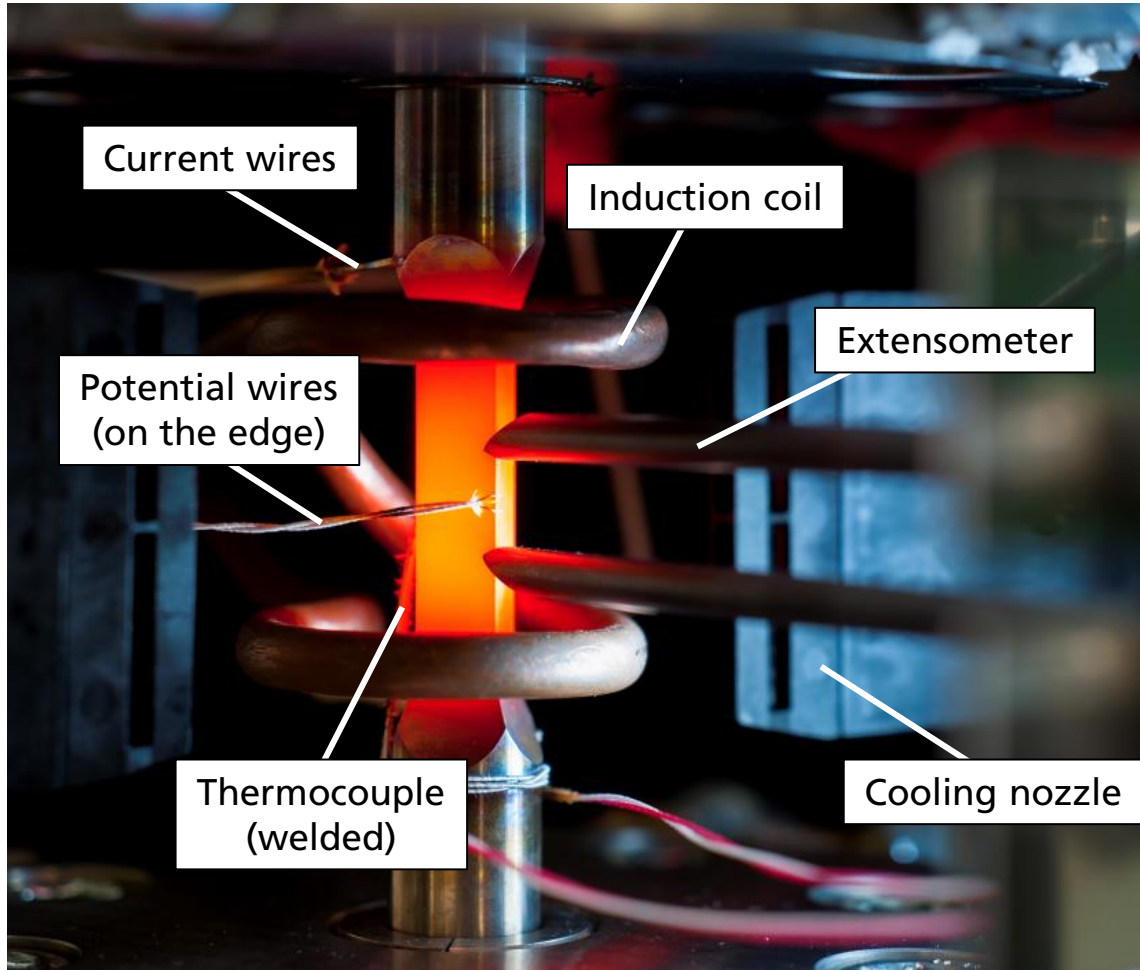


Microstructure MAR-M247 [Oechsner 2011]

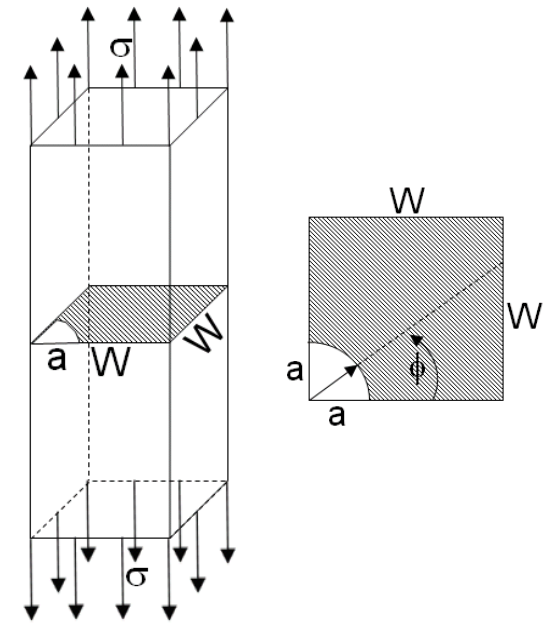
# **NONISOTHERMAL FATIGUE CRACK GROWTH TESTS**

# Nonisothermal fatigue crack growth tests

## Experimental setup



### Corner-Crack Specimen



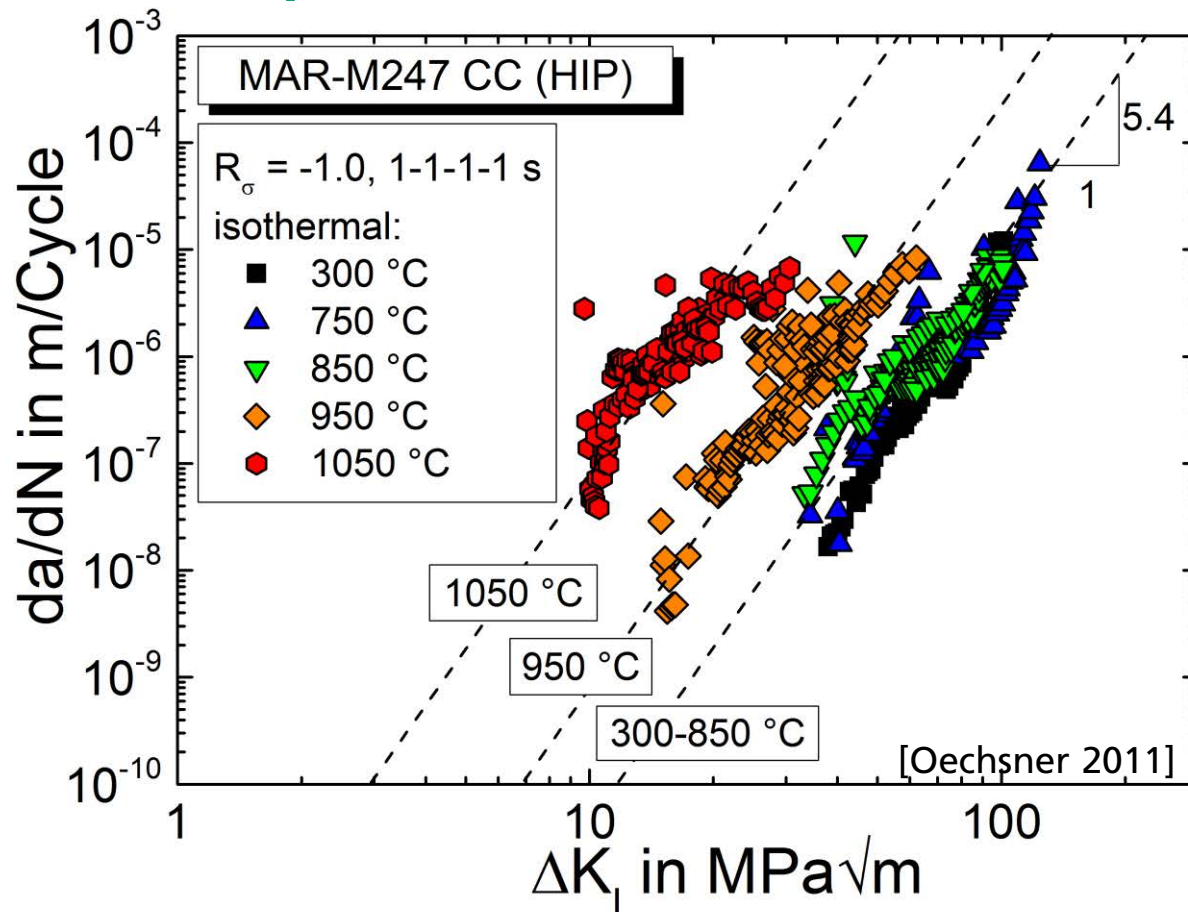
$$W = 8 \text{ mm}$$

$$a_0 = 1.0 \dots 2.5 \text{ mm}$$

© Fraunhofer IWM, Photo by A. Käflein

# Isothermal fatigue crack growth tests

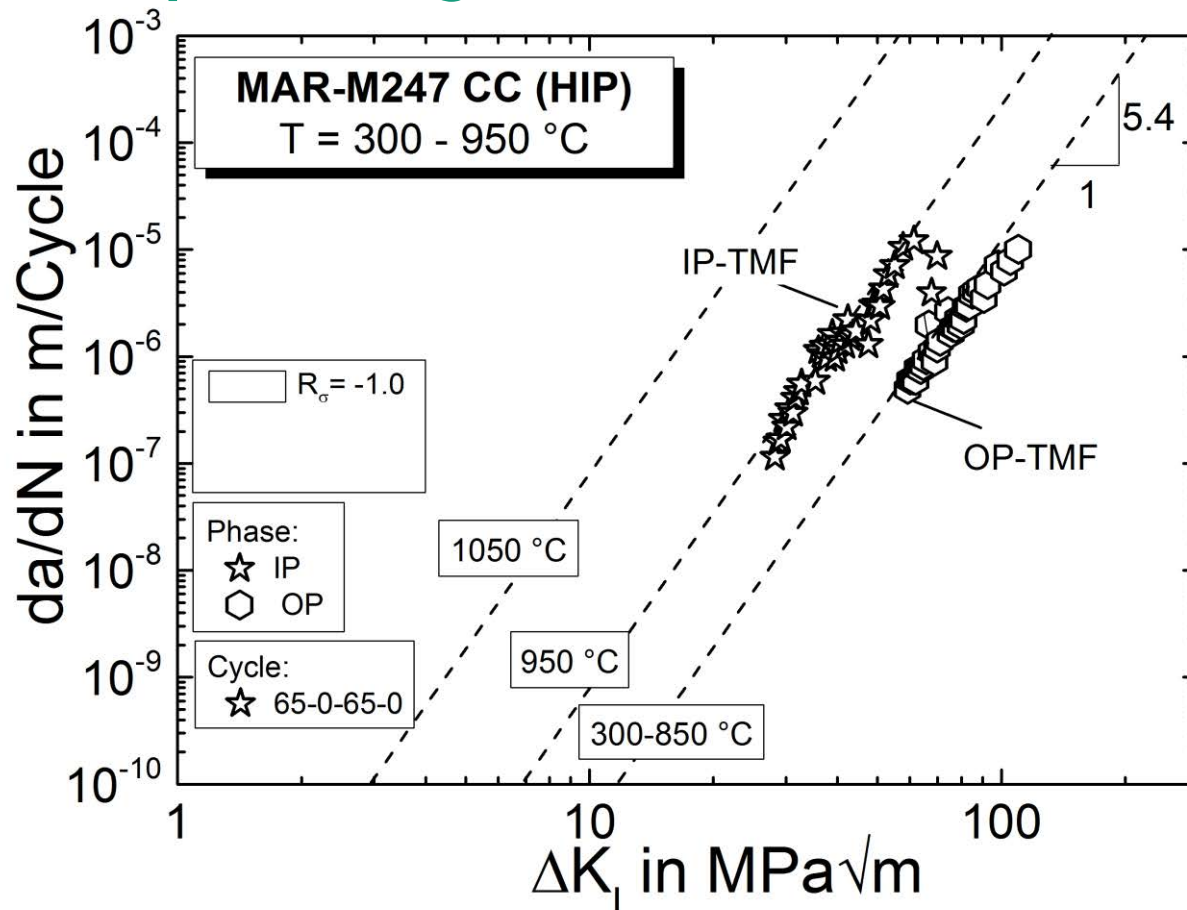
## Influence of temperature



- Strong temperature dependency of fatigue crack growth rate

# Nonisothermal fatigue crack growth tests

## Influence of phase angle: OP ↔ IP

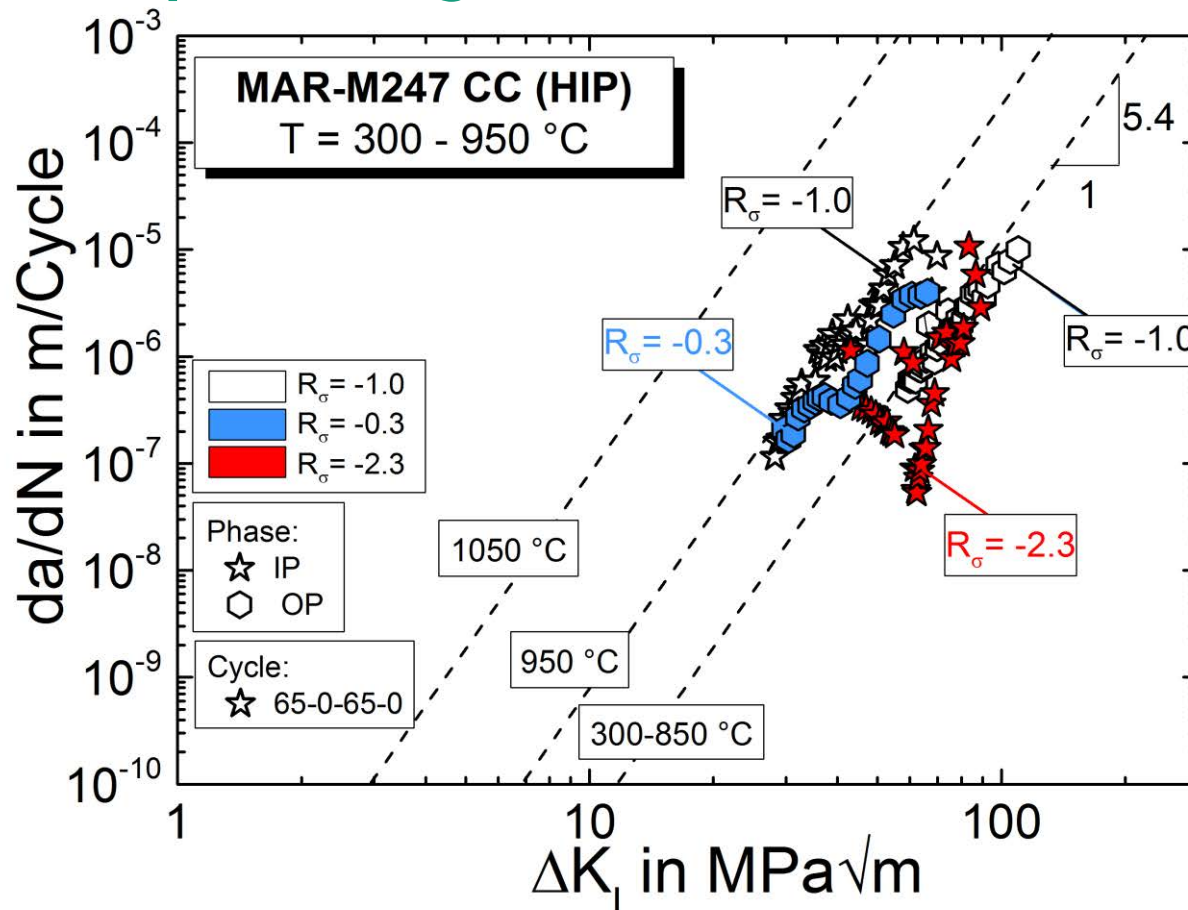


- IP-TMF shows higher crack growth rate than OP-TMF due to creep contribution



# Nonisothermal fatigue crack growth tests

## Influence of phase angle and stress ratio

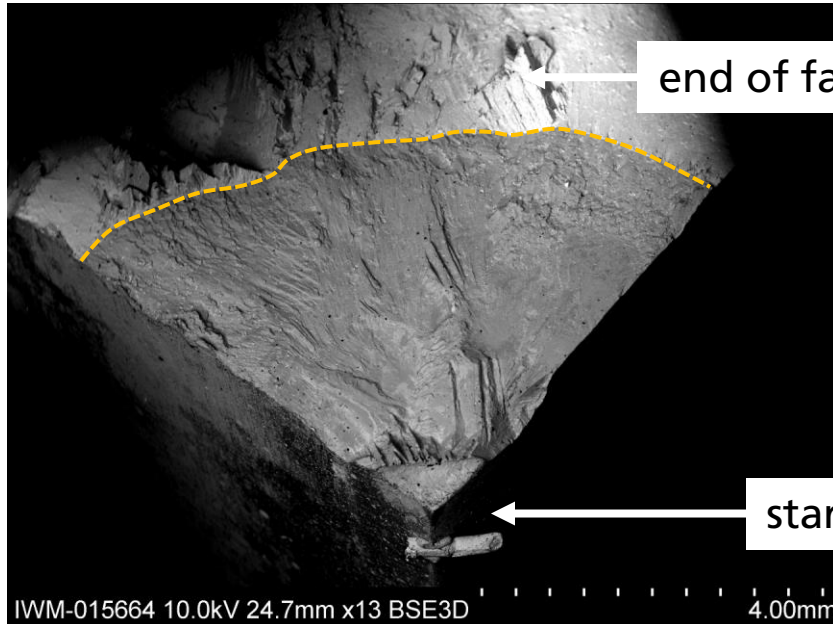


- With more realistic stress ratio, OP-TMF loading shows a higher crack growth rate than IP-TMF

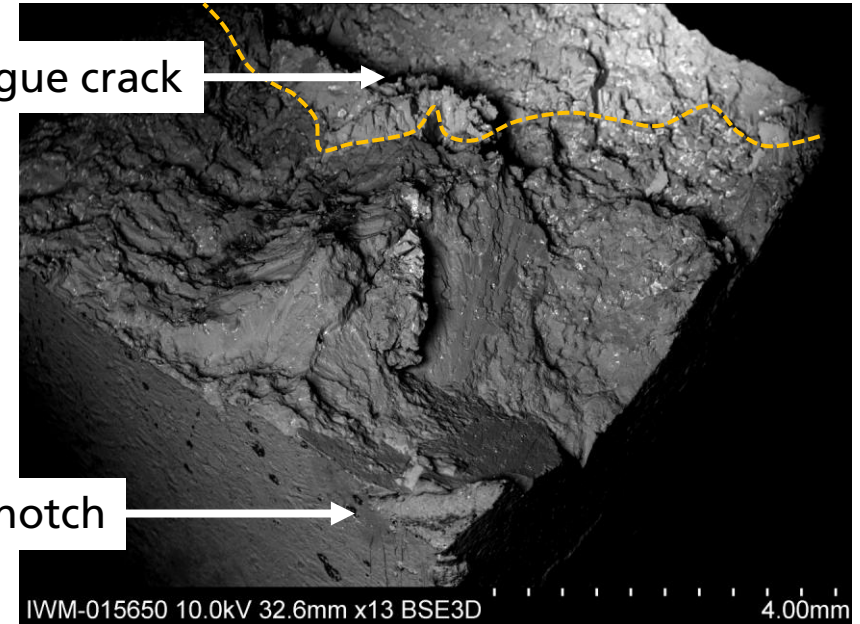
# Nonisothermal fatigue crack growth tests

## Influence of phase angle and stress ratio

OP-TMF,  $R = -0.3$



IP-TMF,  $R = -2.3$



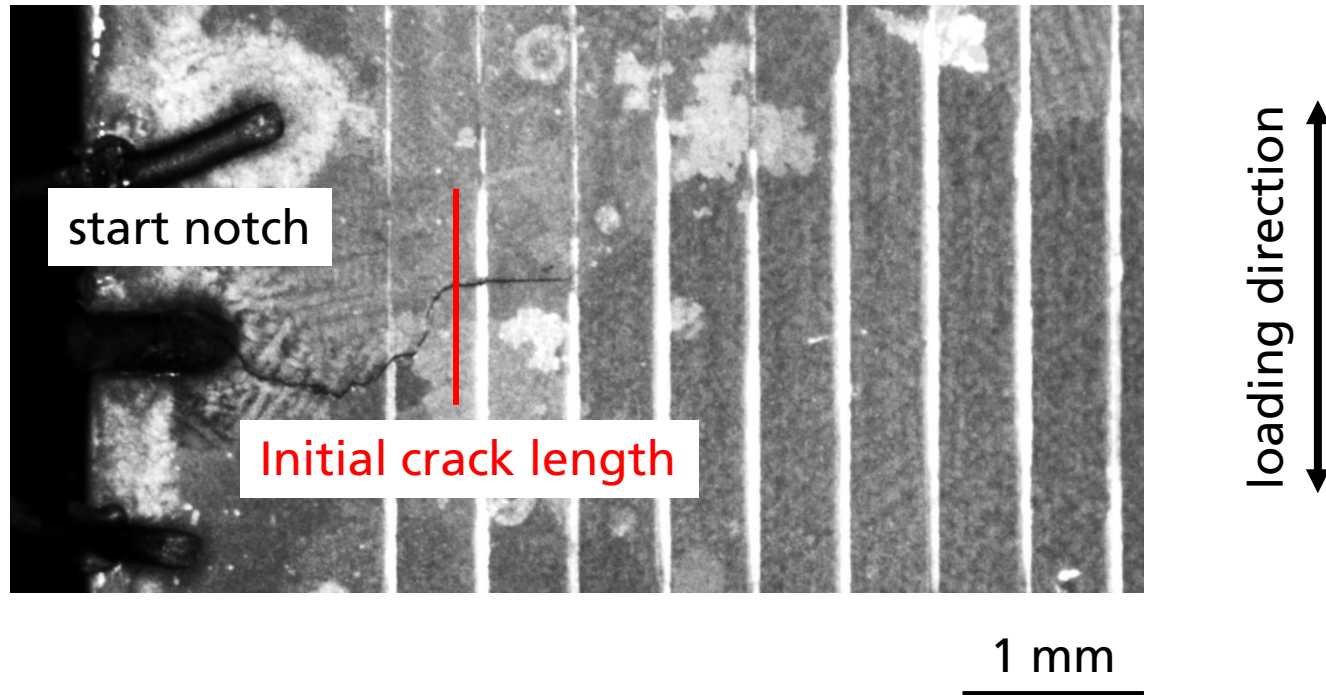
- OP-TMF: smooth fracture surface due to transgranular damage

- IP-TMF: rough surface due to partially interdendritic damage

# Nonisothermal fatigue crack growth tests

## Influence of phase angle and stress ratio

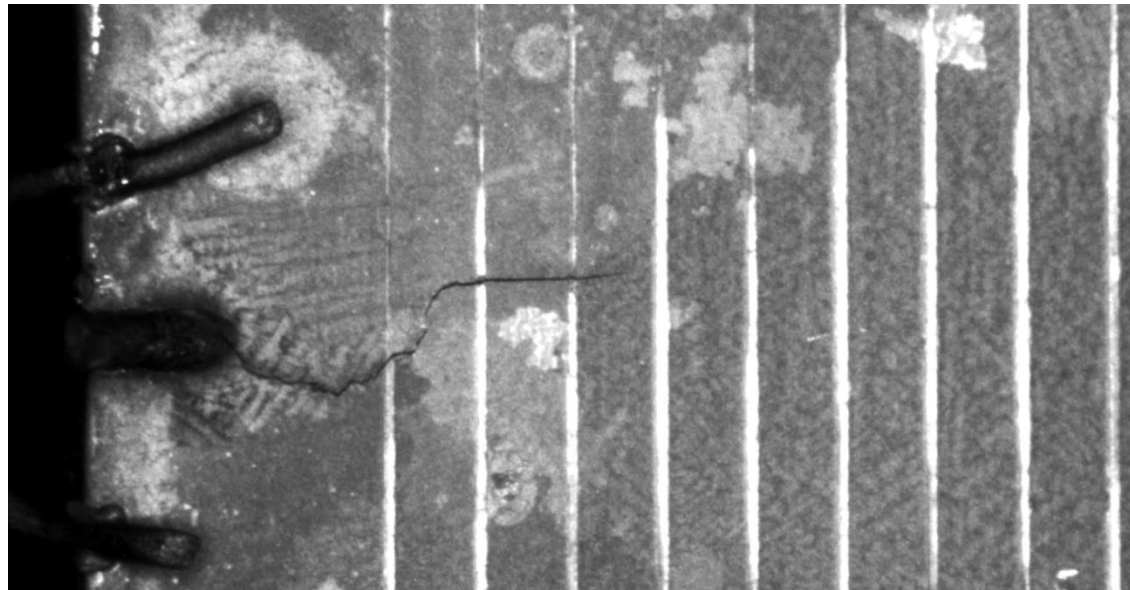
OP-TMF,  $T = 300-950\text{ }^{\circ}\text{C}$ ,  $R_{\sigma} = -0.3$



# Nonisothermal fatigue crack growth tests

## Influence of phase angle and stress ratio

OP-TMF,  $T = 300-950\text{ °C}$ ,  $R_\sigma = -0.3$



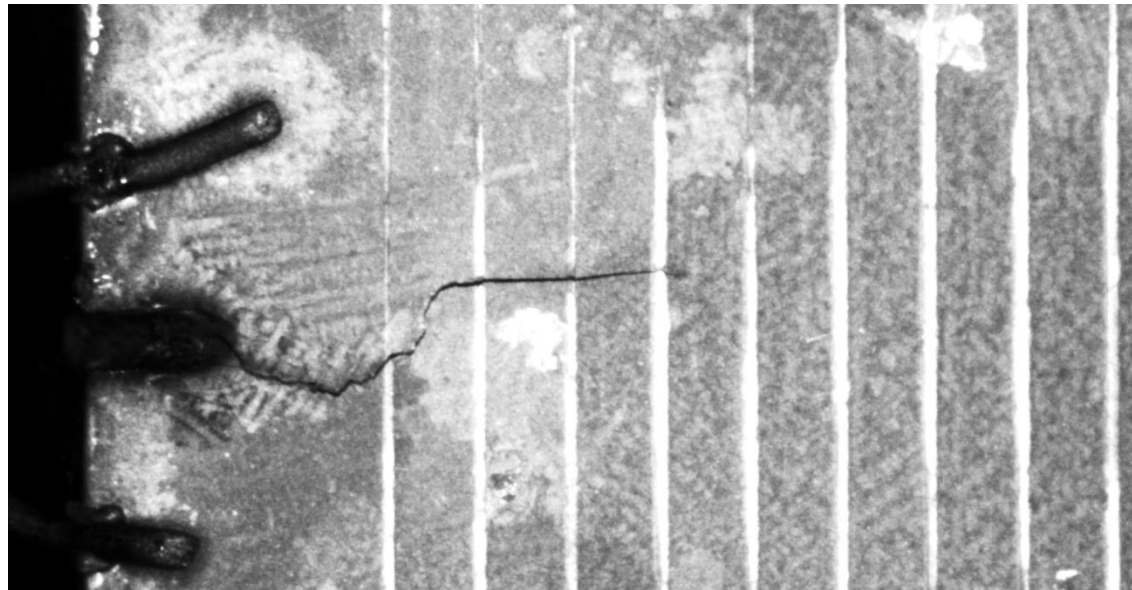
loading direction

1 mm

# Nonisothermal fatigue crack growth tests

## Influence of phase angle and stress ratio

OP-TMF,  $T = 300-950\text{ °C}$ ,  $R_\sigma = -0.3$



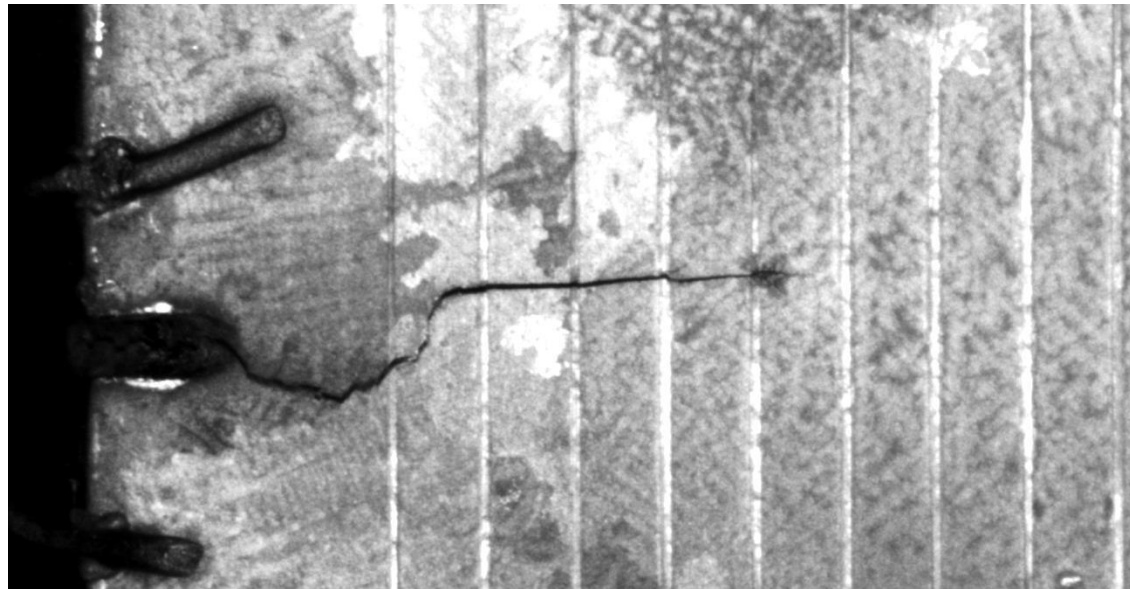
loading direction

1 mm

# Nonisothermal fatigue crack growth tests

## Influence of phase angle and stress ratio

OP-TMF,  $T = 300-950\text{ }^{\circ}\text{C}$ ,  $R_{\sigma} = -0.3$



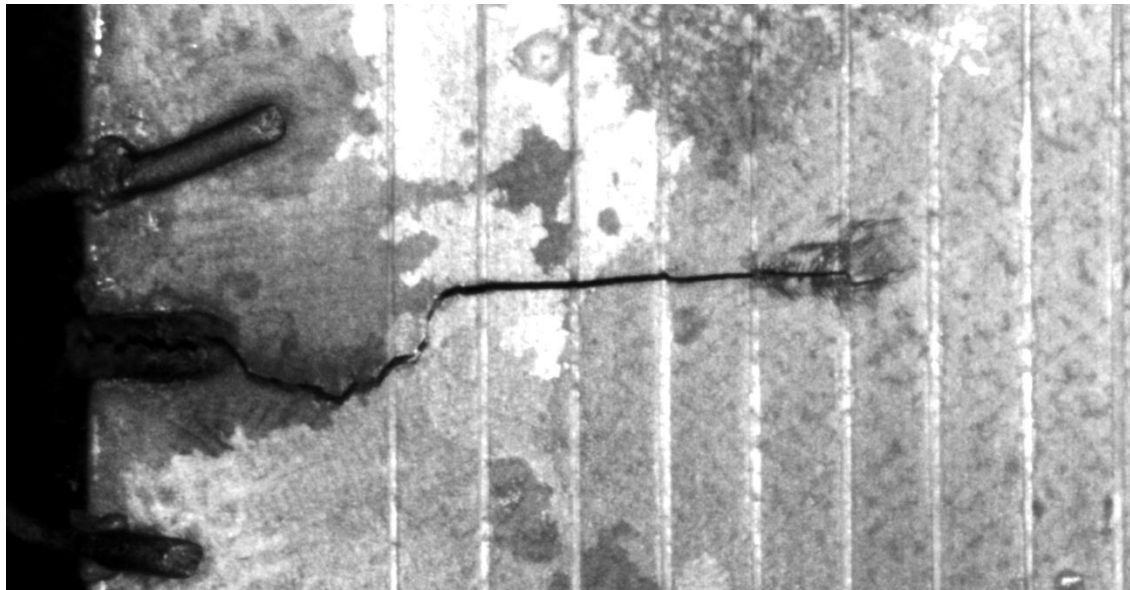
loading direction

1 mm

# Nonisothermal fatigue crack growth tests

## Influence of phase angle and stress ratio

OP-TMF,  $T = 300-950\text{ °C}$ ,  $R_\sigma = -0.3$

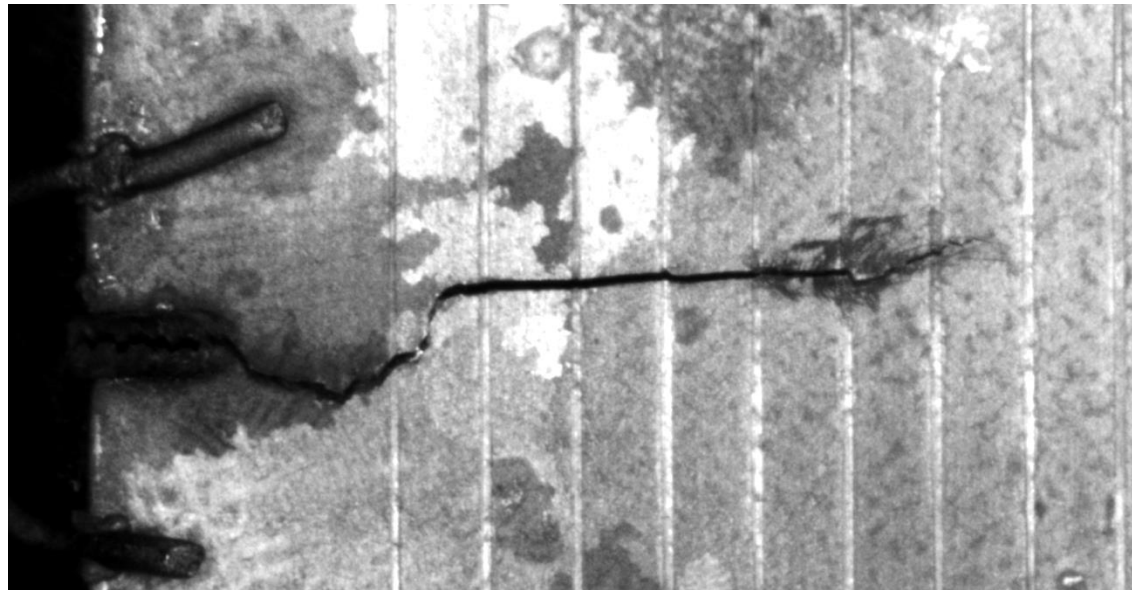


1 mm

# Nonisothermal fatigue crack growth tests

## Influence of phase angle and stress ratio

OP-TMF,  $T = 300-950\text{ }^{\circ}\text{C}$ ,  $R_{\sigma} = -0.3$



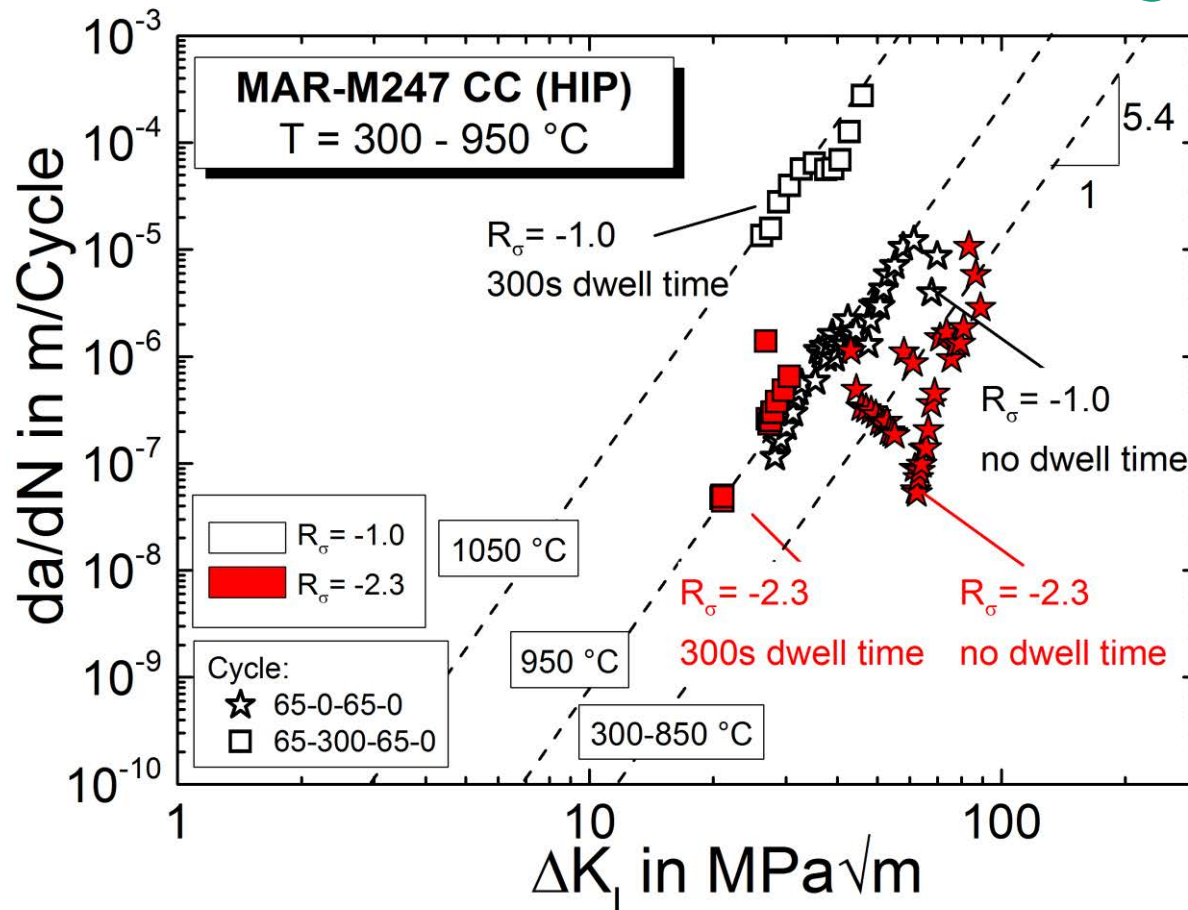
1 mm

- OP-TMF loading leads to transgranular fracture behavior



# Nonisothermal fatigue crack growth tests

## Influence of dwell times under IP-TMF loading

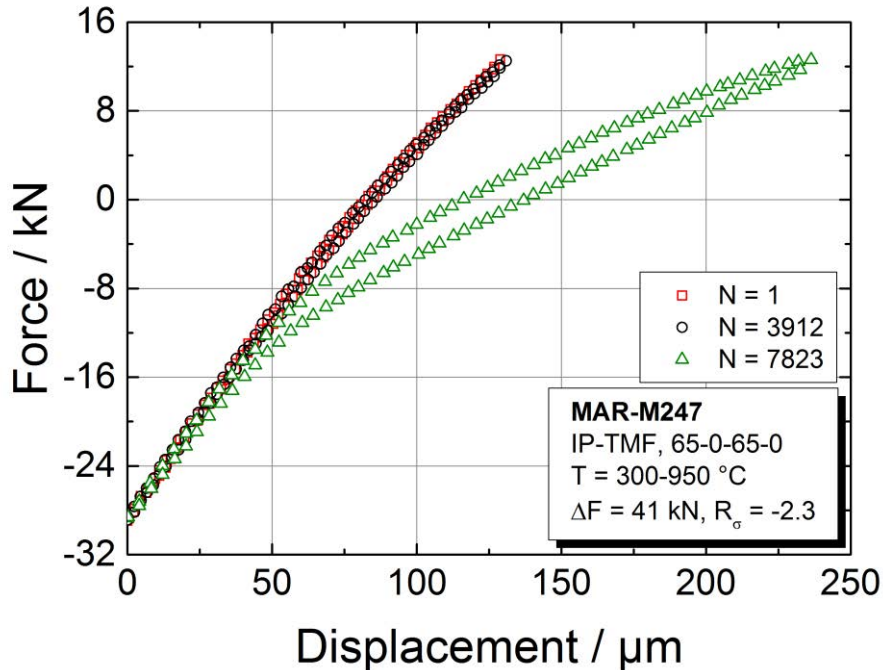


- Introduction of dwell times leads to significantly higher crack growth rates under IP loading

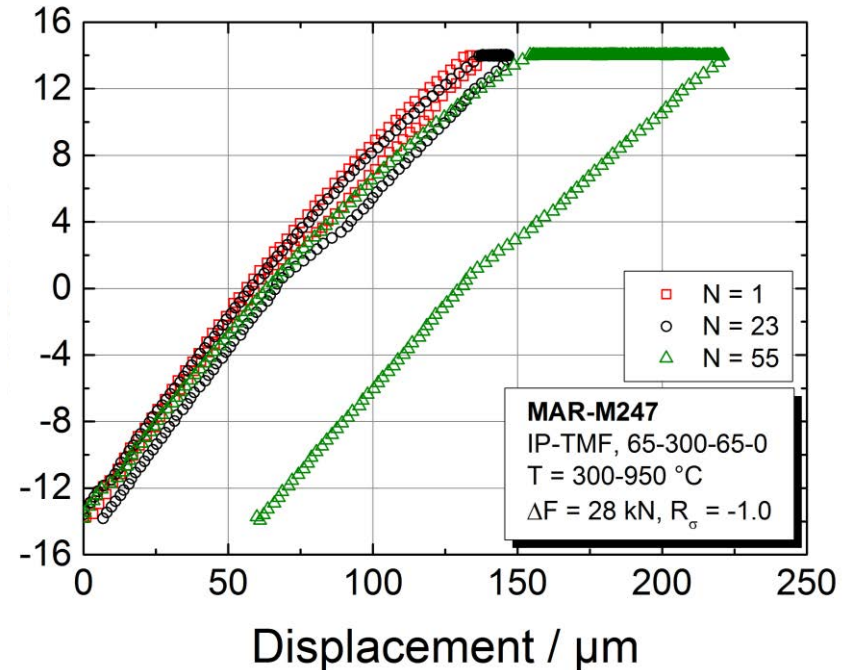
# Nonisothermal fatigue crack growth tests

## Influence of dwell times

IP-TMF,  $R = -2.3$ , without dwell time



IP-TMF,  $R = -1.0$ , 300s dwell time

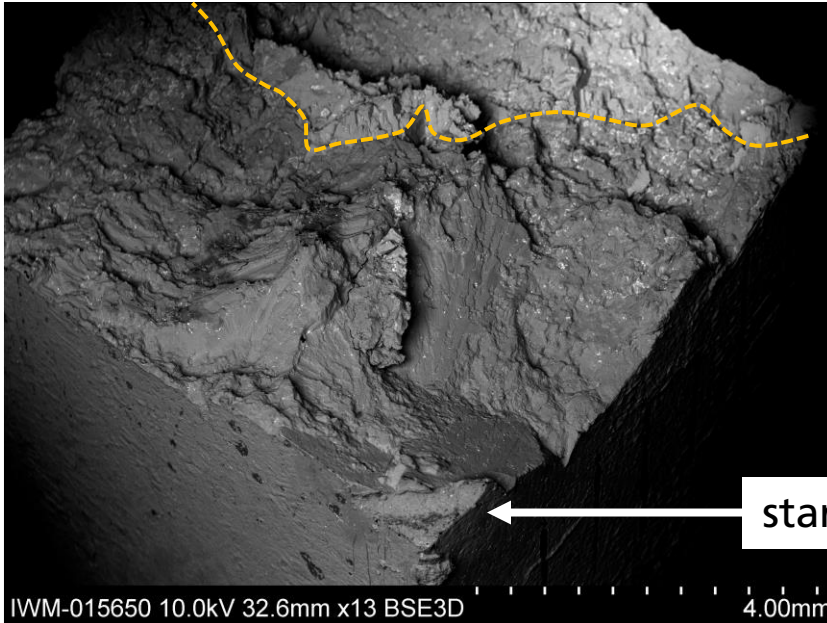


- IP-TMF with dwell time shows creep deformation

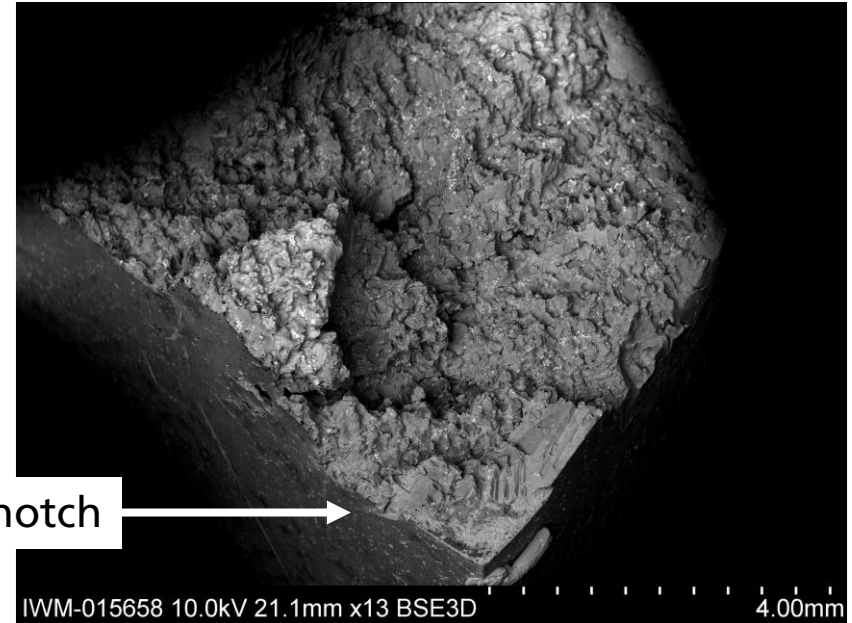
# Nonisothermal fatigue crack growth tests

## Influence of dwell times

IP-TMF, R = -2.3, without dwell time



IP-TMF, R = -1.0, 300s dwell time



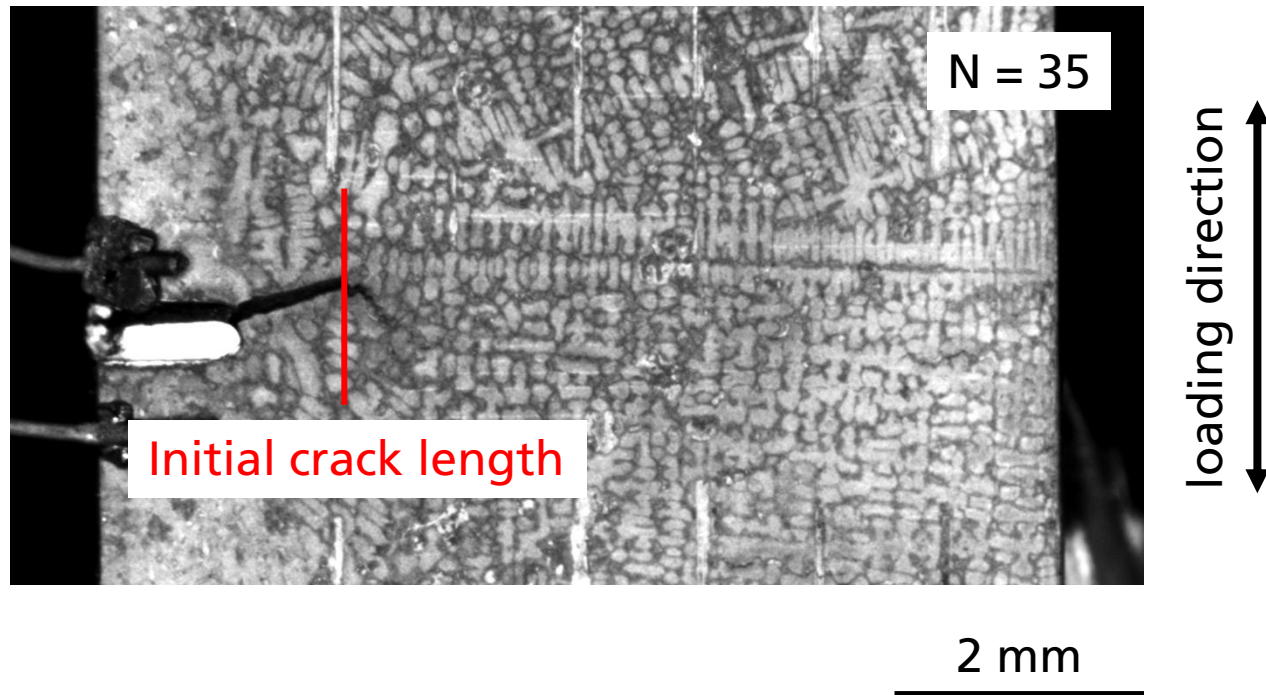
- Without dwell time:  
rough surface due to partially interdendritic damage

- With dwell time:  
mostly interdendritic crack propagation

# Nonisothermal fatigue crack growth tests

## Influence of dwell times

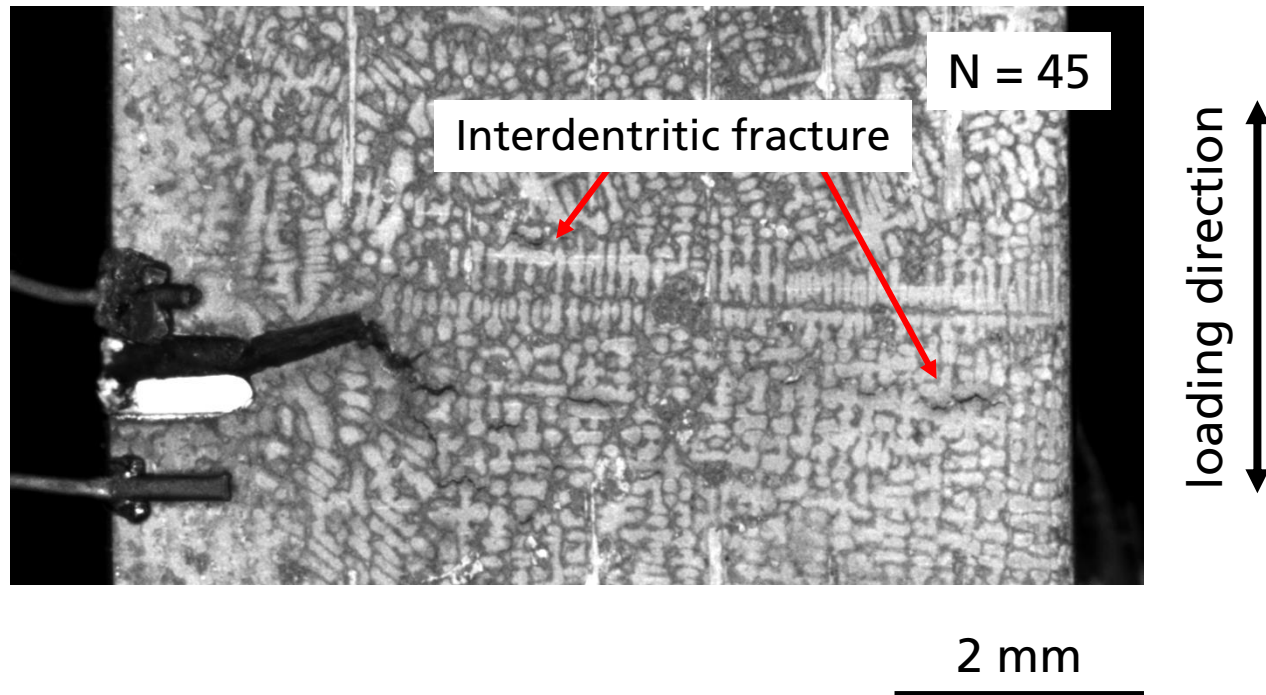
IP-TMF,  $T = 300-950\text{ }^{\circ}\text{C}$ ,  $R_{\sigma} = -1$ , 300 s dwell time in tension



# Nonisothermal fatigue crack growth tests

## Influence of dwell times

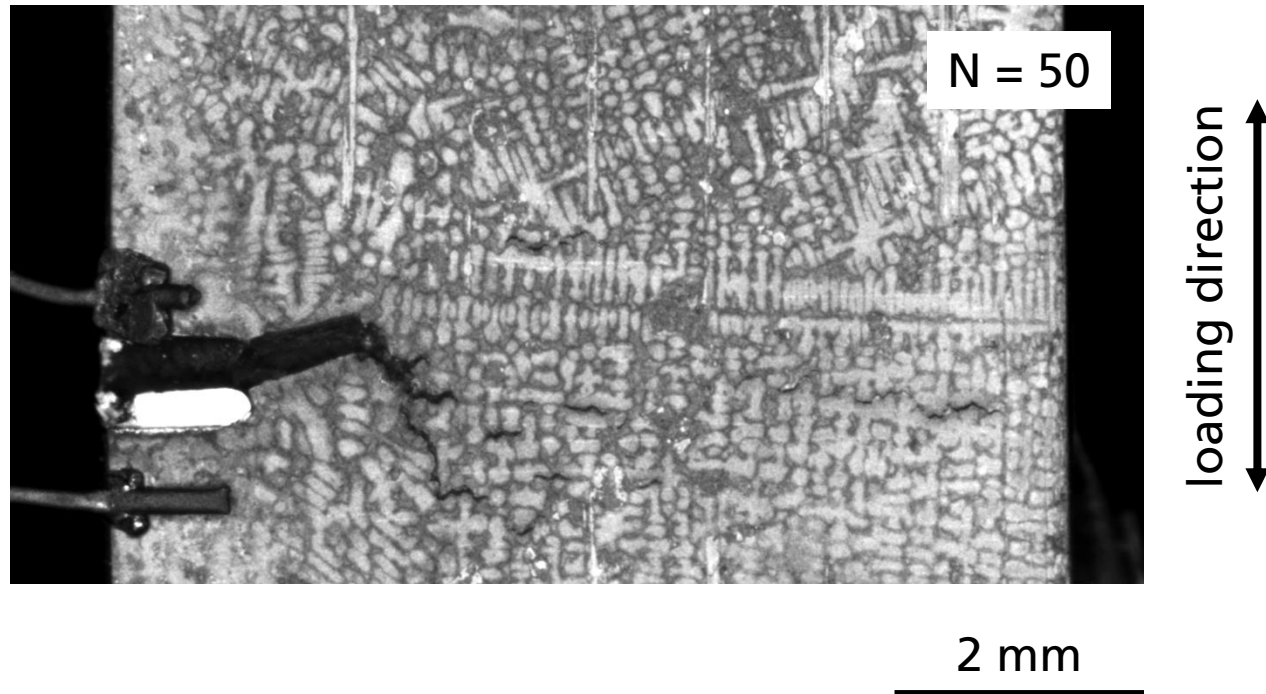
IP-TMF,  $T = 300-950\text{ }^{\circ}\text{C}$ ,  $R_{\sigma} = -1$ , 300 s dwell time in tension



# Nonisothermal fatigue crack growth tests

## Influence of dwell times

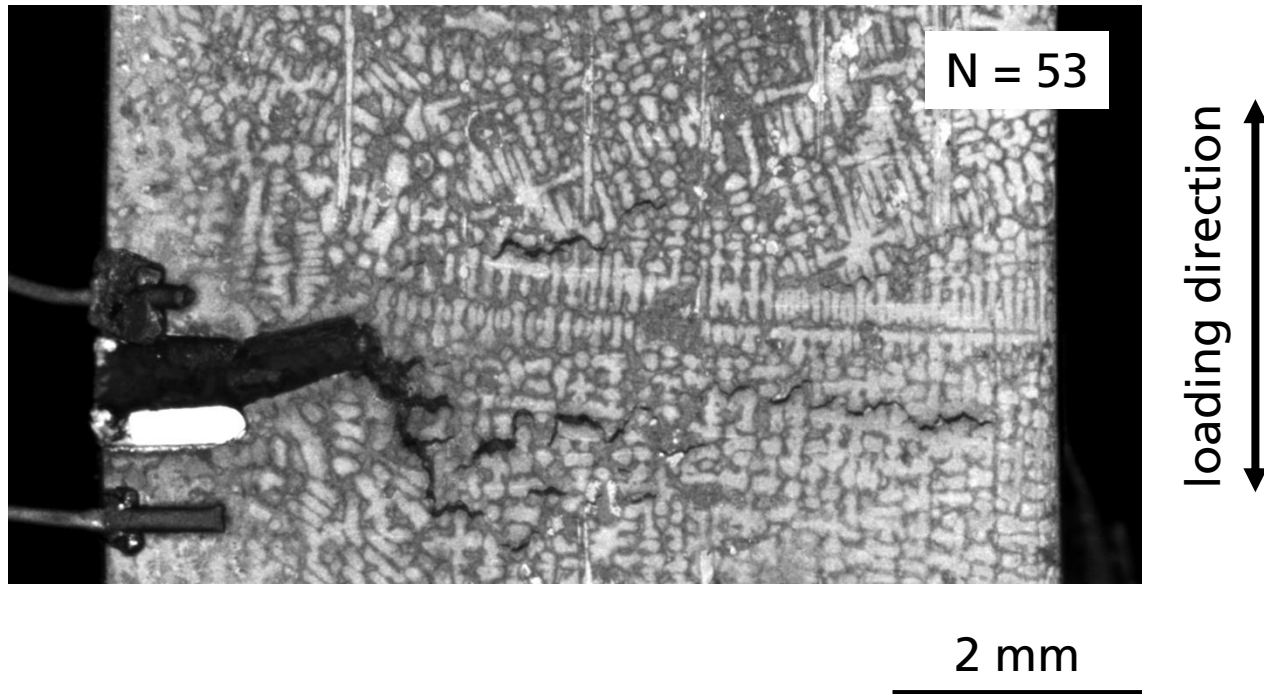
IP-TMF,  $T = 300-950\text{ }^{\circ}\text{C}$ ,  $R_{\sigma} = -1$ , 300 s dwell time in tension



# Nonisothermal fatigue crack growth tests

## Influence of dwell times

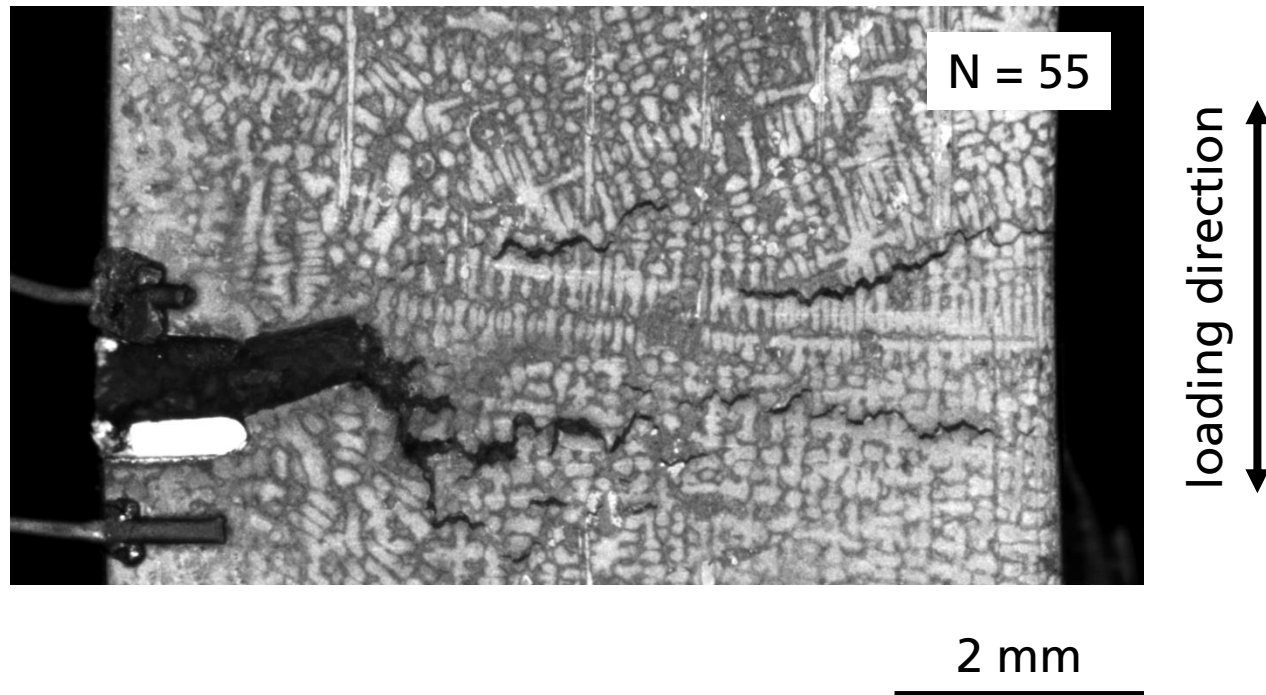
IP-TMF,  $T = 300-950\text{ }^{\circ}\text{C}$ ,  $R_{\sigma} = -1$ , 300 s dwell time in tension



# Nonisothermal fatigue crack growth tests

## Influence of dwell times

IP-TMF,  $T = 300-950\text{ }^{\circ}\text{C}$ ,  $R_{\sigma} = -1$ , 300 s dwell time in tension



- Creep damage during dwell time at 950 °C leads to interdentritic fracture

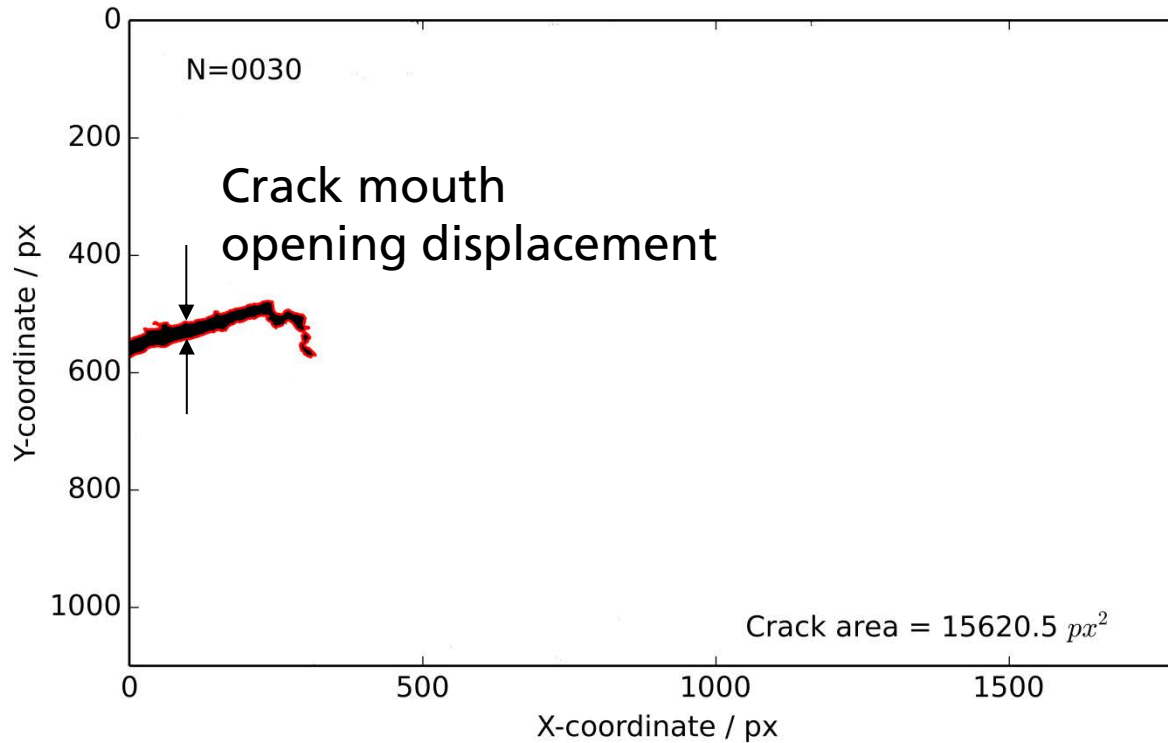


# OUTLOOK – DIGITAL IMAGE PROCESSING

# Outlook

## Correlation of CMOD with damage propagation

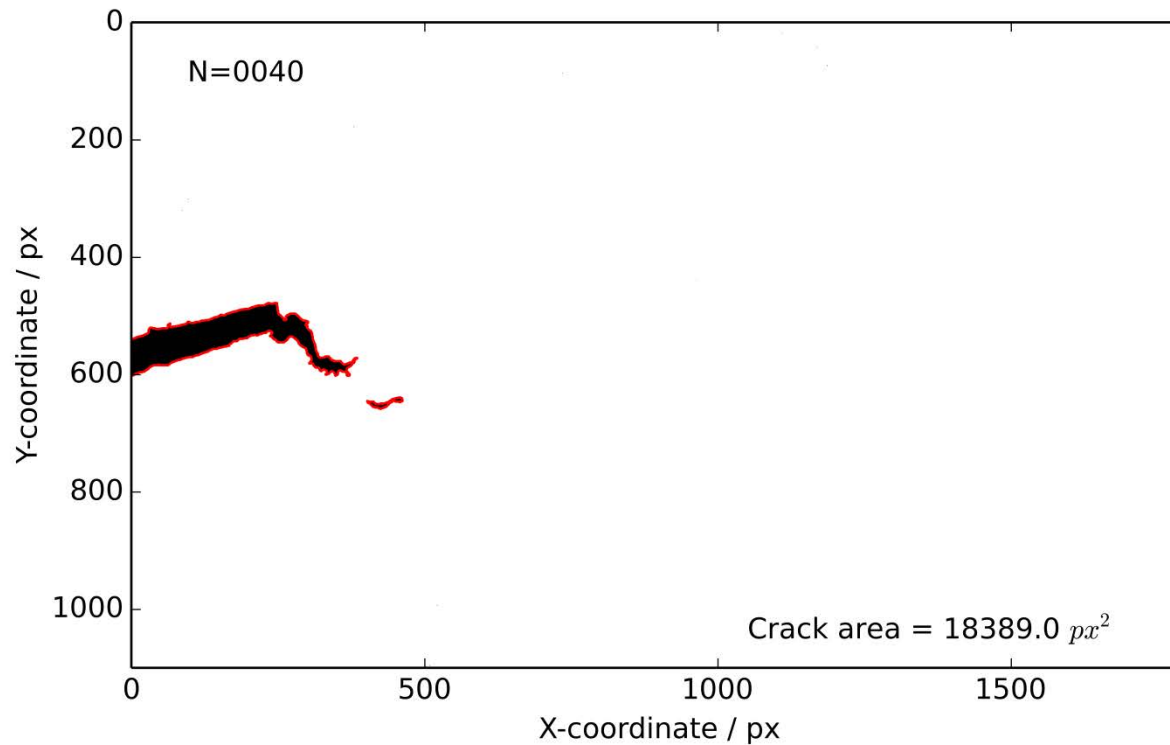
IP-TMF,  $T = 300-950\text{ }^{\circ}\text{C}$ ,  $R_{\sigma} = -1$ , 300 s dwell time in tension



# Outlook

## Correlation of CMOD with damage propagation

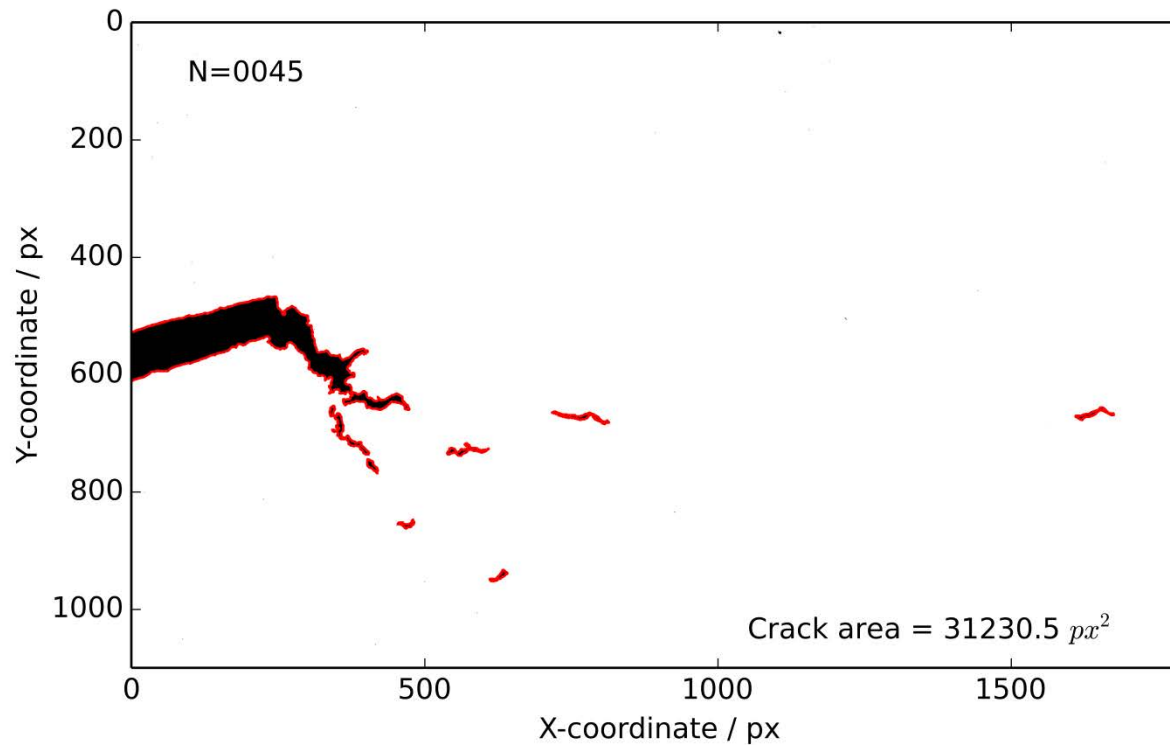
IP-TMF,  $T = 300-950\text{ }^{\circ}\text{C}$ ,  $R_{\sigma} = -1$ , 300 s dwell time in tension



# Outlook

## Correlation of CMOD with damage propagation

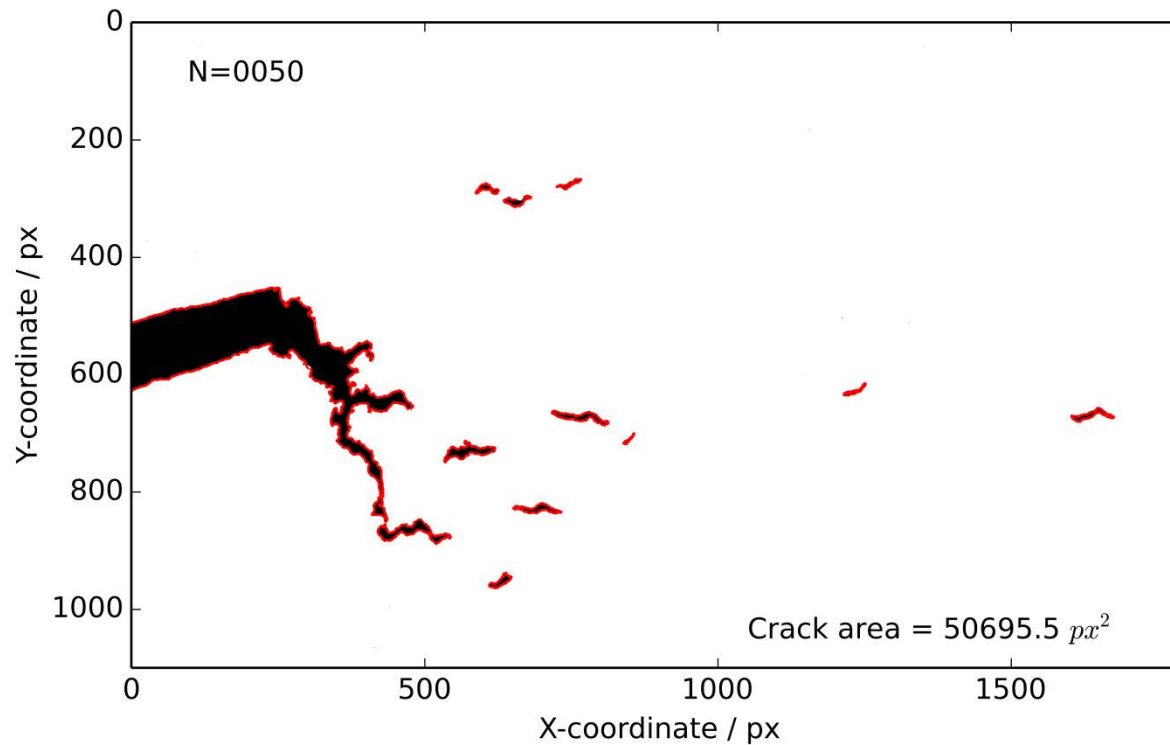
IP-TMF,  $T = 300-950\text{ }^{\circ}\text{C}$ ,  $R_{\sigma} = -1$ , 300 s dwell time in tension



# Outlook

## Correlation of CMOD with damage propagation

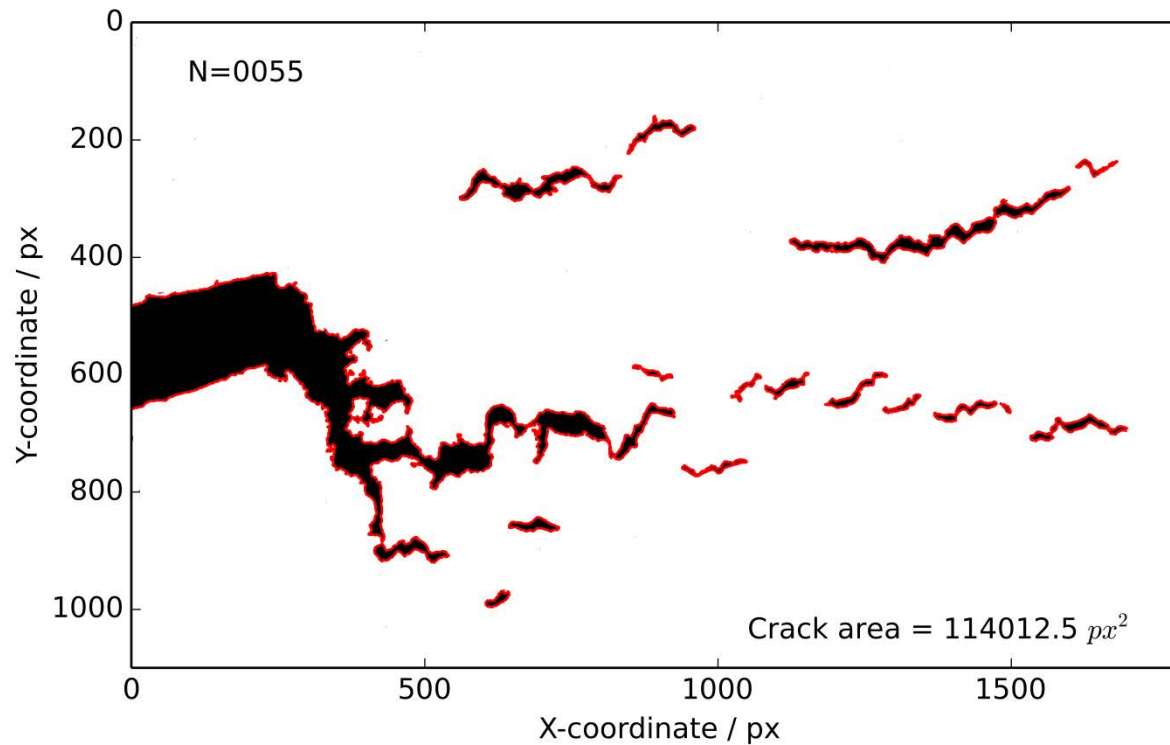
IP-TMF,  $T = 300-950\text{ }^{\circ}\text{C}$ ,  $R_{\sigma} = -1$ , 300 s dwell time in tension



# Outlook

## Correlation of CMOD with damage propagation

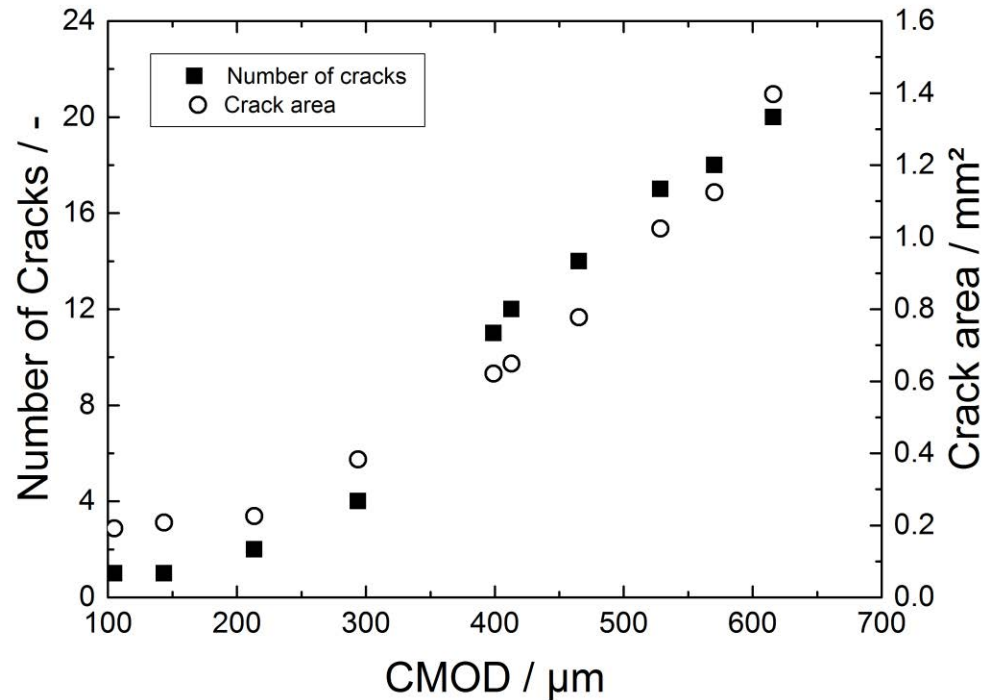
IP-TMF,  $T = 300-950\text{ }^{\circ}\text{C}$ ,  $R_{\sigma} = -1$ , 300 s dwell time in tension



# Outlook

## Correlation of CMOD with damage propagation

IP-TMF,  $T = 300-950\text{ }^{\circ}\text{C}$ ,  $R_{\sigma} = -1$ , 300 s dwell time in tension

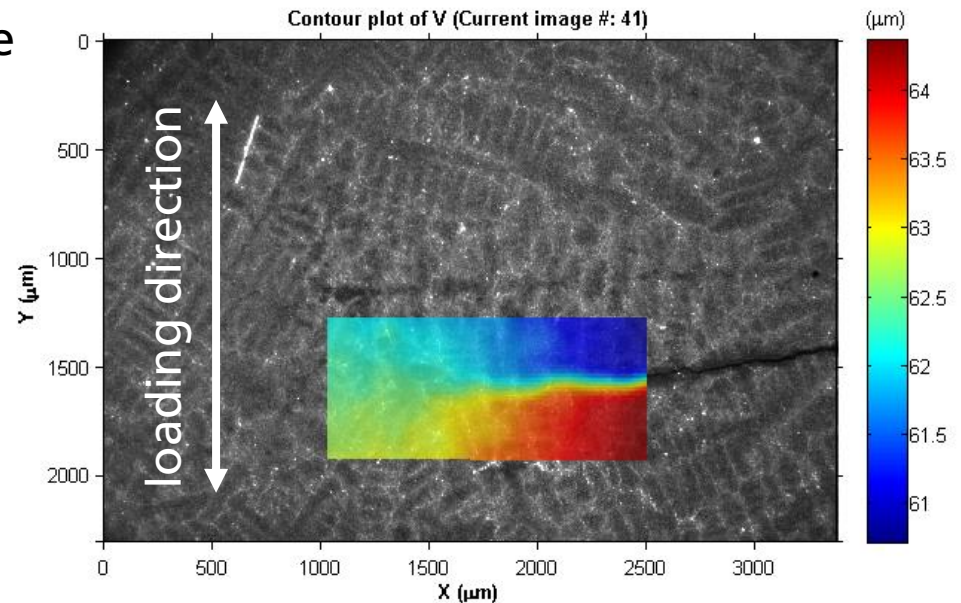


- Nucleation of secondary cracks is increasing with CMOD, i.e. with acc. creep strain

# Outlook

## Digital image correlation (DIC)

- Further investigation of damage mechanism under IP- and OP-TMF loading:
  - DIC to analyse displacement fields at crack tips under different phase angles and dwell times
  - Measurement of fatigue crack closure

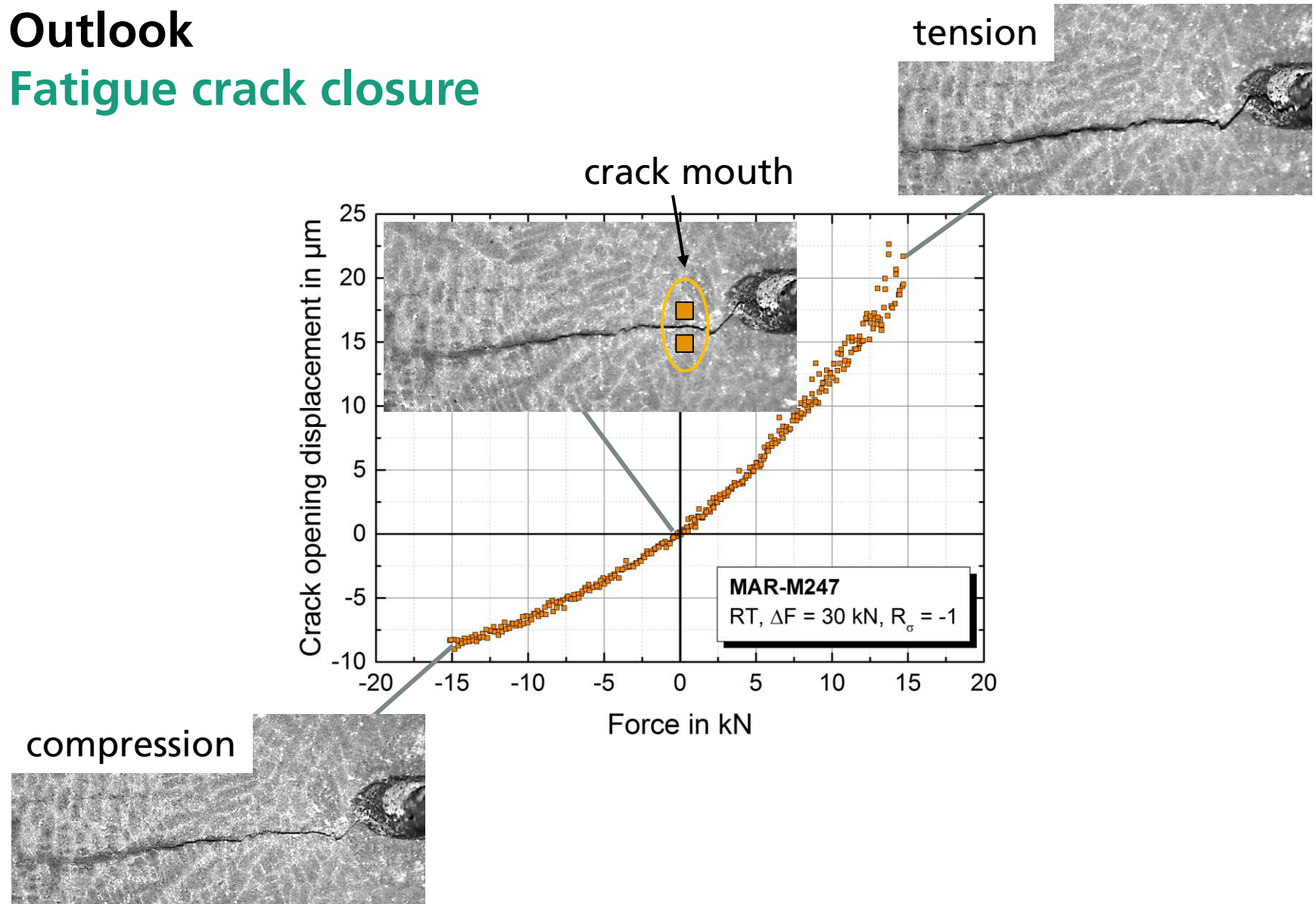


Calculated displacements at the crack tip in loading direction



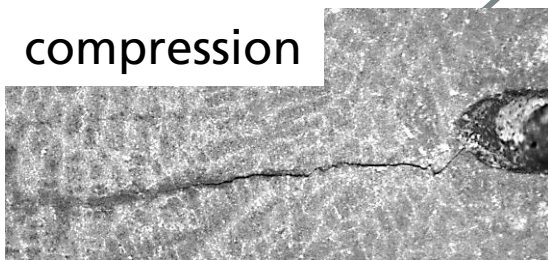
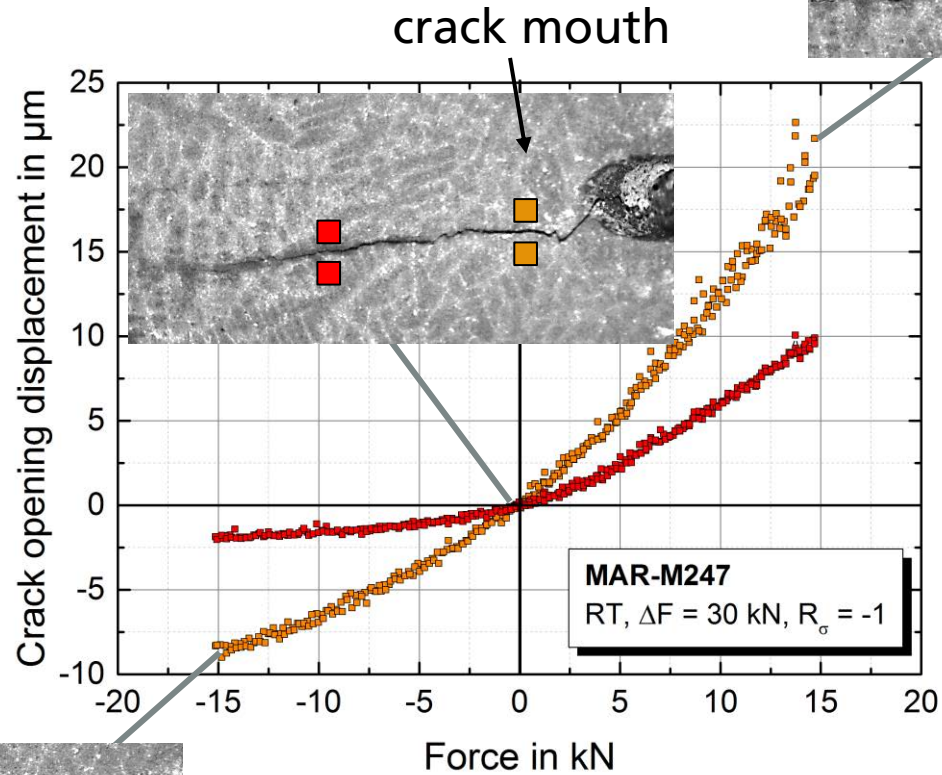
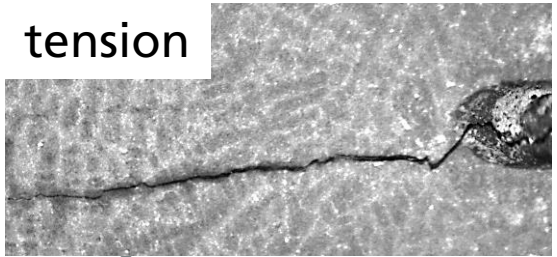
# Outlook

## Fatigue crack closure



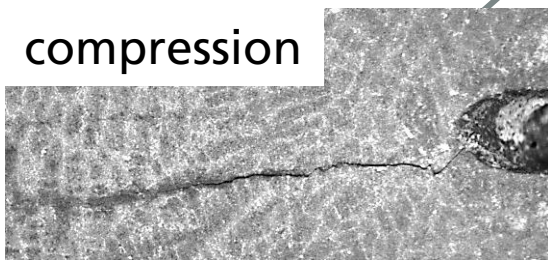
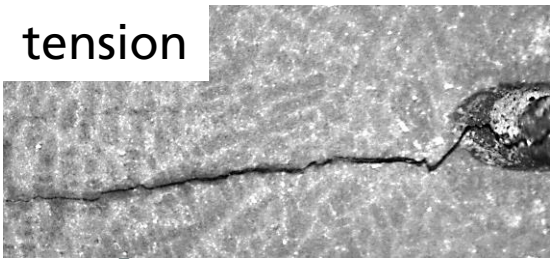
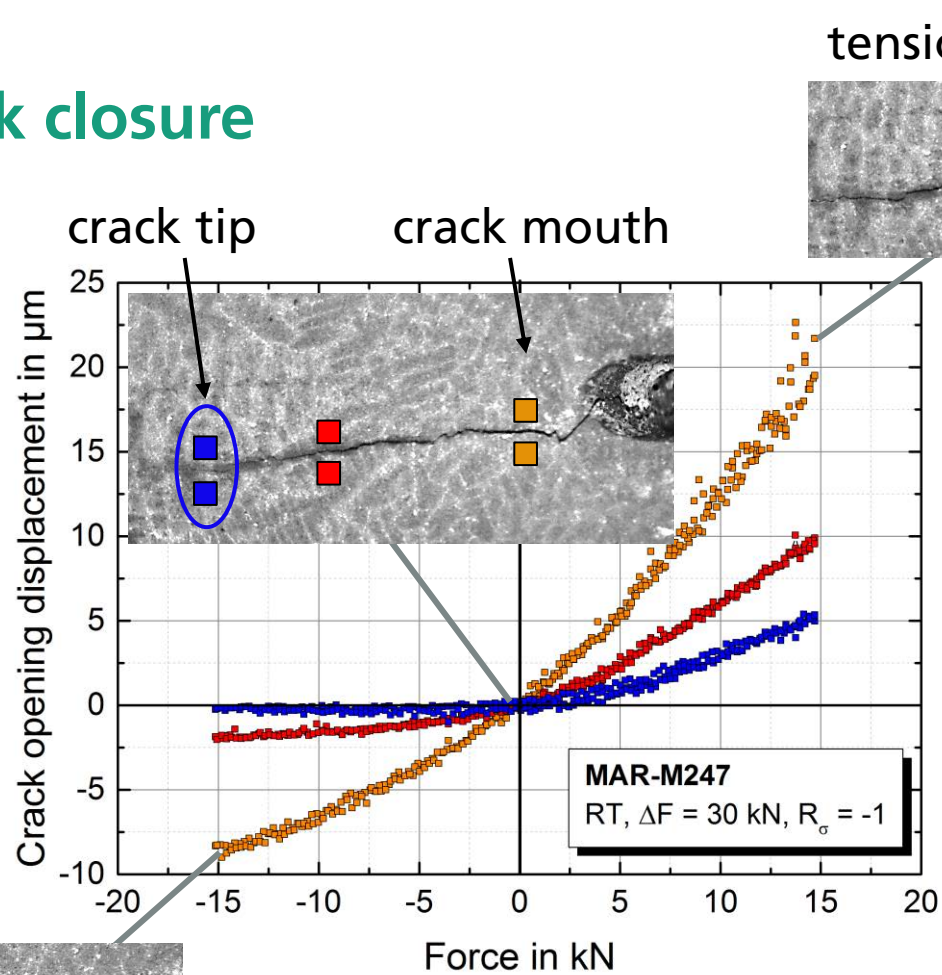
# Outlook

## Fatigue crack closure



# Outlook

## Fatigue crack closure



# Acknowledgement

- This work was supported by
  - the Arbeitsgemeinschaft industrieller Forschungsvereinigungen (AiF)
  - the Forschungsvereinigung Verbrennungskraftmaschinen (FVV)

---

# CHARACTERIZATION OF DAMAGE MECHANISMS OF NICKEL-BASE ALLOY MAR-M247 CC (HIP) UNDER THERMOMECHANICAL CREEP-FATIGUE LOADING USING DIGITAL IMAGE PROCESSING

---

Stefan Eckmann, Christoph Schweizer

Fraunhofer Institute of Mechanics of Materials IWM, Freiburg, Germany

3<sup>rd</sup> TMF-Workshop, Berlin, 27<sup>th</sup> - 29<sup>th</sup> April 2016

# Literature

[Guth 2015]:

Influence of phase angle on lifetime, cyclic deformation and damage behavior of Mar-M247 LC under thermo-mechanical fatigue; S.Guth, S. Doll, K.-H. Lang; Materials Science and Engineering: A Vol. 642; 2015

[Oechsner 2011]:

TMF-Rissverhalten; M. Oechsner et. al. ;FVV-Report 945; 2011

---

# CONSTITUTIVE MODELING AND LIFETIME PREDICTION FOR A CONVENTIONALLY CAST NI-BASE SUPERALLOY UNDER TMF LOADING

S. Grützner<sup>1</sup>, B. Fedelich<sup>1</sup>, B. Rehmer<sup>1</sup>

<sup>1</sup> Federal Institute for Materials Research and Testing, Berlin

---

# Acknowledgements

---



Part of the joint research program AG Turbo 2020.



Support by Siemens AG (financial support & test data) and the Federal Ministry of Economics and Technology (BMWFi, grant number 0327718S).



Thanks to G. Walz and B. Buchholz (Siemens AG) and C. Schweizer (IWM) for helpful discussions.

Thanks to the division Materialography, Fractography and Ageing of Engineering Materials (5.1) of the BAM.





# Outline



---

Deformation behavior of the alloy 247

TMF life time prediction of the alloy 247

Summary

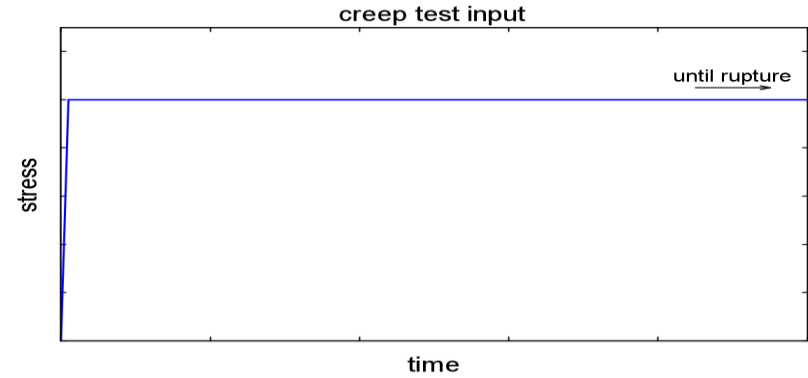
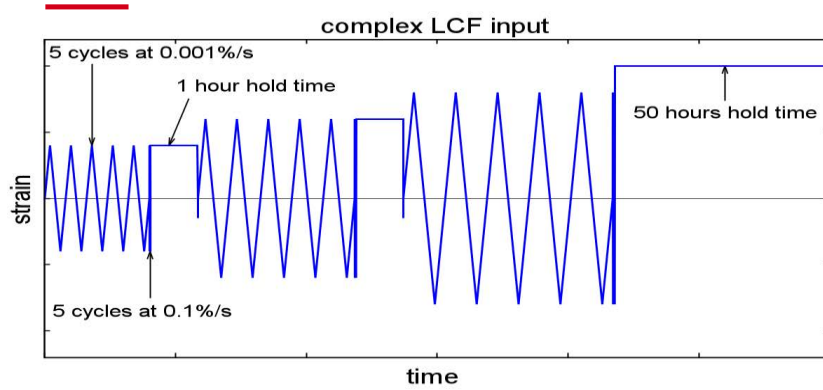
---

---

# Deformation behavior of the alloy 247

---

# Deformation experiments

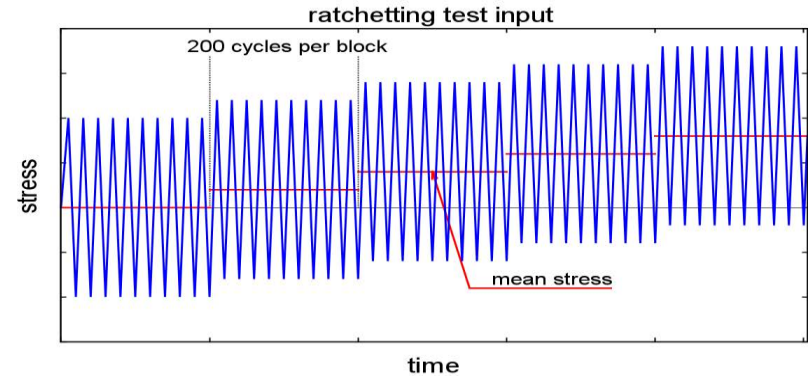


Strain controlled tests:

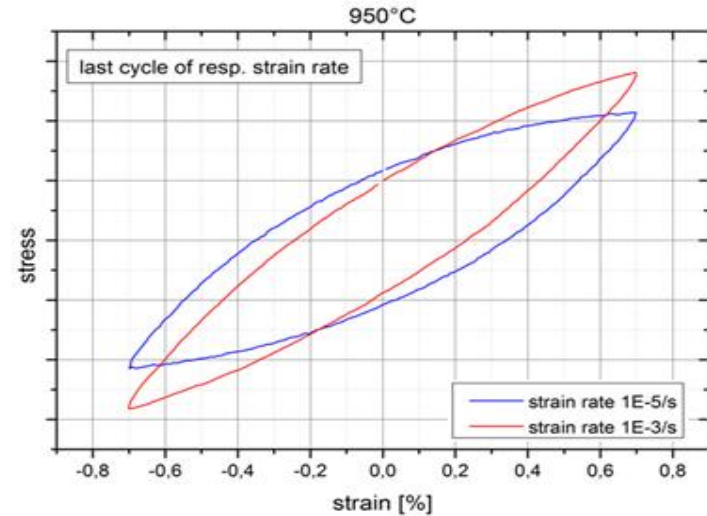
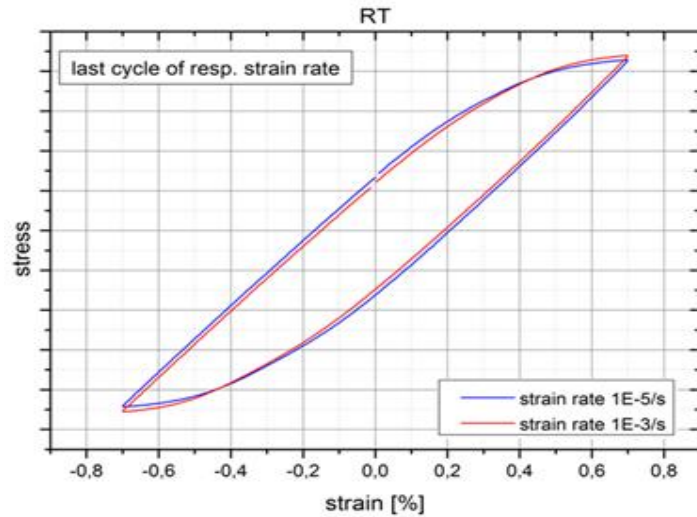
- Complex LCF (CLCF)

Stress controlled tests:

- Creep (Siemens)
- Ratchetting



# Deformation experiments



- Dependency on strain rate
- Stress relaxation
- Creep
- Cyclic strain accumulation (Ratchetting)
- Cyclic plasticity

# Base Deformation model after Chaboche



Hooke's Law

$$\boldsymbol{\sigma} = 2G(\boldsymbol{\varepsilon}' - \boldsymbol{\varepsilon}_{in}) + \frac{E}{3(1-2\nu)} \text{tr}(\boldsymbol{\varepsilon} - \boldsymbol{\varepsilon}_{th}) \mathbf{1}$$

Inelastic strain rate

$$\dot{\boldsymbol{\varepsilon}}_{in} = \frac{3}{2} \left\langle \frac{J_2(\boldsymbol{\sigma}' - \mathbf{X}) - k}{K} \right\rangle^n \frac{\boldsymbol{\sigma}' - \mathbf{X}}{J_2(\boldsymbol{\sigma}' - \mathbf{X})}$$

Backstresses

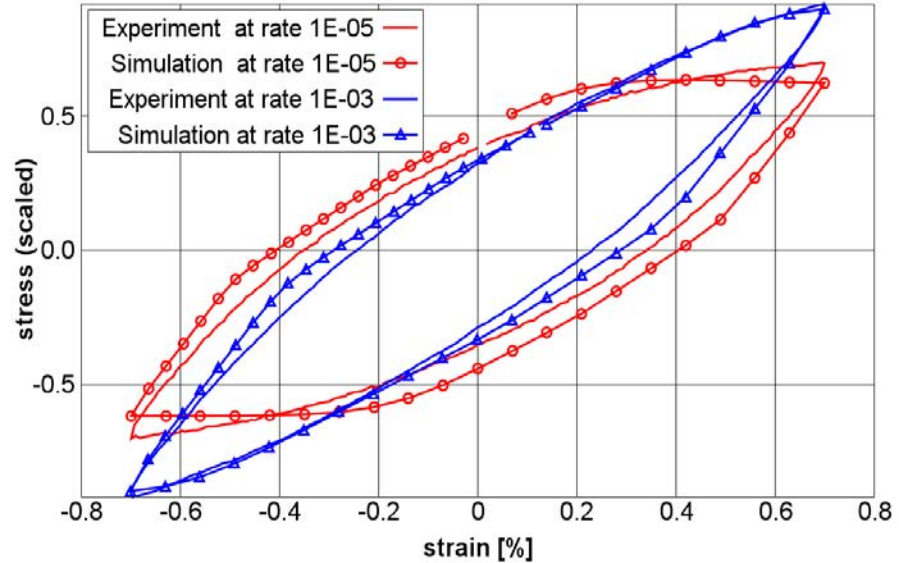
$$\mathbf{X} = \mathbf{X}_1 + \mathbf{X}_2 \quad \mathbf{X}_i = \frac{2}{3} a_i \boldsymbol{\alpha}_i \quad i = 1, 2$$

Hardening / Recovery

$$\dot{\boldsymbol{\alpha}}_i = \dot{\boldsymbol{\varepsilon}}_{in} - \underbrace{\frac{\gamma_i \boldsymbol{\alpha}_i \|\dot{\boldsymbol{\varepsilon}}_{in}\|}{\text{dynamic recovery}}}_{\text{dynamic recovery}} - \underbrace{\frac{3}{2} d_i \left\langle J_2(\gamma_i \boldsymbol{\alpha}_i) \right\rangle^{m_i} \frac{\boldsymbol{\alpha}_i}{J_2(\boldsymbol{\alpha}_i)}}_{\text{static recovery}}$$

# Deformation model

- Dependency on strain rate ✓
- Cyclic plasticity ✓



Hysteresis loops of a CLCF test at 950°C

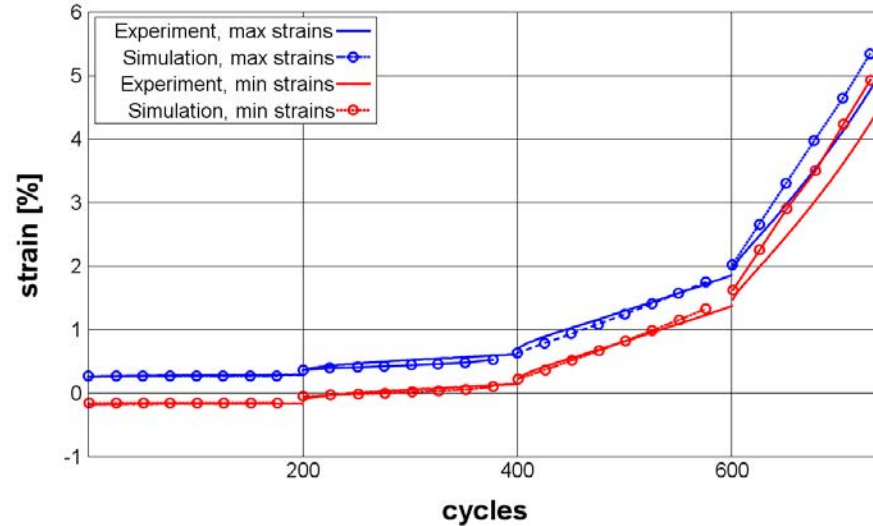
# cyclic strain accumulation (Ratchetting)

$$\gamma_i \boldsymbol{\alpha}_i \|\dot{\boldsymbol{\epsilon}}_{in}\|$$



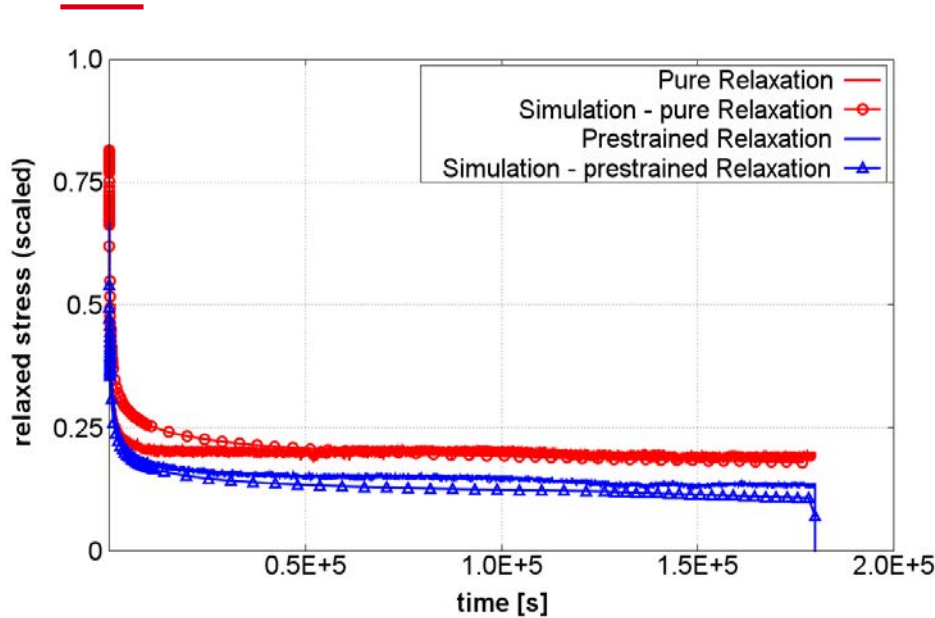
$$\left\langle \frac{\boldsymbol{\alpha}_i}{J_2(\boldsymbol{\alpha}_i)} \right\rangle \left[ \frac{J_2(\gamma_i \boldsymbol{\alpha}_i)}{3/2} \right]^{s_i-1} \left\langle \dot{\boldsymbol{\epsilon}}_{in} : \frac{\boldsymbol{\alpha}_i}{J_2(\boldsymbol{\alpha}_i)} \right\rangle \gamma_i \boldsymbol{\alpha}_i$$

Extended model: (Ohno/Wang)



Ratchetting test at 950°C

# Deformation model: stress relaxation



$$m_i(p) = \left[ m_{\infty,i} + (m_{0,i} - m_{\infty,i}) \exp[-h_i p] \right], \quad \dot{p} = \|\dot{\boldsymbol{\epsilon}}_{in}\|$$

$$\frac{3}{2} d_i \left\langle J_2(\gamma_i \boldsymbol{\alpha}_i) \right\rangle \frac{m_i \boldsymbol{\alpha}_i}{J_2(\boldsymbol{\alpha}_i)}$$

Deformation induced softening after Kindrachuk (2011)

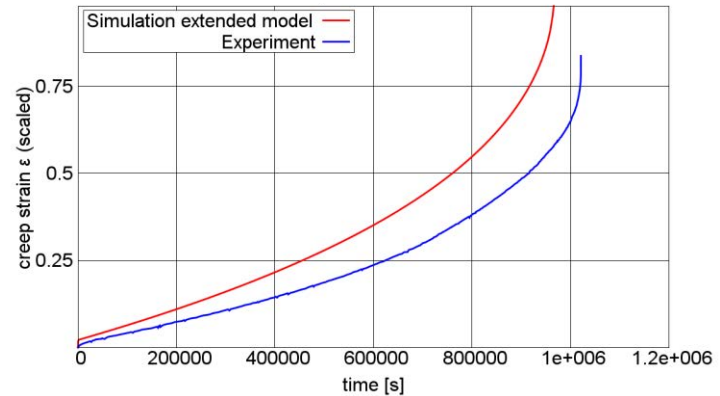
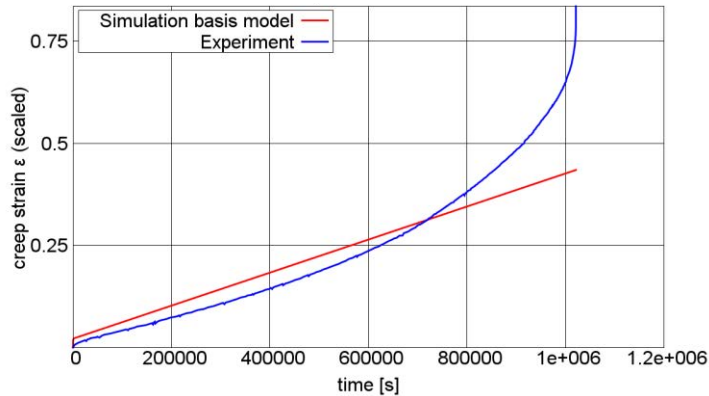


# Deformation model: creep damage (Kachanov)

Effective stress after Kachanov:

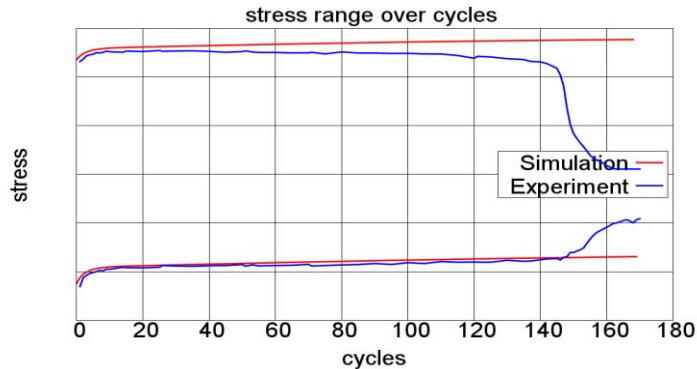
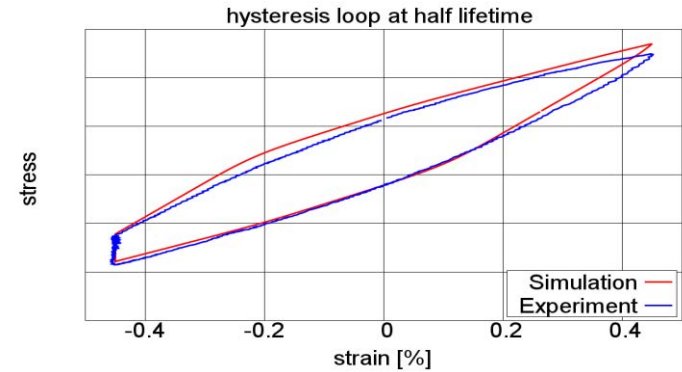
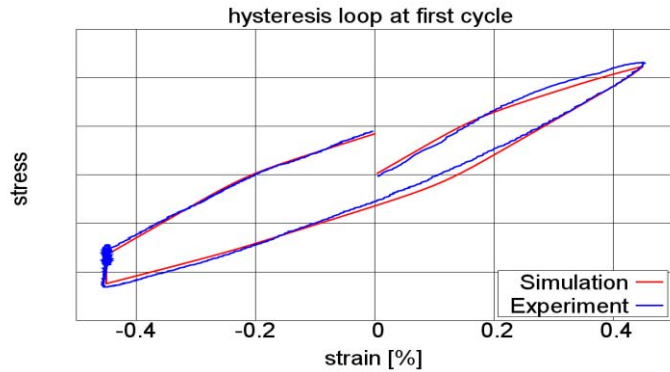
$$\boldsymbol{\sigma} \rightarrow \hat{\boldsymbol{\sigma}} = \frac{\boldsymbol{\sigma}}{1-D}$$

$$\dot{D} = \left( \frac{\chi(\hat{\boldsymbol{\sigma}})}{A} \right)^q (1-D)^{-q}$$



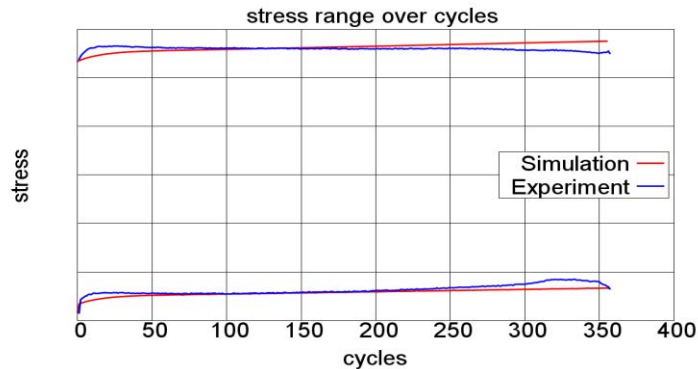
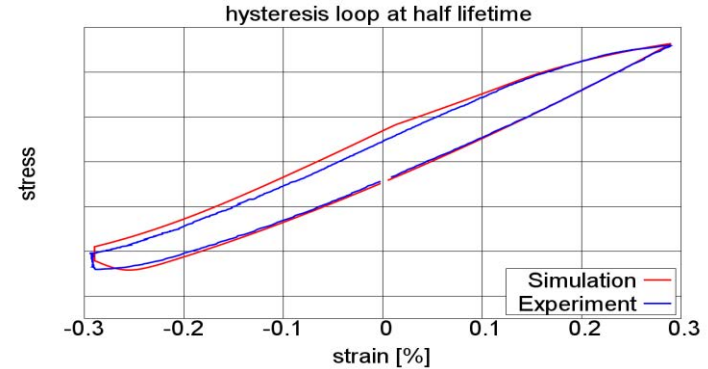
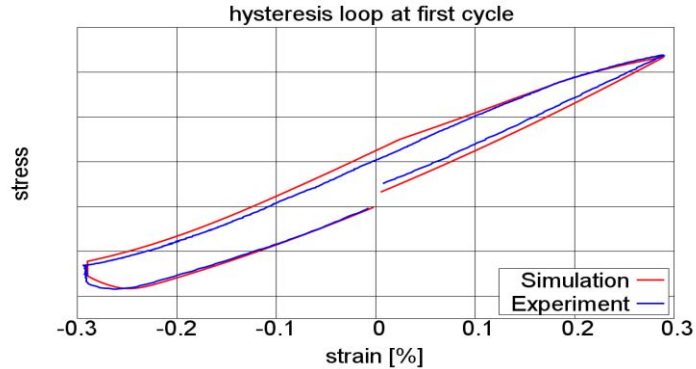
- Creep ✓

# Deformation model: verification



- LCF at 950°C
- Strain amplitude: 0.45%
- Strain ratio:  $R = -1$
- 2 min. hold time

# Deformation model: verification



- TMF OP ( $100^{\circ}\text{C} < T < 950^{\circ}\text{C}$ )
- strain amplitude: 0.29%
- Strain ratio:  $R = -1$
- 3 min. hold time

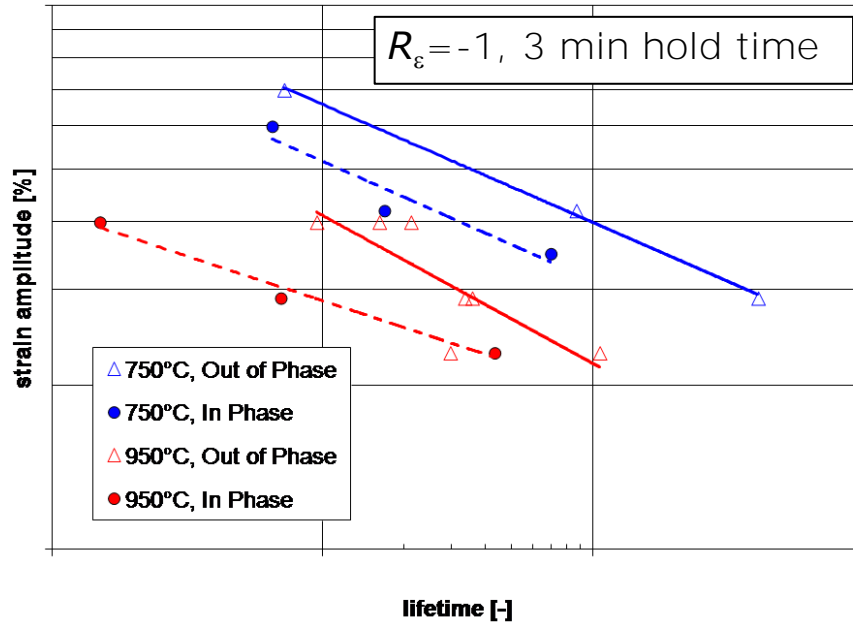
---

# **TMF life time prediction of the alloy 247**

---

- 
- Calibrated on > 120 test data sets (partly from Siemens)
    - LCF / TMF
    - strain ranges 0.3 – 1.5%
    - Load ratios  $R = [-\infty, -1, 0]$
    - Hold times 0 – 600 s at  $T_{\max}$
    - In Phase / Out of Phase TMF
    - $T_{\min} = 100 \text{ }^{\circ}\text{C}$  ,  $T_{\max} = (750^{\circ}\text{C}, 850^{\circ}\text{C}, 950^{\circ}\text{C})$

# Fatigue test results: Case of TMF loading



OP loading: transgranular cracking

IP loading:  $T \uparrow$  or hold time  $\uparrow$

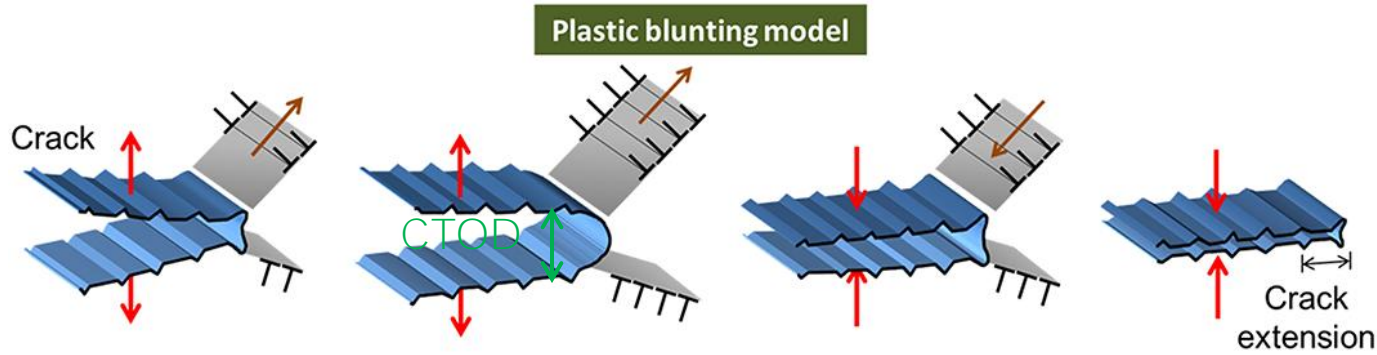
→ intergranular & interdendritic cracking  $\uparrow$

→ number of surface cracks  $\uparrow$

→ number of internal cracks  $\uparrow$

# Lifetime model

— Lifetime = time of growth of microcracks  $\sim 10 \mu\text{m} \rightarrow \sim 1\text{-}5 \text{ mm}$



Source: Chowdhury & Sehitoglu, FFEMS, 2016  
DOI: 10.1111/ffe.12392

$$\frac{da}{dN} = f(CTOD), \quad CTOD = D_{TMF} a \quad \Rightarrow \quad N_F = A D_{TMF}^{-\beta}$$

— Laird & Smith, 1962; Neumann, 1967; Tomkins, 1968; Riedel, 1987

# Approximation of CTOD at low temperatures

$$CTOD = d_n \frac{\Delta J_{eff}}{\sigma_{cyc}}$$

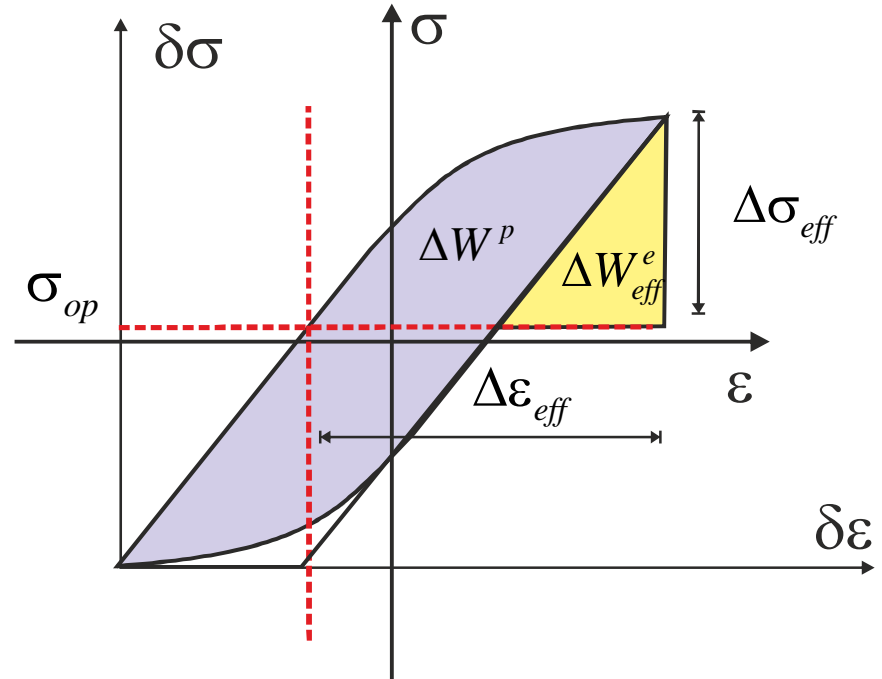
$$\Delta\sigma_{eff} = \sigma_{max} - \sigma_{op} = \Delta\sigma U(R_\sigma), \quad R_\sigma = \frac{\sigma_{min}}{\sigma_{max}}$$

$$a) \Delta J_{eff} = Z_D a, \quad Z_D = 1.45 \frac{\Delta\sigma_{eff}^2}{E} + 2.4 \frac{\Delta\sigma \Delta\varepsilon^p}{\sqrt{1+3n'}},$$

Heitmann, 1983

$$b) \Delta J_{eff} = P_J a, \quad P_J = 1.245 \frac{\Delta\sigma_{eff}^2}{E} + \frac{1.02}{\sqrt{n'}} \Delta\sigma_{eff} \Delta\varepsilon_{eff}^p,$$

Vormwald & Seeger, 1991





# Correction for high temperatures (Riedel, 1987, 2003; Metzger et al. 2013)

---

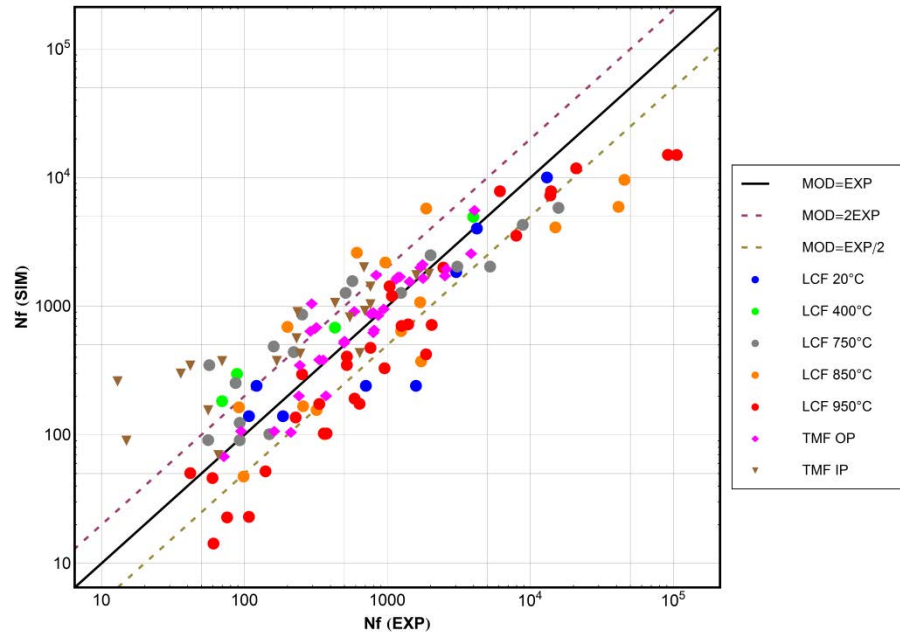
Local creep at crack tip  $\Rightarrow$  *CTOD*  $\nearrow$

$$\text{Creep: } \dot{\varepsilon}^p = B \exp\left(-\frac{Q_{cr}}{RT}\right) \sigma^m, \quad m = 1/n'$$

$$D_{TMF} = \frac{Z_D}{\sigma_{cy}} F(t, T, \sigma)$$

$$F(t, T, \sigma) = \left( 1 + \alpha \exp\left(\frac{Q_{cr}}{RT_{eff}}\right) \int_t \sigma_{cy}^{m-2} \delta\sigma \exp\left(-\frac{Q_{cr}}{RT}\right) dt \right)^{1/m}$$

# Lifetime model with $D_{TMF}$ parameter: comparison experiment/prediction



$$\sigma_{op} = \sigma_{max} [1 - U(R)(1 - R)], \quad R = \frac{\sigma_{min}}{\sigma_{max}}$$

$$U(R) = \left( 0.35 \left( 2.2 - \frac{\sigma_{min}}{\sigma_{max}} \right)^{-2} \right),$$

empirical for MAR-M247 DS, Affeldt (2010)

Simulated stress-strain hysteresis loops

- 
- Deformation behavior can be described satisfyingly for TMF loading with viscoplastic models
  - Fatigue life models based on a measure of the local plastic deformation (CTOD) at the crack tip are a promising tool
  - There is a need for improved estimates of the CTOD and of the crack opening stress under TMF conditions
  - Crack growth model needs to be extended to creep damage
  - Constitutive model implemented as UMAT & TMF life time model implemented as post processing for FEA with Abaqus



---

Thank you for your attention!

# Improved estimate of CTOD (Ainsworth and Budden, 1990; Schweizer, 2013)

---

Combination deformation theory power law creep with same exponent:

$$\varepsilon = \varepsilon^p + \varepsilon^c$$

$$\dot{\varepsilon}^c = B_n(T)\sigma^n, \quad \varepsilon^p = B_0(T)\sigma^n$$

# Improved estimate of CTOD (Ainsworth and Budden, 1990; Schweizer, 2013)

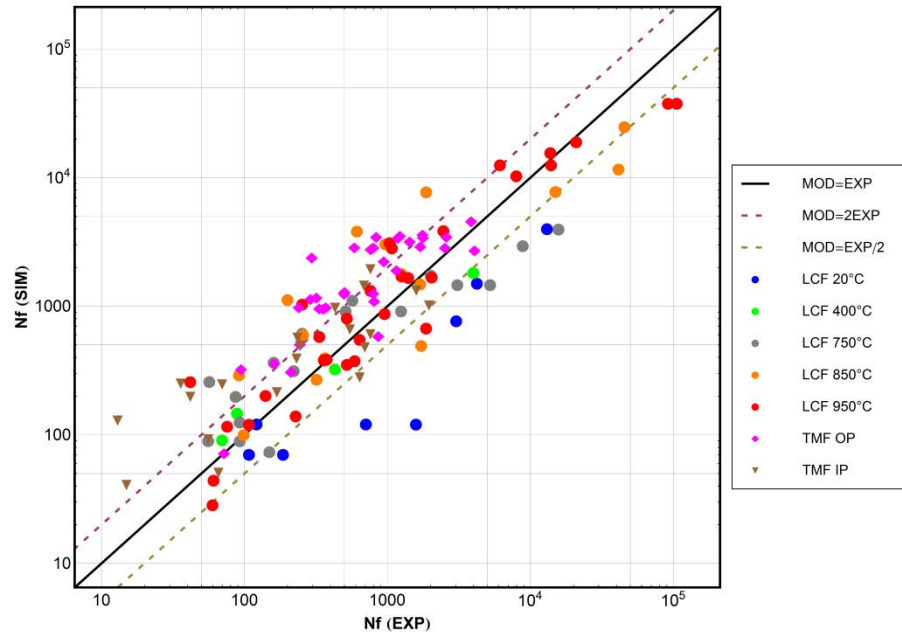
$$D_{TMF} = CTOD / a, \quad CTOD = D_n F^{(n+1)/n} \Rightarrow \frac{dCTOD}{dt} = \frac{n+1}{n} D_n F^{1/n} \dot{F},$$

$$\dot{F} = \left( \frac{C(t)}{B_n} \right)^{n/(n+1)} \left\langle \dot{B}_0 + \frac{n}{n+1} B_0 \left( \frac{\dot{C}}{C} - \frac{\dot{B}_n}{B_n} \right) \right\rangle + B_n \left( \frac{C}{B_n} \right)^{n/(n+1)},$$

$$\dot{C} = (n+1) \frac{B_n C}{B_n J + n B_0 C} \dot{J} + \frac{C J}{B_n J + n B_0 C} \dot{B}_n - \frac{B_n (\dot{B}_0 + B_n)(n+1) - n B_0 \dot{B}_n}{(B_n J + n B_0 C) B_n} C^2,$$

$$\dot{J} = \alpha \langle \sigma^\infty - \sigma_{op} \rangle \dot{\epsilon}^\infty a$$

# Lifetime model with C(t) estimate: comparison experiment/prediction



$$\sigma_{op} = \sigma_{max} \left[ 1 - U(R)(1-R) \right], \quad R = \frac{\sigma_{min}}{\sigma_{max}}$$

$$U(R) = \left( 0.35 \left( 2.2 - \frac{\sigma_{min}}{\sigma_{max}} \right)^{-2} \right),$$

empirical for MAR-M247 DS, Affeldt (2010)

---

# **EXPERIMENTAL AND ANALYTICAL INVESTIGATION OF THE TMF-HCF LIFETIME BEHAVIOR OF TWO CAST IRON ALLOYS**

B. Fedelich<sup>1</sup>, H.-J. Kühn<sup>1</sup>, B. Rehmer<sup>1</sup>, B. Skrotzki<sup>1</sup>

<sup>1</sup> Federal Institute for Materials Research and Testing, Berlin

---



# Outline



---

Experimental results

Assessment of fatigue life reduction due to TMF + HCF loading

Conclusions

---

---

# Experimental Results

---

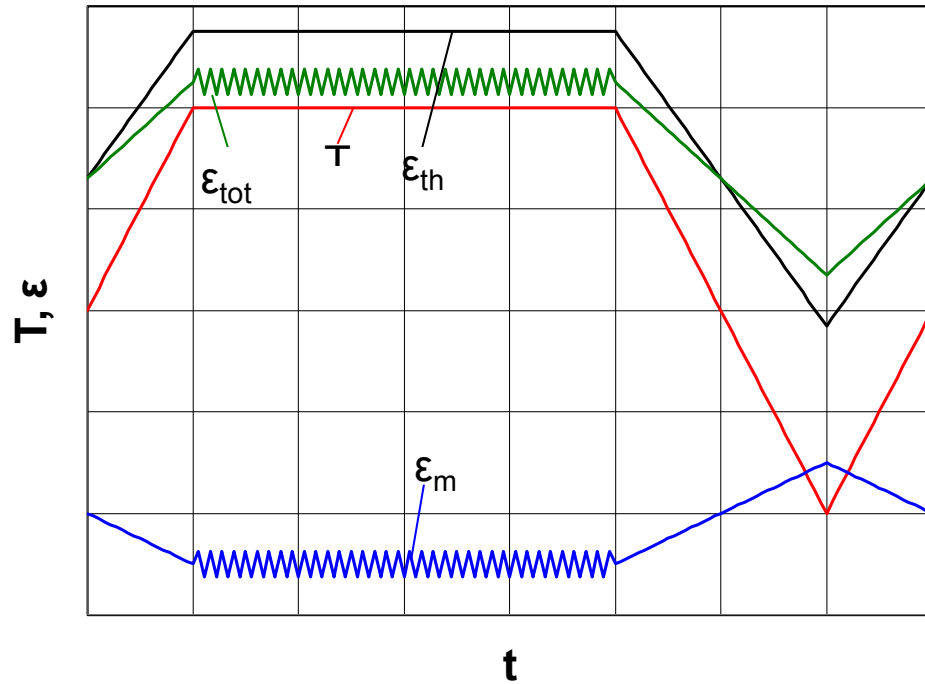
# TMF+HCF - Experimental

---

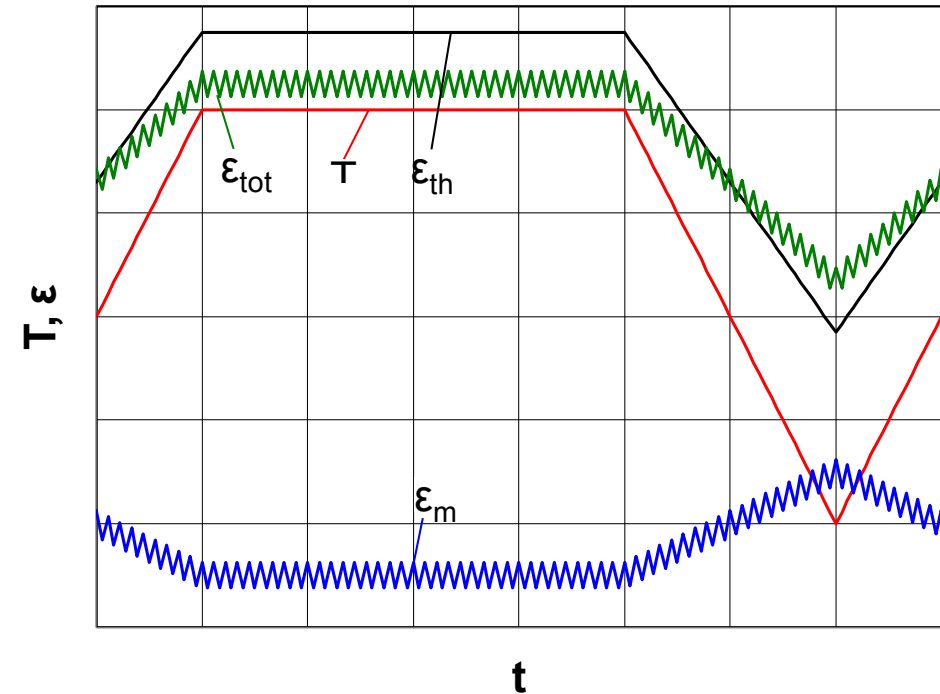
- SiMo 4.05 (ferritic)
    - OP,  $\Delta T$  in 300°C – 700°C
    - $\epsilon_{me, TMF} = 0.12$  or  $0.17$  %
    - $\epsilon^{HCF} = 0.02 - 0.09$  %
    - $f = 5$  or  $20$  Hz
    - LCF-HCF (300 & 700 °C)
- 

- Ni-Resist (austenitic)
  - OP,  $\Delta T = 400^\circ\text{C} - 800^\circ\text{C}$
  - $\epsilon_{me, TMF} = 0.15$  %
  - $\epsilon_{HCF} = 0.017 - 0.09$  %
  - $f = 5$  or  $20$  Hz

# TMF+HCF – Experimental



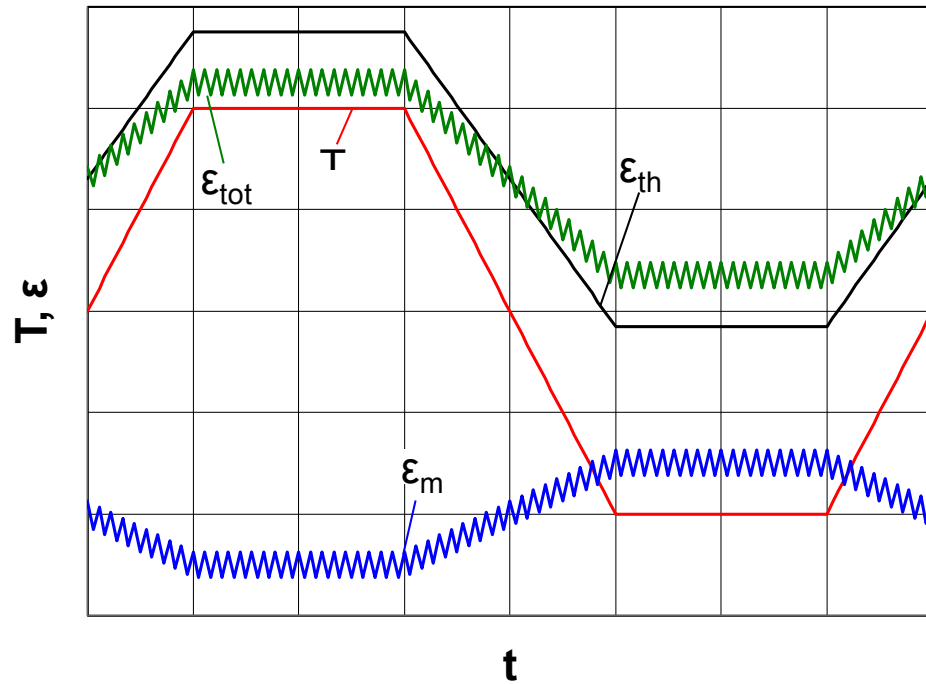
HCF applied only during hold time  
(compression)



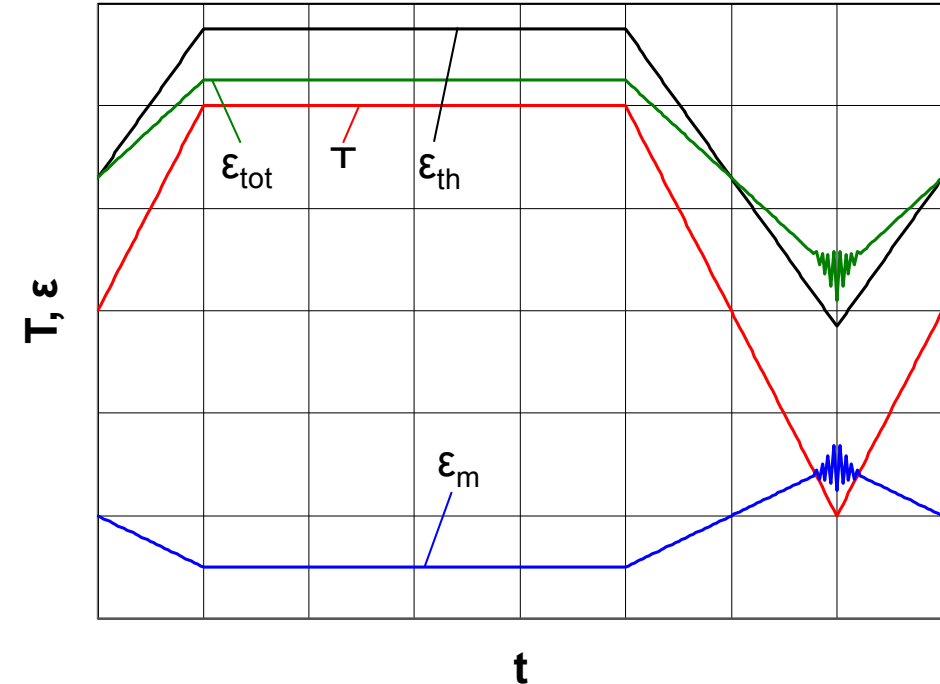
HCF applied continuously during the  
complete cycle

---

# TMF+HCF - Experimental



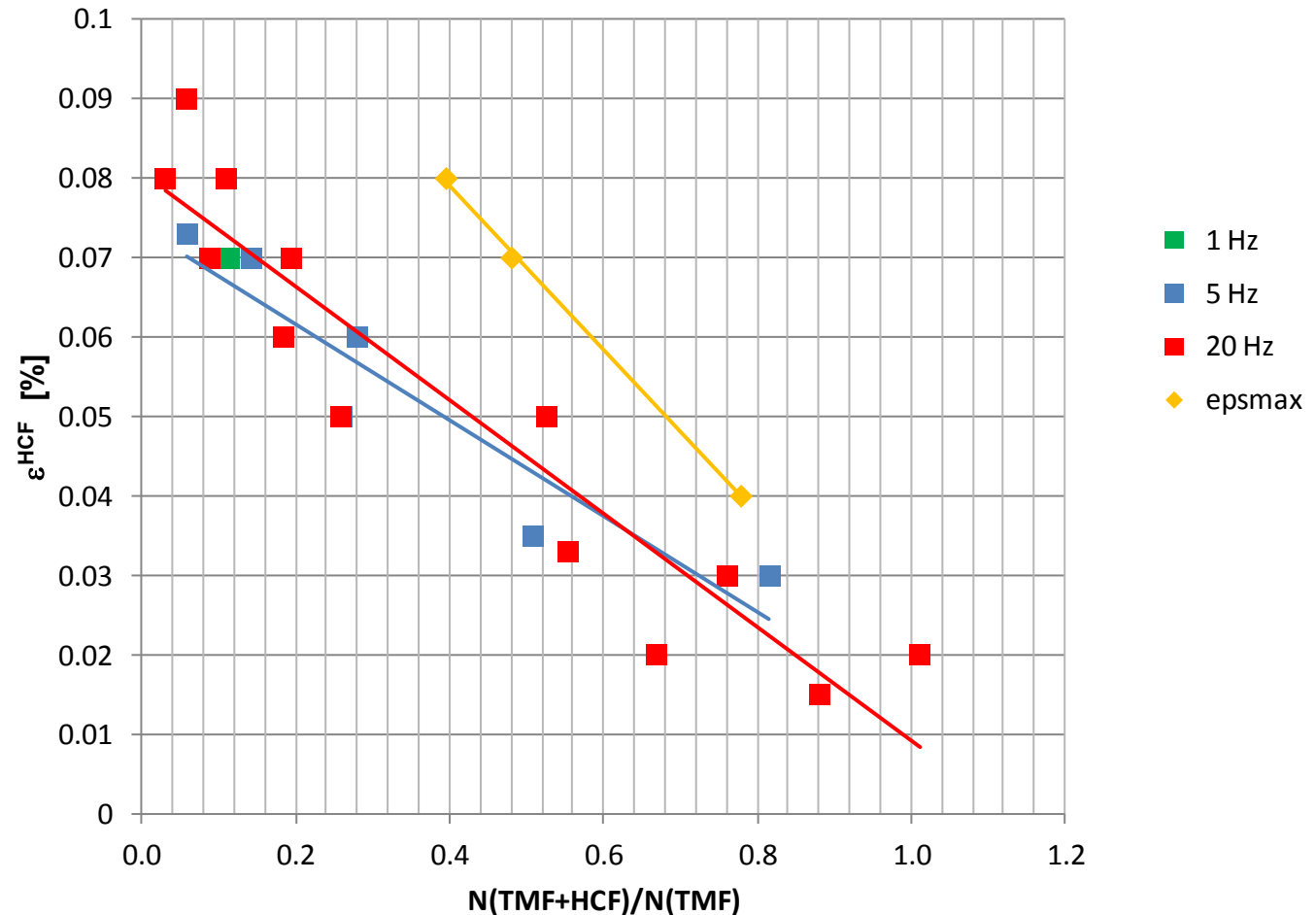
HCF applied continuously during the complete cycle incl. hold time (tensile and compression)



HCF applied only at  $\epsilon_{\max}/T_{\min}$

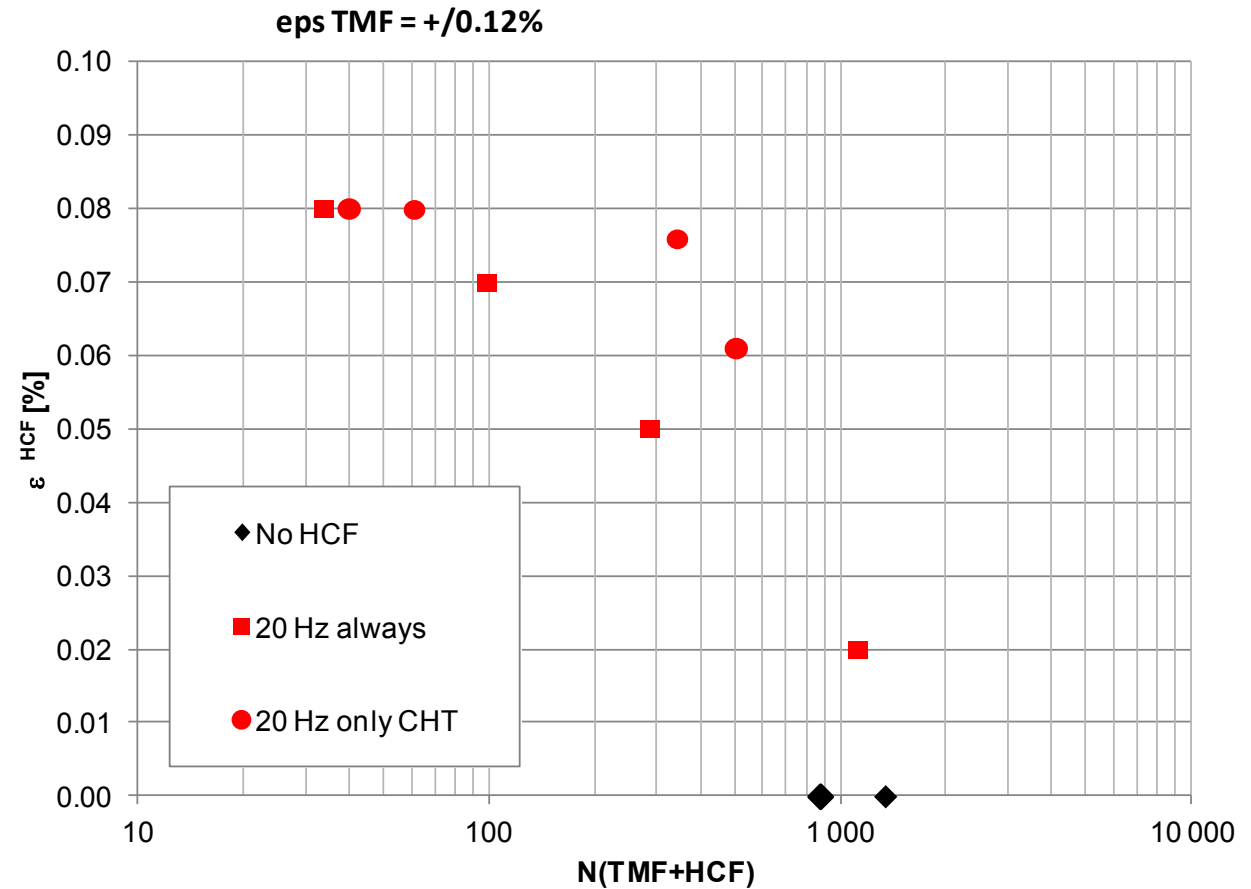
# TMF+HCF Lifetime (SiMo 4.05)

- Effect of HCF-frequency
- Continuous HCF superposition
- $\varepsilon^{\text{TMF}} = 0,1 \% - 0,2 \%$



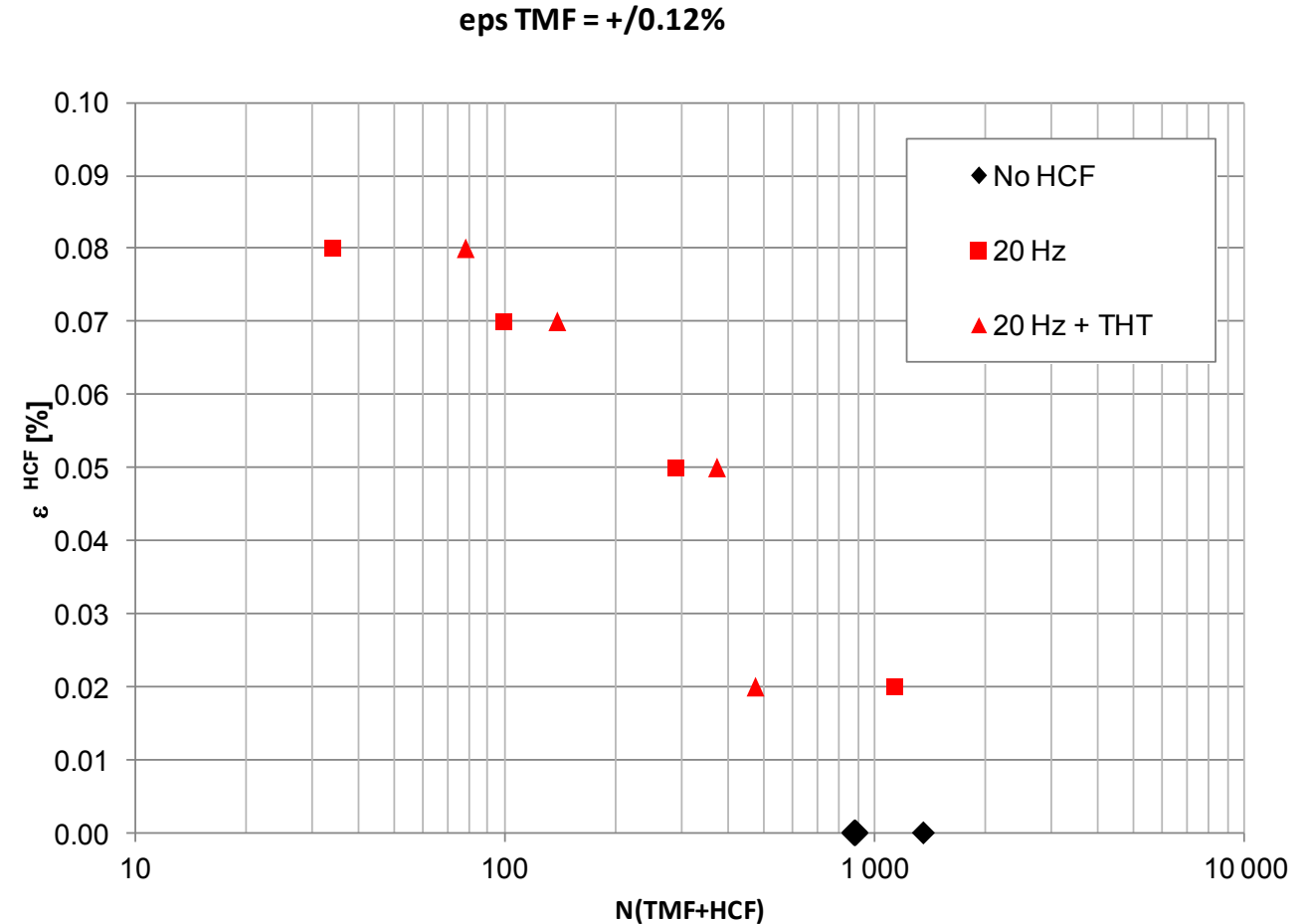
# TMF+HCF Lifetime (SiMo 4.05)

- Effect of HCF-phasing



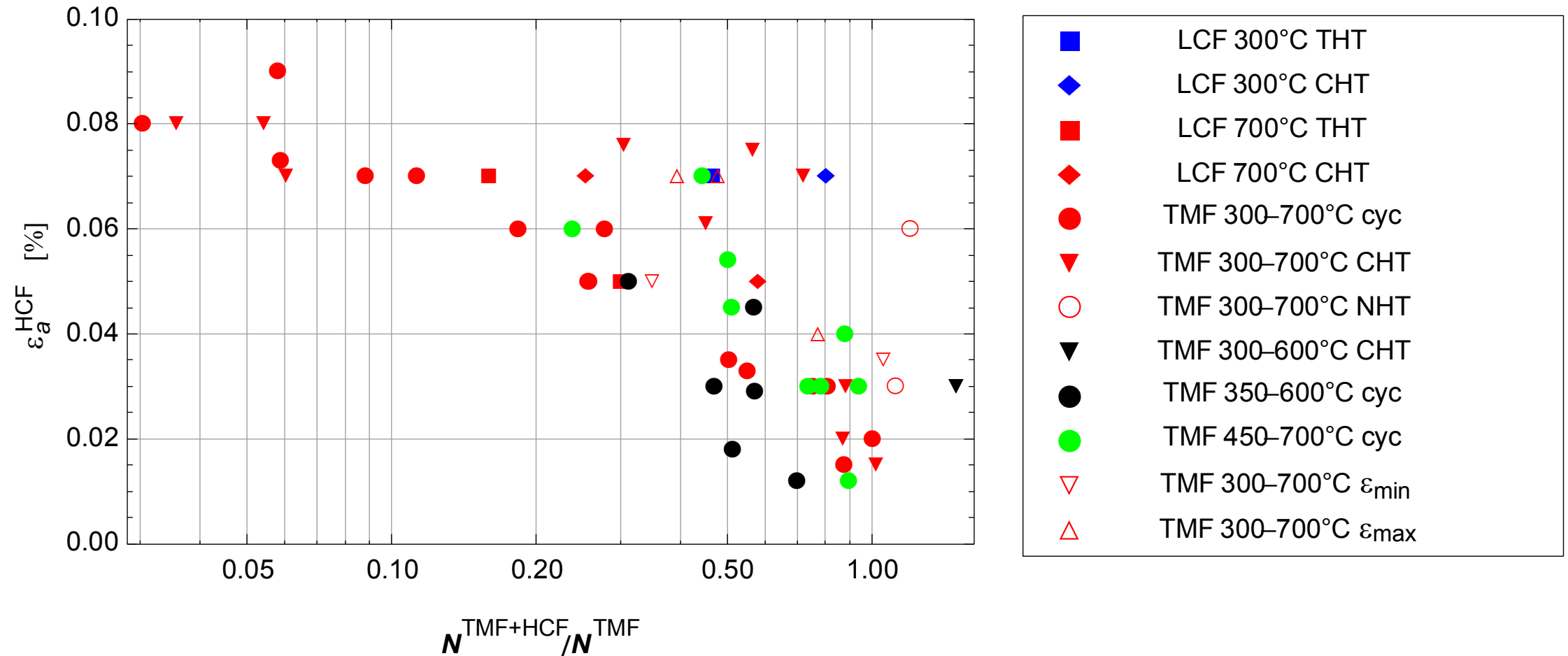
# TMF+HCF Lifetime (SiMo 4.05)

- 
- Effect of additional hold time under tension (THT)



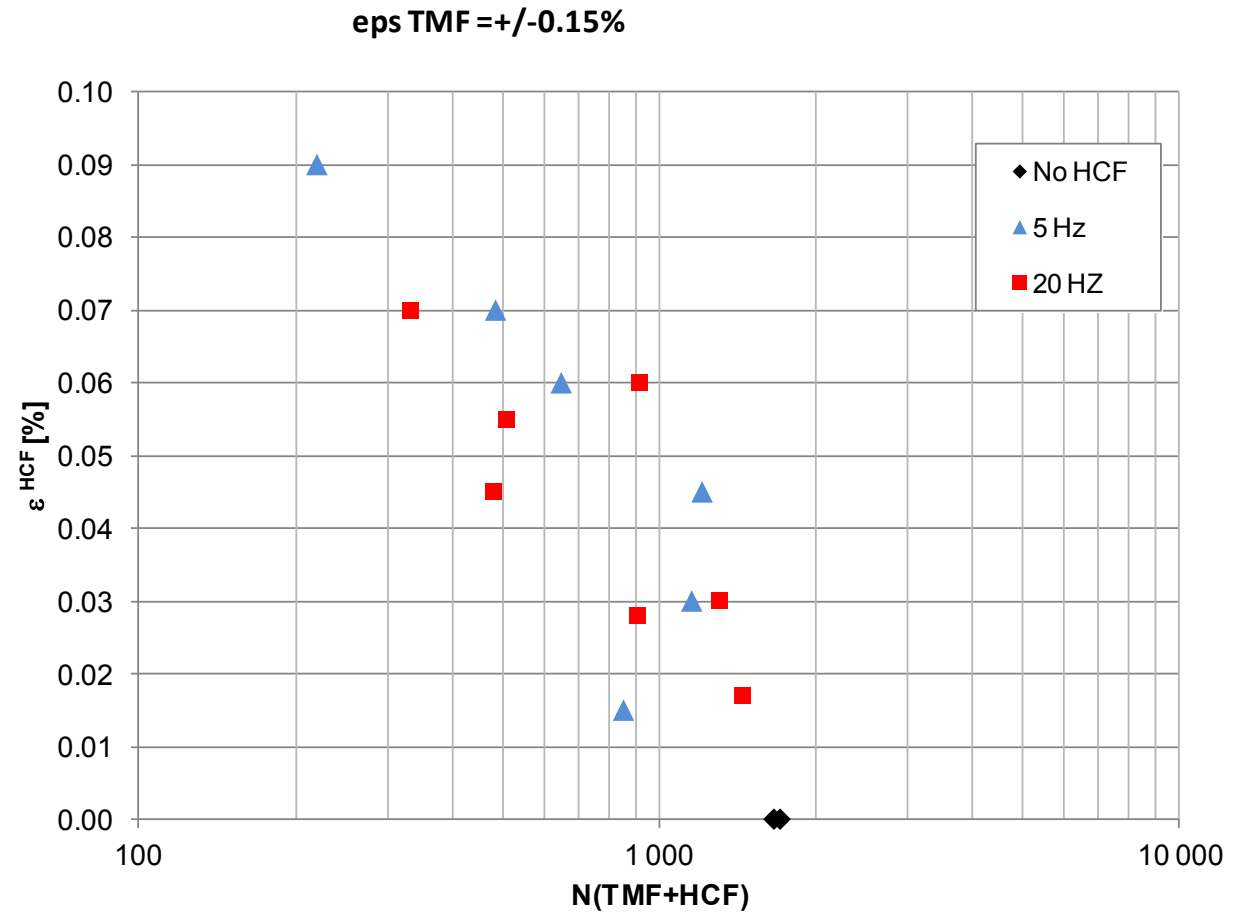


# Effect of HCF amplitude (SiMo 4.05)



# TMF+HCF Lifetime (Ni-Resist)

$T_{\max} = 800^{\circ}\text{C}$

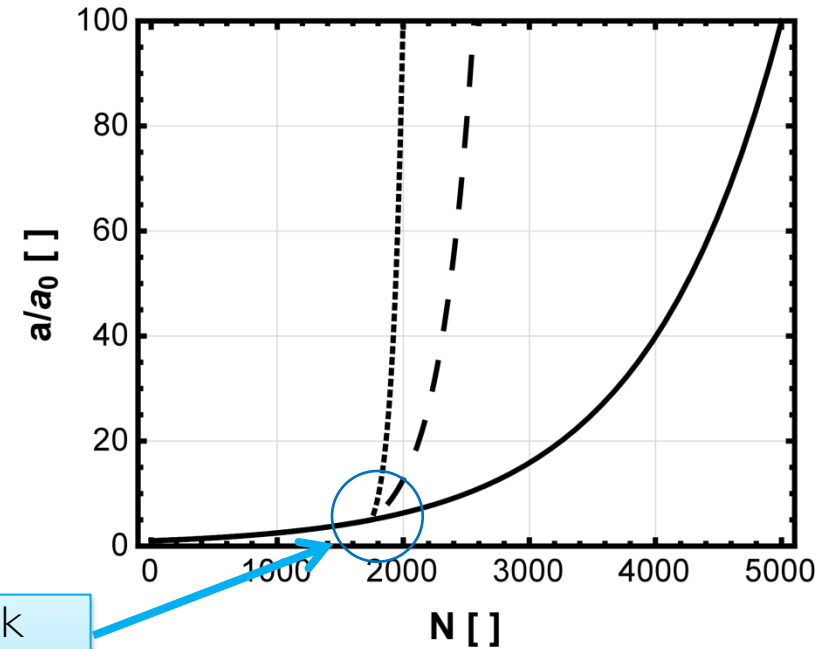
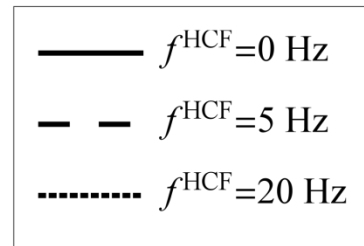
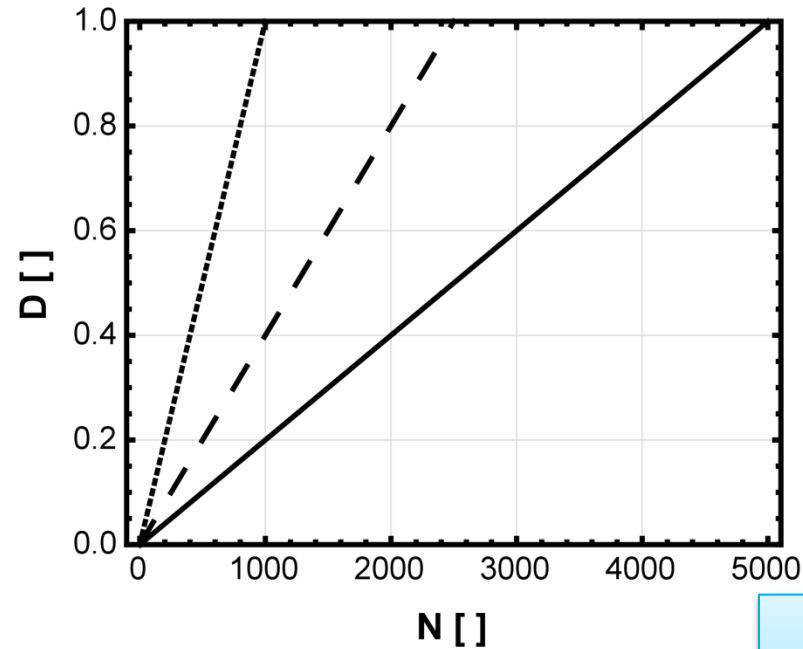


---

# Assessment of fatigue life reduction under TMF+HCF loading

---

# Linear damage accumulation vs. crack growth



Threshold for crack growth under HCF loading (Schweizer et al., 2011)

Linear damage accumulation  $\rightarrow$  large influence of HCF-frequency

Small crack growth  $\rightarrow$  low influence of HCF-frequency

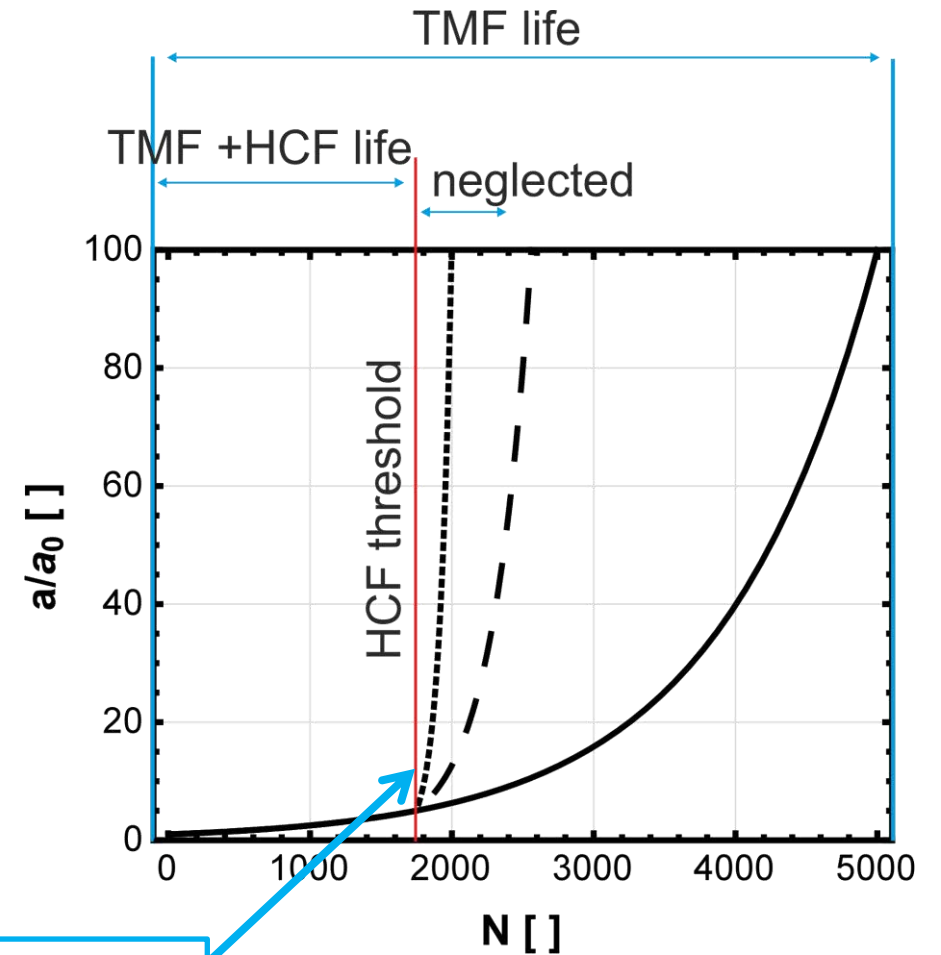
# Estimate of fatigue life reduction ratio

$$\left. \frac{da}{dn} \right|_{TMF+HCF} = \left. \frac{da}{dn} \right|_{TMF} + \sum_{HCF \text{ Cycles}} \left. \frac{da}{dn} \right|_{HCF}, \quad \left. \frac{da}{dn} \right|_{HCF} = \beta \Delta CTOD^{HCF}$$

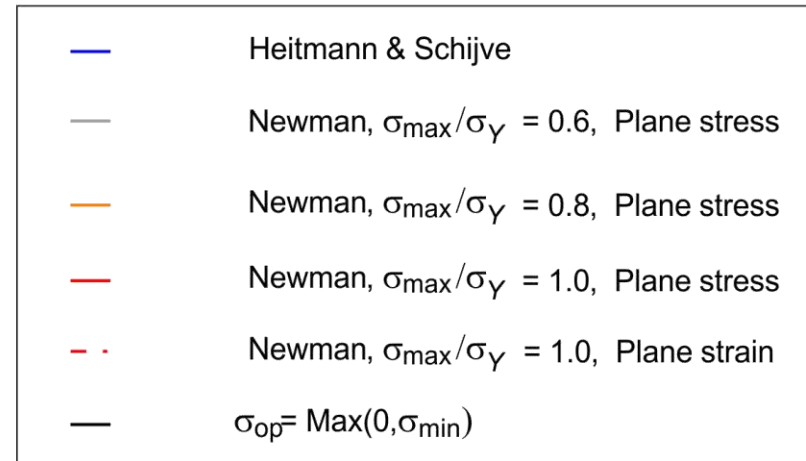
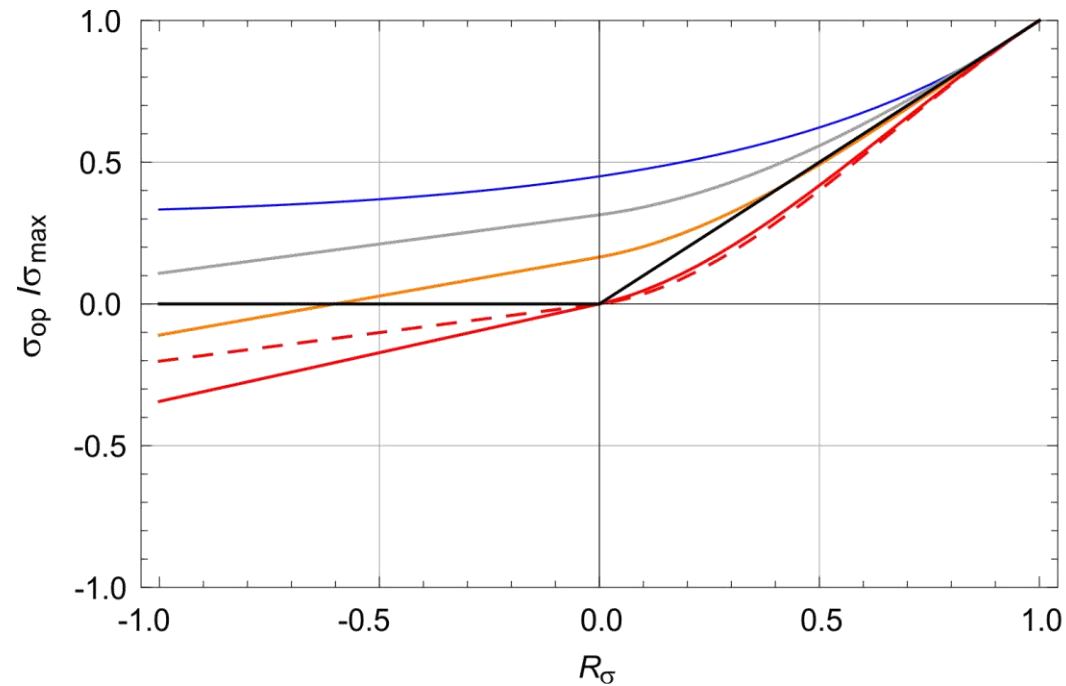
$$\Delta CTOD^{HCF} = d_n \frac{(\Delta \sigma_{eff}^{HCF})^2 \pi a Y^2}{E \sigma_{cyc}}, \quad \Delta \sigma_{eff}^{HCF} = \langle \sigma_{max}^{HCF} - \sigma_{op} \rangle$$

$$\delta_{eff}^{HCF} = \frac{1}{a} \text{Sup}_{HCF \text{ cycles}} \Delta CTOD^{HCF} \rightarrow \frac{N^{TMF+HCF}}{N^{TMF}} = \frac{\text{Log} \left( \frac{\Delta CTOD_{th}}{a_0} \frac{1}{\delta_{eff}^{HCF}} \right)}{\text{Log} \left( \frac{a_f}{a_0} \right)},$$

$$\text{Sup}_{HCF \text{ cycles}} \Delta CTOD^{HCF} = \Delta CTOD_{th}$$



# Crack opening stress function

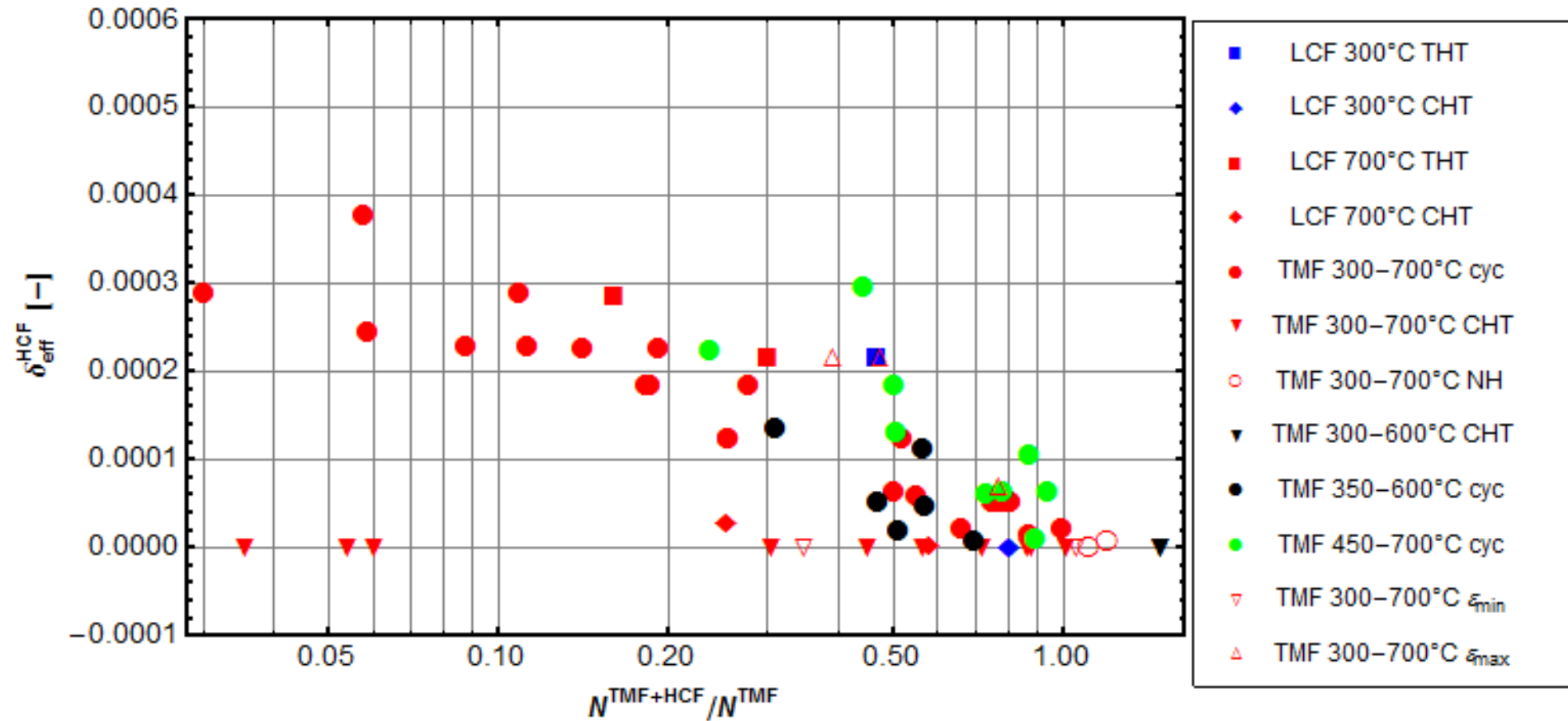


$$\sigma_{op} = \sigma_{\max} \left[ 1 - U(R)(1-R) \right], \quad R = \frac{\sigma_{\min}}{\sigma_{\max}},$$

$$\left\{ \begin{array}{l} U(R) = \frac{3.72}{(3-R)^{1.74}}, \quad \text{Schijve (1981), Heitmann (1984)} \\ U(R) = U(R, \sigma_{\max}/\sigma_Y, \alpha), \quad \text{Newman (1984)} \end{array} \right.$$

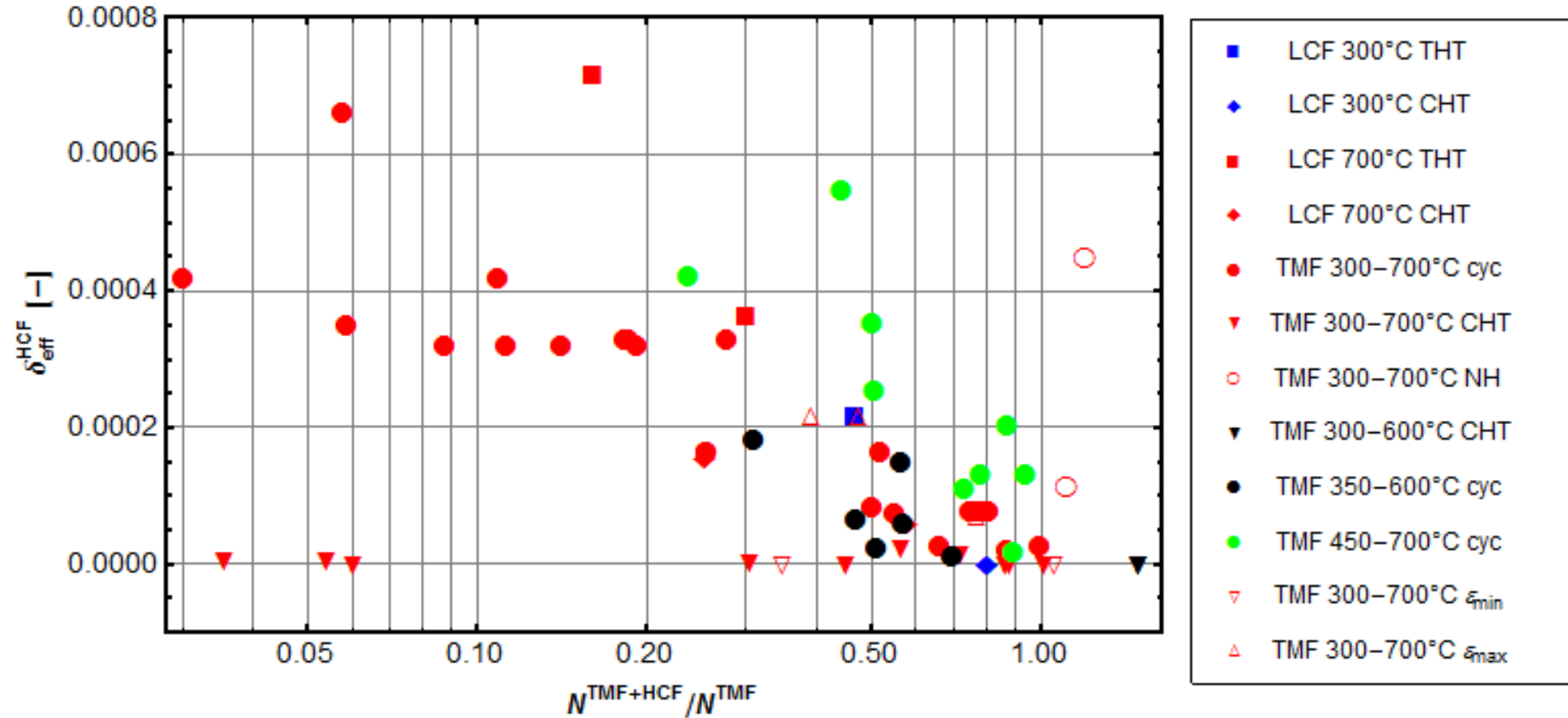
# Opening stress after Heitmann

$$\delta_{eff}^{HCF} = \frac{1}{a} \text{Sup}_{HCF \text{ cycles}} \Delta CTOD^{HCF}$$



# Opening stress after Newman

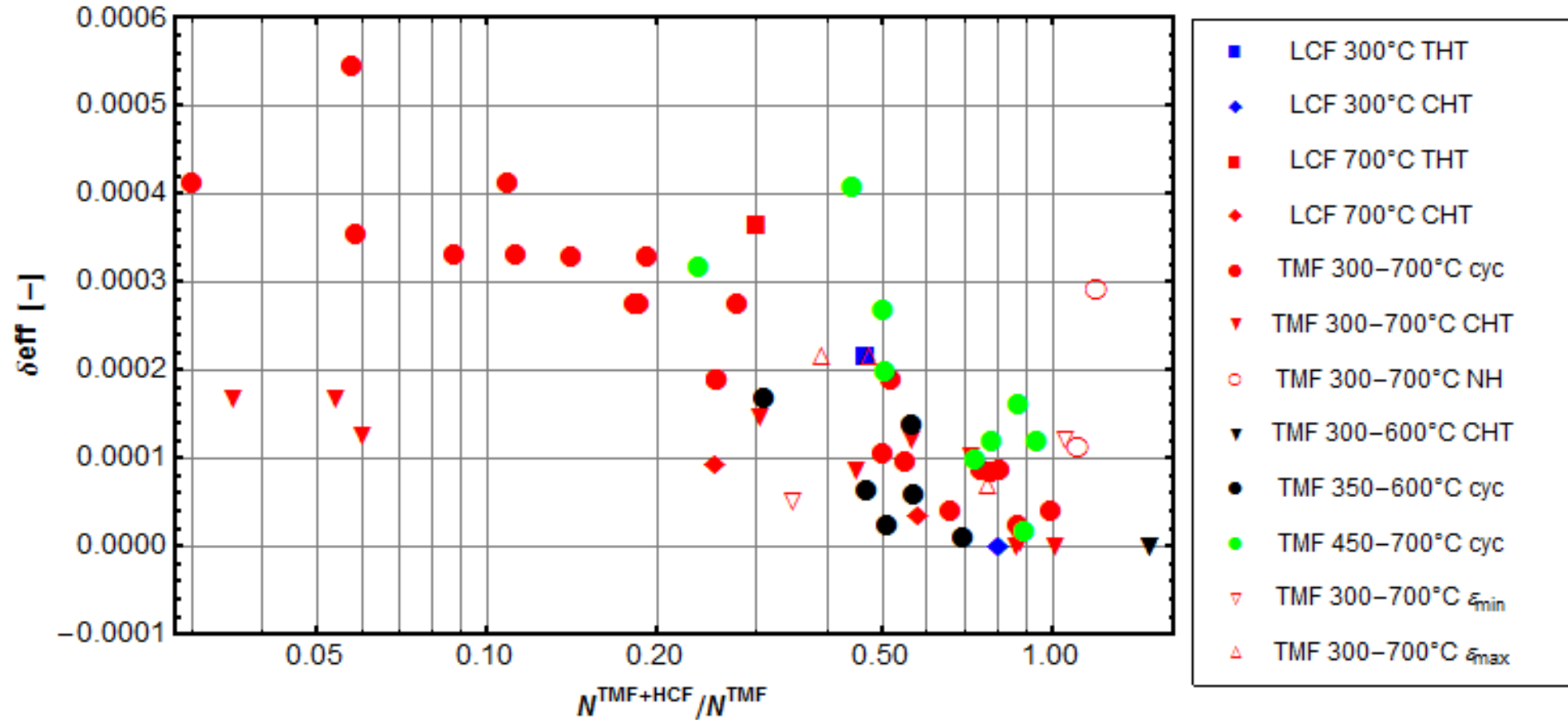
$$\delta_{eff}^{HCF} = \frac{1}{a} \text{Sup}_{HCF \text{ cycles}} \Delta CTOD^{HCF}$$





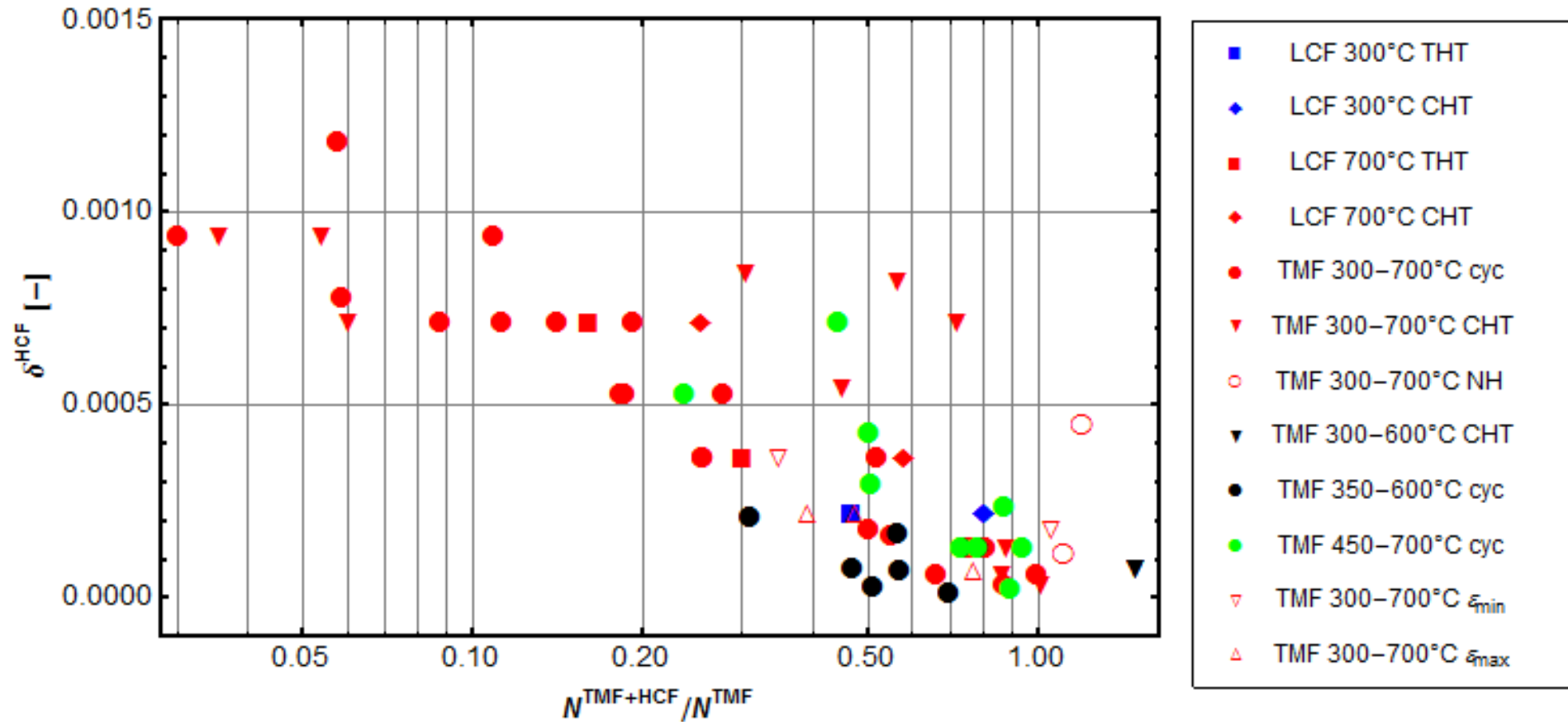
# Opening stress = Max ( 0 MPa, $\sigma_{\min}$ )

$$\delta_{eff}^{HCF} = \frac{1}{a} \text{Sup}_{HCF \text{ cycles}} \Delta CTOD^{HCF}$$

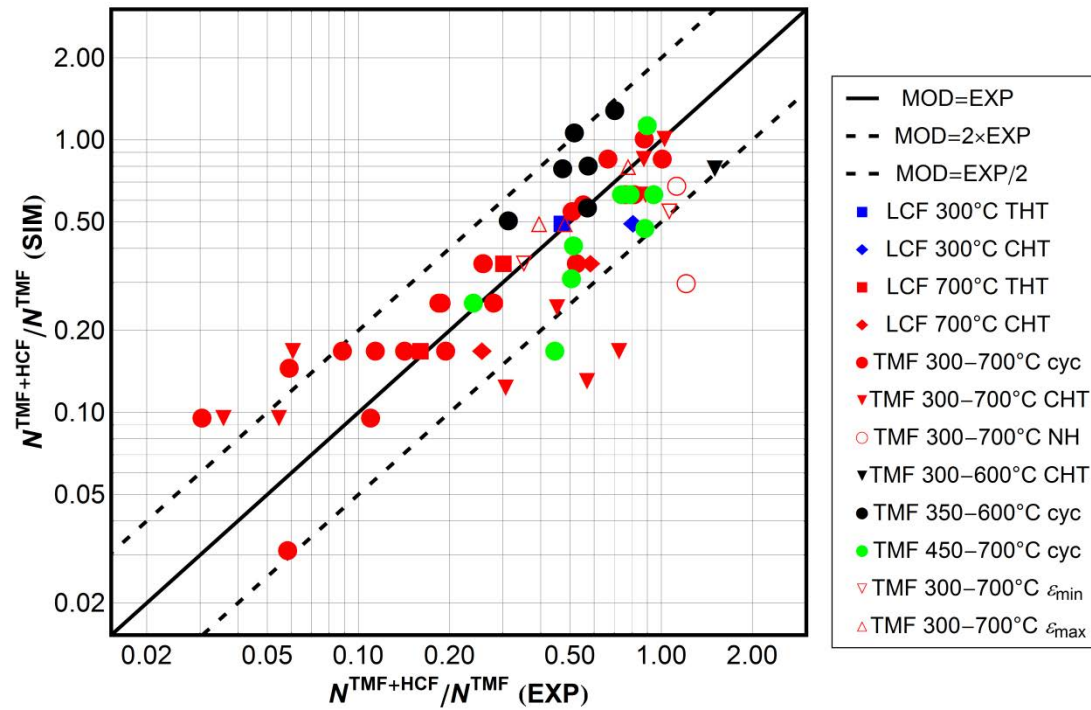


# Total stress range

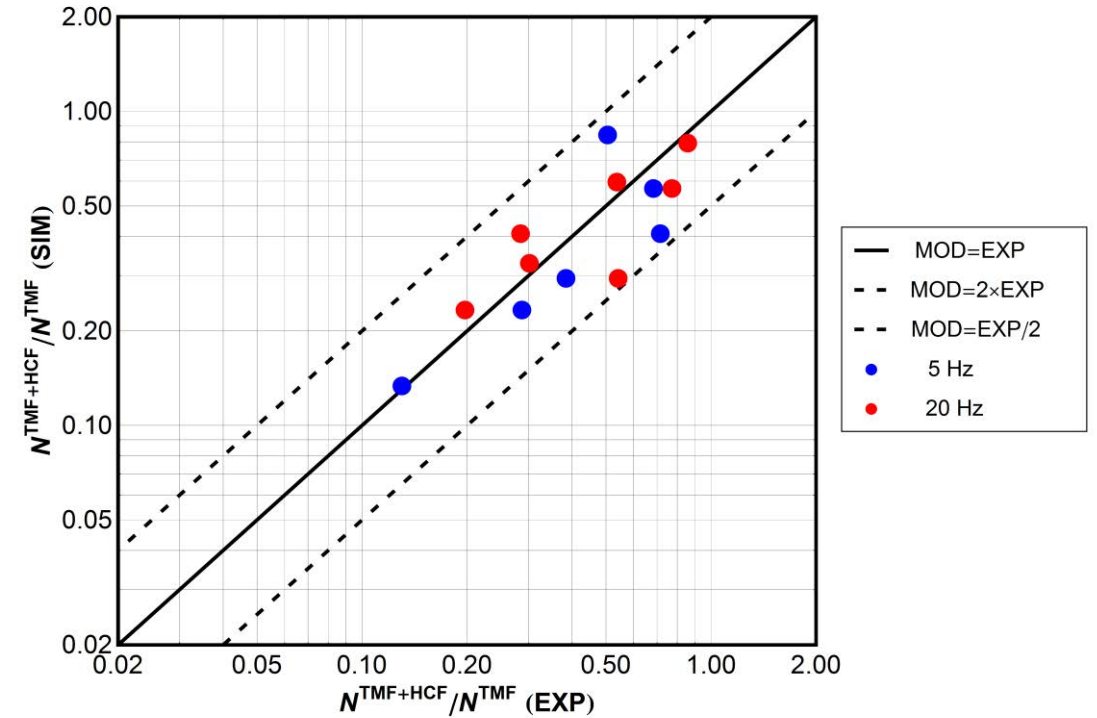
$$\delta_{eff}^{HCF} = \frac{1}{a} \text{Sup}_{HCF \text{ cycles}} \Delta CTOD^{HCF}, \quad \Delta \sigma_{eff}^{HCF} = \sigma_{max}^{HCF} - \sigma_{min}^{HCF}$$



# Experimental vs. predicted fatigue lives (SiMo 4.05)



SiMo 4.05



Ni-Resist

---

# Conclusions

---

# Conclusions

---

- ✓ Weak influence of HCF frequency
  - ✓ Strong influence of HCF strain amplitude
  - ✓ No HCF strain amplitude threshold
  - ✓ Simple assessment rule for the fatigue life reduction ratio
  - ✓ Independent of assessment rule for TMF life
-

# Acknowledgements

---

- Forschungsvereinigung  
Verbrennungskraftmaschinen e. V.

Thank you for your attention!

---



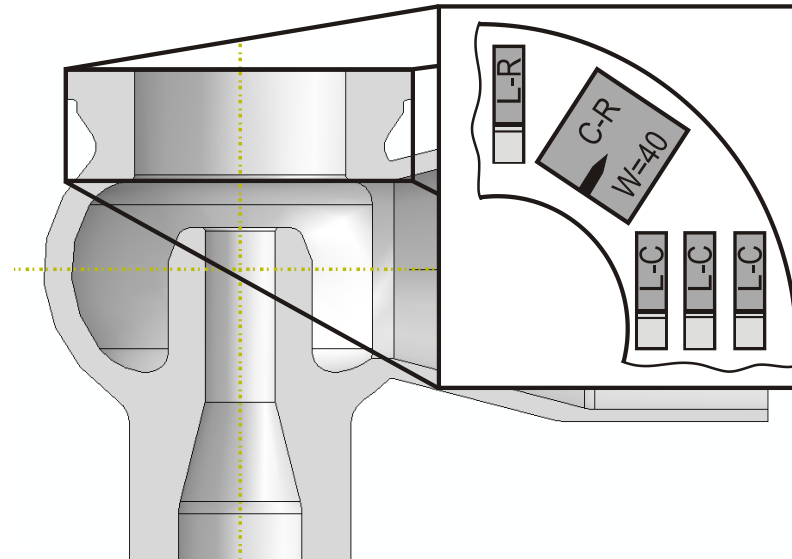
Gefördert durch:



aufgrund eines Beschlusses  
des Deutschen Bundestages



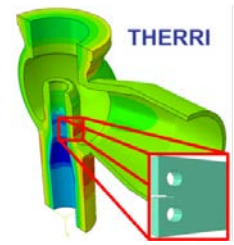
# THERMO-MECHANICAL FATIGUE CRACK GROWTH OF POWER PLANT STEELS



**T. Fischer\***, **B. Kuhn\***, **P. Mutschler\*\***, **M. Paarman\*\***, **M. Sander\*\***,  
**A. Schulz\*\*\***, **D. Rieck\*\*\***

- \* Forschungszentrum Jülich, Institut für Energie und Klimaforschung, Werkstoffstruktur und -eigenschaften (IEK-2)
- \*\* Universität Rostock, Fakultät für Maschinenbau und Schiffstechnik, Lehrstuhl für Strukturmechanik
- \*\*\* TÜV NORD GROUP, Hamburg and Greifswald

# THERMO-MECHANICAL FATIGUE CRACK GROWTH OF POWER PLANT STEELS



## Agenda

- Scope and Intention:  
Thermal Power Plant Operation Challenges
- Thermal Power Plant Component Lifetime:  
Fracture Mechanics Damage Tolerance Concept
- Joint Research Project  
THERRI
  - Objectives and Partners
  - Fatigue Crack Growth Rates Measurements
  - Draft Directive:  
Application of Damage Tolerance Analysis  
to Optimize In-Service Inspection

Gefördert durch:



aufgrund eines Beschlusses  
des Deutschen Bundestages



# SCOPE AND INTENTION: THERMAL POWER PLANT OPERATION CHALLENGES

## Operating Regimes and Components Lifetime Evaluation

- Max. operating temperatures up to 530°C ... 620°C ...720°C (to increase energy conversion efficiency)
- Steam line components:
  - Operation in creep region of materials
  - Start-ups and shut downs as well as load ramps:  $\Delta T$ ,  $\Delta p$
- Components' behaviour and lifetime assessment:
  - Crack propagation rate under creep-fatigue loading [Viswanathan 1989; Speicher, Klenk, Coleman 2013]:

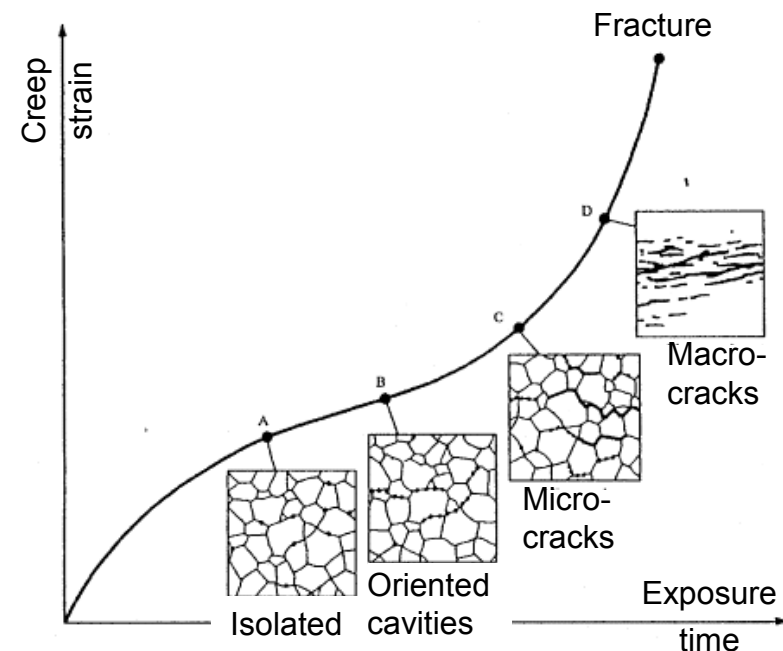


$$\frac{da}{dN} = C_0(\Delta K)^{n_0} + C_1 K^{2m} t_h^{1-m} + C_2 C^* t_h$$

- Thermo-Mechanical fatigue of microcracks (often component lifetime determining) [Schweizer, Seifert, Schlesinger, Riedel 2007]:

$$\frac{da}{dN} \approx \Delta CTOD \approx \frac{a}{2} D_{TMF}$$

$$D_{TMF} = \frac{F(t, T)}{\sigma_{cy}} \left( 1.45 \frac{(\Delta \sigma_{I, eff})^2}{E} + \frac{2.4}{\sqrt{1+3n'}} \frac{(\Delta \sigma_I)^2}{\Delta \sigma_e} \Delta \epsilon_e^{pl} \right)$$



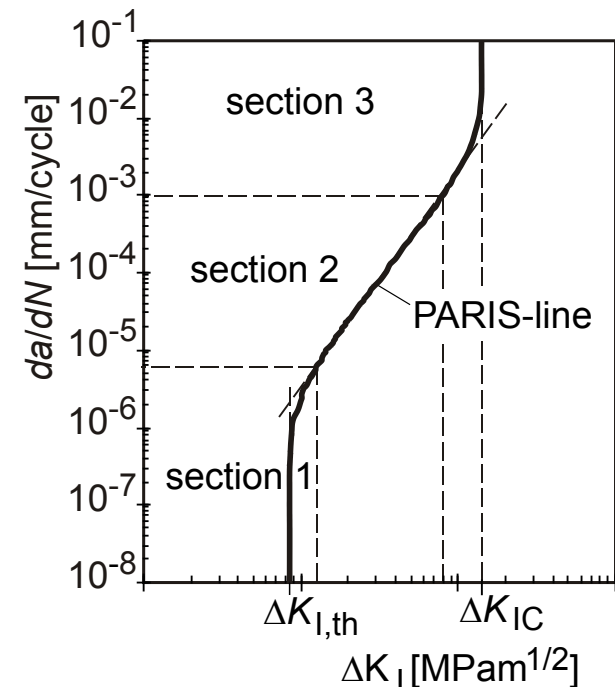
# SCOPE AND INTENTION: THERMAL POWER PLANT OPERATION CHALLENGES

## Change in Operation: Flexibilization

- Energy transition leads to more flexible plant operation with
  - Decreasing full operation time
  - More low-temperature operation and stand-by time
  - Increasing number of load cycles
  - Shorter start-up and shut-down time  
→ high thermal transient loads
- Paradigm shifts in components' lifetime assessment:

$$\frac{da}{dN} = C_0(\Delta K)^{n_0} + C_1 K^{2m} t_h^{1-m} + C_2 C^* t_h$$

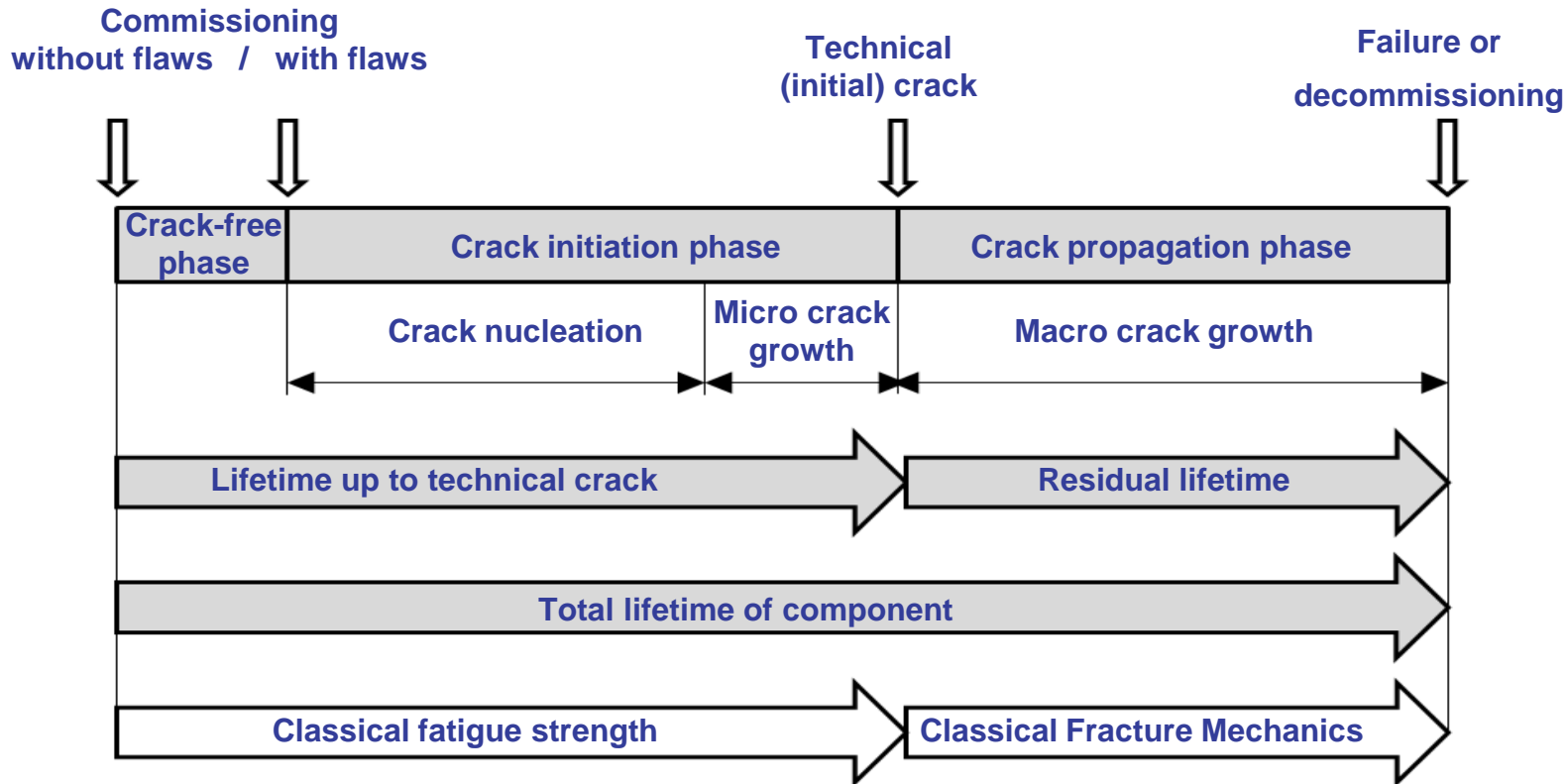
- Dominant degradation: Creep Fatigue → Low Cycle Fatigue
- Mostly strained components:
  - Pipes and bends → thick-walled heaters, valves, fittings, shaped sections
  - Welds → unwelded component areas
- Plain strain constraint in thick-walled components  
→ linear-elastic  $\Delta K$ -concept applicable
- Subcritical long crack growth period



TÜV NORD GROUP

# THERMAL POWER PLANT COMPONENT LIFETIME: FRACTURE MECHANICS DAMAGE TOLERANCE CONCEPT

## Component Lifetime under Dominant Cyclic Loads

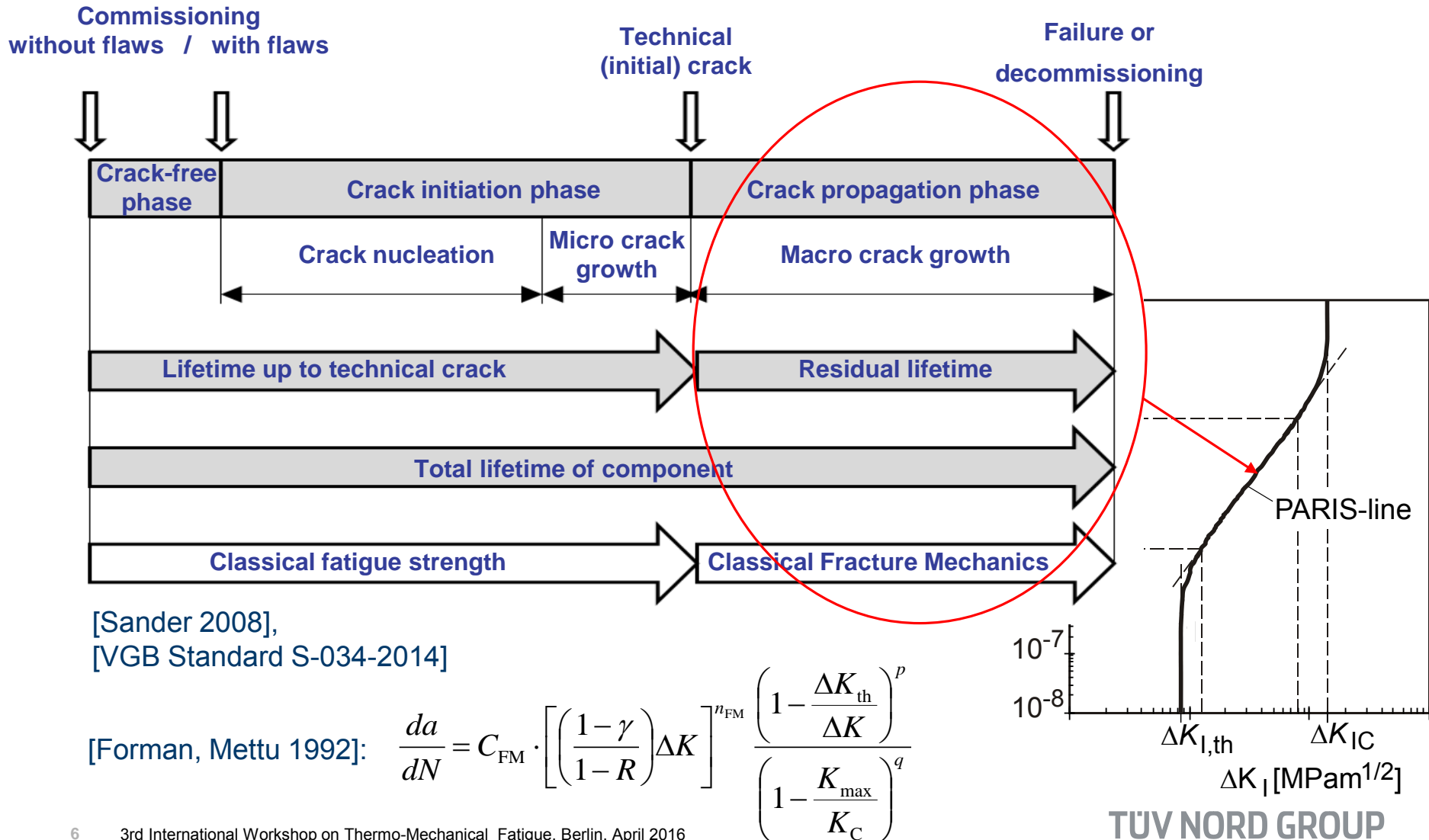


[Sander 2008],

[VGB Standard S-034-2014, Assessment of fatigue loaded components in hydro power plants]

# THERMAL POWER PLANT COMPONENT LIFETIME: FRACTURE MECHANICS DAMAGE TOLERANCE CONCEPT

## Component Lifetime under Dominant Cyclic Loads

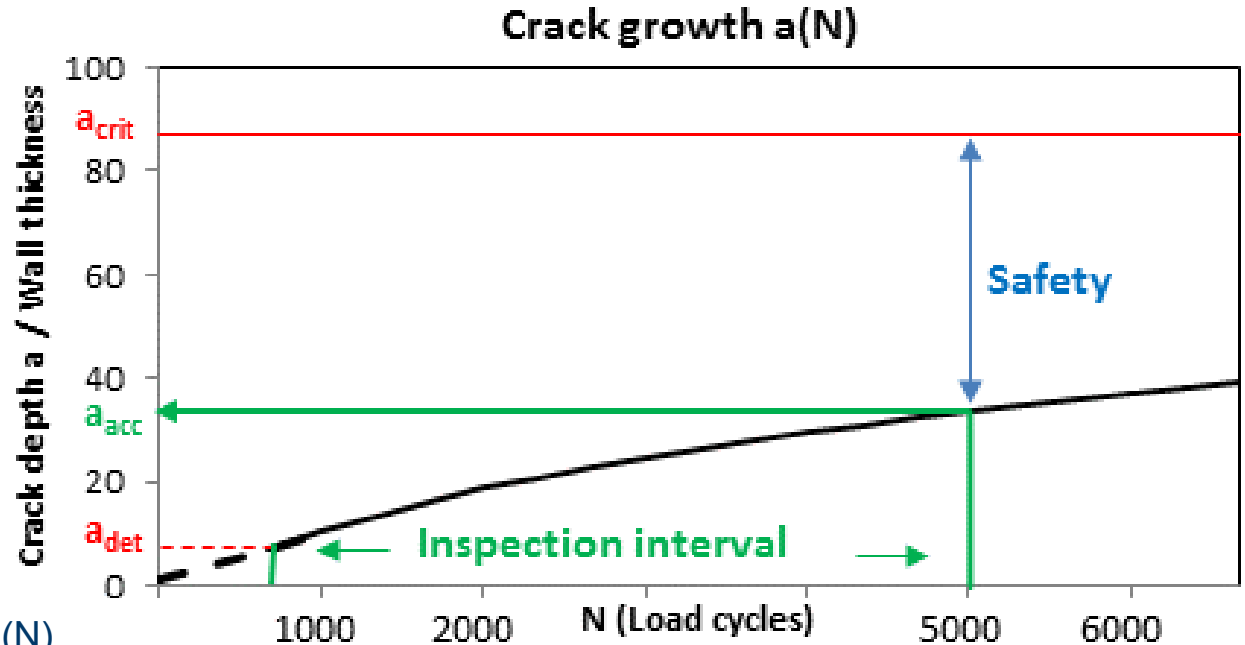


# THERMAL POWER PLANT COMPONENT LIFETIME: FRACTURE MECHANICS DAMAGE TOLERANCE CONCEPT

## Damage Tolerance Analysis and In-Service Inspection

### Work Steps:

- Postulate of an initial crack assumption (crack postulate depth = NDT detection limit  $a_{det}$ )
- Calculation of critical crack depth  $a_{crit}$
- Calculation of fatigue crack growth for predicted cyclic loads
- Comparison of calculated  $a(N)$  and acceptable crack depth  $a_{acc}$  ( $a_{acc} = a_{crit} / \text{safety factor}$ )
- Necessary in-service NDT before reaching acceptable crack depth  $a_{acc}$   
→ max. acceptable inspection interval



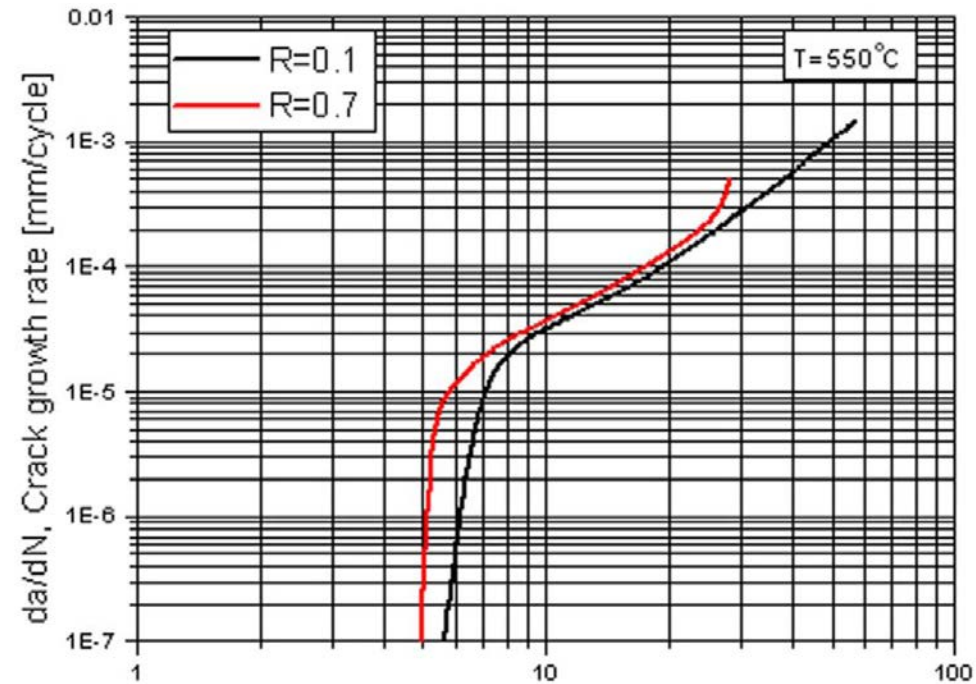
Schematic crack growth diagram  
(Damage Tolerance diagram)

***The Damage Tolerance analysis is the only evaluation method  
to quantify acceptable inspection intervals.  
It is well-regulated and proven in several industries.***

# THERMAL POWER PLANT COMPONENT LIFETIME: FRACTURE MECHANICS DAMAGE TOLERANCE CONCEPT

## Questions and Missing Data Regarding Fatigue Crack Growth of Ferritic-Martensitic Steels at Elevated Temperatures

- Is the small open literature data base conservative?
- What about the influence of
  - medium
  - temperature
- What about the load characteristics
  - T-gradient (slope) of transients
  - dwell time
- Is creep crack growth negligible below a temperature limit?
- Is  $da/dN \sim \Delta K^n$  a sufficient description of thermal crack growth characteristics?
- T-dependent material parameter values of crack growth equation?



[EPRI X20 CrMoV12-1 Steel Handbook 2006]:  
Fatigue crack growth of X20-steel at 550°C

[Forman, Mettu 1992]:

$$\frac{da}{dN} = C_{FM} \cdot \left[ \left( \frac{1-\gamma}{1-R} \right) \Delta K \right]^{n_{FM}} \frac{\left( 1 - \frac{\Delta K_{th}}{\Delta K} \right)^p}{\left( 1 - \frac{K_{max}}{K_C} \right)^q}$$

# JOINT RESEARCH PROJECT THERRI

## Objectives and Partners

- **Experimental Determination of Fatigue Crack Growth Rates**
  - (ferritic-)martensitic steels at **300 – 600°C**
  - **cyclic thermal loads**
  - medium and creep crack growth influence
- **Enhancement of Fracture Mechanics Calculation Methodology**
  - extended FEM (**XFEM**)
  - and analytical solutions for thermal fatigue crack growth analysis
- **Qualification of NDT**
  - verification of flaw detection limit
  - and of crack depth measurement
- **Reference Object**
  - damage tolerance analysis of thermal power plant components
- **Draft Directive**

### Project Partners:

- **TÜV NORD SysTec GmbH & Co. KG**
- **University of Rostock**  
Professorial chair for Technical Thermodynamics
- **University of Rostock**  
Institute of Structural Mechanics
- **Research centre Forschungszentrum Jülich**  
Institute of Energy and Climate Research, IEK-2
- **Coal-fired power plant KNG Rostock**

### Project Runtime:

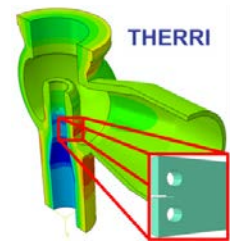
11/2013 – 10/2016

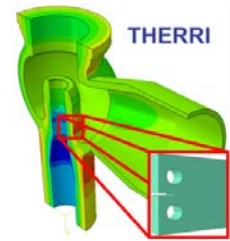
Gefördert durch:



Bundesministerium  
für Wirtschaft  
und Energie

aufgrund eines Beschlusses  
des Deutschen Bundestages





## Fatigue Crack Growth Rates Measurements

- C(T)- and SEN-specimens were taken from a dismantled TBV (turbine bypass valve) provided by industrial partner KNG Rostock
- Material data: martensitic X 20 CrMoV 12 1

Yield strength $R_{p0.2}$ [N/mm <sup>2</sup> ]	Tensile strength $R_m$ [N/mm <sup>2</sup> ]	Elongation $A_5$ [%]
490	690 - 840	≥14

[DIN EN 10216-2]

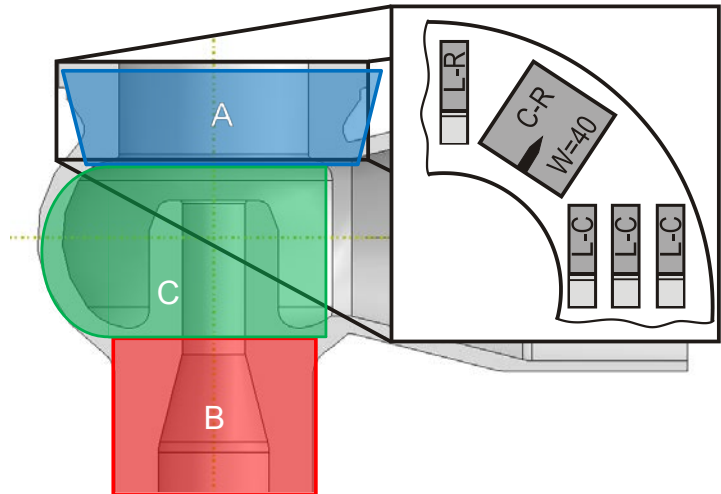


- Measurements are done in Rostock and in Jülich

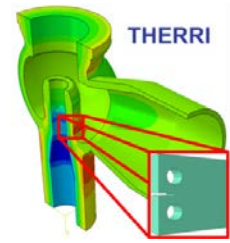


- FCG tests of influence of
  - orientation
  - frequency
  - stress ratio R
 on threshold  $\Delta K_{th}$  and PARIS-region
- FCG tests with thermal transients  $T(t) + p$

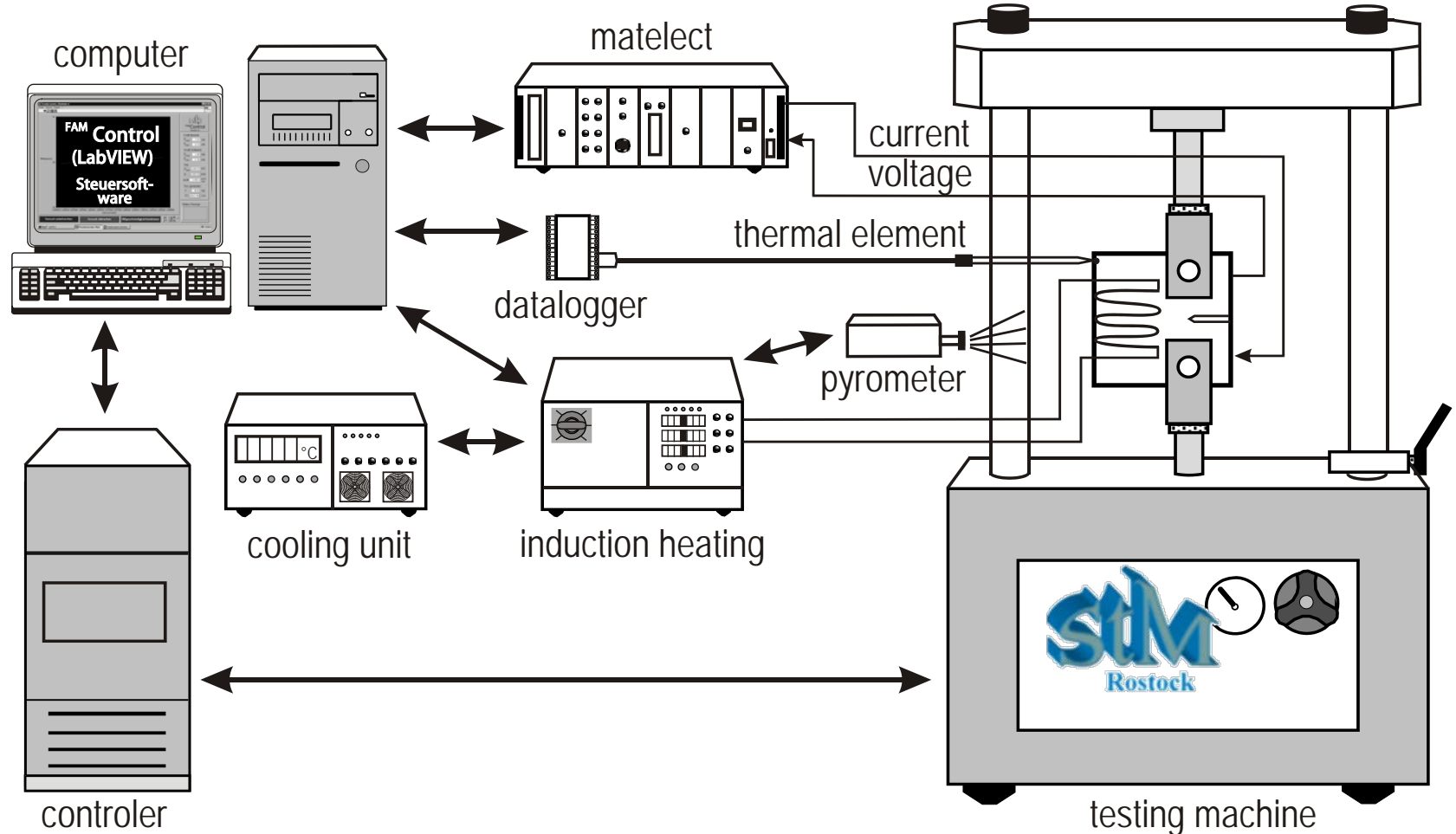
- Tests with holding time
- under steam (Ar/H<sub>2</sub>O) atmosphere
- at elevated temperatures T

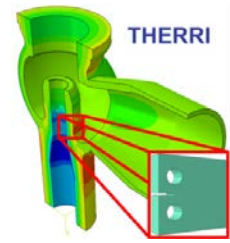






## Fatigue Crack Growth Rates Measurements: Scheme of Test Setup at Uni of Rostock for isothermal FCG tests on CT(T)-specimens

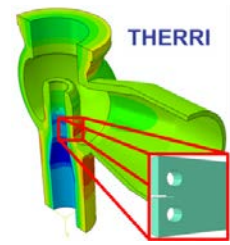




## Fatigue Crack Growth Rates Measurements: Test Setups at FZ Jülich (IEK-2)

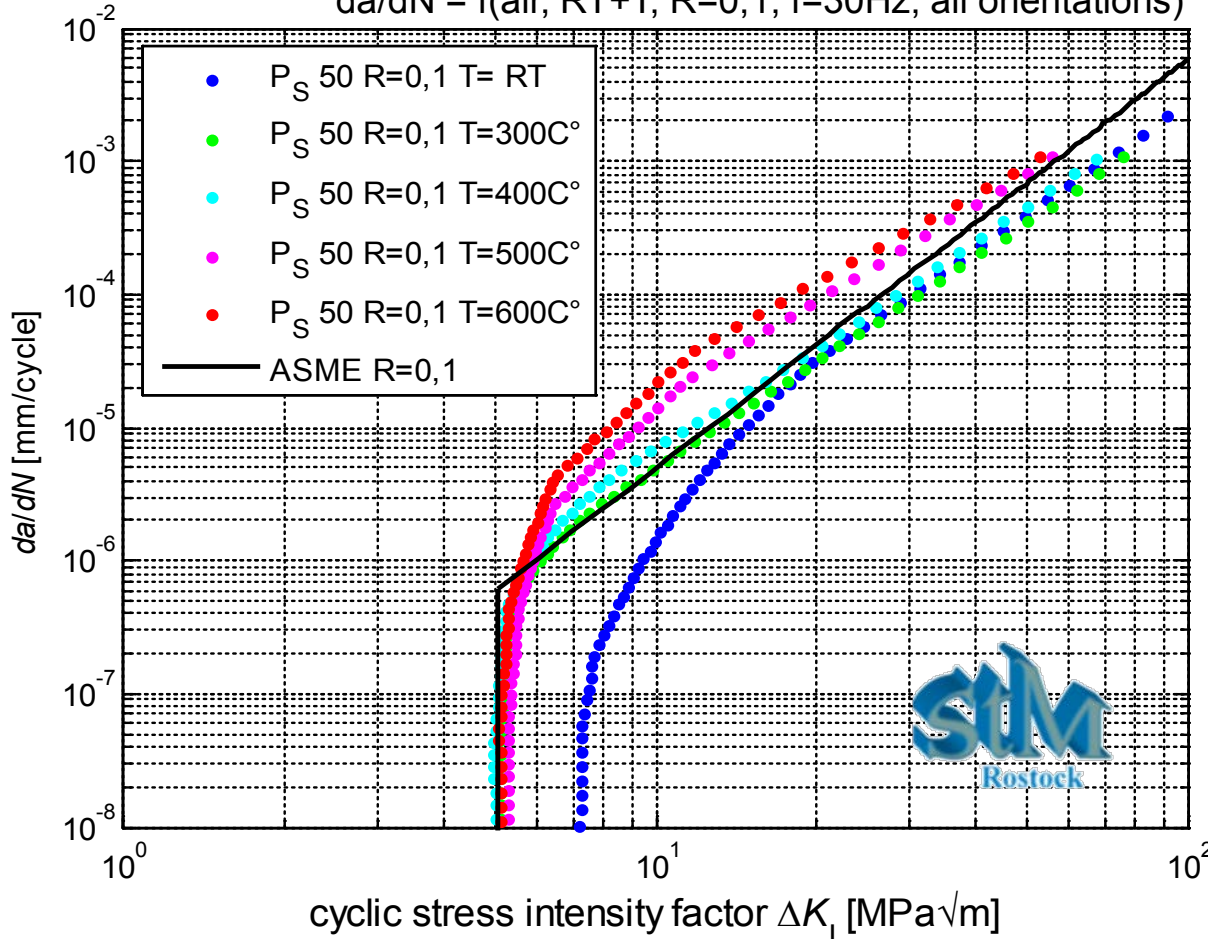


- Tests with and without holding time
- Under air or steam (Ar/H<sub>2</sub>O) atmosphere
- at elevated temperatures



## FCG Tests: Temperature Dependency, Comparison with Standard Crack Propagation Rates

$$da/dN = f(\text{air}, RT+T, R=0,1, f=30\text{Hz}, \text{all orientations})$$



### Paris-line:

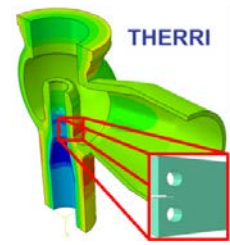
- At  $T = 500^\circ\text{C}$  and  $600^\circ\text{C}$  it has a slightly lower slope and is significantly higher than at lower temperatures

### Threshold $\Delta K_{th}$ :

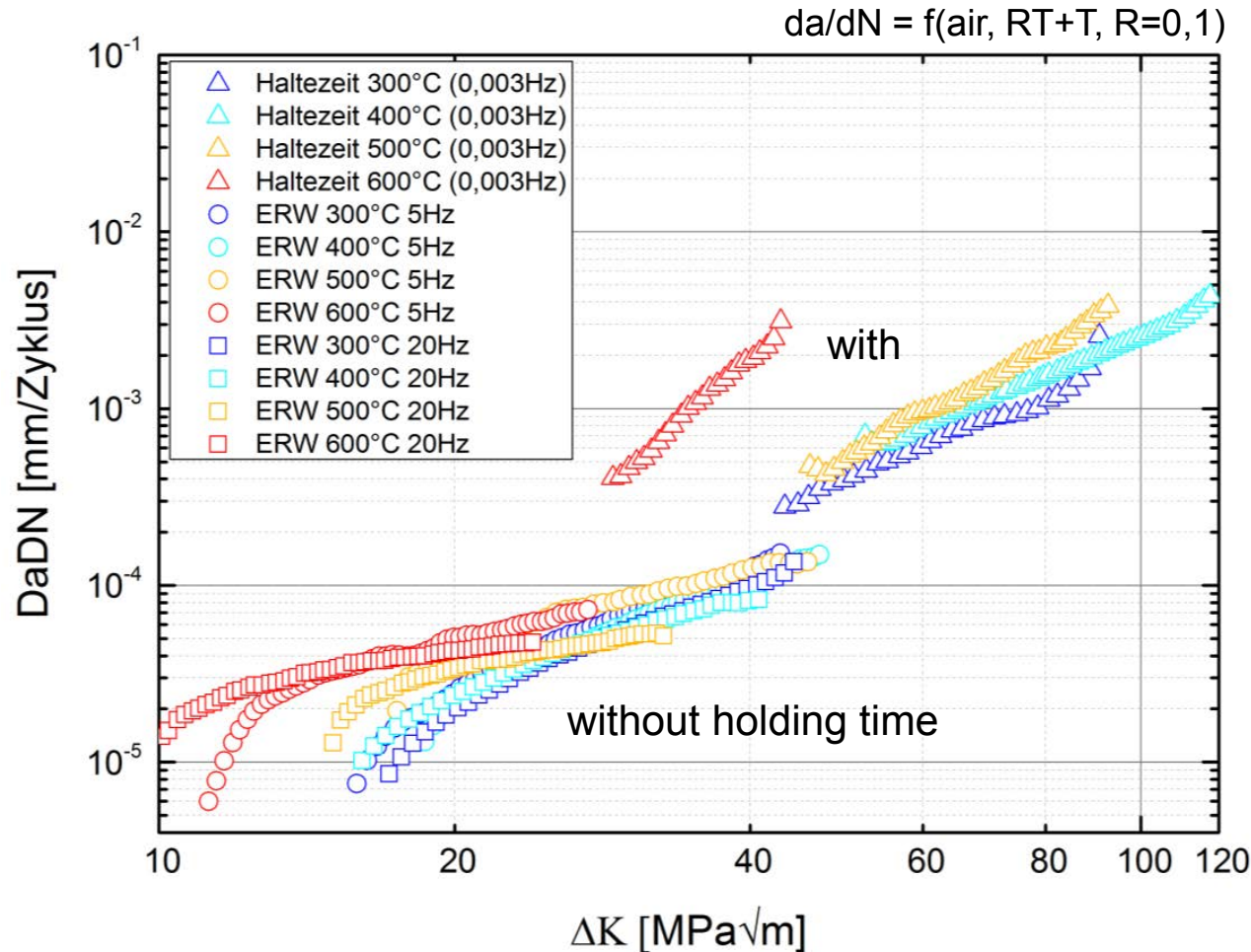
- Significant lower at  $T \geq 300^\circ\text{C}$  than at room temperature
- No temperature dependence between  $300^\circ\text{C}$  and  $600^\circ\text{C}$

### Comparison:

- ASME Code curve for ferritic steels in RPV environment up to  $300^\circ\text{C}$  does not cover  $T > 400^\circ\text{C}$  curves



## FCG Tests with / without 5 Minutes Holding Time: Fatigue Dominated Crack vs. Creep-Fatigue Growth

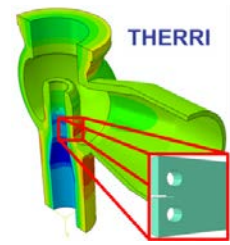


### ■ Paris-line:

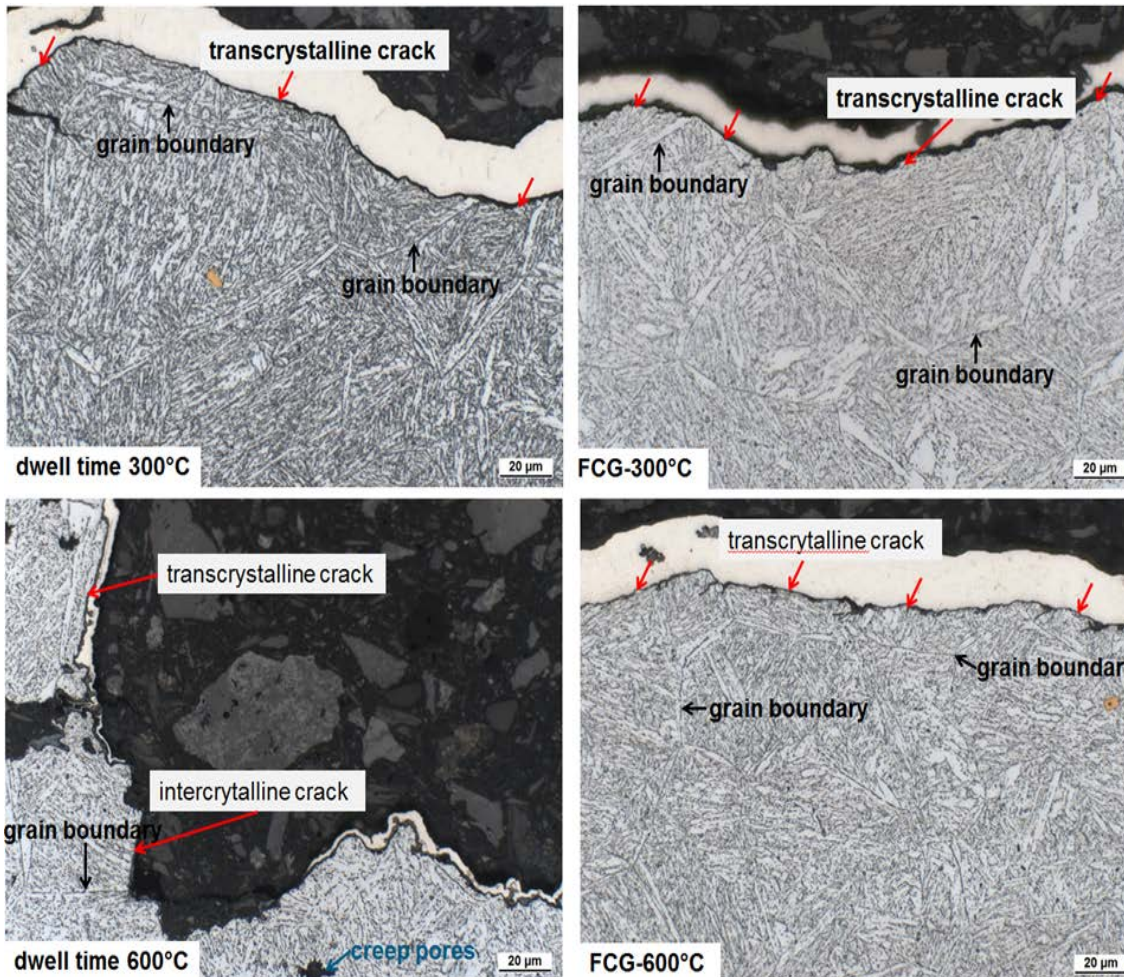
- At all temperatures it has a slightly higher slope and is higher with than without holding time
- Only at  $T = 600^\circ\text{C}$  it is significantly higher with holding time

### ■ Crack initiation:

- Higher at lower frequency (with holding time)



## FCG Tests with / without 5 Minutes Holding Time: Fatigue Dominated Crack vs. Creep-Fatigue Growth



### ■ Microstructural investigations:

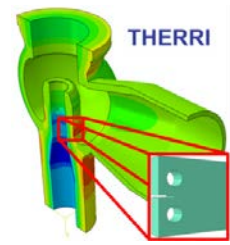
- Crack areas of the C(T) specimens were analysed for trans- or intercrystalline crack growth.
- Only at  $T = 600^{\circ}\text{C}$  there is a superposition of both fatigue (transgranular) and creep (intergranular) damage mechanism.

## FCG Tests in H<sub>2</sub>O Steam Atmosphere

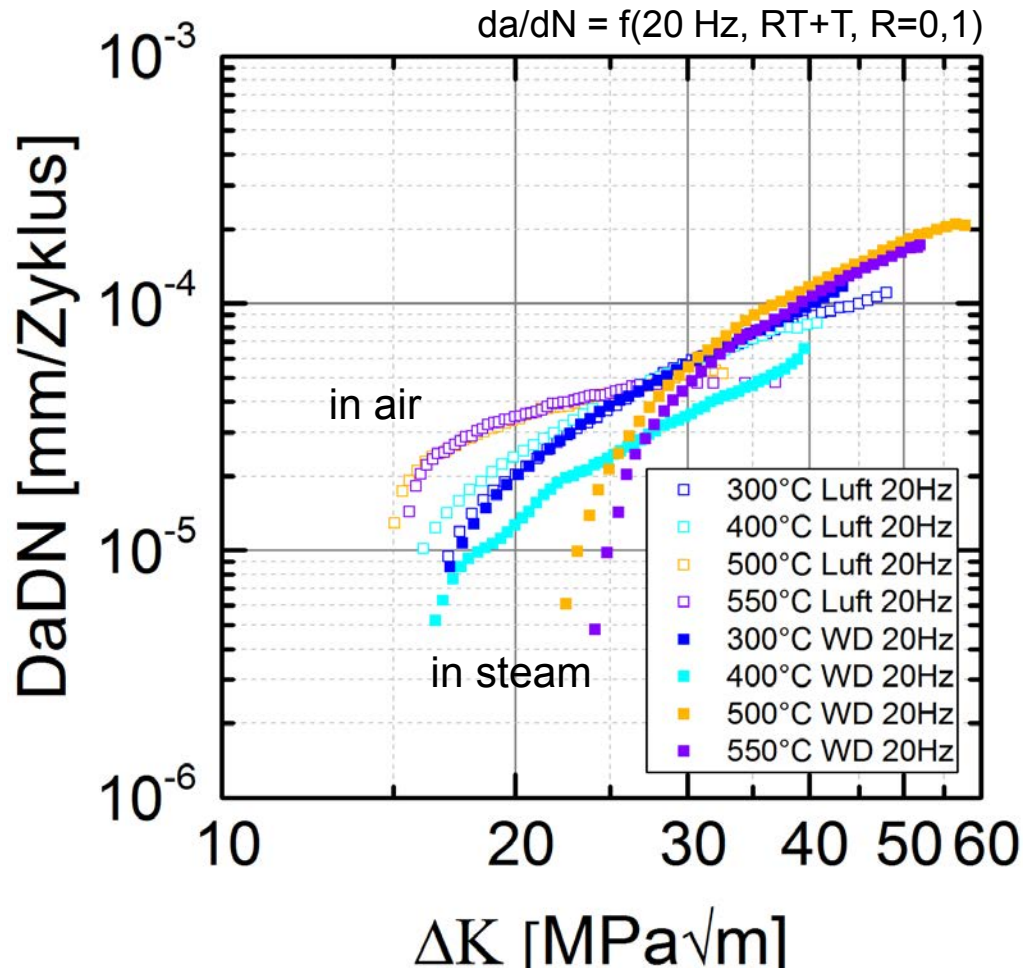
Gefördert durch:



Bundesministerium  
für Wirtschaft  
und Energie



aufgrund eines Beschlusses  
des Deutschen Bundestages



### ■ Paris-line:

- Lowest crack growth rate in steam at  $T \approx 400^\circ\text{C}$
- At  $T \geq 500^\circ\text{C}$  in steam: significant increase of crack growth rates (crack tip corrosion)

### ■ Crack initiation:

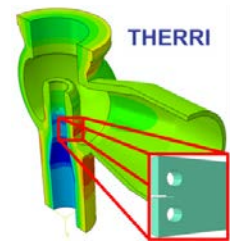
- At  $T \geq 500^\circ\text{C}$  in steam: significant delayed initiation (oxid-induced crack closure)

# JOINT RESEARCH PROJECT THERRI

Gefördert durch:



Bundesministerium  
für Wirtschaft  
und Energie

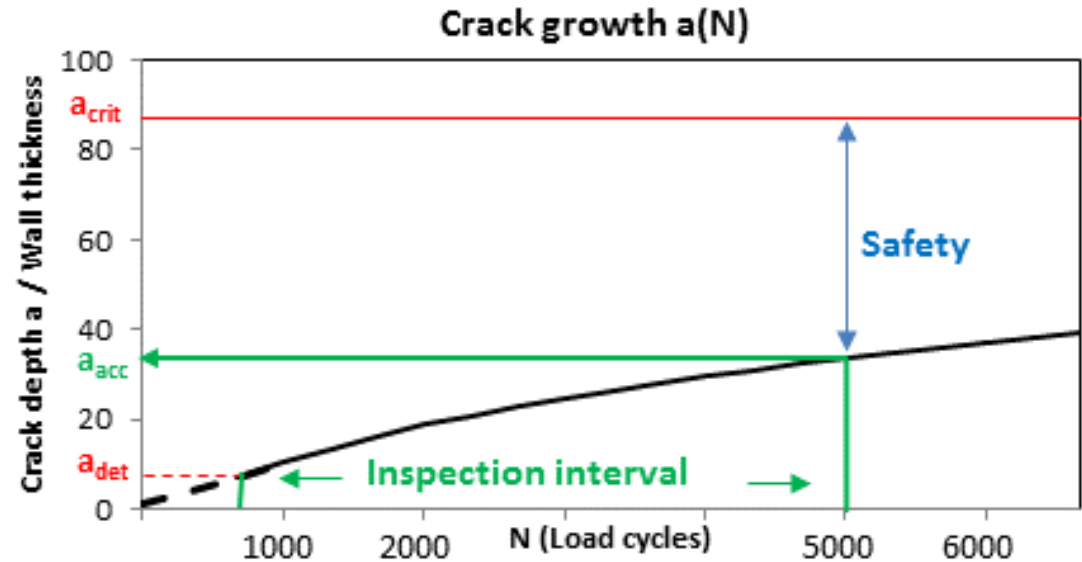


aufgrund eines Beschlusses  
des Deutschen Bundestages

## Draft Directive:

### Application of Damage Tolerance Analysis to Optimize In-Service Inspection

- Methodological concept
  - + THERRI test results
  - + review of open data
    - Draft directive for industrial application
- Structure of the directive is based on existing power plant and Fracture Mechanics standards:
  - R6, BS 7910, SINTAP / FITNET, API 579-1/ASME FFS-1, FKM-R BM, KTA 3206
- Draft directive will be submitted for discussion and validation to the expert bodies (VGB, FDBR, VDI, DVM)
- And is in exemplary applicability examination on thick-walled components in the THERRI industrial partner power plant



- EN 12952
- EN 13445
- VGB S-506

Schematic crack growth diagram  
(Damage Tolerance diagram)

# MANY THANKS FOR YOUR ATTENTION!

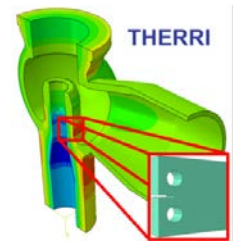
drieck@tuev-nord.de

Gefördert durch:



Bundesministerium  
für Wirtschaft  
und Energie

aufgrund eines Beschlusses  
des Deutschen Bundestages



**TUV NORD**



Thanks to German Federal Ministry for Economic Affairs and Energy (BMWi) for funding the THERRI research project.



---

# A crack opening stress equation for in-phase and out-of-phase thermomechanical fatigue loading

---



Carl Fischer<sup>a</sup>, Christoph Schweizer<sup>a</sup>, Thomas Seifert<sup>b</sup>

<sup>a</sup>Fraunhofer IWM, <sup>b</sup>University of Applied Sciences Offenburg

3<sup>rd</sup> TMF-Workshop, Berlin, 27<sup>th</sup> - 29<sup>th</sup> April 2016

---

---

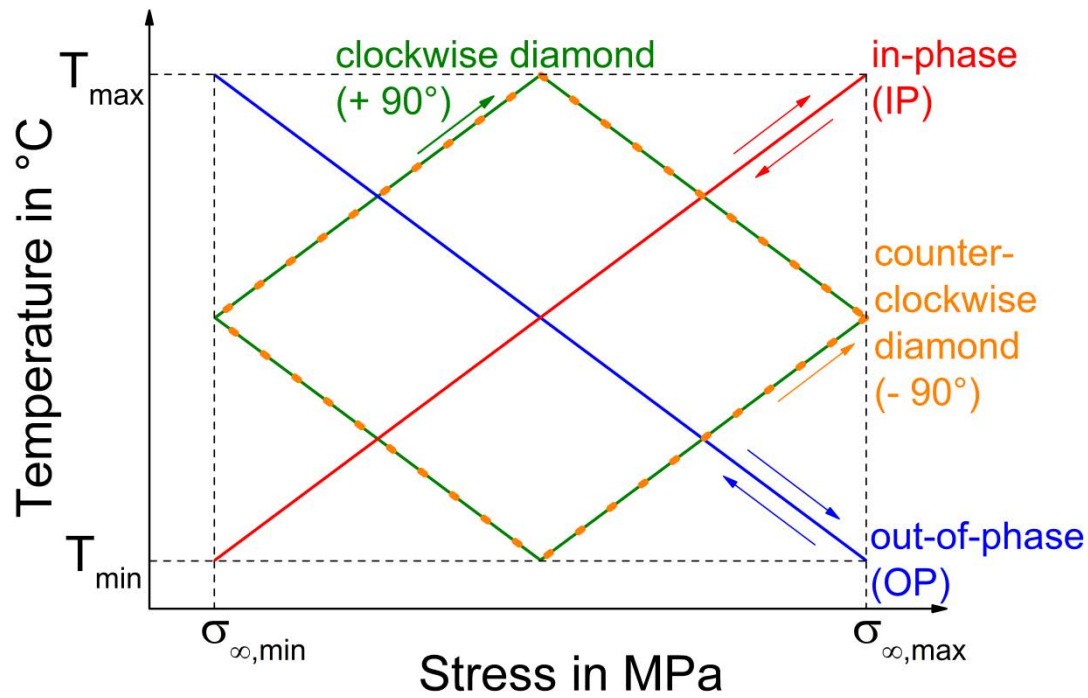
# Overview

---

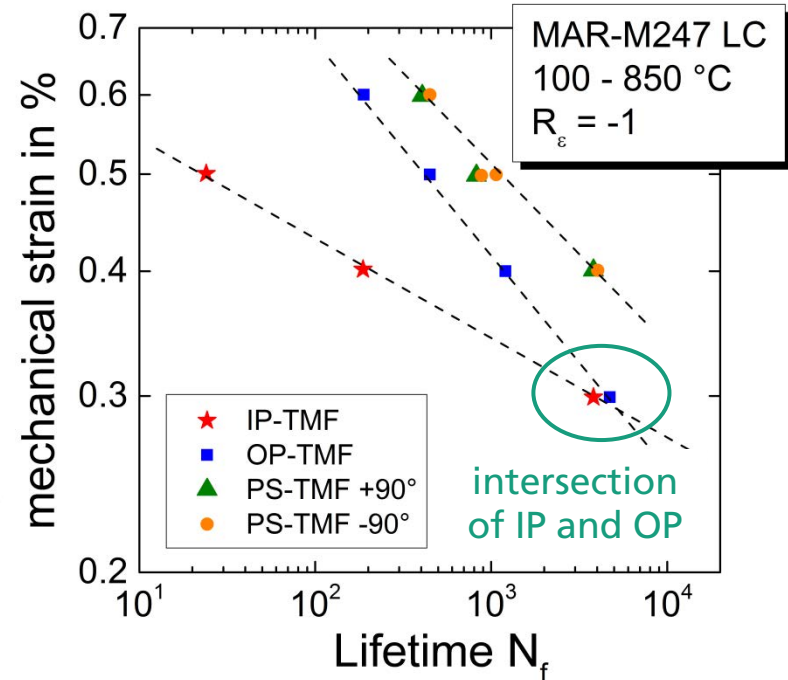
- Motivation:  
Connection between the temperature dependent yield stress and the mean stress under TMF loading
- Crack opening stress calculation with a temperature dependent strip yield model under TMF loading: Plane stress and plane strain conditions
- Scaling relation for describing IP-TMF, OP-TMF and isothermal results in a single diagram
- Application of the scaling relation
- Validation with finite element simulations
- Summary & Outlook

# Motivation

- The fatigue lifetime is influenced by the phase angle between temperature and mechanical strain



Guth et al. (2014). Procedia Engineering 74, 269-272



# Influence of the temperature dependent yield stress on the load ratio

- Introduction: yield stress ratio  $R_Y$ :

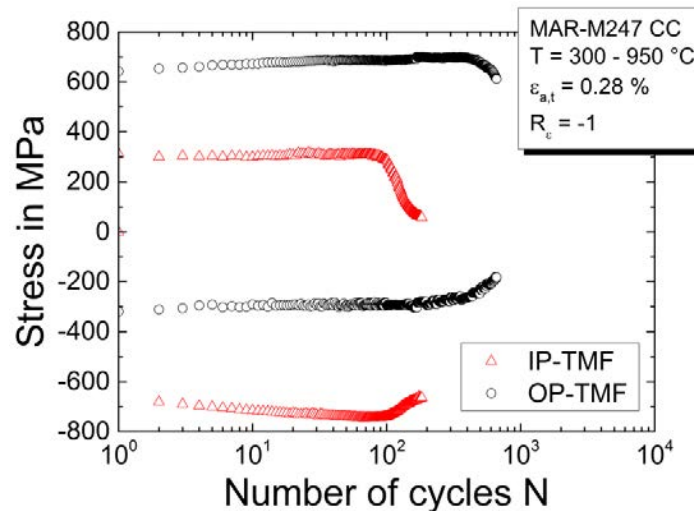
- $\sigma_{Y,c}$ : Yield stress in **c**ompression (at minimum mech. load)
- $\sigma_{Y,t}$ : Yield stress in **t**ension (at maximum mech. load)
- $\alpha$ : considers plane stress ( $\alpha = 1$ ) or plane strain ( $\alpha = 3$ )

$$R_\sigma = \frac{\sigma_{\infty, \min}}{\sigma_{\infty, \max}}$$

$$R_Y = \frac{\sigma_{Y,c}}{\alpha \sigma_{Y,t}}$$

Serrano et al. (2011). FVV report No. 959

$T$ in °C	$E$ in MPa	$\sigma_Y$ in MPa
20	199000	830.5
300	199000	999.5
750	174000	909.5
850	162000	654.5
950	159000	421
1050	142000	235.75



IP-TMF 300-950 °C:

$\sigma_{Y,c} = 999.5$  MPa,  
 $\sigma_{Y,t} = 421$  MPa  
 $\rightarrow R_Y = 2.37$

OP-TMF 300-950 °C:

$\sigma_{Y,c} = 421$  MPa,  
 $\sigma_{Y,t} = 999.5$  MPa  
 $\rightarrow R_Y = 0.42$

➔  $R_\sigma \approx -R_Y$

# Hypothesis

The influence of the mean stress/load ratio  
can be explained by plasticity induced  
fatigue crack closure

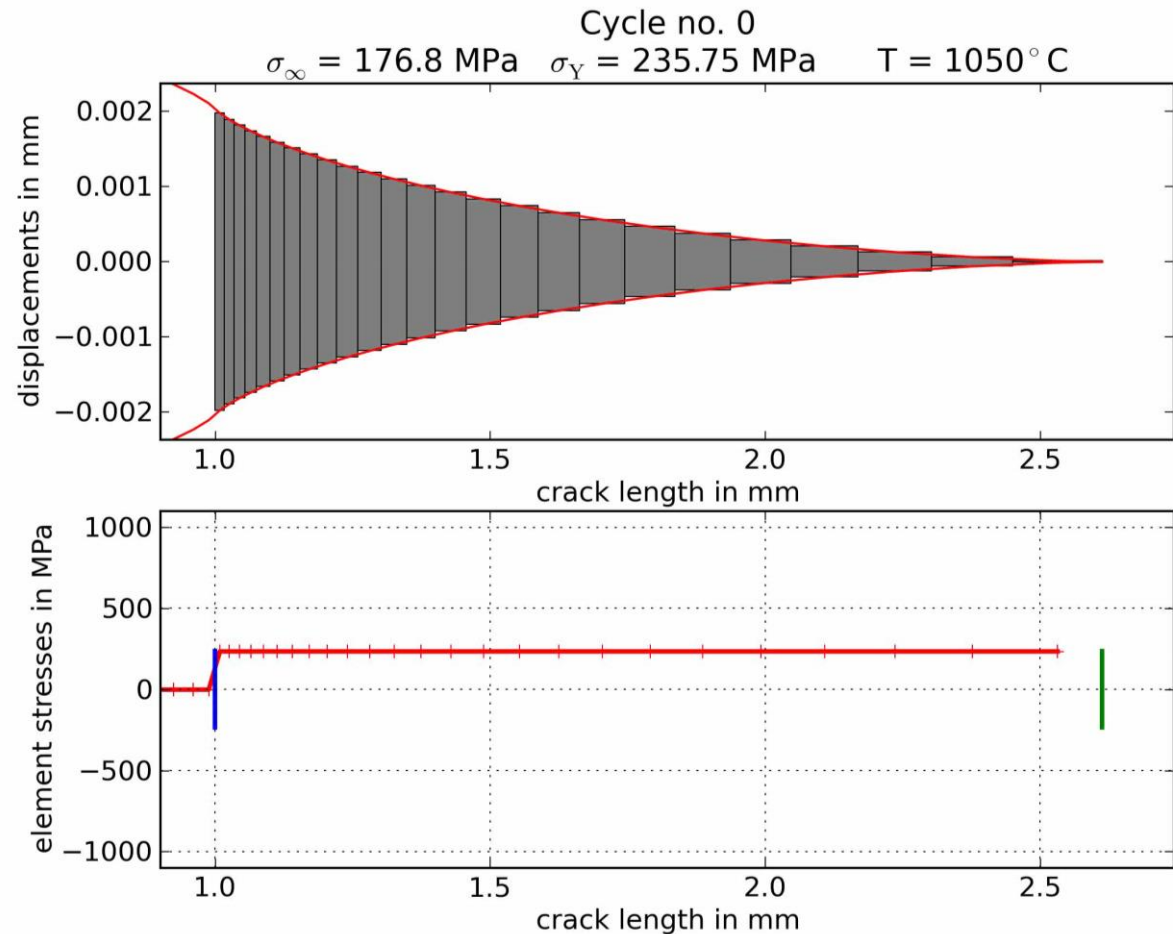


Investigation of fatigue crack closure  
under TMF by using a temperature  
dependent  
strip yield model

# Simulation with the strip-yield model (SYM) – animation

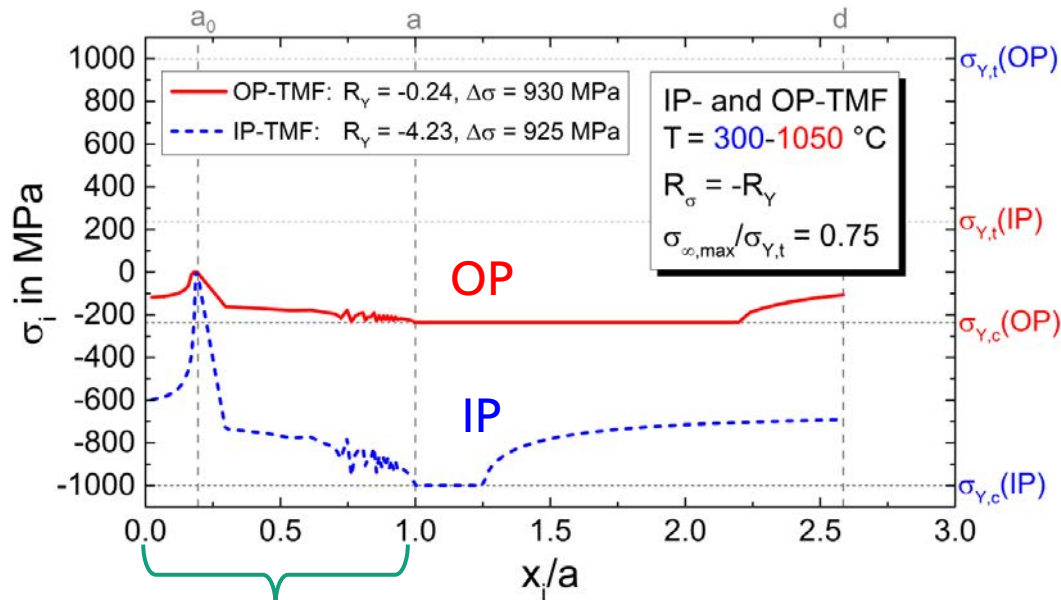
## IP-TMF 300 - 1050 °C

- Elastic perfectly plastic material
- Plastic zone as strips with contact stresses limited to the **temperature dependent yield stress  $\sigma_Y(T)$**
- Crack growth by cracking the first element in the plastic zone at  $\sigma_{\infty, \max}$
- Plastically deformed material behind the advancing crack tip leads to crack closure



# Relationship between contact stresses and the crack opening stress $\sigma_{op}$

- Distribution of the contact stresses  $\sigma_i$  at minimum load:



- Contact stresses are limited to  $\sigma_{Y,c}$ :

$$\sigma_{op} \approx \sigma_{\infty, \min} - \sigma_{Y,c} \sum_{i=1}^{n_{CT}-1} \dots$$

- $\sigma_{op}$  under IP-TMF is higher than under OP-TMF
- Typically used in fatigue crack growth models:

$$\Delta\sigma_{eff} = \sigma_{\infty, \max} - \sigma_{op}$$

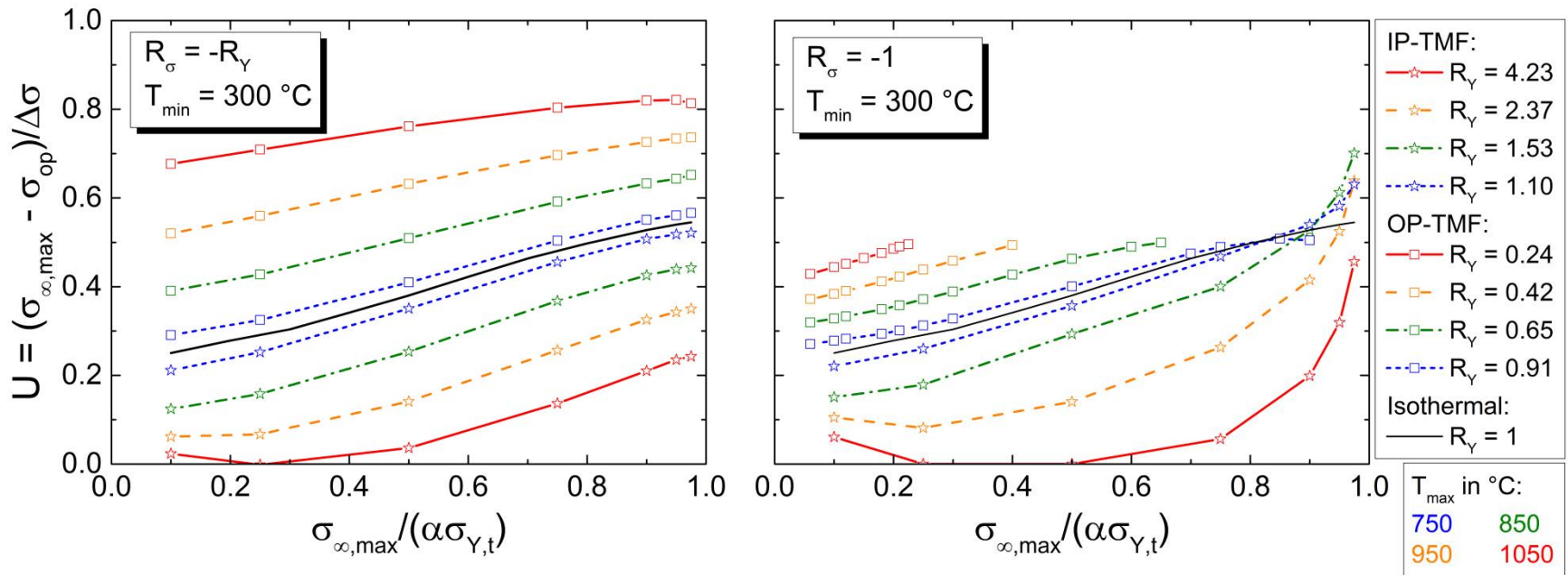
$$U(R_\sigma) = \Delta\sigma_{eff} / \Delta\sigma$$

$$\sigma_{op} = \sigma_{\infty, \min} - \sum_{i=1}^{n_{CT}-1} \sigma_i \left[ \arcsin \frac{b_{2,i}}{a - \Delta a^*} - \arcsin \frac{b_{1,i}}{a - \Delta a^*} \right]$$

# Results of the strip-yield model

## IP- and OP-TMF: Influence of $T_{\max}$

plane stress ( $\alpha = 1$ )



- OP-TMF: less crack closure with increasing maximum temperature
- IP-TMF: more crack closure with increasing maximum temperature

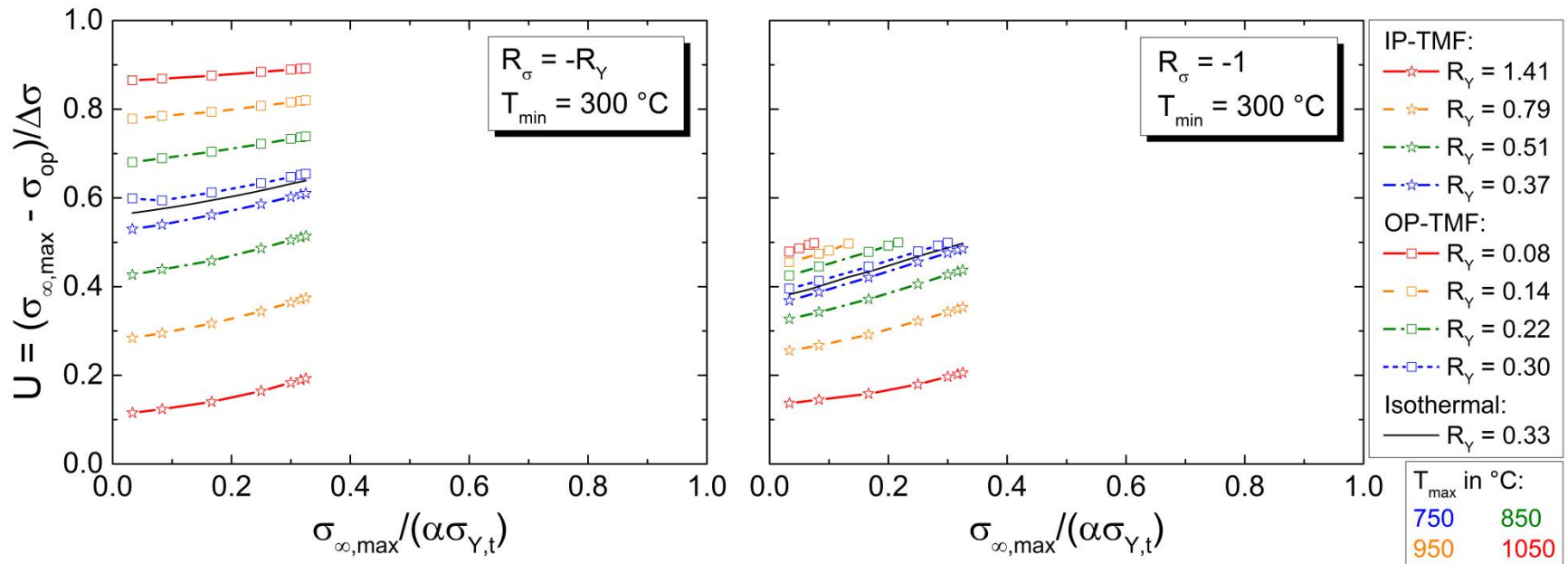
Reason: development of the residual contact stresses at minimum load



# Results of the strip-yield model

## IP- and OP-TMF: Influence of $T_{\max}$

plane strain ( $\alpha = 3$ )



→ The aim is to find a scaling relation, which is capable to describe all IP-TMF, OP-TMF and isothermal results in a single diagram.

# Scaling relation

## Describing IP-TMF results in a single diagram

- Appropriate representation is found by:

- Introducing the yield stress corrected load ratio  $R_\sigma^*$ :

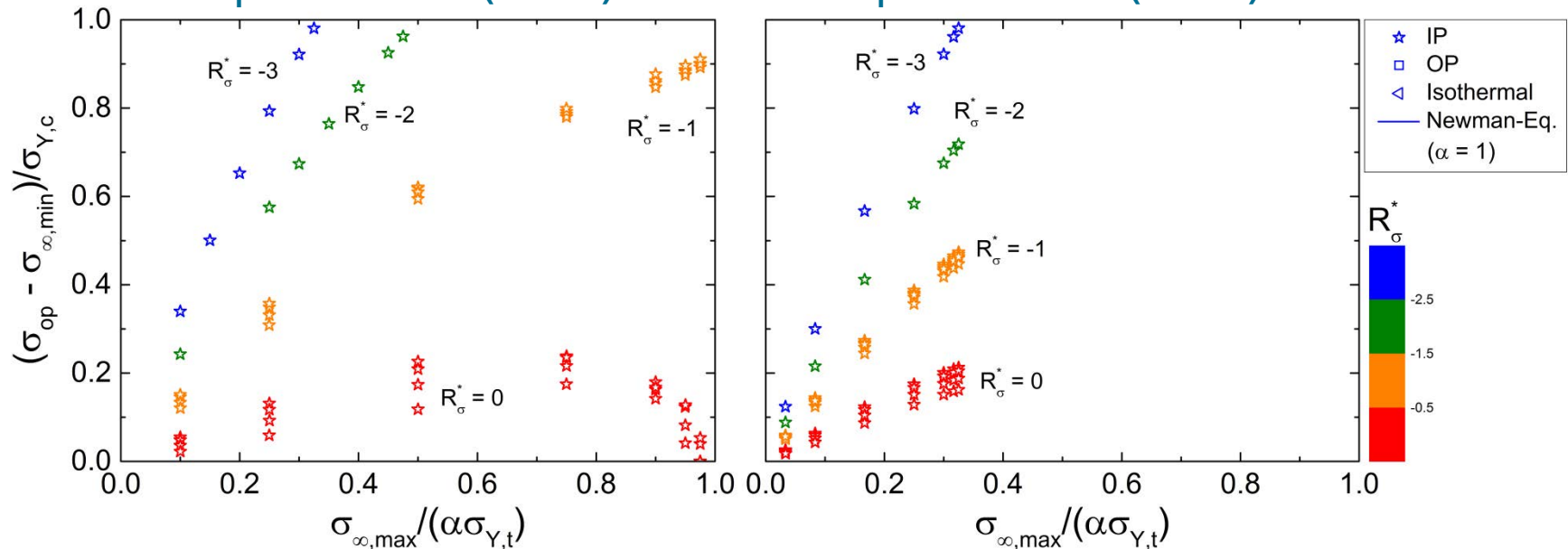
$$R_\sigma^* = \frac{R_\sigma}{R_Y}$$

$$R_Y = \frac{\sigma_{Y,c}}{\alpha\sigma_{Y,t}}$$

- Correlating  $(\sigma_{op} - \sigma_{\infty,min})/\sigma_{Y,c}$  with  $\sigma_{\infty,max}/(\alpha\sigma_{Y,t})$

plane stress ( $\alpha = 1$ )

plane strain ( $\alpha = 3$ )

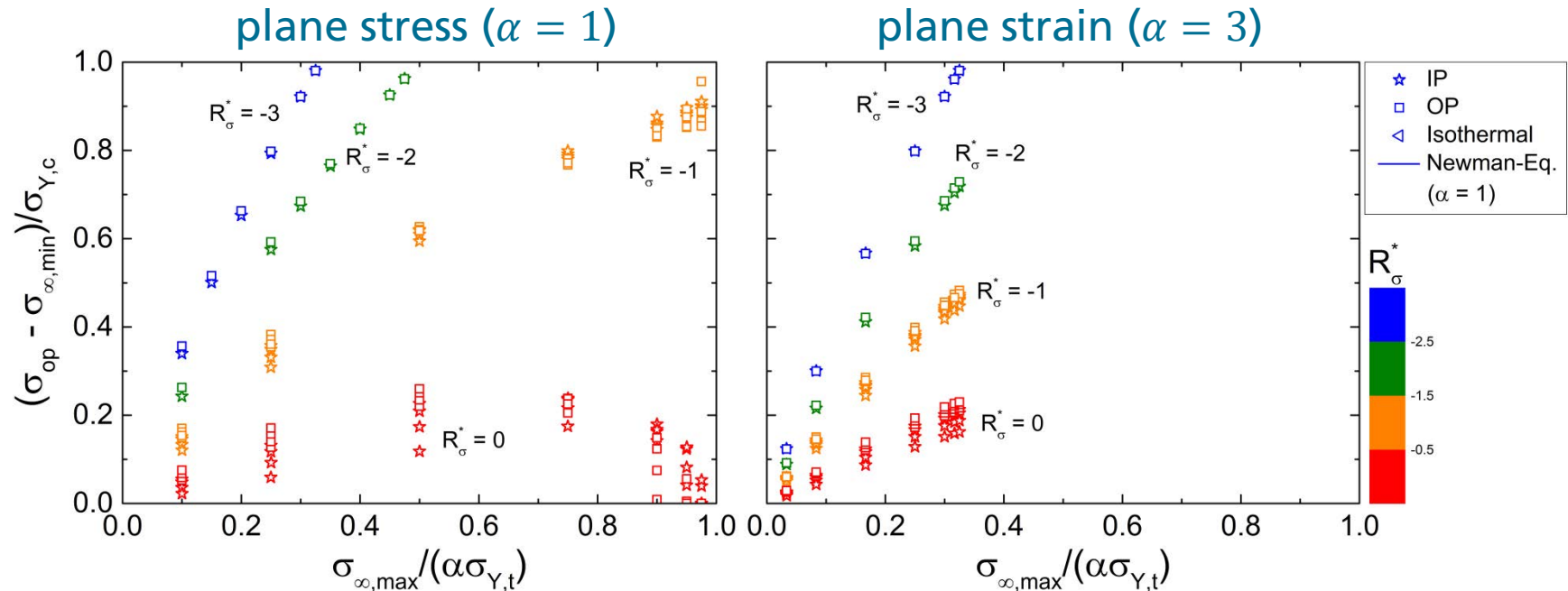


# Scaling relation

## Describing IP-TMF and OP-TMF results in a single diagram

- Appropriate representation is found by:

- Introducing the yield stress corrected load ratio  $R_\sigma^*$ :  $R_\sigma^* = \frac{R_\sigma}{R_Y}$   $R_Y = \frac{\sigma_{Y,c}}{\alpha\sigma_{Y,t}}$
- Correlating  $(\sigma_{op} - \sigma_{\infty,min})/\sigma_{Y,c}$  with  $\sigma_{\infty,max}/(\alpha\sigma_{Y,t})$

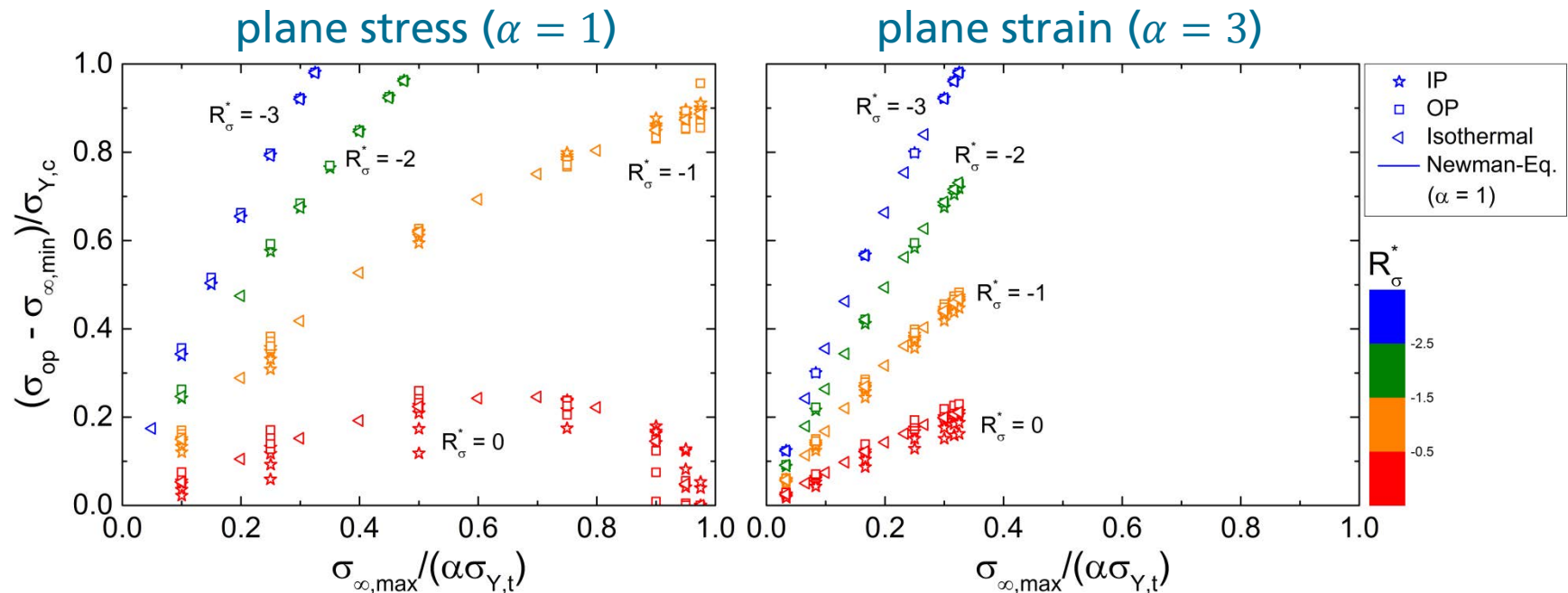


# Scaling relation

## Describing IP-TMF, OP-TMF and isothermal results in a single diagram

- Appropriate representation is found by:

- Introducing the yield stress corrected load ratio  $R_\sigma^*$ :  $R_\sigma^* = \frac{R_\sigma}{R_Y}$   $R_Y = \frac{\sigma_{Y,c}}{\alpha\sigma_{Y,t}}$
- Correlating  $(\sigma_{op} - \sigma_{\infty,min})/\sigma_{Y,c}$  with  $\sigma_{\infty,max}/(\alpha\sigma_{Y,t})$

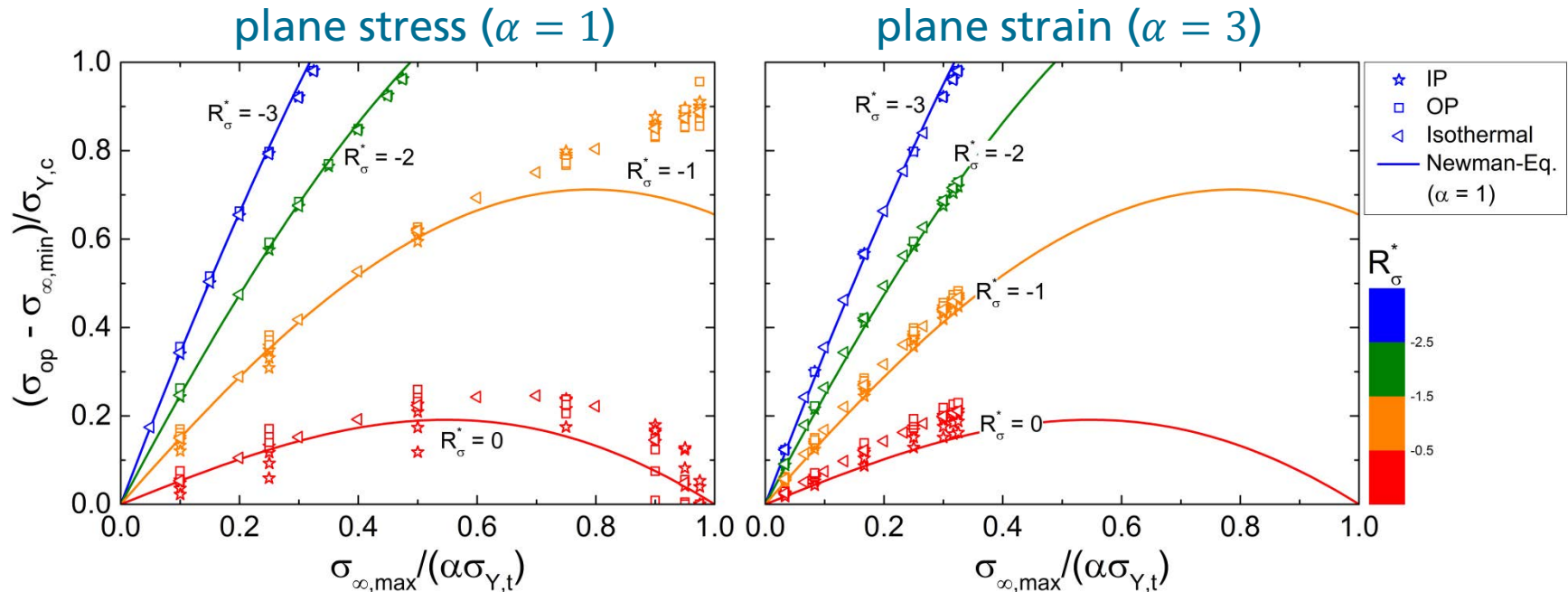


# Scaling relation

## Describing IP-TMF, OP-TMF and isothermal results as well as the Newman equation in a single diagram

- Appropriate representation is found by:

- Introducing the yield stress corrected load ratio  $R_\sigma^*$ :  $R_\sigma^* = \frac{R_\sigma}{R_Y}$   $R_Y = \frac{\sigma_{Y,c}}{\alpha\sigma_{Y,t}}$
- Correlating  $(\sigma_{op} - \sigma_{\infty,min})/\sigma_{Y,c}$  with  $\sigma_{\infty,max}/(\alpha\sigma_{Y,t})$



The scaling relation according to  $(\sigma_{\text{op}} - \sigma_{\infty, \text{min}}) / \sigma_{Y, c}$  and the usage of  $R_{\sigma}^*$  lead to a unified correlation of isothermal and non-isothermal simulation results independent of the stress state and the yield stress ratio  $R_Y$ .



Thus, isothermal results with temperature dependent yield stress can be used to predict results under TMF loading.

# Scaling relation

## Relationship of the normalized crack opening stress for TMF and isothermal loading

- The following conditions have to be fulfilled:

$$\left. \frac{\sigma_{\infty, \max}}{\alpha \sigma_{Y, t}} \right|_{\text{TMF}} = \left. \frac{\sigma_{\infty, \max}}{\alpha \sigma_{Y, t}} \right|_{\text{iso}}$$

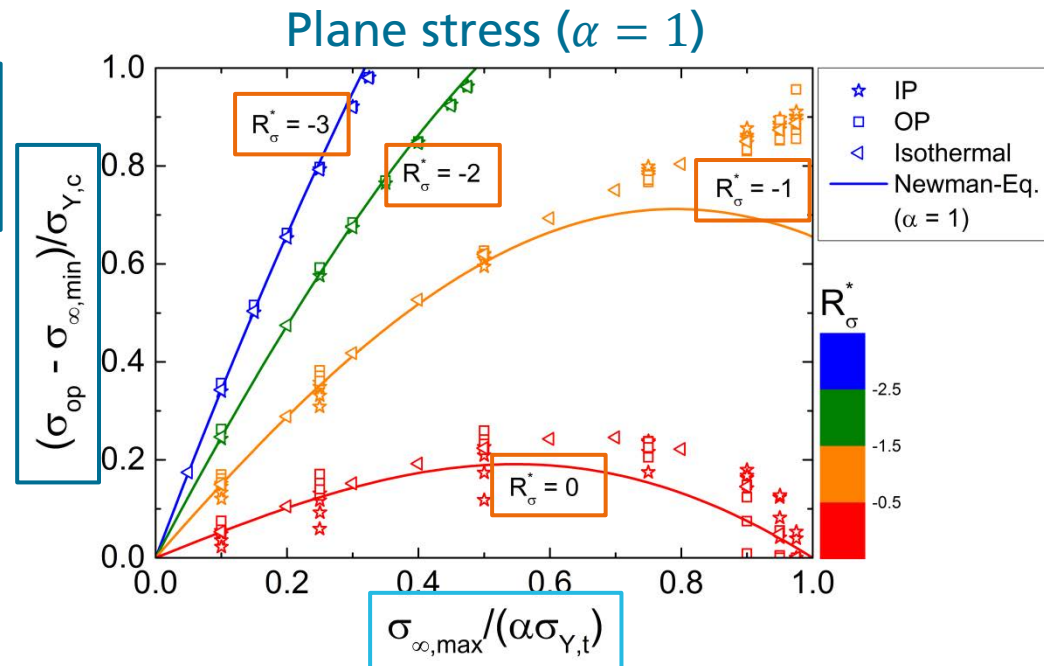
$$R_{\sigma, \text{TMF}}^* = R_{\sigma, \text{iso}}^*$$

- This leads to:

$$\left. \frac{\sigma_{\text{op}} - \sigma_{\infty, \min}}{\sigma_{Y, c}} \right|_{\text{TMF}} = \left. \frac{\sigma_{\text{op}} - \sigma_{\infty, \min}}{\sigma_{Y, c}} \right|_{\text{iso}}$$

- Crack opening equation for TMF loading:

$$\left. \frac{\sigma_{\text{op}}}{\sigma_{\infty, \max}} \right|_{\text{TMF}} = R_{Y, \text{TMF}} \alpha_{\text{iso}} \left. \frac{\sigma_{\text{op}}}{\sigma_{\infty, \max}} \right|_{\text{iso}}$$



# Application of the scaling relation

## Crack opening stress for TMF loading

- Given TMF cycle:  $R_{Y, TMF}$ ,  $R_{\sigma, TMF}^*$  and  $R_{\sigma, TMF}$  are known
- Prediction of  $U$  for TMF loading:

$$U = \frac{\Delta\sigma_{\text{eff}}}{\Delta\sigma} = \frac{1 - \frac{\sigma_{\text{op}}}{\sigma_{\infty, \text{max}}}|_{\text{TMF}}}{1 - R_{\sigma, \text{TMF}}}$$

$$\frac{\sigma_{\text{op}}}{\sigma_{\infty, \text{max}}}|_{\text{TMF}} = R_{Y, \text{TMF}} \alpha_{\text{iso}} \frac{\sigma_{\text{op}}}{\sigma_{\infty, \text{max}}}|_{\text{iso}}$$

- Scaling isothermal results from the strip-yield model with  $\alpha_{\text{iso}} = 1$  at  $R_{\sigma, \text{iso}} = R_{\sigma, \text{iso}}^* = R_{\sigma, \text{TMF}}$
- Using an crack opening stress equation, i. e. from Newman (1984)



# Crack opening stress equation for IP- and OP-TMF

## Modified equation from Newman (1984)

- System of equations for calculating the crack opening stress:

Substitution of  $R_\sigma$  by  $R_{\sigma, \text{TMF}}^* = R_\sigma / R_{Y| \text{TMF}}$ :

$$\frac{\sigma_{\text{op}}}{\sigma_{\infty, \text{max}}} = A_0 + A_1 R_{\sigma, \text{TMF}}^* + A_2 R_{\sigma, \text{TMF}}^{*2} + A_3 R_{\sigma, \text{TMF}}^{*3} \quad \text{for } R_{\sigma, \text{TMF}}^* \geq 0$$

$$\frac{\sigma_{\text{op}}}{\sigma_{\infty, \text{max}}} = A_0 + A_1 R_{\sigma, \text{TMF}}^* \quad \text{for } R_{\sigma, \text{TMF}}^* < 0$$

$$A_0 = 0.535 \cos \left( \frac{\pi}{2} \frac{\sigma_{\infty, \text{max}}}{\alpha \sigma_{Y, t}} \Big|_{\text{TMF}} \right)$$

$$A_1 = 0.344 \frac{\sigma_{\infty, \text{max}}}{\alpha \sigma_{Y, t}} \Big|_{\text{TMF}}$$

$$A_2 = 1 - A_0 - A_1 - A_3$$

$$A_3 = 2A_0 + A_1 - 1$$

$\sigma_{\infty, \text{max}}$  : maximum stress

$\sigma_{\infty, \text{min}}$  : minimum stress

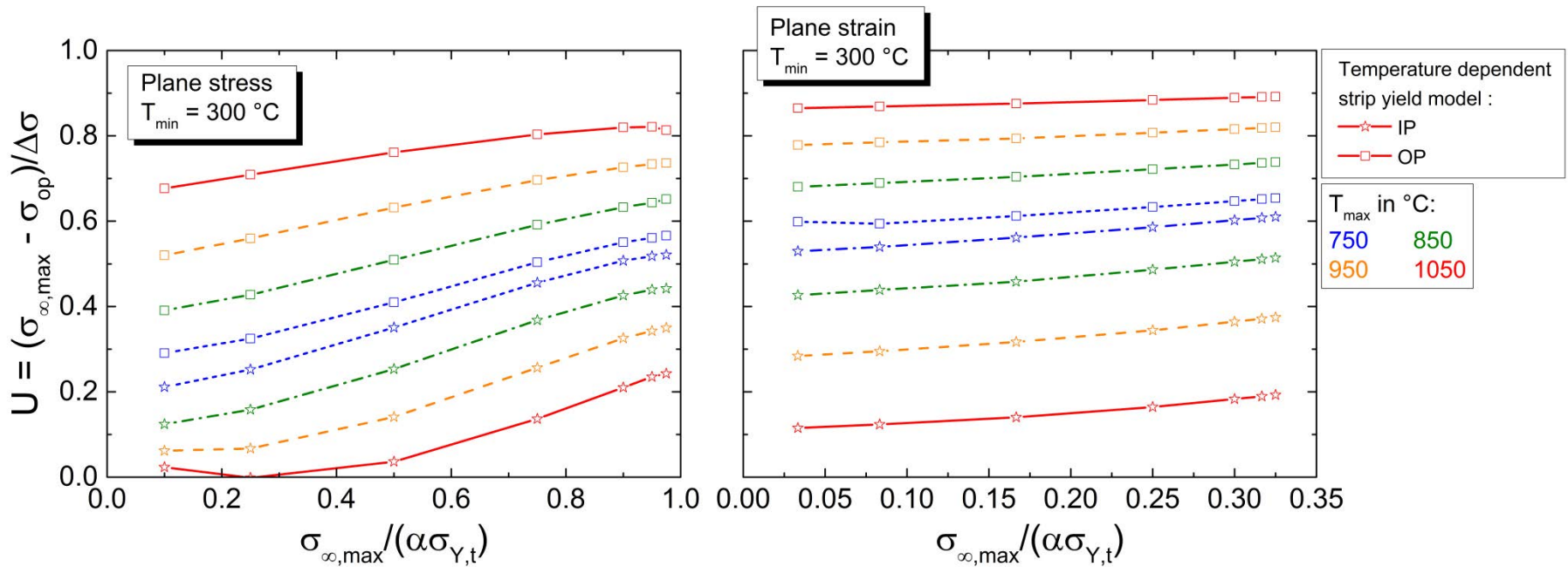
$\sigma_{Y, t}$  : yield stress in tension

$\sigma_{\text{op}}$  : crack opening stress

# Validation of the scaling relation

$$R_\sigma = -R_Y$$

## Results from the temperature dependent strip yield model

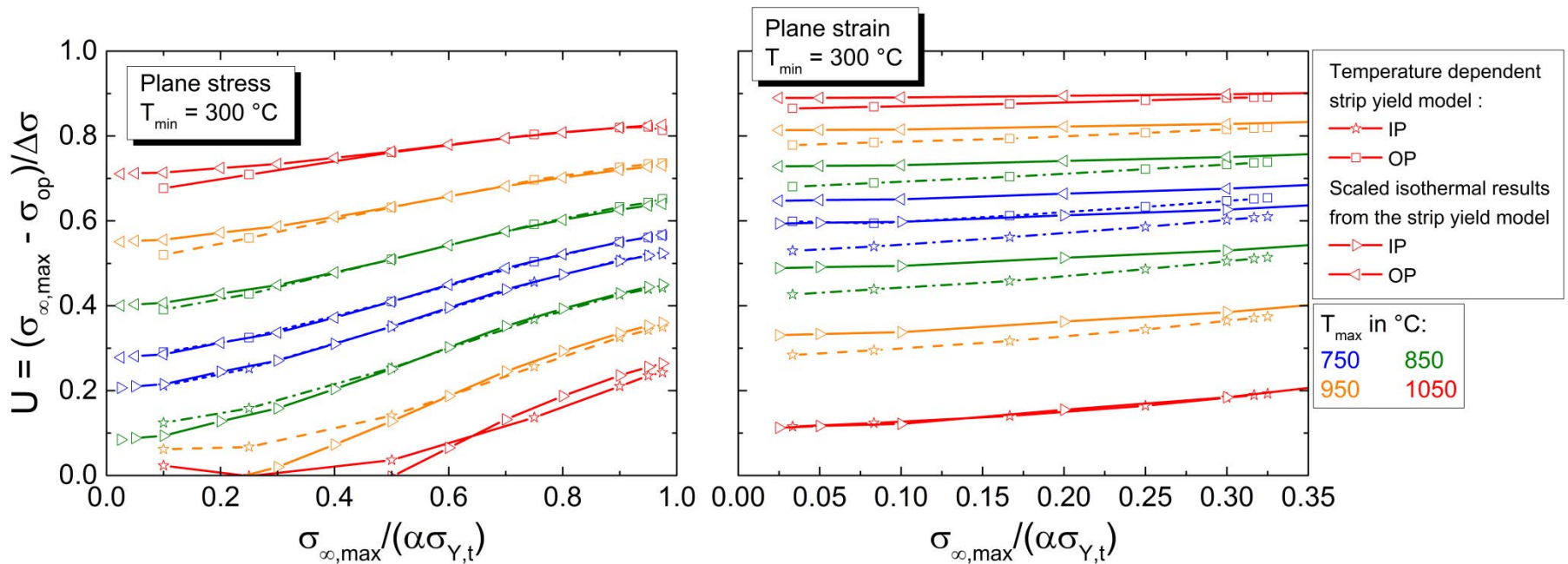


# Validation of the scaling relation

$$R_{\sigma} = -R_Y$$

- OP-TMF: excellent quantitative agreement
- IP-TMF: agreement mostly of comparable quality

## Results from the temperature dependent SYM and scaled isothermal results

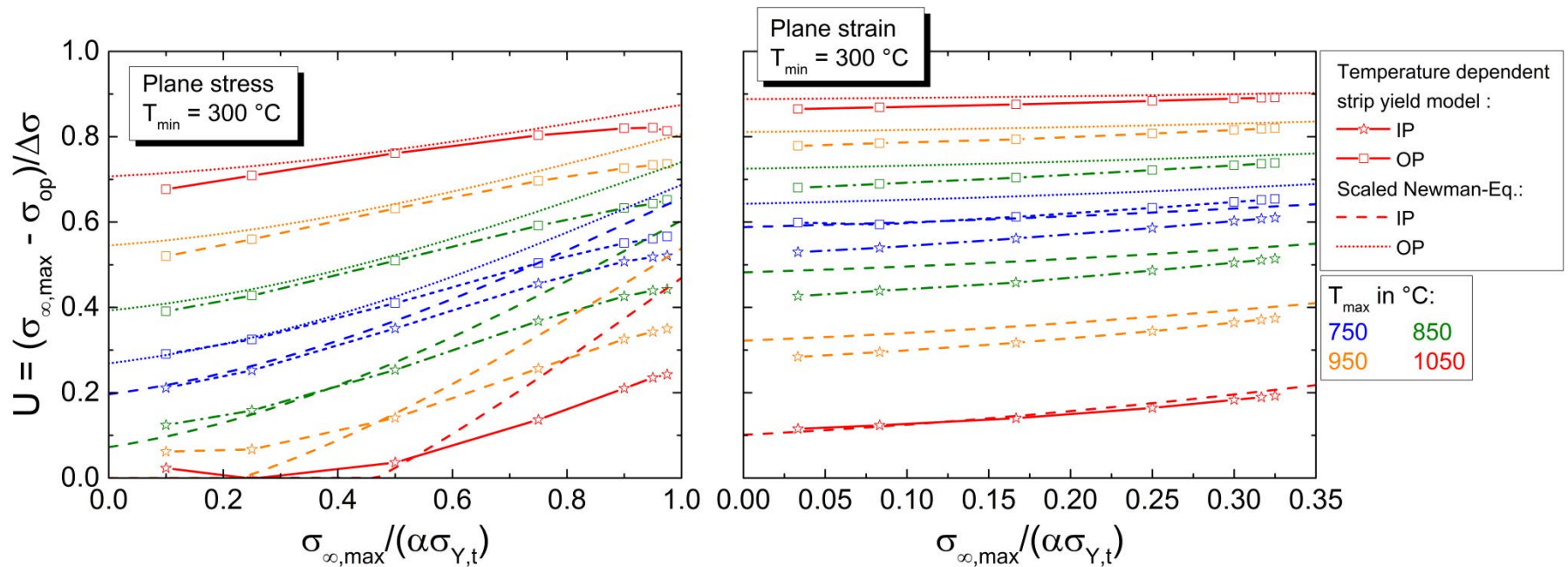


# Validation of the scaling relation

$$R_\sigma = -R_Y$$

- OP-TMF: excellent quantitative agreement
- IP-TMF: results deteriorate under IP-TMF and plane stress conditions

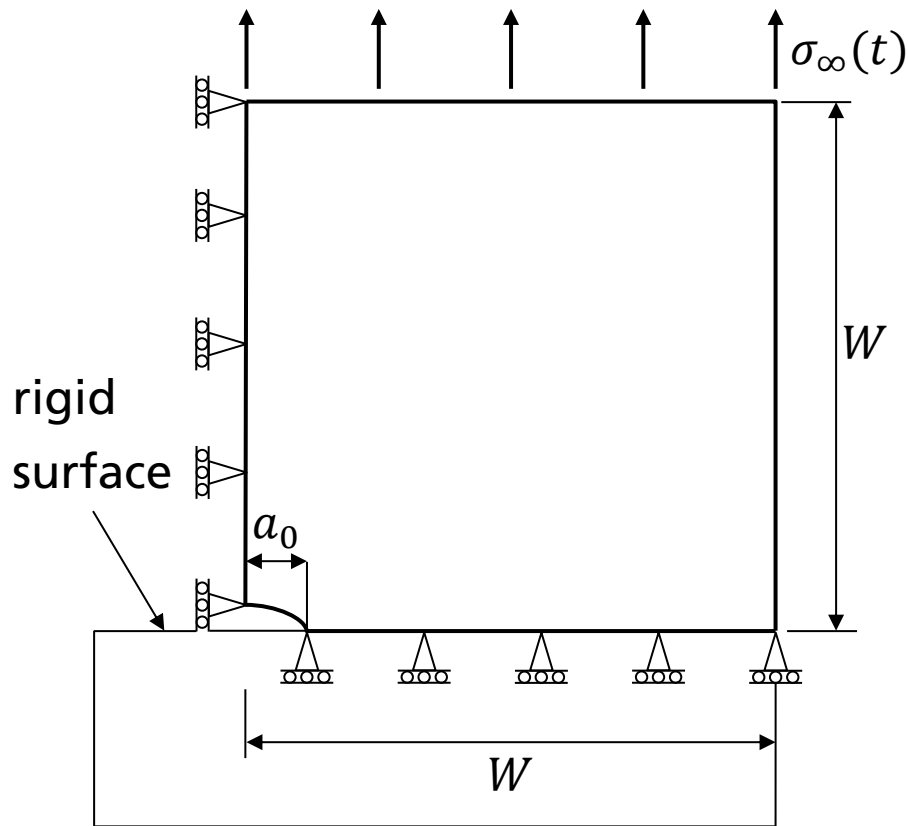
Results from the temp. dependent SYM and scaled results from the Newman eq.



# Finite element simulations

## Model and boundary conditions

■ Model:  $W = 100 \text{ mm}$ ,  $a_0 = 1 \text{ mm}$



■ Boundary conditions:

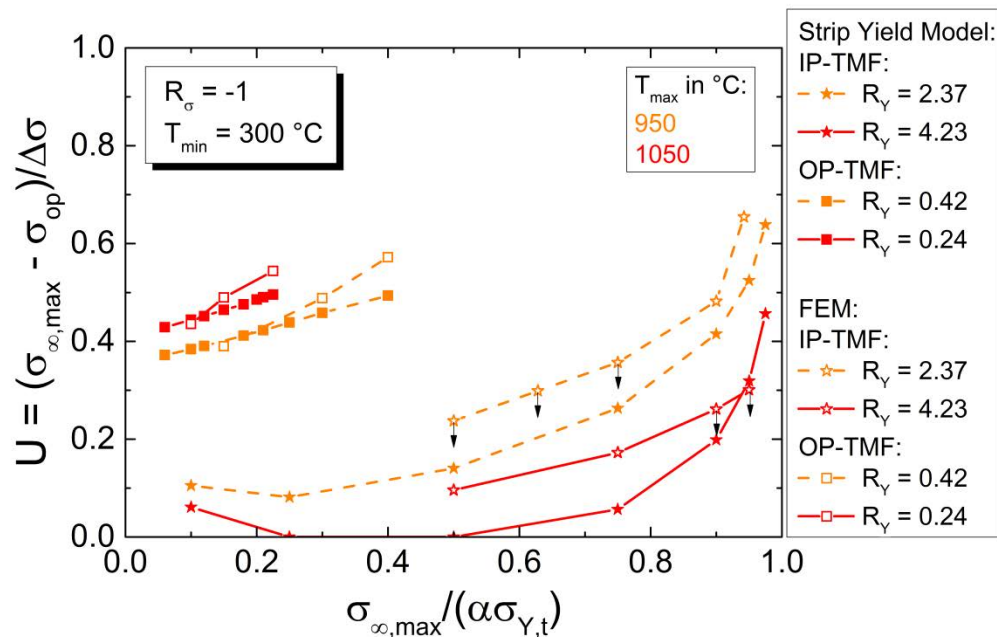
- cyclic loading  $\sigma_\infty(t)$
- $x$ -axis and  $y$ -axis symmetry
- crack growth by releasing the crack tip node at maximum load

■ Calculation of  $\sigma_{op}$ :  
change from compressive to tensile stress at the crack tip node  
→ crack is fully open

# Stress controlled finite element simulations

## Validation of the results with the SYM

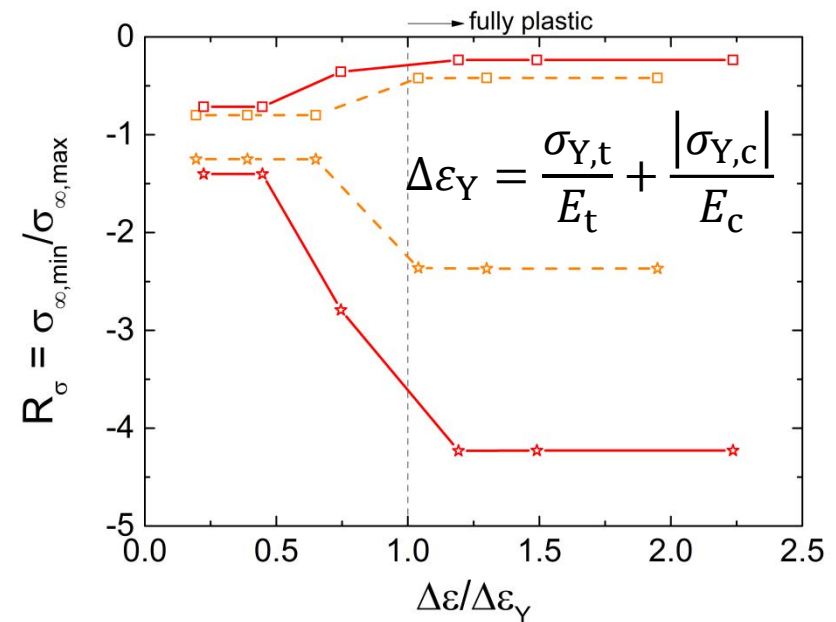
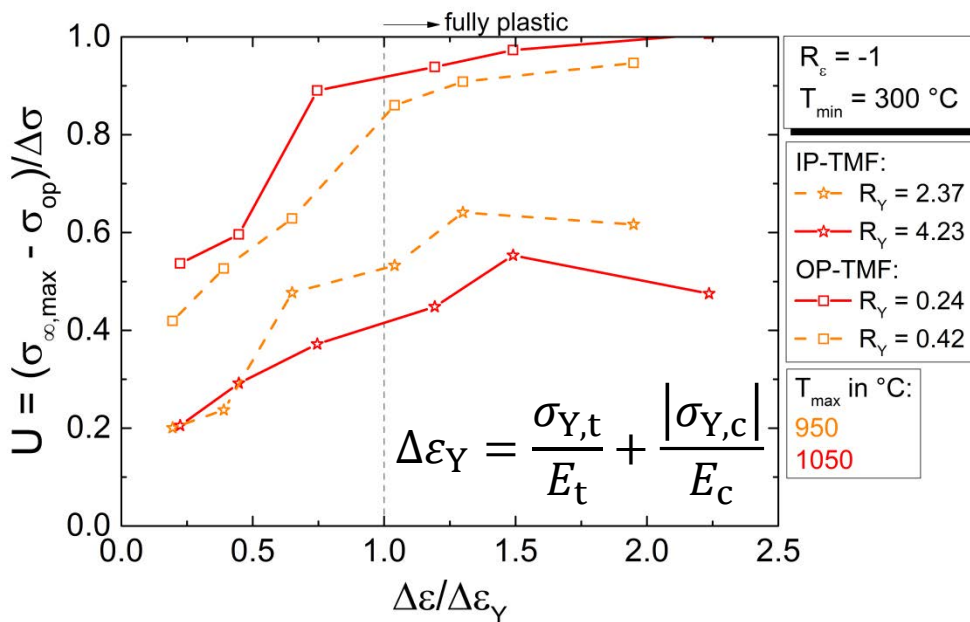
- Good agreement between results obtained with the temperature dependent SYM and finite element simulations
- Less crack closure in the finite element simulations



# Strain controlled finite element simulations

## Large scale yielding conditions

- OP-TMF: no more crack closure for 1050 °C and large mechanical strains
- IP-TMF: crack closure seems to reach a stable level
- The  $R_\sigma$ -values go to  $R_\sigma = -R_Y$



# Summary

- Plasticity-induced crack closure is strongly influenced by the ratio of the yield stress  $R_Y$  and the stress state
- A scaling relation is presented, which allows to predict the crack opening stress under IP- and OP-TMF loading with isothermal results
- Based on the scaling relation an existing crack opening stress equation is extended to thermomechanical fatigue loading

# Outlook

- Finite element simulations under large scale yielding conditions and using isotropic and kinematic hardening material models
- Comparison of different methodologies for the calculation of the crack opening stress
- Experimental measurements of the crack opening stress under thermomechanical fatigue conditions





Contents lists available at [ScienceDirect](#)

## International Journal of Fatigue

journal homepage: [www.elsevier.com/locate/ijfatigue](http://www.elsevier.com/locate/ijfatigue)



### A crack opening stress equation for in-phase and out-of-phase thermomechanical fatigue loading



Carl Fischer<sup>a</sup>, Christoph Schweizer<sup>a,\*</sup>, Thomas Seifert<sup>b</sup>

<sup>a</sup> Fraunhofer Institute for Mechanics of Materials IWM, Wöhlerstrasse 11, 79108 Freiburg, Germany

<sup>b</sup> Offenburg University of Applied Science, Badstrasse 24, 77652 Offenburg, Germany

---

# A crack opening stress equation for in-phase and out-of-phase thermomechanical fatigue loading

---



Carl Fischer<sup>a</sup>, Christoph Schweizer<sup>a</sup>, Thomas Seifert<sup>b</sup>

<sup>a</sup>Fraunhofer IWM, <sup>b</sup>University of Applied Sciences Offenburg

3<sup>rd</sup> TMF-Workshop, Berlin, 27<sup>th</sup> - 29<sup>th</sup> April 2016

---

# Cracking due to Combined TMF and HCF Loading in Cast Iron

**E Hosseini**

*Inspire Centre for Mechanical Integrity, c/o EMPA, Switzerland*

**SR Holdsworth**

*EMPA, Swiss Federal Laboratories for Materials Science & Technology, Switzerland*

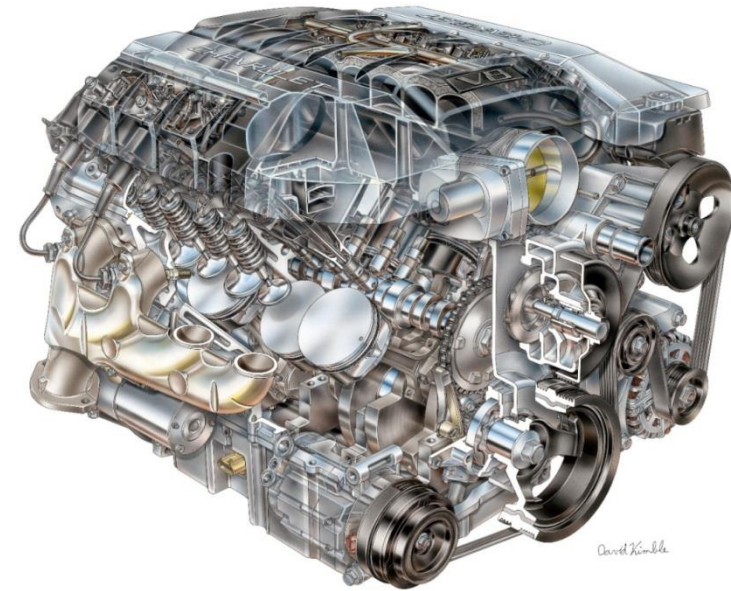
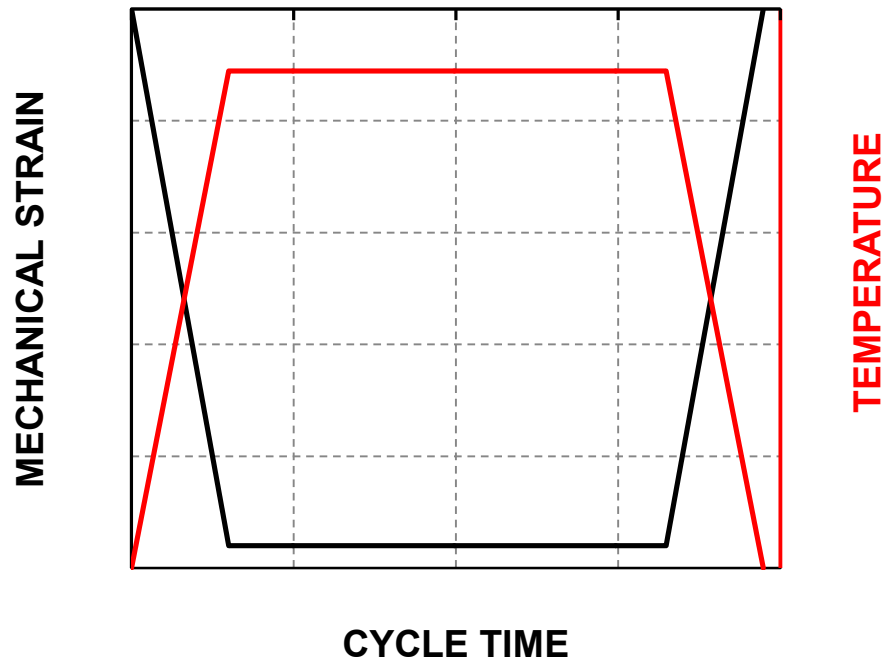
# CONTENTS

---

- Introduction
- OP TMF and TMF/HCF testing
  - New-effective algorithms for control and DAQ of OP TMF test
- Material and testing conditions
- Experimental results and discussions
- Summary

# INTRODUCTION

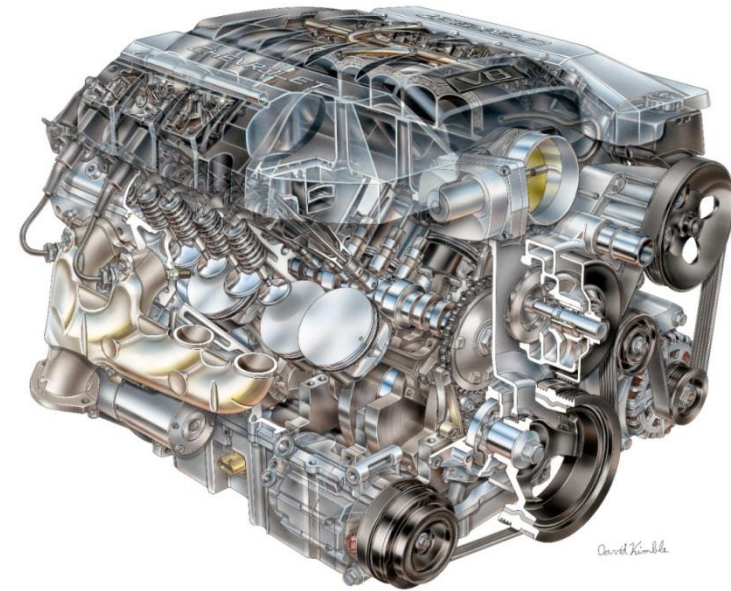
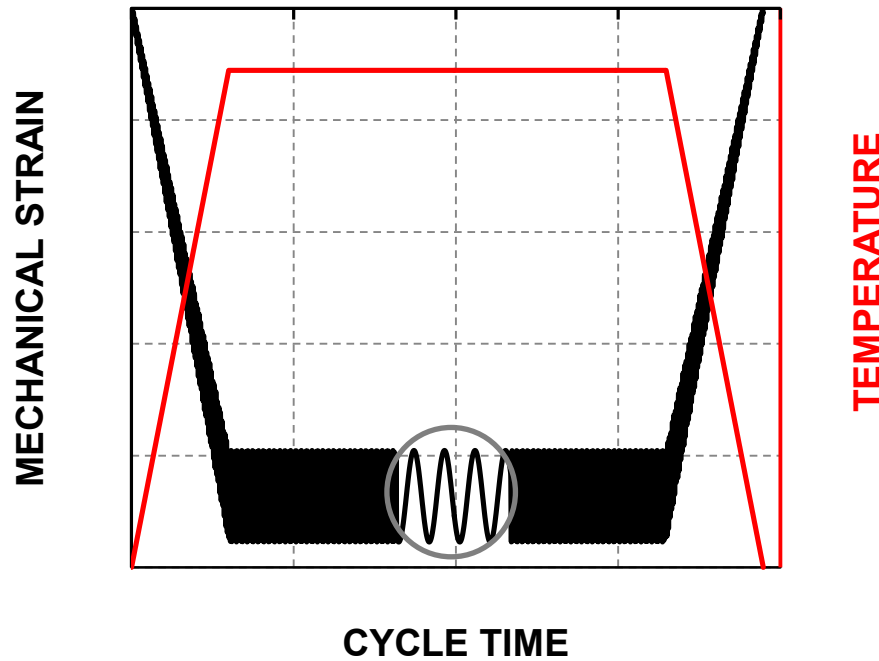
- Out-of-Phase TMF loading



GM 6.2 Liter V8 Small Block LS3 Engine (gmauthority.com)

# INTRODUCTION

- Out-of-Phase TMF/HCF loading



GM 6.2 Liter V8 Small Block LS3 Engine (gmauthority.com)

# INTRODUCTION

- TMF induced crackin

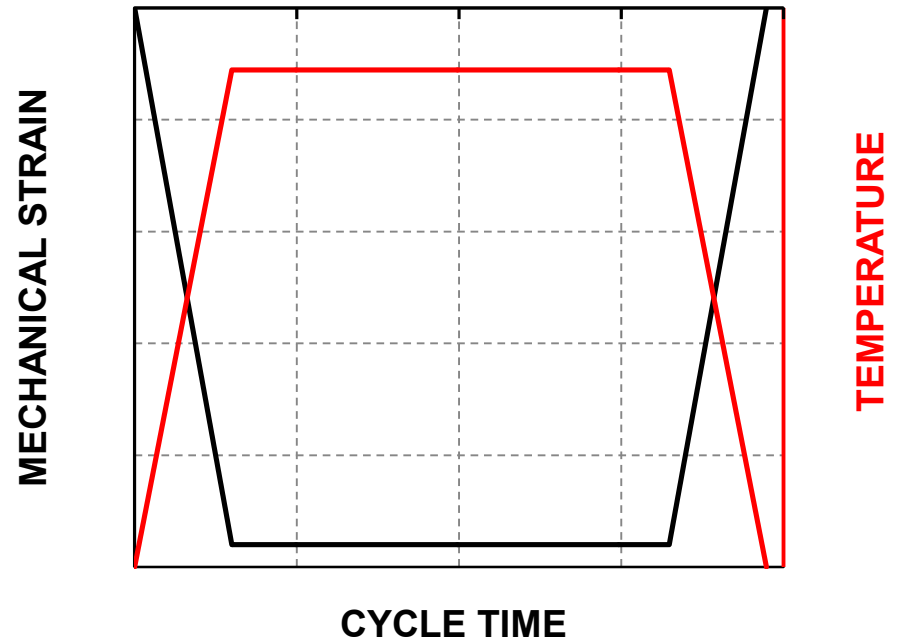
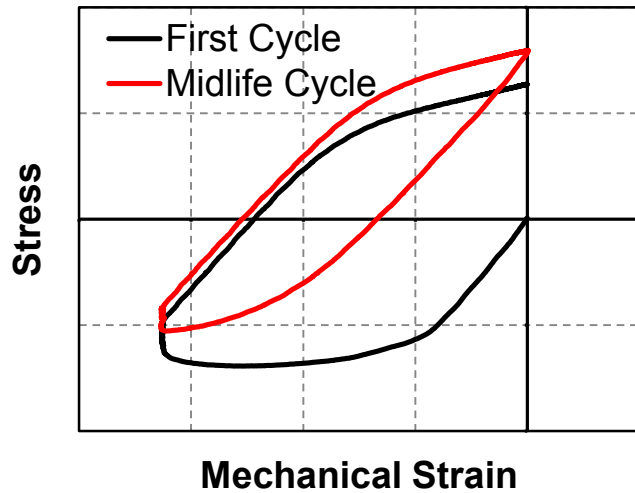


[www.weldangrind.ca](http://www.weldangrind.ca)

# OP TMF AND TMF/HCF TESTING

- OP TMF test

$$\varepsilon_{mech} = -G\varepsilon_{th}^*$$





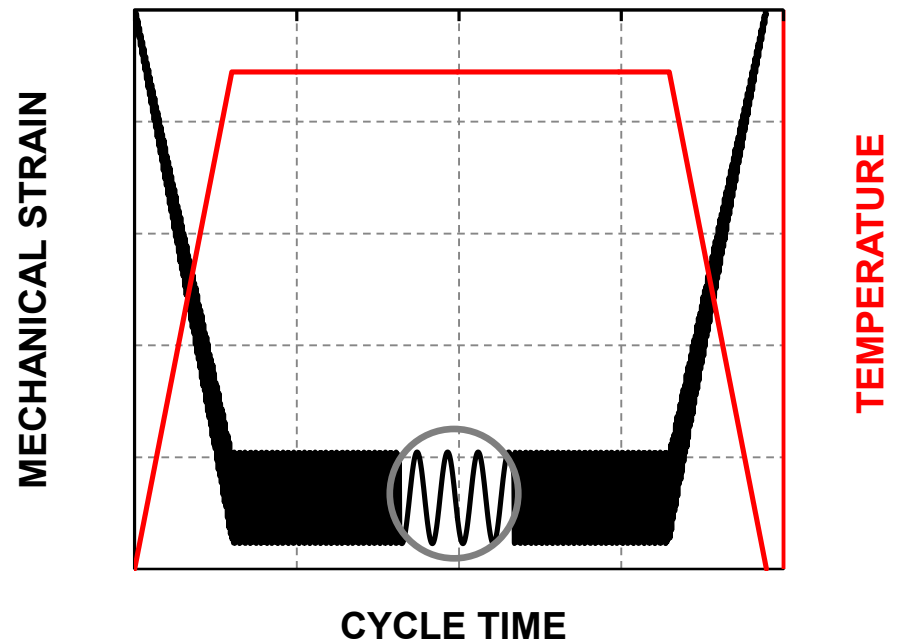
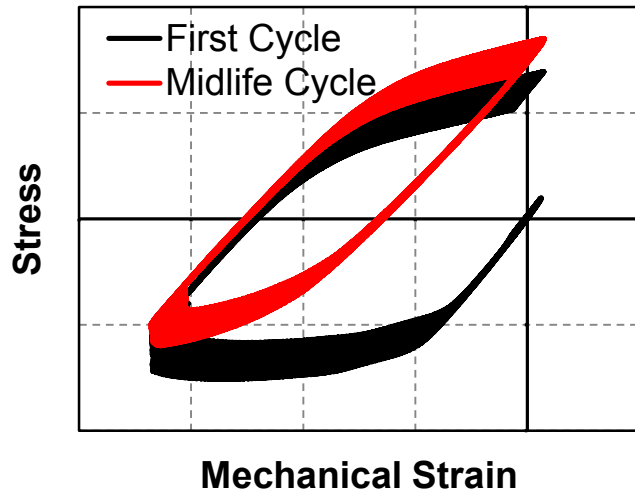
# OP TMF AND TMF/HCF TESTING

- OP TMF test

$$\varepsilon_{mech} = -G\varepsilon_{th}^*$$

- OP TMF/HCF test

$$\varepsilon_{mech} = -G\varepsilon_{th}^* + \varepsilon_{HCF}$$



## OP TMF AND TMF/HCF TESTING

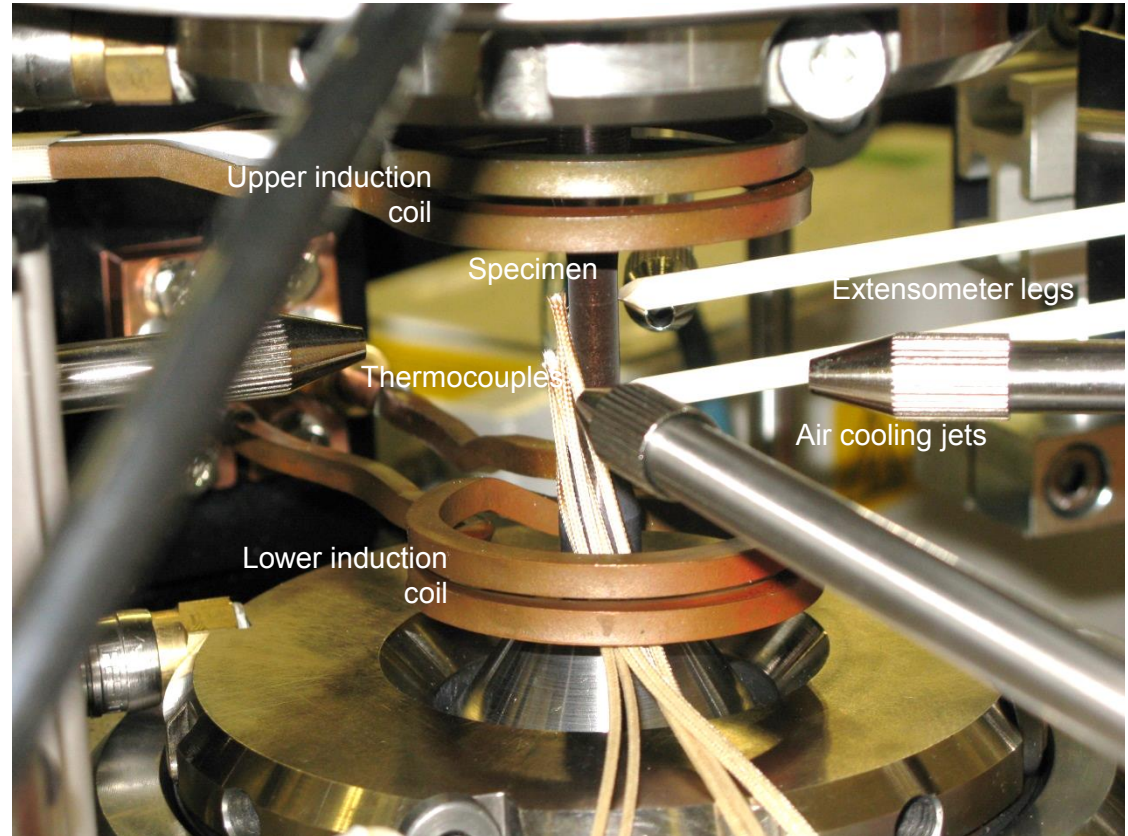
- OP TMF test

$$\varepsilon_{mech} = -G\varepsilon_{th}^*$$

- OP TMF/HCF test

$$\varepsilon_{mech} = -G\varepsilon_{th}^* + \varepsilon_{HCF}$$

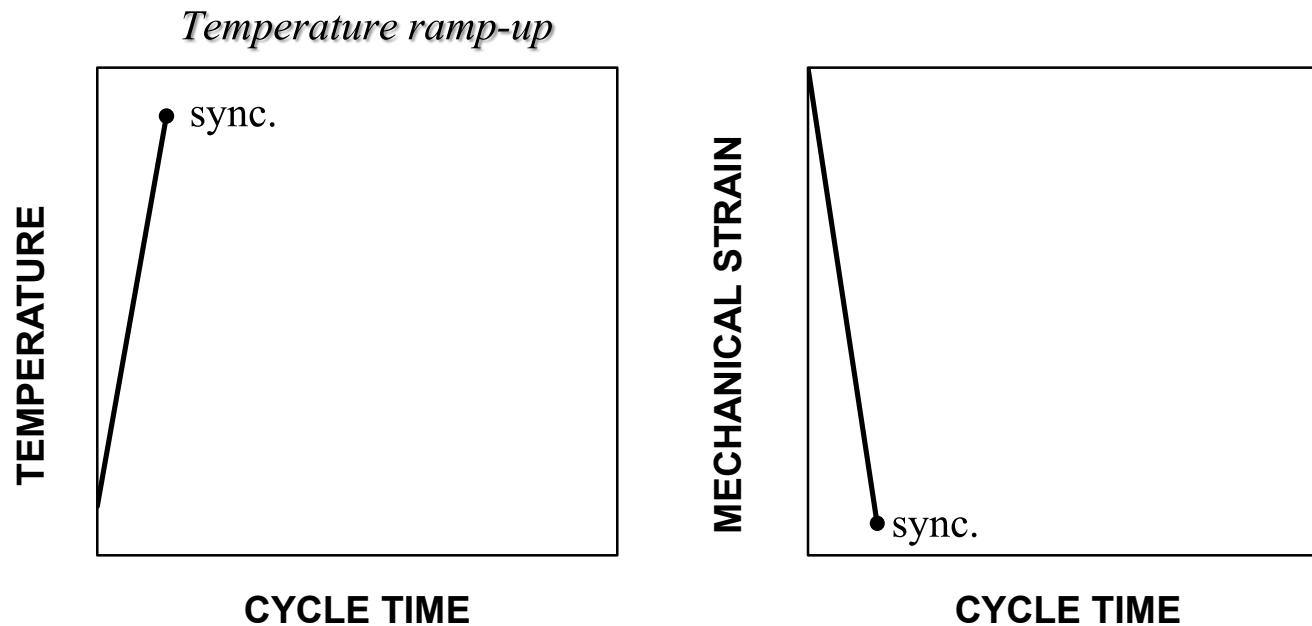
- TMF test set-up



- Test control algorithm
- Test data acquisition strategy

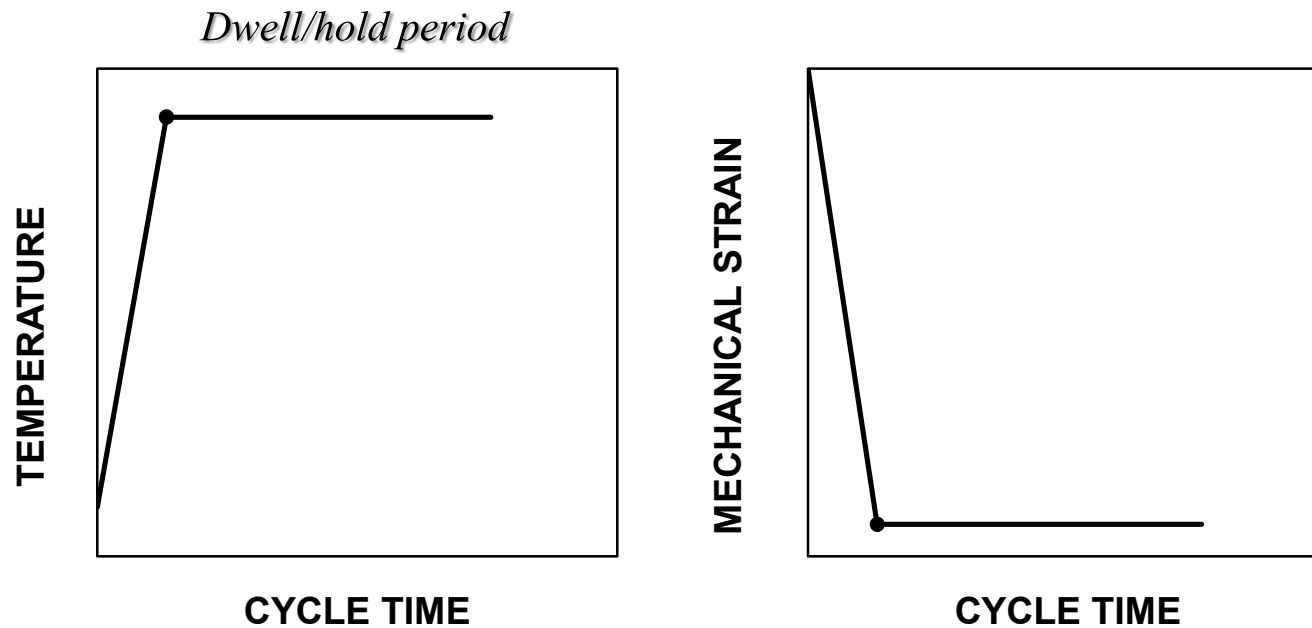
## AN ALGORITHM FOR CONDUCTION OF OP TMF TEST (G-type test)

- Conventional programming algorithm
  - Independent control of temperature and mechanical strain
    - Step synchronisation



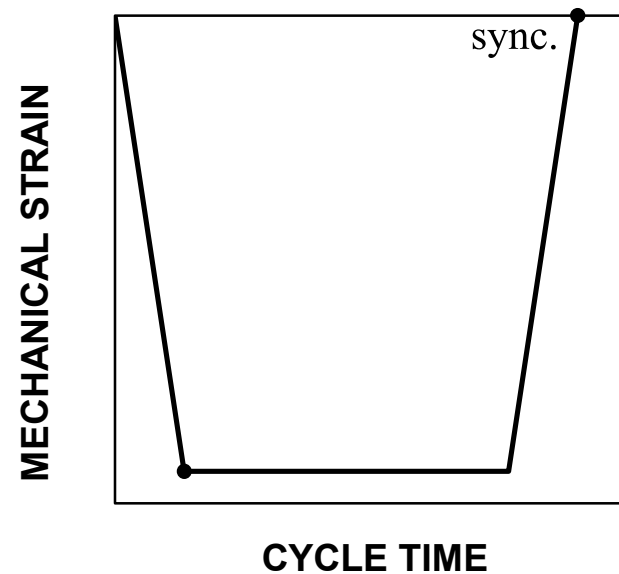
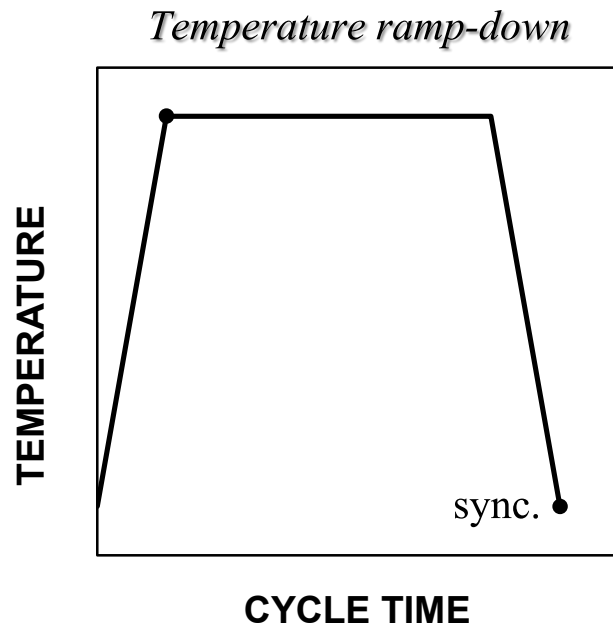
## AN ALGORITHM FOR CONDUCTION OF OP TMF TEST (G-type test)

- Conventional programming algorithm
  - Independent control of temperature and mechanical strain
    - Step synchronisation



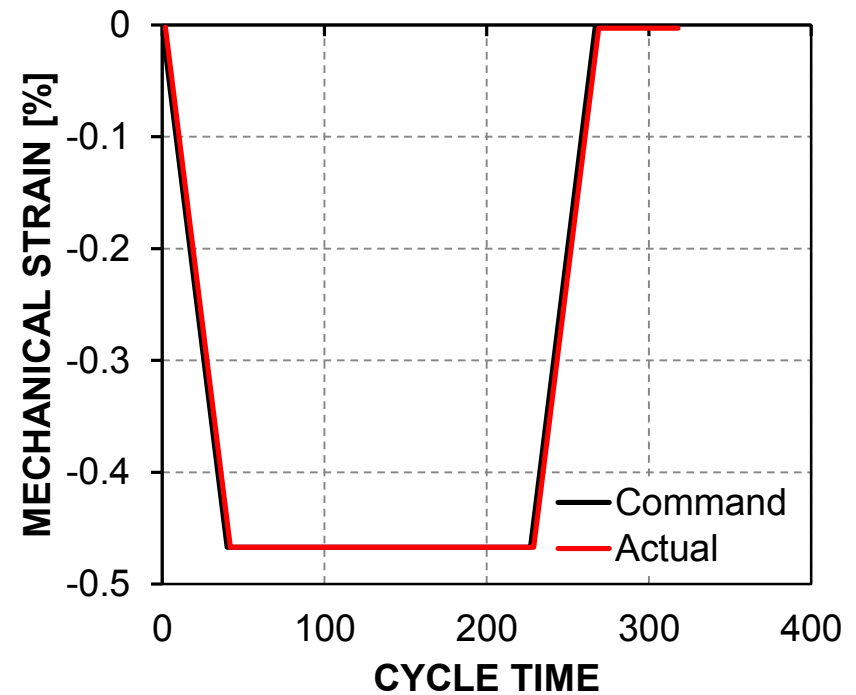
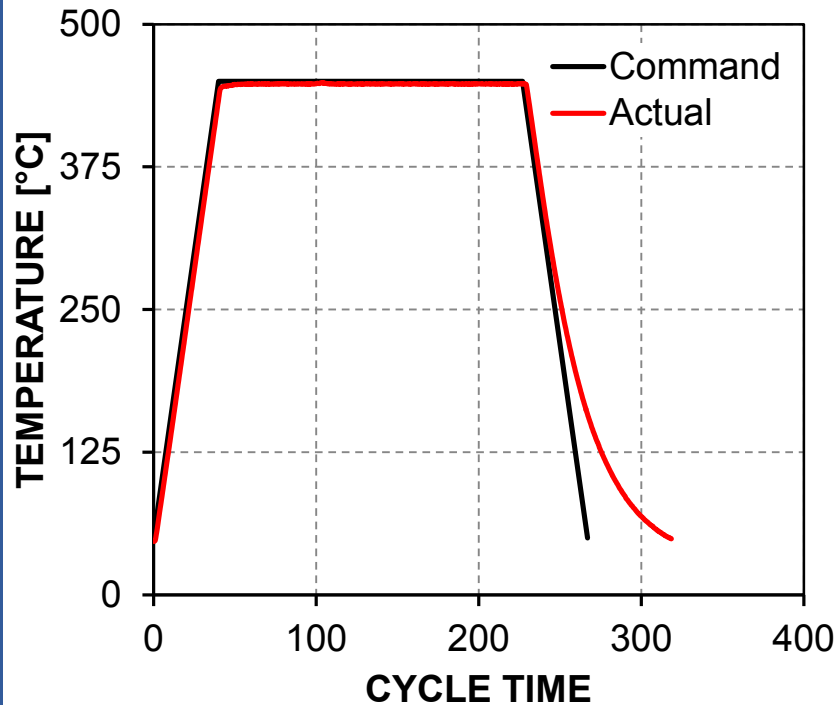
## AN ALGORITHM FOR CONDUCTION OF OP TMF TEST (G-type test)

- Conventional programming algorithm
  - Independent control of temperature and mechanical strain
    - Step synchronisation



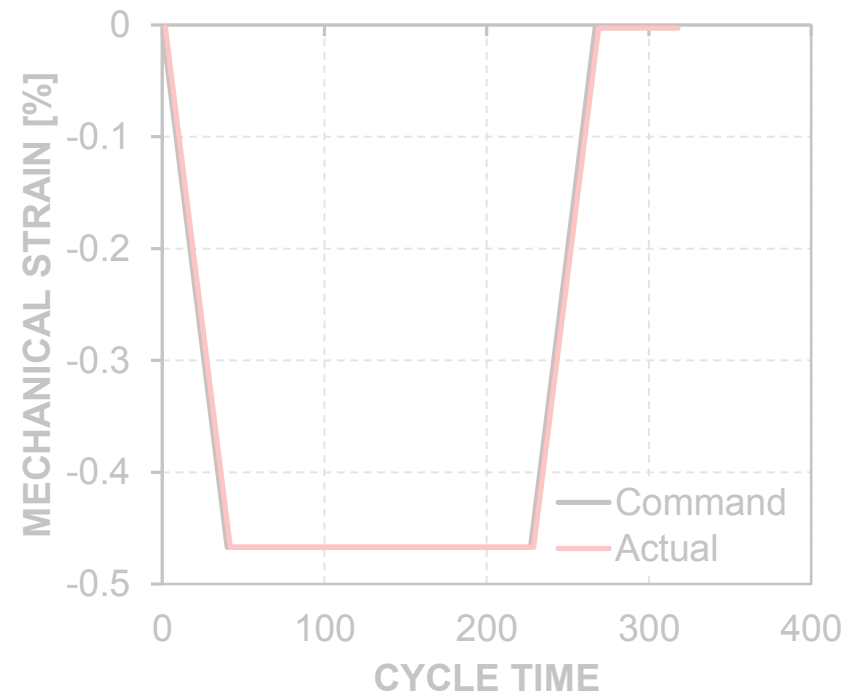
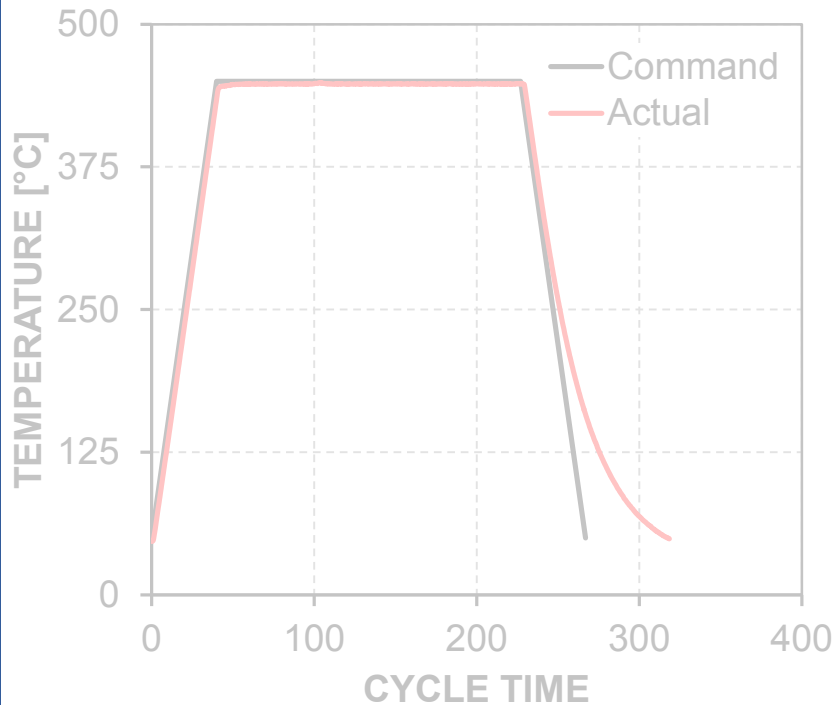
# AN ALGORITHM FOR CONDUCTION OF OP TMF TEST (G-type test)

- Example 1
  - G-type TMF test ( $T_{\max} = 450^{\circ}\text{C}$ ,  $G = 0.8$ )



## AN ALGORITHM FOR CONDUCTION OF OP TMF TEST (G-type test)

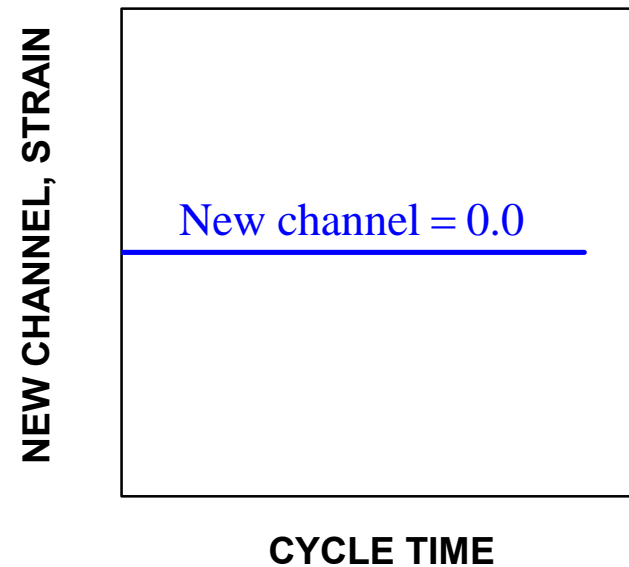
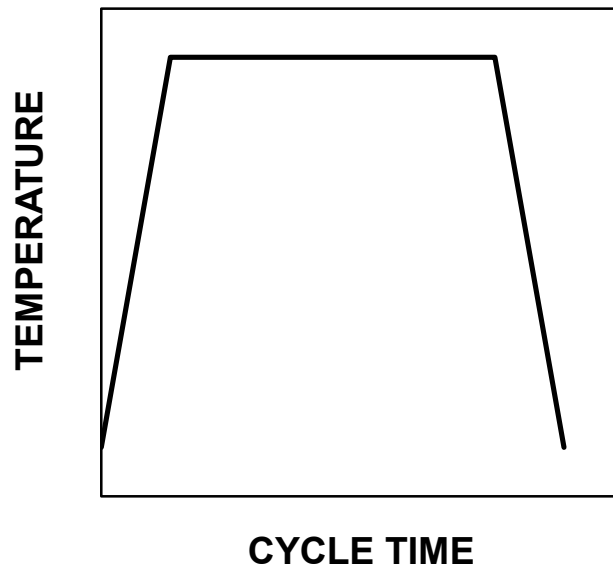
- Example 2
  - G-type TMF test ( $T_{\max} = 450^{\circ}\text{C}$ ,  $G = 0.8$ ) with superimposed HCF  $\pm 0.03\%$ 
    - Possible, but difficult!



## AN ALGORITHM FOR CONDUCTION OF OP TMF TEST (G-type test)

- A new programming algorithm based on a virtual/calculated channel

$$\text{New channel} = G\varepsilon_{th(T)} + \varepsilon_{mech}$$

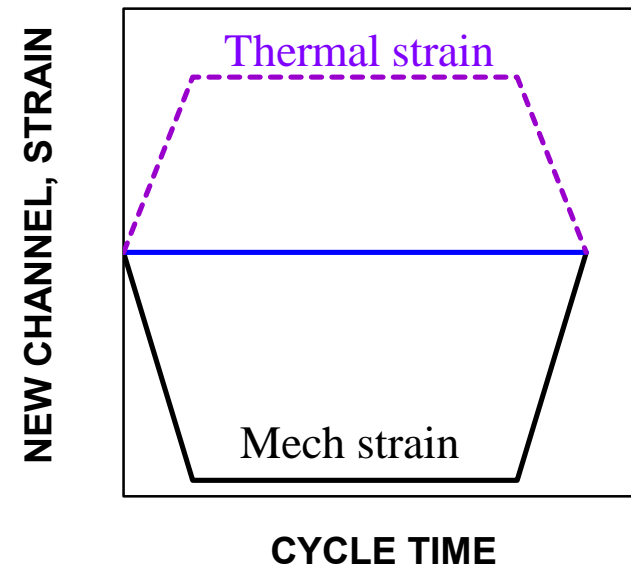
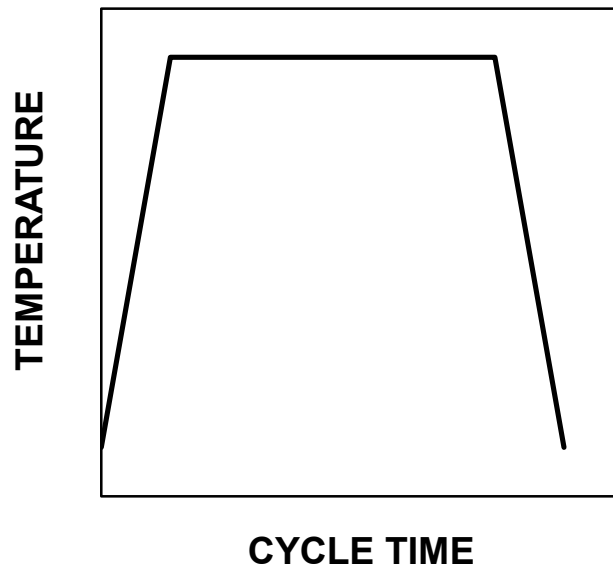




## AN ALGORITHM FOR CONDUCTION OF OP TMF TEST (G-type test)

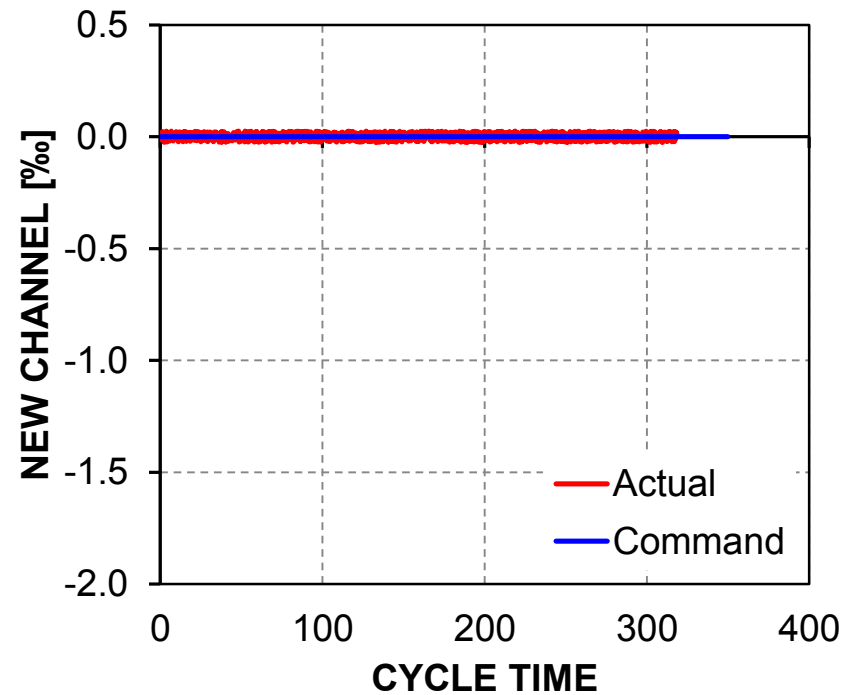
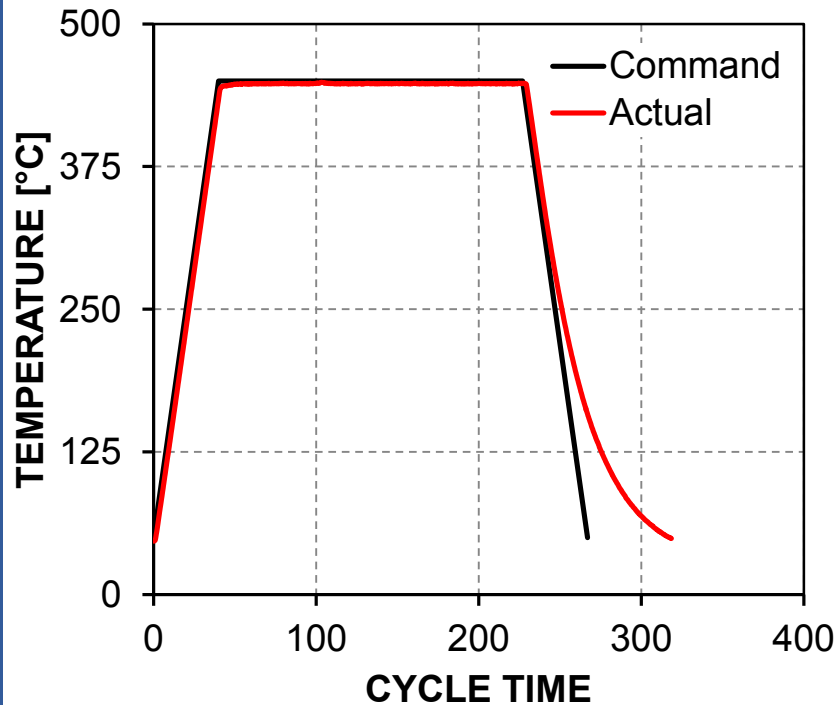
- A new programming algorithm based on a virtual/calculated channel

$$\text{New channel} = G\varepsilon_{th(T)} + \varepsilon_{mech}$$



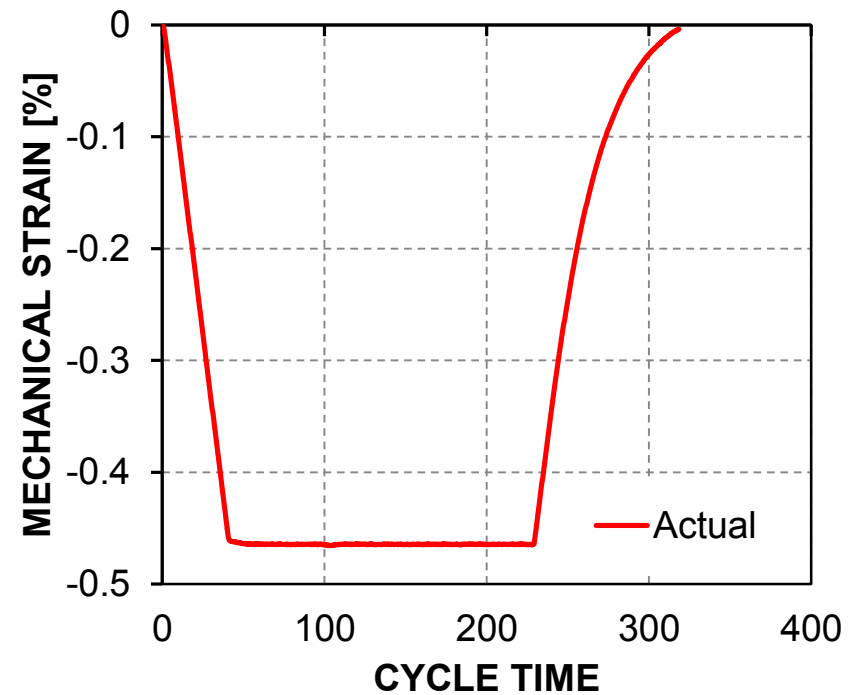
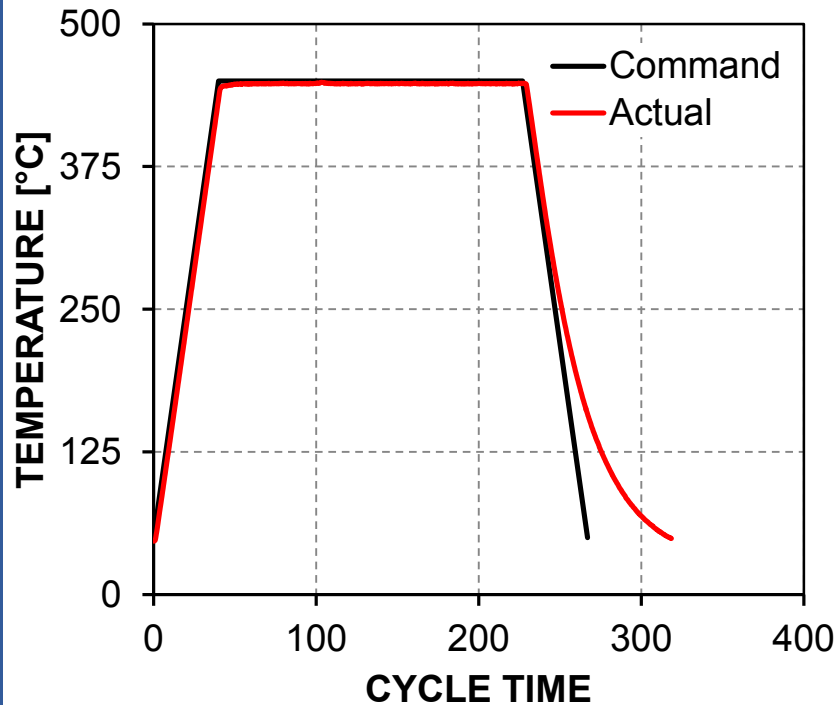
# AN ALGORITHM FOR CONDUCTION OF OP TMF TEST (G-type test)

- Example 1
  - G-type TMF test ( $T_{\max} = 450^{\circ}\text{C}$ ,  $G = 0.8$ )



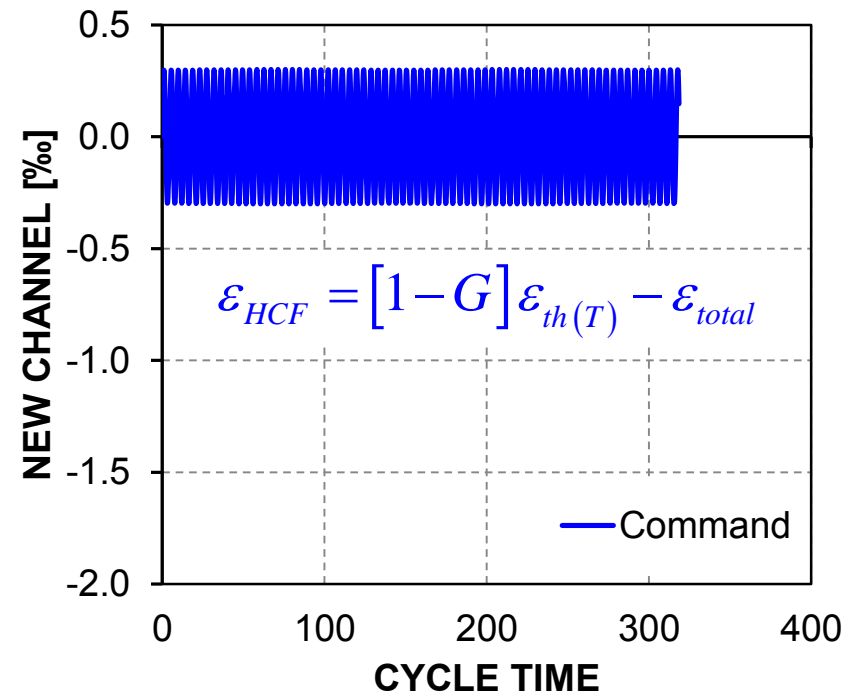
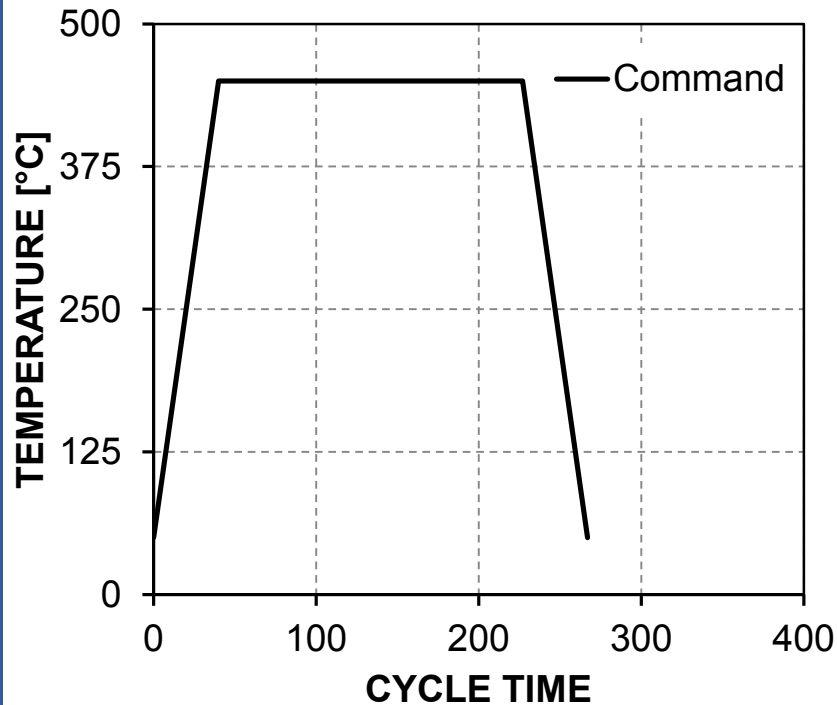
## AN ALGORITHM FOR CONDUCTION OF OP TMF TEST (G-type test)

- Example 1
  - G-type TMF test ( $T_{\max} = 450^{\circ}\text{C}$ ,  $G = 0.8$ )



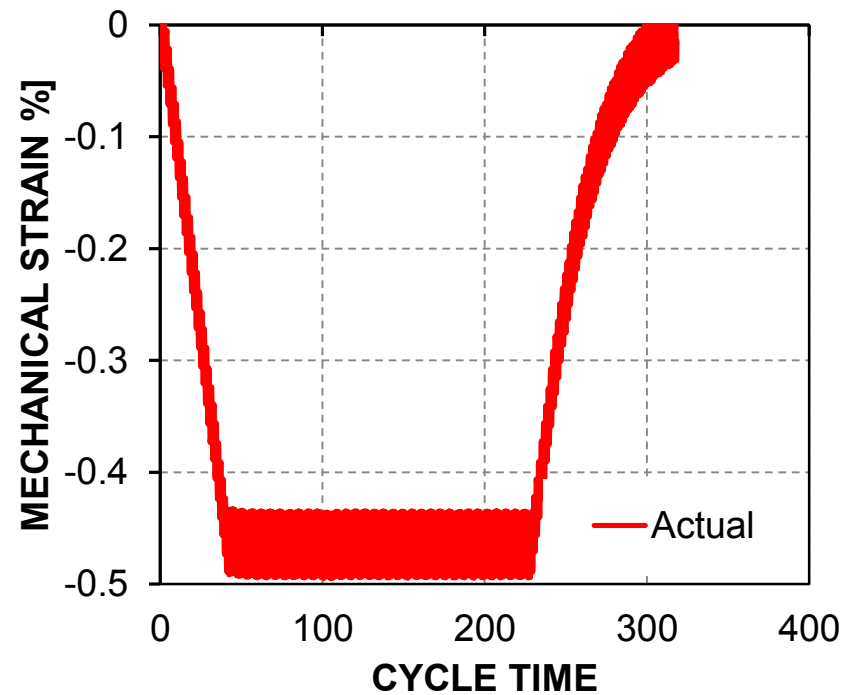
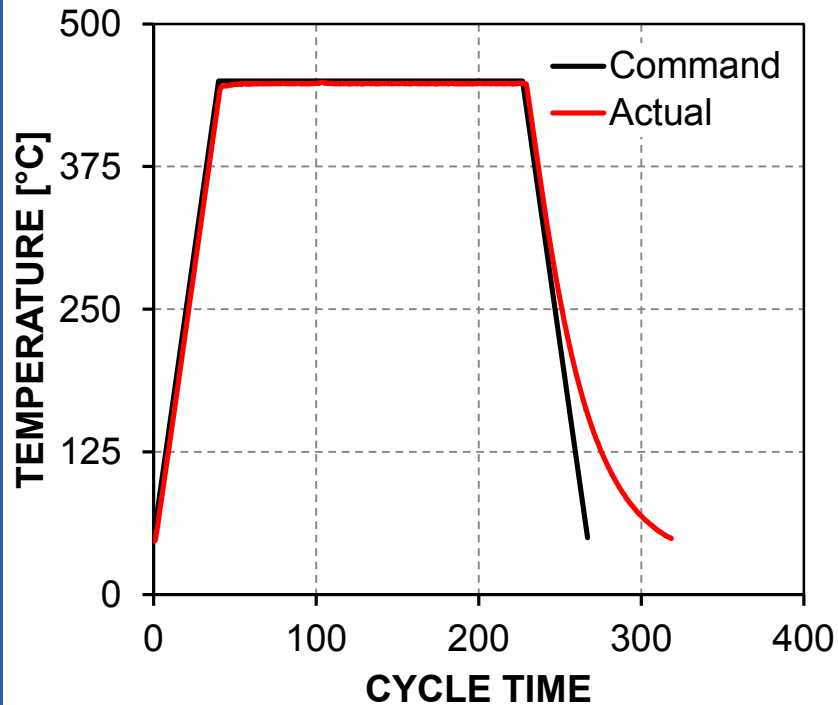
## AN ALGORITHM FOR CONDUCTION OF OP TMF TEST (G-type test)

- Example 2
  - G-type TMF test ( $T_{\max} = 450^{\circ}\text{C}$ ,  $G = 0.8$ ) with superimposed HCF  $\pm 0.03\%$



## AN ALGORITHM FOR CONDUCTION OF OP TMF TEST (G-type test)

- Example 2
  - G-type TMF test ( $T_{\max} = 450^{\circ}\text{C}$ ,  $G = 0.8$ ) with superimposed HCF  $\pm 0.03\%$

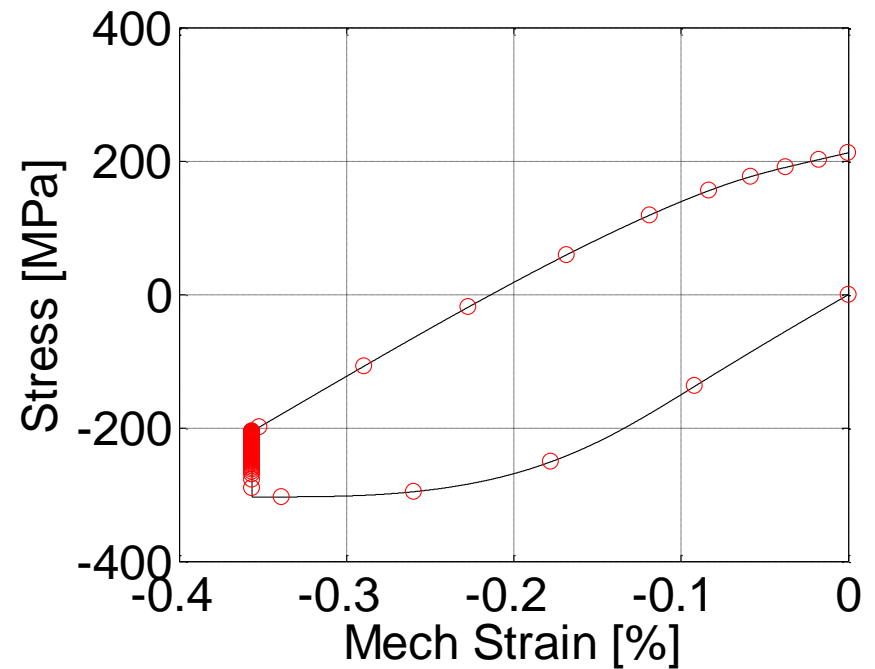
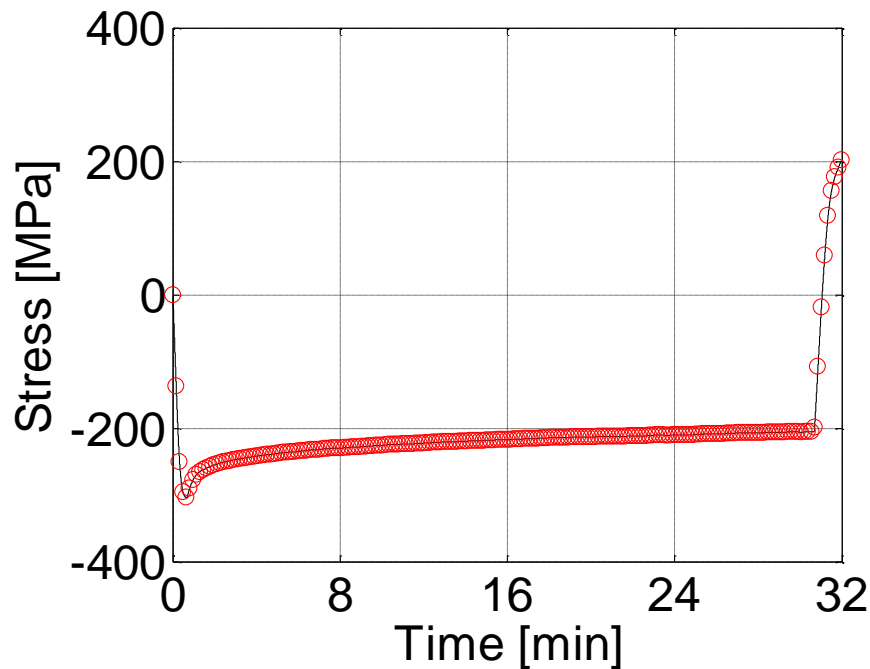


# AN ALGORITHM FOR DATA ACQUISITION DURING TMF TESTS

- Conventional DAQ algorithms
  - Time-based
  - Delta-level (strain, stress, ...)
  - Peak-valley

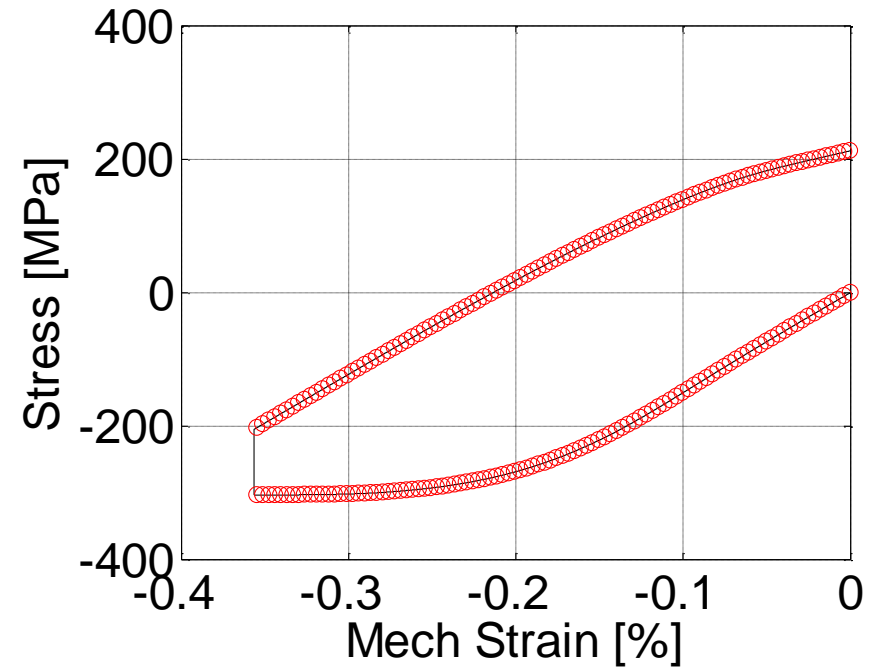
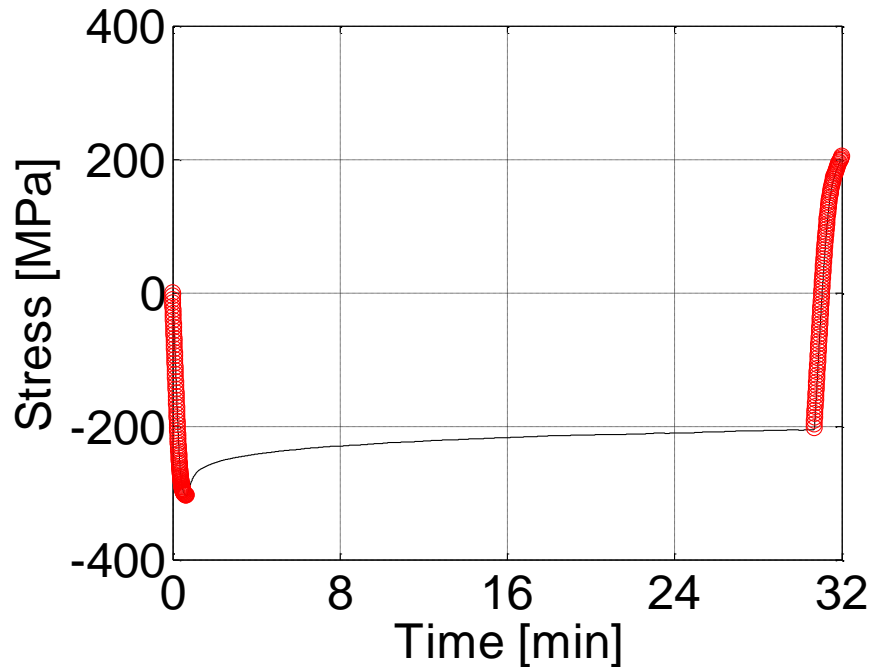
# AN ALGORITHM FOR DATA ACQUISITION DURING TMF TESTS

- Conventional DAQ algorithms
  - Time-based



# AN ALGORITHM FOR DATA ACQUISITION DURING TMF TESTS

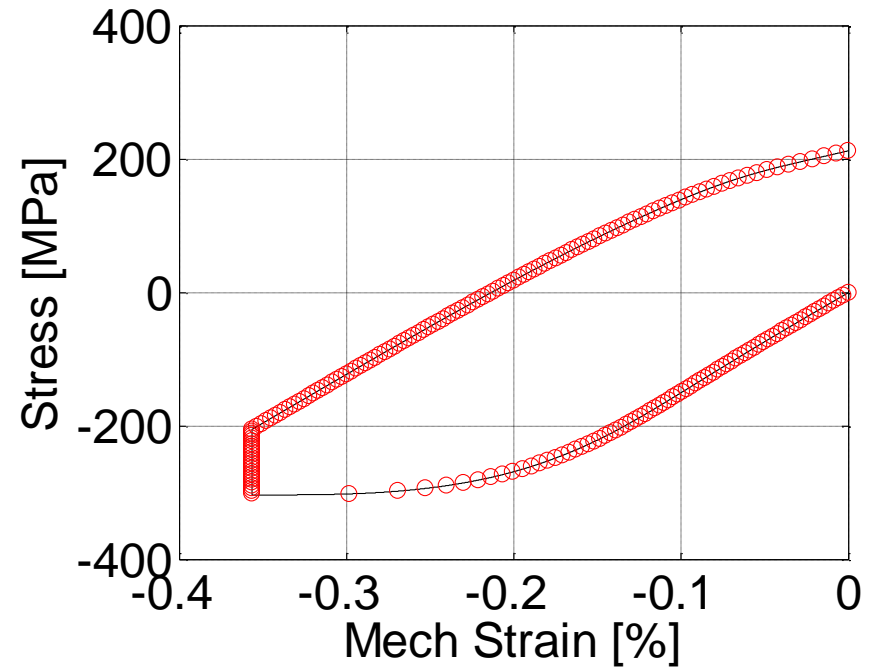
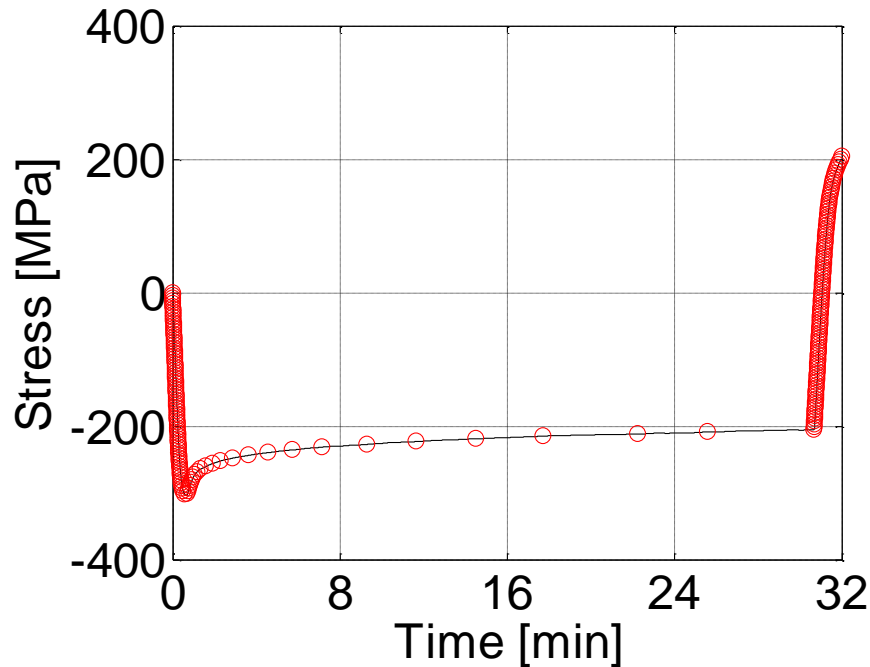
- Conventional DAQ algorithms
  - Delta-level (strain)





# AN ALGORITHM FOR DATA ACQUISITION DURING TMF TESTS

- Conventional DAQ algorithms
  - Delta-level (stress)



# AN ALGORITHM FOR DATA ACQUISITION DURING TMF TESTS

- Employment of multi-DAQ algorithms
  - Time-based
  - Delta-level (strain)
  - Delta-level (stress)
  - ....

**Recording unnecessary large amount of data (big data files!)**

# AN ALGORITHM FOR DATA ACQUISITION DURING TMF TESTS

- A new-effective algorithm
    - Higher frequency data acquisition where there is more variation in signals!
      - Delta-level DAQ ('Csig')
- 'CSig' is a virtual/calculated channel varying between zero and unity!

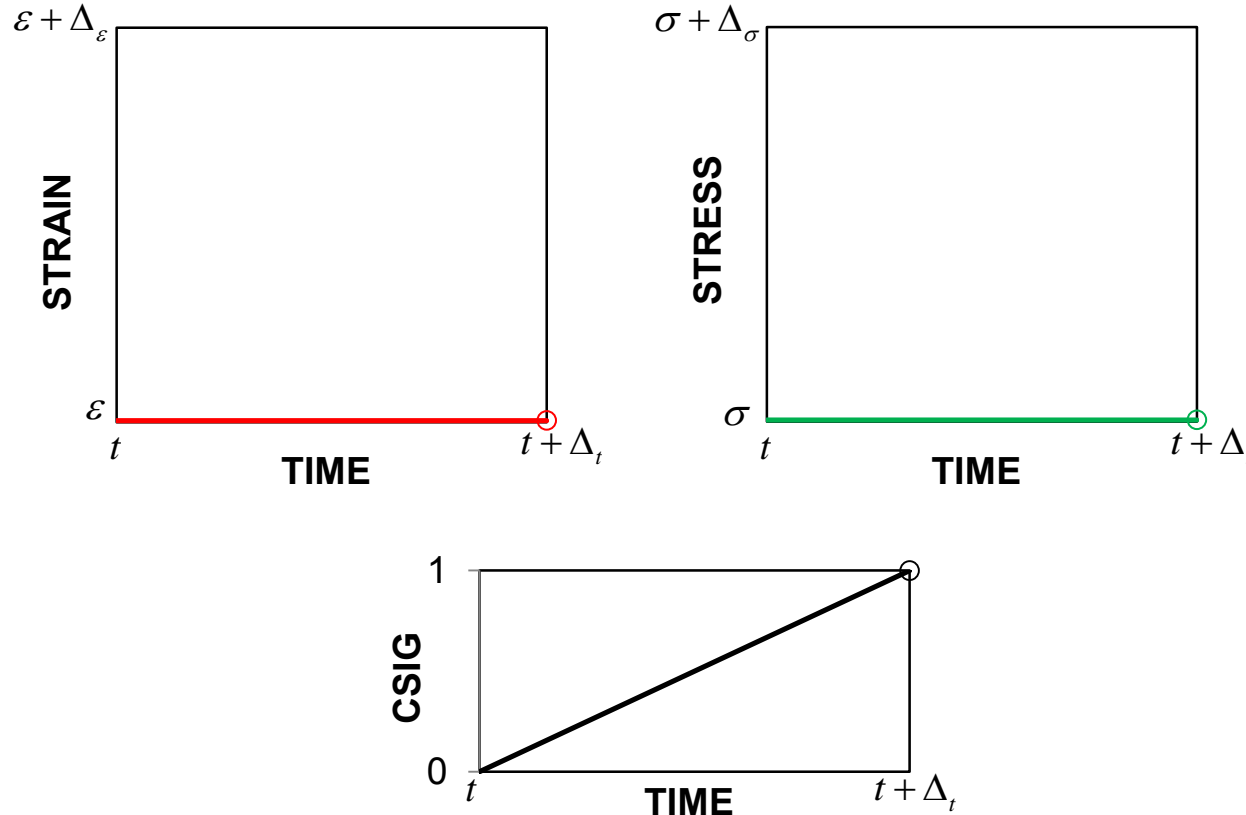
$$A = {}^{n-1}\text{CSig} + {}^{n-1}\text{B} \times \left[ \frac{\Delta t}{\Delta_t} + \left| \frac{\Delta \varepsilon}{\Delta_\varepsilon} \right| + \left| \frac{\Delta \sigma}{\Delta_\sigma} \right| + \dots \right]$$

$${}^n\text{CSig} = \begin{cases} 0 & A < 0 \\ 1 & A > 1 \\ A & \text{else} \end{cases}$$

$${}^n\text{B} = \begin{cases} {}^{n-1}\text{B} & {}^n\text{CSig} = A \\ -{}^{n-1}\text{B} & \text{else} \end{cases}$$

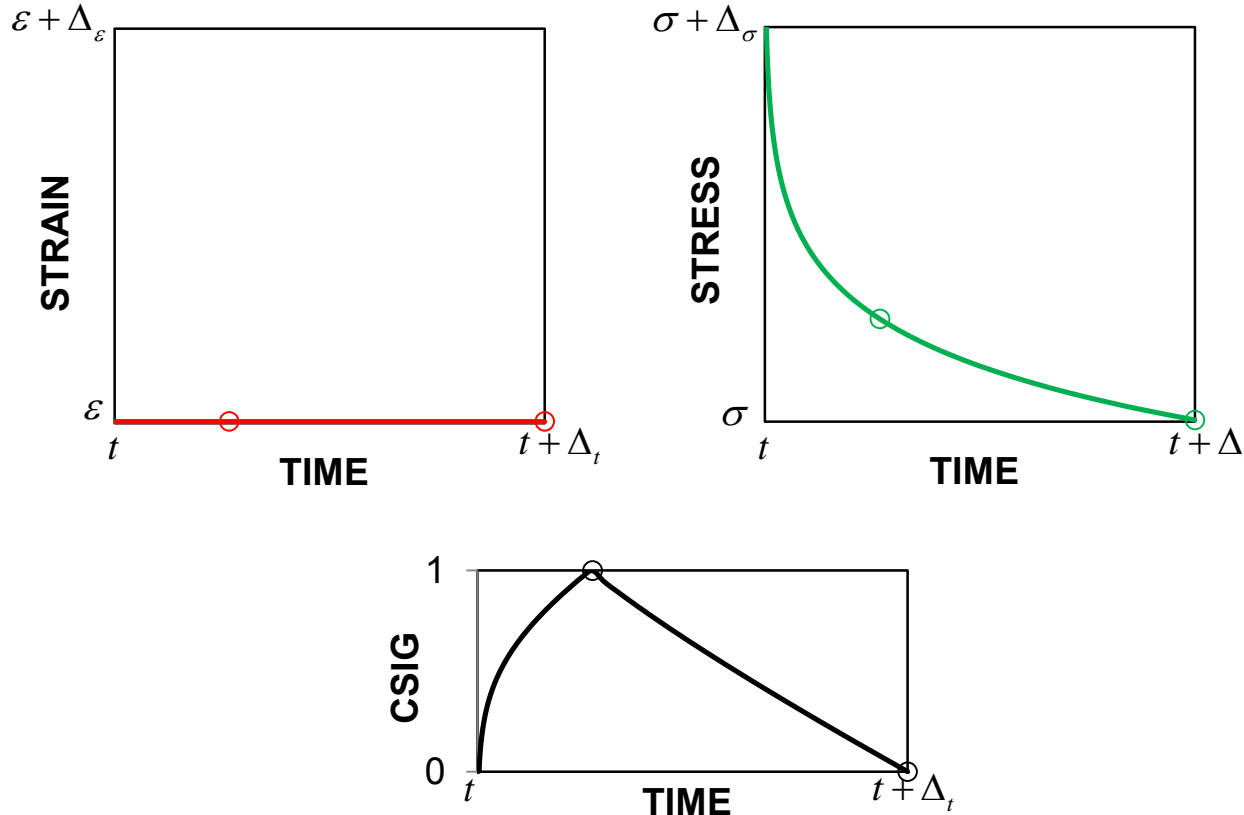
# AN ALGORITHM FOR DATA ACQUISITION DURING TMF TESTS

- A new-effective algorithm
  - Higher frequency data acquisition where there is more variation in signals!



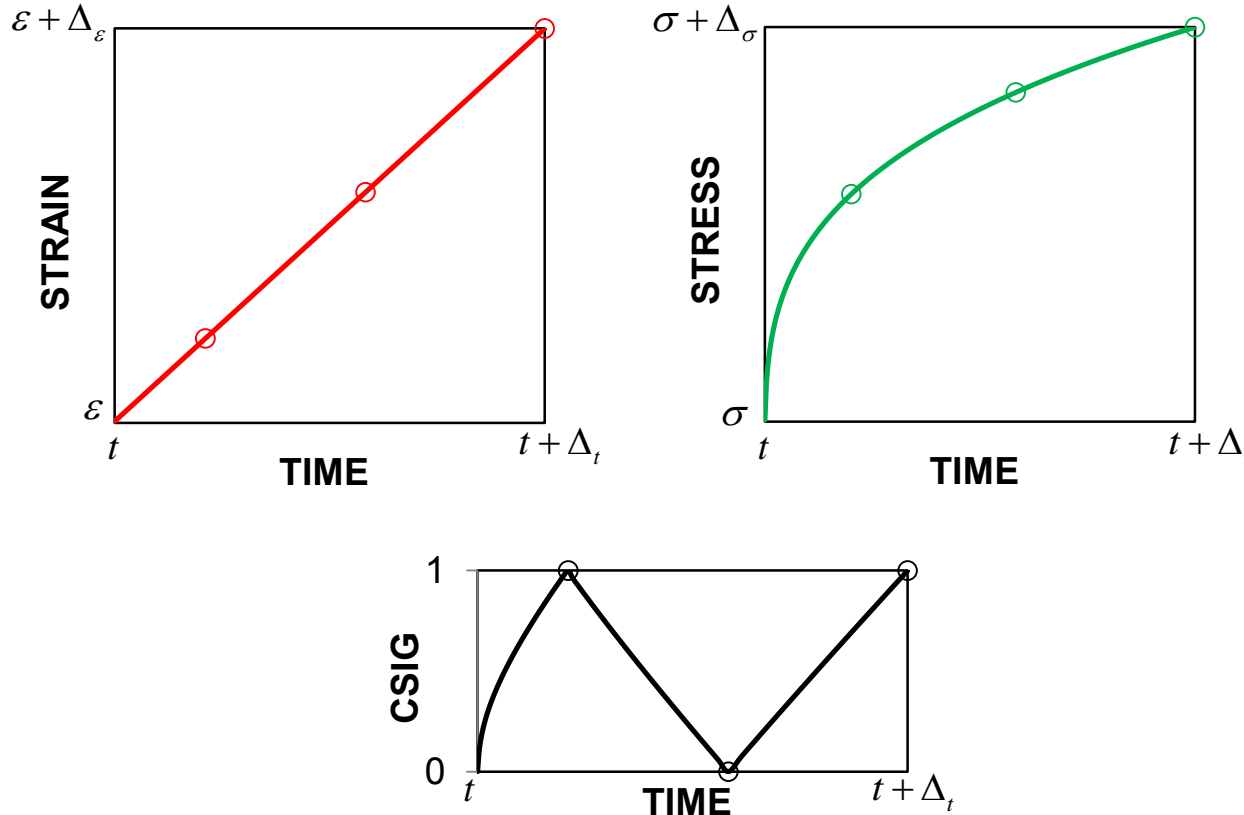
# AN ALGORITHM FOR DATA ACQUISITION DURING TMF TESTS

- A new-effective algorithm
  - Higher frequency data acquisition where there is more variation in signals!



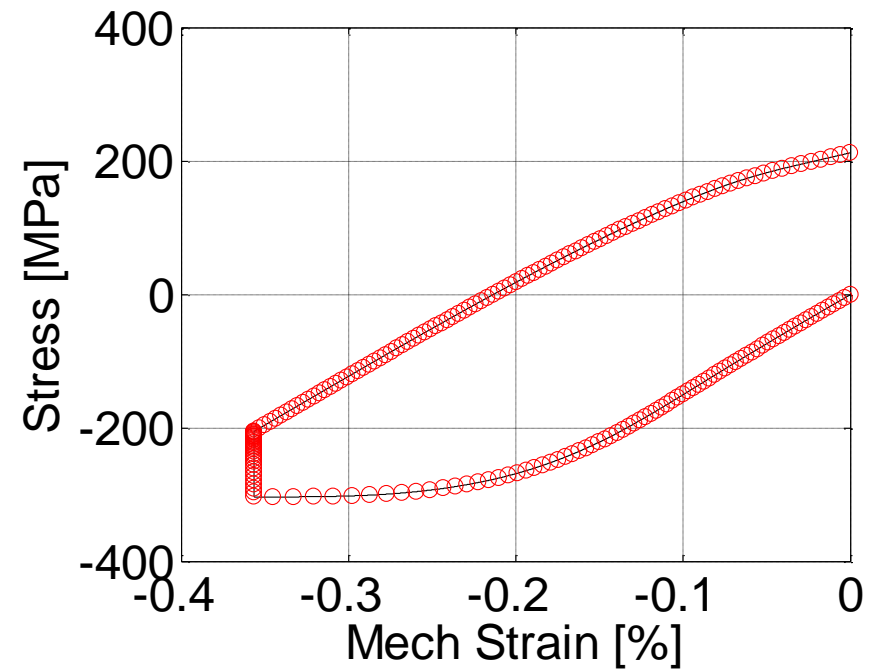
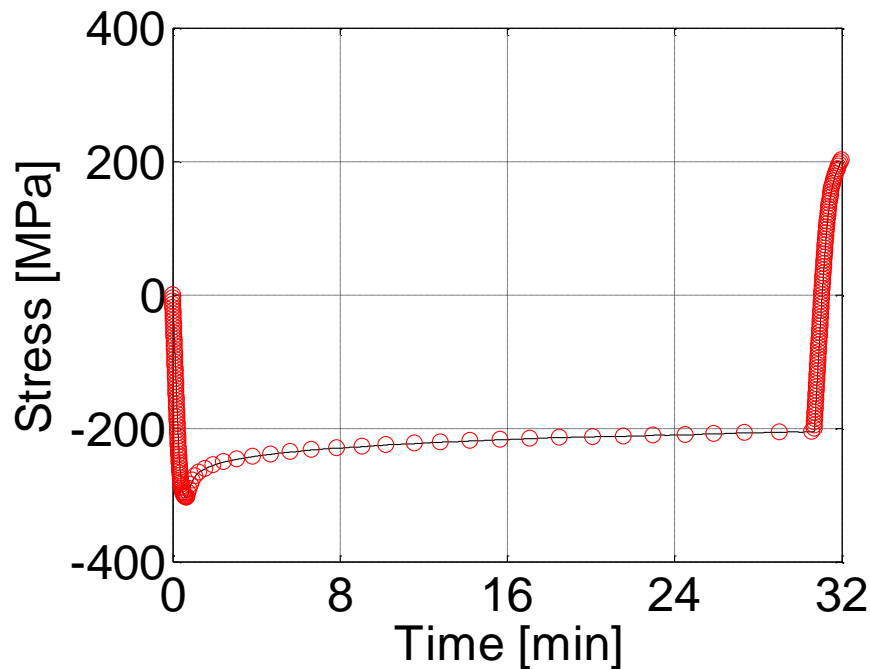
# AN ALGORITHM FOR DATA ACQUISITION DURING TMF TESTS

- A new-effective algorithm
  - Higher frequency data acquisition where there is more variation in signals!

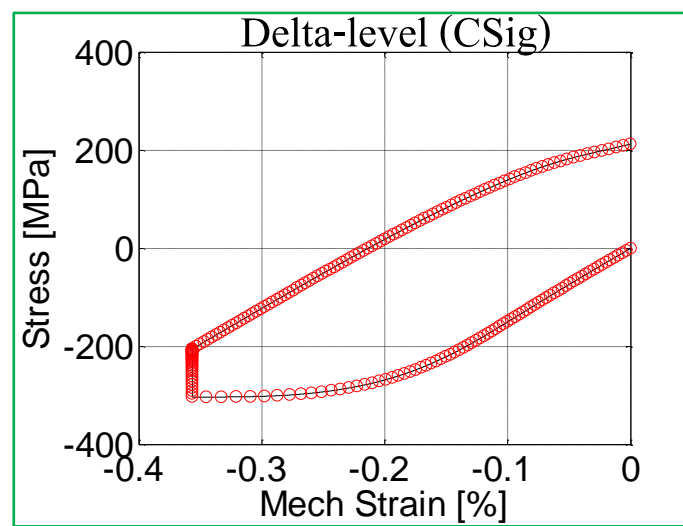
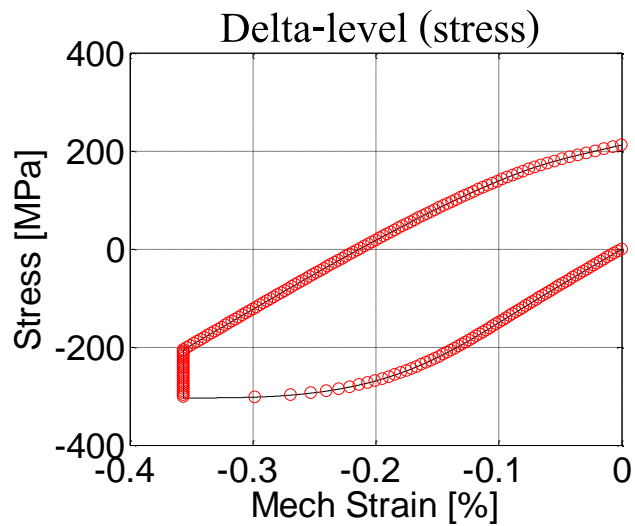
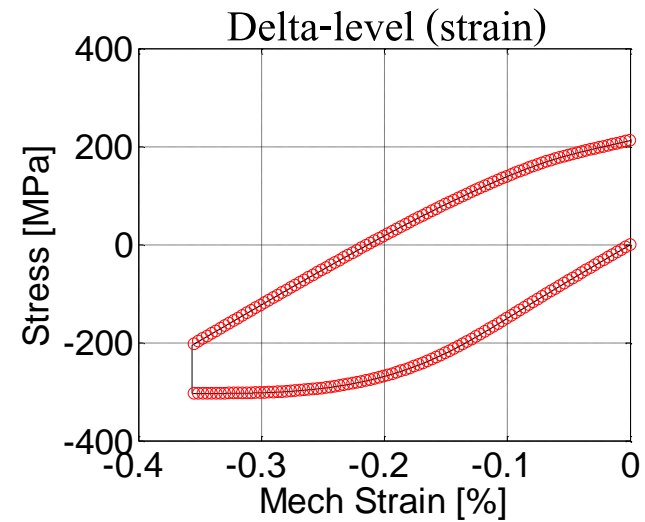
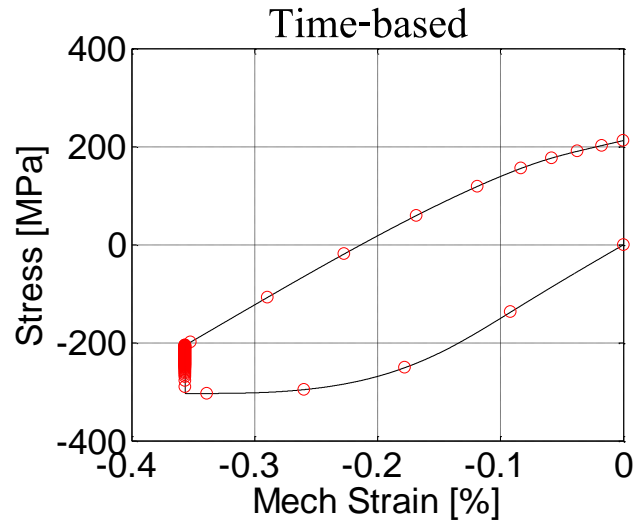


# AN ALGORITHM FOR DATA ACQUISITION DURING TMF TESTS

- A new-effective algorithm
  - Higher frequency data acquisition where there is more variation in signals!



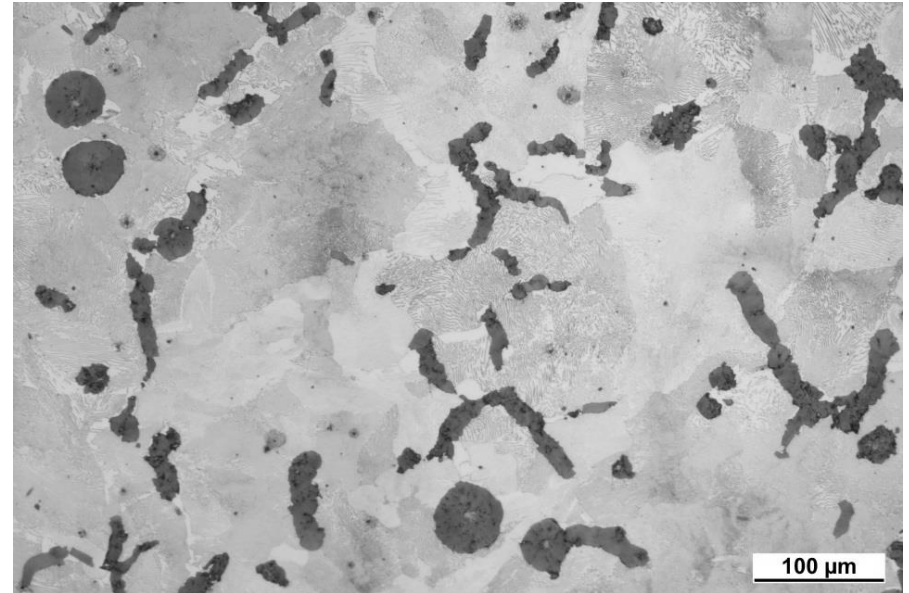
# AN ALGORITHM FOR DATA ACQUISITION DURING TMF TESTS





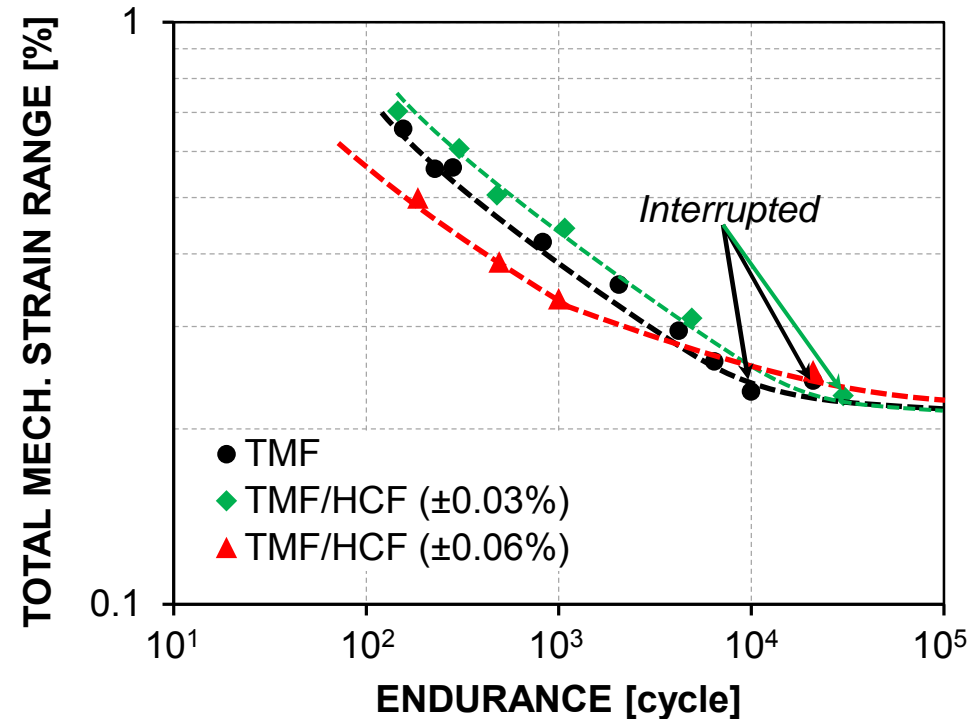
## MATERIAL AND TESTING CONDITIONS

- Material
  - A vermicular cast iron (GJV-450)
- Testing conditions
  - Maximum cycle temperature: 450°C
  - Hold/dwell period at  $T_{\max}$ : 180s
  - Various constraint levels (G: 0.4-1.2)
  - Pure TMF and TMF/HCF tests ( $\pm 0.03\%$  and  $\pm 0.06\%$ , 10Hz)



## EXPERIMENTAL RESULTS AND DISCUSSIONS

- TMF crack initiation endurance

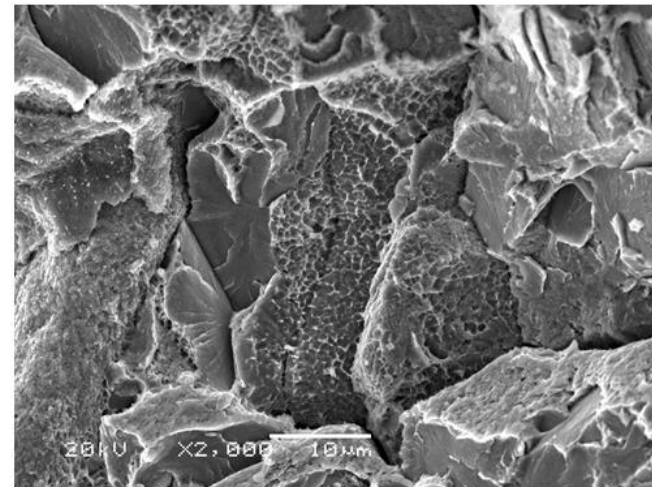


- The threshold HCF strain amplitude is  $\sim 0.03\%$ .
- The fatigue-limits for both TMF and TMF/HCF are similar and correspond to the fatigue-limit for isothermal HCF loading with similar mean stress level.

## SUMMARY

- A set of service-type cycle TMF and TMF/HCF tests with  $T_{\max}$  450°C and a dwell/hold time at peak mechanical strain in compression of 180s has been conducted for a vermicular cast iron (GJV-450).
- New-effective algorithms were introduced for control and DAQ of the OP TMF tests.
- Evidence is presented to show that superimposed HCF loading below a threshold strain amplitude does not reduce the crack initiation endurance. The threshold was  $\sim 0.03\%$  for the conducted experiments.
- Similar fatigue-limits for both TMF and TMF/HCF were observed which coincided with the fatigue-limit of the iron under isothermal HCF loading with similar mean stress level.

**Low Rupture Ductility of Materials**  
(Metallurgical Considerations, Modelling & Testing)  
Thursday 2<sup>nd</sup> – Friday 3<sup>rd</sup> June 2016  
**Burleigh Court, University of Loughborough**  
2<sup>nd</sup> circular



# Infrared Thermography for Temperature Measurement and Control during Mechanical Testing

**Dr. J.P. Jones<sup>1</sup>, Dr. M.T. Whittaker<sup>1</sup>, Dr. S.P. Brookes<sup>2</sup>, Mr. A.L. Dyer<sup>1</sup>**

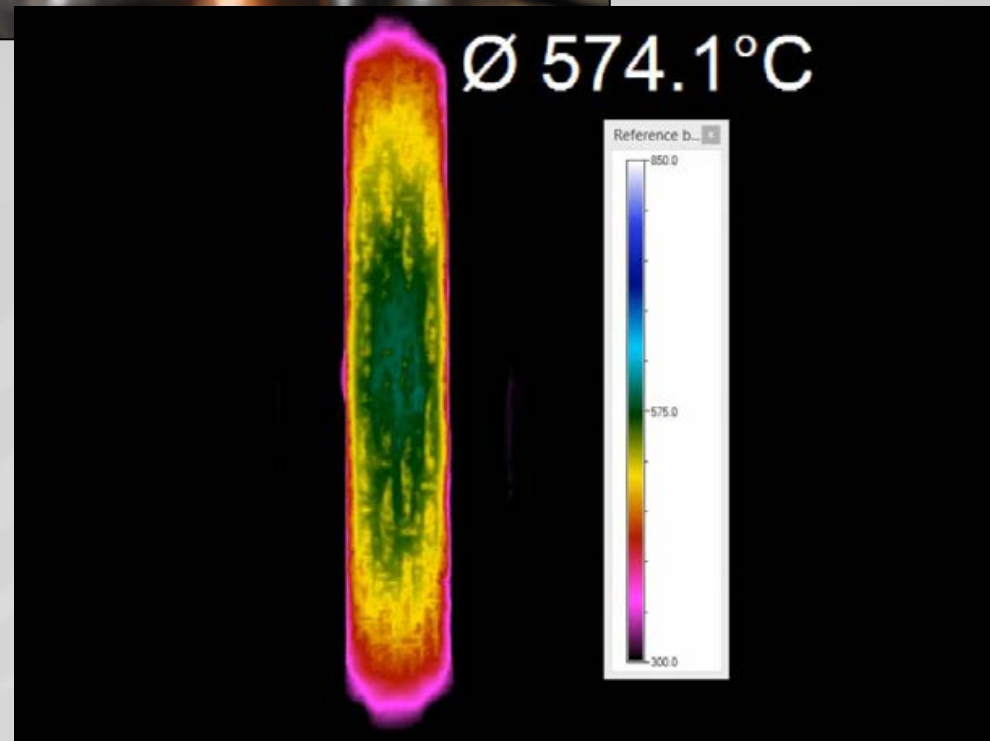
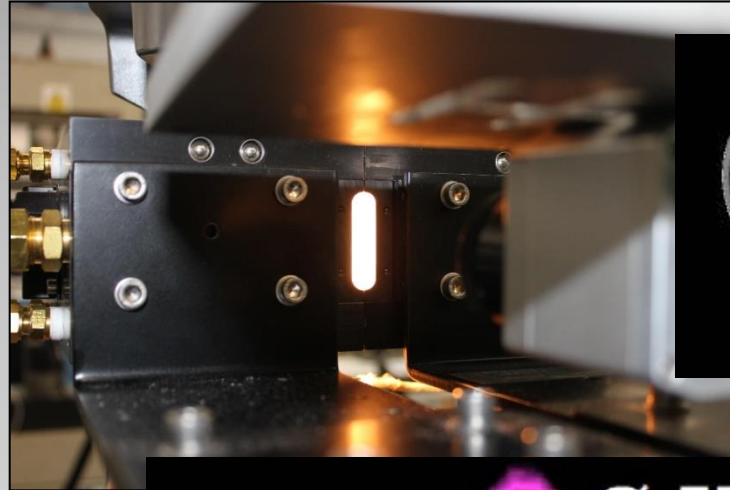
<sup>1</sup> Institute of Structural Materials, Bay Campus, Swansea University, SA1 8EN, United Kingdom.

<sup>2</sup> Rolls-Royce, Mechanical Test Operations Centre, GmbH, 15827 Blankenfelde-Mahlow, Germany.

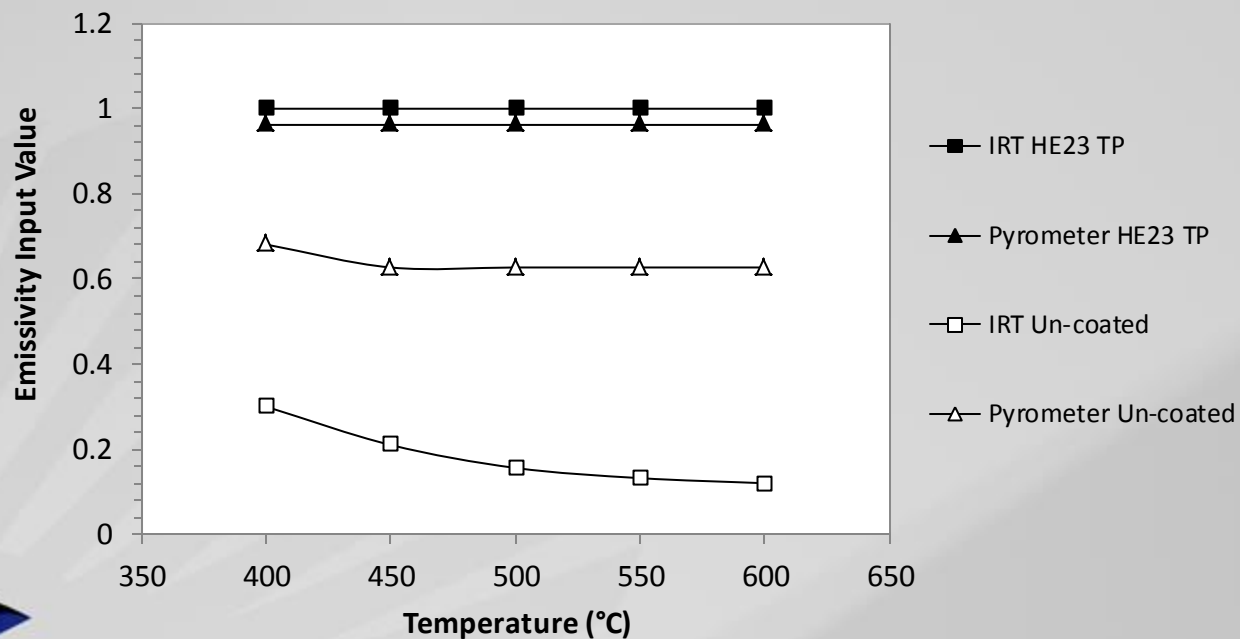
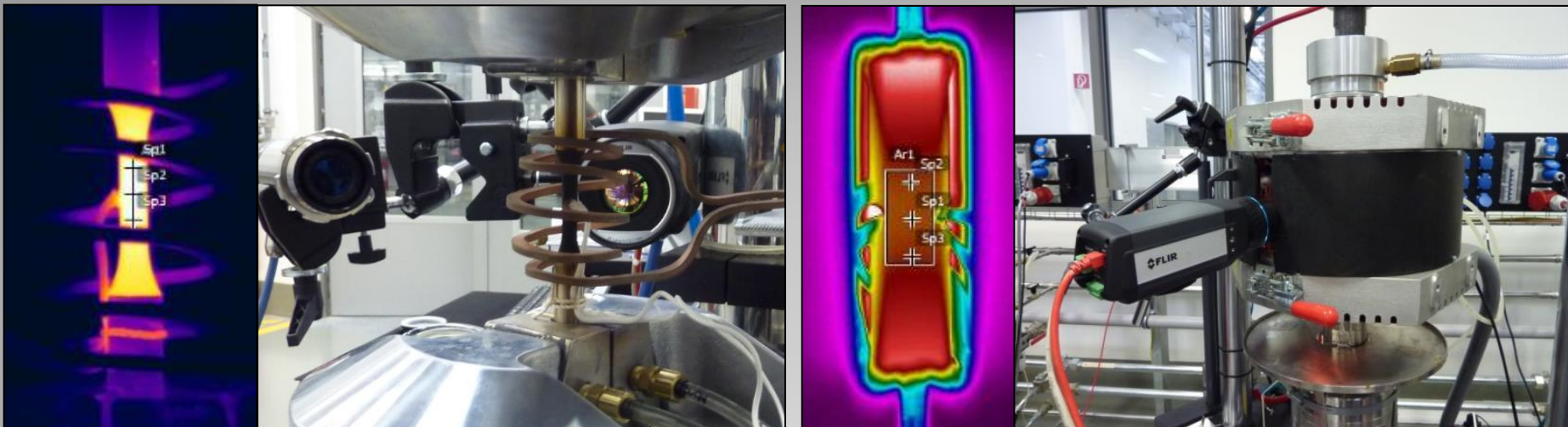


# Introduction - Thermography

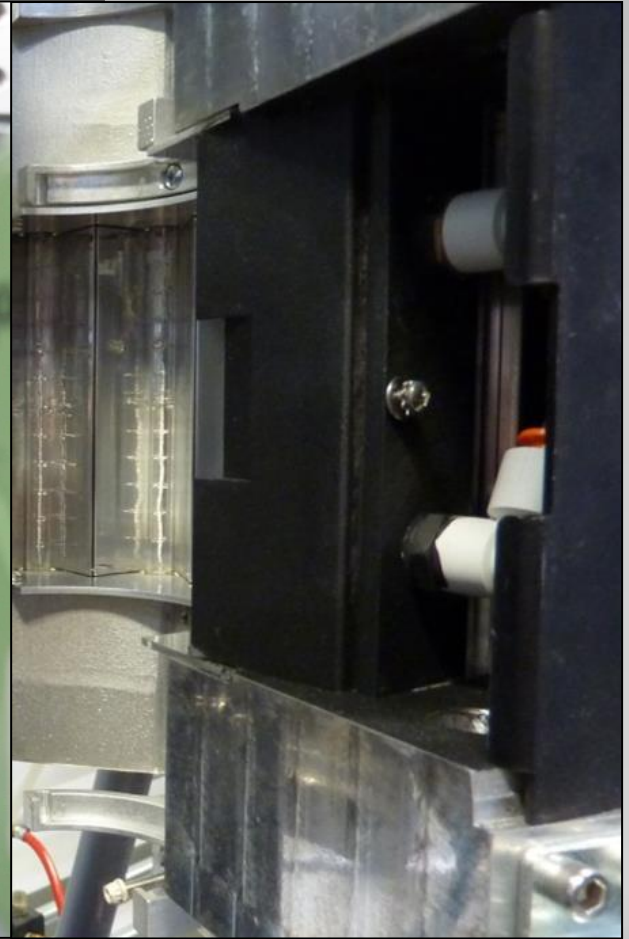
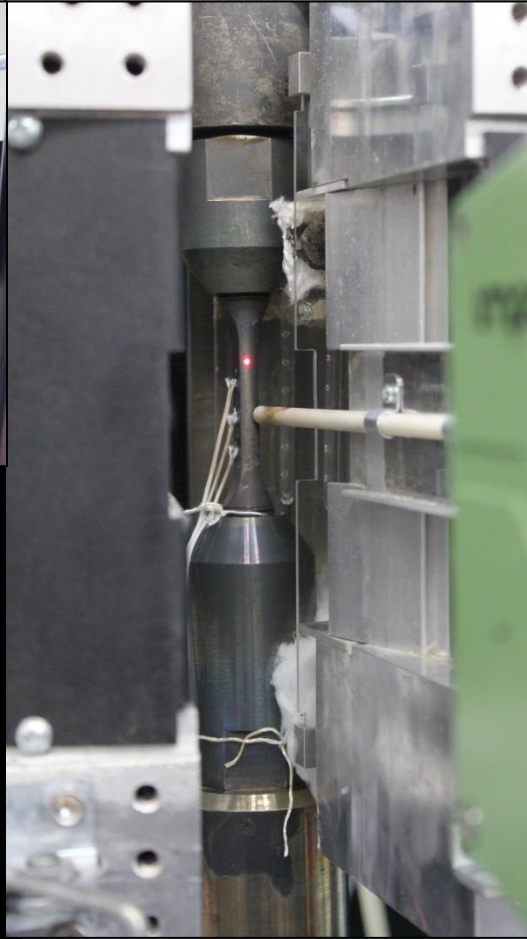
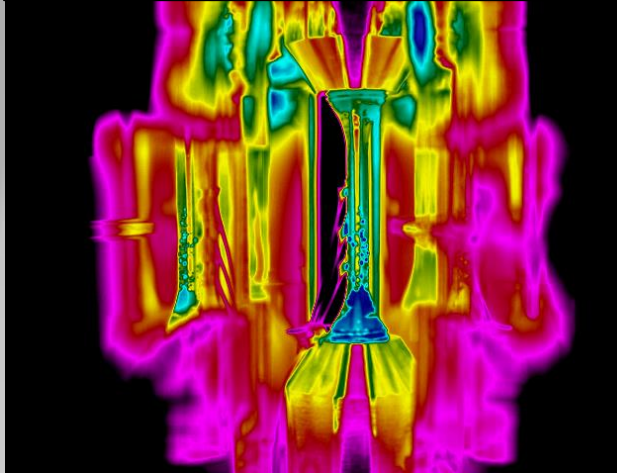
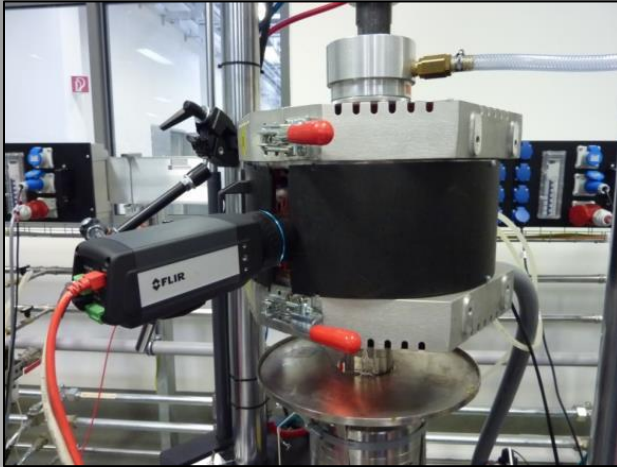
- Previous Work
- Experimental Setup
- Isothermal Stability
- Dynamic Performance
- Thermocouple Complications



# Previous Work – Rolls-Royce, MTOC

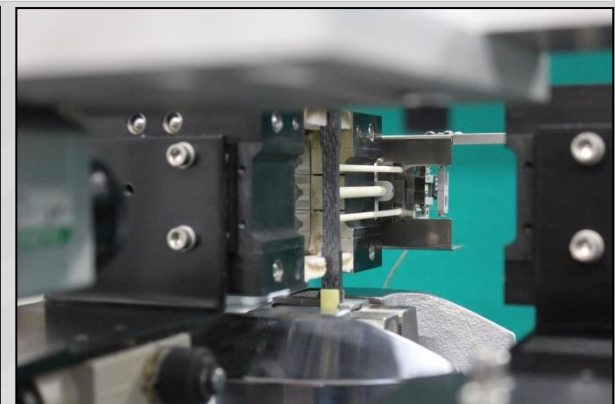
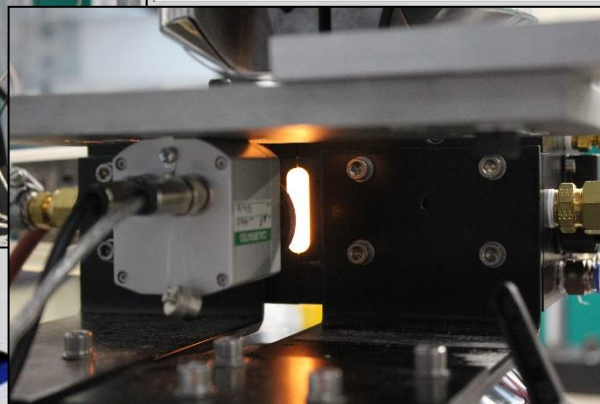


# Previous Work – Rolls-Royce, MTOC

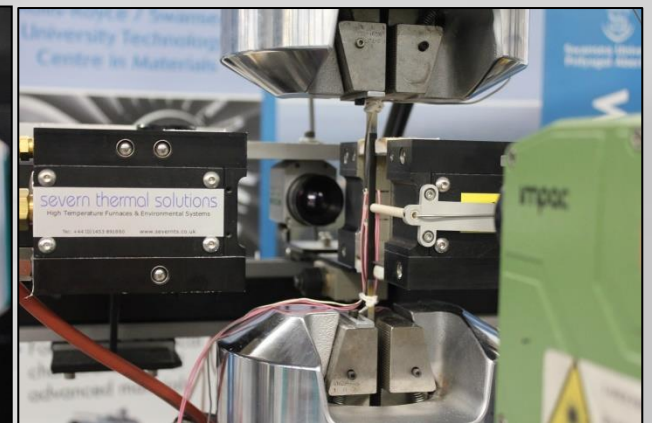




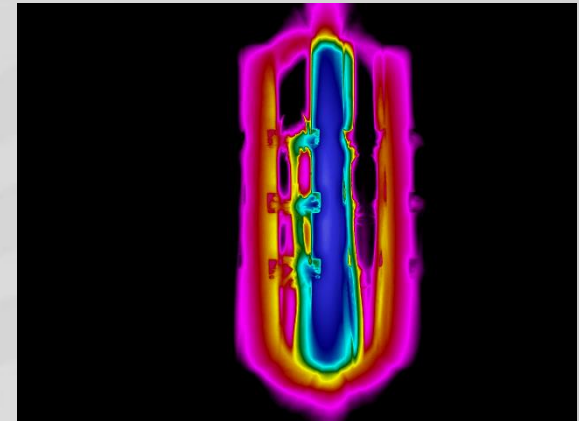
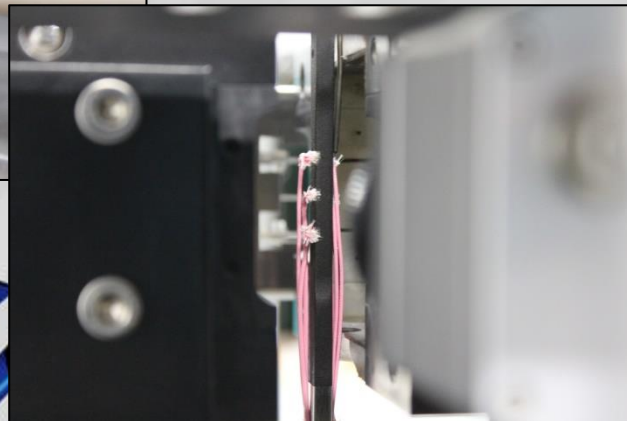
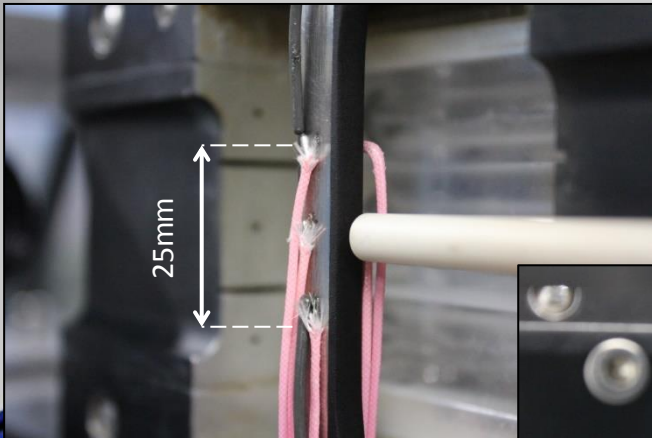
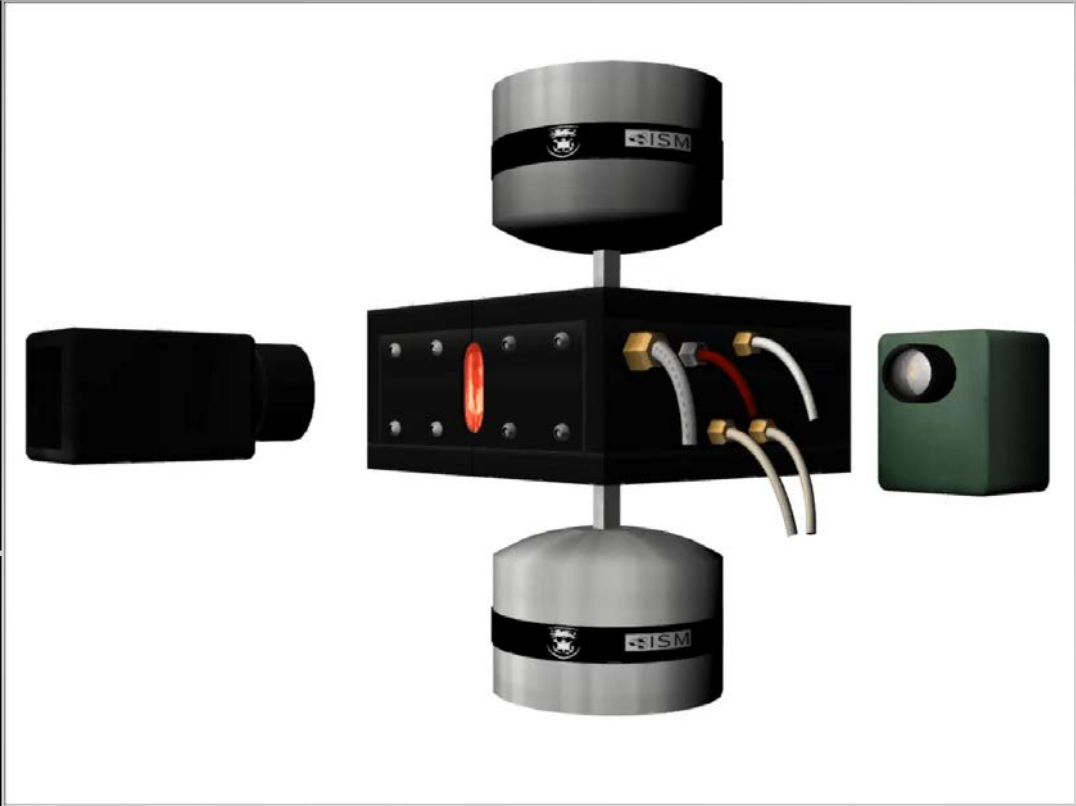
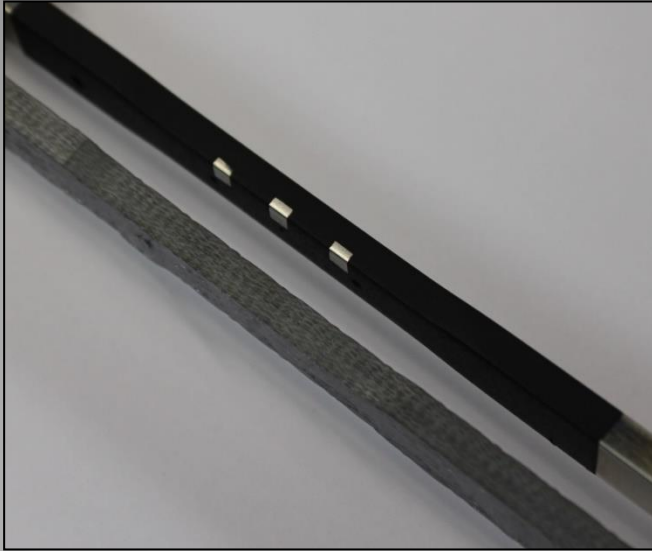
# Experimental Setup – ISM, Swansea



# Experimental Setup – ISM, Swansea

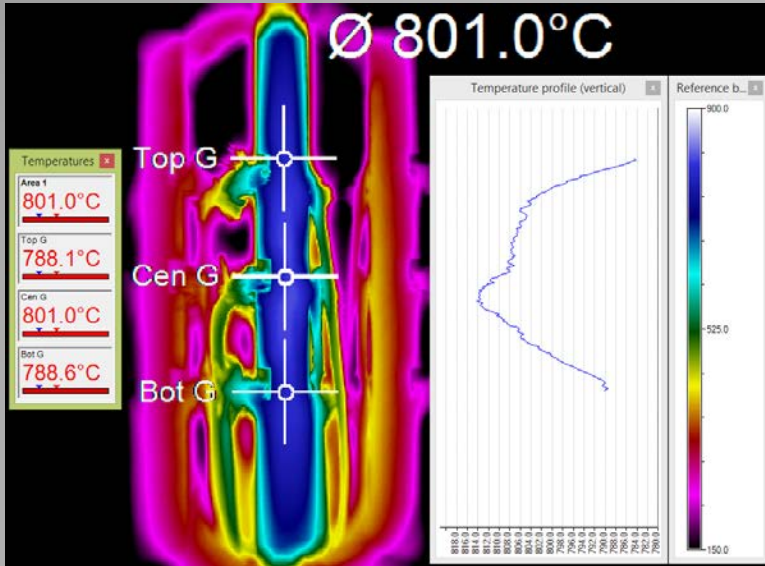


# Temperature Comparisons

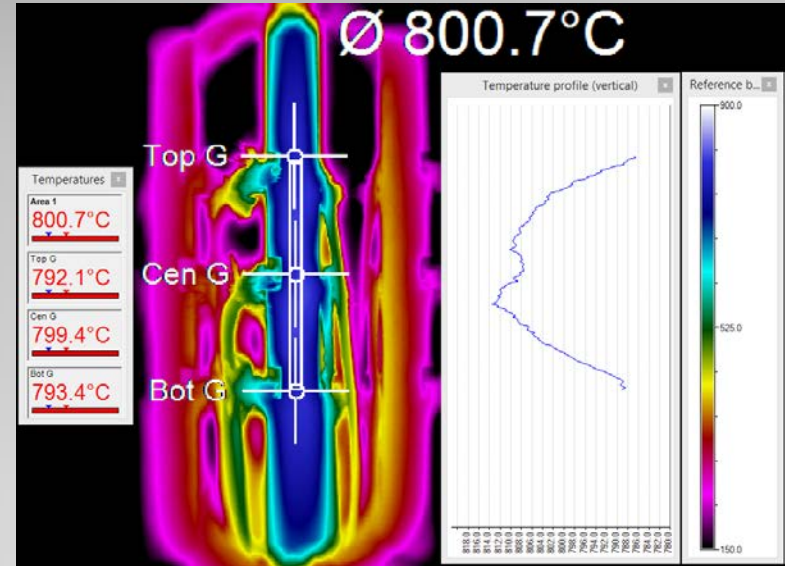


# Control Method Comparison

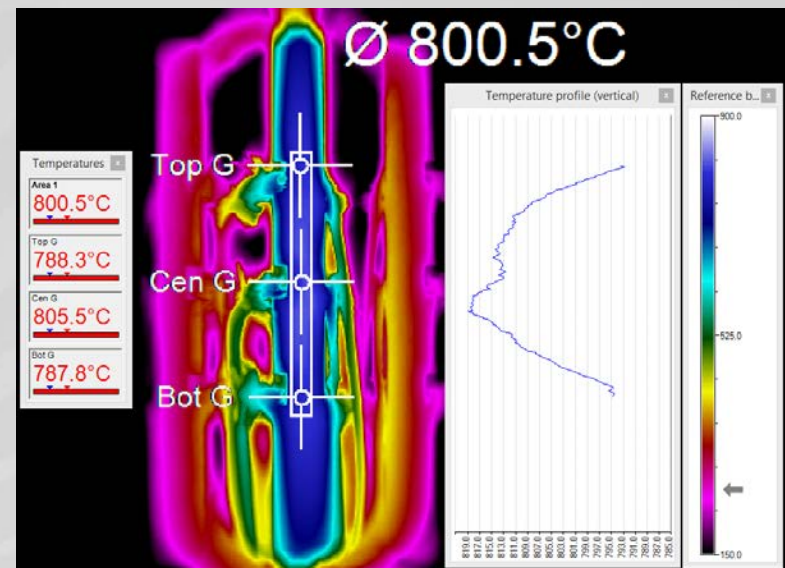
## Single Point Control



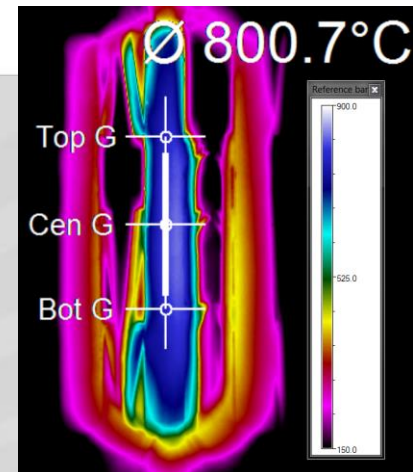
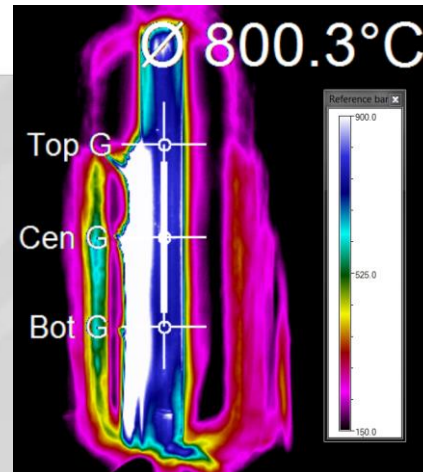
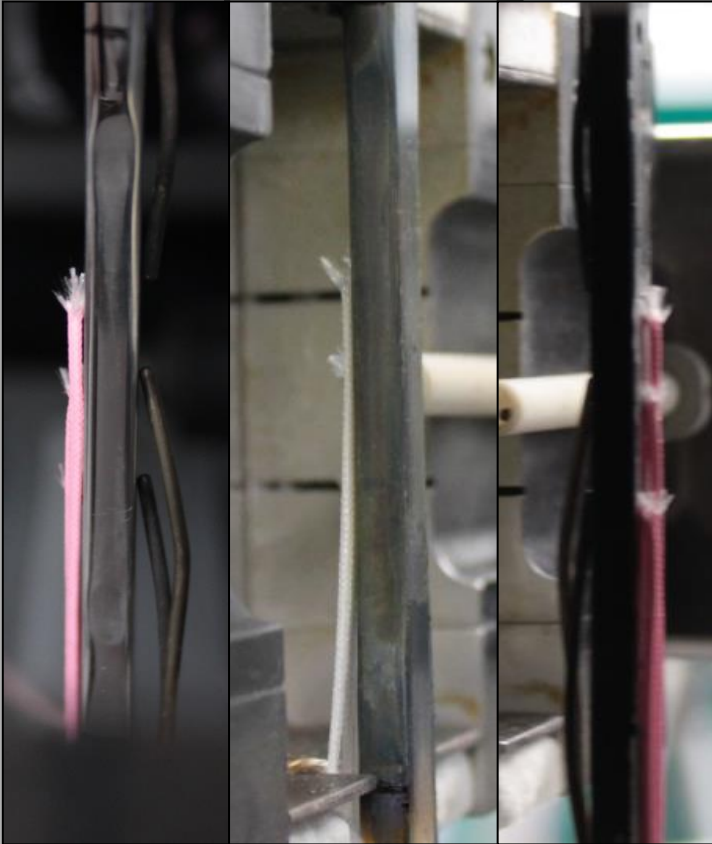
## Small Area Control (2 x 25mm)



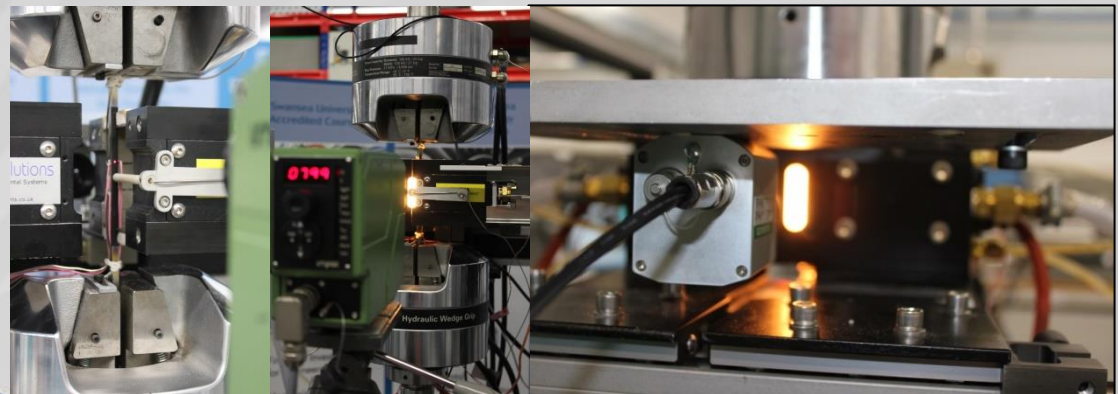
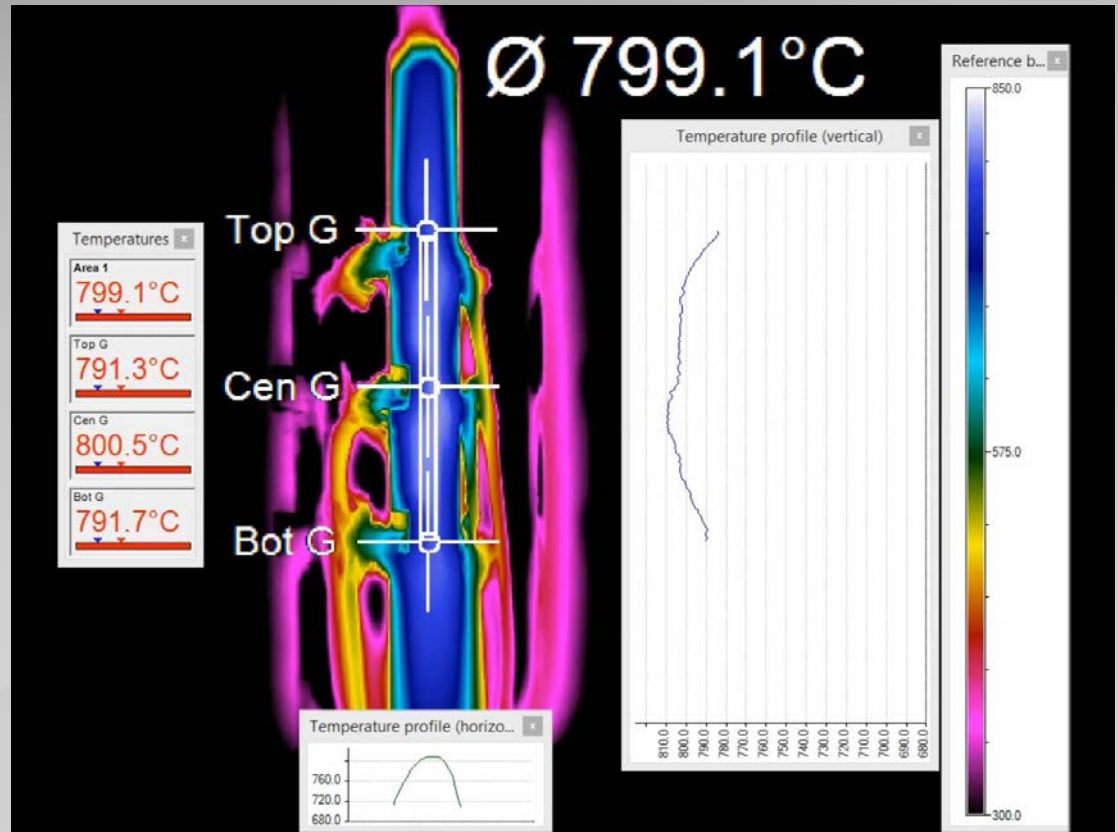
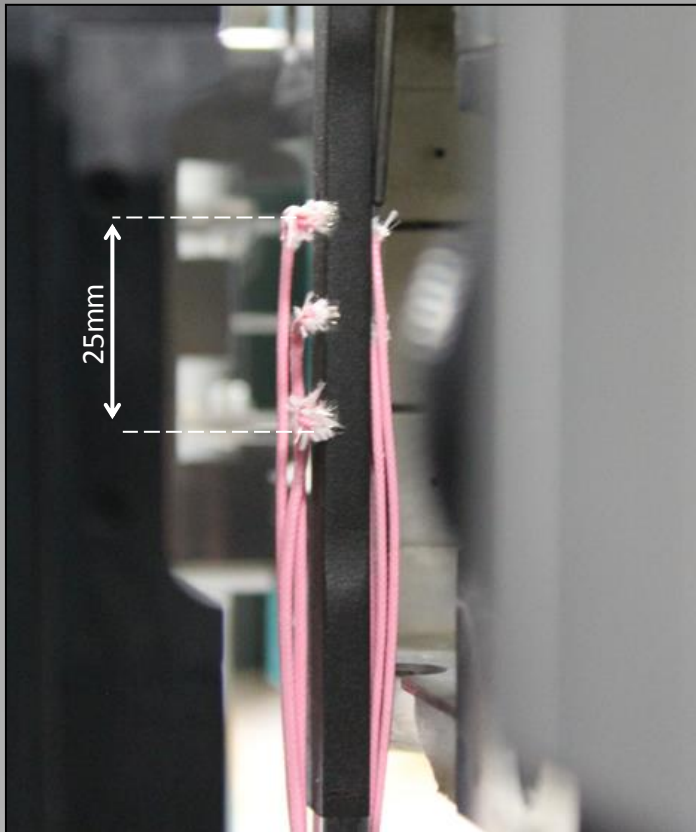
## Large Area Control (3 x 30mm)



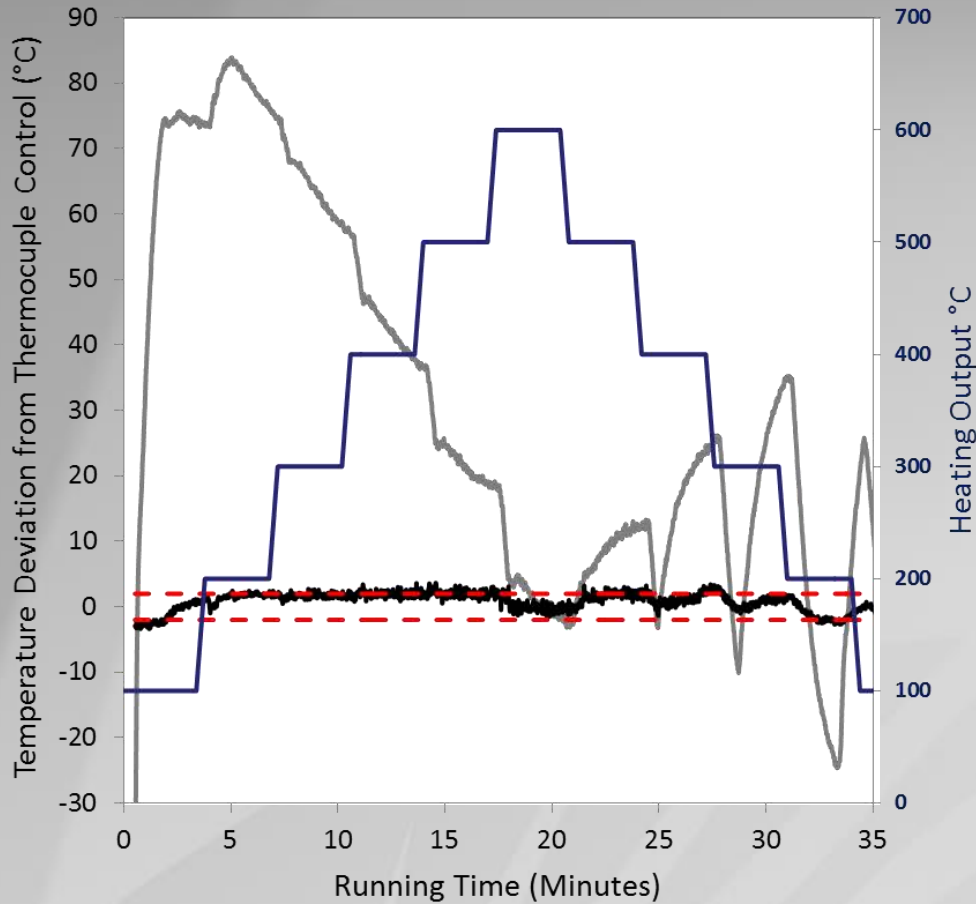
# Temperature Comparisons 2



# Experimental Setup – ISM, Swansea

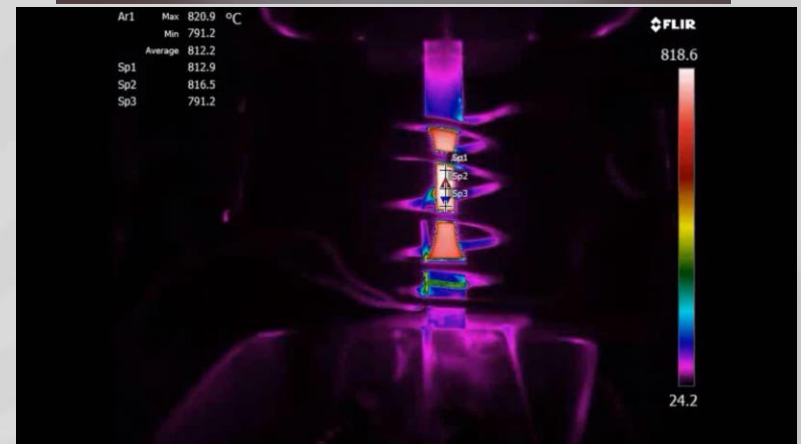
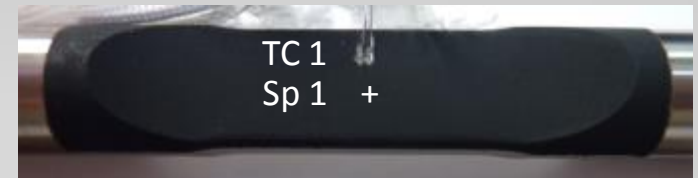


# Previous Work – Rolls-Royce, MTOC

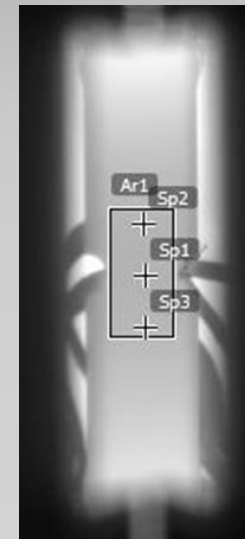
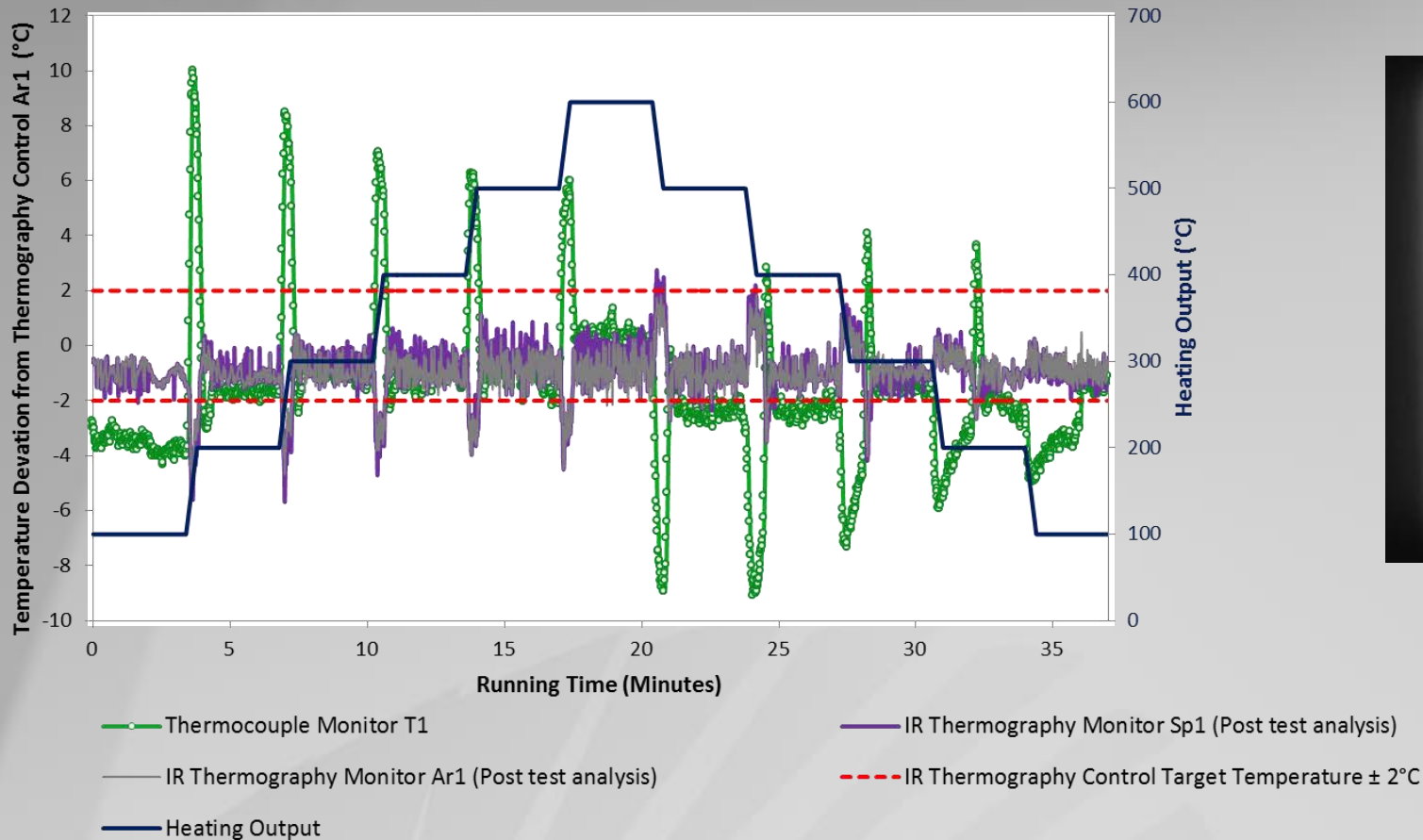


- IR Thermography Monitor
- IR Thermography Monitor HE23
- - - Thermocouple Control Target Temperature  $\pm 2^{\circ}\text{C}$
- Heating Output

Coated Test Piece

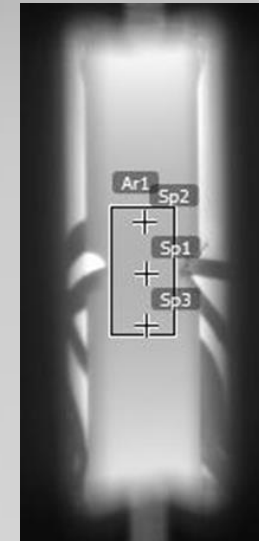
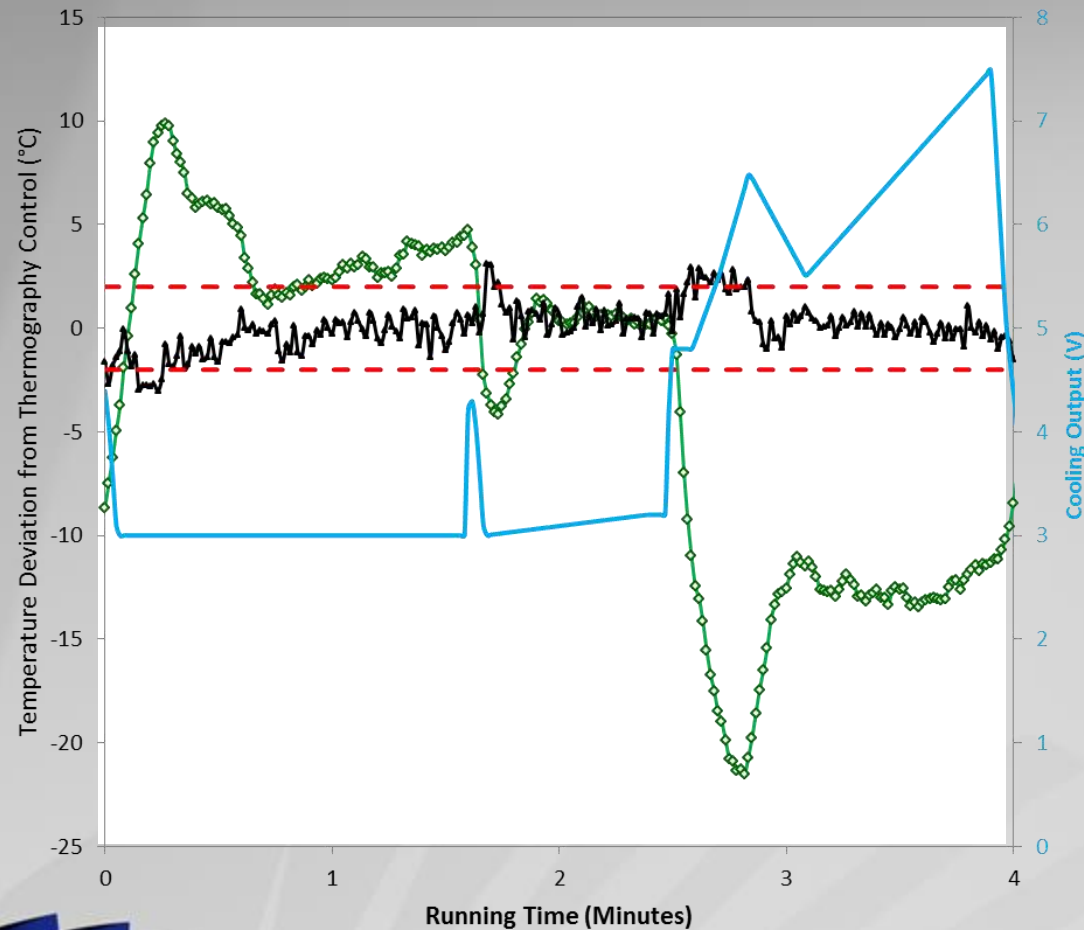


# Previous Work – Rolls-Royce, MTOC



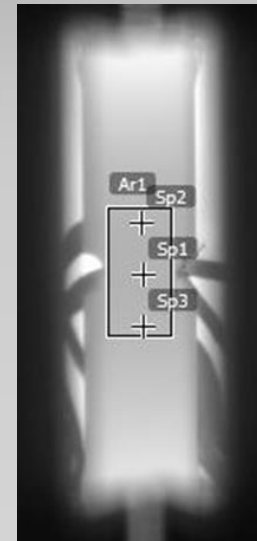
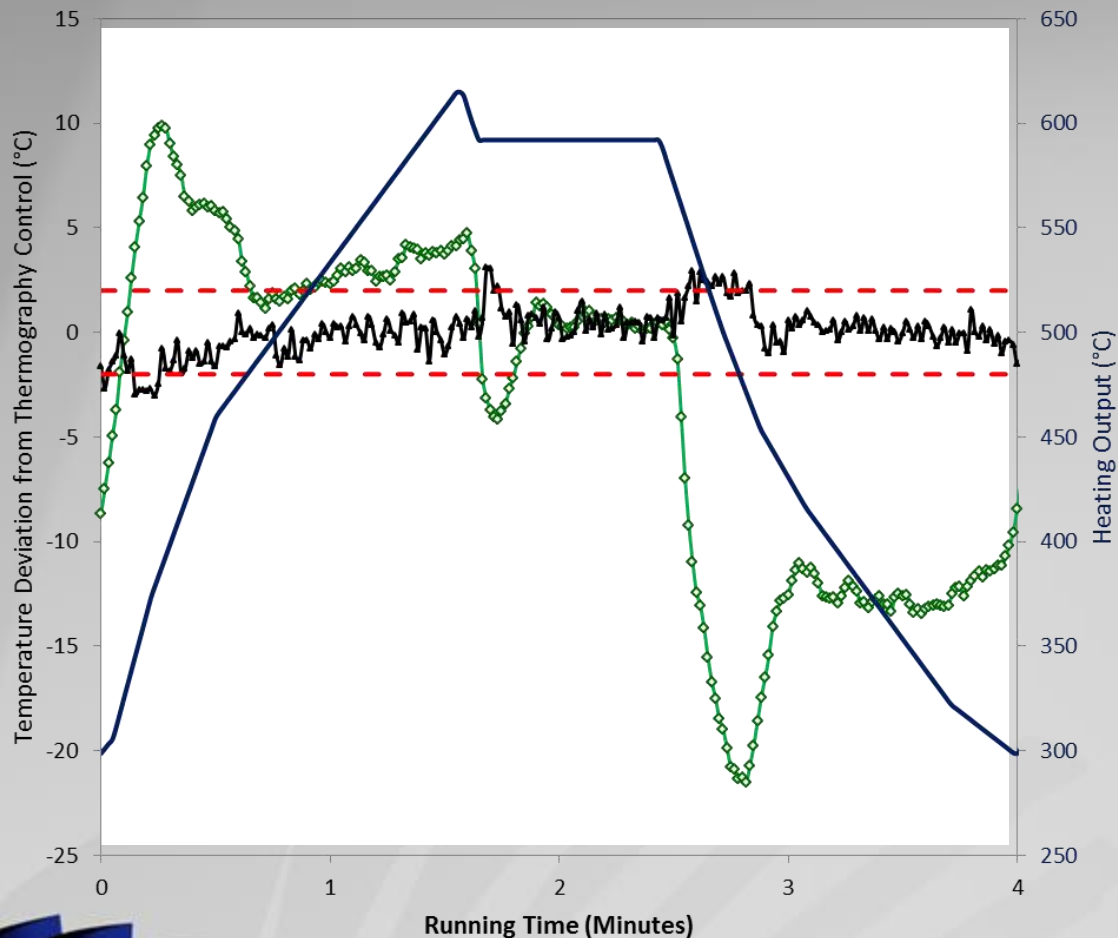


# Previous Work – Rolls-Royce, MTOC



- ◇— Thermocouple Monitor TC1
- IR Thermography Monitor Sp1 (Post test analysis)
- — IR Thermography Control Ar1 Target Temperature  $\pm 2^{\circ}\text{C}$
- Cooling Output

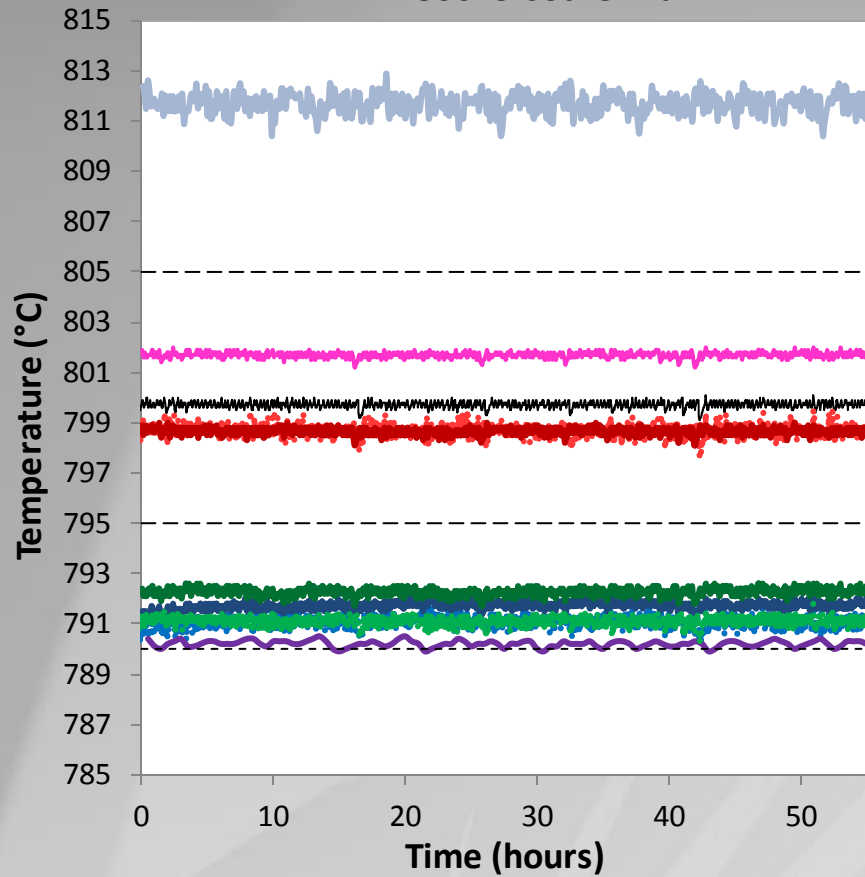
# Previous Work – Rolls-Royce, MTOC



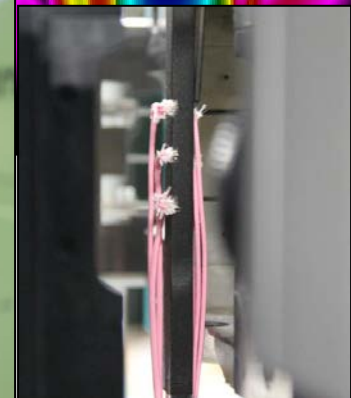
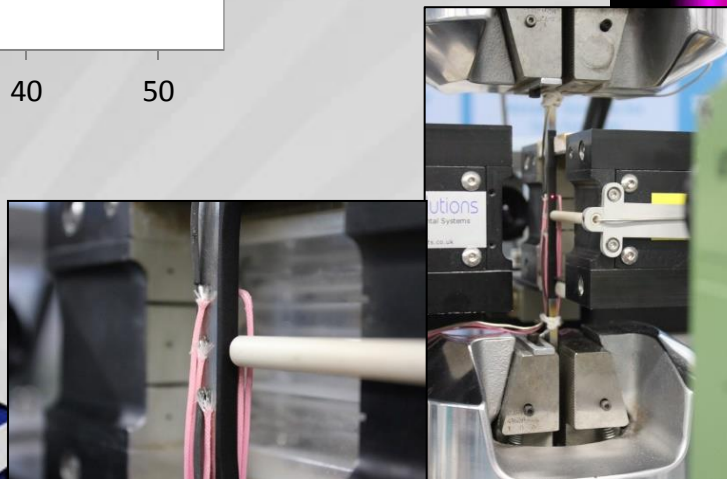
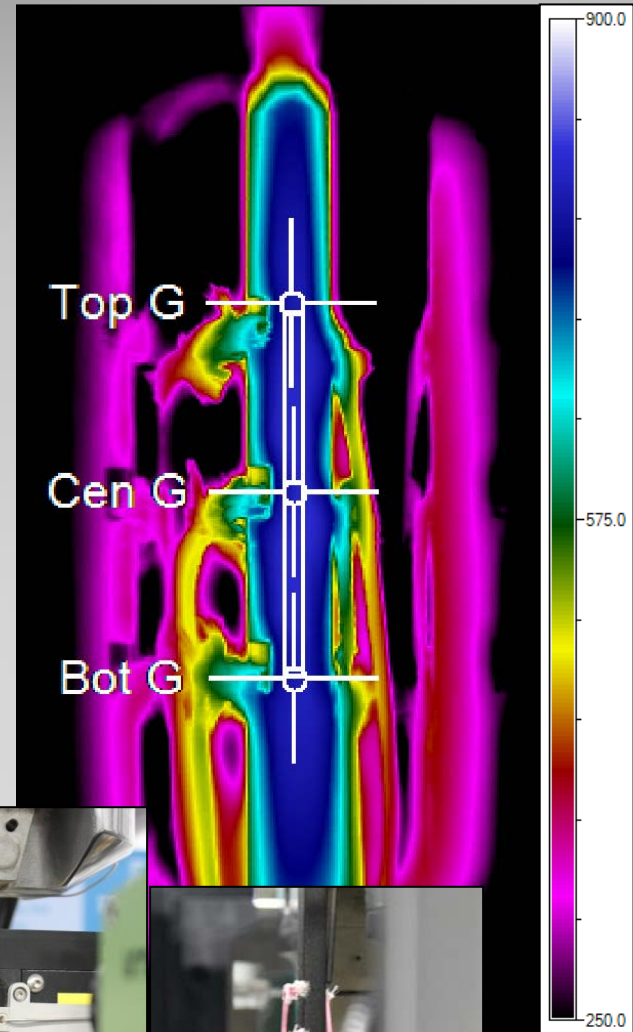
- ◇— Thermocouple Monitor TC1
- IR Thermography Monitor Sp1 (Post test analysis)
- - - IR Thermography Control Ar1 Target Temperature  $\pm 2^{\circ}\text{C}$
- Heating Output

# Isothermal Stability

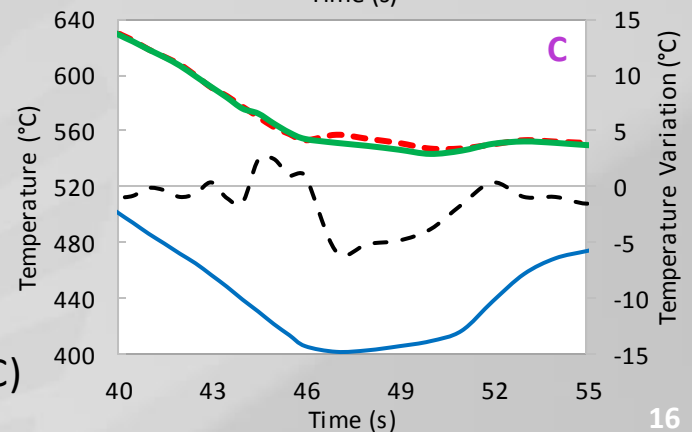
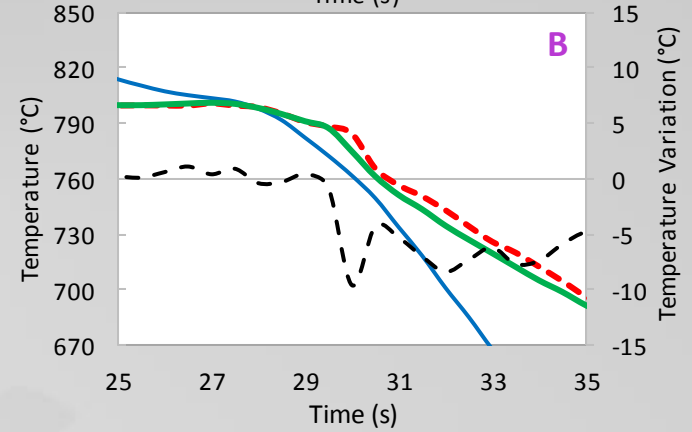
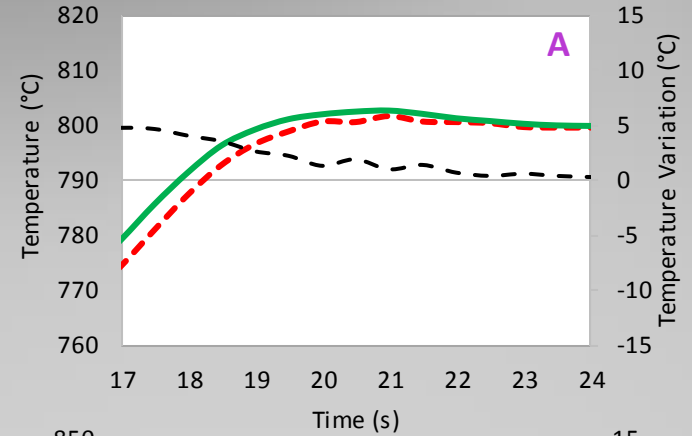
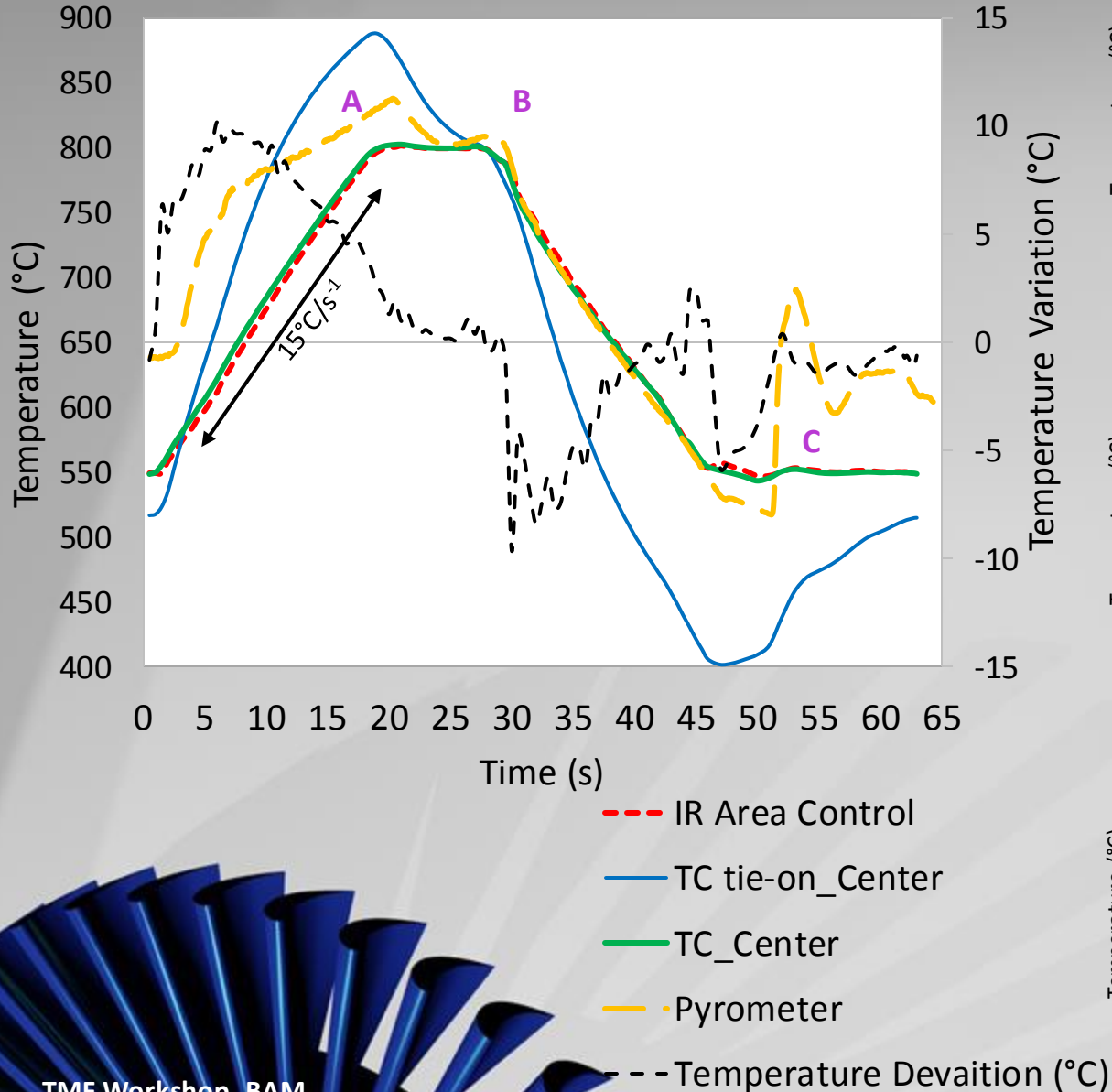
### 800°C Isothermal



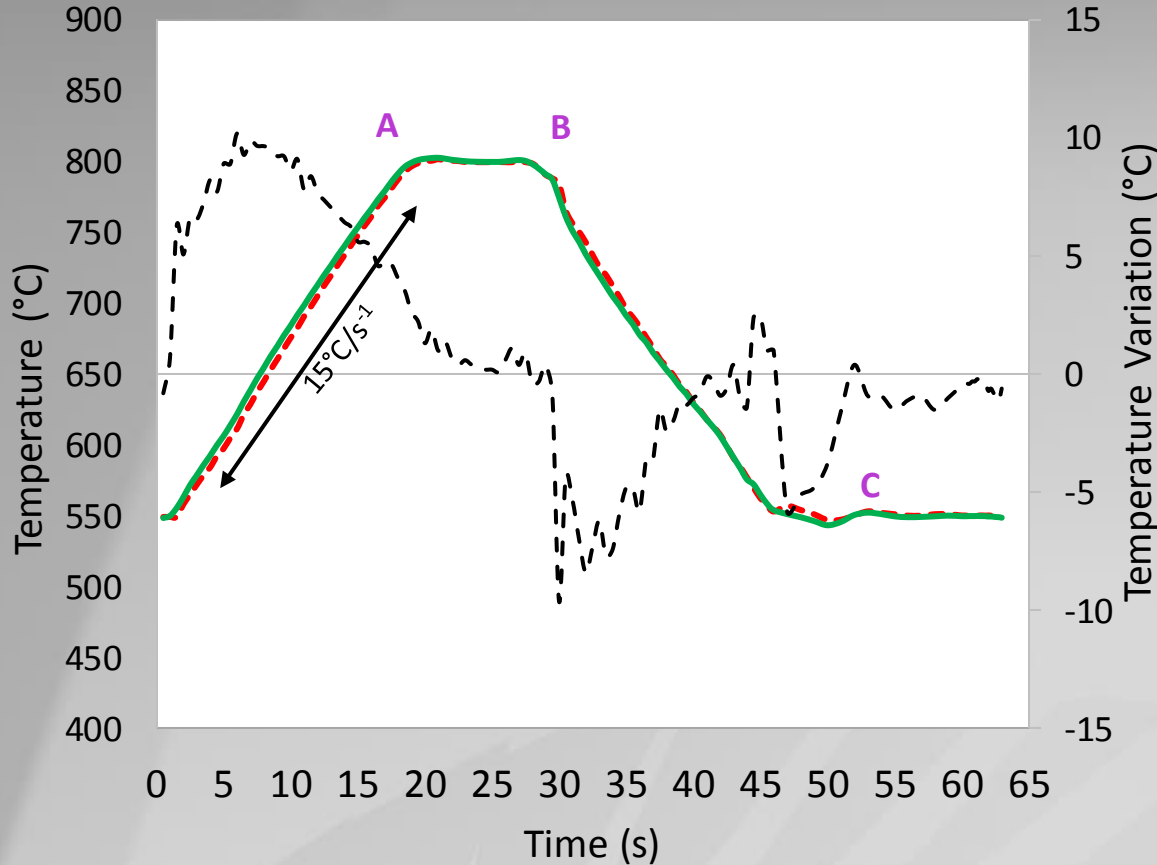
- IR\_Area Control
- ..... IR\_Center
- TC\_Center
- TC\_Center Face
- ..... IR\_Top
- TC\_Top
- Pyrometer\_Top
- ..... IR\_Bottom
- TC\_Bottom
- ±5°C
- ±10°C
- TC tie-on\_Center



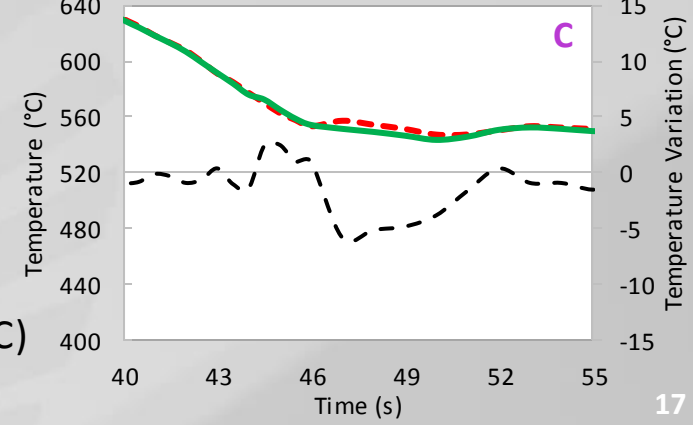
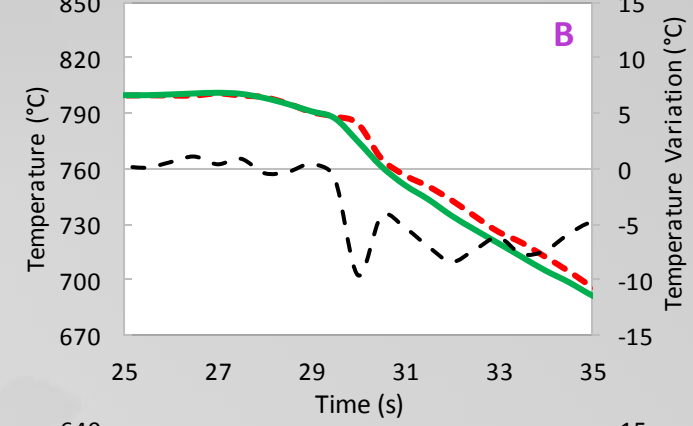
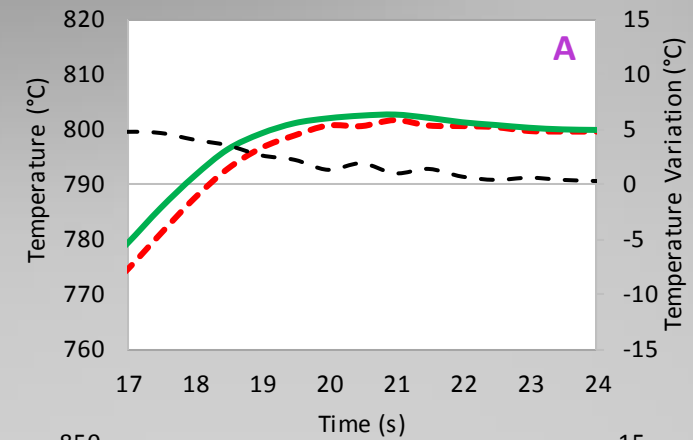
# Dynamic Stability



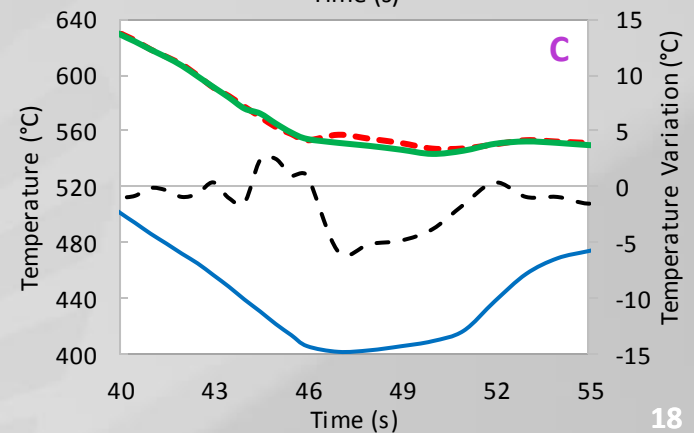
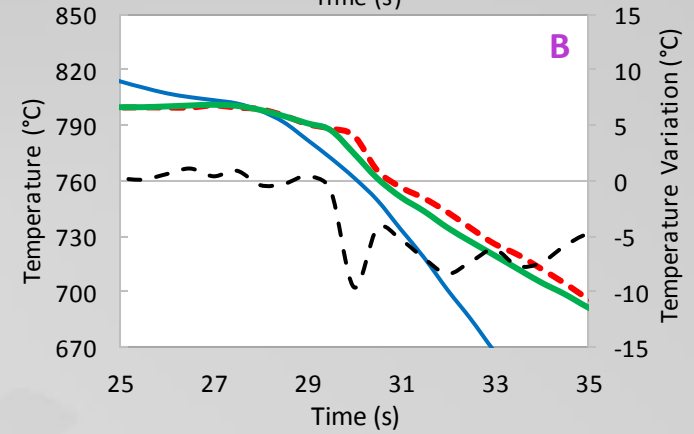
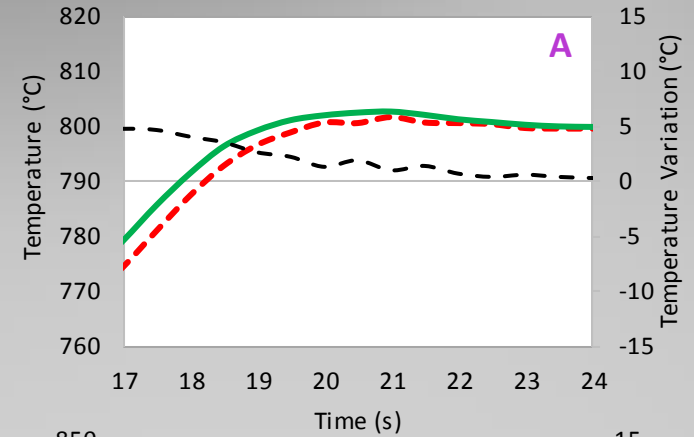
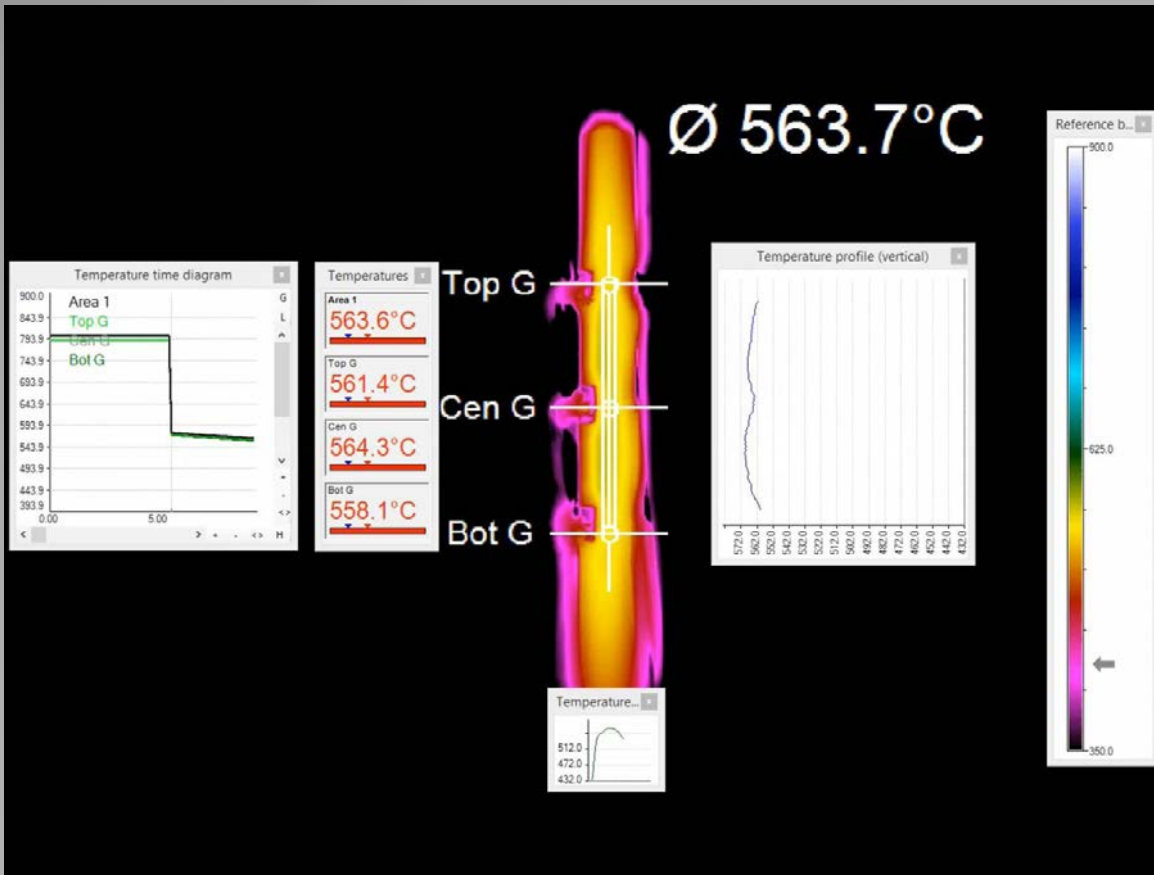
# Dynamic Stability



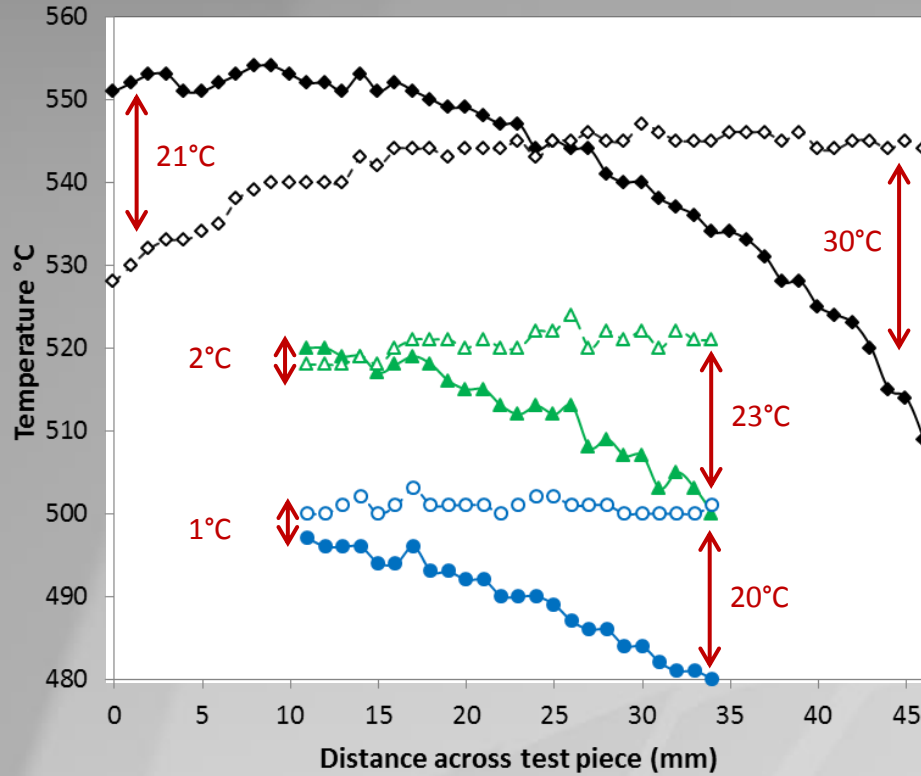
- IR Area Control
- TC\_Center
- Temperature Deviation (°C)



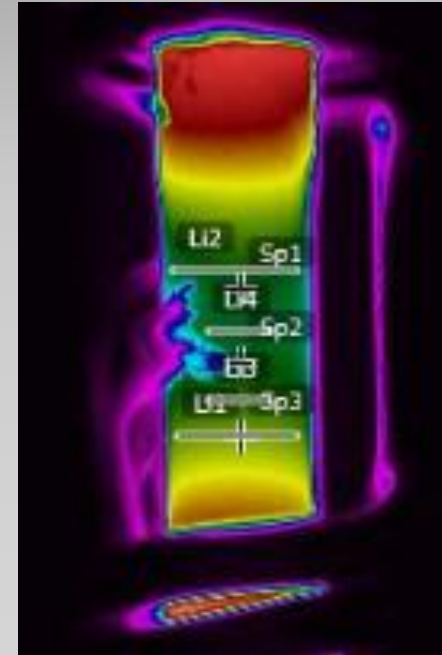
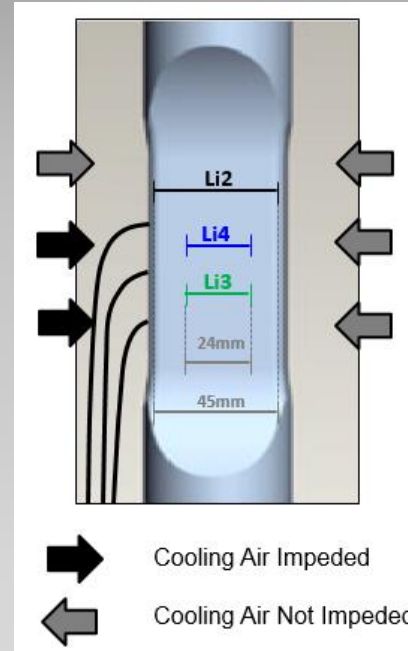
# Dynamic Stability



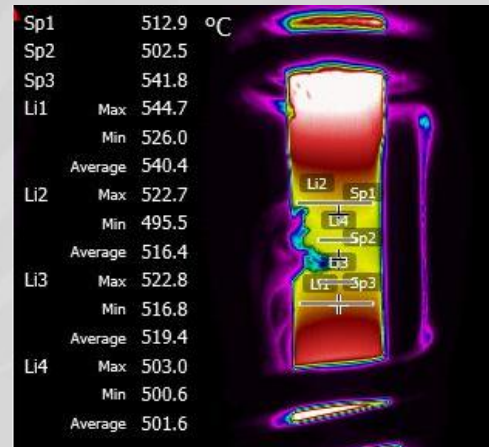
# Previous Work – Rolls-Royce, MTOC



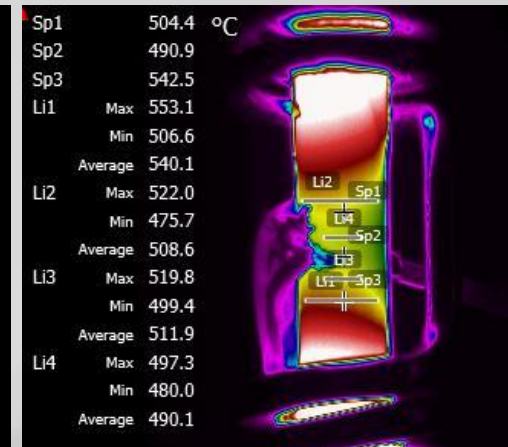
- ◆— Li1 Not Impeded
- ◇— Li1 Air Impeded
- ▲— Li3 Not Impeded
- △— Li3 Air Impeded
- Li4 Not Impeded
- Li4 Air Impeded



Cooling Direction →



← Cooling Direction



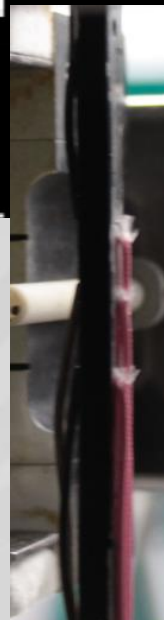
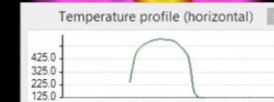
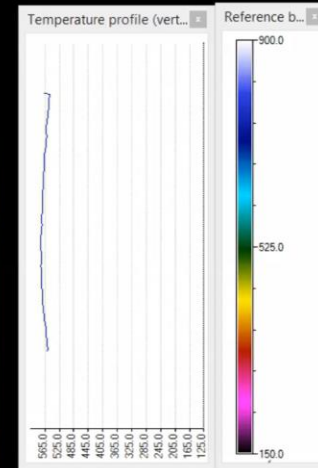
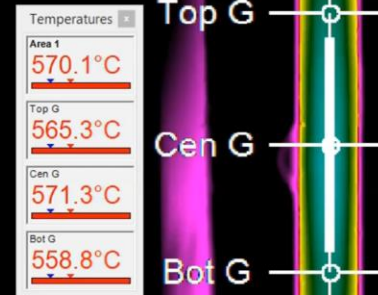
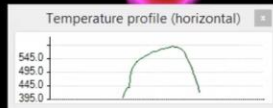
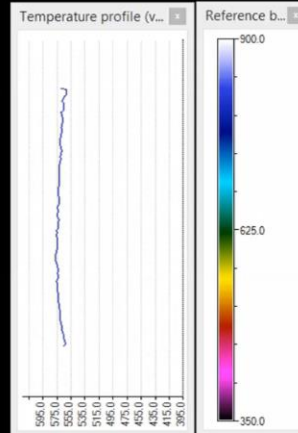
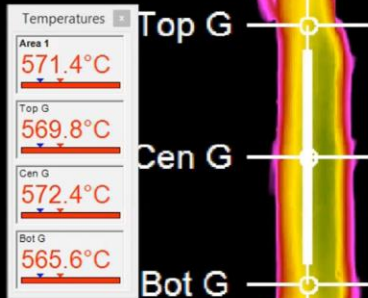
# Thermocouple Complications

Thermocouples

No Thermocouples

Ø 571.4°C

Ø 570.1°C



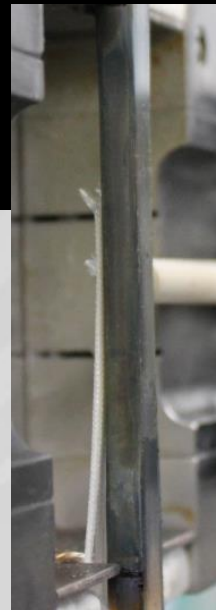
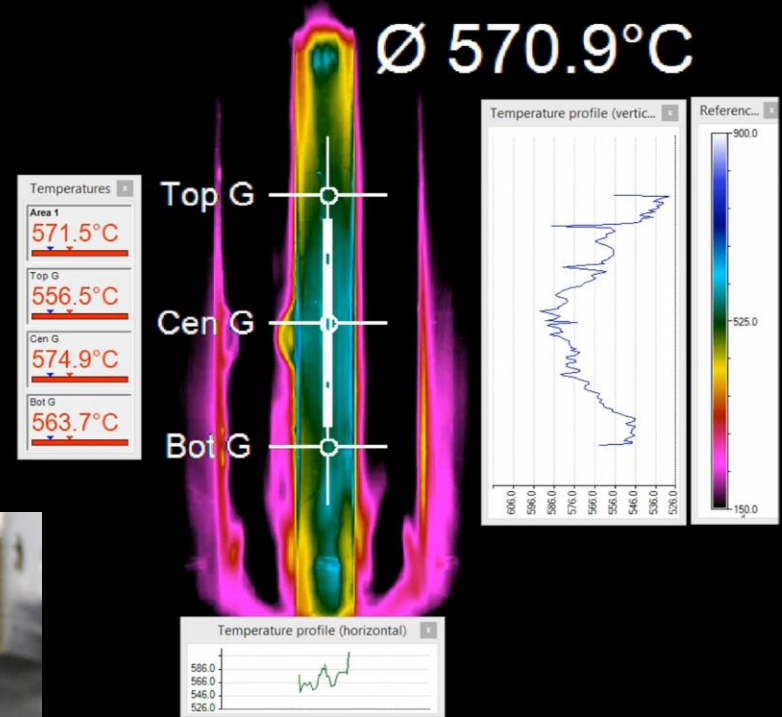
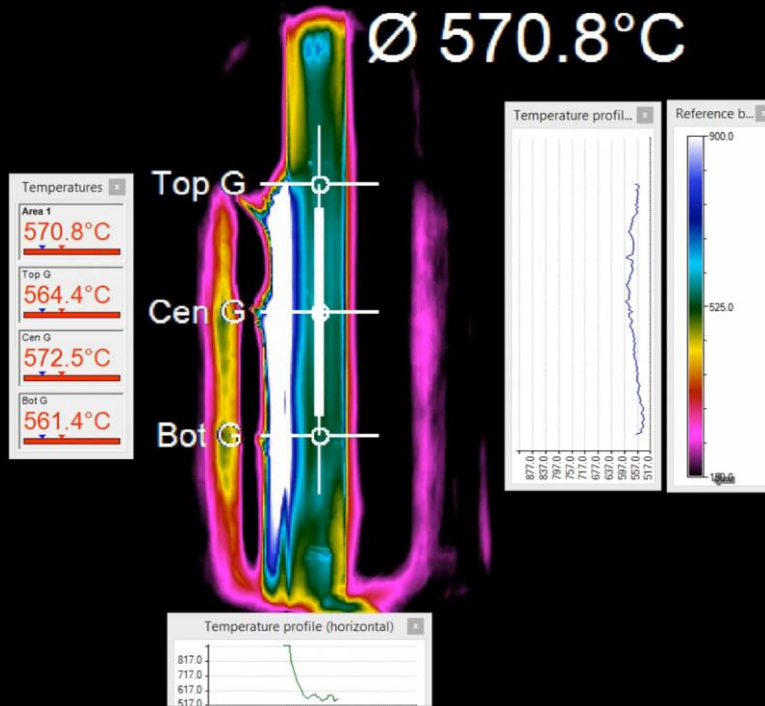
Coated Surface  
 $\epsilon$  used = 0.89



# Thermocouple Complications

Thermocouples

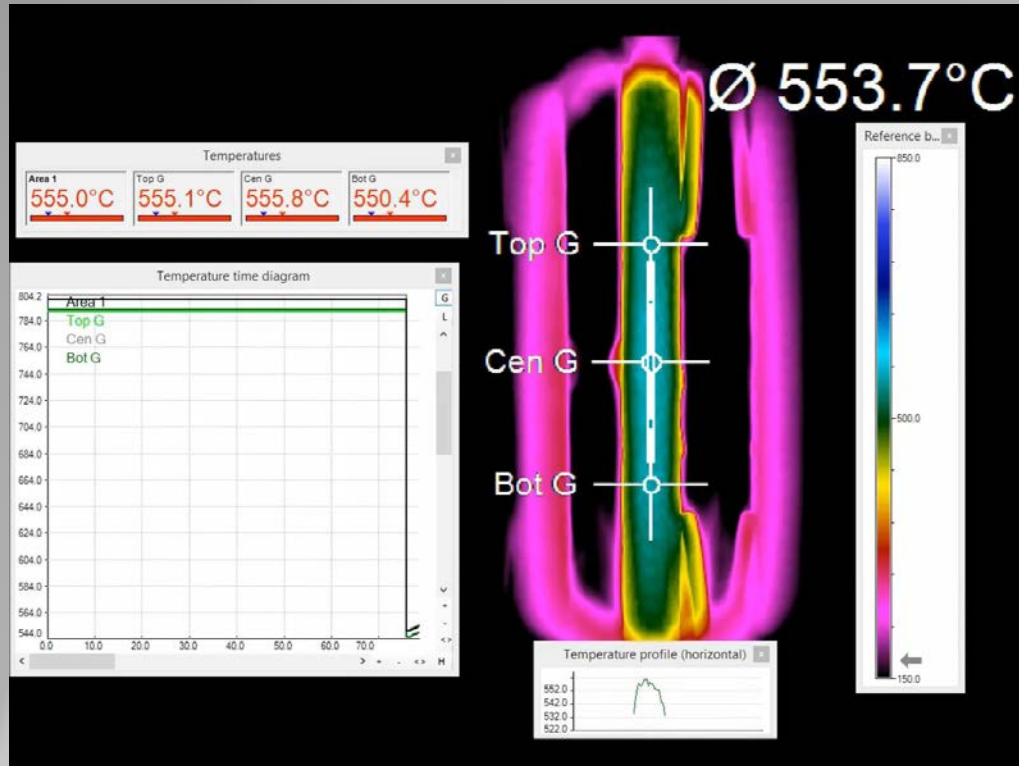
No Thermocouples



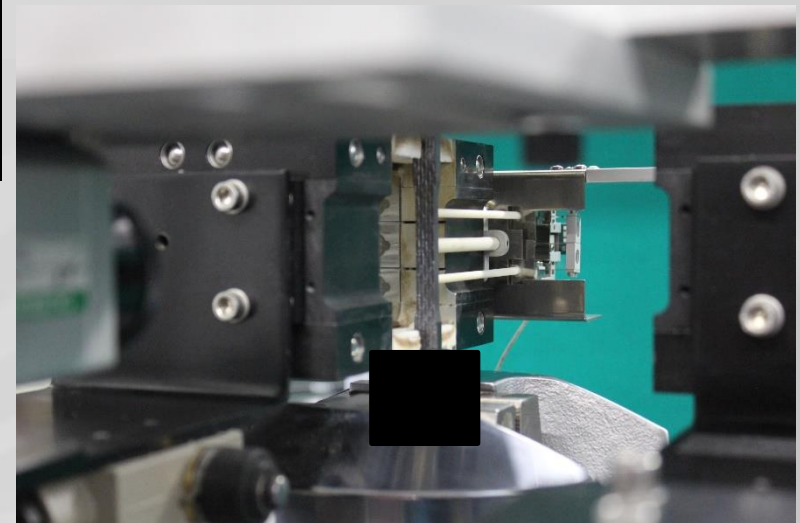
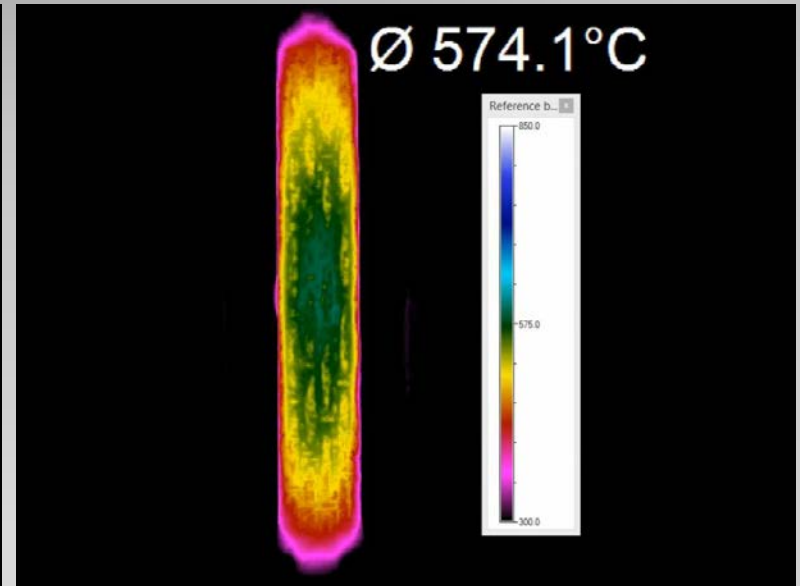
Pre-oxidised Surface  
800°C for 50 hours.  
 $\epsilon$  used = 0.57

# Ceramic Temperature Control

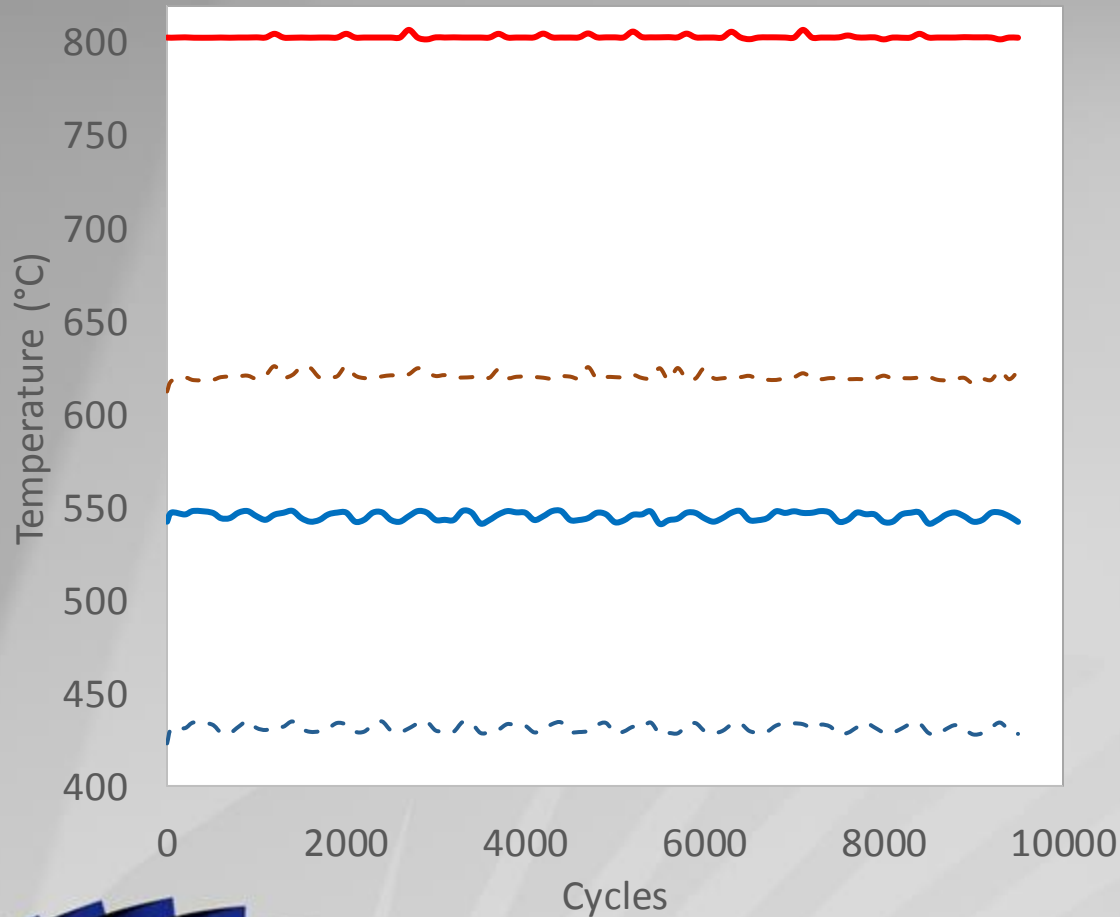
## Ceramic Specimen Side



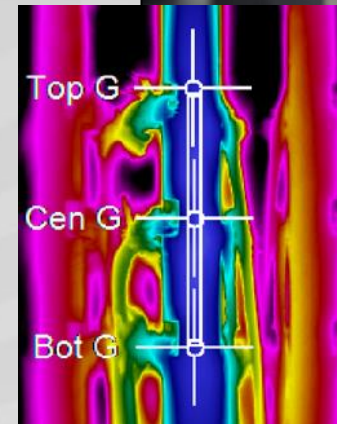
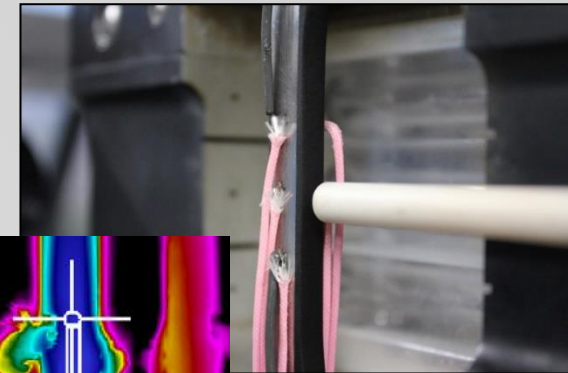
## Ceramic Specimen Face



# Dynamic Temperature Stability



- Max\_IR Control
- Min\_IR Control
- - - Max\_TC Non Contact
- - - Min\_TC Non Contact



10,000 cycles  
= 270 hours

# Advantages / Disadvantages

Measurement	Thermocouple	Pyrometer	Thermography
Mode	Invasive	Non Invasive	Non Invasive
Area	≈ 2mm <sup>2</sup>	≈ 2mm <sup>2</sup>	Entire Gauge Section
Dynamic Accuracy	Externally Influenced	Good	Good
Set up Time	Slow	Fast	Fast
Profiling	Thermocouple Based	Thermocouple Based	Thermography Based
Repeatability	Externally Influenced	Good	Good
Emissivity Influenced	No	Yes	Yes
Post Test Analysis	No	No	Yes
Shadowing Effects	Yes	No	No
Cold Spot Identification	No	No	Yes
In-Situ Adjustments	No	No	Yes
Initial Cost	Low	Ok	High
Calibration Cost	High	Low	Low

# Acknowledgements

The provision of materials and technical support from Rolls-Royce plc is gratefully acknowledged. A special mention must be paid to Veronica Gray and Turan Dirlik.

Email contact: [jonathan.p.jones@swansea.ac.uk](mailto:jonathan.p.jones@swansea.ac.uk)

## *Any Questions?*



# Influence of Phase Angle and Maximum Temperature on the TMF Behaviour of a Polycrystalline Nickel Superalloy

***Dr. J.P. Jones<sup>1</sup>, Dr. M.T. Whittaker<sup>1</sup>, Mr. Stephen Williams<sup>2</sup>, Rob Lancaster<sup>1</sup>***

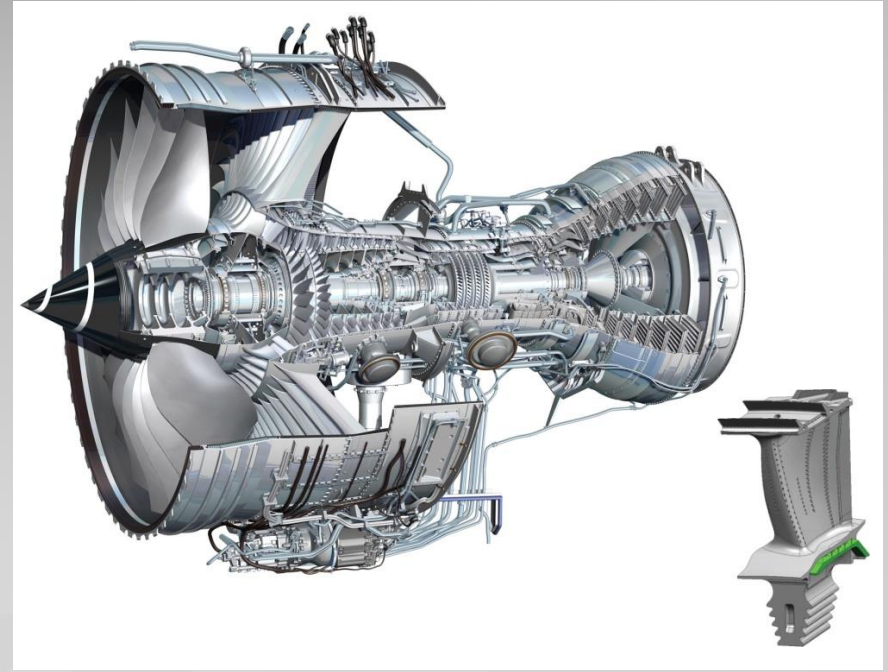
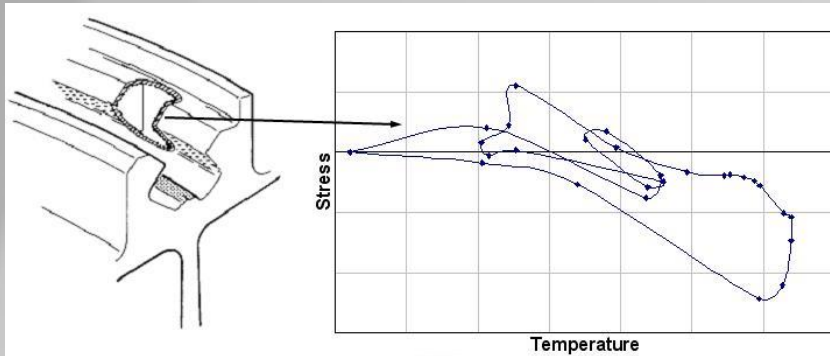
<sup>1</sup> Institute of Structural Materials, Bay Campus, Swansea University, SA1 8EN, United Kingdom

<sup>2</sup> Rolls-Royce plc, P.O. Box 31, Derby, DE24 8BJ, United Kingdom



# Industrial Motivation

- Increased turbine entry temperatures
- Thinner disc rims and advanced cooling systems leading to larger thermal gradients
- Complex loading regimes within the gas turbine leading to diverse phasing between temperature and strain



- Extrapolation of isothermal fatigue (IF) results to incorporate these effects show limited success
- Generation of TMF data is required to allow the development of lifing methodologies under TMF loading

# Thermo-Mechanical Fatigue (TMF)

- Combined effect of:
  - *Cyclic mechanical loading*
  - *Cyclic Temperature*
- Associated with transient effects during start-up/shutdown of engines
- Stresses can be caused by:
  - *Temperature gradients brought about by heating rates/volume effects*
  - *A mismatch in thermal expansion between different materials*
- TMF testing is a closer simulation of component environment, compared to the traditional isothermal fatigue tests, e.g. LCF
- The deformation and damage seen in real components is often better represented by TMF tests



# Thermo-Mechanical Fatigue (TMF)

- Hollow cylindrical specimens
  - Forced air cooling
  - RF Induction heating
  - Tension/torsion servo-hydraulic Strain control
- } Rapid thermal cycles



TMF Workshop\_BAM,  
Berlin, Apr 27-29<sup>th</sup>  
2016.

## TMF Standards:

- **ASTM E2368-10:** Standard Practice for Strain Controlled Thermo-mechanical Fatigue Testing (*Released in 2004, updated in 2010*)
- **ISO 12111:2011:** Metallic materials – Fatigue Testing – Strain Controlled Thermo-mechanical Fatigue Testing Method (*Released 2011*)



# Thermo-Mechanical Fatigue (TMF)

- Cone grip design to reduce heat sink effect
- Non-invasive temperature control and monitoring via IMPAC pyrometry
- Thermal Profiling using thermocouples



## TMF Standards:

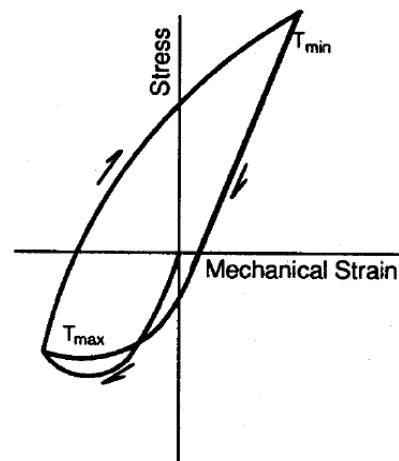
- **ASTM E2368-10:** Standard Practice for Strain Controlled Thermo-mechanical Fatigue Testing (*Released in 2004, updated in 2010*)
- **ISO 12111:2011:** Metallic materials – Fatigue Testing – Strain Controlled Thermo-mechanical Fatigue Testing Method (*Released 2011*)

# Thermo-Mechanical Fatigue (TMF)

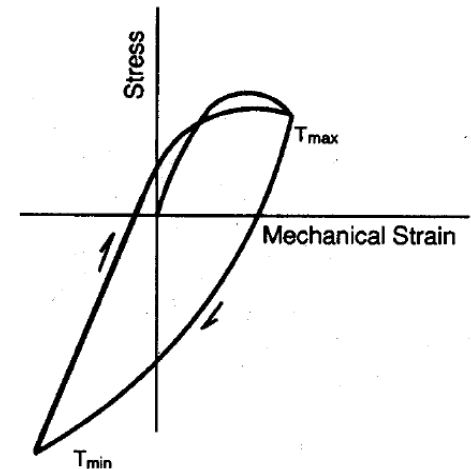
- Diverse mechanisms are involved, Primarily . . .

Fatigue      Creep      Oxidation

- TMF loading can be more damaging than isothermal fatigue at an equivalent  $T_{\max}$
- Complex interaction within diverse *phase angles* between peak temperature and strain range
- Resulting in strain R ratios varying between 0 and  $-\infty$  depending on the phase angle,  $\phi$ .



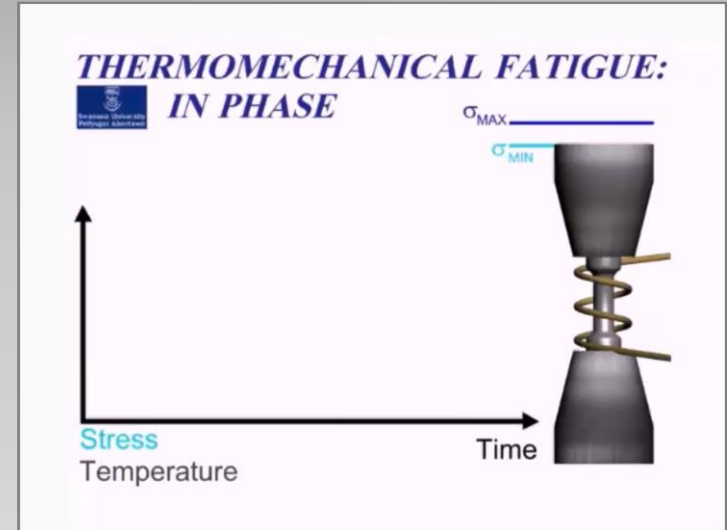
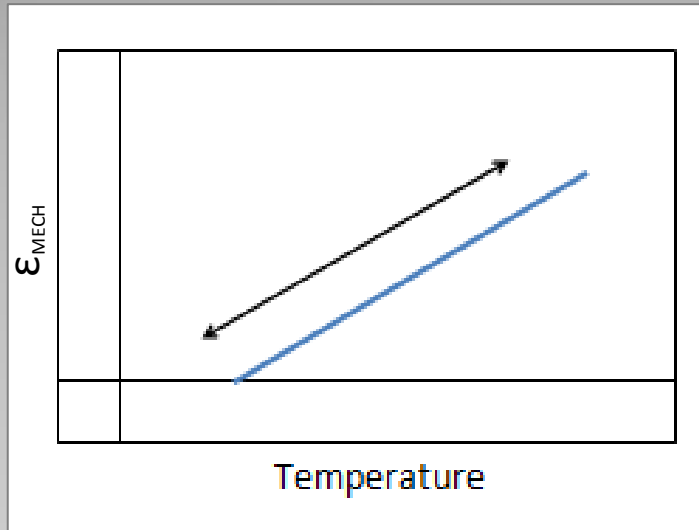
Out-of-Phase



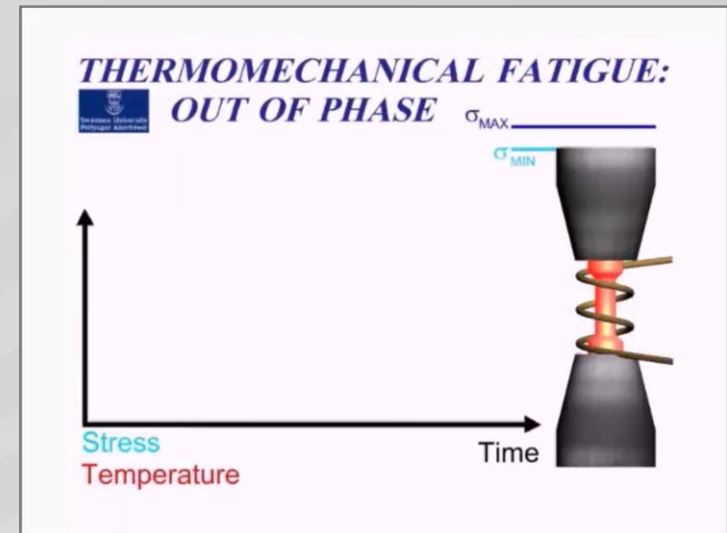
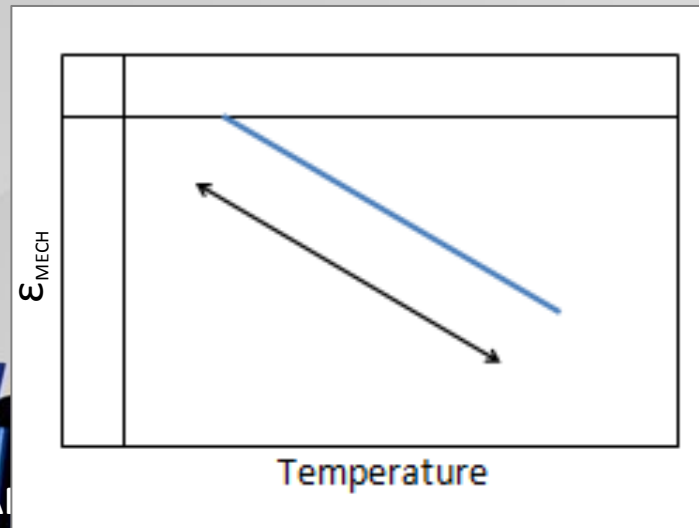
In-Phase

# TMF – Phase Angle ( $\phi$ )

In-Phase  
(IP  $\phi = 0^\circ$ )

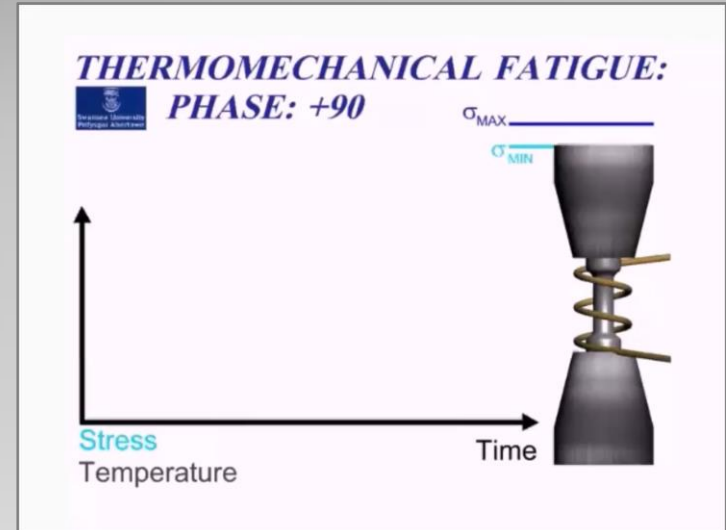
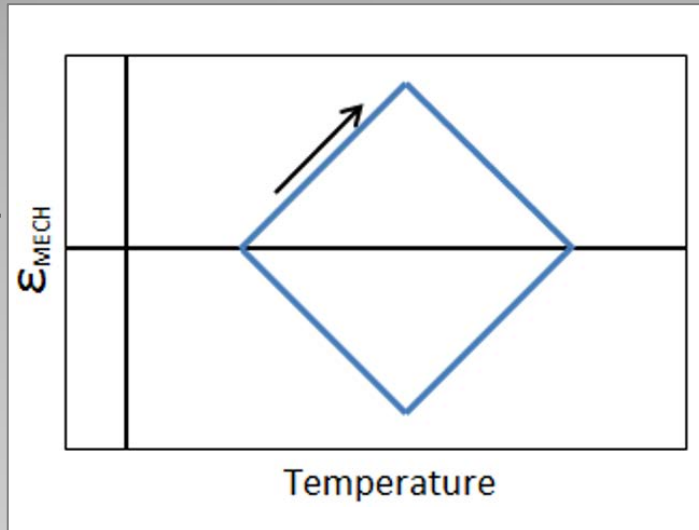


Out of Phase  
(OP  $\phi = -180^\circ$ )

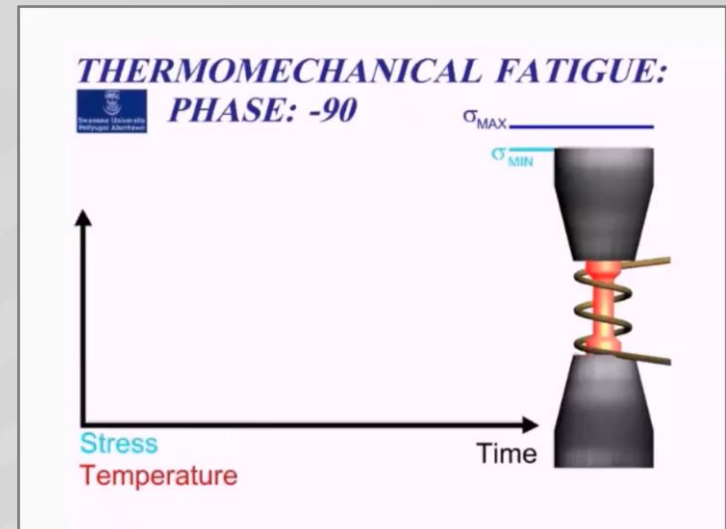
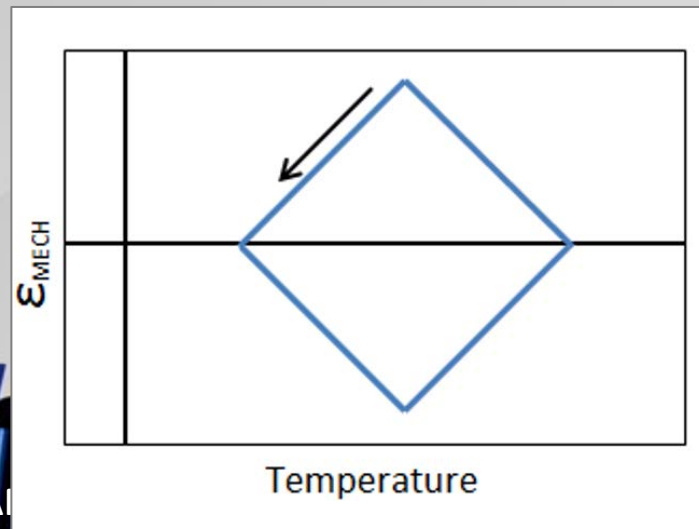


# TMF – Phase Angle ( $\phi$ )

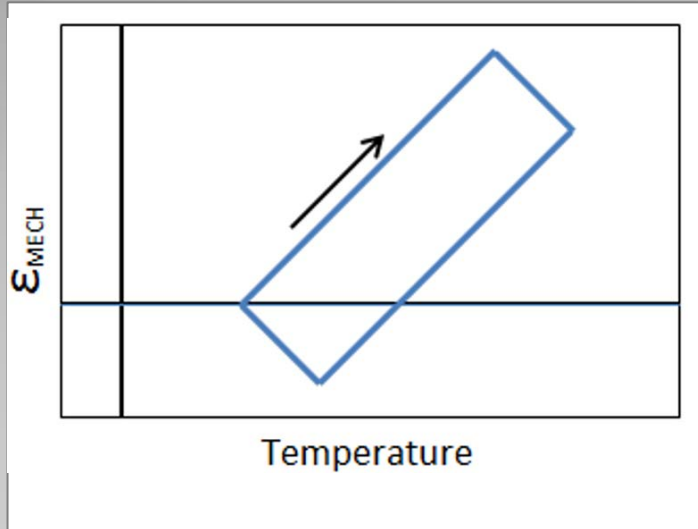
Clockwise Diamond  
(CD90  $\phi = 90^\circ$ )



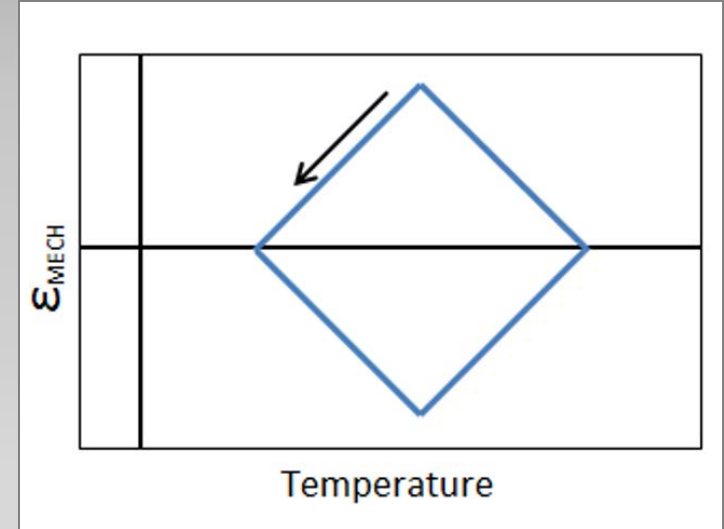
Counter Clockwise  
Diamond  
(CCD  $\phi = -90^\circ$ )



# TMF – Phase Angle ( $\phi$ )



Clockwise 45  
(CW45  $\phi = 45^\circ$ )



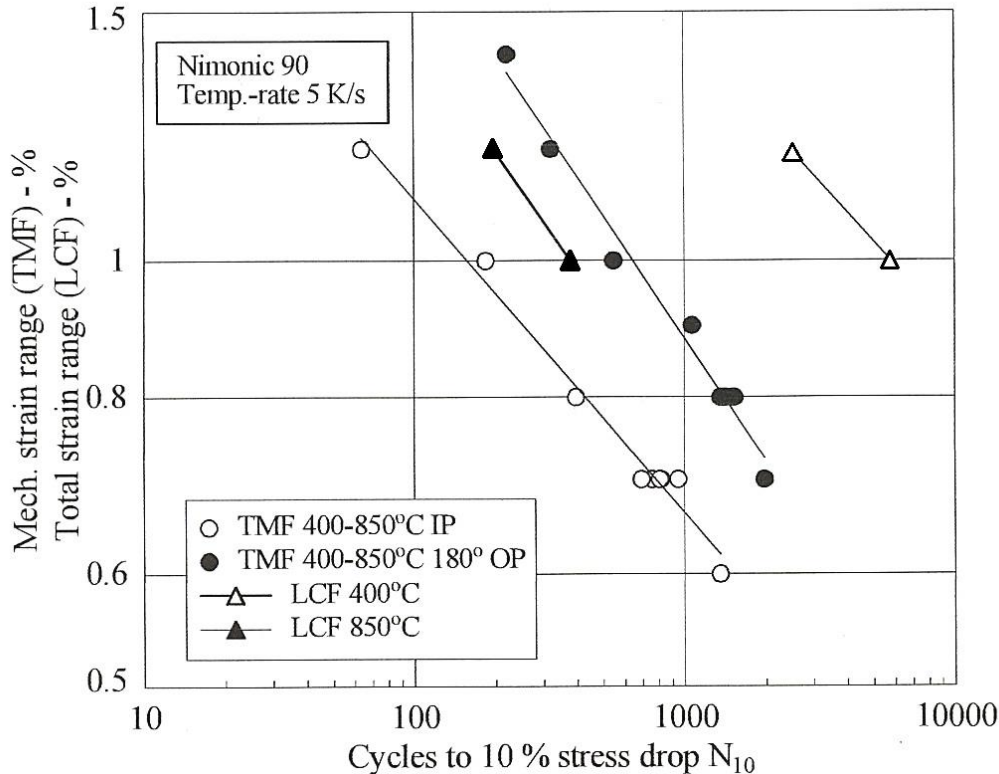
Counter Clockwise  
-135  
(CCW  $\phi = -135^\circ$ )

# Primary Factors Affecting TMF Life

- R ratio
- Peak strain/stress
- Strain/stress range
- Strain rate
- Environment
- $T_{MAX}$
- $T_{MIN}$
- $\Delta T$
- Phase angle
- Loading direction

**Which TMF cycle is the most detrimental?**

# Primary Factors Affecting TMF Life



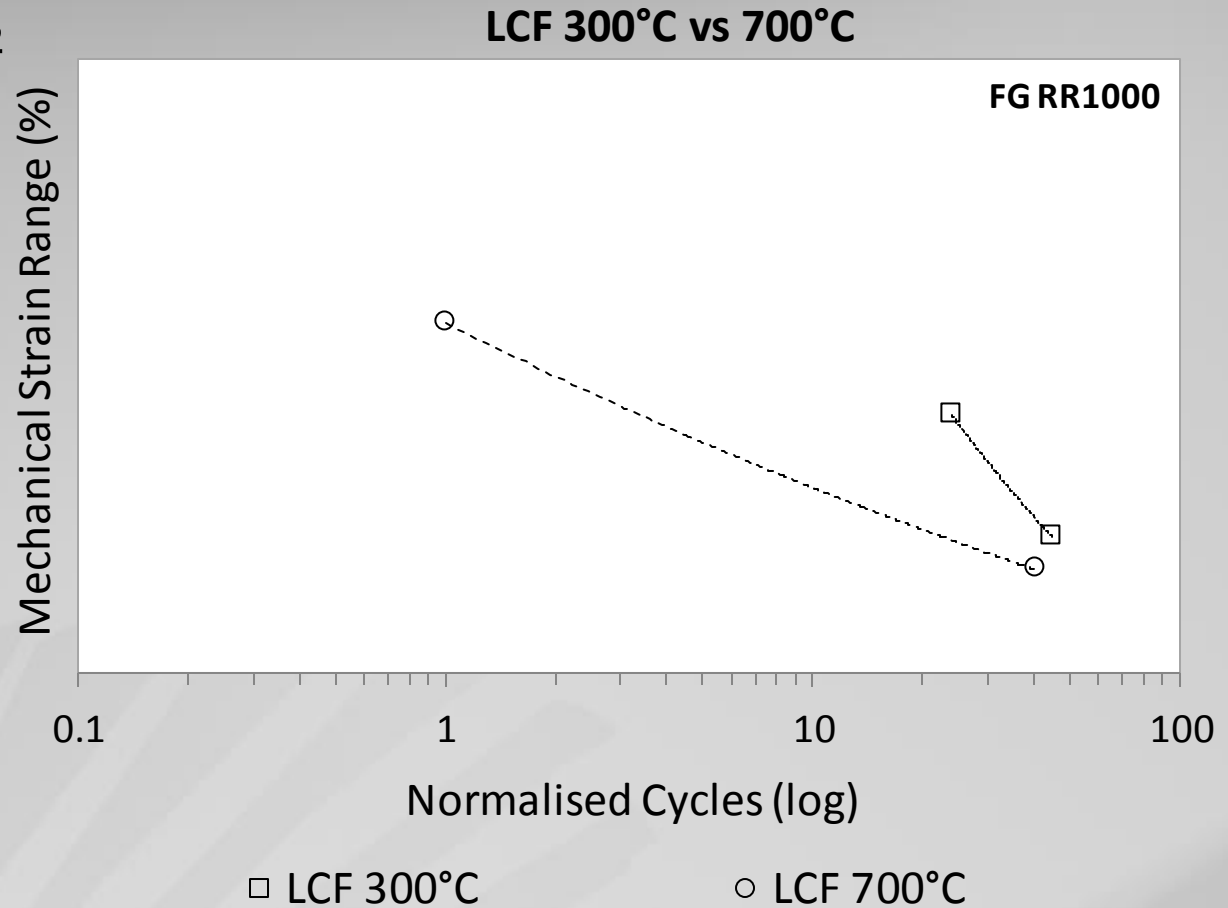
- IP cycles are more damaging than OP cycles
- IP cycles involve:
  - *Tensile stress at  $T_{max}$*
  - *Grain boundary embrittlement*
  - *Reduced resistance to crack initiation and propagation*
  - *Inter-granular cracking*



# Typical RR1000 TMF behaviour

## General TMF Life Trends

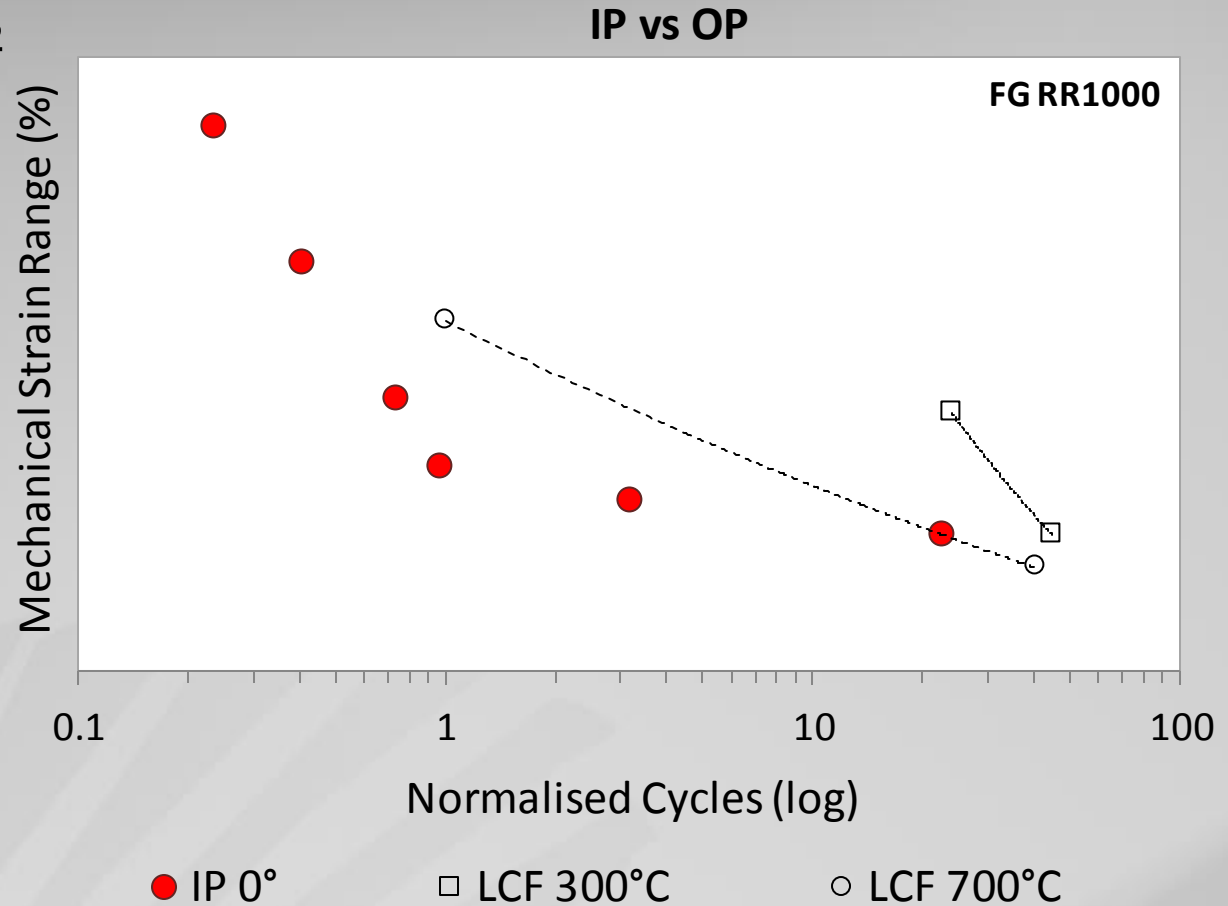
- TMF life  $\leq$  LCF life



# Typical RR1000 TMF behaviour

## General TMF Life Trends

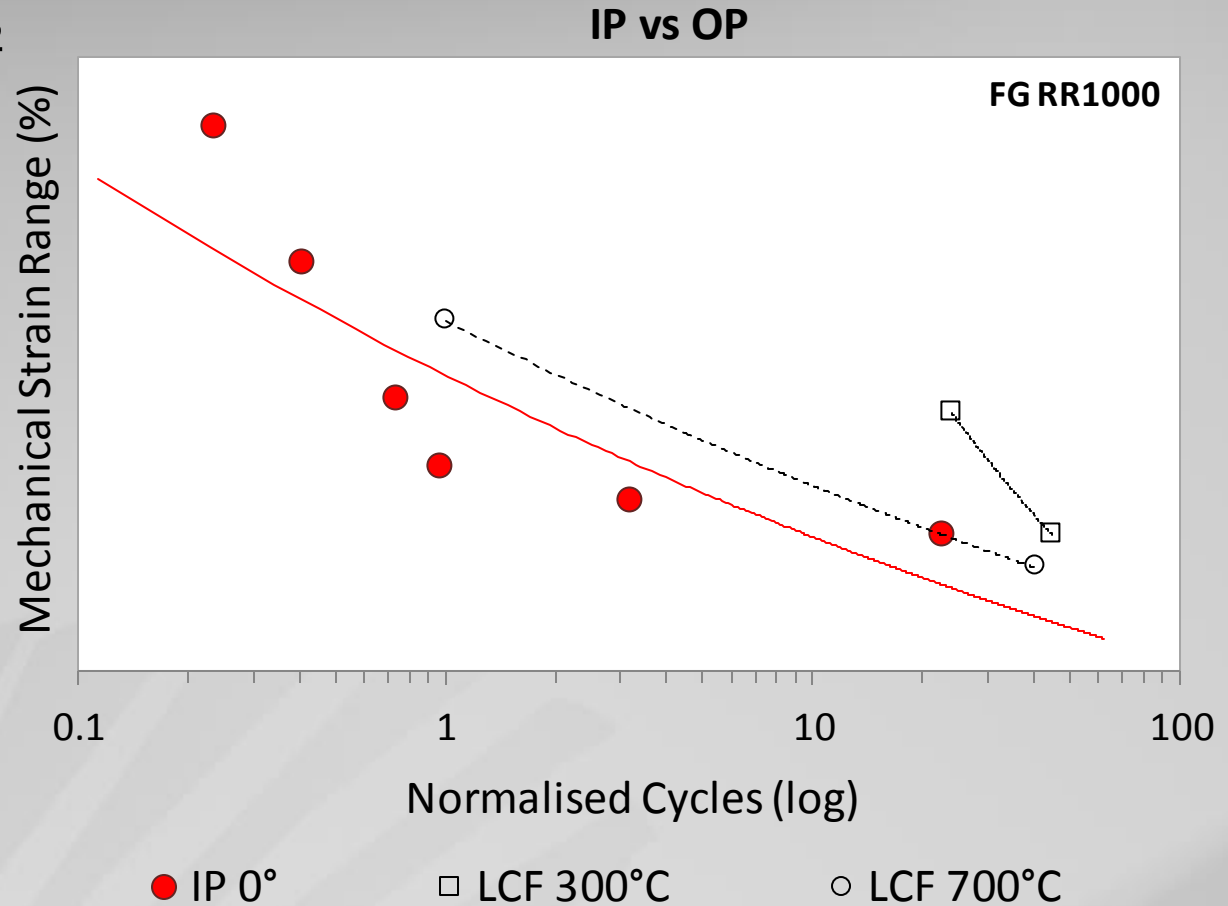
- TMF life  $\leq$  LCF life
- At Intermediate  $\Delta\varepsilon$ 
  - IP life  $\leq$  OP life
  - IP, INTER-granular cracking



# Typical RR1000 TMF behaviour

## General TMF Life Trends

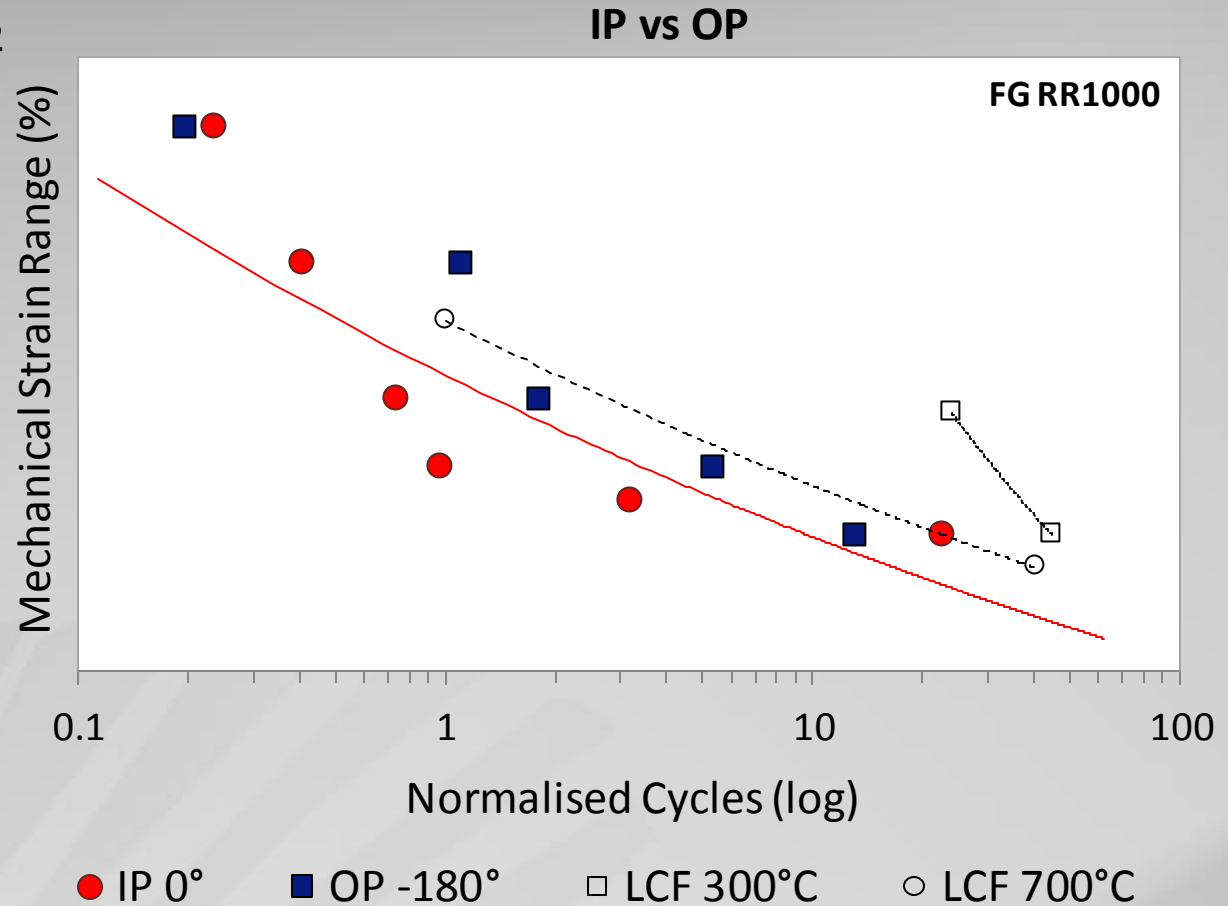
- TMF life  $\leq$  LCF life
- At Intermediate  $\Delta\epsilon$ 
  - IP life  $\leq$  OP life
  - IP, INTER-granular cracking



# Typical RR1000 TMF behaviour

## General TMF Life Trends

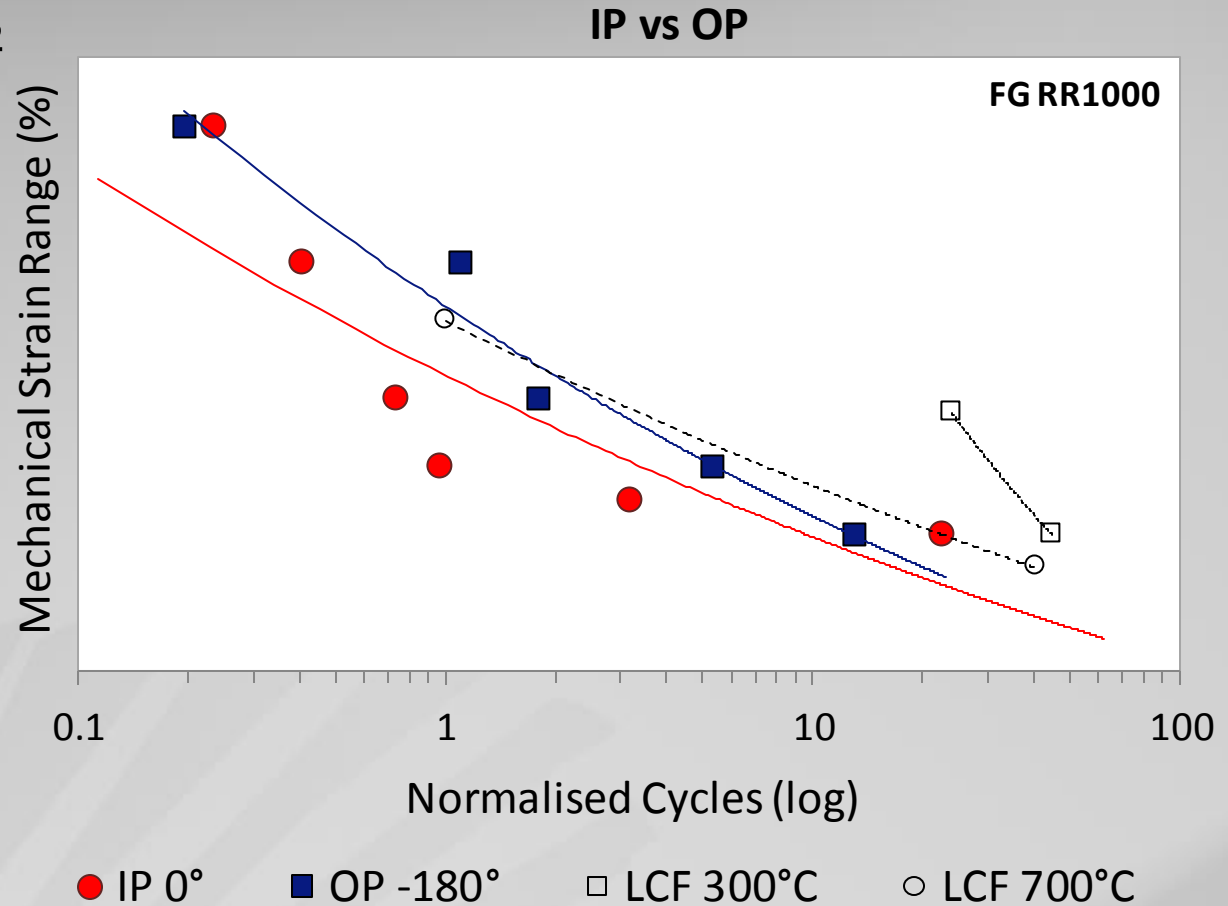
- TMF life  $\leq$  LCF life
- At Intermediate  $\Delta\varepsilon$ 
  - IP life  $\leq$  OP life
  - IP, INTER-granular cracking
- At Low  $\Delta\varepsilon$ 
  - OP life  $\leq$  IP life
  - OP, TRANS-granular cracking



# Typical RR1000 TMF behaviour

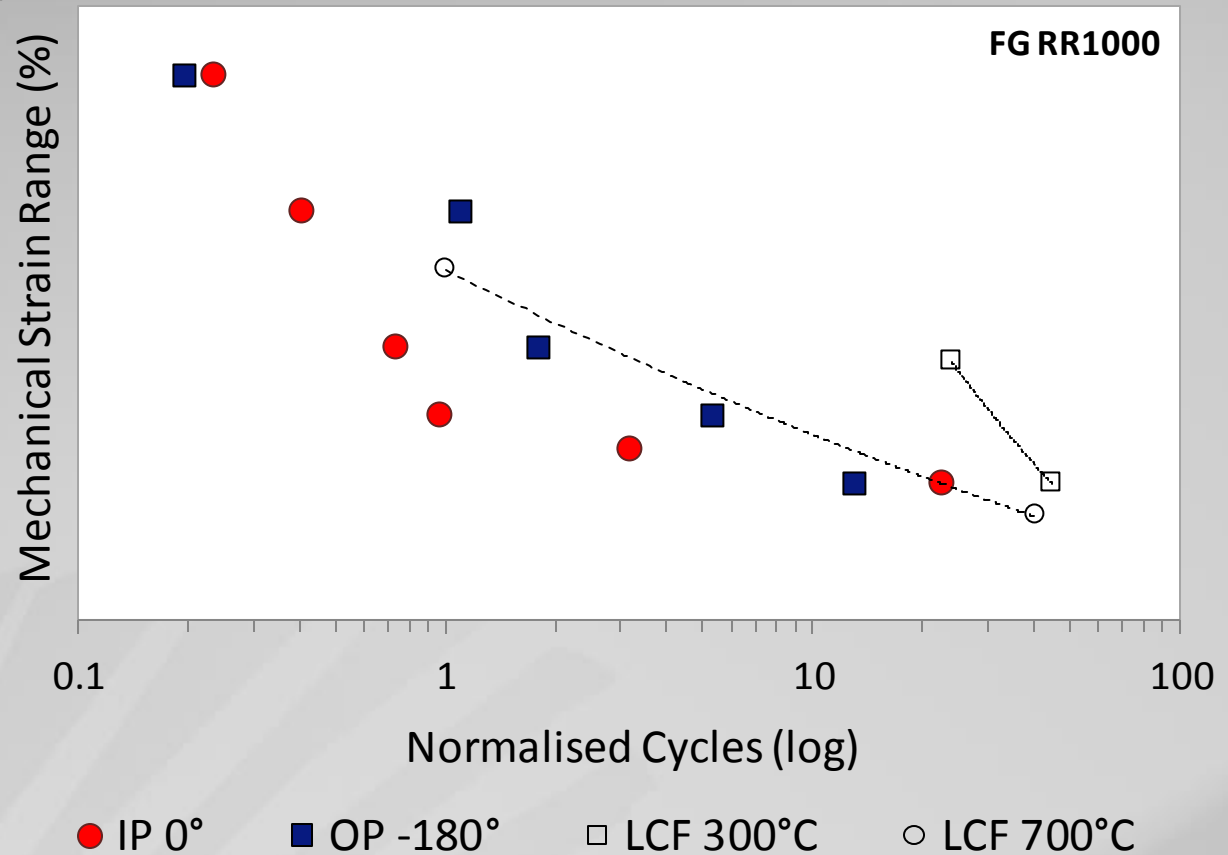
## General TMF Life Trends

- TMF life  $\leq$  LCF life
- At Intermediate  $\Delta\varepsilon$ 
  - IP life  $\leq$  OP life
  - IP, INTER-granular cracking
- At Low  $\Delta\varepsilon$ 
  - OP life  $\leq$  IP life
  - OP, TRANS-granular cracking



# Typical RR1000 TMF behaviour

## General TMF Life Trends



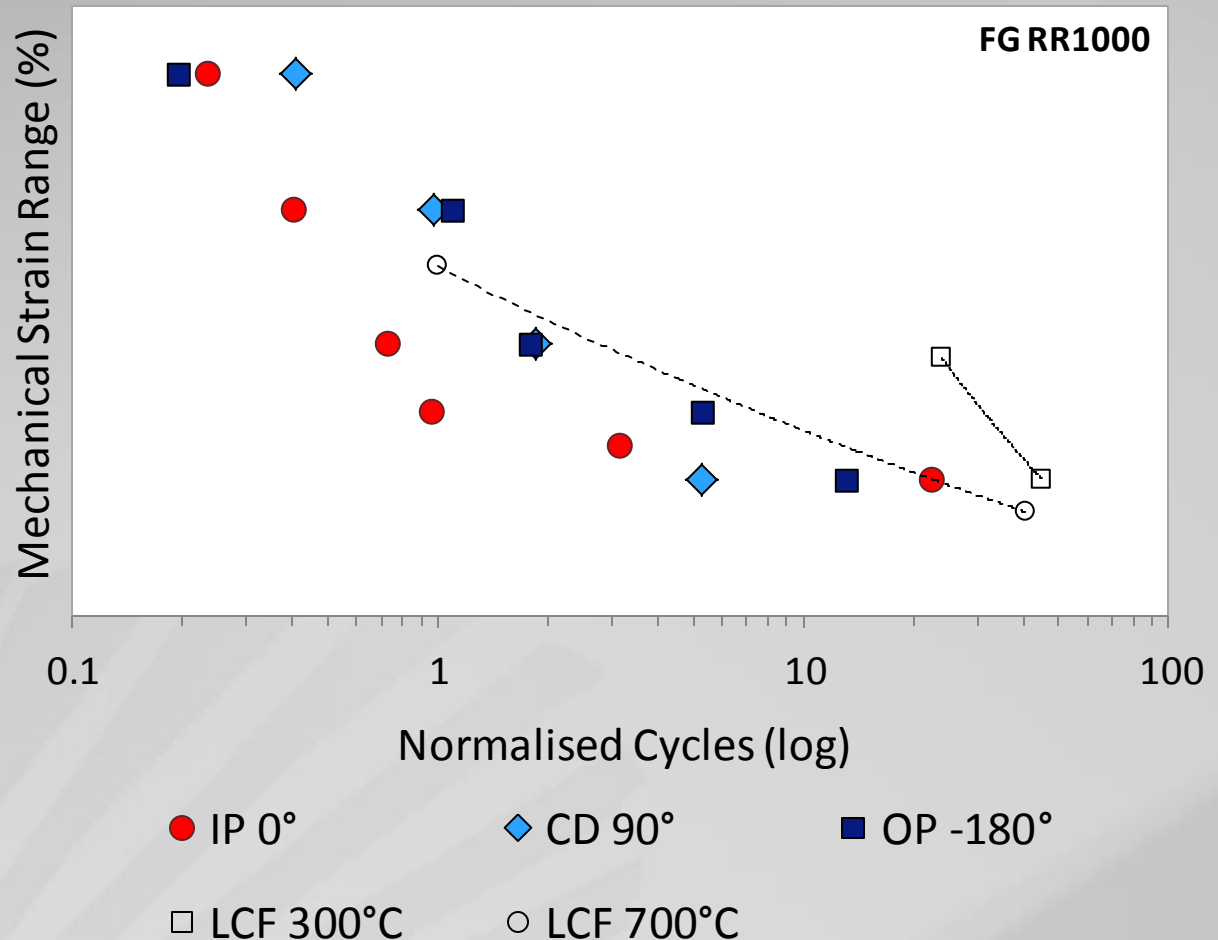
# Typical RR1000 TMF behaviour

## General TMF Life Trends

### ■ At Low $\Delta\varepsilon$

- CD90 life  $\leq$  IP & OP

CD vs CCD



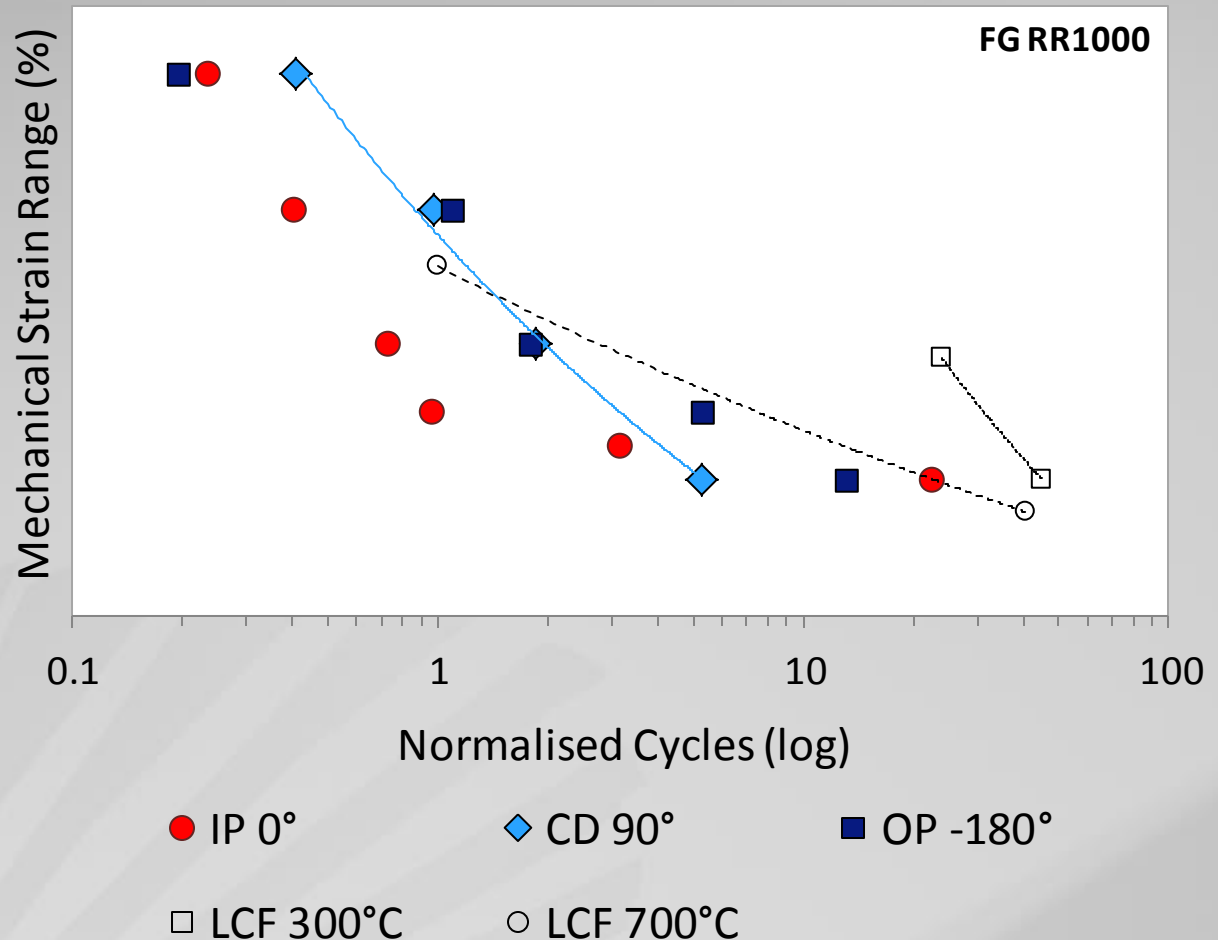
# Typical RR1000 TMF behaviour

## General TMF Life Trends

### ■ At Low $\Delta\varepsilon$

- CD90 life  $\leq$  IP & OP

### CD vs CCD

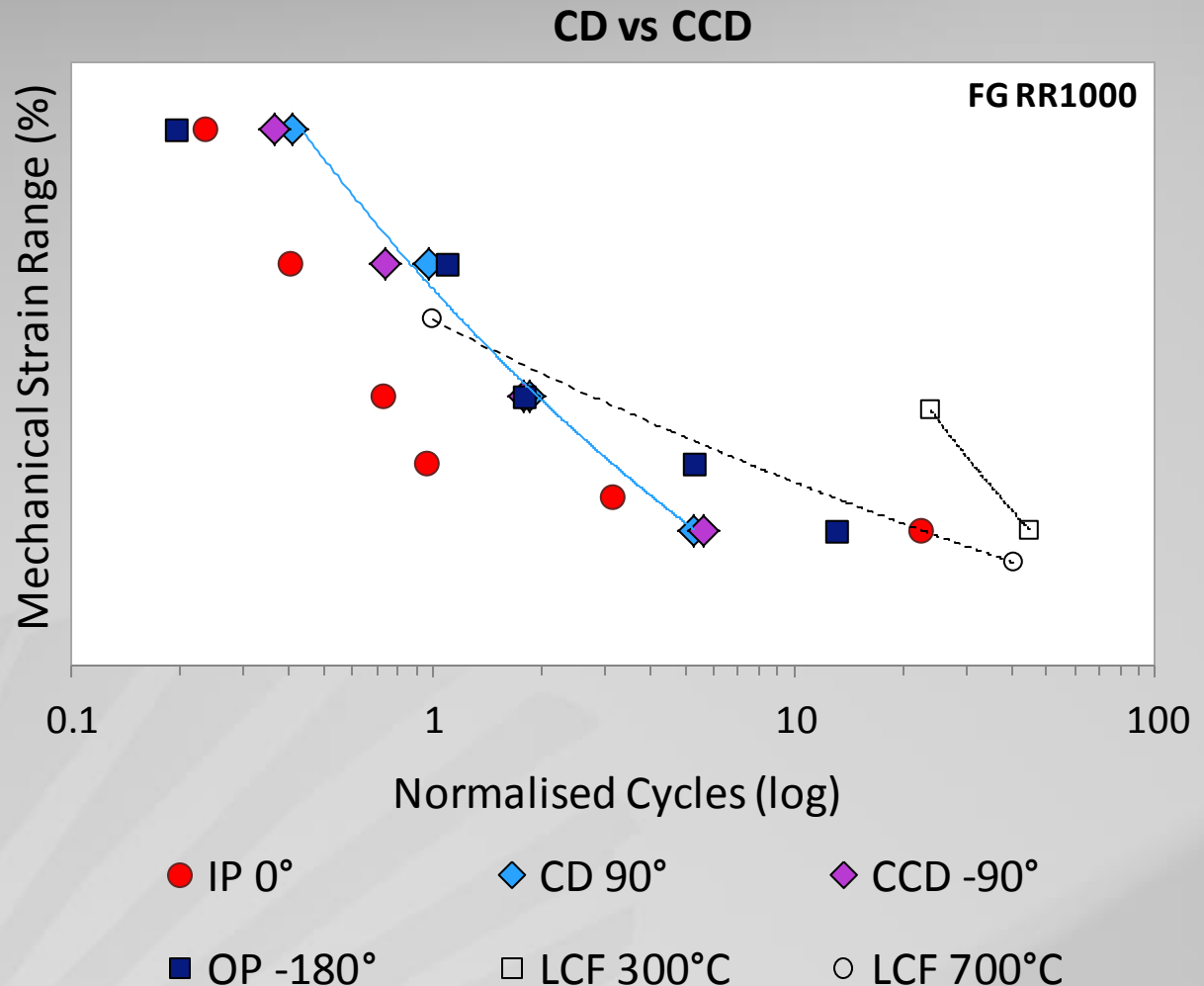




# Typical RR1000 TMF behaviour

## General TMF Life Trends

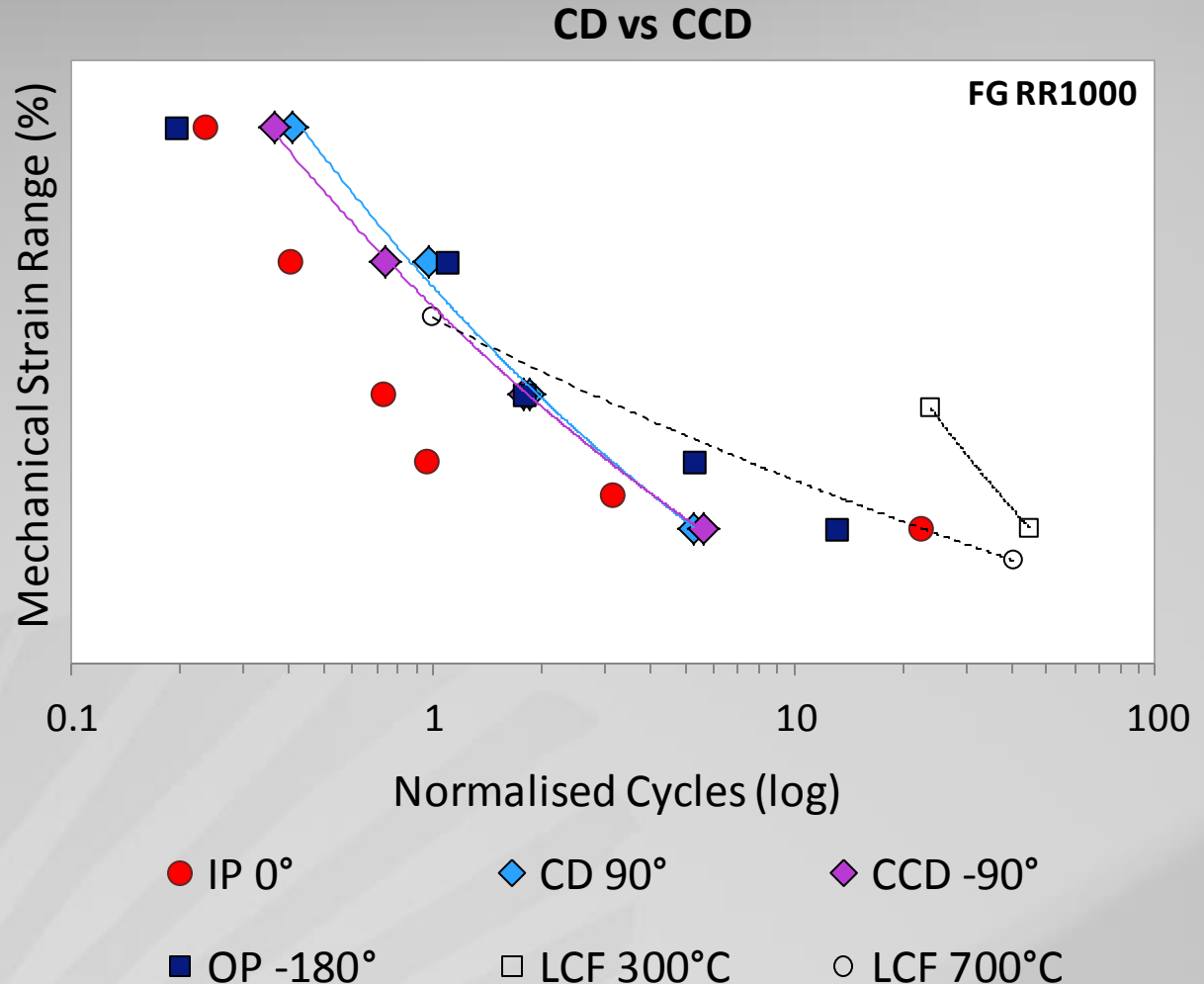
- At Low  $\Delta\varepsilon$ 
  - CD90 life  $\leq$  IP & OP
- CD Life  $\approx$  CCD across all strain ranges



# Typical RR1000 TMF behaviour

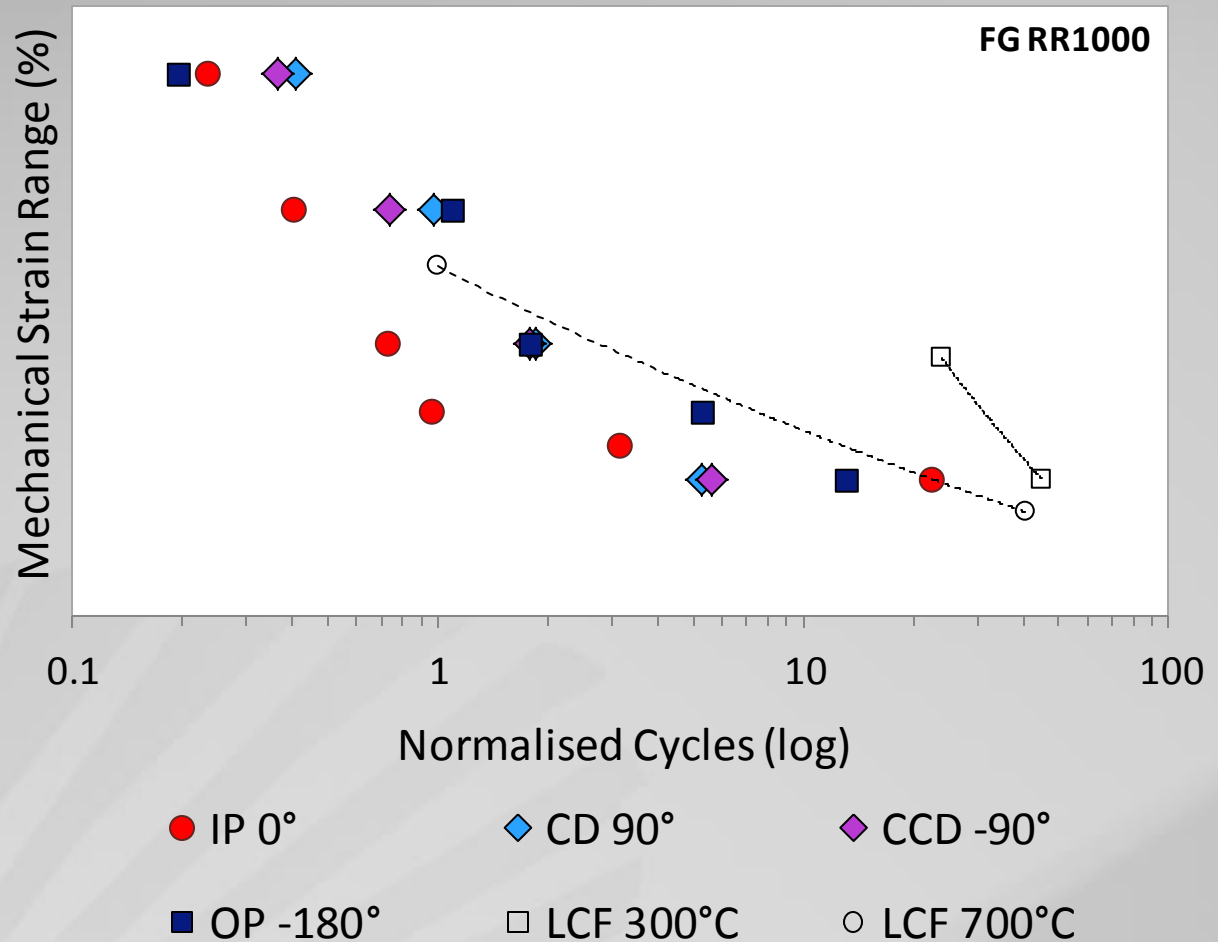
## General TMF Life Trends

- At Low  $\Delta\varepsilon$ 
  - CD90 life  $\leq$  IP & OP
- CD Life  $\approx$  CCD across all strain ranges



# Typical RR1000 TMF behaviour

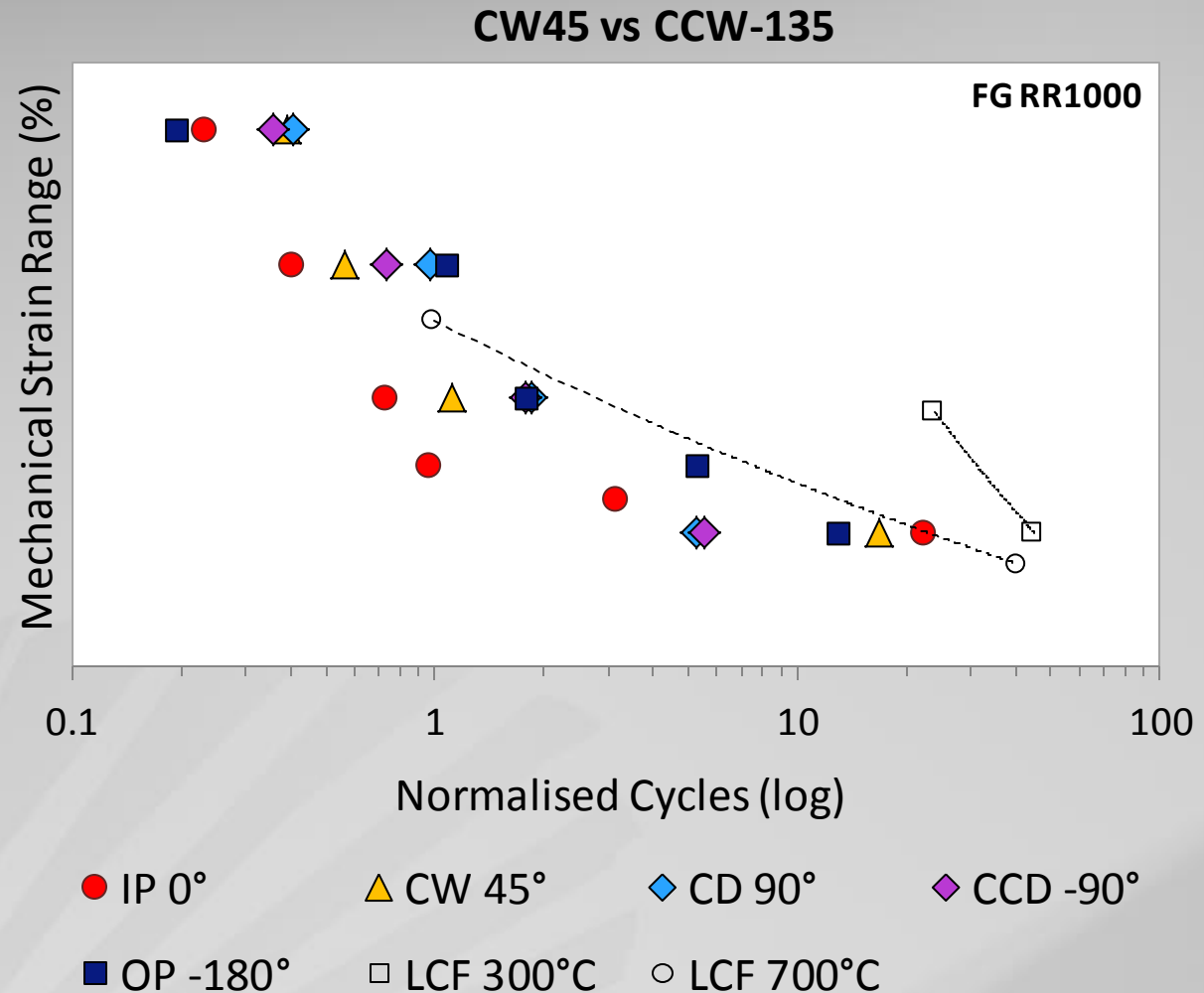
## General TMF Life Trends



# Typical RR1000 TMF behaviour

## General TMF Life Trends

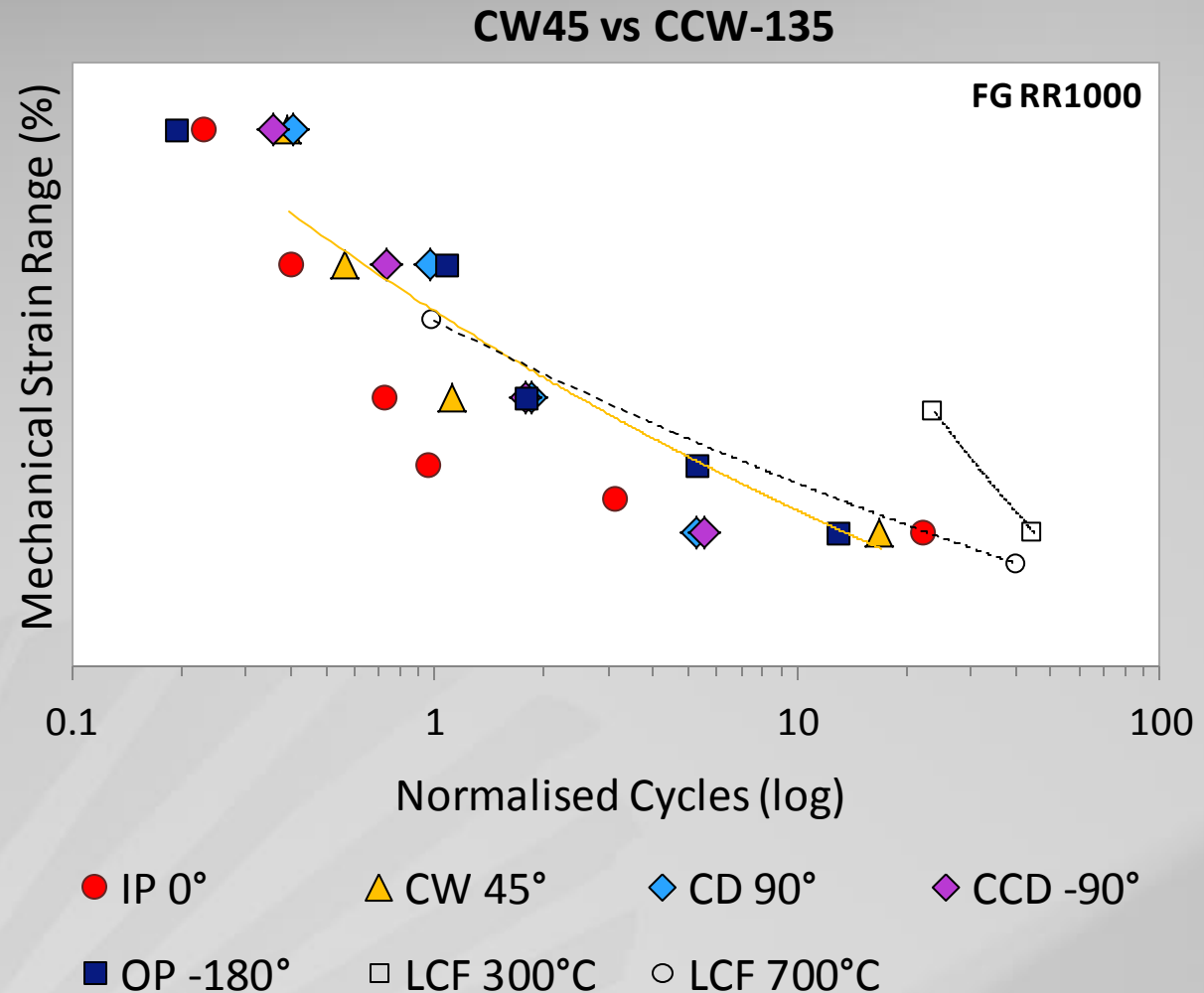
- CW45° loading follows a similar trend to IP loading



# Typical RR1000 TMF behaviour

## General TMF Life Trends

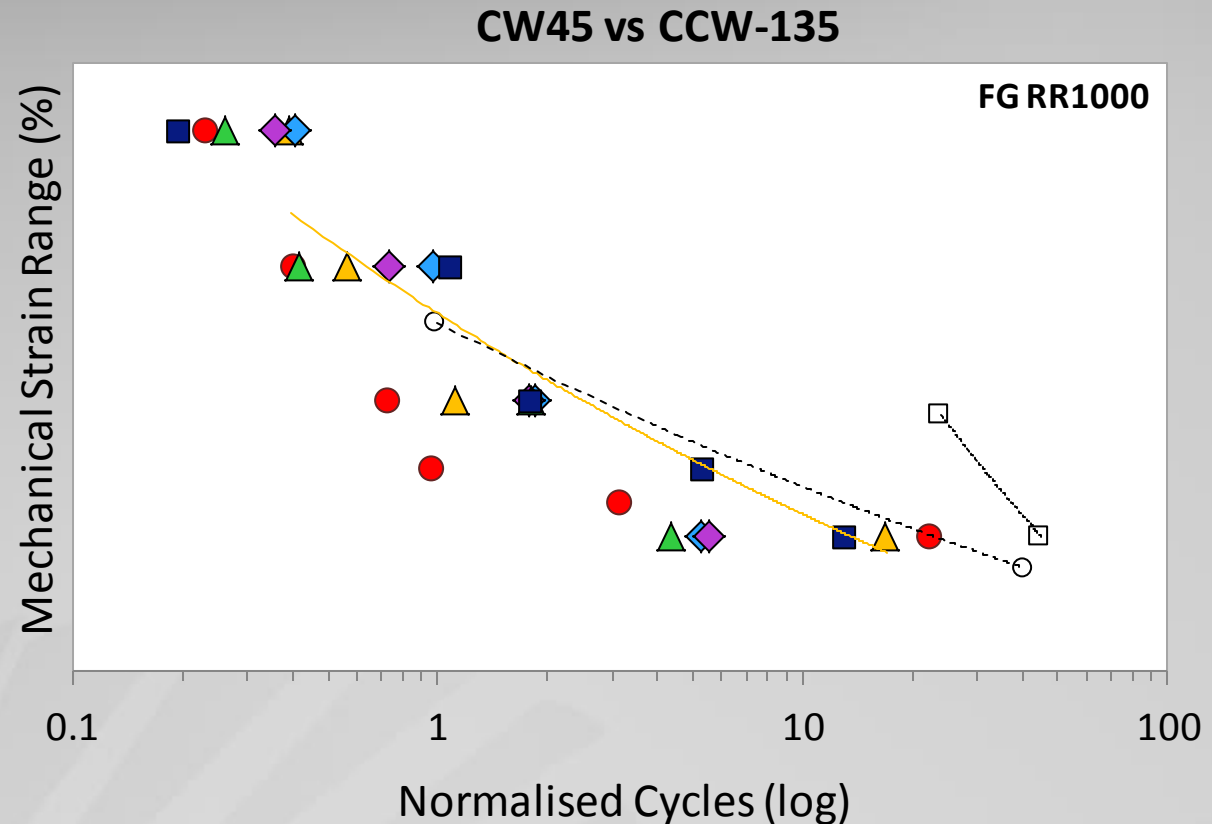
- CW45° loading follows a similar trend to IP loading



# Typical RR1000 TMF behaviour

## General TMF Life Trends

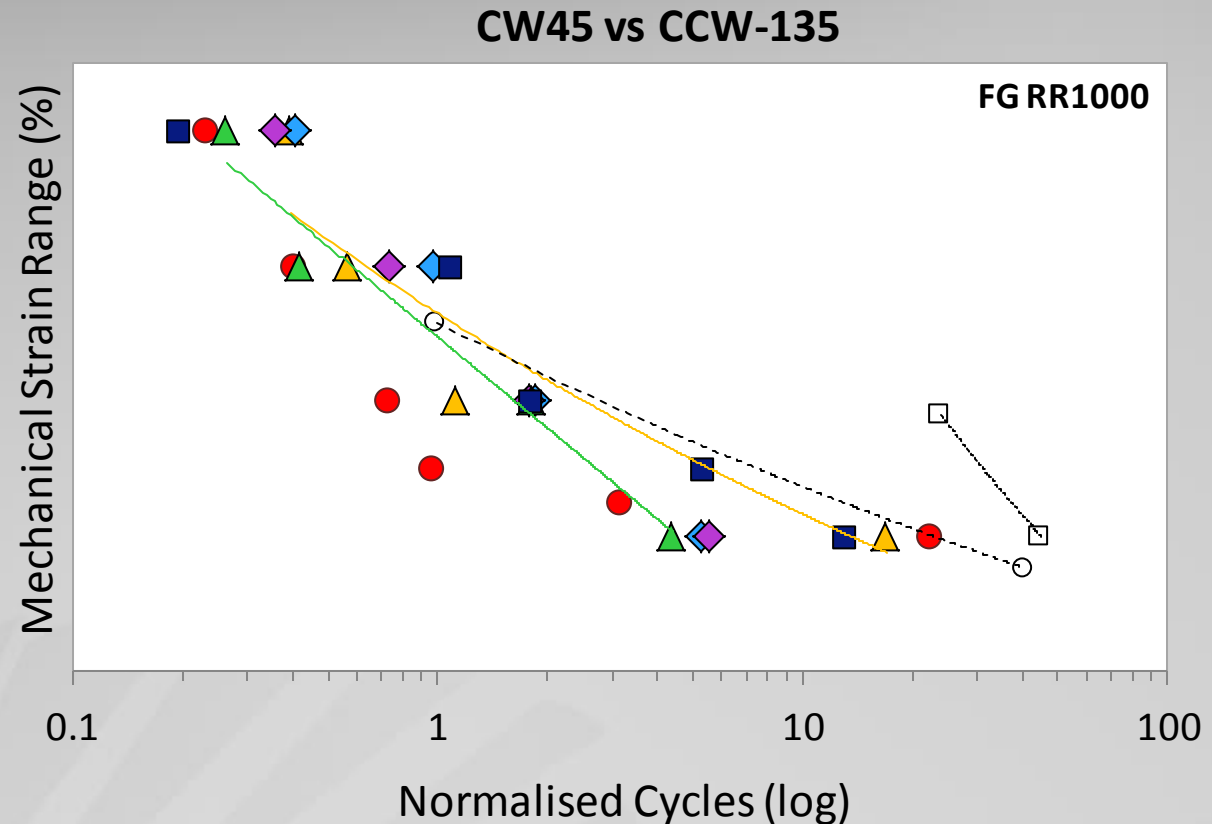
- CW45° loading follows a similar trend to IP loading
- Counter Clockwise -135° loading reduces fatigue life, similar slope to OP loading



# Typical RR1000 TMF behaviour

## General TMF Life Trends

- CW45° loading follows a similar trend to IP loading
- Counter Clockwise -135° loading reduces fatigue life, similar slope to OP loading



● IP 0°

▲ CW 45°

◆ CD 90°

◆ CCD -90°

▲ CCW -135°

■ OP -180°

□ LCF 300°C

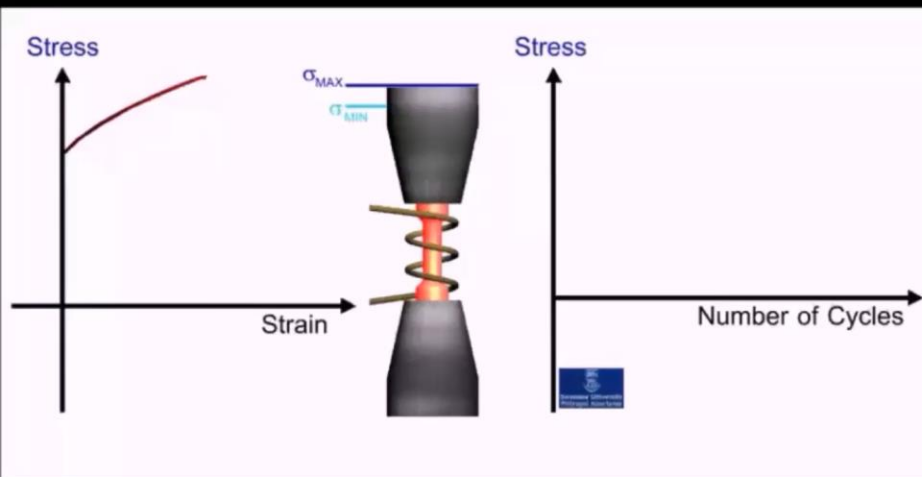
○ LCF 700°C



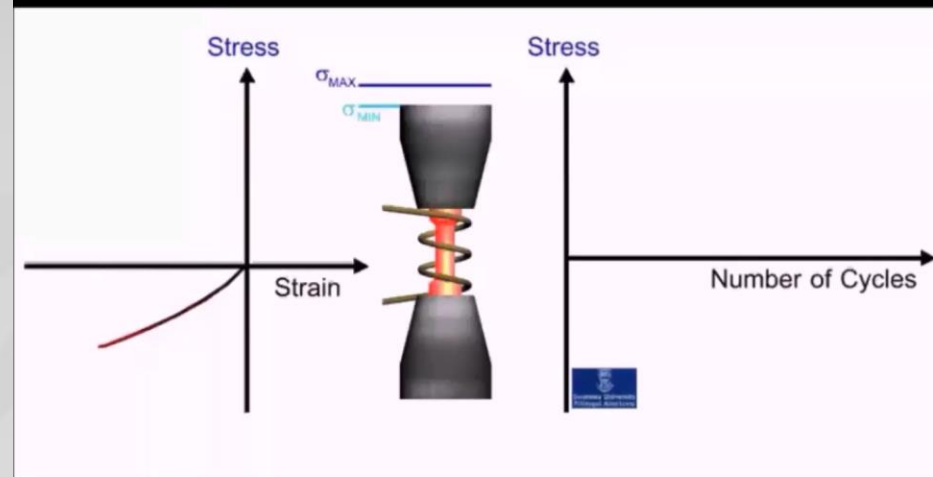
# Typical TMF Hysteresis Behaviour

- Initial material behaviour may change significantly during the test.
- Understanding the stress/strain evolution throughout the test is often critical in order to be able to predict life.
- Cycle may evolve to very different stress conditions due to the interaction of plasticity and creep which often makes TMF tests differ significantly from isothermal fatigue.

## In-Phase ( $\phi = 0^\circ$ )

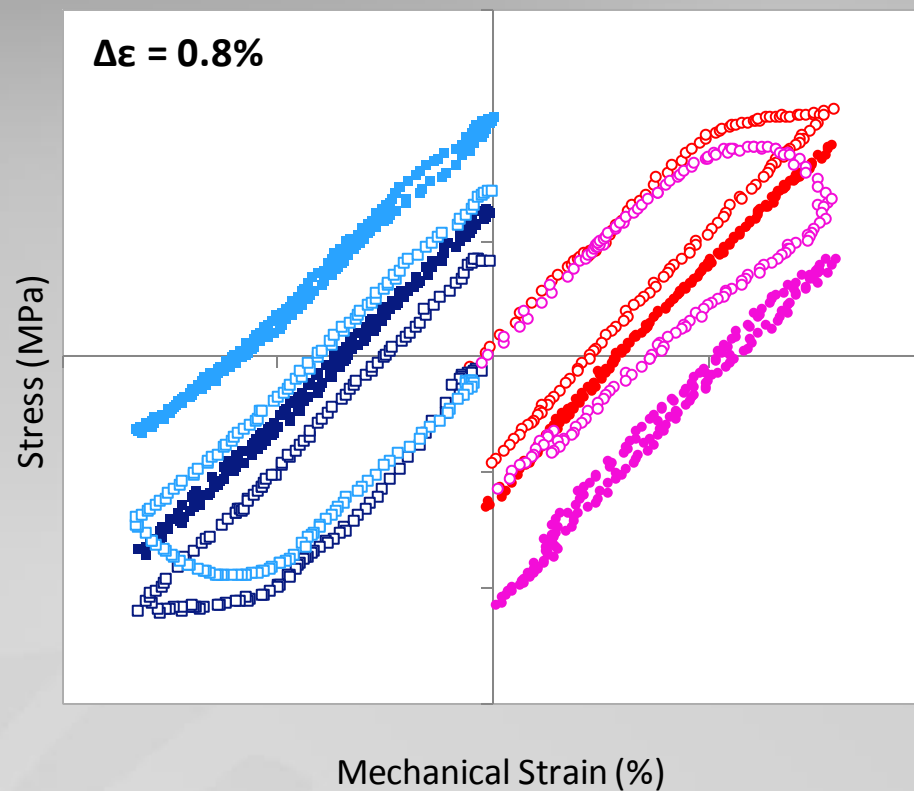
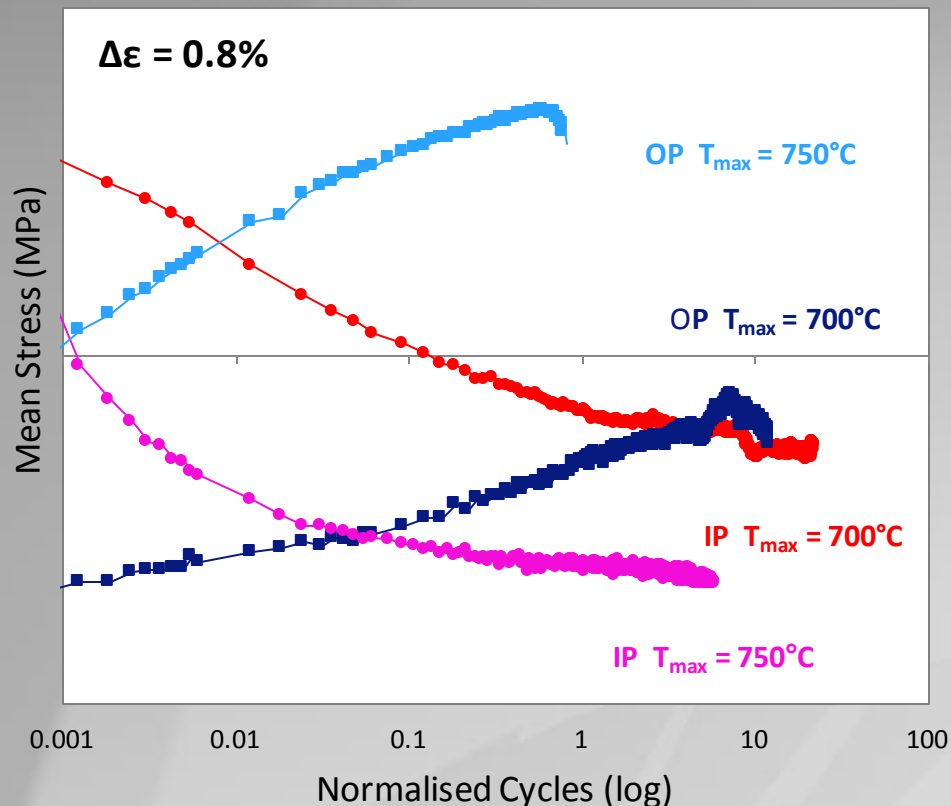


## Out-Phase ( $\phi = -180^\circ$ )





# TMF Hysteresis Behaviour



- 300-700°C    ● IP  $\Delta\epsilon=0.8\%$     ■ OP  $\Delta\epsilon=0.8\%$
- 300-750°C    ● IP  $\Delta\epsilon=0.8\%$     ■ OP  $\Delta\epsilon=0.8\%$

- IP 0.8% 1st
- IP 0.8% Stabilised
- OP 0.8% 1st
- OP 0.8% Stabilised
- IP 0.8%  $\Delta\epsilon$  1st 750°C
- IP 0.8%  $\Delta\epsilon$  Stabilised 750°C
- OP 0.8%  $\Delta\epsilon$  1st 750°C
- OP 0.8%  $\Delta\epsilon$  Stabilised 750°C

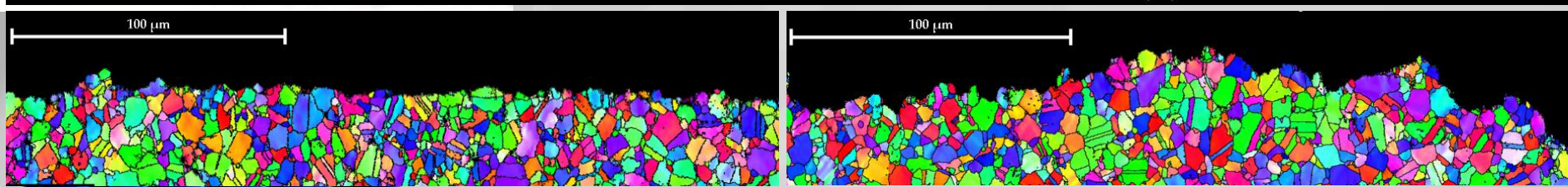
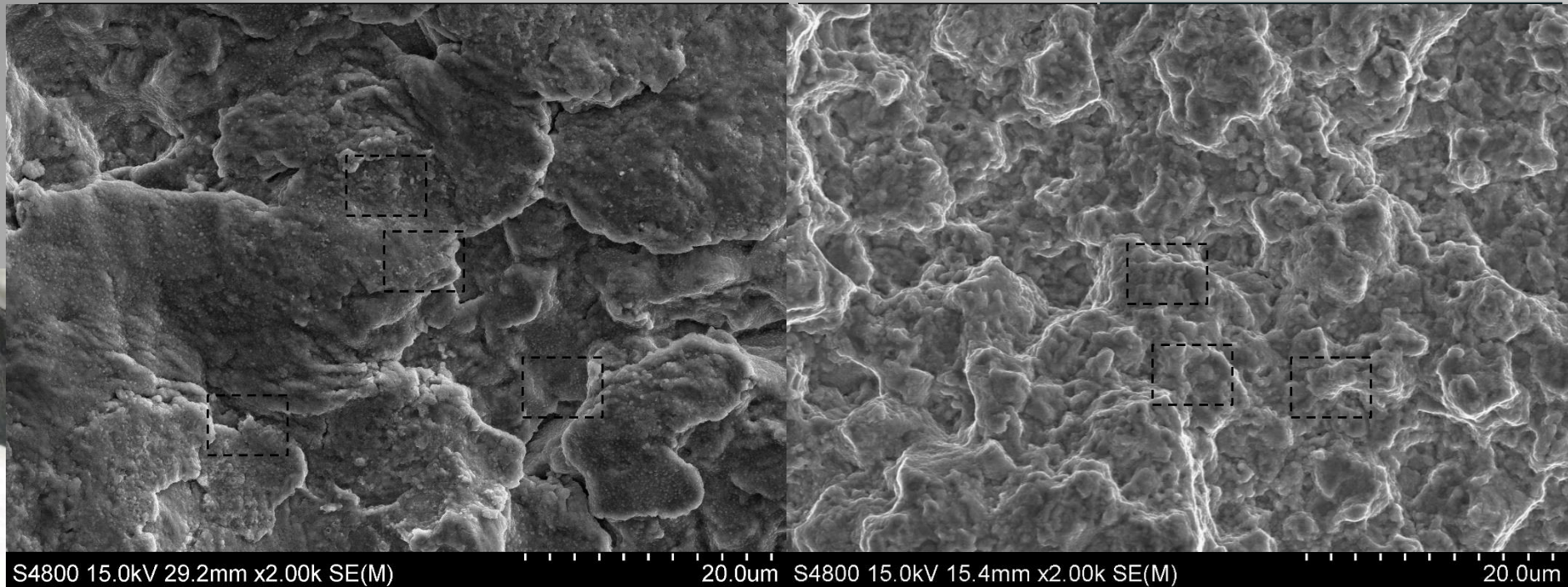


# Fractography

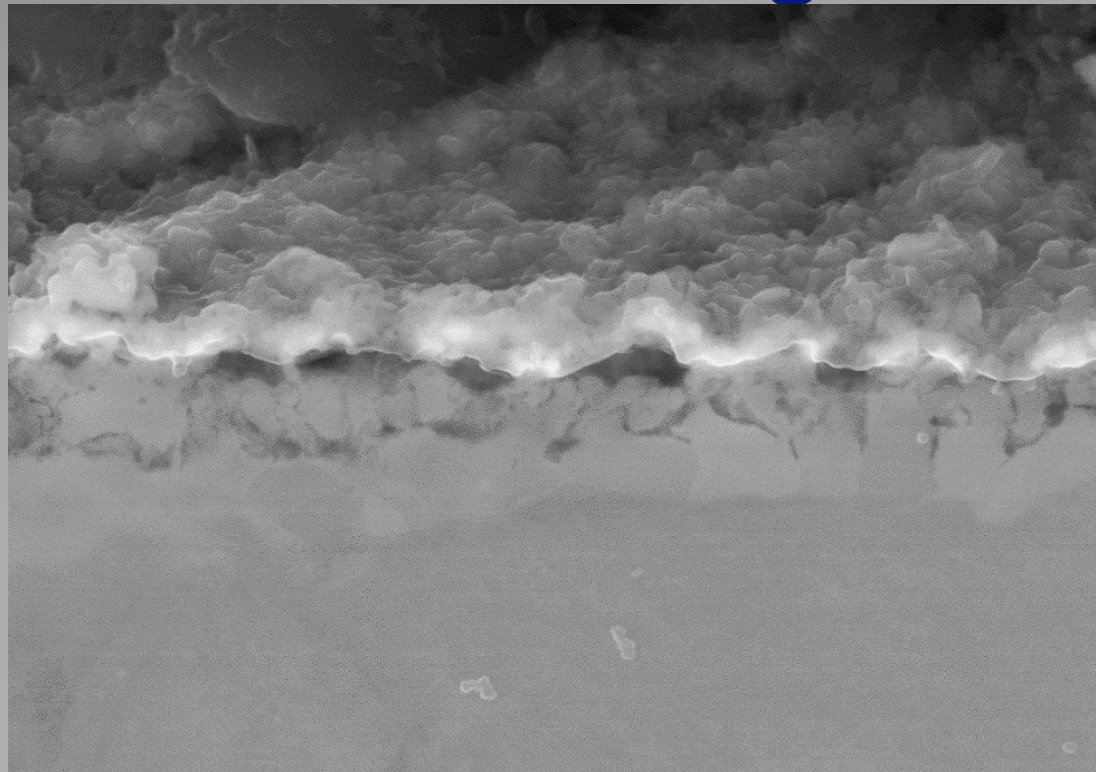
Out of Phase

300-750°C

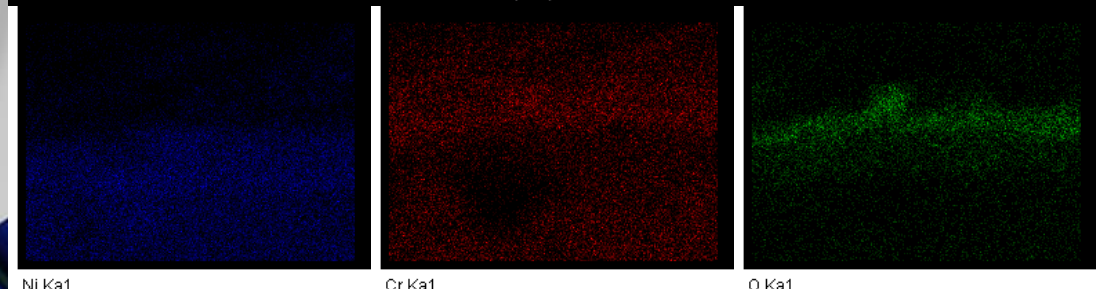
In Phase



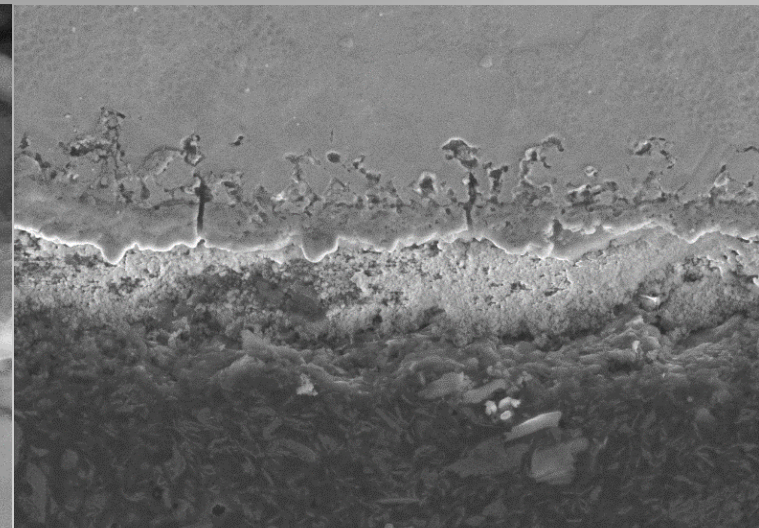
# Oxidation Damage



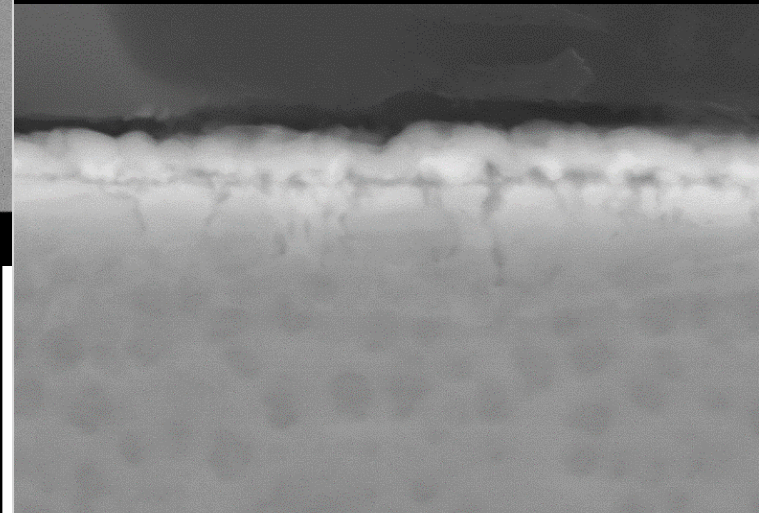
S4800 20.0kV 13.6mm x15.0k SE(M) 3.00um



Ni Ka1 Cr Ka1 O Ka1



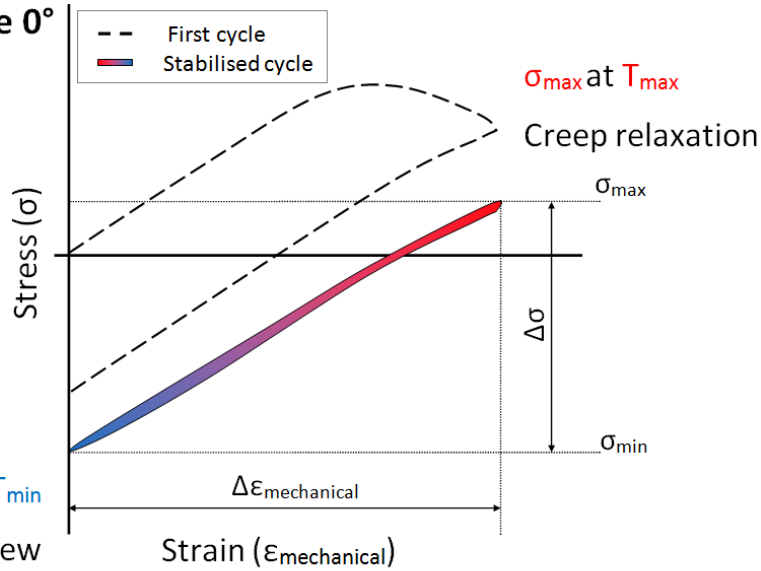
S4800 5.0kV 21.5mm x7.00k SE(M) 5.00um



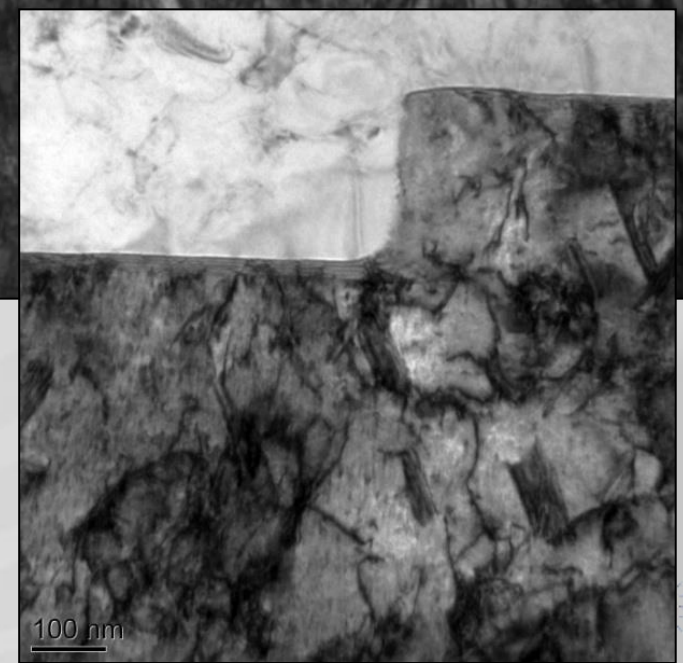
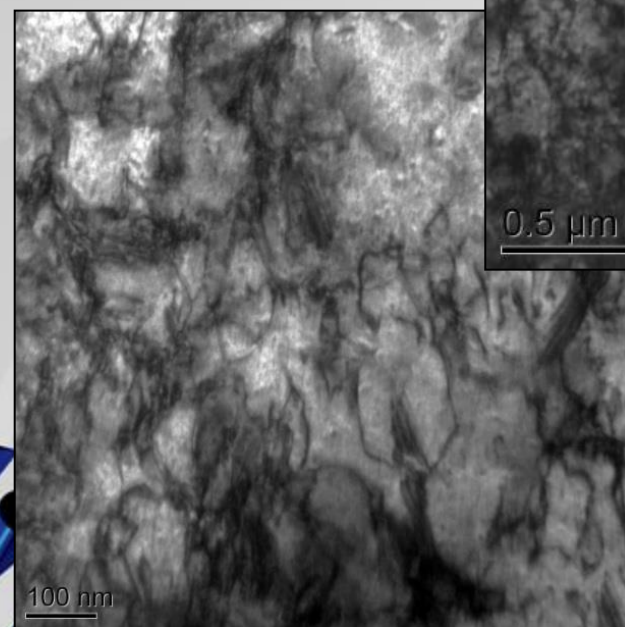
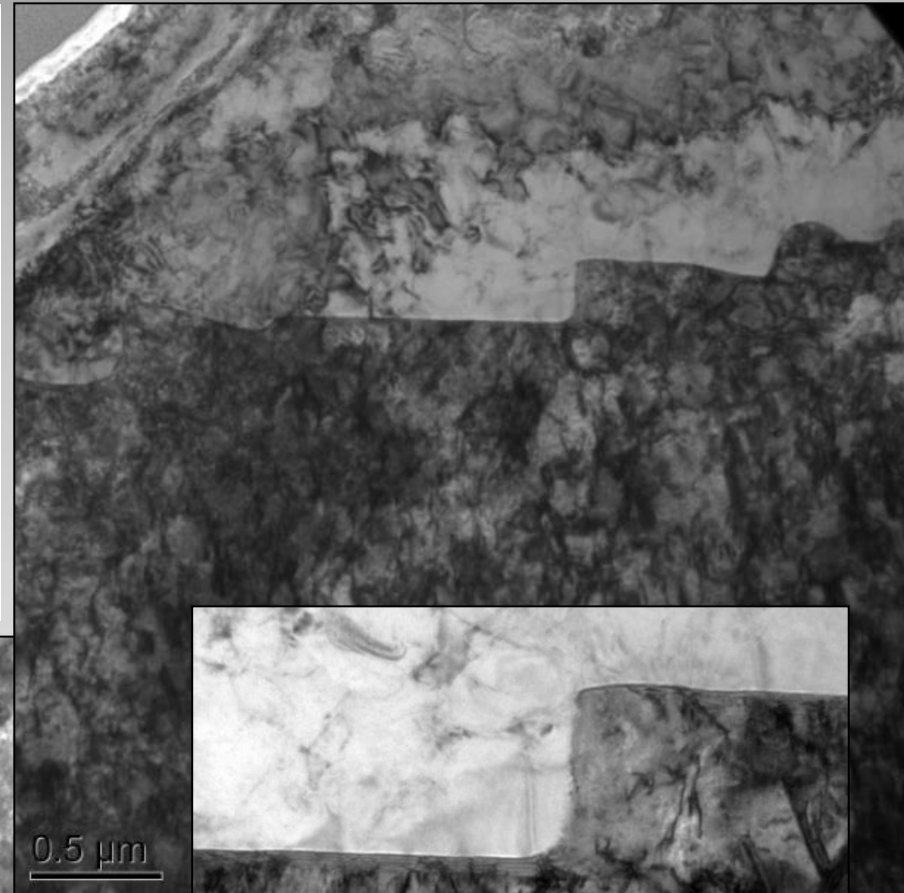
S4800 15.0kV 10.8mm x40.0k SE(M) 1.00um

# Dislocation Mechanisms

In-Phase  $0^\circ$



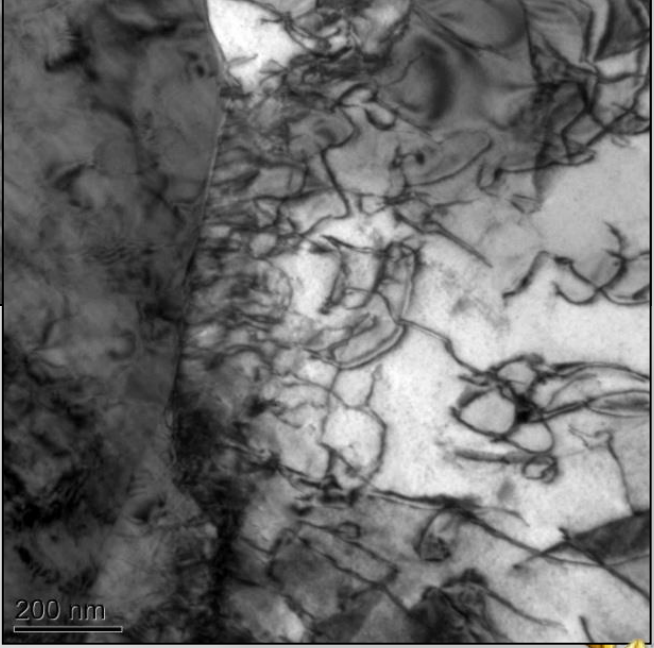
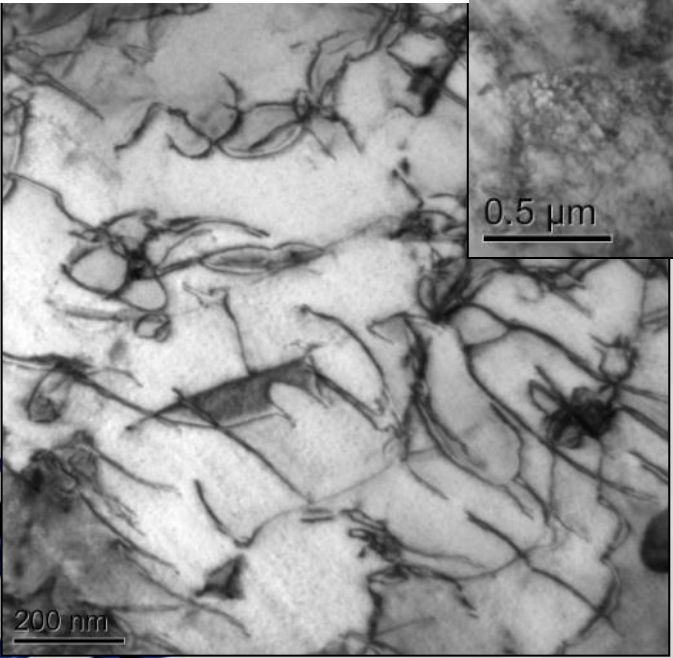
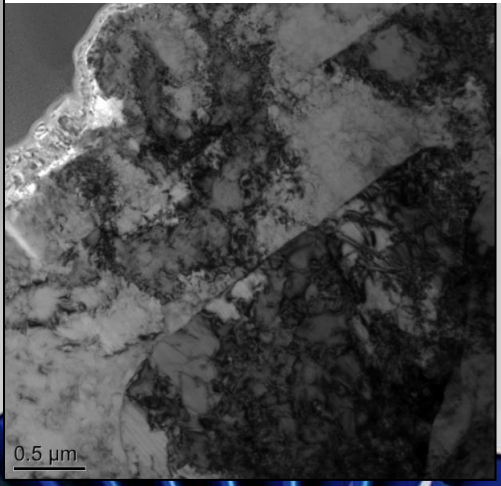
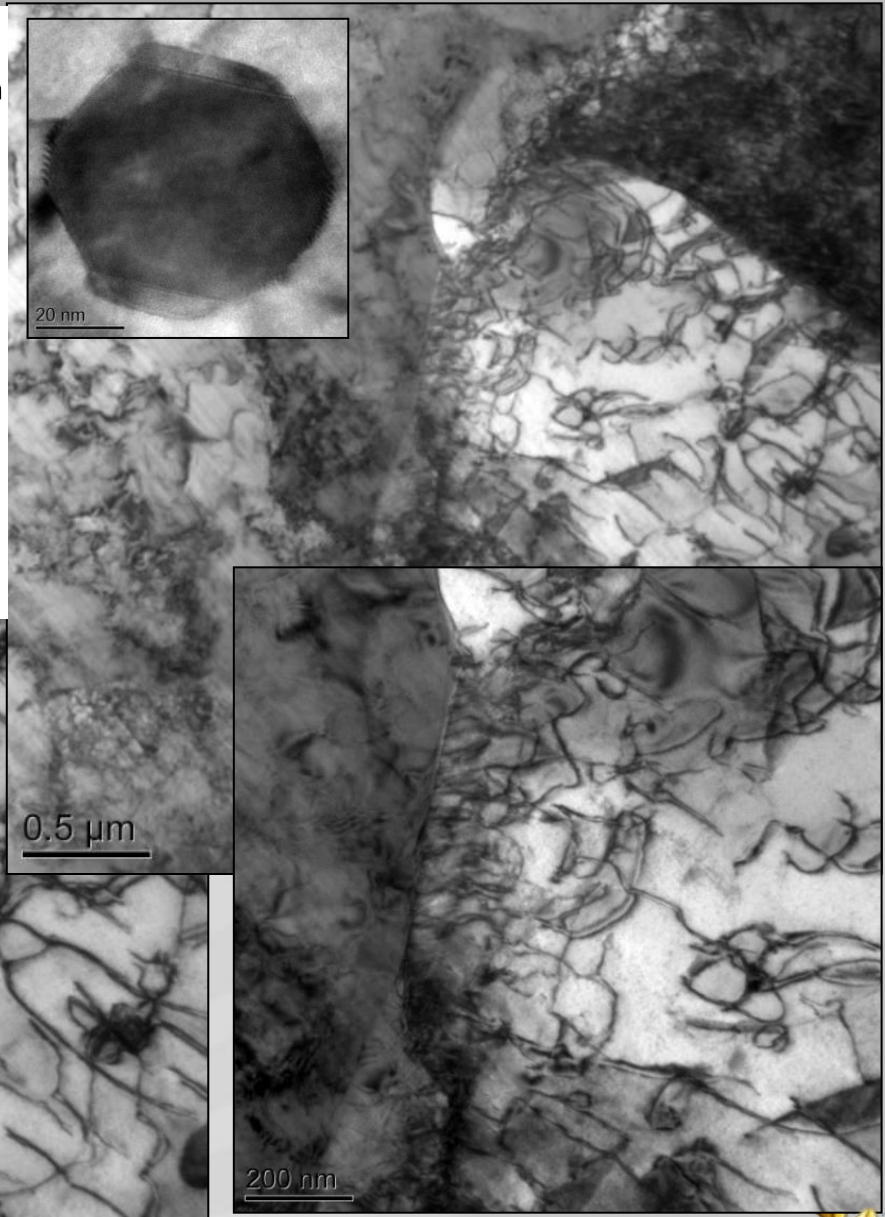
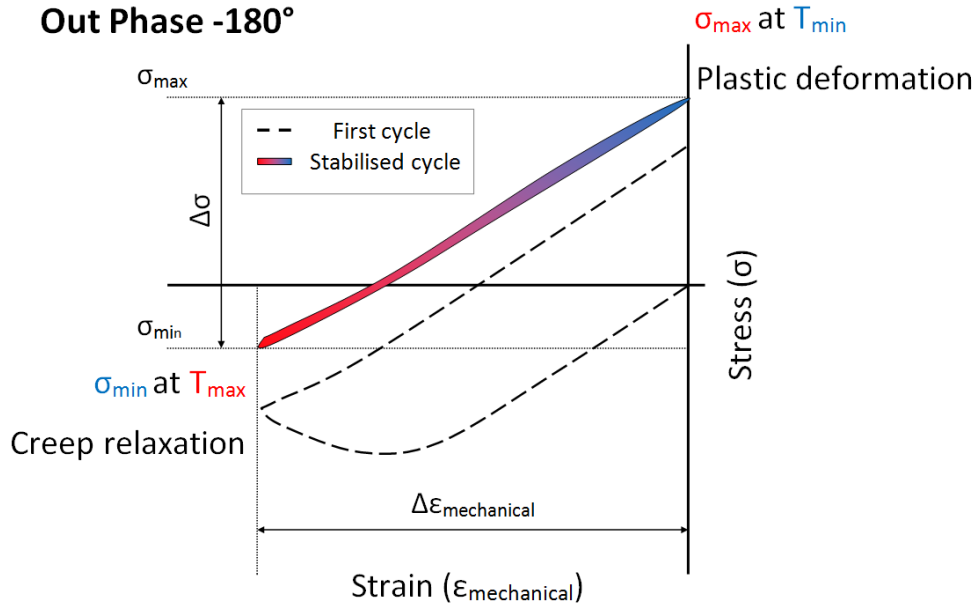
Low Energy, Few Mechanisms



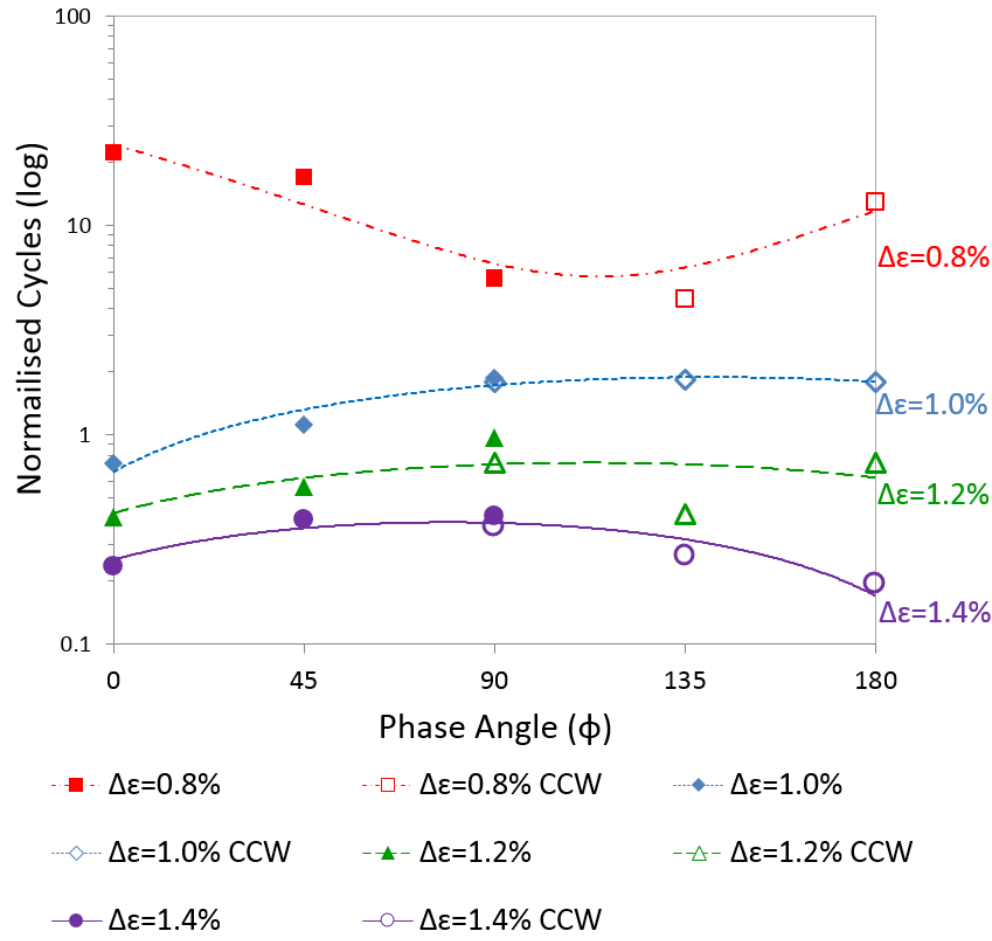
TMF Workshop\_BAM,  
Berlin, Apr 27-29<sup>th</sup>  
2016.

# Dislocation Mechanisms

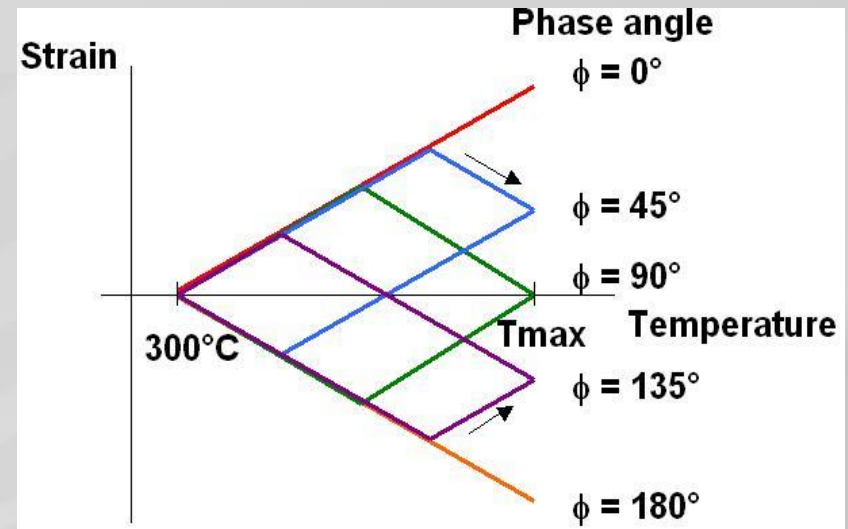
Out Phase -180°



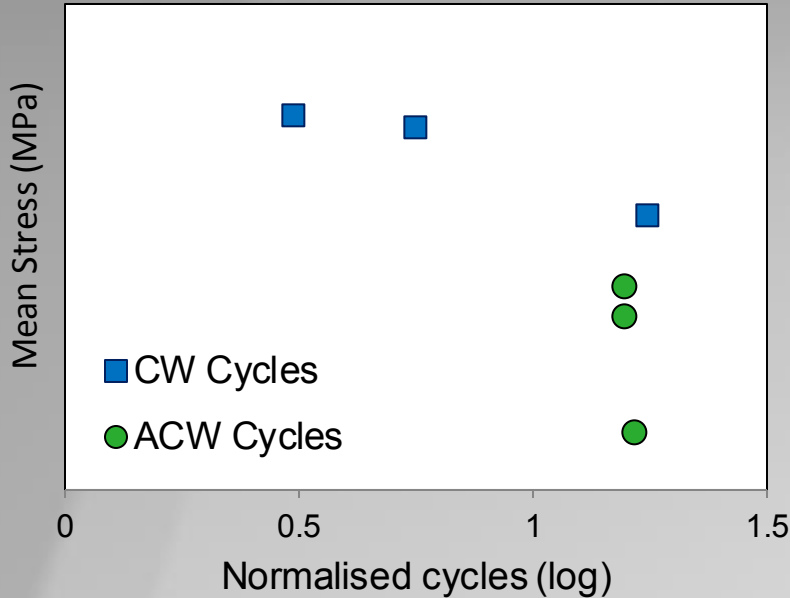
# Phase Angle Effects



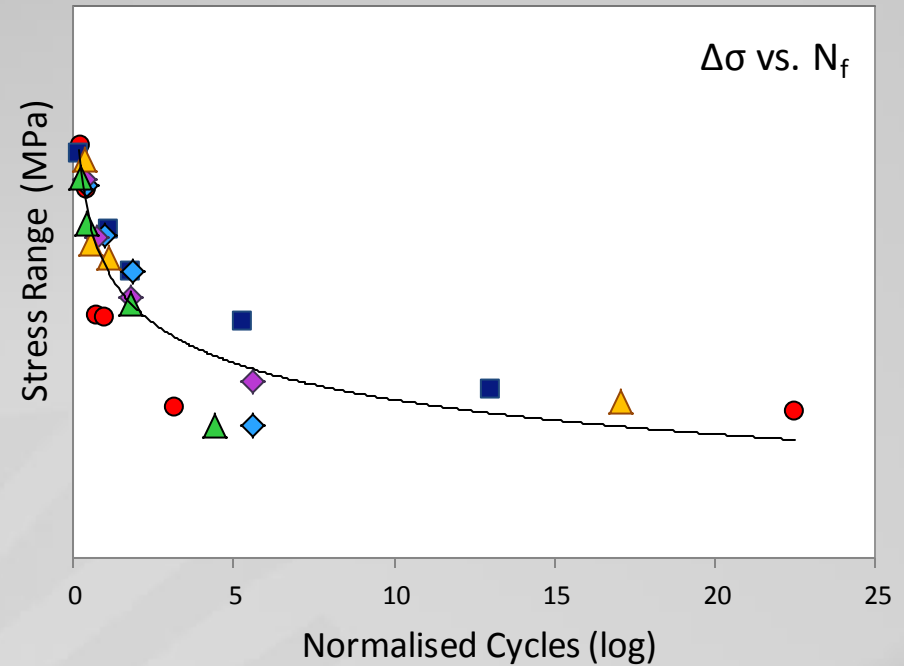
- There is a clear effect of phase angle on TMF life
- The extent of this relationship is dependant on the employed mechanical strain range.
- Although scatter in the data needs to be considered, the relationships are well defined by this data.



# Phase Angle Effects



- Also clear is that there is a relationship with mean stress for varying phase angles at the same strain range.



- IP
- ◆ CD
- ▲ CW45
- OP
- ◆ CCD
- ▲ CCW-135
- Power ( $\Delta\sigma$  vs.  $N_f$ )

- A strong relationship is seen between the stabilised stress range and fatigue life over diverse phase angles and strain ranges.



# Can you predict TMF life based on isothermal data?

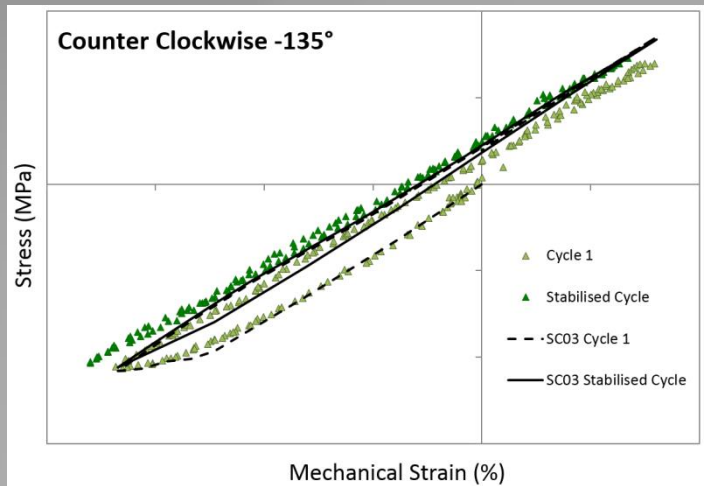


TMF Workshop\_BAM,  
Berlin, Apr 27-29<sup>th</sup>  
2016.

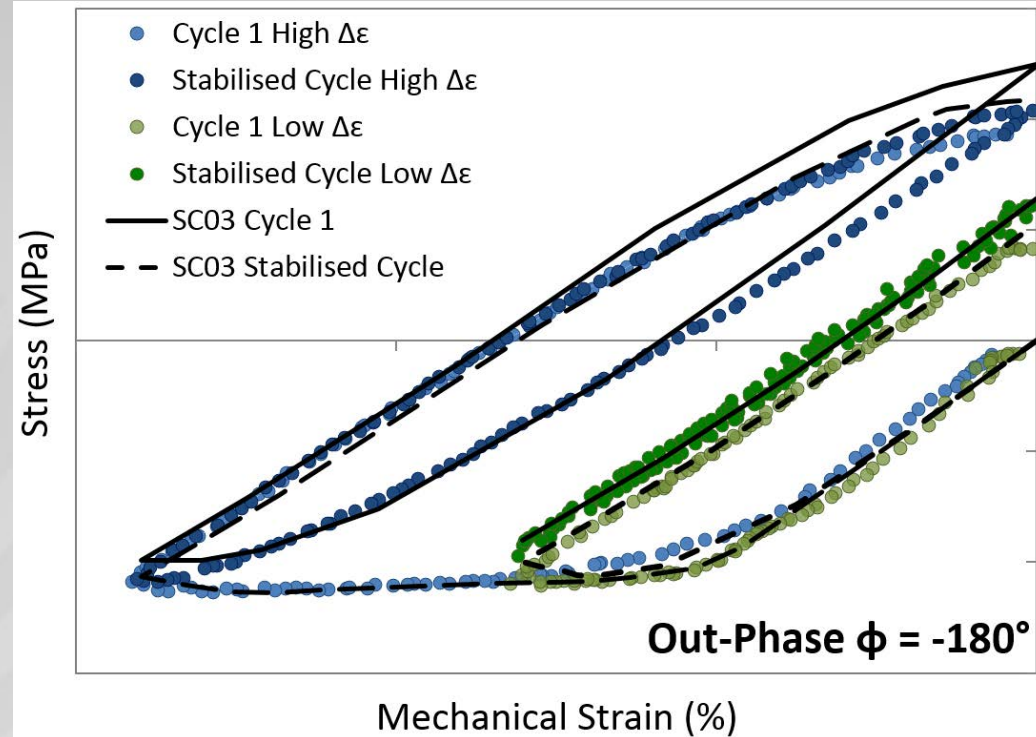
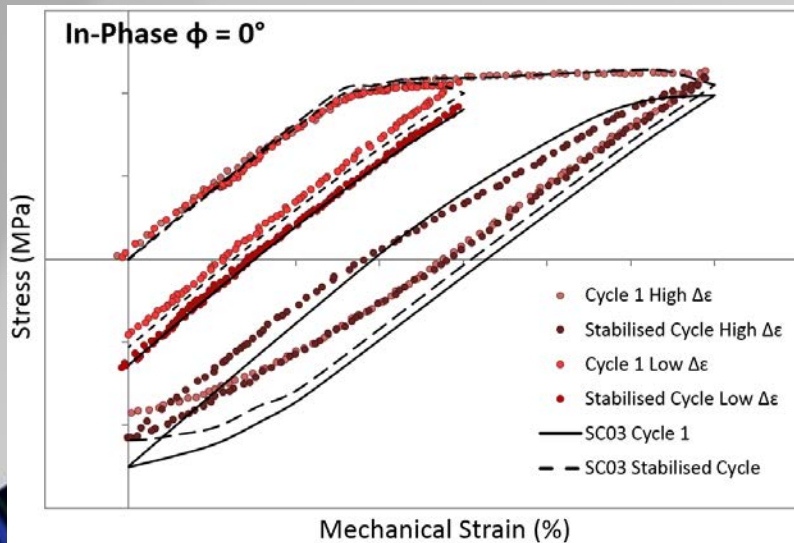




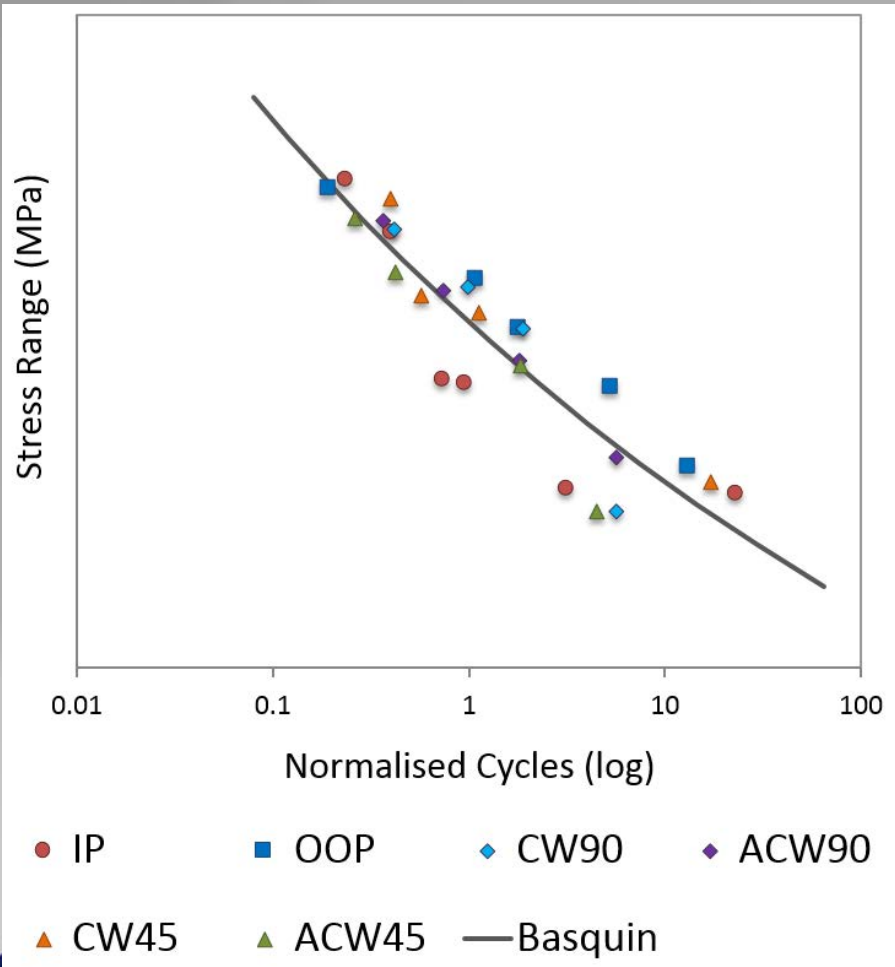
# Modelling and Life Prediction



- TMF loop reproduction in SC03, based on isothermal material properties
- Predictions based on the Mroz multi-layer hardening and the CT07 creep model using life fraction hardening



# Modelling and Life Prediction



$$\frac{\Delta\sigma}{2} = \sigma'_f (2N_f)^b$$

$\Delta\sigma$  = Stabilised Stress Range

$\sigma'_f$  = Fatigue Strength coefficient

$N_f$  = Number of TMF cycles to failure

$b$  = Basquin (fatigue strength exponent)

- Stabilised Stress Range conditions for all phase angles generated in SC03 are entered into the Basquin relationship to give following prediction



# Conclusions

- TMF cycles can be more damaging than LCF cycles at an equivalent  $T_{MAX}$ .
- The phase angle employed strongly influences TMF life, furthermore the  $T_{MAX}$  used can affect the degree of this influence.
- For a fixed strain range, a relationship exists between mean stress and fatigue life, however for increasing strain ranges, this relationship breaks down.
- A relationship between fatigue life and stabilised stress range does exist, enabling a predictive model based on the Basquin rule to predict the life of varying phase angle tests.
- Using isothermal material properties within SC03, accurate predictions of TMF stress-strain loops, thus stabilised stress ranges can be realised. Applying these into the Basquin relationship achieves reasonable predictions of fatigue life.
- Further work is on-going to improve these predictions, by incorporating the effects of crack propagation, the dominating damage mechanism during these TMF cycles



# Acknowledgements

The current research was funded by the EPSRC Rolls-Royce Strategic Partnership in Structural Metallic Systems for Gas Turbines (grants EP/H500383/1 and EP/H022309/1). The provision of materials and technical support from Rolls-Royce plc is gratefully acknowledged.

Email contact: [jonathan.p.jones@swansea.ac.uk](mailto:jonathan.p.jones@swansea.ac.uk)

## *Questions?*



Prifysgol Abertawe  
Swansea University

# ESTIMATION OF THERMO-MECHANICAL FATIGUE CRACK GROWTH USING AN ACCUMULATIVE APPROACH BASED ON ISOTHERMAL TEST DATA



TECHNISCHE  
UNIVERSITÄT  
DARMSTADT

3rd TMF-Workshop, Berlin, 27.-29.04.2016



Karl Michael Kraemer<sup>a,\*</sup>, Falk Mueller<sup>a</sup>, Matthias Oechsner<sup>a</sup>,  
Andrea Riva<sup>b</sup>, Dalila Dimaggio<sup>b</sup>, Erica Vacchieri<sup>b</sup>, Eleonora Poggio<sup>b</sup>

a: *High Temperature Materials, Chair and Institute for Materials Technology,  
Technische Universität Darmstadt, Germany*

b: *Ansaldo Sviluppo Energia, Via Lorenzi 8, Genoa, Italy*

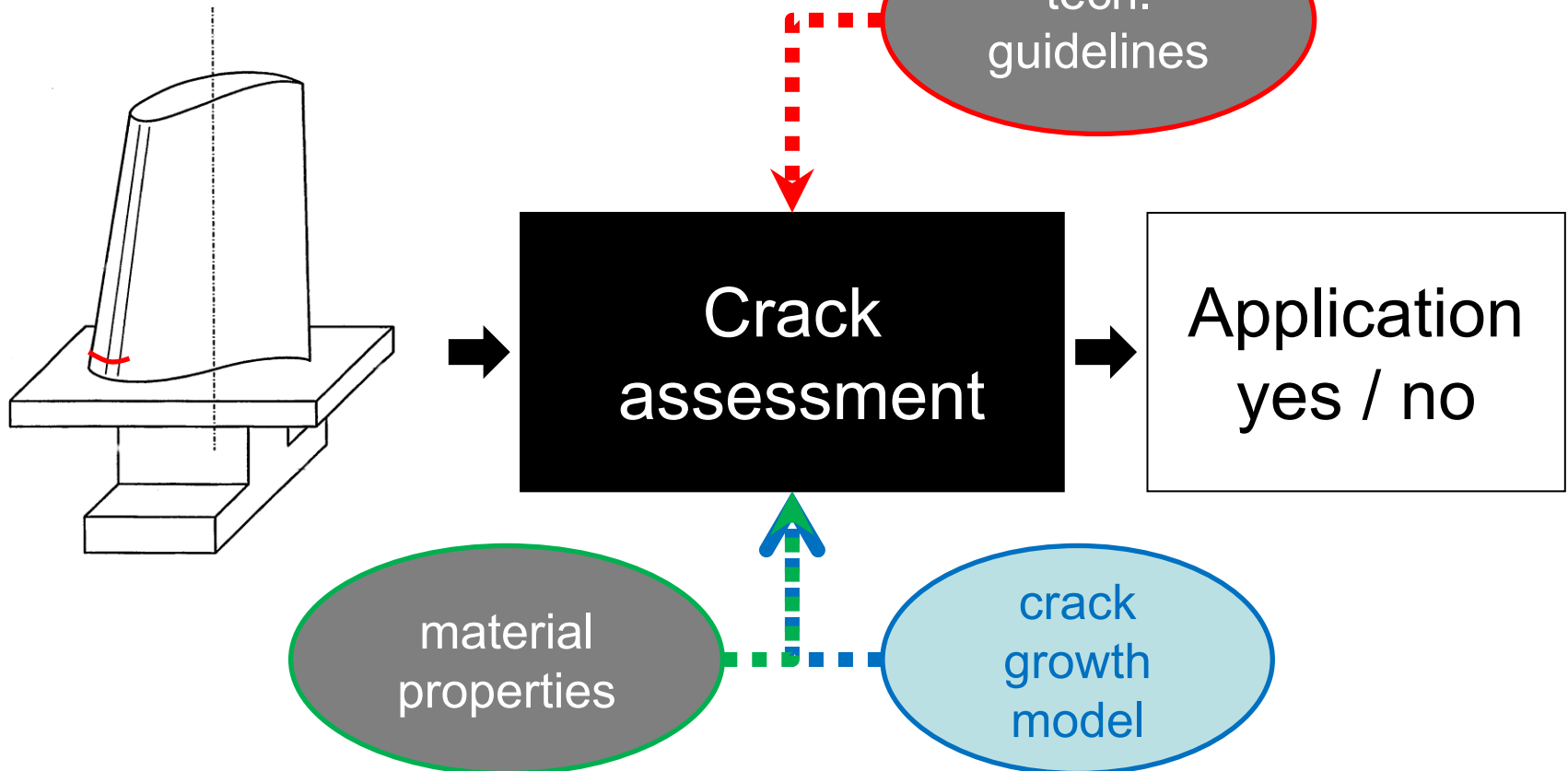
\*email: [kraemer@mpa-ifw.tu-darmstadt.de](mailto:kraemer@mpa-ifw.tu-darmstadt.de)

# Agenda

- I. Motivation, Workflow concept
- II. Concept of accumulated crack growth – the O.C.F. model
- III. Application of experimental results
- IV. Comparison to anisothermal validation experiments
- V. FEM case studies
- VI. Concluding remarks

# I. Motivation: Crack assessment of turbine blades

Foundry / operational defects  
found by NDE



## II. Concept of accumulated crack growth – *O.C.F. model*

- Linear-accumulation of crack growth increments originating from the most significant mechanisms: oxidation, creep crack growth and fatigue crack growth
- Assumptions made within the model:
  - No interactions between mechanisms
  - Time-dependent damage mechanisms are only in effect, if a certain critical temperature is exceeded within a temperature cycle
  - Threshold values are no longer valid above a certain temperature

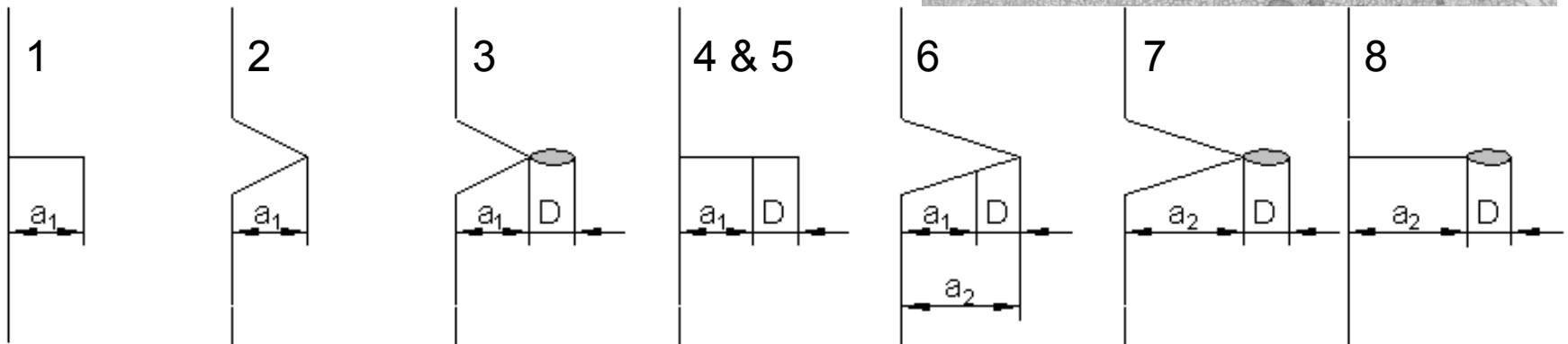
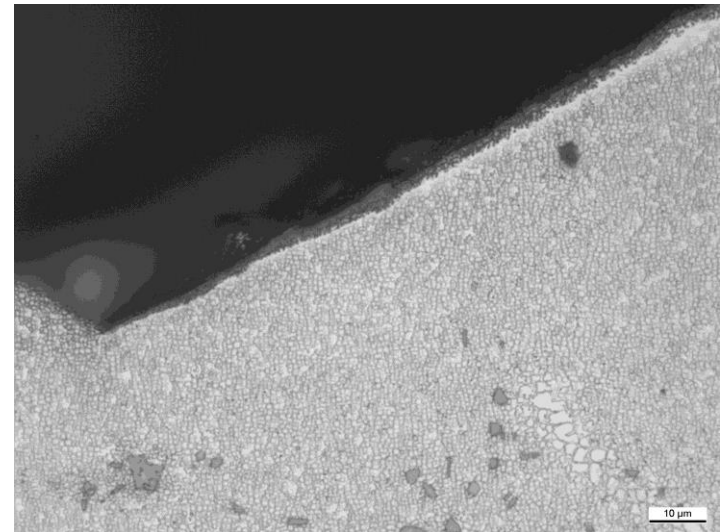
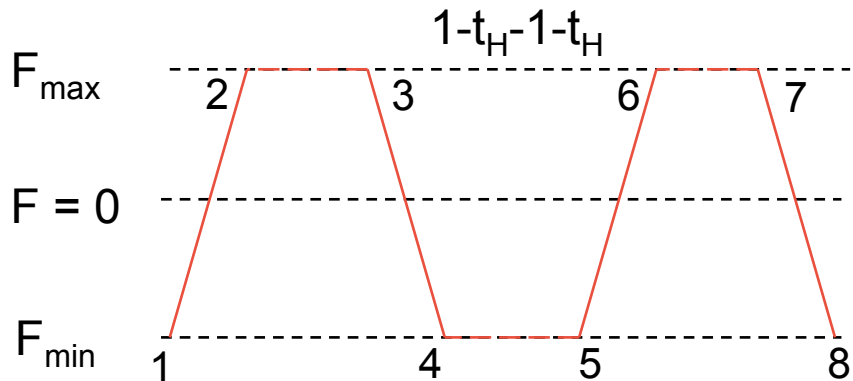
$$\frac{da}{dN}_{O.C.F.} = \sum_{t_i} \Delta a_{O,t_i} + \sum_{t_i} \Delta a_{C,t_i} + \left( \frac{da}{dN} \right)_F \quad ; \sum t_i = t_{cyc}$$

- Creep and oxidation fractions per cycle are calculated as a sum of isothermal growth during cycle increments using intermediate temperatures



# II. Concept of accumulated crack growth – *O.C.F. model*

Example load cycle  
with tension hold time



For M-247: Mueller F, Scholz A, Oechsner M; in Liège Conf. 2014

For C1023: Kraemer KM, Mueller F, Oechsner M; to be published in 2016

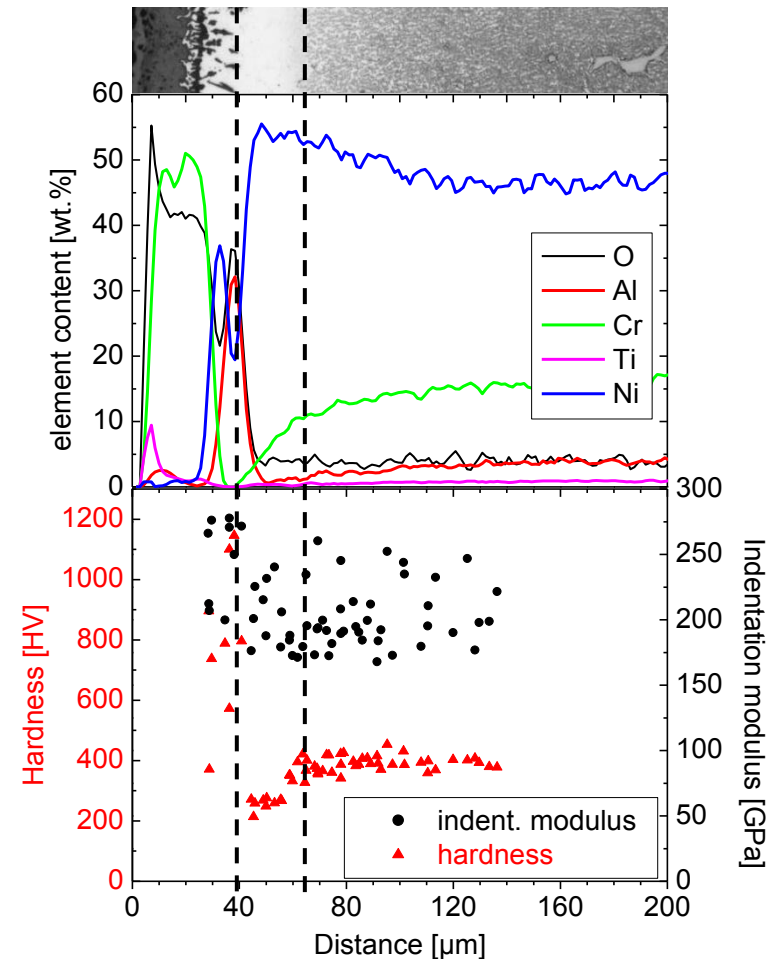
## II. Concept of accumulated crack growth – Q.C.F. model / OXIDATION

- Oxidation accelerates crack growth by depleting alloying elements from the base material
- $\gamma'$ -depletion zones are considered to have a lowered resistance to crack propagation compared to the original microstructure [1]
- Nano-indentation measurements on oxidation test samples of René 80 showed a significant reduction of hardness within the depleted region [2]

[1]: Sengupta A, Putatunda SK.; JMEP 1993

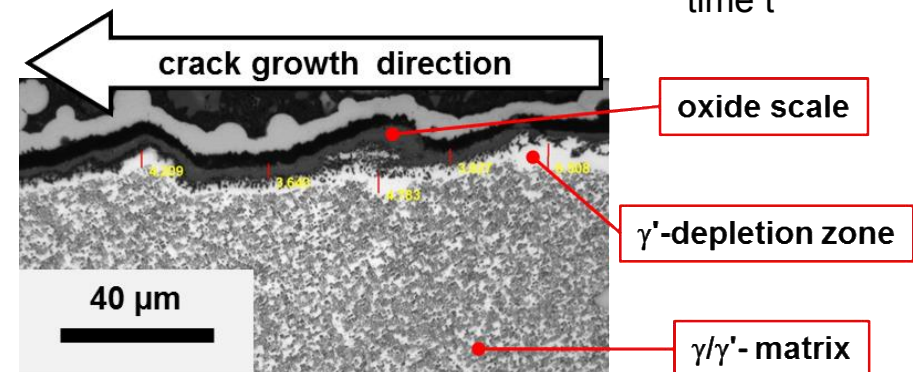
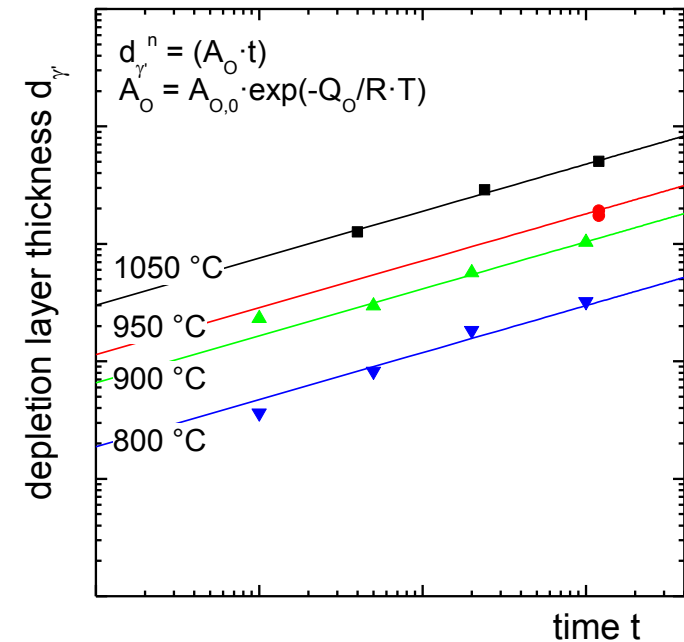
[2]: Kraemer KM et al.; 123himat 2015.

René 80 - 120 h at 1050 °C



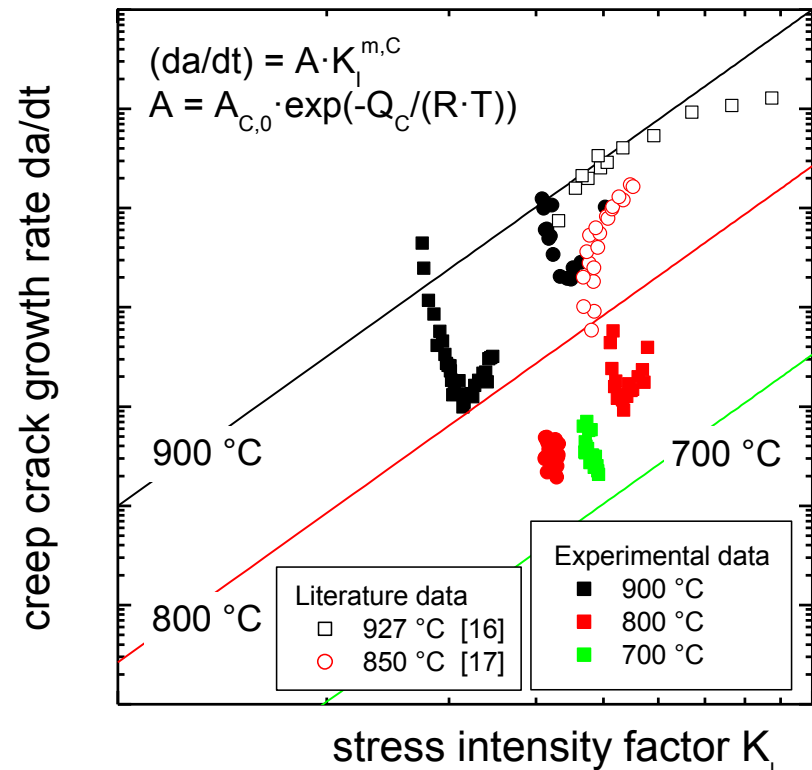
## II. Concept of accumulated crack growth – Q.C.F. model / OXIDATION

- Measurement from isothermal oxidation tests according to ISO 21608
- Modeling of  $\gamma'$ -depletion with sub-parabolic ( $n > 2$ ) approach
- Verification of  $\gamma'$ -depletion zone growth through comparison with metallographic preparation of crack paths from CCG-specimen



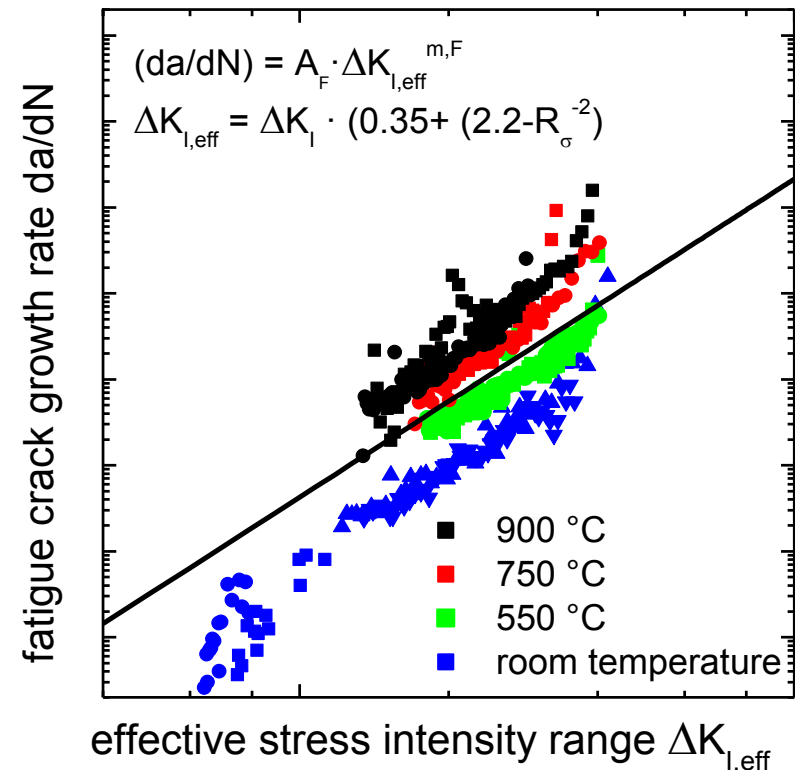
## II. Concept of accumulated crack growth – *O.C.F. model / CREEP*

- Crack propagation delivers  $\Delta a/\Delta t$  in dependence of temperature (here: Norton-like behaviour with Arrhenius dependence)
- Use of stress intensity factor → transferability onto components
- other parameters (e.g.  $C^*$ ) intended in future model editions
- No creep crack growth threshold is considered



## II. Concept of accumulated crack growth – *O.C.F. model / FATIGUE*

- FCG-experiments should be conducted with and without hold times at different temperature levels
- R-ratio and crack closure effects considered by using effective FM-parameters
- Broader scatter band in the low temperature regime should be tolerated because of the heterogeneous compartment of coarse-grain cast materials



## II. Concept of accumulated crack growth – O.C.F. model / MODEL INPUT

- $T_{\text{crit}}$  determines the applicability of O.C.F.  
 → FCG gives conservative description of crack growth if  $T_{\text{max}} < T_{\text{crit}}$
- $T_{\text{crit}}$  is in this case 750 °C since:
  - Oxidation tests at  $T < 750$  °C showed no signs of  $\gamma'$ -depletion
  - Creep crack growth at  $T < 750$  °C was very slow
- Total set of 8 material dependent parameters derived from standardized isothermal tests to fit the model:

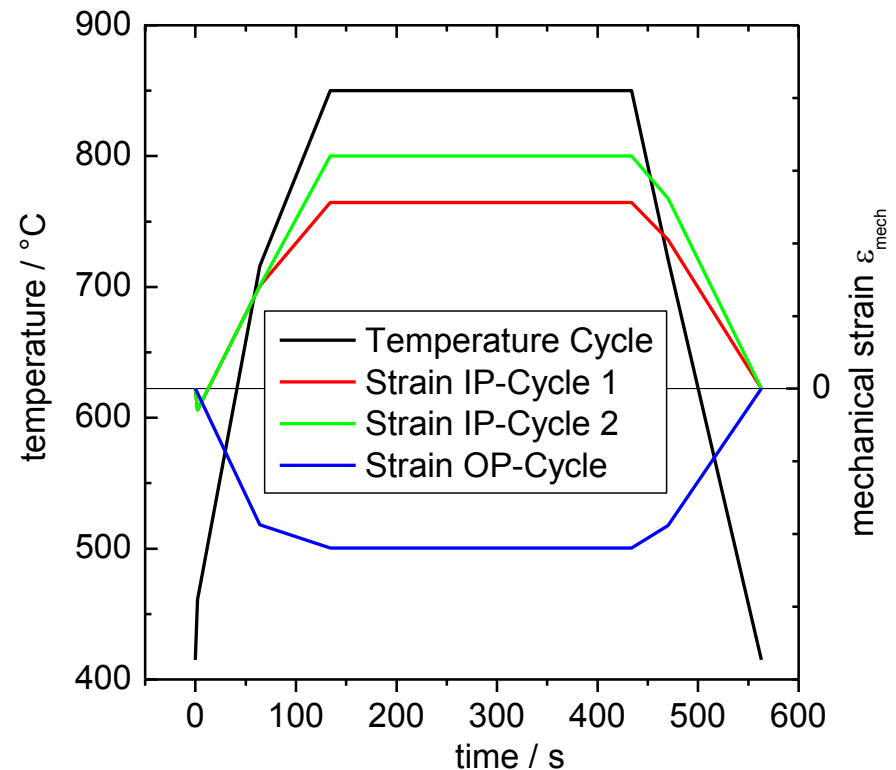
$$\Delta a_{O,t_i} = (A_{O,0} \cdot e^{-\frac{Q_O}{R \cdot T_i}} \cdot t_i)^{1/n} \quad \gamma'\text{-depletion}$$

$$+ \Delta a_{C,t_i} = \begin{cases} 0 & (\sigma_i < 0) \\ A_{C,0} \cdot e^{-\frac{Q_C}{R \cdot T_i}} \cdot K_I^{m_C} \cdot t_i & (\sigma_i > 0) \end{cases} \quad \text{creep crack growth}$$

$$\frac{da}{dN}_{O.C.F.} = \left( \frac{da}{dN} \right)_F = A_F \cdot \Delta K_{I,\text{eff}}^{m_F} \quad \text{fatigue crack growth}$$

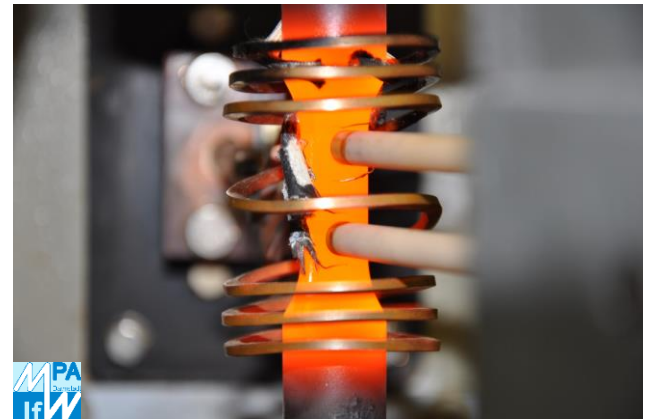
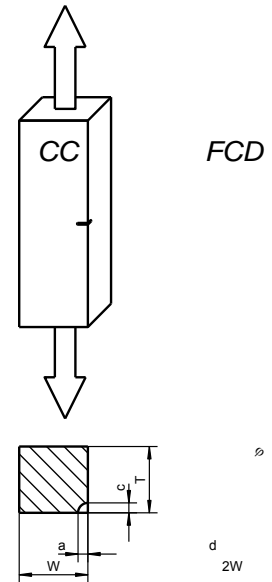
# IV. Comparison to anisothermal validation experiments – Test conditions

- Model validation through TMFCG testing
- 3 different strain cycles imposed on one temperature cycle (Ansaldo TMF benchmark test cycle with reduced hold time)
- Strains and temperatures similar to a turbine warm start
- Temperature gradients  $\sim 3 - 4$  K/s



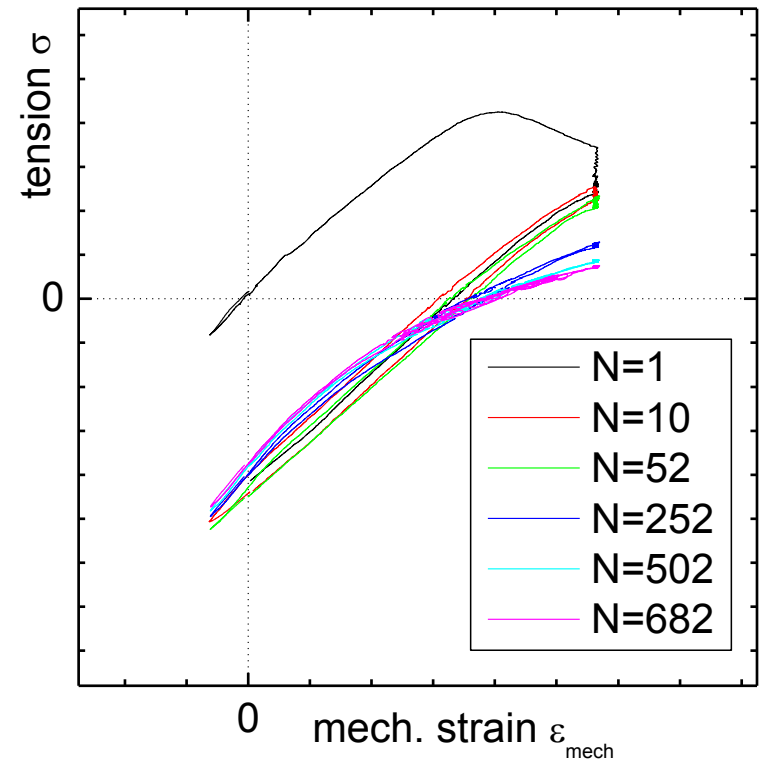
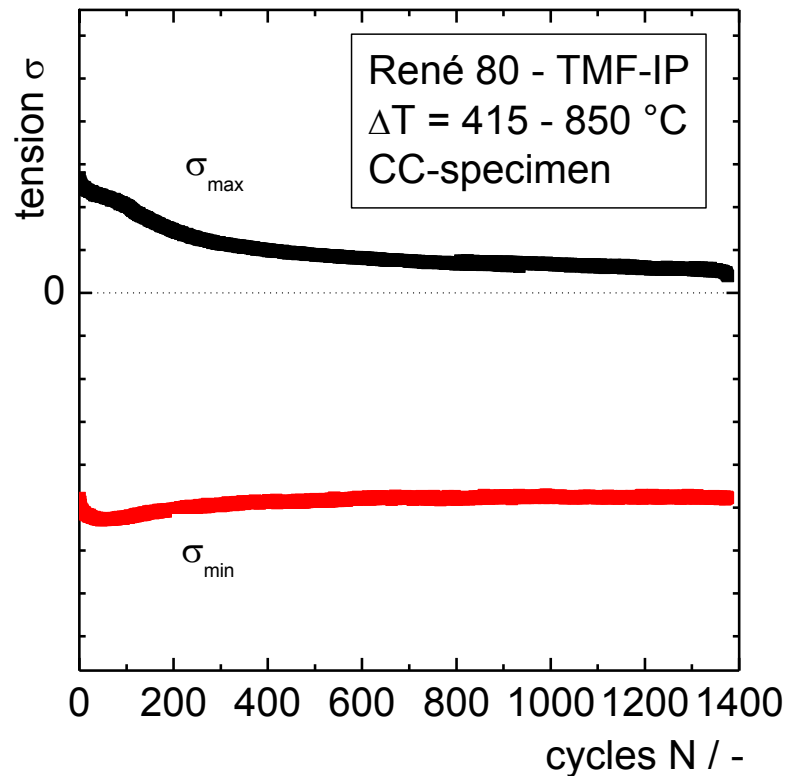
# TMF-test bench at the IfW Darmstadt

- Validation tests on corner crack specimen
- Specimen heating through induction
- Clamping parts water cooled
- Specimen cooling via pressured air
- Maximum validated temperature: 1050 °C
- Maximum temperature gradients: 10 K/s
- Crack growth monitoring via ACPD measurement
- Test conditions comply to ISO 12111
- Crack growth measurement from EN 3873

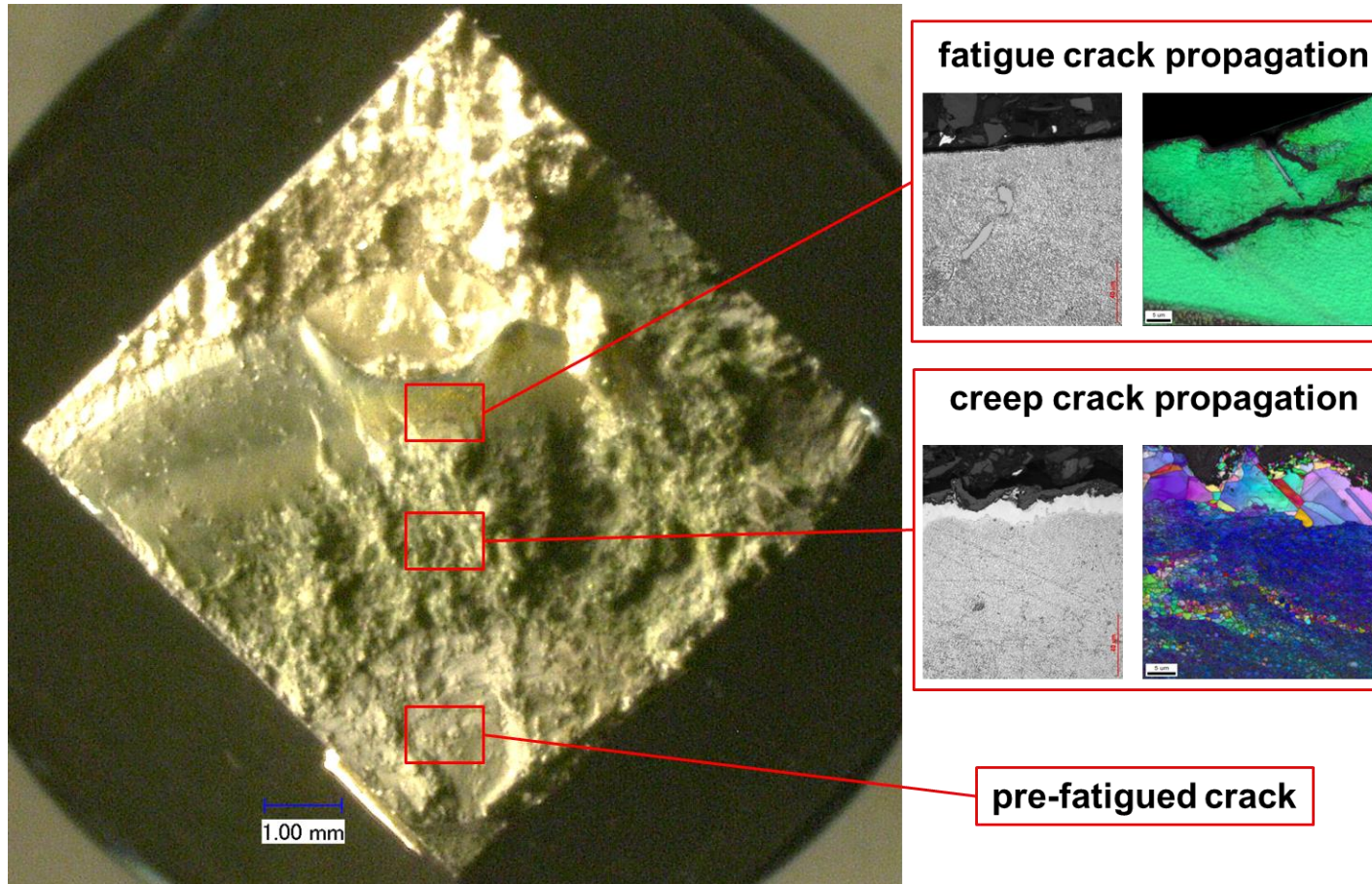




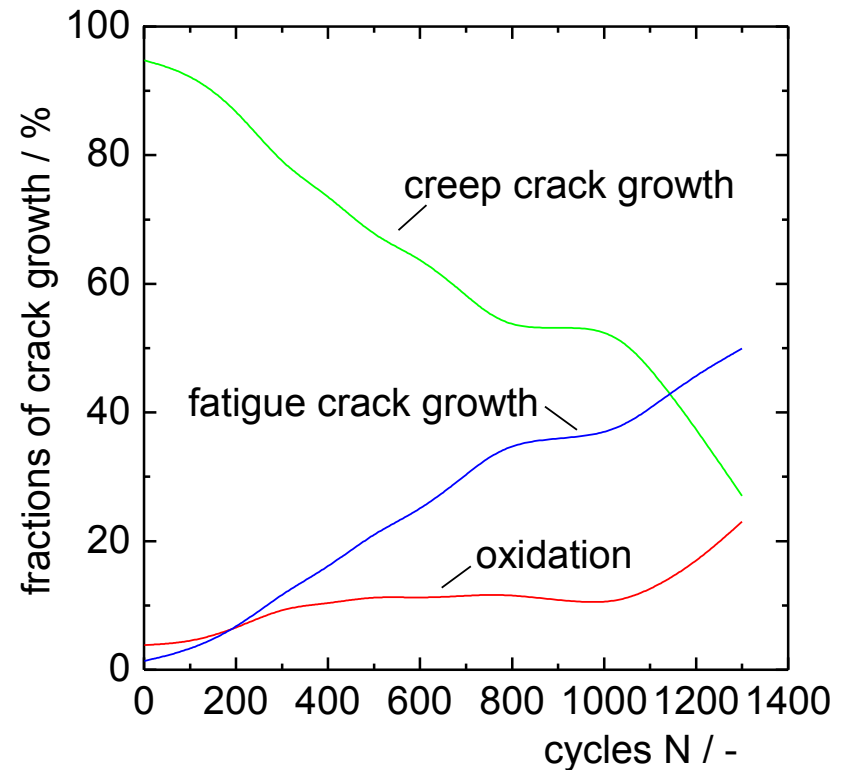
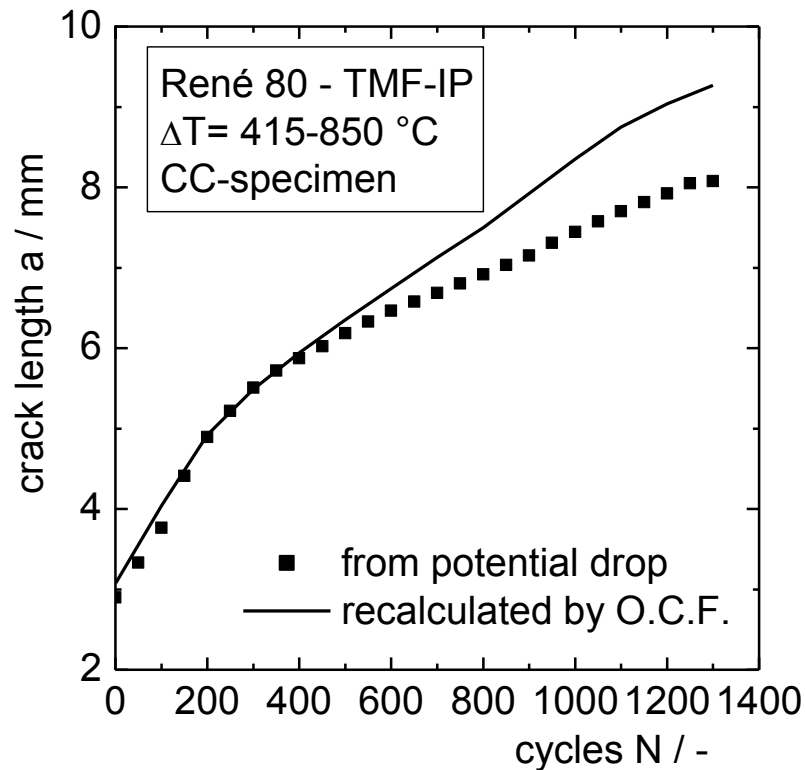
# IV. Comparison to anisothermal validation experiments



# IV. Comparison to anisothermal validation experiments

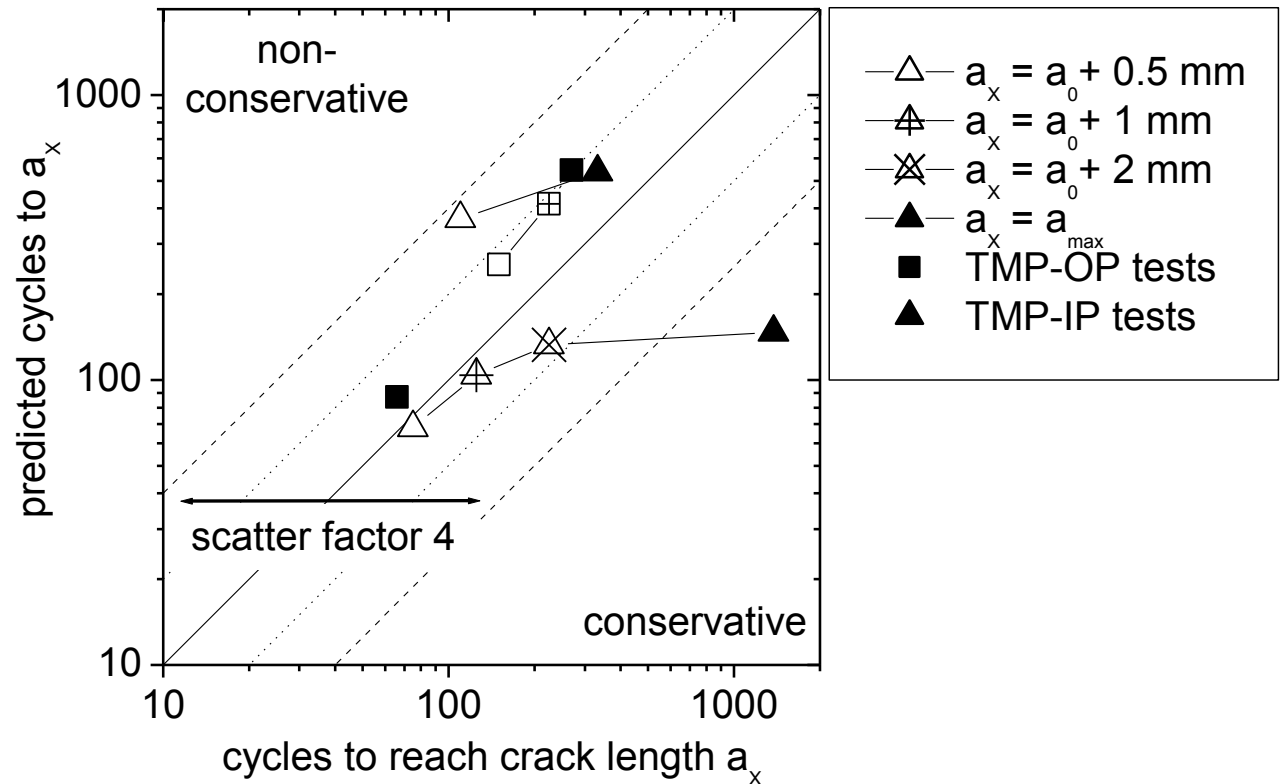


# IV. Comparison to anisothermal validation experiments

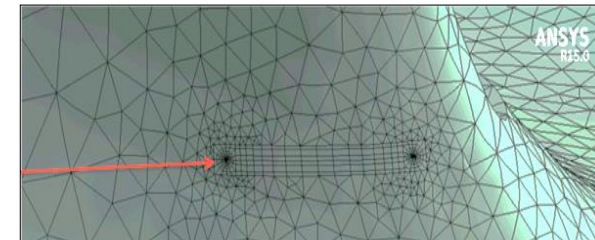
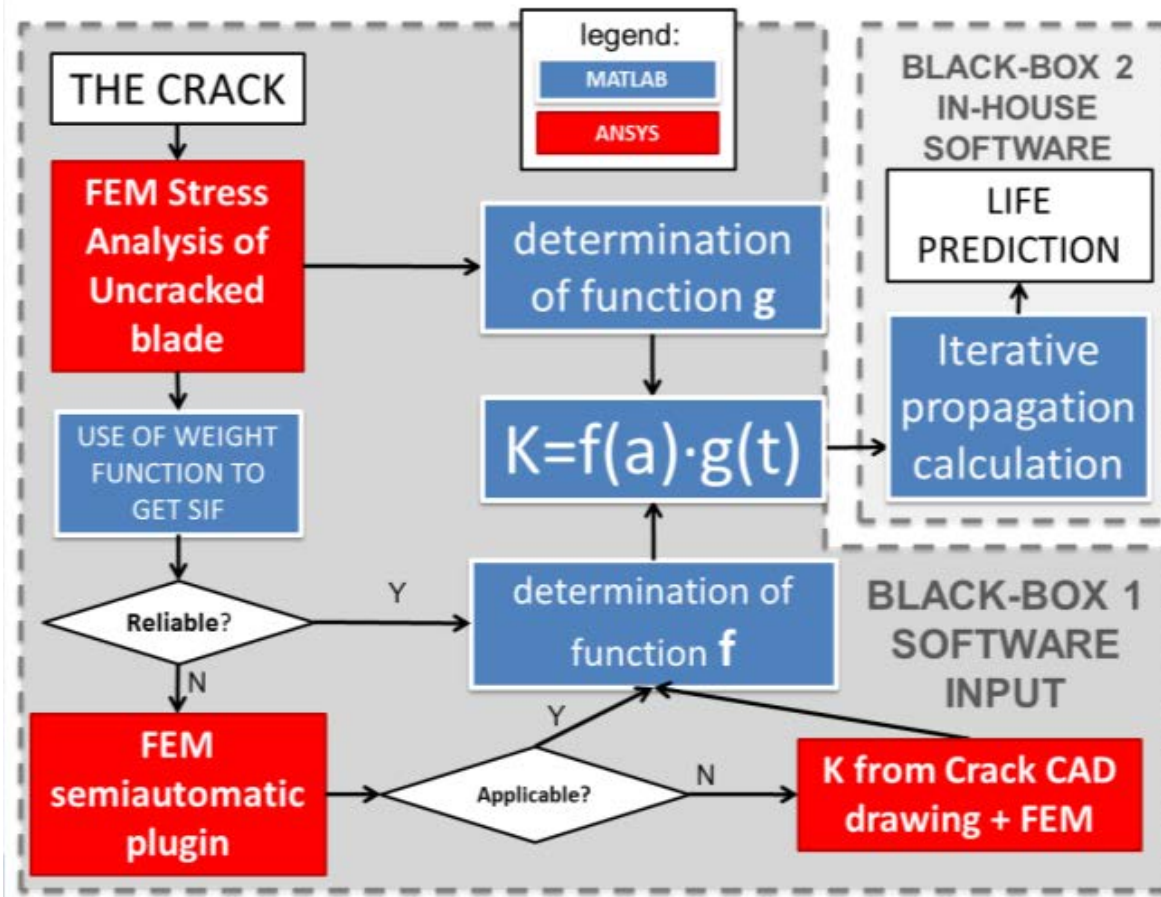


# IV. Comparison to anisothermal validation experiments

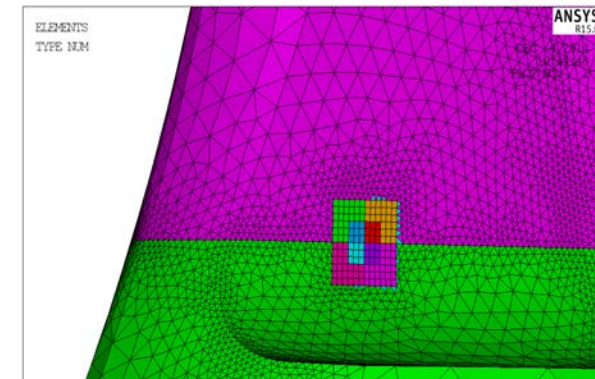
- Model Input :
  - Idealized F,T(t)-cycle using extreme values from experiment
  - Initial crack length
- Scattering of results within the range of natural material scattering



# V. FEM case studies



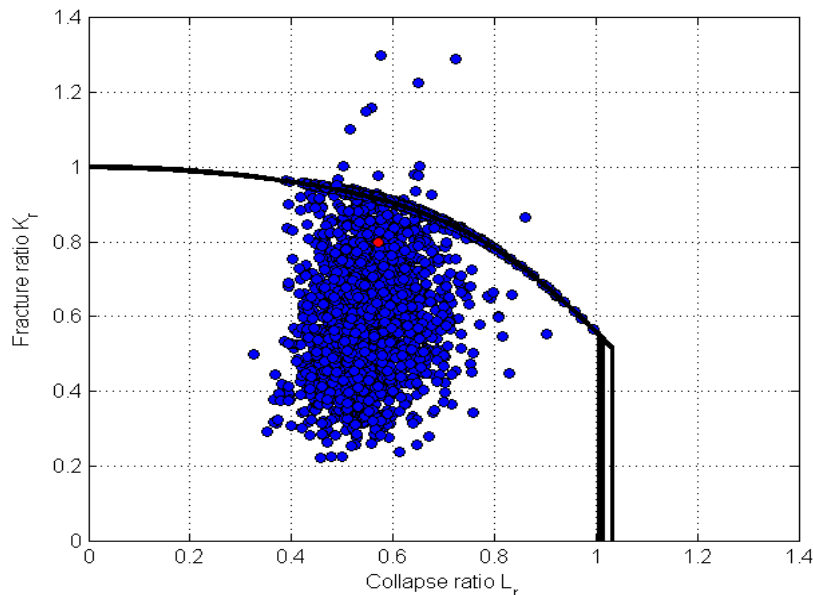
crack modeled via  
ANSYS Plug-In



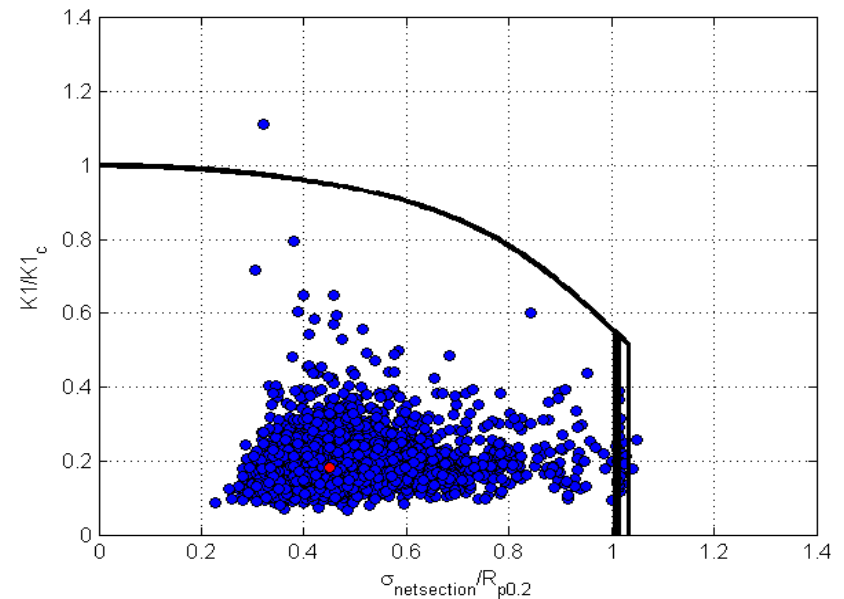
crack modeled  
via released connections

# V. FEM case studies

- Monte Carlo analysis of crack growth with statistical variation of material properties, crack propagation laws and initial defect size  
→ estimation of safety margins / definition of assessment criteria



Case A: fragile component –  
crack propagation through creep



Case B: thin wall –  
crack propagation through oxidation

## VI. Concluding remarks

- The “O.C.F.”- crack propagation model has been fitted on the basis of experimental results.
- Calculation is aimed to provide propagation predictions for a wide number of scenarios. Accuracy depends on the approach adopted (Exact or estimated load cycle data; calculation of stress intensities via FEA or analytic form functions)
- Validated of crack growth model through execution of TMFCG testing.
- Failure analysis software based on the propagation model and crack assessment regulations (e.g. BS 7910/SINTAP) allows the execution of a Monte Carlo analysis, which can serve several purposes:
  - Quantitative estimation of failure probability of a propagating crack.
  - Calibration of safety coefficients
  - Sensitivity analysis to identify the critical input parameters



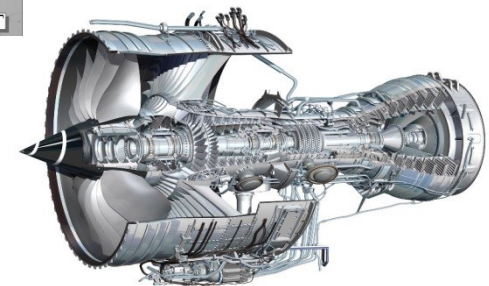
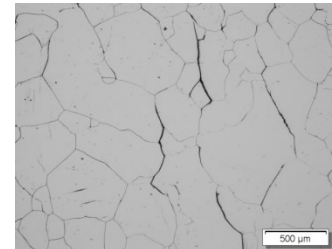
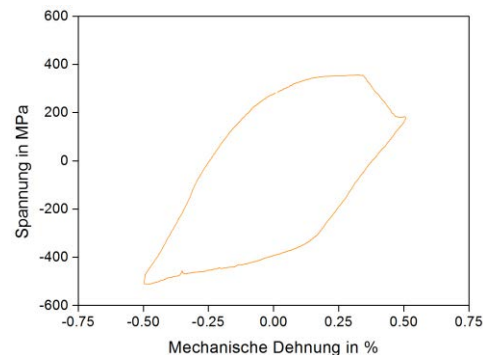
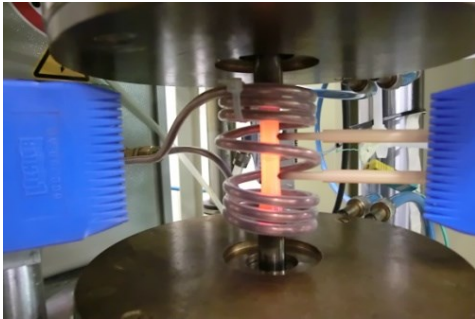
Thank you very much  
for your attention !



# An approach to lifetime prediction for a wrought Ni-base alloy under thermo-mechanical fatigue with various phase angles between temperature and mechanical strain

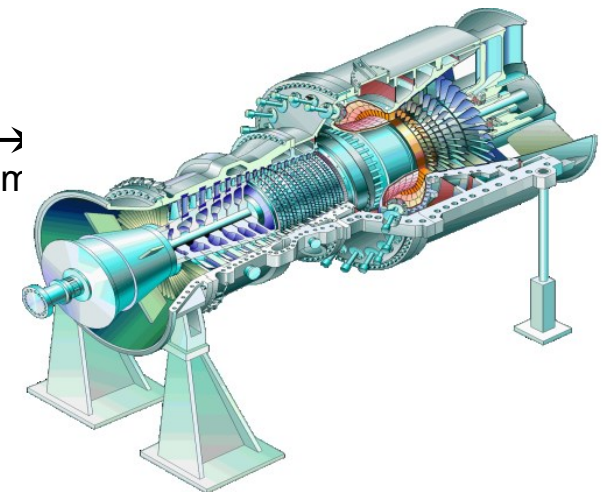
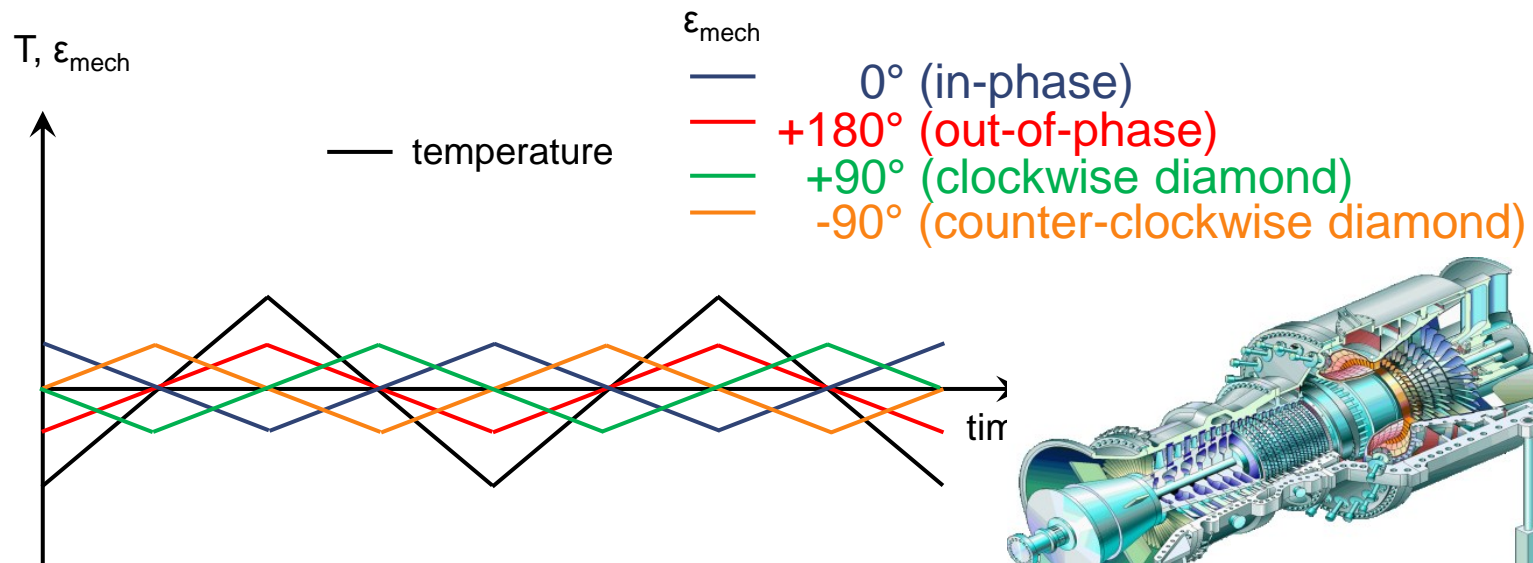
Karl-Heinz Lang, Stefan Guth  
Karlsruhe Institute of Technology (KIT), Institute for Applied Materials (IAM)

Institute for Applied Materials - Materials Science and Engineering (IAM-WK)



Within a component the phase relation between temperature and mechanical strain depends on the cooling situation, the heat transfer, the component geometry, ...

→ various phase angles may occur



$180^\circ, 0^\circ$ , cooled turbine blade

$+90^\circ, -90^\circ$ : uncooled turbine blade

Ziebs et al., ASTM STP 1371, 2000

depending on the phase angle, maximum temperature, loading and time at  $T_{\max}$ , ...  
different damage mechanisms may be dominant:

- fatigue damage
- creep damage
- corrosion damage

Boismier & Sehitoglu, J. Eng. Mater. Technol. , 1990

### **goals of the investigation:**

- improving the understanding of the damage mechanisms which appear at different phase angles and dwell times.
- development of a mechanisms based model to predict damage and lifetime

- material and experimental details
- results
  - lifetime behaviour
  - deformation behaviour
  - investigation of the damage development
  - influence of dwell times
- lifetime model
- summary

## NiCr22Co12Mo9:

- solid solution and carbide solidified nickel-base wrought alloy
- trade names **Inconel Alloy 617** and Nicrofer 5520 Co

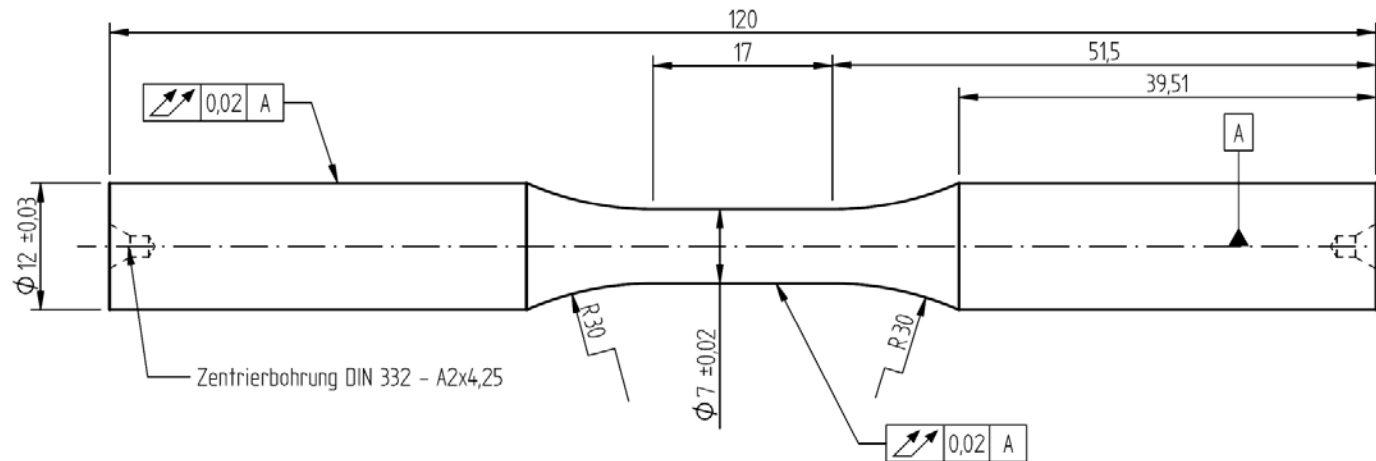
chemical composition:

element	Ni	Cr	Co	Mo	Al	Fe	Ti	Si	C
ma.-%	balance	22.25	11.45	8.88	1.28	0.56	0.40	0.11	0.06

- used for combustion chambers, piping, heat exchangers
- in a modified version candidate material for components of very high temperature reactors (VHTR) and super-critical coal-fired power plants

total strain controlled TMF experiments using a modified servoelectric testing system

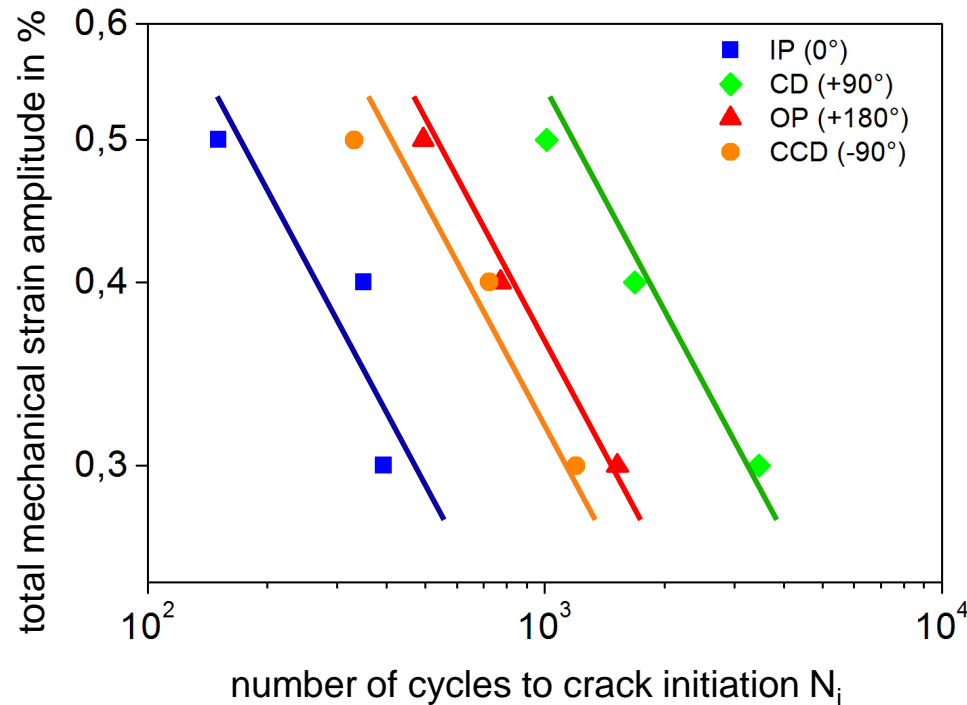
shape an geometry of the specimen:



- temperature range: 100 – 850 °C
- temperature rate: 5 K/s → 5 min per cycle for experiments without dwell time
- optional dwell times of 2, 5 and 30 min at  $T_{\max} = 850$  °C
- $R_{\epsilon} = -1$

- 4 phase angles between temperature and mechanical strain:
  - 0° (in phase, IP)
  - 180° (out of phase, OP)
  - 90° (clockwise diamond, CD)
  - -90° (counter-clockwise diamond, CCD)
  
- lifetime  $N_i$ : macroscopic crack initiation  $\rightarrow$  10 % drop of the stabilised  $\sigma_{\max}$
  
- after the failure:
  - metallographic investigation of micrographs taken longitudinal from gage length

## lifetime behaviour

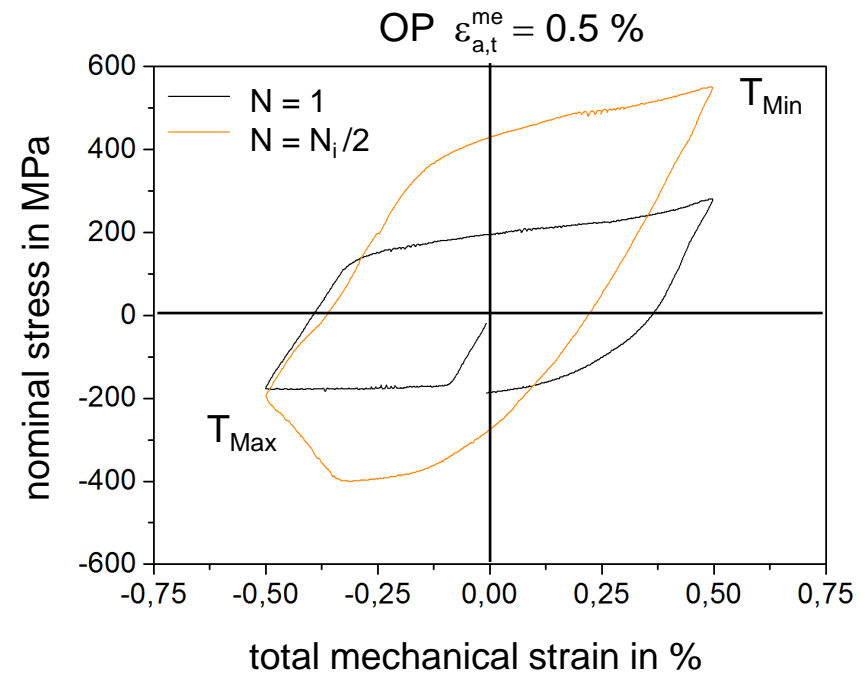
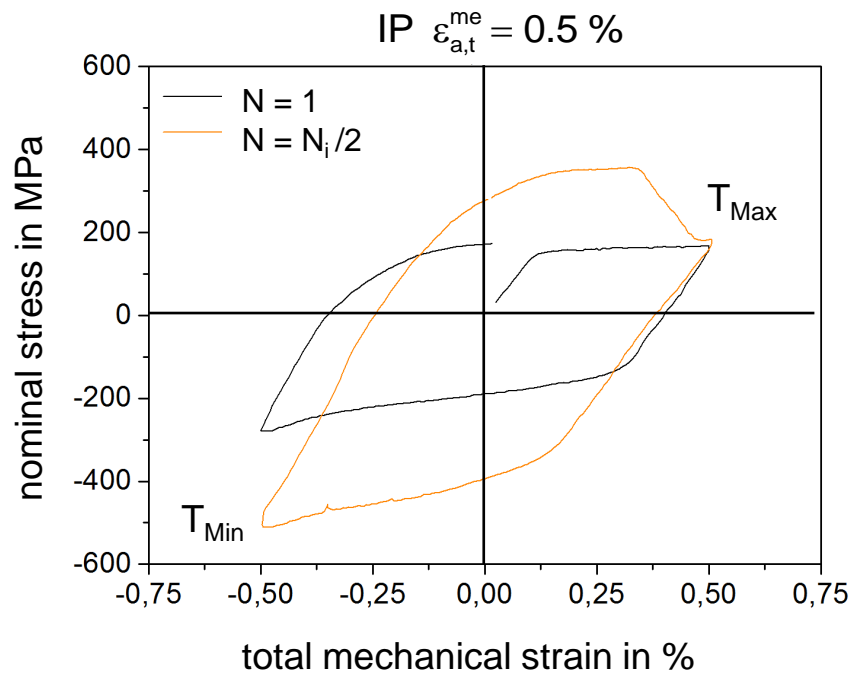


- significant influence of the phase angle on the lifetime
- sequence: IP < CCD < OP < CD
- similar slopes of the lifetime lines



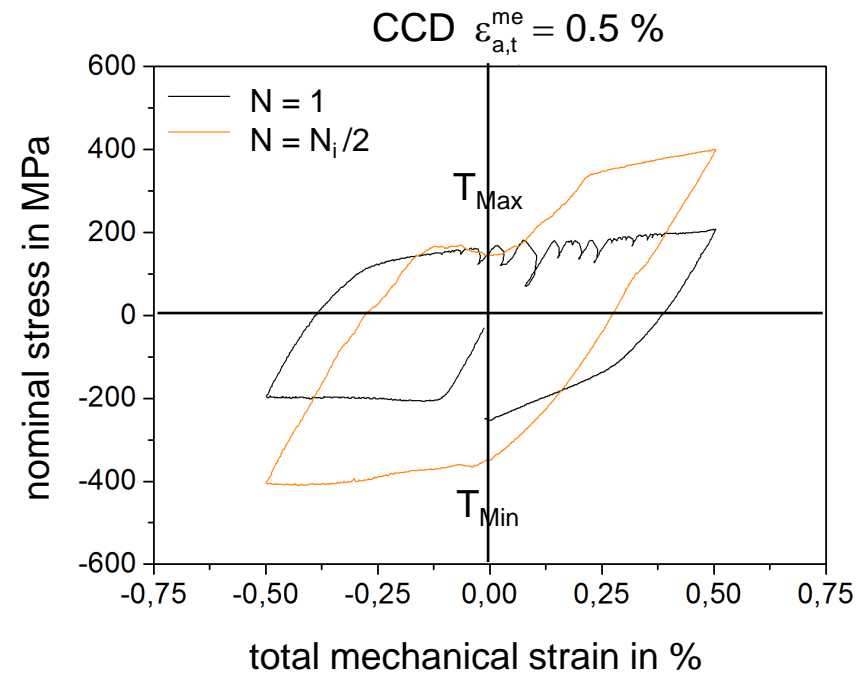
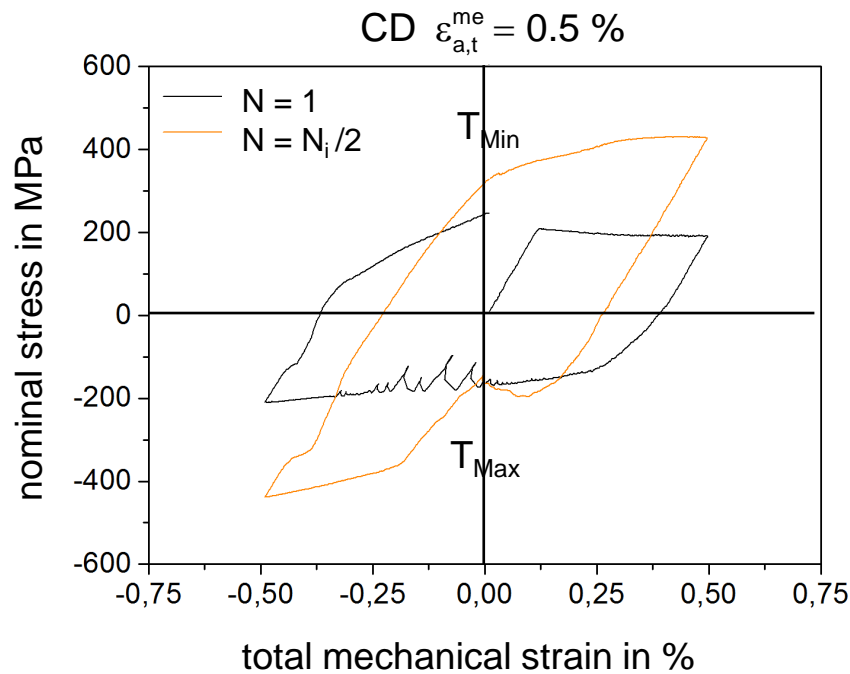
# experiments without dwell time

hysteresis loops for IP and OP-loading



- considerable plastic deformation, distinct cyclic hardening
- negative mean stresses at IP, positive mean stresses at OP
- only weak stress drops due to dynamic strain aging

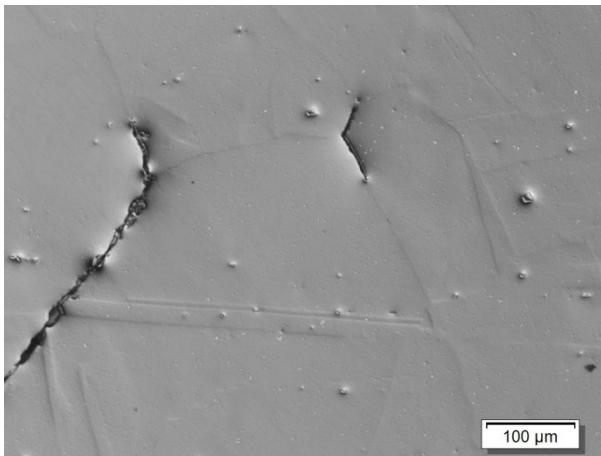
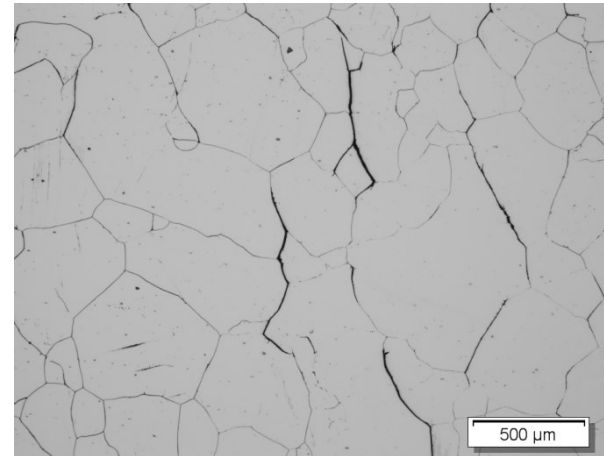
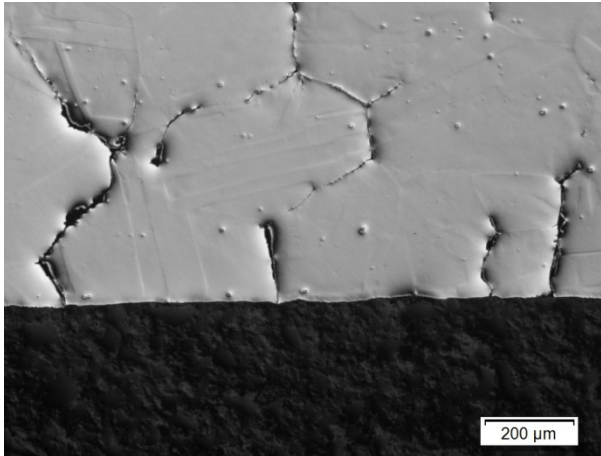
hysteresis loops for CD- and CCD-loading:



- cyclic hardening comparable to IP-/OP-loading
- no mean stresses
- stress drops due to dynamic strain aging more pronounced at the beginning of the tests, declining with increasing number of cycles

## experiments without dwell time

light microscopy after experiments with IP loading:



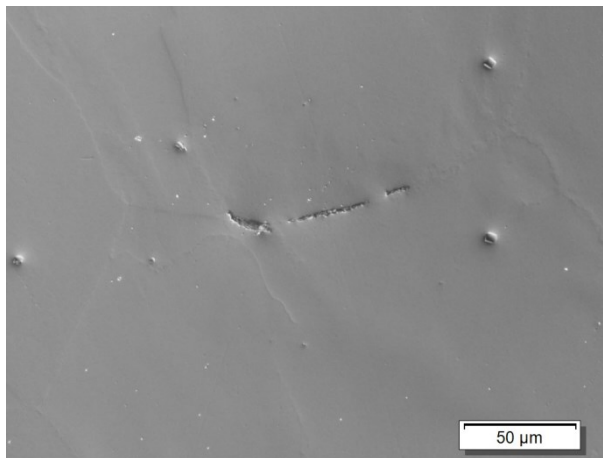
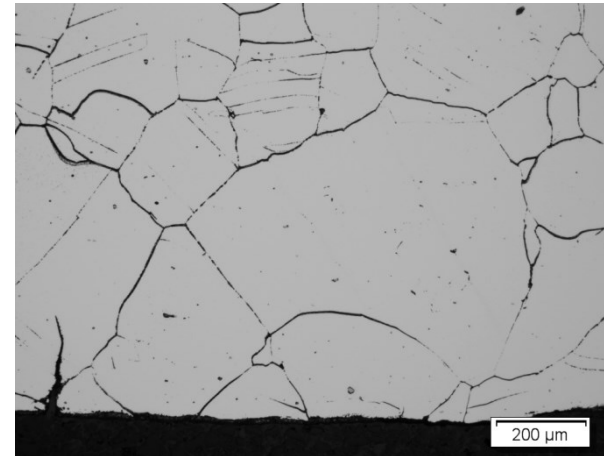
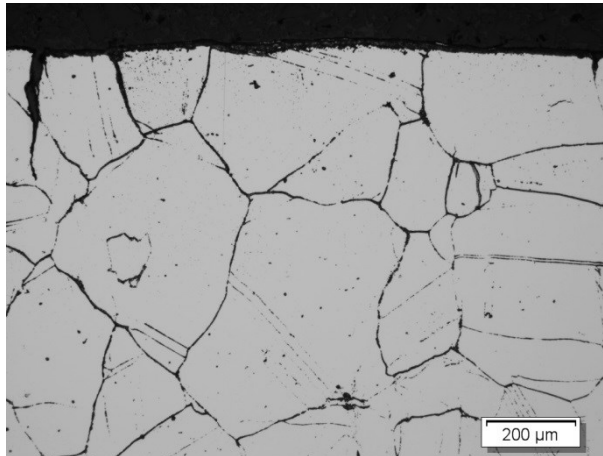
loading direction



- predominant intergranular crack initiation and propagation
- cracks at the surface and in the interior
- wedge-type cracks at triple points
- → creep damage

## experiments without dwell time

light microscopy after experiments with OP loading:



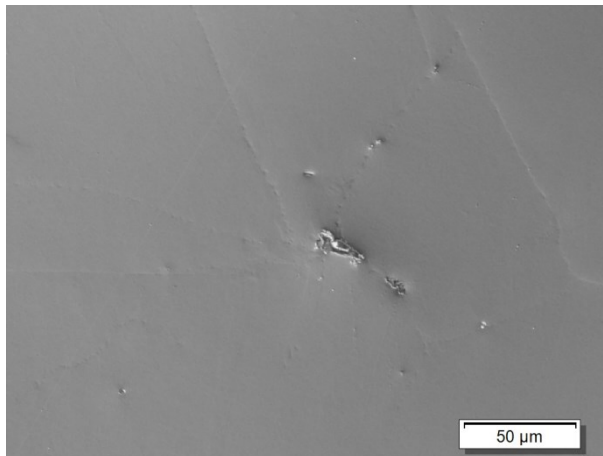
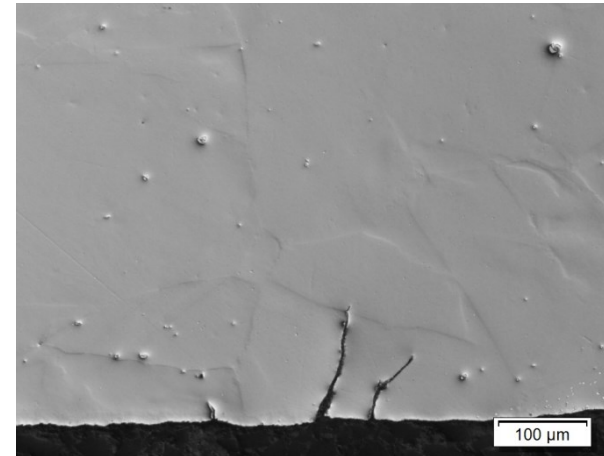
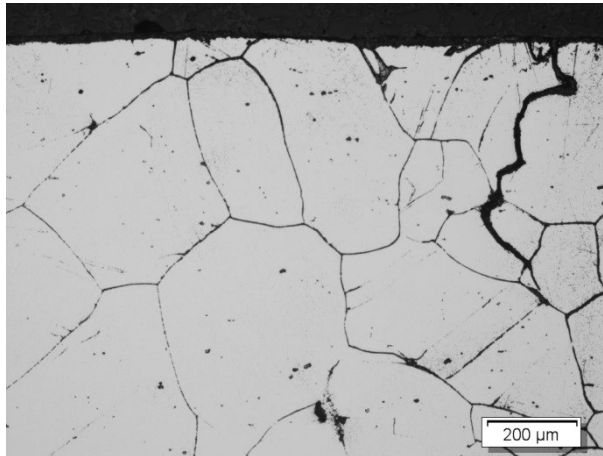
loading direction



- predominant transgranular crack initiation and propagation
- partly intergranular damage parallel to loading direction
- → fatigue and creep damage

## experiments without dwell time

light microscopy after experiments with CD loading:



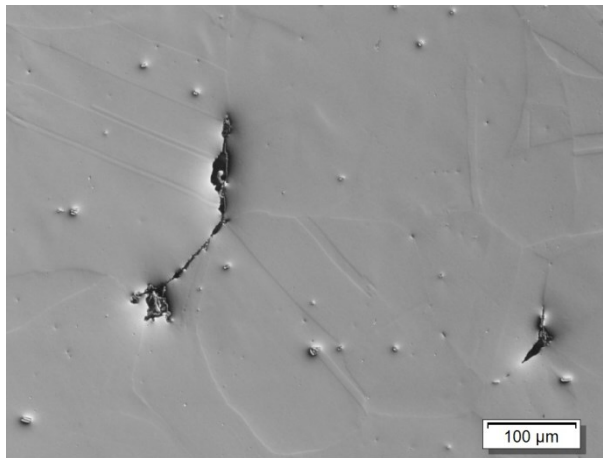
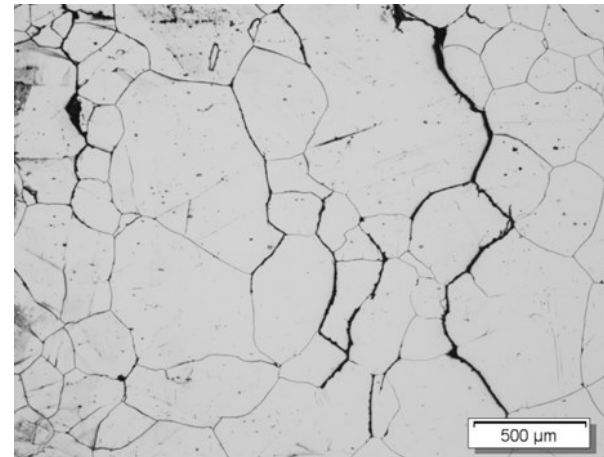
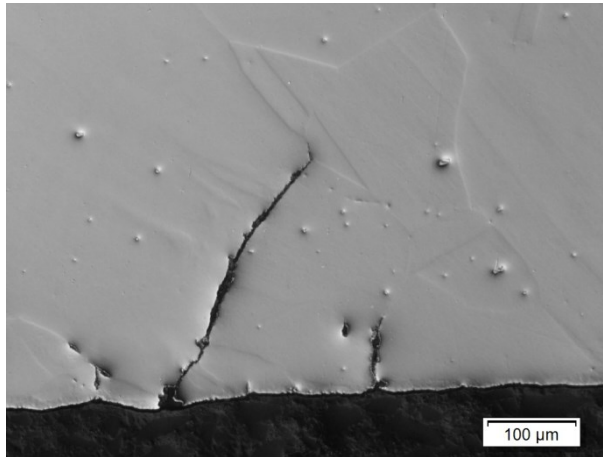
loading direction



- predominant transgranular crack initiation and propagation
- partly wedge-type cracks parallel to loading direction at triple points
- → fatigue and creep damage

## experiments without dwell time

light microscopy after experiments with CCD loading:

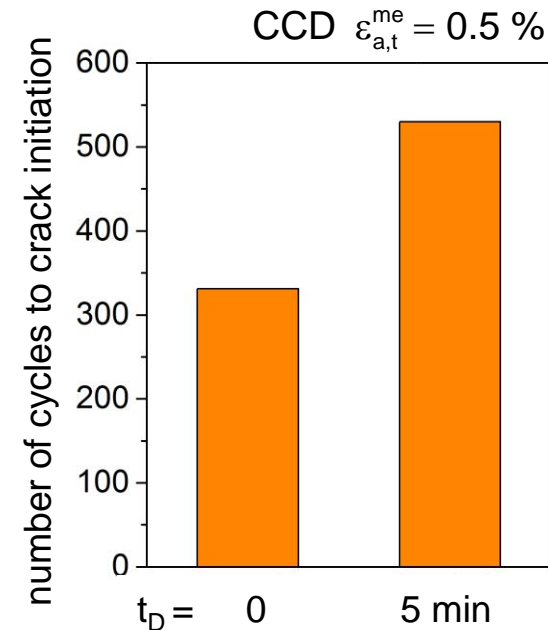
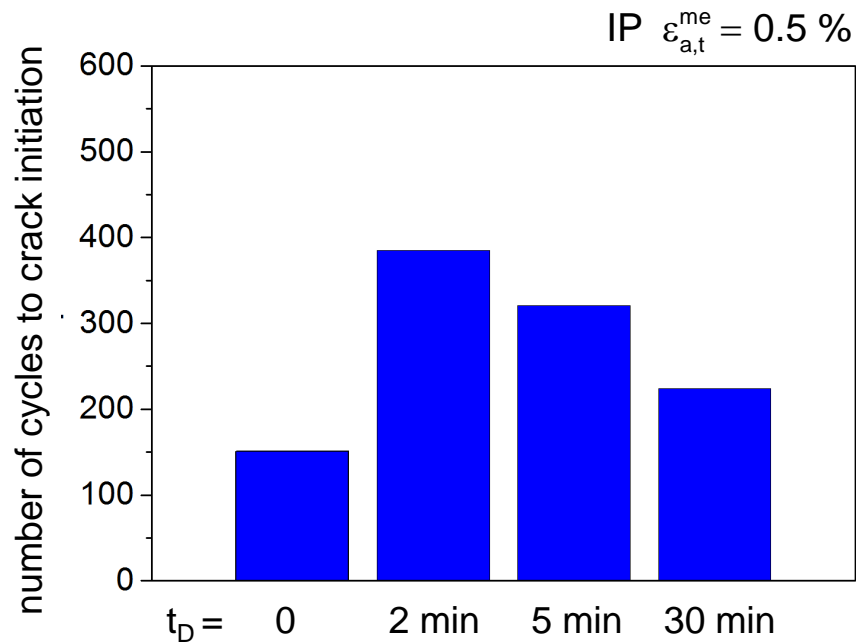


loading direction



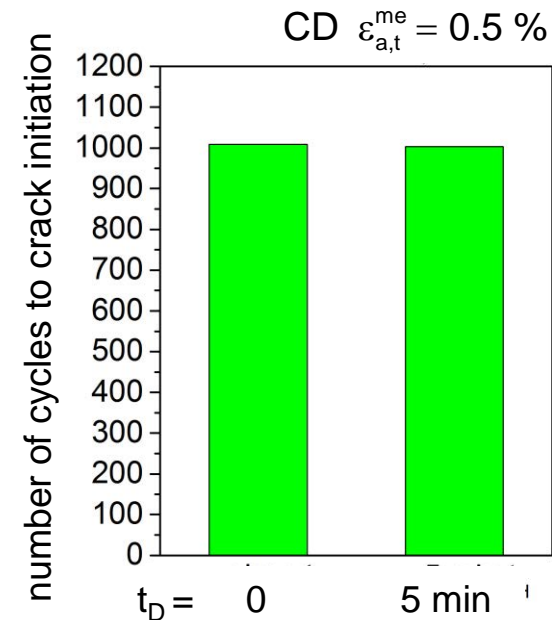
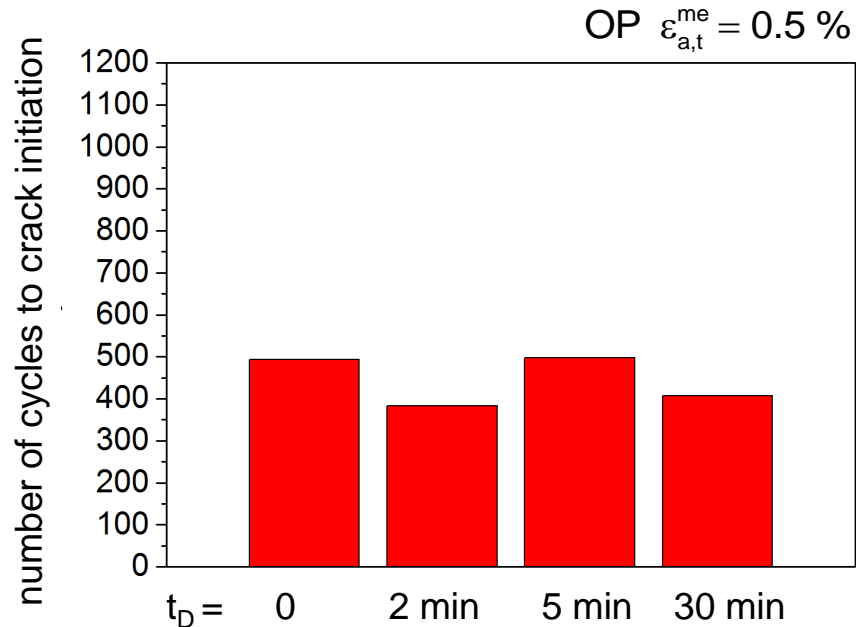
- predominant intergranular crack initiation and propagation
- crack at the surface and the interior
- wedge-type cracks at grain boundaries vertical to loading direction
- → creep damage

lifetime behaviour in experiments with IP and CCD loading:



- lifetime increases by inserting a dwell time
- at IP loading the lifetime decreases with increasing dwell time

lifetime behaviour at OP and CD loading:



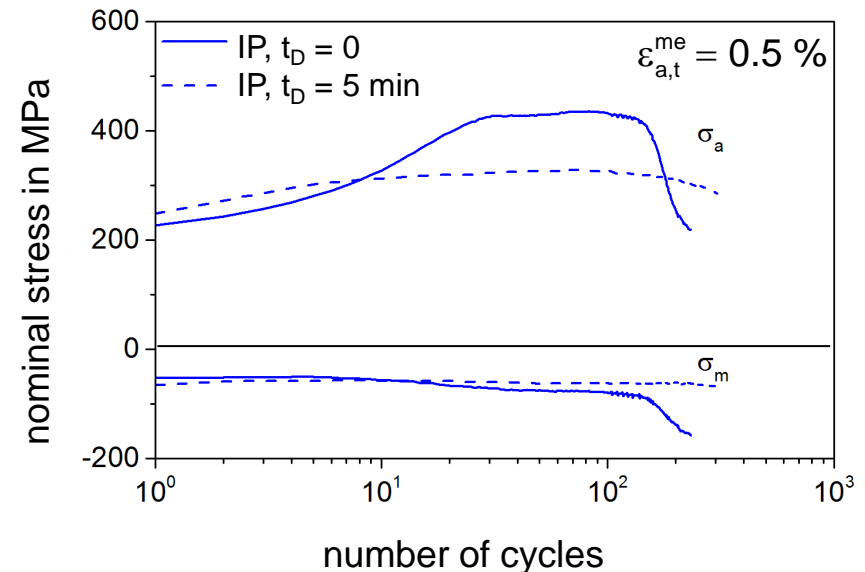
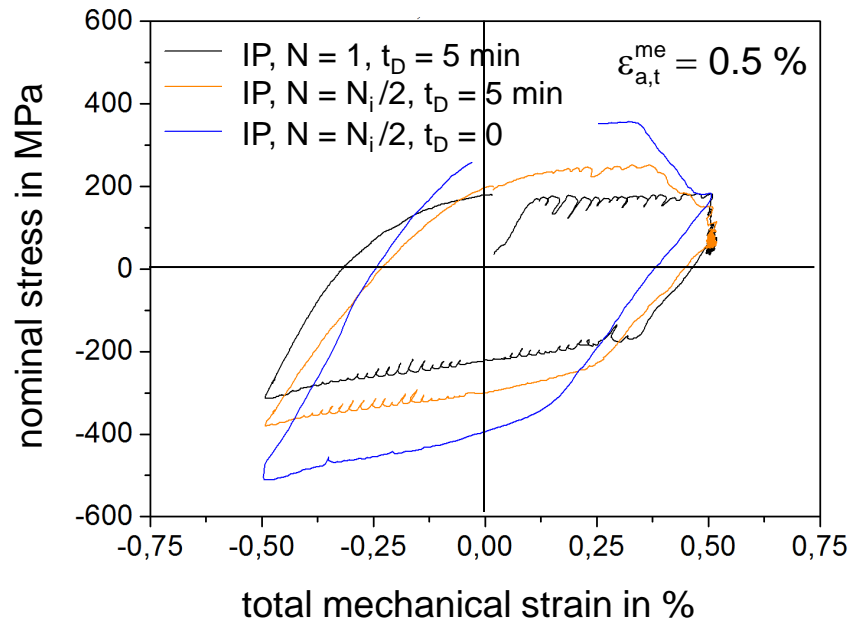
- minor influence of a dwell time on the lifetime, only weak tendency to lifetime reduction with increasing dwell time
- at CD loading no clear dependency between duration of dwell and lifetime



# experiments with dwell time

cyclic deformation behaviour:

→ influence of dwell time for all phase angles comparable



- minor cyclic hardening compared to experiments without dwell time  
→  $\sigma_a \downarrow$ ,  $\epsilon_{a,p} \uparrow$
- more pronounced stress drops due to dynamic strain aging compared to experiments without dwell time, stress drops appear longer



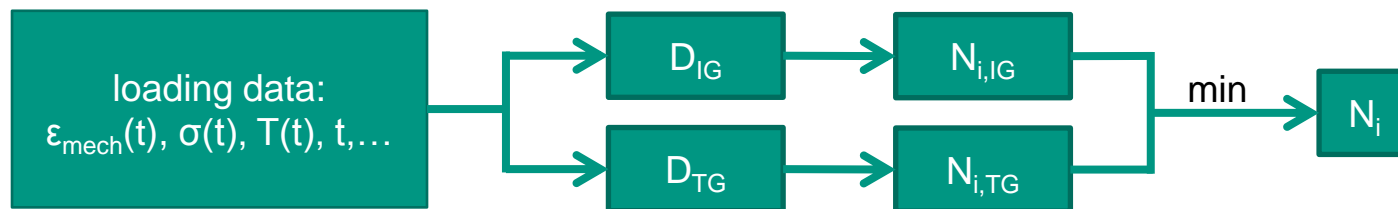
development of a simple empirical model to describe the lifetime behaviour:

- two dominant types of damage depending on temperature and acting tensile stresses:
  - intergranular (IG) damage at IP and CCD loading
  - transgranular (TG) damage at OP und CD loading
- negligible interaction

→ two damage parameter to describe the lifetime:  $D_{IG} = C_{IG} \cdot N_i^{-\alpha_{IG}}$

$$D_{TG} = C_{TG} \cdot N_i^{-\alpha_{TG}}$$

lifetime prediction:



## description of lifetime behaviour

influence values which have to be considered:

- $D_{IG}$ : grain boundary gliding, creep:

$$D_{IG} = \varepsilon_{a,p} \int_{t_1}^{t_2} |\sigma|^n \operatorname{sgn}(\sigma) \frac{\exp\left(-\frac{Q_{cr}}{RT}\right)}{T} dt \quad , \text{ for negative values: } D_{IG} = 0$$

with:  $t_2 - t_1 =$  cycle time;  $n =$  Norton-exponent;  $Q_{cr} =$  activation energy of the acting creep process at high temperatures within the temperature cycle

- $D_{TG}$ : fatigue, maximum tensile stresses, plastic deformation and thickness of the oxide layer:

$$D_{TG} = \varepsilon_{a,p} \sigma_{max} \left( \int_{t_1}^{t_2} \exp\left(-\frac{Q_{ox}}{RT}\right) dt \right)^k$$

with:  $Q_{ox} =$  activation energy for the growth of oxide layer

$D_{TG}$  compares to the frequency modified Ostergren parameter

Ostergren, JTEVA, 1976

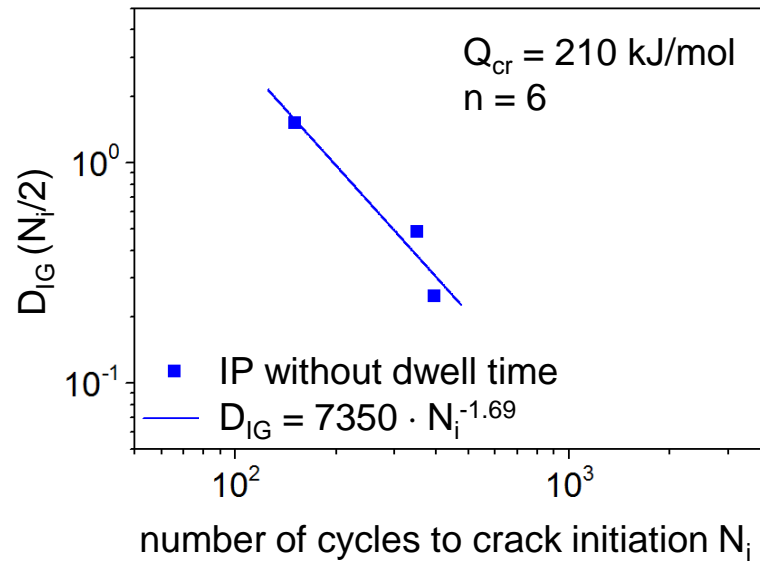
# description of lifetime behaviour

- $n = 6$
- $Q_{cr} = 210$  kJ/mol
- $k = 0.125$
- $Q_{Ox} = 206$  kJ/mol

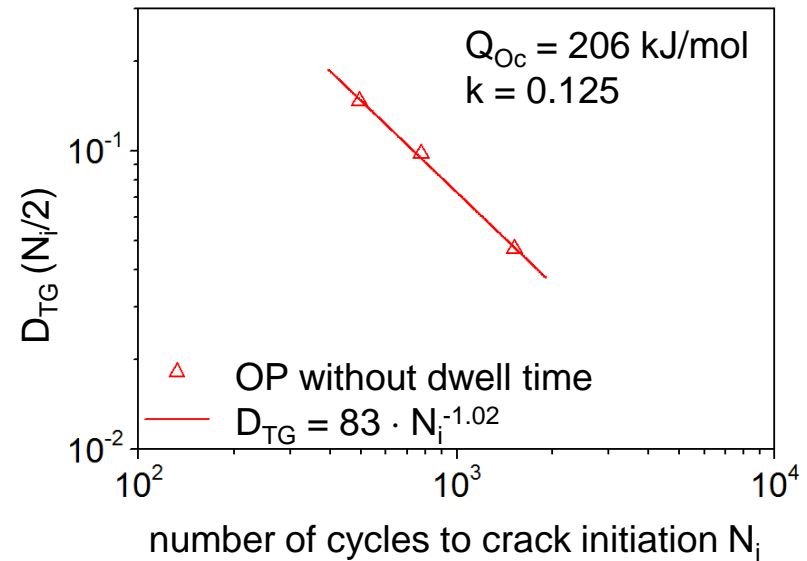
Merckling 1990, Diss. Uni Karlsruhe

Antolovich, Metal Trans A, 1981  
Al-Hattab, Appl Surf Sci, 2014

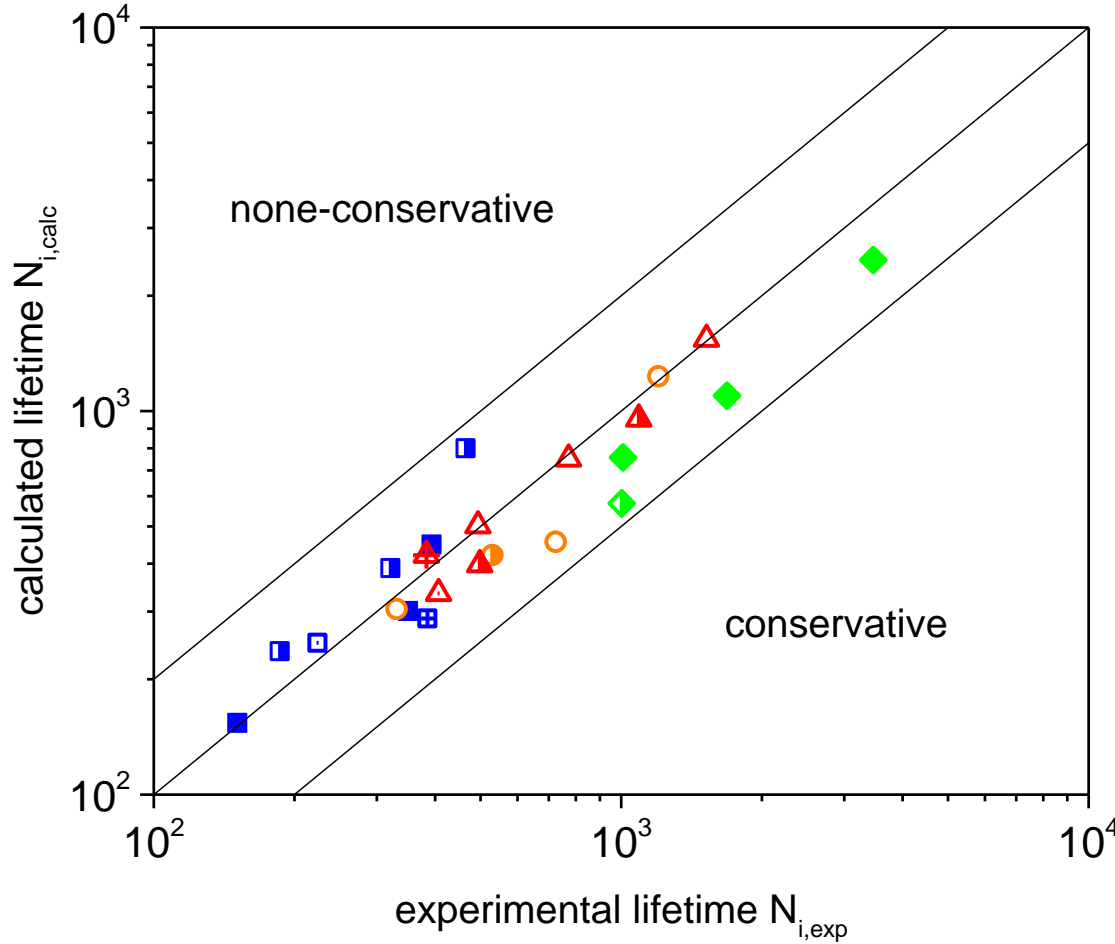
### intergranular damage



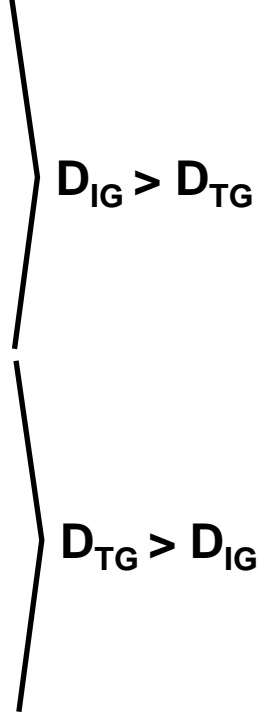
### transgranular damage



# description of lifetime behaviour



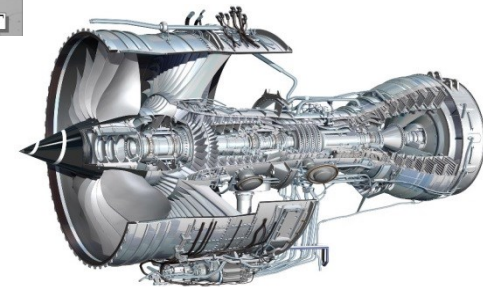
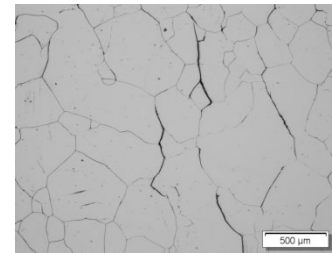
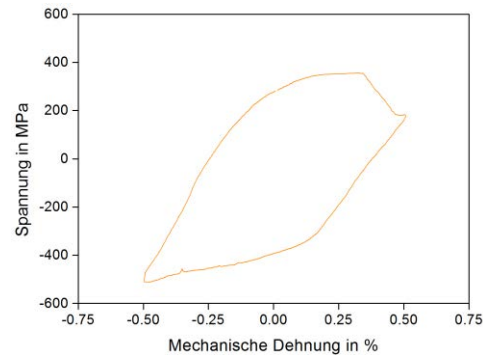
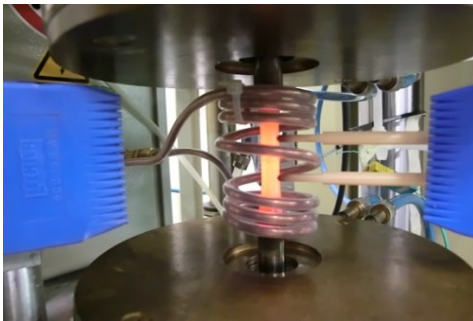
- IP without  $t_D$
- ▣ IP 2 min  $t_D$
- IP 5 min  $t_D$
- ▣ IP 30 min  $t_D$
- CCD without  $t_D$
- CCD 5 min  $t_D$
- △ OP without  $t_D$
- ▣ OP 2 min  $t_D$
- ▲ OP 5 min  $t_D$
- △ OP 30 min  $t_D$
- ◆ CD without  $t_D$
- ◆ CD 5 min  $t_D$



- lifetime prediction is satisfactory
- further validation is desirable

- The thermal-mechanical fatigue behaviour of the Nickel base superalloy NiCr22Co12Mo9 has been studied in TMF tests with different phase angles and optional dwell times.
- The lifetime is strongly influenced by the phase angle. In experiments without dwell time the order is:  $IP < CCD < OP < CD$
- Depending on the phase angle two dominant types of damage were identified:
  - IP, CCD: intergranular damage, W-type-cracks perpendicular to the loading
  - OP, CD: transgranular damage, none-propagable W-type cracks parallel to the loading.
- Two damage parameters have been proposed which
  - predict the emerging type of damage correct,
  - consider the influence of dwell times and
  - correlate satisfactorily with the lifetime.

# Thank you for your kind attention!



## Questions ?





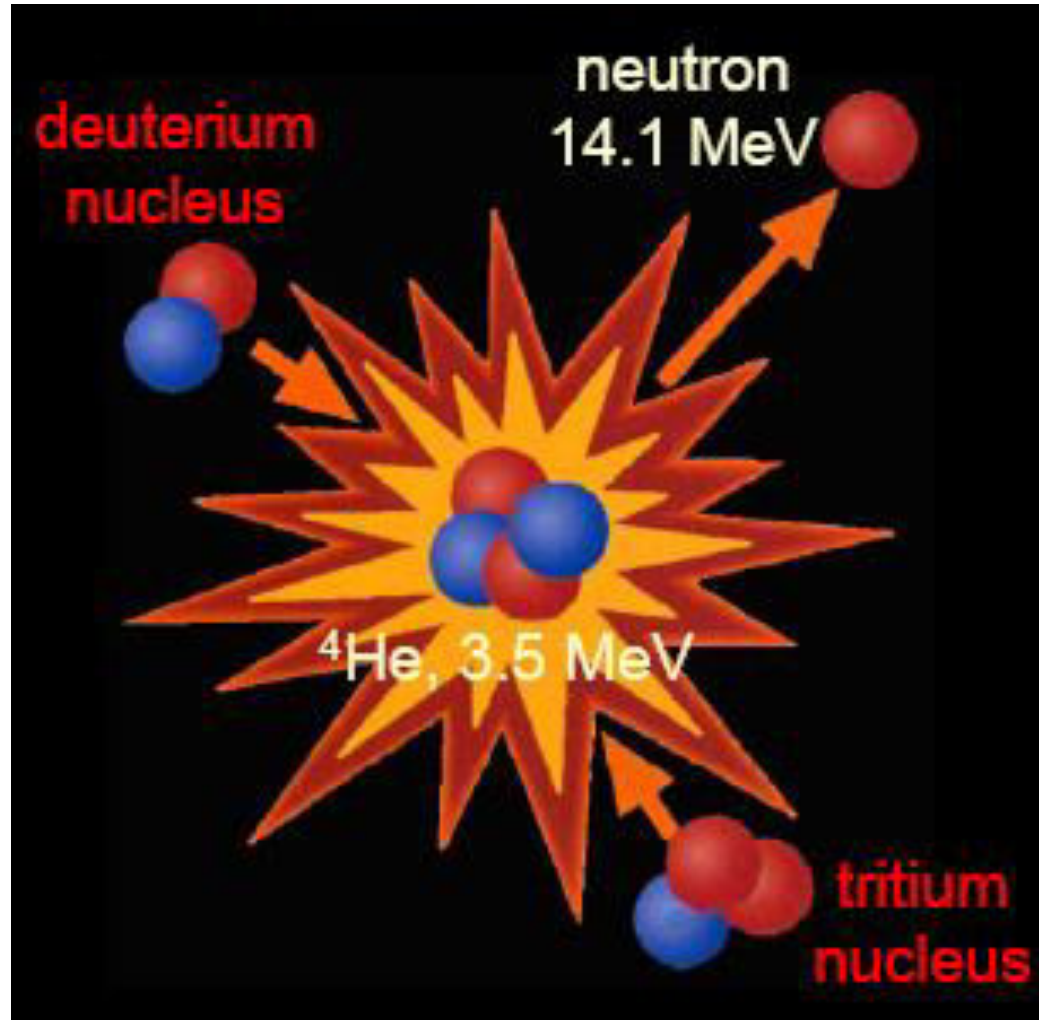
# Thermomechanical fatigue studies on Indian RAFM steel including dwell effects

A. Nagesha, G.V. Prasad Reddy, R. Kannan, R. Sandhya, K. Laha

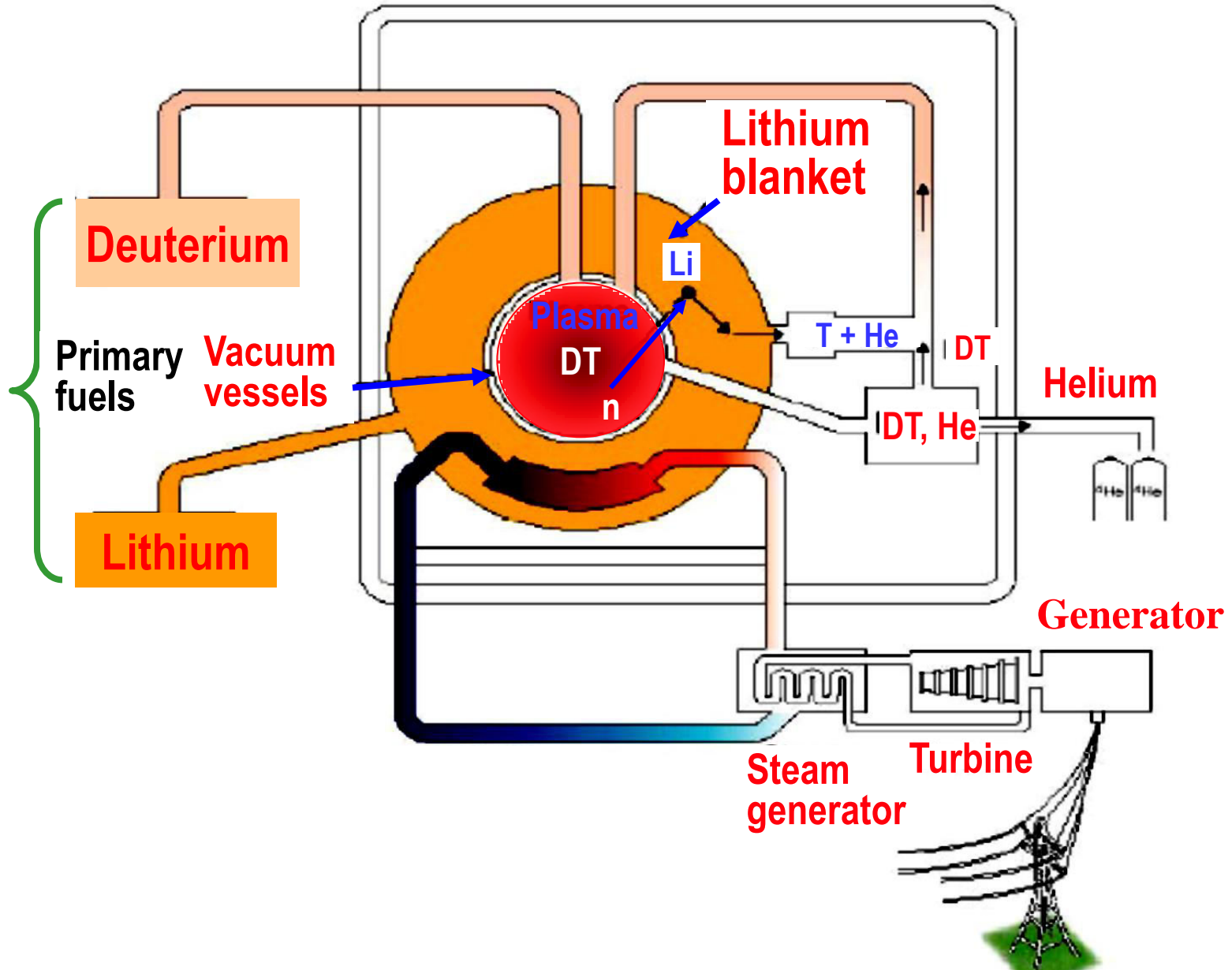
Mechanical Metallurgy Division  
Indira Gandhi Centre for Atomic Research  
Kalpakkam, INDIA

# Fusion Reaction

## D-T Fusion Reaction



# Schematic View of Fusion Reactor



# Materials for first wall and breeding blanket

- **Safety and environmental consideration**
  - **Low specific radioactivity**
  - **Low radioactive decay heat**
  - **Small half-life radio nuclides**
  - **Easy waste disposal**
- **Good resistance to radiation damage**
- **Good mechanical properties**
- **Chemical compatibility**
- **Fabrication and joining**

**Low  
activation  
materials**

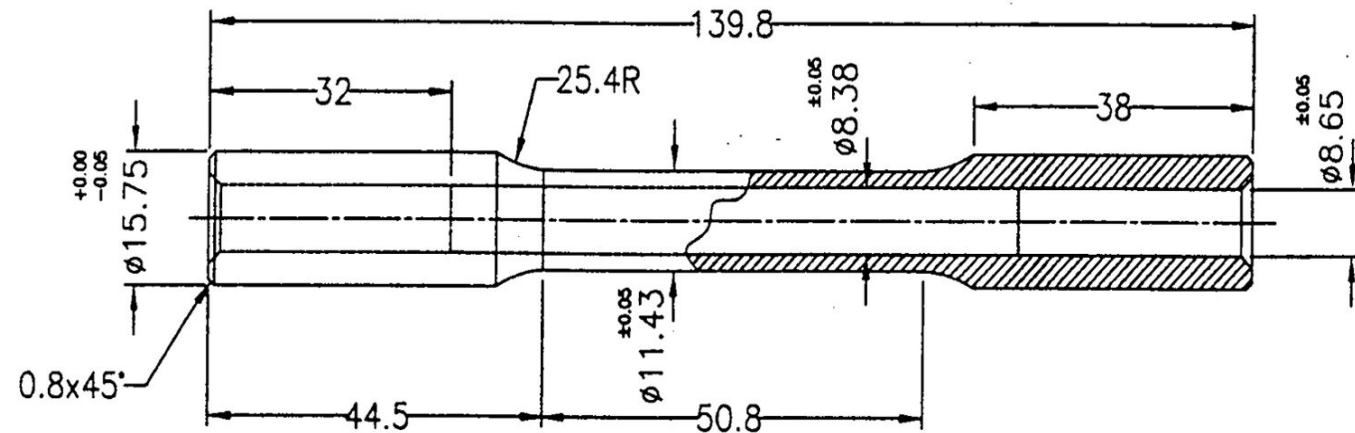
## Objectives

Influence of following factors on the TMF behaviour

- temperature range
- temperature-strain phasing
- dwell time
- chemical composition

# EXPERIMENTAL

- IP and OP tests performed on tubular samples using strain amplitude ( $\Delta\varepsilon_{mech}$ ) of  $\pm 0.4\%$  with  $\dot{\varepsilon} = 1.2 \times 10^{-4} \text{ s}^{-1}$



*Dimensions in mm*

- Temperature ranges: 573-773, 623-823 & 673-873 K
- Dwell times: 1, 5 and 10 min. at peak compressive strain under OP TMF
- Isothermal LCF (IF) tests at the peak temperatures performed at the same  $\Delta\varepsilon_{mech}$  and  $\dot{\varepsilon}$

# TEST SETUP



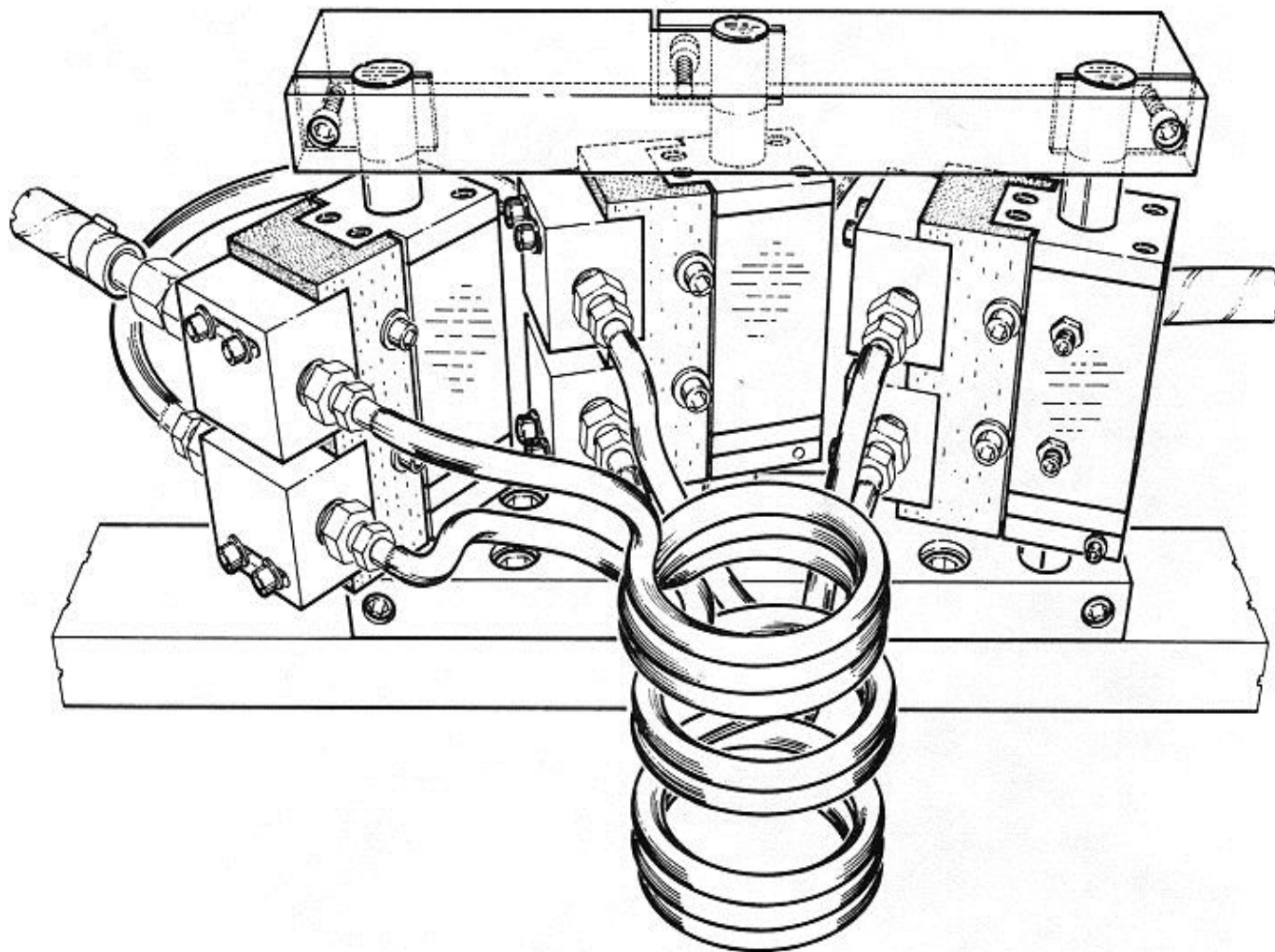
**RAFM Steel:** *Ferromagnetic*

**Problem area:**

Control of axial temperature gradient during induction heating

➤ Use of properly directed air jet to achieve temperature uniformity along the gauge length

- $\pm 100$  kN Servohydraulic
- RF Induction heating
- Air-cooled, side-contacting extensometer



Adjustable work coil fixture for direct induction heating



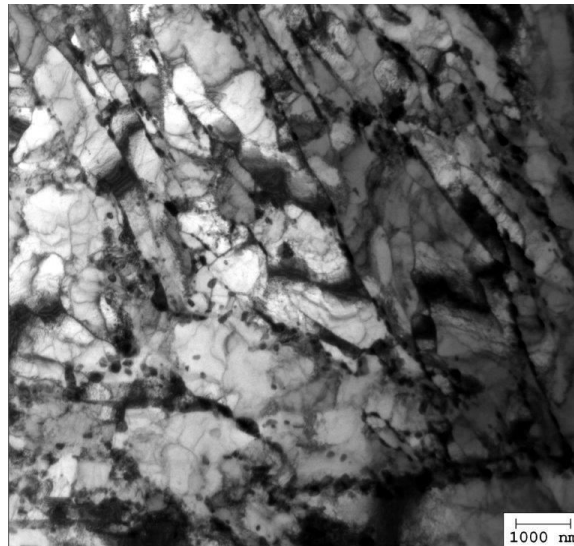
# Chemical composition

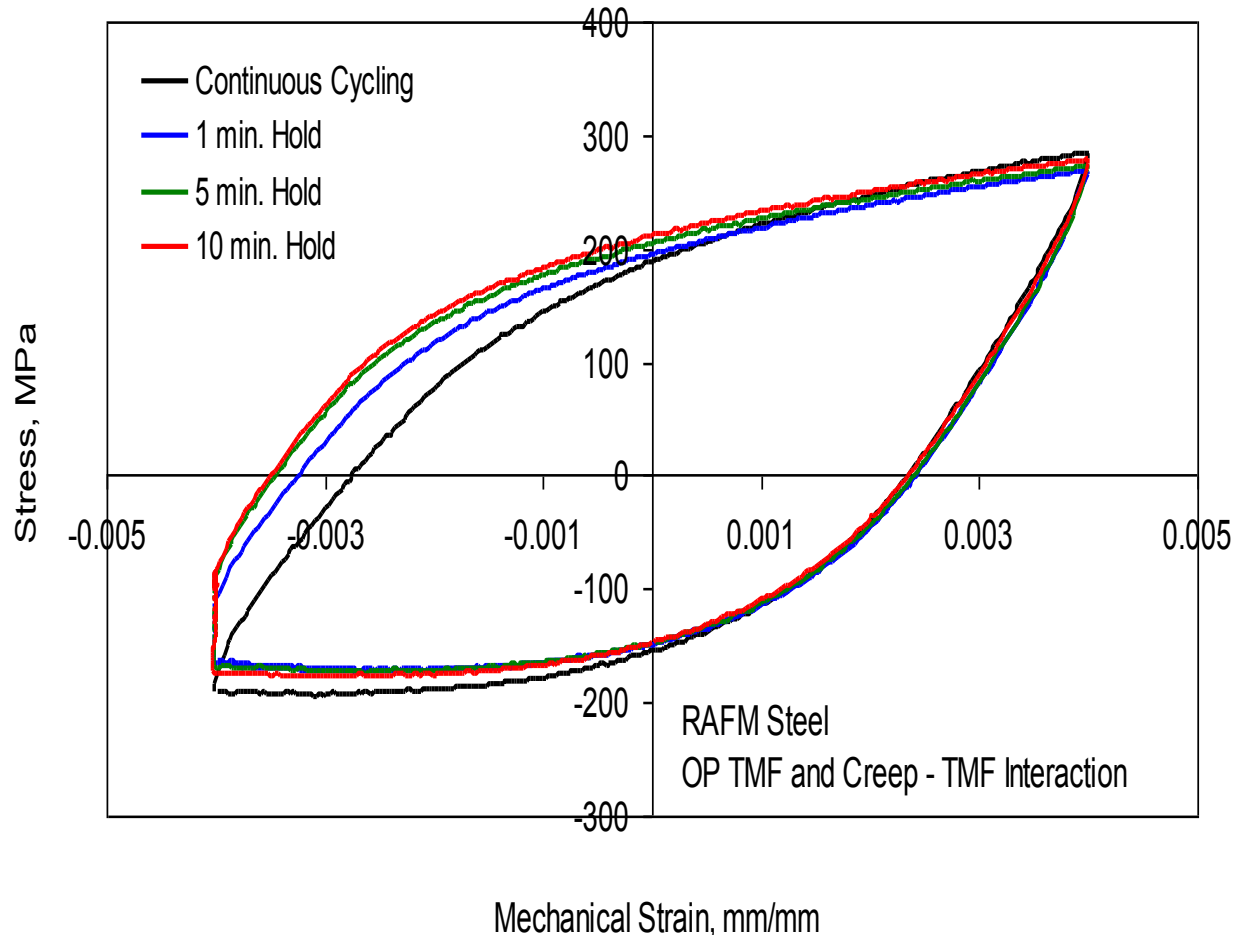
Element	Cr	W	Mn	C	V	Ta	Co	Si
Wt. %	9.03	1.39	0.56	0.126	0.24	0.06	0.005	0.06

## Heat Treatment

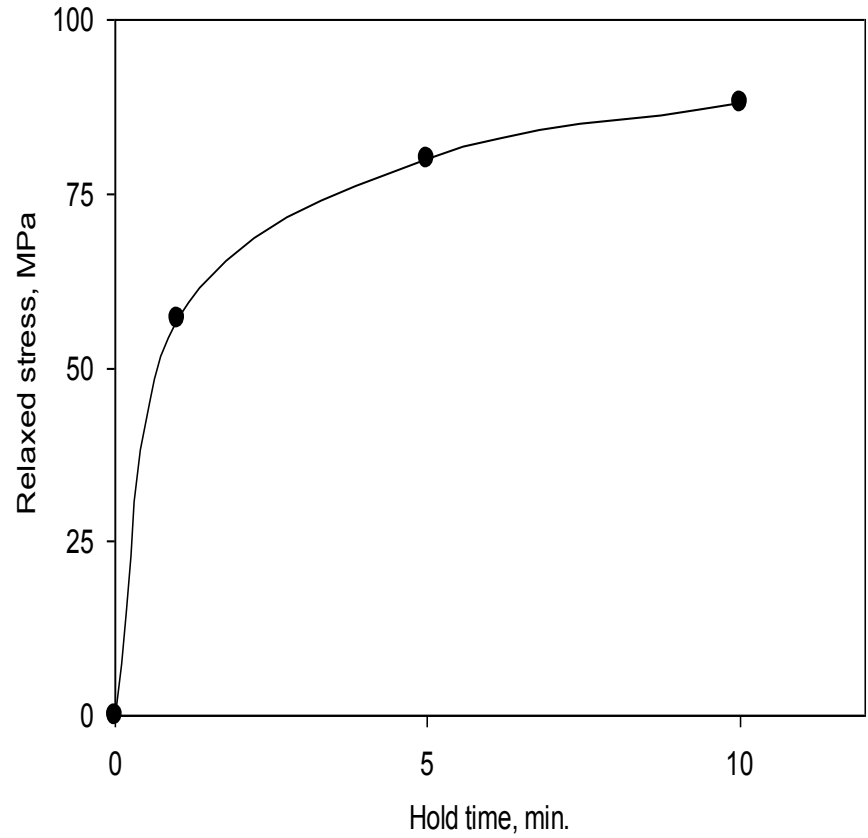
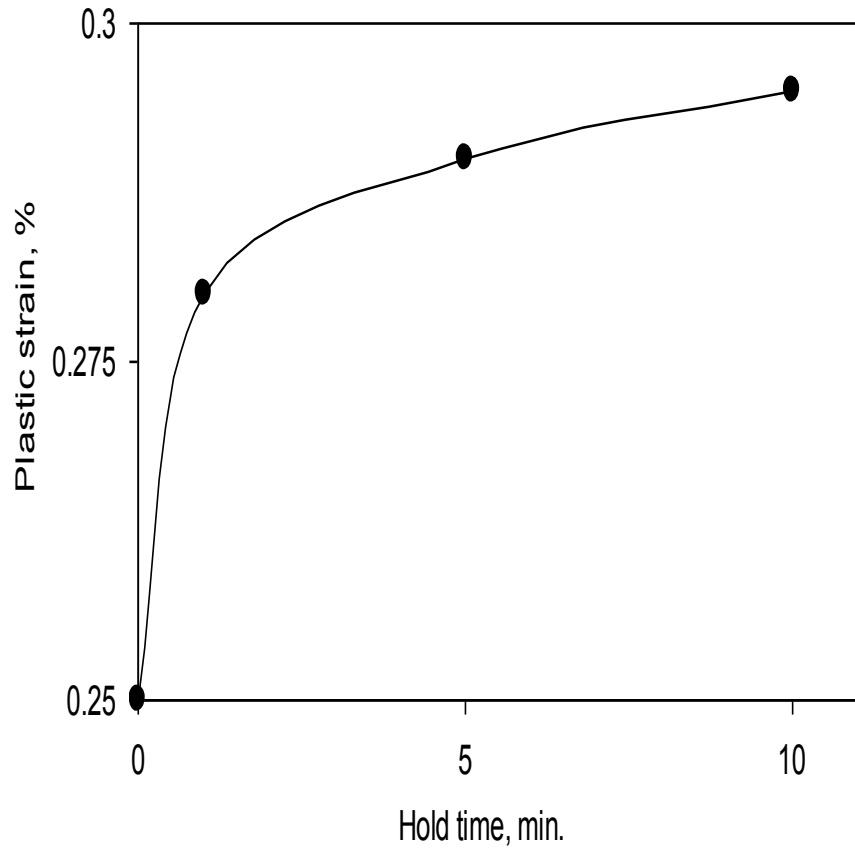
Normalizing (1253 K/30 min + air-cooling)

Tempering (1033 K/60 min + air-cooling)

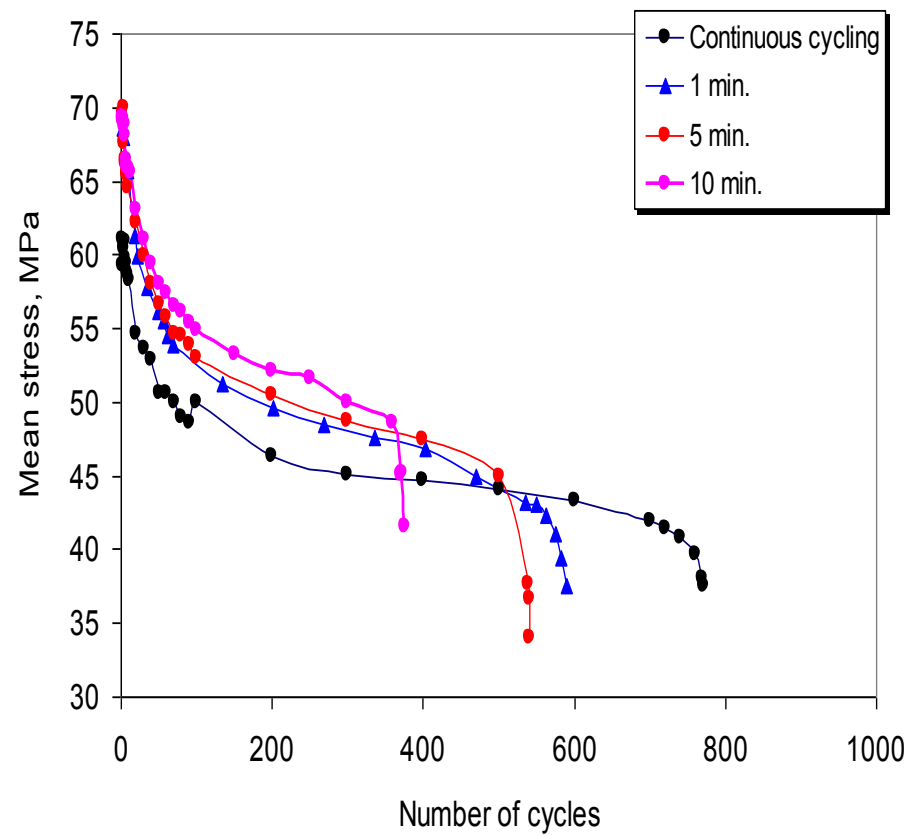




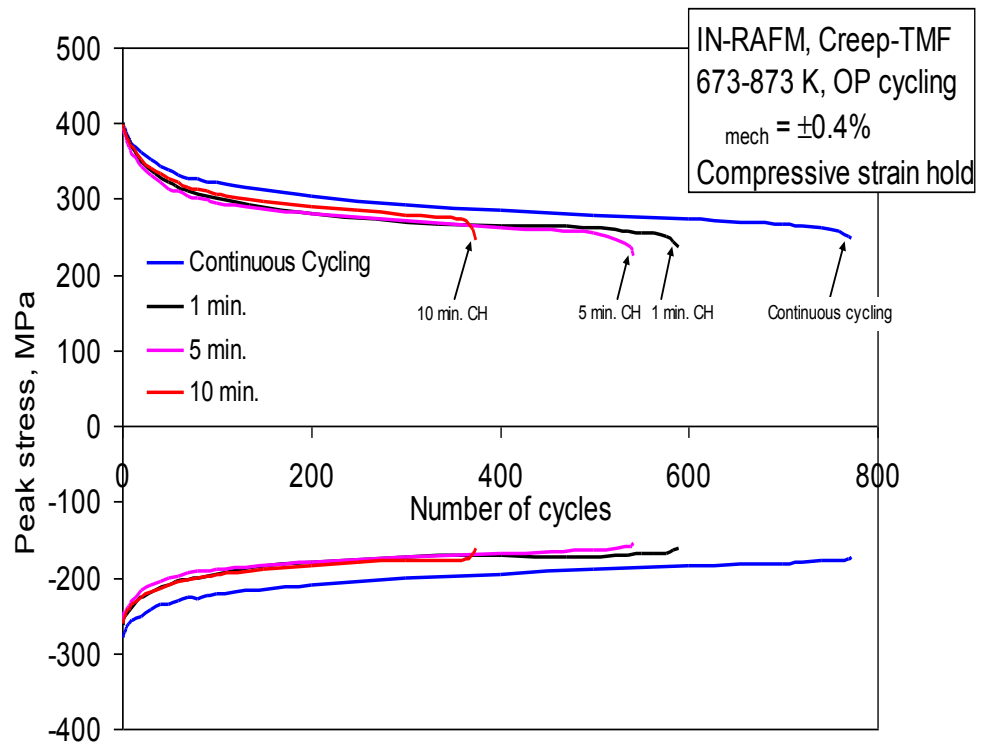
Half-life hysteresis loops under OP TMF and creep-TMF  
(compressive hold time: 60 – 600 s)



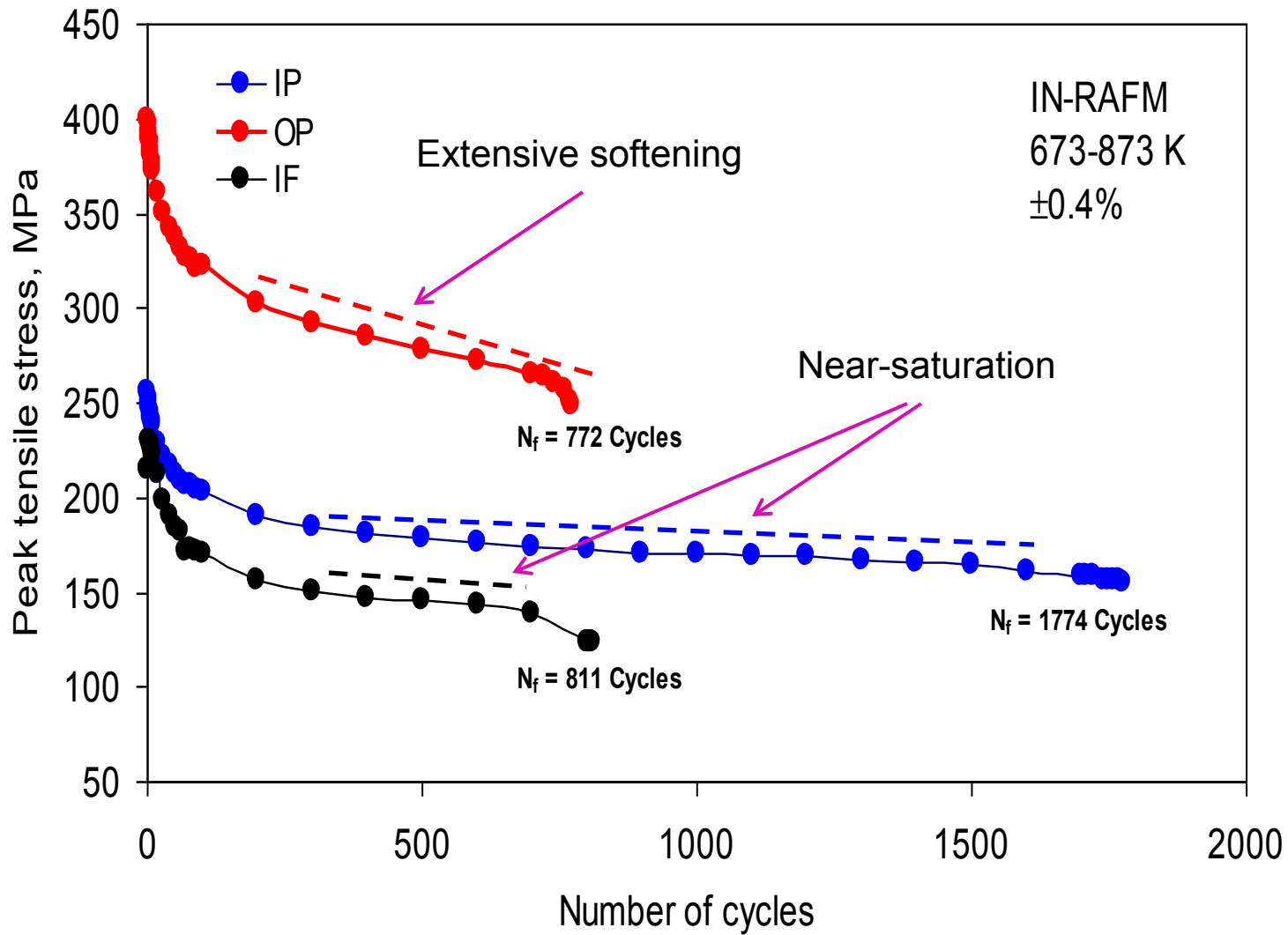
Variation of plastic strain and relaxed stress with hold time



Variation of mean stress with hold time

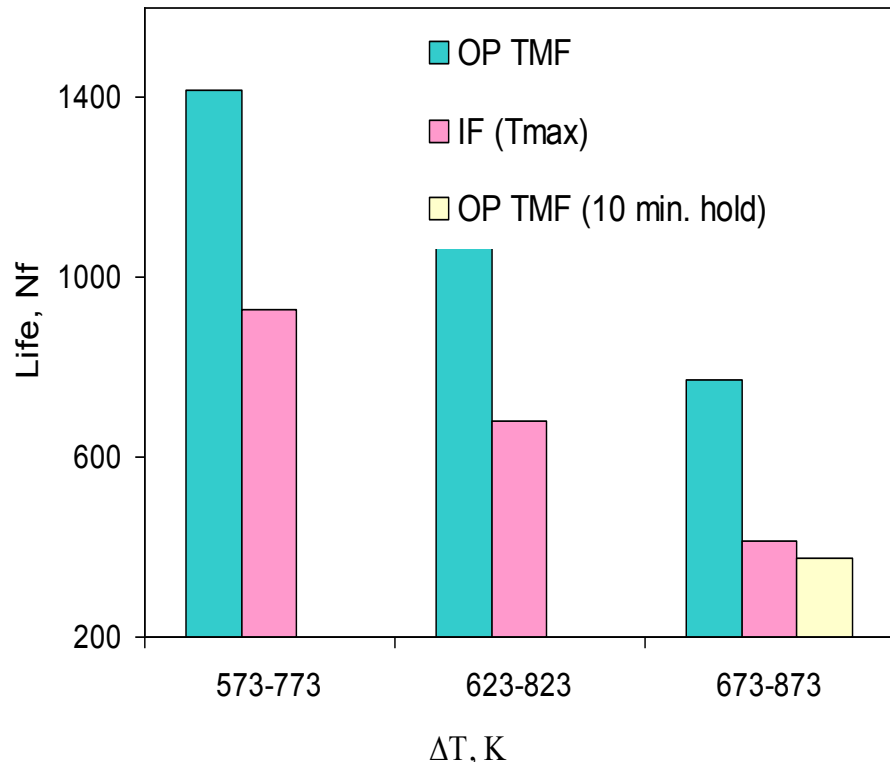


Influence of dwell time on cyclic stress response

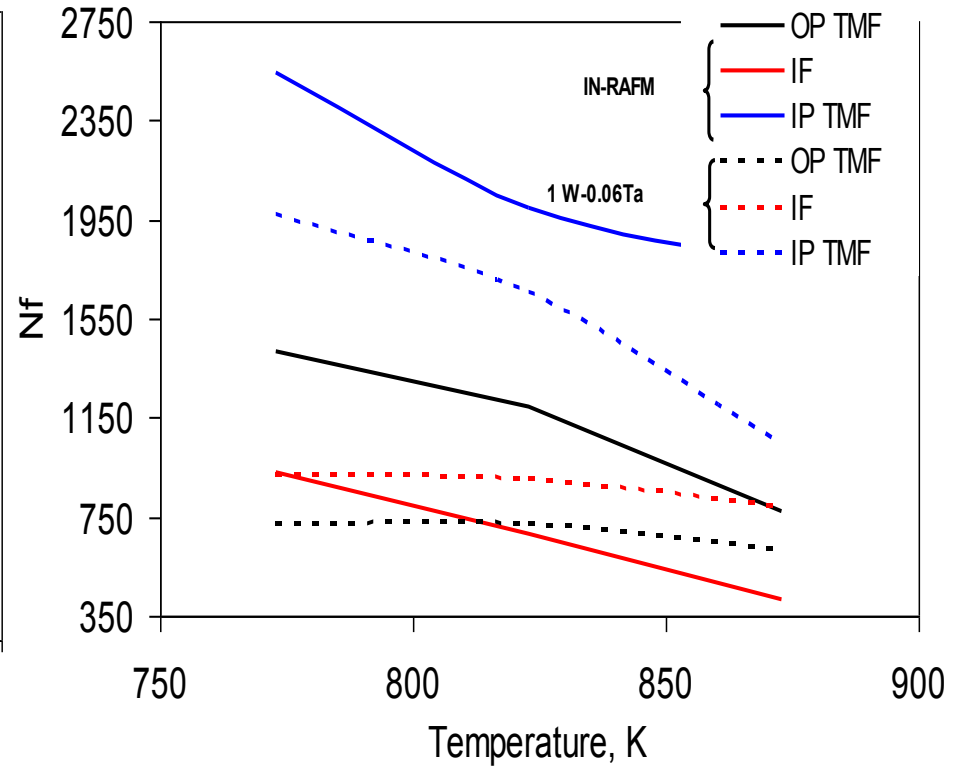


Tensile stress response under IP, OP and Isothermal tests

# Life variation with $T_{max}$

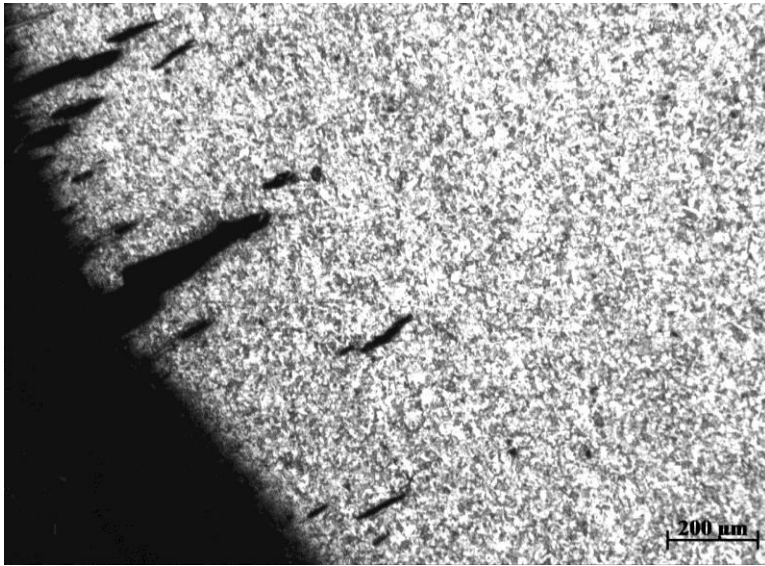


Life vs. temperature range, IN-RAFM steel

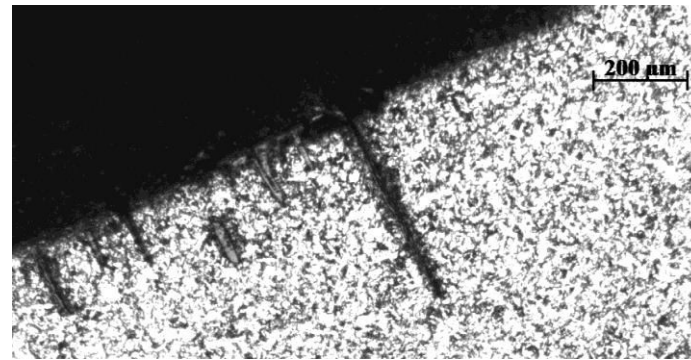


Life vs.  $T_{max}$  – influence of composition

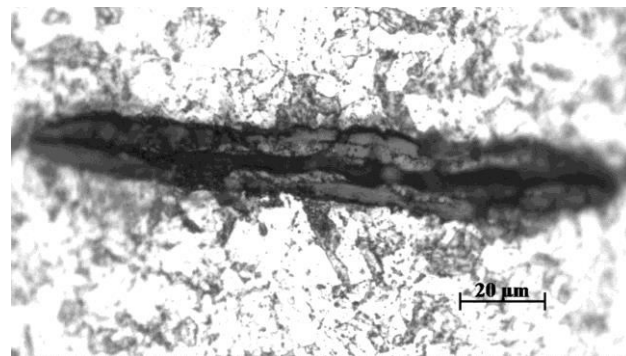
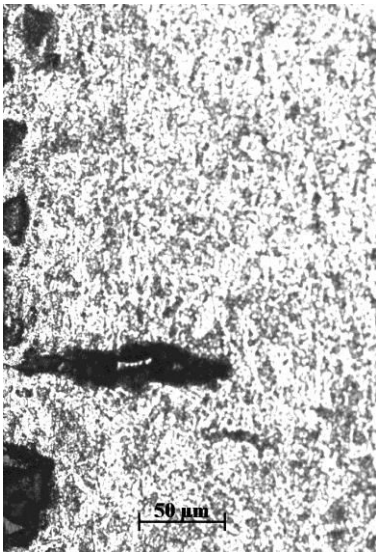
673-873 K, Creep-TMF with comp. hold



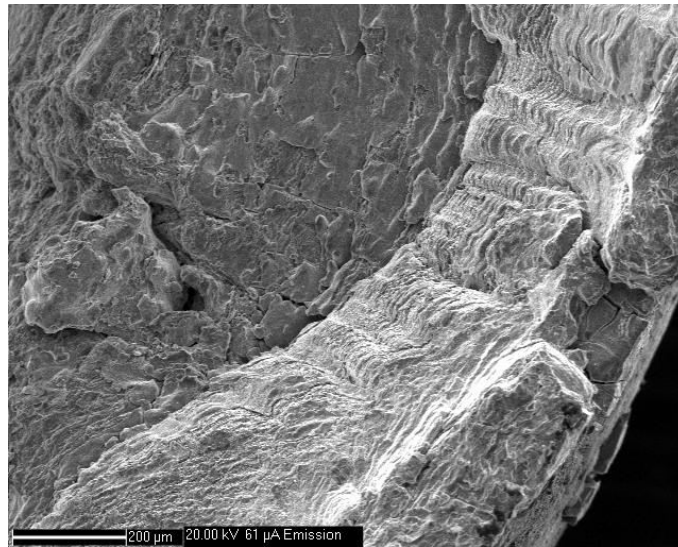
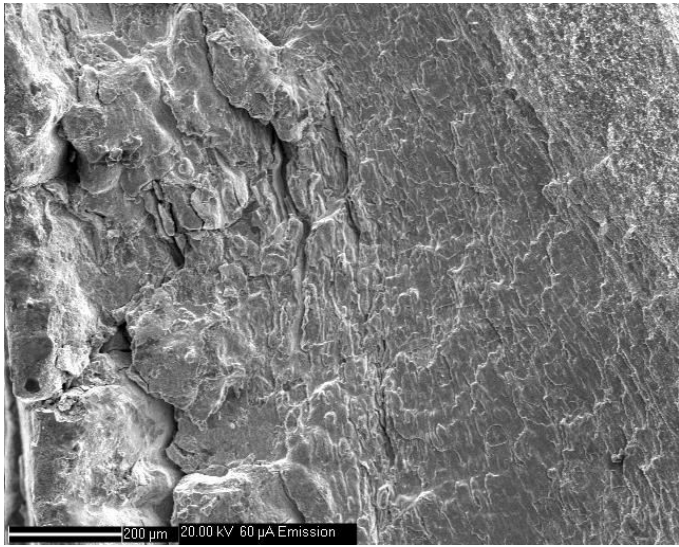
60 s



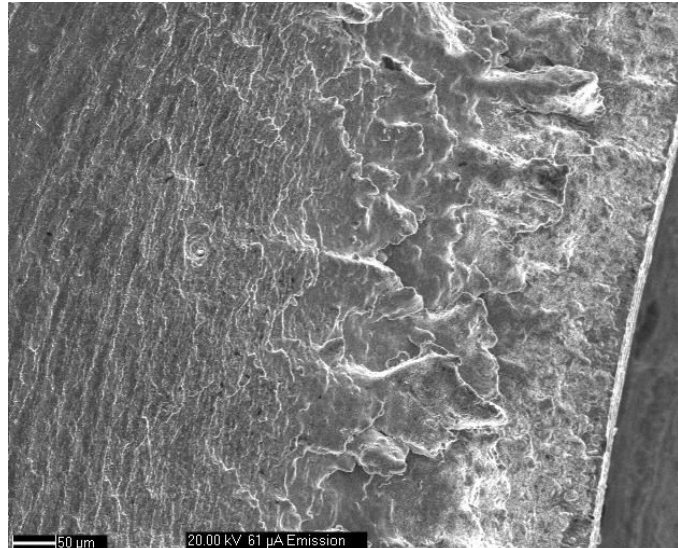
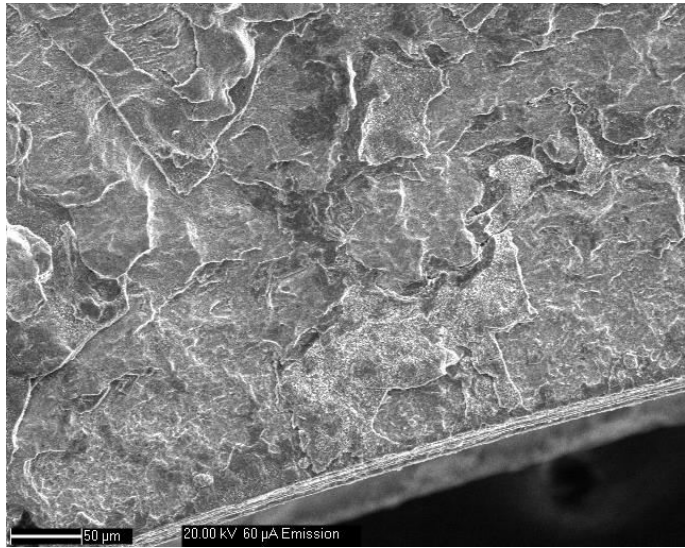
300 s



600 s

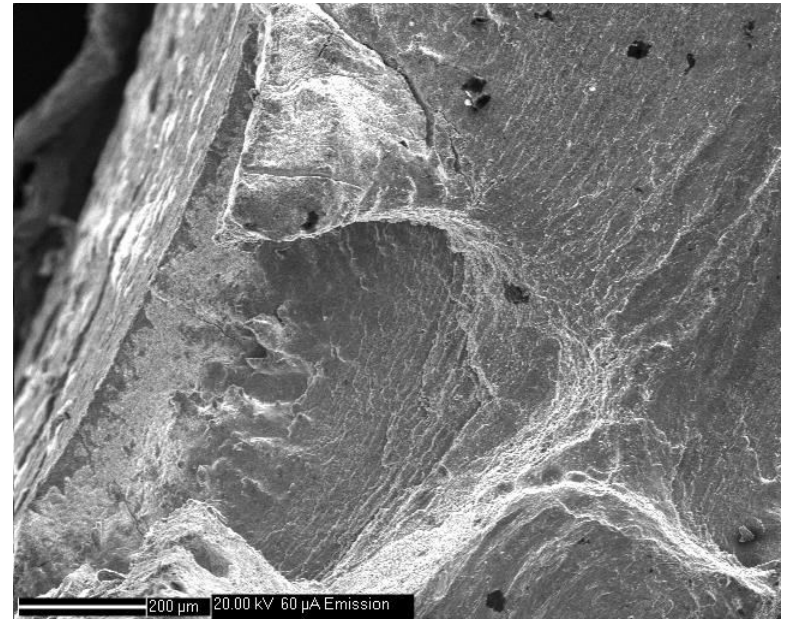
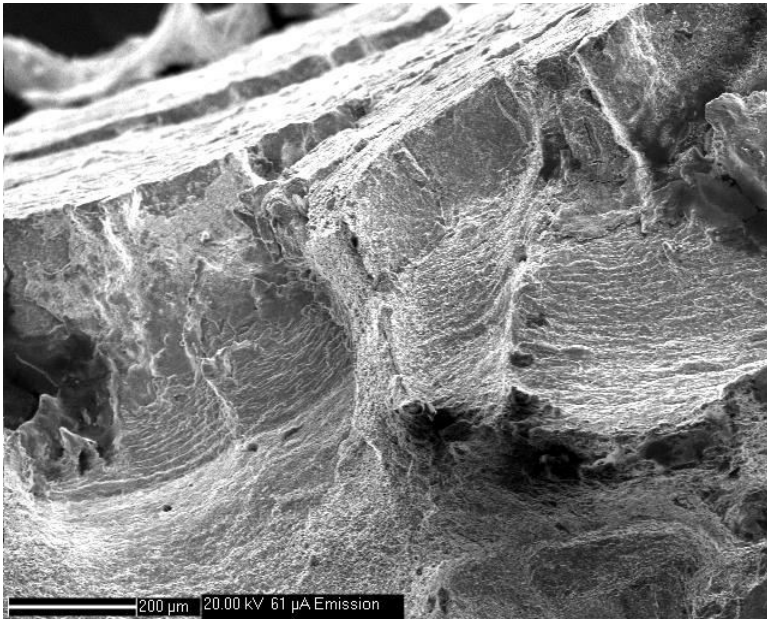


IF cycling, 873 K



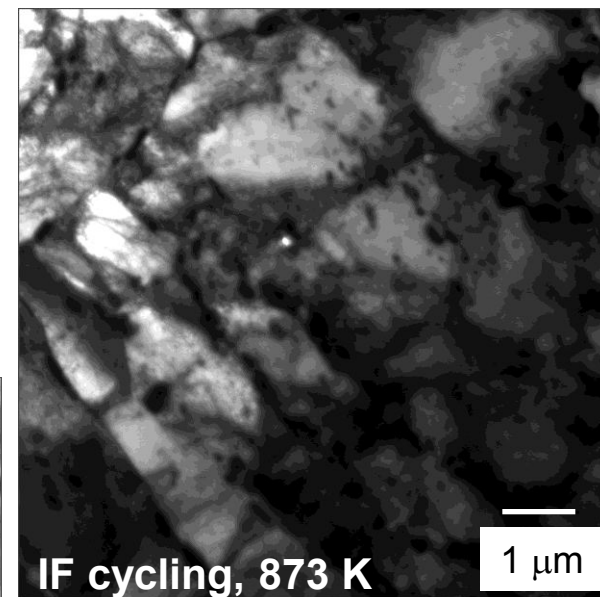
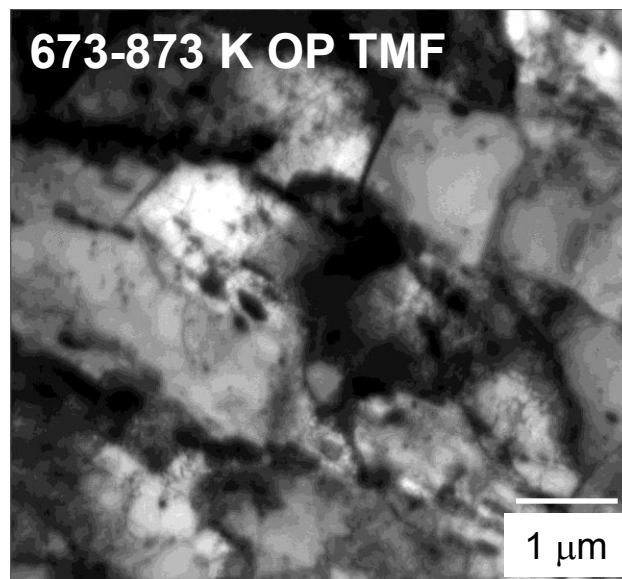
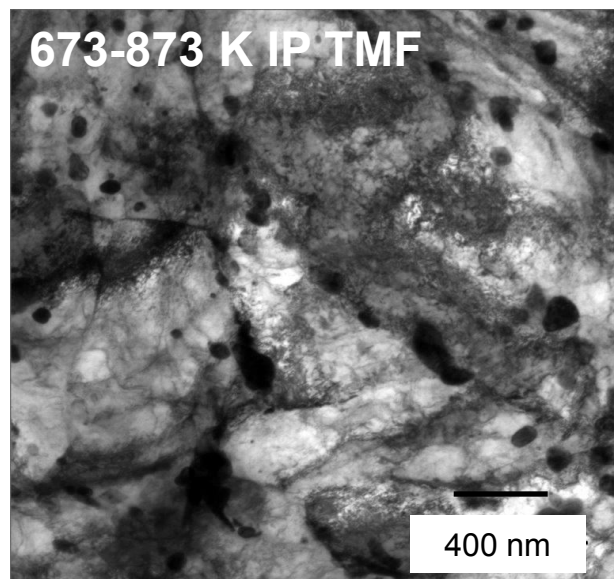
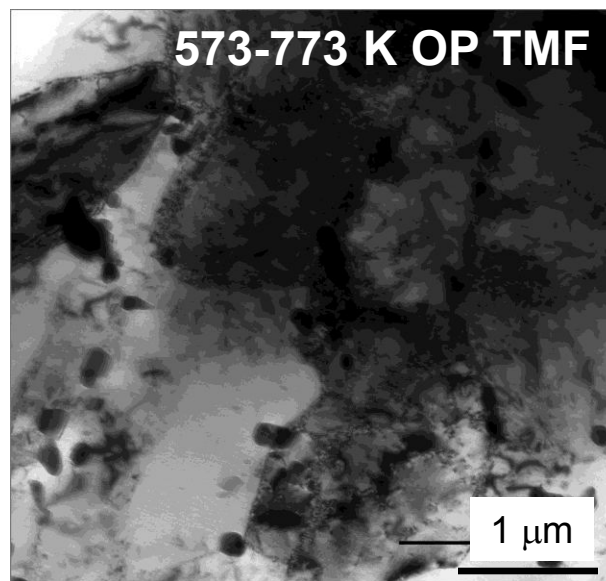
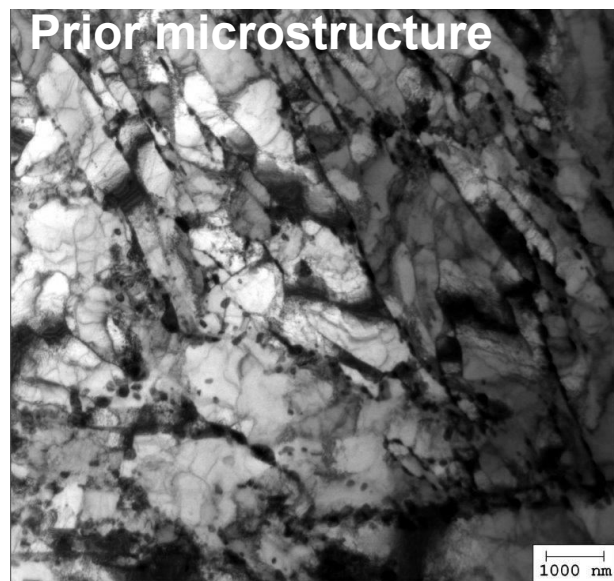
673-873 K, 1 m CH





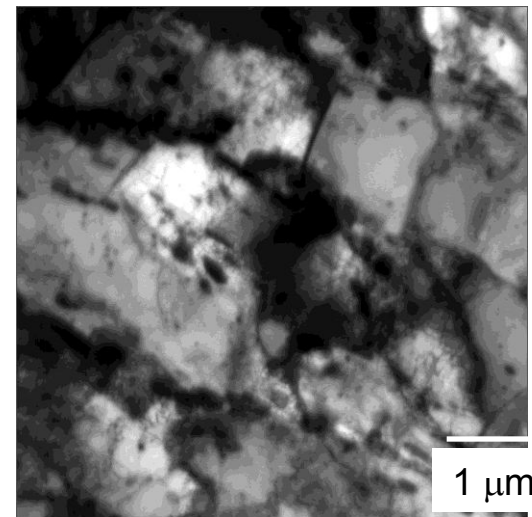
673-873 K, 10 m CH

# Substructural evolution

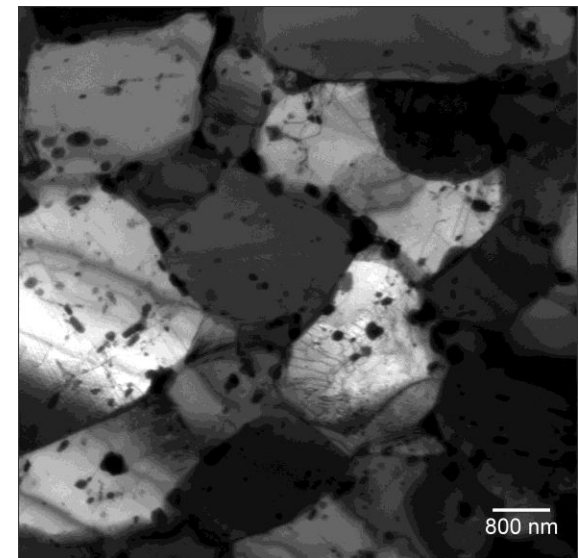
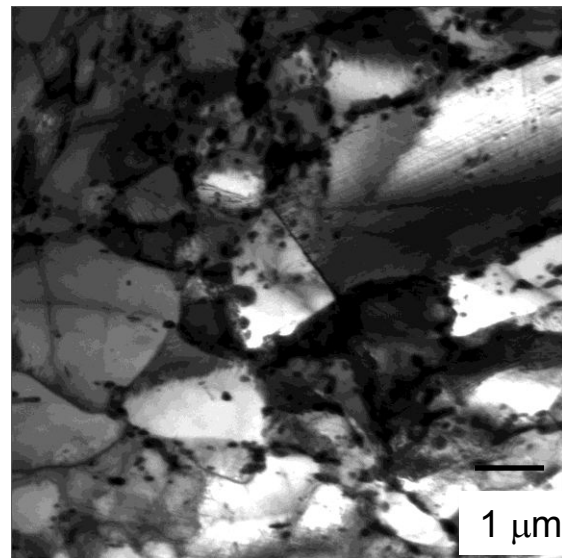
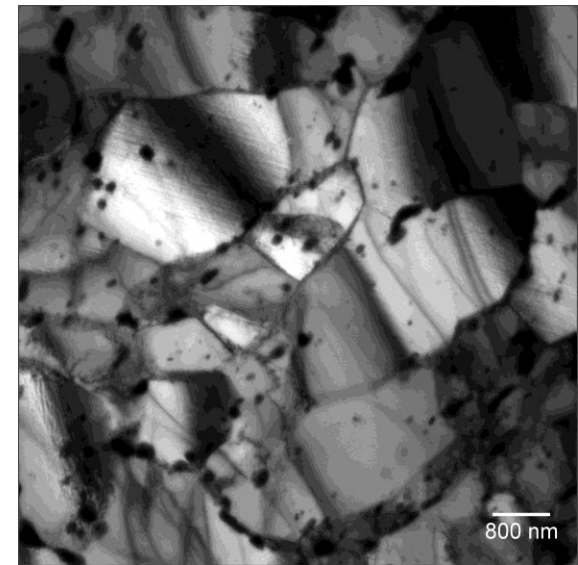
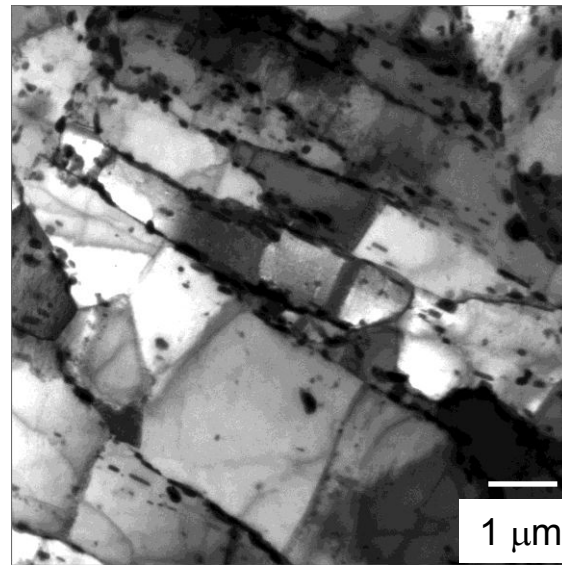


# Influence of dwell

$\Delta T$ : 673-873 K, OP TMF



**Continuous cycling**

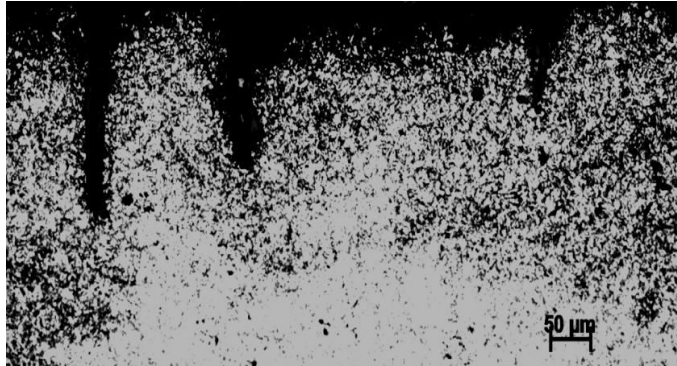


**Compressive hold time**

**1 min. hold**

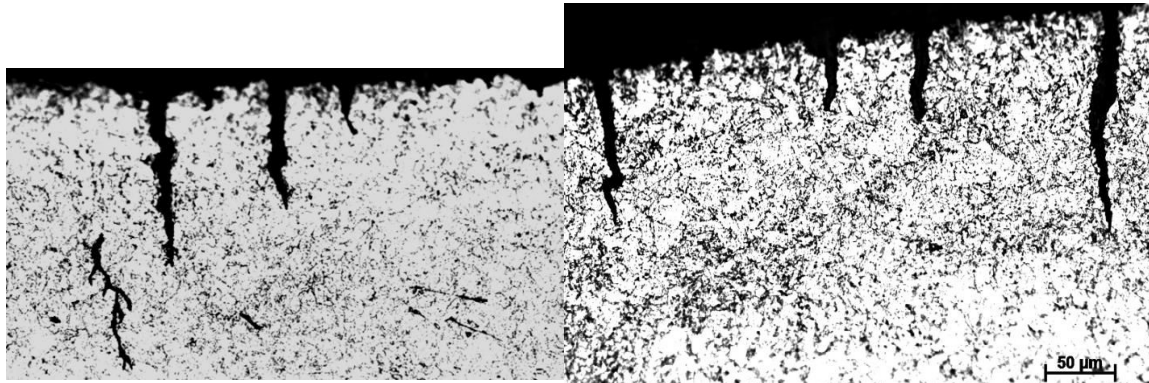
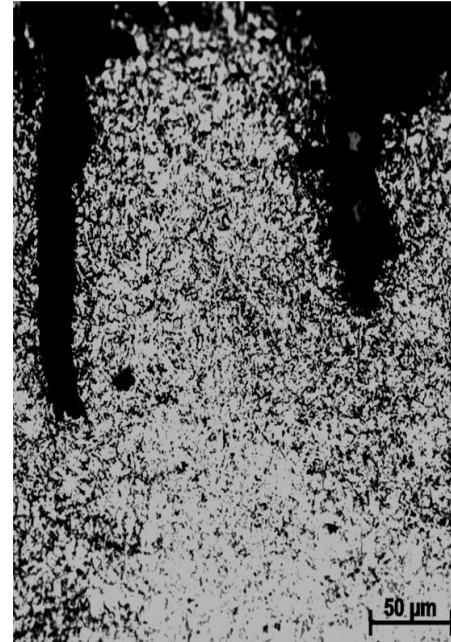
**10 min. hold**

# 1W-0.06 Ta alloy



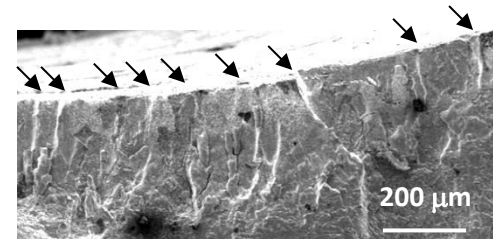
**IP TMF, 673-873 K**

IP TMF:  
Secondary cracks were less in number

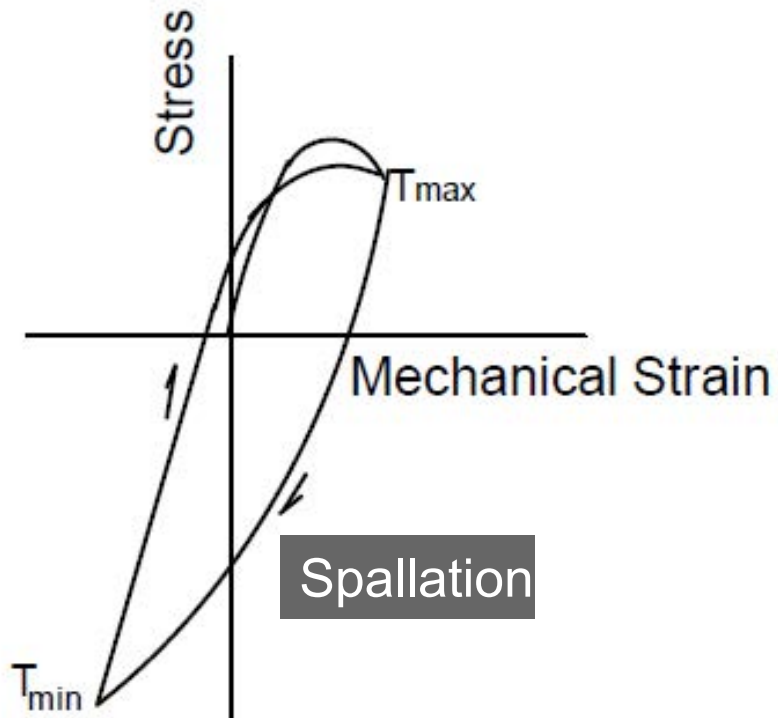


**OP TMF, 623-823 K**

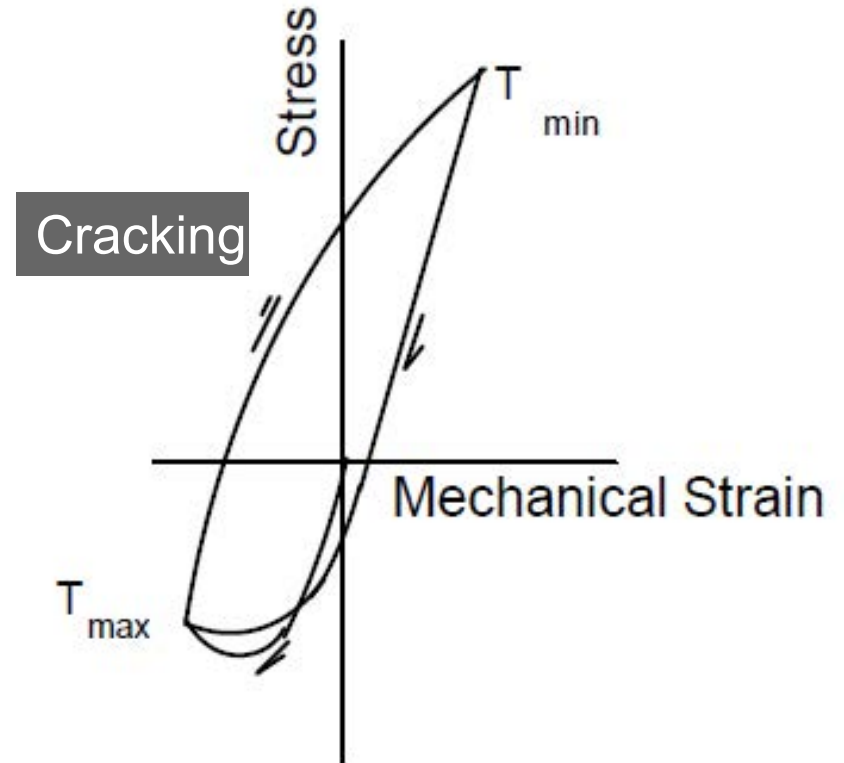
OP TMF:  
Large number of secondary cracks were observed



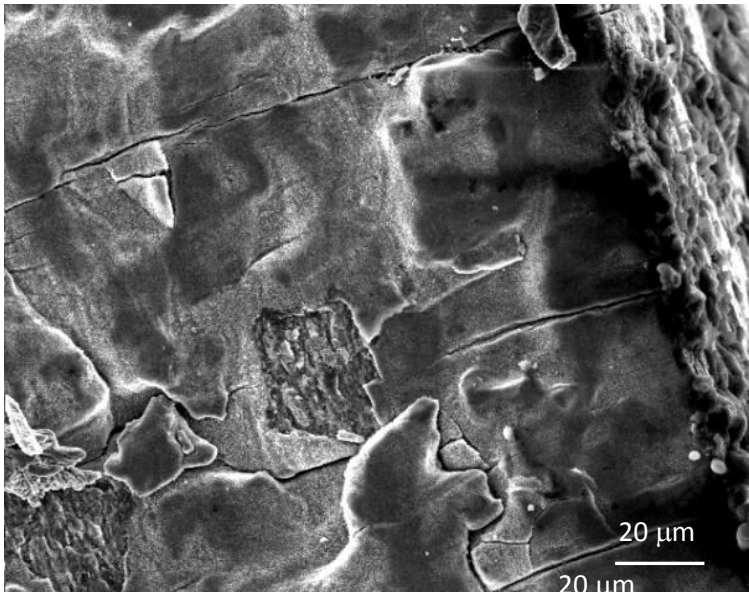
# Oxide behaviour



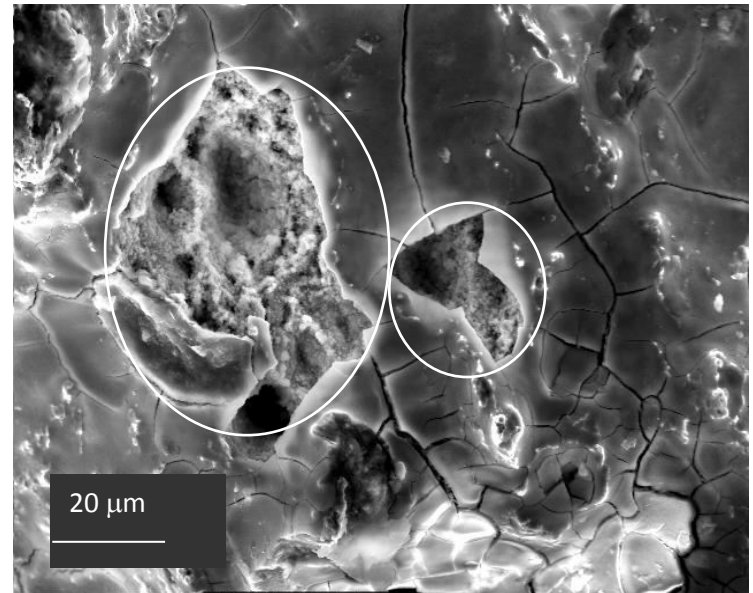
IP TMF



OP TMF



Isothermal cycling at 873 K



OP TMF, 673-873 K

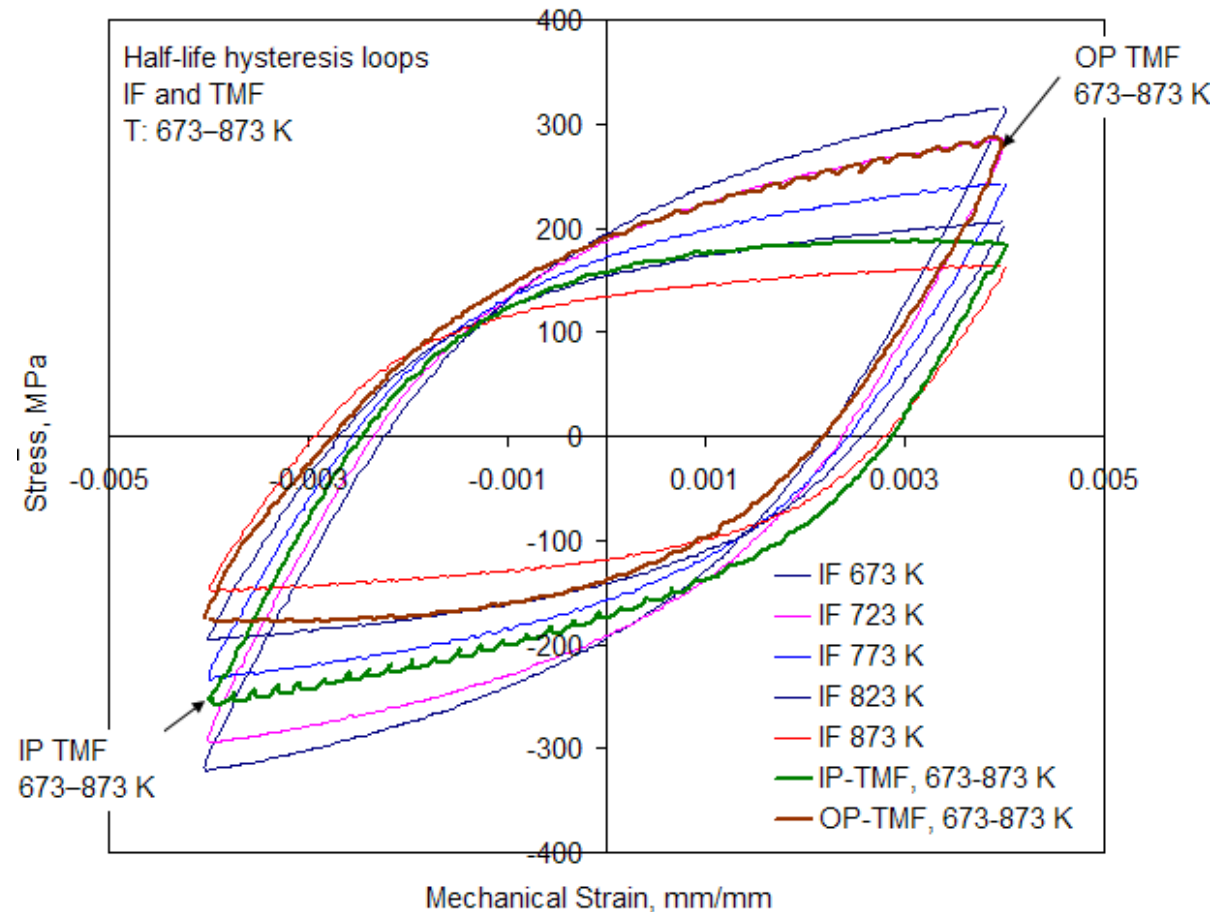


IP TMF, 673-873 K

**1W-0.06 Ta alloy**

# Manifestations of DSA

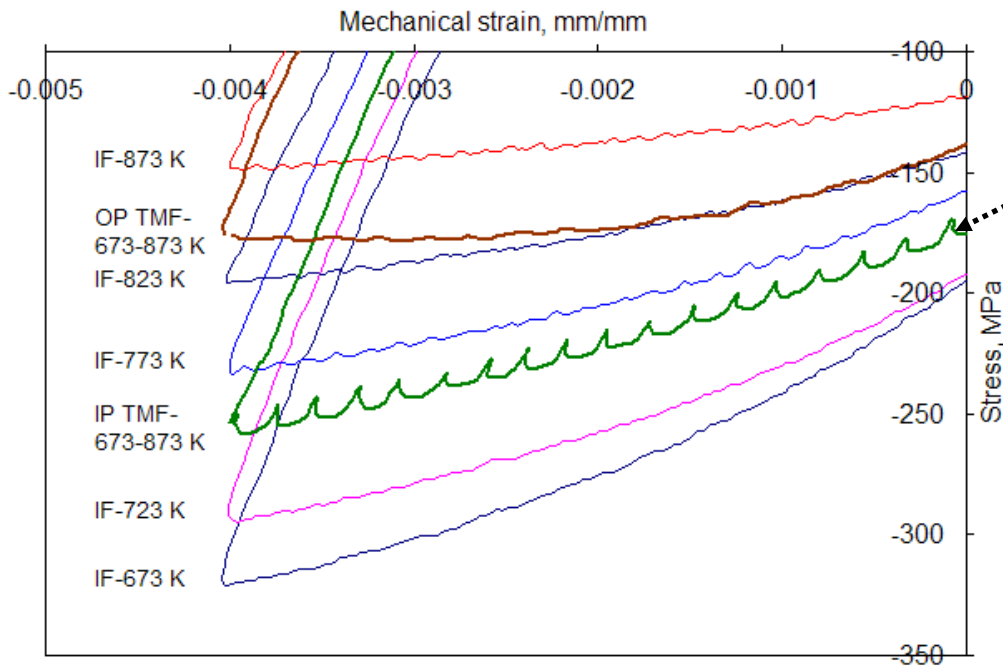
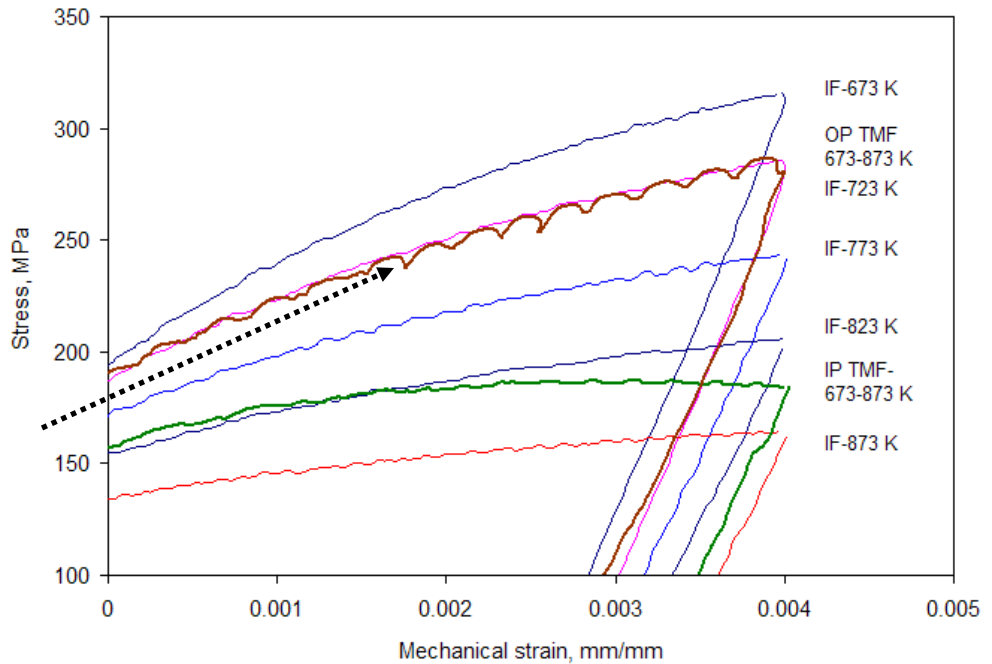
In the case of 1W-0.06Ta alloy, DSA was seen in the form of serrations under TMF cycling. The serrations were observed during the ramp down of temperature.



Stress–strain hysteresis loops at half–life (TMF and isothermal LCF)

# Serrations occurred during the downward ramp of temperature

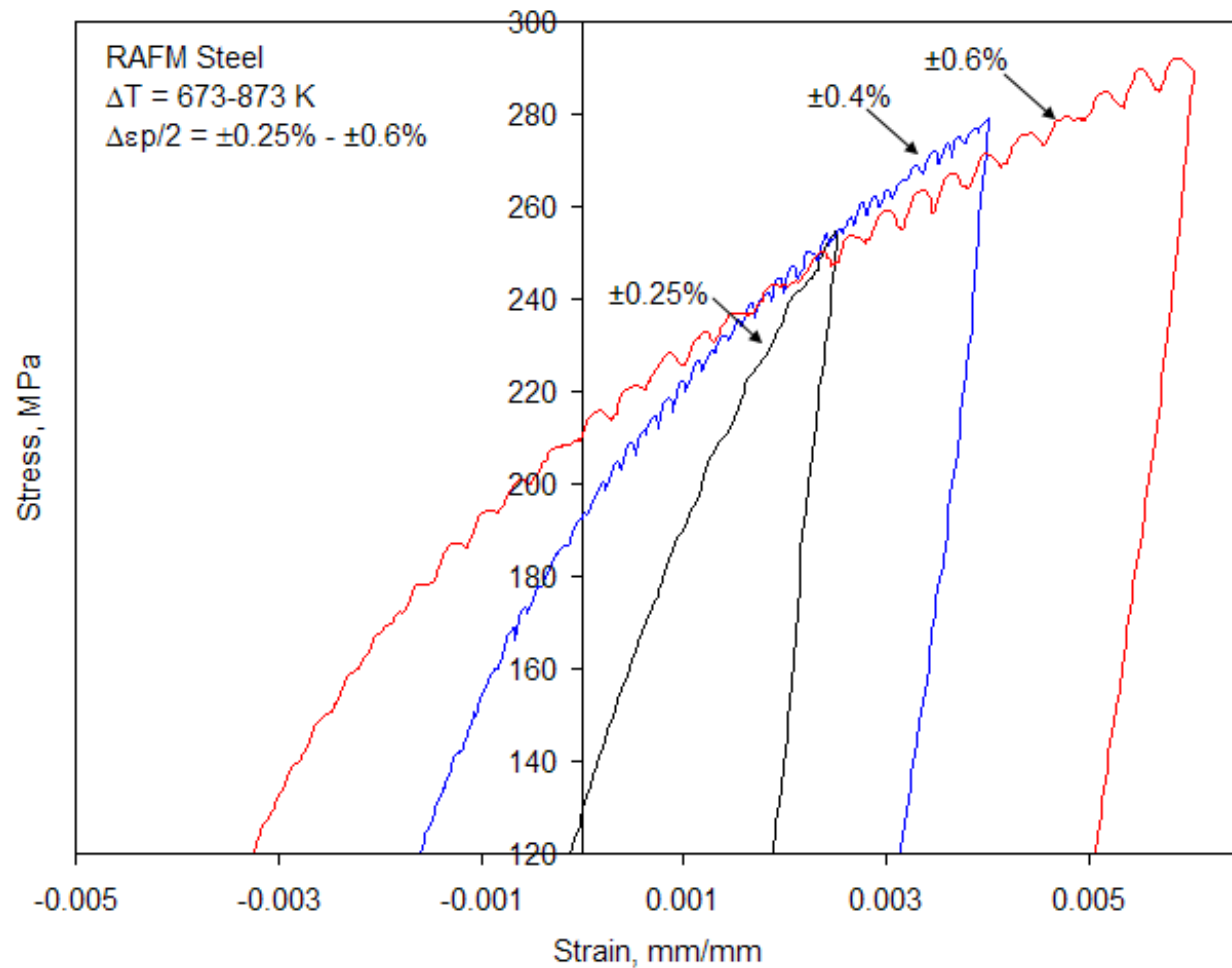
Tensile portion under OP TMF



compressive portion under IP TMF

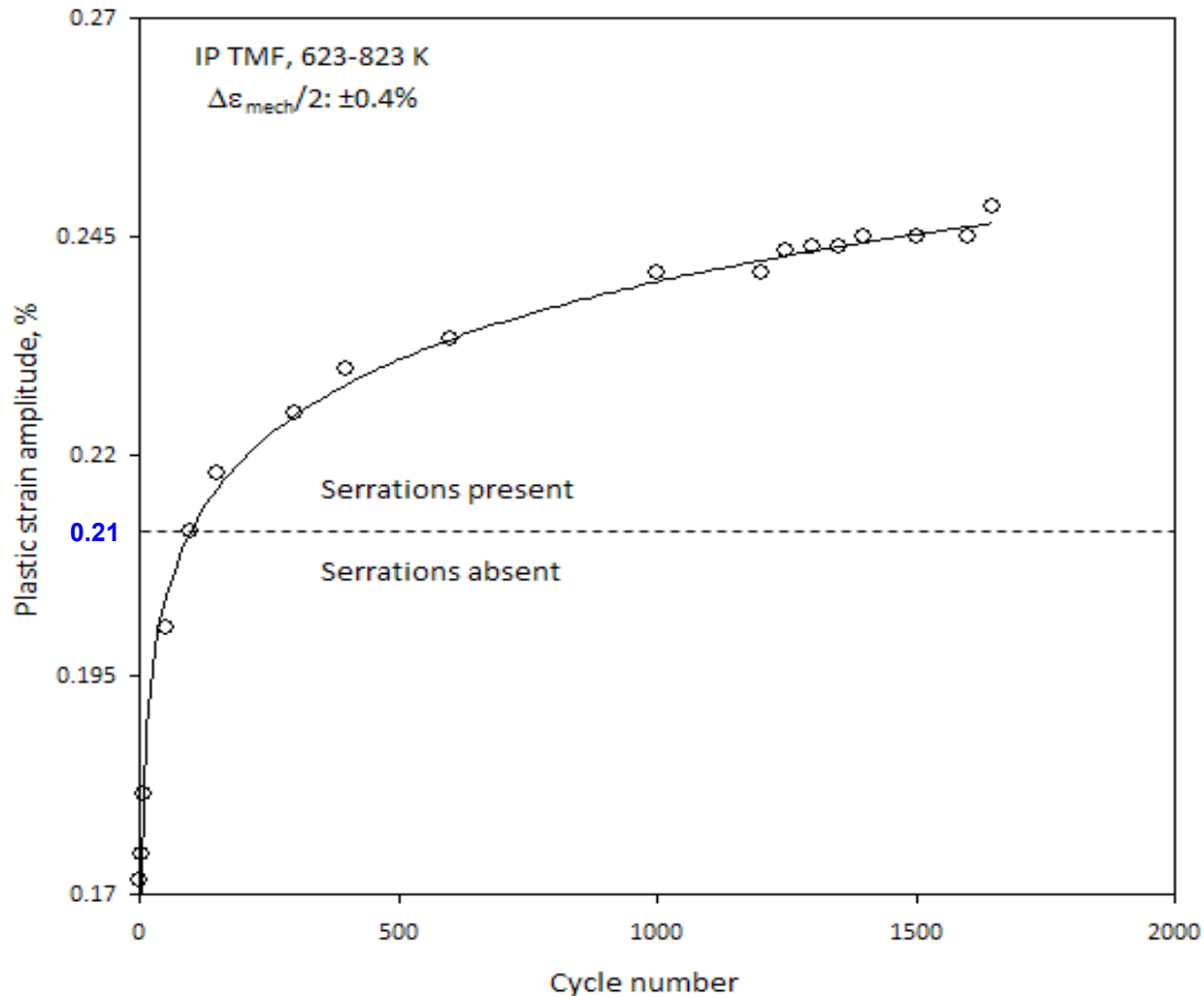
*Serrated flow observed in the range, 800 – 673 K (527 – 400 °C)*





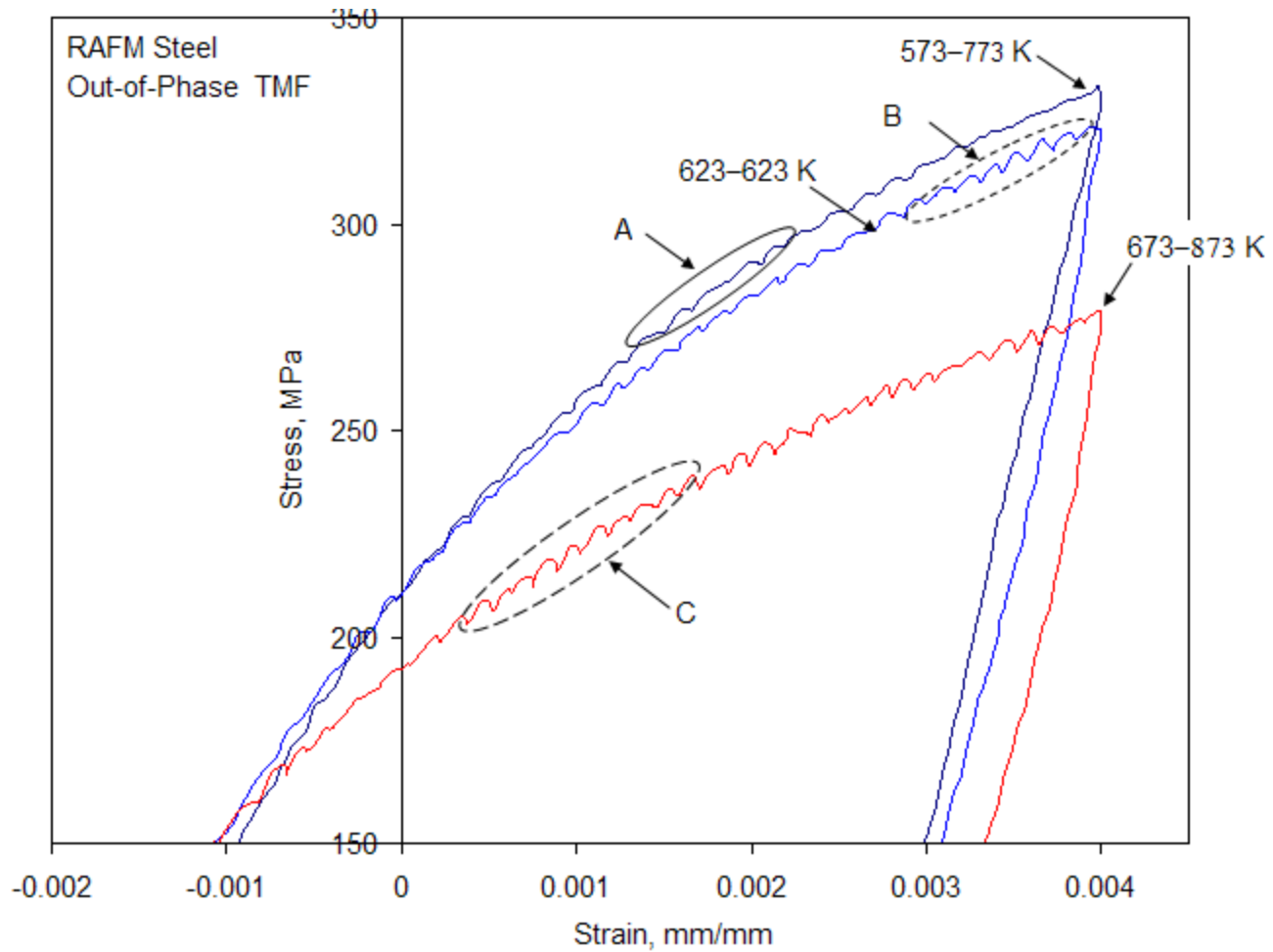
Portions of stress – strain hysteresis loops obtained under OP TMF cycling with a  $\Delta T$  of 673 – 873 K at different  $\Delta \epsilon_{mech}/2$  ( $\pm 0.25\%$  to  $\pm 0.6\%$ ).

Continuous cyclic softening of the alloy has a bearing on the occurrence of serrated flow.

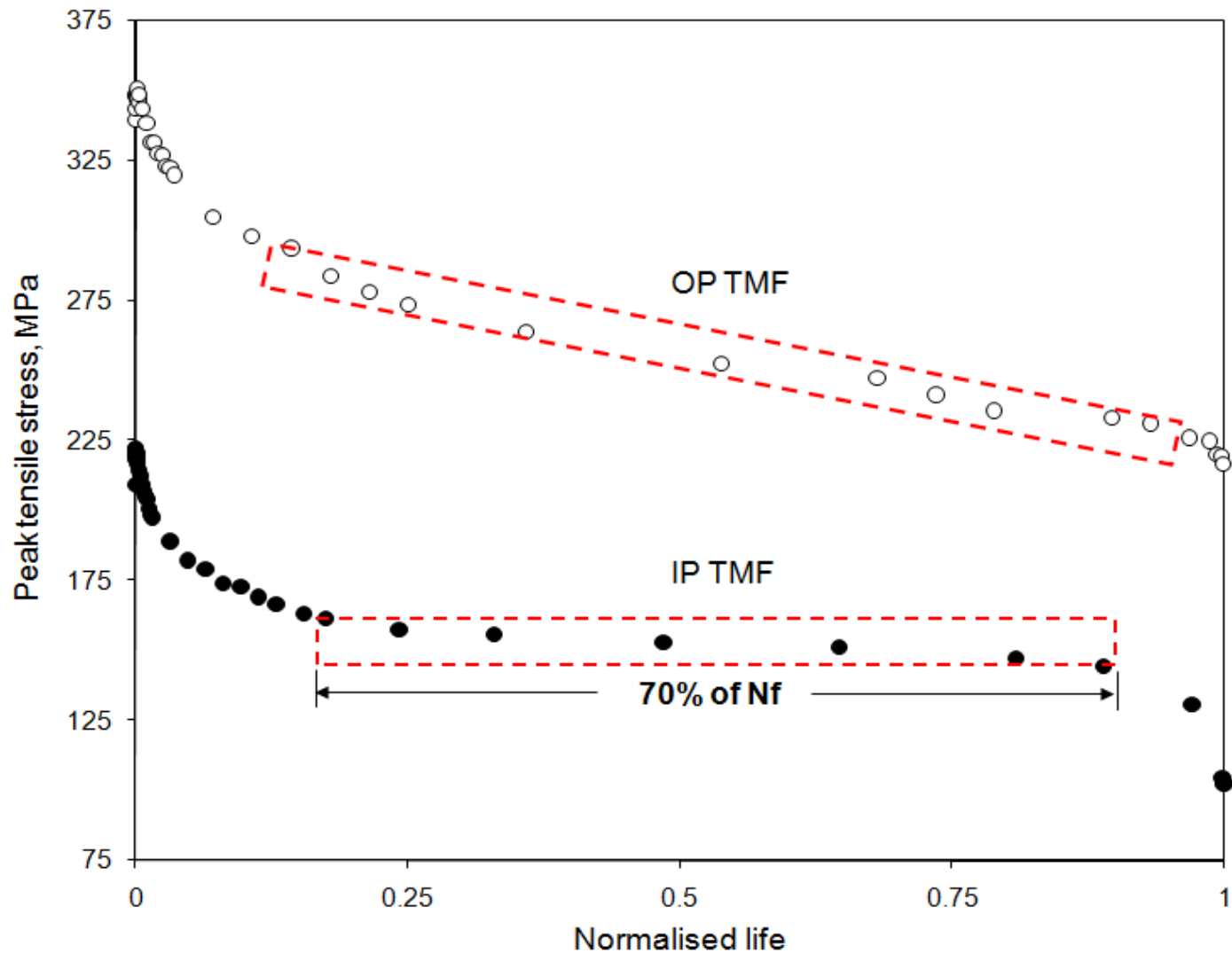


Plastic strain amplitude vs. cycle number IP TMF  $\Delta T = 623 - 823$  K  
 $\Delta\varepsilon_{mech}/2 = \pm 0.4\%$ . A threshold strain of  $\pm 0.21\%$  was observed for the appearance of serrations.

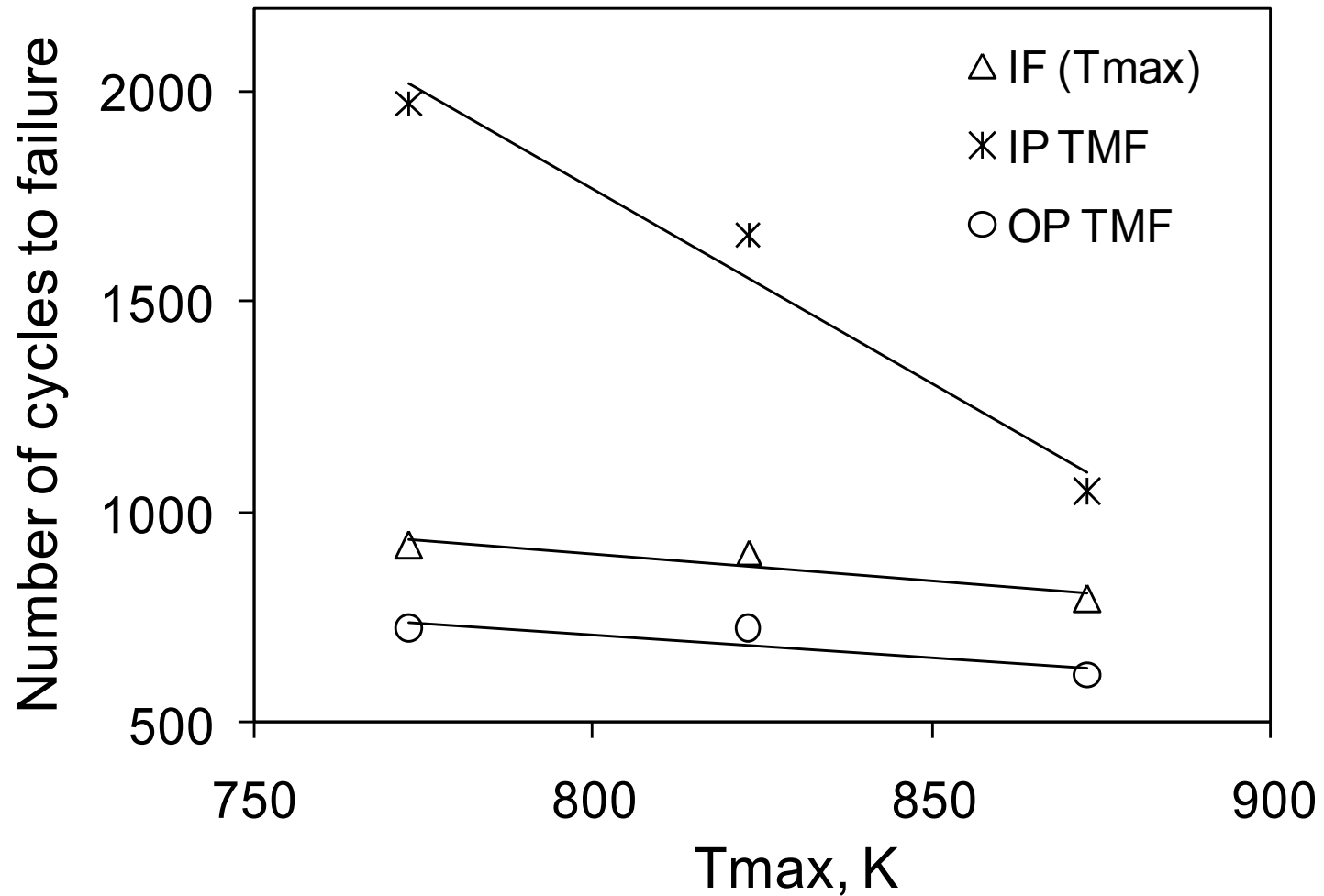
Type of serrations varied from type A to type C with increase in temperature.



Serrations in the tensile portions under OP TMF



Tensile parts of cyclic stress response, normalized with respect to number of cycles under TMF (IP and OP) cycling at  $\Delta\epsilon_{mech}/2: \pm 0.25\%$ ,  $\Delta T = 673-873$  K.



Variation of  $N_f$  with  $T_{max}$

Life under IP TMF was seen to be more sensitive to the  $T_{max}$  compared to OP TMF (1W-0.06 Ta alloy)

# CONCLUSIONS

OP TMF yielded lower life compared to both IP TMF; however, isothermal LCF at the  $T_{max}$  led to lowest life at all temperatures ranges.

Incorporation of dwell led to significant increase in the substructural recovery and a consequent reduction in cyclic life.

Deformation under TMF was characterised by dynamic strain ageing in 1%W-0.06% Ta alloy; however, no evidence of DSA was seen under isothermal cycling.

Conservatism of isothermal database at the  $T_{max}$  depends on the composition for the above steel.

Fatigue Mechanisms in  
Silicon-Molybdenum  
Spheroidal Graphite Irons  
subjected to  
Thermo-Mechanical Fatigue

Viktor Norman

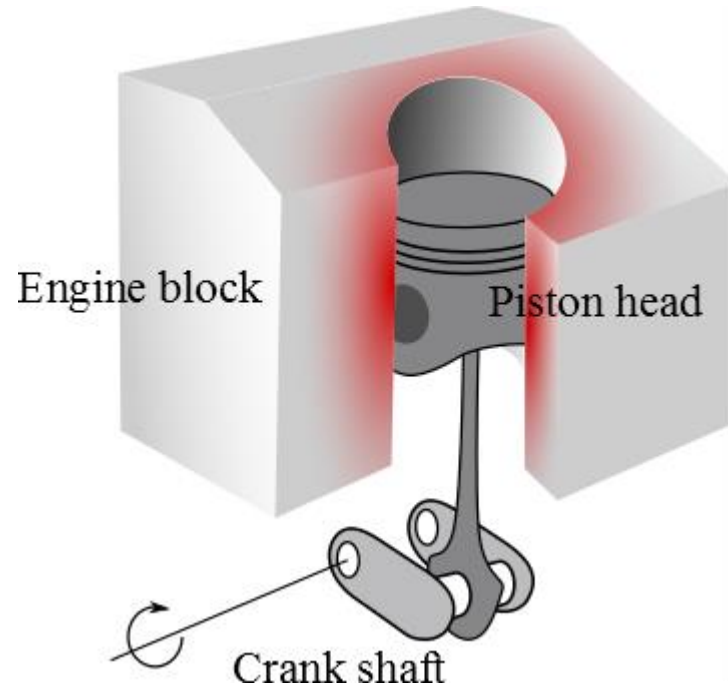
# Outline

- Background and Methodology
- Results
  - TMF and TMF-HCF characterisation
  - Fatigue mechanisms
- Conclusions



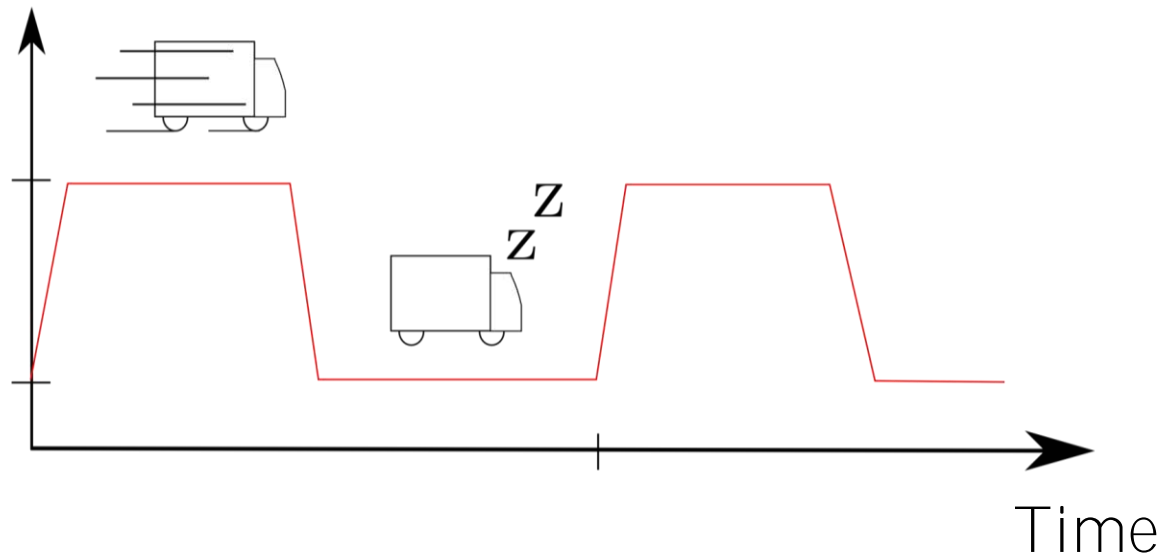
# Engine materials

- Mechanical loads
  - Heat
  - Corrosion
  - Vibrations
- Fatigue

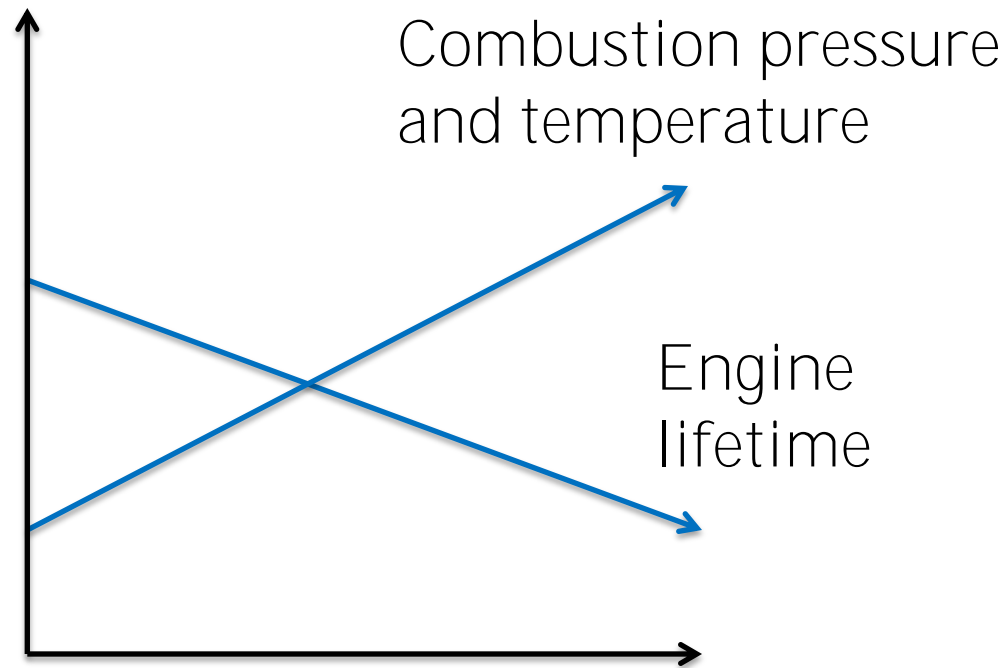


# The start-operate-stop cycle

Engine temperature



# Increasing engine efficiency



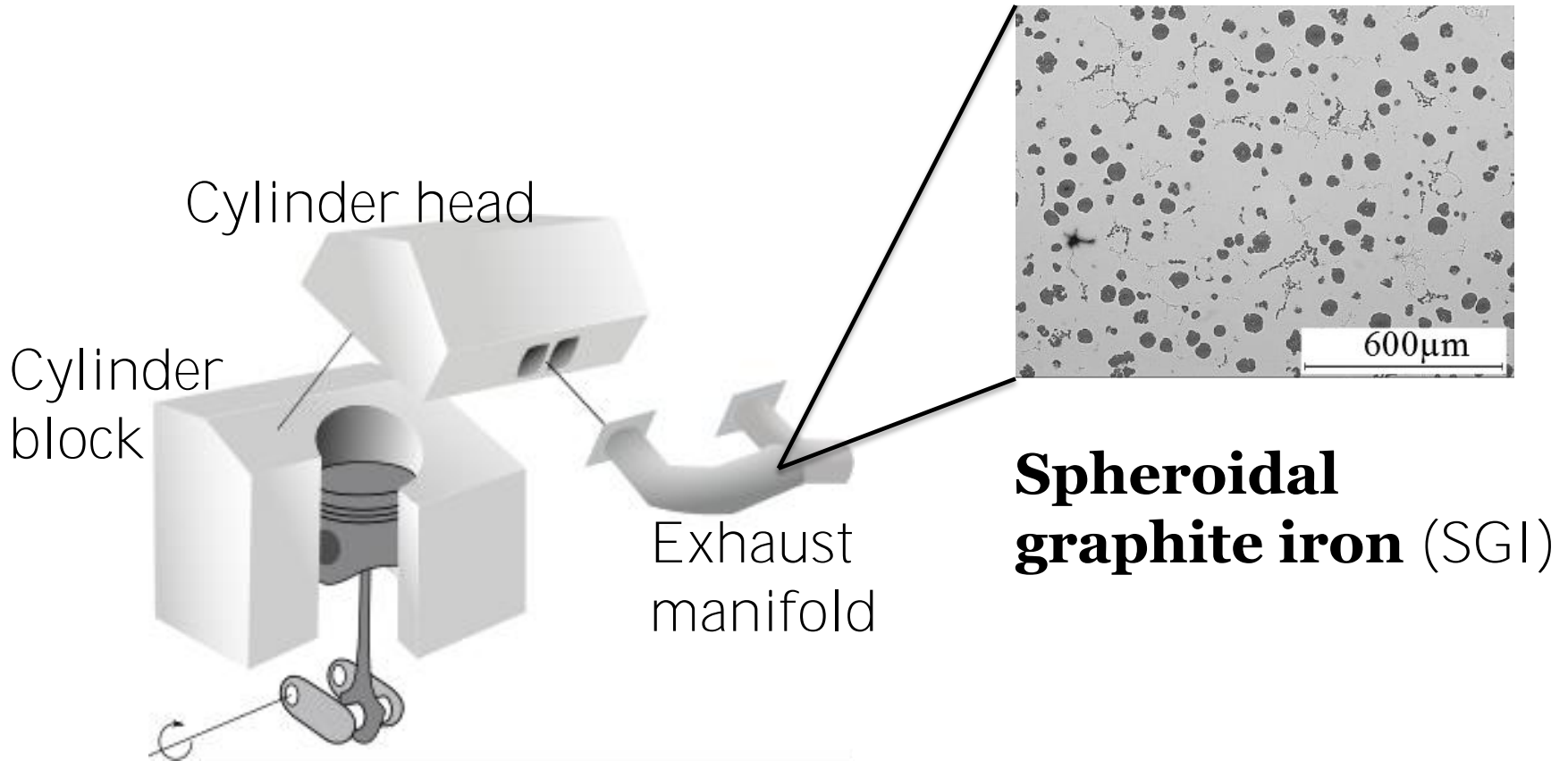
# Research purpose

To push the engine efficiency without risking reduced engine durability

# Strategies

- Replace the material
- Detailed redesign

# The Exhaust manifold



# Investigation objectives

- I) Experimentally study the fatigue mechanisms
- II) Determine the factors controlling the TMF properties

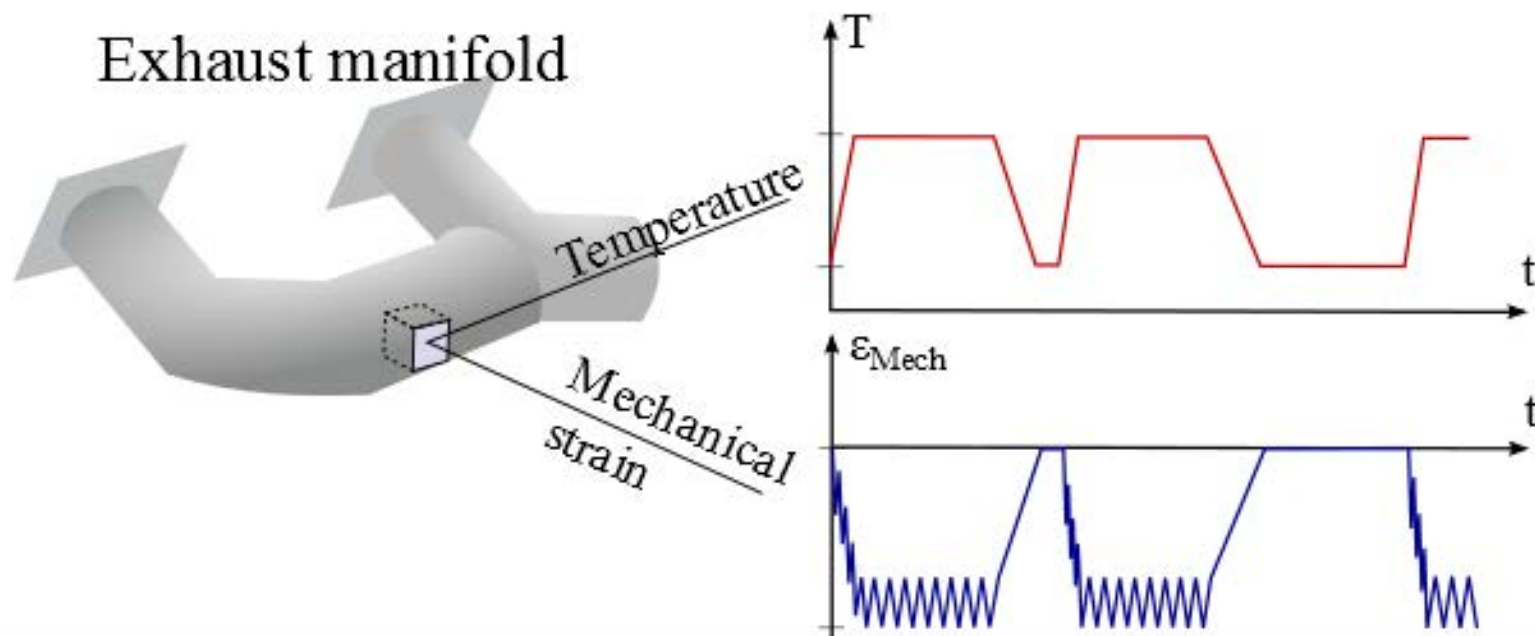
# Methodology



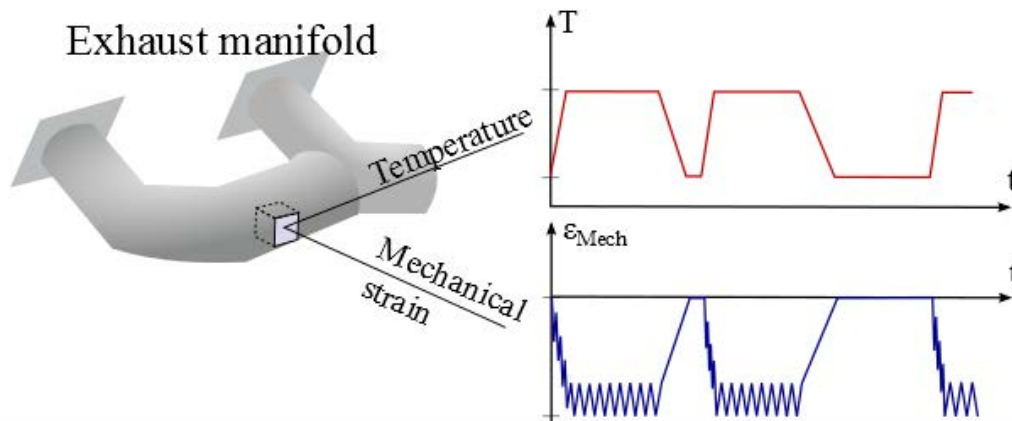
# Experimentals

- TMF and TMF-HCF tests
- Metallographic investigations

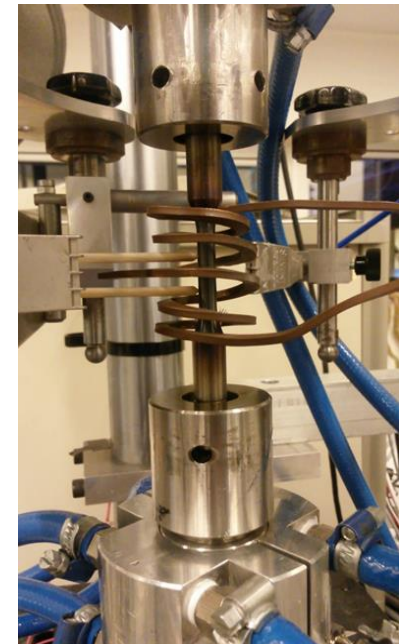
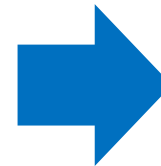
# Experimentals



# Experimental – TMF and TMF-HCF

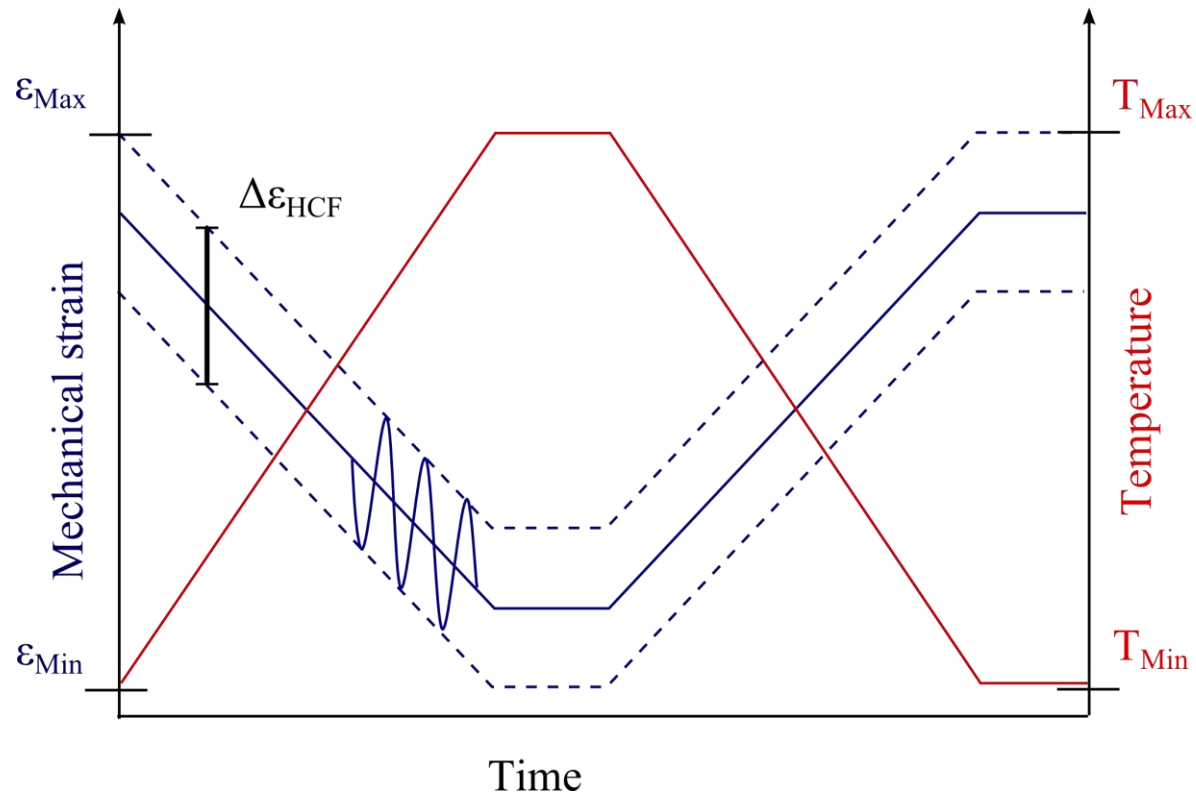


Reality

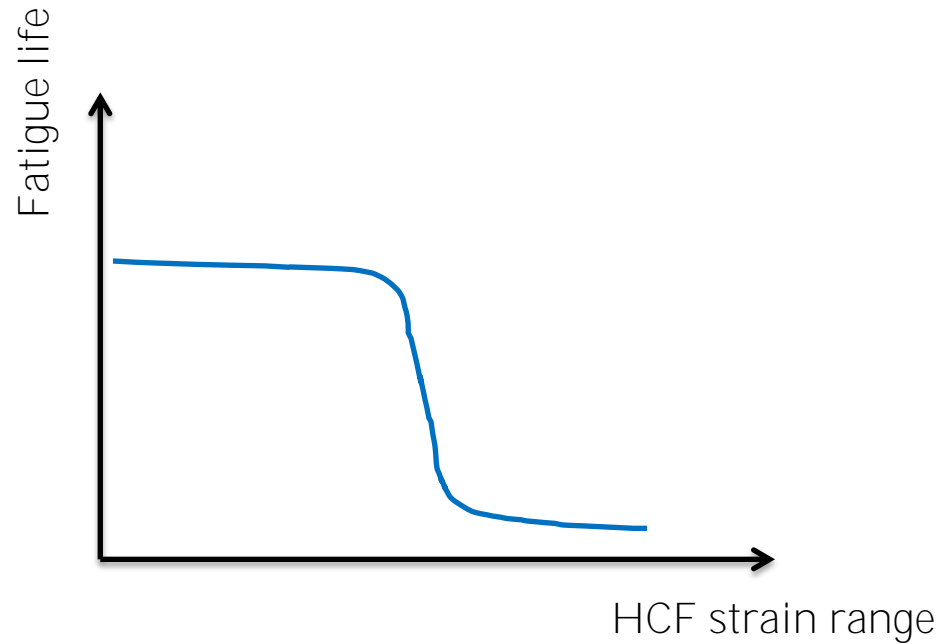


Laboratory

# Experimental - The representative load cycle



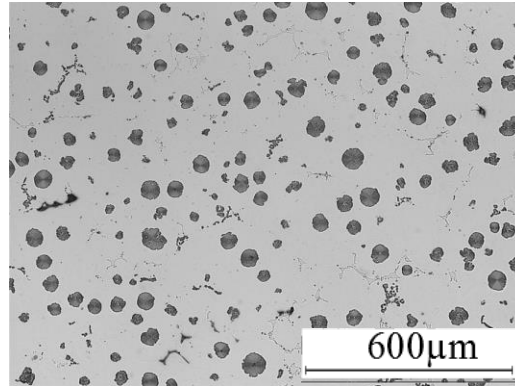
# TMF-HCF characterisation



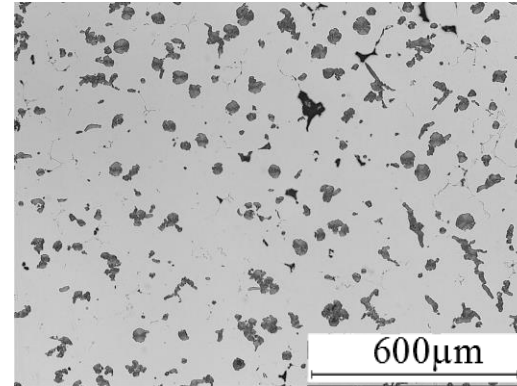
TMF-HCF plot

# Spheroidal graphite irons (SGI)

- Silicon and Molybdenum (SiMo) SGI:
  - EN-GJS-SiMo5-1 (two cooling conditions)
  - SiMo1000



SiMo51



SiMo1000

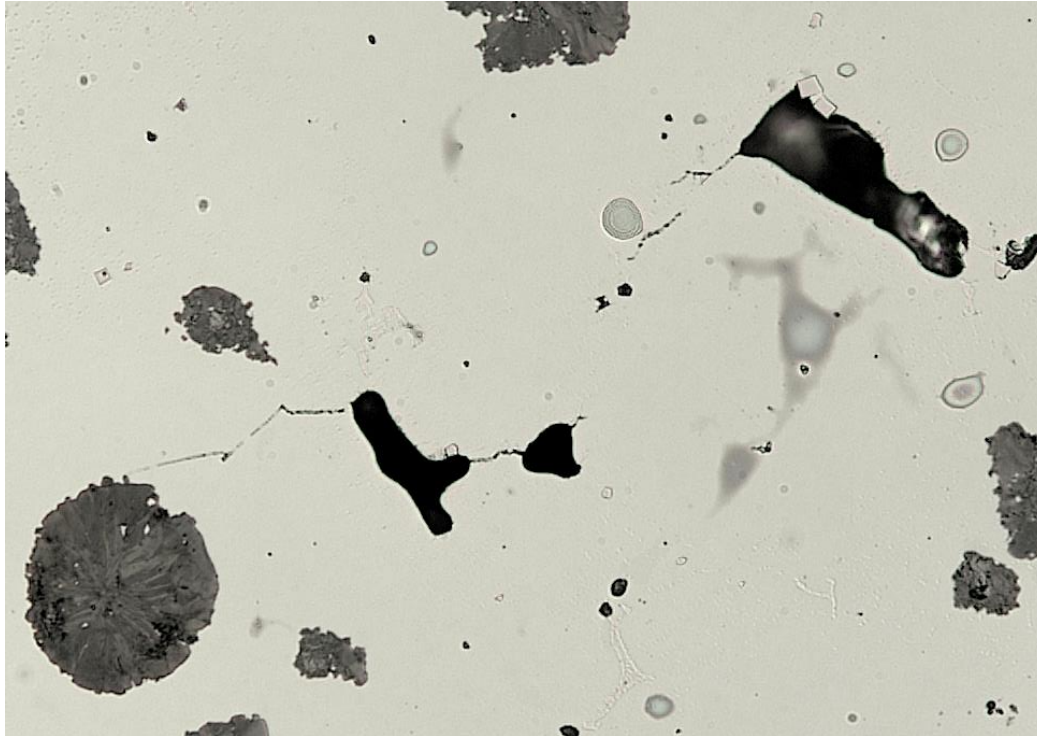
# Spheroidal graphite irons (SGI)

- EN-GJS-SiMo5-1
  - Nodular, ferritic
    - SiMo51 SC, 2.5°C/s
    - SiMo51 RC, 3.5°C/s
- SiMo1000
  - Nodular+compacted, ferritic

# Results: TMF and TMF-HCF characterisation



# Our experience

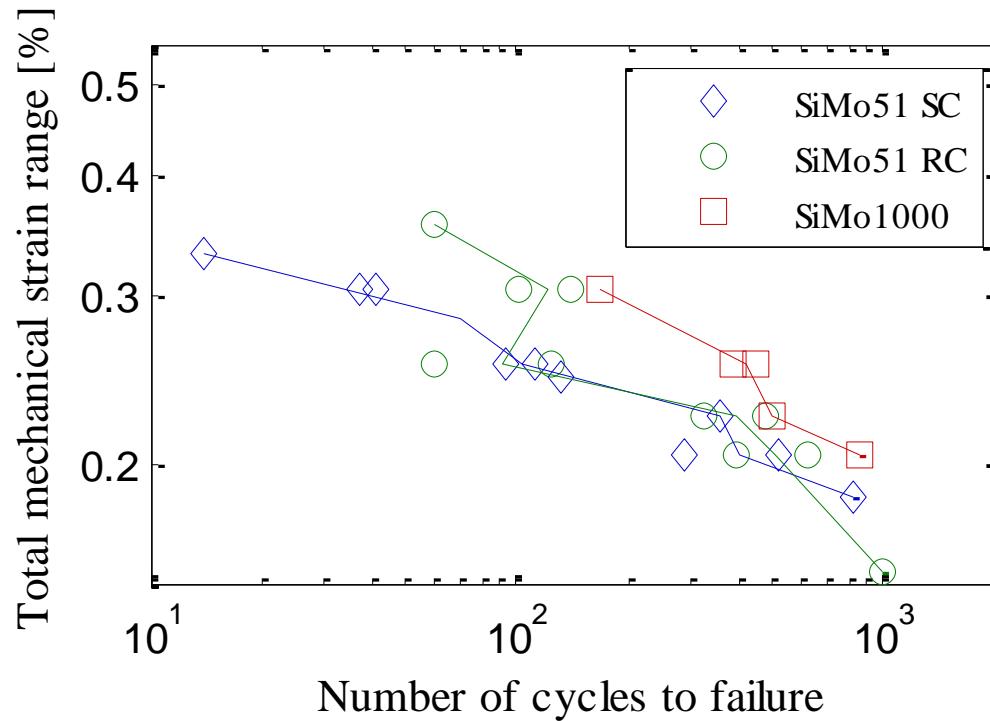


TMF, 100-500°C, SiMo51

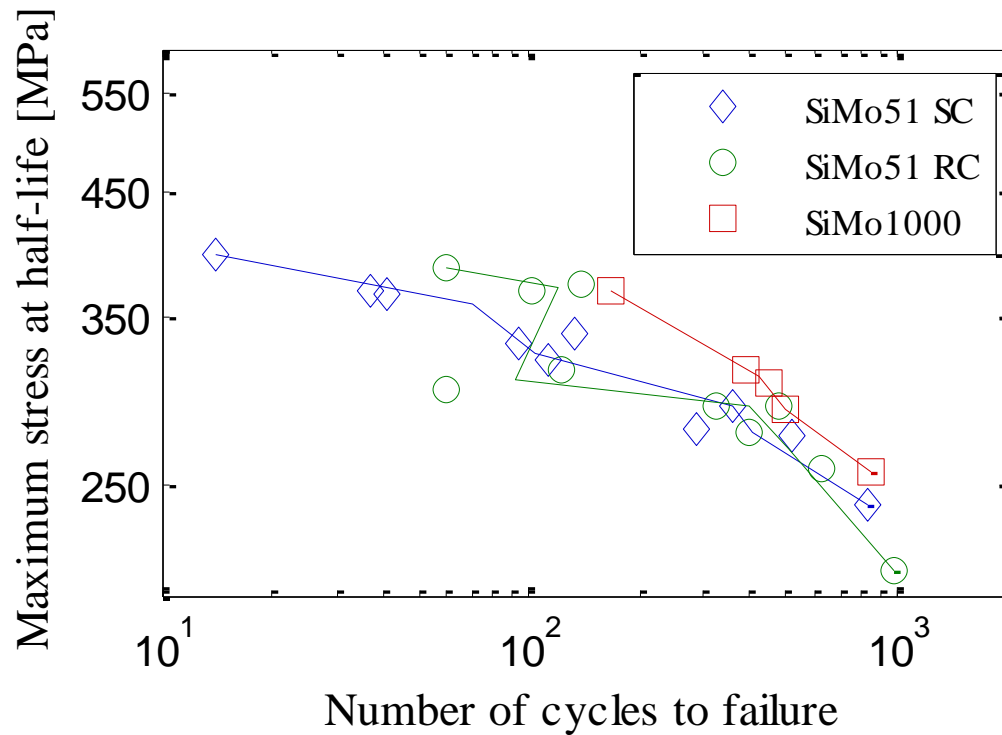
# Casting defects

	Maximum size [ $\mu m$ ]	Average size [ $\mu m$ ]	Density [ $mm^{-2}$ ]
SiMo51 SC	278.7	$92.0 \pm 56.0$	0.80
SiMo51 RC	143.4	$75.4 \pm 23.8$	0.90
SiMo1000	282.9	$96.5 \pm 47.5$	2.34

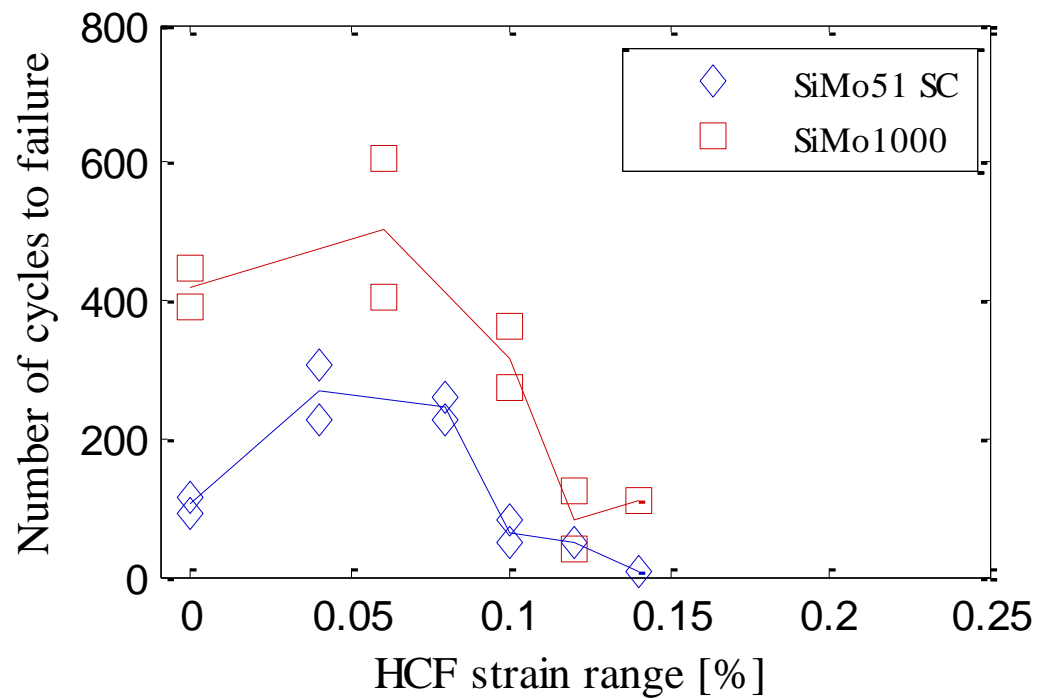
# Thermo-mechanical fatigue (TMF) characterisation



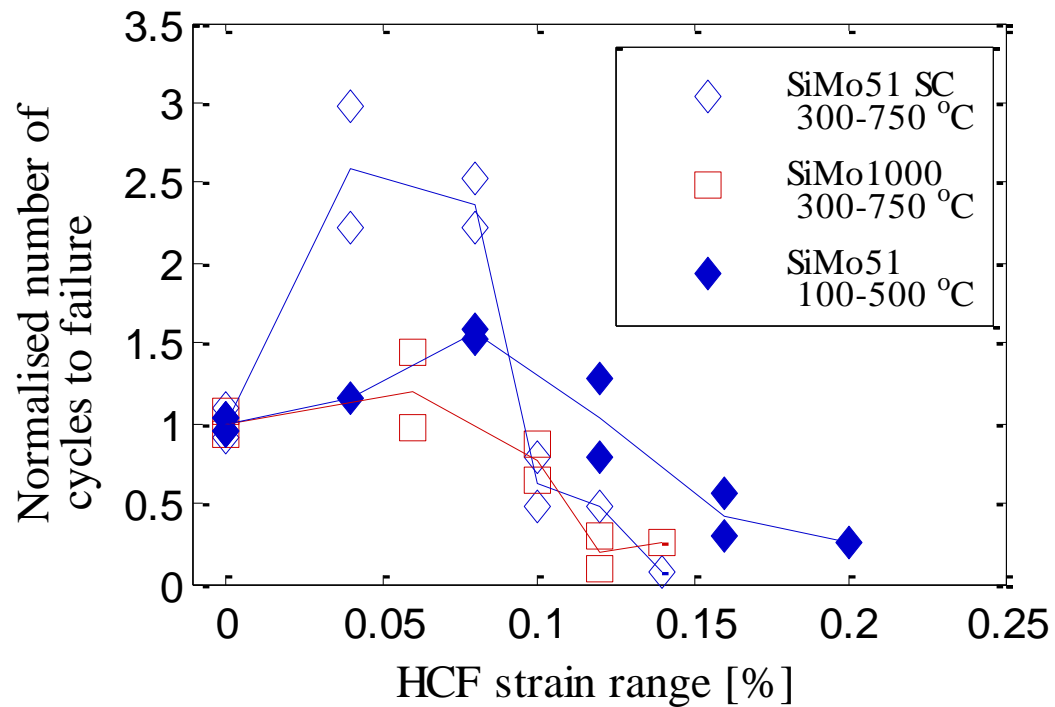
# Thermo-mechanical fatigue (TMF) characterisation



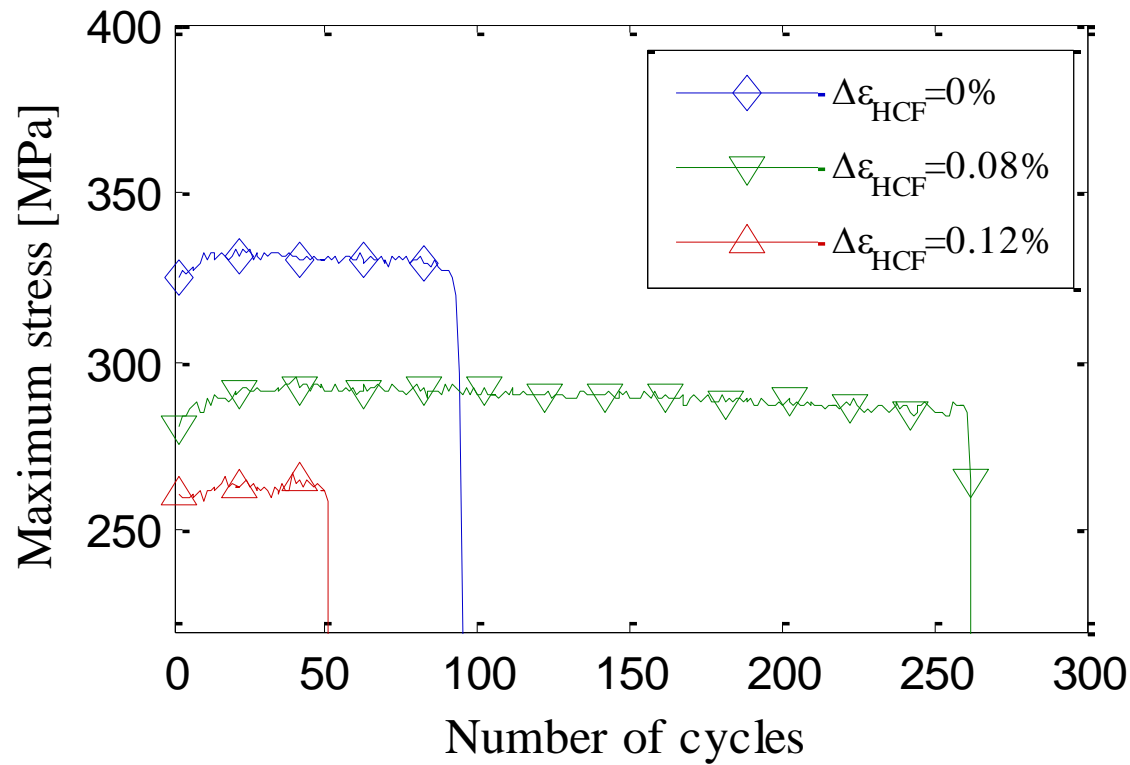
# TMF-HCF characterisation



# TMF-HCF characterisation



# TMF-HCF characterisation



Results:

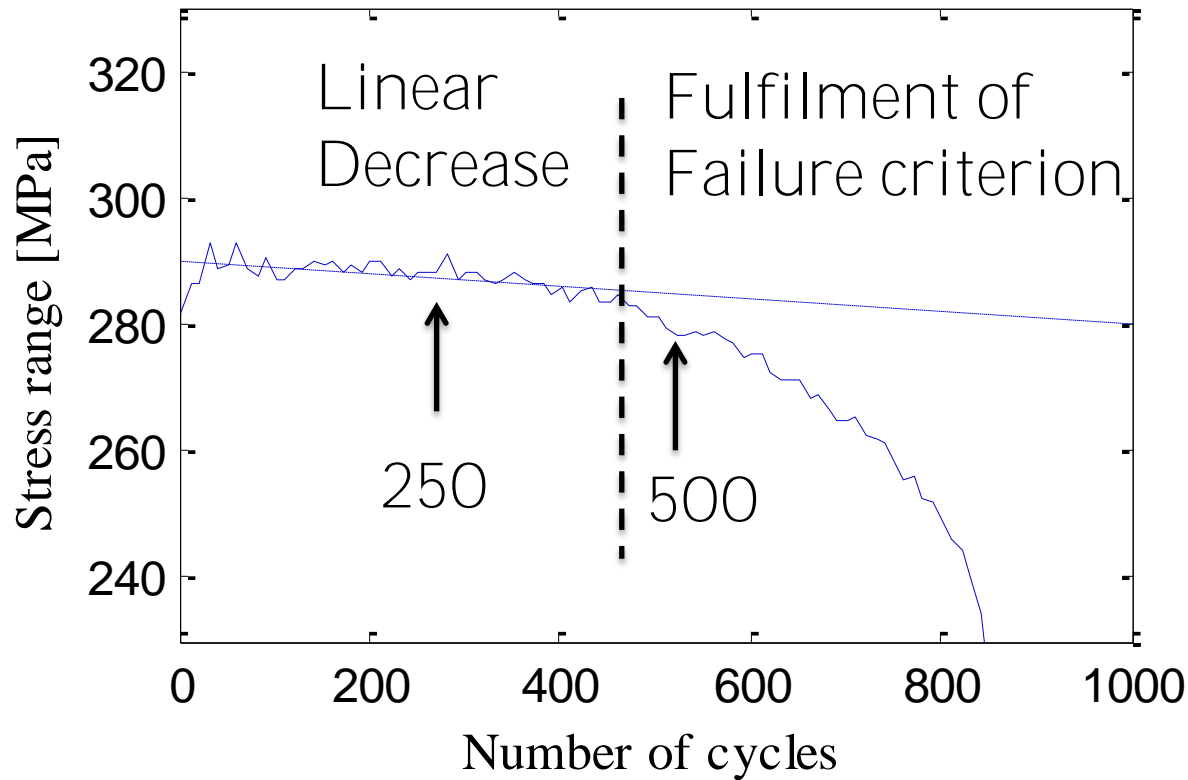
Fatigue mechanisms in TMF



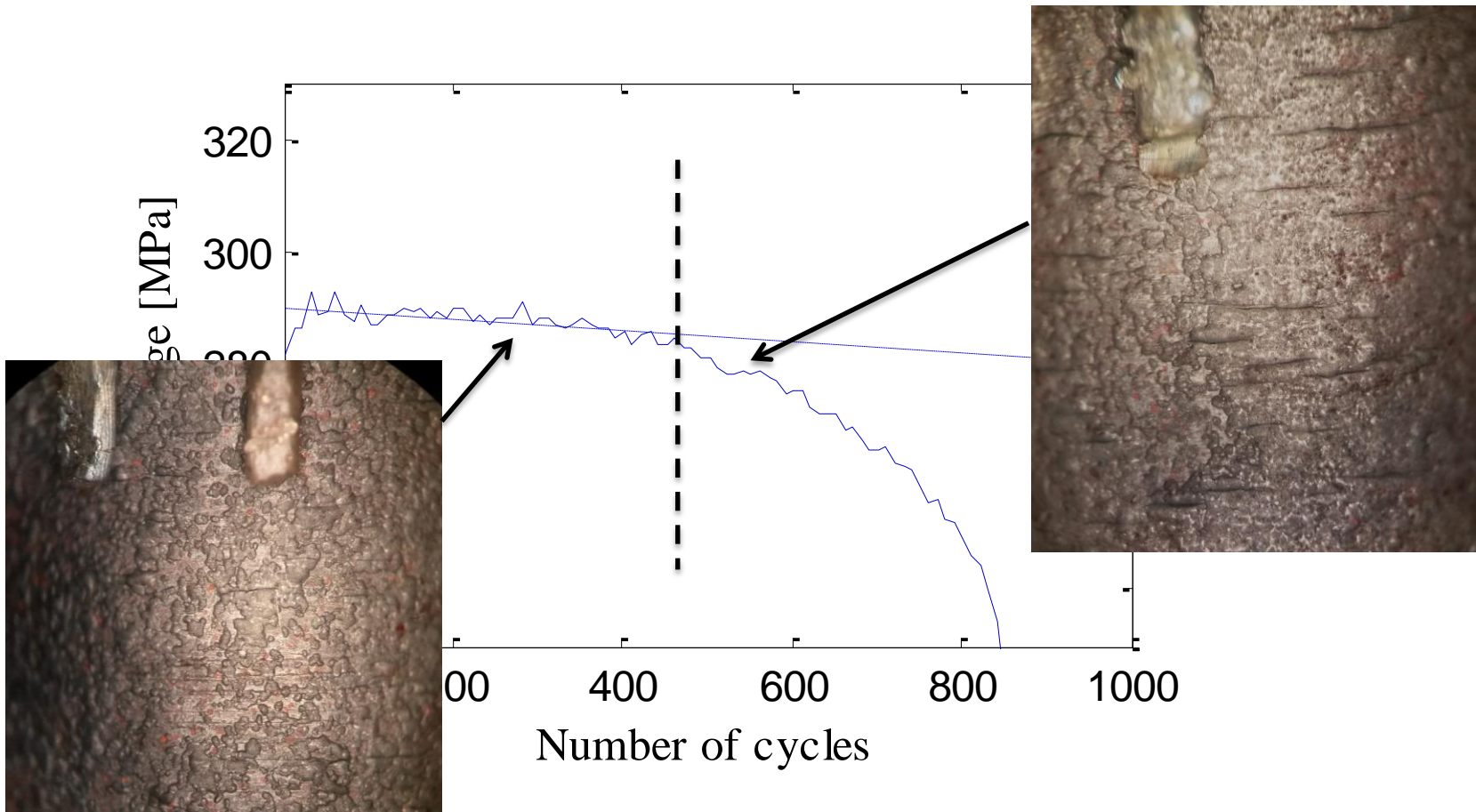
# Interrupted tests

- SiMo51 SC
  - After 250 and 500 cycles
- SiMo51 RC and SiMo1000
  - After 250

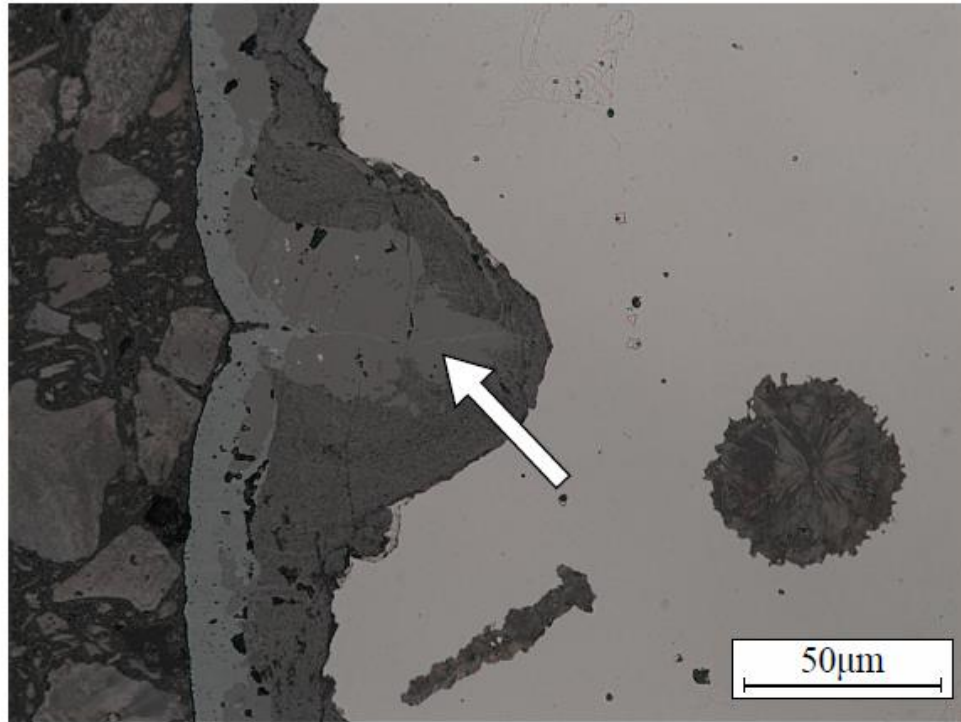
# Interrupted tests, SiMo51 SC



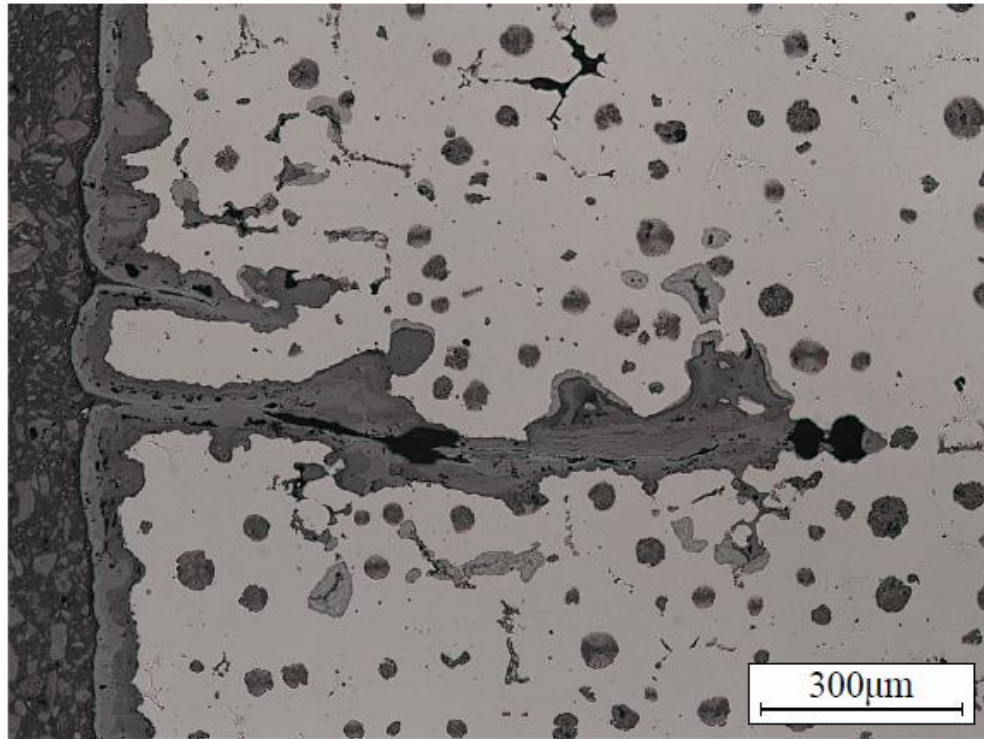
# Interrupted tests, SiMo51 SC



# SiMo51 SC, 250 cycles

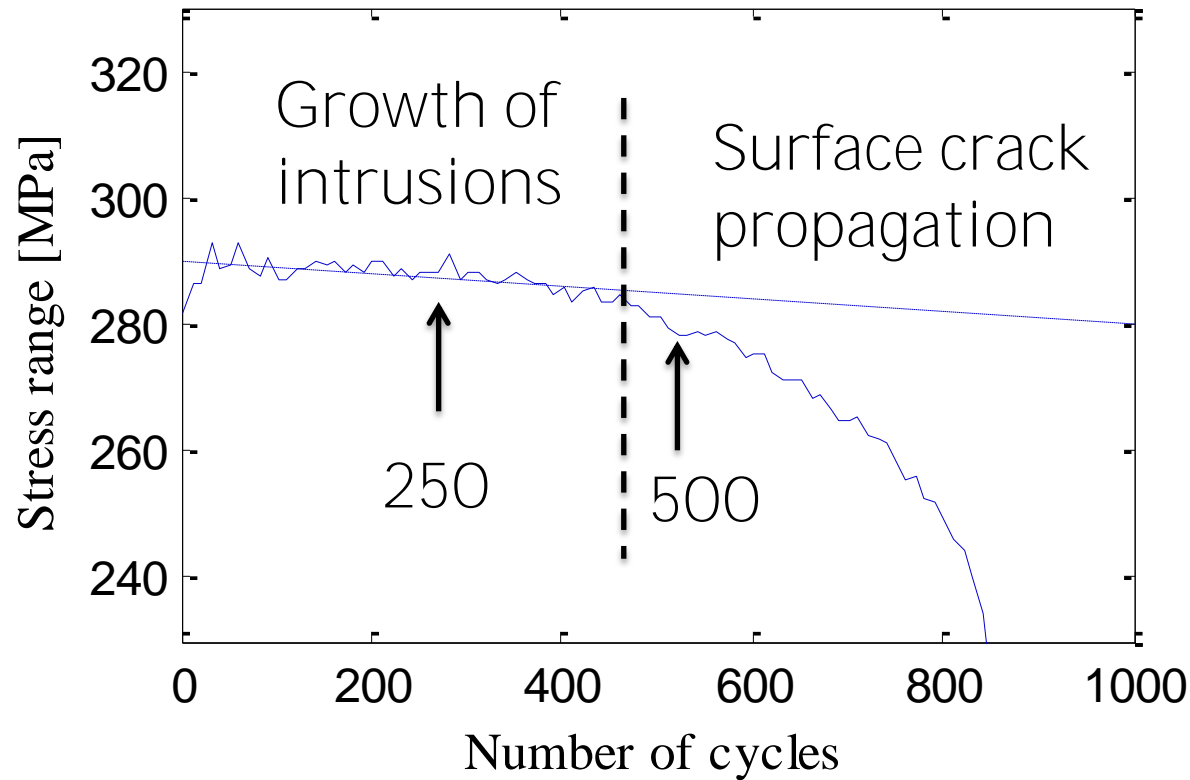


# SiMo51 SC, 500 cycles

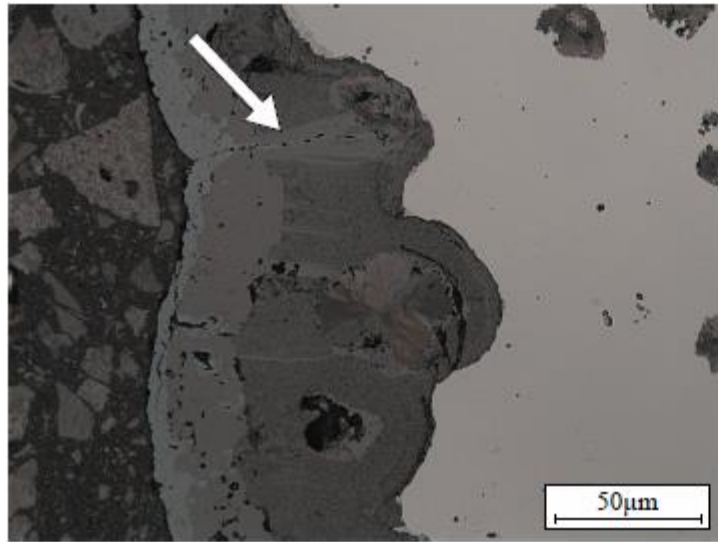


500 cycles, SiMo51

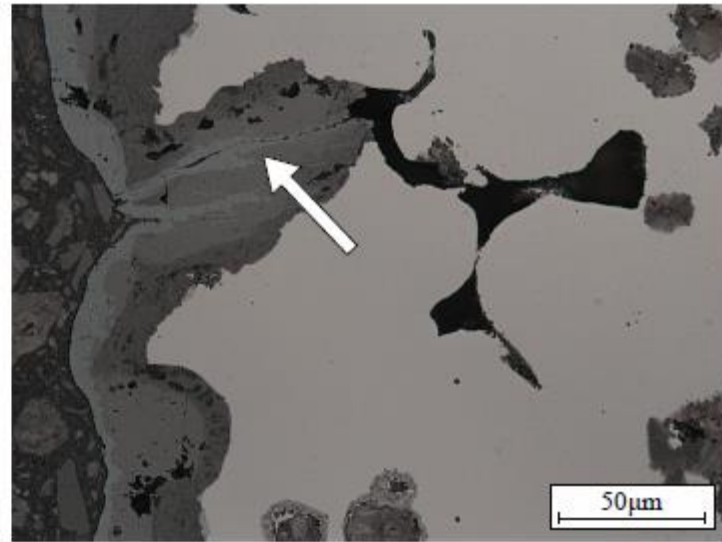
# Interrupted tests, SiMo51 SC



# Interrupted tests: TMF



250 cycles, SiMo51 RC



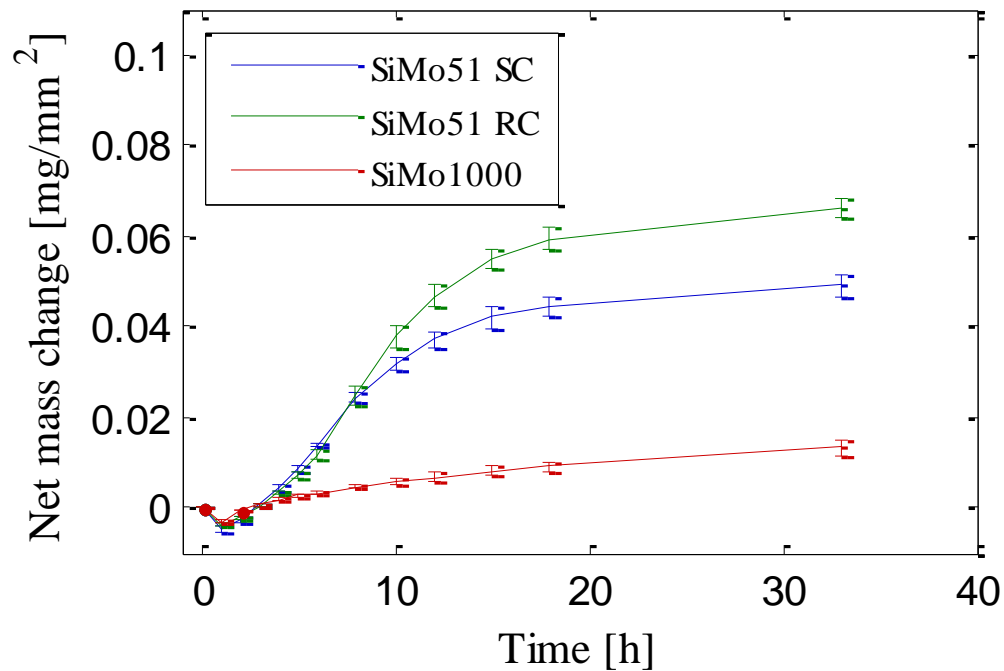
250 cycles, SiMo1000

# Metallographic comparison

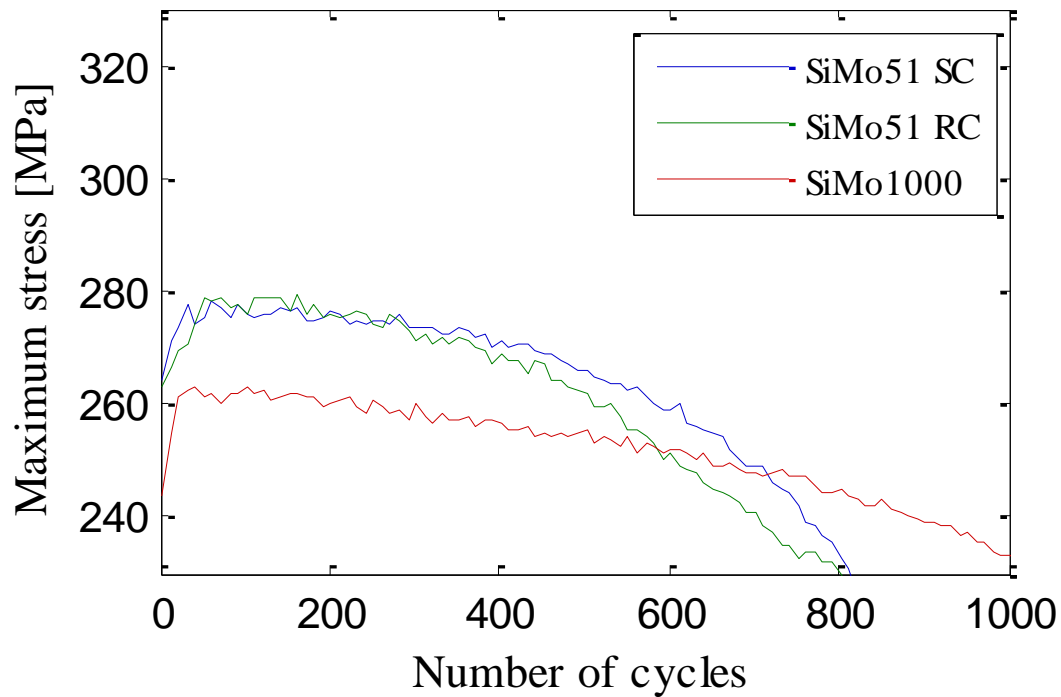
	Maximum length [ $\mu m$ ]	Average length [ $\mu m$ ]
SiMo51 SC	216.0	98.9 $\pm$ 30.0
SiMo51 RC	152.1	109.7 $\pm$ 18.3
SiMo1000	194.9	90.8 $\pm$ 34.5



# Isothermal-exposure oxidation tests



# The difference in maximum stress

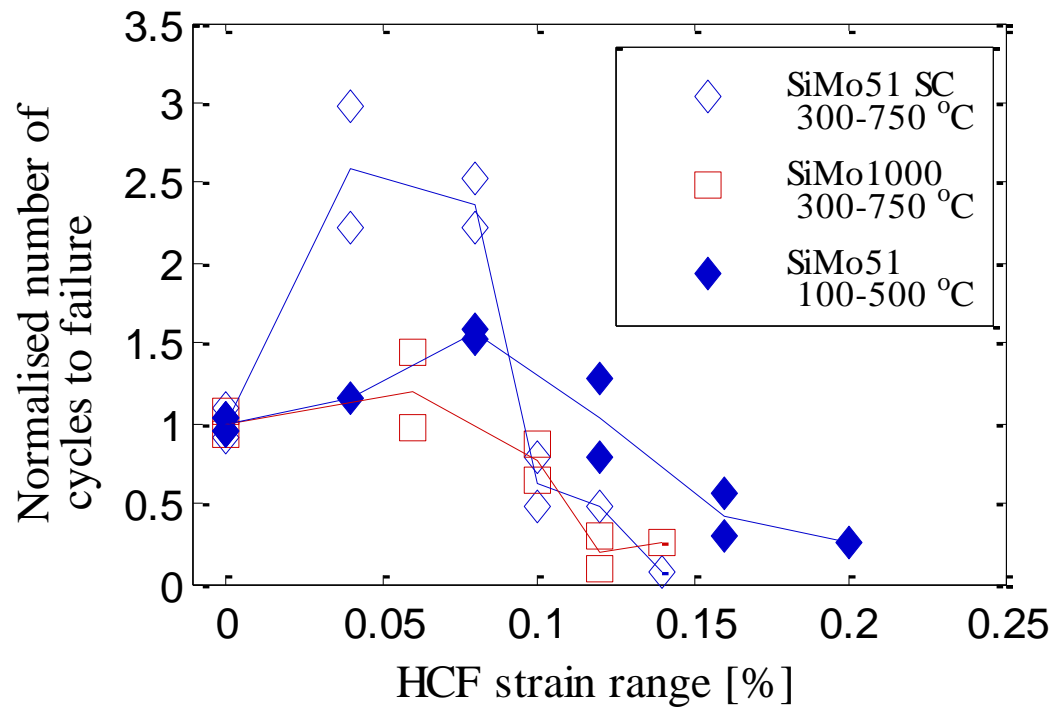


# In conclusion

- The TMF life is more dependent on the stress than the choice of material
- However, oxide intrusions are observed to be favoured by surface defects and low oxidation resistance

# Fatigue behaviour in TMF-HCF

# TMF-HCF characterisation

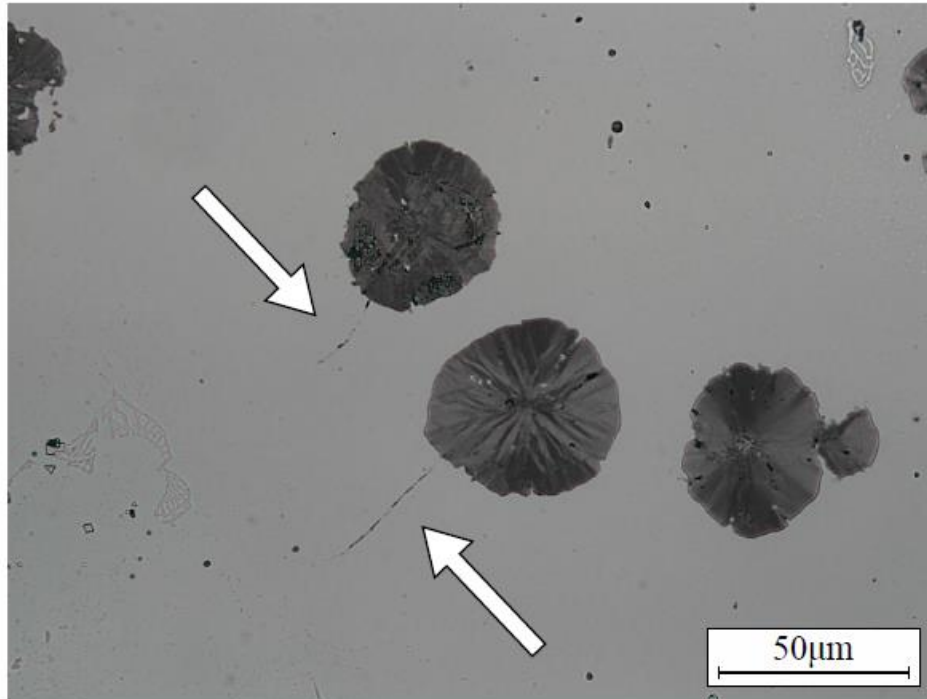


# Interrupted tests: TMF-HCF

	Maximum length [ $\mu m$ ]	Average length [ $\mu m$ ]
SiMo51 SC	216.0	98.9 $\pm$ 30.0
SiMo51 SC, TMF-HCF	232.0	96.6 $\pm$ 33.8

250 cycles, SiMo51,  $\Delta\varepsilon_{HCF} = 0.08\%$

# Interrupted tests: TMF-HCF



250 cycles, SiMo51,  $\Delta\varepsilon_{HCF} = 0.08\%$

# TMF-HCF properties

- Governed by microcracks initiated at internal features such as graphite nodules and casting defects



# Overall conclusions

- The TMF behaviour are governed by the formation of **oxidation intrusion** and the propagation of **surface cracks**
- The TMF-HCF threshold is limited by internal microcrack growth
- The oxide intrusion are affected by oxidation resistance and defect size

[www.liu.se](http://www.liu.se)

*Apr. 27, 2016, Berlin*

# Effect of Ceramic Top Coat on Thermo-Mechanical Fatigue Failure of TBCed Superalloy Specimen.

**M. Okazaki, S. Yamagishi, S. Rajivgandhi**

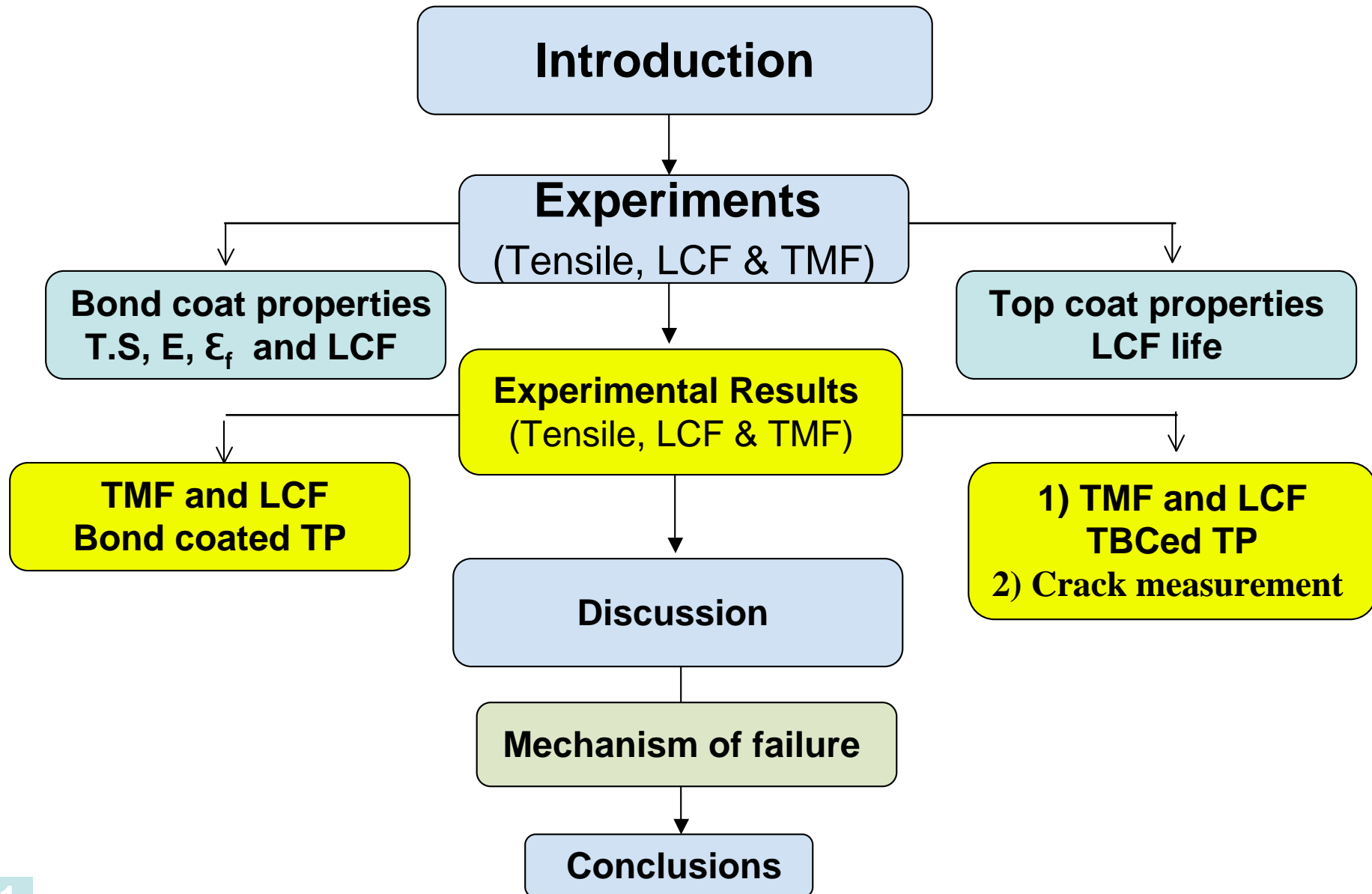


*\*Department of Mechanical Engineering  
1603-1 Kamitomioka-machi, Nagaoka, Niigata,  
Japan.*

*e-mail: [okazaki@mech.nagaokaut.ac.jp](mailto:okazaki@mech.nagaokaut.ac.jp)*

**Acknowledgement:** This work was funded by Grants-in-Aid for scientific research (#25249003) of Japan Society for the Promotion of Science (JSPS).

# METHODOLOGY



*\*Substrate*  
*\*Bond Coated Superalloy*  
*\*TBCed superalloy*  
 +  
*Self-standing bond specimen*

■ Substrate : IN738:

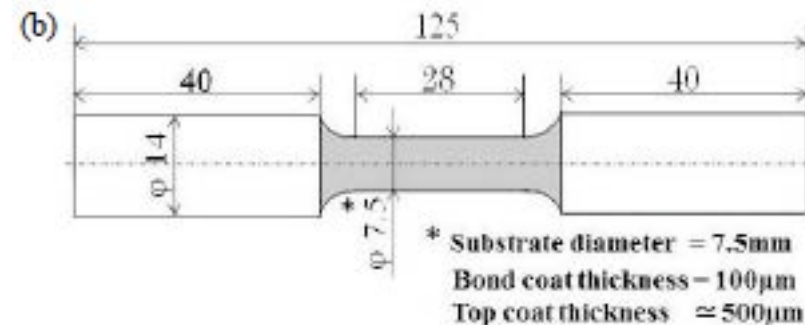
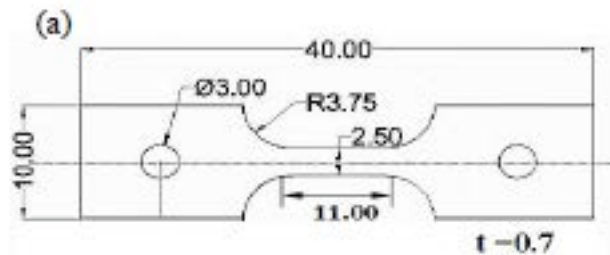
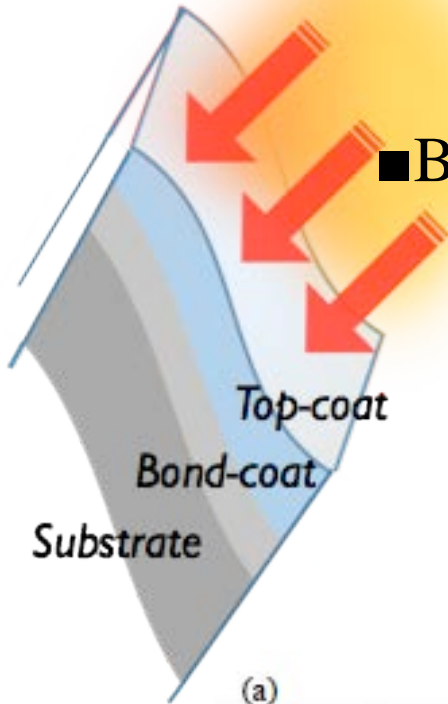
a solution treatment by 1180C for 2 hrs., followed by an aging treatment by 1080 °C for 24hrs.

■ Bond coat : LPPSed CoNiCrAlY (100 μm in thickness)

Co	Ni	Cr	Al	Y
Bal.	32	21	8.5	0.52

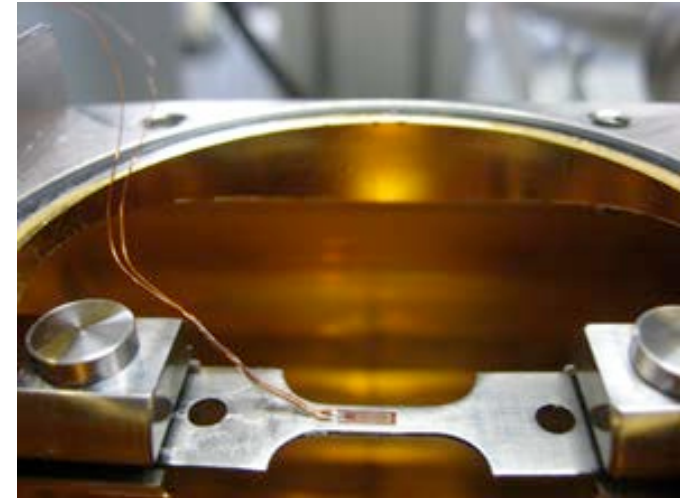
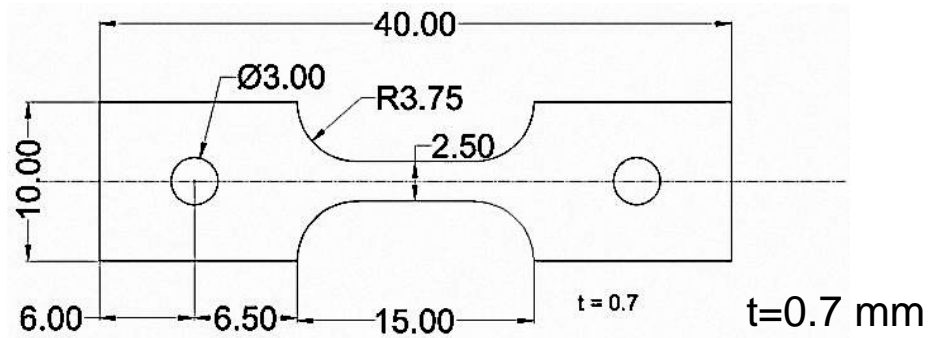
■ Top coat : APSed 8YSZ (500 μm in thick)

ZrO <sub>2</sub>	Y <sub>2</sub> O <sub>3</sub>	CaO	Fe <sub>2</sub> O <sub>3</sub>	SiO <sub>2</sub>	TiO <sub>2</sub>	[wt. %]
Bal.	8.18	0.31	0.3	0.11	0.09	



## 2. Geometry and Composition of the Free standing Bond coat specimen

### Tensile Test Specimen (CoNiCrAlY)



### Composition of the Bond Coat (CoNiCrAlY) specimen

Co	Ni	Cr	Al	Y
Bal.	32	21	8.0	0.52

Tensile Test Equipment

### Test Conditions

Bond coat block  
Coating Block: 15x200x3 mm LPPS  
Aged at 880°C for 1 h;  
Sliced

Strain rate of  $4.1 \times 10^{-4} \text{s}^{-1}$

Temperature: 25 to  
1000°C

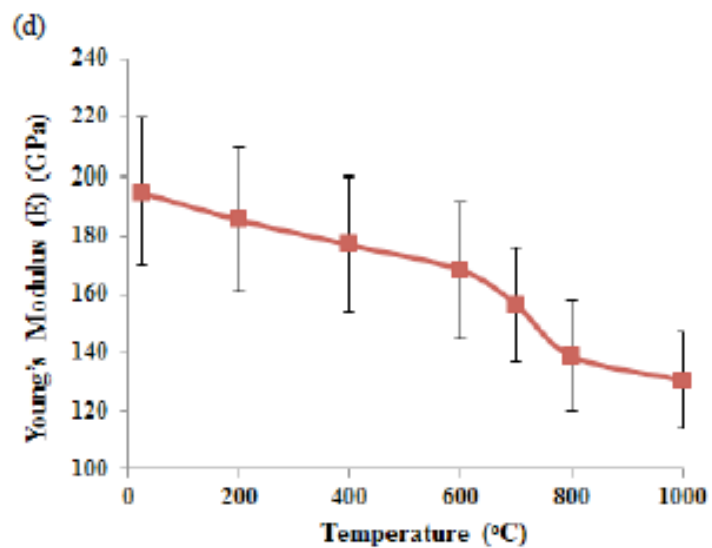
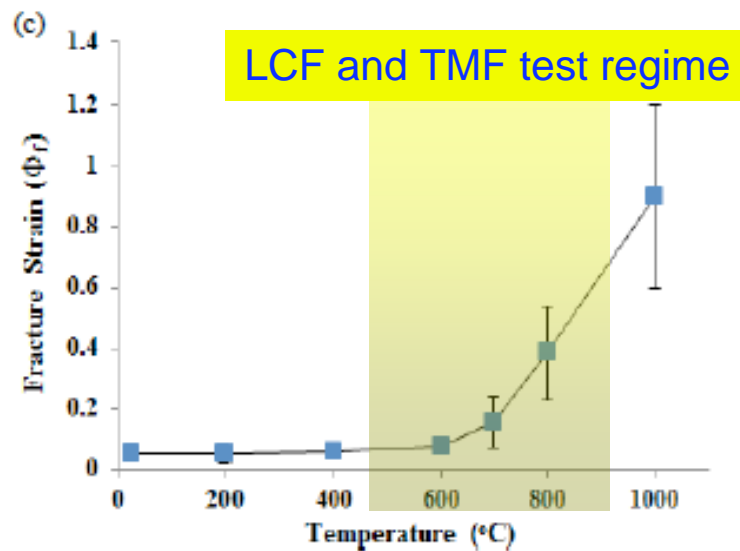
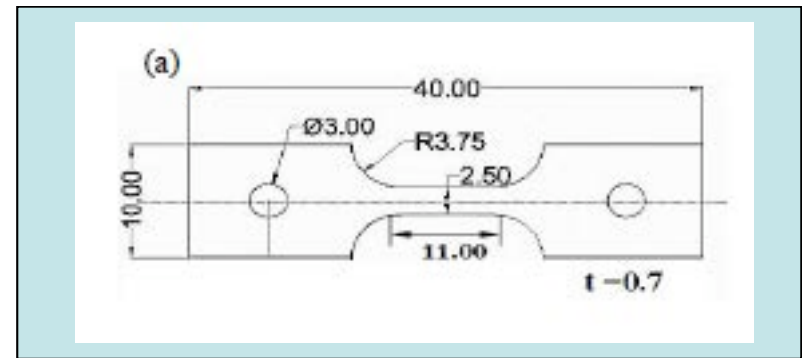
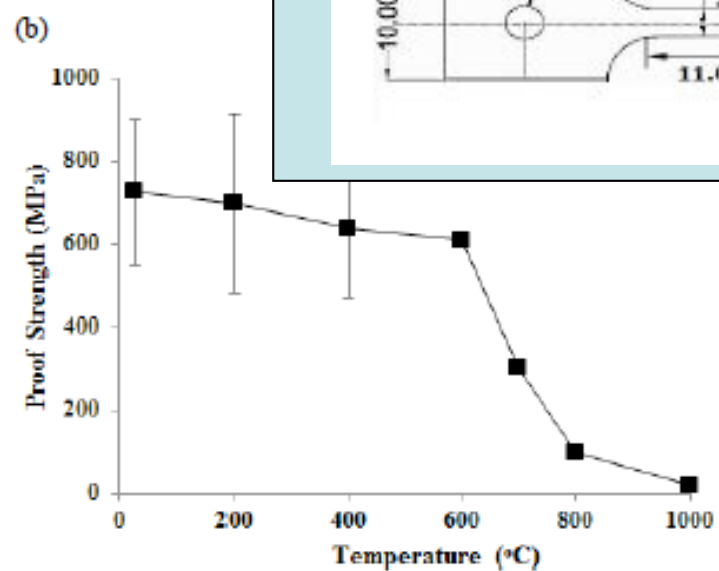
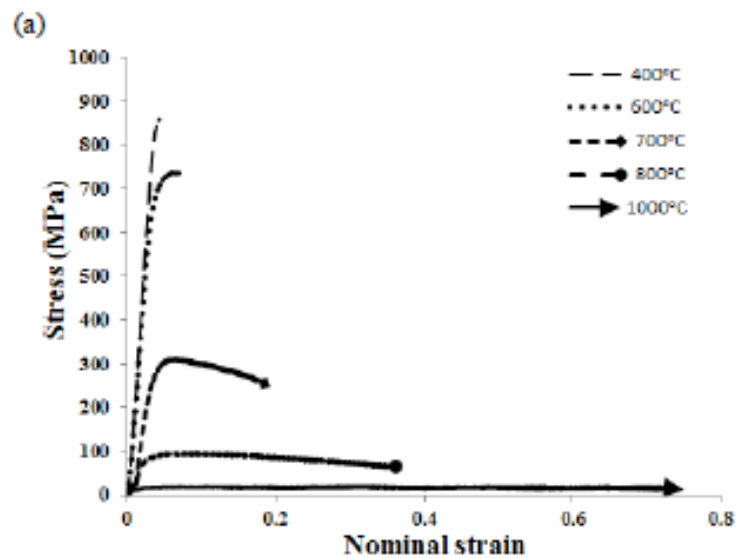


Figure 3. Mechanical properties of CoNiCrAlY bond coat alloy as a function of temperature. (a) stress and strain curve (b) proof strength, (c) fracture strain, and (d) Young's modulus.

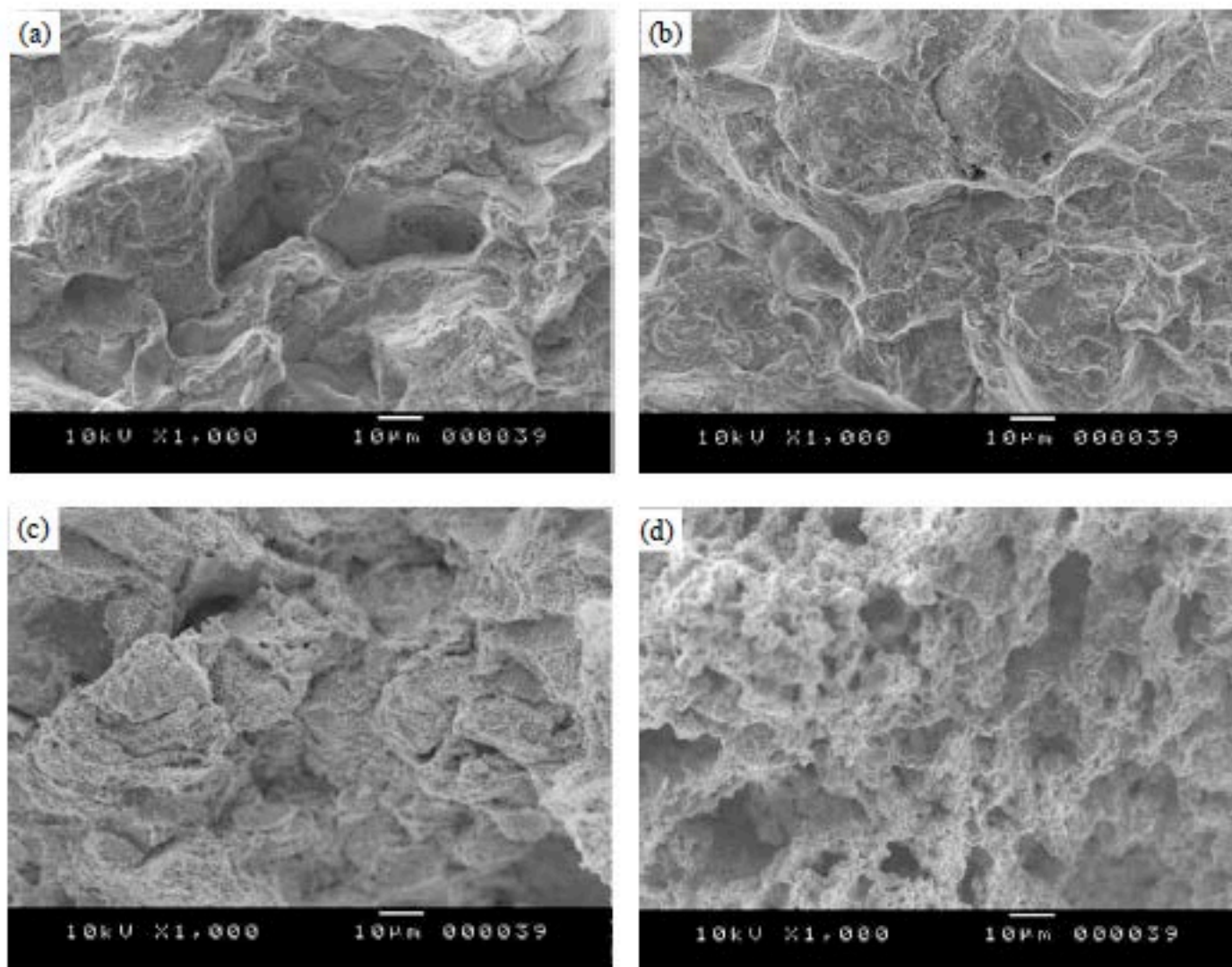
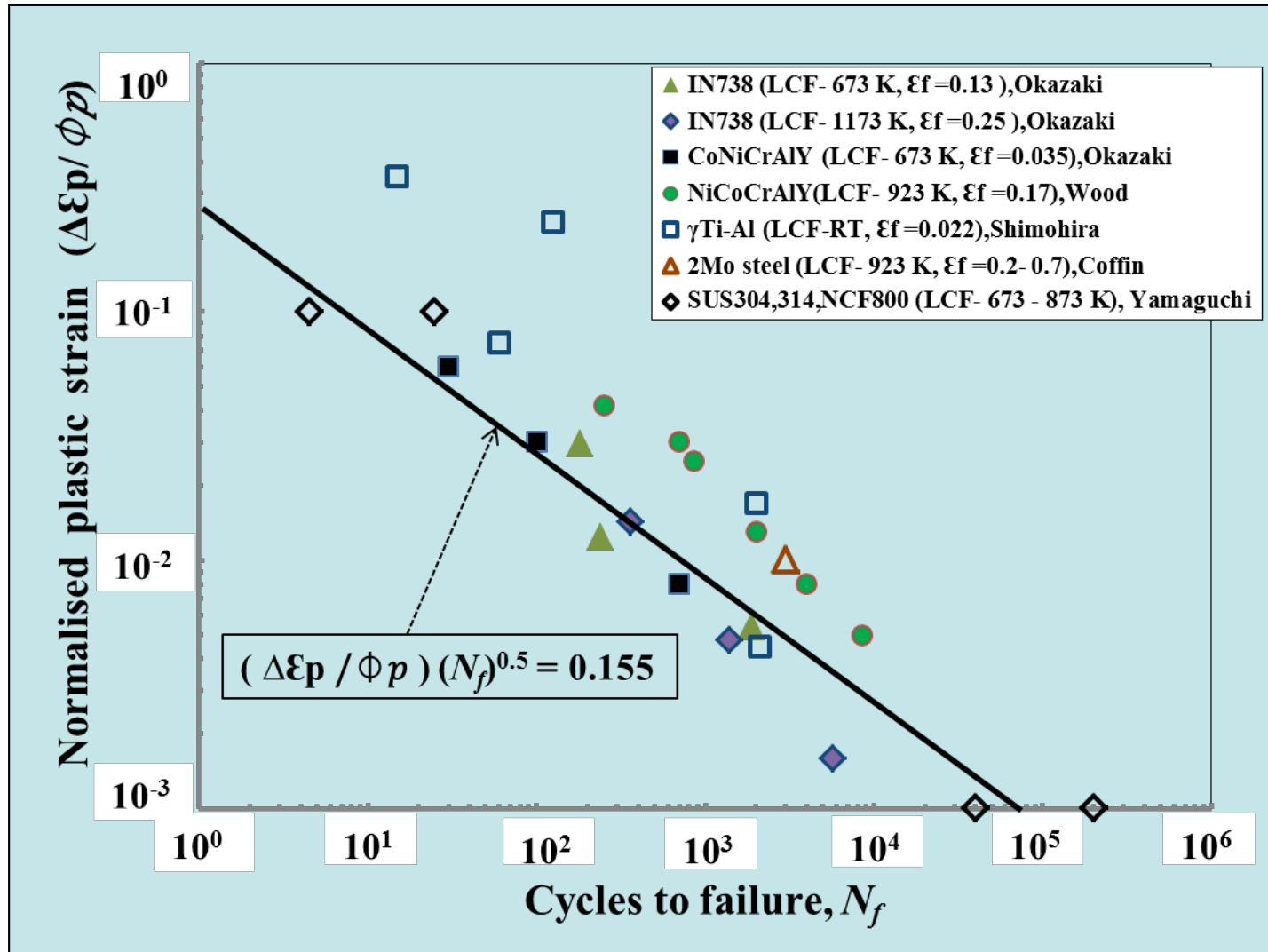


Figure 4. Scanning electron micrographs showing fracture surfaces of the bond coat alloy, (a) 25°C, (b) 600°C, (c) 800°C, and (d) 1000°C.



$$\left( \frac{\Delta \epsilon_p / 2}{\phi_p} \right) (N_f)^a = C', \left\{ \bar{\phi}_p = \frac{1}{T_{max} - T_{min}} \int \phi_p T dt \right\}$$

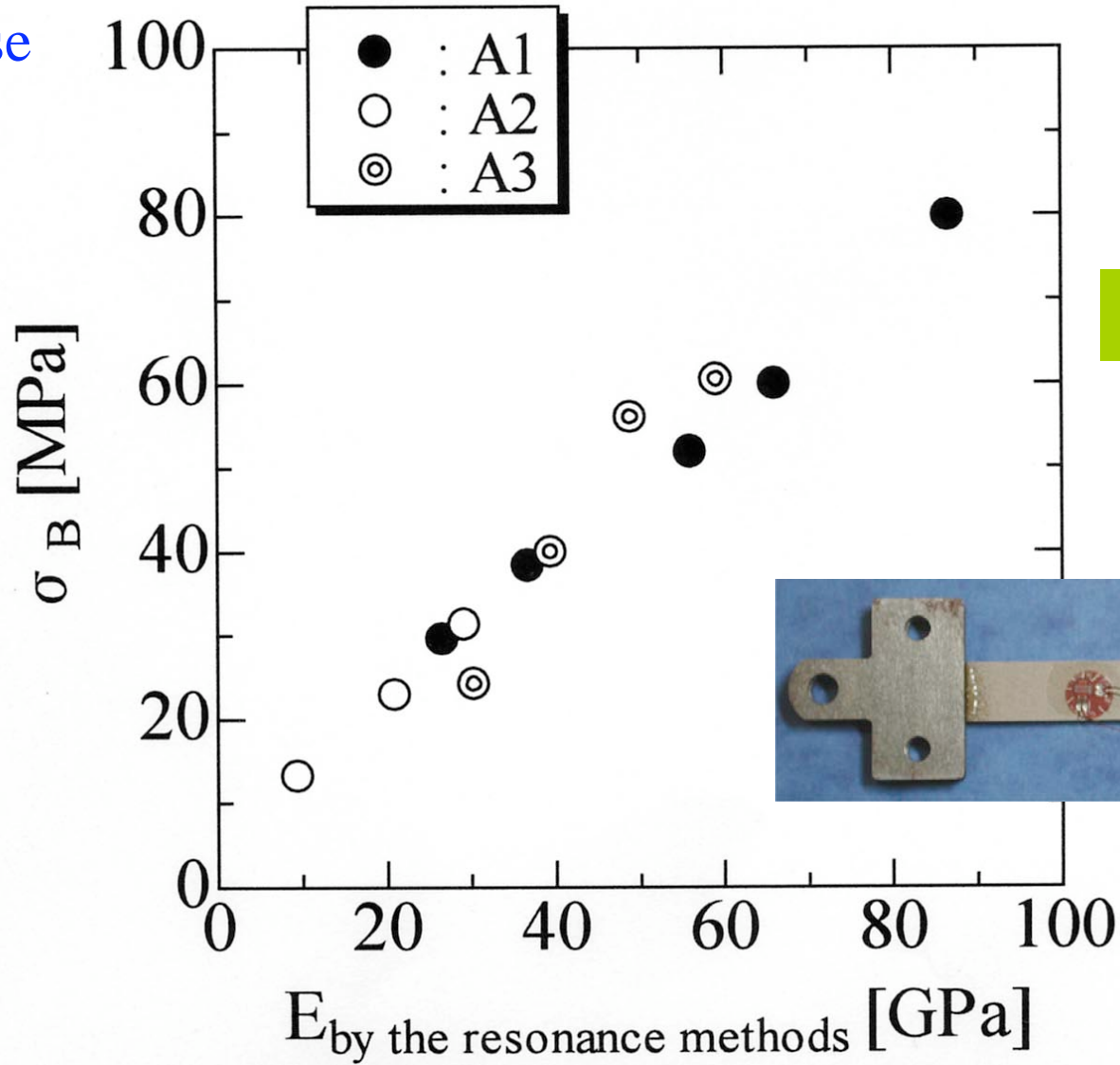
Ductility normalized Manson-Coffin law.



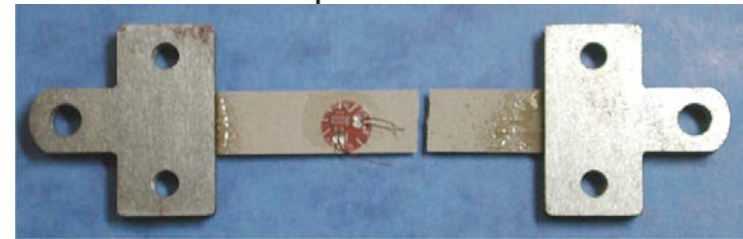
LCF lives of bond coat, as a function of temperature.

Tensile strength of YSZ top coat (collaborative research by JSMS 2011)

Increase with aging



$\epsilon_f = 0.1-0.15 \%$



Increase with aging

# METHODOLOGY

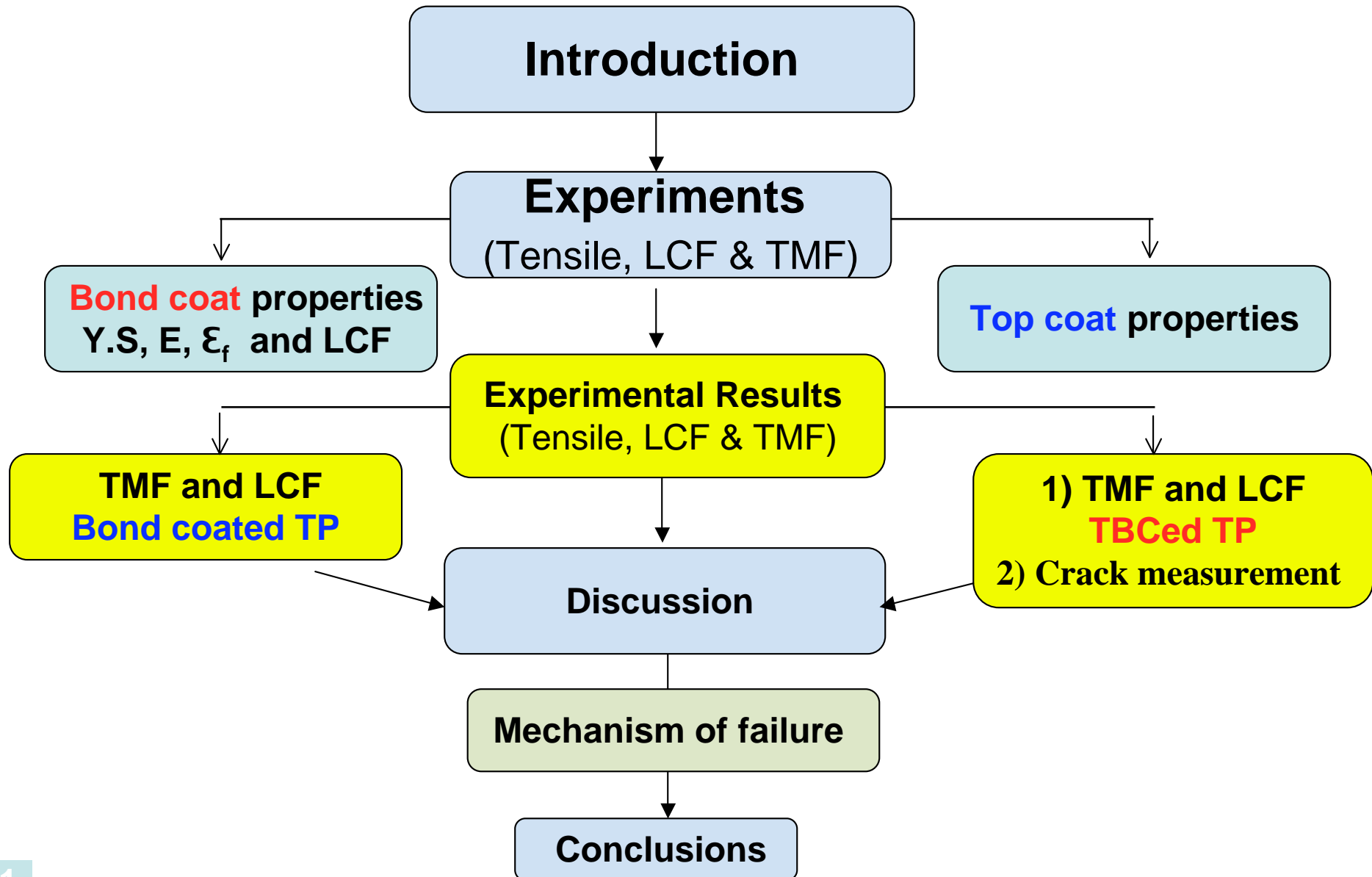


Table 2. Summary of TMF, LCF test conditions

Specimen	Test	$\Delta\epsilon_{mech}$ (%)	Temperature (°C)	Strain rate (1/s)
Substrate, Bond coated, TBCed	LCF	1.0	900	$5.0 \times 10^{-4}$
		0.6		$5.0 \times 10^{-4}$
		0.4		$5.0 \times 10^{-4}$
		0.3		$5.0 \times 10^{-5}$
	LCF	0.6	500 (400)	$5.0 \times 10^{-4}$
	TMF-OP	0.6	500/900 (400/900)	$5.0 \times 10^{-5}$
	TMF-OP	0.4		$3.3 \times 10^{-5}$
TMF-IP	0.6	$5.0 \times 10^{-5}$		
TMF-IP	0.4	$3.3 \times 10^{-5}$		

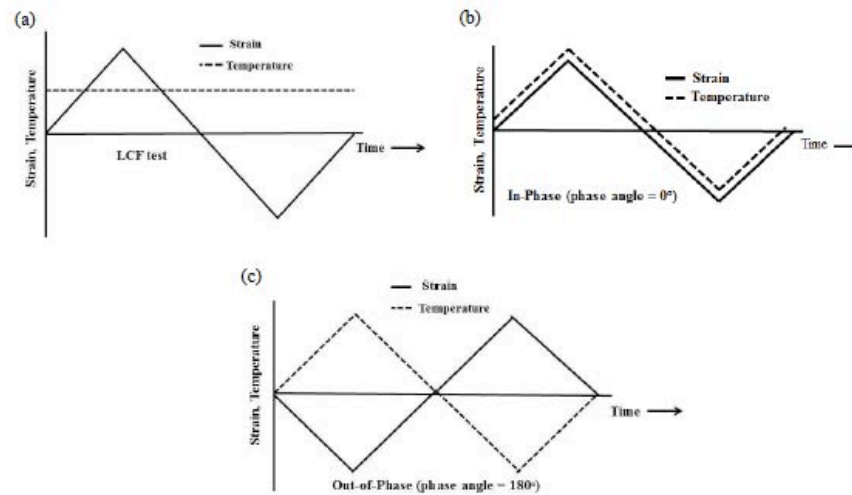
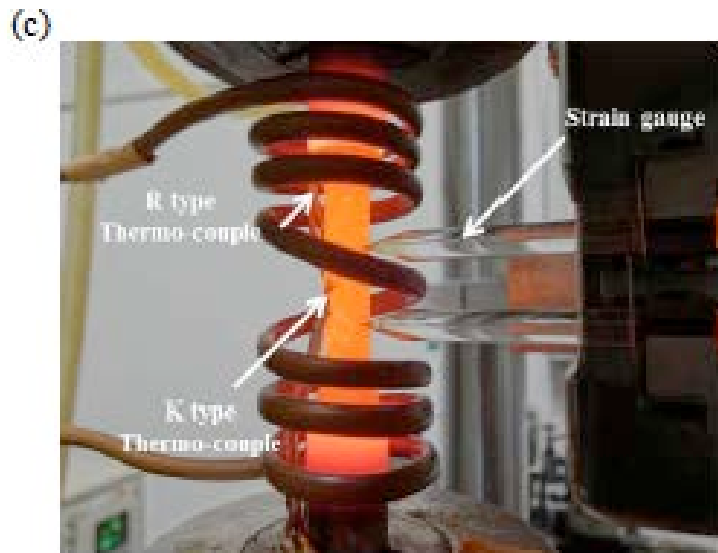
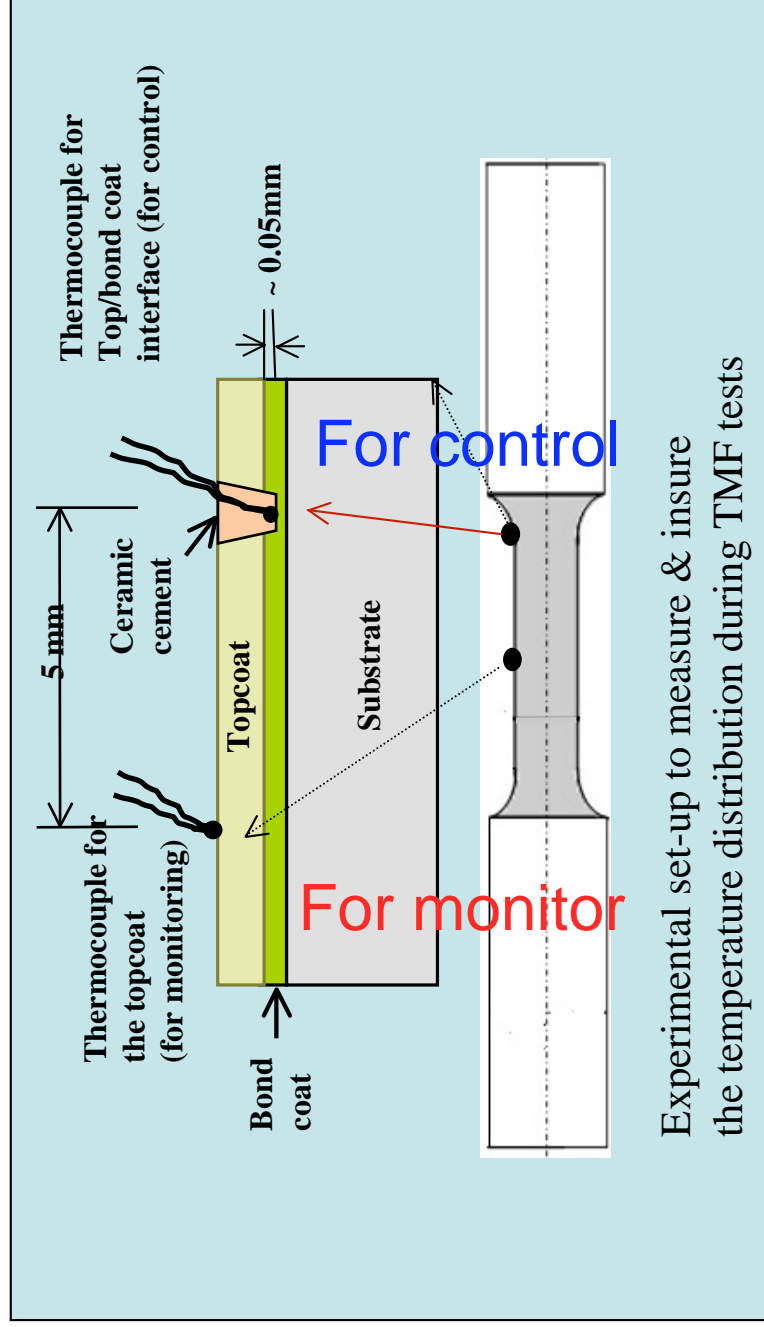
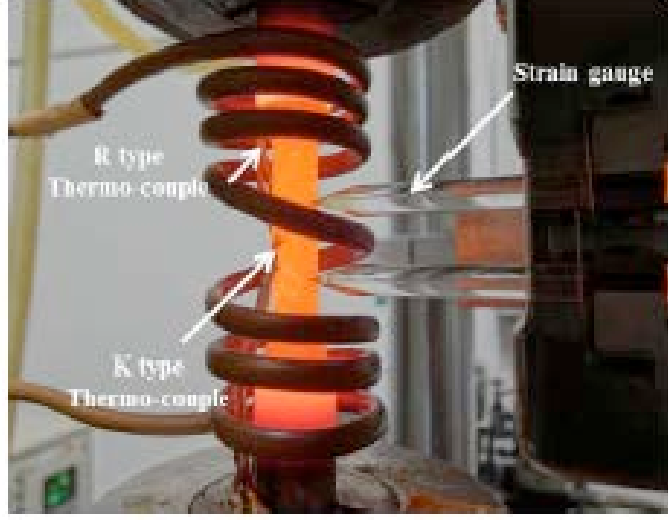
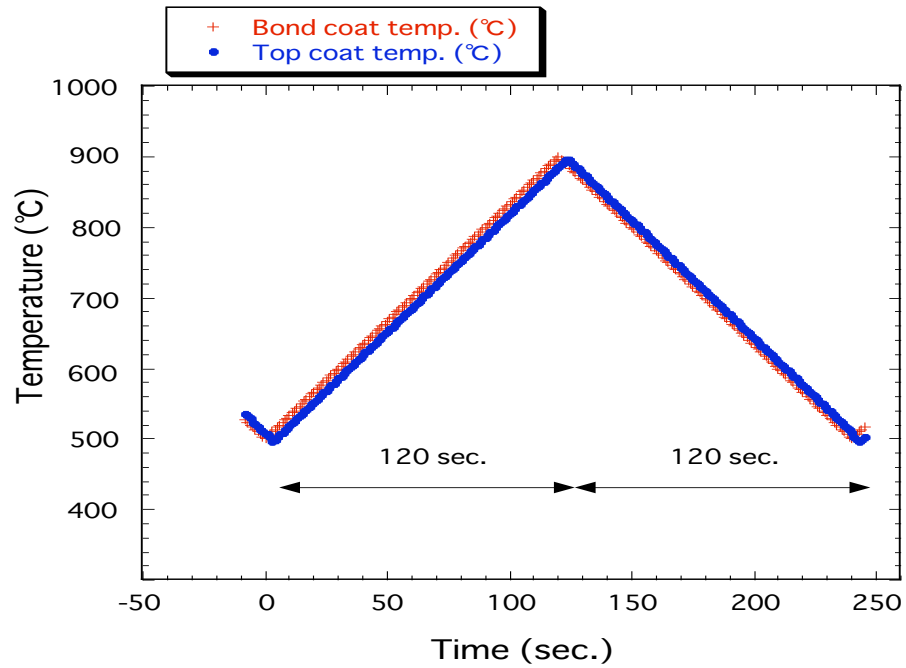


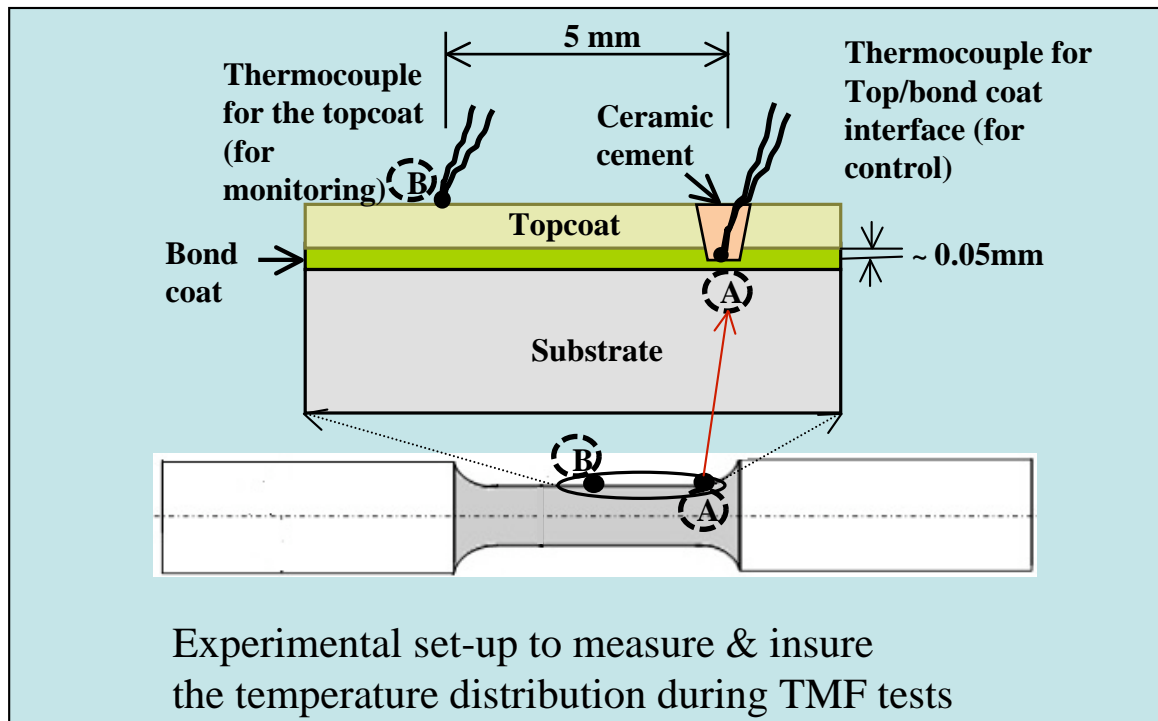
Figure 2. Schematic representation of the thermal and mechanical loading cycles in the : a) LCF test , b) TMF-IP test and c) TMF-OP.

(c)





$$\Delta\varepsilon/dt=5 \times 10^{-5} \text{ sec}$$



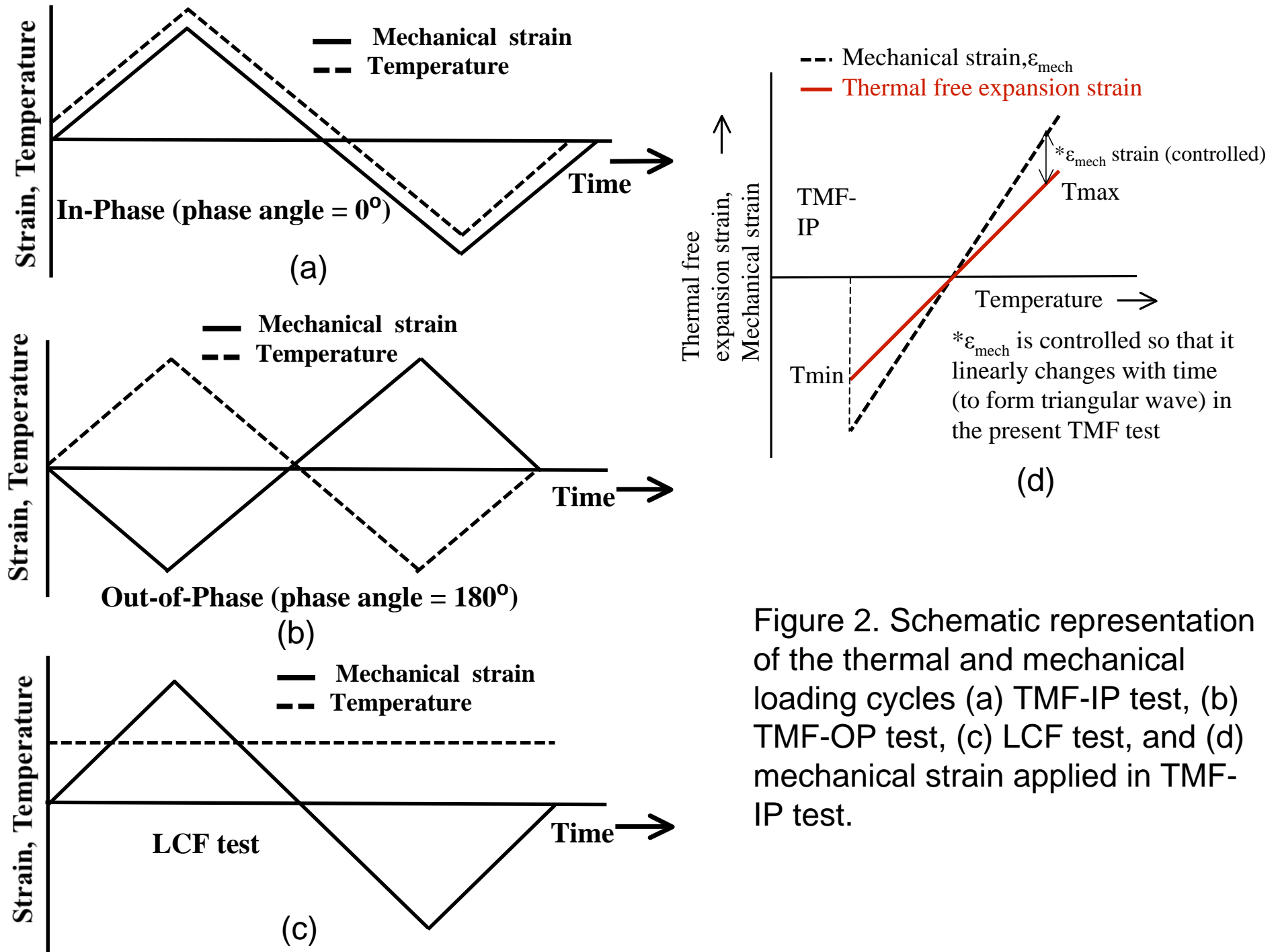
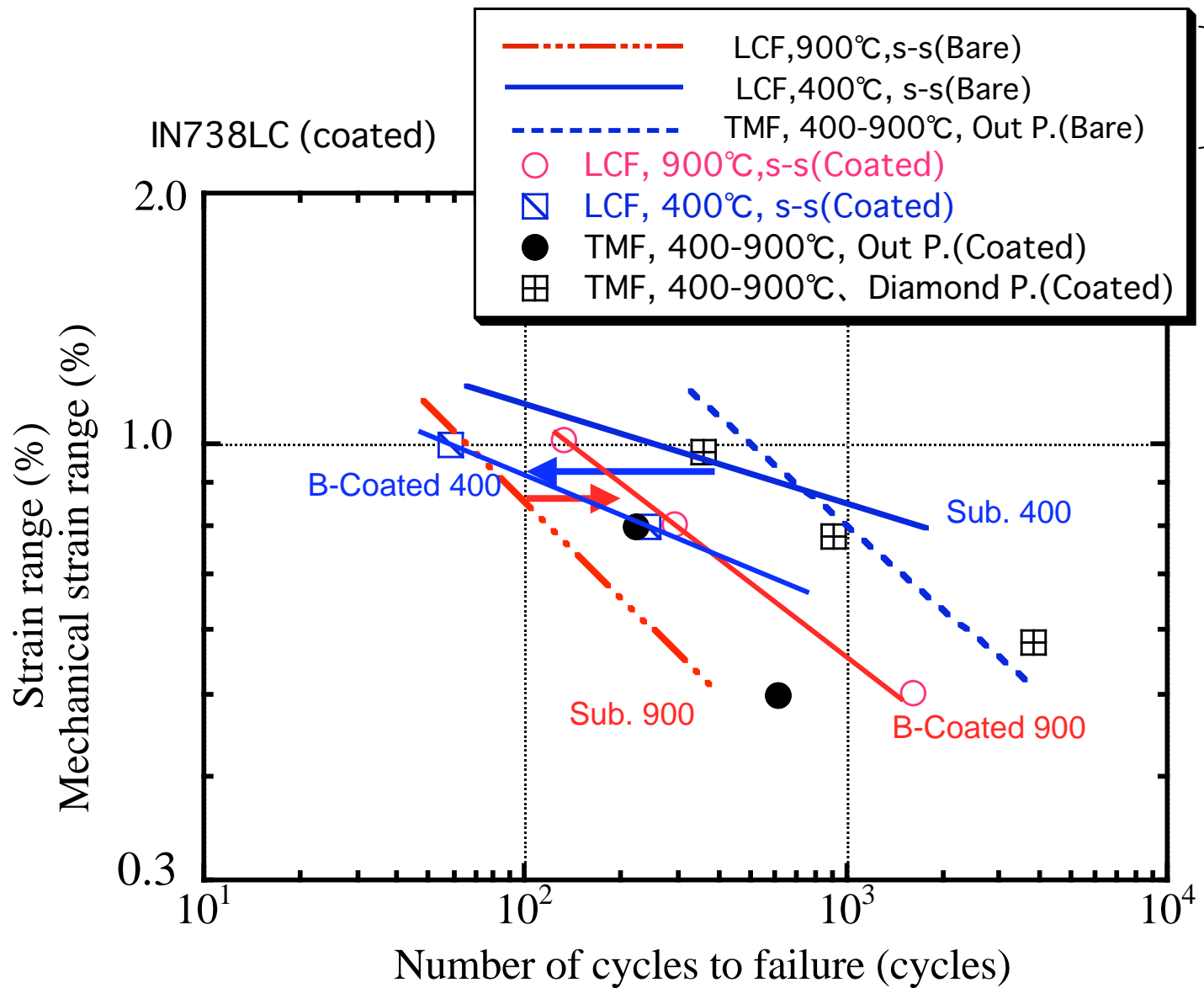


Figure 2. Schematic representation of the thermal and mechanical loading cycles (a) TMF-IP test, (b) TMF-OP test, (c) LCF test, and (d) mechanical strain applied in TMF-IP test.

# Substrate vs. Bond coated specimen under TMF and LCF



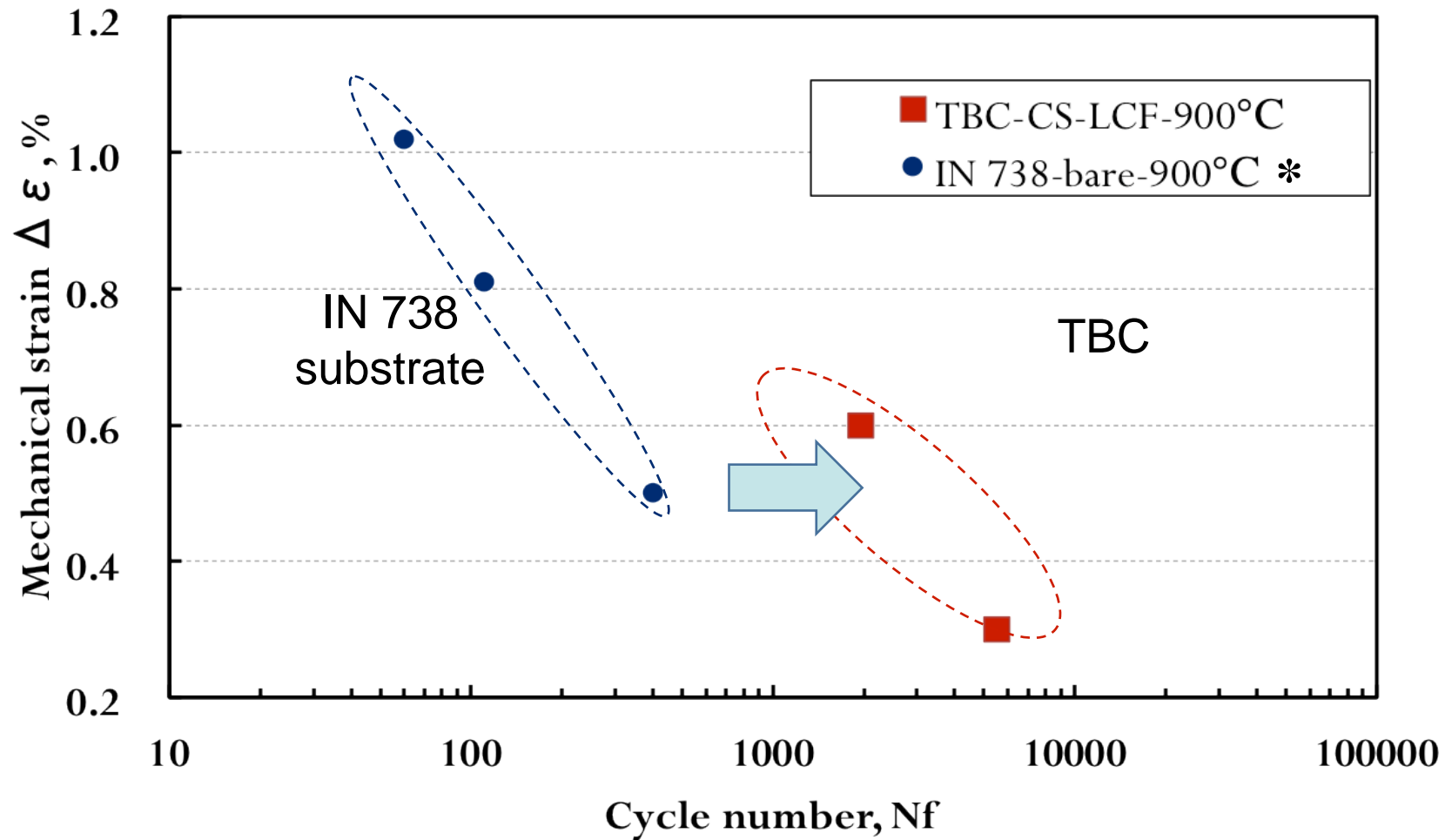
*Okazaki et al*

(a)

*Okazaki et al, ASTM 1480 (2001)*

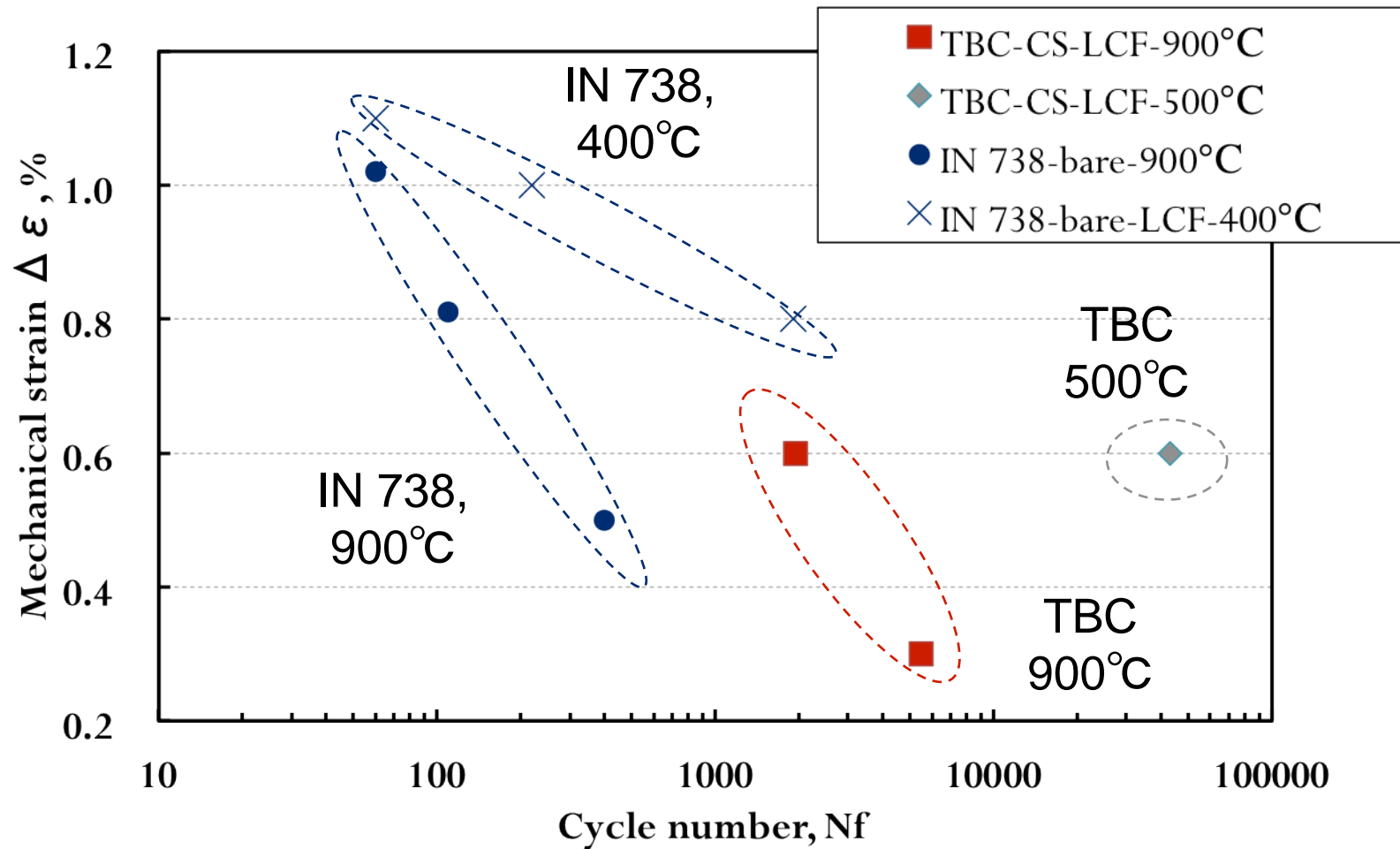


# Substrate vs. TBC specimen under LCF

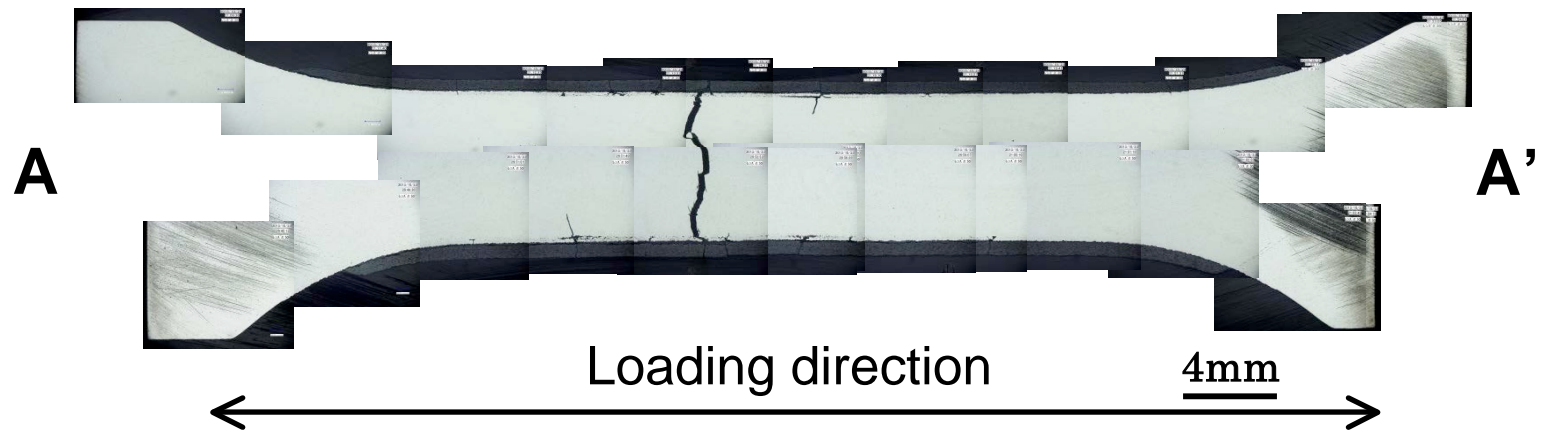


(a)

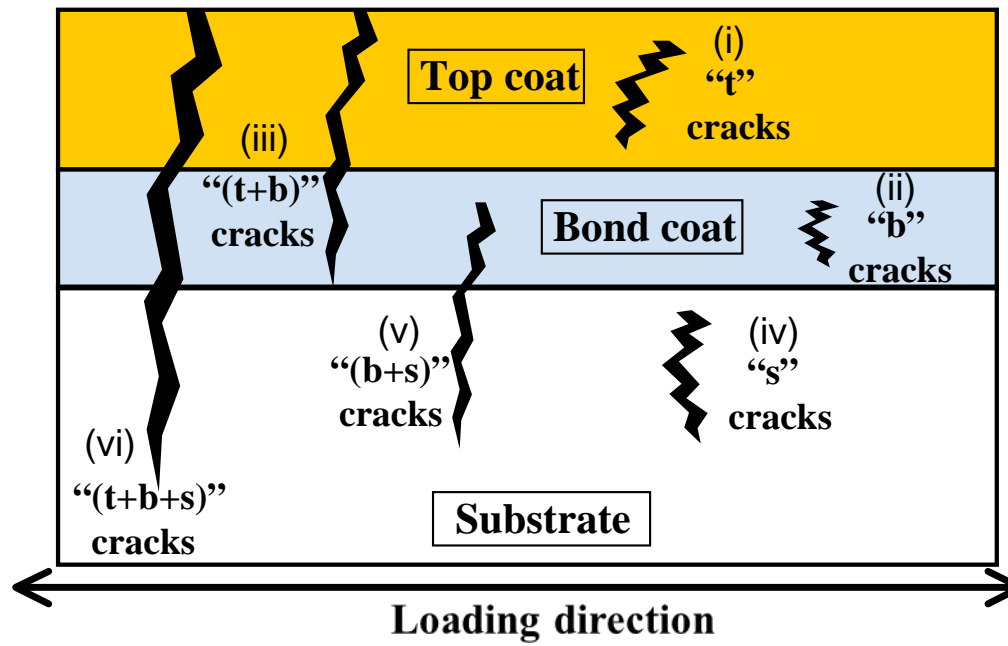
# Influence of ceramic top coat on LCF lives, *sensitive to LCF test temperature*



(b)

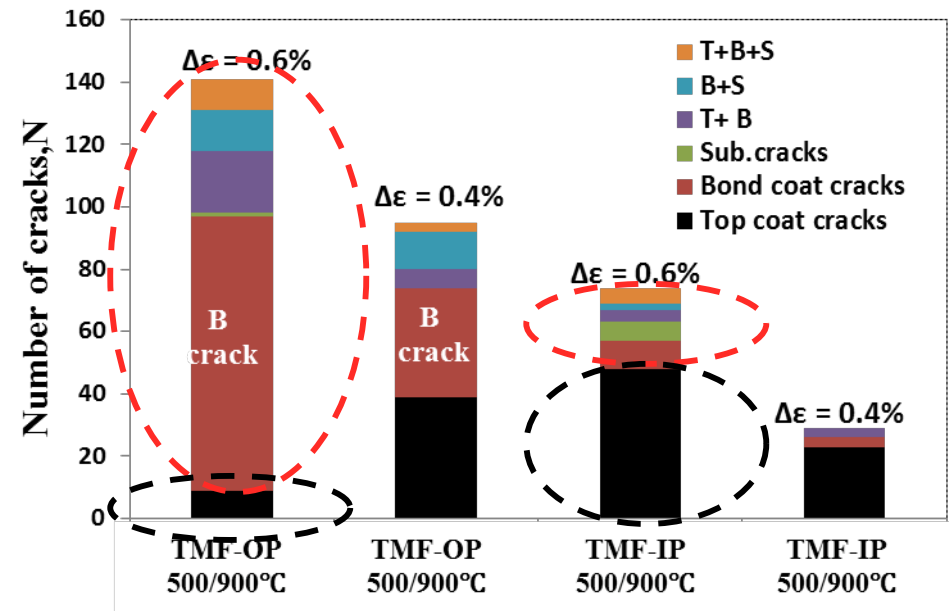
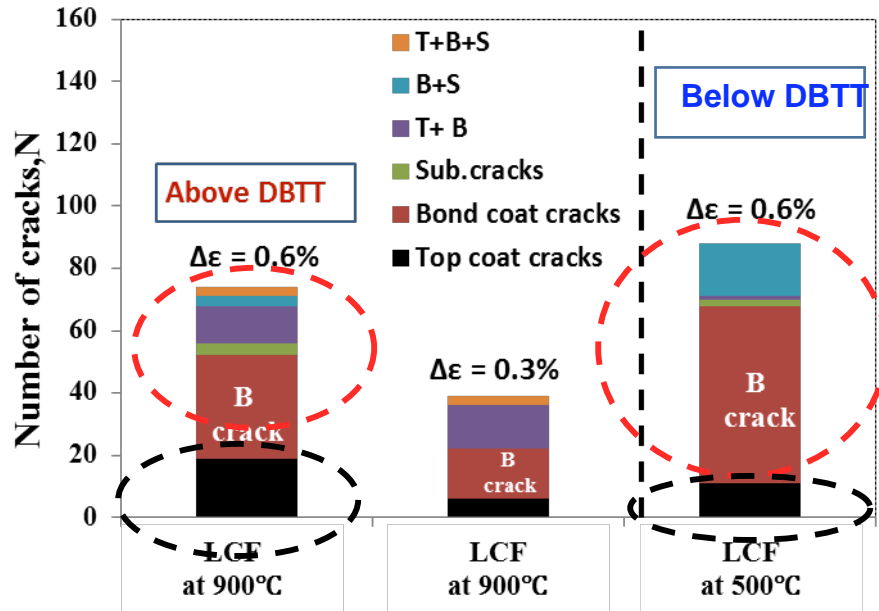


(a)

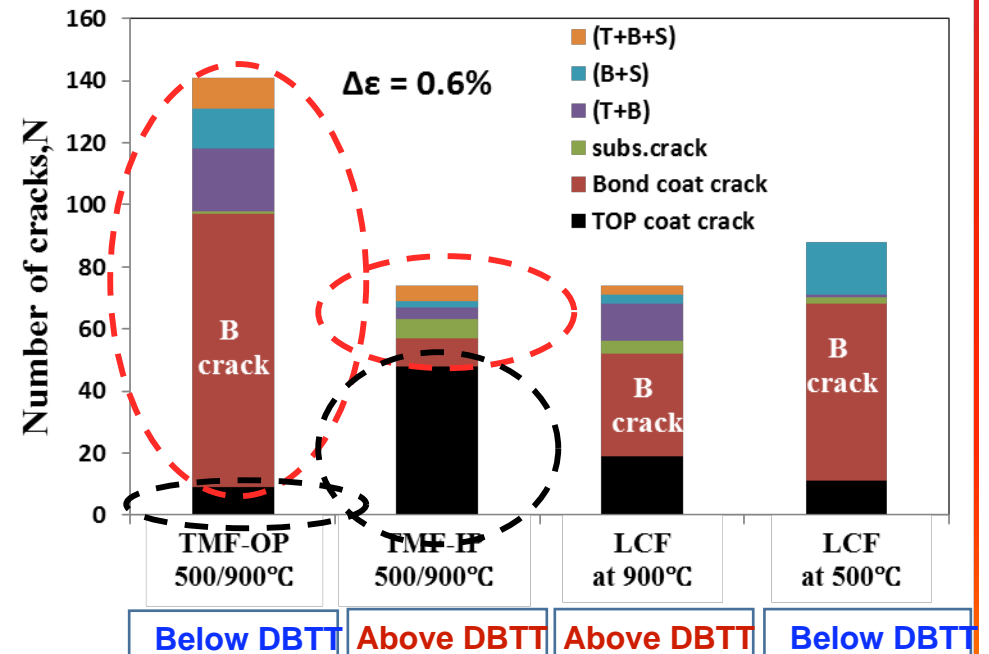


(b)

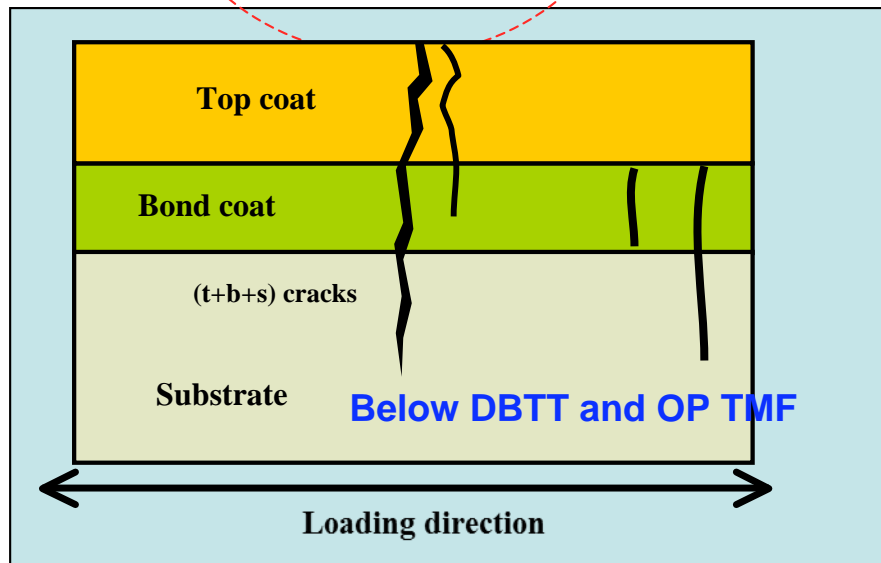
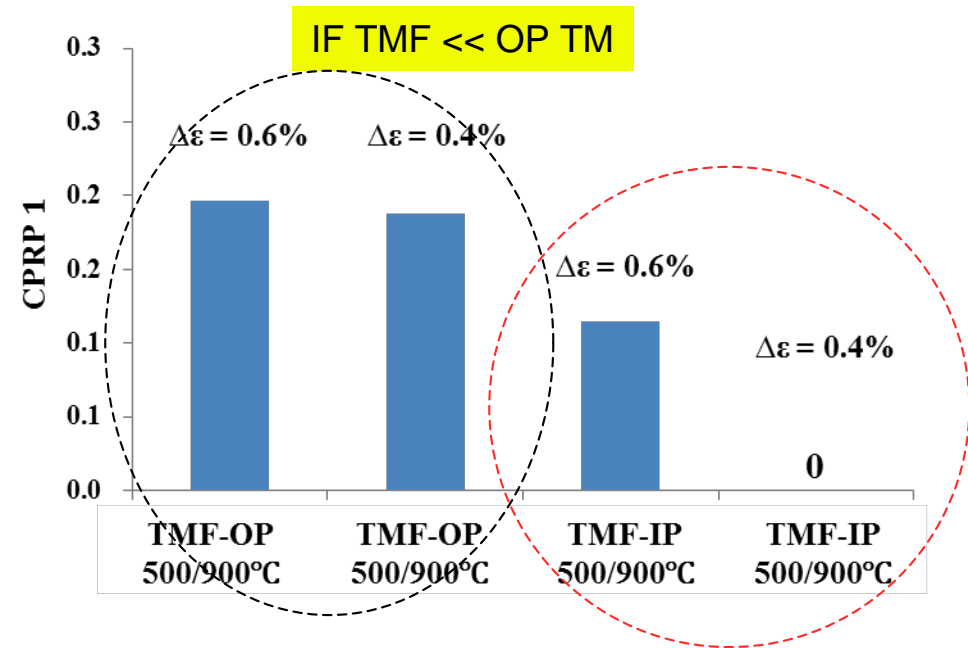
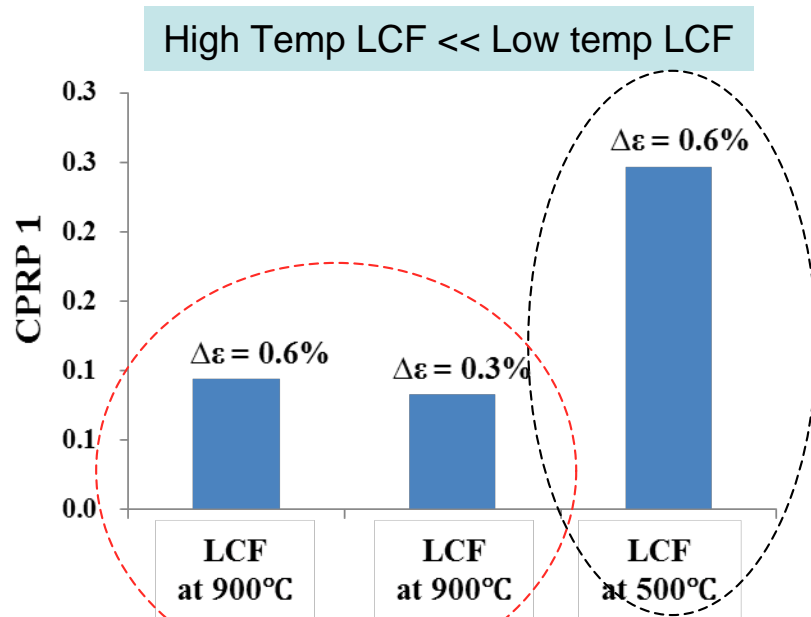
## Number of cracks



- ✓ The bond coat and bond coat related cracks are more predominant at low temperature (500°C) LCF tests.
- ✓ The bond coat and bond coat related cracks are more predominant in OP-TMF tests than in IP-TMF.
- ✓ The top coat related cracks (t cracks) are more predominant at high temperature (900°C) LCF tests.



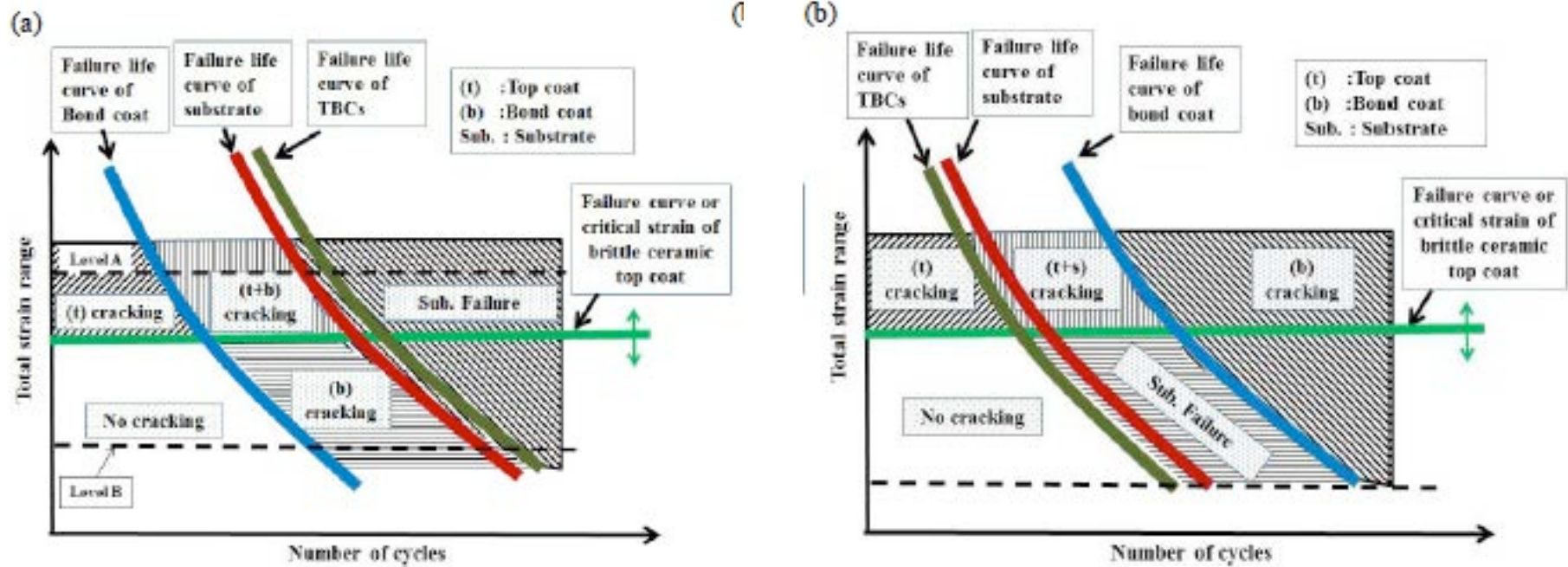
$$Parameter\ 1 = \left( \frac{b_{crack} + s_{crack}}{b_{crack}} \right) + \left( \frac{t_{crack} + b_{crack} + s_{crack}}{t_{crack} + b_{crack}} \right)$$



The **DBTT** surely affects the **crack** penetration probability into the superalloy substrate.

Below DBTT.

Above DBTT.



*Estimated Fatigue life of bond coat, compared with that of substrate.*

Figure 10. The schematic illustrations of cracking morphologies for TBC specimen under TMF and LCF condition (a) cracking morphologies for below DBTT (b) cracking morphologies for above DBTT.

# Conclusions

(1) The present bond coatings exhibited a clear **ductile to brittle transition behavior at around 650°C.**

*Below the DBTT the coatings exhibits low ductility and high yield strength. However, a rapid increase in ductility, steep decrease in yield strength and low young modulus observed above the DBTT.*

(2) Well correlated the LCF life of the bond coat, in terms of the **ductility normalized Manson-Coffin eq.**

(3) **The DBTT significantly affected the LCF and TMF lives.**

*The LCF lives at temperature below the DBTT and OP-TMF test were shorter than that of the substrate. The LCF test at temperature above the DBTT and IP-TMF test were longer than that of the substrate.*

(4) The DBTT may affect the crack **penetration behavior into the superalloy substrate.**

*A penetration probability of the bond coat crack into the substrate was higher in the LCF below the DBTT, and in the OP-TMF.*

# Local stress-strain behaviour of power plant components

J. Okrajni<sup>a</sup>, M. Twardawa<sup>b</sup>, A. Marek<sup>a</sup>

<sup>a</sup> Silesian University of Technology, Faculty of Materials Engineering and Metallurgy,  
ul. Krasińskiego 8, 40-019 Katowice, Poland

<sup>b</sup> RAFAKO S.A., ul. Łąkowa 33, 47-400 Racibórz, Poland

*TMF Workshop, Berlin 2016*

## Plan of the presentation

- Research limitation
- Introduction
- Characteristics of the component
  - Model of the component
  - The role of the heat transfer coefficient in modelling
  - Verification of the model
  - Stress-strain characteristics of the component
- Problems related to an increase of service parameters of power units on characteristics of the processes of thermo-mechanical fatigue
- Discussion and conclusions



## Objectives

The present analysis is part of a complex investigation method, whose main purpose is **increasing the accuracy of the description of the thermo-mechanical fatigue process**. In such a situation the investigations carried out and described here offer a model approach and data for the **comparison of the real behaviour with prior predictions**. However, the work is focused only on the selected component and characteristics of loading.

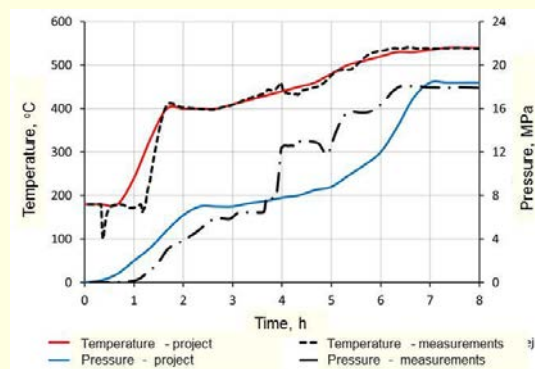
3

TMF Workshop, Berlin 2016

## Introduction to investigation

- Thermal stress based on the difference between the **temperature inside and outside** surfaces of the pressure element.
- Influence of the shape replaced with the **stress intensity factor**
- **Concern quasi steady state** case of operation or start-up of idealized curves
- **Heat transfer coefficient** is assumed as constant

4



Difference between the temperature and the pressure measured during the **real start-up of the power unit** differ from the temperature and pressure assumed during design is usually observed

TMF Workshop, Berlin 2016

## Characteristics of the component

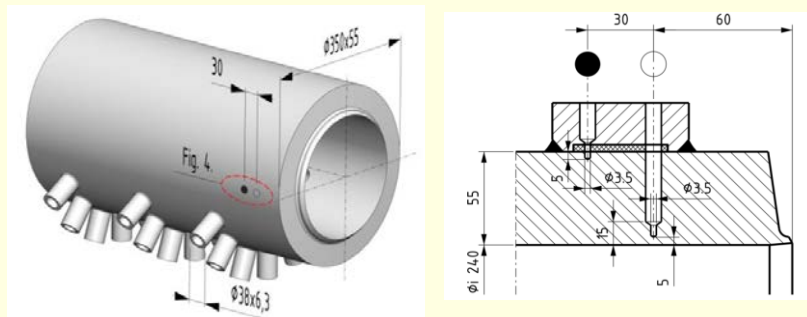
The superheater headers



TMF Workshop, Berlin 2016

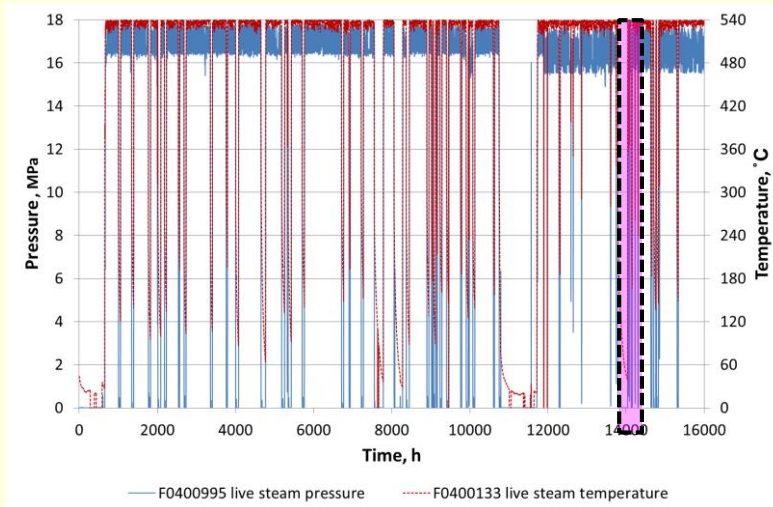
## Characteristics of the component

Localization of the thermocouples



TMF Workshop, Berlin 2016

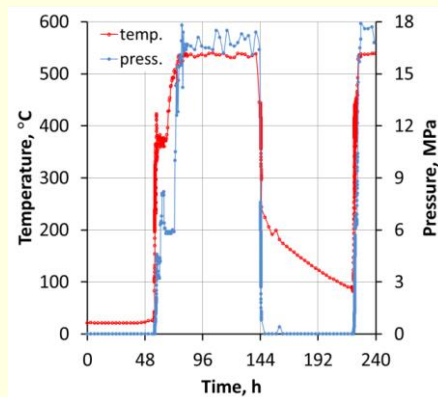
## Thermal and mechanical loading



TMF Workshop, Berlin 2016

## Thermal and mechanical loading

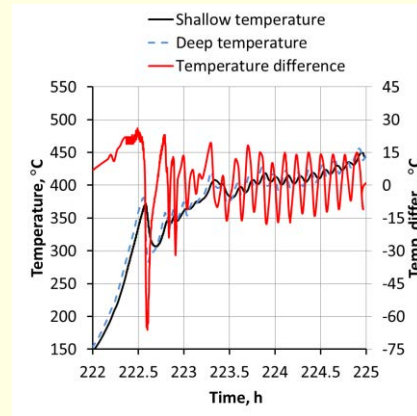
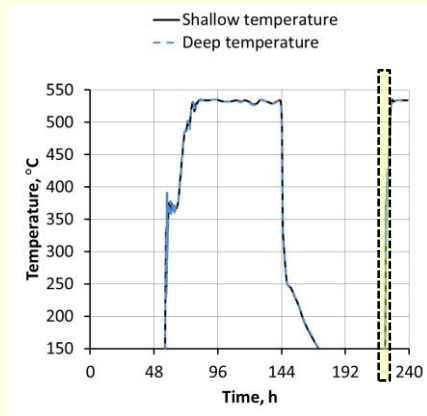
### Cold starting and cooling of the boiler



Inner surface

TMF Workshop, Berlin 2016

## Time-temperature diagrams (results of measurement )

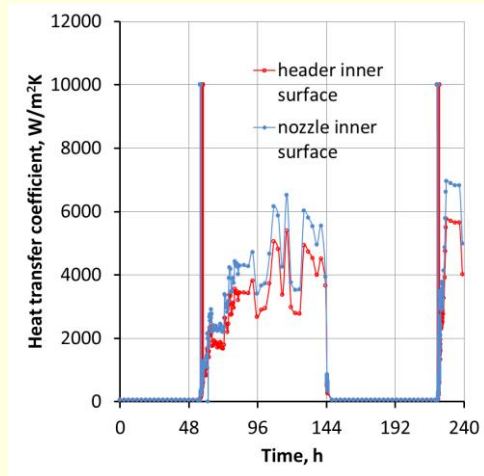
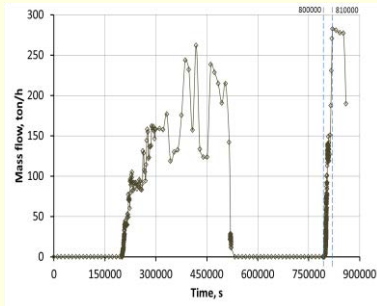


TMF Workshop, Berlin 2016

One of the important features that influence the fatigue behaviour of the component under investigation is a **time-variable heat transfer coefficient** on its inner surface.

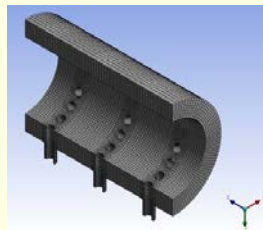
TMF Workshop, Berlin 2016

## Heat transfer coefficient

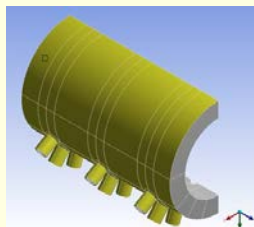
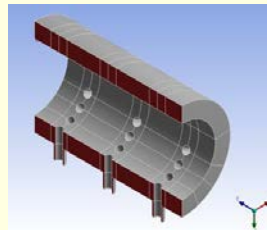


TMF Workshop, Berlin 2016

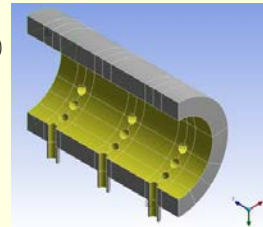
## FEM model. Temperature field analysis



The plane of symmetry



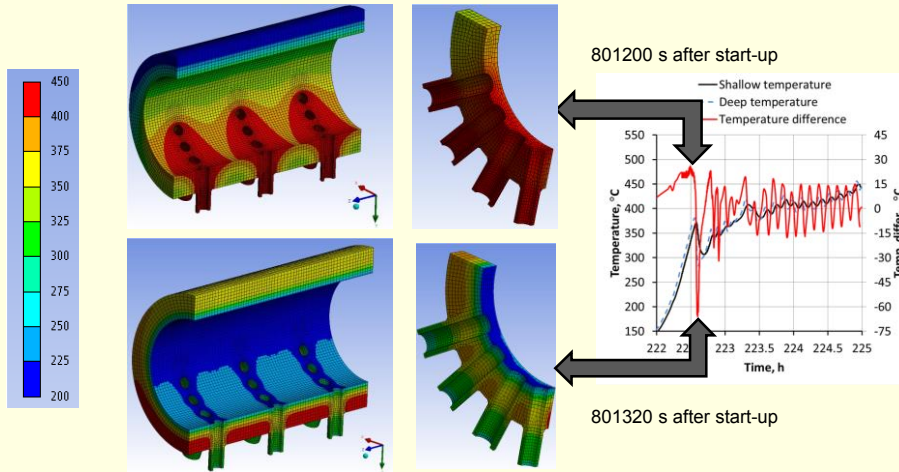
The surface of convective heat exchange (inner surface)



The surface of convective heat exchange (outer surface)

TMF Workshop, Berlin 2016

## FEM model. Temperature field analysis

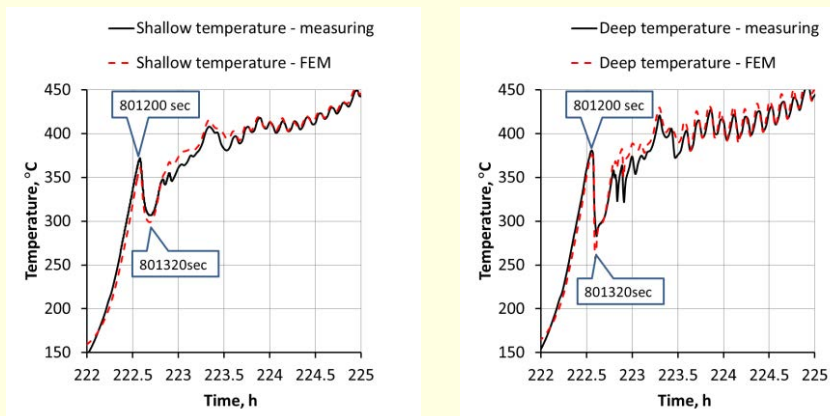


Temperature distribution in the volume of superheater header 801200 and 801320 s after start-up

TMF Workshop, Berlin 2016

## FEM, Temperature field

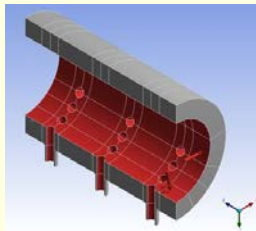
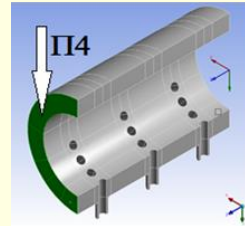
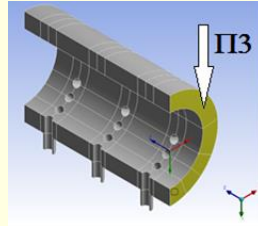
### Verification of the correctness of the model



TMF Workshop, Berlin 2016

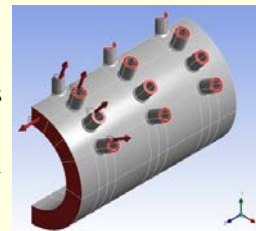
## FEM model. Stress field analysis

Planes which defined the local model



Surface of mechanical load

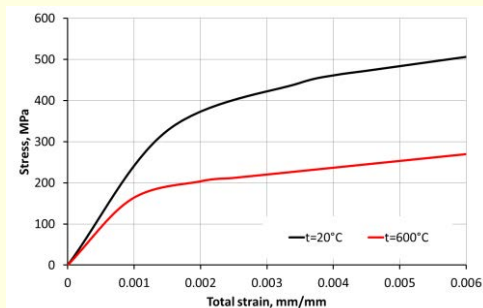
Surfaces on which loads were assumed according to the equilibrium conditions of the thick-walled vessels



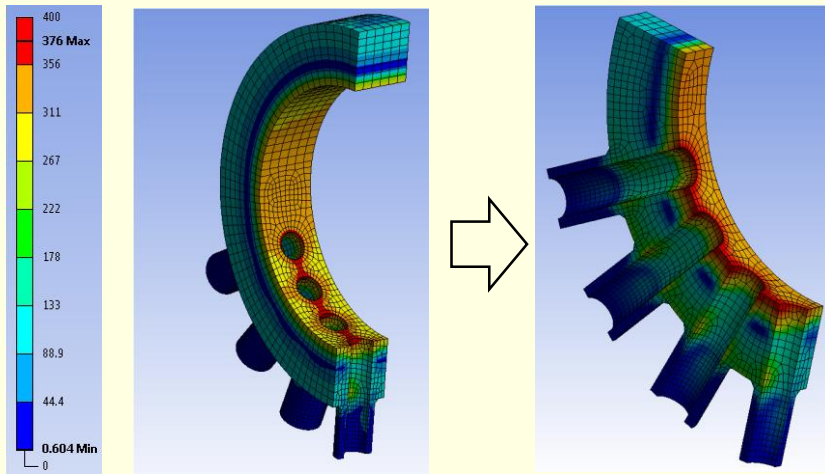
## Stress field (material model)

- The **characteristics of the time-varying** temperature field and of the pressure on the inner surface of the headers served as data for calculating the **time-varying stress** fields.
- A **thermo-elasto-plastic** model of the material was adopted for the investigated case. **Kinematic hardening** was assumed.
- The **elasticity modulus, yield point and hardening curve** were assumed to be **temperature-dependent values**. The dependence of the linear **heat expansion coefficient** on temperature was also taken into account in the calculations .

The **stress-strain** curves that depend on temperature have been assumed as the material characteristics.



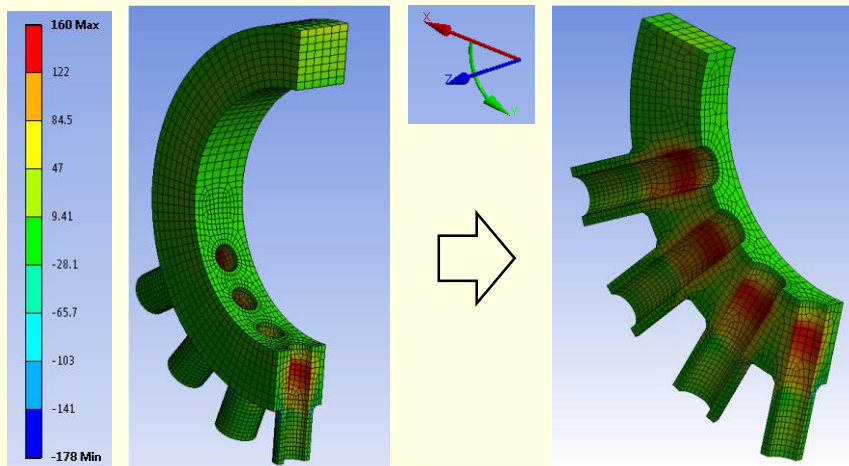
## Stress field



The equivalent stress (in MPa) distribution in the volume of superheater header 801320 s after start-up

*TMF Workshop, Berlin 2016*

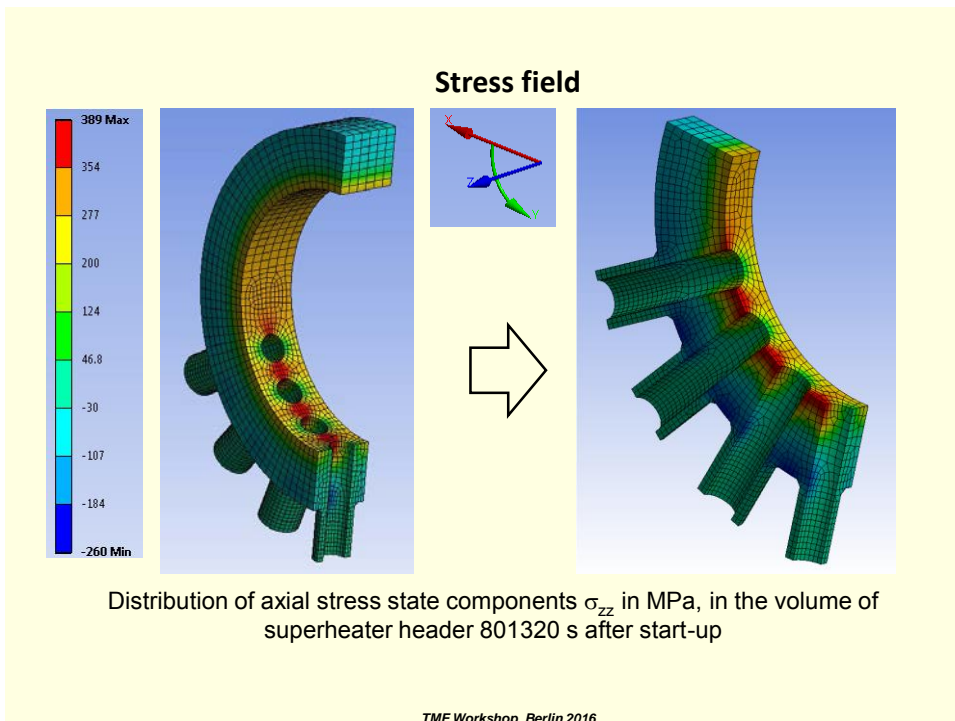
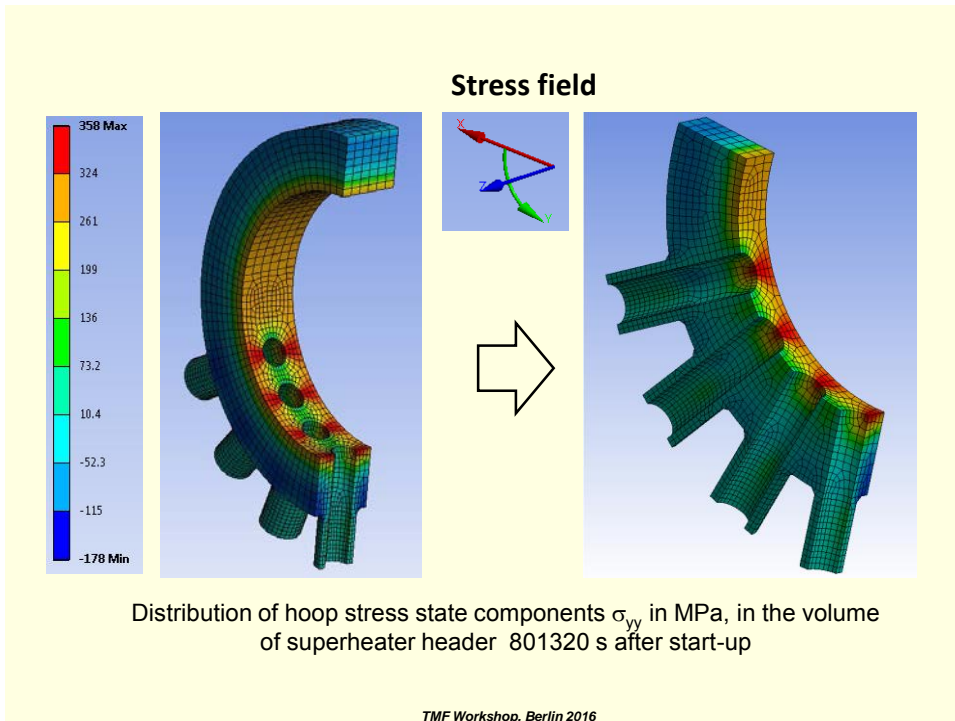
## Stress field

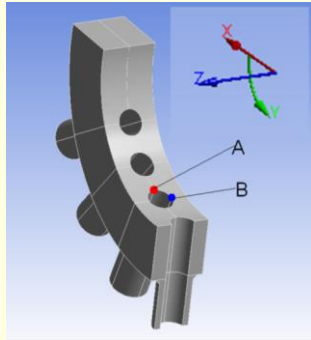


Distribution of stress state components  $\sigma_{xx}$  in MPa, in the volume of superheater header - 801320 s after start-up

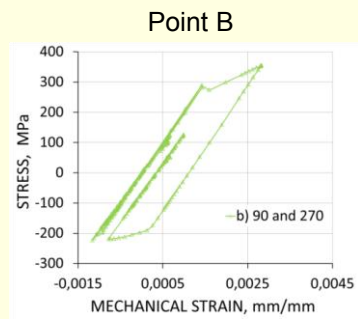
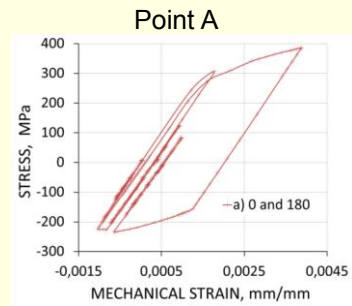
*TMF Workshop, Berlin 2016*







It is important that the hysteresis loops  $\sigma(\epsilon)$  for point A have a higher width, representing the plastic strain range, comparing it with the loops  $\sigma(\epsilon)$  for point B. This might suggest that more intensive damage could be accumulated near point A compared with point B



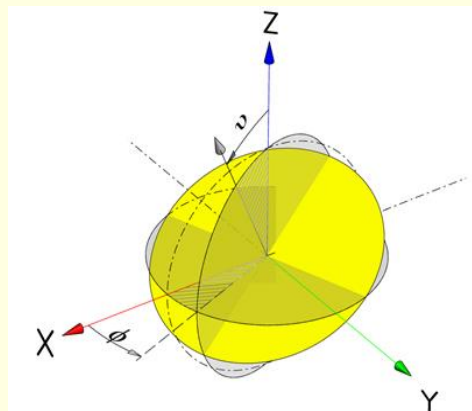
TMF Workshop, Berlin 2016

## Critical plane

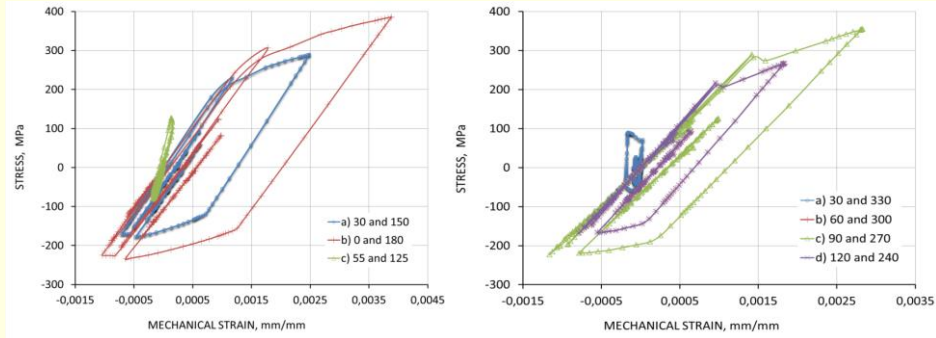
CRITERION

$$P = \Delta \epsilon_p \Delta \sigma T_{max}$$

$$P = f(\phi, \nu)$$



Defining of the position of the plane



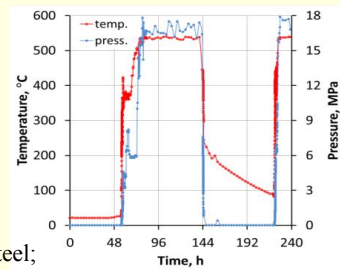
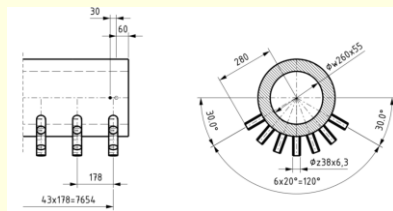
Hysteresis loops depending on the values of angles  $\nu$  with a fixed value of angle  $\phi = 0^\circ - 360^\circ$

Point A

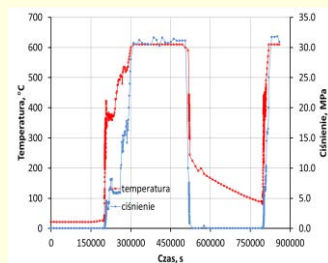
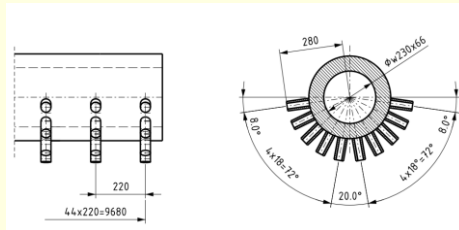
Hysteresis loops depending on the values of angles  $\phi$  with a fixed value of angle  $\nu = 90^\circ$

Point B

**EFFECT OF OPERATING CONDITION CHANGES RELATED TO AN INCREASE OF SERVICE PARAMETERS**

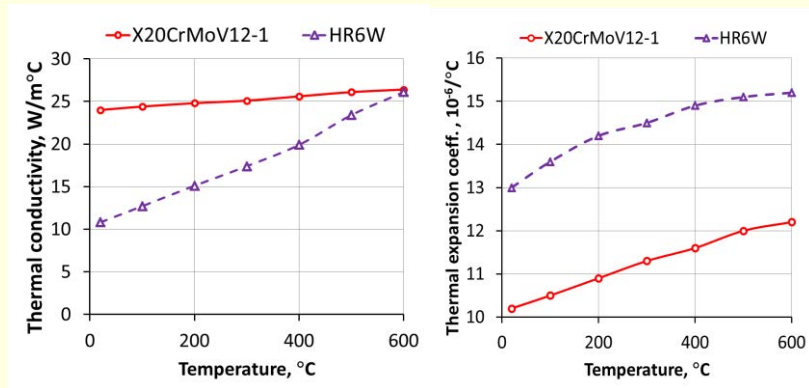


Superheater's header made of the X20CrMoV12-1 steel;



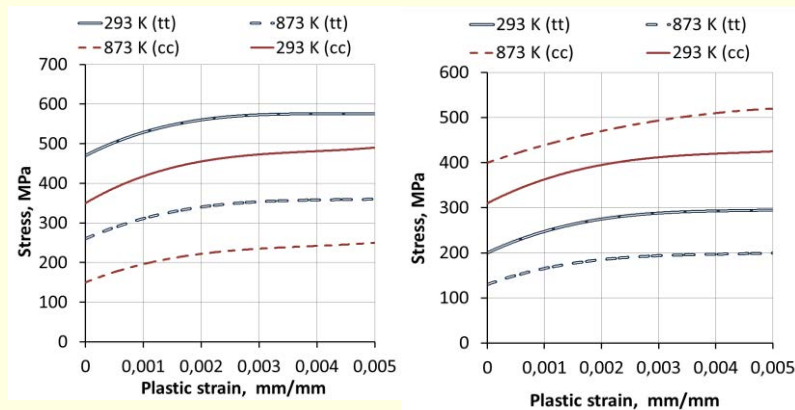
Superheater's header made of the HR6W alloy

Thermal conductivity and thermal expansion coefficient versus temperature for X20CrMoV12-1 and HR6W



TMF Workshop, Berlin 2016

Mechanical characteristics from tensile tests (tt) and cyclic stress – plastic strain curves (cc) at different temperatures

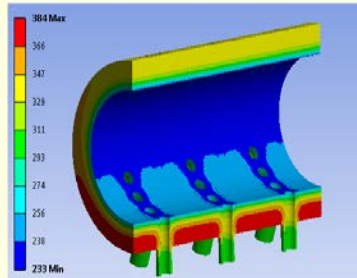


X20CrMoV12-1

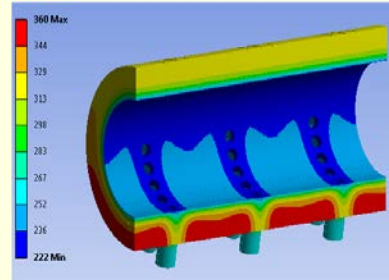
HR6W

TMF Workshop, Berlin 2016

Temperature distributions over time in the headers in the 801320th second following the start-up



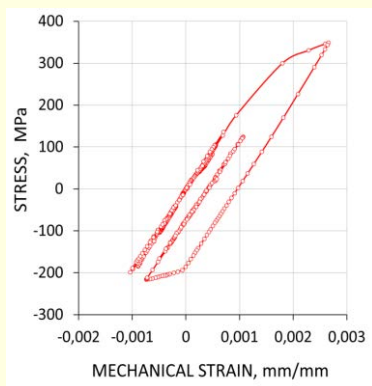
X20CrMoV12-



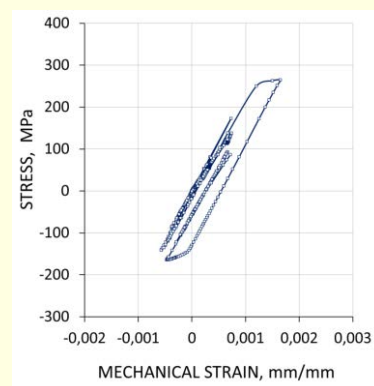
HR6W

TMF Workshop, Berlin 2016

The courses of local strain-stress curves determined for points A and B. Superheater's header made of the X20CrMoV12-1 steel - in the initial state



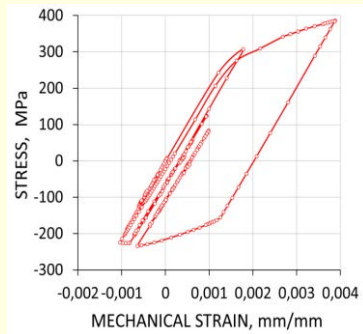
Axial stress as the function of axial strain (point A)



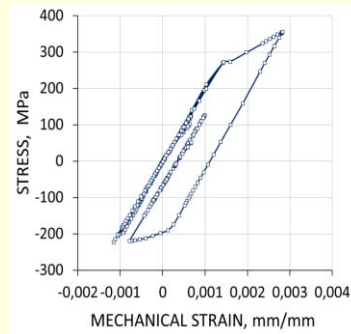
Hoop stress as the function of hoop strain (point B);

TMF Workshop, Berlin 2016

The courses of local strain-stress curves determined for points A and B.  
Superheater's header made of the X20CrMoV12-1 steel - in the state after cyclic softening



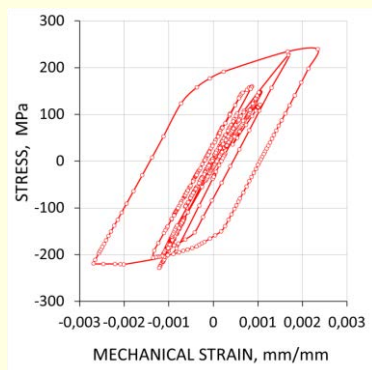
Axial stress as the function  
of axial strain (point A)



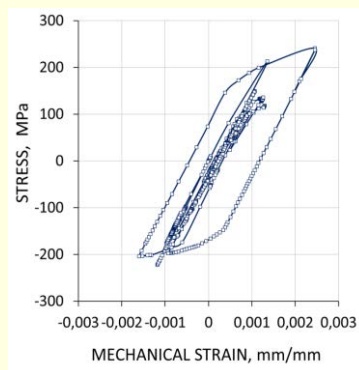
Hoop stress as the function  
of hoop strain (point B);

TMF Workshop, Berlin 2016

The courses of local strain-stress curves determined for points A and B.  
Superheater's header made of the HR6W alloy- in the initial state



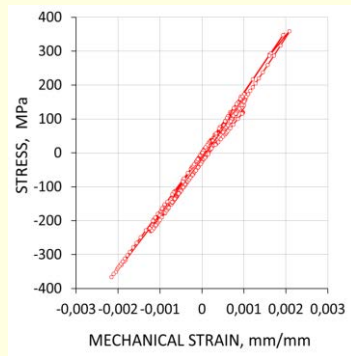
Axial stress as the function  
of axial strain (point A)



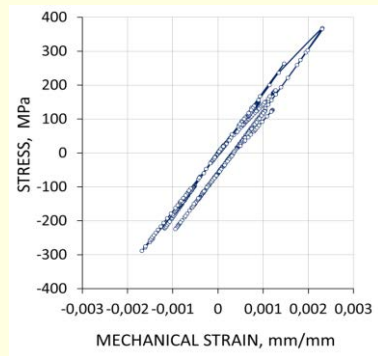
Hoop stress as the function  
of hoop strain (point B);

TMF Workshop, Berlin 2016

The courses of local strain-stress curves determined for points A and B. Superheater's header made of the HR6W alloy- after cyclic hardening



Axial stress as the function of axial train (point A)

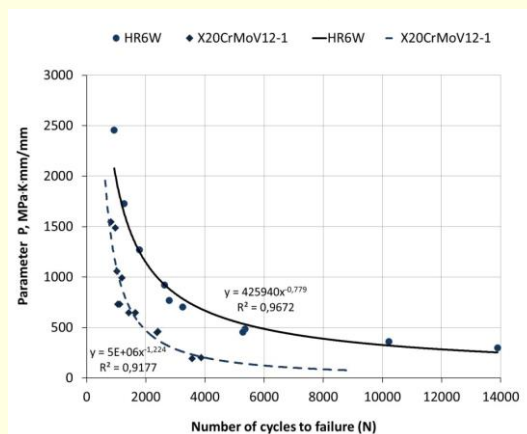


Hoop stress as the function of hoop strain (point B);

TMF Workshop, Berlin 2016

## FATIGUE LIFE CRITERION

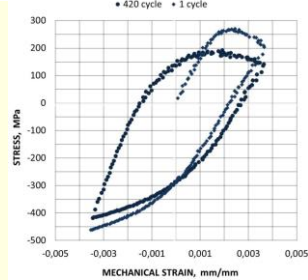
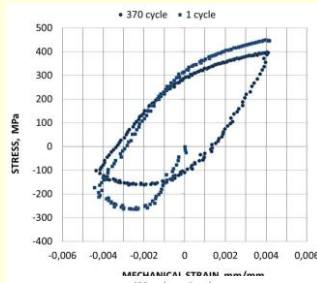
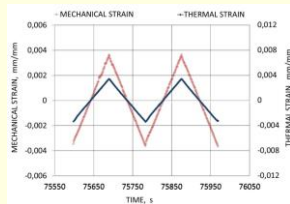
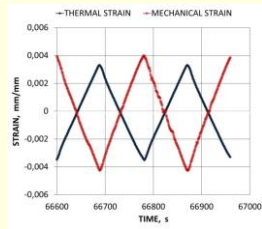
$$N=f(P); P=\Delta\varepsilon_p \Delta\sigma T$$



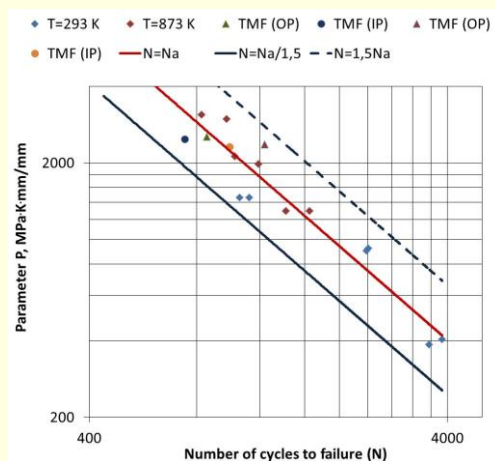
LCF fatigue diagram of X20CrMoV12-1 steel and HR6W alloy

TMF Workshop, Berlin 2016

Characteristics of the thermo-mechanical fatigue tests of X20CrMoV12-1 steel;  
OP (out of phase) cycle and IP (in phase) cycle



TMF Workshop, Berlin 2016



Points marked TMF (IP) - the temperature cycle is in phase with mechanical strain cycle.

Points marked TMF (OP) - the temperature cycle is shifted in time according mechanical strain. The time shift equals half of a period of time of a cycle in this case.

TMF Workshop, Berlin 2016



## Conclusions

- The **main reason** for material fatigue in the components under investigation **is temperature** which fluctuates, especially during transient periods of plant operation.
- One of the important features that influence the fatigue behaviour of the component under investigation is a **time-variable heat transfer coefficient** on its inner surface.
- The **fatigue of thermo-mechanical character** may play a very important role in the power plant component damage.
- Methods from **mechanics of materials, heat flow theory and mechanics of fluids**, combined with **computer modelling** should be used for the derivation of component TMF parameters.

*TMF Workshop, Berlin 2016*

## Conclusions

- Properties of the material of power system components exposed to mechanical and thermal effects may be subject to change under the impact of prolonged mechanical and thermal factors. In the case analysed, the foregoing particularly applies to the **phenomena of their cyclic hardening or softening**, depending on the material type and temperature.
- The studies of the HR6W alloy have revealed **the intense processes of cyclic hardening** taking place in the material. For this specific property, one can clearly distinguish the alloy in question from conventional materials used to manufacture elements of power engineering installations. .

36

*TMF Workshop, Berlin 2016*

Thank you for your kind  
attention



# TMF-Workshop 2016, BAM, Berlin

## Programme

Chairman: Dr.-Ing. Hellmuth Klingelhöffer  
Phone: + 49 30 8104 1501

co-organized by



co-sponsored by



### Wednesday April 27, 2016:

Time Start	Time End	Author(s)/Speaker	Affiliation(s)	Title
09:00	09:10	Klingelhöffer	BAM, chairman	Welcome and Opening
09:10	09:20	Portella	BAM, head of department 5 - Materials Engineering	Welcome to BAM
09:20	09:30	Olbricht	BAM, Berlin, Germany	Development of TMF testing - a little look back
<b>Session 1</b>		<b>Chairman: M. Bache</b>		<b>Thermal Barrier Coatings / Thermal Gradient Mechanical Fatigue</b>
09:35	10:00	Okazaki et al.	Nagaoka Tech. University/... (JP)	Effect of ceramic top coat on thermo-mechanical fatigue failure of TBCed superalloy specimen
10:00	10:25	Mauget et al.	CNRS - ENSMA, Univ. Poitiers (F)	Damage mechanisms in an EBPVD thermal barrier coating system during TMF and TGMF testing conditions under hot gas flow
10:25	10:50	Bartsch et al.	DLR, Köln /...(D)	In situ-strain measurement in a coated superalloy by synchrotron x-ray diffraction during thermal mechanical cycling with superposed thermal gradient (TGMF)
10:50	11:20	Coffee break and poster session		The poster authors and titles can be found on the last page of the program
<b>Session 2</b>		<b>Chairman: T. Beck</b>		<b>TMF properties I: steels, Al- and Mg-alloys</b>
11:20	11:45	Moverare et al.	Linköping Univ. / Sandvik (S)	Thermo-mechanical fatigue behaviour of an advanced heat resistant austenitic stainless steel
11:45	12:10	Azadi et al.	Semnan Univ., Semnan (Iran)	Study of thermo-mechanical fatigue behaviors in light alloys with and without heat treatment
12:10	12:35	Nagesha et al.	Indira Gandhi Centre for Atomic Research, Kalpakkam (India)	Thermomechanical fatigue studies on Indian RAFM steel including dwell effects
12:35	13:00	Hübsch et al.	Fraunhofer IWM, VDM Metals (D)	Impact of phasing, creep effects and microstructural evolution on the thermomechanical fatigue behaviour of alloy 800H
13:00	14:00	Lunch break		

<b>Session 3</b>		<b>Chairman: E. Affeldt</b>		<b>Industrial applications</b>
14:00	14:25	Remy et al.	Mines ParisTech et al	Thermal Mechanical Fatigue of welded ferritic stainless steel structures
14:25	14:50	Rudolph et al.	AREVA, Erlangen (D)	TMF/SHM for thermal power plants
14:50	15:15	Vacchieri, Holdsworth, Poggio, Villari	Ansaldo Sviluppo Energia (I), EMPA, Dübendorf (CH)	Service-like TMF tests for the validation and assessment of a creep-fatigue life procedure developed for GT blades and vanes
15:15	15:45	Coffee break and poster session		The poster authors and titles can be found on the last page of the program
<b>Session 4</b>		<b>Chairman: K.-H. Lang</b>		<b>TMF + HCF</b>
15:45	16:10	Fedelich, Kühn et al.	BAM, Berlin (D)	Experimental and analytical investigation of the TMF-HCF lifetime behavior of two cast iron alloys
16:10	16:35	Hosseini, Holdsworth	Inspire Centre for Mech. Integrity, EMPA, Dübendorf (CH)	Cracking due to combined HCF and TMF loading in cast iron
16:35	17:00	Norman, Skoglund, Leidermark, Moverare	Linköping Univ.; Scania, Södertälje (S)	Combined thermo-mechanical and high-cycle fatigue of high-Silicon-Molybdenum spheroidal graphite irons

<b>Thursday, April 28, 2016:</b>				
<b>Time</b>		<b>Author(s)/Speaker</b>	<b>Affiliation(s)</b>	<b>Title</b>
<b>Start</b>	<b>End</b>			
<b>Session 5</b>		<b>Chairman M. McGaw</b>		<b>Advanced TMF testing techniques / TMF properties Ni-alloys</b>
09:00	09:25	Jones, Whittaker, Brookes, Lancaster et al	Swansea University (UK), Rolls-Royce MTOC (D)	Infrared thermography for cyclic high-temperature measurement and control
09:25	09:50	Brookes et al.	Rolls Royce MTOC (D) et al.	A new code of practice for force controlled thermo-mechanical fatigue testing
09:50	10:15	Hormozi, Biglari, Nikbin	Imperial College London (UK), Amirkabir Univ. of Technology Tehran (Iran)	Experimental procedures of conducting strain-controlled thermo mechanical fatigue & low cycle fatigue tests on type 316 stainless steel
10:15	10:40	Jones, Whittaker, Lancaster, Williams	Swansea University (UK), Rolls-Royce, Derby (UK)	The influence of phase angle, strain range and peak cycle temperature on the TMF crack initiation behaviour and damage mechanisms of the Nickel-based superalloy RR1000
10:40	11:10	Coffee break and poster session		The poster authors and titles can be found on the last page of the program

Session 6		Chairman P.D.Portella		TMF crack growth	
11:10	11:35	Whittaker, Pretty, Williams	Swansea University, Rolls-Royce (UK)	Thermo-mechanical fatigue crack growth of RR1000	
11:35	12:00	Schlesinger, Seifert, Preußner	Fraunhofer IWM, Offenburg University (D)	Experimental investigation of the time and temperature dependent growth of small fatigue cracks in Inconel 718 and mechanism based lifetime prediction	
12:00	12:25	Eckmann, Schweizer	Fraunhofer IWM, Freiburg (D)	Characterisation of damage mechanisms of Nickel-base alloy MAR-M247 CC (HIP) under thermomechanical creep-fatigue loading using digital image processing	
12:25	12:50	Hyde, Buss	Nottingham Univ. (UK)	Thermo-mechanical fatigue crack growth testing of high temperature materials	
13:00	14:00	Lunch break			
14:00	14:25	Fischer, Kuhn, Mutschler, Rieck et al	FZ Jülich, Univ. Rostock, TÜV NORD GROUP (D)	Thermo-mechanical fatigue crack growth of power plant steels	
14:25	14:50	Kraemer, Mueller et al.	IWK Darmstadt (D), Ansaldo Sviluppo Energia (I)	Estimation of thermo-mechanical fatigue crack growth using an accumulative approach based on isothermal test data	
14:50	15:15	Stekovic, Whittaker, Hyde, Messe, Pattison	Linköping Univ. (S), Swansea Univ., Nottingham Univ. Cambridge Univ., Rolls Royce (UK)	Towards the elaboration of the European Code of Practice for thermo-mechanical fatigue crack growth	
15:15	15:30	Coffee break and poster session		The poster authors and titles can be found on the last page of the program	
<b>Round table discussion</b>					
15:30	17:00	discussion chairmen: M. McGaw, E.Affeldt, T.Beck, H.Klingelhöffer		Discussion of potential amendments of TMF testing standards ISO 12111 and ASTM E 2368	
17:00	18:00				Discussion of potential needs for future research and development in the regime of Thermo-Mechanical Fatigue
<b>Buffet dinner</b>					
18:00	Get together reception in the BAM conference center				
21:00					

Friday, April 29, 2016:

Time Start	Time End	Author(s)/Speaker	Affiliation(s)	Title
<b>Session 7</b>		<b>Chairman L. Remy</b>		<b>TMF Modelling and Lifetime Prediction I</b>
09:00	09:25	Christ et al.	Univ. Siegen (D)	Assessing the thermomechanical fatigue life of TiAl-based alloy TNB-V2
09:25	09:50	Faivre, Santacreu et al.	Aperam Isbergues, ArcelorMittal (F)	TMF life prediction model of a Nickel-Chromium alloy
09:50	10:15	Barrett, O'Hara, Li, O'Donoghue, Leen	NUI Gaway (Ireland), Shenzhen Graduate School (China)	A physically based model for microstructural degradation and life prediction in 9-12Cr steels und thermo-mechanical fatigue
10:15	10:40	Grützner, Fedelich, Rehmer	BAM, Berlin (D)	Constitutive modelling and lifetime prediction for a conventionally cast Ni-base superalloy under TMF loading
10:40	11:10	Coffee break and poster session		The poster authors and titles can be found on the last page of the program
<b>Session 8</b>		<b>Chairman H.-J. Christ</b>		<b>TMF Modelling and Lifetime Prediction II / TMF properties</b>
11:10	11:35	Fischer, Schweizer, Seifert	Fraunhofer IWM, Freiburg; Offenburg University (D)	A crack opening stress equation for in-phase and out-of-phase thermomechanical fatigue loading
11:35	12:00	Okrajni et al.	Silesian Univ. of Technology, Katowice (PL)	Local stress-strain behaviour of power plant components
12:00	12:25	Lang, Guth	Karlsruhe Institute Techn. (D)	An approach to lifetime prediction for a wrought Ni-base alloy under thermo-mechanical fatigue with various phase angles between temperature and mechanical strain
12:25	12:50	Kühn, Rehmer, Skrotzki	BAM, Berlin (D)	Thermo-mechanical fatigue of heat resistant austenitic cast iron EN-GJSA-NiSiCr35-5-2 (Ni-Resist D-5S)
12:50	13:00	Closing remarks		
13:00	14:00	Lunch break		
14:00	15:00	Visit of BAM laboratories	Visit options: five parallel visits (please register for one tour at the registration desk; for each visit only a limited number of persons can be accepted)	<a href="#">1. Visit of BAM division 5.2: High temperature mechanical testing incl. TMF testing</a> <a href="#">2. Visit of BAM division 5.1: High temperature corrosion</a> <a href="#">3. Visit of BAM division 2.3: Pyrotechnics for vehicles</a> <a href="#">4. Visit of BAM division 4.1: Biological damage of materials</a> <a href="#">5. Visit of BAM division 8.5: Micro non-destructive testing</a>
15:00	End of event			

<b>Session P</b>	<b>Author(s)/Speaker</b>	<b>Affiliation(s)</b>	<b>Poster Session at coffee breaks Title</b>
P1	von Hartrott, Vorndran, Tandler	Fraunhofer IWM, Freiburg (D)	Investigation on the thermocyclic plasticity of metallic materials for cryogenic hydrogen pressure tanks
P2	Smith, Lancaster, Jones, Mason-Flucke, Bagnall, Jones	Swansea University, Rolls-Royce (UK)	Lifting the thermo-mechanical fatigue behaviour of single crystal superalloys
P3	Prashanth CS, Ragupathy Kannusamy et al.	Honeywell Turbo Technologies, Honeywell Technology Solutions Lab, Bangalore, India	Sensitivity study on effect of cooling and heating rates to control thermal gradient for generation of material data under TMF loading conditions
P4	E.Lopez, S.Ghodrat, L.Kestens, Y.Wu, H.Pirgazi	Ghent University, Ghent, Belgium; Delft University, Delft, The Netherlands	3D EBSD of thermo-mechanical fatigue cracks in compacted graphite iron
P5	Jim Banks, Matt Brooks, Tony Fry, Dave Gorman, John Nunn	National Physical Laboratory, Teddington, UK	Influence of Aluminide coatings on the TMF performance of T91 Steel

29.04.2016

---

# **THERMOMECHANICAL FATIGUE OF HEAT RESISTANT AUSTENITIC CAST IRON EN-GJSA-XNISICR35-5-2 (NI-RESIST D-5S)**

H.-J.Kühn, B.Rehmer, B.Skrotzki

---



# Outline



---

**Introduction**

**Experimental Procedures**

**Thermomechanical fatigue**

**Damage Mechanism**

**Conclusions**

---

# Introduction

---



## **Heat resistant cast iron is characterised by:**

- good resistance to high temperature oxidation and scaling
- high strength at high temperatures
- high ductility
- high creep resistance

## **Alloying with silicon**

- ferritic cast iron with maximum operating temperature of 700 °C

## **Alloying with nickel**

- austenitic cast iron with maximum operating temperature of 800 °C
-

# Introduction



---

**EN-GJSA-XNiSiCr35-5-2 (Ni-Resist D-5S)**  
DIN EN 13835

AiF/FVV research project:  
"TMF lifetime calculation of exhaust-gas turbocharger  
hot parts"

FVV = Research Association for Combustion Engines e.V.  
AiF = German Federation of Industrial Research Associations

---



Eisenwerk Hasenclever & Sohn GmbH

---

# Experimental Procedure

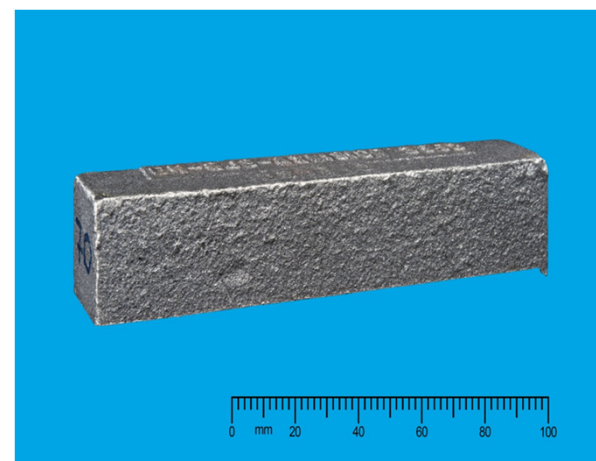
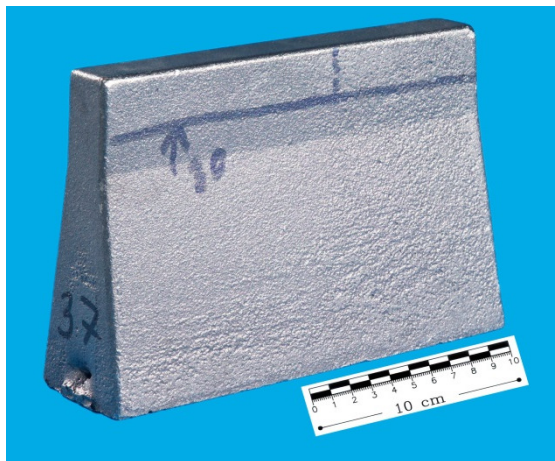
---

# Experimental procedure

---

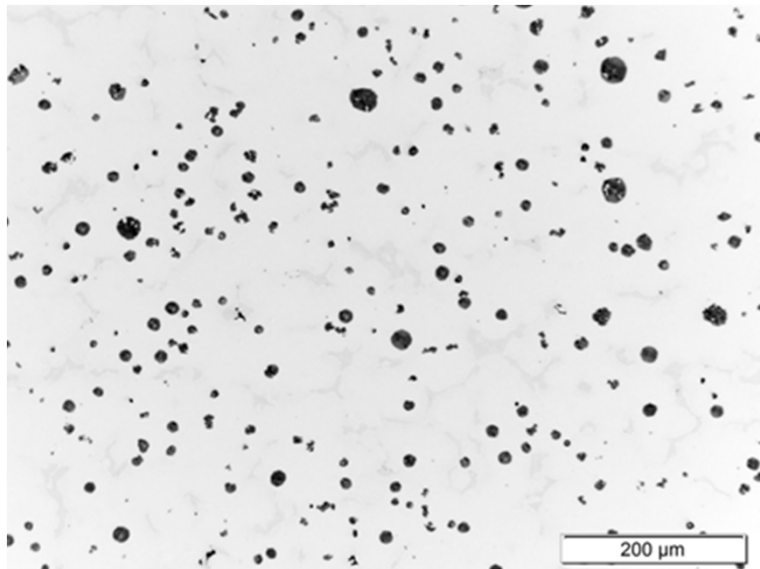
## EN-GJSA-XNiSiCr35-5-2 (Ni-Resist D-5S)

	Fe	C	Si	Mn	Ni	Cr
DIN EN 13835	remaining	max. 2.0	4.0 - 6.0	0.5 - 1.5	34.0 - 36.0	1.5 - 2.5
tested material	remaining	1.76	5.7	1.2	35.8	1.73

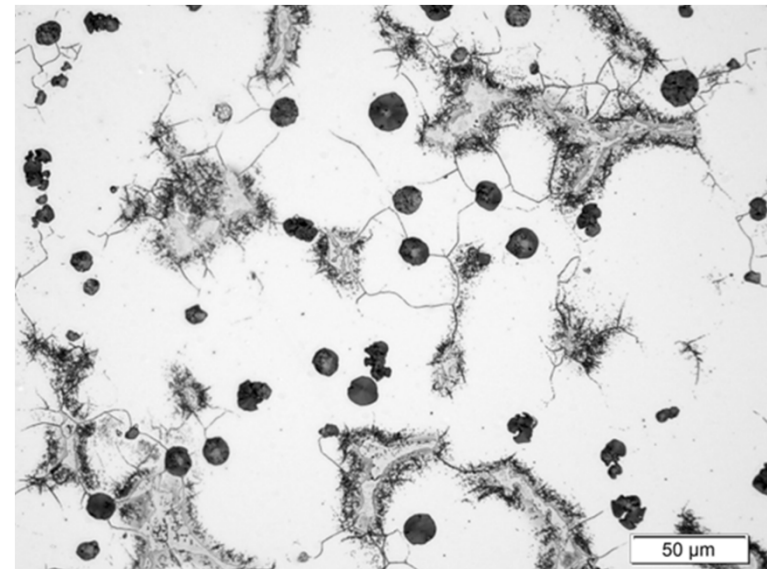


## Experimental procedure

Initial microstructure: homogeneously distributed graphite (4 %),  
carbide network in the remaining solidification area



unetched

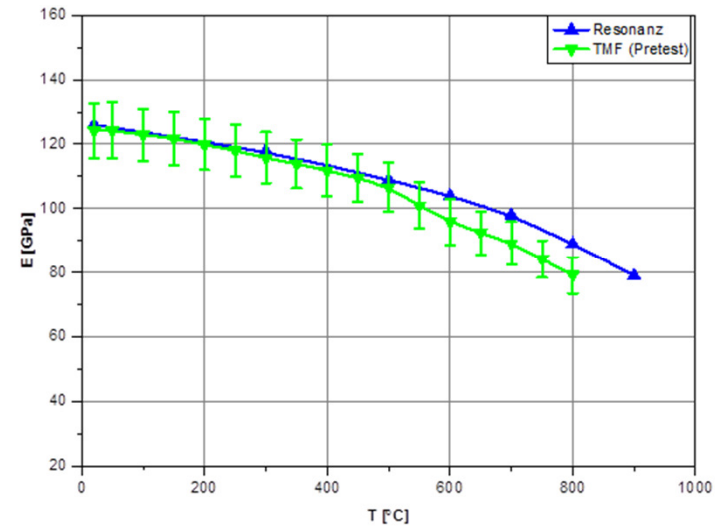
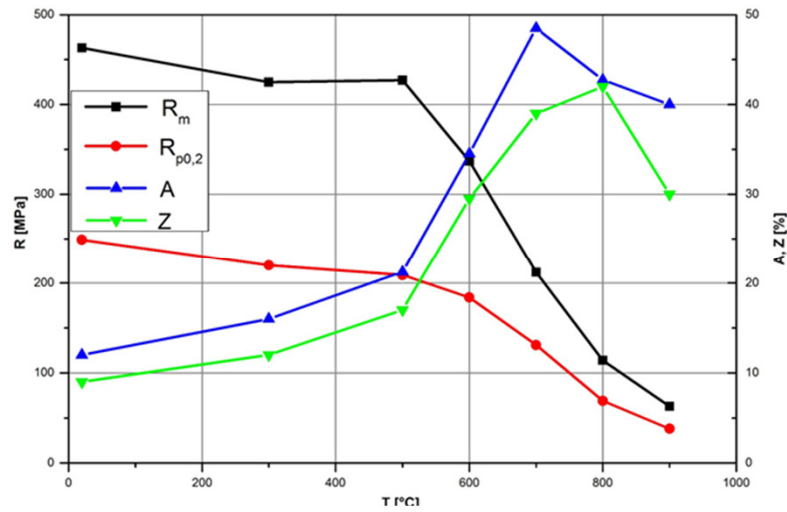


etched with Nital

# Experimental procedure



Temperature dependence of mechanical properties (tensile test, TMF(Pretest) and resonance method)



## Experimental procedure

---

### Strain-Controlled TMF-Tests

$$T_{\min} = 400 \text{ °C}$$

$$T_{\max} = 700 \text{ °C}, 800 \text{ °C}, 900 \text{ °C}$$

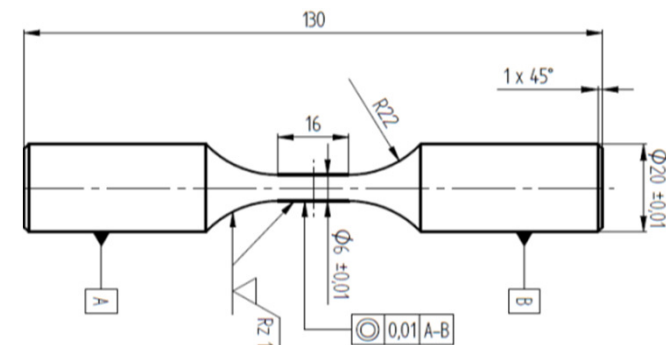
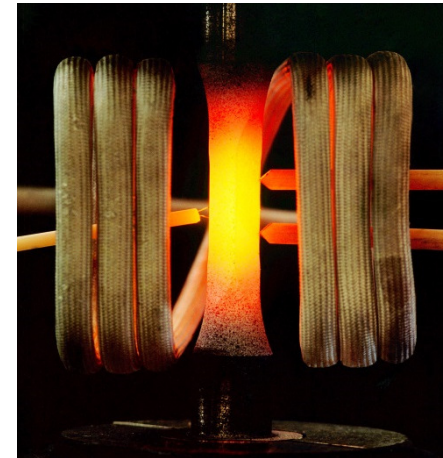
$$R = -1$$

$$T\text{-Rate} = 5 \text{ K/s}$$

$$T_{\text{HZ}} = 180 \text{ s @ } T_{\max}, \text{ IP/OP}$$

$$\epsilon_{\text{mech}} = 0.15 - 0.35\%$$

---

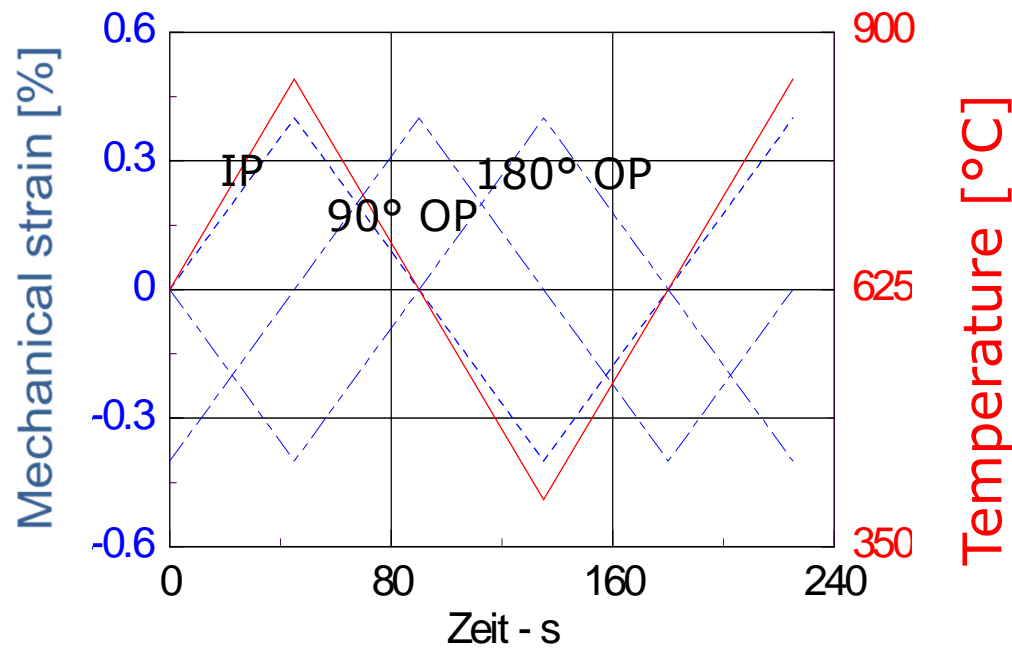




# Experimental procedure



$$\varepsilon_{total}(t) = \varepsilon_{mech.}(t) + \varepsilon_{thermal}(t)$$



**Definition of failure:**

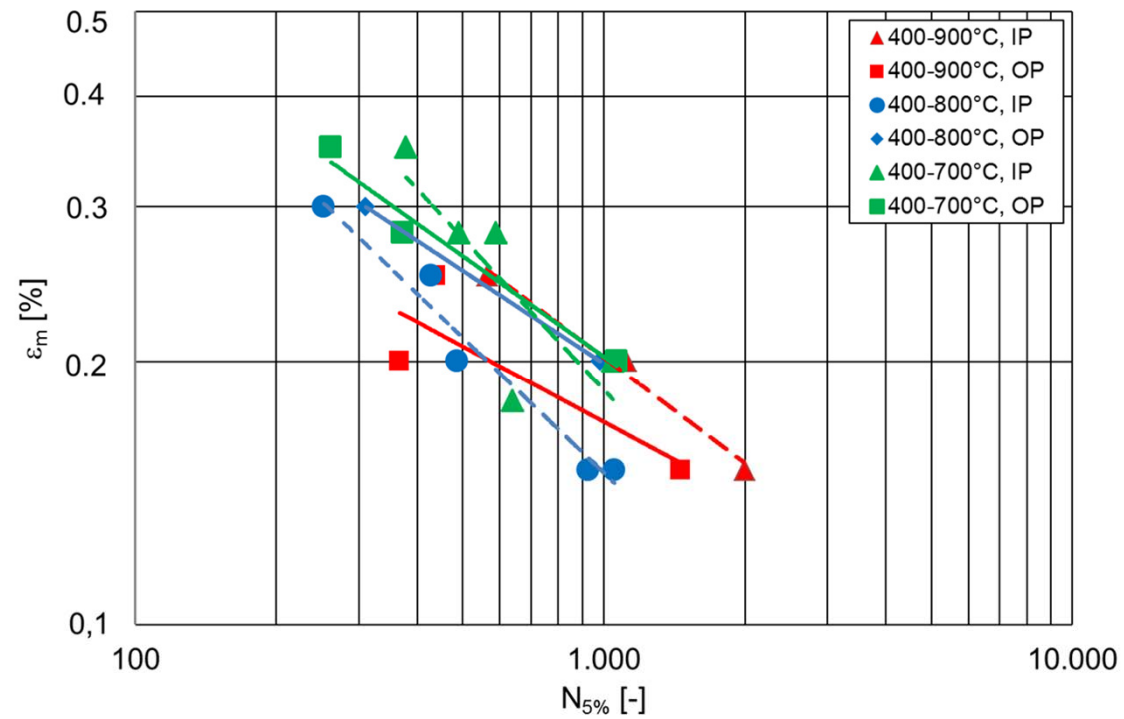
**5 % force drop**

---

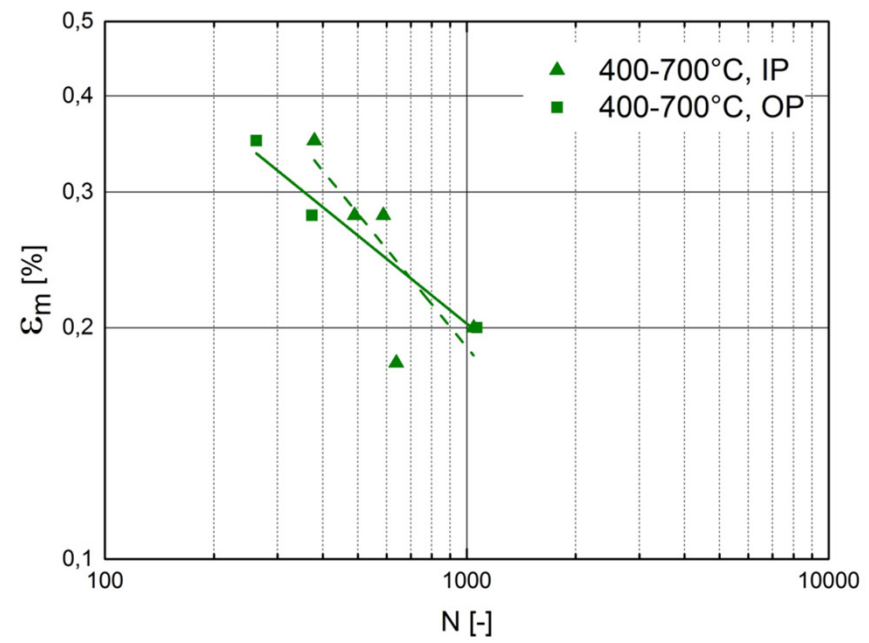
# Thermomechanical fatigue

---

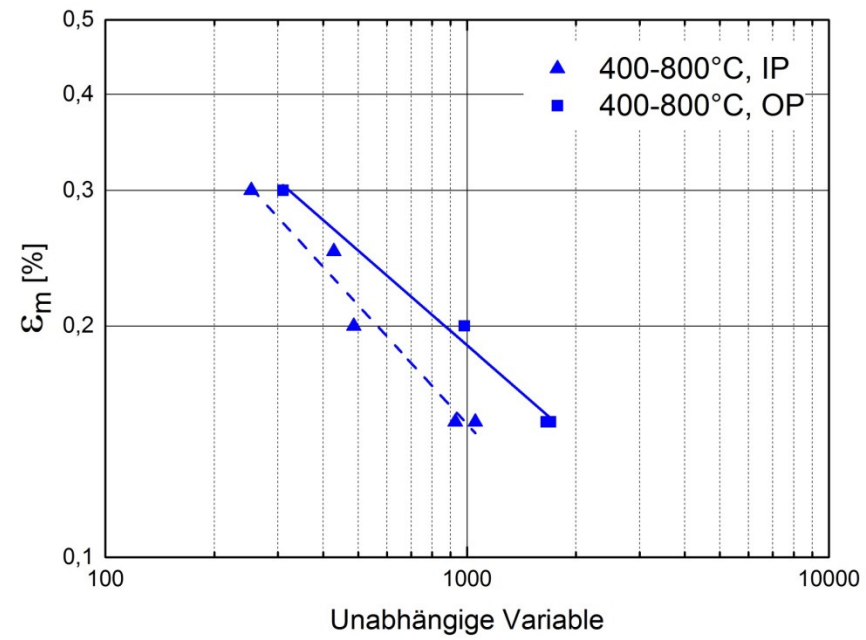
# Thermomechanical Fatigue



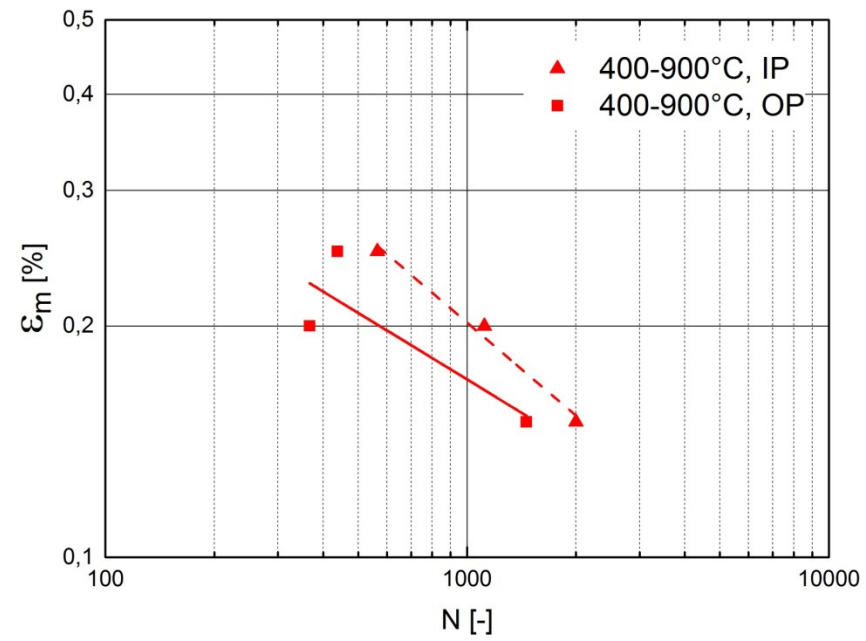
# Thermomechanical Fatigue



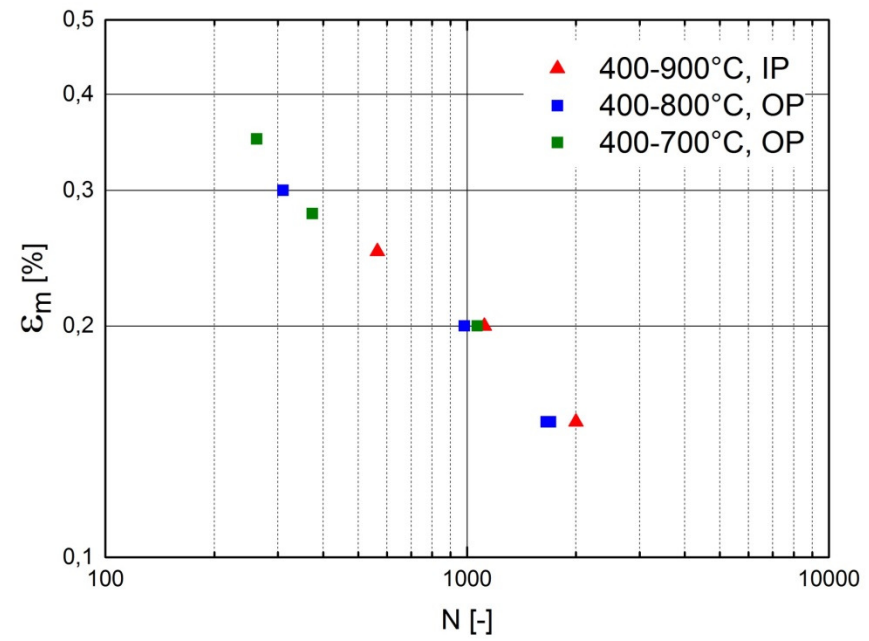
# Thermomechanical Fatigue



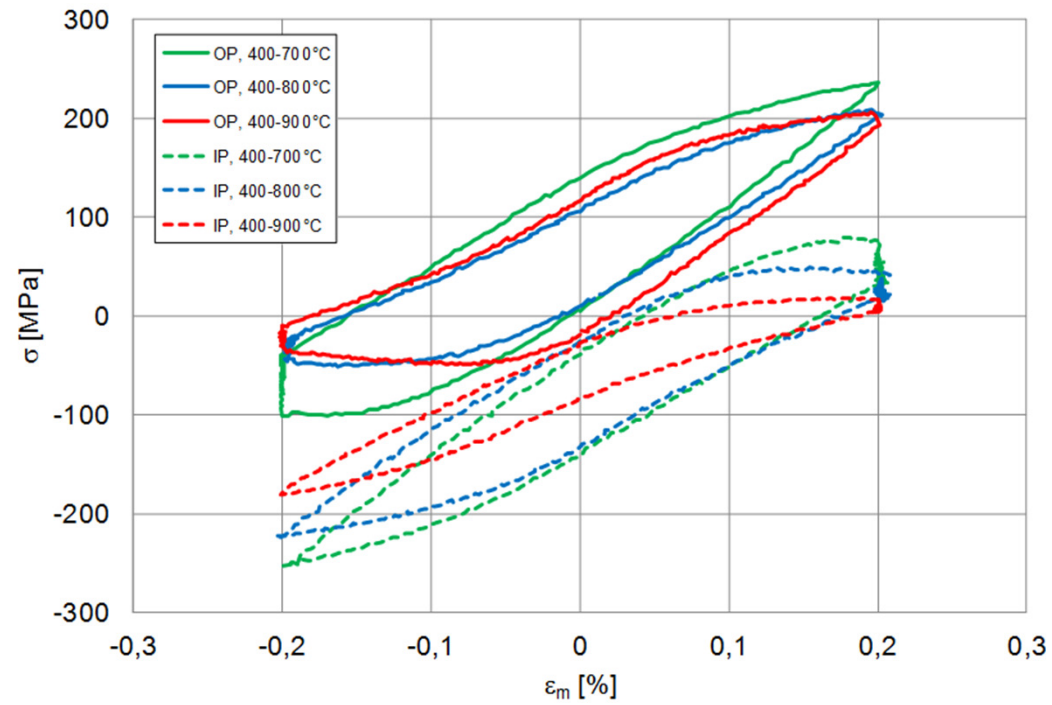
# Thermomechanical Fatigue



# Thermomechanical Fatigue

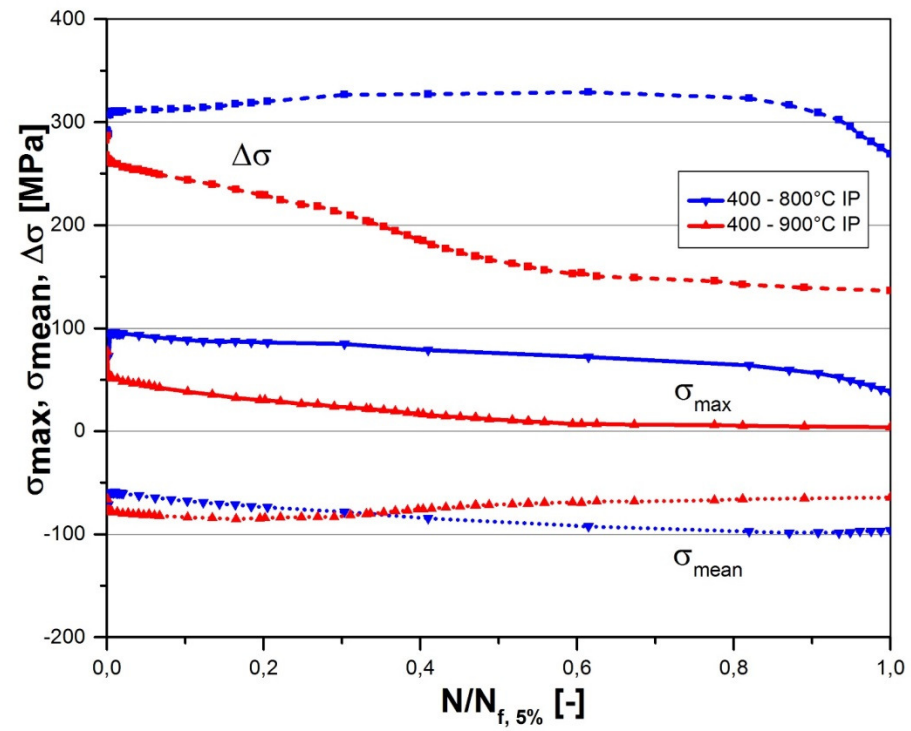


# Thermomechanical Fatigue

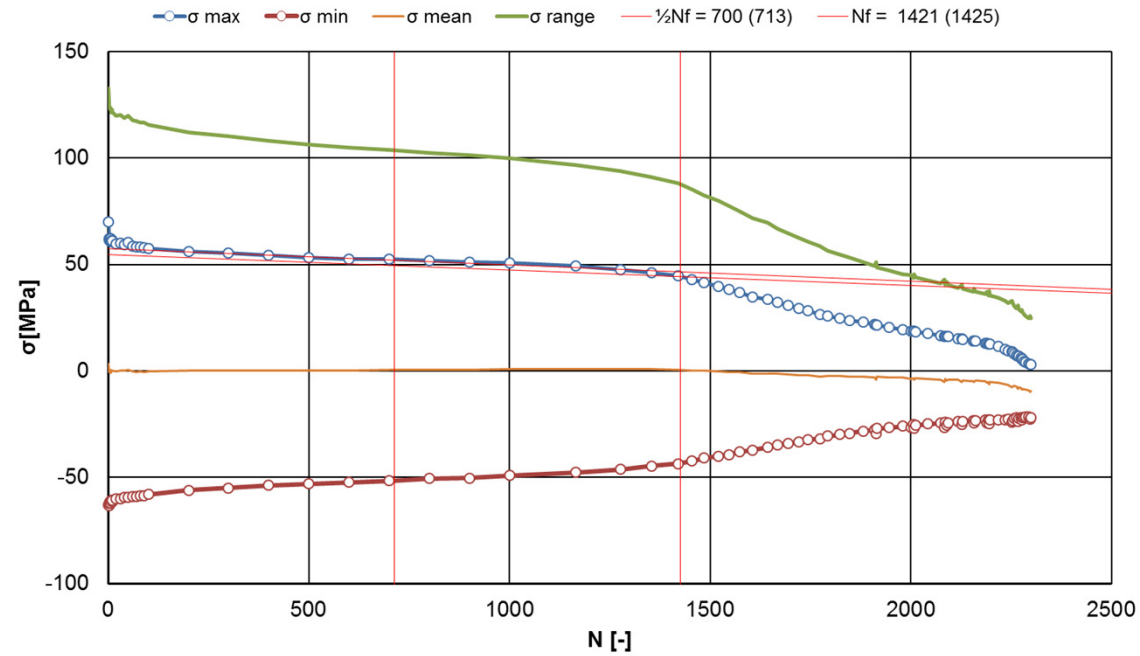




# Thermomechanical Fatigue

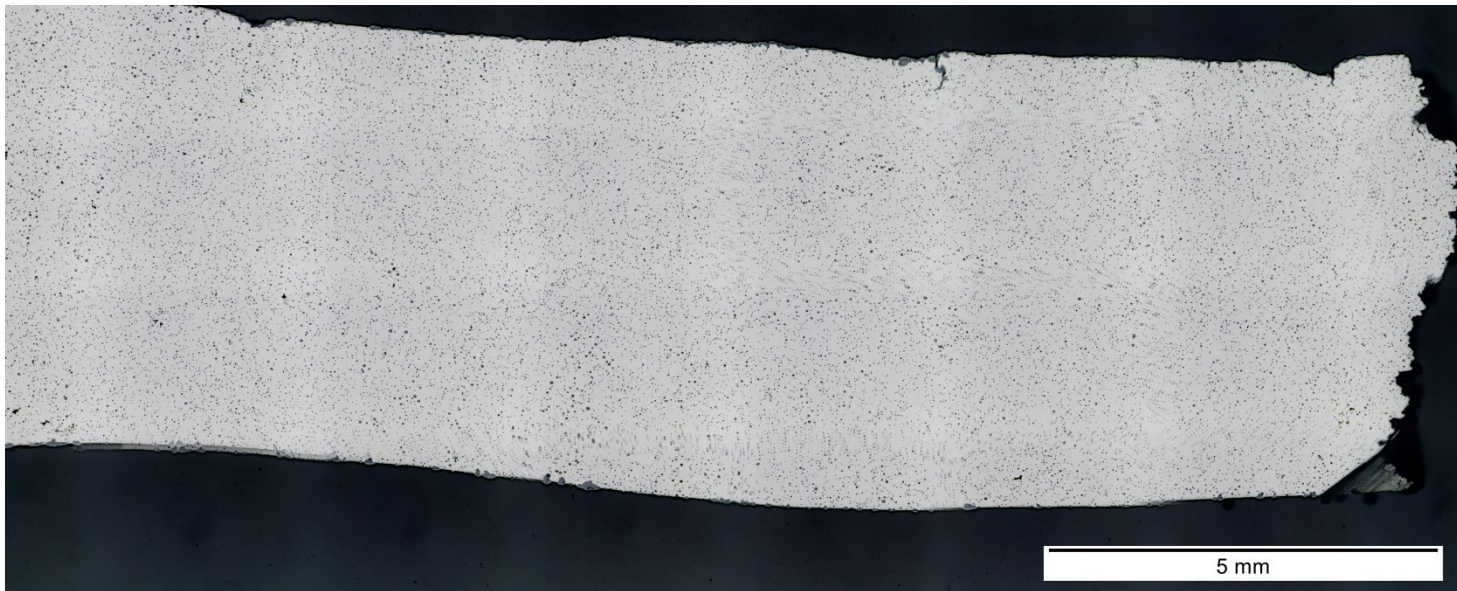


# Thermomechanical Fatigue



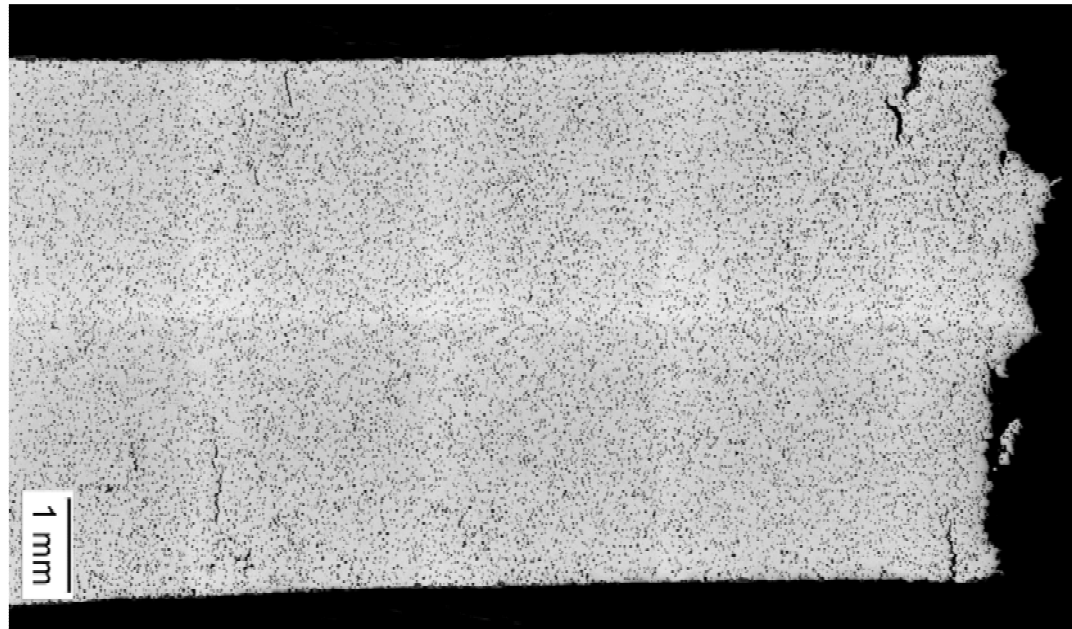
Strain-controlled LCF-Test @ 900°C, 0,3 %,  $R_e = -1$ ,  $\dot{\epsilon} = 10^{-3} \text{ s}^{-1}$

# Thermomechanical Fatigue



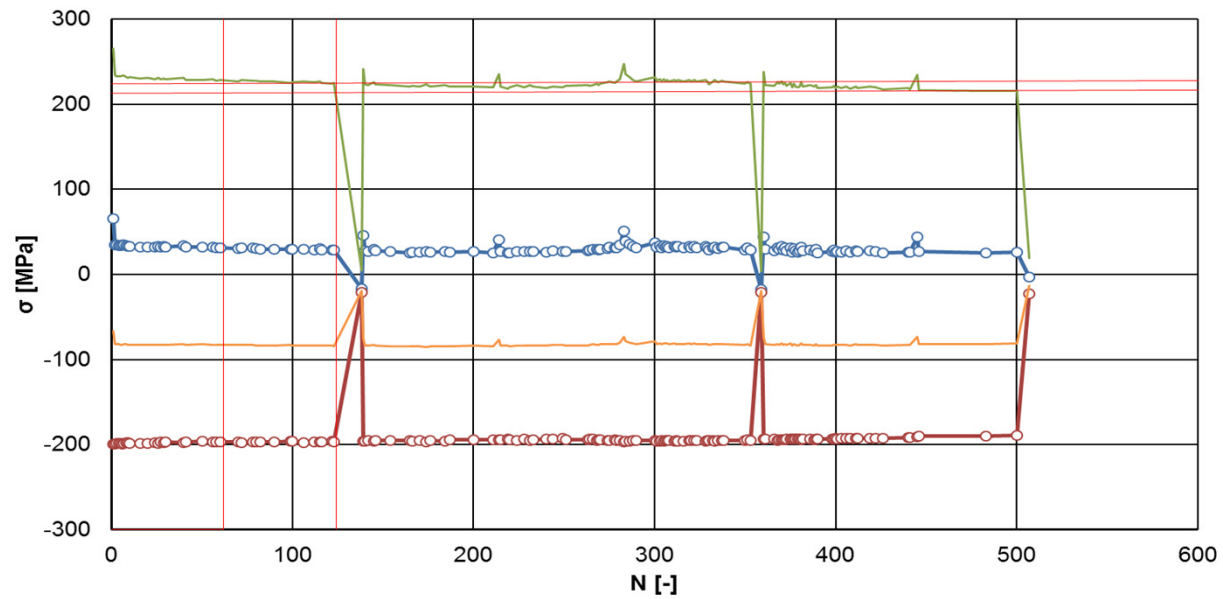
Strain-controlled LCF-Test @ 900°C, 0,3 %,  $R_e = -1$ ,  $\dot{\epsilon} = 10^{-3} \text{ s}^{-1}$

## Thermomechanical Fatigue



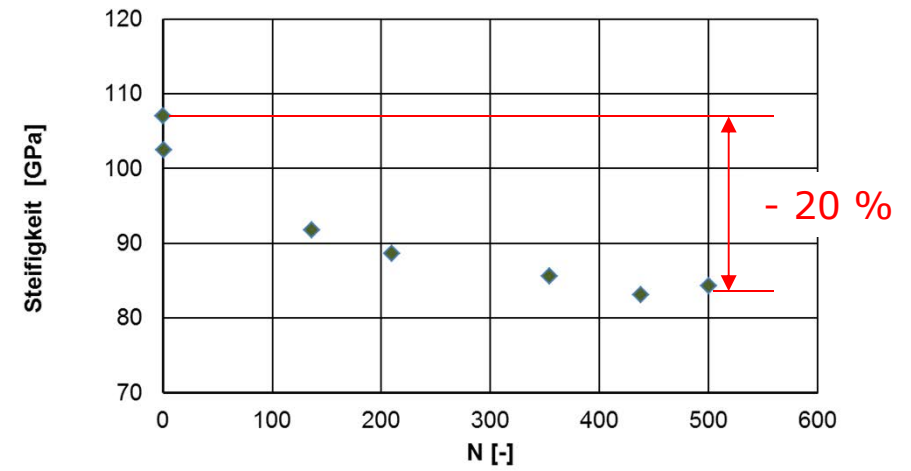
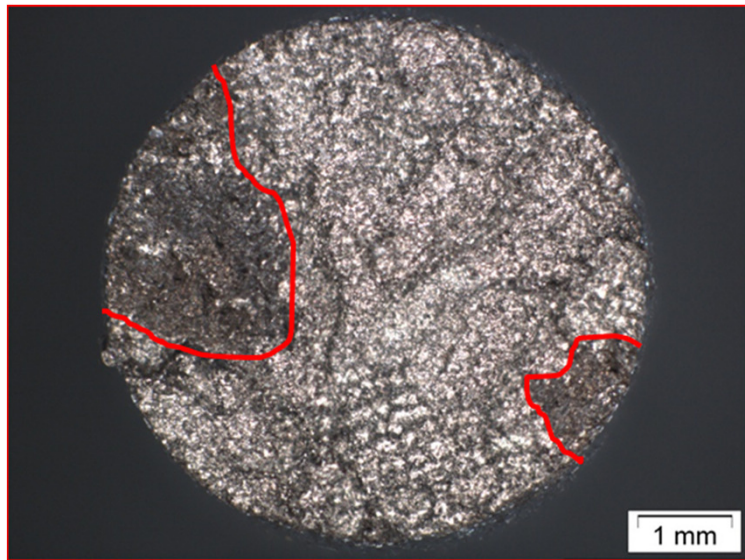
IP,  $T = 400 - 900 \text{ } ^\circ\text{C}$ ,  $\Delta\varepsilon_{\text{mech}} = 0.4 \text{ } \%$

# Thermomechanical Fatigue

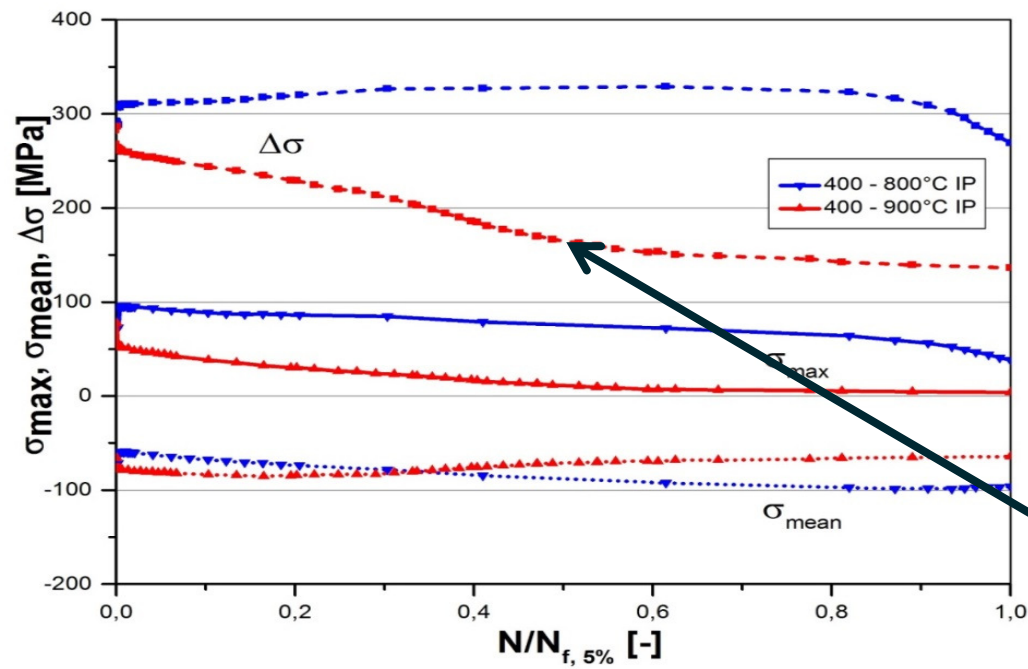


IP,  $T = 400 - 900 \text{ }^\circ\text{C}$ ,  $\Delta\varepsilon_{\text{mech}} = 0.4 \text{ } \%$

# Thermomechanical Fatigue

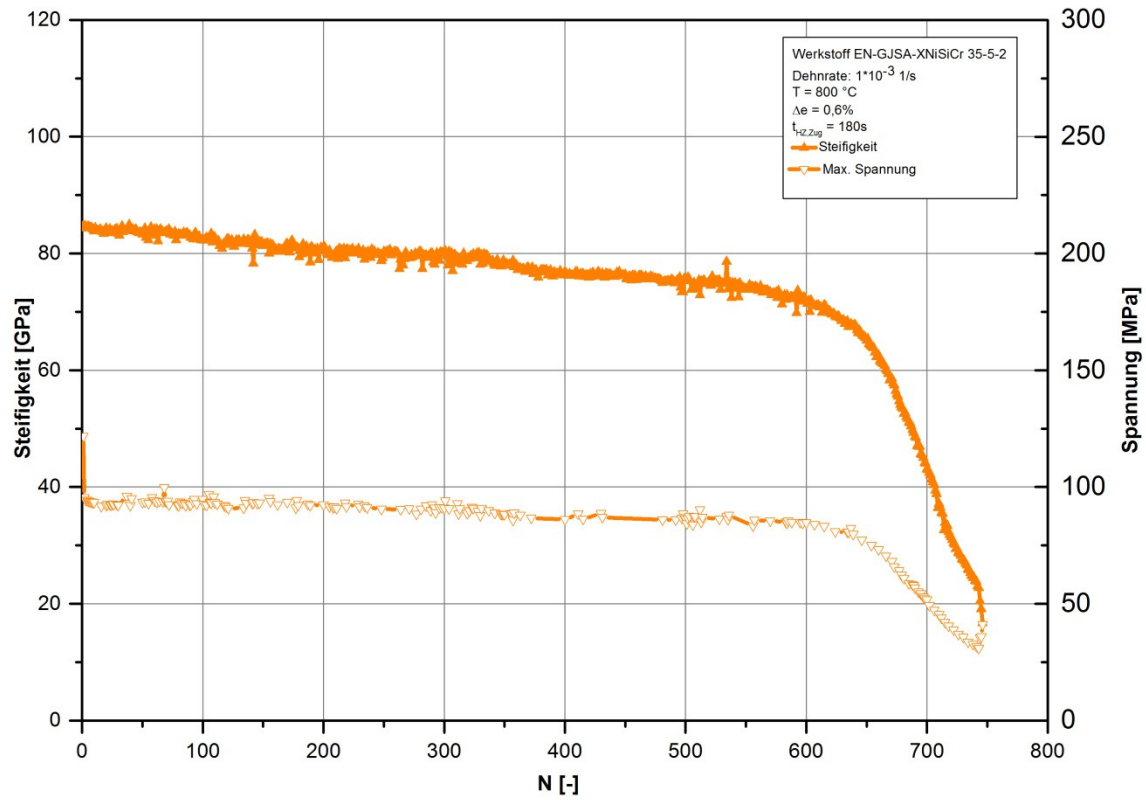


# Thermomechanical Fatigue



Failure criterion 5 % force drop is worthy for discussion

# Thermomechanical Fatigue



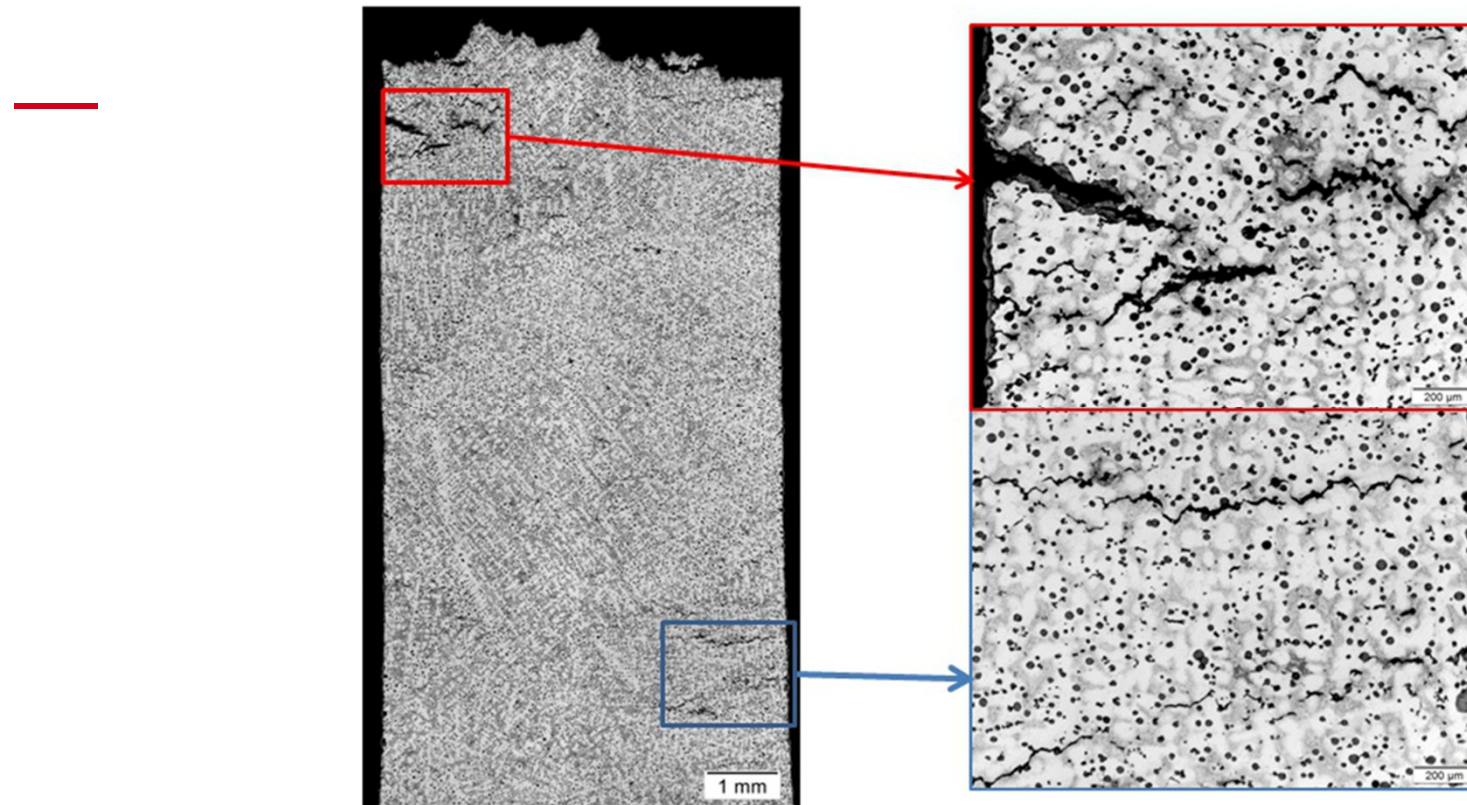


---

## **Damage mechanism**

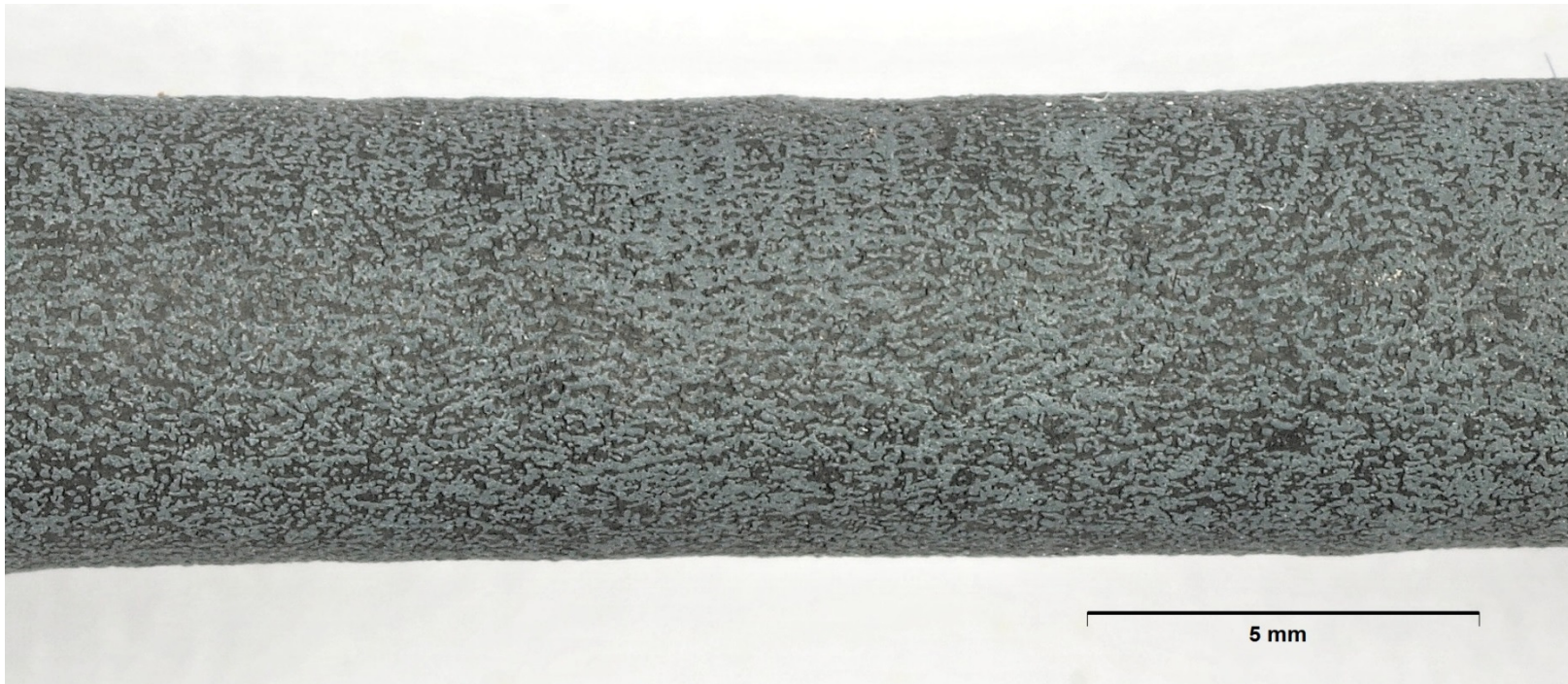
---

## Damage mechanism



— IP,  $T = 400 - 900 \text{ } ^\circ\text{C}$ ,  $\Delta\varepsilon_{\text{mech}} = 0.4 \text{ } \%$ , half lifetime

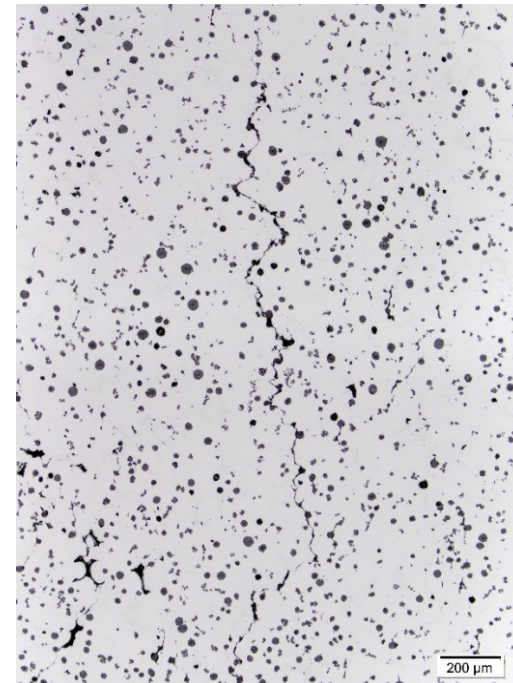
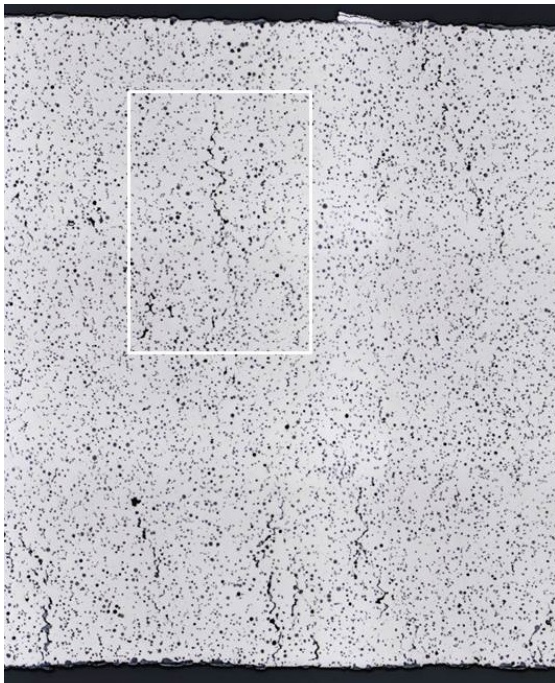
## Damage mechanism



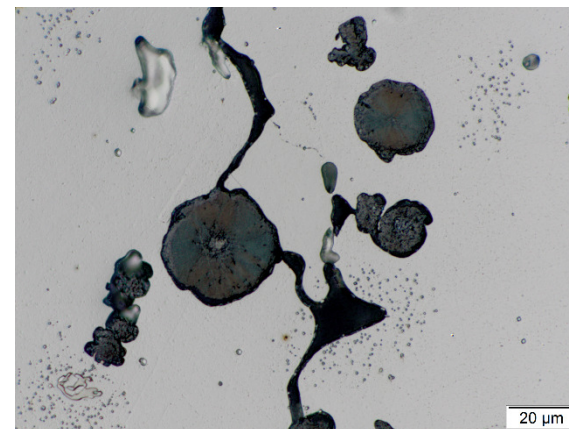
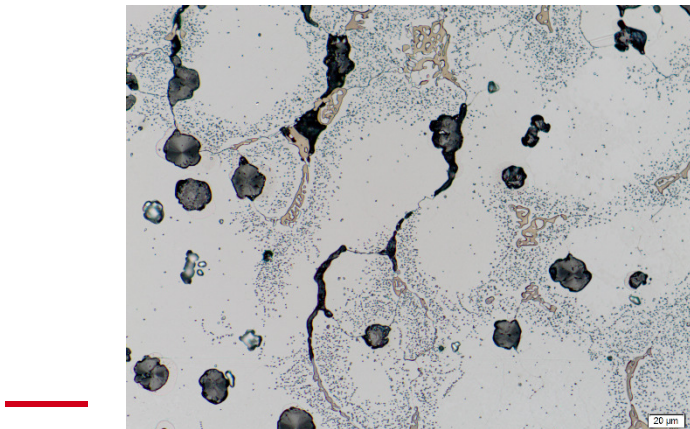
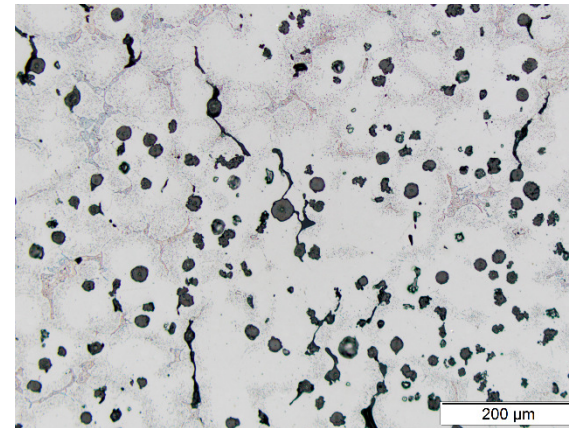
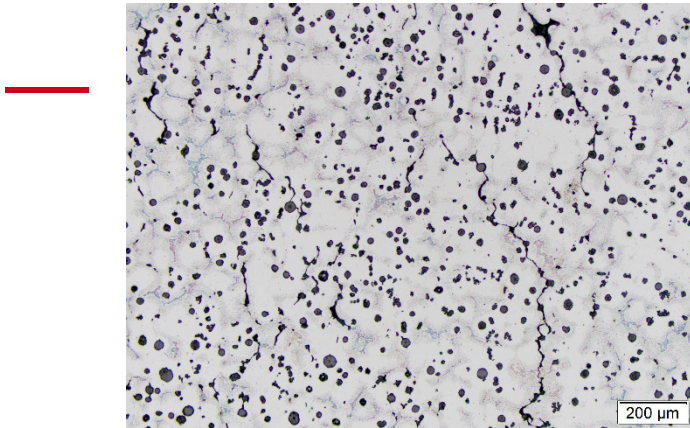
# Damage mechanism



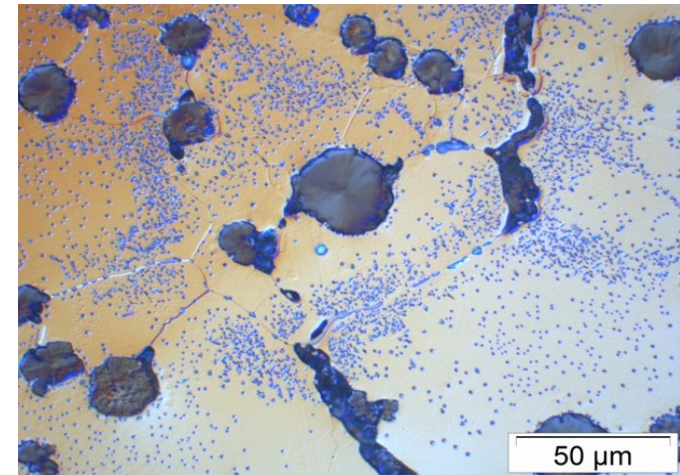
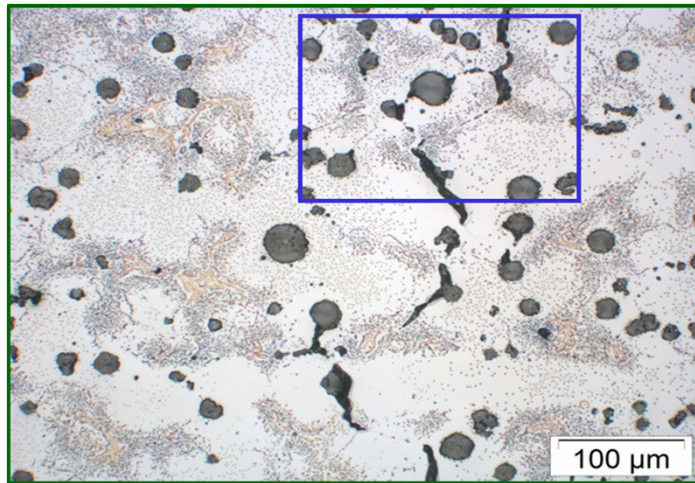
# Damage mechanism



# Damage mechanism



## Damage mechanism



Creep test @ 900 °C,  $\sigma = 15$  MPa

## Damage mechanism

---

Additional damage mechanism:

Microcracks in areas with carbide network in the remaining solidification area



---

Strain-controlled LCF-Test @ 800°C, 0,3 %,  $R_e = -1$ ,  $\dot{\epsilon} = 10^{-3} \text{ s}^{-1}$



---

## **Conclusion**

---

## Conclusion



- 
- Fatigue life of austenitic cast iron Ni-Resist was investigated for  $T_{\min}$  400°C and  $T_{\max}$  700, 800 and 900°C
  - Effect of phase angle (IP, OP) is low
  - IP-TMF tests at  $T_{\max} = 900$  °C show (in contrast to all other TMF tests) continuous cyclic softening right from the start.
  - Reason: creep damage which is also observed in LCF-specimens tested at 800 °C and 900 °C
  - Further research to define stiffness based lifetime criterion t
-

# Acknowledgements



---

Gefördert durch:



Bundesministerium  
für Wirtschaft  
und Energie



IGF-No. 17084



aufgrund eines Beschlusses  
des Deutschen Bundestages

FVV = Research Association for Combustion Engines e.V.

AiF = German Federation of Industrial Research Associations

BAM 5.1 Elke Sonnenburg, BAM 5.2 Benjamin Piesker

---

**Thank you for your kind attention!**



**AREVA**

forward-looking energy



# TMF/SHM for Thermal Power Plants Solutions for load follow operation challenges

Dr. Jürgen Rudolph / Steffen Bergholz / Benoît Jouan

AREVA GmbH, Erlangen

TMF-Workshop 2016, BAM, Berlin, April 27-29

# Contents



- ▶ **Introduction**
- ▶ **Design code requirements**
- ▶ **Creep-fatigue monitoring concept**
- ▶ **Application example**
- ▶ **Summary**

# Chapter 1

## Introduction

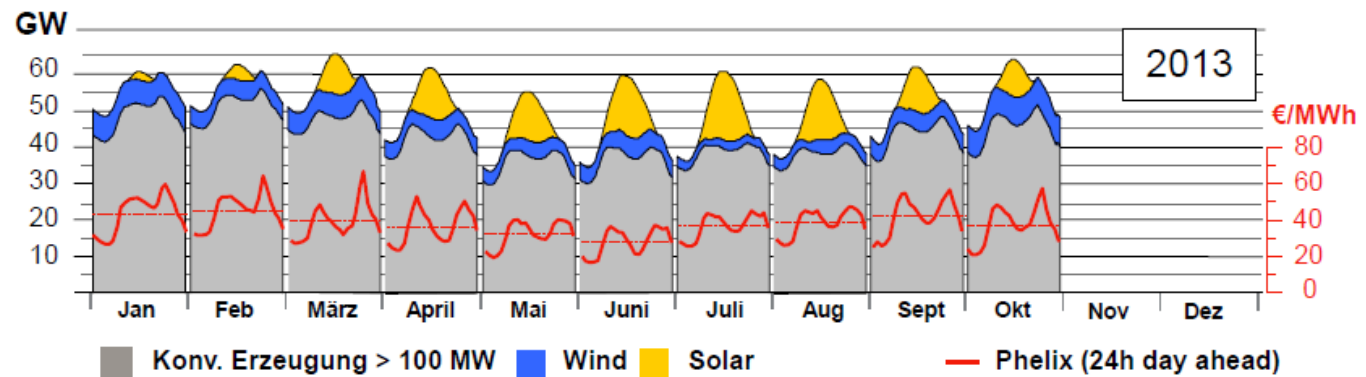


## ▶ Changing energy markets requirement







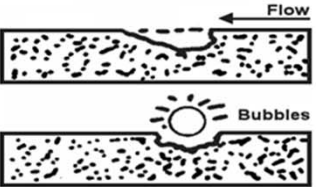
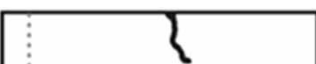
- ◆ Operation of power plants with more flexible loads
- ◆ Load-follow capabilities of conventional power plants essential
- ◆ Reduction of costs
  - Optimization and predictability of maintenance and inspection activities
  - Increase in availability

## ▶ Flexibilization measures

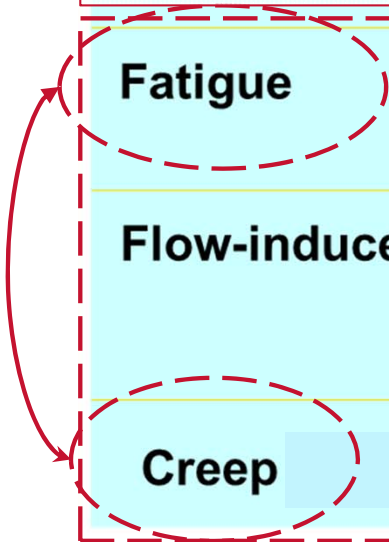
- ◆ Decreasing base load,
- ◆ Start-up time reduction,
- ◆ Increasing load ramps,
- ◆ Optimization of (creep-fatigue) lifetime consumption



# Introduction

<p>General corrosion</p>		<ul style="list-style-type: none"> <li>▪ uniform corrosion</li> <li>▪ shallow pitting</li> </ul>
<p>Microbiological corrosion</p>		<ul style="list-style-type: none"> <li>▪ MIC</li> </ul>
<p>Localized corrosion</p>		<ul style="list-style-type: none"> <li>▪ pitting</li> <li>▪ crevice corrosion</li> </ul>
<p>Stress corrosion cracking</p>		<ul style="list-style-type: none"> <li>▪ Ni-SCC</li> </ul>
<p>Corrosion fatigue</p>		<ul style="list-style-type: none"> <li>▪ strain induced corrosion cracking</li> </ul>
<p><b>Fatigue</b></p>		<ul style="list-style-type: none"> <li>▪ thermal transient fatigue</li> <li>▪ thermal cycling fatigue</li> <li>▪ thermal stratification fatigue</li> </ul>
<p><b>Flow-induced corrosion</b></p>		<ul style="list-style-type: none"> <li>▪ FAC – flow-accelerated corrosion</li> <li>▪ cavitation erosion</li> <li>▪ liquid droplet impingement (LDI)</li> <li>▪ solid particle erosion</li> </ul>
<p><b>Creep</b></p>		<ul style="list-style-type: none"> <li>▪ creep</li> </ul>

AGEING MECHANISMS



# Introduction

*Fatigue damage event at Staudinger power plant May 12, 2014:*

**TÜV Technische Überwachung Hessen GmbH**

Industrie Service

Zusammenfassung der sicherheitstechnischen Beurteilung nach §18 Abs. 2 BetrSichV zum Schadensereignis vom 12.05.2014 am Standort Kraftwerk Staudinger Block 5



6.4.2 E

Auf Grur

Bestimm

Verhältni

den Erschöpfungsgrad.

## Beispiele: Kraftwerk Staudinger LUV Schadensereignis vom 12.05.2014

Im Hinblick auf eine Ermüdungsschädigung besitzt der Lastwechsel „Benson- auf Umwälzbetrieb“ den größten Schädigungsanteil, da dieser die meisten Lastzyklen aufweist. Für die Berechnungsposition 2 der „Alten Geometrie“ ergab sich hierfür Gesamterschöpfung von ca. 2,37 (237%). Für den im Rahmen der Auslegung gem. TRD betrachteten und betrieblich überwachten Saugstutzen (Position 4) errechnete sich eine Gesamterschöpfung von <0,5 (50%). Unter Annahme der gleichen Lastwechsel ergibt sich für die „Neue Geometrie“ an der höchstbeanspruchten Stelle 1 eine Erschöpfung < 0,154 (15,4%).

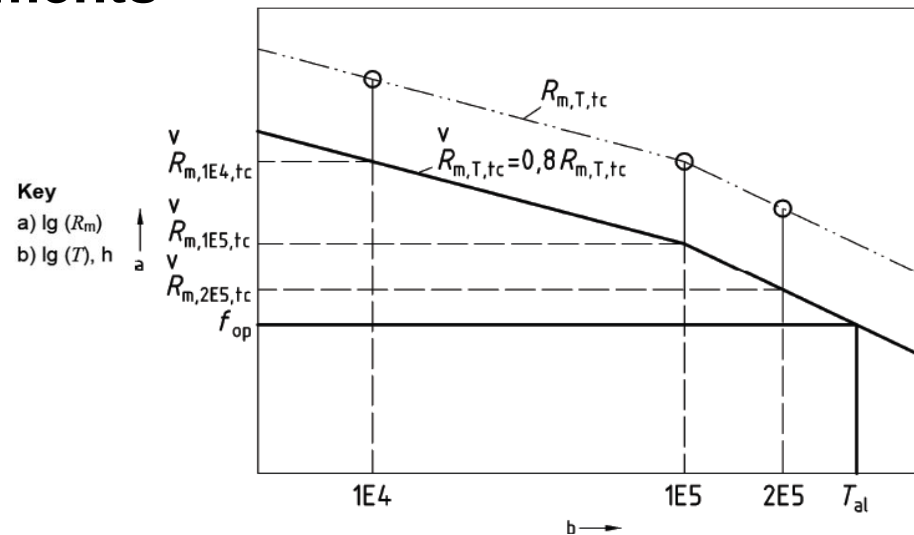
# Chapter 2

## Design code requirements

# Design code requirements / creep

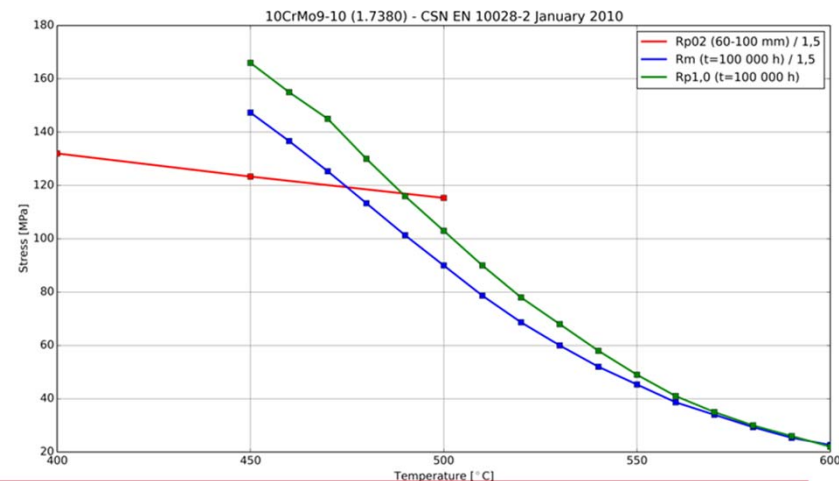
## ► Essential design codes for flexible interfaces meeting the creep-fatigue assessment requirements

- ◆ EN 12952-3
- ◆ EN 12952-4
- ◆ TRD 301
- ◆ TRD 508
- ◆ AD 2000 Merkblatt
- ◆ EN 13445-3
- ◆ ...



## ► Negligible creep

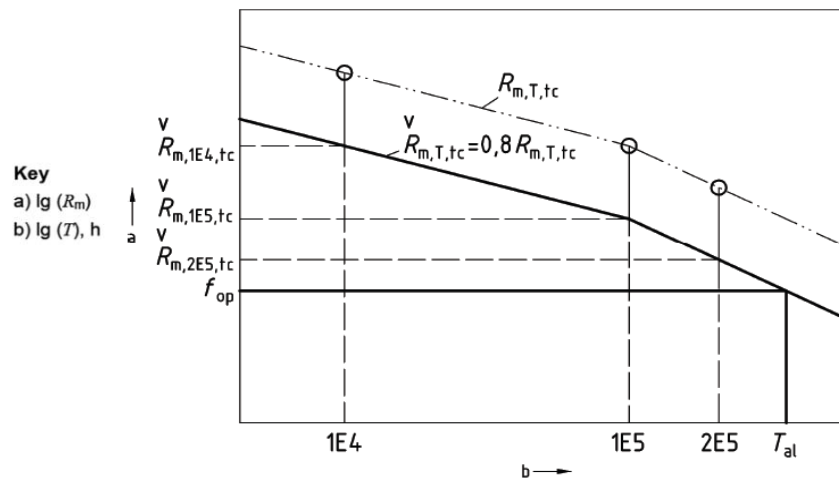
- ◆ Concept to be implemented in EN code



# Design code requirements / creep

► Determination of creep usage factors according to EN 12952-4

◆ Annex A (informative) Calculation of in-service creep damage:



$$\Delta D_{cik} = \frac{T_{op}}{T_{al}}$$

$$D_C = \sum_i \sum_k \Delta D_{cik}$$

Symbol	Description	Unit
$f_{op}$	Membrane stress at operation conditions	MPa
$T_{op}$	Operated time at operating conditions	h
$T_{al} / t_{al}$	Time to reach the theoretical rupture by creep	h
$D_c$	Creep damage	-
$D_{cik}$	Usage portion for each increment	-
$R_{m,T,t}$	Tensile strength at given time and temperature	MPa



**Question:** Does “membrane stress at operation condition” only address internal pressure or also other loads?

# Design code requirements / creep

► Determination of creep usage factors according to EN 12952-4

◆ Annex A (informative) Calculation of in-service creep damage - example:

**Table A.2 — Summation of data for the calculation of in-service creep damage**

User and boiler plant:	XY
Power station:	XY
Boiler:	3
Works-No.:	12345
Year built:	2003
Maximum allowable pressure	HP: 84 bar Reheater: – bar
Superheated steam temperature:	HP: 525 °C Reheater: – °C
Steam output:	128 t/h

1	2	3	4	5	6	7	8	9	10	11	12	13
No.	Component Material; Steel group	a	b	d mm	c	$e_s$ mm	$e_{rs}$ mm	$p_c$ bar	$t_o$ °C	$t_c$ °C	$f_{ap}$ N/mm <sup>2</sup>	$T_{al}$ 10 <sup>3</sup> h
1	HP-line 13CrMo44; 5.1	m	A B	292,0	o	24,0	21,0	75,5	525	530	48,7	208

# Design code requirements / fatigue

► Determination of usage factors according to TRD301, Appendix 1:

◆ ideally elastic mechanical hole edge stress:

$$\sigma_{ip} = \alpha_m * p * \frac{d_m}{2 * sb}$$

◆ ideally elastic hole edge thermal stress

$$\sigma_{iv} = \alpha_v * \frac{\beta_{Lv} * E_v}{1 - \nu} * (v_m - v_i)$$

*under the assumption of a quasi steady-state course of temperature the following equation for the temperature change rate holds true:*

$$\Delta v = v_m - v_i = \text{const.} = \Delta v_\infty = \frac{1}{a_v} * \Phi_f * v_v * s_b^2$$

Stresses are calculated with  $\alpha_v=2.0$  as a function of the temperature change rate  $v_v$

$$\sigma_{iv} = \frac{v_v}{W * V} ; W = \frac{0,35}{\beta_{Lv} * E_v} ; V = \frac{a_v}{\Phi_f * s_b^2}$$



**Question: Is the temperature change rate  $v_v$  an appropriate parameter for the optimization of start-up cycles?**



# Design code requirements / fatigue

## ► What are the relevant sources of stress – time – histories?

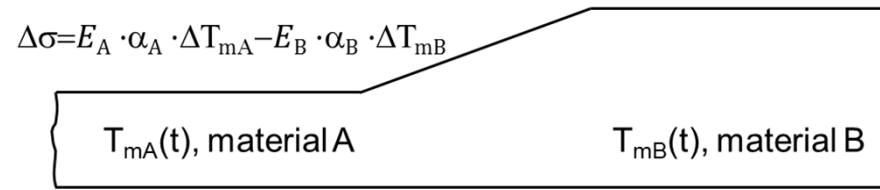
### ◆ Internal Pressure (e.g. start-up, shut-down) → \*C

- Global (membrane) and local (membrane + bending + peak) stresses

### ◆ Thermal stresses in thick-walled component → partially \*C

- quasi steady-state stresses due to temperature difference across the wall thickness
- Unsteady-state stresses due to temperature difference across the wall thickness

### ◆ Thermal stresses due to local structural or material discontinuity (T<sub>A</sub>-T<sub>B</sub> problem) → not directly \*C



### ◆ Additional mechanical loads → not directly \*C

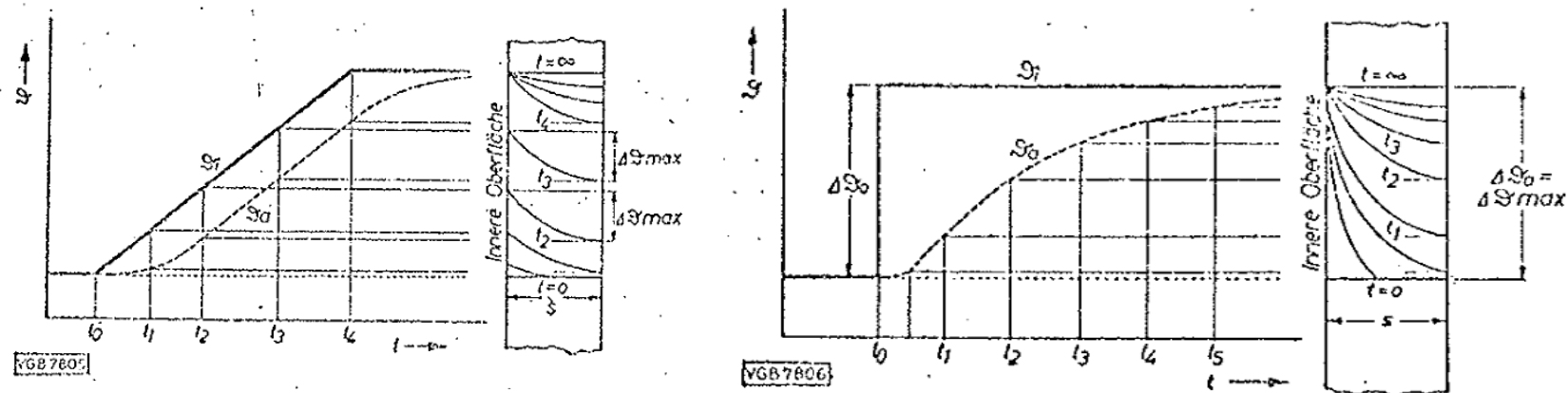
- Nozzle loads
- Thermal loads on piping system resulting in mechanical component loads

\*C ... covered by code procedure

# Design code requirements / fatigue

## ► Theoretical background of thermal stress determination:

- ◆ General case: unsteady-state thermal stresses resulting from transient temperature loads (arbitrary operational load-time histories)
- ◆ Particular cases (with analytical solutions for flat plates, cylinders and spheres):
  - Quasi steady-state temperature changes with constant temperature change rate
  - Ideal thermal shock



Pich, R.: Die Berechnung der elastischen, instationären Wärmespannungen in Platten, Hohlzylindern und Hohlkugeln mit quasistationären Temperaturfeldern. Mitteilungen der VGB, Heft 87/88, 1963/1964

# Design code requirements / fatigue

## ► Theoretical background of thermal stress determination:

### ◆ Fourier's differential equation

$$\frac{\partial \mathcal{G}}{\partial t} = a \cdot \nabla^2 \mathcal{G} + \frac{W}{\rho \cdot c} \quad a = \frac{\lambda}{\rho \cdot c}$$

### ◆ Quasi steady-state temperature changes with constant temperature change rate $V_T$

$$\frac{\partial \mathcal{G}}{\partial t} = V_T = \text{const} \quad \longrightarrow \quad \nabla^2 \mathcal{G} = \frac{V_T}{a}$$

### ◆ Equibiaxial stresses and mean temperature difference at the inside

$$\sigma_i = \frac{\beta_{Lv} * E_v}{1 - \nu} * \Delta \mathcal{G}_m$$

# Design code requirements / fatigue

- ▶ Determination of usage factors according to EN 12952-3 und EN 12952-4:

- ◆ ideally elastic mechanical and thermal stress for cylinder (inside corner of the bore):

$$\sigma = \alpha_m * p * \frac{d_{ms}}{2 * e_{ms}} + \alpha_t * \frac{\beta_{Lt} * Et}{1 - \nu} * \Delta t$$

- ◆ ideally elastic mechanical and thermal stress for sphere (inside corner of the bore):

$$\sigma = \alpha_{sp} * p * \frac{d_{ms}}{4 * e_{ms}} + \alpha_t * \frac{\beta_{Lt} * Et}{1 - \nu} * \Delta t$$

- ◆  $\Delta t$  is calculated according to EN 12952-3, Section 13.2:

*wall temperature difference, defined as integral mean wall temperature minus inside wall surface temperature*

$$\Delta t = t_m - t_i$$



**Question: Does a possible quasi steady-state solution (as in TRD) meet all creep-fatigue monitoring requirements based on realistic load-time histories?**

# Design code requirements / fatigue

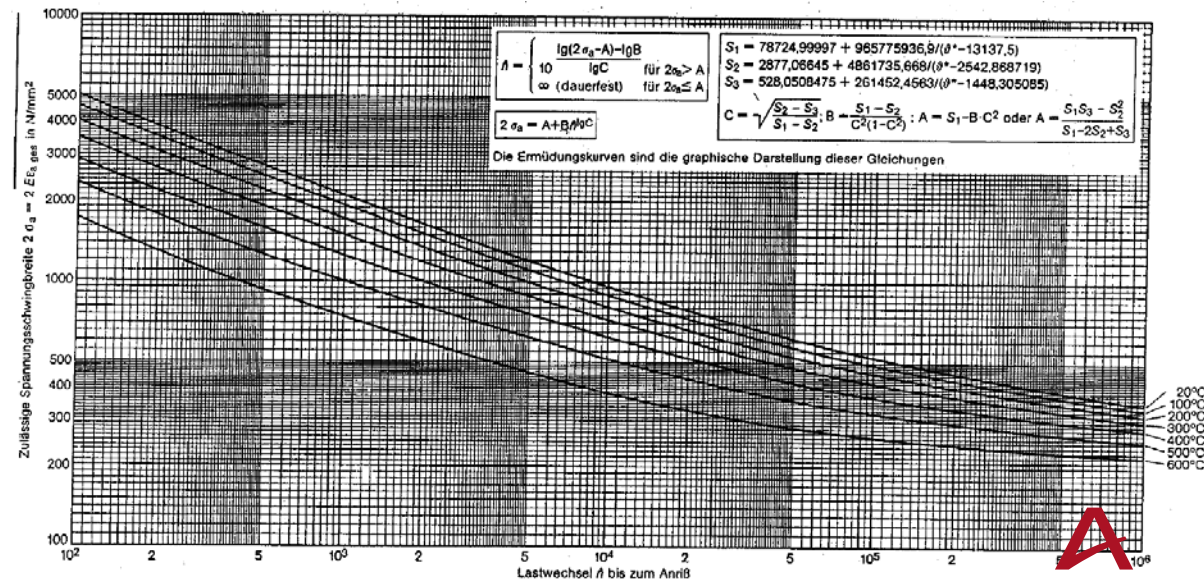
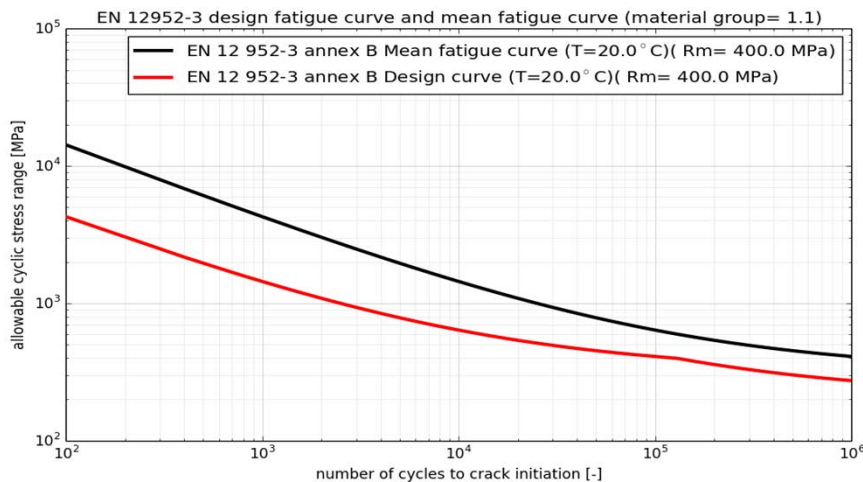
## ► Fatigue Assessment

- ◆ Determination of stress ranges and number of load cycles to technical crack initiation

$$\Delta\sigma_i = \hat{\sigma}_i - \check{\sigma}_i$$

- ◆ Fatigue design curves in terms of stress ranges  $2 * \sigma_a$  are plotted as a function of the ultimate tensile strength
- ◆ Accumulated usage factor D of all load cycles

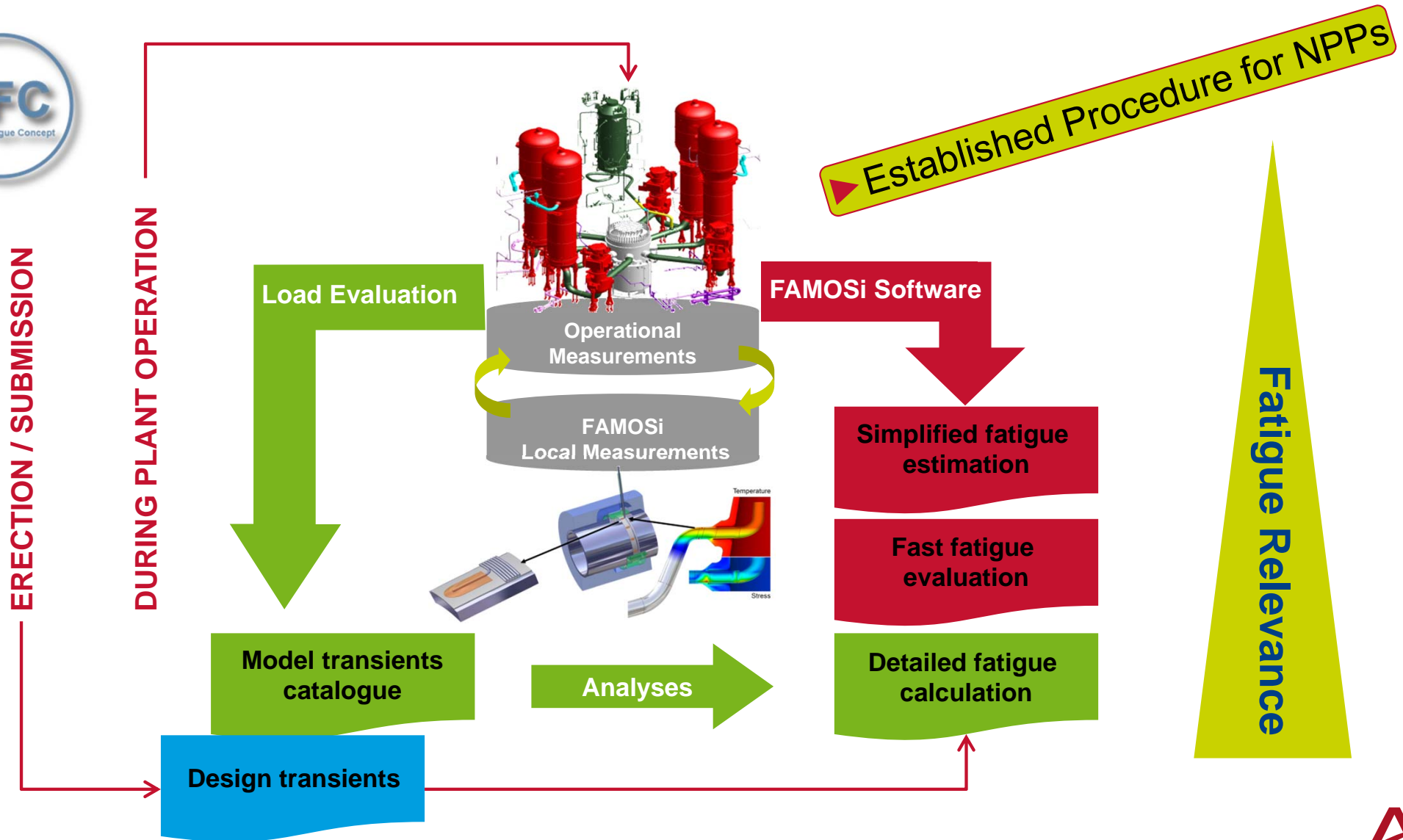
$$D = \frac{n_1}{\hat{n}_1} + \frac{n_2}{\hat{n}_2} + \dots \leq \frac{1}{S_D}$$



# Chapter 3

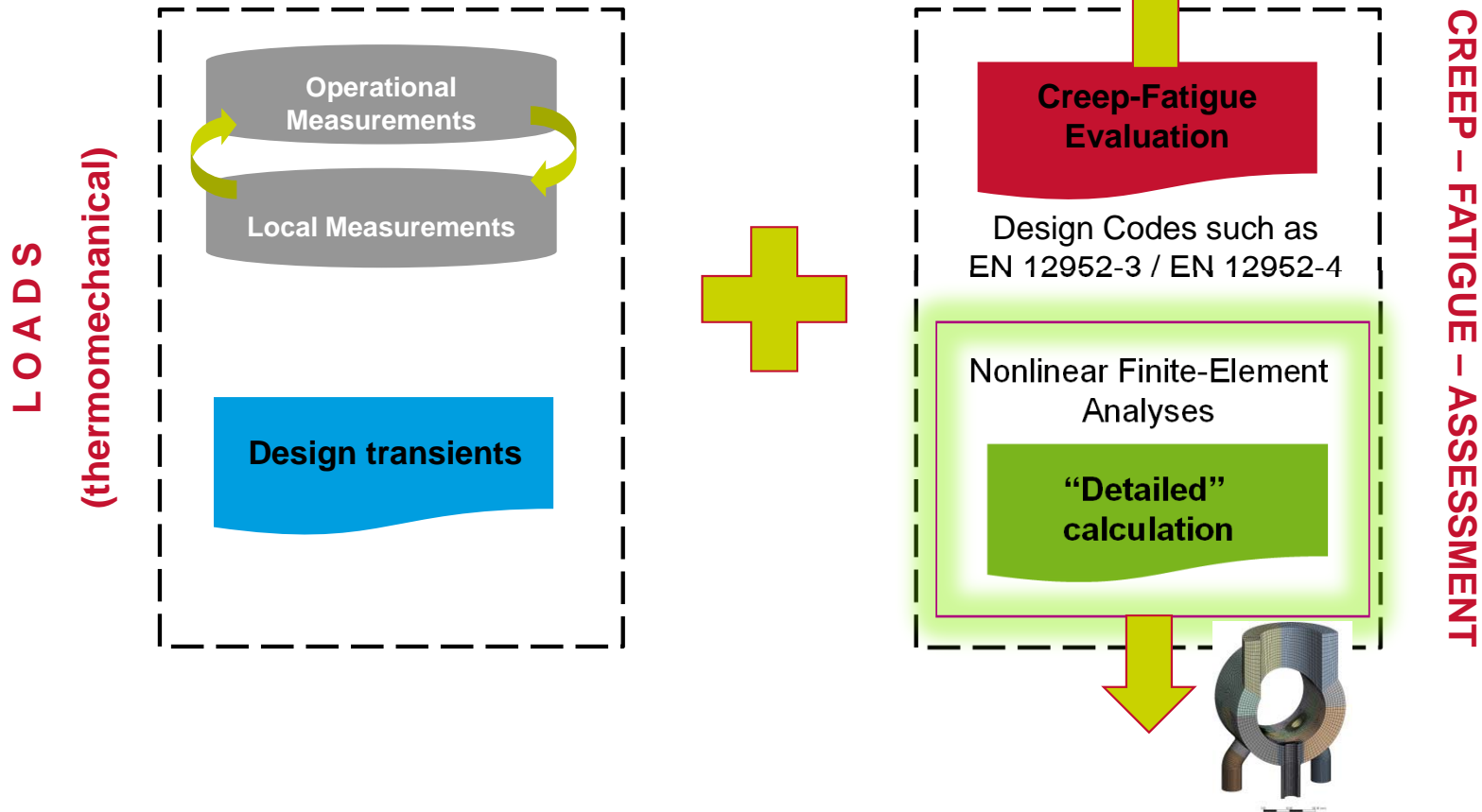
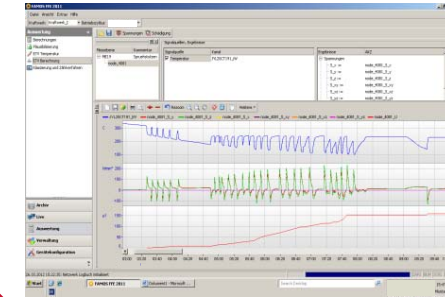
## Creep-fatigue monitoring concept

# Creep-fatigue monitoring concept



# Creep-fatigue monitoring concept

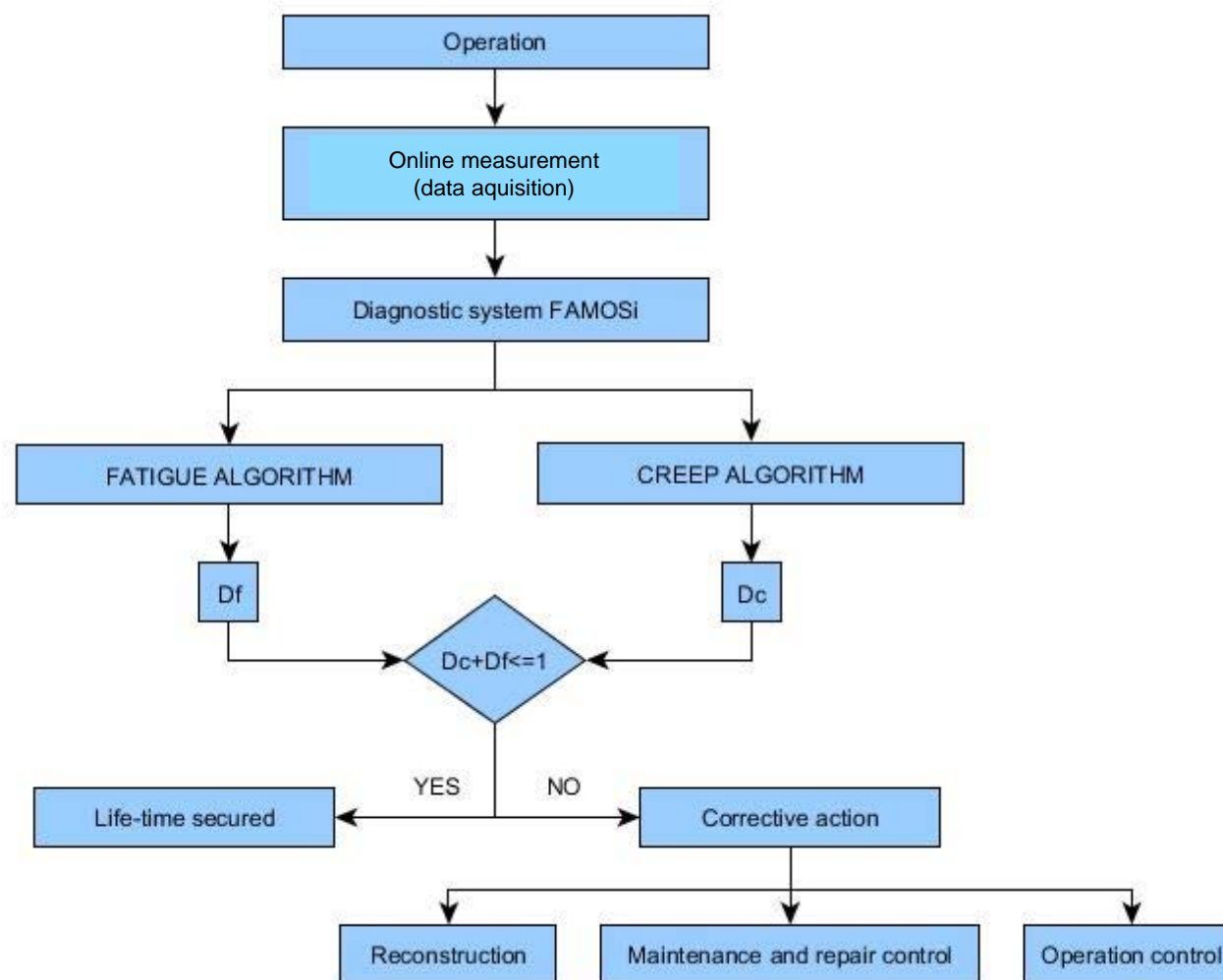
## ▶ AREVA's concept for conventional power plants





# Creep-fatigue monitoring concept

## ► Creep-fatigue interaction layout according to TRD 508 , EN 12952



# Creep-fatigue monitoring concept

## Material Properties:

$E(T)$

$R_{m,200000h}(T), R_m(T), \dots$

Design fatigue curves

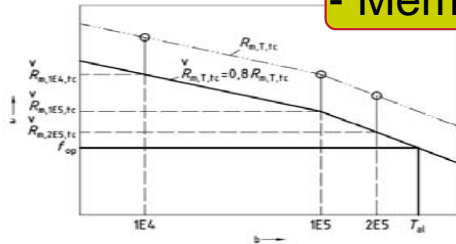
## Stress-time-history

(full stress tensor, total and linearized):  
 $SX(t), SY(t), SZ(t), SXY(t), SYZ(t), SXZ(t)$

## Temperature-time history:

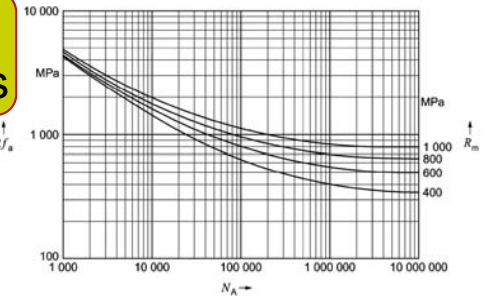
Inner wall / mean temperature  $T_i(t), T_m(t)$

- Membrane stresses



Cycle counting module  
(Rainflow HCM)

- Stress ranges  
- Mean stresses



## Creep evaluation module:

EN 12952-4

Damage  
accumulation

## Fatigue evaluation module:

EN 12952-3 / 4

# Creep-fatigue monitoring concept

## ► Creep evaluation according to EN 12952-4

The usage portion for each increment is given by

$$\Delta D_{ci k} = \frac{T_{op}}{T_{al}} \quad (A.1)$$

The creep damage  $D_c$  during the evaluated period shall be obtained from the linear damage rule by summing up the values  $\Delta D_{ci k}$  for all temperature increments and, if any, pressure as follows:

$$D_c = \sum_i \sum_k \Delta D_{ci k} \quad (A.2)$$

### A.3.2 Online computerized data storage

In the case of on-line data storage by means of a data processing system a separation into increments may be waived. For calculation of the theoretical lifetime  $T_{al}$  the on-line measured values of pressure and temperature including the above mentioned allowances shall be used instead of the mean values of the increments. The increase of creep damage is obtained in this case from the measured time divided by the theoretical lifetime (see Tables A.2 and A.3).

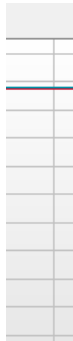
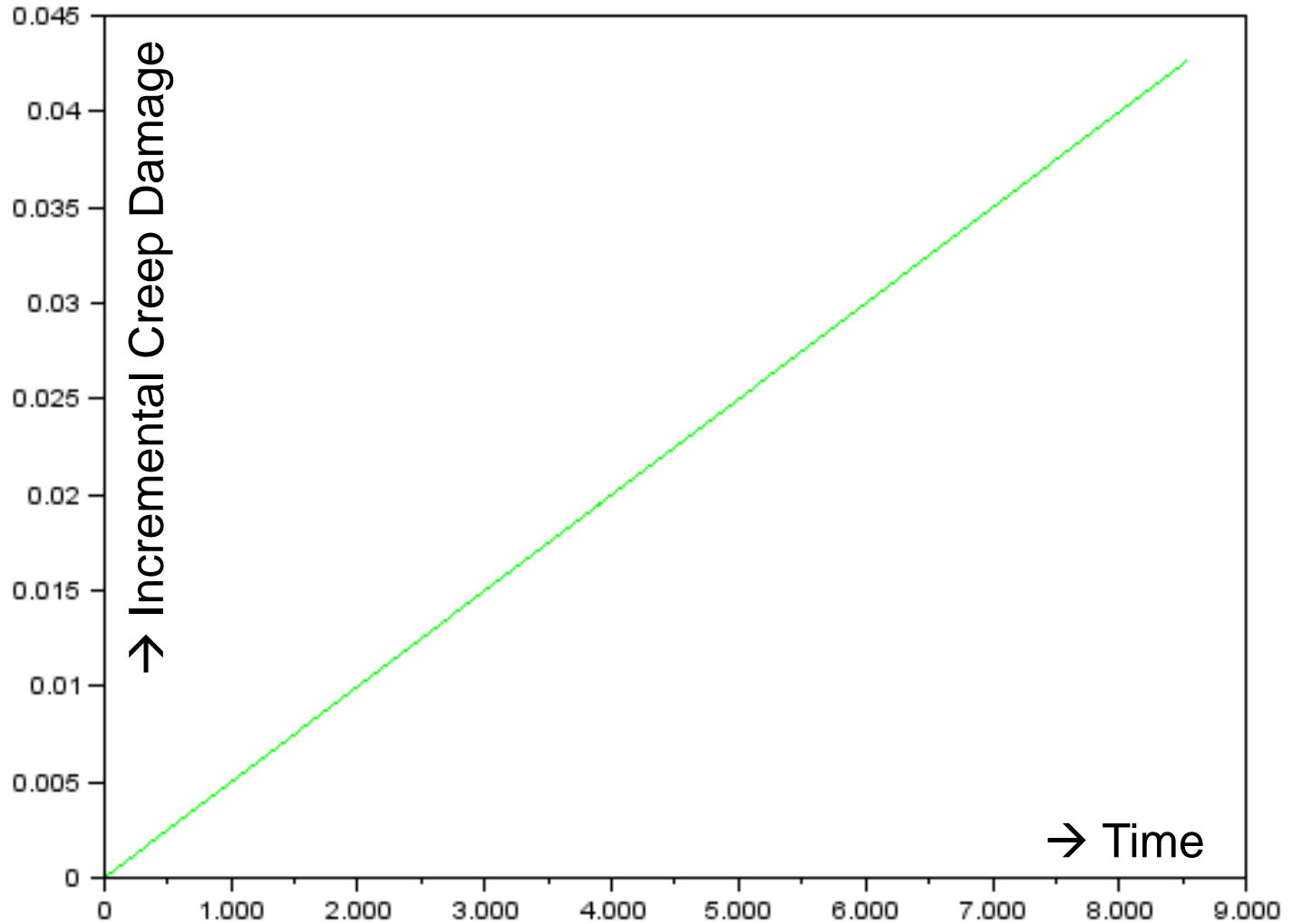
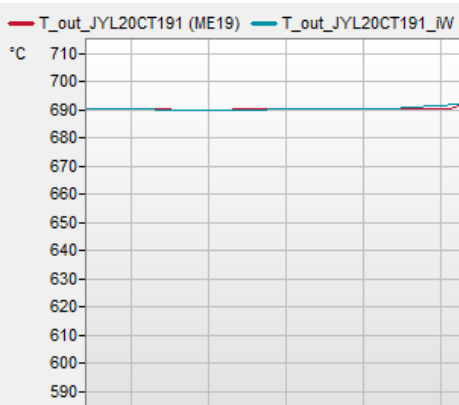
The computer programme used shall permit the results to be verified by at least a random test.

# Creep-fatigue monitoring concept

## ▶ Example of pres



## ▶ Example of temp



# Creep-fatigue monitoring concept

## ► Evaluation of complex load-time histories as a basic feature:

### ◆ Quasi steady state **versus** thermal transient solution

### ◆ Thermal transient solutions by way of

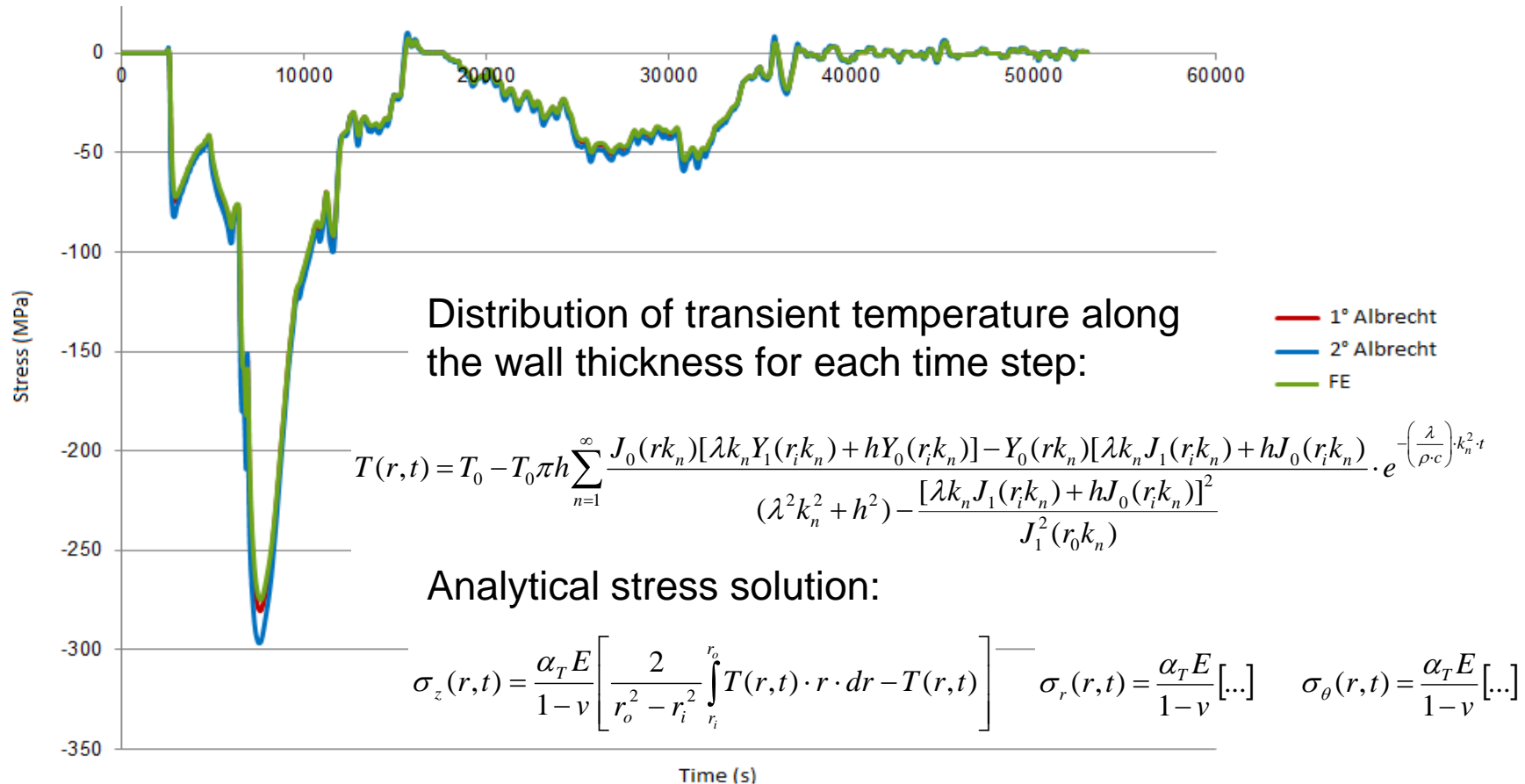
- Coupled thermal transient + mechanical finite elements analyses based on load-time history input
  - not applicable in the sense of monitoring long time histories
- Implementation of specific analytical solutions for simple geometries:
  - *Albrecht, W.: Instationäre Wärmespannungen in Hohlzylindern. Konstruktion 18 (1966), No. 6, pp. 224/231*
  - *Costa, F.; Freire, J.L.; Rudolph, J.; Maneschy, J.E.: A Proposal to Consider Cycle Counting Methods for Fatigue Analysis of Nuclear and Conventional Power Plant Components. Proceedings of the ASME 2016 Pressure Vessels & Piping Conference PVP2016, July 17-21, Vancouver, BC, Canada, Paper No. PVP2016-63931*
- Application of a Green's function (elementary transients) approach:
  - Initializing finite element analyses
  - Storing of elementary stress responses in databases
  - Scaling with realistic load-time history

# Creep-fatigue monitoring concept

## ▶ Exemplary stress-time history for a start-up process

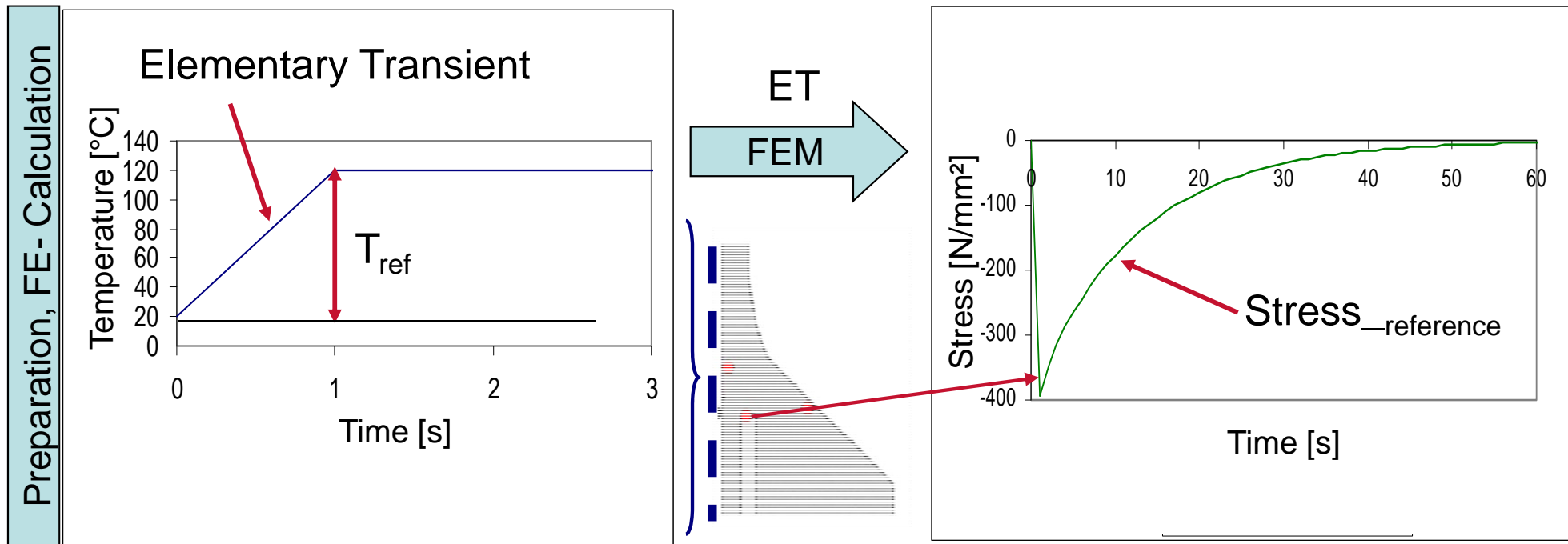
### ◆ Circumferential stress of an exemplary pipe:

- analytical (Albrecht) and numerical (FE) solution



# Creep-fatigue monitoring concept

- ▶ Application of a Green's function (elementary transients) approach
  - ◆ Example for an elementary stress calculation

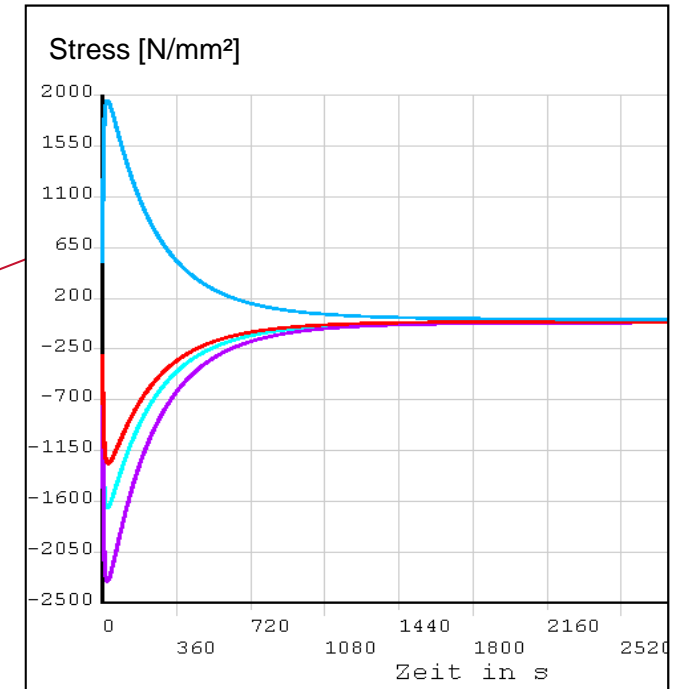
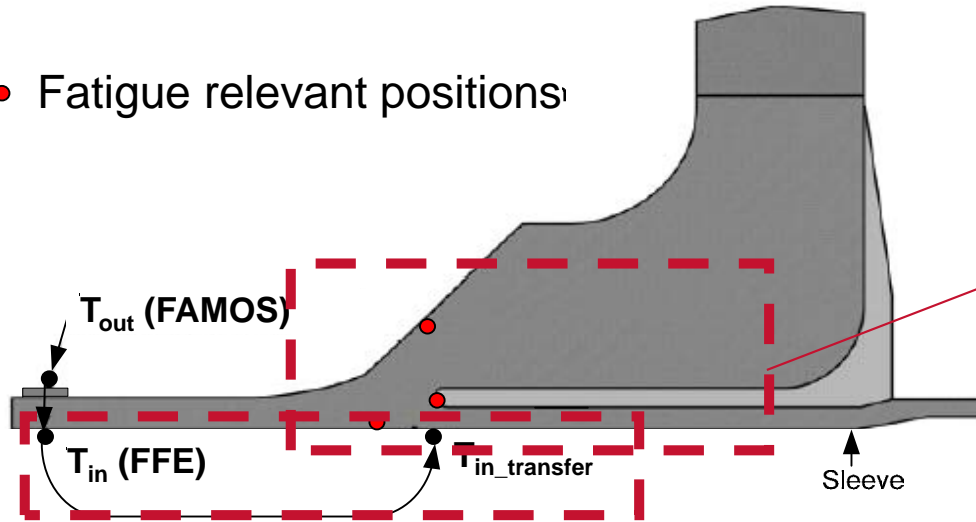


- ▶ The stress references are saved in a database → Initialization

# Creep-fatigue monitoring concept

## ► Fast Fatigue Evaluation principle

- Fatigue relevant positions:



Inner wall temperature at the measured section

Elementary transient

FE- Model of the analyzed structure

Stress reference responses → DATABASE

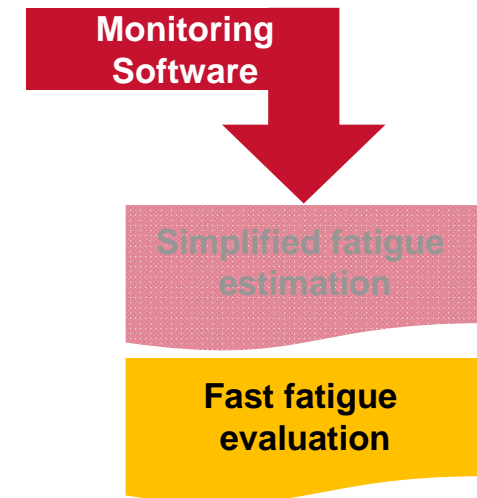
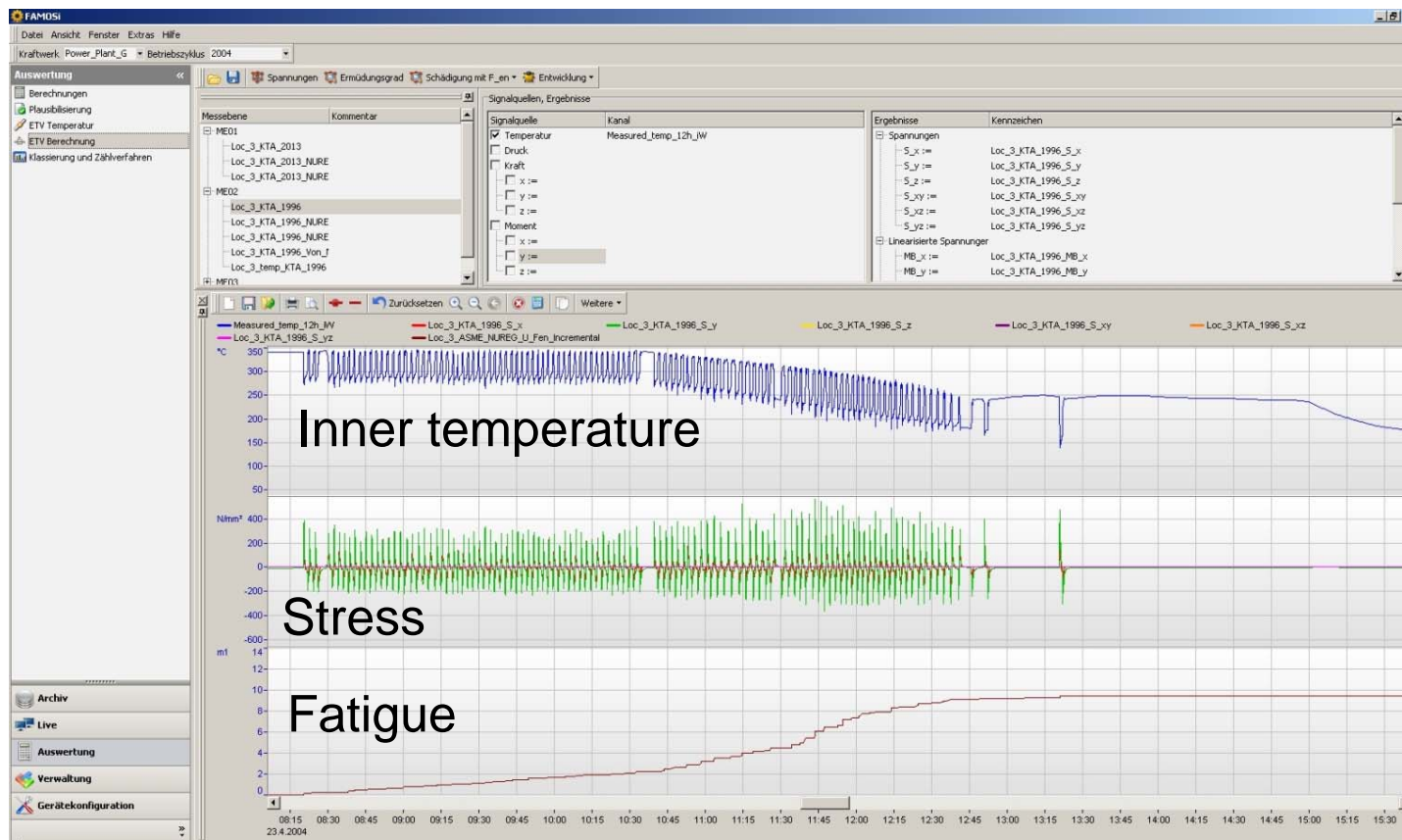
Stress calculation at the fatigue relevant locations

Time dependant stress tensor



# Creep-fatigue monitoring concept

- ▶ After initialization of the Green's functions fatigue evaluation can be done online



- ▶ Scaling process is performed
- ▶ Stress is calculated
- ▶ Rainflow algorithm is implemented for fatigue calculation

# Creep-fatigue monitoring concept

## ▶ Cycle Counting according to EN 12952-4

### ◆ B.5 Detection of load cycles:

- The basis process of load cycle counting shall be the range-pair-method<sup>1)</sup>
- 1) The rain-flow-load cycle counting is based on this method and may also be used, ...

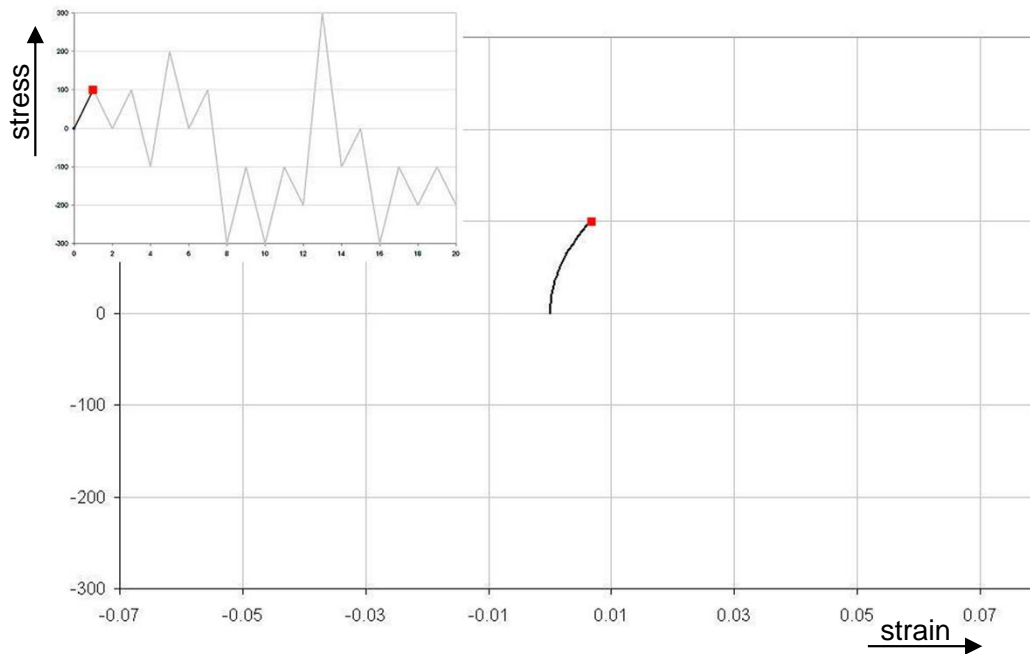
## ▶ Implemented cycle counting algorithm:

### ◆ Hysteresis Counting Method **HCM** as an efficient proposal of a **rainflow** algorithm

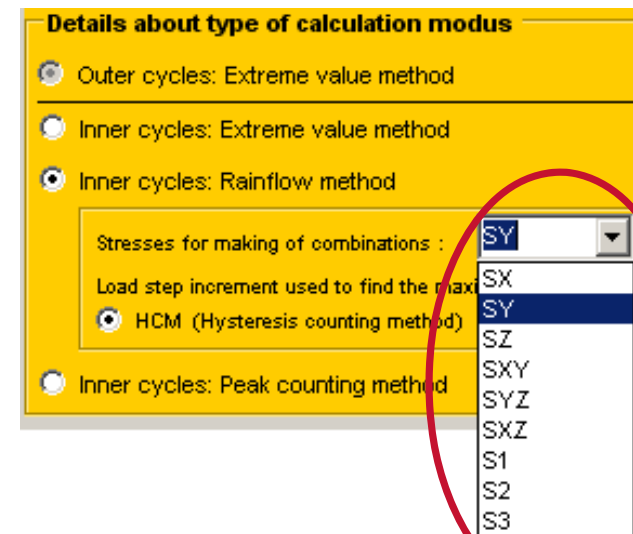
- *Clormann, U.H.; Seeger, T.: Rainflow – HCM. Ein Zählverfahren für Betriebsfestigkeitsnachweise auf werkstoffmechanischer Grundlage. Stahlbau 55 (1986), No. 3, pp. 65/71*
- Easy algorithmic implementation
- Well-proven in engineering practice
- Design code implementation in draft ANNEX NB of EN13445-3

# Creep-fatigue monitoring concept

- ▶ The implemented Rainflow algorithm is according to Clormann and Seeger (HCM = Hysteresis Counting Method / Masing memory material model)



- ▶ It might be necessary to repeat the calculation for different stress directions:



- ▶ **Advantage:**
  - ◆ Enables fast online identification of cycles

# Creep-fatigue monitoring concept

## ► Detailed creep-fatigue calculation based on nonlinear Finite Elements analysis (modified Becker-Hackenberg model)

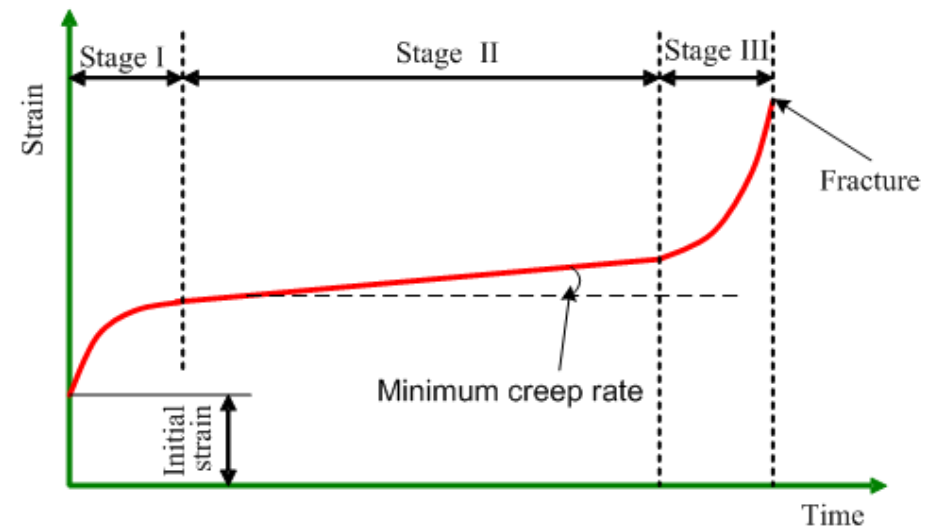
- ◆ Viscoplastic flow rule: ONERA exponential overstress function
- ◆ Kinematic hardening rule: Ohno & Wang – Model II
- ◆ Isotropic hardening rule

Becker M., Hackenberg H.-P., 2011.  
International Journal of Plasticity 27, 596-619.

Wang J., Steinmann P., Rudolph J., Willuweit A., 2015.  
International Journal of Pressure Vessels and Piping 128, 36-47

## ► Presumptions:

- ◆ Calculation based on model / design transients
- ◆ Application for critical components with high usage factors
- ◆ Elimination of the conservatism induced by linearly elastic approach

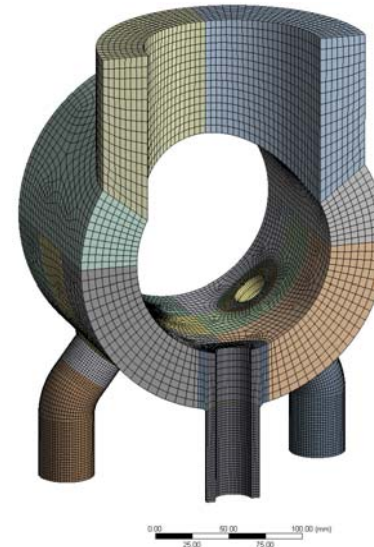


# Chapter 4

Application example

# Application Example

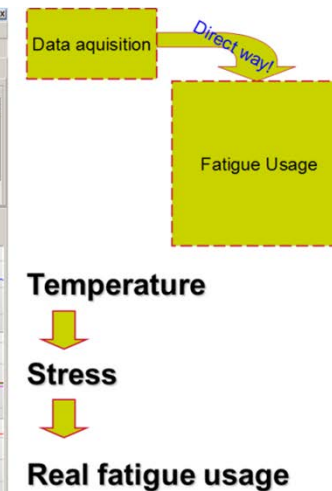
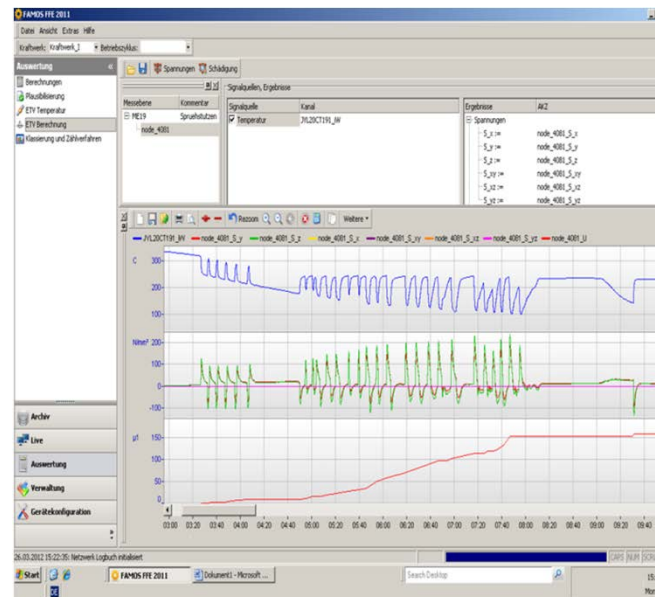
- ▶ Example of detailed fatigue check: Fatigue in drum nozzles of steam generator
- ▶ Instable feeding flow into lower feed water collector causes
  - ◆ Variation of flow rate in the steam generator heating tubes
  - ◆ Height variation water/ steam point
  - ◆ Super heater zone length variation of steam generator pipes
  - ◆ Different average tube temperatures



The instable heat expansion of steam generator tubes produce fatigue cracks after very short normal operation.

# Application example

- ▶ Fatigue in drum nozzles of steam generator
- ▶ Problem statement:
  - ◆ Operational loads induce fatigue at welds of drum nozzles
  - ◆ Fatigue usage factors  $< 1.0$  have to be shown
- ▶ Implemented Solution:
  - ◆ Detailed finite element analysis (FEA)
  - ◆ Detailed fatigue assessment
- ▶ Alternative Solution:
  - ◆ Fast Fatigue Evaluation
    - Temperature
    - Stress
    - Fatigue Usage

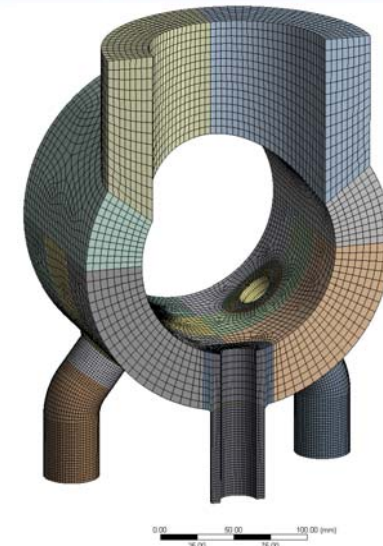
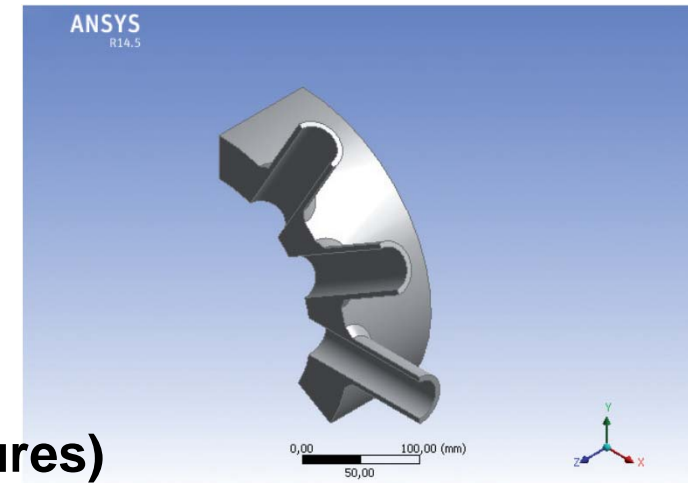



# Chapter 4

## Summary



- ▶ **New challenge: load follow operation**
  - ◆ Potential creep-fatigue damage mechanisms
- ▶ **Proposed solution**
  - ◆ Creep-fatigue monitoring
  - ◆ Acquisition and processing of relevant load data (**time histories** of operational pressure and temperatures)
  - ◆ TMF/SHM Solution for Thermal Power Plants
  - ◆ Integration in inspection concept → including crack propagation
- ▶ **AREVA's creep-fatigue assessment methods**
  - ◆ Established methods e.g. according to EN 12952-3 / 4 in combination with realistic load-time histories
    - Continuous monitoring of creep-fatigue usage
  - ◆ Detailed calculation methods
    - Linear and non-linear finite element analyses





# End of Presentation

## TMF/SHM for Thermal Power Plants

### Solutions for load follow operation challenges

Dr. Jürgen Rudolph / Steffen Bergholz / Benoît Jouan

AREVA GmbH, Erlangen

TMF-Workshop 2016, BAM, Berlin, April 27-29



“

Editor and Copyright [Date]: AREVA GmbH – Paul-Gossen-Straße 100 – 91052 Erlangen, Germany. It is prohibited to reproduce the present publication in its entirety or partially in whatever form without prior written consent. Legal action may be taken against any infringer and/or any person breaching the aforementioned prohibitions.

Subject to change without notice, errors excepted. Illustrations may differ from the original. The statements and information in this brochure are for advertising purposes only and do not constitute an offer of contract. They shall neither be construed as a guarantee of quality or durability, nor as warranties of merchantability or fitness for a particular purpose. These statements, even if they are future-orientated, are based on information that was available to us at the date of publication. Only the terms of individual contracts shall be authoritative for type, scope and characteristics of our products and services.

”

---

# Experimental investigation of the time and temperature dependent growth of small fatigue cracks in Inconel 718 and mechanism based lifetime prediction

---

TMF-Workshop 2016

Michael Schlesinger<sup>1</sup>, Thomas Seifert<sup>2</sup>, Johannes Preußner<sup>1</sup>

<sup>1</sup>Fraunhofer IWM, Germany

<sup>2</sup>Offenburg University of Applied Sciences, Germany

# Topic

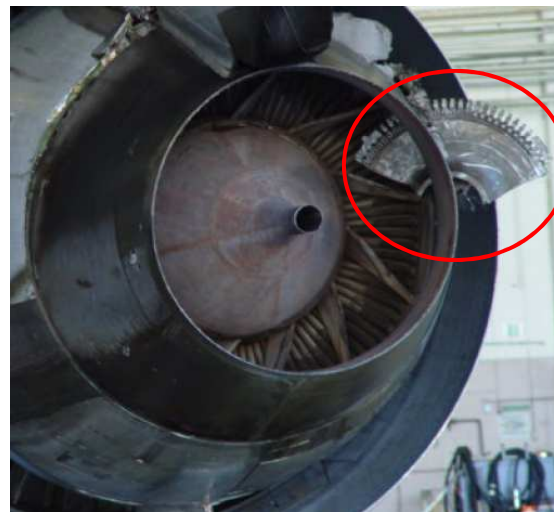
- Introduction
- Material properties of Inconel 718
- Experimental setup
- Time and temperature dependent behavior
  - Deformation
  - Fatigue crack growth
- Mechanism of crack propagation
- Mechanism based modeling
  - Model description
  - Prediction of crack growth and lifetime
- Summary

# Introduction

## Optimizing of future gas turbines with respect to:

- efficiency ➤ elevated turbine inlet temperatures
- flexibility ➤ increasing of start-up and shut-down operations
- operating safety ➤ good knowledge of material behavior and availability of advanced lifetime concepts

Thermomechanical loading leads to initiation and growth of fatigue cracks in hot gas exposed components



Example  
aircraft engine:

Fatigue failure of  
turbine disc out of IN718  
during ground run

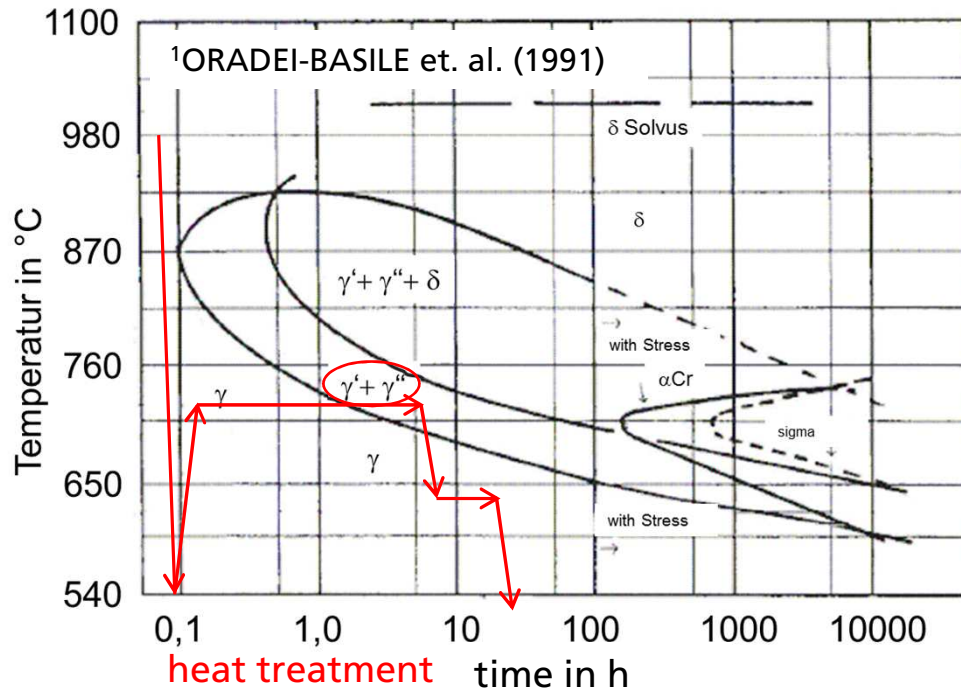
from ROSENKER (2006)

# Material properties of Inconel 718

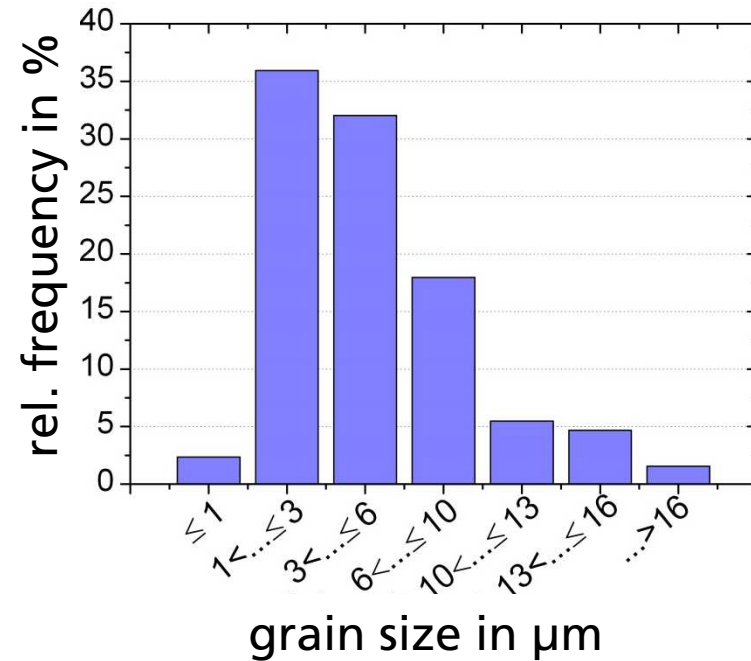
## chemical composition

elem.	Ni	Cr	Fe	Nb	Mo	Ti	Al	Co	Si	Mn	C
value in %	53.1	18.5	18.0	5.4	3.04	1.01	0.44	0.13	0.1	0.07	0.03

## time-temperature precipitation graph<sup>1</sup>

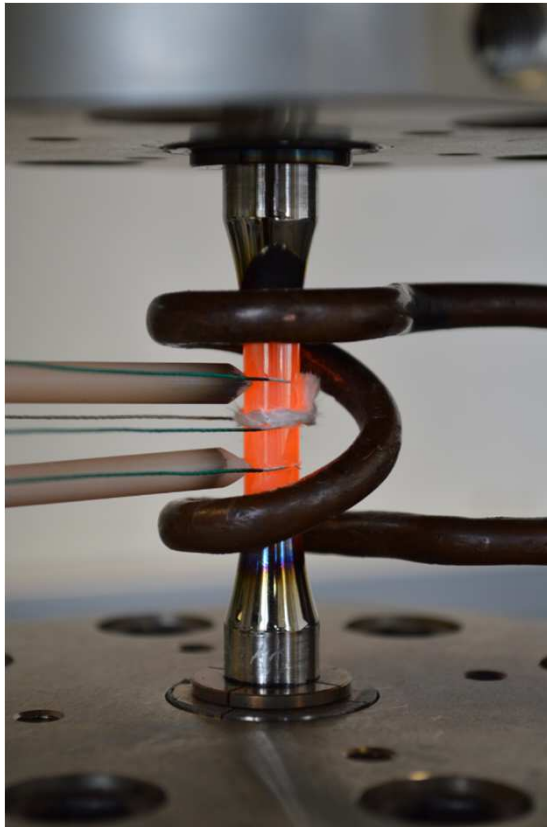



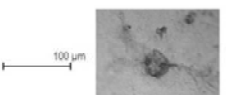
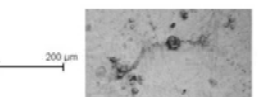
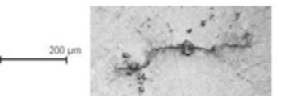

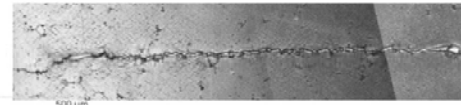
## grain size distribution



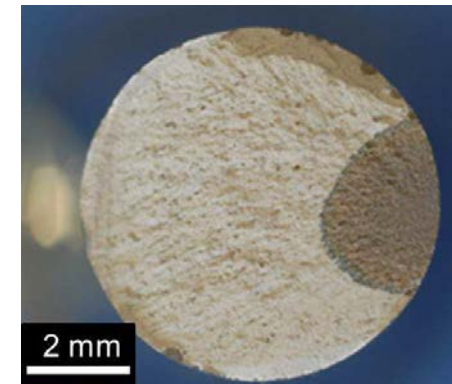
# Experimental setup

## Following of fatigue cracks using the replica technique



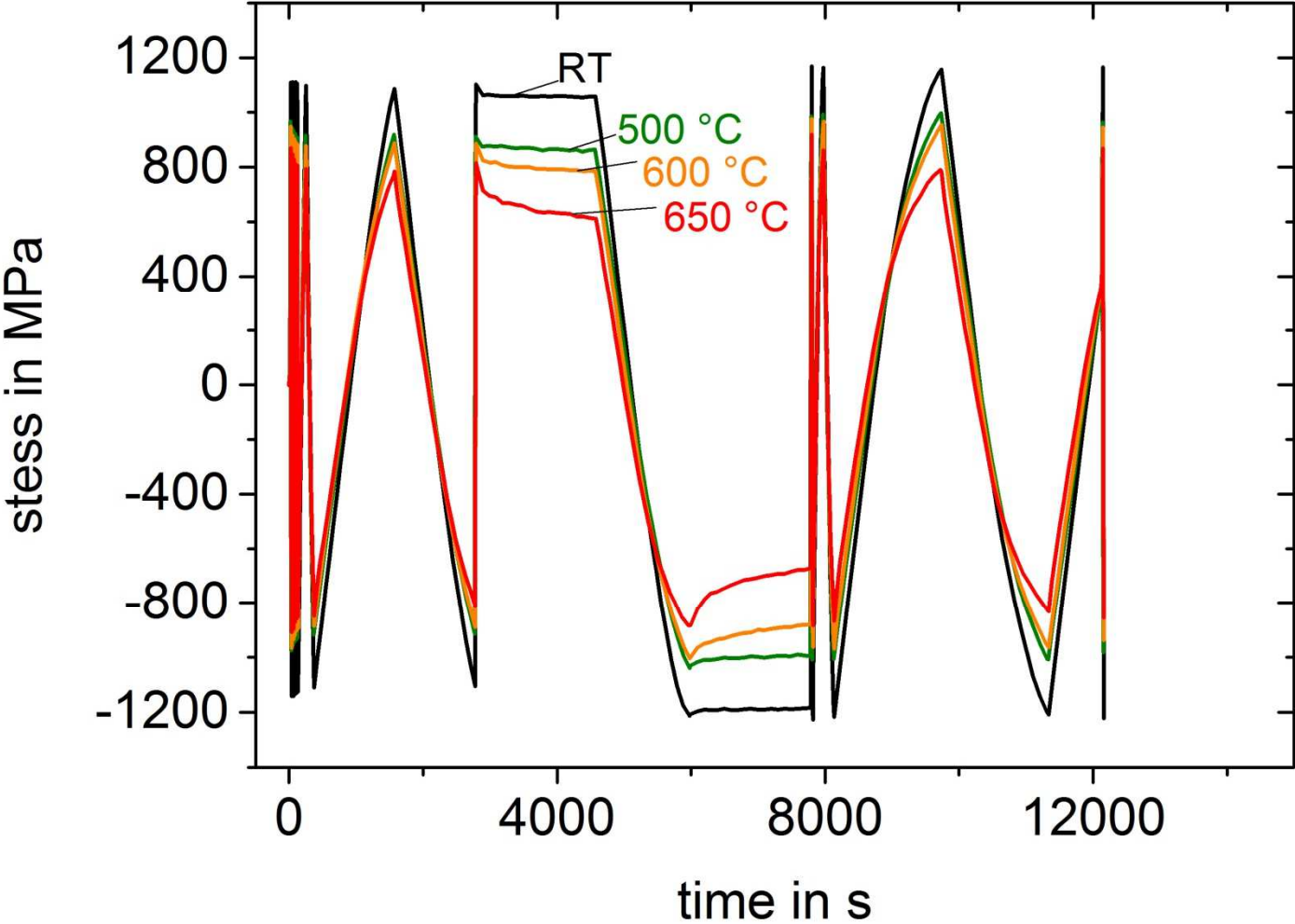
crack length in $\mu\text{m}$	$\times N_f$	
46	$0.2N_f$	
77	$0.6N_f$	
143	$0.7N_f$	
304	$0.8N_f$	
974	$0.9N_f$	
3794	$N_f$	

typical crack length  
0.01...1,5 mm

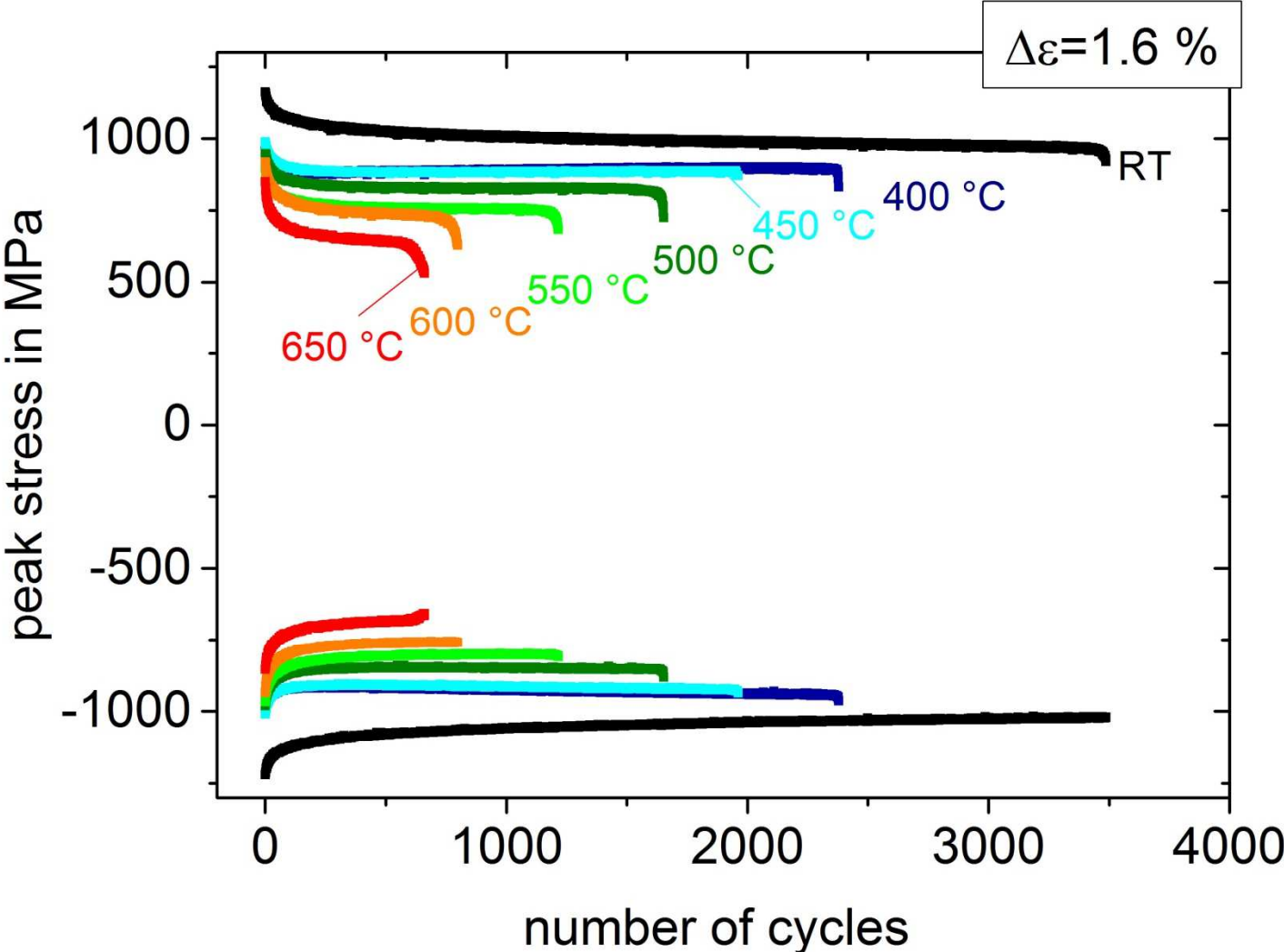




# Temperature dependent material behavior (isothermal)

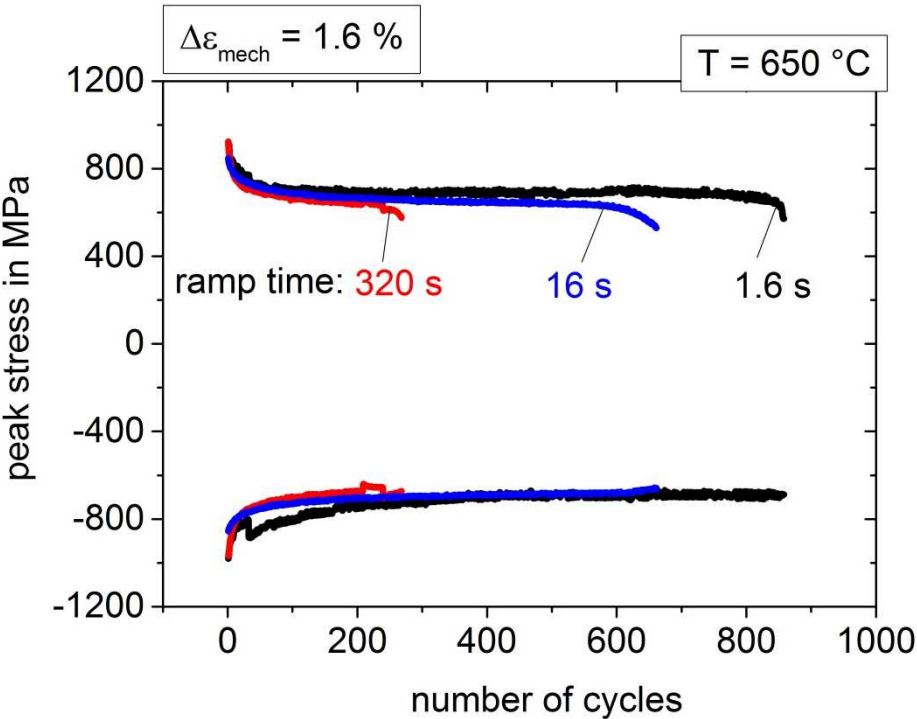


# Temperature dependent material behavior (isothermal)

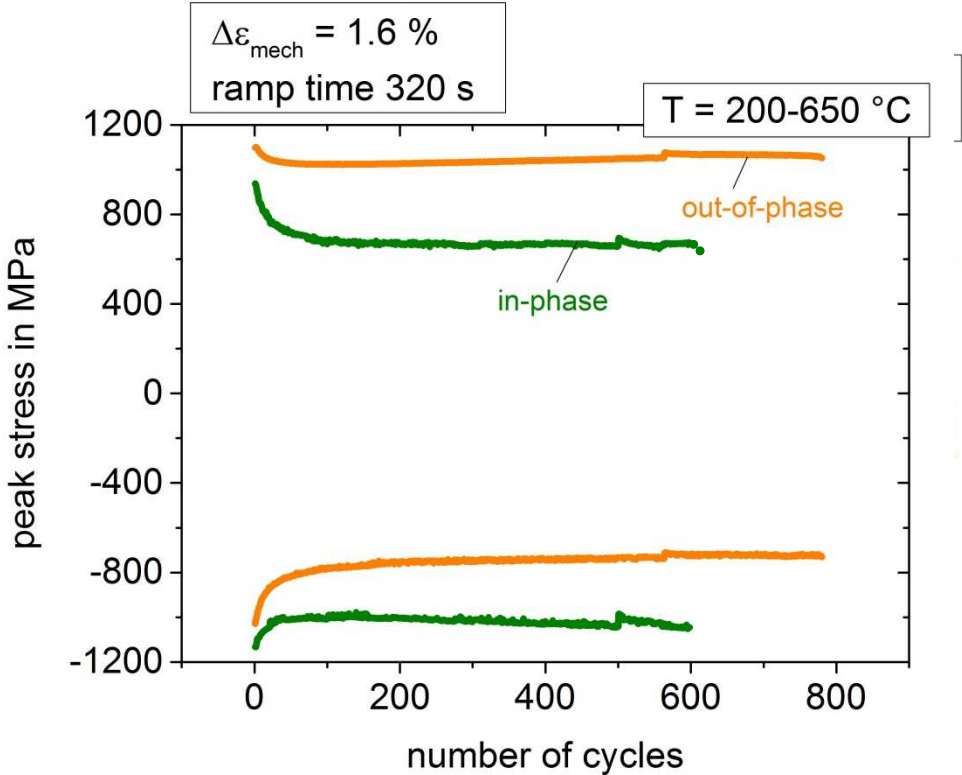


# Time dependent material behavior

## Isothermal tests (LCF)

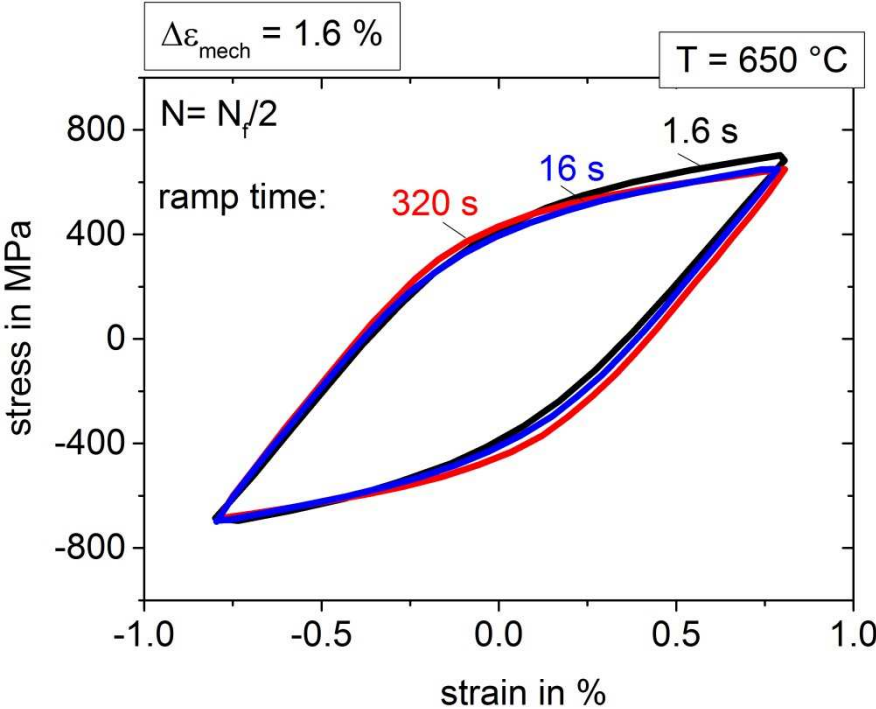


## Non-isothermal tests (TMF)

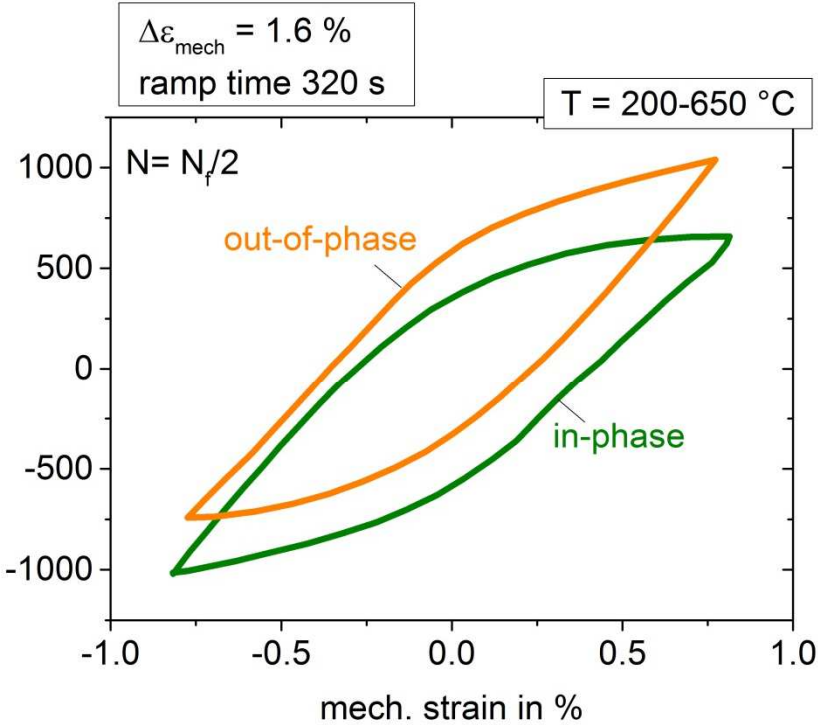


# Time dependent material behavior

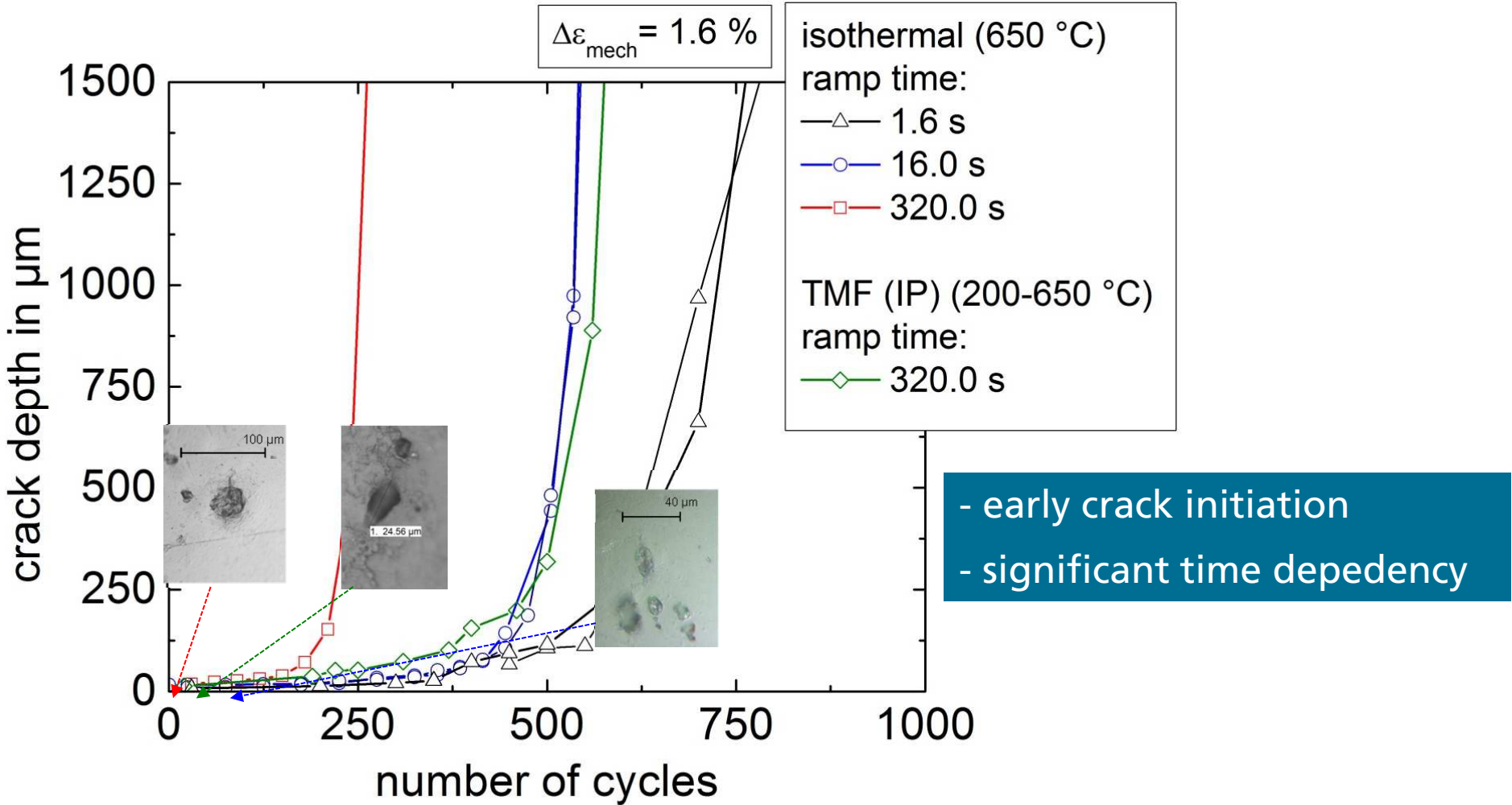
## Isothermal tests (LCF)



## Non-isothermal tests (TMF)



# Time dependent fatigue crack growth behavior

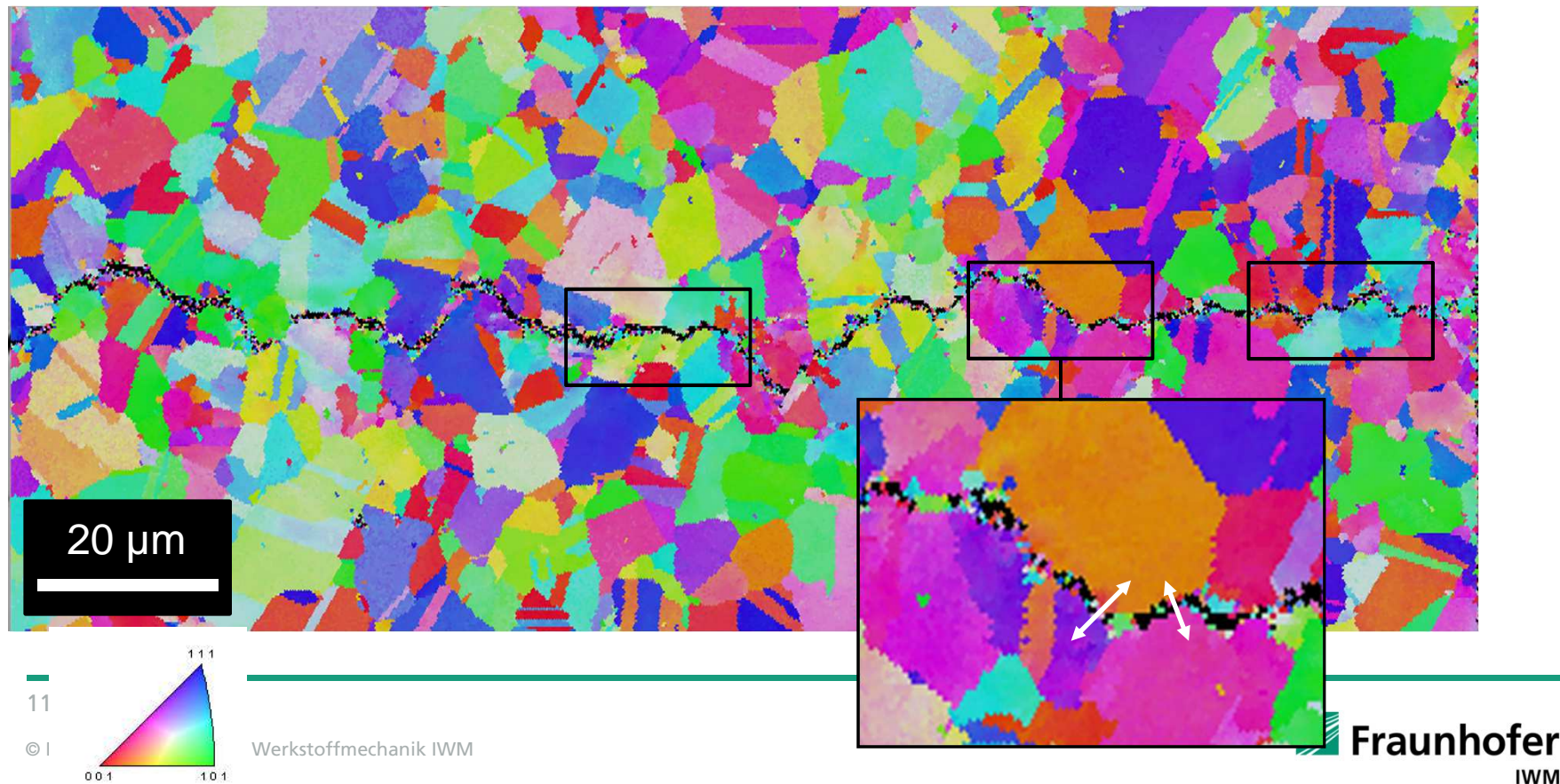


# Mechanism of crack propagation

Electron backscatter diffraction (EBSD)

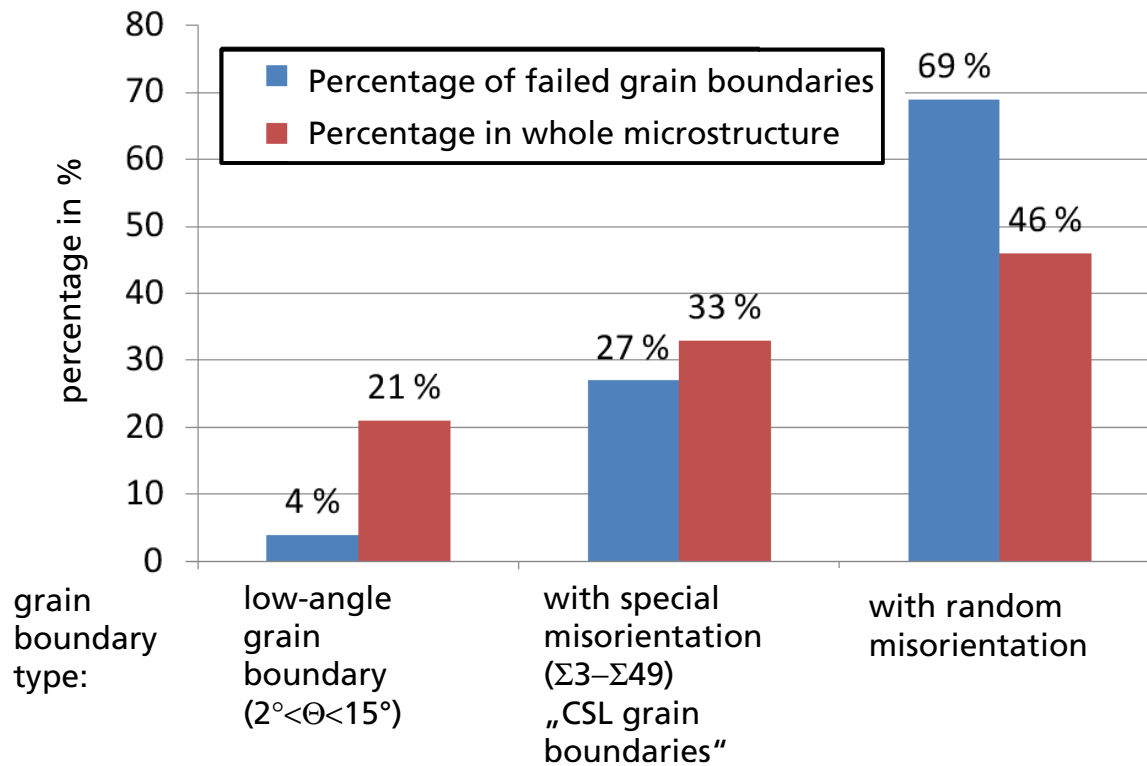
→ Mainly transgranular, in parts intergranular crack growth

Does the grain boundary misorientation influence the mechanism of failure?

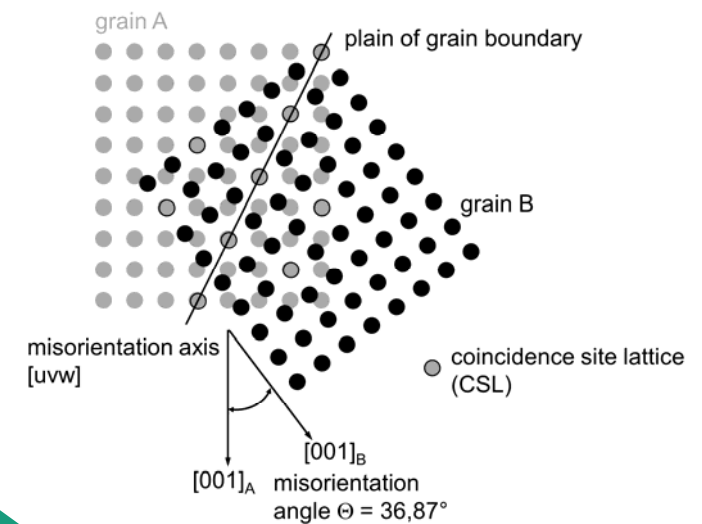


# Mechanism of crack propagation

## Failure frequency of different types of grain boundaries



Coincidence Site Lattice (CSL) grain boundary ( $\Sigma$ -grain boundary):



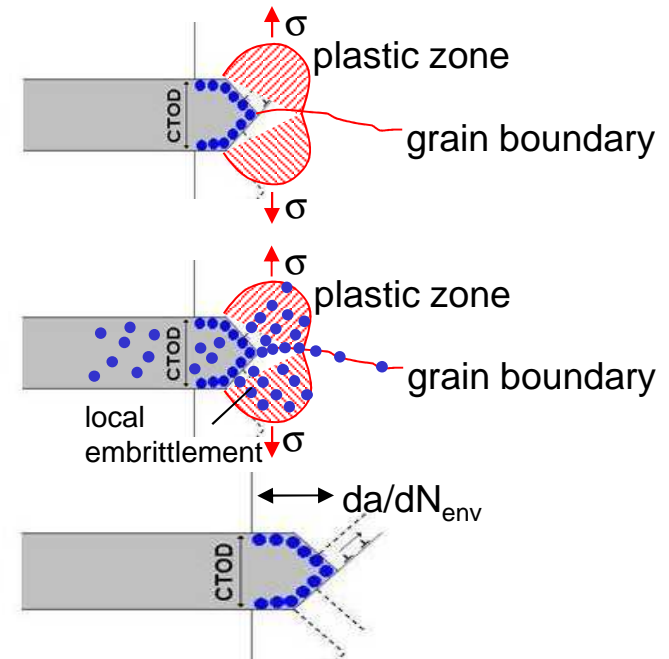
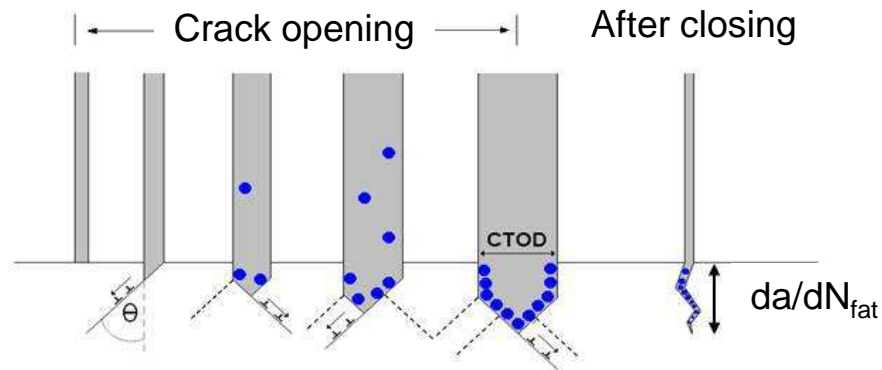
CSL grain boundaries with less susceptibility to intergranular failure

# Mechanism based modeling

$$\frac{da}{dN} = \frac{da}{dN}\Big|_{fat, creep} + \frac{da}{dN}\Big|_{env}$$

alternating slip

oxygen diffusion  
(thermal activated)





# Mechanism based modeling

$$\frac{da}{dN} = \frac{da}{dN}\Big|_{fat,creep} + \frac{da}{dN}\Big|_{env}$$

alternating slip

oxygen diffusion  
(thermal activated)

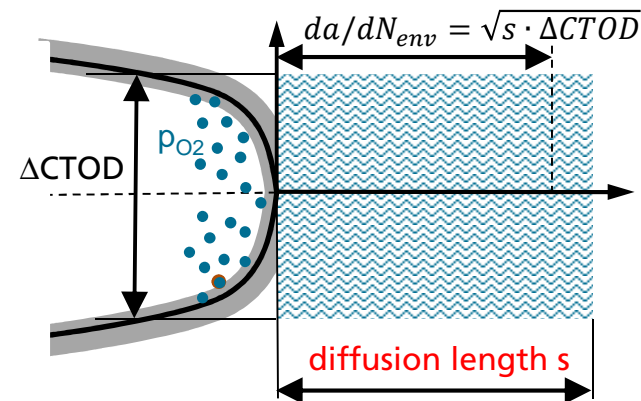
$$\frac{da}{dN}\Big|_{fat,creep} = \beta (\Delta CTOD_{eff}(t))^B$$

$\Delta CTOD_{eff}(t)$  effective, time dependent cyclic crack tip opening displacement

$\beta, B$  parameters for description of alternating slip ( $B \approx 1$ ;  $0.3 < \beta < 1$ )

$$\frac{da}{dN}\Big|_{env} = \left\{ \left[ \left( \frac{p_{O_2}}{p_{atm}} \right)^\lambda D_0 \int_{t_{cyc}} \exp\left(-\frac{Q_{Diff}}{RT}\right) dt \right]^{0,5} \Delta CTOD_{eff}(t) \right\}^{0,5}$$

$t_{cyc}$  cycle time during tensile stress is affecting  
 $D_0, Q_{Diff}$  parameters of parabolic diffusion time law



# Mechanism based modeling

$$\frac{da}{dN} = \frac{da}{dN}\Big|_{fat,creep} + \frac{da}{dN}\Big|_{env}$$

alternating slip

oxygen diffusion  
(thermal activated)

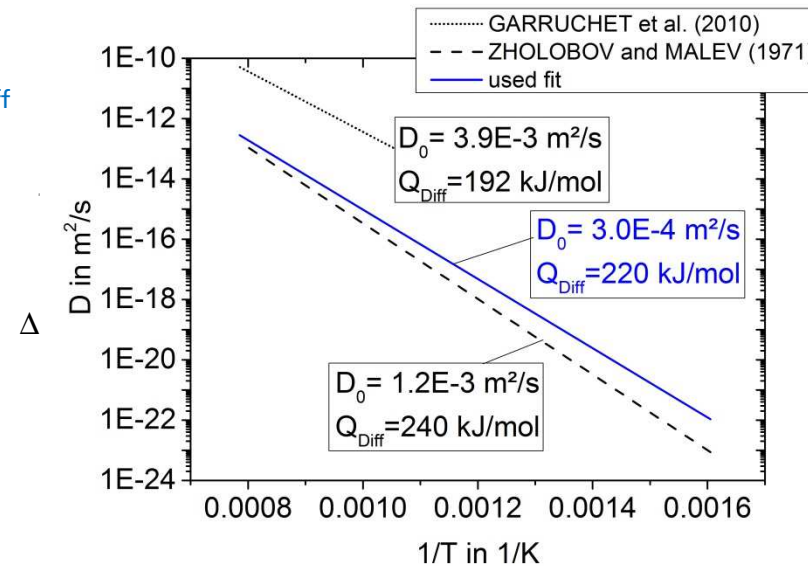
$$\frac{da}{dN}\Big|_{fat,creep} = \beta (\Delta CTOD_{eff}(t))^B$$

$\Delta CTOD_{eff}(t)$  effective, time dependent cyclic crack tip opening displacement

$\beta, B$  parameters for description of alternating slip ( $B \approx 1$ ;  $0.3 < \beta < 1$ )

$$\frac{da}{dN}\Big|_{env} = \left\{ \left[ \left( \frac{p_{o_2}}{p_{atm}} \right)^\lambda D_0 \int_{t_{cyc}} \exp\left(-\frac{Q_{Diff}}{RT}\right) dt \right]^{0,5} \Delta CTOD_{eff}(t) \right\}^{0,5}$$

$t_{cyc}$   
 $D_0, Q_{Diff}$



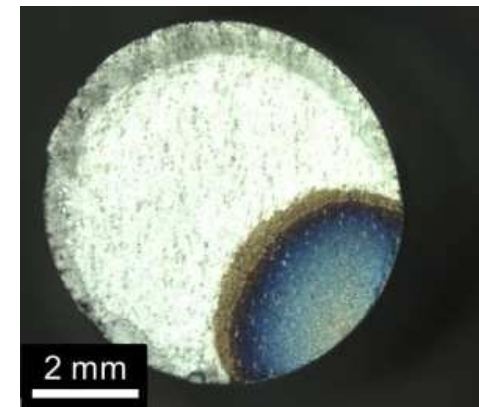
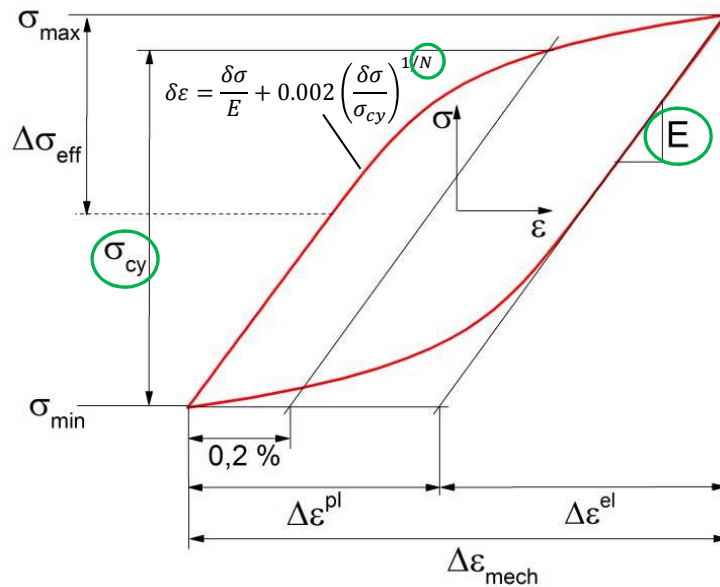
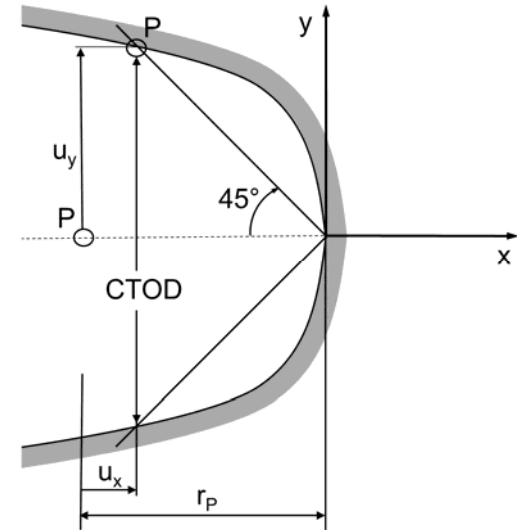
# Cyclic crack tip opening displacement ( $\Delta CTOD$ )

## Fracture Mechanics approach

approach for short, penny-shaped surface cracks:

$$\Delta CTOD_{eff}(t) = d_N \frac{1}{\sigma_{cy}} \left( 1,45 \frac{\Delta\sigma_{eff}^2}{E} + 2,4 \frac{\Delta\sigma \Delta\varepsilon^{pl}}{\sqrt{1+3N}} \right) F(t, T) a$$

$d_{TMF}$  damage parameter      Deformation material parameters



# Cyclic crack tip opening displacement ( $\Delta CTOD$ )

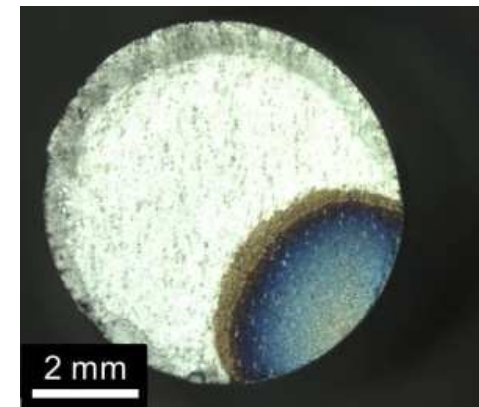
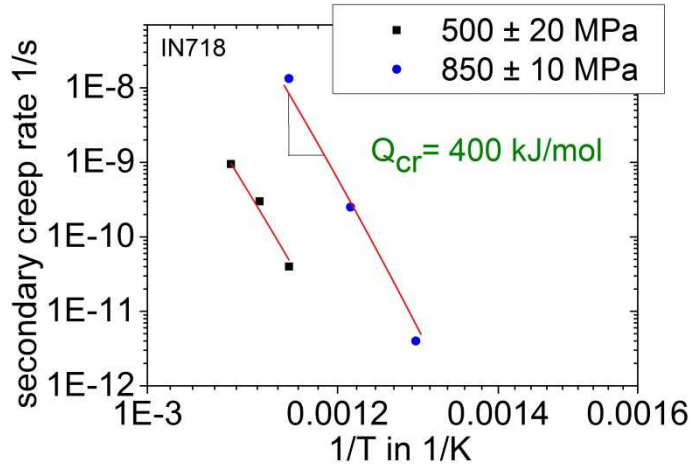
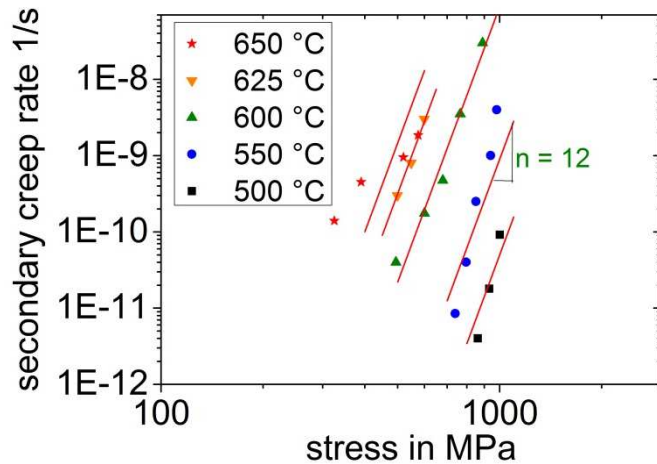
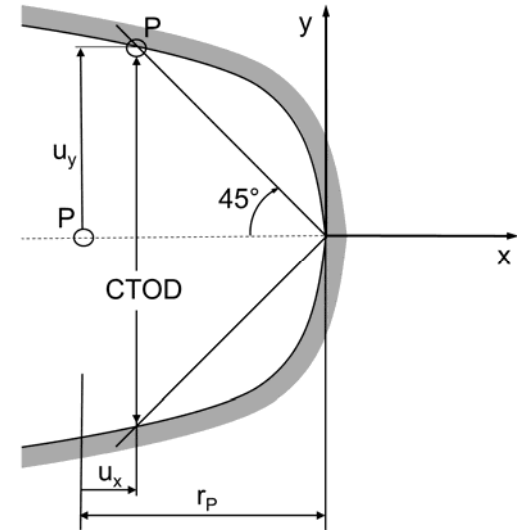
## Fracture Mechanics approach

approach for short, penny-shaped surface cracks

$$\Delta CTOD_{eff}(t) = d_N \frac{1}{\sigma_{cy}} \left( 1,45 \frac{\Delta\sigma_{eff}^2}{E} + 2,4 \frac{\Delta\sigma \Delta\varepsilon^{pl}}{\sqrt{1+3N}} \right) F(t,T) a$$

$D_{TMF}$  damage parameter      Creep deformation material parameters

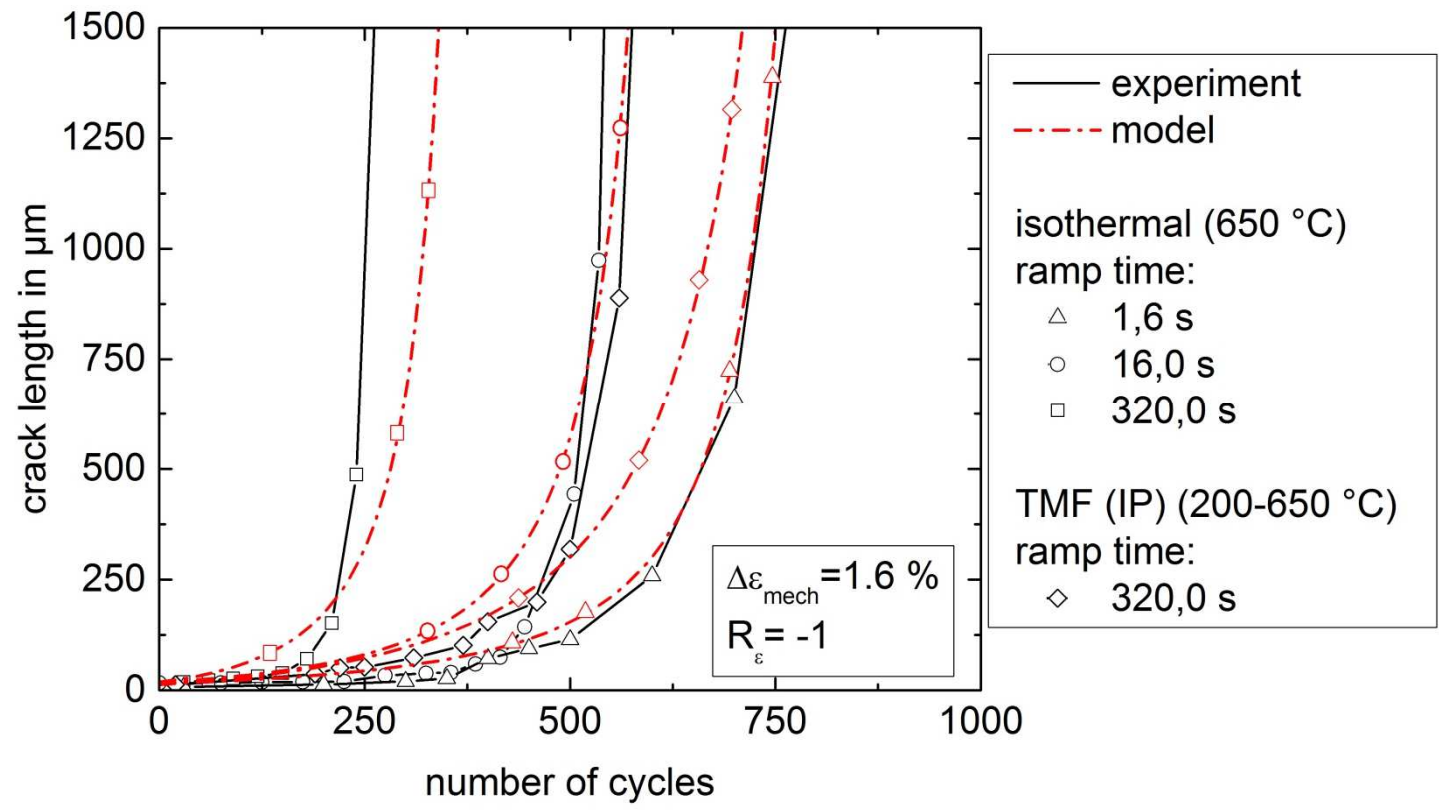
$$F(t,T) = \left( 1 + \alpha_{ref} \exp\left(\frac{Q_{cr}}{RT_{ref}}\right) \int_t \sigma_{cy}^{n-2} \Delta\sigma \cdot \exp\left(-\frac{Q_{cr}}{RT}\right) dt \right)^{1/n}$$



# Prediction of crack growth

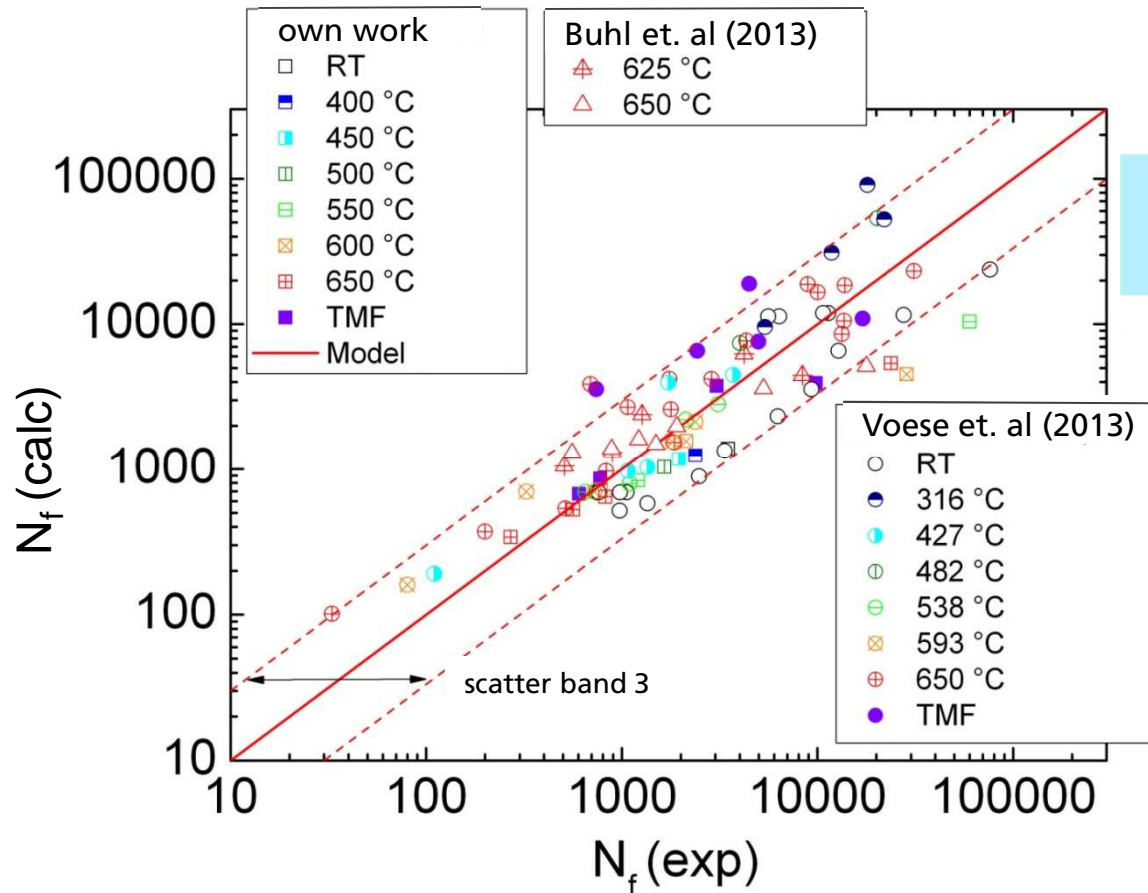
$$a_{i+1} = a_i + \frac{da}{dN} \Big|_{fat, creep} \Delta N + \frac{da}{dN} \Big|_{env} \Delta N \quad a_0 \leq a_i < a_f$$

$a_0$	15...18,5 $\mu\text{m}$
$a_f$	1500 $\mu\text{m}$



# Prediction of lifetime

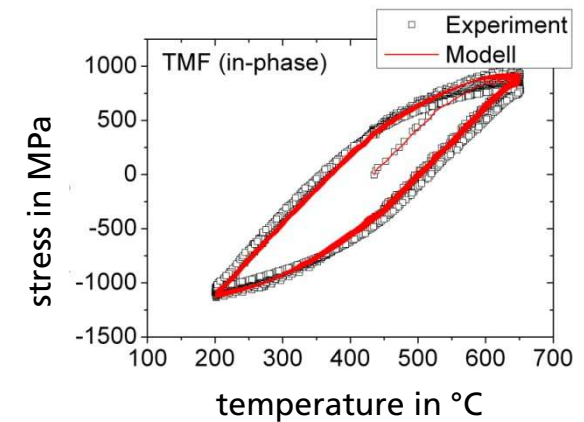
## Uniaxial tests



$$a_{i+1} = a_i + \left. \frac{da}{dN} \right|_{fat, creep} \Delta N + \left. \frac{da}{dN} \right|_{env} \Delta N$$

$$a_0 \leq a_i < a_f$$

hystereses calculated with viscoplastic deformation model

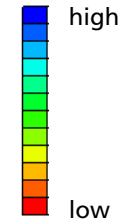


# Summary

- fatigue crack growth with significant time and temperature dependency
- cracks are propagating both trans- and intergranular. Intergranular cracks are propagating preferred at grain boundaries with random misorientation. CSL grain boundaries less susceptible
- mechanism based modeling of fatigue crack growth is based on the „CTOD-concept“ and considers creep and environmental influences at high temperatures and TMF
- all model parameters have a physical meaning
- with the derived lifetime model an improved prediction of uniaxial LCF and TMF tests is achieved
- lifetime model available in finite element post-processing tool

lifetime prediction using FEM & post processing tool

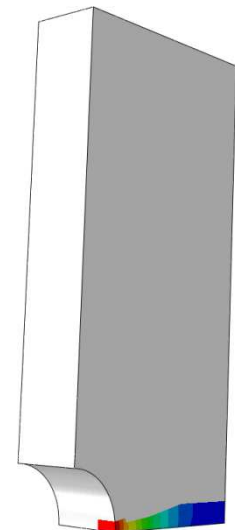
cycles to failure



high

low

The color scale ranges from blue (high) at the top to red (low) at the bottom, with intermediate colors of cyan, green, yellow, and orange.



---

# Experimental investigation of the time and temperature dependent growth of small fatigue cracks in Inconel 718 and mechanism based lifetime prediction

---

TMF-Workshop 2016

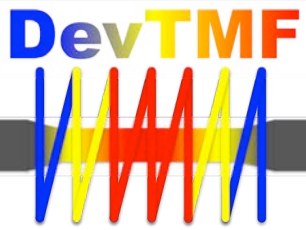
Michael Schlesinger<sup>1</sup>, Thomas Seifert<sup>2</sup>, Johannes Preußner<sup>1</sup>

<sup>1</sup>Fraunhofer IWM, Germany

<sup>2</sup>Offenburg University of Applied Sciences, Germany

Thank you for your  
attention!





# Towards the elaboration of the European Code of Practice for TMF crack growth

S. Stekovic<sup>1</sup>, M. Whittaker<sup>2</sup>, C. Hyde<sup>3</sup>, O.M.D.M Messé<sup>4</sup>, S. Pattison<sup>5</sup> and J. Moverare<sup>1</sup>

<sup>1</sup>Department of Management and Engineering, Linköping University, Sweden

<sup>2</sup>College of Engineering, Swansea University, Swansea, United Kingdom,

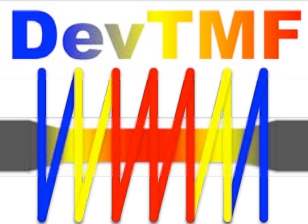
<sup>3</sup>Faculty of Engineering, the University of Nottingham, Nottingham, United Kingdom,

<sup>4</sup>Department of Materials Science & Metallurgy, the University of Cambridge, United Kingdom

<sup>5</sup>Rolls-Royce plc., Derby, United Kingdom.



This project has received funding from the *European Union's Horizon 2020 research and innovation programme* and Joint Undertaking Clean Sky 2 under grant agreement No 686600.



# Content of presentation

- Scope
- What is DevTMF
- Objectives
- Partners
- Approach towards standardisation
- Contact information

# Scope

- Promotion of standardisation of TMF CG method
- Exchange of scientific results and knowledge relating to the field
- Dissemination of the project and its results
- Discuss a way/ways forward

**Objectives:** Development of Experimental Techniques and Predictive Tools to Characterise Thermo-Mechanical Fatigue Behaviour and Damage Mechanisms in two nickel-base superalloys

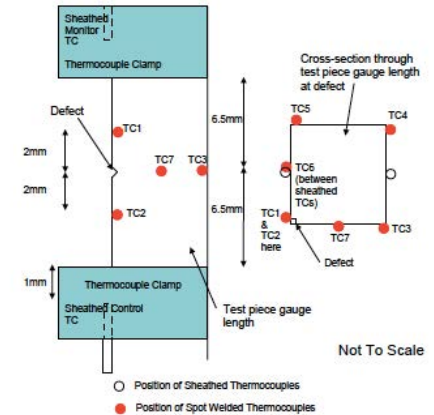
**Funded:** Horizon 2020 and Clean Sky 2

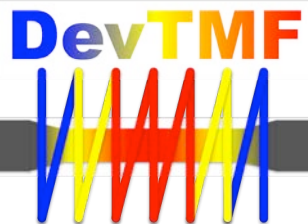
**Start date:** 1<sup>st</sup> of Feb 2016

**Duration:** 48 months

**Consortium:** 3 + 1 partners

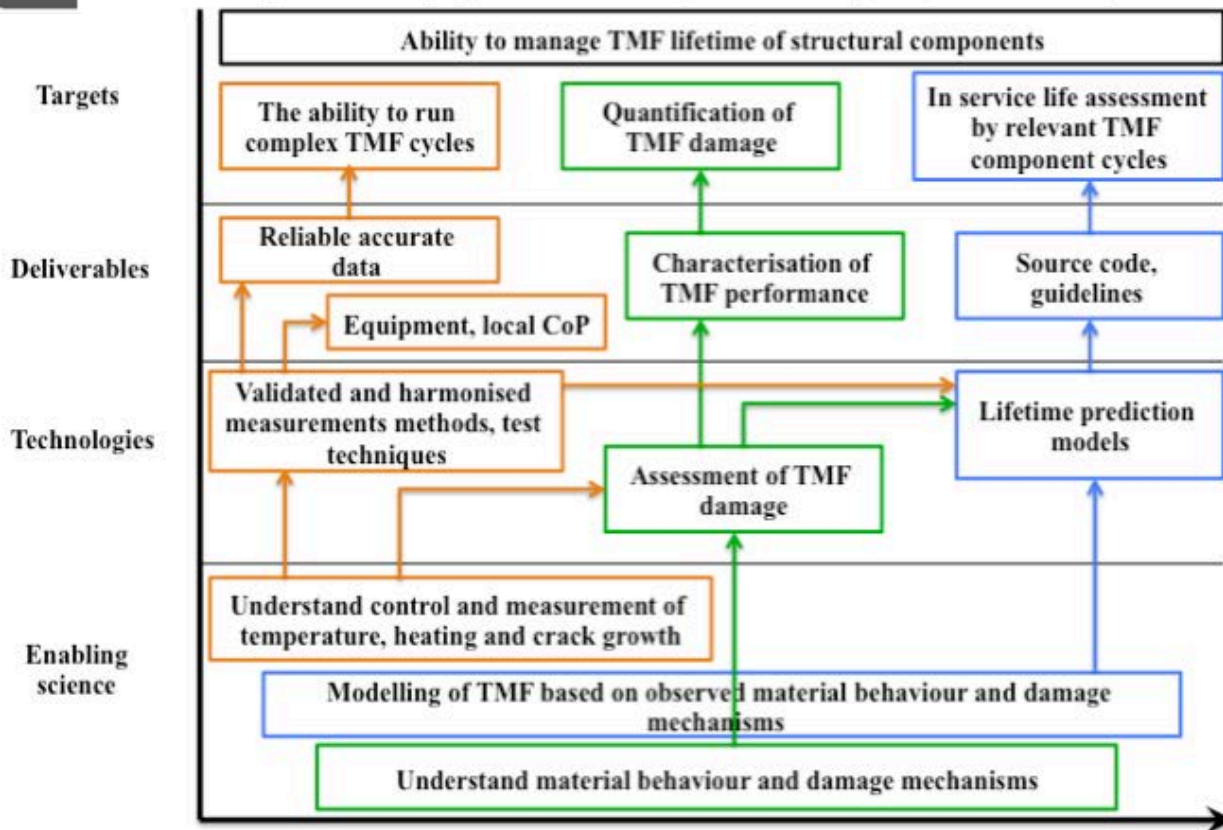
**No of tests:** ≈100 including 15 for the round robin exercise



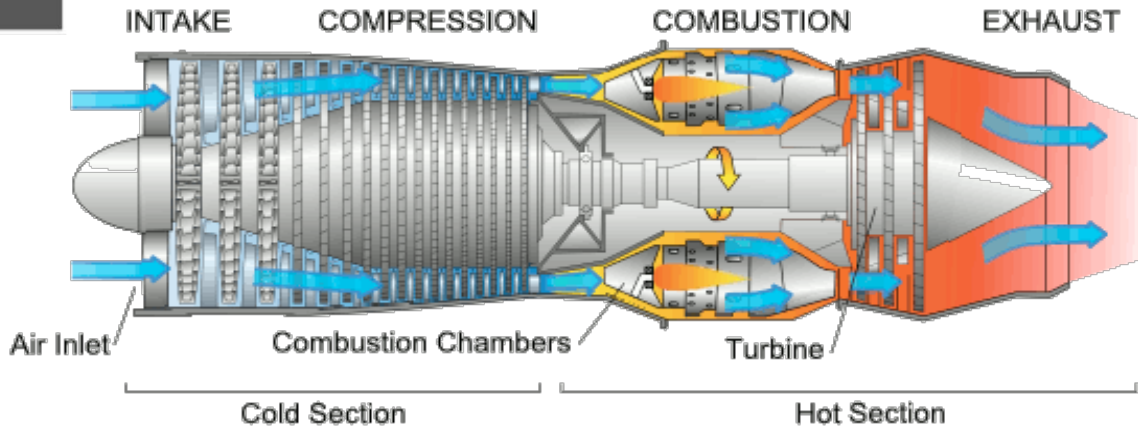


## DevTMF roadmap

Drivers (benefits): environment impact (reduced), sustainability (increased lifetime), competitiveness (improved materials, fuel consumption, market share)



# Grand vision



**Higher turbine temperature**

Cost effective product

Enhance competitiveness

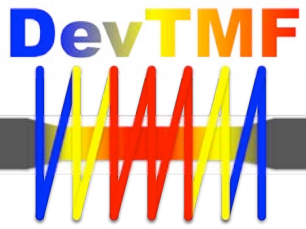
Market advantage

Increase of operation and service life

Optimised performance and efficiency

Reduced overhaul and replacement costs

Lower fuel consumption and environmental impact

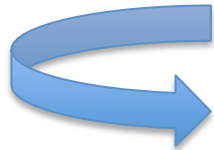


# Grander EU vision

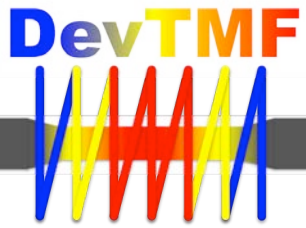
Clean Sky 2: Drivers and technical challenges



- Reduce perceived external noise by **50% by 2020** and **65% by 2050**
- Reduce fuel consumption and CO<sub>2</sub> emissions by **50% by 2020** and **75% by 2050**
- Reduce No<sub>x</sub> emissions by **80% by 2020** and **90% by 2050**



**Vision 2020** and **Flight 2050** targets are for new aircraft technology relative to 2000 performance



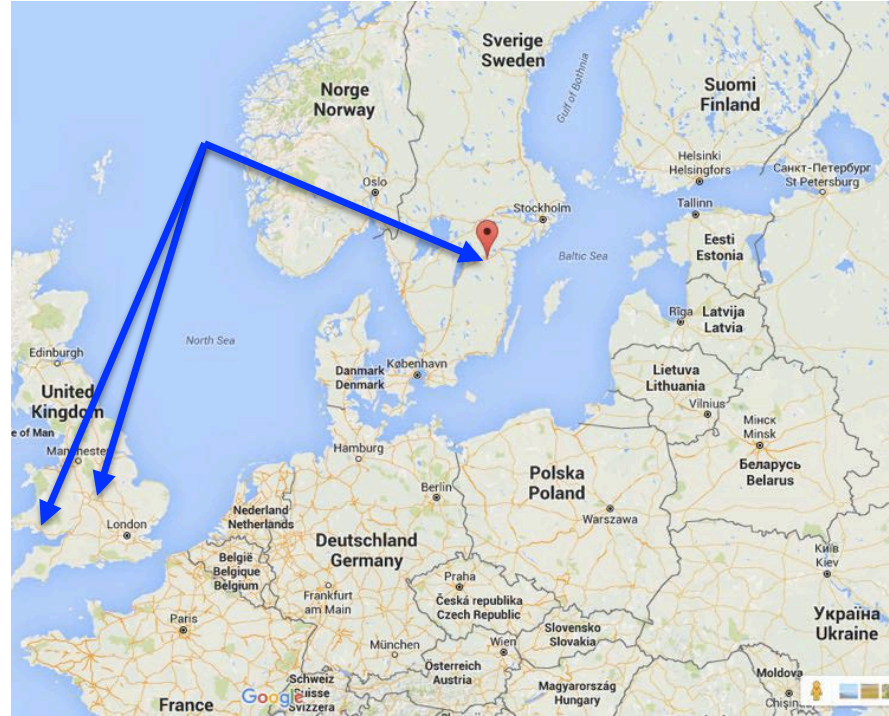
# The Partners



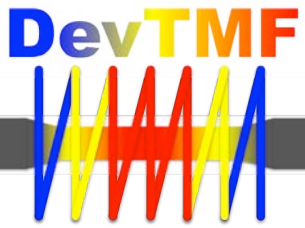
The University of  
Nottingham



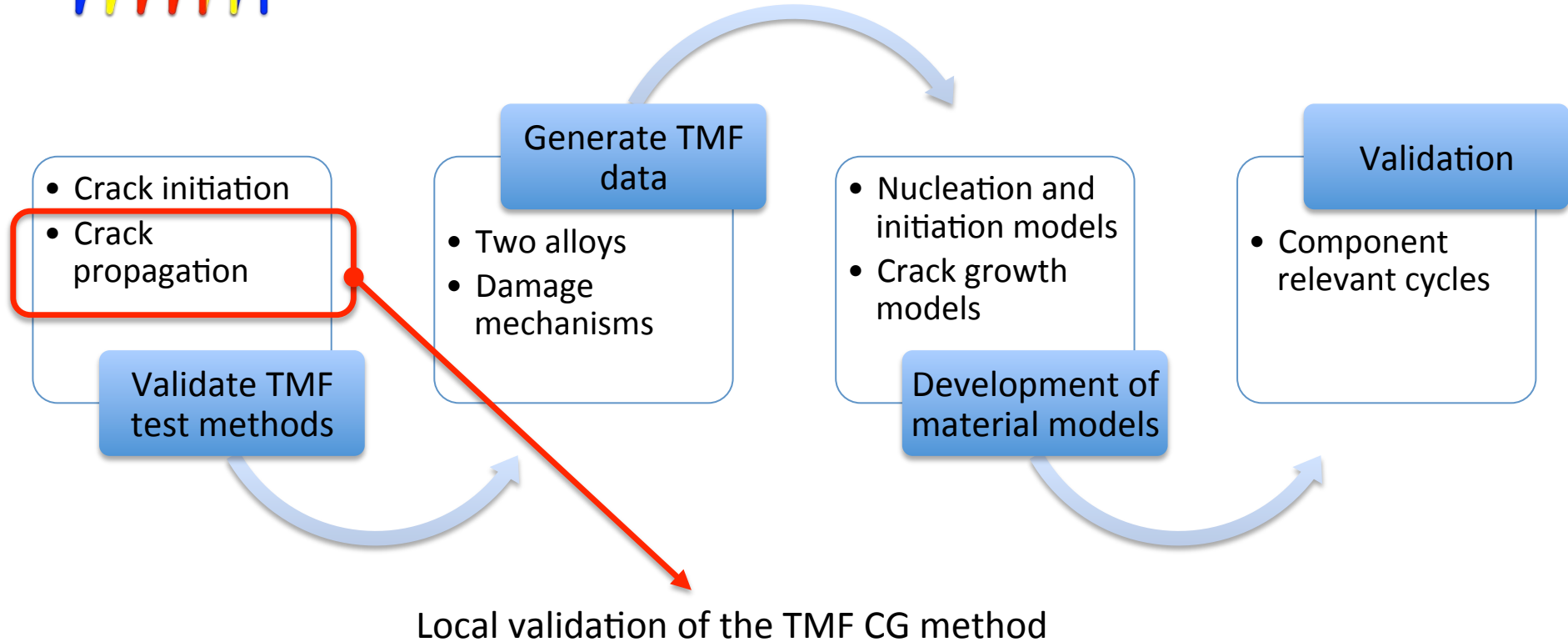
Rolls-Royce

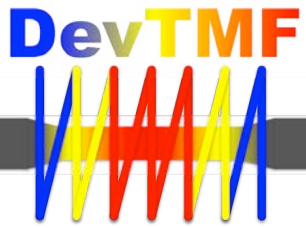






# Specific content addressing TMF CG





# TMF test method status

Existing standards:

Strain controlled TMF:

EU CoP

ASTM E2368 – 10

ISO 12111:2012

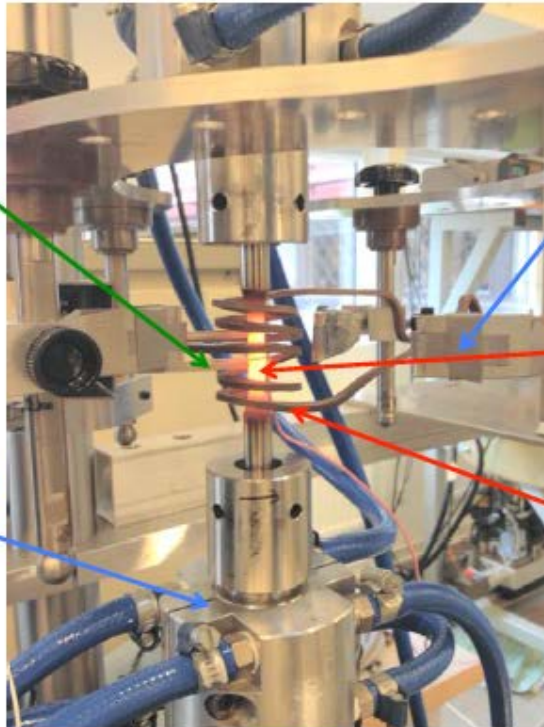
Force controlled TMF:

A CoP developed by Rolls-Royce

MTOC

TMF crack growth:

Not covered by CoP or standard  
Investigated in isolation and with  
limited conditions



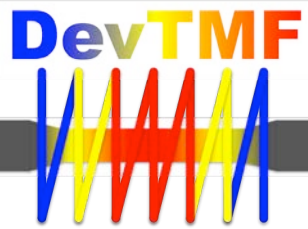
Extensometer

Forced air cooling.

Glowing specimen with thermocouples.

Induction coil.

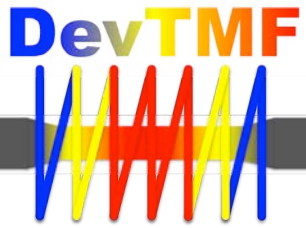
Water cooled grips.



# Approach towards standardisation

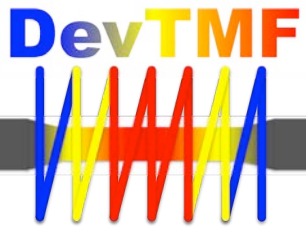
Standardisation of test procedures and methods between the partners:

1. Use same **specimen design and size**: CC and SEN,
2. Compare **crack monitoring** techniques: ACPD and DCPD,
3. Compare **heating/cooling** methods: radiant lamp heating and induction heating,
4. Compare **temperature** measurement methods: TCs, thermography and pyrometry,



# Approach towards standardisation

5. Use **same procedures**, existing standardised protocols for TMF and isothermal crack growth testing,
6. Perform round robin testing with **same conditions** to utilise the experience gained, and pursue a pathway towards standardisation
7. Establish **a local CoP** at the consortium level to ensure repeatability and consistency, and
8. **Dissemination** through the TMF community and further meetings to decide a way forward.

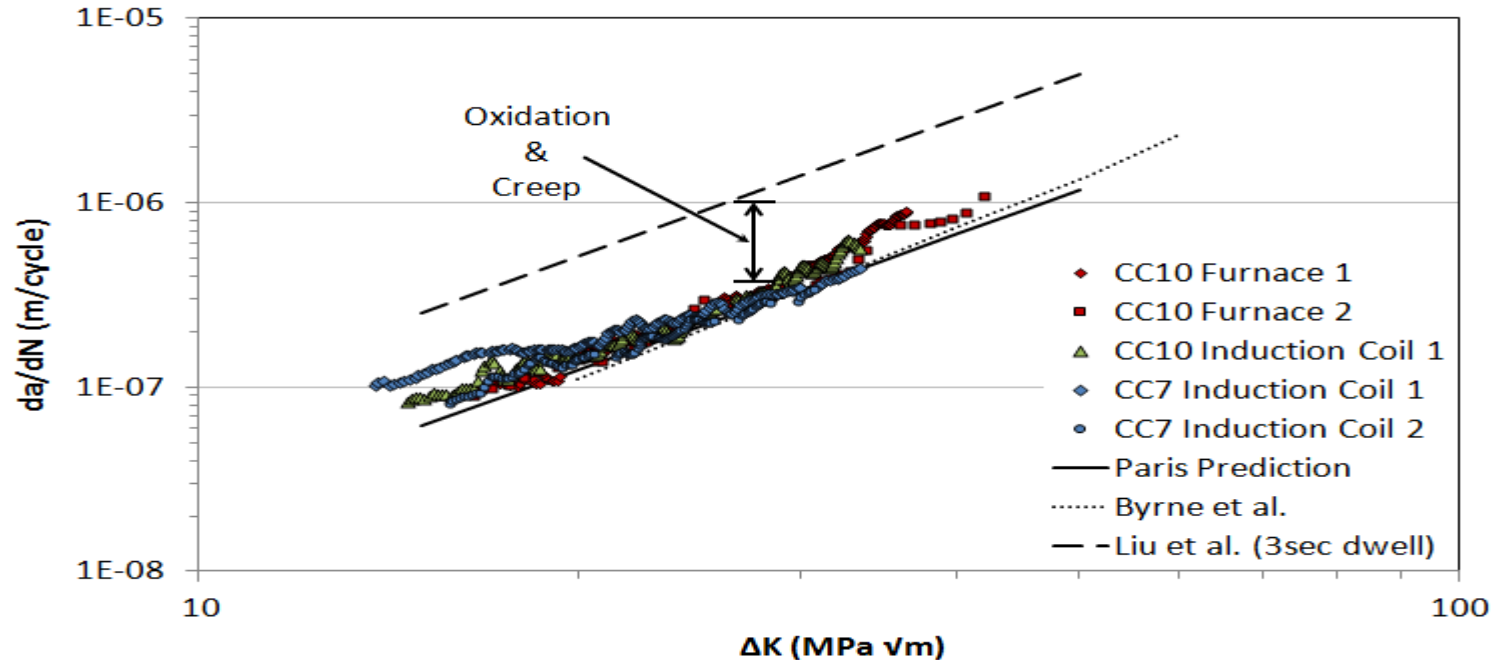


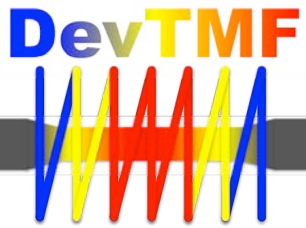
# Approach towards standardisation

1. Assessment of thermal gradients,
2. Ability to heat specimens using different heating sources,
3. Evaluation of stability and accuracy of existing high temperature measurement methods,
4. Interaction of heating methods with crack growth measurements, local crack tip heating, and
5. Applicability of crack detection methods.

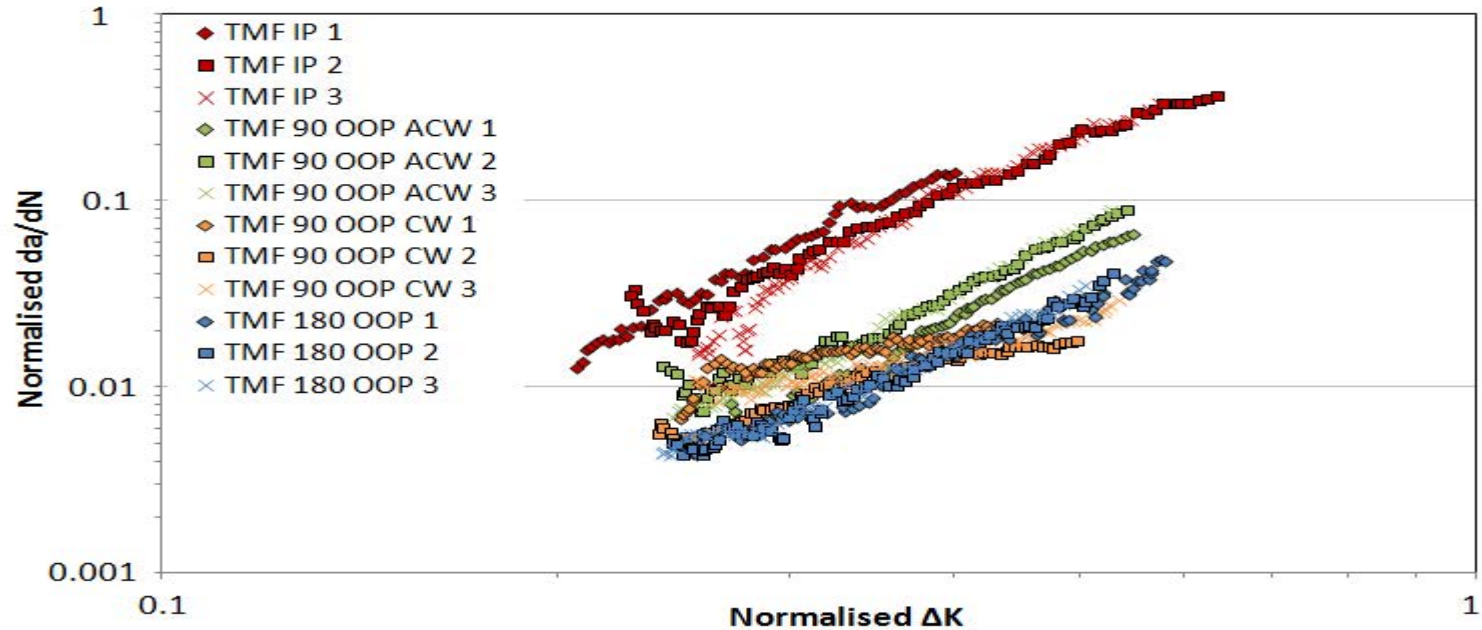
# Induction coil vs furnace validation

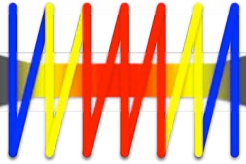
Waspaloy isothermal tests carried out at 650°C and R=0.1 in line with previous literature to ensure comparable and repeatable results





# Previous TMF CG data





# Final words

Starting of with literature review, thermal profile, pre-testing and then a local back-to-back testing

Most of the TMF CG tests to be done at SU

An international seminar will be organised at the end of the project (SU lead) to define further actions but

We are happy to collaborate before and after the end

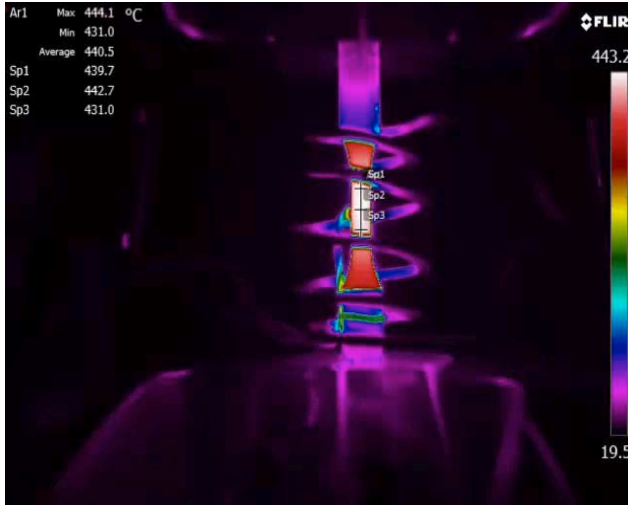
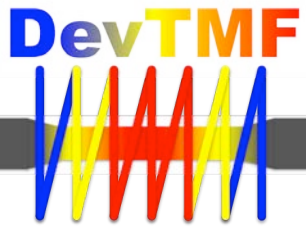


Image from Swansea University





# Contact details

## **For the project:**

Svjetlana Stekovic

E-mail: [svjetlana.stekovic@liu.se](mailto:svjetlana.stekovic@liu.se)

Phone: +46 13 28 69 55

## **For standardisation of TMF CG:**

Mark Whittaker

E-mail: [m.t.whittaker@swansea.ac.uk](mailto:m.t.whittaker@swansea.ac.uk)

Phone: +44 1792 295 573

# Service-like TMF tests for the validation and assessment of a creep-fatigue life procedure developed for GT blades and vanes

E. Vacchieri<sup>1\*</sup>, S.R. Holdsworth<sup>2</sup>, E. Poggio<sup>1</sup>, P. Villari<sup>1</sup>

<sup>1</sup>Ansaldo Sviluppo Energia srl, Genoa, Italy

<sup>2</sup>EMPA Swiss Federal Laboratories for Materials Science and Technology, Dübendorf, Switzerland

[\\*erica.vacchieri@ansaldoenergia.com](mailto:erica.vacchieri@ansaldoenergia.com)



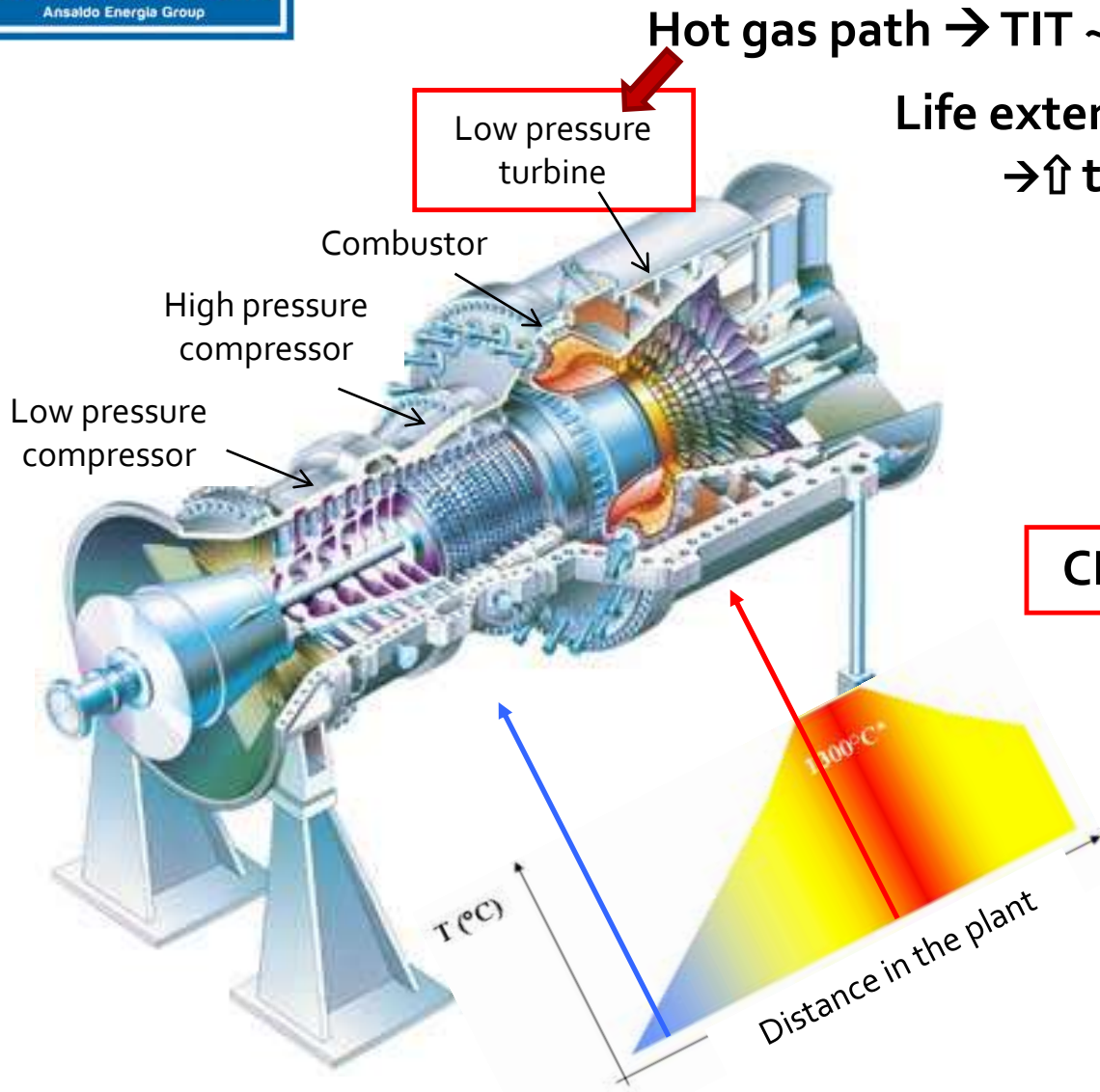
**3<sup>rd</sup> International Workshop on Thermo-Mechanical Fatigue**

April 27<sup>th</sup> – 29<sup>th</sup> 2016, Berlin, Germany

- INTRODUCTION
- MATERIALS and EXPERIMENTAL METHODS
- RESULTS and DISCUSSION
  - ✓ Creep-fatigue Life Assessment Procedure
  - ✓ Service-like TMF Cycle Definition
  - ✓ TMF Test Results
  - ✓ Creep-fatigue Life Procedure Validation
  - ✓ Field Feedback Verification
- CONCLUSIONS and OUTLOOK



# INTRODUCTION



Hot gas path  $\rightarrow$  TIT  $\sim 1300^{\circ}\text{C}$

Life extension  
 $\rightarrow \uparrow t$

Market  
Request

$\uparrow$  efficiency  
 $\rightarrow \uparrow T$

$\uparrow$  cycling

**CREEP**

**FATIGUE**

**CREEP-FATIGUE**

Hot gas path components withstand to:

- **High temperature**
- Multiaxial distribution of mechanical loads due to their **complex geometry** and **strong thermal gradients**

Structural materials for these components have to guarantee resistance to:

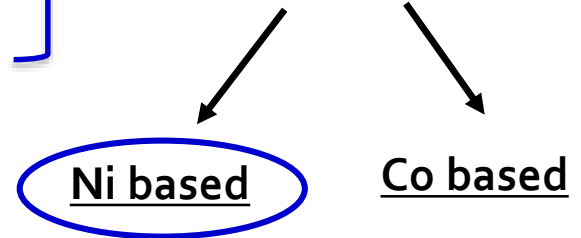
$\rightarrow$  **Oxidation**   **Creep**   **Fatigue**   ...and their combination

## Structural alloys

High temperature material features

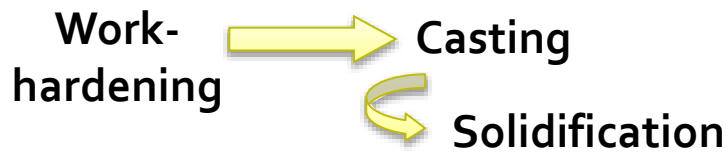
- Mechanical resistance at  $T/T_m \geq 0.6$
- Creep resistance
- LCF and TMF resistance
- Oxidation and corrosion resistance

### Superalloys



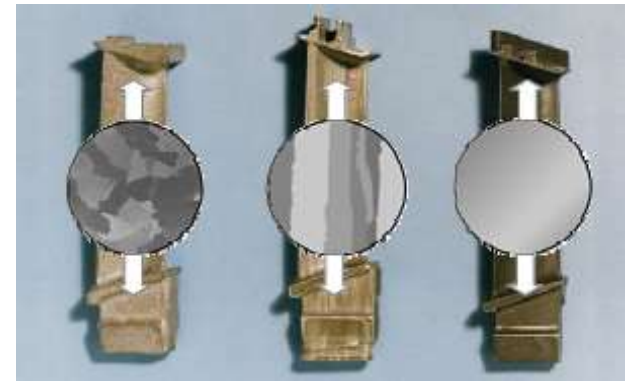
GT components materials evolution

time →



### Strengthening methods:

- Substitutional hardening in the  $\gamma$  matrix
- Carbides precipitation at the grain boundary
- Coherent precipitation of intermetallic phase  $Ni_3Al$ ,  $\gamma'$

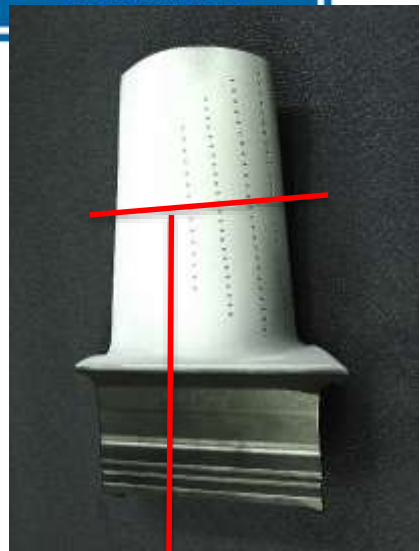


Equiaxed

DS

**SX**

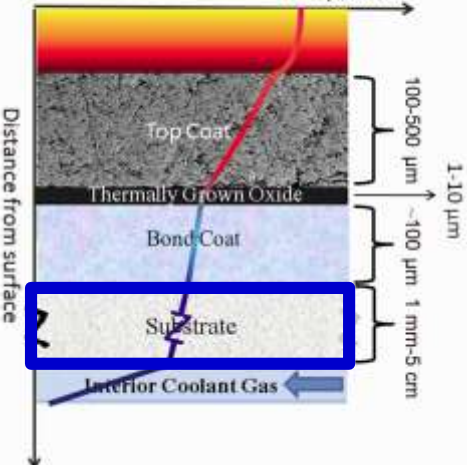
Chemistry



HOT GASES



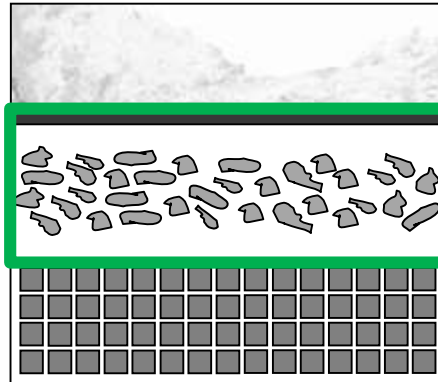
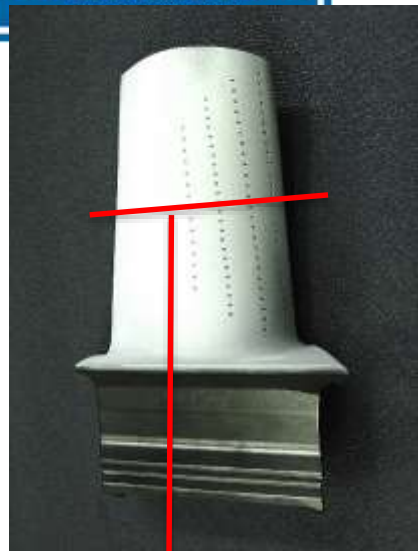
Temperature



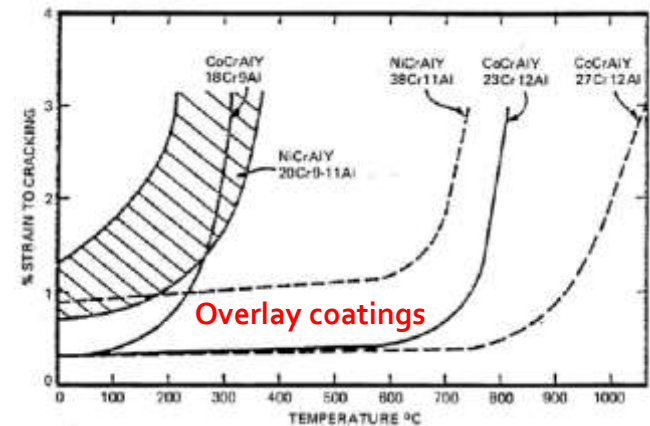
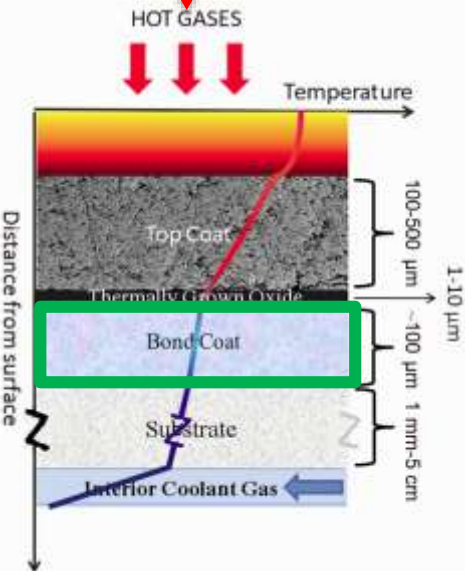
## Metallic coatings

The metallic coatings applied on GT components can be MCrAlY layer that protects the base material from oxidation and corrosion, depending on the operating condition of the considered component

They are very ductile at high temperature and  $\alpha(T)_{coating} \sim \alpha(T)_{base\ material}$  **but** they have relatively high DBTT  $\rightarrow$  TMF resistance can be worsen by these coatings



They are characterized by the presence of  $\beta$  phase, NiAl, that is the Al reservoir, in a  $\gamma$  matrix. Depending on the composition some secondary phases can be present from the production or can precipitate during service



Ductile Brittle Temperature Transition  
DBTT

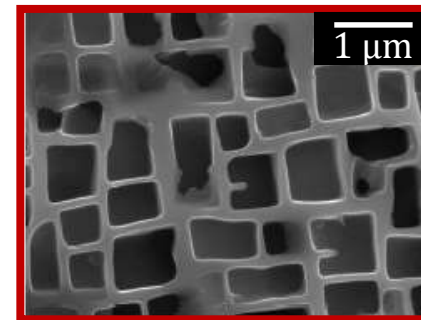
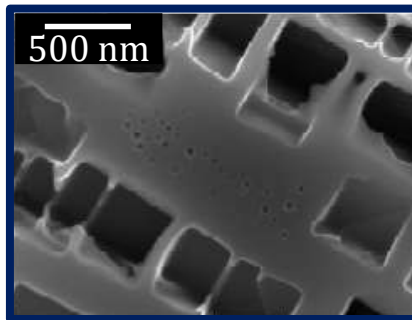
## Motivation

- Benchmark the creep-fatigue life procedure developed for GT blades and vanes through service-like TMF tests
- Benchmark the effect of the metallic coating on TMF endurance and evaluate the influence of its composition
- Exploit the field feedback to verify the TMF test effectiveness through the comparison of the physical damage and to quantitatively validate the design procedure



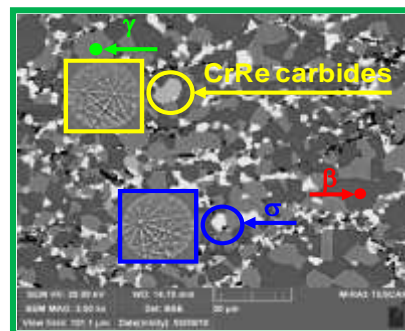
Alloy	Ni	Cr	Co	Al	Ti	Mo	W	Ta	Zr	B	C
<i>René 80</i>	bal.	14.0	9.50	3.00	5.00	4.00	4.00	-	0.03	0.015	0.17
<i>IN792SX</i> *	bal.	12.2	9.00	3.60	4.10	1.80	3.80	5.00	-	-	0.07

\* $\langle 001 \rangle$  Test bars direction with  $\theta$  limit as prescribed in real blades

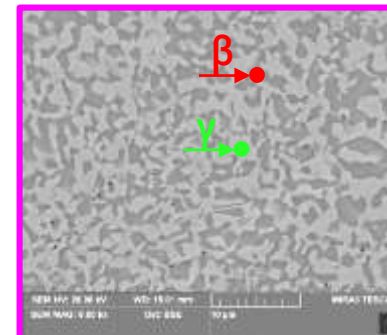


starting  $\gamma/\gamma'$   
microstructure

Coating	Ni	Cr	Co	Al	Re	Y
<i>NiCoCrAlY2Re</i>	bal.	21.0	12.0	11.0	2.00	0.40
<i>NiCoCrAlY1Re</i>	bal.	17.0	25.0	10.0	1.50	0.40

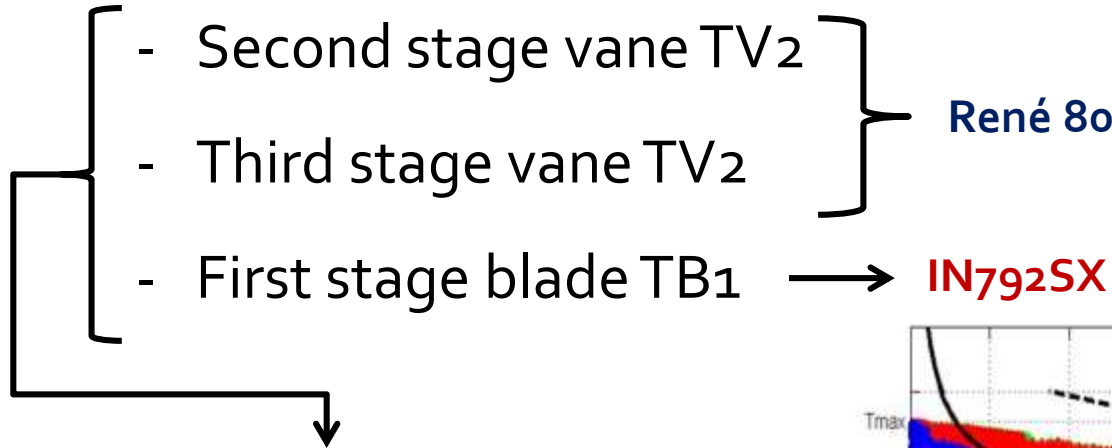


starting coating  
microstructure



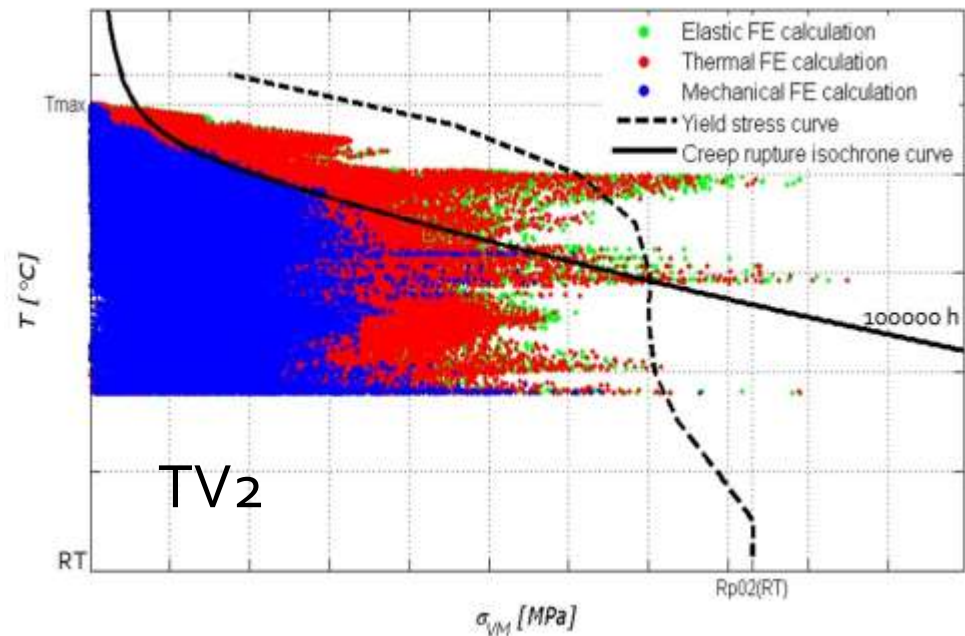


Three case studies from an F-class power plant:



**Strain-driven dominated,**  
also the blade because it is  
hollow and light

**Complex geometry and strong  
thermal gradients characterises  
the three case studies**



The **FE simulations** were conducted using Ansys 15.0

- Elasto-plastic bilinear kinematic hardening cyclic stress-strain (BKIN) model and a secondary creep (Norton) model for the **base material**, considering for the SX blade the elastic and plasticity anisotropy
- The same elastic properties and a time hardening creep model for the **two metallic coatings**

**TMF benchmark cycle** has been defined by post-processing the FE simulation output for the selected critical locations

**TMF tests** were performed in strain-control mode

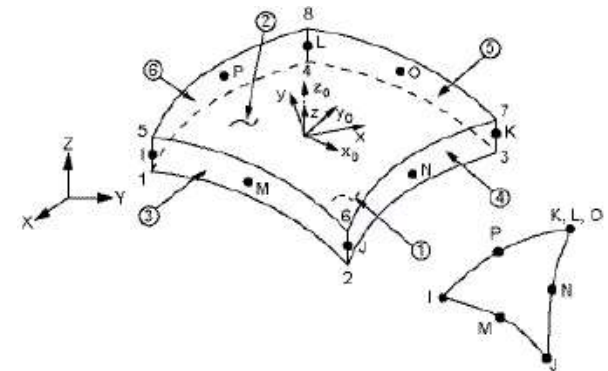
A comprehensive **post-test inspections** was conducted to understand the crack mechanisms and compare the experimental damage to the critical location condition after service



FE calculations simulated a standard start-up/shut-down transient

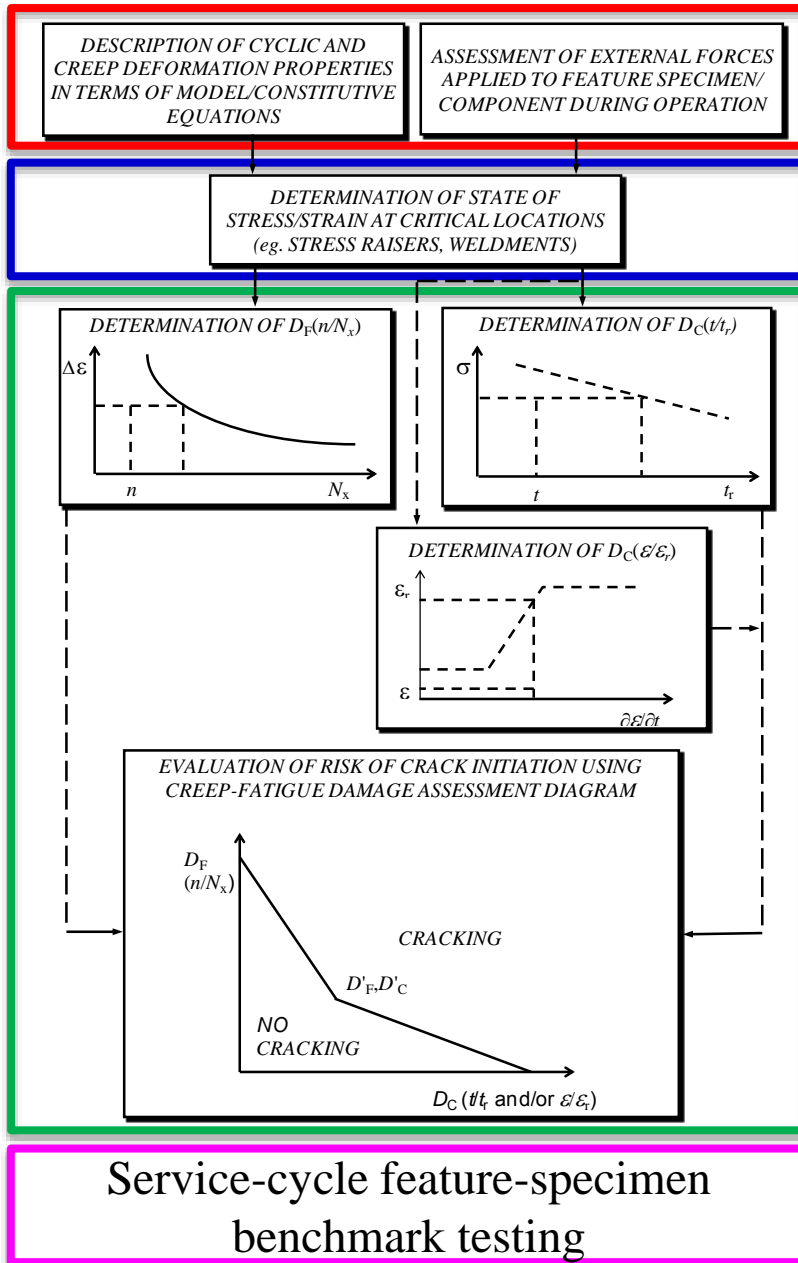
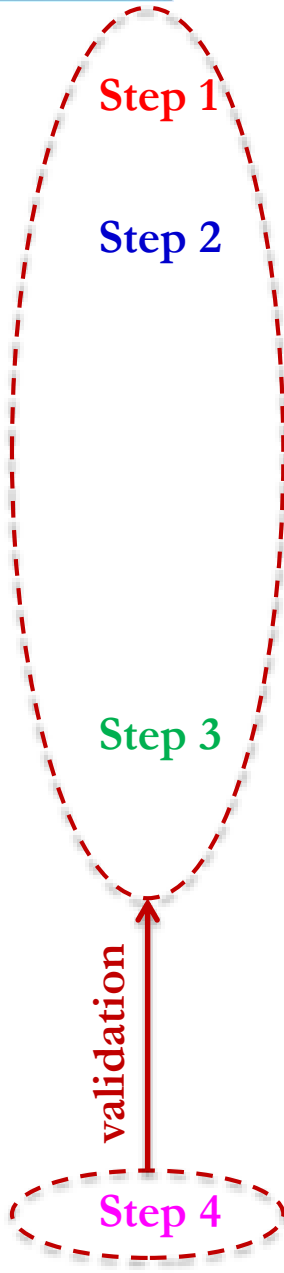
For the SX blade the calculation with the metallic coating reach room temperature

The cycle is repeated **four times** to allow code stabilisation



**Shell elements** have been used to simulate the metallic coating layer on the surface of the blade

## Creep-fatigue life assessment procedure



- Constitutive models
- FE simulation strategy

Component critical location identification

### DAMAGE ASSESSMENT

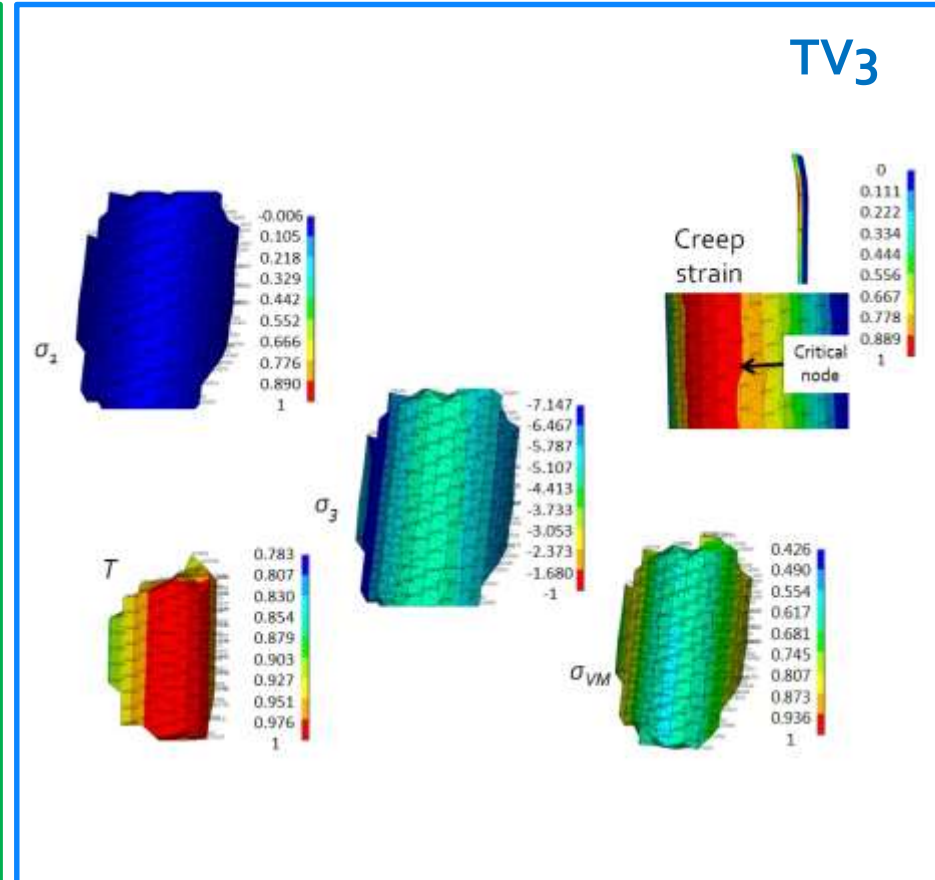
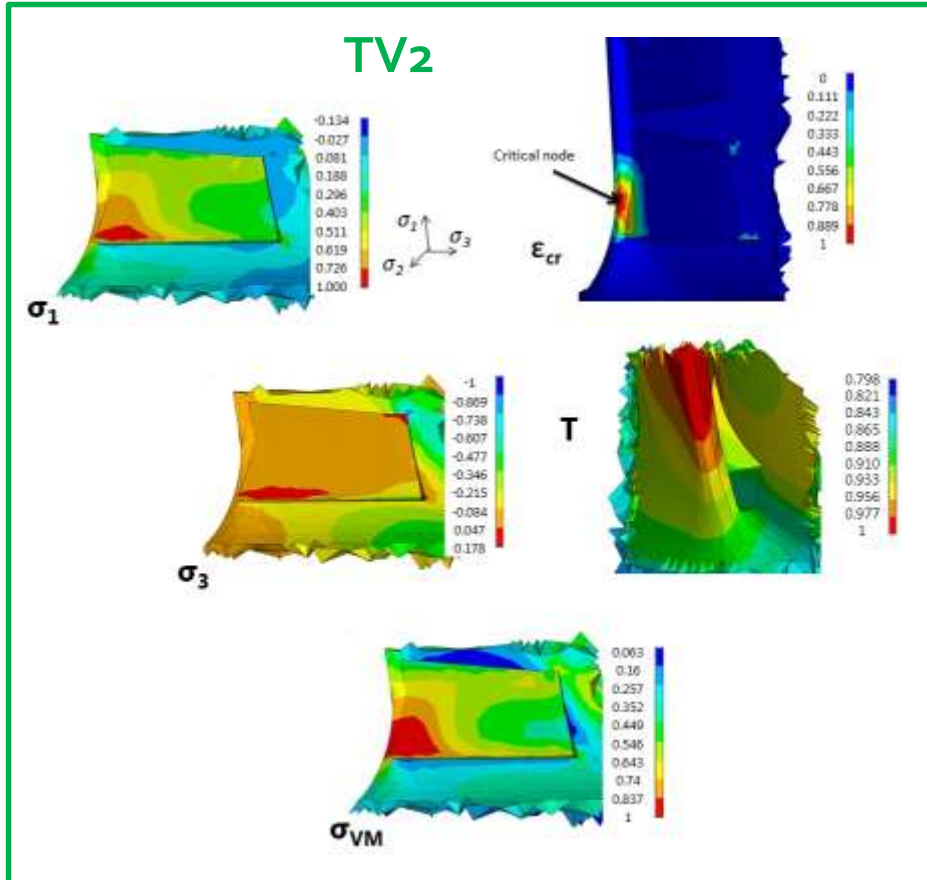
1. Creep-fatigue test execution in condition similar to the one experienced by critical location e.g. T max, strain range, strain ratio, etc..)
2. Damage interaction diagram definition

TMF service-like tests to validate the developed strategy 10

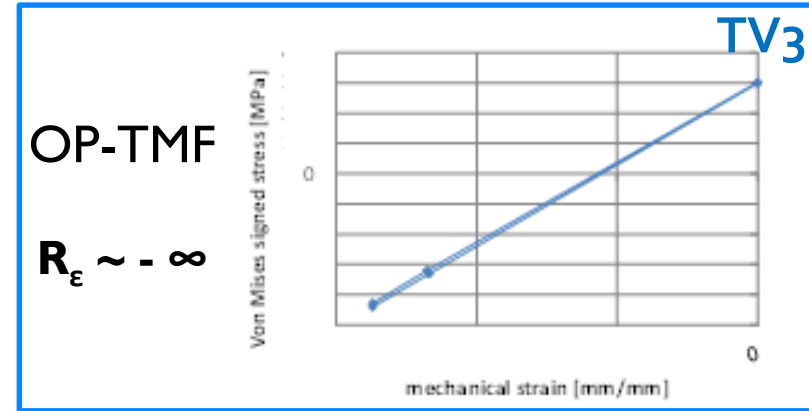
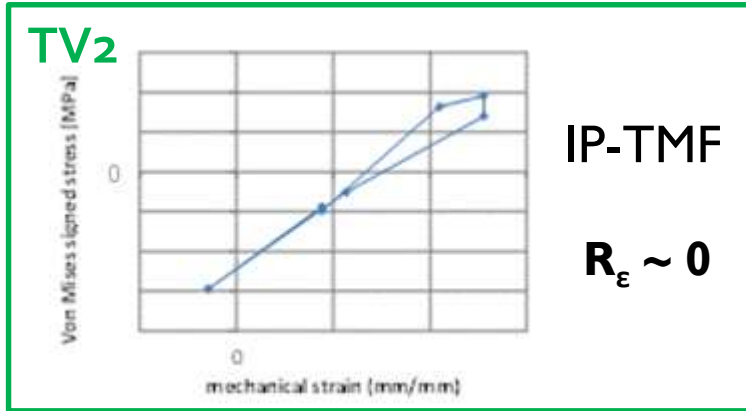


## Service-like TMF Cycle Definition

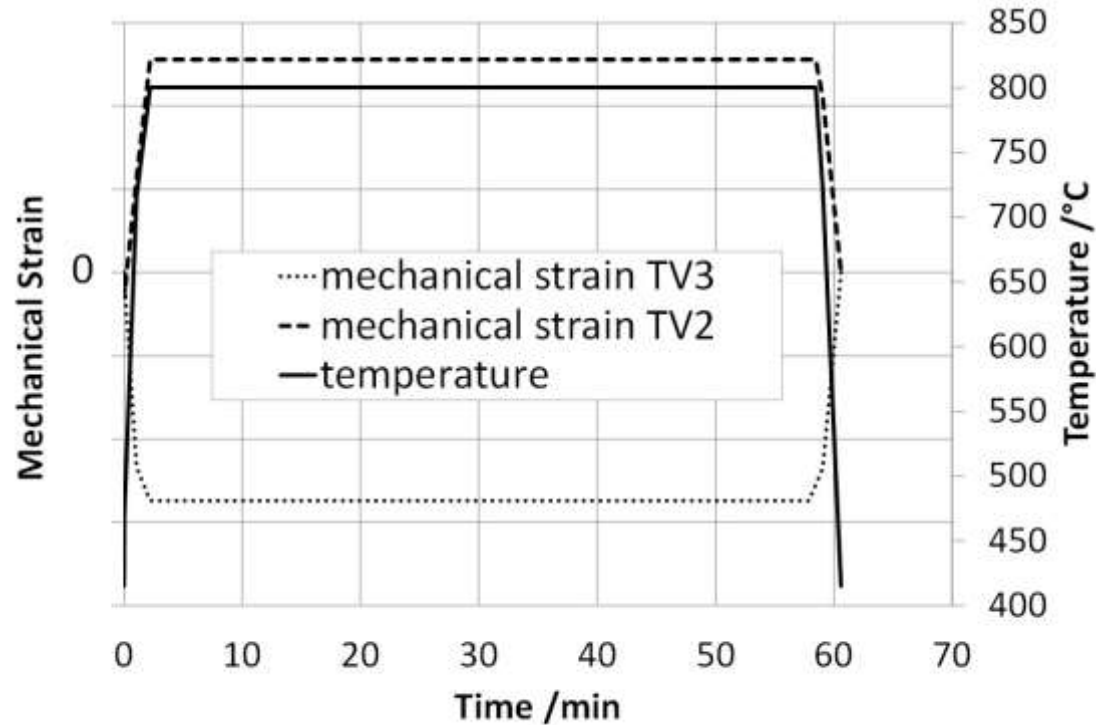
Critical location identification in terms of cumulated plastic and creep strain



## Service-like TMF Cycle Definition



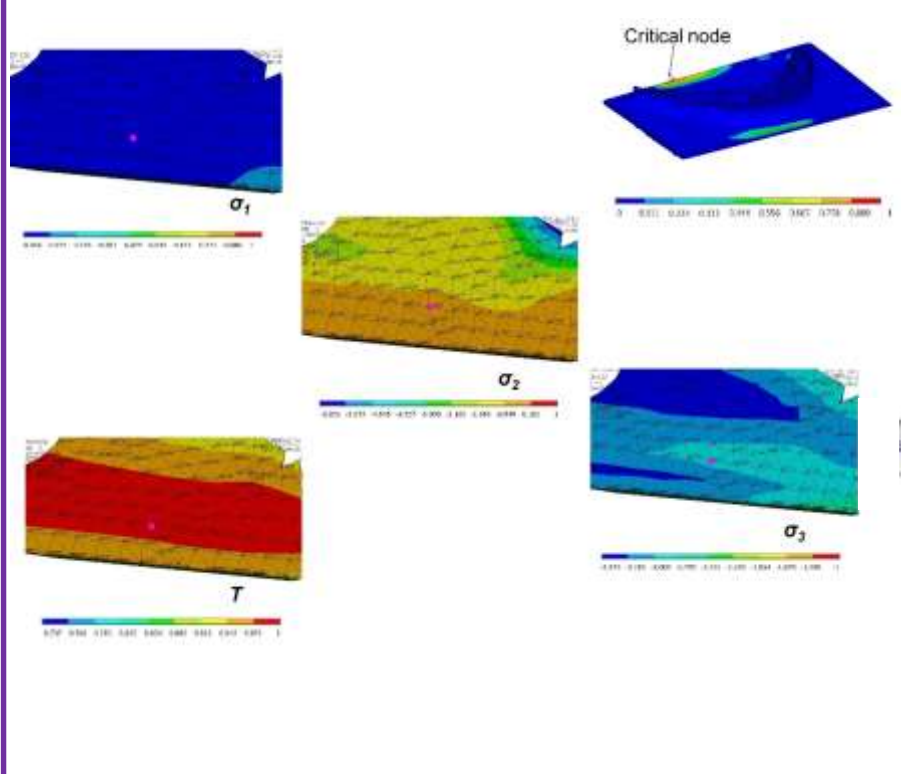
$\dot{\epsilon} \ll 10^{-2} s^{-1}$



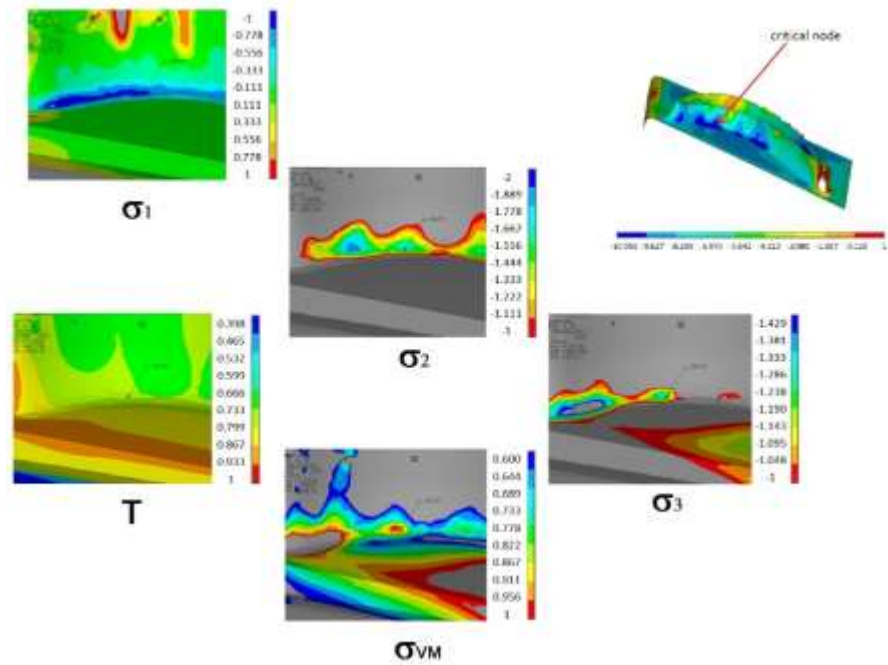
## Service-like TMF Cycle Definition

Critical location identification in terms of cumulated plastic and creep strain

### TB1 –platform edge



### TB1 – fillet radius pressure side



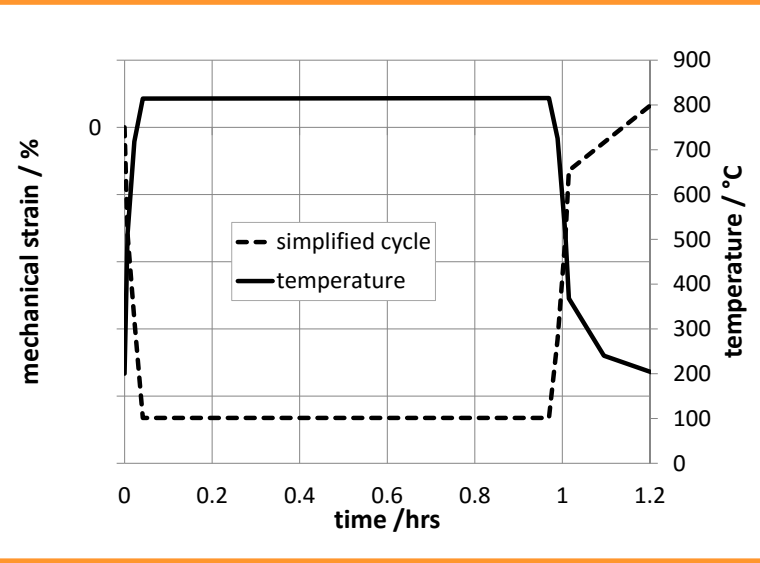
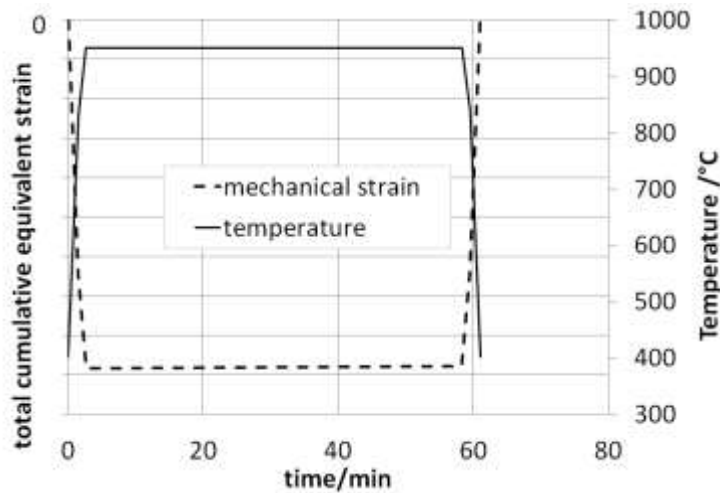
## Service-like TMF Cycle Definition

TB1

OP-TMF

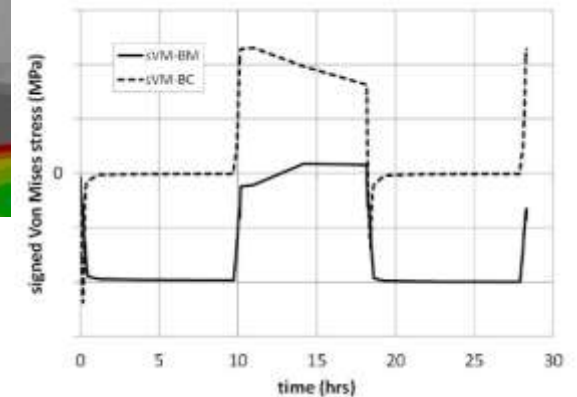
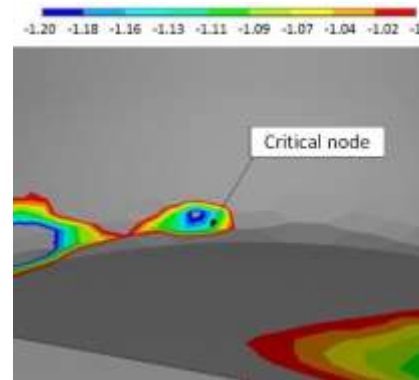
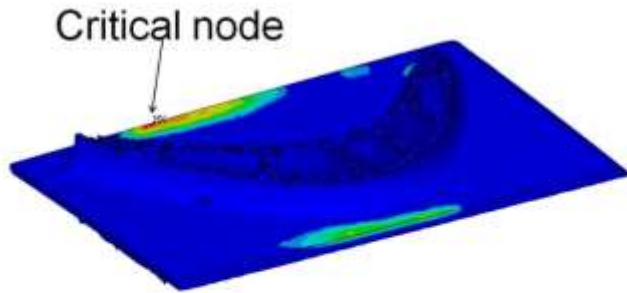
$$R_{\epsilon} \sim -\infty$$

$$\dot{\epsilon} \ll 10^{-2} s^{-1}$$



400°C-950°C

200°C-815°C



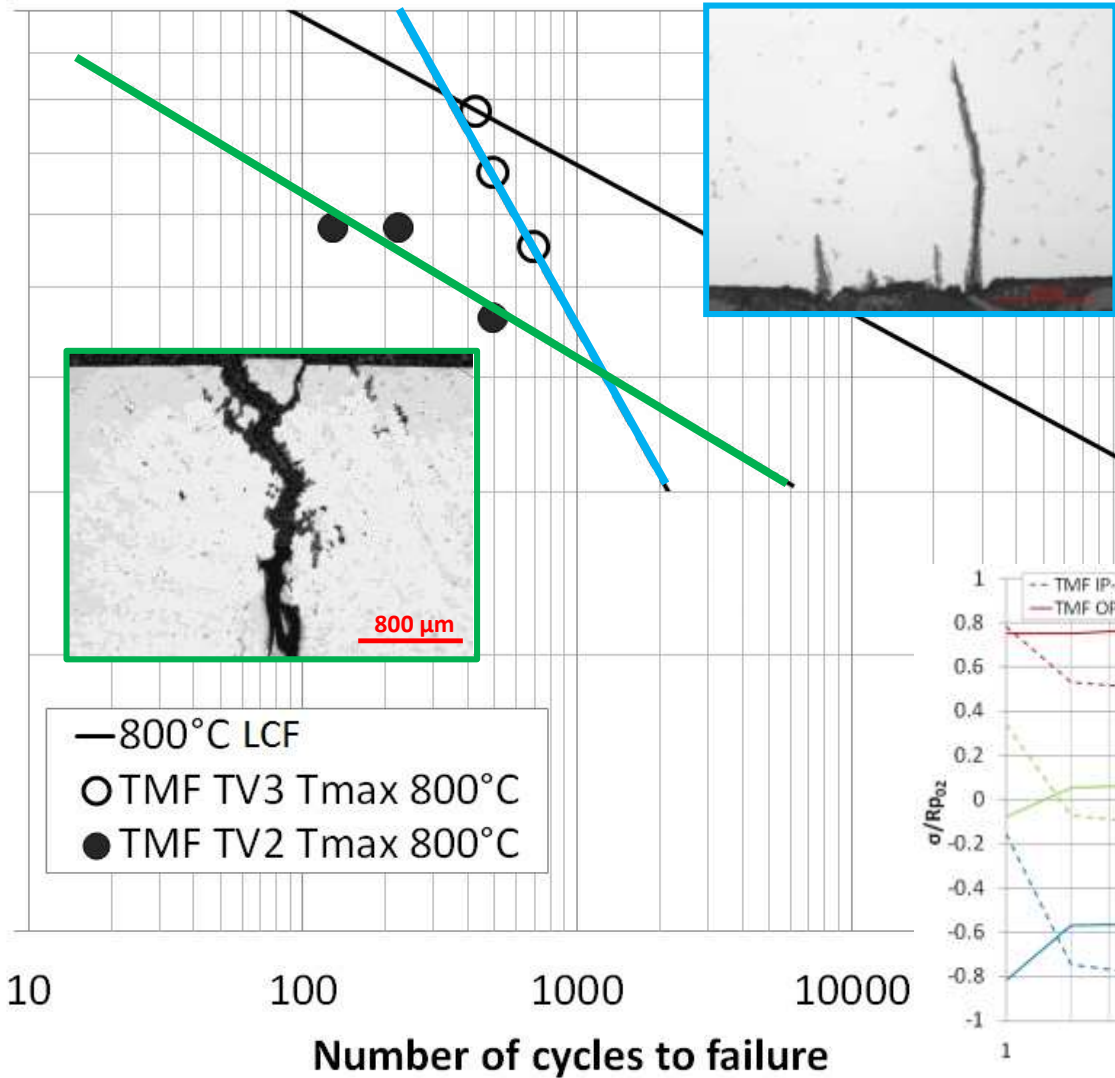
## TMF Test Results

René 80

TV<sub>2</sub>

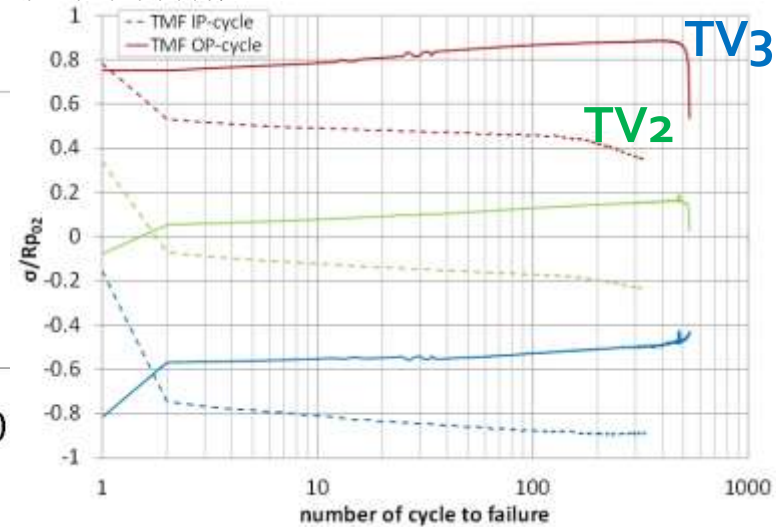
TV<sub>3</sub>

total strain range



Different crack mechanism due to different mechanical cycle

Effect of dwell time on mean stress evolution  
→ creep relaxation

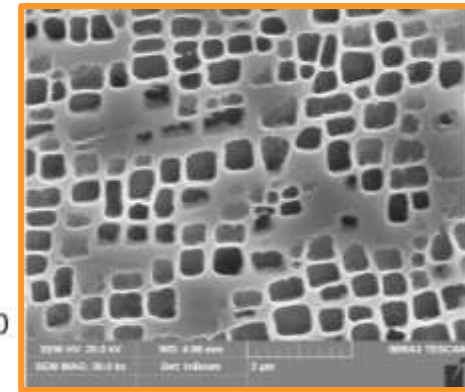
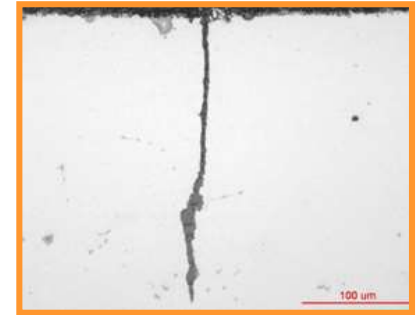
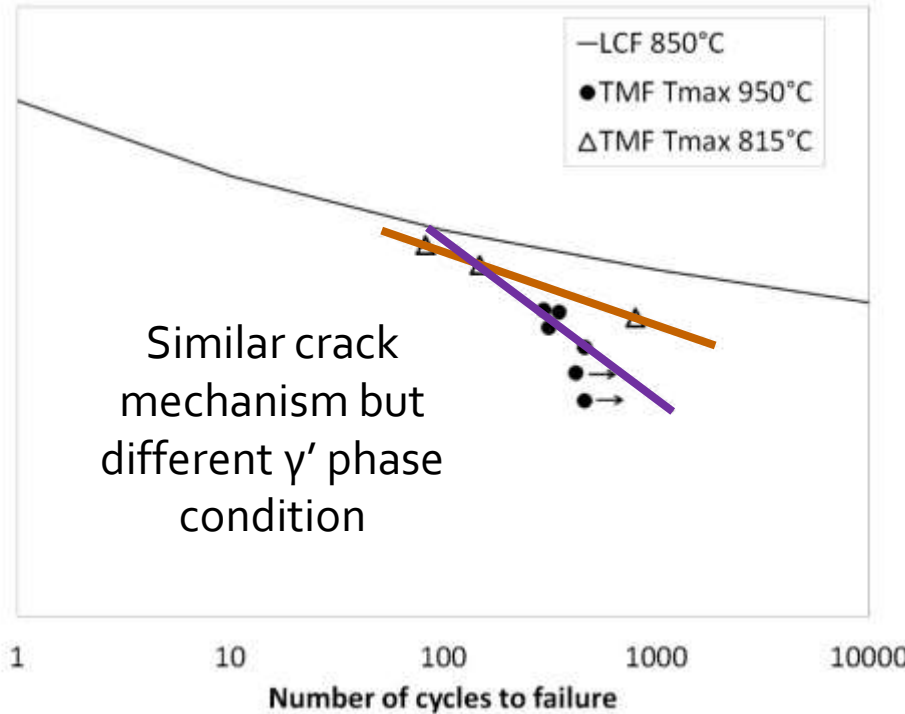




## TMF Test Results

**IN792SX**

**TB1 – fillet radius pressure side**



total strain range / mm/mm

Number of cycles to failure

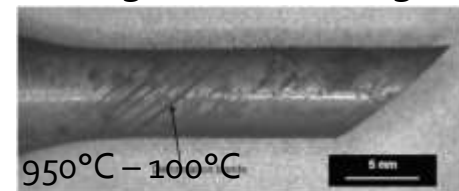
Similar crack mechanism but different  $\gamma'$  phase condition

Slightly greater endurance reduction on uncoated samples for the cycle with the highest maximum temperature ( $T_{max} = 950^{\circ}\text{C}$ )

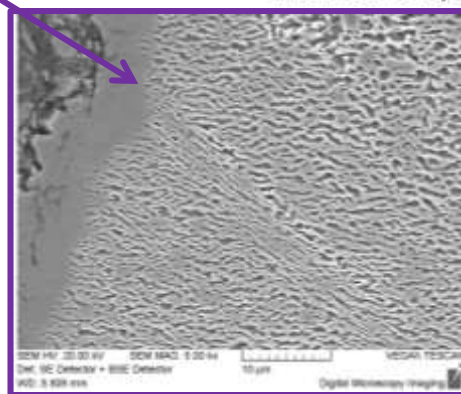
**TB1 – platform edge**



Deformation bands along  $\{111\}$  planes appear on sample surface for the higher strain range



THERMOMECHANICAL FATIGUE OF SINGLE-CRYSTAL SUPERALLOYS: INFLUENCE OF COMPOSITION AND MICROSTRUCTURE  
J J Moverare, et al, Superalloys 2012 pp 369-377

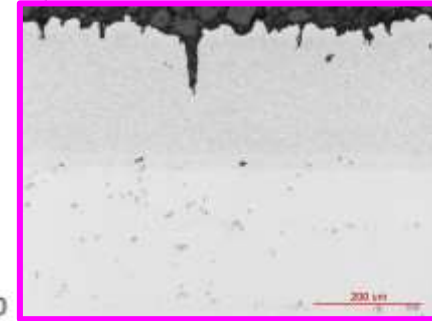
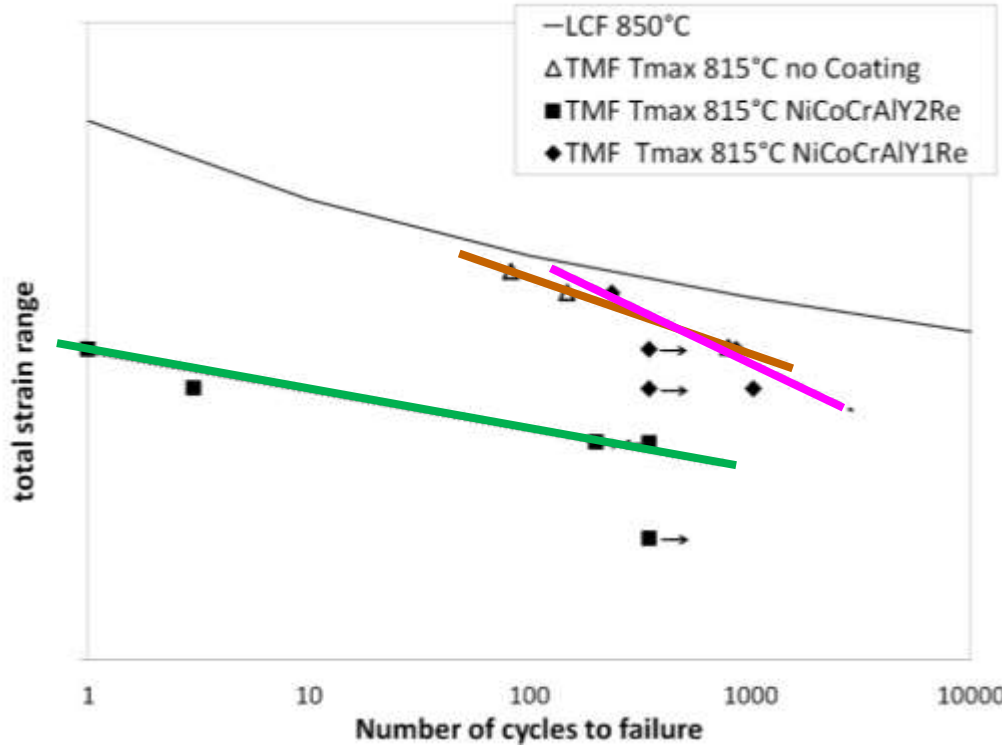
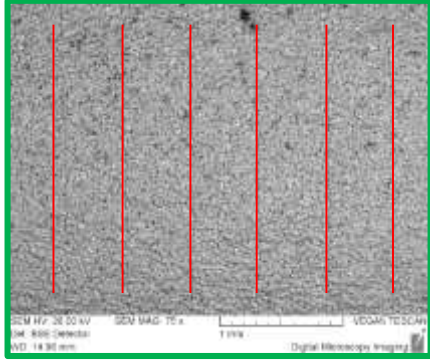


# RESULTS

## TMF Test Results

### TB1 – fillet radius pressure side

NiCoCrAlY<sub>2</sub>Re  
NiCoCrAlY<sub>1</sub>Re



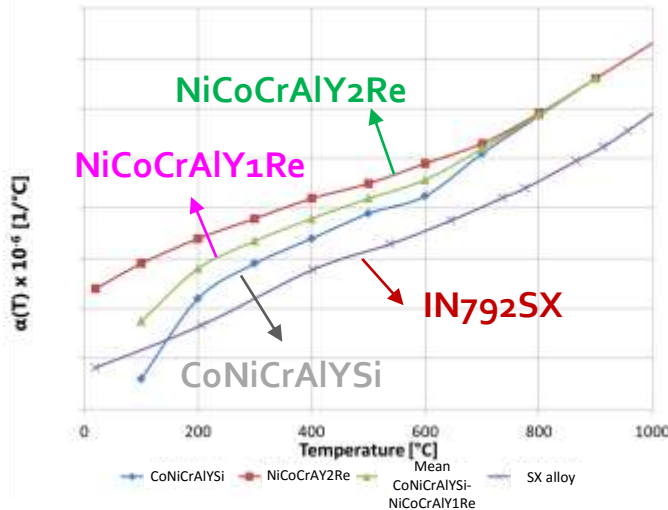
«Instantaneous» cracks during the first cycles for the highest strain ranges  
Cracks are circumferential, straight and nearly constantly spaced

**WHY?**

No difference between uncoated and coated sample  
Completely different cracks, covering the whole surface and resembling roughness

## TMF Test Results

### TB<sub>1</sub> – fillet radius pressure side

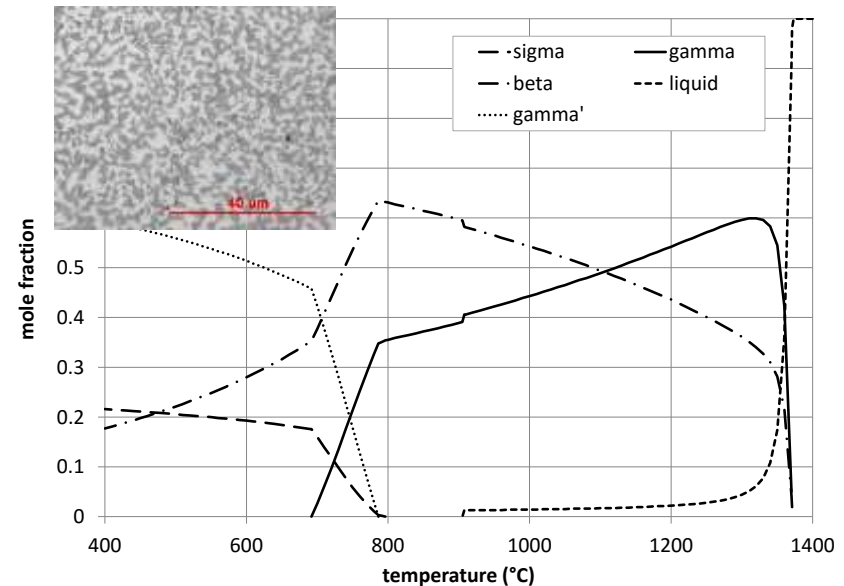
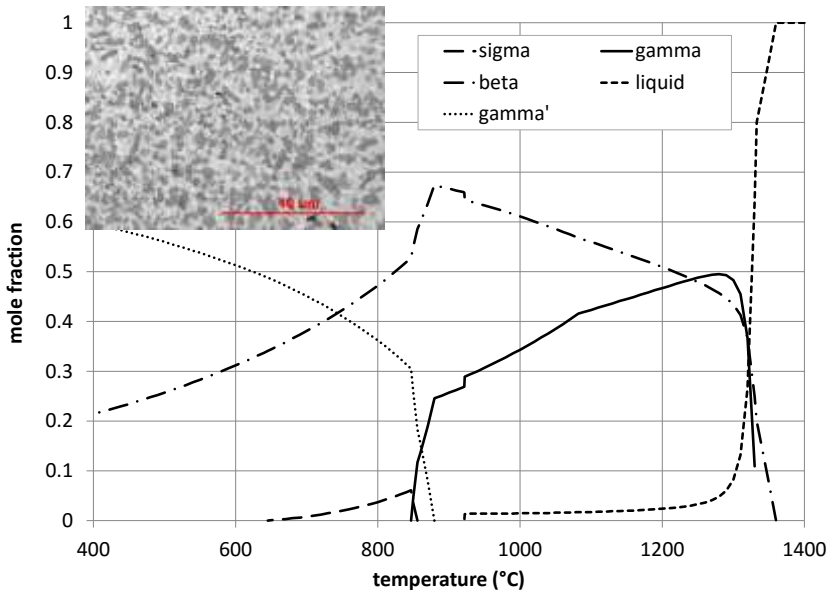


The different coating compositions brings to different thermo-physical and mechanical properties

- ✓  $T_{min}$  for both the coating it is below their DBTT
- ✓ Different  $\alpha(T)$  → Probably **NiCoCrAlY<sub>1</sub>Re** has an  $\alpha(T)$  closer to the IN792SX rather than the one of **NiCoCrAlY<sub>2</sub>Re**
- ✓ Different coating matrix!

✓ **NiCoCrAlY<sub>2</sub>Re** @TMF Tmax →  $\gamma'$  matrix

✓ **NiCoCrAlY<sub>1</sub>Re** @TMF Tmax →  $\gamma$  matrix



## Creep-fatigue life procedure validation

### Fatigue damage

$$D_f = \sum \frac{N}{N_f}$$

$N_f$  has been evaluated through a simplified **Manson-Coffin** model representation

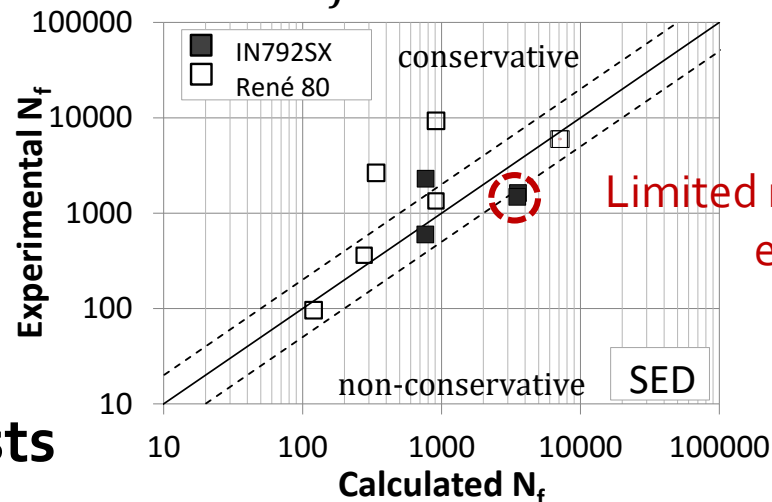
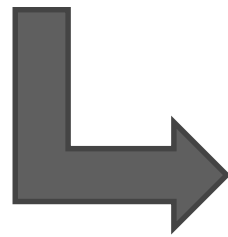
### Creep damage

$$D_c^{SED} = \sum N \int_0^{t_{ht}} \frac{\dot{w}}{w_f(\dot{w}, T)} dt$$

strain energy density  
ductility exhaustion  
(SED)

Evaluation on the mid-life cycle

$$D_f + D_c = 1$$



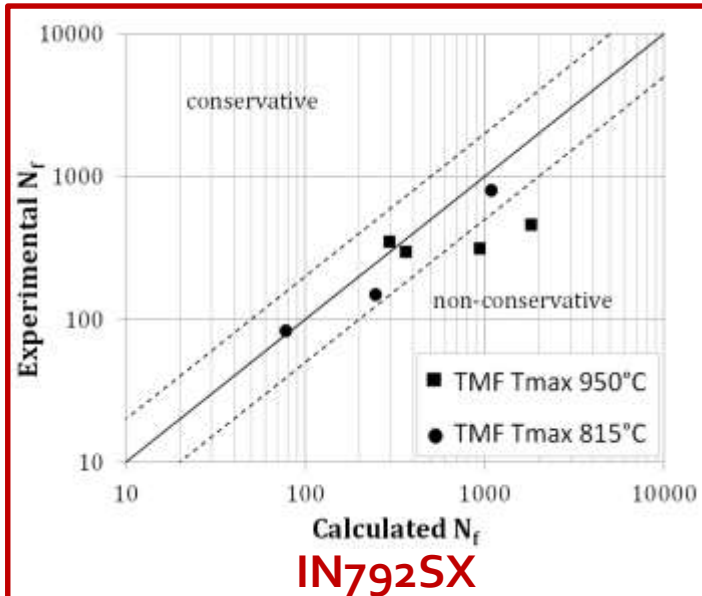
Limited non-conservative evaluation



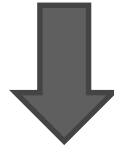
Cyclic-hold time tests

## Creep-fatigue life procedure validation

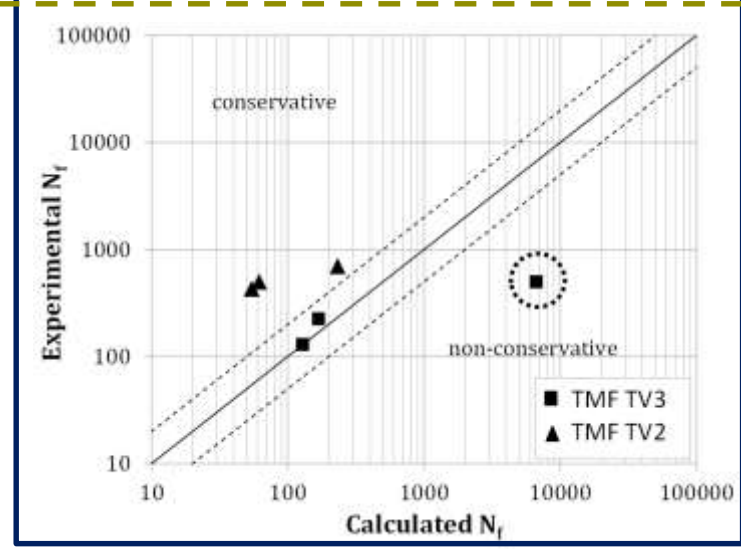
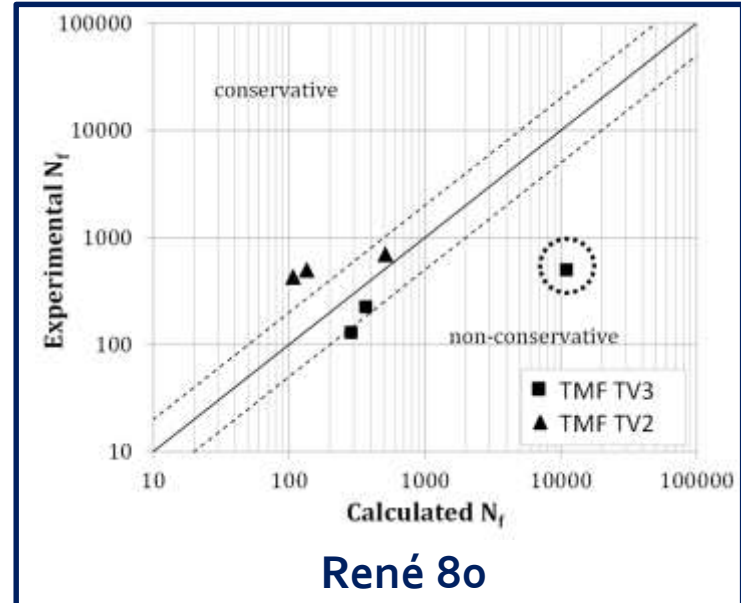
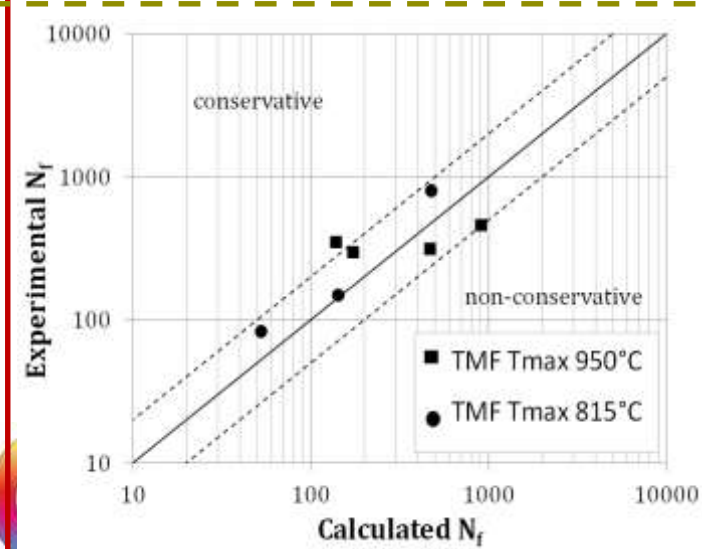
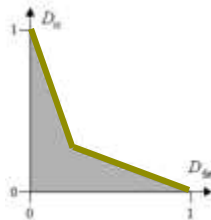
Damage calculation performed on TMF test results



$$D_f + D_c = 1$$

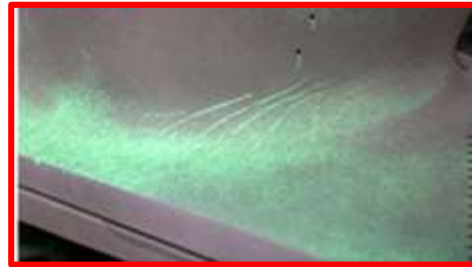
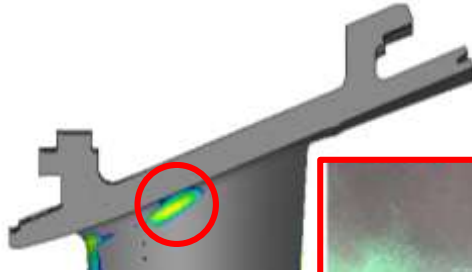


**Interaction Locus**



## Field feedback verification

TV2

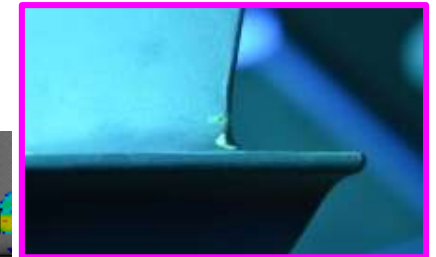
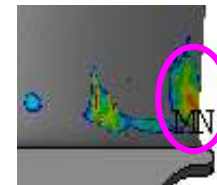
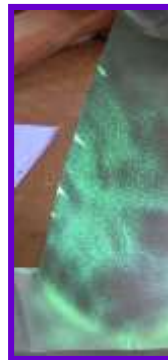
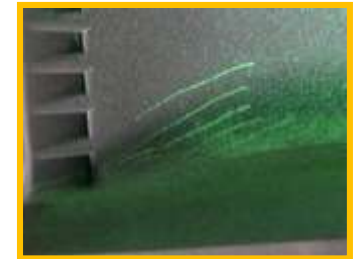
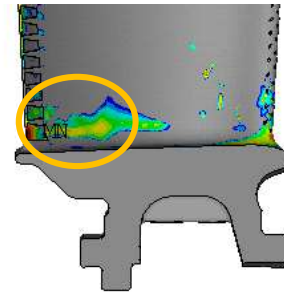


Good correlation with operated vanes

- crack location
- number of cycles

Intermediate and daily cycling components

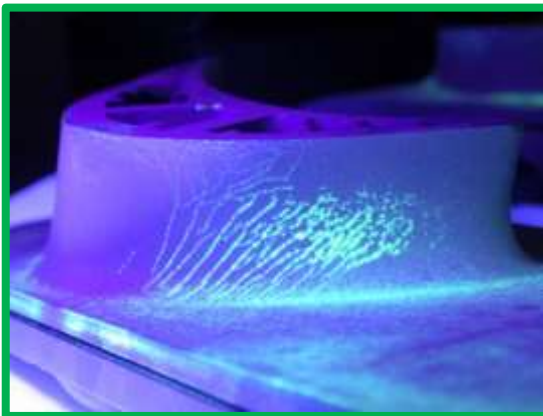
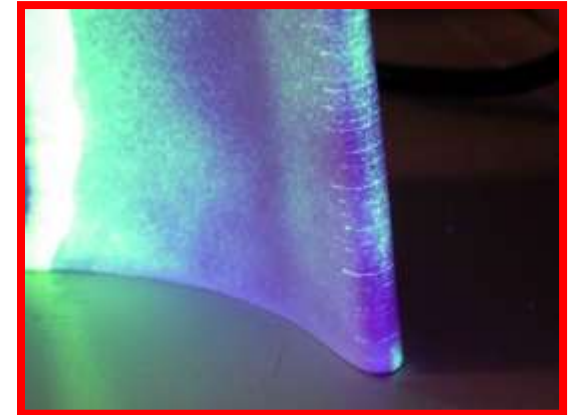
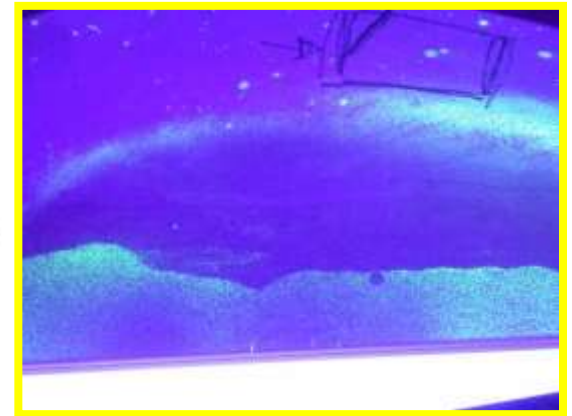
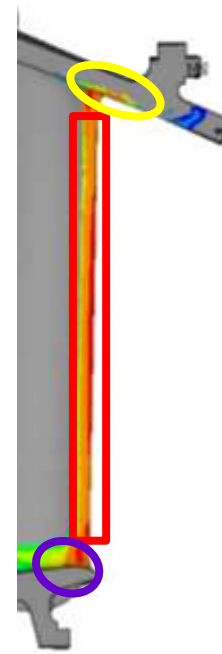
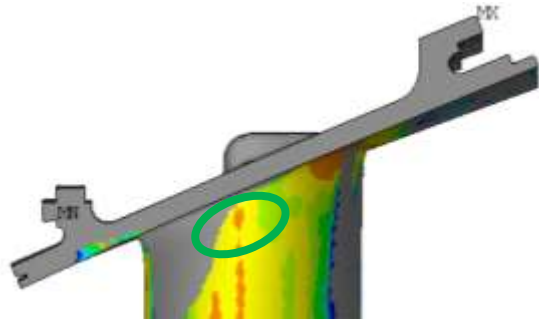
Life maps obtained from FE simulation output  
Damage fractions calculated and summed up through the defined interaction locus



## Field feedback verification

TV<sub>3</sub>

Life maps obtained from FE simulation output  
Damage fractions calculated and summed up  
through the defined interaction locus



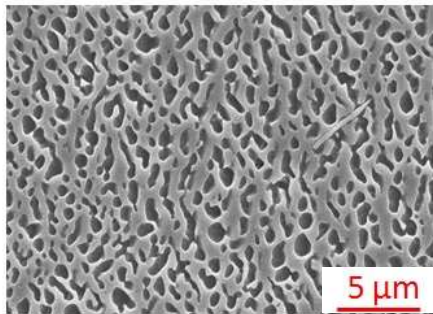
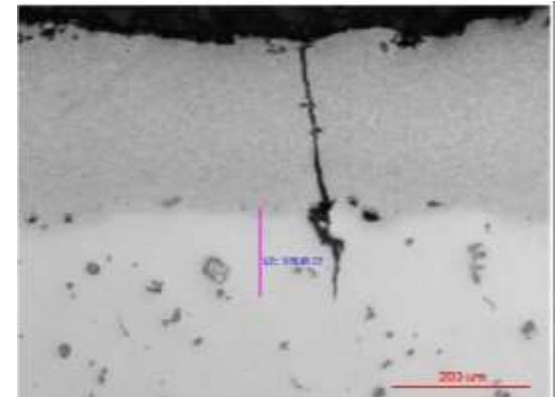
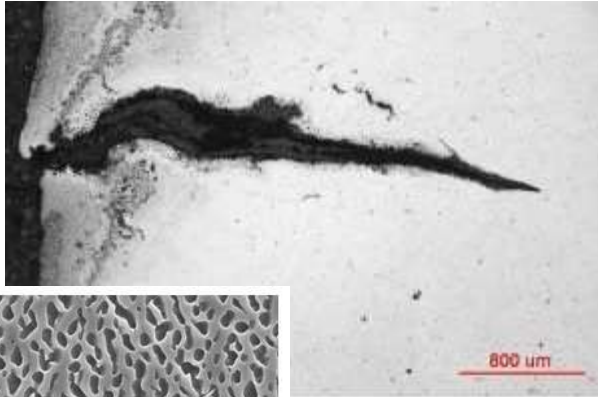
Good correlation with operated vanes  
→ crack location  
→ number of cycles



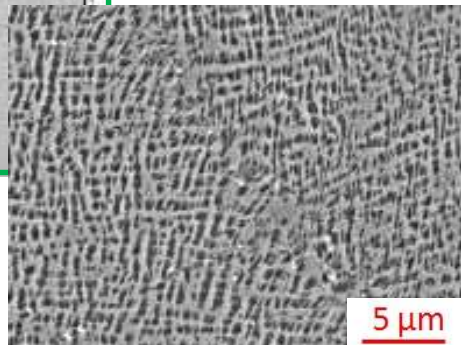
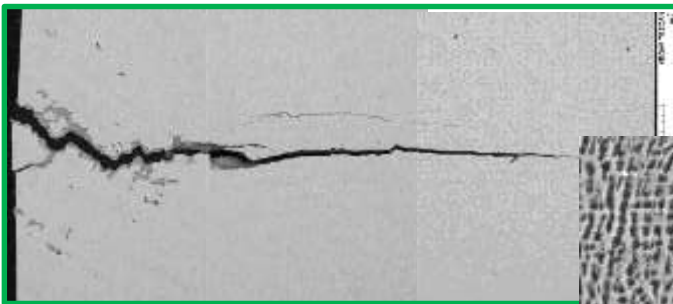
## Field feedback verification

TV<sub>2</sub>

TV<sub>3</sub>



Ex-service vanes



TMF sample



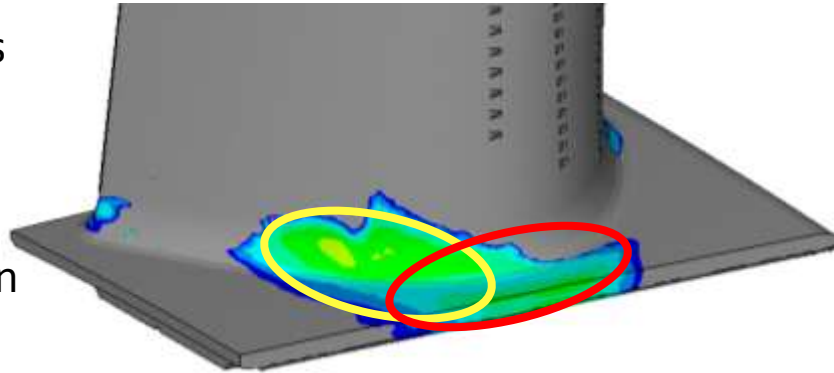


## Field feedback verification

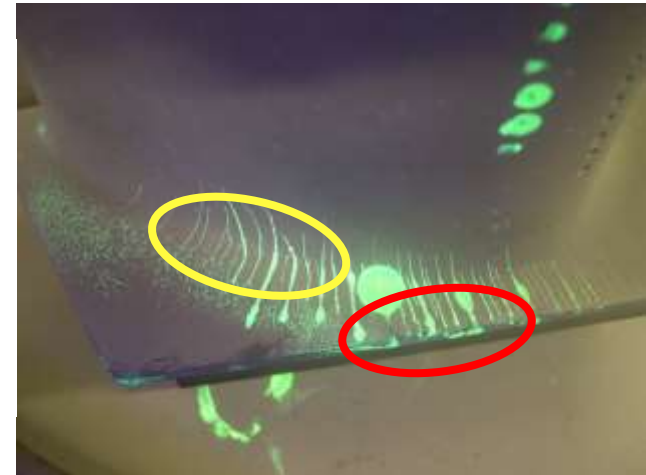
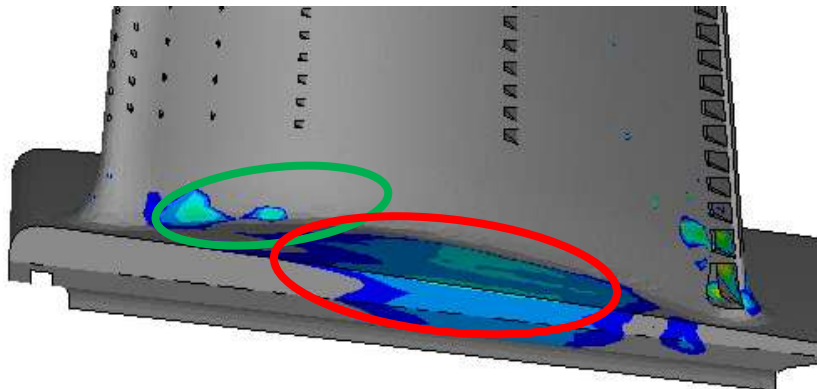
### TB1

Life maps obtained from FE simulation output

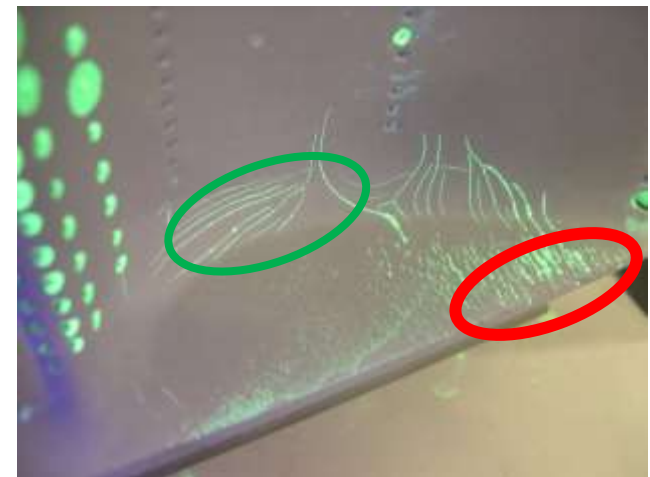
Damage fractions  
calculated and  
summed up  
through the  
defined interaction  
locus



Good correlation with operated blades  
→ crack location  
→ number of cycles



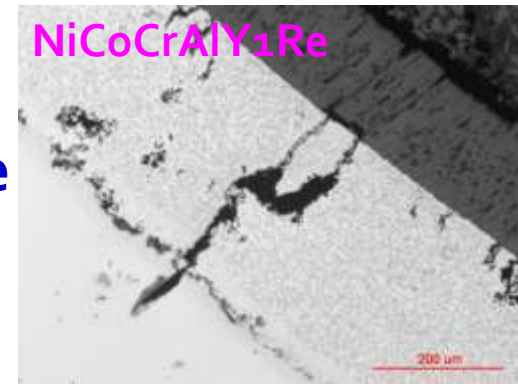
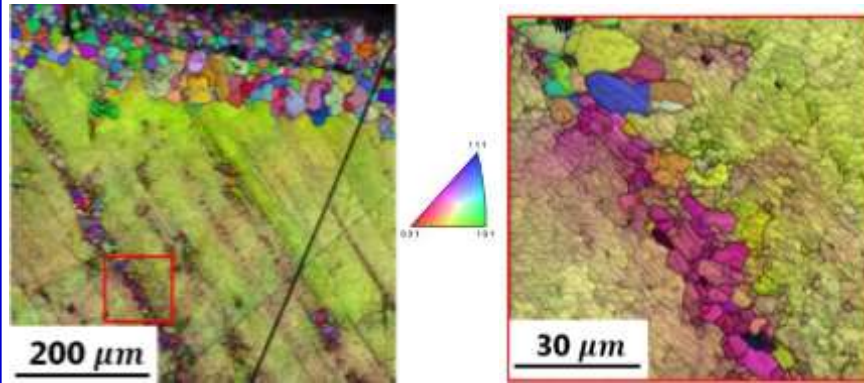
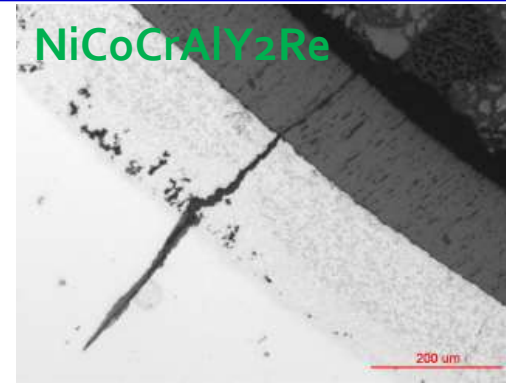
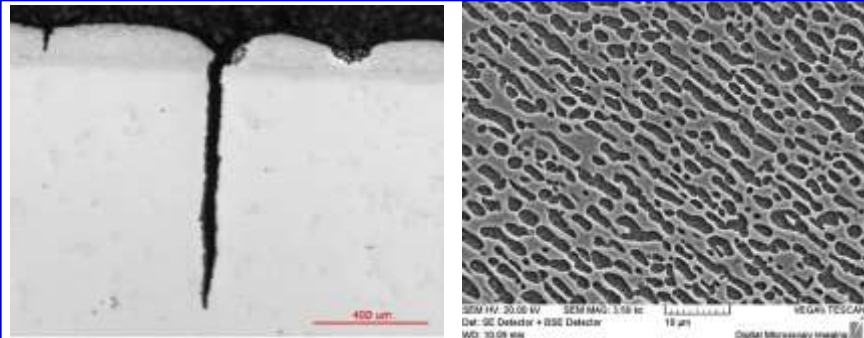
Intermediate and daily  
cycling components



## Field feedback verification

TB<sub>1</sub>-platform edge

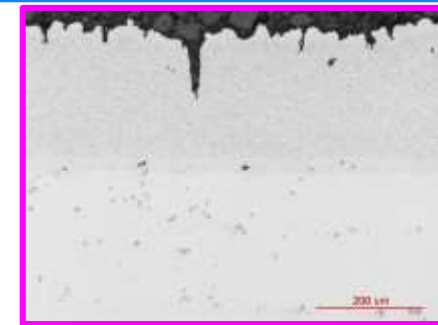
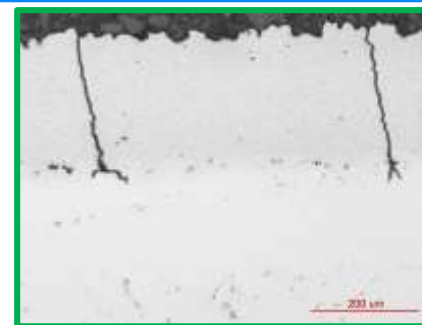
TB<sub>1</sub> – fillet radius pressure side



Ex-service blade



TMF sample



- ✓ **TMF benchmark tests** are fundamental for the assessment and validation of a new life assessment procedure. The great effectiveness of the TMF cycles defined from FE transient simulations has been demonstrated by comparison with the physical damage observed in real components and the one produced in the tested samples
- ✓ **TMF benchmark tests** can be used during the design of new components as it allows the evaluation of critical location behaviour and the validation of the developed design
- ✓ **Service-like TMF tests** can be exploited for the coating effect quantification. By focusing on a critical location, a life reduction factor for each applied coating can be evaluated

In the *next future*:

- The developed life assessment procedure will be applied to other case studies and to other transients, like unexpected stops (i.e. trip or load rejection) or quick ramps from minimum load to peak load
- Improvement of the iterative FE simulations trying to reduce their calculation time
- Progress in damage fraction calculation considering the whole test life and considering the mean stress effect (e.g. using Smith-Watson-Topper parameter)



**Thank you  
for the attention**

**Questions?**

[erica.vacchieri@ansaldoenergia.com](mailto:erica.vacchieri@ansaldoenergia.com)



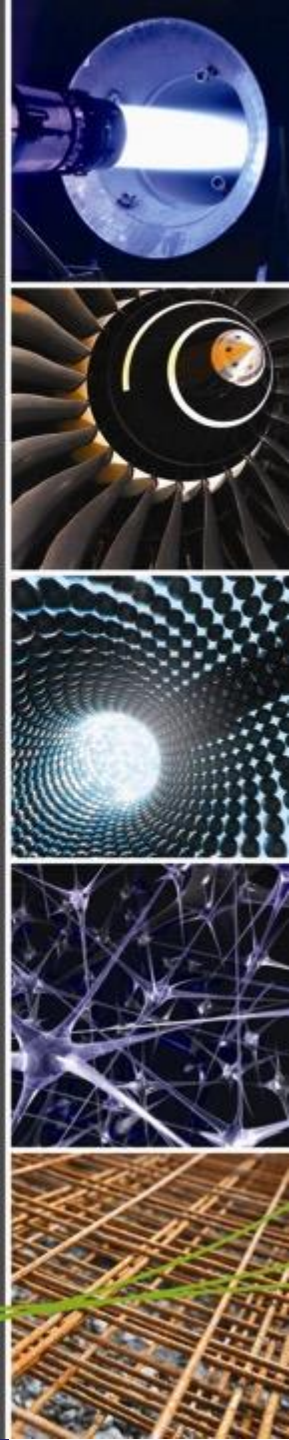
Swansea University  
Prifysgol Abertawe

# Thermo-Mechanical Fatigue Crack Growth of RR1000

Mark Whittaker<sup>1</sup>, Christopher Pretty<sup>1</sup>, & Steve Williams<sup>2</sup>

<sup>1</sup>Institute of Structural Materials, Swansea University, Singleton Park,  
Swansea, SA2 8PP, UK

<sup>2</sup>Rolls-Royce plc, P.O. Box 31, Derby, DE24 8BJ, UK



# Contents

- Introduction
- Experimental
  - Rig Development
  - Validation
- Results
  - Paris Curves
  - Fractography
- Conclusions
- Future Work

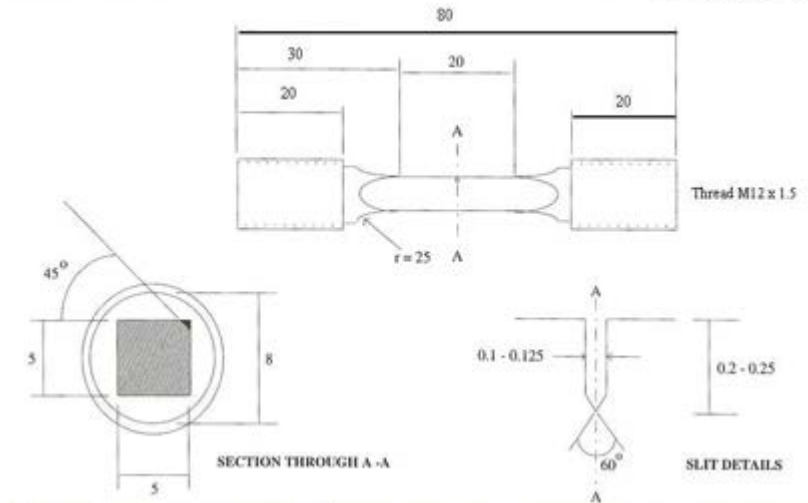
# Introduction: RR1000 Test Material (Fine Grain)

- RR1000 is a heavily  $\gamma'$  stabilised nickel alloy which is expected to be widely used in high temperature applications in the coming years.
- However, the TMF properties of the alloy have not yet been widely examined.
- Crack growth based life predictions under these conditions are thus essential
  - To assess the effects of, for example, handling damage and melt anomalies
  - 5x5mm corner notched specimens developed for method



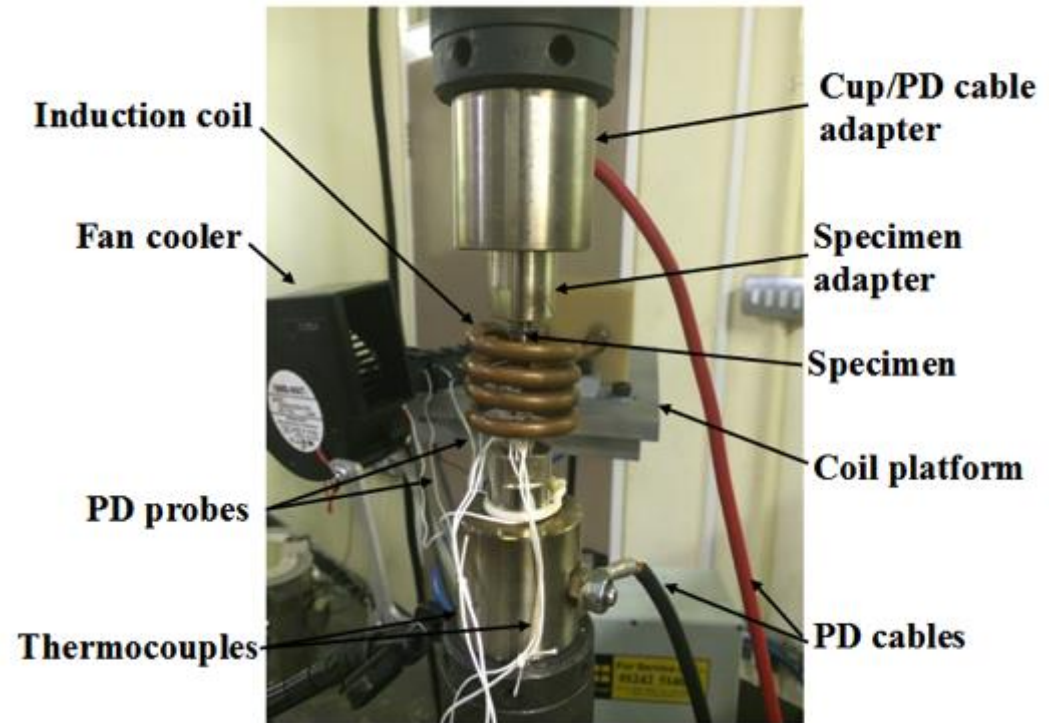
Not to scale

Dimensions in mm



# Experimental: Rig Development

- Specially designed adapters accommodating CC5 specimens and PD wires
- New PD software to allow for phase angle and loading direction variation
- Induction coil platform designed to allow coil position repeatability along with PD and TC box

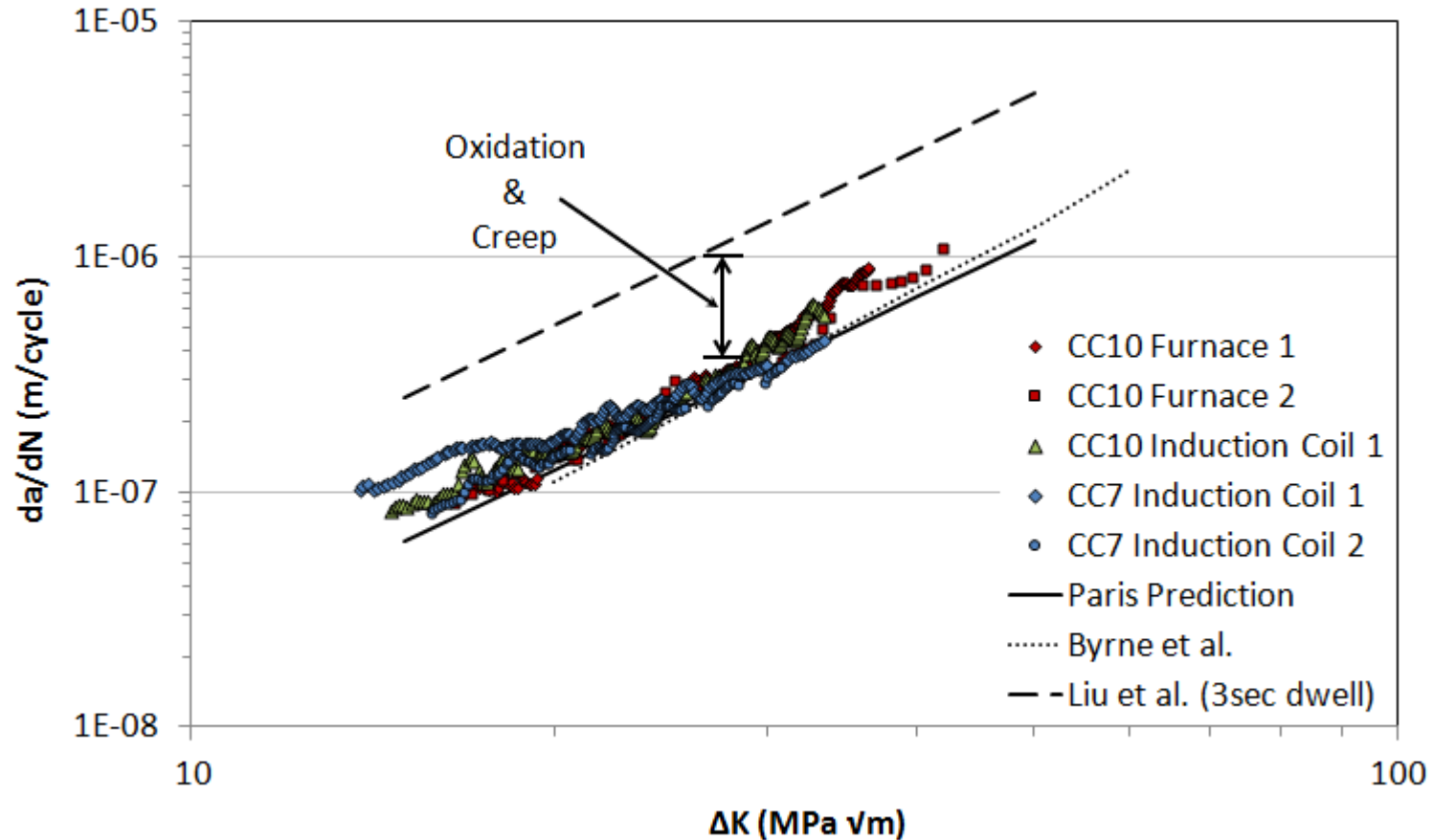


- Air cooler positioned in precise location to allow equal air cooling rates from test to test thus allowing an 80 second TMF cycle (40sec heat + 40sec cool)
- Limited literature on different methods so validation is required first to ensure induction can be used with PD



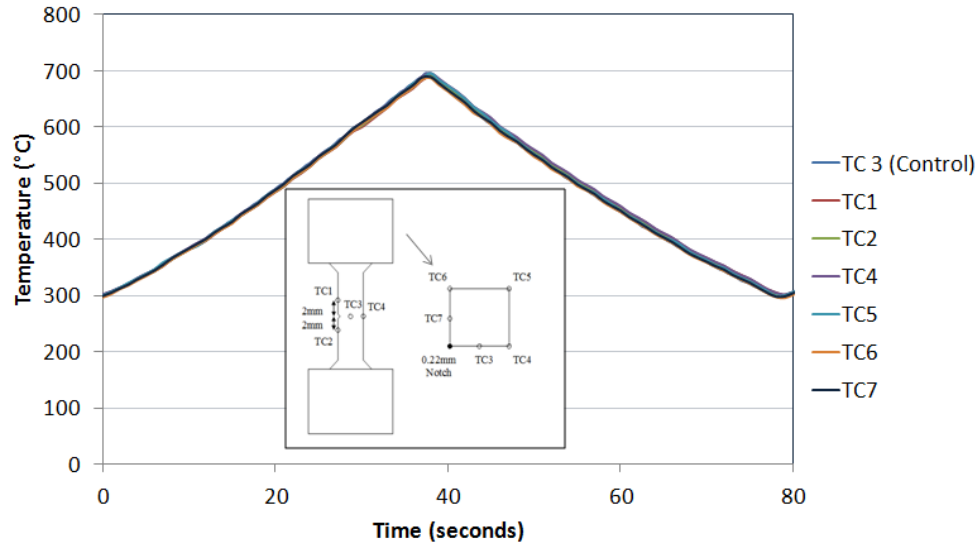
# Experimental: Validation

Waspaloy isothermal tests carried out at 650°C and R=0.1 in line with previous literature to ensure comparable and repeatable results



# Experimental: Validation

Temperature vs. Time: Thermal Profile of 7 Thermocouples over a TMF Cycle



Aimed to produce,

- 10°C/s cooling rate

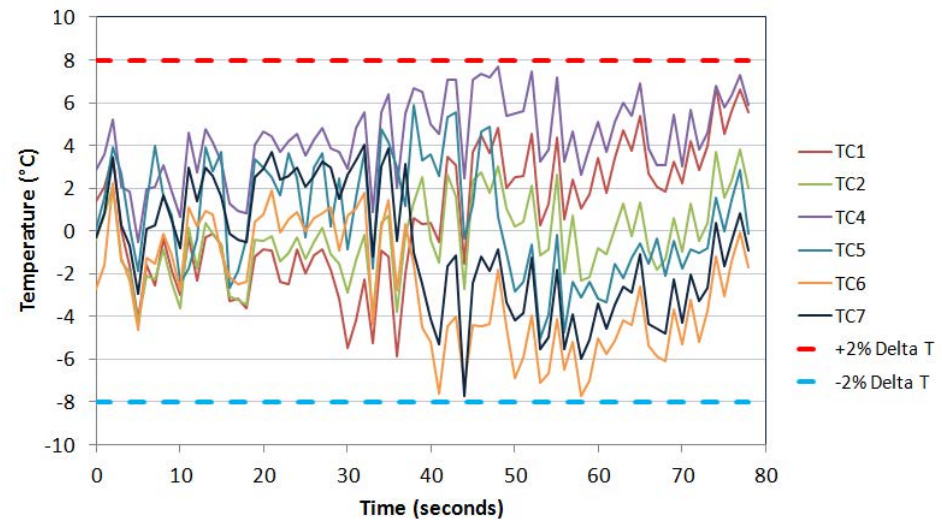
Achieved by,

- 35mm between cooler & specimen
- 1.5m/s flow rate

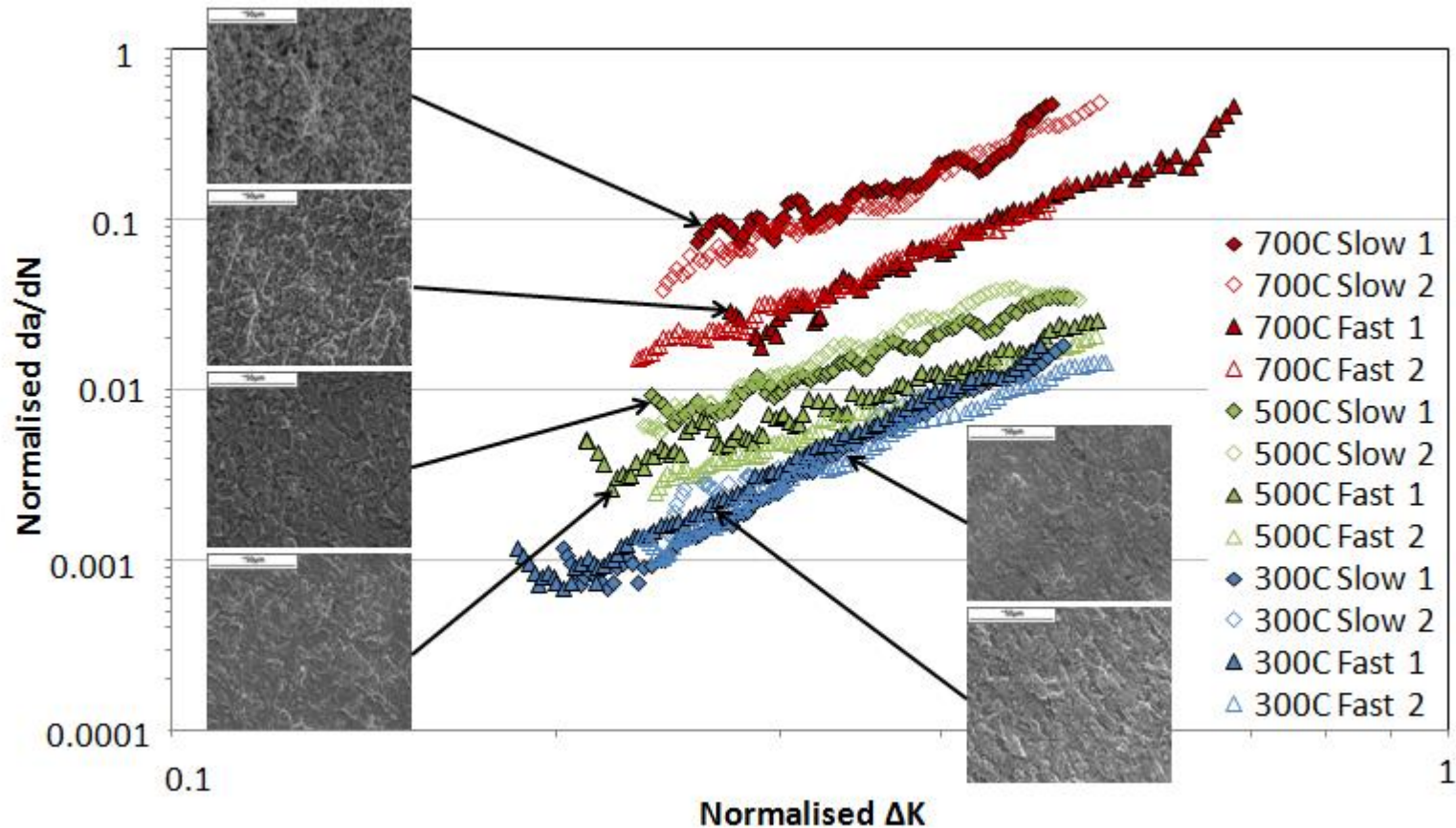
Before TMF acquisition the thermal profiles were measured across the specimen

Very small scatter within 2%  $\Delta T$  as required in TMF strain control code of practice

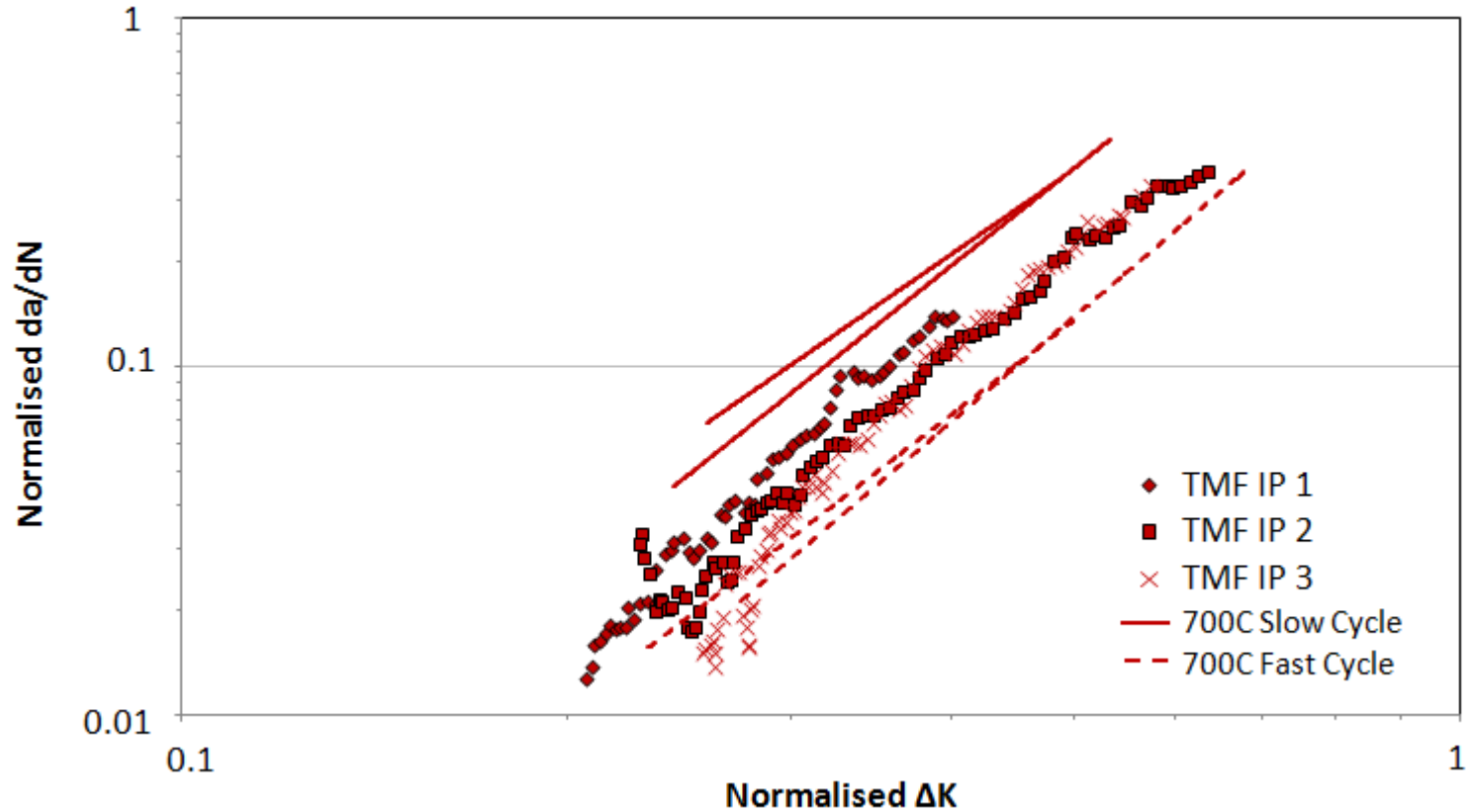
Temperature deviation from the target/control temperature for the other 6 thermocouples



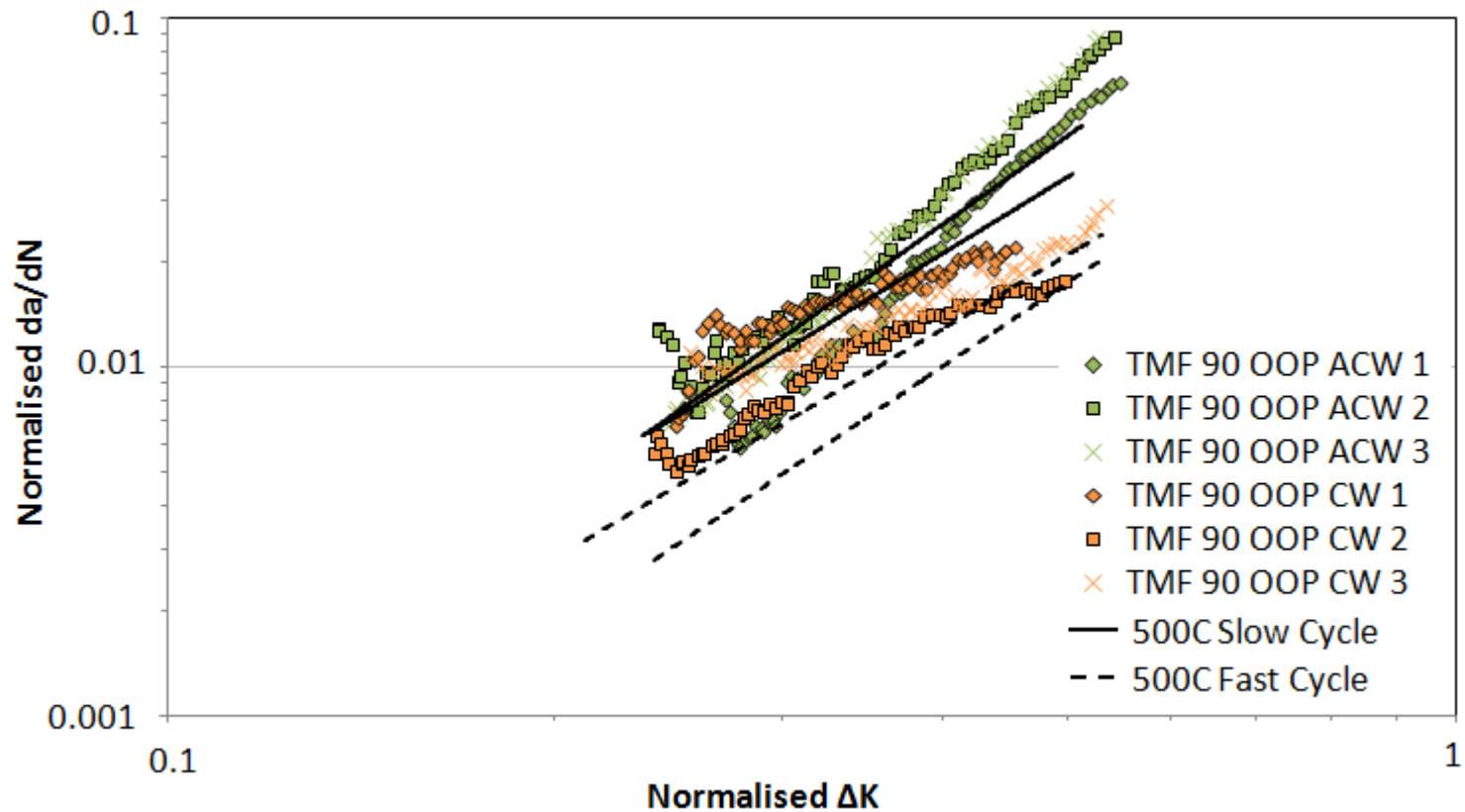
# Results: Isothermal Crack Growth with Fractography



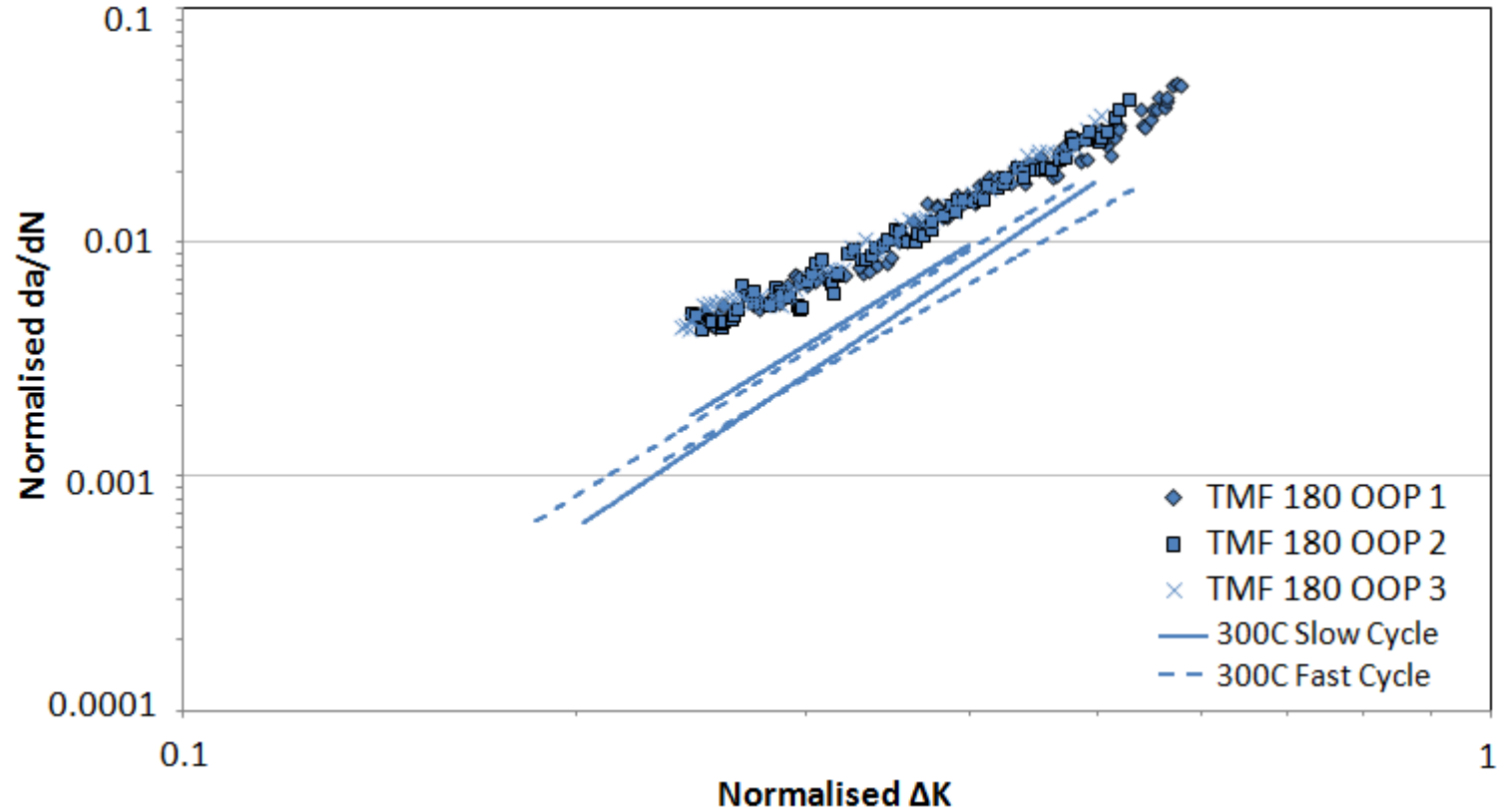
# Results: In-Phase (IP) Crack Growth



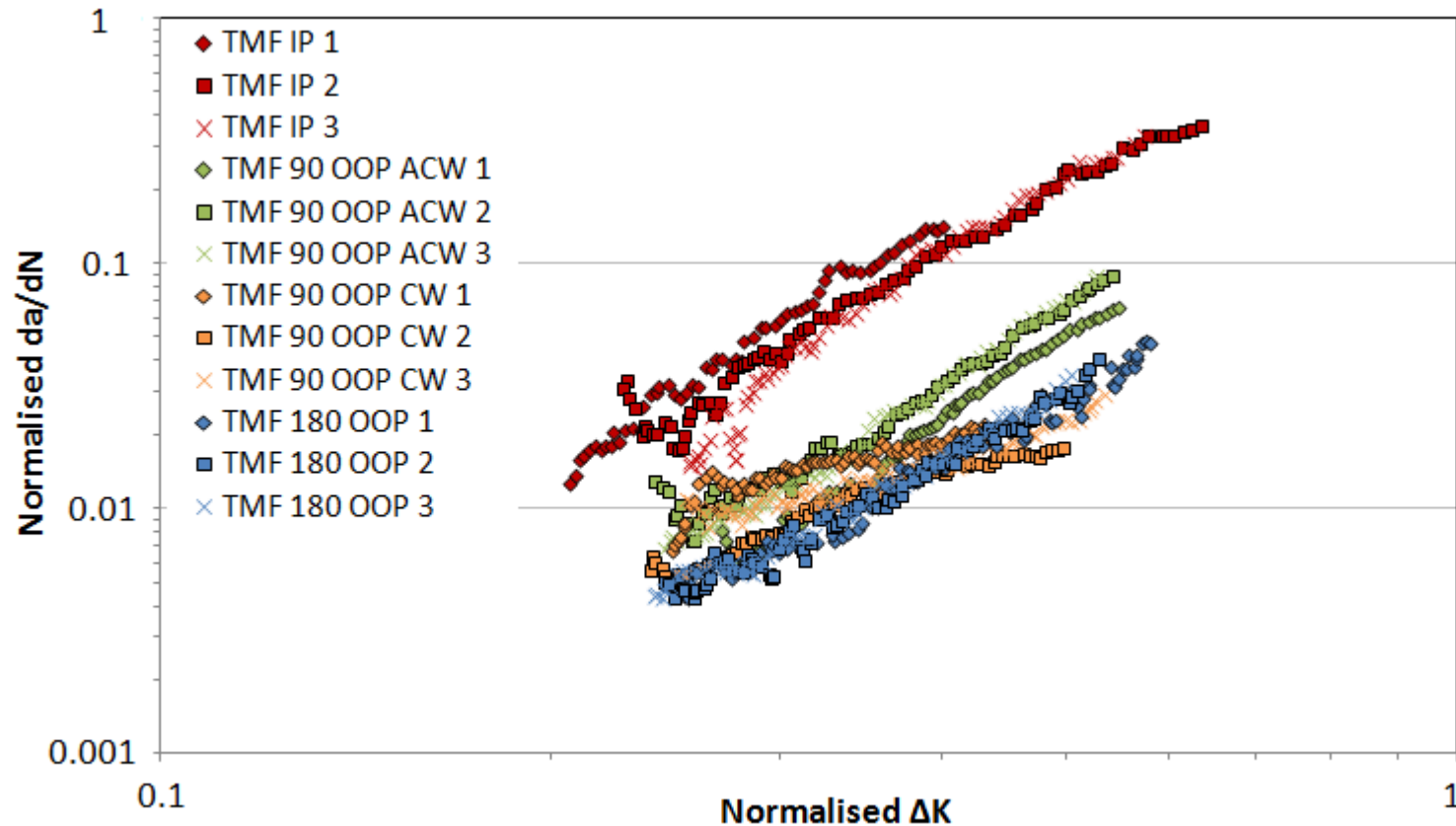
# Results: 90° Out-of-phase (OOP) Crack Growth



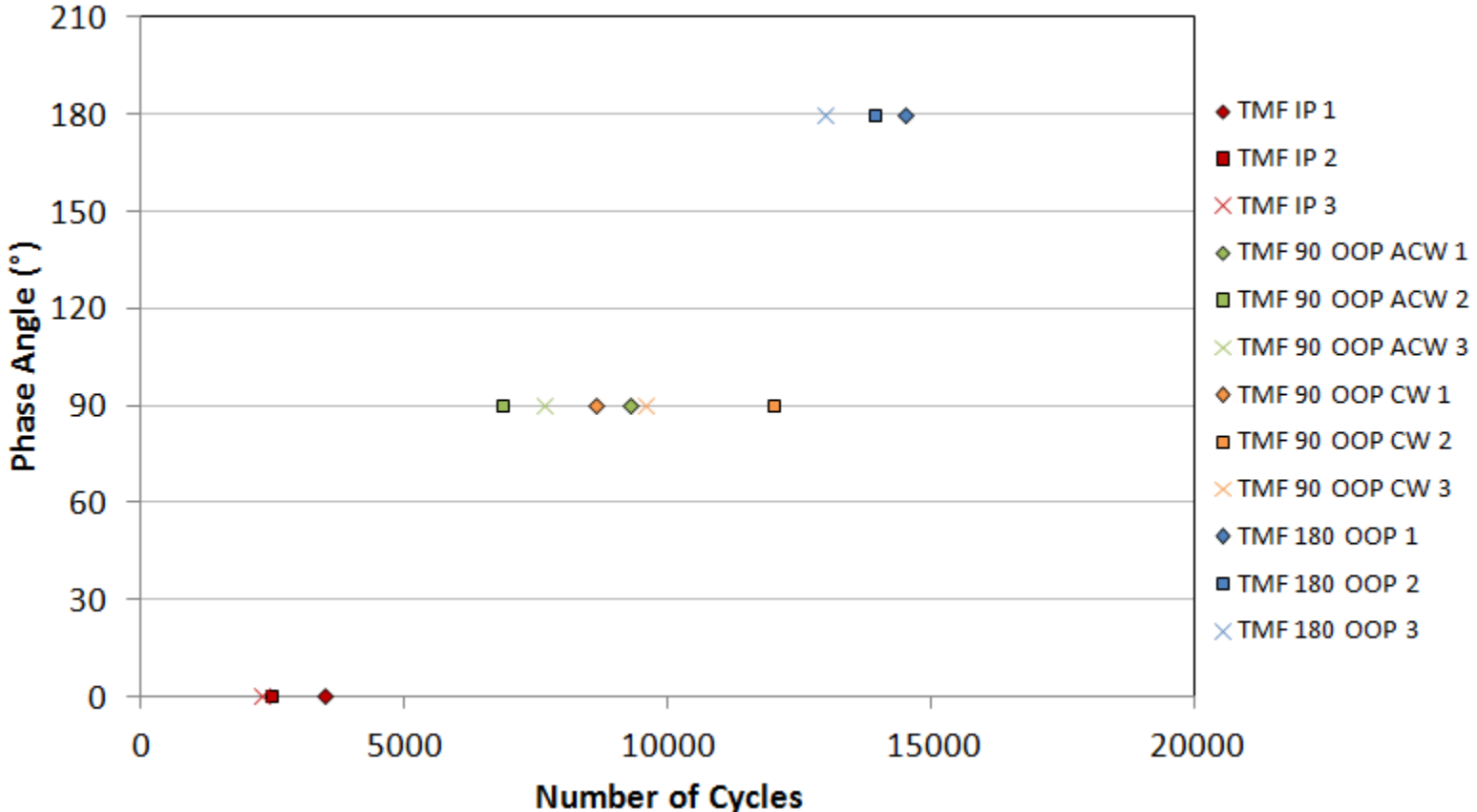
# Results: 180° OOP Crack Growth



# Results: TMF Crack Growth Summary



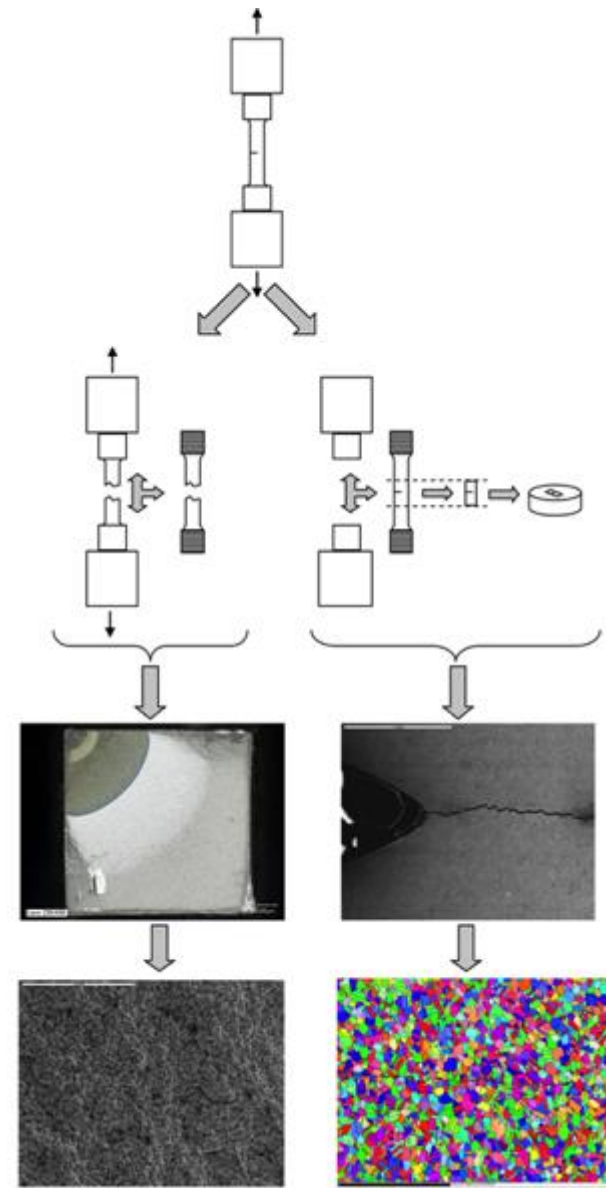
# Results: Phase angle vs. time to 2mm crack length



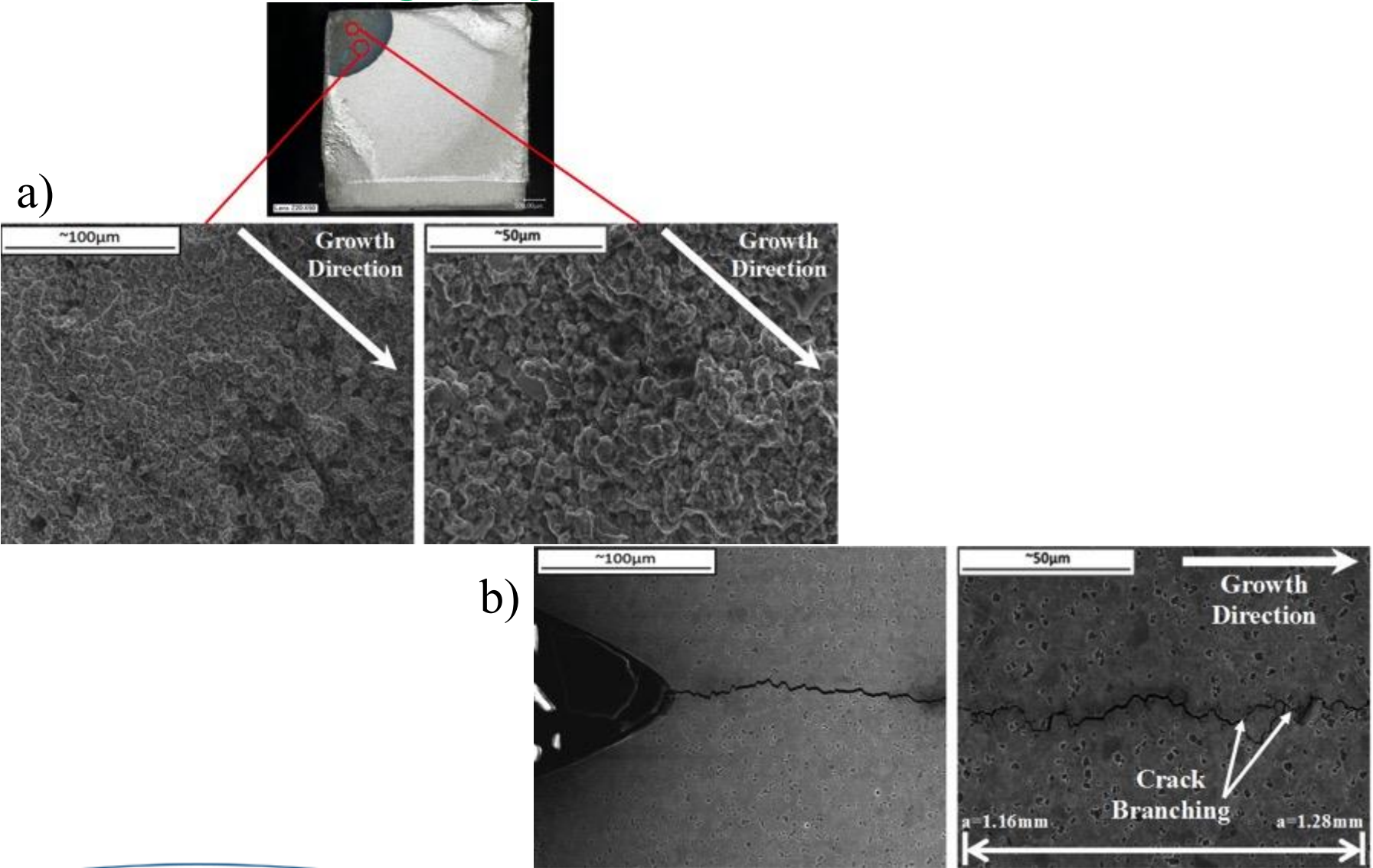


# Results: Analysis Method

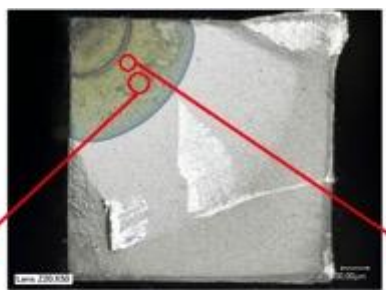
- Two methods used to analyse the crack growth behaviour once the target crack length had been achieved:
  - Applying load to failure to expose the heat tinted fracture surface for SEM
  - Unloading the specimen, sectioning the material around the notch plane and mounting to observe how the crack progresses laterally for EDX or EBSD



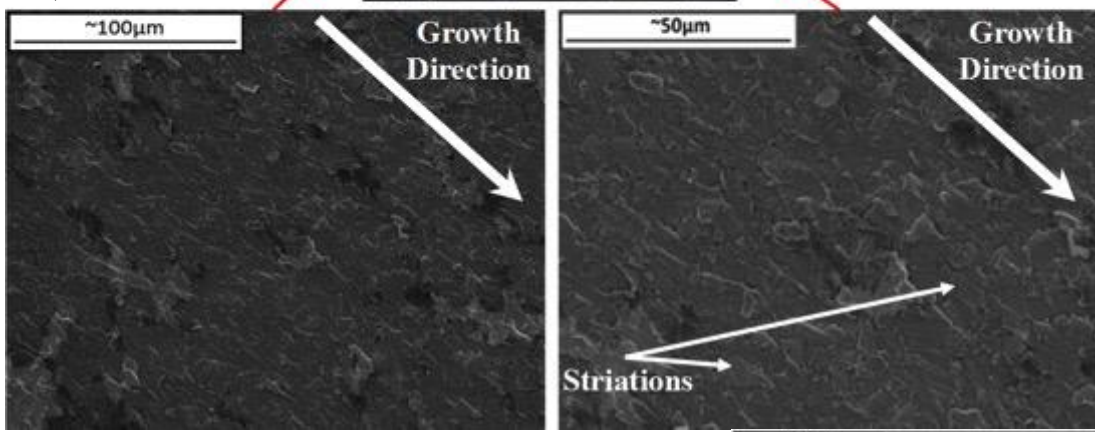
# Results: IP Fractography



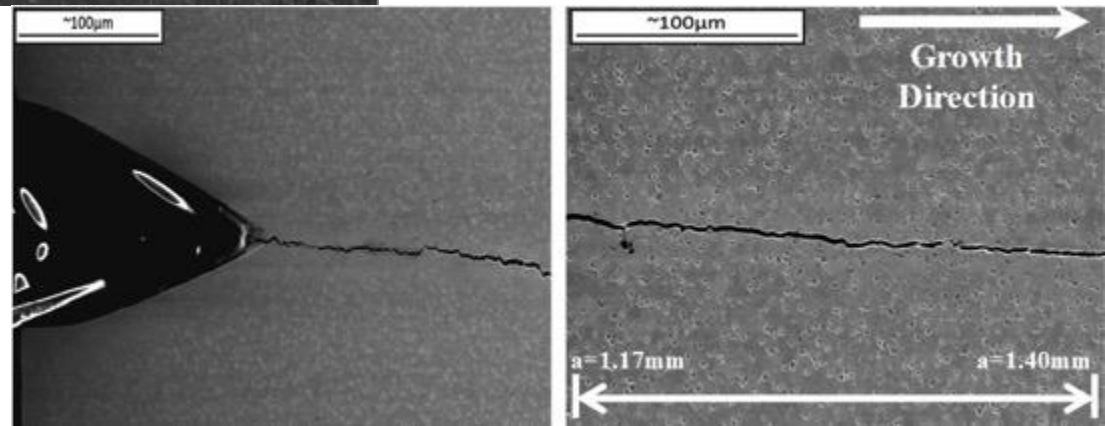
# Results: 180° OOP Fractography



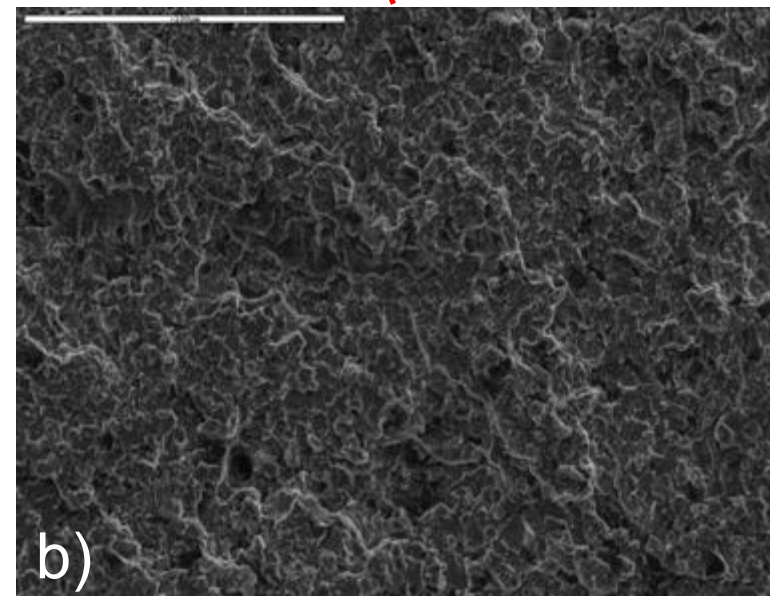
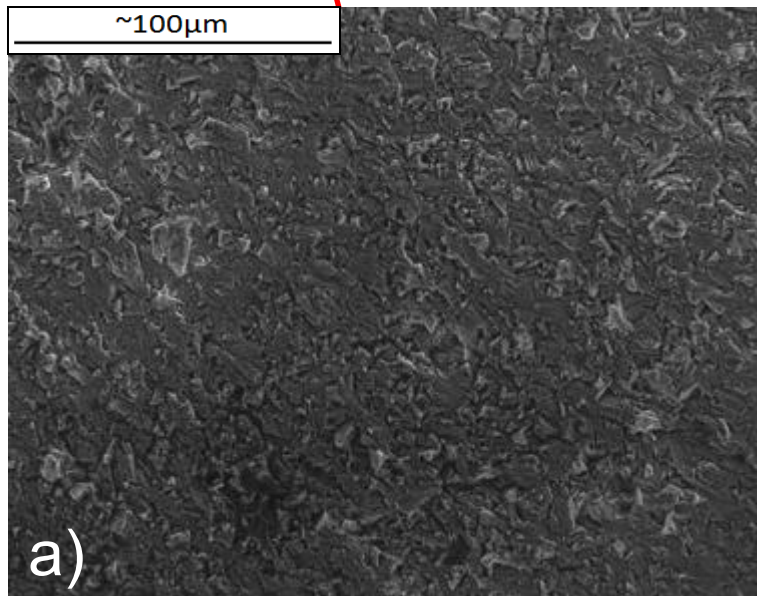
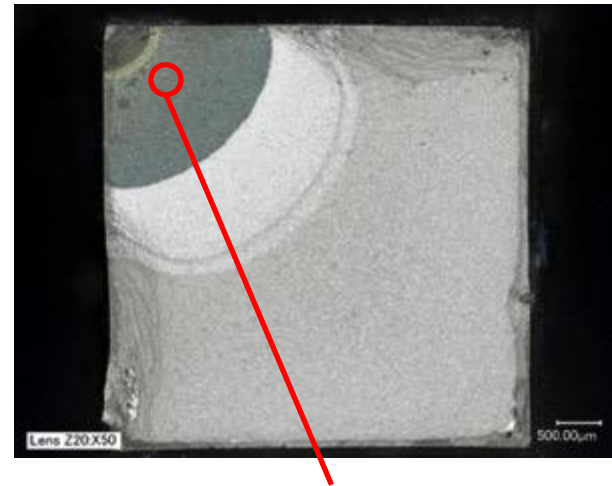
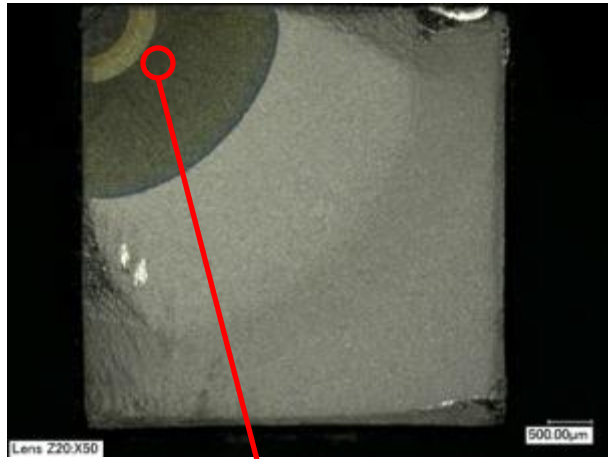
a)



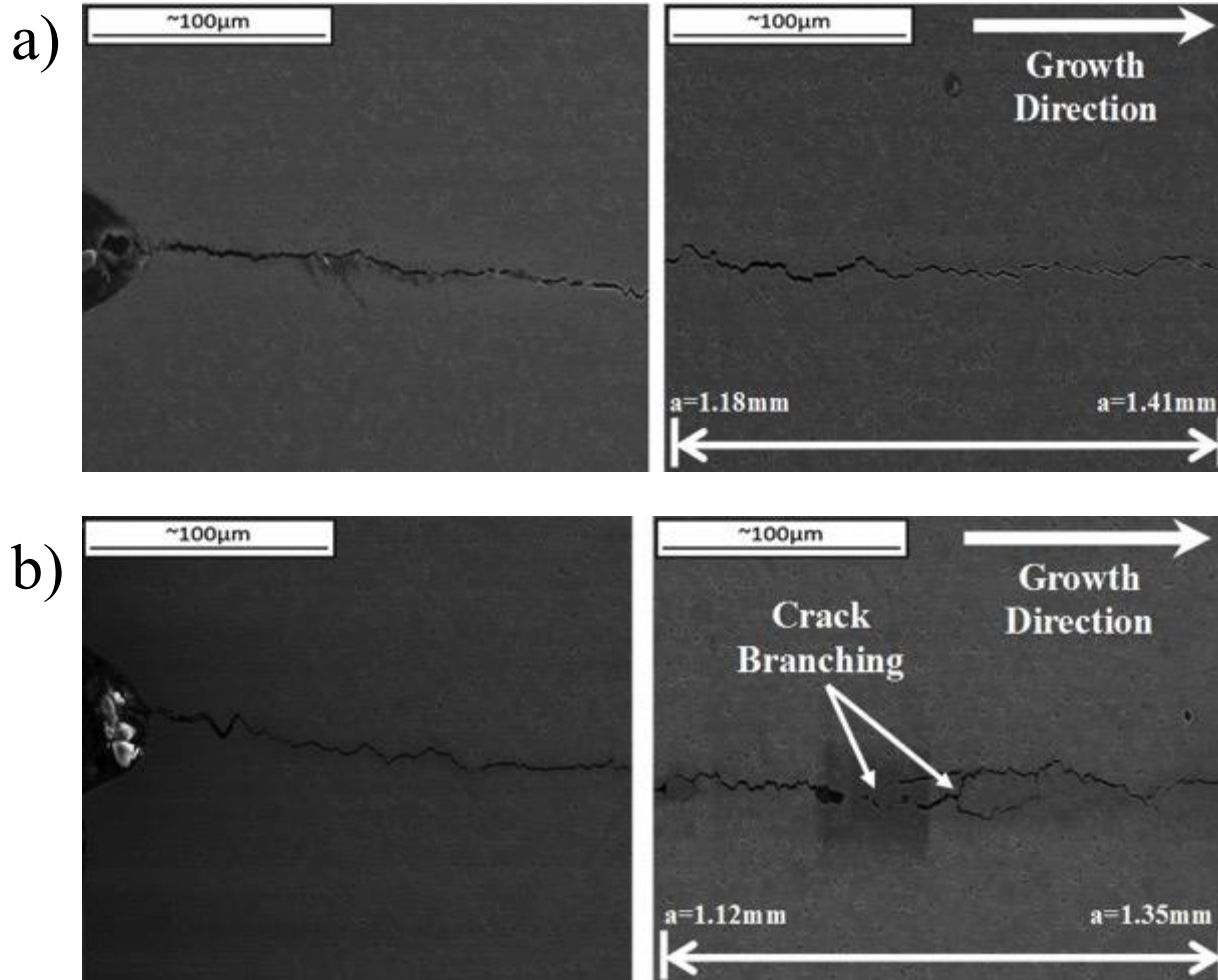
b)



# Results: Fractography of 90° OOP a) ACW and b) CW



# Results: Fractography of 90° OOP a) ACW and b) CW



# Results: 90° OOP CW vs. ACW theory

## ➤ CW:

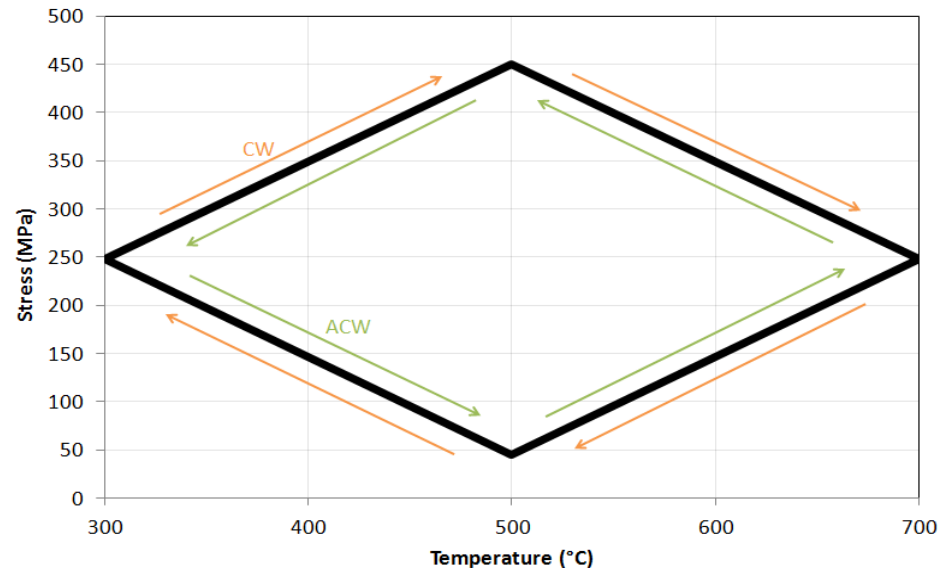
- Unloaded at high temperatures which oxidises crack tip because there is no crack growth so oxides reach a few grains beyond tip
- Loads the oxidised crack tip so crack grows along oxidised grain boundaries causing more of an intergranular failure

## ➤ ACW:

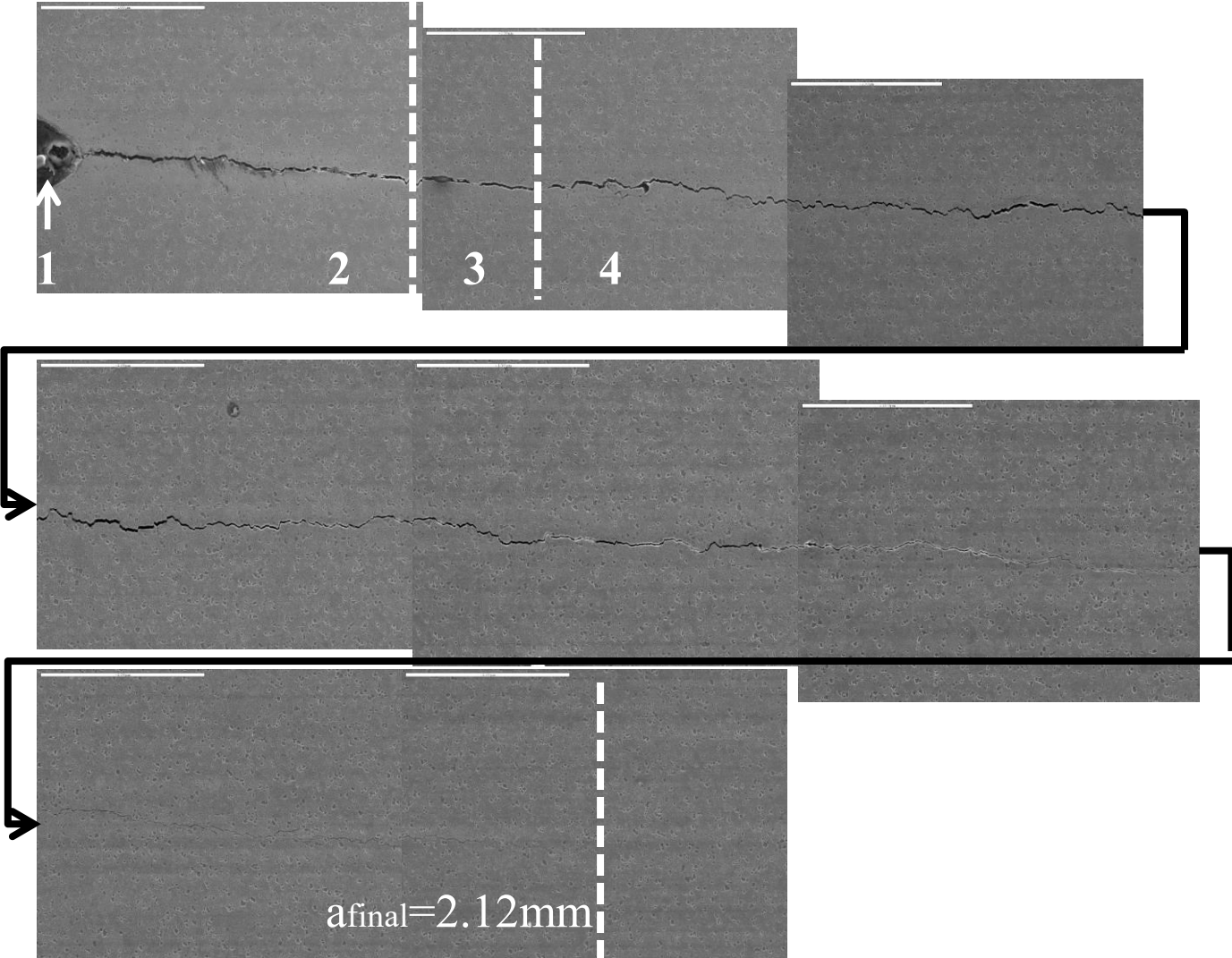
- Unloaded at low temperatures so there is no/less oxidation
- Loaded at higher temperatures so creating new surfaces and preventing oxidation of crack tip causing dynamic transgranular failure i.e. Crack growth faster than oxidation process

## ➤ Theory to the test:

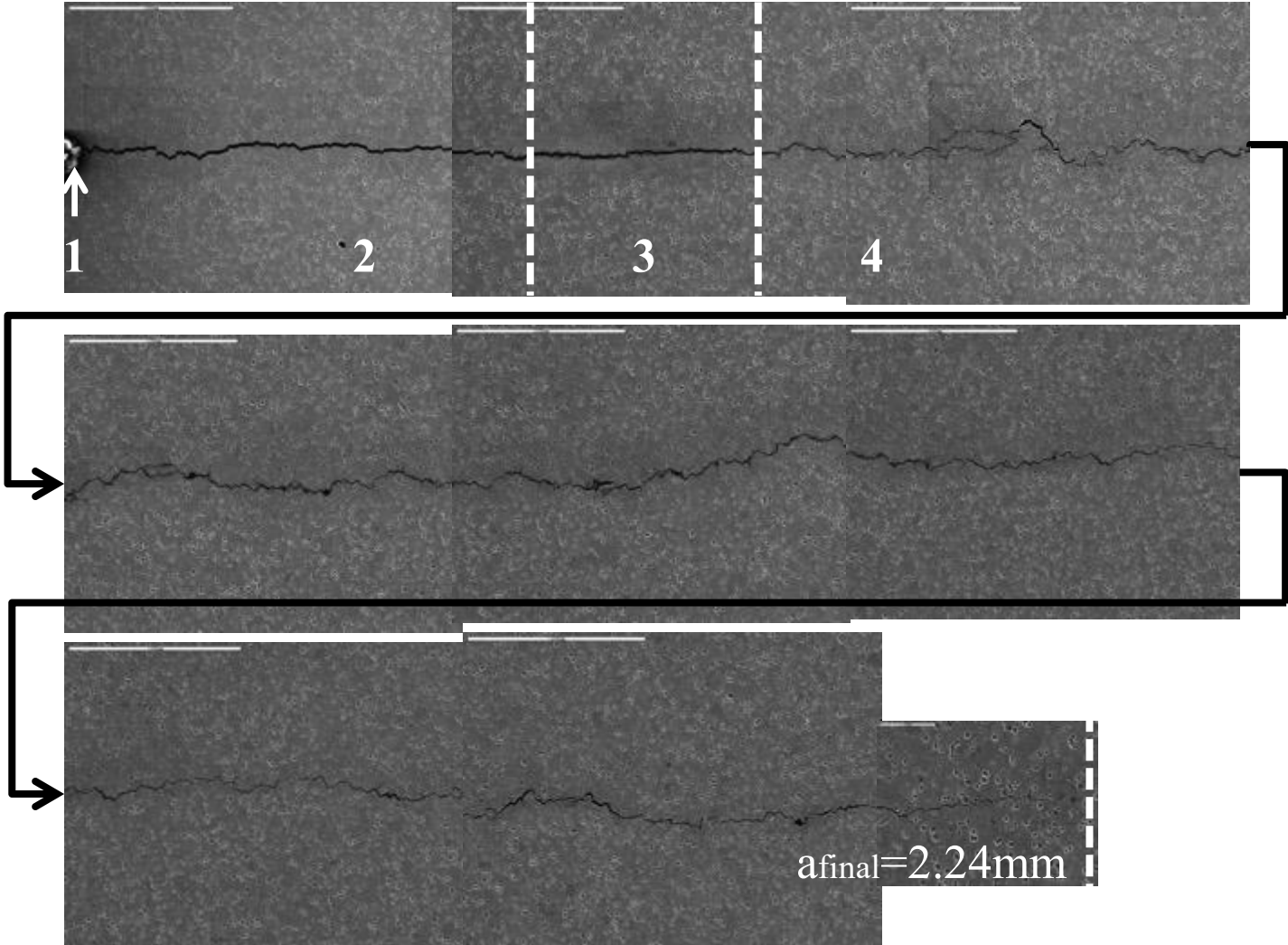
- 500 second cycle TMF OOP90° ACW test to manipulate mechanism
- Check if oxidation surpasses crack growth rate for intergranular failure



# Results: 90° OOP ACW (80 sec) Crack Progression

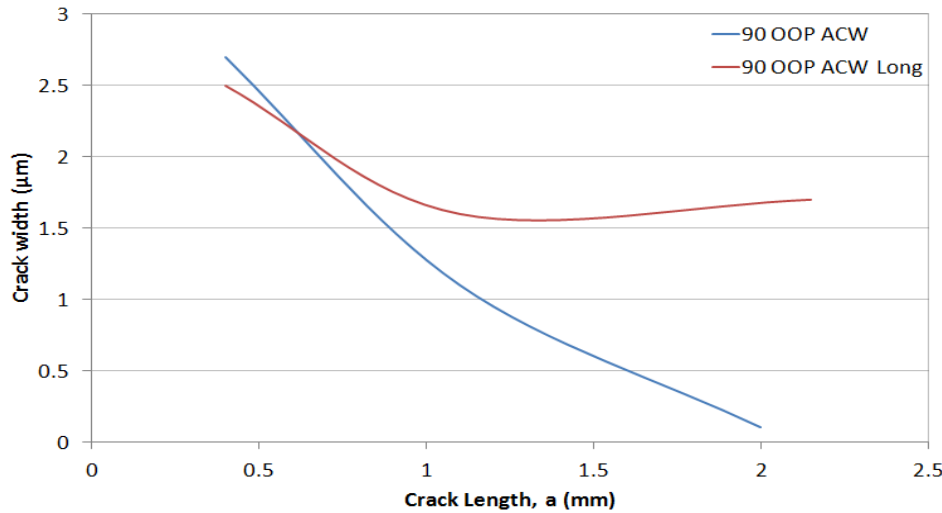


# Results: 90° OOP ACW (500 sec) Crack Progression





# Results: Evidence of Crack Tip Blunting

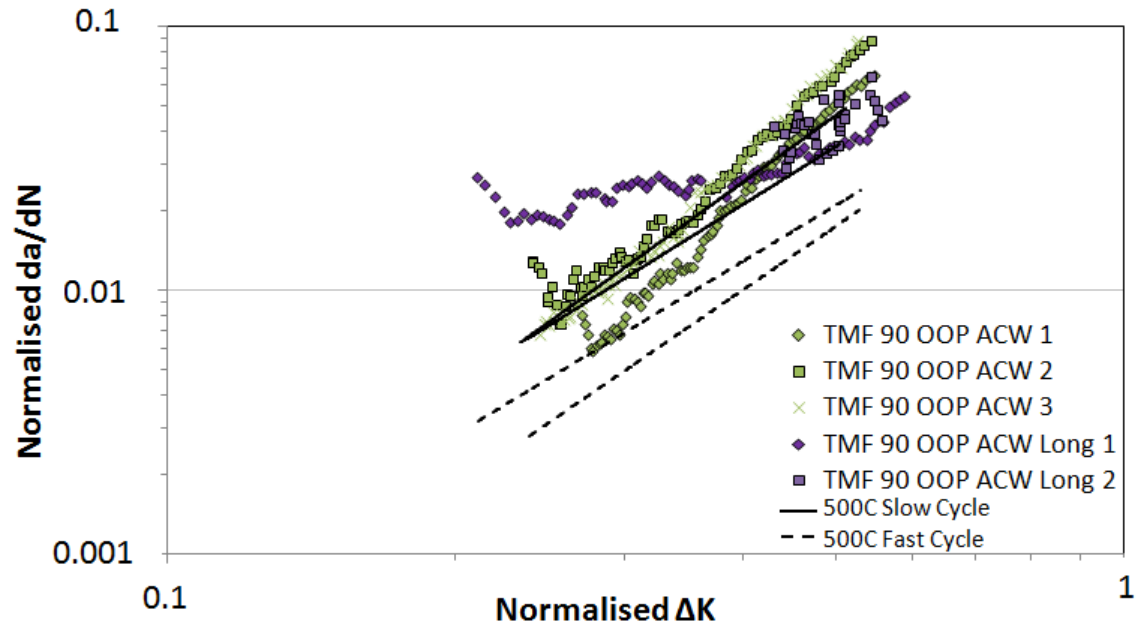


It is clear that the longer cycle results in a wider crack throughout the test

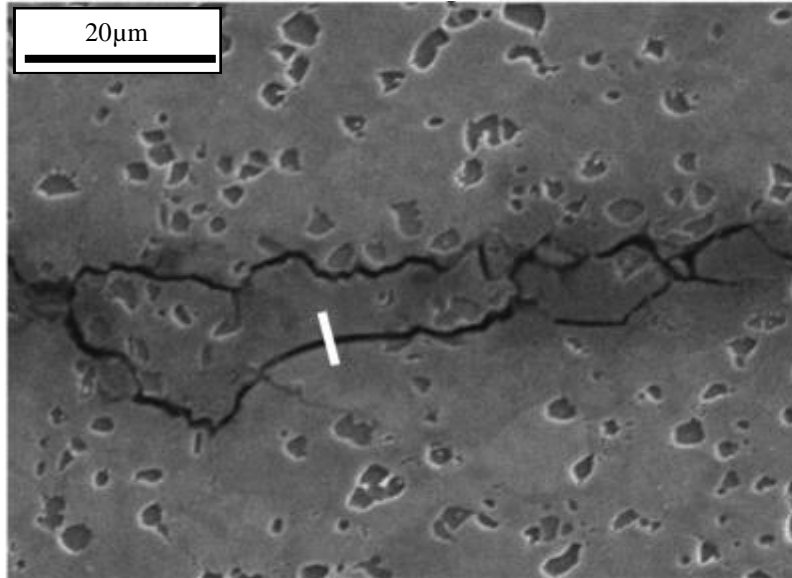
Flat gradient of the Paris curve supports this crack tip blunting theory

The crack growth is retarded by the reduced stress concentration at the crack tip

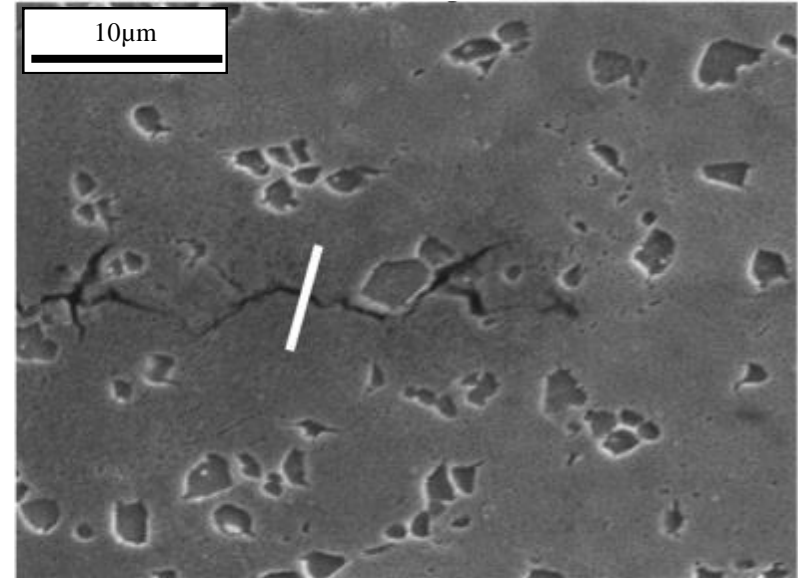
Is this due to oxidation layers on the upper and lower surfaces of the crack?



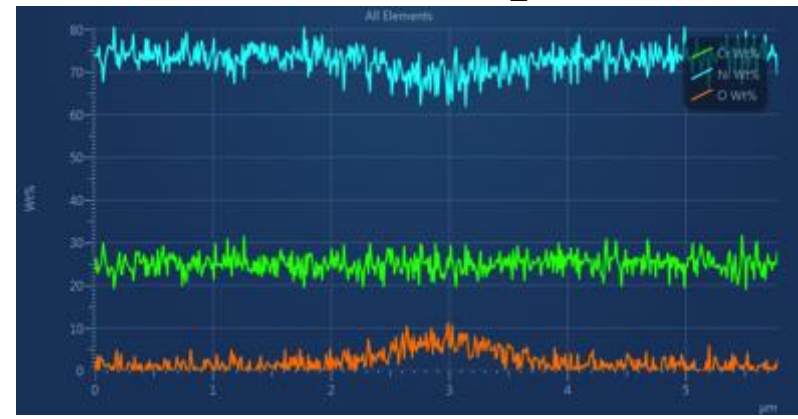
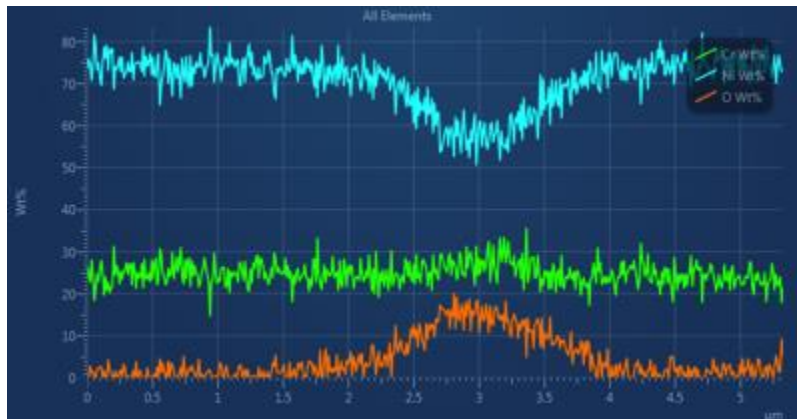
# Results: 90° OOP ACW (80 sec) Oxidation Levels from EDX



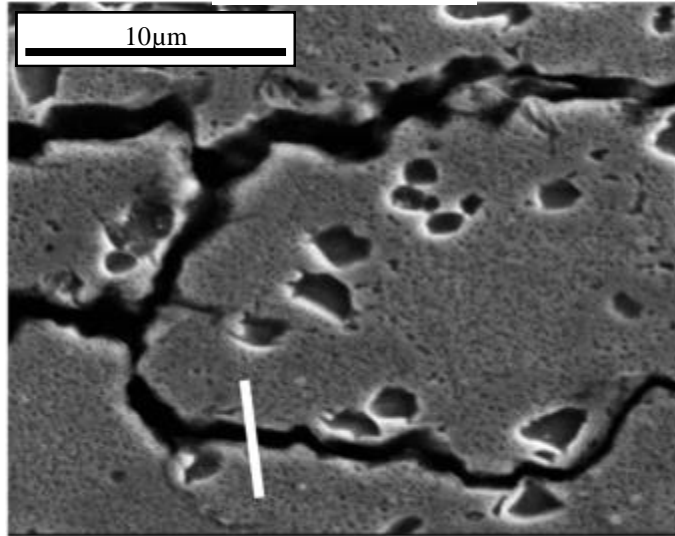
**a) Near notch**



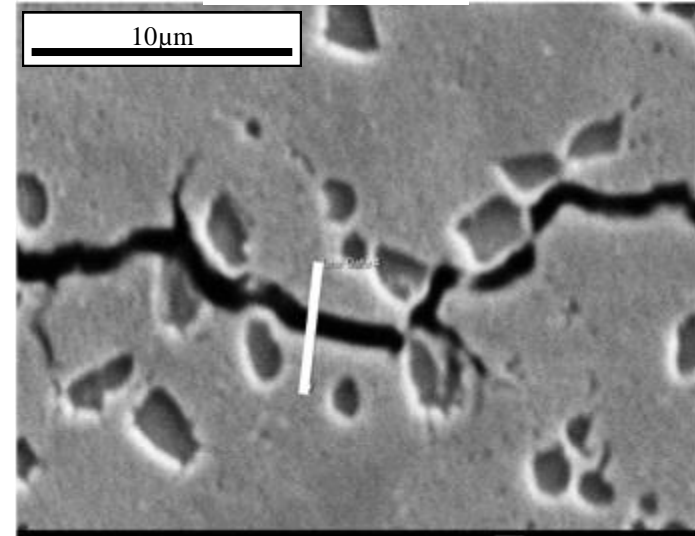
**b) Near tip**



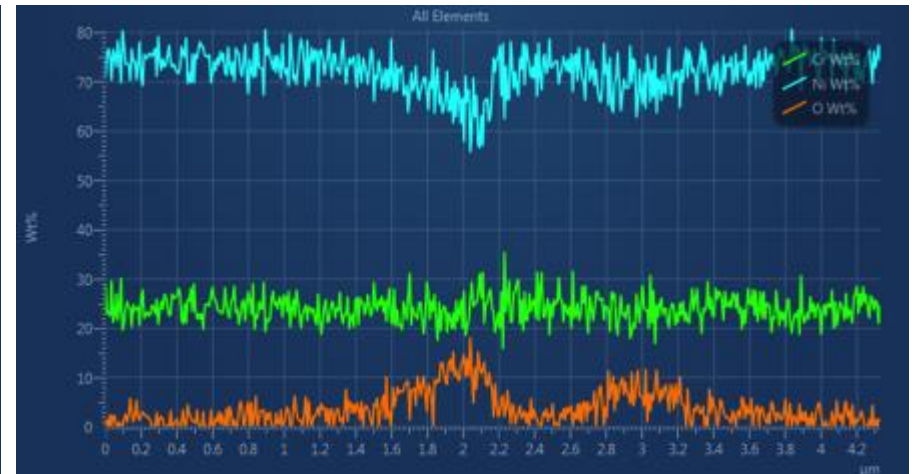
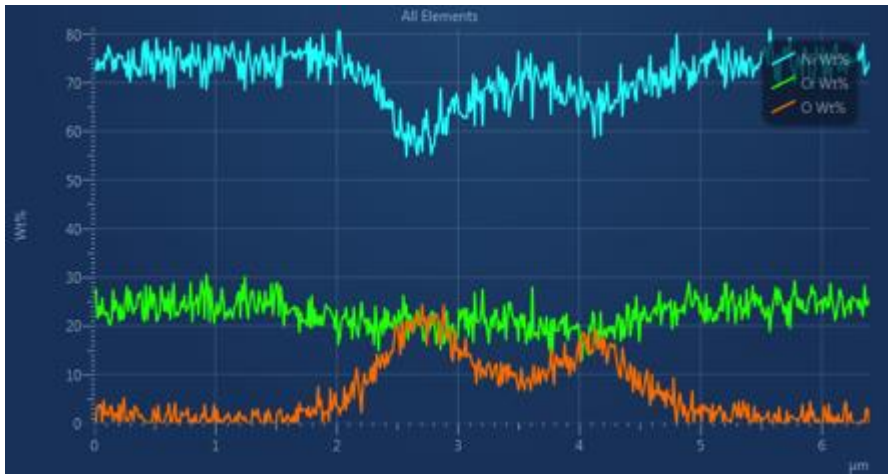
# Results: 90° OOP CW (80 sec) Oxidation Levels from EDX



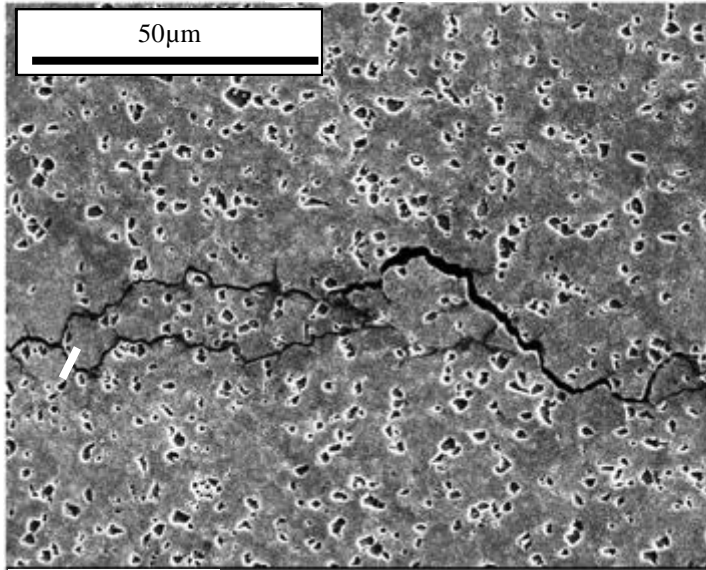
**a) Near notch**



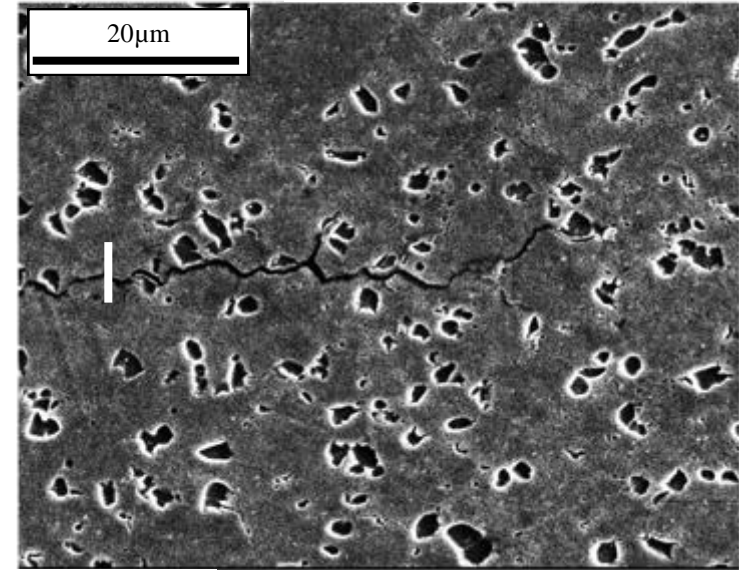
**b) Near tip**



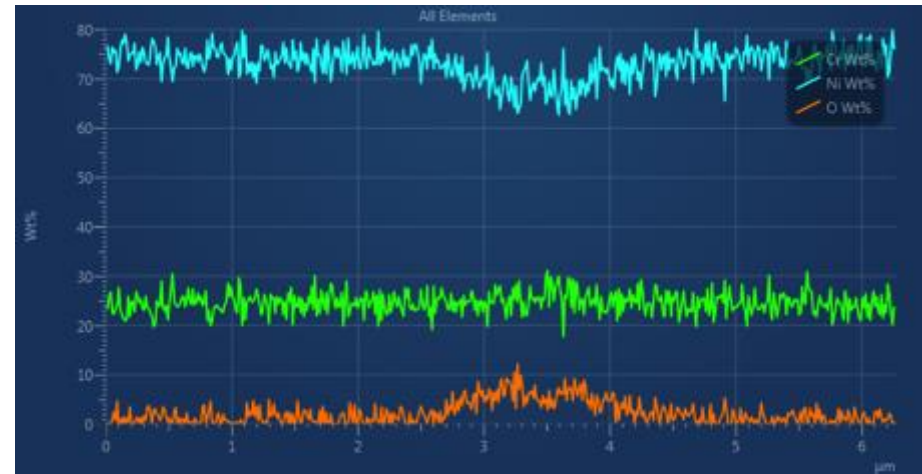
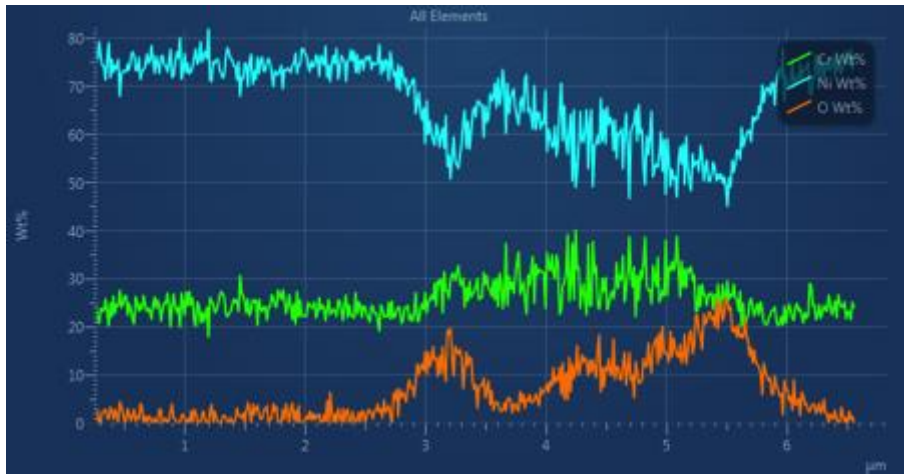
# Results: 90° OOP ACW (500 sec) Oxidation Levels from EDX



**a) Near notch**



**b) Near tip**



## Results: 90° OOP CW vs. ACW Oxidation Levels

- This table quantifies the EDX images for all diamond cycles
- Clearly the CW levels are higher than those of ACW suggesting oxidation does indeed cause the intergranular failure on loading
- The 500 second ACW cycle results in much more oxygen presence than the 80 second ACW cycle implying that the oxidation process is time dependent

Test Condition	Oxidation peak near notch (%)	Oxidation peak near crack tip (%)
90° OOP ACW (80sec)	18	8
90° OOP CW (80sec)	21	13
90° OOP ACW (500sec)	24	10

# Conclusions

- **TMF is becoming a critical life criteria for gas turbine design**
- **A test rig has been designed and validated for TMF crack propagation to investigate effects of various phase angles**
- **Crack growth rates established**
  - **TMF**  
$$\text{OOP180} \leq \text{OOP90} < \text{IP}$$

(Transgranular < Intergranular)
  - **Creep and oxidation effects with high temperature IF slow cycle tests**  
$$\text{Fast } 700^{\circ}\text{C} < \text{IP} < \text{Slow } 700^{\circ}\text{C}$$
$$300^{\circ}\text{C} < \text{OOP180}$$
- **Diamond cycles seem to be sensitive to loading direction due to oxidation rates during the loading cycle**
  - **Longer 500 second cycle has supported this, with evidence of crack tip blunting caused by creep at high temperature/mean stress region and oxidation layers on upper and lower surfaces of the crack**

## Acknowledgements:

The current research was funded by the EPSRC Rolls-Royce Strategic Partnership in Structural Metallic Systems for Gas Turbines (grants EP/H500383/1 and EP/H022309/1). The provision of materials and technical support from Rolls-Royce plc is gratefully acknowledged.

# Thank You

# Questions ?

# 3D EBSD of Thermo-Mechanical Fatigue Cracks in Compacted Graphite Iron

Edwin Lopez<sup>a</sup>, Sepideh Ghodrati<sup>b</sup>, Yaxun Wu<sup>b</sup>, Hadi Pirgazi<sup>a</sup> and Leo Kestens<sup>ab</sup>

<sup>a</sup>Department of Materials Science and Engineering, Ghent University, Technologiepark 903, 9052 Gent, Belgium

<sup>b</sup>Department of Materials Science and Engineering, Delft University of Technology, Mekelweg 2, 2628 CD, Delft, The Netherlands

## Introduction

Out of phase Thermo-Mechanical Fatigue (TMF) occurs in the valve bridge of engines during start-up and shut-down cycles. Compacted graphite iron is the material of choice because of its perfect balance between mechanical and thermal properties. TMF tests were carried out in the lab under uni-axial total constraint condition. The correlation of crack propagation, microstructure and holding time were analyzed in this research.

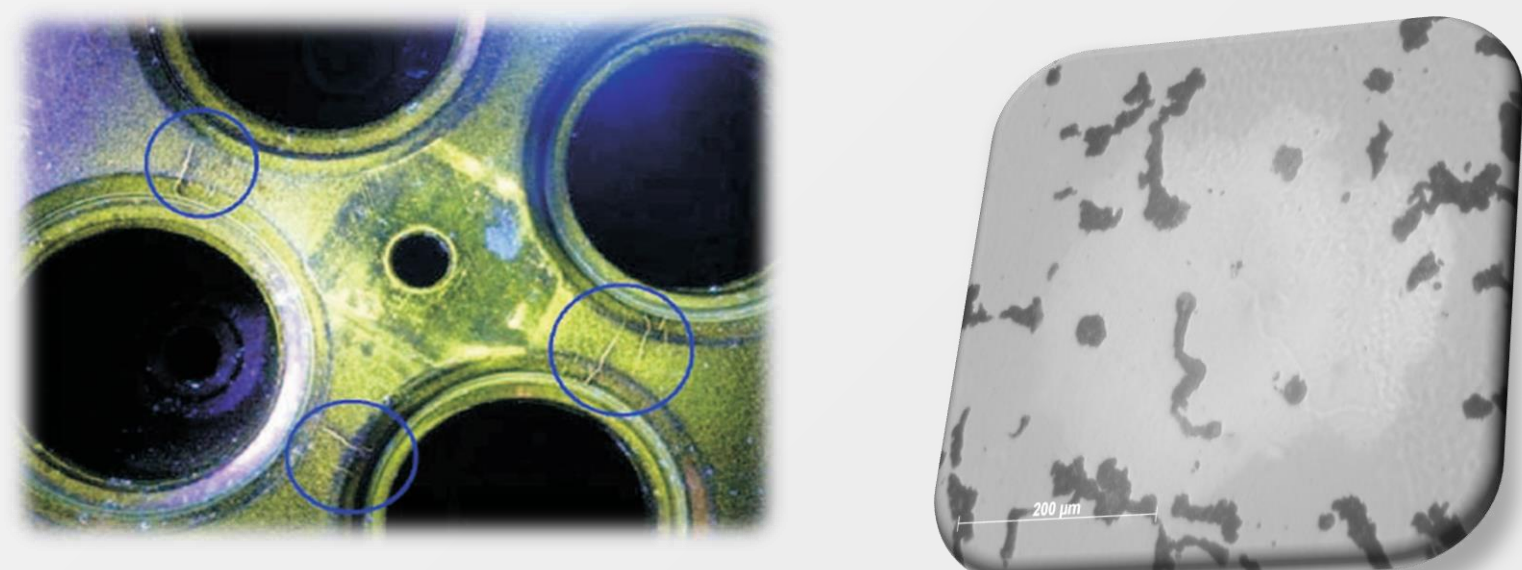
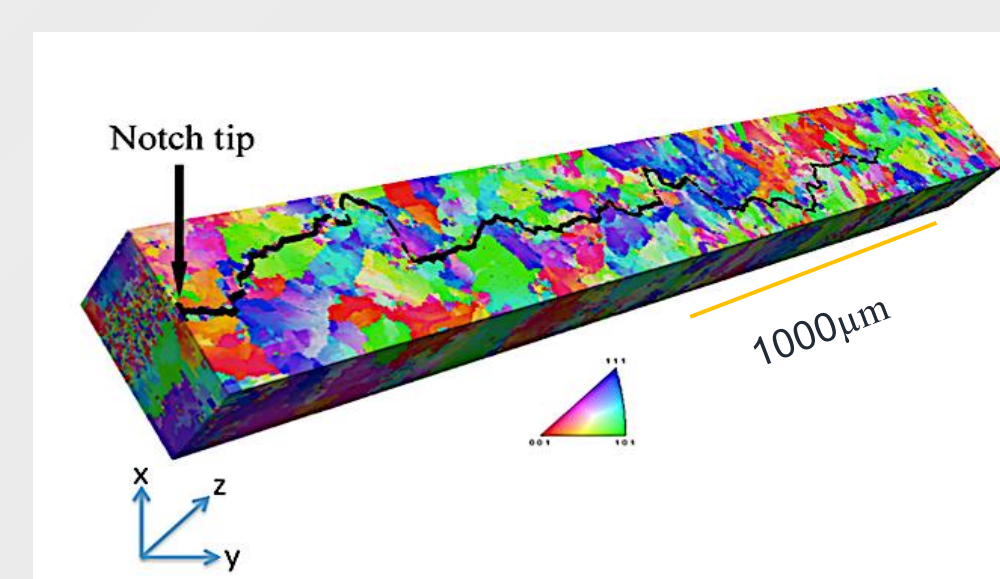


Figure 1: Left, Valve bridge head engine area; Right, Compacted graphite iron

By means of SEM and 3D EBSD measurements, it was found that the volume fraction of graphite in the crack path in the lab sample has considerably increased (2.5x) with respect to a random section. However, in the engine sample no such increase was observed.



	Graphite Fraction Area (%)
LST	18.4
LMT	27.6
ET	8.0

Figure 4: Left, Valve bridge head engine area; Right, Compacted graphite iron

## Materials and procedures

The effect of holding time during high temperature phase of the TMF cycle was investigated, by using three different holding times 30 (LST), 1800 (LMT) and 18000 seconds (LLT). Three additional samples were analyzed: a reference sample from the lab (LR), a sample from an unloaded real engine (RE) and a factory tested engine sample after 3000 cycles (ET). SEM images and EBSD measurements were used to characterize the crack path and analysis the failure.

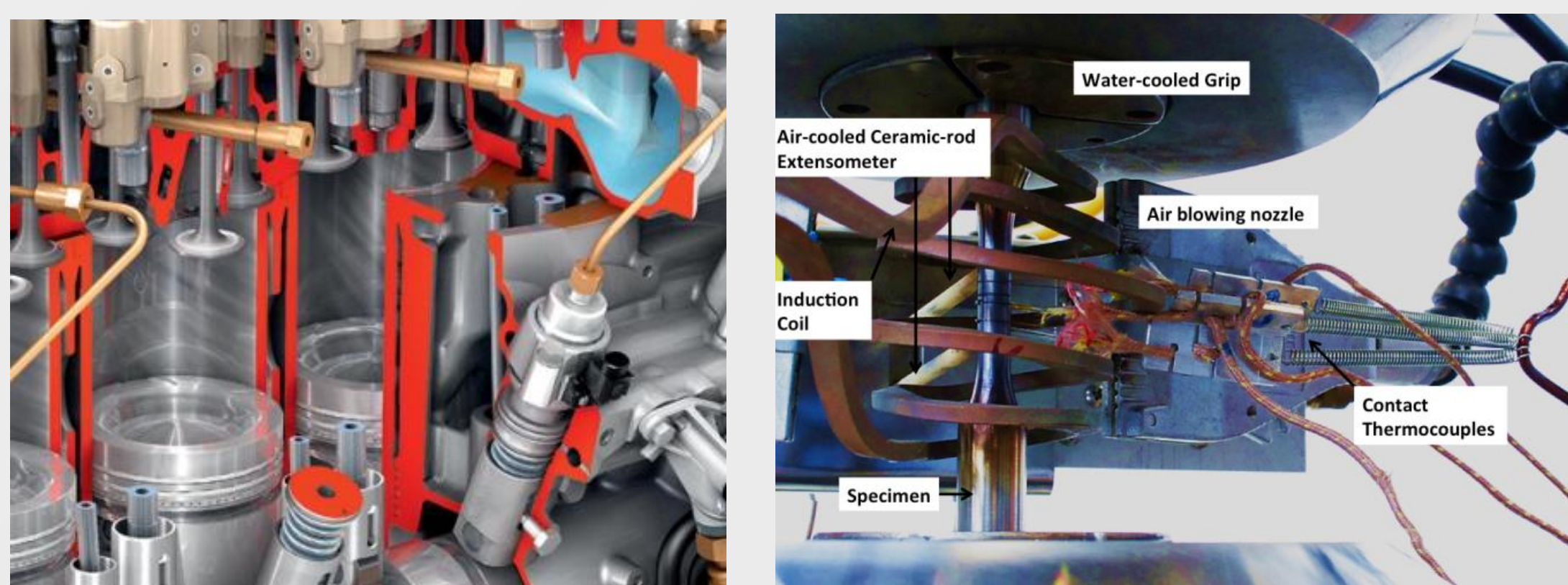


Figure 2: Left, Design of a real engine; Right, Lab Setup

The effect of holding time at high temperature is reflected on the Kernel Average Misorientations (KAM) distribution plotted on figure 5. After TMF tests samples with longer holding times at high temperature shows higher average values of KAM, meaning that the compressive stresses are relaxed in the hot part of the cycle and higher tensile stresses are developed in the cold part of the cycle. However, KAM in real engines are not affected during TMF cycles.

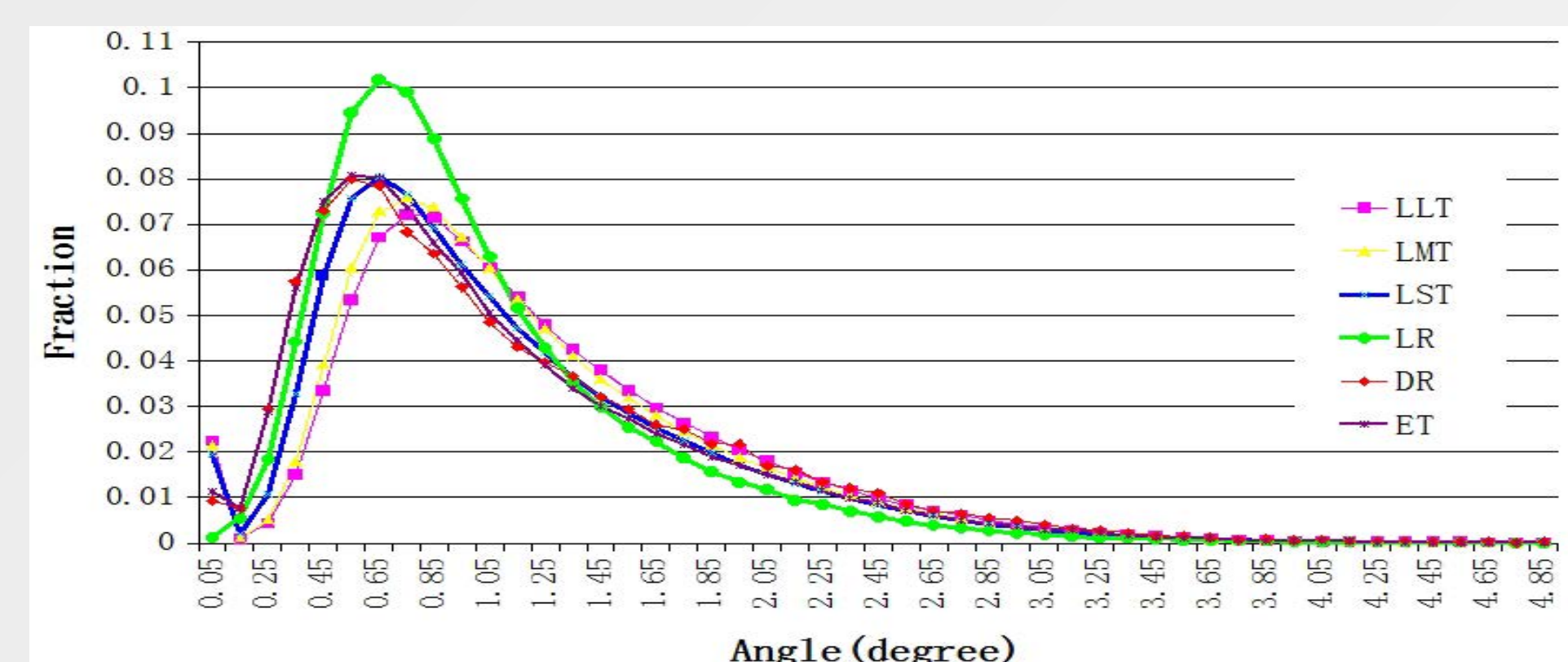


Figure 5: Kernel Average Misorientation

## Results and Analysis

Graphite particle size was of crucial importance in the crack initiation, whereas the spatial distribution of the particles played a decisive role in crack growth. This is in contrast with the branched crack morphology observed in engine samples where the propagation path is not specifically related to the spatial distribution of graphite particles.

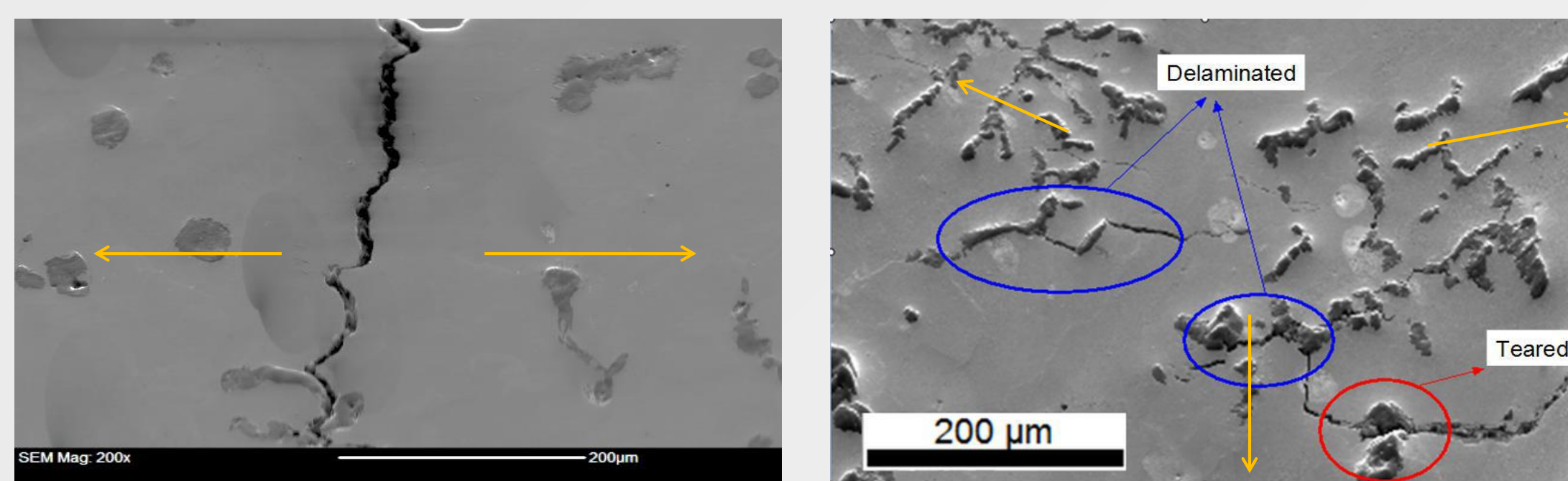


Figure 3: Left, Lab test at uniaxial fatigue; Right, Real engine metallography, multiaxial strain

It was concluded that total constraint test mode (shown in figure 6 Left), perhaps was too severe laboratory tests. Therefore a new experimental setup has to be developed to better mimic the stress-strain conditions of the valve-bridge area, (like partial constraint shown in figure 6 right) However, it remains to be verified whether a uni-axial loading mode of a typical mechanical test is suitable to investigate the complicated 3D stress distributions of real engine.

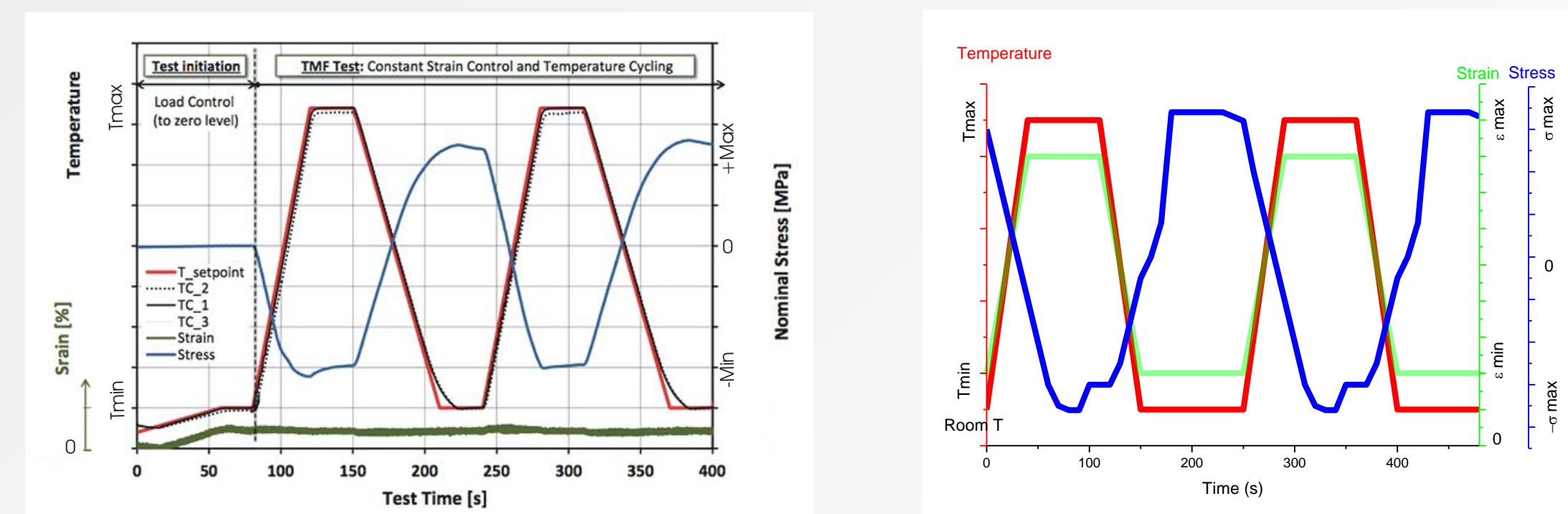


Figure 6: Plot of stresses and strains for Total constraint (left) and partial constraint (right)

## Conclusions

Graphite particle size was of crucial importance in crack initiation and spatial distribution of the particles played a decisive role in crack growth.

By increasing holding time at high temperature, stresses more relaxed in the hot phase and the tensile stresses increased in the cold phase, correspondingly.

Crack morphology in engine tested samples was branched not specifically related to the spatial distribution of graphite particles.

Total constraint is too severe to mimic the real engine test condition; it is necessary to investigate TMF behavior under partial constraint conditions.